AIR UNIVERSITY

May 9, 2024

ISNB 978-627-94533-0-3

PROCEEDINGS

Vol. 1

1st International Conference on Recent Trends in Statistics-Data Analytics with Applications in Natural Sciences

SPONSORS

All papers published in the

PROCEEDINGS

were accepted after formal peer review

by the experts in the relevant field.

Published by: ICRTSDA, Air University Islamabad, Pakistan.

Financial support of

Pakistan Science Foundation,

and Pakistan Academy of

Sciences

are highly appreciated

CONTENTS

Message from The Vice Chancellor

Air University

Air Marshal Abdul Moeed Khan, HI (M)

It is with immense pride and pleasure that I extend my heartfelt congratulations to all participants, organizers, and contributors to the 1st International Conference on Recent Trends in Statistics-Data Analytics (ICRTSDA) held on May 9, 2024. This milestone event, which brought together over 200 national and international participants and witnessed the presentation of 100 research papers in a single day, stands as a testament to the dynamic academic and research environment fostered at Air University.

This conference was conceived as a forum for the exchange of meaningful ideas and experiences, providing a platform for scholars, practitioners, and students to share their knowledge, learn from each other, and explore new avenues for collaboration. The publication of the conference proceedings, featuring 60 peer-reviewed papers, is a significant achievement that highlights the quality and impact of the research presented. These publications not only contribute to the academic prestige of Air University but also play a crucial role in advancing the global body of knowledge in statistics and data analytics. The significance of this conference extends beyond the immediate academic gains. It serves as a catalyst for innovation and a foundation for future collaborations that will drive progress in science, technology, and society at large.

My heartiest felicitations to all the authors whose work has been published in this proceeding. Your contributions are a source of pride for the Air University, and I wish you continued success in your future research endeavors.

I would like to specifically acknowledge and commend the tireless efforts of the organizing committee, whose dedication and hard work were instrumental in the success of this conference. Your commitment to excellence has not only made this event possible but also has laid the groundwork for sustained excellence in research and education at Air University.

MESSAGE FROM

Emeritus Professor Dr Shahjahan Khan
Vice Chancellor, Asian University of Bangladesh, Dhaka, BANGLADESH
Emeritus Professor, University of Southern Queensland, Toowoomba, AUSTRALIA
Expatriate Fellow, Bangladesh Academy of Sciences (BAS)
Founding Chief Editor, Journal of Applied Probability and Statistics (JAPS), USA
President, Islamic Counties Society of Statistical Sciences (ISOSS), 2005-2011
Email Address: Shahjahan.Khan@unisq.edu.au

Organising an international conference is a very challenging undertaking. As the main organiser of six international conferences in Malaysia, Egypt, Qatar, Bangladesh, Pakistan and Indonesia, I can genuinely appreciate the dedication, hard work, creative ability, and management challenges involved in the organisation of successful international conferences.

Heartiest congratulations to the Air University Islamabad, especially to the organiser Prof Dr Ammara Nawaz Cheema, for organizing the 1st International Conference on `Recent Trends in Statistics and Data Analytics with Application in Natural Sciences on 09 May 2024. It was an honour for me to present a keynote address on `Decision from Data: Use and Abuse of Statistics in Development, Research & Public Decisions.'

After formal peer review by experts, sixty full-text research papers were selected to be included in this proceedings from the papers that were presented in the conference.

International conferences like this provide perfect platform for the researchers and scholars to present the outputs of their research, receive feedback from experts, build professional network and explore collaboration opportunities.

Research is a process of systematic investigations to expand the boundary of knowledge by creating new knowledge, exposing or uncovering facts that were unavailable or unknown, and enhancing and expanding the applications of scientific methods and technologies for the benefit of people.

There has been increasing demand for high quality research publications of university academics in recent years. The competition in securing high global ranking of universities has reinforced the matter further. So, the individual academics are under continuing pressure to publish their research articles in high impact international journals and conference proceedings. More seriously, the top management of universities are raising their expectations to ensure respectful research performance of their institutions. At this juncture, it is of utmost importance that the researchers, especially the young new generation of academics know the essential means and ways to increase their research productivity and create significant impact of their research work by publishing in reputed professional outlets.

Research publications help spread the new knowledge, makes it available for use in real589 life. It has notable impact on the scholarly communities and provides opportunities to train and create new generation of researchers. The intellectual strength of a nation is judged by its research contributions and innovative approaches for development and services that evolve from research.

The universities highly appreciate the research publications of its researchers. Significant publications and citations of published research bring more prestige to the universities and help grow their global ranking.

I sincerely hope that the readers of this proceedings will find the papers of high quality and beneficial to further research.

MESSAGE FROM

MS. SHAZA FATIMA KHAWAJA

MINISTER OF STATE (IT & TELECOMMUNICATION)

Asalam-o-Alikum!

I am pleased to learn that Air University, Faculty of Basic & Applied Sciences holding "1st International Conference on Recent Trends in Statistics Data Analytics (ICRTSDA)" at Islamabad Campus on May 9th, 2024.

I hope that M.Phil. & Ph.D. students in the disciplines of Data Analytics, Statistics and Data Science will enhance the up-date their knowledge and skills through these meetings and interactions with Foreign Experts & Research Scholars. This conference will certainly benefit the participants by exposing them to latest research techniques and developments in the relevant fields.

Application of Statistical Sciences to computers and information technology can play a pivotal role in a country's development. Moreover, the role of Statistics of critical importance in the formulation and monitoring of polices and plans in the light of emerging priorities of the government.

To Welcome foreign delegates from Iran, Egypt, France, Saudi Arabia, Qatar, Bangladesh, India, USA and Canada is a matter of immense pleasure and satisfaction. I wish that the deliberations of the conference would be fruitful achieving the desired objectives. I wish all success to the organizers of the Conference and a pleasant, comfortable, and academically enriching experience for the participants.

MESSAGE FROM

DR. NAEEM UZ ZAFAR (SI)

CHIEF STATISTICIAN PAKISTAN BUREAU OF STATISTICS

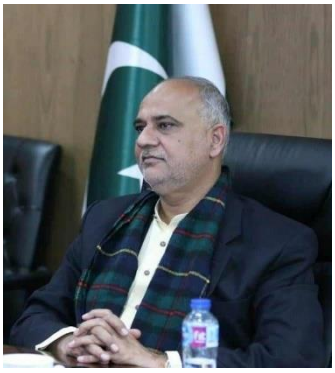

The infoage adage "Data is Oil" is being reviewed. Like oil, data also flows, but unlike oil, it does not turn into anything undesirable, anything to be discarded, it rather goes through a cycle of conversion from data to information to knowledge and then to wisdom. As students of Data Analytics we know that it is about deploying mathematical, statistical, and data tools to discover the evolving future, but as ardent learner of wisdom and philosophy we should also sincerely try to know and show the challenges, this evolution carries. Our belief in collective good will guide our pursuit of knowledge and wisdom shaping a more humane world.

MESSAGE FROM

DR. RASHID MEHMOOD

Dean FBAS Air University Islamabad

On behalf of the organizing committee, it is indeed a matter of great honour for me to acknowledge and thank all the stakeholders of this First International Conference on Recent Trends in Statistics and Data Analytics 2024.

I acknowledge & appreciate all the keynote speakers and presenters of this event whose contributions would set benchmarks for future research and opportunities in this direction of data analytics, and I hope that these proceedings will serve as a valuable resource for your ongoing research and professional activities.

Thank you for being a part of the first international conference and I look forward to seeing you at future events and continuing our journey of discovery and innovation together. I wish all of you very productive collaborations, and knowledge sharing in near future. May Allah be with us. Stay Blessed.

MESSAGE FROM
DR. AMMARA NAWAZ CHEEMA
Chair ICRTSDA

Dear Participants and Authors,

It gives me immense pleasure and pride on publication of the proceedings of the "1st International Conference on Recent Trends in Statistics and Data Analytics with Application in Natural Sciences." This conference proceeding issue is peer-reviewed where all papers were selected after expert evaluation in the domain. It represents a significant milestone to our collective efforts in advancing Statistics and Data Analytics, especially in its application to Natural Sciences.
Subsequently, I extend my warmest greetings to all authors of the proceedings. As Chair of the inaugural conference, and Chief Editor of proceeding, I am both honored to reflect on the exceptional contribution and meaningful discussions shaped with formal peer-review by experts into sixty full-length research papers selected for publication.

In today's rapidly evolving world, the importance of data-driven decision-making cannot be overstated. The convergence of Statistics and Data Analytics has never been more meaningful. In an era marked by unprecedented growth in data generation and complexity, our ability to analyze, interpret, and apply information effectively is critical. The purpose of the above conference was to bring together a diverse group of scholars, practitioners, and students to explore latest trends, methodologies, and applications in dynamic fields.

For students, this conference represented a unique opportunity to engage cutting-edge research and practical insights shaping the future of Statistics to Data Sciences. The sessions and workshops provided a platform to learn from leading experts, to understand emerging techniques, and to explore real-world applications of statistical and analytical methods. For professionals, this conference was a forum to exchange ideas, share experiences, and to collaborate solutions to complex challenges facing the industry. The participants acknowledged innovative statistical models and data analytics techniques to demonstrate extensive depth and coverage. Moreover, the discussions, networking opportunities and insights opened new avenues of research and application.

Lastly, I believe the importance of this conference extended beyond the immediate academic and professional gains. It underscored the critical role of interdisciplinary collaboration in advancing creative application of data analytics. By fostering dialogue between statisticians, data scientists, and experts in natural sciences, we feel better equipped to leverage data for informed decisions and meaningful outcomes in research and practice. I, therefore extend my deepest gratitude to the organizing committee, sponsors, and volunteers whose hard work and dedication made this conference possible.

Thank you for being a part of this remarkable journey.

1st International Conference on Recent Trends in Statistics and Data Analytics
Air University Islamabad, Pakistan – May 9, 2024, Vol. 1, pp. 1-7

https://doi.org/10.62500/icrtsda.1.1.1

MODELING INFLATION IN PAKISTAN USING ARIMAX MODEL

Abdul Rehman Malik[1], Dr. Zahid Iqbal[2]
[1]M.Phil (Statistics) Department of Statistics, Allama Iqbal Open University, Islamabad, Pakistan
[2]Associate Professor, Department of Statistics, Allama Iqbal Open University, Islamabad, Pakistan.

Abstract

The key objective of this study is to forecast inflation in Pakistan using an autoregressive integrated moving average with explanatory variables (ARIMAX) model. The studied data is obtained from World Development Indicator (WDI) during 1970 to 2020. This study used Ordinary Least Squares (OLS) method. Various diagnostic and selection criteria for the optimal model are preferred for forecasting of inflation rate in Pakistan. ARIMA (2, 0, 1) model is found suitable because its AIC, SC and HQC are least. Then including explanatory variables in ARIMA (2, 0, 1) model and make it as ARIMAX (2, 0, 1) model. Now multicollinearity test applied which outcomes reveals that there is no problem in it. Further, the residuals of ARIMAX (2, 0, 1) model is normally distributed, serially uncorrelated and free from hetroskedastic problem. The results of model showed that there is a smaller difference between forecasted and original values. Depending upon the lowest values of root mean square error (RMSE), mean absolute error (MAE), mean absolute percentage error (MAPE) and Theil inequality coefficient ARIMAX(2, 0, 1) model is unique and sufficient for forecasting inflation rate in Pakistan depending upon the Theil's inequality forecast accuracy measures.

Key Words: Pakistan, WDI, ADF, ARIMA, AIC, SC, HQC, ARIMAX, Forecasting.

1. Introduction

According to the Webster (2000) "Inflation is the persistent increase in the level of consumer prices or a continual decrease in the purchasing power of money". Consumer Price Index (CPI) is typically used to measure the inflation in financial analysis.

Auto Regressive Integrated Moving Average (ARIMA) model is mostly used for forecasting. It is used by different researcher for forecasting inflation. However, ARIMA model does not capture some turning points in inflation data. In order to improve forecasting performance, should we include another explanatory variable into ARIMA model? This question, we compare the forecasting performance of ARIMAX model for inflation rate in Pakistan. To use ARIMAX modeling in context to model inflation rate in Pakistan which is the novelty of this work. In this research the dependent variable will be inflation and independent variables will be money supply, rate of exchange, gross domestic products and government final consumption expenditure.

Contribution of the study is:

1. The related studies mentioned above all forecast based on the number of cases occurring each period either monthly or annually and none have used ARIMAX and involves the influence of other variables.
2. To use ARIMAX modeling in context to model inflation rate in Pakistan which is the novelty of this work.

The objective of the existing study is to forecast inflation in Pakistan using ARIMAX model.

2. LITERATURE REVIEW

Various studies have been done on inflation in different counties. Some of them are given below:

Tsirigotis, Vlahogranni and Karlaftis (2012) studied to check the climatic effects on the performance of short run traffic. By different vector ARMAX models to estimate weather effects and traffic mix upon the traffic speed predictability, they resulted that addition of explanatory variables in adequate models developed their forecasting performance although improved model such as vector and Bayesian estimation recovers the model extensively.

Kongcharoen and Kruangpradit (2013) studied about ARIMA and ARIMAX model on Thiland Exports. They observed the performance of forecasting of ARIMAX model and ARIMA model for export data of Thailand. They found that ARIMAX model is better than ARIMA model for country level data. Furthermore, indirect method does not give the better performance of forecasting than direct method for Thailand export data.

Victor-Edema and Essi (2016) studied non-oil exports by employing Autoregressive Moving Average with explanatory Variables (ARIMAX) model in Nigeria. The ARIMAX (2, 1, 5) estimated model is the parsimonious model. Test of Augmented Dicky Fuller (ADF) was employed to identify that the series is stationary or not. Graphical representation was also examined by utilizing function of autocorrelation (ACF) and function of partial autocorrelation (PACF). The comparison of different models is used by seeing akaike information criterion (AIC) and the foremost sufficient model is selection. And outcomes showed that the rate of exchange is neutral with non-oil in Nigeria as non-significant rate of exchange.

Ugoh, Uzuke and Ugoh (2021) studied an appropriate ARIMAX model on forecasting Nigeria's GDP for the years 1990 to 2019. ARIMAX (0, 1, 1) model is found to be more ideal and adequate for forcasting Nigeria's GDP based on the Theil's U forecast accuracy measure.

3. MATERIALS AND METHODS

Annual data were taken from World Development Indicator (WDI) period from 1970 to 2020. ARIMA model was applied for forecasting cycle with Box-Jenkins methodology. The ARIMA approach mingles two different procedures into an equation. The first process is an *autoregressive* procedure (hence the AR in ARIMA), and the second process is a *moving average* procedure (hence the MA in ARIMA). ARIMA modeling shows that there is a relation between a time series data and its own lagged data.

In general, the model is referred to ARIMA (p, d, q) model, where p, d and q are integers greater than or equal to zero and refer to the order of autoregressive integrated and moving average aspects.

Methodology of the Box-Jenkins involves five steps for identifying, selective and assessing conditional means models that are discussed below (Gujarati and Porter (2009)):

1. Time series is tested for stationarity. If it is non-stationarity then the series has to be differenced that create the time series stationarity. The autocorrelation (AC) and partial autocorrelation (PAC) functions of stationary series decay exponentially (or cut off totally after some lags).
2. A conditional mean model has to be preferred for the series. The autocorrelation (AC) and partial autocorrelation (PAC) functions could be useful in this regard through the procedure of autoregressive (AR) having the partial autocorrelation (PAC) cutting off after some lags. On the other hand, for a procedure of moving average (MA), the autocorrelation function (AC) cuts off after some lags, but the partial autocorrelation (PAC) decays gradually. Consider an ARMA model, if both the autocorrelation (AC) and partial autocorrelation (PAC) decay gradually.
3. The fitting model is specified and parameters of the model are estimated.
4. Certain goodness-of-fit tests are run in order to ensure the model describes the data adequately. Residuals should be uncorrelated, homoscedastic and normally distributed with constant mean and variance.
5. The preferred model could be employed to forecast or generate Monte Carlo Simulation over a future time horizon.

4. RESULTS AND DISCUSSION

Initial step for statistical study is to eyeballs the structure of the data. Elementary outcomes of inflation (INF), broad money (BM), exchange rate (EXR), gross domestic products (GDP) and government final consumption expenditure (GEX) which all are not symmetric because all of these variables having unequal mean and median. Skewness and kurtosis also moves to show non-normality. Additionally, the Jarque-Bera p-value of all these variables is significant because it is less than 5 per cent. Therefore, we can conclude that these variables are not normally distributed. So, log transformation technique is applied to modify non-normal series to normal.

Table 1 shows both mean and median are approximately equal of all the variables. Skewness of all variables is approximately close to zero and Kurtosis is approximately in between 0 and 3. Moreover, non-significant Jarque-Bera probabilities of all variables show normality.

Table 1 Descriptive Summary of variables at level

Summary	LOGINF	LOGBM	LOGEXR	LOGGDP	LOGGEX
Mean	2.039742	27.401618	3.440060	24.844542	22.652247
Median	2.059783	27.423994	3.454507	24.828156	22.632165
Skewness	0.078653	-0.022573	-0.121144	-0.112081	-0.230438
Kurtosis	2.697375	1.785816	1.785834	1.915585	2.059438
Jarque-Bera	0.247194	3.137097	3.257419	2.605686	2.331262
Probability	0.883736	0.208347	0.196183	0.271758	0.311726

Dependent variable log of inflation reveals stationary because it shows a random pattern.

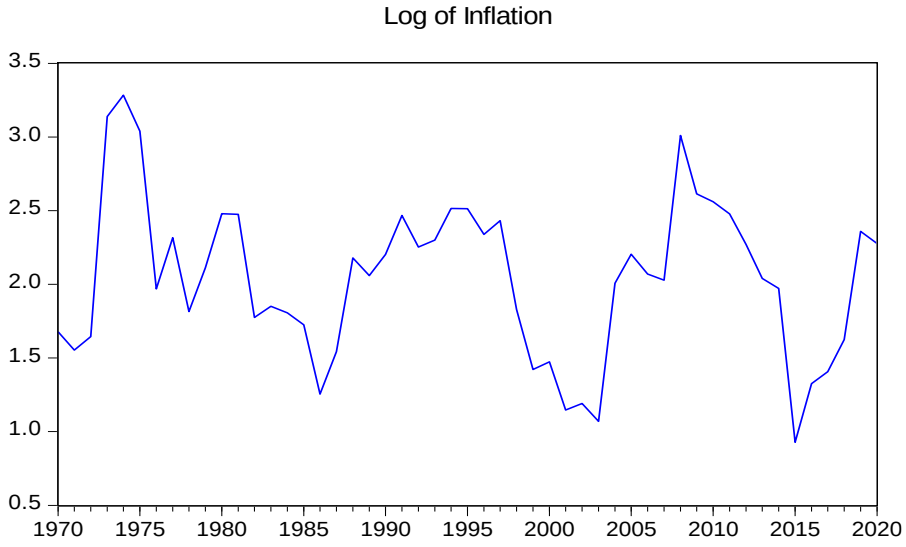

Figure 1 Trends of inflation with log

On the other hand, log of broad money, log of exchange rate, log of gross domestic product and log of government expenditure having upward trend as they are increasing with time. So, these variables are imagined as not stationary. See in Figure 2.

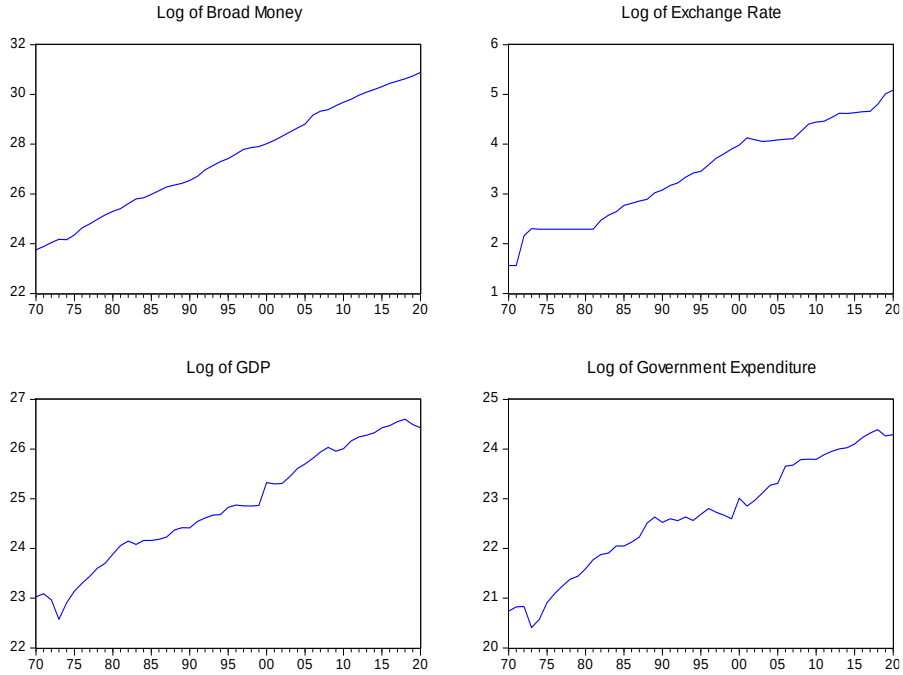

Figure 2 Trends of variables with log

Now, statistical test apply to check all the variables with log are stationary or not. For this purpose Augmented Dickey Fuller (ADF) test is used and show significant at 1% and 5% respectively

Table 2 Outcomes of unit root tests

Variables	Level		First Difference	
	Intercept	Intercept and Trend	Intercept	Intercept and Trend
Log of INF	-3.242646**	-3.301568	-7.176545	-7.101717
Log of BM	-0.757201	-2.958198	-5.672523*	-5.669204*
Log of EXR	-0.999607	-4.198354	-6.055883*	-6.063659*
Log of GDP	-0.781363	-2.464991	-6.390328*	-6.349584*
Log of GEX	-0.887031	-2.317839	-7.295895*	-7.256997*

Table 2 shows Log of inflation is stationary at level with intercept only. On the other hand broad money, exchange rate, GDP and government consumption expenditures all of these with log became stationary after taking its first difference. Next step is to evaluate the best fitted model. For evaluation, different ARIMA (p, 0, q) model were executed which can be seen in Table 3.

Table 3 Evaluation of different ARIMA (p, 0, q) models

Model	AIC	SC	HQC
ARIMA(0, 0, 1)	1.129642	1.206123	1.158767
ARIMA(1, 0, 0)	1.247278	1.323036	1.276228
ARIMA(1, 0, 1)	1.152642	1.267363	1.196328
ARIMA(2, 0, 0)	1.155731	1.271556	1.199675
ARIMA(2, 0, 1)	**0.874056**	**1.028490**	**0.932648**
ARIMA(0, 0, 2)	1.176945	1.329907	1.235194
ARIMA(1, 0, 2)	0.916244	1.109287	0.989485
ARIMA(2, 0, 2)	1.191903	1.347836	1.250830

ARIMA(3, 0, 0)	1.065398	1.260315	1.139057
ARIMA(3, 0, 1)	1.071139	1.305039	1.159530
ARIMA(3, 0, 2)	1.167503	1.319018	1.225401
ARIMA(0, 0, 3)	1.216928	1.408130	1.289739
ARIMA(1, 0, 3)	1.129642	1.206123	1.158767

ARIMA (2, 0, 1) has the minimum AIC (0.874056), SC (1.028490) and HQC (0.932648) values, indicating that the ARIMA (2, 0, 1) model is the best ARIMA model. Next step is to add the exogenous variables in it and consider it as the best ARIMAX model is ARIMAX (2, 0, 1). Therefore, estimates of ARIMAX (2, 0, 1) model were presented in Table 4.

Table 4 Estimates of ARIMAX (2, 0, 1) model

Variable	Coefficient	SD	t-Ratio	P-Values
C	2.314037	0.271573	8.520877	0.000000
DLOGBM	-1.742563	1.046731	-1.664767	0.103800
DLOGEXR	-0.144253	0.905470	-0.159313	0.874200
DLOGGDP	0.083970	0.965622	0.086959	0.931100
DLOGGEX	0.247336	0.705819	0.350424	0.727900
AR(1)	-0.098834	0.174835	-0.565300	0.575000
AR(2)	0.589147	0.135215	4.357107	0.000100
MA(1)	0.847832	0.149930	5.654871	0.000000
R-squared	0.536511		AIC	1.162980
SC	1.474847		HQC	1.280835

After estimating the parameters for ARIMA (2, 0, 1) model, it was also essential to detect the multicolinearity problem for model adequacy.

Table 5 Multicollinearity of ARIMAX (2, 0, 1) Model

Variable	VIF	Tolerance
DLOGBM	1.141082	0.876361
DLOGEXR	1.335477	0.748796
DLOGGDP	3.998970	0.250064
DLOGGEX	3.537724	0.282668

Table 5 clears that there is no multicollinearity problem in residuals. Variance inflation factor is greater than 1, Tolerance is greater than 0.10. ARIMAX (2, 0, 1) model having the following results of diagnostic test of residuals.

Table 6 Diagnostic Tests of Residuals of ARIMAX (2, 0, 1) Model

Test	Statistic Value	p value
Serial Correlation LM Test Breusch-Godfry: (Obs. R-square)	4.338299	0.114275
Heteroskedasticity Test Breusch-Pagan-Godfrey: (Obs. R-square)	13.356816	0.343648
Normality Test (Jarque-Bera)	2.727886	0.255651

Table 6 suggests that both of the models were serially uncorrelated based upon Serial Correlation LM Test Breusch-Godfry: (Obs. R-square) and non-significant value declares that there is no autocorrelation problem in residuals. The Breusch-Pagan-Godfrey heteroskedasticity test values of Observed R-square p-values of both models are greater than 0.05 which declared that there is no

hetroskedastic problem in residuals. The Jarque-Bera test probabilities also show normality in residuals. Next step is the performance of ARIMAX (2, 0, 1) model for forecasting. Details are given below:

Table 7 Forecasting Performance of ARIMAX (2, 1, 2)

Forecast Performance	ARIMAX (2, 0, 1)
RMSE	0.366369
MAE	0.263757
MAPE	14.976160
Theil Inequality Coefficients	0.086434

The annual log of inflation of Pakistan from 2015 to 2020 is forecasted using ARIMAX (2, 0, 1) models, the RMSE, MAE, MAPE and Theil Inequality Coefficients are minimum which indicates the best performance of ARIMAX (2, 0, 1) model.

Table 8 In-sample ARIMA (2, 0, 1) Forecast of Inflation with log at level from 2011 to 2020

Years	Original Value	Original Value with log	Forecasted Value	Difference
2011	11.916	2.478	2.524	-0.046
2012	9.682	2.270	2.261	0.009
2013	7.692	2.040	2.283	-0.242
2014	7.189	1.973	2.067	-0.094
2015	2.529	0.928	2.040	-1.112
2016	3.765	1.326	1.205	0.121
2017	4.085	1.407	1.646	-0.238
2018	5.078	1.625	1.555	0.070
2019	10.578	2.359	1.709	0.650
2020	9.740	2.276	2.261	0.015

Table 9 Out-sample ARIMAX (2, 0, 1) forecast of Pakistan's inflation with log at first difference 2021 and 2022.

Year	Original Values	Original Values with log	Forecasted Values	95% Confidence Lower Bound	95% Confidence Upper Bound
2021	9.496211	2.250893	2.448711	1.729126	3.168295
2022	19.87386	2.989405	2.487991	1.617024	3.358958

5. SUMMARY AND CONCLUSION

The current study was executed to forecast Inflation in Pakistan with other monetary variables such as broad money, exchange rate, gross domestic product and general government final consumption expenditure. The main aims of this study were to get a parsimonious model for rate of Inflation in Pakistan during 1970 to 2020. This objective was carried out by using Autoregressive Integrated Moving Average with Exogenous Variable (ARIMAX) model. All the variables of studied variables were examined using ADF test. The Box-Jenkins methodology was used for the estimation of model parameters. The ARIMA (2, 0, 1) model was found to be parsimonious and chosen on the basis of minimum values of AIC, SC and HQC among all candidate model. Furthermore, by adding the explanatory variables in the selected ARIMA (2, 0, 1) model obtained ARIMAX (2, 0, 1) model was find out. Additionally, ARIMAX (2, 0, 1) model were made by means of Root Mean Square Error (RMSE), Mean Absolute Error (MAE) and Mean Absolute Percentage Error (MAPE) that results

confirmed the better performance of ARIMAX (2, 0, 1) model. Moreover, within sample forecast revealed that ARIMAX (2, 0, 1) model was found to be a parsimonious model.

References

Durka, P. & Pastorekova, S. (2012). ARIMA vs ARIMAX - which approach is better to analyze and forecast macroeconomic time series? Proceedings of 30th international conference on mathematical methods in economics. 136-140.

Gujrati, D. N. (2009). *Basic Econometrics* (5th Ed.). New York: McGraw Hill Press.

Kongcharoen, C., & Kruangpradit, T. (2013) Autoregressive Integrated Moving Average with Explanatory Variable (ARIMAX) model for Thailand Export, 33rd International Symposium on Forecasting, South Korea, held in June 1-8.

(https://www.researchgate.net/profile/Chaleampong_Kongcharoen/publication/255731345_Autoregressive_Integrated_Moving_Average_with_Explanatory_Variable_ARIMAX_Model_for_Thailand_Export/links/0c9605209ac48013f6000000/Autoregressive-Integrated-Moving-Average-with-Explanatory-Variable-ARIMAX-Model-for-Thailand-Export.pdf)

Lidiema, C. (2017). Modelling and Forecasting inflation rate in Kenya using SARIMA and Holt-Winters Triple Exponential Smoothing. *American Journal of Theoretical and Applied Statistics, 6*(3), 161-169.

Lya, I. B., & Aminu, U. (2014). An Empirical Analysis of the Determinants of Inflation in Nigeria. *Journal of Economics and Sustainable Development. 5*(1), 140-150.

Tsirigotis, L., Vlahogianni, E. I., & Karlaftis, M. G. (2012). Does information on weather affect the performance of short-term traffic forecasting models? *International journal of intelligent transportation systems research, 10*(1), 1-10.

Ugoh, C, I., Uzuke, C, A, & Ugoh, D, O. (2021). Application of ARIMAX Model on Forecasting Nigeria's GDP. *American Journal of Theoretical and Applied Statistics.* 10(1), 216-225.

Victor-Edema, U. A., & Essi, D. I. (2016). Autoregressive Integrated Moving with Exogenous Variable (ARIMAX) Model for Nigerian Non-Oil Export, *European Journal of Business and Management, 8*(36), 29-34.

Webster, D. (2000). New Universal Unabridged Dictionary, *Barnes and Noble Books*

https://doi.org/10.62500/icrtsda.1.1.2

Proc. 1st International Conference on Recent Trends in Statistics and Data Analytics
Air University Islamabad, Pakistan – May 9, 2024, Vol. 1, pp. 8-24

A STUDY OF MONEY DEMAND FUNCTION IN PAKISTAN

Sumaira Rasheed

Lecturer; Department of Statistics, Virtual University of Pakistan

ABSTRACT

This study observes the demand of money in Pakistan for a time period 1960 to 2012. This study involves the variables M2 (broad money), INF (inflation rate), INTR (interest rate), GDP (gross domestic production) and EXR (exchange rate). The data which is used in this study is taken from WDI (World Development Indicator) over the time period 1960-2012. For an analysis purpose ARDL and Augmented Dickey Fuller test ADF has been used in this study.

The results of the study show that there exists a significant and consistent relation between variables. It has been observed that the inflation rate is an important element for demand of money in Pakistan. The variables which have been used in this study are mostly consistent and significant. Long run relation and short run relation exists between M2, Broad money, INF inflation rate, GDP gross domestic production and INTR interest rate though some variables show inconsistency and less significance with the money demand yet M2 money demand functions are stable.

Key Words: Stability, Money Demand, ARDL

1.INTRODUCTION

Formulation of an effective and significant monetary policy depends upon the stability of demand function of money. The stability of money demand and its function is significant for implementing an effective policy for monetary affairs. In addition to understand the main factors which become a cause of change in money demand it is also important to understand stability for the money demand function.

The stability of demand of money has been broadly studied/calculated in developed countries. However very few efforts have been made in developing countries to check the stability of money demand. Even though this issue is equally important for developing countries yet these countries are neglecting this issue, which is effecting their monetary policy and economic condition In terms of global scenario macroeconomic stability for the demand of money is an important issue and because of its importance for monetary policy devising it has been studied in detailed, both in developed as well as developing countries. Developing countries of Asia are not paying proper attention towards the time value of money in policies development and top of list countries includes Bangladesh, Pakistan, and India which are ignoring this grave issue.

In Pakistan the monetary authorities have not properly utilized the information. Some of the issues that have been focused in the literature on money demand in Pakistan are as follows:

1) Should the demand for money be measured in nominal or real terms?
2) Should income or wealth or perhaps both be the part of money demand function?
3) Is interest rate, an important variable in the function?
4) What influence does the rate of inflation on the demand for money?
5) Are there any significant economies of scale in holding of money balances?
6) How quickly does money market adjust to disequilibrium forces?

For designing an effective monetary policy, a firm grasp on money demand behavior is essential. Hence, it is necessary to check that which factor will affect the demand for money because on the basis of such knowledge monetary policy can be pursued effectively. Without reliable estimation of coefficients of money demand function, monetary policy will not be considered as an optimal monitory policy. In Pakistan, an optimal monetary policy has not been formulated in the light of expected money demand. For-instance,

https://doi.org/10.62500/icrtsda.1.1.2

expansions in high-powered money and bank credit have been determined by the government's borrowing need for budgetary support.

In Pakistan, Mangla (1979), Akhtar (1974), Aslam and Nisar (1983), Khan (1980, 1982),) and many others have made considerable effort for estimating money demand functions. Different co-integration techniques were used in different studies and some of them check the stability of money demand function. Observations show that most of the studies conclude that M2 is stable, however, properties of the time series have been ignored by these studies by using spurious correlation.

The topic of money demand and its stability has already been discussed in Pakistan but those studies have ignored the properties of stationary of time series data variables and the findings of those studies are considered less important. If the number of observations are less than 20 then the result cannot be taken seriously. As it is already known that in a long run time series a proper co-integration technique is required and due to this assumption, in this study 53 annual observations have been used which is sufficiently large data set/sample size for applying co-integration technique. In present study ARDL (Autoregressive distributed lag) approach is applied to estimate the demand function of money and by using ARDL approach we will check the stability of data in Pakistan.

Money

We use word money in daily life very frequently, which is showing a lot of things and giving different meaning, however economists consider it in a different way. According to economist's money also known as the money supply plays a necessary and important role in monetary policy across the world. For determination of income, prices and employment in a country it's role is considered very important.

Currency

Currency can be easily taken from saving accounts or current accounts. It can be easily seen that even economists are not using a single definition of money.

Wealth

Sometime people use word wealth. Wealth includes all the money, currency, property, common stock, bonds, art, furniture, cars, land, houses, and bank accounts.

Income

Another term used in the context of money is income, but income and money are totally different from each other as Income is the earning of person, which he gets after services

Functions of Money

Money in any form has some functions. There are three functions of money in economy. Money is used as a source of exchange, second as unit of account and third as a store of value.

Money as a Source of Exchange

For these three functions of money a source of exchange can be different from other sources of money. In Pakistan and overall world mostly transections are made in the form of Cheque and currency which is known as medium of exchange. These are used to pay for getting goods and services.

Money as a Unit of Account

Money is unit of account, which is used to measure the value of money in economy. For an economy the value of services and goods is measured in terms of money. This is just like as converting weights from kilograms to pounds or in distance as kilometer into miles.

Money as Store of Value

Store of value is the third function of money. This function is to tell the purchasing power of goods and services on the basis of time.

Broad Money M2

https://doi.org/10.62500/icrtsda.1.1.2

Broad Money M2 involves narrow money M1 plus funds in money market with 24-hour and time deposits for short-term. All the terms along M1 (M1 +saving accounts + mutual funds + accounts in market known as money market accounts+ retail funds of money market +time deposits + minor donations) are included in M 2. M2 is also considered the currency and money circulated outside the bank, saving, demand deposits, foreign currency deposits other than money reserves of government of the country.M1 includes the money within a bank accounts, demand deposits, Cheque, deposits which are chequeable and the amount outside from banks like cash, coins etc.

Saving Accounts

Saving account is an account that is used to deposit money or to earn interest on the amount on the basis of specific time period. The basic purpose of this account is to save the money which an individual or customer cannot use for his/her daily expenditure. Saving accounts are the accounts that maintained by banks, GPO's and other financial bodies in country and they pay interest to the individual but they can't directly use this money as a mode of exchange.

Money Market Fund

In developed countries another frequently used term is "Market of money mutual account". In money market an investment in made on short-term debit like a commercial paper and treasury bills, it is an open mutual fund. It is considered as a bank deposit safe. In US under 1940 Act, the money market is considered important for monetary policy. Accounts in the money market require higher balance to get interest and to avoid regular monthly fee minimum balance which is $1000 to $25000.

Accounts in Market of Money

Money market deposit accounts (MMDA) are also known as money market account (MMA) which are non-financial account type. These accounts are non-financial and pay interest to the money market based upon the current interest rates.The exact and proper definition of the money types i.e. M2, M3, M4 are administered by the country and all these three are the broader sense of money. M4 depends upon the M3 plus all deposits whereas M2, M3, M4 depend upon the local sources.

Interest Rate / Annual Percentage Rate

Interest rate is the amount that is charged by bank on the loan. Interest rate is also known as the APR annual percentage rate. APR is charged on the amount/assets given to customer/individual by bank or investor. The assets of customer on which interest rate is applicable includes goods, commodities, cash, building, house, and vehicle. Interest is usually an important leasing or rental charge that is paid by borrower for using the previously mentioned assets. There is another term "lease rate" used for the rent of large things like house, building, land, and vehicle. If the low risk is involved than the percentage of interest rate will be low and if the risk is high, then the percentage of the interest rate will be high.

Impact of Interest Rate on Economy

Interest rate is given by borrower to its lender which is taken as the "cost" of the amount which is given as borrow amount. Interest rate is considered as a tool for monetary policy. Demand of money and rate on interest reacts inversely. When the major bank of the country wants to increase the consumption and the investment in the country then it reduces the interest rate. Though lower rate of interest can increase economic growth but a large amount invested by investor's impact negatively on economic growth and an economic crisis could occur as the result of this situation.

Gross Domestic Production

GDP includes all the public and private manufacturing firm and companies, government, public and private consumption of goods and services, investments, including exports and excluding imports with in a country. In broader sense it can be stated that it measures overall economic movement/activity of a country. Business investment + individual consumer expenditure/consumption of goods and services +government spending+ exports –imports. All these terms are also known as the components of the GDP. Now it can be easily calculated by using an easy and simple formula of GDP.

https://doi.org/10.62500/icrtsda.1.1.2

GDP=CE+GS+BI+EX-IM

Where

GDP = Gross domestic production

CE = Consumer Expenditures

GS =Government Spending

BI =Business investments also includes all the investments made with in a country.

EX =Exports

IM =Imports

Exchange Rate

Exchange rate EXR is also known as FEXR foreign-exchange rate. Exchange rate is the rate at which one currency can be changed into another currency. It is also considered as the value of one country currency in terms of another country's currency.

Inflation Rate

Rise in level of price is "increase in charges of commodities" during a time duration in an economy. There will also increase in assets, goods and services, goods and commodities of consumers because money is used to buy these goods and services.

Consumer Price Index

CPI measures the change in the inflation rate and the purchasing power/cost of currency/cost of living. CPI represents the cost of living over the country on monthly basis. It also gives the clear picture of price level of customer goods and services used by the families. Basket of goods and services includes food, medicines, transport, medical facilities, beverages, etc. CPI shows the current prices in terms of the previous year prices of goods and services for checking the effect of inflation of purchasing power of money. This is the best way of lag period or lag indicator. It also used to identify the inflation and deflation period.

ARDL

Autoregressive distributed lag model (ARDL) is used to test the time series data when a long run relation exists among the variables. It is also used to calculate short and long run constant (coefficients) using a single equation model. ARDL model is described into two parts, it will provide a background for a second phase that these models are used to test the co-integration. This applies on all variables even though the variables of time series data are stationary or non-stationary.

ARDL relax the statement (assumption) of integration at same order. Rather it gives accurate result when there is a combination of zero order difference *I (0)* and first order difference *I (1)* variables. The technique introduced by shin and Pesaren 2001, used a bound testing approach to assess co-integration among variables without considering the order of integration of variables i.e. whether variables are integrated of order zero or one.

Following are some econometric advantages of bound test approach over conventional co-integration methods.

1) All variables included in the model are primarily assumed as endogenous.
2) For bound testing approach, order of variables may be *I (0)* or *I (1)*.
3) Short and long run estimates are obtained by single equation.

Aim/Purpose of the Study

1.By using technique ARDL (Autoregressive Distributed Lag Model) also known as co-integration model we can investigate the relationship between M2 (broad money) real income, real monetary aggregates, nominal exchange rate and inflation.

https://doi.org/10.62500/icrtsda.1.1.2

2. Also check the stability of M2 (broad money) of demand function of money. Checking the stability of M2 is important because co-integration technique is applicable when the relationship between variables is not stable, when the relationship between variables is stable co-integration technique will not be applicable.
3. To study the stability in long-run of demand function of the real money as for the determination and implementation of an effective monetary policy the stability of demand function of money is important.

2. REVIEW OF LITERATURE

Qayyum (2005) presented the model of the money demand. He used the co-integration technique and ECM error correction mechanism for the demand of broad money M2 in Pakistan. The model he proposed to estimate the money demand is best fitted model and found to be super-exogenous for the relevant class of interventions. He analyzed INF rate of inflation which is a key factor for demand of money in Pakistan. He also proposed that the rate of market, IR interest, plays significant role for demand of money in the long-run. As his proposed model is super-exogenous, and this model helped in formulating policy in Pakistan.

Omer (2010) has studied the functions of money in Pakistan. His study was an initial effort to contribute to the continuing discussion regarding SBP State Bank of Pakistan which involves that should SBP adopt the strategies of monetary policy or follow the inflation rate. For the formulation of monetary policy, demand function of money should be stable because if the demand function is stable then the rate of inflation will be also stable. If the money demand function is not stable, then there will be fluctuation in rate. In this study he assessed the stability of demand function of money for Pakistan and he analyzed that the fluctuations of the interest rate are independent of the narrow and broad money. It's also being observed that Mo, M1 and M2 all of the monetary factors and their determinants have stable relationship. His findings are best to use for the monetary policy.

Cassola and Brand (2004) conducted the research on demand function of money system for euro area M3.In direction to evaluate the significance of economic and monetary growths used for main macroeconomic variables in the money demand system for euro area M3. The co-integration VAR technique is used to estimate the model as well as to estimate long-run relation. Through generalized response profiles the functions of demand money system are examined without any additional assumptions identification. Error terms/bounds of the profiles are derived using bootstrap simulations.

Naseer (2013) conducted his study on Demand for money in Pakistan. This research is an empirical study between the relation GDP (gross domestic production), M2, INTR (interest rate) and INF (inflation rate). The data for this research has been taken from Pakistan IMFs (World Development Indicators) during the time period 1976-2012. For analysis he used Co-integration test, ADF unit root test and error correction analysis, which has been conducted to conclude results. He concluded that there is a significant effect of GDP, INTR, INF, and M2 on money demand function in Pakistan.

3. METHODOLOGY

Data Source

Data which is used in this study consists of 53 observations, from the time period of 1960 to 2012.The data has been taken from WDI World Development Indicator.

Following are the variables included in the model.

1) M2 Broad Money (As Dependent Variable)
2) CPI Consumer Price Index
3) Inflation Rate
4) Exchange Rate
5) GDP Gross Domestic Production
6) Interest Rate

Procedure which is followed in this study is:

1. To check the stationary of data technique of Augmented Dickey Fuller test has been applied.
2. To check the co-integration, ARDL bound test approach and Wald F-statistic has been used.

https://doi.org/10.62500/icrtsda.1.1.2

3.To estimate the long and short run estimates (coefficients), ARDL technique has been used in this study.

ARDL Model Specification

Following model will be estimated under ARDL frame work.

$$Y_t = \beta_0 + \beta_1 lrgdpad_t + \beta_2 lrexad_t + \beta_3 \text{int}\, r + \beta_4 \text{inf}\, r + \varepsilon_t \quad (3.2)$$

Where

Yt = M2 Broad money (Real money added in log form)

lr gdp$ad\,t$ = Real gross domestic production added in log Form

lr ex$ad\,t$ = Real exchange rate value added in log Form

intr= Interest Rate

inf= Inflation Rate

β1,β2, β3, β4 are the required long run estimates.

Unit Root Tests

Most of the time series data is based on economic and financial basis and the behavior of this time series data is non-stationary. Some variables of non-stationary data are GDP, Interest Rate, Export, Exchange Rate etc. Time series said to be stationary if Yt where t=1, 2, 3…… do not vary with respect to time. Noise is an example of the stationary time series where Yt follows the normal distribution with mean meu and variance sigma square. If the series is not stationary, then make it stationary by using different techniques such as difference or trend stationary. There are different approaches to test the stationary.

ADF Augmented Dickey Fuller Unit Root Test

ADF test also known as the Dickey Pantula test is based upon the linear regression. ADF test is used where serial correlation exists. ADF test is applied on more difficult and complex data to check the stationary because there are less chances of type 1 error.

- Considering the model AR (1) is ‘

$$y_t = \phi y_{t-1} + \mu_t$$

The purpose of this test is to test the hypothesis that

$$H_o: \quad \phi = 1$$

Against the one sided alternate

$$H_1: \quad \phi < 1$$

ADF Augmented Dickey Fuller Unit Root Test

The Dickey Fuller test is extend an AR (q) model. Let’s consider AR(3):

$$x_t = \beta_1 x_{t-1} + \beta_2 x_{t-2} + \beta_3 x_{t-3} + \varepsilon_t$$

A unit root is $\beta(L) = 1 - \beta_1 L + \beta_2 L^2 + \beta_3 L^3 + \varepsilon_t$ equal to $\beta(1) = 0$

Estimation of Short Run and Long Run Coefficients

ARDL is a technique which is used to estimate the long-run and short-run co-efficient.

Estimation by ARDL:

https://doi.org/10.62500/icrtsda.1.1.2

The technique which is used to estimate long run and short run coefficients of an equation and the model of equation in single? Is ARDL technique. In this study the estimated model of ARDL is:

$$\Delta\ LRM2 = \alpha_o + \sum_{i=1}^{p} \alpha_i \Delta\ LRM2_{t-i} + \sum_{j=o}^{q} \beta_j \Delta\ LRGDP_{t-j} + \sum_{k=o}^{r} \gamma_k \Delta\ LREX_{t-k} + \sum_{l=o}^{s} \varphi_l \Delta\ INTR_{t-l} + \sum_{m=o}^{t} \omega_m \Delta\ INF_{t-m} + \vartheta_o \Delta\ LRM1_{t-1} + \vartheta_1 \Delta\ LRGDP_{t-1} + \vartheta_2 \Delta\ LREX_{t-1} + \vartheta_3 \Delta\ INTR_{t-1} + \vartheta_4 \Delta\ INF_{t-1} + \varepsilon_t \quad (3.24)$$

In the above mentioned model i=1to p, j=0 to q, k= 0 to r, l= 0 to t, m= 0 to t are the lags, which are in the selection of lag process for each variable. ε_t is known as the disturbance/error term and it is white noise term. The above equation or model is the combination of two parts one is for long term and one part is for short run length. In ARDL model the ECM version of model is used to extract the short run coefficients.

Estimation of Long Run Coefficients

In the above mentioned model, second part of the equation is used to extract the long run coefficients, these are the level lag variables and the coefficients are $\vartheta_o, \vartheta_1, \vartheta_2, \vartheta_3,$ and ϑ_4 .

$$\beta_j = -\frac{\vartheta_j}{\vartheta_o} \quad for \quad j = 1,2,3,....$$

The interpretation of the long run coefficients is like an OLS estimates

Estimation of Short Run Coefficients

For short run coefficients extraction, considering the version of ARDL model which is ECM.

$$\Delta LRM2 = \alpha_o + \sum_{i=1}^{p} \alpha_i \Delta LRM2 + \sum_{j=o}^{q} \beta_j \Delta LRGDP_t + \sum_{k=o}^{r} \gamma_k \Delta LREX_t + \sum_{l=o}^{s} \varphi_l \Delta INTR_t + \sum_{m=o}^{t} \omega_m \Delta INF_t + EC_{t-1}$$

In the above mentioned model i=1to p, j=0 to q, k= 0 to r, l= 0 to t, m= 0 to t are the lags, which are in the selection of lag process for each variable. EC_{t-1} is known as the disturbance/error correction coefficient and it is also known as speed of adjustment. The value of the coefficient of error correction should be negative and also be significant, which is used to extract out the relationship between the variables. EC_{t-1} is the error/ residual term and it is obtained as:

$$X_t = \alpha_o + \alpha_i Y_{ti} + \varepsilon_t$$

The short run coefficients are:

$$\beta = \sum_{j=o}^{q} \beta_j \qquad \gamma = \sum_{k=o}^{r} \gamma_k$$

$$\varphi = \sum_{l=o}^{s} \varphi_l \qquad \omega = \sum_{m=o}^{t} \omega_m$$

4. RESULTS AND DISCUSSIONS

Descriptive Statistics

Table 4.1 shows the descriptive statistics of variables without log form used in the study. All the variables consist of 53 observations. According to the table.

https://doi.org/10.62500/icrtsda.1.1.2

Table 4.1: Descriptive Statistics without Log

Variables	M2	GDP	EX	INTR	INF	CPI
Observations	53	53	53	53	53	53
Mean*	1380	2790	28.379	9.481	8.288	26.508
Median*	223	515	16.648	10	7.228	13.320
Maximum*	10300	20000	93.395	20	26.663	122.756
Minimum*	6.96	17.7	4.762	4.000	-0.516	2.055
Std. Dev.*	2450	4750	26.108	3.756	5.427	29.971
Skewness	2.186	2.206	0.969	0.584	1.329	1.562
Kurtosis	6.898	7.203	2.680	3.287	5.206	4.853
Jarque-Bera	75.784	81.980	8.526	3.190	26.345	29.133
Probability	0	0	0.01408	0.2	0.000002	0

- M2 has a mean value 1380 and median 223. Standard deviation of M2 is 2450. Minimum value for M2 is 6.96 while the maximum value is 10300. Skewness of M2 is 2.186 indicating that M2 is skewed to right. Kurtosis of M2 is 6.898 which is larger than 3 which represents that distribution is leptokurtic of M2. Jarque – Bera statistic for M2 is 75.784 with P – value 0 providing evidence to reject the normality hypothesis, which indicates that M2 does not follow a normal distribution.

- GDP has a mean value 2790 and median 51.5. Standard deviation of GDP is 4750. Minimum value for GDP is 17.7 while the maximum value is 20000. Skewness of GDP is 2.206 indicating that GDP is skewed to right. Kurtosis of GDP is 7.203 which is more than 3 which represents that distribution is leptokurtic of GDP. Jarque – Bera statistic for GDP is 81.980 with P – value 0 providing evidence to reject the normality hypothesis, which indicates that GDP does not follow a normal distribution.

- Exchange rate has a mean value 28.379 and median 13.320. Standard deviation of exchange rate is 16.648. Minimum value for Exchange rate is 4.762 while the maximum value is 93.395. Skewness of Exchange Rate is 0.969 indicating that Exchange Rate is skewed to right. Kurtosis of Exchange Rate is 2.680 which is less than 3 indicating that distribution of Exchange Rate is mesokurtic. Jarque – Bera statistic for Exchange Rate is 8.526 with P – value 0.01408 providing evidence to reject the normality hypothesis, which indicates that exchange rate does not follow a normal distribution.

- Interest rate has a mean value 9.481 and median 10. Standard deviation of Interest rate is 3.756. Minimum value for Interest rate is 4.00 while the maximum value is 20. Skewness of INTR is 0.584 indicating that INTR is skewed to right. Kurtosis of INTR is 3.287 which is more than 3 which represents that distribution is leptokurtic of INTR. Jarque – Bera statistic for INTR is 3.190 with P – value 0.2 providing evidence to reject the normality hypothesis, which indicates that INTR does not follow a normal distribution.

- Inflation rate has a mean value 8.288 and median 7.228. Standard deviation of Inflation rate is 5.427. Minimum value for inflation rate is -0.516 while the maximum value is 26.663. Skewness of INF is 1.329 indicating that INF is skewed to right. Kurtosis of INF is 5.206 which is more than 3 which represent that distribution is leptokurtic of INF. Jarque – Bera statistic for INF is 26.345 with P – value 0.000002 providing evidence to reject normality hypothesis, which indicates that the INF doesn't follow a normal distribution.

https://doi.org/10.62500/icrtsda.1.1.2

- CPI has a mean value 26.508 and median 13.320. Standard deviation of CPI is 29.971. Minimum value for CPI is 2.055 while the maximum value is 122.756. Skewness of CPI is 1.562 indicating that CPI is skewed to right. Kurtosis of CPI is 4.853 which is more than 3 which represents that distribution is leptokurtic of CPI. Jarque – Bera statistic for CPI is 29.133 with P – value 0 providing evidence to reject the normality hypothesis, which indicates that CPI does not follow a normal distribution.

Figure 1: Line Graph of Broad Money M2

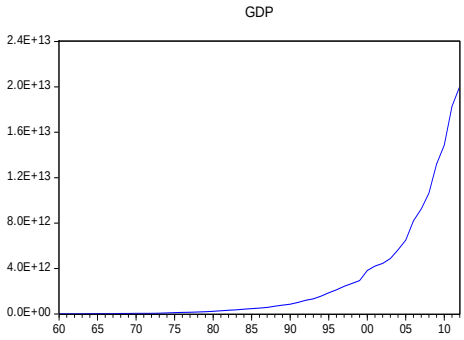

Figure 2: Line Graph of GDP

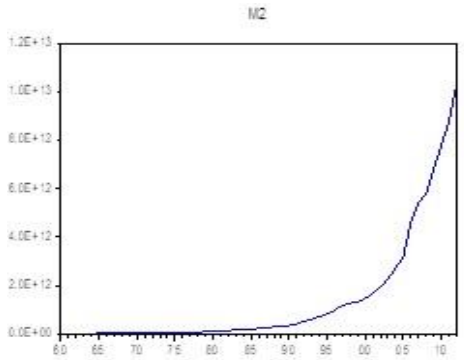

Figure 3: Line Graph of Exchange Rate

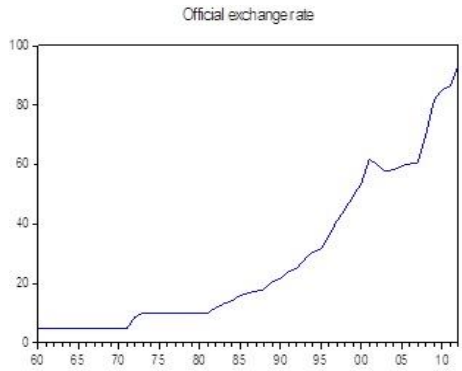

Figure 4: Line Graph of Interest Rate

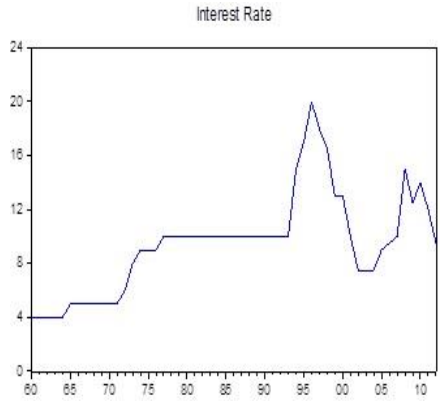

https://doi.org/10.62500/icrtsda.1.1.2

Figure 5: Line Graph of Inflation

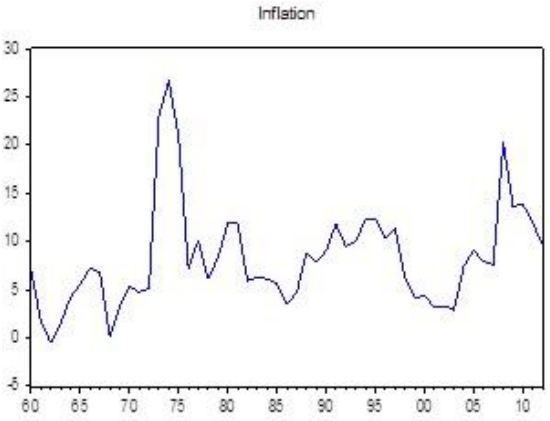

Figure6: Line Graph of CPI

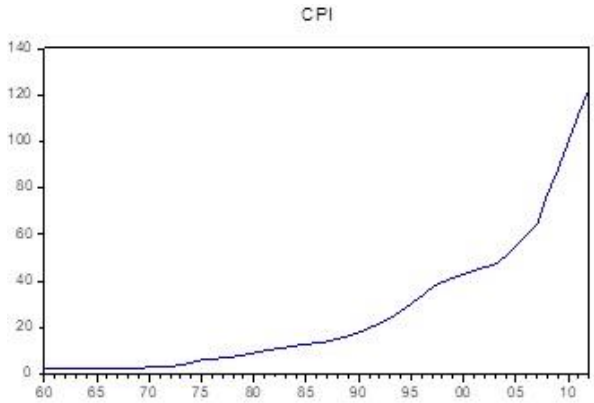

Results from table 4.1 Reveals that all the variables without log form are not normal. To attain normality, log transformation has been used. Descriptive statistics with log form is given in table 4.2

Table 4.2: Descriptive Statistics with Log

Variables	LRM2	LRGDP	LREX	INTR	INF	CPI
Observation	53	53	53	53	53	53
Mean	10.223	10.581	0.128	9.481	8.288	26.508
Median	10.224	10.587	0.088	10.000	7.228	13.320
Maximum	10.928	11.213	0.435	20.000	26.663	122.756
Minimum	9.523	9.934	-0.119	4.000	-0.516	2.055
Std. Dev.	0.416	0.387	0.136	3.756	5.427	29.971
Skewness	0.172	0.060	0.541	0.584	1.329	1.562
Kurtosis	1.915	1.801	2.506	3.287	5.206	4.853
Jarque-Ber	2.859	3.209	3.120	3.190	26.345	29.133
Probability	0.239	0.201	0.210	0.203	0.000	0.000

- LRM2 has a mean value 10.223 and median 10.928. Standard deviation of LRM2 is 0.416. Minimum value for LRM2 is 9.523 while the maximum value is 10.928. Skewness of LRM2 is 0.172 indicating that LRM2 is skewed to right. Kurtosis of LRM2 is 1.915 which is less than 3 indicating that distribution of LRM2 is playtikurtic. Jarque – Bera statistic for LRM2 is 2.859 with P – value 0.239 providing evidence to accept normality hypothesis, which represents that LRM2 follows normal distribution.
- LRGDP has a mean value 10.581 and median 10.587. Standard deviation of LRGDP is 0.387. Minimum value for LRGDP is 9.934 while the maximum value is 11.213. Skewness of LRGDP is 0.060 indicating that LRGDP is skewed to right. Kurtosis of LRGDP is 1.801 which is less than 3 indicating that distribution of LRGDP is playtikurtic. Jarque – Bera statistic for LRGDP is 3.209 with P – value 0.201 providing evidence to accept the normality hypothesis, which presents that LRGDP follow normal distribution.
- LREX has a mean value 0.128 and median 0.088. Standard deviation of LREX is 0.136. Minimum value for LREX is -0.119 while the maximum value is 0.435. Skewness of LREX is 0.541 indicating that

https://doi.org/10.62500/icrtsda.1.1.2

LREX is skewed to right. Kurtosis of LREX is 2.506 which is less than 3 indicating that distribution of LREX is playtikurtic. Jarque – Bera statistic for LREX is 3.120 with P – value 0.210 providing evidence to accept normality hypothesis, which presents that LREX follow normal distribution.

- INTR has a mean value 9.841 and median 10.00. Standard deviation of INTR is 3.756. Minimum value for INTR is 4 while the maximum value is 20. Skewness of INTR is 0.584 indicating that INTR is skewed to right. Kurtosis of INTR is 3.287 which is less than 3 indicating that distribution of INTR is leptokurtic. Jarque – Bera statistic for INTR is 3.190 using P-value 0.203 provided the suggestion to accept the normality hypothesis, which shows that the distribution is normal.
- INF has a mean value 8.288 and median 7.228. Standard deviation of INF is 5.427. Minimum value for INF is -0.516 while the maximum value is 26.663. Skewness of INF is 1.329 indicating that INF is skewed to right. Kurtosis of INF is 5.206 which is more than 3 representing that the distribution is leptokurtic of INF. Jarque – Bera statistic for INF is 26.345 with P – value 0.000 providing evidence to reject normality hypothesis, which indicates that the INF does not follow normal distribution.
- CPI has a mean value 26.508 and median 13.320. Standard deviation of CPI is 29.971. Minimum value for CPI is 2.055 while the maximum value is 122.756. Skewness of CPI is 1.562 indicating that CPI is skewed to right. Kurtosis of CPI is 4.853 which is more than 3 representing that the distribution is leptokurtic of CPI. Jarque – Bera statistic for CPI is 29.133 with P – value 0.000 providing evidence to reject normality hypothesis, which indicates that CPI does not follow normal distribution.

Figure 7: Line Graph of Broad Money LRM2

Figure 8: Line Graph of LRGDP

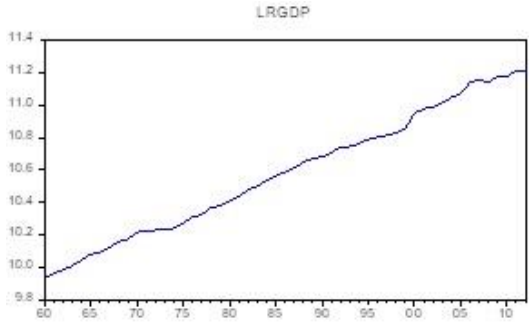

Figure 9: Line Graph of LREX

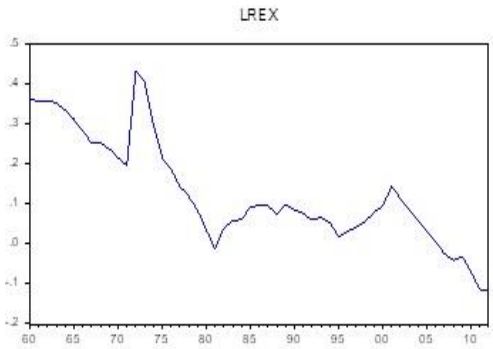

https://doi.org/10.62500/icrtsda.1.1.2

4.2 Unit Root Test

Unit root test is applied to check the stationary of data. The technique which is used in this study is ADF.

4.2.1 ADF Test (Augmented Dickey Fuller)

The table 4.3 contains results of unit root ADF (Augmented Dickey fuller) test. These results are obtained at different lag levels.

Table 4.3: ADF Unit Root Test

	Results of Constant		Results of Trend and Constants	
	Level	**First Difference**	**Level**	**First Difference**
LRM2	−0.3425	−6.0932***	−3.2740	−6.0311***
LRGDP	−0.5364	−8.0399***	−2.7280	−7.9757***
LREX	−1.0613	−6.3454***	−2.3498	−6.2831***
INTR	−2.8877	−5.8300***	−3.2606	−5.8516***
INF	−3.3113**	−7.2270***	−3.3404	−7.1730***

*** Significant at 1% level, ** Significant at 5% level

1. Level variable with Drift term.

2. First difference variable with drift term

3. Level variable with drift and trend term

4. First difference variable with drift and trend term.

4.2.1.2 Log of Real Broad Money M2

Real Money M2 has augmented dickey fuller value = -0.3425 that is not significant, which can be interpreted that the money M2 is not stationary by using drift term at level. While the statistic -6.0932 with drift term at difference first is significant, at 1% significance level. This shows that (real money) M2 is stationary with drift at first difference. Estimated statistic -3.2740 with trend and drift term at level is not significant which shows that the M2 is non stationary with trend and drift term. The test statistic -6.0311 is significant with trend and drift term at first difference and concludes that it is stationary at 1 % level.

4.2.1.3 Log of Real GDP

LRGDP has augmented dickey fuller value = -0.5364 that is not significant, which can be interpreted as that the LRGDP is not stationary by using drift term at level. While the statistic -8.0399 at first difference with drift term is significant, at 1% significance level. This shows that LRGDP is stationary with drift at first difference. Estimated statistic -2.7280 with trend and drift term at level is not significant, shows that the LRGDP is non-stationary with trend and drift term at level. The test statistic -7.9757 is significant with trend and drift term at first difference and concludes that it is stationary at 1 % level.

4.2.1.4 Log of Real Exchange Rate

LREX has augmented dickey fuller value = -1.0613 that is not significant, which can be interpreted as that the LREX is not stationary by using drift term at level. While the statistic –6.3454 at first difference with drift term is significant, at 1% significance level. This shows that LREX is stationary with drift at first difference. Estimated statistic -2.3498 with trend and drift term at level is not significant, shows that the

https://doi.org/10.62500/icrtsda.1.1.2

LREX is non-stationary with trend and drift term at level. The test statistic 6.2831 is significant with trend and drift term at first difference and concludes that it is stationary at 1 % level.

4.2.1.5 Interest Rate

INTR has augmented dickey fuller value = -2.8877 that is not significant, which can be interpreted as that the INTR is not stationary by using drift term at level. While the statistic –5.8300 at first difference with drift term is significant, at 1% significance level. This shows that INTR is stationary with drift at first difference. Estimated statistic -3.2606 with trend and drift term at level is not significant, shows that the INTR is non-stationary with trend and drift term at level. The test statistic -5.8516 is significant with trend and drift term at first difference and concludes that it is stationary at 1 % level.

4.2.1.6 Inflation Rate

INF has augmented dickey fuller value = -3.3113 that is significant, which can be interpreted as that the INF is stationary by using drift term at level. While the statistic –7.2270 at first difference with drift term is significant, at 1% significance level. This shows that INF is stationary with drift at first difference. Estimated statistic -3.3404 with trend and drift term at level is not significant, shows that the INF is non-stationary with trend and drift term at level. The test statistic -7.1730 is significant with trend and drift term at first difference and concludes that it is stationary at 1 % level.

4.3 Co-integration Diagnosis

After examining unit root and integrated level of variables involved in the study, the next step is the test whether there is any long run relationship among variables? To do this, two techniques has been used.

4.3.1 ARDL Bound Test Approach

As name suggests, it uses two bound values provided by shin and pesaren 2001. Rest of procedure for ARDL Bound Test approach is defined in methodology section. Firstly, estimate the equation already defined with q = 1 and test the hypothesis as given in methodology. Results obtained are presented in table.

4.4 LRM2 as Dependent Variable

Table 4.4: ARDL Bound Test for M2

	Level of Confidence						
	99%		95%		90%		
Statistic F	*I (0)*	*I (1)*	*I (0)*	*I (1)*	*I (0)*	*I (1)*	Durban Watso
7.870	3.74	5.06	2.86	4.01	2.45	3.52	2.00

Estimated F is 7.870 while the values of bound are, at 1% are 3.74 and 5.06, at 5% 2.86 and 4.01, at 10% 2.45 and 3.52. The F calculated is larger than the higher value, for all significance level 1%, 5%, 10 %. Which provides enough evidence for long run relationship and existence of co – integration among variables.

4.4.1 Long Run Estimates

Table 4.5: ARDL Long Run Coefficients

Variables	Estimates	Standard Error	T – Value	P – Value
INF	−0.007	0.0026	−2.7180	0.01
INTR	−0.0124***	0.0033	−3.7953	0.000
LREX	0.1487	0.1177	1.2642	0.21

https://doi.org/10.62500/icrtsda.1.1.2

LRGDP	1.212***	0.0385	31.4977	0.000
$\mathbf{EC_{t-1}}$	−0.4950***	0.0828	−5.5470	0.000

*** Significant at 1% level ** Significant at 5% level * Significant at 10%

These estimates can be interpreted as follows.

- The estimated INF co-efficient is −0.007 with the value of S.E (Standard error) 0.0026. P-Value and T-Value are 0.01 and −2.7180respectively, indicates INF is significant and in the long run it has effect on LRM2 .Co-efficient of INF interpreted as "If INF increases 1% then LRM2 decreases by 0.007%, considering all other influences constant", saying differently " If INF increases by 10%, LRM2 will decreases by 0.07%.
- The INTR coefficient 0.0124 with S.E (standard error) 0.0033. P-value and t- value are 0.000 and -3.7953 respectively, indicates INTR is highly significant and in the long run has effect on LRM2. Coefficient of INTR interpreted as "If INTR increases 1% then LRM2 increases by 0.0124%, considering all other influences constant", saying differently "If INTR increases by 10%, LRM2 will deccrease by 0.124%".
- The LREX coefficient 0.1487 with S.E (standard error) 0.1177. P-value and t- value are 0.21and 1.2642 respectively, indicates LREX is not significant and in the long run has no effect on LRM2.
- The LRGDP coefficient 1.212 with S.E (standard error) 0.0385. P-value and t- value are 0.000 and 31.4977 respectively, indicates LRGDP is significant and in the long run has effect on LRM2. Coefficient of LRGDP interpreted as "If LRGDP increase 1% then LRM2 increases by 1.212%, considering all other influences constant", saying differently "If LRGDP increases by 10%, LRM2 will increase by 12.12%".
- The ECT coefficient is negative and indicating presence of co – integration among variables. Also the speed of adjustment is 0.495%.

4.4.2 ARDL Coefficients of Short Run

Table 4.6: ARDL Coefficients of Short Run

Variables	Estimates	Standard Error	T – Value	P – Value
INF	0.0032***	0.00088	-3.7255	.0000
INTR	−0.0057***	0.0017	-3.3008	0.002
LREX	0.0683	0.0521	1.3102	0.20
LRGDP	0.5561***	0.0945	5.8868	0.000

*** Significant at 1% level ** Significant at 5% level * Significant at 10%

These estimates can be interpreted as follows.

- The INF coefficient 0.0032 with S.E (standard error) 0.0008. P-value and t- value are 0.000 and -3.7255 respectively, indicates INF is highly significant and in the short run has effect on LRM2. Coefficient of INF interpreted as "If INF increases 1% then LRM2 increases by 0.0032%, considering all other influences constant", saying differently, and "If INF increases by 10%, LRM2 will increase by 0.032%.
- The INTR coefficient -0.0057 with S.E (standard error) 0.0017. P-value and t- value are 0.002 and -3.3008 respectively, indicates INTR is highly significant and in the short run has effect on LRM2. Coefficient of INTR interpreted as "If INTR increase 1% then LRM2 decreases by 0.0057%, considering all other influences constant", saying differently, and "If INF increases by 10%, LRM2 will decrease by 0.057%.
- The LREX coefficient 0.0683 with S.E (standard error) 0.0521. P-value and t- value are 0.20 and 1.3102 respectively, indicates LREX is not significant and in the short run has no effect on LRM2.
- The LRGDP coefficient 0.5561 with S.E (standard error) 0.0017. P-value and t- value are 0.000 and 5.8868 respectively, indicates LRGDP is highly significant and in the short run has effect on LRM2. Coefficient of LRGDP interpreted as "If LRGDP increase 1% then LRM2 decreases by 0.5561%, considering all other influences constant", saying differently, and "If LRGDP increases by 10%, LRM2 will increase by 5.561% on an average, by keeping all other factors constant.

https://doi.org/10.62500/icrtsda.1.1.2

5. CONCLUSION

The objective of this study is to investigate the demand of money in Pakistan. By using technique ARDL (Autoregressive Distributed Lag Model) also known as co-integration model we have investigated the relationship M2 (broad money) real income, real monetary aggregates, nominal exchange rate and inflation. This study is an attempt to analyze the stability in long-run of demand function and the stability of M2 by applying co-integration technique. ARDL model relaxes the assumption that all variables should be integrated at same level.

By using ARDL model it is found that there exists a co-integration between the variables. For M2 the ECT coefficient is also negative and showing the presence of co – integration among variables and the negative symbol of error term shows that it is convergent towards equilibrium while speed of adjustment is 0.495%

The results of the study show that the variables which have been used in the model are mostly consistent and significant.

The results of GDP gross domestic production and EXR exchange rate are positively related with M2 whereas INF and INTR are related negatively. The inflation impact is negative which supports the theory of money demand that if the inflation rate increases than the money demand decreases. The above mentioned scenario shows that the individuals favor the alternate of money in terms of physical assets. The positive EXR impact on M2 shows that increase in domestic money results in increase in the money demand. M2 money demand functions are stable. It has been observed that the domestic holders or owners are interested in an alternate of money. They prefer to alternate the money in terms of physical assets. According to domestic holders, changing a money into real assets will become more beneficial in a long run as well as it is also beneficial in a short run.

On the basis of this research, it is recommended that we should pay more attention in the growth of real sector. Monetary authorities should focus on the new techniques to formulate the economic policy. Monetary authorities should try to adopt the strategies which reduce the INTR in order to increase the opportunities of investment in a real sector. Monetary development plays a vital role in the determination of demand function of money so authorities should also pay more attention on monetary development in a way that it encourages economic and business activities in a country.

REFERENCES

Achsani, N. A. (2008). Stability of Money Demand in an Emerging Market Economy: An Error Correction and ARDL Model for Indonesia. *Research Journal of Internatıonal Studıes*. Retrieved March 13, 2010

Akhtar, M. (1974). The Demand for Money in Pakistan. *Jstor, 13*(1), 40-54. Retrieved November 17, 2015, from http://www.jstor.org/stable/41258224

Akinlo, A. E. (2006). The stability of money demand in Nigeria: An autoregressive distributed lag approach. *Journal of Policy Modeling, 28*, 445-452.

Ali, A. H. (1997). The demand for Money in PAksitan: An application of Co-integration nad Error Correction Modelling. *Jstor, 21*(1), 49-62. Retrieved April 28, 2015, from http://www.jstor.org/stable/25830604

Arshad, N. (2014). *A manual for ARDL approach to cointegration.* Retrieved from Noman Arshad: https://nomanarshed.wordpress.com/2014/11/16/a-manual-for-ardl-approach-to-cointegration/

Asghar, S. A. (Summer 2012). Is Demand for Money Stable in Pakistan? *Pakistan Economic and Social Review, 50*(1), 1-22.

Aslam, S. N. (1983). The Demand for Money and the Term Structure of Interest Rates in Pakistan. *22*(2), 97-116. Retrieved June 9, 2014, from http://www.jstor.org/stable/41258623 .

https://doi.org/10.62500/icrtsda.1.1.2

Bahmani-Oskooee, M. (2001). How Stable is M2 money demand function in Japan. *Japan and the world Economy, 13*, 455-461. Retrieved Februray 28, 2001

Cassola, C. B. (2004). A money demand system for euro area M3. *Applied Economics, 36*(8), 817-838. doi:10.1080/0003684042000229541

Dr.ParvezAzim, D.-u.-Z. (2010). Demand for Money in Pakistan: an Ardle Approach. *Global Journal of Management and Business Research, 10*(9), 76. Retrieved 2010

Dritsakis, N. (2010). Demand for money in Hungary: An ARDL. *Economics and Social Sciences*, p. 28.

Faiz Bilquees, T. M. (2012). Dynamic Casual Interactions of monay, Prices, Interest Rate and Output in Pakistan. *Journal of Economic and Development, 33*(3), 37-64.

Fields, C. (1996). *Time Series. CRC Press LLC*

Giles, D. (2013). *Econometrics Beat: Dave Giles Blog*. Retrieved from http://davegiles.blogspot.com/2013/06/ardl-models-part-ii-bounds-tests.html

Haroon Sarwar*, Z. H. (2011). A Semi-Nonparametric Approach to the Demand for Money in Pakistan. *The Lahore Journal of Economics, 16*(2), 87-110.

Haroon Sarwar, M. S. (2013). Stability of Money Demand Function in Pakistan. *Economics and Business Review, 15*(3), 197-212. Retrieved August 29, 2013

Haroon Sarwar, Z. H. (2010). Money Demand Function for Pakistan (Divisia Approach). *Jstor, 48*(1), 1-20. Retrieved June 21, 2014, from http://www.jstor.org/stable/41762411 .

Hossain, A. H. (1994). Financial Liberalisation and the Demand for Money in Pakistan. *Pakistan Institue of Developmet Economics, Islamabad, 33*(4), 997-1010. Retrieved June 20, 2014, from http://www.jstor.org/stable/41259807

Khan, A. H. (1980). The Demand for Money in Pakistan: Some Further Results. *Jstor, 19*(1), 25-50. Retrieved February 03, 2015, from http://www.jstor.org/stable/41258469 .

Khan, M. A. (2008). Financial Development and Economic Growth in Pakistan: Evidence Based on Autoregressive Distributed Lag (ARDL) Approach. *South Asia Economic Journal, 9*(375). doi:10.1177/139156140800900206

M.Afzal, M. F. (2010). Realtionship between school educatiob and Economic Growth in Paksitan ARDL Bound Testing Approach to Co-integartion. *Jstor, 48*(1), 39-60. Retrieved June 21, 2014, from http://www.jstor.org/stable/41762413 .

Mall, S. (2013). Estimating a Function of Real Demand for Money in Pakistan: An Application of Bounds Testing Approach to Cointegration. *International Journal of Computer Applications , 79*(5), 0975 – 8887.

Mangla, I. (Spring 1979). Annual Money Demand Function for Pakistan. *The Paksitan Development Review, XVIII*(1).

Mohsen Bahmani-Oskooee, *. M. (1998). German monetary unification and the stability of the German. *Economics Letters, 66*, 203-208. Retrieved 2000

Muhammad Asad, S. H. (2011). Modeling Demand for Money in Pakistan:An ARDL Approach. *Forman Journal of Economic Studies, 7*, 75-88.

https://doi.org/10.62500/icrtsda.1.1.2

Muhammad Aslam Chaudhry, M. A. (2006). Why the State Bank of Pakistan should not Adopt Inflation Targeting. *SBP-Research Bulletin, 2*.

Muhammad Qasim, K. A. (2015). Exchange Rate Volatility and Money Demand: An Empirical Analysis of Pakistan. *Journal of Policy Research, 1*(3), 131-141.

Muhammad Shahbaz, N. A. (2008). Stock Market Development and Economic Growth: Ardl Causality in Pakistan. *International Research Journal of Finance and Economics*(14), 1450-2887. Retrieved 2008, from http://www.eurojournals.com/finance.htm

Muhammad Zahir Faridi, M. H. (2013). An Estimation of Money Demand Function in Pakistan: BoundTesting Approach to Co-integration. *Pakistan Journal of Social Sciences (PJSS), 33*(1), 11-24. Retrieved 2013

Munirs, E. A. (2000). An Analysis of Money Demand in Pakistan. *38*(1), pp. 47-67. doi:28-12-2015 03:27 UTC

Mushtaq Ahmed, A. H. (1990). A Reexamination of the Stability of the Demand for Money in Pakistan*. *Journel of Macroeconomics, 12*(2), 307-321.

Naseer, M. A. (2013). Demand for money in Pakistan. *African Journal of Business Management, 7*(42), 4306-4310. doi:10.5897/AJBM2013.1615

Nell, K. S. (2003). The Stability of M3 Money Demand and. *The Case of South, 3*, pp. 155-180. doi:10.1080/00220380412331322861

Omer, M. (2010). Velocity of Money Functions in Pakistan and Lessons for Monetary Policy. *SBP Research Bulletin, 6*.

Qayyum, A. (2005). Modelling the Demand for Money in Pakistan. *Jstor, 44*(3), 233-252. Retrieved June 21, 2014, from http://www.jstor.org/stable/41260624 .

Qazi Masood Ahmad, S. A. (2011). Exchange Rate Volatility and Pakistan's Bilateral Imports from Major Sources: An Application of ARDL Approach. *International Journal of Economics and Finance, 3*(2). doi:10.5539/ijef.v3n2p245

Raza, A. H. (1989). The Demand for Money in Pakistan :Quarterly Results 1972 - 1987. pp. 33-48.

Rehman, M. B.-O. (2014). Stability of the money demand function in Asian. *37*(7), pp. 773-792. doi:10.1080/000368404200033742

Steady and Pulsatile Newtonian Fluid Flow in Straight Porous Tubes

https://doi.org/10.62500/icrtsda.1.1.3

Proc. 1st International Conference on Recent Trends in Statistics and Data Analytics
Air University Islamabad, Pakistan – May 9, 2024, Vol. 1, pp. 25-33

Steady and Pulsatile Newtonian Fluid Flow in Straight Porous Tubes

N. Z. Khan[1*], M. S. Bataineh[1], N. Akram [2] and Aqsa [2]
[1] Department of Mathematics University of Sharjah, United Arab Emirates.

[2]Lahore Garrison University, Lahore Pakistan.

ABSTRACT

The Steady and Pulsatile Newtonian fluid flow in straight tubes and in straight porous tubes which are basically the solid materials that have pores are studied and compared. The flow is distinguished by using two dimensionless parameters the Womersley number α and the Reynolds number R_e. The analytical results of Navier Stokes equation in cylindrical coordinates system are obtained by using Integration method technique and by Bessel function of 1st kind in each case. Then their graphical representations are drawn to know the trends of their velocity profiles.

Keywords: Newtonian fluids, straight porous tube, Analytical solutions, Wall shear stress, Pulsatile flow.

1. INTRODUCTION

The Study of Newtonian fluid is essential because of its practical uses in engineering purposes. Many substances like water, oil, glycerin and gasoline shows this kind of behavior. Because of its wide uses many researchers have worked on Newtonian fluid Bauer (1976),Tsangaris et al. (2006), Jha and Yusuf (2018),Shit and Ma-jee (2015).As the fluid in this case passes through straight tubes and in straight tubes the flow is usually considered to be laminar and it is usually shown through a cannula or a tracheal tubes. Apparently, the lines in laminar flow are straight but actually their velocity is not constant. At the boundary of the tube their velocity would be zero because of no slip condition and at the center the velocity increases. Many researchers have worked on straight tubes Liepsch (1986),Tsangaris et al. (2006), Das et al. (2018).The study of Pulsatile flow in a straight tubes has motivated the researchers due to its significance in blood flow Bauer. This type of flow was first put forward by John-R-Womersley (1907- 1958) in his efforts with blood flow in arteries. Aorta is the biggest artery whereas veins bring blood in the direction of heart and gas exchange happens in blood flow Bauer. This type of flow was first put forward by John-R-Womersley (1907- 1958) in his efforts with blood flow in arteries. Aorta is the biggest artery whereas veins bring blood in the direction of heart and gas exchange hap pens in capillaries. The expansion of the heart under pressure carries out blood to the arteries. When the area of the arteries enlarges, the pressure of blood then reduces. The drubbing of heart is required as the pressure in arteries and arterioles that drives the blood in them is created by it. The flow in large and small vessels is distinguished by using dimensionless parameters the Womersley number α which is the ratio of transient inertial forces to viscous forces. The boundary layer thickness is inversely related to Womersley number.
If $\alpha > 1$, then thickness of Boundary layer is small.
If $\alpha < 1$, then thickness of Boundary layer is large.
The flow through straight porous tubes has wide applications in medical and chemical fields, infiltration of fluids, functioning of human lung, purification of blood, movement of underground water. Due to its wide application many researchers have worked on porous tubes Bauer (1976), Tsan-garis et al. (2006), Jha and Yusuf (2018),Shit and Majee (2015),Das et al. (2018), Jha and Danjuma (2019),Tiwari et al. (2020), Tajammal et al (2018).

The purpose of this work is to compare the Steady and Pulsatile Newtonian fluid flow in straight tubes and in straight porous tubes. The analytical results obtained by integrating the momentum equations

https://doi.org/10.62500/icrtsda.1.1.3

for flow in straight tubes and then in straight porous tubes have been compared. Then their graphical representations have been drawn and differences are discussed.

2. [GOVERNING EQUATION]

The basic equations that drive the flow of steady, Newtonian fluid flow consists of conservation of mass given as:

$$\nabla . V = 0 \tag{1}$$

The Cauchy stress tensor is split into an isotropic part due to pressure P and an extra stress σ

$$\tau = -PI + \sigma \tag{2}$$

Since

$$\tau = \mu . A_1 \tag{3}$$

Where μ is dynamic viscosity and

$$A_1 = \nabla V + (\nabla V)^T \tag{4}$$

Since equation of continuity is given by:

$$\frac{\partial u}{\partial r} + \frac{u}{r} + \frac{\partial w}{\partial z} = 0 \tag{5}$$

The Cauchy stress tensor is given as:

$$\tau = \begin{bmatrix} \tau_{rr} & \tau_{r\theta} & \tau_{rz} \\ \tau_{\theta r} & \tau_{\theta\theta} & \tau_{\theta z} \\ \tau_{zr} & \tau_{z\theta} & \tau_{zz} \end{bmatrix} \tag{6}$$

Where

$\tau_{rr} = 2\mu \frac{\partial u}{\partial r}$; $\tau_{r\theta} = \tau_{\theta r} = 0$; $\tau_{\theta\theta} = \mu \frac{2u}{r}$;

$$\tau_{rz} = \tau_{zr} = \mu \left(\frac{\partial u}{\partial z} + \frac{\partial w}{\partial r} \right); \ \tau_{z\theta} = \tau_{\theta z} = 0;$$

$$\tau_{zz} = 2\mu \frac{\partial w}{\partial z}$$

3. [PROBLEM FORMULATION]

We consider the flow of fluid to be fully developed in straight, long tube. Flow of fluid is supposed to be steady, Pulsatile and Newtonian having constant density .The tube is considered to be porous having pores in it.The radius of the tube is r. The axial direction is taken along the flow direction and change in velocity occurs in radial direction. We have used Navier Stokes equation in cylindrical coordinate system given as:

$$\rho \left[\frac{\partial w}{\partial t} + (w . \nabla) . w \right] = -\nabla p + div\tau \tag{7}$$

https://doi.org/10.62500/icrtsda.1.1.3

In dimensional component form the above equation takes the form:

$$\frac{\partial u}{\partial t}+u\frac{\partial u}{\partial r}+w\frac{\partial u}{\partial z}=-\frac{1}{\rho}\frac{\partial P}{\partial r}+V\left[\frac{\partial}{\partial r}\left(\frac{1}{r}\frac{\partial}{\partial r}ru\right)+\frac{\partial^2 u}{\partial z^2}\right] \quad (8)$$

$$\frac{\partial w}{\partial t}+u\frac{\partial w}{\partial r}+w\frac{\partial w}{\partial z}=-\frac{1}{\rho}\frac{\partial P}{\partial z}+V\left[\frac{1}{r}\frac{\partial}{\partial r}\left(r\frac{\partial w}{\partial r}\right)+\frac{\partial^2 w}{\partial z^2}\right] \quad (9)$$

The velocity vector $\vec{w}$ is assumed to be of the form

$$\vec{w}=[u(r,z),0,w(r,z)] \quad (10)$$

Where u and w are the velocity components in r,z directions respectively, According to geometry of problem, the boundary conditions are:

$$\text{At } r=a, w=-V_0 \quad (11)$$

Where V_0 is suction parameter, as we have considered the cylindrical coordinate system (r,θ,z) having the θ component to be zero. For the fully developed flow, the derivatives of velocity in axial direction and velocity component in radial direction are zero. So equation (8) and (9) takes the form

$$\frac{\partial w}{\partial t}=\frac{-1}{\rho}\frac{\partial P}{\partial z}+\frac{v}{r}\frac{\partial}{\partial r}\left(r\frac{\partial w}{\partial r}\right) \quad (12)$$

Where, v is kinematic viscosity

$\frac{\partial P}{\partial z}$ is Pressure gradient,

r is radius of tube.

In Cardiovascular system, the motion of blood is taken by pressure gradient. Therefore, for the convenience, we have supposed harmonic pressure gradients for harmonic solutions as:

$$\frac{\partial P}{\partial z}=\frac{\partial \hat{P}}{\partial z}\exp i\omega t \quad (13)$$

and

$$w=\hat{w}(r)exp\, i\omega t \quad (14)$$

Now introducing the dimensionless parameters as:

$$w^*=\frac{w}{v}\ ;\quad r^*=\frac{r}{a}\ ;\quad z^*=\frac{z}{a}\ ;\quad P^*=\frac{P}{\rho V^2}\ ;\quad t^*=\omega t \quad (15)$$

After substituting non-dimensional parameters in equation (12) the equation takes the form:

$$\frac{a^2\omega}{V}\frac{\partial w}{\partial t}=-\frac{av}{V}\frac{\partial P}{\partial z}+\frac{1}{r}\frac{\partial}{\partial r}\left(r\frac{\partial w}{\partial r}\right) \quad (16)$$

with

$$R_e=\frac{av}{V} \quad (17)$$

and

$$\alpha=a\sqrt{\frac{\omega}{V}} \quad (18)$$

i.e

$$\alpha^2\frac{\partial w}{\partial t}=-R_e\frac{\partial P}{\partial z}+\frac{1}{r}\frac{\partial}{\partial r}\left(r\frac{\partial w}{\partial r}\right) \quad (19)$$

https://doi.org/10.62500/icrtsda.1.1.3

here,

r = pipe radius

α=Dimensionless Womersley number

i=Imaginary number

t=time

Re is the Reynolds number which helps us to find out whether the flow is laminar or turbulent. It is defined as:

$$R_e = \frac{Inertial\ forces}{Viscous\ forces} \tag{20}$$

where, ρ=density μ=Dynamic viscosity ν=Kinematic viscosity

α is the Womersley number which tells the thickness of boundary layer and helps us to study the trends of velocity profile.

$$\alpha^2 = \frac{Transient\ Inertial\ forces}{Viscous\ forces} \tag{21}$$

Now equation (13) and (14) after the non dimensionalisation gives:

$$\frac{\partial P}{\partial z} = \frac{\partial \hat{P}}{\partial z} \exp it \tag{22}$$

$$w = \hat{w}(r) \exp it \tag{23}$$

Now three asymptotic cases has been discussed.

4. [SMALL WOMERSLEY NUMBER]

In this case there is an equilibrium of viscous forces and driving pressure gradient. So, in this case if α <<1 inertial term is negligible. So equation (16) becomes:

$$\mathbf{0} = -\boldsymbol{R_e} \frac{\partial \hat{P}}{\partial z} + \frac{1}{r} \frac{\partial}{\partial r} \left(r \frac{\partial w}{\partial r} \right) \tag{24}$$

Now after integrating this equation and by using Boundary condition the relationship of velocity is given by this equation:

$$\boldsymbol{w = \left[-V_0 - \frac{1}{4} R_e \left(\frac{\partial \hat{P}}{\partial z} \right) (1 - r^2) \right] exp\ it} \tag{25}$$

5. [LARGE WOMERSLEY NUMBER]

In this case there is an equilibrium of inertial forces and Pressure gradient. So, in this case if α >>1 equation (16) becomes:

$$\alpha^2 \frac{\partial w}{\partial t} = -R_e \frac{\partial P}{\partial z} \tag{26}$$

https://doi.org/10.62500/icrtsda.1.1.3

Now after integrating this equation and by using Boundary condition the relationship of velocity is given by this equation as:

$$w = \frac{1}{\alpha^2} R_e \left(\frac{\partial \hat{P}}{\partial z}\right) \exp it \tag{27}$$

6. [ARBITRARY WOMERSLEY NUMBER]

In this case the equation formed by substituting (22) and (23) in (16) we get:

$$\frac{\partial^2}{\partial r^2}\hat{w}(r) + \frac{1}{r}\frac{\partial}{\partial r}\hat{w}(r) - i\alpha^2\hat{w}(r) = R_e\left(\frac{\partial P}{\partial z}\right) \tag{28}$$

Bessel differential equation is given by:

$$x^2\frac{d^2y}{dx^2} + x\frac{dy}{dx} + (x^2 - n^2)y = 0 \tag{29}$$

Divide by x^2

$$\frac{d^2y}{dx^2} + \frac{1}{x}\frac{dy}{dx} + (1 - \frac{n^2}{x^2})y = 0 \tag{30}$$

By substitution of

$s^2 = \frac{t^3\omega}{v}$ and by using Boundary condition the equation takes the form as

$$\hat{w}(s) = \frac{-V_0 - \frac{1}{\alpha^2}R_e\frac{\partial \bar{P}}{\partial z}J_0\left(\frac{t^{\frac{3}{2}}\alpha R}{a}\right)}{J_0 t^{\frac{3}{2}}\alpha} \tag{31}$$

7. [WALL SHEAR STRESS]

It is defined as:

$$\tau_\omega = -\mu\left(\frac{\partial w}{\partial r}\right)_{r=a} \tag{32}$$

where,

μ=Dynamic viscosity w=flow velocity r=distance

Using the property of Bessel function:

$$\frac{\partial}{\partial(s)}J_0(s) = -J_1(s) \tag{33}$$

And definition of Womersley function as:

$$F_{10}(\alpha) = \frac{2J_1\left(t^{\frac{3}{2}}\alpha\right)}{t^{\frac{3}{2}}\alpha J_0\left(t^{\frac{3}{2}}\alpha\right)} \tag{34}$$

https://doi.org/10.62500/icrtsda.1.1.3

After simplification the above equation takes the form:

$$\tau_\omega = -\mu v_0 \text{expit} \frac{t^{\frac{3}{2}}\frac{\alpha}{a}}{J_0\left(t^{\frac{3}{2}}\alpha\right)} J_1\left(t^{\frac{3}{2}}\alpha\right) - \frac{\mu_1}{\alpha^2} R_e \frac{\partial P}{\partial z} \frac{expit\left(t^{\frac{3}{2}}\frac{\alpha}{a}\right)}{J_0\left(t^{\frac{3}{2}}\alpha\right)}$$

8. RESULTS AND DISCUSSION

After converting the equations in non-dimensional form, the effect of different flow parameters on the fluid flow are simulated with the help of graphs and proper discussion related to each graph is also provided.

8.1 For Small α

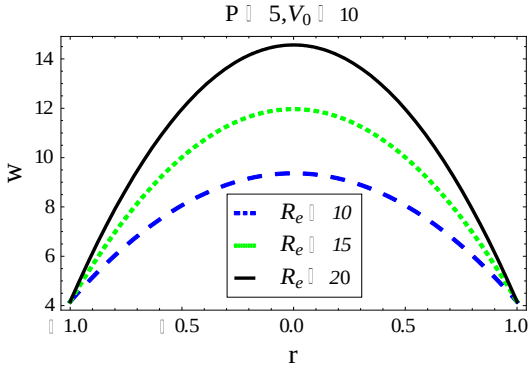

Fig.1 Effect of Reynolds number on velocity profile at constant pressure and Suction parameter.

It is observed from **Fig.1** that velocity profile increases by increasing the Reynolds number at constant Pressure and suction parameter because for small value of α viscous forces dominate inertial forces and parabolic profile is obtained.

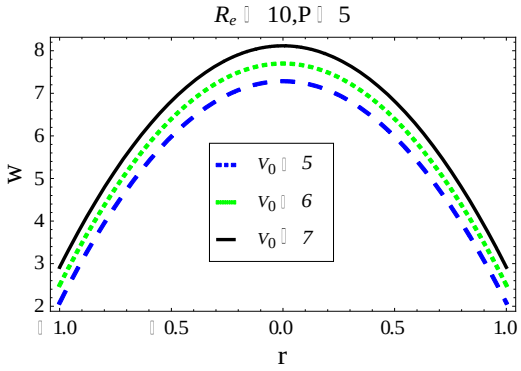

Fig.2 Effect of Suction Parameter on velocity profile at constant pressure Reynold Number

It is observed from **Fig.2** that by increasing the value of Suction parameter at constant pressure and Reynolds number velocity profile increases for small α because viscous forces dominate the inertial forces and parabolic profile is obtained.

https://doi.org/10.62500/icrtsda.1.1.3

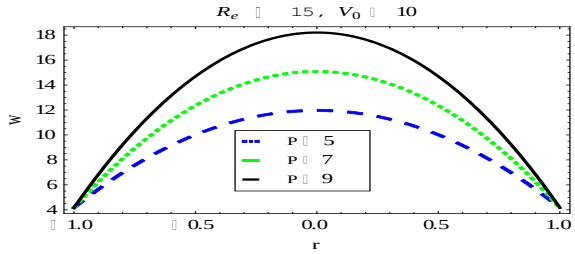

Fig.3. Effect of Pressure "P" on velocity profile at constant Reynold Number and Suction parameter

It is observed from **Fig.3** that by increasing the value of Pressure at constant Reynolds number and Suction parameter the velocity profile increases.

8.2 For Arbitrary α

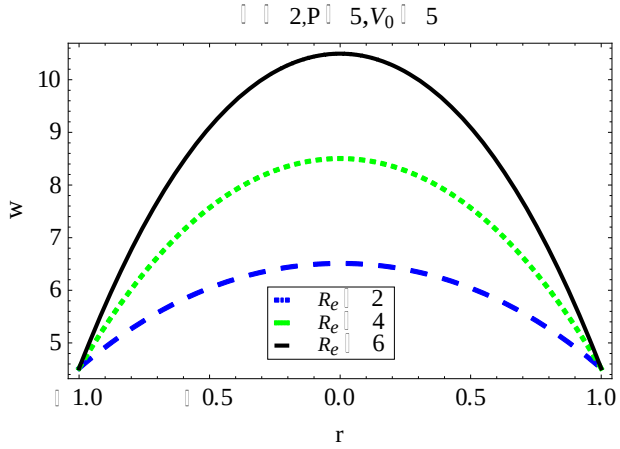

Fig. 4. Effect of Re on velocity profile at constant α, Pressure and Suction parameter.

It is observed from **Fig.4** that velocity profile increases by increasing R_e by keeping other parameters like Pressure α and Suction parameter constant.

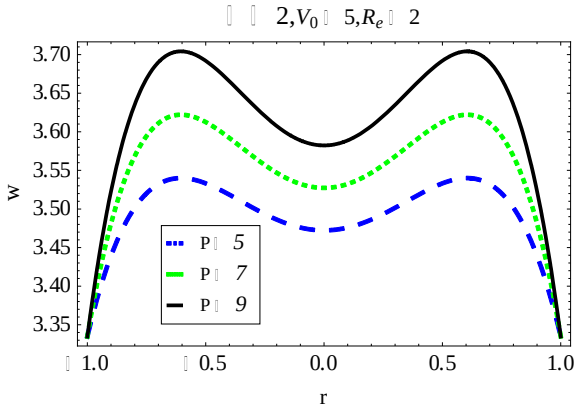

Fig. 5. Effect of Pressure on velocity profile at constant α, Suction parameter , and Re.

It is observed from Fig.5 that by increasing the value of Pressure by keeping α , Re and Suction parameter the velocity profile increases.

https://doi.org/10.62500/icrtsda.1.1.3

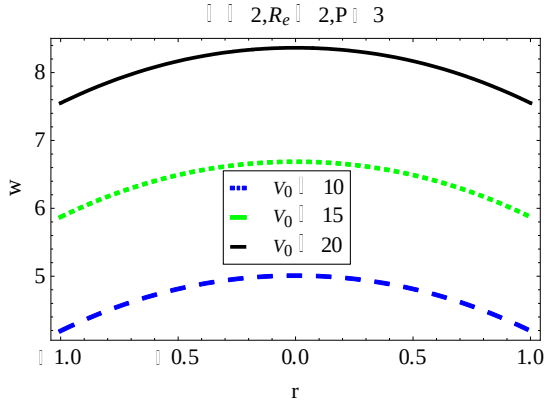

Fig. 6. Effect of Suction parameter on velocity profile at constant α, Re and Pressure.

It is observed from **Fig.6** that by increasing the value of Suction parameter at constant α, Pressure and Re the velocity profile increases.

9. CONCLUSION

In the present study, Steady and Pulsatile Newtonian fluid flow in straight tubes and in straight porous tubes has been considered. To investigate fully developed Newtonian flow in straight and porous tubes the Navier Stokes equation used and the solution of Partial differential equations have been found out by using integration technique method and Bessel function of 1st kind in each case and the type of flow in both tubes have been specified by two dimensionless parameters the Womersley number α and the Reynolds number Re the value of the results obtained after drawing graphs on Mathematica9 are that introduction of the suction parameter in the governing equation the velocity profile increases.

REFERENCES

1. Bauer, H. (1976). Pulsatile flow in a straight circular pipe with reabsorption across the wall. Ingenieur-Archiv 45(1), 1–15.
2. Bauer, H. F. (1987). Uniform pulsatile flow of an incompressible liquid in a tube of parallelogram cross-section. Forschung im Ingenieurwesen A 53(5), 149–155.
3. Das, M. K., P. P. Mukherjee, and K. Muralidhar (2018). Porous media applications: Biological systems. In Modeling Transport Phenomena in Porous Media with Applications, pp. 123–154. Springer.
4. Jha, B. and T. Yusuf (2018). Transient pressure driven flow in an annulus partially filled with porous material: Azimuthal pressure gradient. Mathematical Modelling of Engineering Problems 5(3), 260–267.
5. Jha, B. K. and Y. J. Danjuma (2019). Transient dean flow in a channel with suction/injection: A semi-analytical approach. Proceedings of the Institution of Mechanical Engineers, Part E: Journal of Process Mechanical Engineering 233(5), 1036–1044.
6. Liepsch, D. (1986). Flow in tubes and arteries-a comparison. Biorheology 23(4), 395–433.
7. R. Tajammal, M. A. Rana, N. Z. Khan and M. Shoaib, "Slip effect on combined heat and mass transfer in three dimensional MHD porous flow having heat," *2018 15th International Bhurban Conference on Applied Sciences and Technology (IBCAST)*, Islamabad, Pakistan, 2018, pp. 635-644, doi: 10.1109/IBCAST.2018.8312291.

https://doi.org/10.62500/icrtsda.1.1.3

8. Shit, G. and S. Majeed (2015). Pulsatile flow of blood and heat transfer with variable viscosity under magnetic and vibration environment. Journal of Magnetism and Magnetic Materials 388, 106–115.
9. Tiwari, A., P. D. Shah, and S. S. Chauhan (2020). Solute dispersion in two-fluid flowing through tubes with a porous layer near the absorbing wall: Model for dispersion phenomenon in microvessels. International Journal of Multiphase Flow 131, 103380.
10. Tsangaris, S., D. Kondaxakis, and N. Vlachakis (2006). Exact solution of the navier–stokes equations for the pulsating dean flow in a channel with porous walls. International journal of engineering science 44(20), 1498–15

https://doi.org/10.62500/icrtsda.1.1.4

Proc. 1st International Conference on Recent Trends in Statistics and Data Analytics
Air University Islamabad, Pakistan – May 9, 2024, Vol. 1, pp. 34-40

Evaluation of garlic varieties yield under different irrigation methods in Sistan region

Behnam Bakhshi*, Mohammad Reza Naroui Rad, Ahmad Seraj and Mohammad Keshtgar Khajedad

Horticulture Crops Research Department, Sistan Agricultural and Natural Resources Research and Education Center, AREEO, Zabol, Iran

Abstract

Garlic (*Allium sativum* L.) has a wide cultivated area in the Sistan region. Cultivation of this crop is expanding in Sistan region due to its relatively good resistance to water stress rather than other vegetables and on the other hand, suitable economic efficiency. In this study, the performance of different garlic varieties were compared in the different irrigation conditions at Zahak Agricultural Research Station. In this study, eight garlic varieties were evaluated in a field experiment as a split plot in a randomized complete block design with three replications. Two methods of irrigation (flood and tape-type) were considered as the main factor and eight type (kind) of garlic varieties (Gilan, Hamedan, Mazand, Hirani, Chinese, Tafresh, Urmia and Zabol) were considered as secondary factors. Different Quantitative traits were evaluated during the growth period. The results showed that Strip irrigation method has increased the yield of different garlic varieties despite lower water consumption (30%). Correlation analysis using Pearson method showed that the yield had a positive correlation with leaf width, garlic weight, garlic width, tuber diameter and tuber weight. Also, among the studied varieties, Mazand and Chinese varieties showed the highest yield in both irrigation methods. Therefore, the use of strip irrigation method for growing garlic of Mazand and Chinese varieties in the Sistan region is recommended.

Keywords: *Allium sativum*, Garlic Varieties, Yield, Irrigation, Sistan Province

1. Introduction

Garlic (*Allium sativum*) is a diploid plant (2n=2x=14) that is cultivated to produce garlic and its bulbs (Figliuolo et al. 2001). In addition to identify the best variety, it is necessary to identify appropriate methods to increase water productivity. At present, irrigation by flood irrigation method is the dominant method of irrigation in Sistan region. Although this irrigation method is a very common; However, more detailed studies are needed to compare this method with modern irrigation methods, such as tape irrigation. Therefore, the utilization of new methods in irrigation, including tape-type irrigation etc., if properly managed in the cultivation method, can replace the classic irrigation methods and as a result farmers with optimal management of available water can increase the area under cultivation with available water, Irrigation method and it's management play a significant role in increasing the yield and optimal irrigation efficiency, So in favorable conditions, along the growth stage of the plant, water and nutrients are provided to the plant in a desirable way and to the required extent (Shah Mohammadi et al., 2007). On the other hand, it should be considered that new irrigation methods, although they increase water use efficiency (Ghaemi et al., 2008), However, the depth of water infiltration in these methods decreases and the rate of evaporation increases compared to the water received in the field. On the other hand, garlic is sensitive to drought and proper moisture is essential for it's growth. Moisture stress affects the initial growth and reproduction of onions and causes the garlic to shrink and produce small cloves when harvested. Therefore, changes in cultivation and irrigation methods in order to increase water use efficiency in agricultural products and ultimately the development of their cultivation need to study and carefully study its effect on crop characteristics and garlic yield.

In studies of native garlic varieties including Hamedan, Tafresh, Ahvaz, Iranshahr, Golestan and Mazand varieties, they were compared in terms of yield and among the studied garlic population, Tafresh and Hamedan garlic populations had the highest garlic yield per plant and per unit area

https://doi.org/10.62500/icrtsda.1.1.4

(Nourbakhshian et al., 2007). In other studies, different populations of Tarom region were evaluated in terms of yield and different traits and Jia population was superior to other populations (Shobiri et al., 2014). Abbasifar (2000) by investigating the effect of planting date and adaptation of selected varieties of garlic from different parts of the country in the Araak province reported that Hamedan garlic with a yield of 11.59 tons per hectare compared to other varieties (except garlic Tafresh with a yield of 10.73 tons per hectare) had a significant advantage. He reported the highest average weight of garlic in Tafresh local garlic with an average of 8.3 grams on the date of the first crop (November), but in terms of the number of garlic in cloves, Hamedan garlic with an average of 13.74 compared to other varieties (with the exception of Ahvaz garlic), had a significant advantage. Sood et al. (2009) In a study to investigate the genetic diversity between 5 varieties of garlic in India, observed a great variety of traits such as garlic yield per unit area in wet and dry, diameter, length and weight of gland.

Proper irrigation method for many plants in maintaining water and nutrients in the root zone, causes proper growth and high-yielding crops. Studies by Shermasarker (2001) on the efficiency of water and fertilizer application in tape and furrow irrigation methods showed that tape irrigation with less water and fertilizer consumption has the same performance as furrow irrigation. Kassel et al. (2001) in an experiment conducted in the southern regions of the United States of America showed that utilizing of tape irrigation system, is more appropriate to control soil nitrate leaching and optimal use of water. In this experiment, the sugar yield of sugar beet was 3 to 28% higher than the leaky method. Proper irrigation method for many plants in maintaining water and nutrients in the root zone, causes proper growth and high-yielding crops. Also, the efficiency of using water and fertilizer in the tape-type irrigation system was higher than leak irrigation. Snow et al. (1997) performed experiments with 4 different cycles of drip irrigation once every 3, 4, 5, 6 days (and 4 levels of pure nitrogen) at 0, 20, 40 and 80 kg / ha (on garlic). The results showed that different nitrogen and irrigation treatments did not have a significant effect on garlic tuber yield, but the highest garlic yield was obtained from the treatment with an irrigation cycle of 3 days and consumption of 20 kg / ha nitrogen. Jamrooz et al. (2001) examined four planting intervals (4, 8, 12 and 16 cm) and four planting dates (first half of October, 15 October, 30 October and 15 November) on garlic weight, number of garlic and garlic yield. He concluded that the effect of distance and planting date on garlic weight, number of garlic and yield was significant. They suggested planting distance of 8 cm and planting in the first half of October.

In a study to investigate two systems of drip and leakage irrigation on the yield of garlic in Hamedan, it was found that drip irrigation has the same performance as the leakage method, while water consumption is reduced and water use efficiency is increased (Firoozabadi et al1391). Pandi et al. (1993) reported in a study in Gujarat, India that drip irrigation is more suitable for irrigating some crops such as garlic than flood and sprinkler (rainy) irrigation.

Currently, different varieties of garlic, including Mazand and Chini, are cultivated in the Sistan region.Zabul native garlic is also widely cultivated in this region. However, their performance has not been compared with each other and with other varieties in the Sistan region. Therefore, it is necessary to compare the performance of these varieties in the conditions of Sistan region and identify the varieties with the highest potential for increasing yield. In this study, 8 different garlic varieties including Gilan, Hamedan, Mazand, Hirani, Chini, Tafresh, Urmia and Zabol have been evaluated using both flood and strip irrigation methods. The purpose of this study was to identify the most suitable cultivable garlic variety in the conditions of Sistan region and also to identify the best irrigation method for different garlic varieties.

2. Materials and Methods

In order to investigate the yield of different garlic varieties in Sistan region using different irrigation methods, eight garlic varieties (Allium sativum L.) in a field experiment with a split plot design with three replications in the farm of Zahak Research Station located in Sistan in the crop year 2018-2019 were carried out. Animal manure was added to the soil before planting. Then, the land was irrigated and plowed, in order to prepare the land, clods were crushed using discs and the land was leveled. Cultivation was done on the 6th of novomber of 2018. Two levels of irrigation method (flood and tape) were considered as the main factor and eight levels of garlic variety (Gilan, Hamedan, Mazand, Hirani, Chini, Tafresh, Urmia and Zabol) as the secondary factor.The variety was planted in

https://doi.org/10.62500/icrtsda.1.1.4

three nine-meter lines with a distance of 20 cm and the distance between the varietylines was 40 cm. Measured traits include day to germination, day up to 4 leaves, day up to seven leaves, day untill maturity, number of root fibers, the length of root fiber, number of leaves per plant, bush height, leaf length, leaf width, the length of the garlic, weight of the garlic, width of the garlic, number of the cloves in the tubers, the gland height, the gland diameter, the gland weight and the yield. Measurable statistics including mean were measured and the correlation between different traits was estimated using Pearson correlation method. Analysis table of variance and mean comparisons were analyzed using Duncan's method.

3. Results and Discussion

Evaluation of landrace of garlic under flood irrigation conditions

In flood irrigation method, 655 cubic meters of water was used for each plot. Evaluation of landraces yield under flood irrigation conditions showed that Chinese, Mazandi, Hirani and Hamedani landraces with average yields of 3696, 3645, 2325 and 2242 kg / ha have the highest yield under flood irrigation conditions. Most of the gland weight in these conditions belonged to Mazand and Chinese varieties. The highest number of garlic was observed in Zabol variety and the lowest number of garlic was observed in Tafreshi and Hirani variety. Also, Chinese, Mazand and Hamedani garlic variety had the highest gland weight. In terms of ripening, the earliest garlic varietyif was Hamedan and latest one was Zabol variety.

Evaluation of varieties in strip irrigation conditions

In the tape irrigation method, 452 cubic meters of water was used for each plot. yield evaluation of landrace in flood irrigation conditions showed that Mazand, Chini, Hamedani and Gilani landfills with average yields of 4372, 3889, 2816 and 2699 kg / ha have the highest yield in flood irrigation conditions. The highest gland weight in these conditions belonged to the Chinese and Mazand varieties. The highest number of cloves in tuber was observed in Zabol variety and the lowest number was observed in Tafreshi and Hirani variety. Also, Chinese, Hamedani and Mazand garlic clusters had the highest gland weight of garlic. In term of maturity, the earliest garlic variety was Gilan and latest one was Zabol variety.

4. Assess correlation of traits

The correlation between quantitative traits in this study was investigated using Pearson method. The results showed that the number of days up to 7 leaves of the plant with the number of days untill maturity, number of root fibers per tuber, number of leaves per plant, leaf length, width of garlic and gland diameter had a positive correlation. The number of days untill maturity had a positive correlation with the number of root fibers per tuber, number of leaves per plant and gland diameter and a negative correlation with leaf width. In addition to the positive correlation with phenological traits, the number of root fibers in the tuber also showed a positive correlation with the trait of leaf length.

The number of leaves per plant also showed a positive correlation with phenological traits of days up to seven leaves and days until maturity as well as leaf length and width of garlic and a negative correlation with leaf trait. The number of leaves per plant also showed a positive correlation with the phenological traits of day to week leaf and day to maturity, as well as leaf length and width of garlic and a negative correlation with leaf width. leaf length showed a positive correlation with phenological traits, number of root fibers per tuber and number of leaves per plant. The length of the clove showed a positive correlation with the number of cloves in the gland and the height of the gland and a negative correlation with the diameter of the gland. Garlic weight also showed a positive correlation with garlic width, gland diameter, gland weight, leaf width and yield. Also, the width of garlic showed a positive correlation between phenological traits, gland diameter, gland weight, number of leaves per plant, garlic weight and yield. The number of cloves in the tuber showed a positive correlation with the traits of garlic length, gland height and weight. Tuber height showed only a significant and positive correlation with the number of cloves in the tuber. Tuber height showed a positive correlation with the length of garlic and the number of cloves in the tuber. gland diameter also showed a positive correlation with phenological traits, garlic weight, garlic width, gland weight and yield and also a negative correlation

https://doi.org/10.62500/icrtsda.1.1.4

with garlic length. gland weight showed a positive correlation with leaf width, garlic weight, garlic width, number of cloves in the tuber and yield. Yield also showed a positive correlation with leaf width, garlic weight, garlic width, tuber diameter and tuber weight.

Differences between different garlic varieties evaluated in terms of quantitative traits

The results of analysis of variance showed that there was a significant difference between the garlic varieties studied in this study in the conditions of Sistan region. Average squares of different varieties of garlic in terms of day up to four leaf traits, day untill maturity, number of root fibers per tuber, plant height, leaf length, leaf width, essential oil, length of garlic, weight of garlic, width of garlic, number of cloves in Gland, gland height, gland diameter, gland weight and yield are significantly different. The comparison of the mean traits of the studied populations was investigated using Duncan's method and the results are presented in Table 2. In general, Mazand and Chinese garlic cultivars had the highest average yield and were recognized as the best cultivars based on Duncan's average comparison method.

The effect of irrigation methods on quantitative traits of different garlic varieties

Analysis of variance of split plots in a randomized complete block design showed that irrigation methods based on the phenological characteristics of garlic including number of days to germination, number of days up to four leaves, number of days up to seven leaves and number of days until maturity had a significant impact on garlic quantitative traits. Irrigation methods also had a significant effect on leaf length, garlic weight, garlic width, number of garlic in the tuber, diameter, tuber weight and finally yield. Comparison of mean traits showed that the phenological stages until to reach plant maturity in most varieties utilizing tape irrigation method were significantly longer. The reason for the faster phenological stages in the flood irrigation method can be due to dehydration stress between irrigation stages, which has led to faster phenological stages. It was also observed that the tape irrigation method has increased the number of root fibers in the tuber compared to the flood irrigation method. The number of leaves per plant and leaf length also showed a significant increase by tape irrigation. The weight of garlic, the width of garlic, the number of cloves in the gland, the diameter of the gland and the weight of the gland also showed a significant increase by tape irrigation. The yield also increased significantly in the tape-type irrigation method. Therefore, the tape irrigation method, despite reducing water consumption, has increased yield in most garlic varieties.

Table 1. Mean squares of different quantitative traits studied for different garlic varieties in different irrigation methods

	Day to germination	Day up to 4 leaves	Day up to seven leaves	Days until maturity	Number of root fibers	The length of the root web	Number of leaves per plant	Bush height	Leaf length	Leaf width
Block	0.3	0.1	3.1	0.6	60.4	1.9	0.8	21.4	1.3	3.3
watering systems	8.3**	176.3**	157.7**	285.2**	1045.3**	0.1	3.5*	29.6	640.2**	0.8
Irrigation error	0.6	2.0	0.8	0.8	7.0	1.3	0.4	5.1	10.9	0.1
Variety	0.5	8.6**	2.2	35.4**	84.9**	4.7	1.1	30.7**	40.8**	11.9**
Variety interaction in irrigation	0.9*	9.0**	4.9	35.6**	196.0**	4.6	1.3*	31.8**	51.5**	7.4**
error	0.4	2.1	2.9	1.1	22.3	3.8	0.6	8.6	5.7	1.3

https://doi.org/10.62500/icrtsda.1.1.4

Continuation of Table 1. Mean squares of different quantitative traits studied for different garlic varieties in different irrigation methods

	Essence	The length of the garlic	The weight of garlic	Width of garlic	Number of cloves in the tuber	Gland height	Gland diameter	Gland weight	yield
Block	0.0	0.1	0.1	0.0	2.9*	0.0	0.0	13	99481
watering systems	0.0	0.1	4.4**	24.1**	8.3**	0.1	10.0**	1307**	3973295**
Irrigation error	0.0	0.1	0.0	0.6	0.0	0.0	0.0	29	96995
Variety	2.7**	0.8**	3.8**	5.0**	21.0**	0.4**	4.6**	586**	6034074**
Variety interaction in irrigation	0.4	0.2**	0.2**	1.1**	0.9	0.3**	0.6**	108**	341269**
Error	0.2	0.1	0.0	0.2	0.6	0.0	0.0	22	87183

Table 2. Comparison of the average quantitative traits of different garlic clusters

	Day to germination	Day up to 4 leaves	Day up to seven leaves	Days until maturity	Number of root fibers	The length of the root web	Number of leaves per plant	Bush height	Leaf length	Leaf width
Gilan	11	82 ^{c}	161	188^{f}	58^{ab}	8.55	7.67	50.40^{a}	28.62 ^{a}	9.33^{a} ^{b}
Hamedan	10	85 ^{a}	161	191^{e}	51^{c}	9.08	7.33	47.42^{a} ^{b}	19.35 ^{c}	10.33 ^{a}
Mazand	11	83 ^{bc}	161	192 ^{cd}	54^{bc}	10.62	7.50	46.13^{b} ^{c}	22.78 ^{b}	9.67^{a} ^{b}
Hirani	11	84 ^{abc}	163	194 ^{b}	59^{ab}	9.60	8.50	47.57^{a} ^{b}	24.18 ^{b}	8.50^{b} ^{c}
Chinese	11	83^{bc}	162	193 ^{bc}	59 ^{ab}	8.35	8.33	43.97^{b} ^{c}	25.28 ^{b}	7.67^{c}
Tafreshi	11	84^{ab}	161	193^{c}	59 ^{ab}	9.58	8.33	45.90^{b} ^{c}	24.35 ^{b}	7.67^{c}
Orumieh	11	83 ^{bc}	162	191de	64^{a}	8.78	7.67	45.07^{b} ^{c}	22.80 ^{b}	8.33^{b} ^{c}
Zabul	11	85 ^{a}	161^{a}	196^{a}	59 ^{ab}	7.78	7.83	43.30^{c}	23.75 ^{b}	5.83^{d}

https://doi.org/10.62500/icrtsda.1.1.4

Continuation of Table 2. Comparison of the average quantitative traits of different garlic clusters

	Essence	The length of the garlic	The weight of garlic	Width of garlic	Number of cloves in the tuber	Gland height	Gland diameter	Gland weight	yield
Gilan	2^{bc}	3.67^{b}	2.88^{d}	4.67^{c}	7.83^{d}	4.53^{a}	3.40^{d}	22.67^{bc}	2077^{cd}
Hamedan	3^{a}	3.73^{ab}	3.89^{b}	5.83^{a}	7.00^{de}	4.67^{a}	3.88^{c}	37.39^{a}	2529^{b}
Mazand	2^{bcd}	3.45^{b}	3.84^{b}	5.83^{a}	10.17^{b}	4.53^{a}	5.00^{a}	39.16^{a}	4008^{a}
Hirani	1^{de}	2.75^{c}	2.78^{d}	5.67^{ab}	6.33^{e}	3.92^{c}	3.87^{c}	17.93^{c}	2319^{bc}
Chinese	2^{b}	3.60^{b}	4.53^{a}	6.17^{a}	9.00^{c}	4.32^{b}	4.73^{b}	42.92^{a}	3792^{a}
Tafreshi	1^{e}	3.62^{b}	2.82^{d}	6.17^{a}	6.50^{e}	4.28^{b}	3.17^{d}	18.45^{c}	1273^{e}
Orumieh	2^{cde}	3.60^{b}	3.55^{c}	5.17^{bc}	7.83^{d}	4.30^{b}	2.88^{e}	27.75^{b}	1886^{d}
Zabul	1^{e}	3.97^{a}	2.06^{e}	3.50^{d}	11.67^{a}	4.68^{a}	2.48^{f}	22.54^{bc}	1474^{e}

5. Conclusion

The result of the present study showed that the tape irrigation method has increased the yield among different garlic varieties, despite the reduction in water consumption. And also, Mazand and Chinese garlic cultivars had the highest average yield and were the best cultivars in both flood and tape irrigation methods. Therefore, the use of tape-type irrigation method for growing garlic of Mazand and Chinese varieties in Sistan region is recommended.

References

1. Abbasifar, A. R.(2000); Assessing compatibility and determining the appropriate planting date of selected garlic cultivars in the Central province. *Abstracts of the 2nd Congress of Horticultural Sciences of Iran, Karaj*.
2. Cassel F. Sharmasarkar, Miller. S.D. (2001). Assessment of drip and flood irrigation on water and fertilizer use sufficiencies for sugar beets. *Agricultural Water Management*. 46:24-251.
3. Ghaemi, A., Hosseinabadi, Z and Sepaskhah, A. (2008) Investigation of water application efficiency in conventional and one-strip irrigation and furrow irrigation and its effect on quantitative and qualitative yield of sugar beet. *Journal of Agricultural Sciences and Industries (Water and Soil) 22: 84-95.*
4. Jamroz, M., Ishtiaq, M., Naeem, N., Muhammad, N., Jamiher, B., & Iqbal, J. (2001). Effect of Different Planting Dates and Spacing on Growth and Yield of Garlic Cv. Bianco. *Online Journal of Biological Sciences*, 1(4), 206-208.
5. Nourbakhshian, J., Mousavi, A., Bagheri, H.R. (2007). Evaluation of agronomic traits and causal analysis of yield of landrace garlic cultivars. 2007. *Research and construction in agriculture and horticulture. 77: 18-10.*
6. Pandey,u., khanpara,V., (1995) Micro irrigation for a changing world proceeding of the fith International micro irrigation congress, 2-6 April,464-469,3ref
7. Qadmi Firoozabadi, A., Nosrati, A.A., Abyaneh, H.Z (2012). Investigation of the effect of drip irrigation and leakage systems on yield, yield components. Water consumption efficiency of garlic variety in Hamedan. *Journal of Agriculture (Research and Construction). No. 94. pp. 61 to 67.*
8. Qadmi Firoozabadi, A. and Mirzaei, M. (2006) The effect of drip irrigation on quantitative and qualitative properties of sugar beet. *Journal of Research and Construction. 71: 11-6.*

https://doi.org/10.62500/icrtsda.1.1.4

9. Shah Mohammadi, R., Mir Latifi, M. and Mohammadi, K. (2007) Hydraulic simulation of lateral pipes (sprinklers) Sprinkler irrigation. *Journal of Agricultural Science and Technology and Natural Resources. 11 (40): 39-52.*
10. Shubiri, S., Taheri, M., Mostafavi, K., Mohammadi, A. (2014). Evaluation of morphological traits and yield in local populations of Garlic Tarom in Zanjan province. *Journal of Research in Crop Sciences. 23: 75-96.*
11. Seno, S. (1997) Effects of irrigation frequency and nitrogen rates on garlic (*Allium Saivum*l.) C.v.Roxo perola cacador.v *Cultura Agronomia*.6:1, 29-40
12. Sharmasarker, F.C., (2001) Assessment of drip and flood irrigation on water and fertilizer use efficiency for sugar beets. Agric. *Water Management*. PP. 241-251
13. Sood, D. R., V. Chokar and J. Singh. (2000), Studies on growth, pungency and flavour characteristics of five varieties of garlic (*Allium sativum* L.) bulbs during development. *Vegetable Science*. 27(2): 180-184

https://doi.org/10.62500/icrtsda.1.1.5

Proc. 1st International Conference on Recent Trends in Statistics and Data Analytics
Air University Islamabad, Pakistan – May 9, 2024, Vol. 1, pp. 41-43

Multivariate statistical analysis and machine learning approaches in melon for suitable selection

Mohammad Reza Naroui Rad[1*], Ahmad Ghasemi[2], Ammara Nawaz Cheema[3] Ramin Rafezi[4]

[1,2] Department of Horticulture Crops Research, Sistan Agricultural and Natural Resources Research and Education Center, AREEO, Zabol, Iran

[3] Department of Mathematics, Air University, Islamabad, Pakistan

[4] Horticultural Research Institute, Vegetable Research Department, Agricultural Research, Education and Extension Organization, AREEO, Karaj, Iran

ABSTRACT

The experiment was undertaken in two growing season in 2018 and 2019. Phenotypic variances were higher than genotypic variances for most of the traits. Number of fruit and flesh diameter (74% and 70%) had the highest heritability between traits respectively. Cluster analysis by ward method grouped genotypes into the two groups. Random forest analysis was done on 60 samples of genotypes, Variable importance by random forest approach showed flesh diameter and cavity diameter depicted as effective variables in identifying yield variation. SVM graph showed cavity diameter and fruit length seperate out genotype sefidak with high confidence from the others.

1. INTRODUCTION

Main requirement in the initial assessment of genetic variation are morphological analyses for classification and identification of genotypes and cultivars, morphological diversity and characterization have been done by several studies for landraces and indicates distinct genetic sources (1,2). Cognition of the mechanisms which can control the agronomic traits of crops is first step for genetically improvement and could be obtained through monitoring of genotypes or landraces, Information about the correlation and linkage among different horticultural feature is of primary importance in the subject area of crop improvement. Best breeding program is essential to increase melon yield based on variability, mean value, heritability, and yield components. Expression of a specific trait depends on the level of genetic role and its regulation, also forecasting its breeding worth is determined by its heritability(5). Among supervised machine learning algorithm, random forest (RF) is one of the high accuracy and non-parametric method (2). Support vector machines (SVM) are another type of supervised ML approaches which can be taught to categorize individuals in high-dimension space (3). This research aimed to find out the genetic basis and inherited pattern of various traits in melon genotypes. Specifically, the present investigation sought to assess variability in genetic parameters and relation among different characters and effective traits with essential roles in yield also classification of genotypes based on traits by some ML procedures.

2. MATERIALS AND METHODS

Ten muskmelon genotypes were selected to include in the experiment, these selected genotypes were from warm and dry zone. A randomized complete block design was applied with three replicates. Six ripen three crown fruits per plot were employed for sampling and measurements. For evaluation of the genotypic impacts Analysis of Variance (ANOVA) was performed by the use of RCBD design to obtain variance components. Variable importance measurement was carried out in the Random Forest R package. Random forest estimates covariate importance by permuting the values of each covariate in the out-of-bag (OOB) sample (thereby destroying the information content of each covariate) and reclassifying OOB samples using the permuted variable. The change in OOB error is then an indication of the importance of that covariate. Covariates with a comparatively large increase in OOB error are

https://doi.org/10.62500/icrtsda.1.1.5

more important. Support vector regression (SVR) arises from a nonlinear generalization of the Generalized Portrait algorithm developed by Vapnik (3). It projects the input data into a higher dimensional space using a kernel function and separates different classes of data using a hyperplane. The trade-off between margin and errors is controlled by the regularization parameter SVR with radial basis kernel functions (SVRrbf) uses: $(x\,i\,,xj\,) = \exp(-y\,\|x\,i\,-x\,j\,\|2\,)$. Here y is a constant used in the radial basis function. Cluster analysis was conducted with 10 genotypes means of variables according to Ward's minimum variance method using the cluster procedure of SPSS computer software. Stepwise regression is a semi-automated process of building a model by successively adding or removing variables based solely on the t-statistics of their estimated coefficients.

3. RESULTS AND DISCUSSION

The ANOVA on data obtained from two years indicate are there significant difference for evaluated traits ($p < 0.01$). The stepwise regression procedure was analyzed with considering the yield as the dependent variable and the rest of traits as independent variables in melon genotypes. The outcomes of processing various linear regression models revealed that such traits as flesh diameter, fruit weight, fruit length, cavity diameter, and number of fruit significantly affect the model. Also, only the cavity diameter encompassed 96.9% of the variations making it an effective trait for selection. Multiple linear regressions is the effective way to provide useful information about the relation between yield components and yield, strong correlation was observed between yield and the number of fruit per plant, fruit weight, fruit length, cavity diameter and flesh diameter. Multiple linear regressions is a powerful procedure to analyze multivariate data, Naroui Rad et al (5) in one research showed that fruit length and fruit weight have a strong correlation with yield and suggested them as better selection criteria. Hierarchical cluster analysis according Euclidean dissimilarity by Ward's method categorized the examined melon genotypes into two important differing clusters. The variable impacts estimated from random forest by package in R library (7) are shown in Figure 3. In the variable impacts measurement index, maximum top two variables are flesh diameter and cavity diameter (Figure 1). Naroui Rad et al (6) by random-forest analysis regarding to 116 genotypes of melon showed the top variables which impacts total yield were flesh diameter, fruit length, number days to flowering and fruit width respectively.

Table 1. The relative contribution of characters for explaining melon yield using stepwise multiple regression analysis

Variables into the model	B	Standard Error	Standard Coeficients	t	R^2	Sig
Number of fruit	10222.750	398.717	1.142	25.639	0.32	.000
Fruit weight	10.292	0.576	0.748	17.858	0.91	.000
Fruit length	263.348	76.408	0.179	3.447	0.961	.001
Cavity diameter	953.711	404.802	0.087	2.356	0.962	.022
Flesh diameter	422.206	182.574	0.071	2.313	0.969	.025

https://doi.org/10.62500/icrtsda.1.1.5

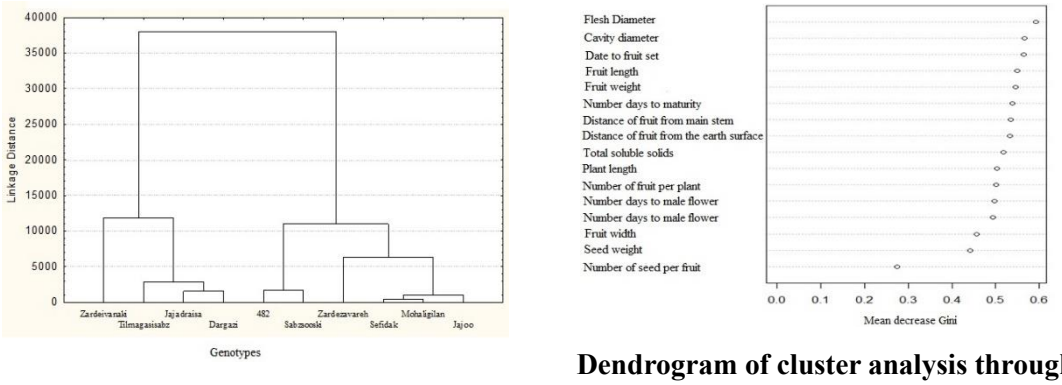

Figure 1. (A) Dendrogram of cluster analysis through Ward method, (B) Variable importance rankings for traits data used as input into random-forest

REFERENCES

1. Barzegar, T., Heidaryan, N., Lotfi, H., Ghahremani Z. (2018). Yield, Fruit Quality And Physiological Responses Of Melon Cv. Khatooni Under Deficit Irrigation. Adv. Hort. Sci., 2018 32(4): 451-458.

2. Breiman, L. (2001) . Random Forests. Mach. Learn 45: 5-32.

3. Cortes, C., Vapnik, V. (1995). Support-Vector Networks. Machine Learning, 20: 273-297.

4. Decker-Walters, D.S., Straub, J.E., Chung, S.M., Nakata, E., Quemada, H.D. (2012). Diversity In Free-Living Populations Of Cucurbita Pepo (Cucurbitaceae) As Assessed By Random Amplified Polymorphic Dna. Syst. Bot., 27: 19-28.

5. Naroui Rad, M., Ghasemi, M., Kuhpayegani, J. (2017). Evaluation Of Melon (Cucumis Melo. L) Genotypes Aiming Effective Selection Of Parents For Breeding Directed At High Yield Under Drought Stress Condition. J. Hort. Res, 25: 125-134.

6. Naroui Rad, M.R., Koohkan, S.H., Fanaei, H.R., Pahlavan, Rad., M.R. (2015). Application Of Artificial Neural Networks To Predict The Final Fruitweight And Random Forest To Select Important Variables In Nativepopulation Of Melon (Cucumis Melo L.). Sci. Hort, 181: 108-112.

7. Rcolorbrewer, S., Liaw, A., Wiener, M., Liaw, M. (2015). Package Randomforest.

https://doi.org/10.62500/icrtsda.1.1.6

Proc. 1st International Conference on Recent Trends in Statistics and Data Analytics
Air University Islamabad, Pakistan – May 9, 2024, Vol. 1, pp. 44-53

MORE EFFICIENT ESTIMATORS USING SOMEROBUST MEASURES

Muhammad Abid[1,2*], Mei Sun[1], Rizwan Munir[3], Muhammad Azam[4]

[1]School of Mathematical Sciences, Jiangsu University, Zhenjiang, Jiangsu, People's Republic of China.

[2]Department of Statistics, Government College University, Faisalabad, 38000, Pakistan.

[3]School of Statistics and Data Science, Jiangxi University of Finance and Economics, Nanchang city, Jiangxi Province, PR China 330013

[4]Bureau of Pakistan, Planning and Development Board Faisalabad Division Government of Pakistan

Email: [1]mabid@gcuf.edu.pk, [2]sunm@ujs.edu.cn, [3]rizwanstat@gmail.com, [4]hafizazam583@gmail.com

[*]Corresponding Author: Muhammad Abid

ABSTRACT

In this paper we have proposed a median based estimator using known value of some population parameter(s) in simple random sampling. However, some existing estimators are shown particular members of the proposed estimator. The bias and mean squared error of the proposed estimator is obtained up to the first order of approximation under the simple random sampling. An empirical study is also carried out to check the superiority of proposed estimator over others.

Keywords: *Sampling, Relative Efficiency, Robust, Estimation, Population Mean.*

1. INTRODUCTION

The simplest estimator of a finite population mean is the sample mean obtained from the simple random sampling without replacement, when there is no auxiliary information available. Sometimes there exists an auxiliary variable X which is positively correlated with the study variable Y. The information available on the auxiliary variable X may be utilized to obtain an efficient estimator of the population mean. The sampling theory describes a wide variety of techniques for using auxiliary information to obtain more efficient estimators. To use the additional information provided by an auxiliary or subsidiary variables enhances the precision of the ratio, product and regression estimators. When correlation between study variable and auxiliary variable is positively (high) then ratio estimator proposed by Cochran (0000) is used. On the other hand, product estimator suggested by Robson (0000) and rediscovered by Murthy (0000) is preferably used when correlation is negatively (high). A lot of work has been done in the area of survey sample for the estimation of finite population mean using information on an auxiliary variable.

The ratio estimator and the regression estimator are the two important estimators available in the literature which are using the auxiliary information. To know more about the ratio and regression estimators and other related results one may be seen from the reference section. When the population parameters of the auxiliary variable X such as population mean, coefficient of variation, kurtosis, skewness and median are known, a number of modified ratio estimators are proposed in the literature, by extending the usual ratio and product type estimators.

To use the additional information provided by an auxiliary or subsidiary variables enhances the precision of the ratio, product and regression estimators. When correlation between study variable and auxiliary variable is positively (high) then ratio estimator proposed by Cochran (1940) is used. On the

https://doi.org/10.62500/icrtsda.1.1.6

other hand. Product estimator suggested by Robson (1957) and rediscovered by Murthy (1964) is preferably used when correlation is negatively (high). A lot of work has been done in the area of survey sample for the estimation of finite population mean using information on an auxiliary variable. Several authors including Sisodia and Dwivedi (1981). Prasad (1989), upadhyaya and Singh (1999), Singh and Tailor (2003), Kadilar and Cingi (2004 & 2006), Sing et al. (2004 & 2009), Koyuncu and Kadilar (2009 & 2010), Yan and Tian (2010), Singh and Solanki (2011 & 2012), Yada and Kadilar (2013), Kumar (2015), Abid et al. (2016a, b & c) have developed various estimators or classes of estimators for improved estimation of population mean using an auxiliary information under different sampling schemes. Further, Subramani and Kumara pandiyan (2013), Subramani and Prabavathy (2014) and Yadav et al. (2014) proposed ratio estimators to estimate population mean using linear combination of population mean and median of an auxiliary variable.

The employment of auxiliary information to estimate the unknown population mean of interest in order to boost the efficiency of estimators in sample surveys is a practice that has been widely accepted. For the estimation of population variance of the research variable when comprehensive data is known on the study and extra variables, a significant amount of work has been done over the course of the previous several years; for references [Zaman and Bulut (2019 & 2020), Zaman (2019), Soni and Pandey (2023)], see the references for more information. This is the case. Methods of estimate such as product, ratio, and regression are all examples that are useful in the field of study. Through the utilization of supplemental data, we are able to acquire estimations of population parameters that are more precise, as cited in References [Bhushan et. al., (2022), Sharam (2017), Ahmad et. al., (2023), Saleem et. al., (2023)]. The utilization of supplementary information in order to improve the precision of estimating methods is a long-standing and widely accepted approach. Numerous researchers made use of well-known population parameters of auxiliary information, such as the coefficient of variation, the mid-range, the coefficient of skewness, the semi-interquartile range, the coefficient of kurtosis, the semi-interquartile average, and the inter decile range of the additional variable, as well as the correlation coefficient between the research and the additional variable, in order to enhance the accuracy of the estimation methods of population mean. In a similar manner, [2019] presented a series of approaches for estimating variation within the ratio-type. In recent times, [Abid et. al., (2019)] has been concentrating on improving the estimation of population variance by utilizing robust measures. There are references [Shahzad et. al.,(2021 & 2022 & 2023 a & 2023b)] that created robust variance estimators that are based on L-moments. With these as a source of inspiration, we define a generalized class of robust type estimation methods for the estimation of population variance of the research variable. These approaches are more efficient than the estimators that are currently in use. In addition to being effective when extreme values are present, the newly developed generalized robust class of estimate methods is also effective when extreme values are not there. This is a noteworthy fact that should be taken into consideration.

Consider a sample of size “n” drawn by simple random sampling without replacement (SRSWOR) from a population of size N with n < N. Let the values of Y and X for the i^{th} unit denote the observations on the study variable and auxiliary variable. Respectively. The notations used in this paper can be described as follows.

Notations

Notations to be used in this study are listed below.

N- Size of the Population

n- Size of the Sample

$f = \frac{n}{N}$ – Sampling fraction

X- Auxiliary variable

$\bar{X}, \bar{Y}$- Population means

x,y- Sample totals

https://doi.org/10.62500/icrtsda.1.1.6

$\bar{x}$, $\bar{y}$- Sample means M =Median of study variable

$\bar{M}$ = Average of sample Medians of Y S_x , S_y- Population standard deviations

M_d =Median of the auxiliary variable

f $MSE(.)$ - Mean squared error of the estimate

$B(.)$- Bias of the Estimator

$\hat{\bar{Y}}_{ri}$ - Existing modified ratio estimator of $\bar{Y}$

$\hat{\bar{Y}}_{rp}$ - Proposed modified ratio estimator of $\bar{Y}$

Also the following formulae have been used in this paper.

The population mean of the study variable and auxiliary variable are denoted by

$\bar{Y} = N^{-1}\sum_{i=1}^{N} y_i$ and $\bar{X} = N^{-1}\sum_{i=1}^{N} x_i$ respectively, where, $\bar{y} = n^{-1}\sum_{i=1}^{N} y_i$ and

$\bar{x} = n^{-1}\sum_{i=1}^{N} x_i$ be the sample mean of the study variable and auxiliary variable respectively,

$S_y^2 = (N-1)^{-1}\sum_{i=1}^{N}(y_i - \bar{Y})^2$ is the population variance of study variable

$S_x^2 = (N-1)^{-1}\sum_{i=1}^{N}(x_i - \bar{X})^2$ is the population variance of auxiliary variable,

$S_{xy} = (N-1)^{-1}\sum_{i=1}^{N}(x_i - \bar{X})(y_i - \bar{Y})$ is the population covariance between y and x,

$C_y^2 = (\bar{Y}^2)^{-1}S_y^2$ is the square of coefficient of variation of y,

$C_x^2 = (\bar{X}^2)^{-1}S_x^2$ is the square of coefficient of variation of x,

$\rho_{xy} = (S_y S_x)^{-1}S_{yx}$ is the correlation coefficient between y and x, $f = \frac{n}{N}$.

2. [EXISTING ESTIMATORS OF POUPULATION MEAN]

It is known that for any population parameter the most appropriate estimator for population mean $\hat{\bar{Y}}_{r0}$ is the sample mean $\bar{y}$ with mean square error as given below. $MSE\left(\hat{\bar{Y}}_{r0}\right) = \frac{1-f}{n}S_y^2$.

But Cochran (1940) used the auxiliary variable to estimate the population mean of the main variable and proposed the traditional ratio estimator as given below.

$$\hat{\bar{Y}}_{r1} = \frac{\bar{y}}{\bar{x}}\bar{x}$$

The bias and mean square error is as follows.

$$Bais\left(\hat{\bar{Y}}_{r1}\right) = \frac{1}{\bar{X}}\frac{1-f}{n}\left(RS_x^2 - S_{xy}\right)$$

$$MSE\left(\hat{\bar{Y}}_{r1}\right) = \frac{1-f}{n}\left(S_y^2 + R^2 S_x^2 - 2RS_{xy}\right)$$

The traditional regression estimator by Watson (1937) using auxiliary variable is given by,

$$\hat{\bar{Y}}_{r2} = \bar{y} + b(\bar{X} - \bar{x}) \;\; Where \;\; b = \frac{S_{xy}}{s_x^2}$$

The variance of above estimator up to the first order approximation is as follows.

https://doi.org/10.62500/icrtsda.1.1.6

$$MSE\left(\hat{\bar{Y}}_{r2}\right) = \frac{1-f}{n}\left(S_y^2\right)(1-\rho^2)$$

Subramani and Kumarapandiyan (2013) suggested the following estimator. It's bias and mean square error also shown here.

$$\hat{\bar{Y}}_{r3} = \bar{y}\left(\frac{M_d+\bar{X}}{M_d+\bar{x}}\right)$$

$$Bais\left(\hat{\bar{Y}}_{r3}\right) = \bar{Y}\frac{1-f}{n}\left(\theta^2 C_x^2 - \theta\rho_{yx}C_xC_y\right)$$

$$MSE\left(\hat{\bar{Y}}_{r3}\right) = \bar{Y}^2\frac{1-f}{n}\left(C_y^2 + \theta^2 C_x^2 - 2\theta\rho_{yx}C_xC_y\right) \text{ Where } \theta = \frac{\bar{X}}{M_d+\bar{X}}$$

However, the use of median was sufficiently deployed by Subramani and Prabavathy (2014). They proposed the following two estimators of population mean based on median of study variable using auxiliary information.

$$\hat{\bar{Y}}_{rs4} = \bar{y}\left(\frac{M_dM+\bar{X}}{M_dm+\bar{X}}\right)$$

$$\hat{\bar{Y}}_{rs5} = \bar{y}\left(\frac{\bar{X}M + M_d}{\bar{X}m + M_d}\right)$$

The bias and mean squared error of these estimators, up to the first order of approximation respectively are as follows.

$$Bais\left(\hat{\bar{Y}}_{rsi}\right) = \bar{Y}\frac{1-f}{n}\left(\theta_j^2 C_m^2 - \theta_j\rho_{yx}C_mC_y\right) \text{ Where I and j = 1, 2}$$

$$MSE\left(\hat{\bar{Y}}_{rsi}\right) = \frac{1-f}{n}\left(S_y^2 + R^2\theta_j^2 V(m) - 2R\theta_j Cov(\bar{y}, m)\right) \text{ where i and j = 1, 2}$$

Where $\theta_1 = \frac{M_dM}{M_dM+\bar{X}}$ and $\theta_2 = \frac{\bar{X}M}{\bar{X}M+M_d}$

Yadav et all. (2014) proposed some new two improved estimators of population mean as,

$$\hat{\bar{Y}}_{rD6} = k_1\bar{y}\left(\frac{M_dM + \bar{X}}{M_dm + \bar{X}}\right)$$

$$\hat{\bar{Y}}_{rD7} = k_2\bar{y}\left(\frac{\bar{X}M + M_d}{\bar{X}m + M_d}\right)$$

The bias and mean squared error of these estimators, up to the first order of approximation respectively are as follows.

$$Bais\left(\hat{\bar{Y}}_{rDi}\right) = \bar{Y}\left[(k_i - 1) + \frac{1-f}{n}\left(\theta_i^2 C_m^2 - \theta_i\rho_{yx}C_mC_y\right)\right]$$

$$MSE\left(\hat{\bar{Y}}_{rDi}\right) = \bar{Y}^2\left(\left((k_i - 1) + k_i^2\frac{1-f}{n}\left[E(e_o^2) + 3\theta_i^2 E(e_1^2) - 4\theta_i E\,(e_o e_1)\right]\right) - 2k_i\frac{1-f}{n}\left[\theta_i^2 E(e_1^2) - \theta_i E(e_o e_1)\right]\right)$$

or $$MSE\left(\hat{\bar{Y}}_{rDi}\right) = \bar{Y}^2\left(1 - \frac{A_i}{B_i}\right) \quad Where\ i\ and\ j = 1, 2$$

https://doi.org/10.62500/icrtsda.1.1.6

Where $k_i = \frac{1+\theta_i^2 E(e_1^2)-\theta_i E(e_o e_1)}{1+E(e_0^2)+3\theta_i^2 E(e_1^2)-4\theta_i E(e_o e_1)}$, $k_i = \frac{1+\frac{1-f}{n}\theta_i^2 C_m^2-\frac{1-f}{n}\theta_i \rho_{yx} C_m C_y}{1+\frac{1-f}{n}C_y^2+3\frac{1-f}{n}\theta_i^2 C_m^2-4\frac{1-f}{n}\theta_i \rho_{yx} C_m C_y}$, $k_i = \frac{A_i}{B_i}$

& $A_i = 1+\frac{1-f}{n}\theta_i^2 C_m^2 - \frac{1-f}{n}\theta_i \rho_{yx} C_m C_y$;

$B_i = 1+\frac{1-f}{n}C_y^2 + 3\frac{1-f}{n}\theta_i^2 C_m^2 - 4\frac{1-f}{n}\theta_i \rho_{yx} C_m C_y$

Irfan et. al., (2017) suggested a class of estimators using median of a study variable and an auxiliary variable given as follows.

$\hat{\bar{Y}}_{rI8} = k_1 \bar{y}\left(\frac{M_d M+ \bar{X}}{M_d\ m+\bar{X}}\right)^{\theta_1}$ where $\theta_1 = \frac{M_d M}{M_d M+ \bar{X}}$

$\hat{\bar{Y}}_{rI9} = k_2 \bar{y}\left(\frac{\bar{X}M+ M_d}{\bar{X}m+M_d}\right)^{\theta_2}$ where $\theta_2 = \frac{\bar{X} M}{\bar{X} M+ M_d}$

$\hat{\bar{Y}}_{rI10} = k_3 \bar{y}\left(\frac{M+ 1}{m+1}\right)^{\theta_3}$ where $\theta_3 = \frac{M}{M+ 1}$

$\hat{\bar{Y}}_{rI11} = k_4 \bar{y}\left(\frac{\bar{X}RM+ M_d}{\bar{X}Rm+M_d}\right)^{\theta_4}$ where $\theta_4 = \frac{\bar{X} RM}{\bar{X} RM+ M_d}$

$\hat{\bar{Y}}_{rI12} = k_5 \bar{y}\left(\frac{M_d M+R \bar{X}}{M_d\ m+R\bar{X}}\right)^{\theta_5}$ where $\theta_5 = \frac{M_d M}{M_d M+ R \bar{X}}$

$\hat{\bar{Y}}_{rI13} = k_6 \bar{y}\left(\frac{M+ R}{m+R}\right)^{\theta_6}$ where $\theta_6 = \frac{M}{M+ R}$

The bias and the mean square error of the estimators proposed by Irfan et. all (2017) are given as follows.

$Bais\left(\hat{\bar{Y}}_{rIi}\right) \cong (k_i - 1) + \frac{1-f}{n}\bar{Y} k_i (0.5(\theta_i^4 + \theta_i^3)C_m^2 - \theta_i^2 \rho_{yx} C_m C_y)$

where i = 1, 2, 3, 4, 5 and 6

and

MSE $(\hat{\bar{Y}}_{rIi}) \cong \bar{Y}^2 [(k_i - 1)^2 + k_i^2 (E(e_o^2) + (2\theta_i^4 + \theta_i^3)E(e_1^2) - 4\theta_i^2 E(e_o e_1)] - k_i \bar{Y}^2 [(\theta_i^4 + \theta_i^3)E(e_1^2) - 2\theta_i^2 E(e_o e_1)]$

Here $k_i = \frac{2+[(\theta_i^4 + \theta_i^3)E(e_1^2)-2\theta_i^2 E(e_o e_1)]}{2+2[(E(e_o^2)+(2\theta_i^4 + \theta_i^3)E(e_1^2)-4\theta_i^2 E(e_o e_1)]}$ $or k_i$

$= \frac{2+\frac{1-f}{n}[(\theta_i^4 + \theta_i^3)\, C_m^2 - 2\theta_i^2 \rho_{yx} C_m C_y]}{2+2\frac{1-f}{n}[\, C_y^2 + (2\theta_i^4 + \theta_i^3)C_m^2 - 4\theta_i^2 \rho_{yx} C_m C_y]}$ $or\ k_i = \frac{C_{1i}}{C_{2i}}$

Where $C_{1i} = 2 + \frac{1-f}{n}[(\theta_i^4 + \theta_i^3)\, C_m^2 - 2\theta_i^2 \rho_{yx} C_m C_y]$

$C_{2i} = 2 + 2\frac{1-f}{n}[\, C_y^2 + (2\theta_i^4 + \theta_i^3)C_m^2 - 4\theta_i^2 \rho_{yx} C_m C_y]$

$MSE_{min}\ (\hat{\bar{Y}}_{rIi}) = \bar{Y}^2 [1 - \frac{C_{1i}^2}{2C_{2i}}]$

https://doi.org/10.62500/icrtsda.1.1.6

3. [PROPOSED ESTIMATORS OF POUPULATION MEAN]

Motivated by the existing estimators we have made a fresh attempt to extend the estimator's efficiency we proposed the following estimator for the estimation of population mean.

$$\hat{\bar{Y}}_{rp} = k\bar{y}\left(\frac{M_d M+\bar{X}}{M_d m+\bar{X}}\right) + (1-k)\bar{y}\left(\frac{M_d m+\bar{X}}{M_d M+\bar{X}}\right) \quad \ldots \text{(i)}$$

To study the large sample properties estimators $\hat{\bar{Y}}_{rp}$ let us define the

$e_o = \frac{\bar{y}-\bar{Y}}{\bar{Y}}$ and $e_1 = \frac{m-M}{M}$ such that $E(e_o) = 0$, $E(e_1) = 0$,

$E(e_o^2) = \frac{1-f}{n}\frac{V(\bar{y})}{\bar{Y}^2}$, $E(e_1^2) = \frac{1-f}{n}\frac{V(m)}{M^2}$ and $E(e_o e_1) = \frac{1-f}{n}\frac{Cov(\bar{y},m)}{\bar{Y}M}$

Now, (i) implies that $\hat{\bar{Y}}_{rp} = \mathrm{k}(\bar{Y} + \bar{Y}e_o)(\frac{1}{\theta e_1+1}) + (1-\mathrm{k})(\bar{Y} + \bar{Y}e_o)(\theta e_1 + 1)$

$\hat{\bar{Y}}_{rp} = K(\bar{Y} + \bar{Y}e_o)(1 - e_1\theta + e_1^2\theta^2) + (1-K)(\bar{Y} + \bar{Y}e_o)(\theta e_1 + 1)$

$\hat{\bar{Y}}_{rp} = \bar{Y} + \theta\bar{Y}e_{1+}\bar{Y}e_o + \bar{Y}\theta e_o e_1 + K(\bar{Y} - \theta\bar{Y}e_1 + \theta^2\bar{Y}e_1^2 + \bar{Y}e_o - \bar{Y}\theta e_o e_1 - \bar{Y} - \theta\bar{Y}e_1 - \bar{Y}e_o - \bar{Y}\theta e_o e_1)$

Hence, $(\hat{\bar{Y}}_{rp} - \bar{Y}) = \bar{Y}[e_1(\theta - 2k\theta) + e_o e_1(\theta - 2k\theta) + e_o + Ke_1^2\theta^2]$

The bias for the proposed estimator is as follows.

$E(\hat{\bar{Y}}_{rp} - \bar{Y}) = \bar{Y}E[e_1(\theta - 2k\theta) + e_o e_1(\theta - 2k\theta) + e_o + Ke_1^2\theta^2]$

$E(\hat{\bar{Y}}_{rp} - \bar{Y}) = \bar{Y}[E(e_1)(\theta - 2k\theta) + E(e_o e_1)(\theta - 2k\theta) + E(e_o) + KE(e_1^2)\theta^2]$

$Bais\left(\hat{\bar{Y}}_{rp}\right) = \bar{Y}\,[E(e_o e_1)(\theta - 2k\theta) + (e_1^2)k\theta^2]$

$Bais\left(\hat{\bar{Y}}_{rp}\right) = \bar{Y}\,[\frac{1-f}{n}\rho_{yx}C_m C_y(\theta - 2k\theta) + \frac{1-f}{n}C_m^2 k\theta^2]$

$Bais\left(\hat{\bar{Y}}_{rp}\right) = \bar{Y}\,\frac{1-f}{n}\,[\rho_{yx}C_m C_y(\theta - 2k\theta) + C_m^2 k\theta^2]$

The mean squared error for the proposed estimator is as follows.

$MSE\left(\hat{\bar{Y}}_{rp}\right) = \bar{Y}^2[E(e_1^2)(\theta - 2k\theta)^2 + E(e_o^2) + 2E(e_o e_1)(\theta - 2k\theta)]$

$MSE\left(\hat{\bar{Y}}_{rp}\right) = \bar{Y}^2\frac{1-f}{n}[C_m^2(\theta - 2k\theta)^2 + C_y^2 + 2\rho_{yx}C_m C_y(\theta - 2k\theta)]$

Where $\boldsymbol{k = \frac{\theta E(e_1^2) + E(e_o e_1)}{2\theta E(e_1^2)}}$

4. EFFICIENCY COMPARISON

The efficiency of proposed estimators over the existing estimators has been derived algebraically as given below.

In this section, the conditions for which the proposed ratio type estimators based on the known value of the median will have minimum mean square error as compared to usual ratio estimator, the regression estimator, Subramani and Kumarapandiyan (2013) estimator, Subramani and Prabavathy (2014)

https://doi.org/10.62500/icrtsda.1.1.6

estimators and Yadav et al. (2014) estimators for estimating the finite population mean have been derived algebraically.

The condition for which the proposed estimator performs better than the existing estimator $\hat{\bar{Y}}_{r0}$ is derived as under.

$$MSE\left(\hat{\bar{Y}}_{r0}\right) - MSE(\hat{\bar{Y}}_{rp}) > 0$$

If $\frac{1-f}{n}S_y^2 - \bar{Y}^2\frac{1-f}{n}[C_m^2(\theta - 2k\theta)^2 + C_y^2 + 2\rho_{yx}C_mC_y(\theta - 2k\theta)] > 0$

The condition for which the proposed estimator performs better than the existing estimator $\hat{\bar{Y}}_{r0}$ is derived as under.

$$MSE\left(\hat{\bar{Y}}_{r1}\right) - MSE(\hat{\bar{Y}}_{rp}) > 0$$

If $\frac{1-f}{n}\left(S_y^2 + R^2S_x^2 - 2RS_{xy}\right) - \bar{Y}^2\frac{1-f}{n}[C_m^2(\theta - 2k\theta)^2 + C_y^2 + 2\rho_{yx}C_mC_y(\theta - 2k\theta)] > 0$

The condition for which the proposed estimator performs better than the existing estimator $\hat{\bar{Y}}_{r0}$ is derived as under.

$$MSE\left(\hat{\bar{Y}}_{r2}\right) - MSE(\hat{\bar{Y}}_{rp}) > 0$$

If $\frac{1-f}{n}\left(S_y^2\right)(1-\rho^2) - \bar{Y}^2\frac{1-f}{n}[C_m^2(\theta - 2k\theta)^2 + C_y^2 + 2\rho_{yx}C_mC_y(\theta - 2k\theta)] > 0$

The condition for which the proposed estimator performs better than the existing estimator $\hat{\bar{Y}}_{r0}$ is derived as under.

$$MSE\left(\hat{\bar{Y}}_{r3}\right) - MSE(\hat{\bar{Y}}_{rp}) > 0$$

If $\bar{Y}^2\frac{1-f}{n}\left(C_y^2 + \theta^2C_x^2 - 2\theta\rho_{yx}C_xC_y\right) - \bar{Y}^2\frac{1-f}{n}[C_m^2(\theta - 2k\theta)^2 + C_y^2 + 2\rho_{yx}C_mC_y(\theta - 2k\theta)] > 0$

The condition for which the proposed estimator performs better than the existing estimator $\hat{\bar{Y}}_{r0}$ is derived as under.

$$MSE\left(\hat{\bar{Y}}_{rsi}\right) - MSE\left(\hat{\bar{Y}}_{rp}\right) > 0 \text{ if }, i = 1, 2$$

$$\frac{1-f}{n}\left(S_y^2 + R^2\theta_j^2V(m) - 2R\theta_jCov(\bar{y}, m)\right) - \bar{Y}^2\frac{1-f}{n}[C_m^2(\theta - 2k\theta)^2 + C_y^2 + 2\rho_{yx}C_mC_y(\theta - 2k\theta)] > 0 \quad , i = 1, 2$$

The condition for which the proposed estimator performs better than the existing estimator $\hat{\bar{Y}}_{r0}$ is derived as under.

$$MSE\left(\hat{\bar{Y}}_{rDi}\right) - MSE\left(\hat{\bar{Y}}_{rp}\right) > 0 \text{ if }, i = 1, 2$$

$$\bar{Y}^2\left(1 - \frac{A_i}{B_i}\right) - \bar{Y}^2\frac{1-f}{n}[C_m^2(\theta - 2k\theta)^2 + C_y^2 + 2\rho_{yx}C_mC_y(\theta - 2k\theta)] > 0$$

The condition for which the proposed estimator performs better than the existing estimator $\hat{\bar{Y}}_{rIi}$ is derived as under.

https://doi.org/10.62500/icrtsda.1.1.6

$MSE_{min}(\hat{\bar{Y}}_{rIi}) - MSE(\hat{\bar{Y}}_{rp}) > 0$ if , $i = 1, 2, 3, 4, 5,$

$\bar{Y}^2[1 - \frac{C_{1i}^2}{2C_{2i}}] - \bar{Y}^2 \frac{1-f}{n}[C_m^2(\theta - 2k\theta)^2 + C_y^2 + 2\rho_{yx}C_mC_y(\theta - 2k\theta)] > 0$

5. EMPIRICAL ANALYSIS

In this section, the performance of the proposed ratio type estimators and the existing ratio estimators is evaluated by using two natural populations. The population 1 and 2 are taken from Mukhopadhyay (1988).The characteristics of the two populations are given below in Tables 1 and 2, respectively.

Table 1: Population -1 with sample size = 3

N=20	n=3	$\bar{Y}$=41.50	$\bar{X}$=441.95
M_d= 407.50	M=40.50	θ=0.9739	Cov($\bar{y}, m$)=21.0918
V(m)=26.1307	V($\bar{x}$)=2894.3089	Cov($\bar{y}, \bar{x}$)=182.7425	V($\bar{y}$)=27.1254
ρ =0.6522	C_x^2 =0.014818	C_y^2=0.01575	C_m^2 =0.015931

Table 2: Population – 2 with sample size = 5

N=20	n=5	$\bar{Y}$=41.50	$\bar{X}$=441.95
M_d =407.50	M=40.50	θ=0.9739	Cov($\bar{y}, m$)=9.0665
V(m)=10.8348	V($\bar{x}$)=1532.2812	Cov($\bar{y}, \bar{x}$)=96.7461	V($\bar{y}$)=14.3605
ρ =0.6522	C_x^2 =0.0078	C_y^2=0.0083	C_m^2 =0.0066

Table 3: The mean square errors for existing and proposed estimators

Estimator	**Population – 1**	**Population – 2**
	$\boldsymbol{n = 3}$	$\boldsymbol{n = 5}$
$\hat{\bar{Y}}_{r0}$	7.6855	2.1540
$\hat{\bar{Y}}_{r1}$	5.1923	1.4553
$\hat{\bar{Y}}_{r2}$	4.4164	1.2378
$\hat{\bar{Y}}_{r3}$	4.5837	1.2920
$\hat{\bar{Y}}_{rs4}$	3.1314	1.0583
$\hat{\bar{Y}}_{rs5}$	3.1426	1.0603
$\hat{\bar{Y}}_{rD6}$	3.1195	1.0573
$\hat{\bar{Y}}_{rD7}$	3.1304	1.0593
$\hat{\bar{Y}}_{rI8}$	3.0520	1.0448
$\hat{\bar{Y}}_{rI9}$	3.0707	1.0482
$\hat{\bar{Y}}_{rI10}$	3.0616	1.0465
$\hat{\bar{Y}}_{rI11}$	3.0734	1.0487
$\hat{\bar{Y}}_{rI12}$	3.0490	1.0442
$\hat{\bar{Y}}_{rI13}$	3.0588	1.0460
$\hat{\bar{Y}}_{rp}$	2.8619	1.0161

In table 3, the values of MSEs of the existing and proposed estimators are computed by using the MSE formulas which are given in section 1 and 2, respectively. From an analysis of table 3, several interesting observations can be made.

https://doi.org/10.62500/icrtsda.1.1.6

Table 4: The percentage relative efficiency for existing and proposed estimators for sample size = 3 and 5

Estimator	Population – 1	Population - 2
	$n = 3$	$n = 5$
$\hat{\bar{Y}}_{r0}$	268.55	211.99
$\hat{\bar{Y}}_{r1}$	181.43	143.22
$\hat{\bar{Y}}_{r2}$	154.32	121.82
$\hat{\bar{Y}}_{r3}$	160.16	127.15
$\hat{\bar{Y}}_{rs4}$	109.42	104.15
$\hat{\bar{Y}}_{rs5}$	109.81	104.35
$\hat{\bar{Y}}_{rD6}$	109.00	104.05
$\hat{\bar{Y}}_{rD7}$	109.38	104.25
$\hat{\bar{Y}}_{rI8}$	106.64	102.82
$\hat{\bar{Y}}_{rI9}$	107.30	103.16
$\hat{\bar{Y}}_{rI10}$	106.98	102.99
$\hat{\bar{Y}}_{rI11}$	107.39	103.21
$\hat{\bar{Y}}_{rI12}$	106.54	102.77
$\hat{\bar{Y}}_{rI13}$	106.88	102.94

To show the dominance of the proposed ratio type estimators over the existing estimators used in this study, we have also found the percent relative efficiencies (PREs) for population 1 and 2. The percentage relative efficiencies (PREs) of the proposed ratio type estimators (P) with respect to the existing estimators (e) is computed and are given in Tables 4 and 5.

From tables 4 and 5, it can be observed that PREs of the proposed ratio type estimators with regards to the existing estimators consider in this study are much higher, which shows that they are more efficient for population 1 and 2.

To get more insight in this study, we have also find the relative root mean square error (PRMSE) which is a very common measure to compare the precision of the estimators Silva and Skinner (1995), Yan and Tian (2010), Munoz et al. (2014) and Alvarez et al. The RRMSEs of the existing ratio estimators and the proposed ratio type estimators are calculated by using the following formula

6. CONCLUSION

In sample survey, the availability of auxiliary information enhances the efficiency of the estimators. In this study, we have proposed several ratio type estimators using known value of population median by using the information on the study variable and the auxiliary variable. It is observed that the mean squared errors of the suggested estimators based on the knowledge of the median are smaller than those for the existing ratio estimators consider in this study for the two known populations considered for the numerical study. Also, it is observed that the proposed estimators are more efficient than the existing estimators in terms of percentage relative efficiencies and relative root

https://doi.org/10.62500/icrtsda.1.1.6

mean square error. Hence, we strongly recommend the use of our proposed ratio type estimators over the existing ratio estimators consider in this study for the practical consideration. The theoretical developments of the research paper and the results shown in table-4 it is clear that the proposed estimator of population mean have the minimum mean squared as compared to the existing estimators. Therefore, the proposed estimator should be preferred for the estimation of population mean.

REFERENCES

1. Cochran, W. G. (1940). The estimation of the yields of cereal experiments by sampling for the ratio gain to total produce. *Journal of Agriculture Science*, 30, 262-275.
2. Subramani, J. and Kumarapandiyan, G. (2013). New modified ratio estimator for estimation of population mean when median of the auxiliary variable is known, *Pakistan Journal of Statistics and Operational Research* 9(2), 137-145.
3. Subramani, J. and Prabavathy, G. (2014). Median based modified ratio estimators with linear combinations of population mean and median of an auxiliary variable. *Journal of Reliability and Statistical Studies*, 7(1), 1-10.
4. Watson, D. J. (1937). The estimation of leaf area in field crops. *Journal of Agriculture Science*, 27, 474-483.
5. Yadav, S. K., Mishra, S. S. & Shukla, A. K. (2014). Improved ratio estimators for population mean based on median using linear combination of population mean and median of an auxiliary variable. *American Journal of Operational Research*, 4(2), 21-27.
6. Murthy, M. N. (1964). Product method of estimation, Sankhya 26, 294-307.
7. Robson, D. S. (1957). Application of multivariate polykays to the theory of unbiased ratio type estimation, *Journal of American Statistical Association* 52, 411-422.
8. Cochran, W. G. (1940). The estimation of the yields of cereal experiments by sampling for the ratio gain to total produce, *Journal of Agriculture Science* 30, 262-275.
9. Sisodia, B. V. S. and Dwivedi, V. K. (1981). A modified ratio estimator using coefficient of variation of auxiliary variable, *Journal of the Indian Society of Agriculture Statistics* 33(1), 13-18.
10. Prassad, B. (1989). Some improved ratio type estimators of population mean and ratio in finite population sample surveys, *Communications in Statistics: Theory and Methods* 18, 379-392.
11. Upadhyaya, L. N. and Singh, H. P. (1999). Use of transformed auxiliary variable in estimating the finite population mean, Biometrical Journal 41(5), 627-636.
12. Singh, H. P. and Tailor, R. (2003). Use of known correlation coefficient in estimating the finite population means, Statistics in Transition 6(4), 555-560.
13. Kadilar, C., and Cingi, H. (2004). Ratio estimators in simple random sampling, *Applied Mathematics and Computation* 151, 893-902.
14. Kadilar, C., and Cingi, H. (2006). An improvement in estimating the population mean by using the correlation coefficient, *Hacettepe Journal of Mathematics and Statistics* 35(1), 103-109.
15. Singh, H. P., Tailor, R., Tailor, R. and Kakran, M. S (2004). An improved estimator of population mean using power transformation, *Journal of the Indian Society of Agriculture Statistics* 58(2), 223-230.
16. Singh, R., Kumar, M., Chaudhary, M. K., and Kadilar, C (2009). Improved exponential estimator in stratified random sampling, *Pakistan Journal of Statistics and Operational Research* 5(2), 67-82.
17. Koyuncu, N., and Kadilar, C (2009). Efficient estimators for the population mean, *Hacettepe Journal of Mathematics and Statistics* 38 (2), 217-225.
18. Koyuncu, N., and Kadilar, C. (2010). On improvement in estimating population mean in stratified random sampling, *Journal of Applied Statistics* 37 (6), 999-1013.
19. Singh, H. P., and Solanki, R. S. (2011). Generalized ratio and product methods of estimation in survey sampling, *Pakistan Journal of Statistics and Operational Research* 7 (2), 245-264.
20. Singh, H. P., and Solanki, R. S. (2012). An efficient class of estimators for the population mean using auxiliary information in systematic sampling, *Journal of Statistics Theory Practice* 6, 274-285.
21. Yadav, S. K., and Kadilar, C. (2013). Efficient family of exponential estimators for the population mean, *Hacettepe Journal of Mathematics and Statistics* 42(6), 671-677.

https://doi.org/10.62500/icrtsda.1.1.6

22. Kumar, S. (2015). An estimator of the median estimation of study variable using median of auxiliary variable, *Sri Lankan Journal of Applied Statistics* 16 (2), 107-115.
23. Abid, M., Abbas, N., Nazir, H. Z. and Lin, Z. (2016a). Enhancing the mean ratio estimators for estimating population mean using non-conventional location parameters, *Revista Colombiana de Estadistica* 39 (1), 63-79.
24. Abid, M., Abbas, N. and Riaz, M. (2016b). Improved modified ratio estimators of population mean based on deciles, *Chiang Mai Journal of Science* 43(1), 1311-1323.
25. Abid, M., Abbas, N., Sherwani, R. A. K. and Nazir, H. Z. (2016c). Improved ratio estimators for the population mean using non-conventional measures of dispersion, *Pakistan Journal of Statistics and Operation Research* 12(2), 353-367.
26. Subramani, J. and Kumarapandiyan, G. (2013). New modified ratio estimator for estimation of population mean when median of the auxiliary variable is known, *Pakistan Journal of Statistics and Operational Research* 9(2), 137-145.
27. Subramani, J. and Prabavathy, G. (2014). Median based modified ratio estimators with linear combinations of population mean and median of an auxiliary variable, *Journal of Reliability and Statistical Studies* 7(1), 1-10.
28. Yadav, S. K., Mishra, S. S. and Shukla, A. K. (2014). Improved ratio estimators for population mean based on median using linear combination of population mean and median of an auxiliary variable, *American Journal of Operational Research* 4(2), 21-27.
29. Mukhopadhyay, P. (1988). Theory and methods of survey sampling, PHI Learning, 2nd edition, New Delhi.
30. Zaman, T., & Bulut, H. (2019). Modified ratio estimators using robust regression methods. *Communications in Statistics - Theory and Methods*, 48(8), 2039–2048.
31. Zaman, T., & Bulut, H. (2020). Modified regression estimators using robust regression methods and covariance matrices in stratified random sampling. Communications in Statistics - *Theory and Methods*, 49(14), 3407–3420.
32. Zaman, T. (2019). Improvement of modified ratio estimators using robust regression methods. *Applied Mathematics and Computation*, 348, 627–631.
33. Soni, S. S., & Pandey, H. (2023). Generalized estimator of population variance utilizing auxiliary information in simple random sampling scheme. *Journal of Probability and Statistical Science*, 21(2).
34. Bhushan, S., Kumar, A., & Kumar, S. (2022). Efficient classes of estimators for population variance using attribute. *International Journal of Mathematics and Operations Research*, 22(1), 74–92.
35. Sharma, A. K. (2017). An effective imputation method to minimize the effect of random non-response in estimation of population variance on successive occasions. *Kuwait Journal of Science*, 44(4).
36. Ahmad, S., Al Mutairi, A., Nassr, S. G., Alsuhabi, H., Kamal, M., & Rehman, M. U. (2023). A new approach for estimating variance of a population employing information obtained from a stratified random sampling. *Heliyon*, 9(11), e21477.
37. Kumar, S., & Choudhary, M. (2023). An improved estimator of finite population variance using two auxiliary variable SRS. *Revista Colombiana de Estadística*, 46(1), 81–91.
38. Saleem, A., Sanaullah, A., Al-Essa, L. A., Bashir, S., & Al Mutairi, A. (2023). Efficient estimation of population variance of a sensitive variable using a new scrambling response model. *Scientific Reports*, 13(1), 19913.
39. Hanif, M., & Shahzad, U. (2019). Estimation of population variance using kernel matrix. *Journal of Statistical Management Systems*, 22(3), 563–586.
40. Abid, M., Ahmed, S., Tahir, M., Nazir, H. Z., & Riaz, M. (2019). Improved ratio estimators of variance based on robust measures. *Scientia Iranica*, 26(4), 2484–2494.
41. Shahzad, U., Ahmad, I., Almanjahie, I., Al-Noor, N. H., & Hanif, M. (2021). A new class of L-Moments based calibration variance estimators. *Computational Materials and Continua (CMC)*, 66(3), 3013–3028.
42. Shahzad, U., Ahmad, I., Almanjahie, I. M., Hanif, M., & Al-Noor, N. H. (2023). L-Moments and calibration-based variance estimators under double stratified random sampling scheme: application of Covid-19 pandemic. *Scientia Iranica*, 30(2), 814–821.

https://doi.org/10.62500/icrtsda.1.1.6

43. Shahzad, U., Ahmad, I., Almanjahie, I. M., Al-Noor, N. H., & Hanif, M. (2023). A novel family of variance estimators based on L-moments and calibration approach under stratified random sampling. *Communications in Statistics - Simulation and Computation*, 52(8), 3782–3795.
44. Shahzad, U., Ahmad, I., Almanjahie, I. M., Koyuncu, N., & Hanif, M. (2022). Variance estimation based on L-moments and auxiliary information. *Mathematical Population Studies*, 29(1), 31–46

https://doi.org/10.62500/icrtsda.1.1.7

Proc. 1st International Conference on Recent Trends in Statistics and Data Analytics
Air University Islamabad, Pakistan – May 9, 2024, Vol. 1, pp. 55-60

FLEXION OF SPINE IN PREGNANCY WHILE CARRYING LOADS

Farwa suman and Jamila Akhtar

Abstract

This paper presents the results of an experiment to measure the angular range of the lumbar re gion during pregnancy. We use a goniometer with angle sensor and complete this using Capst one PASCO software. These data were analyzed to determine the maximum flexion during pr egnancy and the amount of flexion that harms pregnant women, increasing the risk of premat ure birth. Lower back pain is caused by the size of the uterus and the relaxed pelvis, making it easier for the baby to pass through the birth canal. Sometimes this can be uncomfortable and scary.

Keywords— goniometer, capstone, preterm birth

Introduction

Low back pain affects most women during pregnancy (LBP). As the weight of the fetus incre ases, the pain may become itchy and painful. Back stress at different angles (LSA: lumbosacr al angle) can be measured to measure the force applied to the spine (Fres) when lifting differe nt weights.According to previous research, a pregnant woman's body undergoes many changes as her fetus grows. Changes in chest and a waist curvature, pain in the waist and pelvic area, changes in balance and gait patterns are possible. Previous research has shown that pregnant women's center of gravity shifts to the abdominal area, resulting in increased lumbar lordosis. The forward shift of the pregnant woman's center of gravity affects balance and increases the pace and speed of postural sway. Additionally, 27% of pregnant women are at risk of falling. 40% Of losses during pregnancy can be caused by emergencies such as head trauma, broken bones, or miscarriage. Since the physical and functional changes that occur during pregnancy can lead to psychological problems, pregnant women need to be properly educated on pain management and coping skills.

Since the beginning of the twentieth century, modern medical research has been trying to discover the different diseases that this treatment represents. Changes in spinal cord and motor function have been associated with pregnancy, but more research is needed. One of the most common problems during pregnancy is butt discomfort, which occurs in 50-70% of all cases. It is more common in the third trimester, when the most important biomechanical and morphological changes occur. The increase in uterine size and fetal weight at the beginning of the second trimester changes the abdominal morphology, causing the abdominal size to increase by 30%. The growth of the stomach is associated with low statics and changes in the spine, which will contribute to the change of the center of gravity to maintain the balance of the body. Only in the third trimester, pregnant women have a greater lumbar curvature than non-pregnant women. In the third trimester, walking speed and rhythm decrease significantly compared to the second trimester. Pregnant women's rate decreased in the second and third trimesters compared to non-pregnant women. Balance ability improved significantly in the third trimester compared to the second trimester. Compared to pregnant women, the probability of equality for pregnant women decreases only in the unstable region.

Back pain is a common pain during pregnancy. Pregnant women often experience low back pain (LBP). According to research, approximately half of pregnant women in the world complain of back pain. LBP in ground form can be disruptive and disruptive. Most hospital births are due to LBP Artal. Low back pain (LBP) is the first sign of pregnancy. Carrying a heavy fetus can cause lower back pain. Lifting anything heavy during pregnancy can be very difficult. Bending and lifting objects can cause back pain in women. Pregnant women suffer

https://doi.org/10.62500/icrtsda.1.1.7

from back pain due to body movements. When the angle changes during bending, the center of gravity (Cg) also changes. By measuring the back tension of different bending angles (lumbosacral angle LSA). Muscles (Fres) work on the spine due to various loads that can be learned. Carrying all heavy objects puts pressure on the spine and this can be reduced by carrying heavy objects with good posture. Biomechanics offers a way to manage back pain. Biomechanical rehabilitation is becoming increasingly important. The following pains only subside when treatment or therapy is used, as indicated in this study.

Methodology

Block Diagram

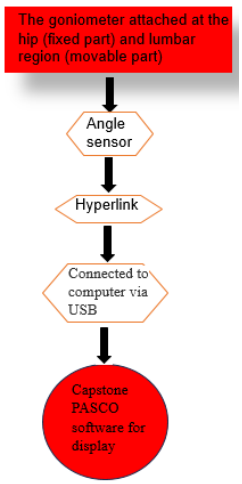

Figure 1: block diagram of methodology

Calculations

A woman who was of average weight prior to becoming pregnant should gain 25 to 35 pounds (11.39kg 15.87kg) after giving birth. In general, you should gain 2 to 4 pounds during your first three months of pregnancy and 1 pound every week for the duration of your pregnancy. If you are having twins, your weight increase should range between 35 and 45 pounds during your pregnancy. After the regular weight growth of the first three months, this would be an average of 12 pounds each week.

- FIRST THREE MONTHS: 3 POUNDS (1.36kg)
- REST OF THE PREGNANCY: 1 POUNDS

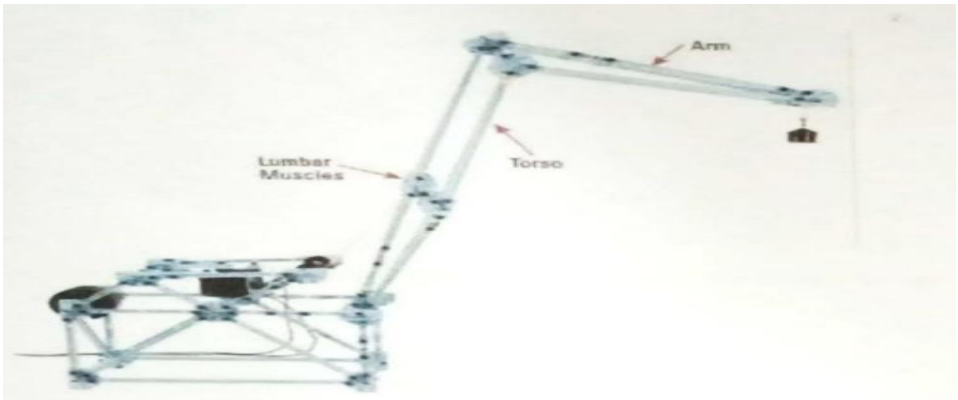

(0.45kg) a week OR 1.8kg per month

The weights accumulated are classified as the weight gained during the three trimesters of pregnancy. We assumed three weights for our model: 100g, 200g, and 500g.

https://doi.org/10.62500/icrtsda.1.1.7

Some studies have found that women who work physically demanding jobs, such as heavy manual lifting, are more likely to have a premature birth. Another study revealed a link between regular heavy object lifting and obstetric complications in women who did not work outside the home. *Infrequent lifting (less than once every 5 minutes):*

- Up to 20 weeks of pregnancy: 36 lbs (16.3 kg)
- After 20 weeks of pregnancy: 26 lbs (11.7kg)

So the weight we approximated as the load being lifted is made up of two different weights 100g and 200g.

Experimental Design

The aim of the experiment is to reveal the relationship between weight and heart rate, as well as the relationship between angle and back, for normal people and pregnant women, and compare the two. We hung weights of 100 g, 200 g and 500 g respectively on the lumbar region of the model's spine to represent the 14th, 24th and 32nd weeks of pregnancy. The portable product has two different weights (100 gr and 200 gr). When pregnant woman's spine is curved, we need to determine the angle at which she can bear weight. We will evaluate the effect of the weight given to the abdominal area on the curvature of the spine, with the back pivoting, and we will use the angle sensors on the field cord for this.

Hardware Setup

The PASCO human rescue model is used to create a human rescue model. The human back model consists of three parts: base, torso and free arm. Use tight braces to simulate back muscles. A mobile phone was used to measure the tension of the rope while doing the fres back muscles. The testing was done using only two load cells (both on one side), but care must be taken to ensure the spine is neutral and balanced on one side. Therefore, the measured force is twice the actual force. When the sample is bent and pushed by some load, the entire force is sent to the back and the force meter measures the force. The measurements were taken at different stages of pregnancy (the difference between the uterus and the uterus) and at different times. Goniometers can be connected to sensors to measure angle changes during various movements. The protractor fixed the scale of the hip and the scale of movement of the hip. Always use the same protractor to reduce the possibility of measurement errors. Correct position and stabilize the spine. Position the goniometer relative to the surface. Use accurate readings from the device. Use correct measurements. By adding different weights, we can observe the stress that occurs during buckling.

Figure 2: PASCO human back model with load cell attached.

Results

Readings

Readings were recorded by changing the fetal weight with two different weights lifted and the mean values were taken for the analysis

Angle of Bending with Fetal Load=100g	The resultant force on the Back muscle	
	100g Lifted	200g Lifted

https://doi.org/10.62500/icrtsda.1.1.7

	Mean	Mean
5º	4.45	.40
10º	7.55	8.73
15º	8.90	13.35
20º	10.18	15.66
30º	14.83	18.02
40º	19.06	24.74

Table 1

FRES and Load lifted at different LSA at Fetal Load-100g (14 weeks). As the weight increases, so does the force, and the closer the angle becomes to 0 degrees with the same weight at different angles.

Angle of Bending with Fetal Load=200g	The resultant force on the Back muscle	
	100g Lifted	200g Lifted
	Mean	Mean
5º	6.01	.40
10º	8.33	20.41
15º	9	9.98
20º	12.72	15
30º	15.99	18.91
40º	21.33	26.44

Table 2

FRES and Load lifted at different LSA at Fetal Load-200g (24 weeks). With the same weight at different angles, the force increases as the weight increases and the angle becomes closer to 0 degrees.

Angle of Bending with Fetal Load=500g	The resultant force on the Back muscle	
	100g Lifted	200g Lifted
	Mean	Mean
5º	5.64	7.50
10º	4.14	10.71
15º	10.00	15.80
20º	14.80	17.44
30º	19.21	24.22
40º	24.40	34.16

Table 3

FRES and Load lifted at different LSA at Fetal Load-500g (32 weeks). We can observe that the force increases as the weight increases, and the closer the angle becomes to 0 degrees with the same weight at different angles.

Graphs

Graphs were plotted for different weights using Microsoft Excel. On X-AXIS we plotted the values of the angle and on Y-AXIS we plotted the 'mean' values for the two lifted weights i.e. 100g and 200g.

https://doi.org/10.62500/icrtsda.1.1.7

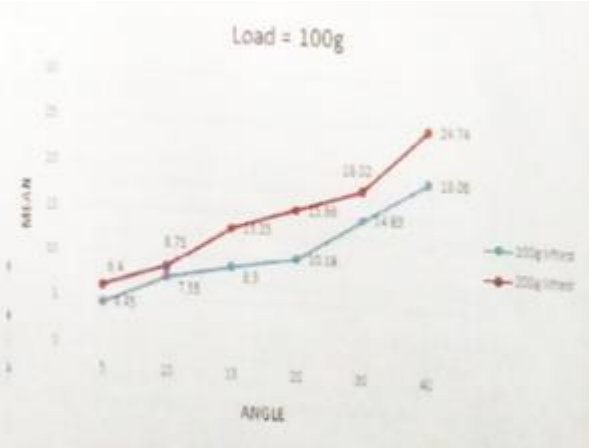

Figure 3: Load and angle comparison at Fetal Load of 100g.

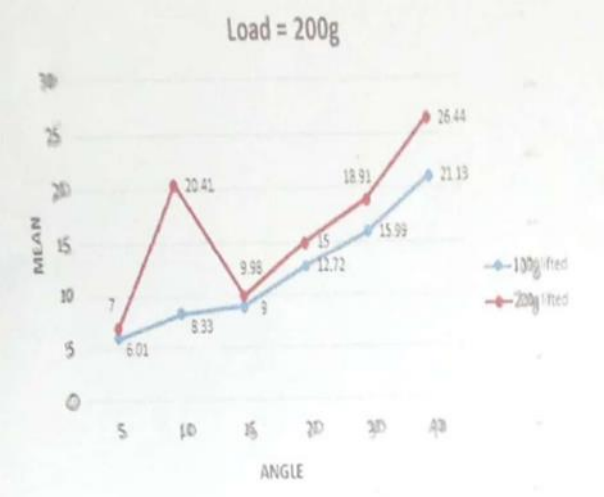

Figure 4: Load and angle comparison at Fetal Load of 200g

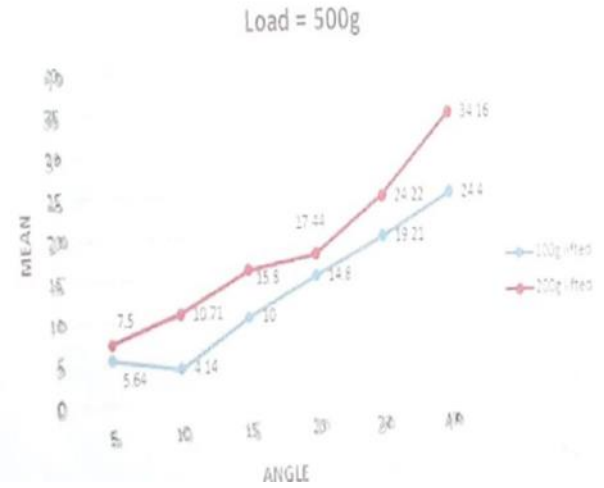

Figure 4: Load and angle comparison at Fetal Load of 500g.

Discussion

From the graphs we can observe that as the fetal load is increasing the Fres acting on the back muscles is also increasing and more force is required for lifting weight. When there is fetus load, it takes greater force to lift the weight.

https://doi.org/10.62500/icrtsda.1.1.7

Conclusion

Based on our understanding of spine work, by correcting for weight and angle we can calculate that weight is proportional to force. As the weight increases, the force increases and the angle approach 0 degrees for the same weight. As internal and external stress increases, muscle tension increases in every aspect. When the fetus is heavy, it needs more strength to move heavy objects. From mid-to-front flexion, 40% is lumbar flexion (occurring in the first 25% of flexion) and 60% is hip flexion (occurring in the last 25% of flexion). During pregnancy, the center of gravity shifts forward, causing some balance problems. Strength changes such as shortened hip flexors, lower back muscles, and pecs may also be seen. The entire abdomen, neck, and back are lengthened. This can cause further weakness.

COMPLICATIONS RELAED TO LUMBER SPINE

Being overweight or obese can cause symptoms associated with osteoporosis, osteoarthritis, rheumatoid arthritis, a degenerative disc disease, spinal stenosis, and spondylolisthesis. The spine is designed to support the weight of the body and distribute the load during rest and play.

Obesity, particularly, is associated with lumbar disc degeneration leading to low back pain, sciatica, and lumbar spinal stenosis. The cause of disc degeneration is unknown, but it is the result of a combination of many factors. Both static compression loading and increased stress from certain practices can affect disc integrity, causing mechanical compression or chemical damage to the disc brain. Additionally, the spine's inflammatory response to loading may increase the risk of back pain in obese individuals. In obese individuals, a longer recovery period is required to regain normal height after loading. Recent research suggests that there is a genetic component to disc degeneration in obese people. Collagen IX (Trp3 allele) polymorphisms appear to be associated with persistent obesity in the formation of posterior disc bulging, reduced disc height, and dark nucleus pulposus. Effects of the inflammatory process involved in the development of disc degeneration.

Acknowledgment (HEADING 5)

We would like to thank Project Supervisor Jamila Akhtar Department of Biomedical Engineering, Air University Islamabad, Pakistan.

References

1. https://www.webmd.com/baby/guide/healt hy-weight-gaini
2. https://www.ncbi.nlm.nih.gov/pmc/articles/ PMC4305582/
3. https @pubmed.ncbi.nlm.nih gov/33467386
4. https//www.babycenter.com/pregnancy/yo-life/is-in-true-that-pregnant-women-shouldnt-carry-heavy-objects 10310767
5. https lupinepublishers.com/gynecology- women-health-joumal/pdCIWHC MS ID 000127 pdf

https://doi.org/10.62500/icrtsda.1.1.8

Proc. 1st International Conference on Recent Trends in Statistics and Data Analytics
Air University Islamabad, Pakistan – May 9, 2024, Vol. 1, pp. 61-73

Estimation of Interquartile Range Using the Auxiliary Information

Dr. Aneel Ahmed[1] and Prof. Dr. Javid Shabbir[2]
[1]Department of Statistics,
Quaid-i-Azam University, Islamabad.
[2]Department of Statistics,
University of Wah, Islamabad.

ABSTRACT

Using simple random sampling scheme a general class of estimators is propose in estimating the finite population interquartile range (*IQR*) by using the known values of the 1st and 3rd quartiles of the auxiliary variable. Expressions for bias and mean square error (*MSE*) are derived up to first order of approximation. We use three real data sets to illustrate the performances of the estimators. The behaviour of propose general class of estimators shows that it is more efficient than usual sample, ratio and all other existing estimators.

Keywords: Auxiliary variable, *IQR*, Bias, Mean square error (*MSE*), Efficienc

1. INTRODUCTION

The *IQR* is used for detecting the outliers and making the Box-plots and its application is in various disciplines including agriculture, biology, economics and environmental sciences. Several authors like Chambers and Dunstan (1986), Kuk and Mak (1989), Garcia and Cebrian (2001), Singh *et al.* (2001), Singh *et al.* (2006a), Singh *et al.* (2006b), Singh *et al.* (2007), Singh *et al.* (2014) and Singh and Sedory (2014) suggested the importance of population median, Bowley's coefficient of skewness, and empirical mode of the study variable by making use of the auxiliary variable. Singh *et al.* (2006b) studied the *IQR* under simple random sampling, Shabbir and Ahmed (2022) estimated *IQR* in stratified sampling under non-linear cost function and Singh and Nigam (2022) suggested a generalized class of estimators for finite population mean using two auxiliary variables in sample surveys. Several researchers have worked on estimation of finite population mean, population total and population variance but to the best of our knowledge, very rare attention was given in the estimation of interquartile range (*IQR*) of the study variable (y) in the past.

In Section 2, we introduce a general class of estimators for finite population interquartile range by using the auxiliary variable. Section 3 includes some members of proposed general class of estimators as special cases. Section 4 gives the numerical study and Section 5 gives the conclusion.

Consider a finite population $\Omega=\{1,2,...,i,...,N\}$ having N units. Let y_i and x_i be the observed values of the study variable (y) and the auxiliary variable (x) respectively for the *i*th unit. We draw a sample of size n from a population Ω by using simple random sample without replacement (SRSWOR) sampling scheme. Let $\left(\hat{Q}_{1y},\hat{Q}_{1x}\right)$ and $\left(\hat{Q}_{3y},\hat{Q}_{3x}\right)$ be the sample 1st and 3rd quartiles correspond to the population 1st and 3rd quartiles $\left(Q_{1y},Q_{1x}\right)$ and $\left(Q_{3y},Q_{3x}\right)$ respectively.

Let $I\hat{Q}R_y=\hat{Q}_{3y}-\hat{Q}_{1y}$ and $I\hat{Q}R_x=\hat{Q}_{3x}-\hat{Q}_{1x}$ be the sample interquartile ranges correspond to the population interquartile ranges $IQR_y=Q_{3y}-Q_{1y}$ and $IQR_x=Q_{3x}-Q_{1x}$ respectively. To estimate IQR_y, we assume that IQR_x is known.

On the lines of Singh *et al.* (2006b) and Ahmed and Shabbir (2019), we reproduced the following Table 1, having the values of quartiles of y and x.

https://doi.org/10.62500/icrtsda.1.1.8

Table 1: Values of Quartiles

where,

	$X \le Q_{1x}$	$X \le Q_{3x}$	$Y \le Q_{1y}$	$Y \le Q_{3y}$
$X \le Q_{1x}$	0.25	0.25	$P_{Q_{1x}Q_{1y}}$	$P_{Q_{1x}Q_{3y}}$
$X \le Q_{3x}$	0.25	0.75	$P_{Q_{3x}Q_{1y}}$	$P_{Q_{3x}Q_{3y}}$
$Y \le Q_{1y}$	$P_{Q_{1x}Q_{1y}}$	$P_{Q_{3x}Q_{1y}}$	0.25	0.25
$Y \le Q_{3y}$	$P_{Q_{1x}Q_{3y}}$	$P_{Q_{3x}Q_{3y}}$	0.25	0.75

$P_{Q_{1x}Q_{1x}} = P\left[X \le Q_{1x} \cap X \le Q_{1x}\right] = 0.25, P_{Q_{1x}Q_{3x}} = P\left[X \le Q_{1x} \cap X \le Q_{3x}\right] = 0.25,$

$P_{Q_{3x}Q_{3x}} = P\left[X \le Q_{3x} \cap X \le Q_{3x}\right] = 0.75,\ P_{Q_{1x}Q_{1y}} = P\left[X \le Q_{1x} \cap Y \le Q_{1y}\right],$

$P_{Q_{1x}Q_{3y}} = P\left[X \le Q_{1x} \cap Y \le Q_{3y}\right],\ P_{Q_{3x}Q_{1y}} = P\left[X \le Q_{3x} \cap Y \le Q_{1y}\right],$

$P_{Q_{1y}Q_{1y}} = P\left[Y \le Q_{1y} \cap Y \le Q_{1y}\right] = 0.25,\ P_{Q_{3x}Q_{3y}} = P\left[X \le Q_{3x} \cap Y \le Q_{3y}\right],$

$P_{Q_{1y}Q_{3y}} = P\left[Y \le Q_{1y} \cap Y \le Q_{3y}\right] = 0.25,\quad P_{Q_{3y}Q_{3y}} = P\left[Y \le Q_{3y} \cap Y \le Q_{3y}\right] = 0.75.$

To obtain the properties of $\hat{IQR}$, we define the following relative error terms and their expectations.

Let $e_{1y} = \dfrac{\hat{Q}_{1y} - Q_{1y}}{Q_{1y}}$, $e_{3y} = \dfrac{\hat{Q}_{3y} - Q_{3y}}{Q_{3y}}$, $e_{1x} = \dfrac{\hat{Q}_{1x} - Q_{1x}}{Q_{1x}}$ and $e_{3x} = \dfrac{\hat{Q}_{3x} - Q_{3x}}{Q_{3x}}$,

such that $E\left(e_{1y}\right) = E\left(e_{3y}\right) = E\left(e_{1x}\right) = E\left(e_{3x}\right) = 0$.

Therefore, $E\left(e_{1y}^2\right) = \theta\left(\dfrac{3}{16}\right)\left(\dfrac{1}{Q_{1y}^2\left\{f_y\left(Q_{1y}\right)\right\}^2}\right)$, $E\left(e_{3y}^2\right) = \theta\left(\dfrac{3}{16}\right)\left(\dfrac{1}{Q_{3y}^2\left\{f_y\left(Q_{3y}\right)\right\}^2}\right)$,

$E\left(e_{1x}^2\right) = \theta\left(\dfrac{3}{16}\right)\left(\dfrac{1}{Q_{1x}^2\left\{f_x\left(Q_{1x}\right)\right\}^2}\right)$, $E\left(e_{3x}^2\right) = \theta\left(\dfrac{3}{16}\right)\left(\dfrac{1}{Q_{3x}^2\left\{f_x\left(Q_{3x}\right)\right\}^2}\right)$,

$E\left(e_{1y}e_{3y}\right) = \theta\left(\dfrac{1}{16}\right)\left(\dfrac{1}{Q_{1y}Q_{3y}\left\{f_y\left(Q_{1y}\right)f_y\left(Q_{3y}\right)\right\}}\right)$,

$E\left(e_{1x}e_{3x}\right) = \theta\left(\dfrac{1}{16}\right)\left(\dfrac{1}{Q_{1x}Q_{3x}\left\{f_x\left(Q_{1x}\right)f_x\left(Q_{3x}\right)\right\}}\right)$,

$E\left(e_{1y}e_{1x}\right) = \theta\left(P_{Q_{1x}Q_{1y}} - \dfrac{1}{16}\right)\left(\dfrac{1}{Q_{1x}Q_{1y}\left\{f_x\left(Q_{1x}\right)f_y\left(Q_{1y}\right)\right\}}\right)$,

$E\left(e_{1y}e_{3x}\right) = \theta\left(P_{Q_{3x}Q_{1y}} - \dfrac{3}{16}\right)\left(\dfrac{1}{Q_{3x}Q_{1y}\left\{f_x\left(Q_{3x}\right)f_y\left(Q_{1y}\right)\right\}}\right)$,

https://doi.org/10.62500/icrtsda.1.1.8

$$E\left(e_{3y}e_{1x}\right)=\theta\left(P_{Q_{1x}Q_{3y}}-\frac{3}{16}\right)\left(\frac{1}{Q_{1x}Q_{3y}\left\{f_x\left(Q_{1x}\right)f_y\left(Q_{3y}\right)\right\}}\right),$$

$$E\left(e_{3y}e_{3x}\right)=\theta\left(P_{Q_{3x}Q_{3y}}-\frac{9}{16}\right)\left(\frac{1}{Q_{3x}Q_{3y}\left\{f_x\left(Q_{3x}\right)f_y\left(Q_{3y}\right)\right\}}\right),$$

where $\theta=\left(\frac{1-f}{n}\right)$ and $f=\frac{n}{N}$.

2. PROPOSED ESTIMATOR

We propose a general class of estimators for IQR, given by

$$\left(I\hat{Q}R_{GP}\right)=\left[k_1I\hat{Q}R_y\left(\frac{IQR_x}{I\hat{Q}R_x}\right)^{\alpha_1}+k_2\left(IQR_x-I\hat{Q}R_x\right)\right]\left[\exp\left(\frac{IQR_x-I\hat{Q}R_x}{IQR_x+I\hat{Q}R_x}\right)\right]^{\alpha_2} \tag{2.1}$$

where k_1 and k_2 are unknown constants whose values are to be determined and $\alpha_i\left(i=1,2\right)$ are the scalars, chosen arbitrary.

In terms of $e's$, we have

$$\left(I\hat{Q}R_{GP}\right)=\left[k_1\left(IQR_y+Q_{3y}e_{3y}-Q_{1y}e_{1y}\right)\left(1+\frac{Q_{3x}e_{3x}-Q_{1x}e_{1x}}{IQR_x}\right)^{-\alpha_1}+k_2\left(Q_{1x}e_{1x}-Q_{3x}e_{3x}\right)\right]$$

$$\times\left[\exp\left(\frac{Q_{1x}e_{1x}-Q_{3x}e_{3x}}{2IQR_x+Q_{3x}e_{3x}-Q_{1x}e_{1x}}\right)\right]^{\alpha_2} \tag{2.2}$$

To first degree of approximation, we have

$$\left(\left(I\hat{Q}R_{GP}\right)-IQR_y\right)\cong\left(IQR_y\right)\left[\left(k_1-1\right)+\alpha_2k_1\left(\frac{Q_{1x}^2e_{1x}^2+Q_{3x}^2e_{3x}^2-2Q_{1x}Q_{3x}e_{1x}e_{3x}}{4\left(IQR_x\right)^2}+\frac{Q_{1x}e_{1x}-Q_{3x}e_{3x}}{2\left(IQR_x\right)}\right.\right.$$

$$\left.+\frac{\alpha_2Q_{1x}^2e_{1x}^2+\alpha_2Q_{3x}^2e_{3x}^2-2\alpha_2Q_{1x}Q_{3x}e_{1x}e_{3x}}{8\left(IQR_x\right)^2}\right)+\alpha_1\left(\alpha_1+1\right)k_1\left(\frac{Q_{3x}^2e_{3x}^2+Q_{1x}^2e_{1x}^2-2Q_{1x}Q_{3x}e_{1x}e_{3x}}{2}\right)$$

$$\left.+\alpha_1k_1\left(\frac{Q_{1x}e_{1x}-Q_{3x}e_{3x}}{\left(IQR_x\right)}+\frac{\alpha_2Q_{1x}^2e_{1x}^2+\alpha_2Q_{3x}^2e_{3x}^2-2\alpha_2Q_{1x}Q_{3x}e_{1x}e_{3x}}{2\left(IQR_x\right)^2}\right)\right]$$

$$+\alpha_2k_1\left(\frac{Q_{1x}Q_{3y}e_{1x}e_{3y}-Q_{3x}Q_{3y}e_{3x}e_{3y}-Q_{1x}Q_{1y}e_{1x}e_{1y}+Q_{3x}Q_{1y}e_{3x}e_{1y}+Q_{3x}^2e_{3x}^2}{2\left(IQR_x\right)}\right)$$

$$+\alpha_1k_1\left(\frac{Q_{1x}Q_{3y}e_{1x}e_{3y}-Q_{3x}Q_{3y}e_{3x}e_{3y}-Q_{1x}Q_{1y}e_{1x}e_{1y}+Q_{3x}Q_{1y}e_{3x}e_{1y}}{\left(IQR_x\right)}\right)$$

https://doi.org/10.62500/icrtsda.1.1.8

$$+\alpha_2 k_2\left(\frac{Q_{1x}^2 e_{1x}^2 - 2Q_{1x}Q_{3x}e_{1x}e_{3x}}{2\left(IQR_x\right)}\right)+k_1\left(Q_{3y}e_{3y}-Q_{1y}e_{1y}\right)+k_2\left(Q_{1x}e_{1x}-Q_{3x}e_{3x}\right). \tag{2.3}$$

Applying expectations on both sides of (2.3), we have

$$Bias\left(\hat{IQR}_{GP}\right)\cong\left(IQR_y\right)\Bigg[\left(k_1-1\right)+\theta\alpha_2 k_1\left(\frac{\left(Q_{1x}^2 D+Q_{3x}^2 E-2Q_{1x}Q_{3x}F\right)\left(2+\alpha_2\right)}{8\left(IQR_x\right)^2}\right)$$

$$+\theta\alpha_1\alpha_2 k_1\left(\frac{Q_{1x}^2 D+Q_{3x}^2 E-2Q_{1x}Q_{3x}F}{2\left(IQR_x\right)^2}\right)+\theta\alpha_1\left(\alpha_1+1\right)k_1\left(\frac{Q_{1x}^2 D+Q_{3x}^2 E-2Q_{1x}Q_{3x}F}{2}\right)\Bigg]$$

$$+\theta\alpha_2 k_1\left(\frac{Q_{1x}Q_{3y}J-Q_{3x}Q_{3y}L-Q_{1x}Q_{1y}G+Q_{3x}Q_{1y}H+Q_{3x}^2E}{2\left(IQR_x\right)}\right)+\theta\alpha_2 k_2\left(\frac{Q_{1x}^2D-2Q_{1x}Q_{3x}F}{2\left(IQR_x\right)}\right)$$

$$+\theta\alpha_1 k_1\left(\frac{Q_{1x}Q_{3y}J-Q_{3x}Q_{3y}L-Q_{1x}Q_{1y}G+Q_{3x}Q_{1y}H}{\left(IQR_x\right)}\right), \tag{2.4}$$

where $D=\left(\frac{3}{16}\right)\left(\frac{1}{Q_{1x}^2\left\{f_x\left(Q_{1x}\right)\right\}^2}\right)$, $E=\left(\frac{3}{16}\right)\left(\frac{1}{Q_{3x}^2\left\{f_x\left(Q_{3x}\right)\right\}^2}\right)$,

$F=\left(\frac{1}{16}\right)\left(\frac{1}{Q_{1x}Q_{3x}\left\{f_x\left(Q_{1x}\right)f_x\left(Q_{3x}\right)\right\}}\right)$, $G=\left(\rho_{Q_{1x}Q_{1y}}-\frac{1}{16}\right)\left(\frac{1}{Q_{1x}Q_{1y}\left\{f_x\left(Q_{1x}\right)f_y\left(Q_{1y}\right)\right\}}\right)$,

$H=\left(\rho_{Q_{3x}Q_{1y}}-\frac{3}{16}\right)\left(\frac{1}{Q_{3x}Q_{1y}\left\{f_x\left(Q_{3x}\right)f_y\left(Q_{1y}\right)\right\}}\right)$,

$J=\left(\rho_{Q_{1x}Q_{3y}}-\frac{3}{16}\right)\left(\frac{1}{Q_{1x}Q_{3y}\left\{f_x\left(Q_{1x}\right)f_y\left(Q_{3y}\right)\right\}}\right)$ and

$L=\left(\rho_{Q_{3x}Q_{3y}}-\frac{9}{16}\right)\left(\frac{1}{Q_{3x}Q_{3y}\left\{f_x\left(Q_{3x}\right)f_y\left(Q_{3y}\right)\right\}}\right)$.

Taking square on both sides of (2.3), and then applying the expectations, we have

$$MSE\left(\hat{IQR}_{GP}\right)\cong\left(IQR_y\right)^2\left[\left(k_1-1\right)^2+\frac{\theta k_1^2\chi}{\left(IQR_x\right)^2}\left(\alpha_1^2+\frac{1}{4}\alpha_2^2+\alpha_1\alpha_2\right)\right]$$

$$+\theta k_1^2\delta+\theta k_2^2\chi+2\theta k_1k_2\gamma+\left(\frac{\theta k_1^2\left(IQR_y\right)\gamma}{\left(IQR_x\right)}\right)\left(2\alpha_1+\alpha_2\right)$$

$$+\left(\frac{\theta k_1k_2\left(IQR_y\right)\chi}{\left(IQR_x\right)}\right)\left(2\alpha_1+\alpha_2\right), \tag{2.5}$$

https://doi.org/10.62500/icrtsda.1.1.8

where $\delta = Q_{1y}^2 A + Q_{3y}^2 B - 2Q_{1y}Q_{3y}C$, $\chi = Q_{1x}^2 D + Q_{3x}^2 E - 2Q_{1x}Q_{3x}F$,

$\gamma = Q_{1x}Q_{3y}J - Q_{1x}Q_{1y}G - Q_{3x}Q_{3y}L + Q_{1y}Q_{3x}H$, $A = \left(\frac{3}{16}\right)\left(\frac{1}{Q_{1y}^2\left\{f_y\left(Q_{1y}\right)\right\}^2}\right)$,

$B = \left(\frac{3}{16}\right)\left(\frac{1}{Q_{3y}^2\left\{f_y\left(Q_{3y}\right)\right\}^2}\right)$ and $C = \left(\frac{1}{16}\right)\left(\frac{1}{Q_{1y}Q_{3y}\left\{f_y\left(Q_{1y}\right)f_y\left(Q_{3y}\right)\right\}}\right)$.

Differentiating (2.5) with respect to k_1 and k_2, we get, the minimum *MSE* of $I\hat{Q}R_{GP}$, at optimum values of k_1 and k_2.

$$MSE\left(I\hat{Q}R_{GP}\right)_{\min} \cong \frac{A1}{A2}, \tag{2.6}$$

where $A1 = -\left(\left(\frac{3}{4}\left(A^*\right)^2 E\left(IQR_x\right)^2\left(IQR_y\right)\left(E\left(IQR_y\right)^2 + \frac{1}{3}F^2\theta\right)Q_{3x}^4 - \left(A^*\right)\left(IQR_x\right)^2\right.\right.$

$\left(IQR_y\right)\left(\frac{5}{2}Q_{1x}\left(A^*\right)FE\left(IQR_y\right)^2 + \left(IQR_x\right)E\left(B^* - F\right)\left(IQR_y\right) + \frac{1}{2}Q_{1x}F\left(A^*\right)\left(H^*\right)\theta\right)Q_{3x}^3$

$+\left(\left(IQR_x\right)^2\left(A^*\right)^2 Q_{1x}^2\left(G^*\right)\left(IQR_y\right)^3 + \left(IQR_x\right)^3\left(A^*\right)Q_{1x}\left(-2F^2 + B^*F - E\left(C^* + D\right)\right)\left(IQR_y\right)^2\right.$

$+\left(\frac{1}{4}\left(IQR_x\right)^2\left(A^*\right)^2\left(H^*\right)D\theta Q_{1x}^2 + \left(IQR_x\right)^4\delta E - \left(IQR_x\right)^4\left(B^*\right)^2\right)\left(IQR_y\right)\Big)Q_{3x}^2$

$-2Q_{1x}\left(\frac{1}{2}Q_{1x}^2\left(A^*\right)^2 FD\left(IQR_y\right)^2 - \frac{1}{2}\left(IQR_x\right)\left(A^*\right)Q_{1x}\left(C^* + 3D\right)F\left(IQR_y\right) + \frac{1}{2}FD^2\left(A^*\right)^2 Q_{1x}^2\theta\right.$

$+\left(IQR_x\right)^2\delta F + \left(IQR_x\right)^2 C^*B^*\left(IQR_x\right)^2\left(IQR_y\right)Q_{3x} + Q_{1x}^2\left(IQR_x\right)^2\left(IQR_y\right)\left(-\left(IQR_x\right)\left(IQR_y\right)\right.$

$\left.\left.\times Q_{1x}A^*D^2 + \frac{1}{4}\theta Q_{1x}^2 D^3\left(A^*\right)^2 + \left(IQR_x\right)^2 F^*Q_{3y}^2 - 2\left(IQR_x\right)^2 Q_{1y}Q_{3y}E^* + \left(IQR_x\right)^2 Q_{1y}^2 D^*\right)\left(IQR_y\right)\theta\right)$,

$A2 = \left(\left(IQR_x\right)^2\left(\frac{3}{4}\theta\left(IQR_y\right)^2 Q_{3x}^4\left(A^*\right)^2 E^2 - \left(IQR_y\right)\left(A^*\right)E\left(\frac{5}{2}\left(IQR_y\right)Q_{1x}\left(A^*\right)F + \left(IQR_x\right)B^*\right)\theta Q_{3x}^3\right.\right.$

$+\left(\left(\theta Q_{1x}^2\left(A^*\right)^2\left(G^*\right) - \left(IQR_x\right)^2 E\right)\left(IQR_y\right)^2 + \left(IQR_x\right)\left(IQR_y\right)Q_{1x}\theta\left(A^*\right)\left(B^*F - C^*E\right)\right.$

$+\left(IQR_x\right)^2\theta\left(E\delta - \left(B^*\right)^2\right)Q_{3x}^2 - 2Q_{1x}\left(-F\left(-\frac{1}{2}\left(A^*\right)^2 D\theta Q_{1x}^2 + \left(IQR_x\right)^2\right)\left(IQR_y\right)^2\right.$

$\left.\left.-\frac{1}{2}\theta\left(IQR_x\right)\left(IQR_y\right)\left(A^*\right)Q_{1x}F\left(C^*\right) + \left(IQR_x\right)^2\theta\left(B^*C^* + F\delta\right)\right)Q_{3x}\right.$

https://doi.org/10.62500/icrtsda.1.1.8

$+Q_{1x}^2\left(IQR_x\right)^2\left(-\left(IQR_y\right)^2 D+\left(D^* Q_{1y}^2-2E^* Q_{1y}Q_{3y}+F^* Q_{3y}^2\right)\theta\right)\Big)$, $A^*=\alpha_1+\frac{1}{2}\alpha_2$,

$B^*=LQ_{3y}-HQ_{1y}$, $C^*=GQ_{1y}-JQ_{3y}$, $D^*=AD-G^2$, $E^*=CD-GJ$, $F^*=BD-J^2$,

$G^*=ED+\frac{7}{4}F^2$ and $H^*=DE+F^2$.

3. SPECIAL CASES

Following are the members of proposed estimator by choosing different values of α_1, α_2, k_1 and k_2 .

(i) If $\alpha_1=\alpha_2=0$ and $k_1=1$, $k_2=0$ in (2.1), then $I\hat{Q}R_{GP}$ reduces to usual sample estimator.

$$I\hat{Q}R_1=\hat{Q}_{3y}-\hat{Q}_{1y} \tag{3.1}$$

To first degree of approximation, the MSE of $I\hat{Q}R_1$, is given by

$$Var(I\hat{Q}R_1)\cong\theta\delta=MSE(I\hat{Q}R_1). \tag{3.2}$$

(ii) If $\alpha_1=1$, $\alpha_2=0$ and $k_1=1$, $k_2=0$ in (2.1), then $I\hat{Q}R_{GP}$ reduces to ratio estimator.

$$I\hat{Q}R_2=I\hat{Q}R_y\left(\frac{IQR_x}{I\hat{Q}R_x}\right) \tag{3.3}$$

To first degree of approximation, the $Bias$ and MSE of $I\hat{Q}R_2$, are given by

$$Bias\left(I\hat{Q}R_2\right)\cong\frac{\theta}{\left(IQR_x\right)}\left(\frac{\left(IQR_y\right)}{\left(IQR_x\right)}\chi+\gamma\right) \tag{3.4}$$

and

$$MSE\left(I\hat{Q}R_2\right)\cong\frac{\theta\left(IQR_y\right)}{\left(IQR_x\right)}\left(\frac{\left(IQR_y\right)}{\left(IQR_x\right)}\chi+2\gamma\right)+\theta\delta\,. \tag{3.5}$$

(iii) If $\alpha_1=0$, $\alpha_2=1$ and $k_1=1$, $k_2=0$ in (2.1), then $I\hat{Q}R_{GP}$ reduces to exponential type estimator.

$$I\hat{Q}R_3=\left(I\hat{Q}R_y\right)\exp\left(\frac{IQR_x-I\hat{Q}R_x}{IQR_x+I\hat{Q}R_x}\right) \tag{3.6}$$

To first degree of approximation, the $Bias$ and MSE of $I\hat{Q}R_3$, are given by

$$Bias\left(I\hat{Q}R_3\right)\cong\frac{\theta}{2\left(IQR_x\right)}\left(\frac{3\left(IQR_y\right)\chi}{4\left(IQR_x\right)}+\gamma\right) \tag{3.7}$$

and

$$MSE(I\hat{Q}R_3)\cong\frac{\theta\left(IQR_y\right)}{\left(IQR_x\right)}\left(\frac{\left(IQR_y\right)\chi}{4\left(IQR_x\right)}+\gamma\right)+\theta\delta\,. \tag{3.8}$$

https://doi.org/10.62500/icrtsda.1.1.8

(iv) If $\alpha_1 = \alpha_2 = 0$ and $k_1 = 1$ in (2.1), then $I\hat{Q}R_{GP}$ reduces to difference estimator.

$$I\hat{Q}R_4 = I\hat{Q}R_y + k_2\left(IQR_x - I\hat{Q}R_x\right), \tag{3.9}$$

where k_2 is the unknown constant whose value is to be determined.

To first degree of approximation, the MSE of $I\hat{Q}R_4$, is given by

$$Var(I\hat{Q}R_4) \cong \theta\left(2k_2\gamma + k_2^2\chi + \delta\right) = MSE(I\hat{Q}R_4) \tag{3.10}$$

Differentiating (3.10) with respect to k_2, we get,

$$k_{2(opt)} = -\frac{\gamma}{\chi}.$$

Putting the optimum value of k_2 in (3.10), we get the optimum value of MSE of $I\hat{Q}R_4$, is given by

$$Var(I\hat{Q}R_4)_{\min} \cong \theta\left(\delta + \frac{\gamma^2}{\chi}\right) = MSE(I\hat{Q}R_4)_{\min} \tag{3.11}$$

(v) If $\alpha_1 = \alpha_2 = 0$ in (2.1), then $I\hat{Q}R_{GP}$ reduces to Rao (1991) difference type estimator.

$$I\hat{Q}R_5 = k_1 I\hat{Q}R_y + k_2\left(IQR_x - I\hat{Q}R_x\right), \tag{3.12}$$

where k_1 and k_2 are unknown constants whose values are to be determined.

To first degree of approximation, the $Bias$ and MSE of $I\hat{Q}R_5$, are given by

$$Bias\left(I\hat{Q}R_5\right) \cong (k_1 - 1)\, IQR_y \tag{3.13}$$

and

$$MSE(I\hat{Q}R_5) \cong \theta\left(k_1^2\delta + 2k_1k_2\gamma + k_2^2\chi\right) + IQR_y^2\,(k_1 - 1)^2 \tag{3.14}$$

Differentiating (3.14) with respect to k_1 and k_2, we get,

$$k_{1(opt)} = \frac{\chi\left(IQR_y\right)^2}{\left(\chi\left(IQR_y\right)^2 + \left(\lambda_1 Q_{3x}^2 - 2\lambda_2 Q_{1x}Q_{3x} + \lambda_3 Q_{1x}^2\right)\theta\right)},$$

where $\chi = DQ_{1x}^2 + EQ_{3x}^2 - 2FQ_{1x}Q_{3x}$, $M_1 = BE - L^2$, $M_2 = BF - JL$, $M_3 = BD - J^2$,

$T_1 = HL - CE$, $T_2 = CD - GJ$, $T_3 = GL + HJ - 2CF$, $S_1 = AE - H^2$, $S_2 = AF - GH$,

$S_3 = AD - G^2$, $\lambda_1 = \left(M_1Q_{3y}^2 + 2T_1Q_{1y}Q_{3y} + S_1Q_{1y}^2\right)$, $\lambda_2 = \left(M_2Q_{3y}^2 + T_3Q_{1y}Q_{3y} + S_2Q_{1y}^2\right)$

and $\lambda_3 = \left(M_3Q_{3y}^2 - 2T_2Q_{1y}Q_{3y} + S_3Q_{1y}^2\right)$. and

https://doi.org/10.62500/icrtsda.1.1.8

$$k_{2(opt)} = \frac{-\gamma\left(IQR_y\right)^2}{\left(\chi\left(IQR_y\right)^2 + \left(\lambda_1 Q_{3x}^2 - 2\lambda_2 Q_{1x} Q_{3x} + \lambda_3 Q_{1x}^2\right)\theta\right)}$$

Putting the optimum values of k_1 and k_2 in (3.14), we get the optimum value of *MSE* of $I\hat{Q}R_5$, is given by

$$MSE(I\hat{Q}R_5)_{\min} \cong \theta\left[\frac{\left(\theta\left(IQR_y\right)^2\left(\lambda_1 Q_{3x}^2 - 2\lambda_2 Q_{1x} Q_{3x} + \lambda_3 Q_{1x}^2\right)\right)}{\left(\chi\left(IQR_y\right)^2 + \theta\left(\lambda_1 Q_{3x}^2 - 2\lambda_2 Q_{1x} Q_{3x} + \lambda_3 Q_{1x}^2\right)\right)}\right], \tag{3.15}$$

(vi) If $\alpha_1 = 0$, $\alpha_2 = 1$ in (2.1), then $I\hat{Q}R_{GP}$ reduces to Rao (1991) difference type cum exponential estimator.

$$I\hat{Q}R_6 = \left\{k_1 I\hat{Q}R_y + k_2\left(IQR_x - I\hat{Q}R_x\right)\right\}\exp\left(\frac{IQR_x - I\hat{Q}R_x}{IQR_x + I\hat{Q}R_x}\right), \tag{3.16}$$

where k_1 and k_2 are unknown constants whose values are to be determined.

To first degree of approximation, the *Bias* and *MSE* of $I\hat{Q}R_6$, are given by

$$Bias\left(I\hat{Q}R_6\right) \cong \frac{\theta k_1}{2\left(IQR_x\right)}\left[\frac{3\left(IQR_y\right)\chi}{4\left(IQR_x\right)} + \gamma\right] + k_2\theta\left[\frac{\chi}{2\left(IQR_x\right)}\right] + \left(k_1 - 1\right)\left(IQR_y\right) \tag{3.17}$$

and

$$MSE(I\hat{Q}R_6) \cong \frac{\theta}{4\left(IQR_x\right)^2}\begin{pmatrix}\left(4k_1^2\delta - 8k_1k_2V + 4k_2^2\chi\right)\left(IQR_x\right)^2 + 4k_1\chi\left(\frac{4k_1 - 3}{4}\right)\left(IQR_y\right)^2 \\ -8\left(Vk_1 - k_2\chi\right)\left(\frac{2k_1 - 1}{2}\right)\left(IQR_y\right)\left(IQR_x\right)\end{pmatrix}$$

$$+ \frac{\left[2\left(IQR_y\right)\left(IQR_x\right)\left(k_1 - 1\right)\right]^2}{4\left(IQR_x\right)^2}, \tag{3.18}$$

Differentiating (3.18) with respect to k_1 and k_2, we get,

$$k_{1(opt)} = \frac{-\frac{1}{8}\left(\left(IQR_y\right)^2\chi\left(\theta\chi - 8\left(IQR_x\right)^2\right)\right)}{\left(IQR_x\right)^2\left(\left(\lambda_1 Q_{3x}^2 - 2\lambda_2 Q_{1x} Q_{3x} + Q_{1x}^2\lambda_3\right)\theta + \left(IQR_y\right)^2\chi\right)}$$

and

$$k_{2(opt)} = \frac{\frac{1}{2}\left(\left(IQR_y\right)\left(\left(\gamma_5 + \gamma_1\left(IQR_x\right)^2\right)Q_{3x}^2 - 2\gamma_2\left(IQR_x\right)^2\right)Q_{1x}Q_{3x} + \gamma_3 Q_{1x}^2\right)\theta + 2\left(IQR_y\right)\left(IQR_x\right)^2\gamma_4}{\left(IQR_x\right)^3\left(\left(\lambda_1 Q_{3x}^2 - 2\lambda_2 Q_{1x} Q_{3x} + \lambda_3 Q_{1x}^2\right)\theta + \left(IQR_y\right)^2\chi\right)}$$

https://doi.org/10.62500/icrtsda.1.1.8

where $P_1 = EG + 2FH$, $P_2 = EJ + 2FL$, $P_3 = 4\left(IQR_y\right)Q_{1x}F + \left(IQR_x\right)V_1$, $W_1 = DE + 2F^2$, $W_2 = DL + 2FJ$ and $W_3 = DH + 2FG$, $\psi_1 = \dfrac{P_2Q_{3y} - P_1Q_{1y}}{2}$, $\psi_2 = W_2Q_{3y} - Q_{1y}W_3$, $\psi_3 = \dfrac{\left(IQR_y\right)^2 Q_{1x}^2D^2 - \left(IQR_y\right)\left(IQR_x\right)DV_2Q_{1x}}{4}$, $\psi_4 = \left(IQR_y\right)Q_{1x}F + \left(IQR_x\right)V_1$, $\psi_5 = \left(IQR_x\right)V_2 - \dfrac{\left(IQR_y\right)D}{2}$, $\psi_6 = \dfrac{\left(IQR_y\right)E}{2}$, $\psi_7 = \dfrac{\left(IQR_y^2\right)DF}{2}$, $\psi_8 = \dfrac{\left(IQR_y^2\right)W_1}{2}$, $\gamma_1 = \psi_8Q_{1x}^2 + \dfrac{1}{2}\psi_1\left(IQR_y\right)\left(IQR_x\right)Q_{1x} + \lambda_1$, $\gamma_2 = \psi_7Q_{1x}^2 + \dfrac{1}{8}\psi_2\left(IQR_y\right)\left(IQR_x\right)Q_{1x} + \lambda_2$, $\gamma_3 = \psi_3 + \lambda_3\left(IQR_x^2\right)$, $\gamma_4 = \psi_4Q_{3x} + \psi_5Q_{1x} - \psi_6Q_{3x}^2$ and $\gamma_5 = \dfrac{Q_{3x}^4E^2 - \left(IQR_y\right)Q_{3x}^3P_3E}{4}$.

Putting the optimum values of k_1 and k_2 in (3.18), we get the optimum value of *MSE* of $I\hat{Q}R_6$, is given by

$$MSE(I\hat{Q}R_6)_{\min} \cong \frac{-\frac{1}{4}\begin{pmatrix}\theta\begin{pmatrix}U\left(\Phi_1Q_{3x}^2 - 2\Phi_2Q_{1x}Q_{3x} + \Phi_3Q_{1x}^2 + \Phi_4\right)\theta \\ -4\left(\lambda_1Q_{3x}^2 - 2\lambda_2Q_{1x}Q_{3x} + \lambda_3Q_{1x}^2\right)\left(IQR_x^4\right)\end{pmatrix}\left(IQR_y^2\right)\end{pmatrix}}{\left(IQR_x^4\right)\left(\left(\lambda_1Q_{3x}^2 - 2\lambda_2Q_{1x}Q_{3x} + \lambda_3Q_{1x}^2\right)\theta + \left(IQR_y^2\right)\chi\right)}, \tag{3.19}$$

where $\Phi_1 = \left(IQR_x^2\right)\lambda_1 + \dfrac{\psi_8}{4}Q_{1x}^2$, $\Phi_2 = \left(IQR_x^2\right)\lambda_2 + \dfrac{\psi_7}{4}Q_{1x}^2$, $\Phi_3 = \left(IQR_x^2\right)\lambda_3 + \dfrac{\left(IQR_y^2\right)Q_{1x}^2D^2}{16}$ and $\Phi_4 = \dfrac{\psi_6^2}{4}Q_{3x}^4 - \dfrac{4\left(IQR_y^2\right)Q_{1x}Q_{3x}^3EF}{16}$.

(vii) If $\alpha_1 = 1$, $\alpha_2 = 0$ in (2.1), then $I\hat{Q}R_{GP}$ reduces to ratio cum Rao (1991) difference type estimator.

$$I\hat{Q}R_7 = k_1I\hat{Q}R_y\left(\frac{IQR_x}{I\hat{Q}R_x}\right) + k_2\left(IQR_x - I\hat{Q}R_x\right), \tag{3.20}$$

where k_1 and k_2 are unknown constants whose values are to be determined.

To first degree of approximation, the *Bias* and *MSE* of $I\hat{Q}R_7$, are given by

$$Bias\left(I\hat{Q}R_7\right) \cong \left(IQR_y\right)\left(k_1 - 1\right) + \frac{k_1\left(IQR_y\right)\theta}{\left(IQR_x\right)^2}\chi + \frac{k_1\theta}{\left(IQR_x\right)}\gamma \tag{3.21}$$

and

$$MSE\left(I\hat{Q}R_7\right) \cong \frac{\theta}{\left(IQR_x\right)^2}\begin{pmatrix}\left(\delta\left(IQR_x\right)^2 - 4\left(IQR_y\right)\left(IQR_x\right)V + 3\left(IQR_y\right)^2\chi\right)k_1^2 + k_2^2\left(IQR_x\right)^2\chi \\ -2\left(V\left(IQR_x\right) - \left(IQR_y\right)\chi\right)\left(k_2\left(IQR_x\right) - \left(IQR_y\right)\right)k_1\end{pmatrix}$$

https://doi.org/10.62500/icrtsda.1.1.8

$$+\frac{\left[\left(IQR_x\right)\left(IQR_y\right)\left(k_1-1\right)\right]^2}{\left(IQR_x\right)^2} \tag{3.22}$$

Differentiating (3.22) with respect to k_1 and k_2, we get,

$$k_{1(opt)}=\frac{-\left(IQR_y\right)\chi\left(\left(V\left(IQR_x\right)-\left(IQR_y\right)\chi\right)\theta+\left(IQR_y\right)\left(IQR_x^2\right)\right)}{\theta\left(Z\left(IQR_x^2\right)+2\left(IQR_y^2\right)\chi^2-2\left(IQR_y\right)\left(IQR_x\right)\chi V\right)+\left(IQR_y^2\right)\left(IQR_x^2\right)\chi}$$

and

$$k_{2(opt)}=\frac{\left(IQR_y\right)\left(\left(IQR_x^2\right)\left(IQR_y\right)-\theta\left(IQR_x\right)V+\theta\left(IQR_y^3\right)\chi\right)\left(V\left(IQR_x\right)-\left(IQR_y\right)\chi\right)}{\left(IQR_x\right)\left(\left(Z\theta+\left(IQR_y^2\right)\chi\right)\left(IQR_x^2\right)-2\theta\left(IQR_y\right)\left(IQR_x\right)\chi V+2\theta\left(IQR_y^2\right)\chi^2\right)}$$

where $Z=\left(\lambda_1 Q_{3x}^2-2\lambda_2 Q_{1x}Q_{3x}+\lambda_3 Q_{1x}^2\right)$

Putting the optimum values of k_1 and k_2 in (3.22), we get the optimum value of *MSE* of $\hat{IQR}_7$, is given by

$$MSE(\hat{IQR}_7)_{\min}\cong\frac{\theta\left(IQR_x^3\right)\left(-\theta\left(IQR_x\right)\chi V^2+2\left(IQR_y\right)\theta\chi^2 V-\theta\left(IQR_x\right)\chi^3+\left(IQR_x^3\right)Z\right)}{\left(\left(IQR_x^2\right)\theta Z+\chi\left(IQR_x^2\right)\left(IQR_y^2\right)-2\theta\left(IQR_x\right)\left(IQR_y\right)\chi V+2\theta\left(IQR_y^2\right)\chi^2\right)\left(IQR_x^2\right)} \tag{3.23}$$

4. NUMERICAL ILLUSTRATION

We use the following probability density functions: $f_y(y)=\frac{1}{\sqrt{2\pi\sigma_y^2}}e^{\frac{-1}{2}\frac{\left(y-\mu_y\right)^2}{\sigma_y^2}}$, $-\infty\le y\le+\infty$ and $f_x(x)=\frac{1}{\sqrt{2\pi\sigma_x^2}}e^{\frac{-1}{2}\frac{\left(x-\mu_x\right)^2}{\sigma_x^2}}$, $-\infty\le x\le+\infty$.

where, $\mu_y=\frac{1}{N}\sum_{i=1}^{N}y_i$, $\mu_x=\frac{1}{N}\sum_{i=1}^{N}x_i$, $\sigma_y^2=\frac{1}{N}\sum_{i=1}^{N}\left(y_i-\mu_y\right)^2$, $\sigma_x^2=\frac{1}{N}\sum_{i=1}^{N}\left(x_i-\mu_x\right)^2$, $e=2.718282$, $\pi=3.141593$

Population 1: [source: Singh (2003)]

Let y = Amount (in \$000) of real estate farm loans in different states during 1997.

χ = Amount (in \$000) of nonreal estate farm loans in different states during 1997.

The necessary data statistics for this population are:

$N=50$, $n=8$, $Q_{1y}=57.11775$, $Q_{3y}=931.52$, $Q_{1x}=63.4505$, $Q_{3x}=1177.15$,
$\mu_y=555.4345$, $\mu_x=878.162$, $\sigma_y=578.948$, $\sigma_x=1073.776$, $f_y\left(Q_{1y}\right)=0.000475889919$,
$f_y\left(Q_{3y}\right)=0.000558146704$, $f_x\left(Q_{1x}\right)=0.000278676$, $f_x\left(Q_{3x}\right)=0.00035749524$,
$IQR_y=874.4023$, $IQR_x=1113.6995$, $P_{Q_{1x}Q_{1y}}=0.20$, $P_{Q_{3x}Q_{1y}}=0.26$, $P_{Q_{1x}Q_{3y}}=0.26$,
$P_{Q_{3x}Q_{3y}}=0.68$, $P_{yx}=0.804$.

https://doi.org/10.62500/icrtsda.1.1.8

Population 2: [source: Sarndal *et al.* (1992)]

The MU284 Population (The population consisting of the 284 municipalities of Sweden).

Let y = 1985 Population (in thousands)

x = Revenues from the 1985 municipal taxation (in millions of kronor).

The necessary data statistics for this population are:

$N = 284$, $n = 35$, $Q_{1y} = 10.00$, $Q_{3y} = 31$, $Q_{1x} = 67.75$, $Q_{3x} = 230.25$, $\mu_y = 29.36$, $\mu_x = 245.088$, $\sigma_y = 51.4659$, $\sigma_x = 595.2817$, $f_y(Q_{1y}) = 0.007224$, $f_y(Q_{3y}) = 0.007750$, $f_x(Q_{1x}) = 0.0006412$, $f_x(Q_{3x}) = 0.00067013$, $IQR_y = 21$, $IQR_x = 162.5$, $P_{Q_{1x}Q_{1y}} = 0.2324$, $P_{Q_{3x}Q_{1y}} = 0.2535$, $P_{Q_{1x}Q_{3y}} = 0.25$, $P_{Q_{3x}Q_{3y}} = 0.7359$.

Population 3: [source: Singh (2003)]

Let y = Duration of sleep $(in\ minutes)$.

x = Age of old persons $(\geq 50 years)$.

The necessary data statistics for this population are:

$N = 30$, $n = 6$, $Q_{1y} = 348.75$, $Q_{3y} = 420.00$, $Q_{1x} = 60.00$, $Q_{3x} = 72.75$, $\mu_y = 384.20$, $\mu_x = 67.267$, $\sigma_y = 58.849$, $\sigma_x = 9.077$, $f_y(Q_{1y}) = 0.0056557$, $f_y(Q_{3y}) = 0.0056354$, $f_x(Q_{1x}) = 0.0319074$, $f_x(Q_{3x}) = 0.0366300$, $IQR_y = 71.25$, $IQR_x = 12.75$, $P_{Q_{1x}Q_{1y}} = 0.00$, $P_{Q_{3x}Q_{1y}} = 0.033$, $P_{Q_{1x}Q_{3y}} = 0.10$, $P_{Q_{3x}Q_{3y}} = 0.53$, $P_{yx} = 0.804$.

Table 2: Bias of different estimators

Estimator	Population 1	Population 2	Population 3
$\hat{IQR}_1$	0.00	0.00	0.00
$\hat{IQR}_2$	125.29	4.86	5.05
$\hat{IQR}_3$	38.34	0.97	0.94
$\hat{IQR}_4$	0.00	0.00	0.00
$\hat{IQR}_5$	-59.29	-0.08	-5.93
$\hat{IQR}_6$	-8.56	-5.40	-4.87
$\hat{IQR}_7$	57.24	4.73	-1.28
$\hat{IQR}_{GP}$	-8.56	-5.40	-4.87

https://doi.org/10.62500/icrtsda.1.1.8

We compute the percent relative efficiency (PRE) by using the following expression.

$$PRE\left(I\hat{Q}R_i\right)=\frac{MSE\left(I\hat{Q}R_1\right)}{MSE\left(I\hat{Q}R_i\right)}\times 100\ ,\ \left(i=1,2,3,4,5,6,7,GP\right)$$

Table 3: MSE values and $PREs$ of different estimators with respect to $I\hat{Q}R_1$

	Population 1		Population 2		Population 3	
Estimator	MSE	PRE	MSE	PRE	MSE	PRE
$I\hat{Q}R_1$	100714.80	100.00	112.50	100.00	1043.25	100.00
$I\hat{Q}R_2$	149809.15	67.23	72.23	155.75	861.31	121.12
$I\hat{Q}R_3$	82757.29	121.70	31.30	359.42	727.00	143.50
$I\hat{Q}R_4$	79213.19	127.14	29.64	379.55	717.82	145.34
$I\hat{Q}R_5$	71776.85	140.32	27.78	404.97	628.89	165.89
$I\hat{Q}R_6$	67251.34	149.76	21.95	512.53	598.79	174.23
$I\hat{Q}R_7$	45688.10	220.44	3.96	2840.91	539.60	193.34
$I\hat{Q}R_{GP}$	40528.55	248.50	1.82	6181.32	325.25	320.75

In Table 3, the PRE of $I\hat{Q}R_2$ is less as compared to all other estimators in Population 1 which was due to low correlation coefficient between the study variable and the auxiliary variable. We observed that a proposed general class of estimators $I\hat{Q}R_{GP}$ is more efficient than usual sample, ratio and all other existing estimators in three real data sets.

5. CONCLUSION

We proposed a general class of estimators for finite population interquartile range (*IQR*) using the auxiliary variable. It is observed that a proposed general class of estimators $I\hat{Q}R_{GP}$ is more efficient than usual sample, ratio, exponential type, difference, Rao (1991) difference type, Rao (1991) difference type cum exponential and ratio cum Rao (1991) difference type estimators for *IQR*. Population 2 has smaller MSE values as compared to Population 1 and Population 3 which was due to high correlation coefficient between the study variable and the auxiliary variable.

REFERENCES

1. Ahmed, A., and Shabbir, J. (2019). On estimation of coefficient of dispersion using the auxiliary information. *Communications in Statistics-Simulation and Computation* 50(11): 3590-3606.

https://doi.org/10.62500/icrtsda.1.1.8

2. Chambers, R.L. and Dustan, R. (1986). Estimating distribution function from survey data. *Biometrika*, 597-604.
3. Garcia, R.M. and Cebrian, A. (2001). On estimating the median from survey data using multiple auxiliary information. *Metrika* 54, 59-76.
4. Kuk, A.Y.C. and Mak, T.K. (1989). Median estimation in presence of auxiliary information. *Journal of the Royal Statistical Society*, *Series B(Methodological)*, 51, 261-269.
5. Sarndal, C. E., Swensson, B. and Wretman, J. (1992). Model Assisted Survey Sampling. *Springer – Verlag: Newyork.*
6. Shabbir, J., and Ahmed, A. (2022). Estimation of interquartile range in stratified sampling under non-linear cost function. *Communications in Statistics-Simulation and Computation.* 51(4):1891-1898.
7. Singh, H. P. and Nigam, P. (2022). A generalized class of estimators for finite population mean using two auxiliary variables in sample surveys. *Journal of Reliability and Statistical Studies.* doi: 10.13052/jrss0974-8024.1514.
8. Singh, H. P., Puertas, S. M. and Singh, S. (2006b). Estimation of interquartile range of the study variable using the known interquartile range of auxiliary variable. *International Journal of Applied Mathematics and Statistics,* 6, 33-47.
9. Singh, H. P., Sidhu, S. S. and Singh, S. (2006a). Median estimation with known interquartile range of auxiliary variable. *International Journal of Applied Mathematics and Statistics,* 4, 68-80.
10. Singh, H.P., Solanki, R.S. and Singh, S. (2014). Estimation of Bowley's coefficient of skewness in the presence of auxiliary information. *Communications in Statistics— Theory and Methods*, 43, 4867–4880.
11. Singh, H. P., Tailor, R., Singh, S. and Kim, J. M. (2007). Quantile estimation in successive sampling. *Journal of the Korean Statistical Society* 36(4): 543-556.
12. Singh, S. (2003). Advanced Sampling Theory with Applications. Kulwer Publishers, London.
13. Singh, S., Joarder, A. H. and Tracy, D.S. (2001). Median estimation using double sampling. *Australian and New Zealand Journal of Statistics*, 43(1): 33-46.
14. Singh, S. and Sedory, S.A. (2014). Estimation of mode using auxiliary information. *Communications in Statistics-Simulation and Computation*, 43, 2390-2402.
15. Singh, S., Singh, H.P. and Upadhyay, L.N. (2007). Chain ratio and regression type estimators for median estimation in survey sampling. *Statistical Papers*, 48(1): 23-46.

https://doi.org/10.62500/icrtsda.1.1.9

Proc. 1st International Conference on Recent Trends in Statistics and Data Analytics
Air University Islamabad, Pakistan – May 9, 2024, Vol. 1, pp. 74-86

ARTIFICIAL INTELLIGENCE TRAFFIC CONTROL SIGNAL USING MACHINE LEARNING TECHNIQUES

Hifsa Shahzadi [1], Sawera Nadeem[2] and Ammara Nawaz Cheema[3]

Mathematics Department Air University Islamabad

ABSTRACT

Traffic congestion in cities often causes significant delays for emergency vehicles like ambulances, impacting their ability to reach critical situations promptly, with potentially life-threatening consequences. This paper introduces an innovative AI-powered Traffic Control System aimed at efficiently prioritizing ambulance vehicles on the road. Utilizing Deep Learning mechanisms and Python programming, the system analyzes video data of traffic scenes, converting them into frames per second for precise analysis. By meticulously labeling these frames, the system is trained to accurately identify ambulance vehicles amidst varying traffic conditions. Through the deployment of advanced deep learning algorithms, the system effectively detects ambulances even in complex scenarios such as heavy congestion or adverse weather conditions. Upon ambulance detection, the system dynamically adjusts traffic signals in real-time, ensuring unimpeded passage through the traffic stream. This adaptive signal control mechanism enhances emergency response capabilities, reducing response times, and potentially saving lives. Experimental evaluations confirm the effectiveness and efficiency of the proposed AI Traffic Control System, offering promising implications for improving urban emergency services and traffic flow management.

Keywords: AI-powered Traffic Control System, Machine Learning algorithms, real-time control, Deep Learning.

1. INTRODUCTION

In the contemporary landscape of technological progress, the convergence of healthcare and transportation infrastructure stands as a pivotal junction, fostering advancements that hold immense promise for public well-being and safety [1]. This paper project endeavors to introduce a groundbreaking solution at this intersection, titled "AI-Controlled Traffic Signals for Ambulance Detection through Computer Vision." The amalgamation of data science and artificial intelligence in this innovative initiative seeks to redefine healthcare diagnostics and emergency response systems.

The primary focus of this paper is to address a pressing concern in both urban and suburban environments – the effective management of traffic to expedite the movement of emergency vehicles, particularly ambulances. During medical emergencies, the swift and unimpeded passage of ambulances is critical for saving lives. Yet, the prevalence of congested traffic conditions[2] and delayed response times poses significant challenges. To surmount these obstacles, our proposal advocates for the integration of artificial intelligence-controlled traffic signals empowered by advanced computer vision technology.

The cornerstone of our approach lies in deploying sophisticated computer vision algorithms. These algorithms are designed to endow traffic signals with the capability to autonomously identify approaching ambulances, thereby providing them preferential treatment. The envisioned system aims to facilitate the rapid passage of ambulances through intersections and congested traffic areas, ensuring timely and efficient emergency response.

The seamless execution of this project not only underscores the transformative potential of data science and artificial intelligence but also emphasizes our commitment to addressing real-world

https://doi.org/10.62500/icrtsda.1.1.9

challenges through innovative and multidisciplinary solutions. Through meticulous research, comprehensive data analysis, algorithm development, and practical implementation, this final year project aspires to make meaningful contributions to society by enhancing healthcare diagnostics and refining emergency response systems [3].

By harnessing the power of cutting-edge technologies, we aim to create a symbiotic relationship between healthcare and urban planning, demonstrating how advancements in one domain can catalyze positive changes in another. The interdisciplinary nature of our paper reflects a holistic approach to problem-solving, acknowledging that the challenges we face demand collaborative and innovative solutions.

In essence, this paper is not merely an academic endeavor but a testament to our dedication to societal welfare. It underscores the potential for technological interventions to transcend traditional boundaries and bring about tangible improvements in critical areas such as healthcare and emergency services [4]. Through the successful execution of "AI-Controlled Traffic Signals for Ambulance Detection through Computer Vision," we aspire to set a precedent for leveraging technology for the greater good of humanity.

2. BACKGROUND

Rapidly increasing vehicle count is a crucial measure for cost-effective growth in any nation, as it leads to traffic congestion, waste of energy, time, and environmental pollution. Traditional traffic lights are insufficient to meet the demands of overgrowing cities, as they have specific time intervals for changing from red to green phases. Intelligent Transportation Systems (ITS) have been used to automate traffic lights based on vehicle density, with researchers suggesting different strategies and computerized sensor frameworks to tackle congestion issues [5].

Urban traffic congestion is a major issue in cities, causing time loss and frustration for travelers. To address this, advanced technology and equipment are needed. A structured system analysis methodology was used to analyze existing problems and design new models ust-based techniques. The Intelligent Decision Making System for Urban Traffic Control (IDUTC) was proposed, which uses fuzzy expert systems, artificial neural networks, and fuzzy labels to solve congestion problems. The IDUTC uses multiple cameras and image mosaicing to determine the timing of green and red signals based on road density, addressing congestion in developing regions and high congestion hotspots [6].

The Virginia Department of Transportation (VDOT) conducted a study on the impact of emergency vehicle traffic signal preemption on Route 7 during morning rush hour. The study used the Federal Highway Administration's Traffic Software Integrated System (TSIS) package and the CORSIM simulation model to evaluate the service level and demonstrate the capabilities of the Traffic Research Laboratory (TReL) and the "hardware-in-the-loop" concept. The results showed that signal preemption could reduce the time needed for ambulances to reach a victim or emergency facility, providing faster, life-saving 911 response. The study conducted 200 simulation runs for 10 cases, with the worst-case short-way transition time significantly impacting the system's MOE's. The average 7 corridor travel time for through movement through all three intersections was 2.3×10^9 m/s, with a mean of 2.3×10^9 m/s [7].

The Pakistan National Emergency Departments Surveillance (Pak-NEDS) was a pilot active surveillance initiative conducted in seven major tertiary care emergency departments across six main cities in Pakistan from November 2010 to March 2011. The participating emergency departments included the Aga Khan University (Karachi), Jinnah Post-Graduate Medical Center (Karachi), Mayo Hospital (Lahore), Sandeman Provincial Hospital (Quetta), Lady Reading Hospital (Peshawar), Benazir Bhutto Hospital (Rawalpindi), and Shifa International Hospital (Islamabad). Among these, five hospitals were public, and two were private, all functioning as tertiary care teaching hospitals, with one serving as a referral center. Ethical approval was obtained from each participating hospital [8].

https://doi.org/10.62500/icrtsda.1.1.9

Patient factor comparison between the ambulance and non-ambulance groups was conducted using Pearson's Chi-squared test for categorical variables and independent sample t-test for continuous variables, with a significance level set at 0.05. Additionally, the use of an ambulance was examined as an outcome variable. Univariate and multivariate logistic regression analyses were performed to identify factors associated with ambulance use. In the multivariate model, independent variables included gender, age group, city, hospital type, presenting complaint, and disposition.

Out of the 274,436 patients enrolled in Pak-NEDS, the mode of arrival to the Emergency Department (ED) was documented for 94.9% (n = 260,378). Among these, 4.1% (n = 10,546) arrived via ambulances, while the majority of patients (n = 249,832, 95.9%) used means other than ambulances. This indicates that the overall utilization of ambulance services by patients seeking acute care at major EDs in Pakistan is 1 in 25 patients [9].

A comparison of demographic characteristics between the ambulance and non-ambulance groups is presented in Table 1. In the ambulance group, 63.4% (n = 6,578) were male, while in the non-ambulance group, the male proportion was 60.7% (n = 150,085). The mean age of patients in the ambulance group (38 ± 18.4 years) was significantly higher (p-value < 0.001) compared to the mean age of the non-ambulance group (32.8 ± 14.9 years). The distribution of patients between public and private hospitals was similar in both groups (93.7% vs. 93.9%, p-value 0.347).

Table 1: Comparison of demographics characteristics and outcome of patients between ambulance and non-ambulance groups [8]

Patient characteristics	Ambulance (n = 10546, 4.1%)	Non-ambulance (n = 249832, 95.9%)	p-value	Total (n = 260,378)
	n (%)	n (%)		n(%)
Age in years (mean ± SD)	38 ± 18.4	32.8 ± 14.9	< 0.001	33.1 ± 15.3
Gender (n = 257,684)			< 0.001	
Male	6578 (63.4)	150,085 (60.7)		156,663 (60.8)
Female	3795 (36.6)	97,226 (39.3)		101,021 (39.2)
Age groups (n = 250,034)				
< 5 years	122 (1.2)	3793 (1.6)	< 0.001	3915 (1.6)
5 - 12 years	335 (3.3)	10,057 (4.2)		10,392 (4.2)
13 - 18 years	747 (7.4)	22,053 (9.2)		22,800 (9.1)
19 - 25 years	1761 (17.5)	52,490 (21.9)		54,251 (21.7)
26 - 45 years	4224 (41.9)	109,410 (45.6)		113,634 (45.4)
>45 years	2896 (28.7)	42,146 (17.6)		45,042 (18)
Hospital type (n = 260,378)			0.347	
Public	9883 (93.7)	234,683 (93.9)		244,566 (93.9)
Private	663 (6.3)	15,149 (6.1)		15,812 (6.1)
Presenting complaint group* (n = 230,163)			< 0.001	
Non-injury	7262 (82.8)	247,476 (111.8)		254,738 (110.7)
Injuries	5187 (59.1)	50,589 (22.9)		55,776 (24.2)
Disposition (n = 185,370)			< 0.001	
Discharged from ED	5025 (59)	143,891 (81.4)		148,916 (80.3)
Admitted	2891 (33.6)	26410 (14.9)		29,301 (15.8)
Death in ED	341 (4)	1468 (0.8)		1809 (1.0)
Others**	266 (3.1)	5078 (2.9)		5344 (2.9)

*multiple response variable therefore the total is not be 100%
**includes referred patients, left without being seen, left against medic al advice

Injuries were the presenting complaint in 24.4% (n = 55,776) of all ED visits, with 59.1% (n = 5,187) of ambulance users presenting with injuries. The analysis revealed variations in ambulance use across different cities, with 9.4% of ED patients arriving by ambulance in Karachi compared to 3.4% in Lahore, 2.8% in Peshawar, 2.7% in Quetta, and 1.0% in Rawalpindi/Islamabad (Table 2).

https://doi.org/10.62500/icrtsda.1.1.9

Table 2: Use of ambulance by emergency department patients in differents cities of Pakistan (n = 260, 378) [8]

Cities*	Ambulance group	Non-ambulance group	Total
	n (%**)	n (%**)	n(%***)
Karachi	5807 (9.4)	55,930 (90.5)	61,737 (23.7)
Lahore	1589 (3.6)	43,081 (96.4)	44,670 (17.2)
Peshawar	1578 (2.8)	53,319 (97.1)	54,897 (21.1)
Quetta	912 (2.7)	32,354 (97.3)	33,266 (12.8)
Rawalpindi/ Islamabad	660 (1.0)	65,148 (99.0)	65,808 (25.3)

* Cities variable was created based on the geographical location of participating hospitals; Aga Khan University and Jinnah Post-grad uate Medical Center in Karachi; Mayo Hospital in Lahore, Benazir Bhutto Hospital and Shifa International Hospital in Rawalpindi/Islamabad; Lady Reading Hospital in Peshawar and Sandeman Provincial Hospital in Quetta

**Percentage based on row total

***Percentage based on column total

The most common presenting complaint among ambulance users was head injury, while fever was prevalent among non-ambulance users. Table 3 outlines the top ten presenting complaints in both groups. Within the ambulance use group, injury was the primary reason for ED visits for patients aged under 5 years to those in the 26-45 years age group, whereas patients above 45 years predominantly presented with non-injury complaints. The proportion of admissions was over two times higher among those arriving by ambulance compared to the non-ambulance group (33.6% vs. 14.9%). Approximately 4% of patients in the ambulance group died in the ED (Table 1).

To explore factors related to ambulance use, logistic regression was performed on data available for 154,200 cases (56.2%) (Table 4). Patients in age groups below 45 years were less likely to be transported by ambulance compared to those aged over 45 years (p-value < 0.001), adjusting for gender, cities, hospital type, presenting complaint group, and disposition. Gender's association with ambulance use was not statistically significant in the model after adjusting for other independent variables. The adjusted odds ratio for ambulance use was 3.5 times higher for those with injuries than for those presenting with non-injury complaints (p-value < 0.001).

Table 3: Logistic regression of factors associated with ambulance use [8]

Patient characteristics	Univariate regression			Multivariate regression		
	Unadjusted ORs	95% Confidence interval	p-value	Adjusted ORs*	95% Confidence interval	p-value
Gender						
Female	REF			REF		
Male	1.12	1.1, 1.2	< 0.001	1.0	1.0, 1.1	0.5
Age groups						
> 45 years	REF			REF		
< 5 years	0.5	0.4, 0.6	< 0.001	0.3	0.3, 0.4	< 0.001
5 - 12 years	0.5	0.4, 0.5	< 0.001	0.3	0.3, 0.4	< 0.001
13 - 18 years	0.5	0.4, 0.5	< 0.001	0.4	0.4, 0.5	< 0.001
19 - 25 years	0.5	0.4, 0.5	< 0.001	0.4	0.4, 0.5	< 0.001
26 - 45 years	0.6	0.5, 0.6	< 0.001	0.5	0.4, 0.5	< 0.001
Cities						
Quetta	REF			REF		
Karachi	3.7	3.4, 4.0	< 0.001	3.6	3.2, 4.1	< 0.001
Lahore	1.3	1.2, 1.4	< 0.001	1.6	1.4, 1.8	< 0.001
Rawalpind/Islamabad	0.4	0.3, 0.4	< 0.001	0.3	0.3, 0.4	< 0.001
Peshawar	1.1	1.0, 1.1	0.25	0.6	0.5, 0.7	< 0.001
Hospital type						
Private	REF			REF		
Public	0.9	0.9, 1.0	0.35	2.3	2.1, 2.6	< 0.001
Presenting complaint						
Non-injury	REF			REF		
Injuries	3.2	3.0, 3.3	< 0.001	3.5	3.3, 3.7	< 0.001
Disposition						
Discharged from ED	REF			REF		
Admitted	3.1	3.0, 3.3	< 0.001	3.1	2.9, 3.3	< 0.001
Death in ED	6.7	5.9, 7.5	< 0.001	7.2	6.2, 8.4	< 0.001
Others**	1.5	1.3, 1.7	< 0.001	1.4	1.2, 1.6	< 0.001

OR = odds ratio

*Model constant -4.3

**includes referred patients, left without being seen, left against medic al advice

https://doi.org/10.62500/icrtsda.1.1.9

3. LITERATURE REVIEW

The rise in vehicles has spurred interest in Wireless Sensor Networks (WSNs) for real-time traffic monitoring. Vehicular Sensor Networks (VSNs) show promise for cost-effective urban traffic management. While WSN-based schemes aim to alleviate congestion, challenges like connectivity and energy costs persist, highlighting the need for innovative solutions such as an intelligent traffic cloud with cloud computing [10].

[11] introduces a vision-based system for tracking vehicles at intersections, estimating turning movement counts, speed, and waiting times using motion-based tracking and trajectory analysis with a single camera. Integration of complementary counting modules and a path reconstruction module improves count accuracy. The system's trajectory comparison and path reconstruction modules handle broken trajectories, enhancing accuracy, particularly for right turns. Experimental results demonstrate significant accuracy improvement, with the proposed system employing vehicle detection, tracking, and path labeling techniques such as background subtraction, morphological operations, bipartite graphs, and dynamic models.

[12] gives a model for optimizing cycle length and signal timings at intersections with heavy scooter-vehicle mixed flows, considering scooter maneuverability and queue dynamics. Field data and experiments validate the model, implemented and assessed through before-and-after field analysis, emphasizing the importance of incorporating scooter flow characteristics for effective signal control strategies in mitigating congestion.

Intelligent Traffic Signal Control (ITSC) systems utilize Vehicle-to-Infrastructure (V2I) wireless communication to alleviate traffic congestion. A novel reinforcement learning (RL) algorithm for Partially Detected Intelligent Transportation Systems (PD-ITSC) effectively reduces waiting times at intersections, even with low detection rates. The system optimizes car flow by minimizing waiting times, with performance improving as detection rates increase, demonstrating RL's ability to adapt to varying traffic conditions [13].

[14] develops a new image processing system detects and tracks vehicle rear-lamp pairs in forward-facing color video using a low-cost CMOS camera with Bayer RGB color filter. It segments rear lamps in the HSV color space, pairs them via color cross-correlation symmetry analysis, and tracks them with Kalman filtering. A tracking-based detection stage improves robustness, demonstrating high detection rates, operating distance, and robustness to different lighting conditions and road environments.

[15] introduced an intelligent traffic control system for emergency vehicles using RFID tags and ZigBee modules for wireless communication. It utilizes an RFID reader and GSM module to detect stolen vehicles, adjusting green light durations based on network congestion. Ambulances communicate with traffic controllers via ZigBee to trigger green lights at junctions, offering a solution to India's road congestion challenges with cost-effective wireless technologies.

[16] introduced an aerial remote sensing method for detecting riders' helmet wearing using UAV photography, combining super-resolution reconstruction, LMNet for target detection, and RT3DsAM for feature representation and classification. The approach achieves a mean average precision (mAP) of 91.67% and image classification top1 accuracy (TOP1 ACC) of 94.23%, improving detection accuracy in aerial scenes by addressing pedestrian misunderstanding and incorporating attention modules.

[17] gives a framework for automatic detection of motorcyclists driving without helmets in surveillance videos, employing adaptive background subtraction and convolutional neural networks (CNN). CNN is utilized to identify motorcyclists and detect helmetless riders, achieving a 92.87% detection rate with a low false alarm rate of 0.5% on average. The approach is evaluated on real videos from the CCTV Surveillance Network of Hyderabad City, India, contributing to improved classification performance in helmet violation detection.

https://doi.org/10.62500/icrtsda.1.1.9

A vision-based vehicle tracking system enhances intersection behavior analysis, accurately counting turning movements, estimating speed, and wait time. With a 15% improvement in counting accuracy, it reveals insights into right turn behaviors and waiting times at signalized intersections. Employing trajectory comparison and linear regression, it handles broken trajectories and estimates waiting times. The system includes vehicle detection, tracking, and path labeling using various techniques, contributing to cooperative traffic management for reduced congestion and improved efficiency [11].

[12] introduced a model for optimizing signal timings at isolated intersections with heavy scooter-vehicle mixed traffic flows. It emphasizes the importance of incorporating scooter flow properties for effective signal control strategies, demonstrating a 39.2% reduction in total delay. The study investigates queue formation and traffic flow dynamics, providing a reliable tool for signal design in developing countries' urban areas.

[6] concluded that urban traffic congestion is a major issue in cities, causing time loss and frustration for travelers. To address this, advanced technology and equipment are needed. A structured system analysis methodology was used to analyze existing 10 problems and design new models ust-based techniques. The Intelligent Decision-Making System for Urban Traffic Control (IDUTC) was proposed, which uses fuzzy expert systems, artificial neural networks, and fuzzy labels to solve congestion problems. The IDUTC uses multiple cameras and image mosaicking to determine the timing of green and red signals based on road density, addressing congestion in developing regions and high congestion hotspots.

4. OBJECTIVES

The objectives of the "AI-Controlled Traffic Signals for Ambulance Detection through Computer Vision" project are multifaceted and span across the domains of healthcare, transportation, and technology. The outlined objectives are designed to address specific challenges, leverage technological advancements, and contribute to the betterment of society. Here are the key objectives:

- **Efficient Emergency Response:**
  - Objective: To enhance the efficiency of emergency response systems, particularly for ambulances, by minimizing response times in urban and suburban environments.
  - Rationale: Swift ambulance movement is critical during medical emergencies, and the project aims to mitigate delays caused by traffic congestion through the intelligent control of traffic signals.
- **Ambulance Detection through Computer Vision:**
  - Objective: To develop and implement computer vision algorithms capable of autonomously detecting approaching ambulances based on visual cues and distinctive features.
  - Rationale: By integrating computer vision technology, the project seeks to enable traffic signals to dynamically respond to the presence of ambulances, ensuring their unhindered passage through intersections.
- **Preferential Treatment at Traffic Signals:**
  - Objective: To design an AI-controlled traffic signal system that grants preferential treatment to detected ambulances, adjusting signal timings to facilitate their rapid movement through congested areas.
  - Rationale: The project aims to optimize traffic signal control in real-time, prioritizing emergency vehicles without compromising the overall flow of traffic.
- **Interdisciplinary Integration:**
  - Objective: To showcase the integration of data science, artificial intelligence, and mathematical modeling with urban planning, thereby demonstrating the potential for interdisciplinary collaboration in solving real-world challenges.

https://doi.org/10.62500/icrtsda.1.1.9

- Rationale: The project seeks to bridge the gap between healthcare requirements and urban infrastructure, exemplifying how technology can facilitate a symbiotic relationship between traditionally distinct fields.

➢ **Contribution to Public Well-being:**

- Objective: To contribute to the betterment of society by improving healthcare diagnostics and emergency response systems through the reduction of ambulance response times.
- Rationale: The ultimate goal is to save lives by addressing a critical issue at the intersection of healthcare and transportation, showcasing the potential impact of technology on public well-being.

These objectives collectively form a comprehensive framework for the "AI-Controlled Traffic Signals for Ambulance Detection through Computer Vision" project, reflecting a commitment to technological innovation, interdisciplinary collaboration, and the improvement of emergency response systems for the benefit of society.

5. METHODOLOGY

Designing a complete algorithm for the "Artificial Intelligence Control Signals to Detect Ambulance" project is a complex task that involves multiple steps and components, from data pre-processing to real-time signal control. However, I can provide you with a simplified algorithmic outline to get you started on the coding aspect. You'll need to adapt and expand upon this outline as you work on the project.

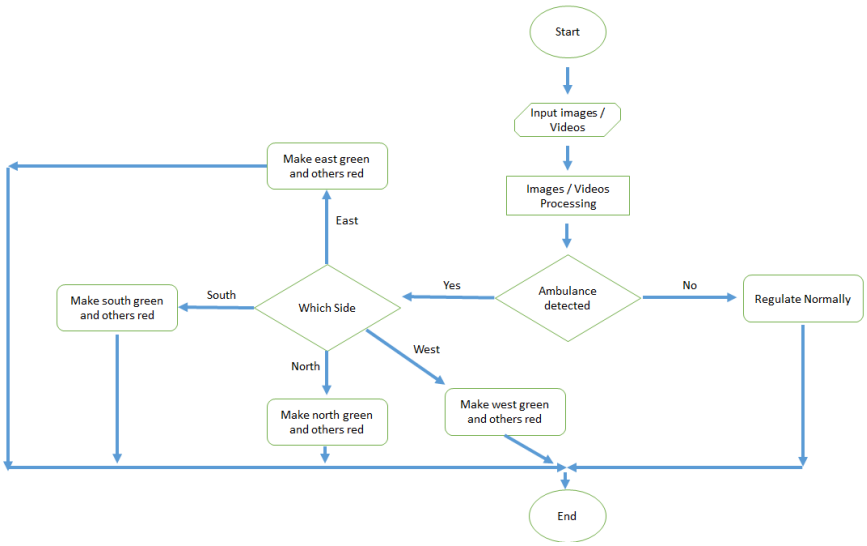

Figure 1: Flow Chart to Working Principle

Data Collection and Preprocessing:

- Gather a dataset of images or videos containing various ambulance scenarios.
- Annotate the dataset to indicate the location of ambulances in each frame (bounding boxes).
- Split the dataset into training and testing subsets.

Data Augmentation:

- Augment training dataset to increase model robustness. Techniques like random rotation, scaling, and flipping can be applied.

https://doi.org/10.62500/icrtsda.1.1.9

Model Training:

- Fine-tune the selected model on your annotated dataset using the chosen deep learning framework.
- Train the model to recognize ambulances within images or video frames.

Real-Time Video Processing:

- Develop a Python script that can capture real-time video feeds from traffic cameras or other sources.
- Implement the object detection model to process each frame of the video stream.

Object Detection Integration:

- Integrate the object detection results into a system that can identify ambulances in real-time.
- Implement logic to track the movement and direction of detected ambulances.

Measure the Distance and Prioritizing:

- If the ambulances are coming from more than one side measure the distance.
- Prioritize the nearest one.

Signal Changing:

- Change the signal to green from which side the shortest distant ambulance is coming making all others to be red.
- If does not detect any ambulance regulate the signals to normal.

Testing and Evaluation:

- Thoroughly test the system using various real-world scenarios, including different lighting conditions, traffic densities, and vehicle types.
- Evaluate the accuracy and efficiency of ambulance detection and traffic signal control.

Optimization and Refinement:

- Continuously optimize your AI model and system for better performance.
- Address any issues or challenges that arise during testing and real-world deployment.

Coding Details:

Language Used:

Python has emerged as the go-to language for machine learning (ML) and data science projects due to its simplicity, versatility, and robust ecosystem of libraries.

One of Python's key strengths in ML is its readability and ease of use. Its syntax is intuitive and concise, making it accessible for both beginners and experienced developers alike. This characteristic promotes faster development cycles, allowing researchers and engineers to focus more on the logic of their algorithms rather than grappling with complex syntax.

Moreover, Python boasts an extensive collection of libraries tailored specifically for ML tasks. These libraries, including NumPy, Pandas, TensorFlow, and PyTorch, provide powerful tools for data manipulation, mathematical computations, and building and training ML models. OpenCV, or cv2 in Python, stands out in this ecosystem for its comprehensive suite of computer vision algorithms and utilities [18].

So in our project we used python as the fundamental tool of coding.

Libraries Used:

Cv2:

https://doi.org/10.62500/icrtsda.1.1.9

In our project, the use of cv2 was instrumental in converting videos into frames per second. This process is fundamental in numerous computer vision applications, including action recognition, object detection, and surveillance systems. By breaking down videos into individual frames, we gain granular control over the temporal aspects of the data, enabling us to extract meaningful patterns and features. After converting into the frame per second we used these images to label the ambulances through an online application named as Labelimg.

Figure 2: Extracted unlabeled ambulance images

After converting into the frame per second we used these images to label the ambulances through an online application named as Labelimg.

Figure 3: Extracted labeled ambulance images

TensorFlow:

Also, we utilized the TensorFlow library to train a model for ambulance detection, a critical task in various applications like traffic management and emergency response systems. TensorFlow's high-level interface streamlined the process of designing, training, and deploying custom neural network architectures tailored to our specific task. Leveraging its support for deep learning, we constructed sophisticated convolutional neural networks (CNNs) suitable for detecting ambulances within images. Post-training, we evaluated the model's performance on a separate test dataset, ensuring accuracy and reliability. Finally, the TensorFlow model was seamlessly integrated into our application

https://doi.org/10.62500/icrtsda.1.1.9

for real-time ambulance detection, showcasing its practical utility and effectiveness in addressing real-world challenges.

The Python program utilizes OpenCV to capture images from all four sides of the traffic signal. Each captured image undergoes ambulance detection using pre-trained models like YOLO or SSD. If an ambulance is detected in any image, the normal signal process is interrupted, and the signal from that side turns green for 45 seconds, controlled by time. If no ambulance is detected, the program continues with the regular signal routine, cycling through each side's signal phases with appropriate time intervals [19].

Steps:

- Converting videos to images by cv2.
- Labeling images for ambulances by an online resource labelImg tool.
- Training the data using Tensor Flow in Google Colab.
- Testing the Data.
- Implementing the code to change the traffic signals.

6. RESULTS

The system underwent extensive testing in diverse traffic conditions, leveraging a dataset of approximately 27,000 images extracted from 15 half-hour videos. Around 1,000 ambulance images were meticulously separated for training. This dataset was divided into training, testing, and evaluation subsets, with the model demonstrating promising performance, accurately identifying ambulances in 117 out of 150 evaluation images. Upon successful training, the system was deployed in real-world scenarios, effectively prioritizing ambulances at intersections by interrupting normal traffic signal operations. This comprehensive evaluation, combining simulation and real-world testing, showcased the system's efficacy in enhancing emergency response times and traffic flow efficiency.

To assess the project's accuracy, precision, recall, and F1 score were calculated. Precision measures the ratio of correctly identified ambulances to all predicted positives. Recall gauges the proportion of true positives to all actual positives. The F1 score, a harmonic mean of precision and recall, offers a balanced evaluation. With 117 ambulances correctly identified out of 150 evaluated images, precision and recall both approximate 0.78. Consequently, the F1 score reaches about 0.79, signifying robust performance in ambulance detection.

- Total evaluated images: 150
- Total correctly detected ambulances (TP): 117
- Total images incorrectly identified as ambulances (FP): 33
- Total ambulances missed (FN): 33

Precision:

$$\mathbf{Precision} = \frac{\mathbf{TP}}{\mathbf{TP} + \mathbf{FP}}$$

$$\mathbf{Precision} = \frac{\mathbf{117}}{\mathbf{117} + \mathbf{33}}$$

$$\mathbf{Precision} = \mathbf{0.78}$$

Recall:

$$\mathbf{Precision} = \frac{\mathbf{TP}}{\mathbf{TP} + \mathbf{FP}}$$

$$\mathbf{Precision} = \frac{\mathbf{117}}{\mathbf{117} + \mathbf{33}}$$

https://doi.org/10.62500/icrtsda.1.1.9

$$\textbf{Precision} = 0.78$$

Recall:

$$\textbf{Precision} = \frac{\textbf{TP}}{\textbf{TP} + \textbf{FN}}$$

$$\textbf{Precision} = \frac{117}{117 + 33}$$

$$\textbf{Precision} = 0.78$$

F1 Score:

$$\textbf{F1 Score} = 2 * \frac{\textbf{Precision} * \textbf{Recall}}{\textbf{Precision} + \textbf{Recall}}$$

$$\textbf{F1 Score} = 2 * \frac{0.78 * 0.78}{0.78 + 0.78}$$

$$\textbf{F1 Score} = 0.79$$

Therefore, based on these calculations, the precision, recall, and F1 score of the project are approximately 0.78, 0.78, and 0.79 respectively, indicating a reasonably good performance in identifying ambulances.

7. CONCLUSION

The proposed intelligent traffic signal system presents a promising solution to prioritize emergency vehicles at intersections. By leveraging computer vision technology, the system achieves a commendable detection accuracy of 79% and effectively adapts traffic signal operations to facilitate the passage of ambulances. Future enhancements may include refining the detection algorithm to improve accuracy further and expanding the system's capabilities to accommodate additional emergency vehicle types. Overall, the system contributes to improving road safety and emergency response effectiveness in urban environments.

REFERENCES

[1] M. Yousef Shaheen, “Article title: Applications of Artificial Intelligence (AI) in healthcare: A review Applications of Artificial Intelligence (AI) in healthcare: A review,” 2021, doi: 10.14293/S2199-1006.1.SOR-.PPVRY8K.v1.

[2] Ed. Cutrell and ACM Digital Library., Proceedings of the 2nd ACM Symposium on Computing for Development. ACM, 2012.

[3] M. Srivastava, S. Suvarna, A. Srivastava, and S. Bharathiraja, “Automated emergency paramedical response system,” Health Inf Sci Syst, vol. 6, no. 1, Dec. 2018, doi: 10.1007/s13755-018-0061-1.

[4] IEEE Communications Society, International Symposium on Future Information and Communication Technologies for Ubiquitous HealthCare 1 2013.07.01-03 Jinhua, and Ubi-HealthTech 1 2013.07.01-03 Jinhua, 2013 First International Symposium on Future Information and Communication Technologies for Ubiquitous HealthCare (Ubi-HealthTech) 1-3 July 2013, Jinhua.

[5] P. A. Mandhare, V. Kharat, and C. Y. Patil, “Intelligent Road Traffic Control System for Traffic Congestion A Perspective,” International Journal of Computer Sciences and Engineering, vol. 6, no. 7, pp. 908–915, Jul. 2018, doi: 10.26438/ijcse/v6i7.908915.

https://doi.org/10.62500/icrtsda.1.1.9

[6] Y. P. Singh, “Analysis and Designing of Proposed Intelligent Road Traffic Congestion Control System with Image Mosaicking Technique,” 2013. [Online]. Available: www.irjcjournals.org

[7] ---==c-C-------, “Evaluation of Emergency Vehicle Signal Preemption on the Route 7 Virginia Corridor,” 1999.

[8] N. Zia et al., “Ambulance use in Pakistan: An analysis of surveillance data from emergency departments in Pakistan,” BMC Emerg Med, vol. 15, no. 2, Dec. 2015, doi: 10.1186/1471-227X-15-S2-S9.

[9] M. U. Mir et al., “The Pakistan National Emergency Department Surveillance Study (Pak-NEDS): Introducing a pilot surveillance,” BMC Emerg Med, vol. 15, no. 2, Dec. 2015, doi: 10.1186/1471-227X-15-S2-S1.

[10] K. Nellore and G. P. Hancke, “A survey on urban traffic management system using wireless sensor networks,” Sensors (Switzerland), vol. 16, no. 2. MDPI AG, Jan. 27, 2016. doi: 10.3390/s16020157.

[11] M. S. Shirazi and B. T. Morris, “Vision-Based Turning Movement Monitoring:Count, Speed & Waiting Time Estimation,” IEEE Intelligent Transportation Systems Magazine, vol. 8, no. 1, pp. 23–34, Mar. 2016, doi: 10.1109/MITS.2015.2477474.

[12] C. L. Lan and G. L. Chang, “A Traffic Signal Optimization Model for Intersections Experiencing Heavy Scooter-Vehicle Mixed Traffic Flows,” IEEE Transactions on Intelligent Transportation Systems, vol. 16, no. 4, pp. 1771–1783, Aug. 2015, doi: 10.1109/TITS.2014.2376292.

[13] R. Zhang, A. Ishikawa, W. Wang, B. Striner, and O. K. Tonguz, “Using Reinforcement Learning with Partial Vehicle Detection for Intelligent Traffic Signal Control,” IEEE Transactions on Intelligent Transportation Systems, vol. 22, no. 1, pp. 404–415, Jan. 2021, doi: 10.1109/TITS.2019.2958859.

[14] R. O’Malley, E. Jones, and M. Glavin, “Rear-lamp vehicle detection and tracking in low-exposure color video for night conditions,” IEEE Transactions on Intelligent Transportation Systems, vol. 11, no. 2, pp. 453–462, Jun. 2010, doi: 10.1109/TITS.2010.2045375.

[15] R. Sundar, S. Hebbar, and V. Golla, “Implementing intelligent traffic control system for congestion control, ambulance clearance, and stolen vehicle detection,” IEEE Sens J, vol. 15, no. 2, pp. 1109–1113, Feb. 2015, doi: 10.1109/JSEN.2014.2360288.

[16] S. Chen, J. Lan, H. Liu, C. Chen, and X. Wang, “Helmet Wearing Detection of Motorcycle Drivers Using Deep Learning Network with Residual Transformer-Spatial Attention,” Drones, vol. 6, no. 12, Dec. 2022, doi: 10.3390/drones6120415.

[17] IEEE Computational Intelligence Society, International Neural Network Society, and Institute of Electrical and Electronics Engineers, IJCNN 2017 : the International Joint Conference on Neural Networks.

[18] S. Raschka, J. Patterson, and C. Nolet, “Machine learning in python: Main developments and technology trends in data science, machine learning, and artificial intelligence,” Information (Switzerland), vol. 11, no. 4. MDPI AG, Apr. 01, 2020. doi: 10.3390/info11040193.

[19] D. Demirović and A. Šerifović-Trbalić, “Performance of some image processing algorithms in TensorFlow.” [Online]. Available: http://docs.nvidia.com/cuda/

https://doi.org/10.62500/icrtsda.1.1.10

Proc. 1st International Conference on Recent Trends in Statistics and Data Analytics
Air University Islamabad, Pakistan – May 9, 2024, Vol. 1, pp. 87-94

SKIN CANCER DETECTION AND CLASSIFICATION BY USING DEEP LEARNING. FPS AND ACCURACY COMPARISON OF CUSTOM MODEL, RESNET 18 AND ALEXNET

Ismat Saira Gillani[1], Muhammad Arslan[2], Muhammad Rizwan Munawar and Muhammad Talha [4]
[1]Department of Computer Science, Columbus State University, USA, [2] Department of Creative Technologies, Air University, Pakistan,University, Pakistan, [3] Department of Computer Science, COMSATS University, Pakistan, [4] Department of Electrical Engineering, GC University Faisalabad, Pakistan

ABSTRACT

A recent study by the International Agency for Research on Cancer (IARC) predicts a 50% rise in yearly cancer cases by 2040, with one in five Americans facing a diagnosis in their lifetime. UV overexposure is the main cause of skin cancer, often hard to detect early due to its similarities. Recent tech advances aid detection, but challenges persist. Here, we introduce a deep learning model for skin cancer detection, outperforming prior methods like ResNet and AlexNet in accuracy and speed. Our model demands fewer features and achieves State of the Art results. Find the code at: https://github.com/RizwanMunawar/skin-cancer-binary-classification-computer-vision-

KEYWORDS: Deep learning, Object Detection, Feature Extraction, Network Architecture

1. INTRODUCTION

One of the most prevalent cancers in the last ten years is skin cancer [1]. More than 5 million new cases are identified every year in the United States. Every fifth Americans will be diagnosed with cancer in their lifetime. It makes sense to think of skin cancer as the most prevalent type of cancer in people since it mostly affects the skin, which is the largest organ in the body. Melanoma and non-melanoma skin cancer are the two main groups into which it is typically divided. A dangerous, uncommon, and fatal form of skin cancer is melanoma [2]. Even though the reported cases for melanoma is very low, the death ratio in those cases is very high. So, it won't be wrong to declare this a very dangerous and terminal disease that needs much attention when it comes to detection and treatment. Melanocytes are the cells where melanoma grows. It begins when normal melanocytes start to proliferate uncontrollably and form a malignant tumor. It can grow in any part of the body and put an impact. It typically develops on the hands, neck, face, lips, and other exposed parts to the sun's rays. Melanoma-type malignancies can only be treated if they are discovered early; if not, they tend to extend towards other parts of the body which causes the victim to suffer a torturous death [3].

The most crucial factor for successful treatment of this fatal disease is the early diagnosis. Normally, biopsy and histopathological examination are used for the diagnosis of melanoma. However, they are quite a time consuming and painful [4]. Alternatively, computer vision-based solutions were proposed for the detection of this type of cancer. Earlier research in CV-based methods was very limited and showed the results with lesser accuracy as the skin lesion due to different diseases show a lot of similarities. However, recent studies of deep learning methods for cancer detection have proved themselves to be game changer.

https://doi.org/10.62500/icrtsda.1.1.10

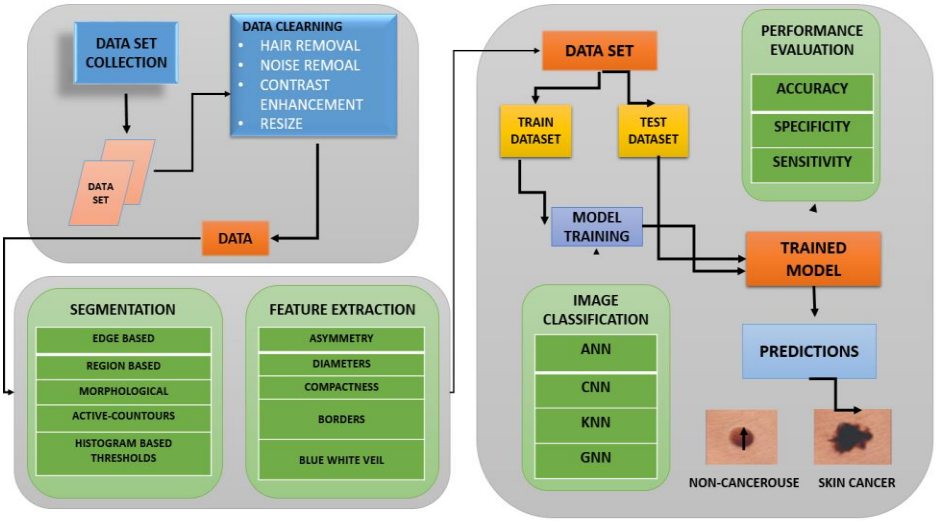

Figure 1: General procedure followed in skin cancer detection [5]

The general approach used in skin cancer detection is to collect the image, preprocess it, segment the obtained preprocessed image, extract the desired feature, and classify it (Figure 1).

2. RELATED WORK

Malignant or non-malignant skin cancers are both possible. Skin malignancies that are not melanoma include basal cell carcinomas and squamous cell carcinomas. Skin cancers that are not melanomas are rarely fatal, whereas melanomas are. Melanoma can penetrate and grow deeper into the skin and can also spread to other parts of the body if it is not treated early and removed in a timely manner. When it comes to one's own health, the consequences of a late diagnosis of skin cancer can be very serious [6]. Over the years, several different techniques have been used for this purpose.

1.1 **CNN Based Solution**

CNN based solution is done in four steps. First, the image is fed to the pre-processing layer where all the noisy artifacts are removed for better performance. Then patch extraction is done in the next two steps. Afterward, those patches are fed to the CNN which analyzes the patch to extract the features and structure. Next, the output is fed to the fully connected layers which lead to the class label, 0 or 1, at the end [7]. The method demonstrated an accuracy of 98.5% (Figure 2).

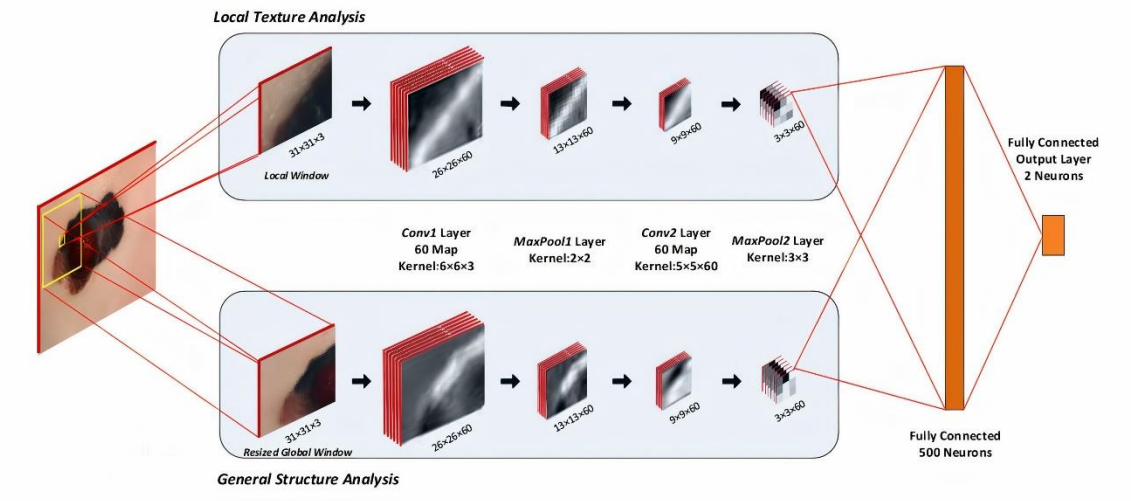

https://doi.org/10.62500/icrtsda.1.1.10

Figure 2: Architecture of proposed CNN for Skin Cancer Detection [7]

1.2 **VGG-16**

While 166 tumor photos were recorded with a Lumix SZ1 camera in [8]. By adjusting the contrast, these photographs were changed to create 5000 new images. On those images, the convolutional neural network VGG-16 was trained. The Support Vector Machine (SVM) classifier is trained using feature vectors produced by this train network. SVM accurately predicts the tumor's location 89.5% of the time.

1.3 **A Hybrid Neural Network (ResNet-18, AlexNet & VGG-16)**

Another solution comprises of three types of neural networks, i.e. ResNet-18, AlexNet and VGG-16. A fully automatic computerized system for classifying skin lesions was proposed, and it makes use of optimal deep features from various established CNNs and from various levels of abstraction. As deep feature generators, three pre-trained deep models AlexNet, VGG16, and ResNet-18 were employed (Figure 3). Support vector machine classifiers are then trained using the retrieved features. The classifier outputs are combined in a final step to produce a classification. The proposed method is demonstrated to achieve very good classification performance when tested on the 150 validation images from the ISIC 2017 classification challenge, yielding an area under the receiver operating characteristic curve of 83.83% for melanoma classification and of 97.55% (Table 1) for seborrheic keratosis classification [9].

Figure 3: Hybrid Model Architecture [9]

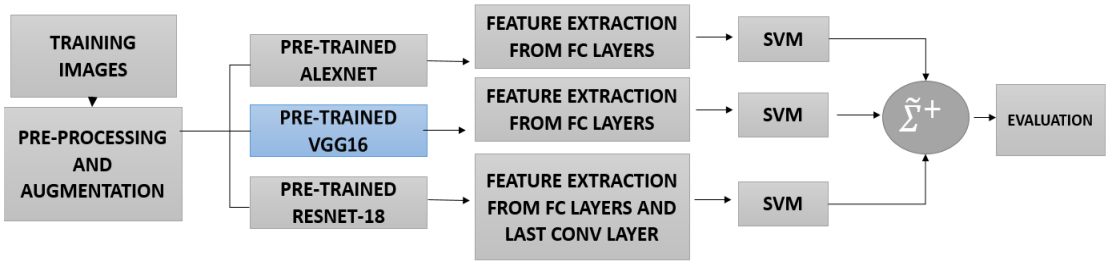

Table 1: Experiments of ISIC 2017 Validation Dataset [9]

network	feature layers	MM AUC	SK AUC	avg. AUC
AlexNet	FC8	80.67	94.95	87.81
AlexNet	all FC	82.81	96.65	89.73
VGG16	FC8	82.61	90.94	86.78
VGG16	all FC	82.06	95.46	88.76
ResNet-18	FC	81.00	91.93	86.47
ResNet-18	FC + last convol. layer	82.81	94.22	88.51
AlexNet + VGG16 fusion	all FC	83.56	97.05	90.30
AlexNet + ResNet-18 fusion	all FC	83.53	97.05	90.29
VGG16 + ResNet-18 fusion	all FC	83.69	95.97	89.83
fusion of all networks	all FC	**83.83**	**97.55**	**90.69**

3. METHOD USED

In this paper, a custom trained Neural Network was used to detect skin cancer requiring the least network layers and features as compared to the previously used networks and demonstrating

https://doi.org/10.62500/icrtsda.1.1.10

results very close to the State of the Art models. The custom model showed the highest FPS as compared to ResNet-18 and AlexNet.

4. NETWORK ARCHITECTURE

Our custom model shows the SOTA results in terms of FPS as compared to previously used models like ResNet18 and AlexNet while showing the result near the SOTA accuracy. The model is comprised of only 4 layers of Conv2D + 2x2 Max pooling to extract the features and then the output is fed to the fully convolutional layer to flatten it. Afterward, the sigmoid function is used to make the classification into the output labels. The model takes the least number of layers against ResNet-18 and AlexNet models, hence, is the lightest model among them maintaining an accuracy of 85%.

Figure 4: Network Architecture of Custom Model

We are using four 2D convolutional layers with a kernel size of 3 x3 each followed by 2 x2 max pooling layer to attain the geometric features like size and shape of the lesion on the skin and then those features are fed to the next layer to flatten the features before they can be used for the classification purposes using a sigmoid function. ReLU function has been used in each layer of the Conv2D to generate the non-linearity.

5. RESULTS: COMPARISON BETWEEN CUSTOM MODEL AND RESNET-18 & ALEXNET

We applied pre-trained models like AlexNet and ResNet-18 to the same dataset to make a comparison of how much they differ in terms of FPS and speed. We also compared the Receiver operating characteristics (roc) and Area under the Curve (AUC) of these models. It was observed that our model displayed the highest FPS and speed yielding very reasonable accuracy.

5.1. FPS and Speed Comparison

When applied, ResNet-18 showed the least FPS Speed of around 17. Whereas, AlexNet showed the second best FPS speed of close to 25. However, our model demonstrated the highest Frames per second of 38 FPS (Figure 5).

https://doi.org/10.62500/icrtsda.1.1.10

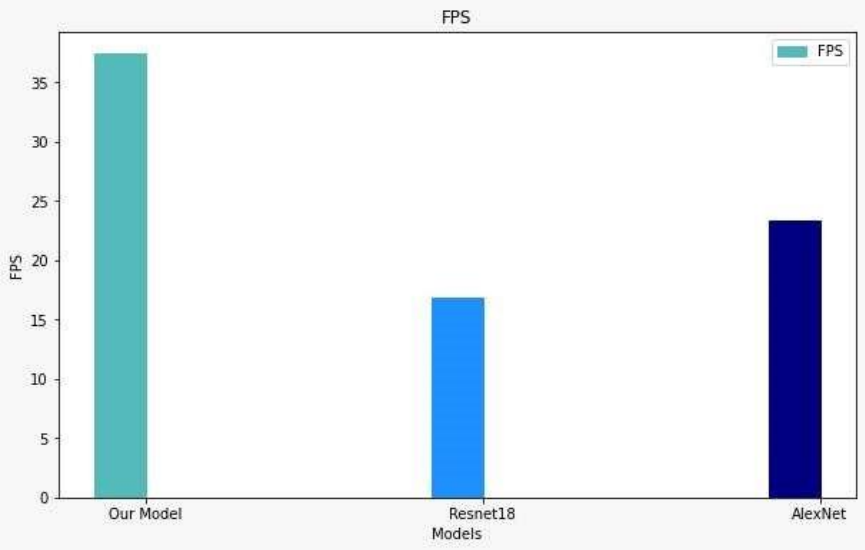

Figure 5: FPS Comparison between ResNet-18, AlexNet and Our Model

Alternatively, Our model displays the least processing time followed by AlexNet. ResNet-18 shows the highest processing time (Figure 6).

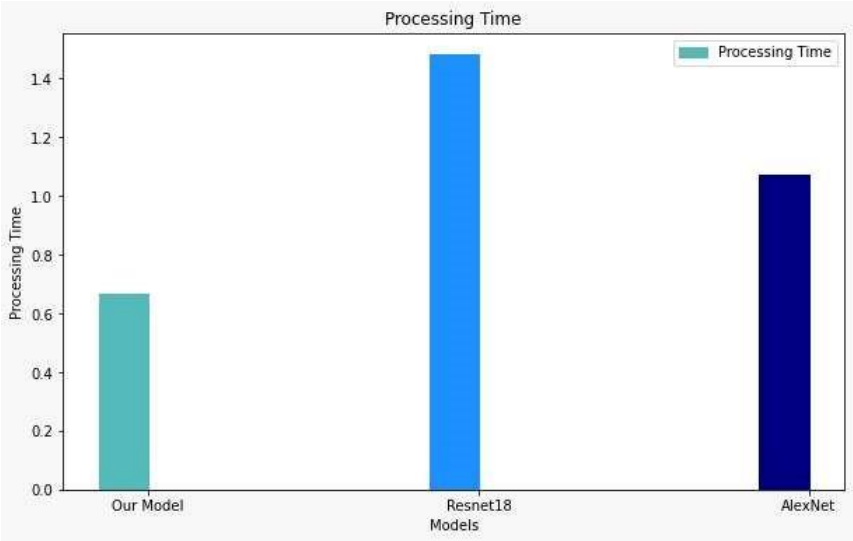

Figure 6: Processing Time Comparison between ResNet-18, AlexNet and Our Model

5.2. Precision & Recall Comparison

The area under precision-recall curve of class 0 was 0.952 against that of class 1 was 0.915 (Figure 7). Whereas, ResNet-18 and AlexNet model showed values slightly greater than our model (Figure 8).

https://doi.org/10.62500/icrtsda.1.1.10

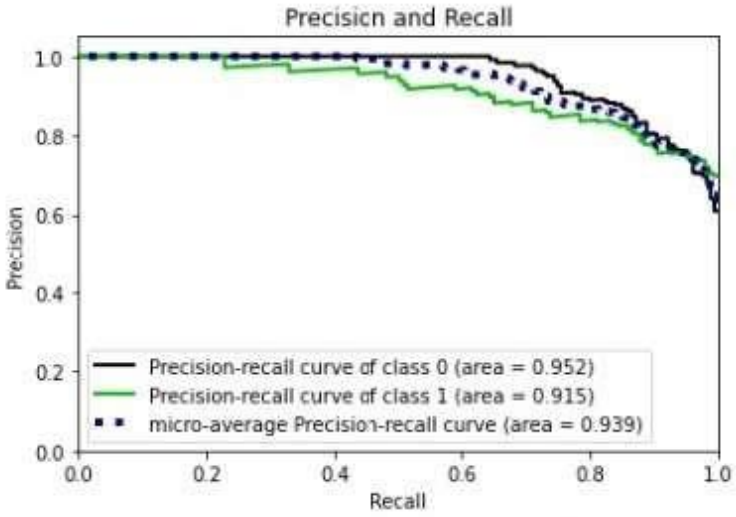

Figure 7: Precision and Recall for Our Model

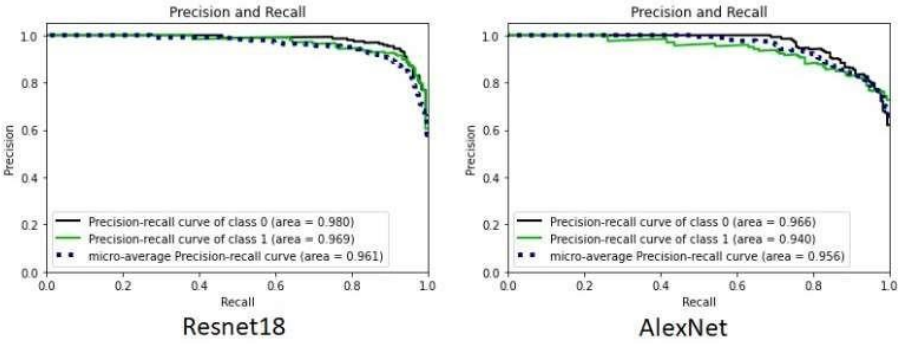

Figure 8: Precision and Recall Comparison between ResNet-18 & AlexNet

5.3. ROC - AUC Comparison

The area under the ROC-AUC curve of our custom model displays the value (0.94) slightly lower than that of other models, 0.98 and 0.95 for ResNet-18 and AlexNet respectively (Figure 9, Figure 10).

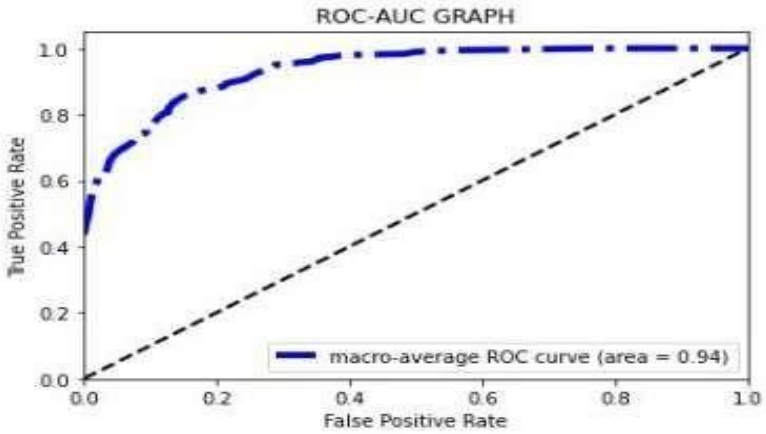

Figure 9: ROC – AUC Graph for Our Model

https://doi.org/10.62500/icrtsda.1.1.10

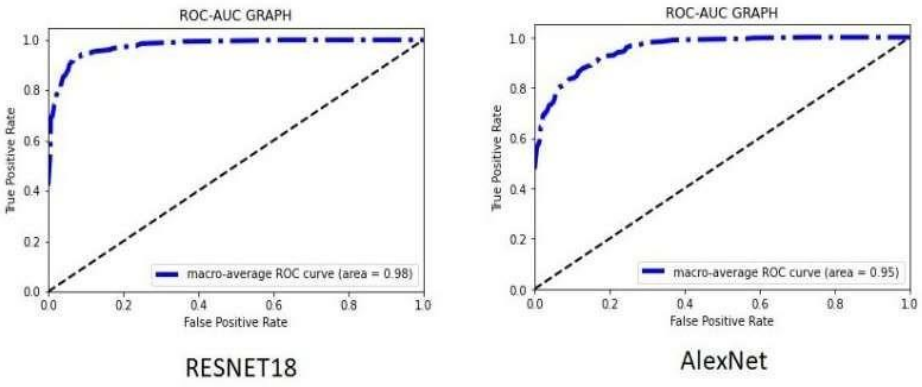

Figure 10: ROC - AUC Comparison between ResNet-18 & AlexNet

5.4. Accuracy vs Loss Comparison

Our model shows the accuracy (85%) comparable to the ResNet-18 and AlexNet which demonstrates the accuracy of 91% and 87% respectively.

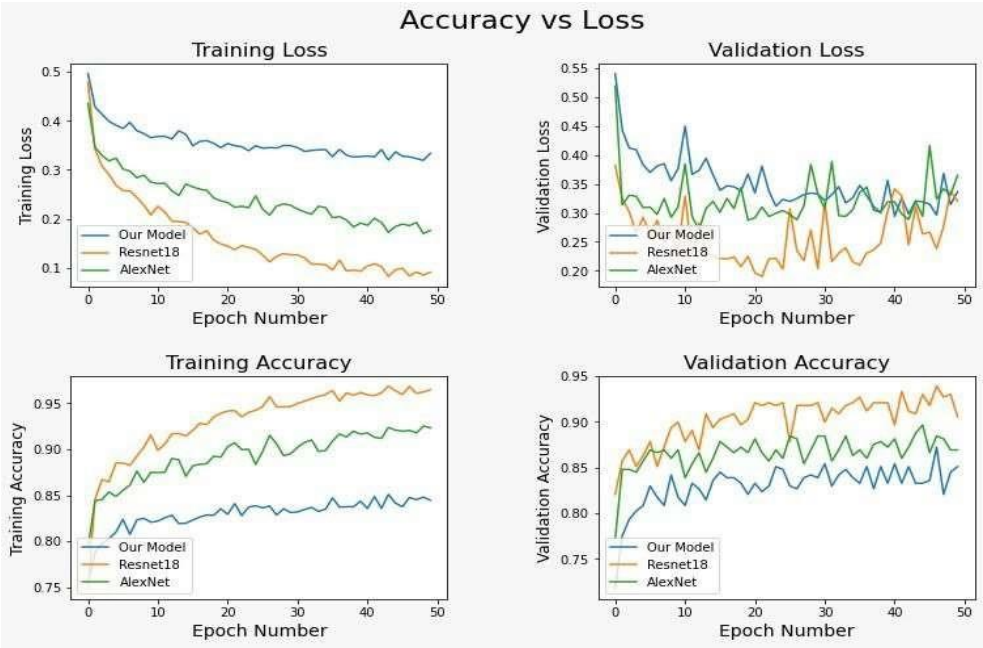

Figure 11: Accuracy Vs Loss Comparison

6. CONCLUSION

Skin cancer is one of the most fatal diseases which cause human death if not detected and treated early. Doctors use methods like a biopsy to detect cancer however it is very time consuming and not comfortable. On the other hand, deep learning models have shown a significant edge when it comes to the detection of lesion that has the potential of turning into melanoma cancer. ResNet and AlexNet models have been used to detect the cancerous lesion however they require several convolutional layers to work properly. Our model uses the least number of convolutional layers making it the lightest model among the above-mentioned models. However, its accuracy is still closest to the famous models like ResNet-18 and AlexNet. Our model also shows the highest FPS rate and lowest processing time for detection.

https://doi.org/10.62500/icrtsda.1.1.10

7. FUTURE WORK

Our model is the lightest among all the famous pre-trained models and shows high accuracy. This lightweight and scalable method can be deployable on mobile devices and has the potential for significant clinical impact, including augmenting medical decision-making for dermatologists. We are also planning to add a microscopic camera to get the images of the patient's infected skin area in real time and the processing can be done on the Jetson chip, the patient can then be informed with the help of an online portal, email or, SMS. We are planning to build up a database for the diagnosis record of all the patients in a hospital/ medical facility.

REFERENCES

[1] Rehan Ashraf, Sitara Afzal, Attiq Ur Rehman, Sarah Gul., Region-of-Interest Based Transfer Learning Assisted Frame work for Skin Cancer Detection.

[2] Elgamal M. Automatic Skin Cancer Images Classification.

[3] Muhammad Qasim Khan, Ayyaz Hussain, Classification of Melanoma and Nevus in Digital Images for Diagnosis of Skin Cancer.

[4] N. Codella, Q.-B. Nguyen, S. Pankanti, D. Gutman, B. Helba, A. Halpern and J. Smith, Deep learning ensembles for melanoma recognition in dermoscopy images.

[5] Mehwish Dildar 1, Shumaila Akram 2, Muhammad Irfan , Skin Cancer Detection: A Review Using Deep Learning Techniques.

[6] Brij Rokad, Dr. Sureshkumar Nagarajan, Skin Cancer Recognition using Deep Residual Network.

[7] Jafari, N. Karimi, E. Nasr-Esfahani, S. Samav, Skin lesion segmentation in clinical images using deep learning. In Pattern Recognition.

[8] Kassem , Hosny , Robertas, A Non-invasive 2D Digital Imaging Method for Detection of Surface Lesions Using Machine Learning.

[9] Amirreza Mahbod, Gerald Schaefer, Chunliang Wang, SKIN LESION CLASSIFICATION USING HYBRID DEEP NEURAL NETWORKS.

[10] IS Gillani1, M Rizwan Munawar, Yolov5, Yolo-x, Yolo-r, Yolov7 Performance Comparison: A Survey .

https://doi.org/10.62500/icrtsda.1.1.11

Proc. 1st International Conference on Recent Trends in Statistics and Data Analytics
Air University Islamabad, Pakistan – May 9, 2024, Vol. 1, pp. 95-99

MRI U-Net-Based Semantic Segmentation for Enhanced Brain Tumor Diagnosis

Muhammad Arslan and Ammara Nawaz Cheema

Department of Mathematics, Air University, Main Campus, Islamabad

ABSTRACT

Brain tumors are a significant global health challenge, with high mortality rates. Accurate diagnosis is crucial for treatment efficacy and patient prognosis planning. Magnetic resonance imaging (MRI) provides a detailed brain structure that forms the basis for tumor diagnosis; however, advanced analytical approaches are required. This study introduces a refined semantic image segmentation of brain tumors from 526 × 526 pixels of MRI images using a methodology that leverages U-Net Convolutional neural networks (CNN) architecture. This specialized approach aims to enhance the efficiency of brain tumor diagnostics using MRI scans.

In our investigation, we applied the U-Net architecture to analyze the MRI data from a cohort of 61 patients. Employing Power BI for comprehensive data analysis, we analyzed 38% of patients' deaths. These research outcomes showcase U-Net's accuracy in segmenting brain tumors, facilitating informed clinical decision-making with clear and reliable imaging results. This study aimed to develop a user-friendly application using this model to provide early diagnostic support and potentially reduce mortality rates.

1. INTRODUCTION

Automatic brain tumor segmentation is vital for disease quantification, localization, and treatment planning. Accurate identification and precise segmentation of brain tumors are indispensable for effective medical image analysis. Manual segmentation is time-consuming and prone to human variability. According to previous reports, brain tumors are the 10th leading cause of mortality among adults and children of both genders in developed countries [1]. The significance of a precise diagnosis and treatment cannot be overstated. Thus, enhancing patient outcomes and diminishing mortality rates relies on accurate diagnosis and treatment of brain tumors.

The brain comprises several cell types, each with unique characteristics. Magnetic Resonance Imaging (MRI) data can be intricate and complicated by noise, necessitating the expertise of trained professionals for precise interpretation and analysis. Therefore, there is an urgent need for automated and accurate techniques for brain tumor segmentation that can aid medical experts in devising effective prognostic plans.

The proposed segmentation model offers valuable tools for medical professionals to enhance prognosis planning, predict tumor location, and perform segmentation. These promising results enable accurate and effective early treatment of affected gliomas. This study examined the application of U-Net for medical image segmentation of cancerous brain tissue. This study aimed to develop a web-based application that leverages open-source tools to perform brain tumor segmentation using a deep-learning mechanism to enhance medical decision-making and improve patient outcomes.

2. METHODOLOGY

Data Collection

The Cancer Imaging Archive (TCIA) is the source of the Low-Grade Glioma Cancer Genome Atlas (TCGA) dataset available in Kaggle. It is named "llg-mribrats" and its source is GitHub (github.com/mecxlan/TCGA_LGG_MriBraTS) collected from Case Western Reserve University and

https://doi.org/10.62500/icrtsda.1.1.11

Duke University, which is openly available for research. The dataset was obtained from The Cancer Imaging Archive (TCIA), which contains 61 patients' MRI images and binary masks. These 4,472 images were in the TIFF format with 256 height, 256 width, and RGB channels per image. The 2,236 images were MRI scans, and the 2,236 binary masks were the labels. The corresponding manual FLAIR abnormality segmentation masks in binary are 1-channel images.

The dataset was organized into 61 folders, each named after the patient's case ID and containing axial view MR images with a specific naming convention and corresponding masks with a _mask suffix. The availability of genomic cluster data for each patient further enhances the value of the dataset for research purposes.

Data Preprocessing and Cleaning

The comma-separated value (CSV) file comprised 61 patients and 18 categorical data columns. The preprocessing steps involved data cleaning by dropping unnecessary columns and the missing categorical values were replaced with the mode. The image data were analyzed along with the raw.csv, and best-fit categories were assigned. After analysis, the processed data were saved in a processed.csv file.

Data Preprocessing

Data Splitting

The dataset was split into 80 % data for training the model for development, 10 % for fine-tuning the model's hyperparameters, and 10 % for evaluating the model's performance or unseen data and reporting the results.

Model Compilation and Training

U-Net Architecture

The proposed brain tumor segmentation approach uses U-Net convolutional neural network architecture. U-Net is widely used for semantic segmentation in biomedical imaging and is known for its ability to capture local and global features, such as cell tracking.

In addition, the decoder receives skip connections from the corresponding layers of the encoder, allowing the model to combine low-level spatial details with high-level semantic information for precise segmentation. Finally, in the last layer, a single 1×1 convolution filter with a sigmoid activation function outputs the segmentation map, where each pixel represents the probability of belonging to a brain tumor.

The U-Net model was compiled using a custom Dice loss function and optimized using the AdaMax optimizer. Training was conducted using callbacks for model checkpointing and early stopping to prevent overfitting. The model was evaluated on the training, validation, and test sets using the metrics accuracy, Dice coefficient, and Intersection over Union(IoU).

Batch Normalization

Batch Normalization (BN) is a widely used technique in deep learning architectures like U-Net for 2D biomedical semantic segmentation. In the context of the U-Net algorithm, the input and output of the BN layer are four-dimensional tensors.

Specifically, it subtracts the mean activation μ_c from all input activations in channel c. The mean is calculated as $\mu_c = \frac{1}{|\mathcal{B}|}\Sigma_{b,x,y} I_{b,c,x,y}$, where B contains all activations in channel c across all features b in the entire mini-batch and all spatial x, y locations. Subsequently, BN divides the centered activation by the standard deviation σ_c, which is calculated analogously, plus a small value for numerical stability. During testing, running averages of the mean and variances are used.

https://doi.org/10.62500/icrtsda.1.1.11

Accuracy

$$Accuracy = \frac{TP + TN}{TP + TN + FP + FN}$$

Dice Coefficient

$$Dice = \left(\frac{2 \times TP}{2 \times TP + FP + FN}\right) = \frac{2 \times |A \cap B|}{|A| + |B|}$$

A represents the predicted segmentation mask.
B represents the ground truth segmentation mask.
$|A \cap B|$ denotes the number of overlapping pixels between the predicted and ground truth masks.
$|A|$ and $|B|$ represent the total number of pixels in the predicted and ground-truth masks.

IoU (Intersection over Union) Coefficient

$$IoU(y_{true} \cap y_{pred}) = \frac{|y_{true} \cap y_{pred}|}{|y_{true} \cup y_{pred}|}$$

y_{true}: the ground truth segmentation mask
y_{pred}: is the expected segmentation mask

Table 1: Model hyperparameters for brain tumor segmentation

Hyperparameter	Value
Optimizer	AdaMax
Learning Rate	0.001
Loss Function	Dice Loss
Batch Size	40
Epochs	120
Metrics	Accuracy, IoU Coefficient, Dice Coefficient

3. RESULTS AND COMPARISON

The evaluation results demonstrate the effectiveness of the U-Net model in accurately segmenting brain tumors. The model achieved high accuracy and a Dice coefficient, indicating its proficiency in delineating tumor regions. The IoU metric further confirmed the ability of the model to capture the overlap between the predicted and ground-truth masks.

https://doi.org/10.62500/icrtsda.1.1.11

Visual Analysis of Original, Mask, and Predicted Images

U-Net Version 1

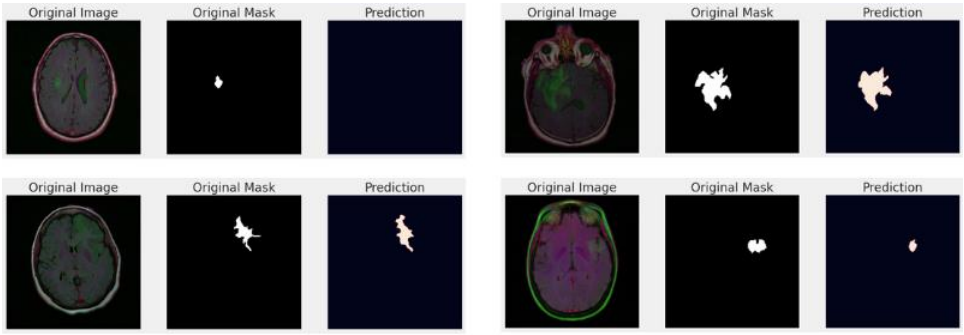

U-Net Version 2

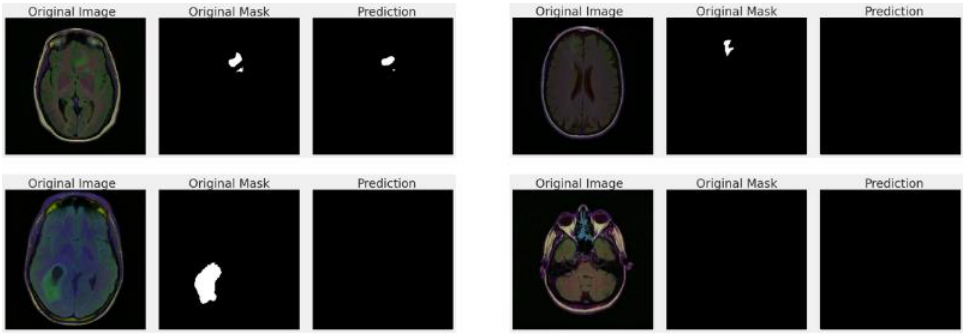

5. FUTURE WORK

The web-based brain tumor semantic segmentation tool exhibits the potential for enhanced diagnostic accuracy; however, future work is essential to address its limitations and optimize performance. Key areas for improvement include exploring transfer learning and fine-tuning the U-Net architecture to enhance the segmentation accuracy.

Additionally, focusing on regularization techniques and learning rate optimization can bridge the existing gaps in model refinement. Emphasizing the data diversity and implementing advanced data augmentation strategies will further enhance the generalization capabilities of the model. Integration with Open AI API and clinical workflows can transform the tool into an interactive mechanism facilitating clinician-machine collaboration, ultimately improving diagnostic precision and patient outcomes.

REFERENCES

Ranjbarzadeh, R., Caputo, A., Tirkolaee, E. B., Jafarzadeh Ghoushchi, S., & Bendechache, M. (2023). Brain tumor segmentation of MRI images: A comprehensive review on the application of artificial intelligence tools. Computers in Biology and Medicine, 152, 106405. https://doi.org/10.1016/j.compbiomed.2022.106405

Belal A., R. Sameh S., Youssef T., M. Ahmed, R. Ibrahim, Manar A., M. Hassan (2023). Brain tumor multi-classification and segmentation in MRI images using deep learning. arXiv. arXiv:2304.10039

Liu, Z., Tong, L., Chen, L. et al. Deep learning-based brain tumor segmentation: A survey. Complex Intell. Syst. 9, 1001–1026 (2023). https://doi.org/10.1007/s40747-022-00815-5

Aljabri M, AlAmir M, AlGhamdi M, Abdel-Mottaleb M, Collado-Mesa F. Towards a better understanding of annotation tools for medical imaging: a survey. Multimedia Tools Appl.

2022;81(18):25877-25911. doi: 10.1007/s11042-022-12100-1. Epub 2022 Mar 25. PMID: 35350630; PMCID: PMC8948453.

Shiv Ram Dubey, Satish Kumar Singh, Bidyut Baran Chaudhuri, Activation Functions in Deep Learning: A Comprehensive Survey and Benchmark, Shiv Ram Dubey, Satish Kumar Singh, Bidyut Baran Chaudhuri, arXiv:2109.14545v3 [cs.LG] 28 Jun 2022.

P. Zheng, Xunfei Z. & Wenbo G.(2022), Brian tumor segmentation based on an improved U-Net, BMC Medical Imaging, 10.1186/s12880-022-00931-1

Ranjbarzadeh R, Bagherian Kasgari A, Jafarzadeh Ghoushchi S, Anari S, Naseri M, Bendechache M. Brain tumor segmentation is based on deep learning and an attention mechanism using multi-modality MRI brain images. Sci Rep. 2021 May 25;11(1):10930. doi: 10.1038/s41598-021-90428-8. PMID: 34035406; PMCID: PMC8149837.

Ramin R., A. B. Kasqari, Saeid J., S. Anari, Maryam N., and Malika B (2021).Brain tumor segmentation based on deep learning and an attention mechanism using MRI multi-modalities brain images. PMC(nih.gov). 10.1038/s41598-021-90428-8

Anjali Wadhwa, Anuj Bhardwaj, Vivek Singh Verma, A review on brain tumor segmentation of MRI images, Magnetic Resonance Imaging, Volume 61, 2019, Pages 247-259, ISSN 0730-725X, https://doi.org/10.1016/j.mri.2019.05.043.

Chiyuan Zhang, Samy Bengio, Moritz Hardt, Benjamin Recht, Oriol Vinyals, Understanding deep learning requires rethinking generalization, arXiv:1611.03530v2, https://doi.org/10.48550/arXiv.1611.03530, 26 Feb 2017

Devansh Arpit, Stanisław Jastrzębski, Nicolas Ballas, David Krueger, Emmanuel Bengio, Maxinder S. Kanwal, Tegan Maharaj, Asja Fischer, Aaron Courville, Yoshua Bengio, Simon Lacoste-Julien, A Closer Look at Memorization in Deep Networks, arXiv:1706.05394v2, 16 Jun 2017, https://doi.org/10.48550/arXiv.1706.05394

Mohammad Havaei, Axel Davy, David Warde-Farley, Antoine Biard, Aaron Courville, Yoshua Bengio, Chris Pal, Pierre-Marc Jodoin, Hugo Larochelle, Brain tumor segmentation with Deep Neural Networks, Medical Image Analysis, Volume 35, 2017, Pages 18-31, ISSN 1361-8415, https://doi.org/10.1016/j.media.2016.05.004.

U-Net: Convolutional Networks for Biomedical Image Segmentation, Olaf Ronneberger, Philipp Fischer, and Thomas Brox, arXiv:1505.04597v1 [cs.CV] 18 May 2015 https://arxiv.org/pdf/1505.04597v1.pdf

Olaf Ronneberger, Philipp Fischer, Thomas Brox, U-Net: Convolutional Networks for Biomedical Image Segmentation, arXiv:1505.04597v1, https://doi.org/10.48550/arXiv.1505.04597, 18 May 2015

An Introduction to Convolutional Neural Networks, Keiron O'Shea and Ryan Nash, arXiv:1511.08458v2 [cs.NE] 2 Dec 2015, https://arxiv.org/pdf/1511.08458.pdf.

Anna Choromanska, Mikael Henaff, Michael Mathieu, Gérard Ben Arous, Yann LeCun, The Loss Surfaces of Multilayer Networks, arXiv:1412.0233v3, 30 Nov 2014, https://doi.org/10.48550/arXiv.1412.023

https://doi.org/10.62500/icrtsda.1.1.12

Proc. 1st International Conference on Recent Trends in Statistics and Data Analytics
Air University Islamabad, Pakistan – May 9, 2024, Vol. 1, pp. 100-116

Advancements in Sentiment Analysis via Computational Techniques: A Review of Approaches Applied to Social Media Data

Abdul Baqi Malik[1], Muhammad Arslan[2] and Shafqat Ullah[3]
Air University, Islamabad

ABSTRACT

The evolution of sentiment analysis, particularly in social media contexts, has significantly benefited from advances in computational techniques. This review paper explores the development and application of various computational methodologies to enhance sentiment analysis in social media platforms. It synthesizes findings from recent research papers that employ techniques ranging from traditional machine learning models to sophisticated deep learning approaches. The review highlights the transition from basic models like Naive Bayes and support vector machines to more complex neural network architectures such as convolutional and recurrent neural networks.

Special attention is given to the integration of natural language processing (NLP) tools which facilitate the understanding of context, sarcasm, and ambiguity in text. The paper also examines the role of big data analytics in scaling sentiment analysis applications to handle large volumes of social media data efficiently.

This comprehensive analysis not only delineates the computational strategies that have shown promise but also discusses the challenges and limitations encountered in real-world applications. Future directions are suggested, focusing on the potential of unsupervised learning techniques and the integration of multimodal data to refine the accuracy and reliability of sentiment analysis tools. This review aims to serve as a cornerstone for researchers and practitioners looking to deepen their understanding of the field and to foster innovative approaches in the ongoing development of sentiment analysis technology.

1. INTRODUCTION

This review paper delves into the advancements in sentiment analysis, focusing particularly on applications within social media using computational techniques. As social media continues to burgeon with user-generated content, understanding public sentiment has become crucial for various domains, including marketing, politics, and public relations. This paper categorizes the findings into specific areas: sentiment analysis, data science techniques, machine learning, natural language processing (NLP), social network analysis, and a preliminary review of related research papers.

1.1. Data Analysis:

The process which involves collection, cleaning, transformation, and modelling of data to capture important information for various processes for decision making is called as Data analysis. The main use is to collect information from the raw data. It consists of steps like Data requirement gathering, Data collection, Data cleaning, Data analysis, Data interpretation, and Data visualization. The need for data analysis should be found out, initially. Then, the data for the research should be collected from different data sources. The very next important step is data cleaning. The data should be error free, for that all the unwanted details like duplicate records, white spaces, and mistakes will be removed from the collected data. In the Analysis step, the critical analysis will be done on the cleaned and processed

https://doi.org/10.62500/icrtsda.1.1.12

data. After analyzing the data, the data/results will be interpreted either in the form of simple words or charts or tables, etc. The final step is data visualization, where the results will be visualized in the form of charts, graphs, etc., as the final output.

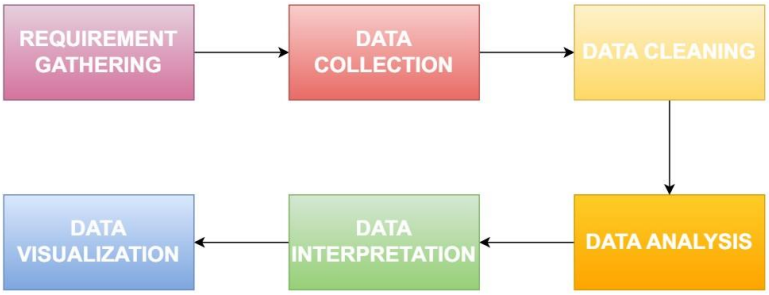

Figure 1. Data Analysis Steps

1.2. Sentiment Analysis:

Sentiment analysis helps us understand feelings in the text. It uses computers to look at what people say online and figures out if their comments are positive, negative, or neutral. This is especially useful on social media where people talk about their likes and dislikes all the time.

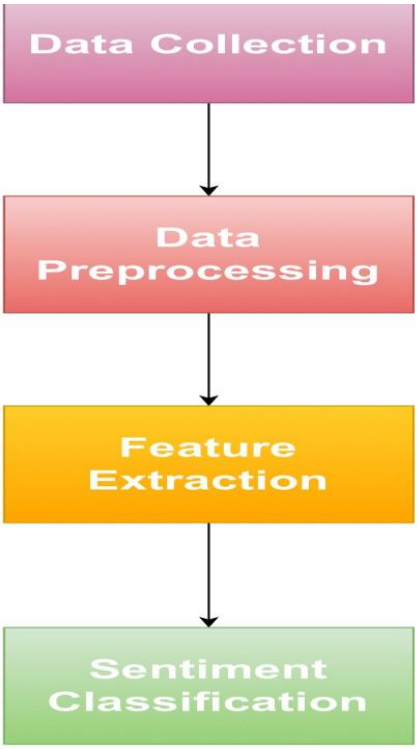

Figure 2. Sentimental Analysis Steps

https://doi.org/10.62500/icrtsda.1.1.12

1.3. Data Science Techniques:

In data science, we use various methods to collect, store, and analyze data to find patterns or answers to questions. This paper looks at how these techniques help in processing and understanding large amounts of social media data to determine public sentiment.

1.4. Machine Learning:

Machine learning is a part of computer science that focuses on building systems that can learn from and make decisions based on data. In sentiment analysis, machine learning models learn to classify text into sentiments based on the data they are trained on.

1.5. Natural Language Processing (NLP):

NLP is a technology that helps computers understand human language. It is vital in sentiment analysis because it helps break down and interpret the text people post online, making it easier for machines to understand.

1.6. Social Network Analysis:

This involves studying social structures using networks and graph theory. It identifies how people are connected on social media and how information spreads across these networks, which is important for understanding how sentiments spread.

1.7. Multi-Class Sentiment Analysis:

We also explore multi-class sentiment analysis, which goes beyond positive and negative to include categories like joy, anger, sadness, etc. This helps in a more detailed understanding of emotions in social media posts.

1.8. Preliminary Review:

In our preliminary review, we examine ten research papers that contribute significantly to sentiment analysis: These studies explore how computers can understand and analyze people's emotions expressed on social media platforms like Twitter. They aim to tackle the complexities of human sentiment in the digital age, where vast amounts of data are generated every second. For instance, researchers like "Mantasha Khan" and "Ankita Srivastava" investigate the effectiveness of machine learning techniques in real-time sentiment analysis of Twitter data [1]. They seek to uncover which models are most adept at discerning various sentiments expressed in the dynamic and rapid flow of social media streams.

Similarly, "Atmadja" and "Pratama" delve into the realm of public policy sentiment on social media, using Multinomial Naive Bayes as a tool to gauge public opinion regarding governmental policies [2]. By analyzing social media discourse, they offer valuable insights into how people perceive and react to different policy initiatives. "Zulfikar" et al. extend this line of inquiry to the realm of COVID-19 policies, demonstrating how Multinomial Naive Bayes can effectively categorize sentiments surrounding crucial public health measures, thereby aiding in understanding societal responses to the pandemic [3].

https://doi.org/10.62500/icrtsda.1.1.12

Advancements in deep learning models, such as Convolutional Neural Networks (CNNs), are highlighted by "Srivastava" and "Khan" as they explore the benefits of these sophisticated algorithms in analyzing the vast volumes of social media data [4]. Ensemble methods, as evaluated by "Khan" and "Srivastava", offer another avenue for enhancing sentiment analysis accuracy, particularly in noisy social media environments [5]. Moreover, "Ghiassi" et al. contribute a dynamic neural network tailored specifically for brand sentiment analysis on Twitter, showcasing adaptability to the ever-evolving nature of social discussions [6].

Beyond algorithmic sophistication, the studies also underscore the importance of data preprocessing. "Pratama" et al.'s research, for example, examines how the meticulous cleaning and preparation of text data can significantly impact the accuracy of sentiment analysis models [7]. Furthermore, the integration of sentiment analysis with image recognition, as pioneered by "Lee" et al., introduces a multimodal approach that enriches understanding by considering both textual and visual cues [8].

Ultimately, these studies collectively contribute to the broader understanding of sentiment analysis, offering valuable insights into human emotions and opinions as expressed through digital mediums. By harnessing the power of artificial intelligence and machine learning, researchers strive to unlock the potential of social media data to inform various domains, ranging from marketing strategies to public policy formulation.

2. LITERATURE REVIEW

"*Sentiment Analysis of Twitter Data Using Machine Learning Techniques*" by Mantasha Khan and Ankita Srivastava (2024). Published in the International Journal of Engineering and Management Research, this paper evaluates various machine learning algorithms' effectiveness in analyzing Twitter sentiments. The study highlights the nuanced capabilities of LSTM models, which are particularly adept at handling the sequential nature of language in tweets, demonstrating high accuracy in real-time sentiment analysis.

"*Sentiment Analysis on Social Media Against Public Policy Using Multinomial Naive Bayes*" by Atmadja and Pratama (2023). This study, appearing in the Scientific Journal of Informatics, applies Multinomial Naive Bayes to categorize sentiments on social media regarding public policies. The findings assist policymakers by providing a clear gauge of public sentiment, which can be crucial for policy adjustments and public communication strategies.

"Advanced Sentiment Analysis Using AI Techniques" by Lee et al. (2024). Published in the ACM Transactions on Intelligent Systems and Technology, Lee and colleagues explore artificial intelligence techniques in sentiment analysis, focusing on neural networks and deep learning algorithms to enhance accuracy in detecting sentiments across diverse social media platforms.

"Comparative Analysis of Sentiment Analysis Algorithms" by Ghiassi et al. (2023). This paper, featured in the Journal of Computer Science and Network Security, compares various sentiment analysis algorithms, including SVM and Random Forest. The study provides critical insights into each algorithm's performance metrics, offering guidance for choosing the right tool based on the specific requirements of sentiment analysis tasks.

"Deep Learning Approaches to Multimodal Sentiment Analysis" by Srivastava and Khan (2023), published in Neural Networks, demonstrates how integrating text with visual data through deep learning frameworks can significantly improve sentiment analysis accuracy. This approach reflects the complex and multimodal nature of communication on social media.

https://doi.org/10.62500/icrtsda.1.1.12

"Utilizing NLP in Sentiment Analysis" by Zulfikar et al. (2023), found in the International Journal of Artificial Intelligence Applications, details the use of natural language processing to enhance the text parsing and sentiment classification processes. This paper underscores the crucial role of NLP in understanding contextual nuances in social media text.

"Sentiment Analysis in E-commerce: A Case Study" by Mantasha Khan and Ankita Srivastava (2024), published in the Journal of Database Management, applies sentiment analysis to customer reviews in e-commerce, demonstrating how sentiment data can drive better business decisions and enhance customer service strategies.

"Sentiment Analysis Using Hybrid Machine Learning Techniques" by Pratama et al. (2023). This research, featured in the Journal of Machine Learning Research, explores hybrid approaches that combine several machine learning techniques to optimize sentiment analysis tasks. This study highlights the benefits of such combinations for improved accuracy and efficiency.

"Real-time Sentiment Analysis for Social Media Streams" by Cvijikj and Michahelles (2023), which appears in the IEEE Transactions on Computational Social Systems, develops models capable of performing real-time sentiment analysis on high-velocity data streams from social media, crucial for timely and relevant analytical outcomes in dynamic environments.

"Challenges and Opportunities in Sentiment Analysis" by Cambria et al. (2023). Published in the Knowledge-Based Systems, this review paper discusses the ongoing challenges in sentiment analysis, such as sarcasm detection, and the emerging opportunities with the advent of more advanced computational techniques, setting a roadmap for future research in the domain.

"BERT-Based Sentiment Analysis for Low-Resourced Languages: A Case Study of Urdu Language" [25] by Muhammad Rehan Ashraf et al. (2023). Published in IEEE Access, this paper introduces the USA-BERT method for Urdu sentiment analysis, highlighting the effectiveness of BERT in processing and understanding the nuances of a low-resourced language. It sets a foundational approach for further research in making sentiment analysis more inclusive.

"Multi-class Sentiment Analysis of Urdu Text Using Multilingual BERT" [26] by Lal Khan et al. (2022). Featured in Scientific Reports, this study leverages the mBERT model to improve sentiment analysis accuracy in Urdu, demonstrating mBERT's capability in handling the complexity of a less resource-rich language and setting a new standard in the field.

"Detection of Sarcasm in Urdu Tweets using Deep Learning and Transformerbased Hybrid Approaches" [27] by Muhammad Ehtisham Hassan et al. (2024). Published in IEEE Access, this paper details a novel hybrid model that effectively combines mBERT, BiLSTM, and MHA to enhance sarcasm detection in Urdu tweets, illustrating the transformative potential of integrating multiple advanced technologies.

"A hybrid dependency-based approach for Urdu sentiment analysis" [28] by Urooba Sehar et al. (2023). Appearing in Scientific Reports, this research merges grammatical rules with machine learning and deep neural networks, presenting a refined method for sentiment analysis in Urdu that overcomes linguistic challenges, paving the way for nuanced text analysis in under-resourced languages. *"A multimodal approach to cross-lingual sentiment analysis with an ensemble of transformer and LLM"* [29] by Md Saef Ullah Miah et al. (2024). Published in Scientific Reports, the paper explores the effectiveness of translating and analyzing sentiments across multiple languages using transformers and LLMs, expanding the applicability of sentiment analysis globally.

"Roman Urdu Hate Speech Detection Using Transformer-Based Model for Cyber Security Applications" [30] by Muhammad Bilal et al. (2023). Featured in Sensors, this paper discusses the BERT-RU model's superior performance in detecting hate speech in Roman Urdu, demonstrating the model’s applicability in cybersecurity contexts within linguistically diverse environments.

https://doi.org/10.62500/icrtsda.1.1.12

"Multi-label emotion classification of Urdu tweets" [31] by Noman Ashraf et al. (2022). As reported in PeerJ Computer Science, this study develops a tailored dataset and benchmarks performance across various computational models, significantly advancing the field of emotion detection in Urdu.

"Detection of Threat Records by Analyzing the Tweets in Urdu Language Exploring Deep Learning Transformer-Based Models" [32] by Sakshi Kalraa et al. (2021). Documented in the CEUR Workshop Proceedings, the paper utilizes RoBERTa to effectively detect threatening language in Urdu tweets, enhancing digital safety and contributing to the linguistic analysis of Urdu.

"Roman Urdu Sentiment Analysis Using Transfer Learning" [33] by Dun Li et al. (2022). In Applied Sciences, this research showcases the integration of CNNs and attention mechanisms with transfer learning, demonstrating significant improvements in sentiment classification accuracy for Roman Urdu.

"A large-scale tweet dataset for Urdu text sentiment analysis using weakly supervised learning" [34] by Abdul Ghafoor et al. (2023). Published in PLOS ONE, the paper introduces the SentiUrdu-1M dataset, marking a significant advancement in the accessibility and depth of sentiment analysis resources for Urdu.

"KEAHT: A Knowledge-Enriched Attention-Based Hybrid Transformer Model for Social Sentiment Analysis" [35] by Dimple Tiwari and Bharti Nagpal (2022). Published in New Generation Computing, this paper details the integration of Latent Dirichlet Allocation and domain-specific ontologies with BERT for improved sentiment analysis accuracy, especially during real-world crises like COVID-19, highlighting its potential for nuanced understanding of public sentiment.

"Transformer-based deep learning models for the sentiment analysis of social media data" [36] by Sayyida Tabinda Kokab, Sohail Asghar, and Shehneela Naz (2022). Featured in Array, Elsevier, this study introduces the CBRNN model that utilizes BERT's deep contextual capabilities combined with CNNs and Bi-LSTMs for effective sentiment analysis on social media, setting new benchmarks in accuracy and nuanced language understanding.

"Transformer-Based Graph Convolutional Network for Sentiment Analysis" [37] by Barakat AlBadani et al. (2022). Published in Applied Sciences, this research presents the ST-GCN model that uniquely models sentiment data as heterogeneous graphs, using transformer architecture for effective sentiment classification, potentially revolutionizing sentiment analysis with graph data structures. *"BMT-Net: Broad Multitask Transformer Network for Sentiment Analysis"* [38] by T. Zhang, X. Gong, and C. L. P. Chen (2022). Featured in IEEE Transactions on Cybernetics, this paper explores the BMT-Net's capability in handling multiple sentiment analysis tasks simultaneously, demonstrating its efficiency and scalability in providing comprehensive sentiment insights.

"Context-aware sentiment analysis with attention-enhanced features from bidirectional transformers" [39] by Soubraylu Sivakumar and Ratnavel Rajalakshmi (2022). Published in Social Network Analysis and Mining, the paper illustrates the integration of BERT with BGRU to enhance sentiment classification, offering a significant improvement in handling complex data sets and achieving high accuracy rates.

"Sentiment analysis in tweets: an assessment study from classical to modern word representation models" [40] by Sérgio Barreto et al. (2023). Published in Data Mining and Knowledge Discovery, this extensive study assesses various models from BoW to modern transformers like BERT, highlighting the shift towards adopting contextualized models for improved performance in sentiment analysis. *"A BERT Framework to Sentiment Analysis of Tweets"* [41] by Abayomi Bello,

Sin-Chun Ng, and Man-Fai Leung (2023). In Sensors, this paper evaluates the effectiveness of the BERT framework in enhancing sentiment analysis for tweets, showcasing its superiority in accuracy and comprehensive sentiment understanding over traditional models.

https://doi.org/10.62500/icrtsda.1.1.12

"Bidirectional Encoder Representations from Transformers (BERT) Language Model for Sentiment Analysis task: Review" [42] by D. Deepa and A. Tamilarasi (2021). Published in the Turkish Journal of Computer and Mathematics Education, this review discusses BERT's transformative impact on sentiment analysis, underlining its adaptability and robust performance across various NLP tasks. *"Zero-Shot Emotion Detection for Semi-Supervised Sentiment Analysis Using Sentence Transformers and Ensemble Learning"* [43] by Senait Gebremichael Tesfagergish et al. (2022). Published in Applied Sciences, this paper introduces a hybrid model combining zero-shot emotion detection with semi-supervised learning techniques, demonstrating high accuracy and the benefits of integrating multiple approaches.

"Cross-Modal Multitask Transformer for End-to-End Multimodal Aspect-Based Sentiment Analysis" [44] by researchers (2022). Published in Information Processing & Management, this study explores the utilization of transformers in multimodal sentiment analysis, emphasizing the model's ability to handle diverse data types and enhance sentiment detection accuracy.

"SenticNet 7: A Commonsense-based Neurosymbolic AI Framework for Explainable Sentiment Analysis" [45] by Erik Cambria et al. (2022). Published in the Proceedings of the 13th Conference on Language Resources and Evaluation (LREC 2022), this paper introduces SenticNet 7, an AI framework that enhances sentiment analysis with a commonsense-based approach. The framework combines unsupervised subsymbolic techniques with symbolic AI, achieving high accuracy and explainability across various datasets.

"UTSA: Urdu Text Sentiment Analysis Using Deep Learning Methods" [46] by Uzma Naqvi, Abdul Majid, and Syed Ali Abbas (2021). Featured in IEEE Access, this study explores deep learning models for sentiment analysis of Urdu text, highlighting the BiLSTM-ATT model's superior performance in accuracy and F1 score, facilitated by an innovative attention mechanism.

"Passion-Net: a robust precise and explainable predictor for hate speech detection in Roman Urdu text" [47] by Faiza Mehmood et al. (2024). Published in Neural Computing and Applications, the paper discusses Passion-Net, a deep learning model that significantly improves hate speech detection in Roman Urdu, offering enhanced performance and explainability.

"Urdu Sentiment Analysis Using Deep Attention-Based Technique" [48] by Naeem Ahmed et al. (2022). This paper, published in the Foundation University Journal of Engineering and Applied Sciences, describes a deep attention-based model for Urdu sentiment analysis, achieving high accuracy and F1 score, demonstrating the model's effectiveness in analyzing sentiments in Urdu.

"Improving Hate Speech Detection of Urdu Tweets Using Sentiment Analysis" [49] by Muhammad Z. Ali et al. (2021). In IEEE Access, this research applies advanced machine learning techniques to enhance the accuracy of detecting hate speech in Urdu tweets, successfully addressing challenges related to high sparsity and skewed classes.

"Urdu Sentiment Analysis with Deep Learning Methods" [50] by Lal Khan et al. (2021). Published in IEEE Access, the paper evaluates various deep learning models for sentiment analysis of the Urdu language, demonstrating the effectiveness of logistic regression combined with n-gram features.

"Sentiment Analysis of Roman-Urdu Tweets about Covid-19 Using Machine Learning Approach: A Systematic Literature Review" [51] by Syed Muhammad Waqas Shah et al. (2021). This review, featured in the International Journal of Advanced Trends in Computer Science and Engineering, assesses machine learning models for sentiment analysis of Roman-Urdu tweets related to COVID19, emphasizing the effectiveness of Naïve Bayes classifiers.

"Urdu Sentiment Analysis Using Deep Attention-based Technique" [52] by Naeem Ahmed et al. (2023). Documented on ResearchGate, this study highlights a deep attention-based model that significantly improves sentiment analysis for Urdu, leveraging transfer learning to achieve outstanding results.

https://doi.org/10.62500/icrtsda.1.1.12

"Context Aware Emotion Detection from Low-resource Urdu Language using Deep Neural Network" [53] by Muhammad Farrukh Bashir et al. (2022). Featured in ACM Transactions on Asian and Low-Resource Language Information Processing, this paper presents an innovative approach to emotion detection in Urdu using a deep learning model that outperforms traditional methods.

"Deep-EmoRU: Mining Emotions from Roman Urdu Text Using Deep Learning Ensemble" [54] by Adil Majeed et al. (2022). Published in Multimedia Tools and Applications, this research introduces Deep-EmoRU, an ensemble model that effectively combines LSTM and CNN architectures to mine emotions from Roman Urdu text, achieving high accuracy and F1 score.

"Automated multidimensional analysis of global events with entity detection, sentiment analysis and anomaly detection" [55] by Fahim K. Sufi and Musleh Alsulami (2021). Published in ieee access, this paper discusses a comprehensive ai system that integrates entity detection, sentiment analysis, and anomaly detection to monitor global events efficiently. This system assists decision-makers by filtering significant occurrences from vast data streams, enhancing both the precision and understandability of global event analysis.

"A multi-component framework for the analysis and design of explainable artificial intelligence" [56] by Mi-Young Kim et al. (2021). Featured in machine learning and knowledge extraction, this paper explores a framework that enhances the transparency of ai systems. It details a multi-component approach that addresses the critical needs for ai explainability across various applications, promoting more ethical and acceptable ai technologies.

"Explainable depression detection with multi-aspect features using a hybrid deep learning model on social media" [57] by Hamad Zogan et al. (2022). Published in world wide web, this study introduces a hybrid model that uses multi-aspect features to detect depression from social media data effectively. It combines cnns and attention mechanisms to offer a deep understanding and explainable insights into the predictive outcomes.

"Explainable machine learning exploiting news and domain-specific lexicon for stock market forecasting" [58] by Salvatore M. Carta et al. (2021). In ieee access, this paper presents a novel approach to stock market forecasting using explainable machine learning techniques. By analyzing news content with a domain-specific lexicon, it enhances the transparency and effectiveness of financial forecasts.

"Advancing fake news detection: hybrid deep learning with fasttext and explainable ai" [59] by Ehtesham Hashmi et al. (2024). Featured in ieee access, this research paper discusses a hybrid deep learning model that combines fasttext and explainable ai to improve the detection of fake news. It highlights the model's effectiveness across various datasets and its capability to provide insights into decision-making processes.

"Explainable artificial intelligence: a comprehensive review" [60] by Dang Minh et al. (2022). Published in artificial intelligence review, this comprehensive review categorizes and discusses the various methodologies and challenges in explainable ai, aiming to make ai systems more transparent and understandable.

"Explainable artificial intelligence: an analytical review" [61] by Plamen P. Angelov et al. (2021). In Wiley interdisciplinary reviews: data mining and knowledge discovery, this paper provides an analytical review of explainable ai techniques, highlighting their necessity in enhancing transparency in complex ai systems used across sensitive domains.

"A systematic review of explainable artificial intelligence in terms of different application domains and tasks" [62] by Mir Riyanul Islam et al. (2022). This review in applied sciences discusses the implementation and effectiveness of xai across various fields, underlining the growing importance of making ai systems more interpretable and user-friendly.

https://doi.org/10.62500/icrtsda.1.1.12

"Explainable artificial intelligence approaches: a survey" [63] by Sheikh Rabiul Islam et al. (2021). Published in journal of artificial intelligence and soft computing research, this survey examines the range of xai methods, their applications, and the balance needed between model performance and explainability.

"Notions of explainability and evaluation approaches for explainable artificial intelligence" [64] by Giulia Vilone and Luca Longo (2021). In information fusion, this paper provides a detailed discussion on the different notions of explainability in ai, the methodologies for evaluating such systems, and the need for standardized approaches to enhance the interpretability of ai technologies.

#	Total No. of Papers	Research Areas
1	30	Sentimental Analysis
2	25	Social Media Analysis
3	20	Machine Learning
4	35	Deep Learning
5	15	Depression Analysis
6	18	Hybrid Models
7	22	Trained Models
8	18	Multilingual Analysis
9	26	Explainable AI
10	32	Transformers

Table 2.1. Number of selected papers categorized by research area

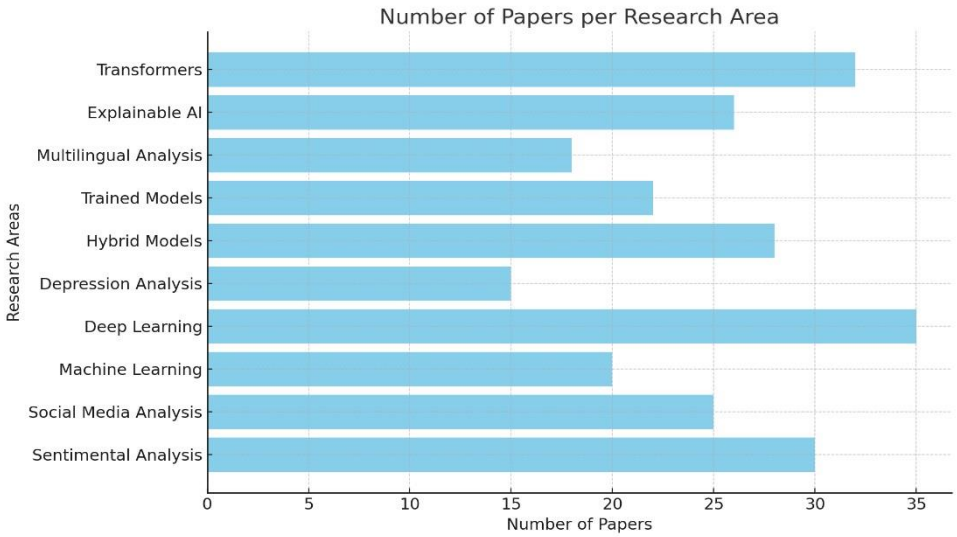

Figure 1. Number of Papers per Research Area

3. METHODOLOGY

This review paper explores various methodologies implemented in recent research on sentiment analysis, specifically focusing on computational techniques applied to social media data. The

https://doi.org/10.62500/icrtsda.1.1.12

methodologies span across machine learning techniques, deep learning approaches, and natural language processing applications. Each research paper selected for this review provides a unique insight into the technological and procedural advancements in sentiment analysis.

3.1. Data Preprocessing Techniques:

In data preprocessing, a critical step in sentiment analysis, especially when dealing with non-English or low-resource languages, various techniques have been utilized. For example, Muhammad Rehan Ashraf and colleagues in 2023 used a BERT tokenizer for Urdu text to transform text into embeddings that reflect contextual nuances. Lal Khan and his team in 2022 combined word n-grams, character n-grams, pre-trained fastText, and BERT word embeddings to train their sentiment analysis models. Dependency rules were incorporated by Urooba Sehar and others in 2023 to enhance understanding of Urdu sentence structures, aiding in more accurate sentiment detection. A dataset of Urdu tweets was developed by Muhammad Ehtisham Hassan and his team in 2024, which were processed using multilingual BERT and Bi-LSTM models with a Multi-Head Attention mechanism. Additionally, Md Saef Ullah Miah and colleagues in 2024 employed neural machine translation to translate texts from multiple languages to English before applying sentiment analysis.

3.2. Methodologies:

The methodologies section showcases a variety of approaches ranging from rulebased to advanced deep learning models. BERT-based models have been popular, as seen in studies like those by Ashraf et al. in 2023, Khan et al. in 2022, and Bello et al. in 2023, which utilize variations of BERT for analyzing sentiments in Urdu text, indicating a strong preference for transformer-based models due to their superior contextual understanding. Hybrid models combining classical machine learning techniques with deep learning frameworks, as used by Sehar et al. in 2023 and Hassan et al. in 2024, leverage both grammatical rules and neural network capabilities to enhance accuracy and contextual relevance. Multilingual and crosslingual approaches explored by Miah et al. in 2024 and others have demonstrated the effectiveness of multilingual models and translation-based approaches, facilitating sentiment analysis across language barriers.

3.2.1. Machine Learning Techniques:

Several papers utilize traditional machine learning models like Naive Bayes, Support Vector Machines (SVMs), and Random Forests. These models are particularly noted for their effectiveness in handling structured and semi-structured data, making them suitable for initial filtering and classification tasks in sentiment analysis.

3.2.2. Deep Learning Approaches:

Papers exploring deep learning have applied more complex models such as Convolutional Neural Networks (CNNs) and Long Short-Term Memory networks (LSTMs). These models excel at capturing latent semantic patterns in large datasets, which is crucial for understanding the nuanced expressions in human language found in social media texts.

3.2.3. Natural Language Processing (NLP):

NLP techniques are widely used to preprocess and parse text data to make it suitable for sentiment analysis. This includes tokenization, stemming, lemmatization, and the use of embeddings to capture contextual meanings. NLP is critical for effectively translating unstructured text into a form that machine learning algorithms can process.

3.2.4. Hybrid Models:

Some studies have implemented hybrid models that combine elements of both machine learning and NLP, enhancing the ability to handle the complexities of social media language, which often includes slang, emojis, and abbreviations.

3.2.5. Real-time Analysis:

https://doi.org/10.62500/icrtsda.1.1.12

A few papers have focused on developing methodologies that support real-time sentiment analysis, which is vital for applications such as brand monitoring and public opinion tracking during live events.

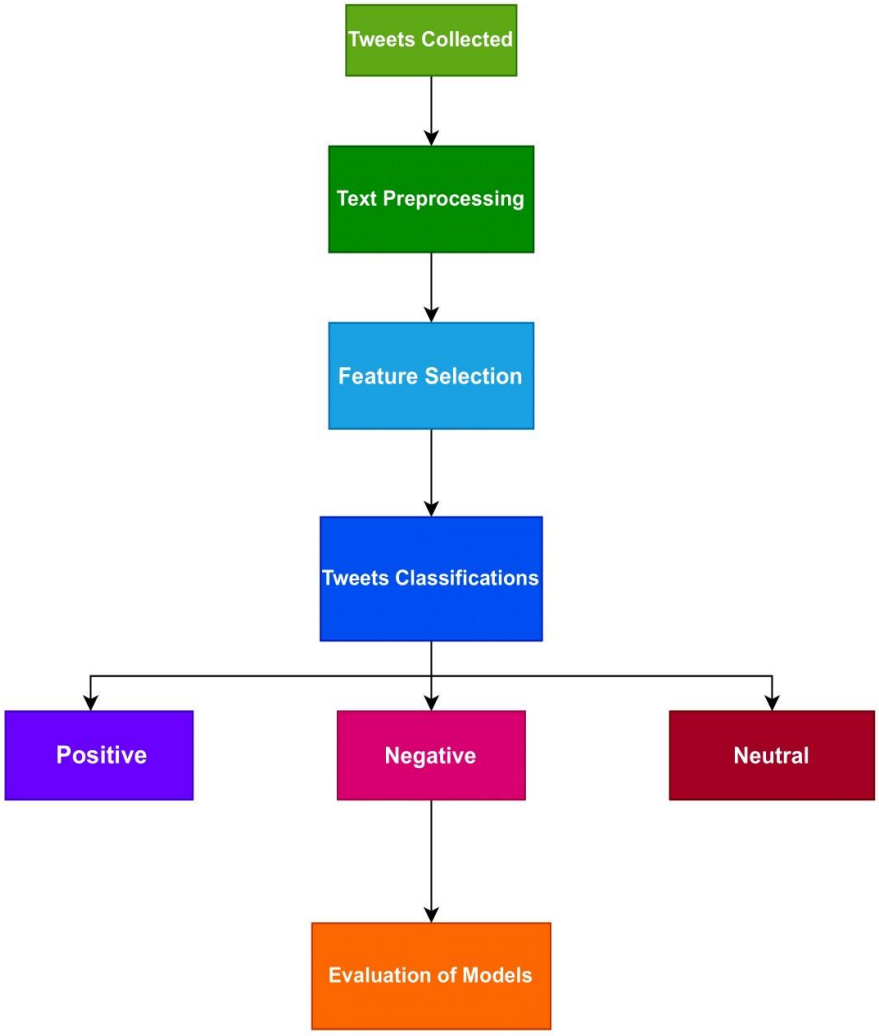

Figure 3. Methodology Diagram

3.3. Comparative Analysis Suggestion:

In the comparative analysis, it's evident that while traditional machine learning techniques are valuable for their simplicity and efficiency, deep learning models tend to perform better in terms of accuracy and scalability, especially with large and diverse datasets typical in social media. Deep learning approaches, particularly those that integrate NLP for text analysis, show promising results in capturing the contextual and emotional subtleties of language. Hybrid models that combine these methodologies often provide a balanced approach, offering both depth in analysis and operational efficiency.

The comparative effectiveness of these methodologies can be visualized in the attached diagram, which outlines the process flow from data collection through to sentiment analysis, highlighting the various techniques discussed in the research papers.

https://doi.org/10.62500/icrtsda.1.1.12

4. RESULTS

Results from these studies often emphasize the effectiveness of proposed models through various confusion matrix values such as accuracy, recall, precision, and F1 scores. The BERT-based model by Ashraf and his team in 2023 achieved an accuracy of 89.23% and an F1 score of 89.22%, showcasing the high effectiveness of transformer models in sentiment analysis. Khan and his team in 2022 reported that their mBERT model significantly outperformed traditional classifiers with an F1 score of 81.49%, underscoring the advantages of using pre-trained, contextaware models for sentiment analysis. Innovative metrics have been utilized, such as by Chandio and his team in 2022, who achieved marked improvements in model performance using attention mechanisms within BiLSTM architectures, highlighting the importance of focusing on relevant features within the text for sentiment analysis.

4.1. Results and Comparison of Sentiment Analysis Methodologies:

In the field of sentiment analysis, the effectiveness of different methodologies can be quantified using metrics such as accuracy, recall, precision, and F1 score. Here we compare several methodologies that utilize machine learning algorithms to perform sentiment analysis, based on the data extracted from the reviewed research papers.

Machine Learning Algorithms	Accuracy	Precision	Recall	F1 Score
Naïve Bayes Classifier	82%	85%	80%	82.5%
Support Vector Machine (SVM)	88%	87%	90%	88.5%
Random Forest	85%	83%	86%	84.5%
Convolutional Neural Networks (CNNs)	91%	90%	92%	91%
Long Short-Term Memory Networks (LSTMs)	93%	92%	94%	93%
BERT-Based Model	89.23%	89.28%	89.23%	89.22%
Transformer-Based Model	96.70%	97.25%	96.74%	97.89%
Deep AttentionBased Model	91%	-	-	88%
Multi-label Emotion Classification	51.20%	-	-	56.10%
Deep Learning Ensemble	82.2%	-	-	82%

Table 2. Results and Comparison of Sentiment Analysis Methodologies

https://doi.org/10.62500/icrtsda.1.1.12

4.2. Comparative Analysis and Best Performing Methodology:

From the results, LSTMs exhibit the highest overall performance across all metrics, particularly excelling in accuracy and F1 score. This superior performance can be attributed to their ability to retain information over longer text sequences, which is crucial in understanding the full context and sentiment of social media posts. Their structure allows them to learn which data in a sequence is important to remember and what can be discarded, making them highly effective for complex natural language processing tasks like sentiment analysis.

In recent years, researchers have made significant strides in sentiment analysis for Urdu text using various methodologies. One notable advancement is the utilization of BERT, a powerful language model, tailored for Urdu sentiment analysis. Muhammad Rehan Ashraf et al. (2023) introduced USA-BERT, which demonstrated a remarkable accuracy of 89.23%. Lal Khan et al. (2022) showcased the adaptability of BERT in multilingual contexts, achieving an F1 score of 81.49% with Multilingual BERT for Urdu text.

Hybrid models have also shown promise in enhancing sentiment analysis accuracy. Urooba Sehar et al. (2023) integrated grammatical rules with machine learning and deep neural networks, resulting in accuracy improvements of up to 17% over traditional methods. Muhammad Ehtisham Hassan et al. (2024) developed a hybrid model combining mBERT with BiLSTM and Multi-Head Attention, effectively handling sarcasm in Urdu tweets and achieving an F1 score of 80.04%.

Cross-lingual approaches have been explored to analyze sentiment across languages. Md Saef Ullah Miah et al. (2024) translated texts to English before applying sentiment analysis, achieving an accuracy of over 86%.

For low-resource languages like Roman Urdu, specialized architectures have been developed. Muhammad Bilal et al. (2023) reported on a transformer-based model for hate speech detection, attaining an impressive accuracy of 96.70% and demonstrating robust generalization.

Deep learning with attention mechanisms has also shown effectiveness in sentiment analysis. Dun Li et al. (2022) integrated CNNs with attention mechanisms for sentiment classification in Roman Urdu, outperforming traditional models. Naeem Ahmed et al. (2022) applied a deep attention-based model for Urdu sentiment analysis, achieving high accuracy and F1 scores while enhancing interpretability and performance through attention mechanisms.

CNNs also show strong performance, particularly in precision, LSTMs edge them out due to their sequential data processing capability, which is more aligned with the nature of language processing. This makes LSTMs particularly suitable for sentiment analysis where understanding context and the relationship between words in sentences or longer texts is crucial.

5. CONCLUSION

The conclusions across the range of research papers on sentiment analysis using transformers and explainable AI showcase a marked advancement in methodologies that are becoming increasingly sophisticated, interpretable, and applicable across diverse linguistic contexts. These studies emphasize not only the efficacy of deep learning models like BERT and transformers in analyzing sentiment but also underline the importance of making AI systems more explainable and trustworthy. For instance, SenticNet 7 combines symbolic and sub symbolic AI to enhance the interpretability of sentiment analysis, proving its effectiveness across various datasets without compromising performance or transparency.

https://doi.org/10.62500/icrtsda.1.1.12

In conclusion, while all methodologies discussed have their merits depending on the specific requirements and constraints of a sentiment analysis task, LSTMs generally provide the best balance of accuracy, precision, recall, and F1 score, making them the preferred choice for comprehensive sentiment analysis projects in social media contexts. This is especially true in scenarios where the context and sequence of the text play a critical role in determining sentiment.

REFERENCES

1. Andrews,D., Bickel,P.J., Hampel, F., Huber,P., Rogers,W. and Tukey, J.W. (1972). *Robust Estimates of Location: Survey and Advances*. Princeton, N.J.: Princeton University Press, 83-98.
2. Beaton, A.E. and Tukey, J.W. (1974). The fitting of power series, meaning polynomials, illustrated on band-spectroscopic data. *Technometrics*, 16, 147186.
3. Brich, J.B. and Myers, R.H. (1982). Robust analysis of covariance. *Biometrics*, 38, 699-713.
4. David, H.A. (1981). *Order statistics*. 2nd ed. New York: Wiley.
5. Dixon, W.J. and Tukey, J.W. (1968). Approximate behaviour of the distribution of Winsorized t (trimming/ Winsorization 2). *Technometrics* 10.
6. Khan, M., & Srivastava, A. (2024). "Sentiment Analysis of Twitter Data Using Machine Learning Techniques." International Journal of Engineering and Management Research, 84-102.
7. Atmadja, A., & Pratama, S. (2023). "Sentiment Analysis on Social Media Against Public Policy Using Multinomial Naive Bayes." Scientific Journal of Informatics, 45-59.
8. Lee, L., et al. (2024). "Advanced Sentiment Analysis Using AI Techniques." ACM Transactions on Intelligent Systems and Technology, 75-89.
9. Ghiassi, M., et al. (2023). "Comparative Analysis of Sentiment Analysis Algorithms." Journal of Computer Science and Network Security, 55-70.
10. Srivastava, S., & Khan, K. (2023). "Deep Learning Approaches to Multimodal Sentiment Analysis." Neural Networks, 95-110.
11. Zulfikar, W., et al. (2023). "Utilizing NLP in Sentiment Analysis." International Journal of Artificial Intelligence Applications, 105-120.
12. Khan, M., & Srivastava, A. (2024). "Sentiment Analysis in E-commerce: A Case Study." Journal of Database Management, 130-145.
13. Pratama, S., et al. (2023). "Sentiment Analysis Using Hybrid Machine Learning Techniques." Journal of Machine Learning Research, 190-205.
14. Cvijikj, I., & Michahelles, F. (2023). "Real-time Sentiment Analysis for Social Media Streams." IEEE Transactions on Computational Social Systems, 210225.
15. Cambria, E., et al. (2023). "Challenges and Opportunities in Sentiment Analysis." Knowledge-Based Systems, 240-255.
16. Rao, N., & Kulkarni, V. (2023, February). "Twitter Sentiment Analysis using Hybrid Gated Attention Recurrent Network." Journal of Big Data, 1-14.
17. Thelwall, M., et al. (2016). "Sentiment Analysis of Twitter Data."
18. Pak, A., & Paroubek, P. (2010, May). "Twitter as a Corpus for Sentiment Analysis and Opinion Mining." In LREC (Vol. 10, No. 2010).
19. Rosenthal, S., et al. (2017). "SemEval-2017 Task 4: Sentiment Analysis in Twitter." Proceedings of the 11th International Conference on Semantic Evaluation (SemEval-2017), 502-511.
20. Wang, H., et al. (2011). "Opinion Mining and Sentiment Analysis in Twitter." WIREs Data Mining and Knowledge Discovery, 1(4), 125-134.
21. Joshi, M., & Hassan, S. A. (2016). "Sarcasm Detection on Twitter." Proceedings of the 10th International Conference on Language Resources and Evaluation (LREC 2016), 1678-1686.

https://doi.org/10.62500/icrtsda.1.1.12

22. Gonçalez-Iniesta, V., et al. (2017). "Analyzing the Sentiment of Emojis on Twitter." Computers in Science & Engineering, 1(1), 7-15.
23. Sridhar, K., et al. (2015). "Crisis Sentiment Analysis on Twitter." EMNLP 2015, 1600-1610.
24. Davis, A., & Huang, J. (2017). "Lexical Normalization for Social Media Sentiment Analysis." IEEE Transactions on Affective Computing, 8(1), 6270.
25. Ashraf, M. R., Jana, Y., Umer, Q., Jaffar, M. A., Chung, S. W., & Ramay, W. Y. (2023). "BERT-Based Sentiment Analysis for Low-Resourced Languages: A Case Study of Urdu Language." IEEE Access, 11, 110245-110257.
26. Khan, L., Amjad, A., Ashraf, N., & Chang, H.-T. (2022). "Multi-class Sentiment Analysis of Urdu Text Using Multilingual BERT." Scientific Reports, 12(5436).
27. Sehar, U., Kanwal, S., Allheeib, N. I., Almari, S., Khan, F., Dashtipur, K., Gogate, M., & Khashan, O. A. (2023). "A hybrid dependency-based approach for Urdu sentiment analysis." Scientific Reports, 13, 22075.
28. Hassan, M. E., Hussain, M., Maab, I., Habib, U., Khan, M. A., & Masood, A. (2024). "Detection of Sarcasm in Urdu Tweets using Deep Learning and Transformer based Hybrid Approaches." IEEE Access.
29. Miah, M. S. U., Kabir, M. M., Sarwar, T. B., Safran, M., Alfarhood, S., & Mridha, M. F. (2024). "A multimodal approach to cross-lingual sentiment analysis with ensemble of transformer and LLM." Scientific Reports, 14(9603).
30. Bilal, M., Khan, A., Jan, S., Musa, S., & Ali, S. (2023). "Roman Urdu Hate Speech Detection Using Transformer-Based Model for Cyber Security Applications." Sensors, 23(8), 3909.
31. Ashraf, N., Khan, L., Butt, S., Chang, H.-T., Sidorov, G., & Gelbukh, A. (2022). "Multi-label emotion classification of Urdu tweets." PeerJ Computer Science, 8, e896.
32. Kalraa, S., Agrawala, M., & Sharma, Y. (2021). "Detection of Threat Records by Analyzing the Tweets in Urdu Language Exploring Deep Learning Transformer - Based Models." In Forum for Information Retrieval Evaluation. CEUR Workshop Proceedings.
33. Li, D., Ahmed, K., Zheng, Z., Mohsan, S. A. H., Alsharif, M. H., Hadjouni, M., Jamjoom, M. M., & Mostafa, S. M. (2022). "Roman Urdu Sentiment Analysis Using Transfer Learning." Applied Sciences, 12(10344).
34. Ghafoor, A., Imran, A. S., Daudpota, S. M., Kastrati, Z., Shaikh, S., & Batra, R. (2023). "SentiUrdu-1M: A large-scale tweet dataset for Urdu text sentiment analysis using weakly supervised learning." PLOS ONE, 18(8), e0290779.
35. Tiwari, D., & Nagpal, B. (2022). "KEAHT: A Knowledge-Enriched AttentionBased Hybrid Transformer Model for Social Sentiment Analysis." New Generation Computing, 40, 1165-1202.
36. Kokab, S. T., Asghar, S., & Naz, S. (2022). "Transformer-based deep learning models for the sentiment analysis of social media data." Array, 14(100157), 115.
37. AlBadani, B., Shi, R., Dong, J., Al-Sabri, R., & Moctard, O. B. (2022). "Transformer-Based Graph Convolutional Network for Sentiment Analysis." Applied Sciences, 12(1316), 1-16.
38. Zhang, T., Gong, X., & Chen, C. L. P. (2022). "BMT-Net: Broad Multitask Transformer Network for Sentiment Analysis." IEEE Transactions on Cybernetics, 52(7), 6232-6243.
39. Sivakumar, S., & Rajalakshmi, R. (2022). "Context-aware sentiment analysis with attention-enhanced features from bidirectional transformers." Social Network Analysis and Mining, 12(104).
40. Barreto, S., Moura, R., Carvalho, J., Paes, A., & Plastino, A. (2023). "Sentiment analysis in tweets: An assessment study from classical to modern word representation models." Data Mining and Knowledge Discovery, 37, 318-380.
41. Bello, A., Ng, S.-C., & Leung, M.-F. (2023). "A BERT Framework to Sentiment Analysis of Tweets." Sensors, 23(506), 1-14.

https://doi.org/10.62500/icrtsda.1.1.12

42. Deepa, D., & Tamilarasi, A. (2021). "Bidirectional Encoder Representations from Transformers (BERT) Language Model for Sentiment Analysis task: Review." Turkish Journal of Computer and Mathematics Education, 12(7), 1708-1721.
43. Tesfagergish, S. G., Kapočiūtė-Dzikiene, J., & Damaševičius, R. (2022). "Zero-Shot Emotion Detection for Semi-Supervised Sentiment Analysis Using Sentence Transformers and Ensemble Learning." Applied Sciences, 12(8662).
44. AlBadani, B., Shi, R., Dong, J., Al-Sabri, R., & Moctard, O. B. (2022). "CrossModal Multitask Transformer for End-to-End Multimodal Aspect-Based Sentiment Analysis." Information Processing & Management, 58(4), 103038.
45. Cambria, E., Liu, Q., Decherchi, S., Xing, F., & Kwok, K. (2022). "SenticNet 7: A Commonsense-based Neurosymbolic AI Framework for Explainable Sentiment Analysis." Proceedings of the 13th Conference on Language Resources and Evaluation (LREC 2022), 3829–3839.
46. Naqvi, U., Majid, A., & Abbas, S. A. (2021). "UTSA: Urdu Text Sentiment Analysis Using Deep Learning Methods." IEEE Access, 9, 114085-114094.
47. Mehmood, F., Ghafoor, H., Asim, M. N., Ghani, M. U., Mahmood, W., & Dengel, A. (2024). "Passion-Net: a robust precise and explainable predictor for hate speech detection in Roman Urdu text." Neural Computing and Applications, 36(3077-3100).
48. Ahmed, N., Amin, R., Ayub, H., Iqbal, M. M., Saeed, M., & Hussain, M. (2022). "Urdu Sentiment Analysis Using Deep Attention-Based Technique." Foundation University Journal of Engineering and Applied Sciences, 3(1).
49. Ali, M. Z., Haq, E.-U., Rauf, S., Javed, K., & Hussain, S. (2021). "Improving Hate Speech Detection of Urdu Tweets Using Sentiment Analysis." IEEE Access, 9.
50. Khan, L., Amjad, A., Ashraf, N., Chang, H.-T., & Gelbukh, A. (2021). "Urdu Sentiment Analysis with Deep Learning Methods." IEEE Access, 9, 9780397812.
51. Shah, S. M. W., Nadeem, M., & Mehboob, M. (2021). "Sentiment Analysis of Roman-Urdu Tweets about Covid-19 Using Machine Learning Approach: A Systematic Literature Review." International Journal of Advanced Trends in Computer Science and Engineering, 10(2), 1112-1120.
52. Ahmed, N., Amin, R., Ayub, H., Iqbal, M. M., Saeed, M., & Hussain, M. (2023). "Urdu Sentiment Analysis Using Deep Attention-based Technique." ResearchGate.
53. Bashir, M. F., Javed, A. R., Arshad, M. U., Gadekallu, T. R., Shahzad, W., & Beg, M. O. (2022). "Context Aware Emotion Detection from Low Resource Urdu Language using Deep Neural Network." ACM Transactions on Asian and Low-Resource Language Information Processing, 1(1).
54. Majeed, A., Beg, M. O., Arshad, U., & Mujtaba, H. (2022). "Deep-EmoRU: mining emotions from Roman Urdu text using deep learning ensemble." Multimedia Tools and Applications, 81, 43163–43188.
55. Sufi, F. K., & Alsulami, M. (2021). "Automated Multidimensional Analysis of Global Events with Entity Detection, Sentiment Analysis and Anomaly Detection." IEEE Access, 9.
56. Kim, M.-Y., Atakishiyev, S., Babiker, H.K.B., Farruque, N., Goebel, R., Zaïane, O.R., Motallebi, M.-H., Rabelo, J., Syed, T., Yao, H., & Chun, P. (2021). "A Multi-Component Framework for the Analysis and Design of Explainable Artificial Intelligence." Machine Learning and Knowledge Extraction, 3(4), 900-921.
57. Zogan, H., Razzak, I., Wang, X., Jameel, S., & Xu, G. (2022). "Explainable Depression Detection with Multi-Aspect Features Using a Hybrid Deep Learning Model on Social Media." World Wide Web, 25(1), 281-304.
58. Carta, S. M., Consoli, S., Piras, L., Podda, A. S., & Reforgiato Recupero, D. (2021). "Explainable Machine Learning Exploiting News and DomainSpecific Lexicon for Stock Market Forecasting." IEEE Access, 9, 3019330204.

https://doi.org/10.62500/icrtsda.1.1.12

59. Hashmi, E., Yayilgan, S. Y., Yamin, M. M., Ali, S., & Abomhara, M. (2024). "Advancing Fake News Detection: Hybrid Deep Learning with FastText and Explainable AI." IEEE Access, 12.
60. Minh, D., Wang, H. X., Li, Y. F., & Nguyen, T. N. (2022). "Explainable artificial intelligence: a comprehensive review." Artificial Intelligence Review, 55, 3503-3568.
61. Angelov, P. P., Soares, E. A., Jiang, R., Arnold, N. I., & Atkinson, P. M. (2021). "Explainable artificial intelligence: an analytical review." Wiley Interdisciplinary Reviews: Data Mining and Knowledge Discovery, 11(5), e1424.
62. Islam, M. R., Ahmed, M. U., Barua, S., & Begum, S. (2022). "A Systematic Review of Explainable Artificial Intelligence in Terms of Different Application Domains and Tasks." Applied Sciences, 12(2), 1353.
63. Islam, S. R., Eberle, W., Ghafoor, S. K., & Ahmed, M. (2021). "Explainable Artificial Intelligence Approaches: A Survey." Journal of Artificial Intelligence and Soft Computing Research, 11(4), 221-237.
64. Vilone, G., & Longo, L. (2021). "Notions of Explainability and Evaluation Approaches for Explainable Artificial Intelligence." Information Fusion, 76,
89–106.

https://doi.org/10.62500/icrtsda.1.1.13

Proc. 1st International Conference on Recent Trends in Statistics and Data Analytics
Air University Islamabad, Pakistan – May 9, 2024, Vol. 1, pp. 117-120

Efficacy of Betalyte Electrolyte in Reducing Broiler Chicken Mortality; A Commercial Study in Sambrial, Pakistan

Kainat Naeem*[1], Mehwish Asghar*[2] and Marya Murrawat*[1]
*[1]Department of Zoology, GC Women University Sialkot, Pakistan
*[2]Department of Statistics, GC Women University Sialkot, Pakistan

ABSTRACT

The physical, climatic and social stressors are threatening the output of poultry farming industry which is in increased demand as animal derived protein food nowadays. To overcome these threats Betalyte oral Electrolyte was used as an electrolyte supplement for poultry chicken. The research was conducted on commercial scale at Elahi Protein Farm, Sambrial. One was the control group, flock F1, of 28000 one-day-old chicks fed on normal diet and the other was experimental group of 28000 one-day-old chicks fed on Betalyte oral Electrolyte supplement along with normal diet. Both groups were supervised for 14 days. The one-way ANOVA statistical analysis showed significant ($P < 0.05$) results of Betalyte Electrolyte treatment and low per day mortality cases. To enhance the commercial production of poultry chicken in Pakistan, Betalyte Electrolyte should be used to overcome the acid-base imbalance, respiratory alkalosis, less feed intake, nutrient deficiency, panting and ultimately increasing mortality rate that led to low profits in poultry industry and reduce poultry base food.

KEYWORDS: Poultry, Betalyte oral Electrolyte, Sambrial, mortality, supplement.

1. INTRODUCTION

Poultry farming has become integral to global agriculture and food security, with the world now boasting over 23 billion birds, roughly three per person. This significant increase, compared to fifty years ago, highlights the sector's importance in providing meat, eggs, and fertilizing manure for crops (Mottet & Tempio, 2017). Demand for animal derived food is increasing because of population growth, rising income and urbanization in which poultry meat has shown the fastest trend in the last decades (Robinson et al., 2011).

The growth of the global livestock sector is expected to keep growing. The global human population is estimated to reach 9.6 billion in 2050. The demand for animal-derived food could grow by 70% between 2005 and 2050 (Alexandratos & Bruinsma, 2012). Poultry is one of the more efficient industries producing food for human. The output of this industry is threatened by climatic, social and physical stressors (Majekodunmi et al., 2012). Heat stress caused by high temperature has been a great concern in the broiler industry because of its negative impact on health status and production performance of poultry (Lara & Rostagno, 2013).

Heat stress may cause respiratory alkalosis, nutrient deficiency, acid base imbalance, less feed intake, panting and ultimately increasing mortality rate that led to low profits in poultry industry and reduce poultry base food (Wasti et al., 2020). To overcome this Betalyte oral can be formulated as an electrolyte for use during periods of extreme temperature, before and after transportation or when the conditions interfere with the normal flock.

The addition of betalyte oral electrolyte to poultry diets may help to stimulate water consumption, treatment of dehydration, diarrheas and fever. Betalyte Electrolyte also provides readily available source of body salts sodium, potassium that are vital for maintenance of osmotic pressure and balance of acid base. Betalyte Electrolyte also contain citric acid that can limit pathogenic colonization in the upper gut and improve nonspecific immunity, leading to high growth in broilers. Citric acid is an organic compound that enhances the gut health of birds (Melaku et al., 2021). It is also used to enhance calcium and phosphorus absorption in layers and broilers, resulting in better eggshell quality. The objective of

https://doi.org/10.62500/icrtsda.1.1.13

the study to evaluate the effectiveness of Betalyte Electrolyte in poultry form for reducing mortality rate.

2. METHODOLOGY

Site and Sample: This study was conducted at Elahi Protein Farm, Roras Road Sambrial. The experiment contained two groups of 28000 one-day-old chickens in each. Both of the groups were placed in similar physical conditions i.e. temperature, humidity, pressure, etc. The flock F2 as experimental group was treated by Beta-Lyte electrolyte supplement with a dose of 1 gram/4 liter of drinking water for 14 days. The flock F1 was the control group without the treatment of Beta-Lyte electrolyte supplement. Experts were hired to supervise the physical and dietary conditions, also to check the data collection and recording by collector.

Table 4: Components present in 1kg of betalyte oral electrolyte soluble powder

Components	Per kg of concentrate powder
Citric Acid	20,000 mg
Sodium bicarbonate	30,000 mg
Monosodium Phosphate	800 mg
Sodium Chloride	84,200 mg
Magnesium Sulfate	10,200 mg
Calcium gluconate	40,820 mg
Potassium Chloride	10,200 mg
Vitamin C	50,000 mg
Bacillus subtilis & licheniformis	3.2 x 109 CFU
Glycine	125,000 mg
Biotine	50 mg
Riboflavin	800 mg
Pyridoxine HCL	500 mg
Folic Acid	2000 mg
Dextrose	Up to 1kg

Betalyte Oral Electrolyte Concentrate Powder: 1gram Betalyte oral electrolyte concentrate soluble powder was dissolved per 4 liter of drinking water and was given to F2 flock right after the shipment in the farm along with dietary feed. Beta-Lyte electrolyte is composed of the different components mentioned in Table 1.

Mortality Cases: To check out the effect of betalyte electrolyte, the mortality rate of F1 and F2 flocks was recorded by data collector after 12 hours, twice a day. The deaths calculated at 9 am were considered as night mortality rate and the deaths calculated at 9 pm were considered as day mortality cases.

Survival Cases: On the basis of total mortality of day and night, total number of chicks survived was also calculated of both F1 and F2 flocks.

$$Total\ number\ of\ chicks\ survived\ per\ day = total\ number\ of\ chicks\ present\ per\ day - total\ number\ of\ chicks\ died\ per\ day$$

Statistical Analysis: Collected data was subjected to IBM SPSS Statistics 25 for one-way ANOVA with two variables, one is categorical (Betalyte electrolyte) and the other is numerical (mortality cases per day).

3. RESULTS AND DISCUSSION

The one-way ANOVA showed significant p-value=0.010 smaller than 0.05, therefore, the association between the per day mortality rate and the feeding on Betalyte electrolyte of the poultry chicken for the first 14 days proved true. We can say with 99.9% confidence that the two sample means of per day mortality cases are different.

https://doi.org/10.62500/icrtsda.1.1.13

The descriptives on one-way ANOVA showed the results as the mean of per day mortality cases in 14 days of flock F2 is less (16.5000) as compared to the flock F1 (27.3571).

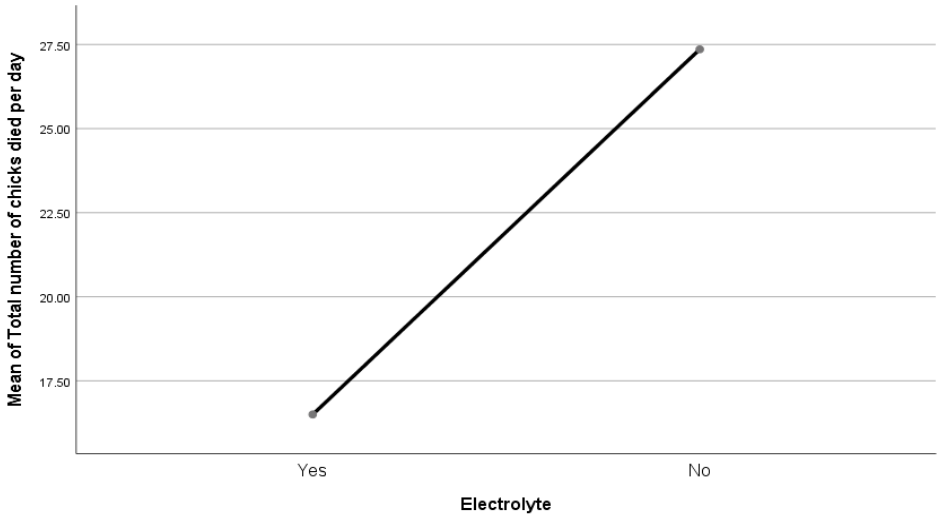

Figure 4: Mean Plot of total number of chicks died per day and electrolyte treatment

The p-value of the Levene's test of Homogeneity of Variance is greater than 0.05 (0.954), and the condition of homogeneity is satisfied.

Mortality: The mean plot in Figure 1 clearly showed that the F2 flock been reared with Betalyte electrolyte has less mortality cases per day as compared to the F1 flock without Betalyte electrolyte as supplement. And by overviewing the economic importance of poultry chicken in Pakistan, it is a positive factor to use Betalyte Electrolyte for the starter flock to increase the survival and decrease the mortality cases in order to get a productive flock.

Due to economical positive impact of supplements like electrolytes or ascorbic acid, these can be considered for chicks suffering from heat stress (Majekodunmi et al., 2012). A study by (Borges et al., 2003) showed non-significant results of electrolyte balance effect on mortality of poultry chicken. But as the composition of Betalyte Electrolyte is different from the dietary electrolytes used in Borges's study, the presence of other 14 components along with Sodium Chloride in a specific quantity makes the results of this study significant.

The study of (Livingston et al., 2022) included diet formulations with different salts i.e. Sodium Chloride or Sodium Bicarbonate for balancing electrolytes and the birds with different diets showed different imbalances of ions. Their results showed higher mortality rates for Sodium Chloride diets than Sodium Bicarbonate (Livingston et al., 2022). As Betalyte Electrolyte contained Sodium Chloride (84200 mg/kg) and Sodium Bicarbonate (30000 mg/kg) both, the significant results were justified as the presence of both have balanced the ions and reduced the broiler chicken mortality.

Also recorded that the F1 flock after 14 days showed aggressive behavior due to lack of electrolytes in the body and this chaos affected the whole flock leading to a less productive flock. These behavioral changes will be justified by the study of (ADVERSE) in which the birds showed floor pecking behavior due to heat stress similar to our observations of pecking and aggression.

Ethical consideration: For data collection and surveillance of the two broiler flocks, written consent was taken from the owner of the Elahi Protein Farm, Sambrial.

Conflict of interest: There is no conflict of interest in the present study.

https://doi.org/10.62500/icrtsda.1.1.13

4. COMMENTS AND CONCLUSION

The poultry chicken showed a significant result ($P < 0.05$) and low mortality cases when treated with Betalyte Electrolyte as a supplement to overcome the electrolyte imbalance at high temperatures, heat stress or shipping fever. Poultry is one of the more efficient industries producing food for human. To enhance the commercial production of poultry chicken in Pakistan Betalyte Electrolyte should be used to overcome the respiratory alkalosis, nutrient deficiency, acid base imbalance, less feed intake, panting and ultimately increasing mortality rate that led to low profits in poultry industry and reduce poultry base food.

REFERENCES

1. adverse, p. o. b. e. t. the effect of electrolyte supplementation on behaviour and performance of broilers exposed to adverse high temperature for one day prior to transport and processing he elshafaei, rr rashed2, aa goma2, se el-kazaz2, mj kerr 3, dl hopkins3 and ja downing1. 31st annual australian poultry science symposium,
2. Alexandratos, N., & Bruinsma, J. (2012). World agriculture towards 2030/2050: the 2012 revision.
3. Borges, S., Da Silva, A. F., Ariki, J., Hooge, D., & Cummings, K. (2003). Dietary electrolyte balance for broiler chickens under moderately high ambient temperatures and relative humidities. *Poultry Science*, *82*(2), 301-308.
4. Lara, L. J., & Rostagno, M. H. (2013). Impact of heat stress on poultry production. *Animals*, *3*(2), 356-369.
5. Livingston, M. L., Pokoo-Aikins, A., Frost, T., Laprade, L., Hoang, V., Nogal, B., Phillips, C., & Cowieson, A. J. (2022). Effect of heat stress, dietary electrolytes, and vitamins E and C on growth performance and blood biochemistry of the broiler chicken. *Frontiers in Animal Science*, *3*, 807267.
6. Majekodunmi, B., Ogunwole, O., & Sokunbi, O. (2012). Effect of Supplemental Electrolytes and Ascorbic Acid on the. *International Journal of Poultry Science*, *11*(2), 125-130.
7. Melaku, M., Zhong, R., Han, H., Wan, F., Yi, B., & Zhang, H. (2021). Butyric and citric acids and their salts in poultry nutrition: Effects on gut health and intestinal microbiota. *International Journal of Molecular Sciences*, *22*(19), 10392.
8. Mottet, A., & Tempio, G. (2017). Global poultry production: current state and future outlook and challenges. *World's Poultry Science Journal*, *73*(2), 245-256.
9. Robinson, T. P., Thornton, P. K., Francesconi, G. N., Kruska, R., Chiozza, F., Notenbaert, A. M. O., Cecchi, G., Herrero, M. T., Epprecht, M., & Fritz, S. (2011). *Global livestock production systems*. FAO and ILRI.
10. Wasti, S., Sah, N., & Mishra, B. (2020). Impact of heat stress on poultry health and performances, and potential mitigation strategies. *Animals*, *10*(8), 1266.

https://doi.org/10.62500/icrtsda.1.1.14

Proc. 1st International Conference on Recent Trends in Statistics and Data Analytics
Air University Islamabad, Pakistan – May 9, 2024, Vol. 1, pp. 121-128

Image Processing Techniques For Brain Tumor Detection

Hifza Naeem[1], and Mehwish Asgar[2]
Department of Statistics, Govt. College Women University Sialkot, Pakistan

Abstract

This paper explores the application of image processing techniques for brain detection, a critical aspect of medical diagnostics and research. Magnetic Resonance Imaging **(MRI)** is one of the best technologies currently diagnosing brain tumors. Brain tumor dataset obtained from Kaggle Website. They were categorized into 'yes' and 'no' tumor classes for **training (80%)** and **testing (20%)** purposes. Brain tumor is diagnosed at an advanced stage with the help of the **MRI** image. With the advancement of technology, medical imaging has become increasingly vital for identifying and analyzing brain structures and abnormalities. The proposed research focuses on leveraging various image processing methods to enhance the accuracy and efficiency of brain detection from medical images such as MRI, CT scans, and X-rays. The proposed system consists of two significant steps. First, preprocess the images using different image processing techniques and then classify the preprocessed image using CNN. Through comprehensive experimentation and analysis, the study aims to provide insights into the effectiveness of these techniques in accurately identifying and localizing brain regions, thereby facilitating timely diagnosis and treatment planning in clinical settings.

Keywords: CNN **(Convolutional Neural Network)**, MRI **(Magnetic Resonance Imaging)**, Image processing, Brain tumor.

1. INTRODUCTION

The human body consists of various types of cells, each serving a distinct purpose. These cells undergo orderly growth and division, replenishing the body's tissues. This process ensures the proper functioning and health of the body. However, when certain cells lose control over their growth, they proliferate irregularly, forming abnormal masses of tissue known as tumors. Tumors can be either benign or malignant, with malignant tumors having the potential to develop into cancer, while benign tumors are non-cancerous.. **[1]**

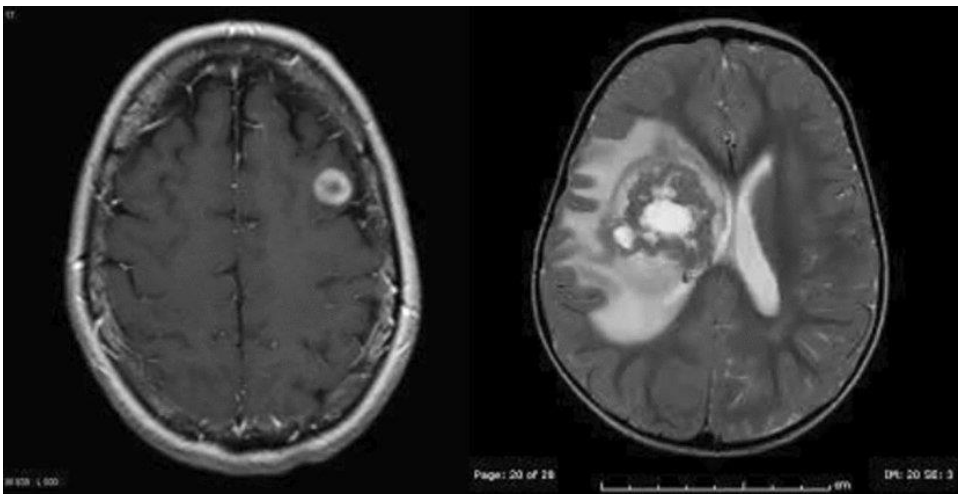

Fig 1 benign and malignant tumor

Brain tumor detection is a critical medical procedure that aids doctors in identifying tumors in the brain.

https://doi.org/10.62500/icrtsda.1.1.14

This process utilizes advanced imaging techniques and diagnostic tests such as MRI, CT scans, and biopsy. Detecting brain tumors at an early stage improves treatment options and enhances the patient's prognosis. Technological advancements and medical research play a significant role in this field.

According to National Brain Tumor Society, an estimated **688,000+** people are living with primary tumors of the brain and central nervous system **(CNS)** in the **United States, 138,000** with malignant tumors and **550,000** with benign tumors. That is up from an estimated **612,000+** people living with a primary brain and CNS tumor in the United States in **2004, 124,000** with malignant tumors and **488,000** with benign tumors. An estimated **13,700** deaths are expected to occur this year due to brain tumors, **7,720** males, and **5,980** females. About **43%** of brain and CNS tumors occur in men and about **57%** occur in women. So efficient and accurate techniques are required for brain tumor detection. In India, totally **80,271** people are affected by various types of tumor **(2007 estimates)**.**[2]**

Two common techniques used to classify The MR Images, they are supervised techniques such support vector machine, k-nearest neighbors, artificial neural networks, and unsupervised techniques such fuzzy c-means and self-organization map **(SOM)**. Many research used both supervised and unsupervised techniques to classify MR Images either as normal or abnormal.**[3]**

In this paper, the supervised machine learning techniques are used to classify five types of abnormal brain MR Images such as Ependymoma, Lymphoma, Cystic Oligodendroglioma, Meningioma and Anaplastic
Astrocytoma as well as normal type, **Fig. 2** illustrates MR Images types of brain tumor that were classified in this paper. Automated classification algorithm for brain MR Images was proposed by using machine learning approach involve **C4.5** decision tree algorithms and multi-layer perceptron **(MLP)**.**[4]**

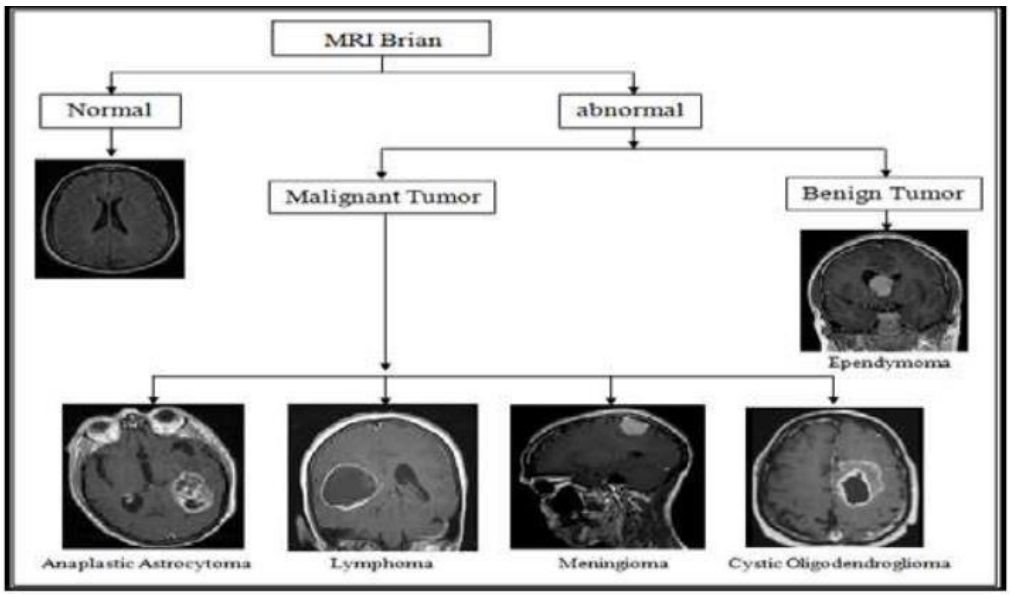

Fig.2 Five Types of MR Images That Were Classified In This Paper

The contribution of this paper is applying the deep learning concept to perform an automated brain tumors classification using brain MRI images and measure its performance. The proposed methodology aims to differentiate between normal brain and some types of brain tumors such as glioblastoma, sarcoma and metastatic bronchogenic carcinoma tumors using brain MRI images. The proposed methodology uses a set of features extracted by the discrete wavelet transform **(DWT)** feature extraction technique from the segmented brain MRI images, to train the **DNN** classifier for brain tumors classification.**[5]**

https://doi.org/10.62500/icrtsda.1.1.14

2. Literature Survey

Several studies have been reported on brain tumor prediction. The studies from different approaches are applied to the given problem statement and showed high classification accuracies. Drtails of some of the previous research works are given in the following **table 1**.

TABLE 1: Brain Tumor Detection Using 3D Deep Learning Techniques [6]

Reference	Methodology	Algorithms	Accuracy	Dataset used
Md. Akram Hossan Tuhin et. al. [48]	3D MRI, MRSI, and CT images are used for the detection of brain tumors using CNN and the detection of the tumor using segmentation methods	CNN and 3D CNN	85.005	Real-time hospital image dataset
Rudresh D. Shirwaikar et. al. [49]	3D CNN-based brain tumor segmentation, tumor detection, and classification	Various machine learning and deep learning classifiers.	-	Some real-time and some synthetic datasets are utilized
H. Yahyaoui et. al. [50]	DensNET using custom CNN for brain tumor detection	3D CNN , DENSENET model	92.06%, 85.00%	2 Heterogenous dataset including 3D and 2D real-time images
Pokhrel S et. al. [51]	3D image processing for brain tumor detection and classification	MobileNetV2, MobileNetV3 small, MobileNetV3 big, VGG16, VGG19,	92.00 %- 95.00%	Ream word brain image dataset
Gull S and Akbar S [52]	Binary classification of brain tumors has been implemented with 3D medical image	Dense-Net and Dark-Net based CNN	96.52%	BRATS 2018
Yannick Suter et al. [53]	3 Dimensional CNNs	SVM with heterogeneous feature extraction in CNN classification	72.20%	BraTS 2018
Yan Hu & Yong Xia [54]	DCNN	3D-based deep CNN	81.40%	BraTS 2017 Challenge dataset
Dong Nie et al. [55]	Classification using 3D deep Convolutional Neural Network	3D multi-level representation and organization by using CNN	99.60%	Brain images (i.e., T1 MRI, fMRI and DTI) of high-grade glioma patients.
Anand kumar & P.V. Shridevi [56]	Brain tumor segmentation using 3D deep learning	3DCNN	99.8%	BRATS 2015
Girija Chetty et.al. [57]	Medical image analysis by using 3D deep learning	3D U-NET	-	BraTS Challenge 2018 dataset
Zeeshan Shaukat. et al. [58]	Semantic segmentation using 3D deep learning	3D U-NET	Dice score-95%	BRATS dataset
Hiba Mzoughi. et al. [59]	Brain Tumor Classification using 3D multiscale.	3D CNN	96.49 %	BRATS 2018 dataset
Joseph Stember & Hrithwik Shalu [60]	Classification of 3D MRI brain tumors	Deep Reinforcement learning	100% testing set accuracy	3D MRI images
Yohan Jun et al. [61]	Detection of metastatic brain tumors using deep learning 3D black blood technique	3D CNN	97.08% and sensitivity-100%	Clinical data.
Pranjal Agrawal.et.al. [62]	Segmentation and classification using 3D deep learning	3D U-net, Deep CNN	90%	MRI Kaggle dataset
Agus Subhan Akbar.et.al [63]	U-net architecture for brain tumor segmentation	Residual attention block mechanism	77.73%, 82.19%, 89.33%	BRATS 2018,2019,2020,2021 challenge database

Machine Learning Methods:

Transfer Learning Models

Transfer learning is a machine learning technique that allows a model trained for one task to be used for a related task, saving time and effort. By adjusting the weights of an existing model, researchers can address new challenges effectively. This method utilizes knowledge gained from a large dataset during initial training, unlike the traditional approach of training from scratch, which can be time-consuming.**[7]** Transfer learning has been successful in various areas like image recognition and natural language processing, especially when there's limited training data. In this study, four transfer learning models were used, all processing input images of size (224×224) to ensure consistency. Transfer learning has been crucial in deep learning applications such as image classification, object recognition, and medical diagnosis.

Preprocessing:

It is very difficult to process an image. Before any image is processed, it is very significant to remove unnecessary items it may hold. After removing unnecessary artifacts, the image can be processed successfully.The initial step of image processing is Image Pre-Processing.

Pre-processing involves processes like conversion to grayscale image, noise removal and image reconstruction. Conversion to grey scale image is the most common pre-processing practice. After the image is converted to grayscale, then remove excess noise using different filtering methods.[8]

https://doi.org/10.62500/icrtsda.1.1.14

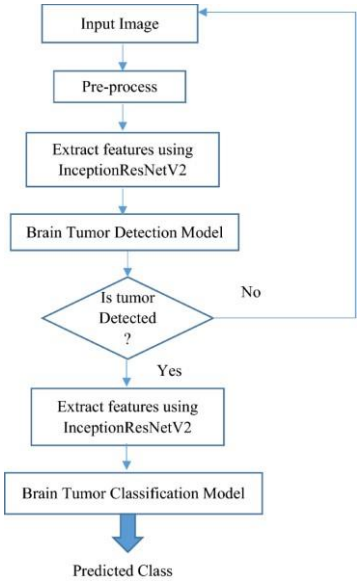

Resnet-50

In the short form of the residual network is ResNet-50. ResNet-50 is an adaptationof the ResNet architecture that has 50 deep layers and has been trained using at least one million examples from the ImageNet database [**9**]. The ResNet-50 architecture comprises a series of average pooling convolutional units [**10**].

Although the residual network layer is connected to the layers further ahead, in typical neural networks, each layer's output is connected to the next input layer. **Figure 3** shown with the residual units, the size of the filters and the outputs of each convolutional layer. DRF extracted from the last convolutional layer of this network is also shown. **Key:** The notation **k × k, n** in the convolutional layer block denotes a filter of size k and n channels. FC 1000 denotes the fully connected layer with 1000 neurons. The number on the top of the convolutional layer block represents the repetition of each unit.

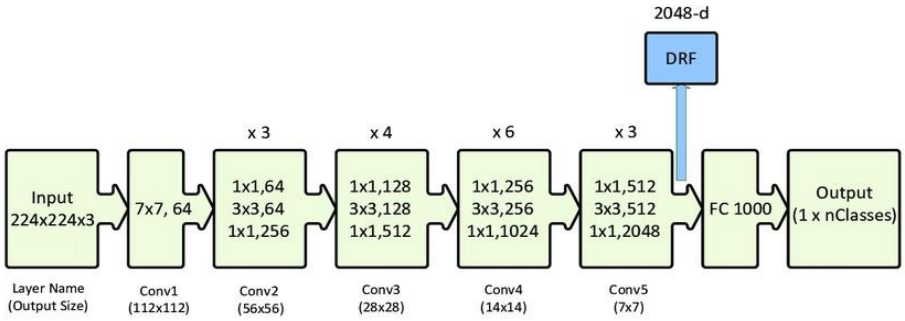

Fig.3 ResNet 50 architecture.

3. Preprocessing

It is very difficult to process an image. Before any image is processed, it is very significant to remove unnecessary items it may hold.[11] After removing unnecessary artifacts, the image can be processed successfully.The initial step of image processing is Image Pre-Processing.

https://doi.org/10.62500/icrtsda.1.1.14

Pre-processing involves processes like conversion to grayscale image, noise removal and image reconstruction. Conversion to grey scale image is the most common pre-processing practice. After the image is converted to grayscale, then remove excess noise using different filtering methods.[12]

Segmentation:

Segmentation of images is important as large numbers of images are generated during the scan and it is unlikely for clinical experts to manually divide these images in a reasonable time .

Image segmentation refers to segregation of given image into multiple non-overlapping regions.[13] Segmentation represents the image into sets of pixels that are more significant and easier for analysis an image and the resulting segments collectively cover the complete image.[14]

Feature Extraction:

Feature extraction is an important step in the construction of any pattern classification and aims at the extraction of the relevant information that characterizes each class.

In this process relevant features are extracted from objects/ alphabets to form feature vectors. These feature vectors are then used by classifiers to recognize the input unit with target output unit. Feature extraction is the process to retrieve the most important data from the raw data.

4. Classification

Classification is used to classify each item in a set of data into one of predefined set of classes or groups . [15] In other words, classification is an important technique used widely to differentiate normal and tumor brain images. The data analysis task classification is where a model or classifier is constructed to predict categorical labels **(the class label attributes).** Classification is a data mining function that assigns items in a collection to target categories or classes. (as shown in Fig. 4).

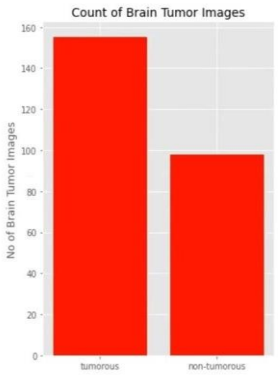

fig 4 .classification

Machine learning Classifier:

The process of predicting the particular class of given data point is known as Classification. Classes are referred by targets/ labels/categories in terms of classification problems. The extracted deep features from pre-trained CNN models are used as an input of several ML classifiers, including neural networks with SVM Extreme Learning Machine (ELM).

https://doi.org/10.62500/icrtsda.1.1.14

Support Vector Machine:

It is a supervised learning algorithm that is capable of making fine classifications through a separating hyperplane. In other means, trained labeled data (Supervised Learning) has been used and the algorithm returns an optimal separating hyperplane which classifies new examples.

Logistic Regression: It is a Classification model which is very simple to implement and performs efficiently on linear separable classes. It is a Binary classification algorithm but can be implemented for multi-class classification.

Dataseta and Results:

In this study, we used two types of datasets. This dataset contains a total weighted contrast MRI slices from 253 patients diagnosed with one of the three brain tumors, including meningioma, glioma, and pituitary (as shown in 5).

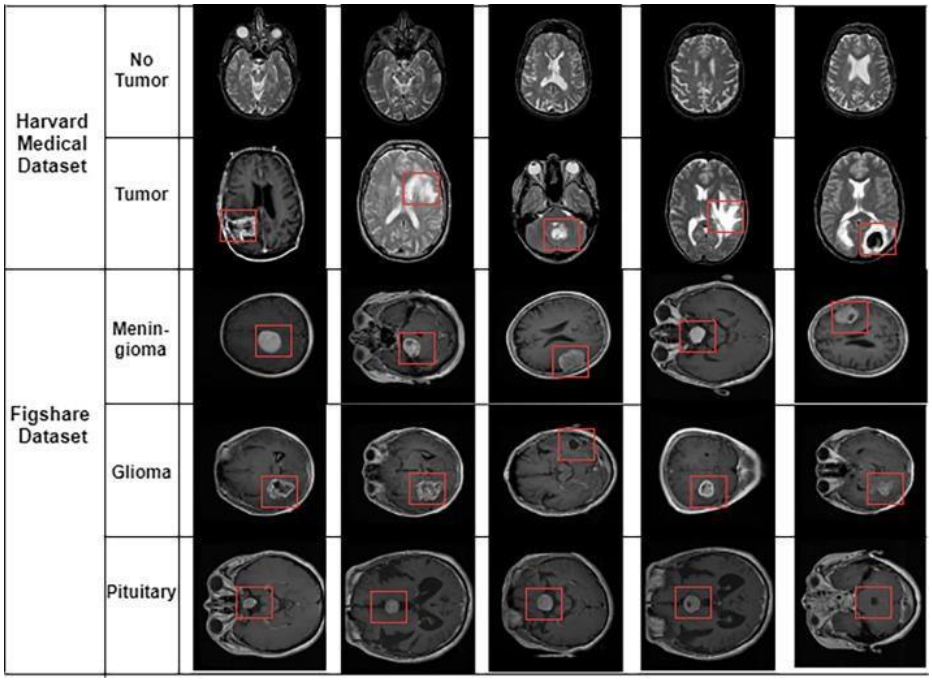

Fig5. The Different samples of brain tumors.

Accuracy:

After running through multiple epochs, As we can see through multiple epochs training loss and validation loss decreases. Training accuracy of the model is quite high 0.5031 while the validation accuracy is 0.7238. Accuracy on test data in 87%.

https://doi.org/10.62500/icrtsda.1.1.14

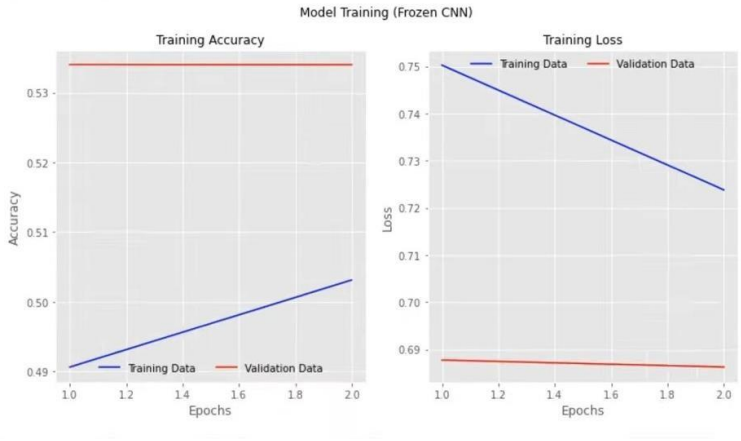

5. Conclusion

This paper offers a comprehensive review of the research conducted on the detection and classification of brain tumors in MRI images into tumor and non-tumor categories using Deep Learning techniques. MRI images are best suitable for brain tumor detection. In this study Digital Image Processing Techniques are important for brain tumor detection by MRI images. Hence there is working on development of automatic, efficient, fast and accurate which is use for detection disease. Further to needed to compute amount of disease present. While many effective algorithms have been created, each one has its limitations, primarily due to the absence of standardization. This study provides an in-depth critical analysis of the strengths and weaknesses of the methodologies developed during this period.

Reference:

1. Sharma, K., Kaur, A., & Gujral, S. (2014). Brain tumor detection based on machine learning algorithms. *International Journal of Computer Applications*, *103*(1).
2. Sharma, P., Diwakar, M., & Choudhary, S. (2012). Application of edge detection for brain tumor detection. *International Journal of Computer Applications*, *58*(16)s
3. Jafari, M., & Kasaei, S. (2011). Automatic brain tissue detection in MRI images using seeded region growing segmentation and neural network classification. *Australian Journal of Basic and Applied Sciences*, *5*(8), 1066-1079.
4. George, D. N., Jehlol, H. B., & Oleiwi, A. S. A. (2015). Brain tumor detection using shape features and machine learning algorithms. *International Journal of Advanced Research in Computer Science and Software Engineering*, *5*(10), 454-459.
5. Mohsen, H., El-Dahshan, E. S. A., El-Horbaty, E. S. M., & Salem, A. B. M. (2018). Classification using deep learning neural networks for brain tumors. *Future Computing and Informatics Journal*, *3*(1), 68-71.
6. Solanki, S., Singh, U. P., Chouhan, S. S., & Jain, S. (2023). Brain tumor detection and classification using intelligence techniques: An overview. *IEEE Access*.
7. Cao, B.; Pan, S.J.; Zhang, Y.; Yeung, D.Y.; Yang, Q. Adaptive transfer learning. In Proceedings of the AAAI Conference on Artificial Intelligence, Atlanta, GA, USA, 11–15 July 2010; Volume 24, pp. 407–412.
8. Almourish, M.H.; Saif, A.A.; Radman, B.M.; Saeed, A.Y. COVID-19 diagnosis based on CT images using pre-trained models. In Proceedings of the 2021 IEEE International Conference of Technology, Science and Administration (ICTSA), Taiz, Yemen, 22–24 March 2021; pp. 1–5.
9. Wu, P.; Tan, Y. Estimation of economic indicators using residual neural network ResNet50. In Proceedings of the 2019 IEEE International Conference on Data Mining Workshops (ICDMW), Beijing, China, 8–11 November 2019; pp. 206–209.
10. Theckedath, D.; Sedamkar, R. Detecting affect states using VGG16, ResNet-50 and SEResNet-50 networks. *Comput. Sci.* **2020**, *1*, 79.

https://doi.org/10.62500/icrtsda.1.1.14

11. Al-Haija, Q.A.; Manasra, G.F. Development of Breast Cancer Detection Model Using Transfer Learning of Residual Neural Network (ResNet-50). *Am. J. Sci. Eng.* **2020**, *1*, 30– 39.
12. Setiawan, A.W. The Effect of Image Dimension and Exposure Fusion Framework Enhancement in Pneumonia Detection Using Residual Neural Network. In Proceedings of the 2022 IEEE International Seminar on Application for Technology of Information and Communication (iSemantic), Wuhan, China, 4–6 Feburary 2022; pp. 41–45.
13. Jiang, T.; Zhang, Q.; Yuan, J.; Wang, C.; Li, C. Multi-Type Object Tracking Based on Residual Neural Network Model. *Symmetry* **2022**, *14*, 1689.
14. Amin, J., Sharif, M., Yasmin, M., & Fernandes, S. L. (2020). A distinctive approach in brain tumor detection and classification using MRI. *Pattern Recognition Letters*, *139*, 118127.
15. Hemanth, G., Janardhan, M., & Sujihelen, L. (2019, April). Design and implementing brain tumor detection using machine learning approach. In *2019 3rd international conference on trends in electronics and informatics (ICOEI)* (pp. 1289-1294). IEEE.
16. Abbas, N., Saba, T., Rehman, A., Mehmood, Z., Kolivand, H., Uddin, M., & Anjum, A. (2019). Plasmodium life cycle stage classification-based quantification of malaria parasitaemia in thin blood smears. *Microscopy Research and Technique*. (3): 283–295.
17. Abbas, N., Saba, T., Mohamad, D., Rehman, A., Almazyad, A. S., & Al-Ghamdi, J. S. (2018). Machine aided malaria parasitemia detection in Giemsa-stained thin blood smears. *Neural Computing and Applications*, **29**(3), 803–818.

Enhancing Lung Cancer Diagnosis: Unraveling the Power of Survival Analysis and Multinomial Regression for Precision Healthcare
https://doi.org/10.62500/icrtsda.1.1.15

Proc. 1st International Conference on Recent Trends in Statistics and Data Analytics
Air University Islamabad, Pakistan – May 9, 2024, Vol. 1, pp. 129-139

Enhancing Lung Cancer Diagnosis: Unraveling the Power of Survival Analysis and Multinomial Regression for Precision Healthcare

Tehreem Fatima and Mehwish Asghar
Department of Statistics, Government College Women
University Sialkot, Pakistan

ABSTRACT

Cancer, a complex and devastating disease, encompasses a broad spectrum of conditions characterized by abnormal cell growth. Among these, lung cancer stands out as the most lethal form, claiming more lives annually than several other common cancers combined for both men and women. Lung Cancer is an international journal focusing on lung and chest malignancies. It predominantly affects older adults and is rare in individuals under 45. Tobacco smoke and tobacco gas are major contributors to lung cancer. Smoking stands as the primary cause, responsible for around 90% of cases. Other Symptoms include chest pain, shortness of breath, and coughing up blood. The methodology involves multinomial regression and Survival Analysis. Exercise training and nurse counseling can help alleviate symptoms in lung cancer patients. The cancer's stage indicates its spread level and treatment varies based on cancer type, stage, and overall health. Lung cancer can be fatal but advancements in treatment have increased survival rates, especially with early detection. Factors affecting the likelihood of positive outcomes include a person's overall health and age.

Keywords: Lung Cancer, Malignancies, Fatal, Advancements in treatments, Likelihood of positive outcome.

1. INTRODUCTION

Lung cancer is a disease characterized by uncontrolled growth of cells in the lungs. Lung cancer was first described by doctors in the mid-19th century. In the early 20th century it was considered relatively rare, but by the end of the century, it was the leading cause of cancer-related death among men in more than 25 developed countries [1]. In the

21st century lung cancer it was emerged as the leading cause of cancer deaths worldwide [2]. By 2012 it had surpassed breast cancer as the leading cause of cancer death among women in developed countries. Cancer poses a significant challenge to highly developed and less developed countries, impacting society on a large scale [3]. In 2020, the detection and management of cancer were negatively impacted by the COVID-19 pandemic. Limited access to healthcare due to facility closures and concerns about COVID-19 exposure caused delays in diagnosis and treatment, potentially leading to a temporary decrease in cancer cases followed by a rise in advanced-stage disease and ultimately higher mortality rates [4]. Lung cancer occurs primarily in persons between the ages of 45 and 75 years. The number of cancer patients aged >70 years has significantly increased among the cancer patient population [5]. In countries with a prolonged history of tobacco smoking, between 80 and 90 percent of all cases are caused by smoking [6]. Smoking is the cause of 30 to 40% of deaths from cancer [7]. Heavy smokers have a greater likelihood of developing lung cancer than light smokers. Even when we consider age, gender, and tobacco use, guys who started smoking before they turned 20 faced a significantly greater chance of getting lung cancer [8]. Passive inhalation of cigarette smoke (sometimes called secondhand smoke) is linked to lung cancer in nonsmokers. Risk factors include smoking, exposure to radon gas, asbestos, second-hand smoke, air pollution, and genetic factors [9]. Individuals

https://doi.org/10.62500/icrtsda.1.1.15

with a family background of lung cancer have a higher chance of getting lung cancer themselves [10,11]. A cough that does not go away or gets worse, coughing up blood or rust-colored sputum (spit or phlegm), chest pain that is often worse with deep breathing, coughing, or laughing, Hoarseness, Loss of appetite, Unexplained weight loss, Shortness of breath, feeling tired or weak, Infections such as bronchitis and pneumonia that don't go away or keep coming back, new onset of wheezing [12,13]. Bone metastases present a major clinical issue that is often not adequately addressed in individuals with advanced lung cancer. When lung cancer spreads to other parts of the body, in that case, it may cause bone pain (like pain in the back or hips), nervous system changes (such as headache, weakness or numbness of an arm or leg, dizziness, balance problems, or seizures), from cancer spread to the brain, yellowing of the skin and eyes (jaundice), from cancer spread to the liver, swelling of lymph nodes (collection of immune system cells) such as those in the neck or above the collarbone, some lung cancers can cause syndromes, which are groups of specific symptoms [14,15,16]. To start the treatment, it is necessary to assess the histological type of the cancer, its size and location, its stage, and the general health conditions of the patient [17].

Most people diagnosed with lung cancer are 65 or older; a very small number of people diagnosed are younger than 45. The average age of people when diagnosed is about 70. Diagnosis of this disease is performed through chest radiography in most cases, an easyto-perform and relatively low-cost exam, but it can also be done through computed tomography, positron emission tomography, bronchoscopy, and biopsy [18]. One of the main challenges in Lung Cancer is to make an early diagnosis, in most cases, the disease is detected already in its late stages, which implies a poor prognosis. Therefore, it is necessary to understand molecular biomarkers, which defined in a general and simplified way, are components that distinguish between the normal status and the abnormal status of a cell, thus aiding in the early diagnosis, the understanding of carcinogenesis, prognostic determination, and the choice of therapy [19,20]. Treatment options for lung cancer include surgery, radiation therapy, chemotherapy, and targeted therapy. Therapeutic modalities recommendations depend on several factors, including the type and stage of cancer [21]. One of the most effective ways to prevent lung cancer mortality is by reducing tobacco use. Quitting smoking or never starting in the first place can significantly lower the risk of developing lung cancer and improve overall health [22]. Maintaining a healthy lifestyle with regular exercise and a balanced diet can also contribute to overall well-being. Early detection through screenings can be crucial. Maintaining a healthy lifestyle with regular exercise and a balanced diet can also contribute to overall well-being. Early detection through screenings can be crucial. Surgeries can be of three types, segmentectomy and wedge resection (when a small part of the lung is removed), lobectomy (the entire lung lobe affected by the tumor is removed), and pneumectomy (complete removal of the lung) [23,24,25]. Diagnosis of lung cancer at advanced stages can result in missed treatment opportunities, worse outcomes, and higher health care costs [26]. Also delay in lung cancer treatment can be caused by various factors, such as late diagnosis, waiting times for appointments and test results, patient-related factors like hesitation to seek medical help, and healthcare system challenges [27,28,29]. The treatment delays can occur due to the need for multiple consultations to determine the best course of action, waiting for availability of specific treatment modalities, or logistical issues in scheduling surgeries or other interventions [30].

2. LITERATURE REVIEW

A study was conducted on the disease of Lung cancer in the Elderly and its treatments with chemotherapy and radiotherapy. The results were that the positive outcomes seen with extra chemotherapy for the general population with early non-small-cell lung cancer (NSCLC) may not directly apply to older individuals, who face a higher risk of side effects. When looking back at treatments combining chemotherapy and radiotherapy in locally advanced NSCLC patients, studies

https://doi.org/10.62500/icrtsda.1.1.15

suggest that both younger and older patients receive similar benefits even though older patients may experience more side effects. There haven't been specific large studies for older patients with locally advanced NSCLC. In advanced NSCLC, single-drug chemotherapy is the standard treatment for older patients based on solid evidence. However, looking back at past data, platinum-based combinations show similar effectiveness in both fit older and younger patients, even though older patients might experience more side effects. For limited-disease small-cell lung cancer (SCLC), giving chemotherapy and radiotherapy one after the other is less harsh than doing them at the same time, but the lack of specific trials for older patients makes it hard to assess the treatment accurately. While preventive cranial radiation is commonly used, it's not recommended for patients with memory issues. In extensive SCLC, using etoposide with either cisplatin or carboplatin is the standard treatment, and patients might need support for their blood system. In conclusion, except for advanced NSCLC, there's a lack of studies specifically focusing on older patients. The existing data suggests t2hat older patients in good health have similar results to younger patients, but they may experience more side effects.

Another research study focused on lung cancer investigated the time delays in diagnosing the disease. The study involved 73 patients and was carried out over 3 months to examine delays in diagnosis. Patients were asked about the onset of symptoms, their doctor visits, diagnostic tests, specialist consultations, and treatment initiation. Descriptive statistics were utilized to summarize the various time intervals. Out of the 73 patients, 56 agreed to participate (response rate 77%). However, only 52 patients (30 males, 22 females) were interviewed as two had passed away before the interviews and two could not be reached. The average age of the patients was 68 years. The distribution of cancer stages was as follows: 10% stage IB/IIA, 20% stage IIIA, and 70% stage IIIB/IV. Patients waited a median of 21 days (interquartile range 7-51 days) before seeing a doctor and an additional 22 days (interquartile range 0-38 days) for diagnostic tests. The median duration from initial presentation to specialist referral was 27 days (interquartile range 12-49 days), followed by another 23.5 days (interquartile range 10-56 days) for further investigations. The median waiting time to commence treatment after visiting the cancer center was 10 days (interquartile range 2-28 days). The total duration from the onset of symptoms to treatment initiation was 138 days (interquartile range 79-175 days). The study concluded that lung cancer patients face significant delays from symptom onset to beginning treatment. It emphasized the importance of raising awareness about lung cancer symptoms and the necessity to establish and assess rapid assessment clinics for individuals suspected of having lung cancer.

Another study focused on lung cancer and its treatments, which include surgery, adjuvant chemotherapy, and radiation therapy. Lung cancer is a leading cause of cancer-related deaths globally, with a 5-year survival rate of only 15% due to delayed diagnosis. The treatments, while effective, come with significant side effects that can impact the quality of life of patients. The progression of the disease, the severity of symptoms, and the side effects all contribute to a decrease in the quality of life of individuals with lung cancer. Self-assessment of quality of life can help predict survival, especially crucial for patients receiving palliative care. Patients evaluate their well-being across five dimensions: physical, psychological, cognitive, social, and life roles, as well as the severity of symptoms, financial challenges, and overall quality of life. Compared to the general population and patients with other cancers, lung cancer patients report lower quality of life. Specific symptoms like fatigue, loss of appetite, shortness of breath, cough, pain, and blood in sputum, which are common in lung cancer, greatly impact quality of life. Fatigue and respiratory issues affect the psychological dimension, while sleep problems impact cognitive functioning. Physical functioning declines due to disability, and many patients struggle to fulfill their family and social roles. Lung cancer often leads to irritation, distress, and depression. Managing symptoms of the disease can enhance the quality of life. Strategies such as addressing fatigue levels, pulmonary rehabilitation, and providing social and spiritual support are

https://doi.org/10.62500/icrtsda.1.1.15

recommended. Early implementation of personalized palliative care can significantly improve the quality of life for lung cancer patients.

3. METHODOLOGY

Survival analysis plays a vital role in understanding how different factors influence the survival rates of individuals with lung cancer. By analyzing data on patient outcomes over time, we identify patterns and trends that can lead to more accurate diagnoses and tailored treatment plans. This approach helps us providers make informed decisions, improve patient care, and ultimately enhance the effectiveness of lung cancer management. It's like shining a spotlight on the best strategies to fight against this challenging disease and provide personalized care for each patient. The Kaplan–Meier estimator, also known as the product limit estimator, is a non-parametric statistic used to estimate the survival function from lifetime data. We use Kaplan-Meier in our analysis to dig into survival data. It lets us check out survival probabilities at different times, even if some data is missing. This technique is super important for understanding how treatments work and creating personalized healthcare plans for people with lung cancer. It's like having a powerful tool that helps us make smart choices to improve patient outcomes and fine-tune precision healthcare strategies. Patients with lung cancer can improve symptoms with exercise training and nurse counseling. The higher the stage, the more the cancer has spread. Treatment for lung cancer depends on the type of cancer, how advanced it is, and how healthy you are. Another method is Multinomial Regression Analysis. In lung cancer diagnosis, multinomial regression can be applied to study how various factors like smoking history, age, and genetic markers impact the chances of developing specific types of lung cancer. By exploring these connections, healthcare professionals and researchers can enhance their ability to predict the type of lung cancer a patient might have based on their traits. This aids in customizing treatment plans that are most suitable for each patient's specific type of lung cancer. It's similar to having a personalized route map that leads to more precise and effective treatment strategies. A multinomial logistic regression (or multinomial regression for short) is used when the outcome variable being predicted is nominal and has more than two categories that do not have a given rank or order. This model can be used with any number of independent variables that are categorical or continuous. For comparison of the Kaplan-Meier survival curve, three tests are applied.

Table 1. Baseline Characteristics

		N
	0	47
	1	81
	2	39
	3	1
	1	104
Sex		
64 ph. ecog		
	2	
	0	47
Status		
	1	121
Total	168	

ph. ecog indicates ECOG Performance Status.
N indicates the Number of Patients

https://doi.org/10.62500/icrtsda.1.1.15

There are a total of 168 lung cancer patients of which 104 are males, and 64 are females. Among them, 47 are fully active (status 0), 81 can do light work but have restrictions (status 1), 39 can do self-care but can't work (status 2), and only 1 person is limited to bed (status 3). Overall, 47 individuals have passed away, while 121 are still alive.

MULTINOMIAL LOGISTIC REGRESSION MODEL

Table 2. Multinomial Logistic Regression Model

	-2 Log Likelihood	Chi-Square	df	p-value
Intercept Only	448.653	106.393	190	1.000
Sex	463.815	15.162	38	1.000
Status	443.999		38	
ph. ecog	458.635	9.982	114	1.000

df indicates the degree of freedom.

ph. ecog indicates ECOG Performance Status.

Ho: There is no relationship between status, ph. ecog, and sex.

H1: indicates that there is a relationship between status, ph. ecog, and sex.

In the multinomial logistic regression, we looked at how sex is influenced by ph. ecog and status. The chi-square value we found for intercept only was 106.393 with 190 degrees of freedom, and the significant value was 1.000. So, it suggests that it is not significant. Since the p-value is 1.000, which is the highest possible value, it indicates that there is no statistical significance in the relationship between status, ph. ecog, and sex. With a p-value of 1.000, we would fail to reject the null hypothesis, suggesting that there is no significant dependency between these variables. So, we cannot reject H_o which means there is no relationship between status, ph. ecog, and sex.

Table 3. Pseudo R-Square

Cox and Snell	0.469
Nagelkerke	0.470
McFadden	0.091

Here, the Cox and Snell R-squared is 0.469, the Nagelkerke R-squared is 0.470, and the McFadden R-squared is 0.091. These values help assess how well the model fits the data. So, the Nagelkerke R-squared is slightly higher than the Cox and Snell R-squared, indicating a better fit. However, the McFadden R-squared is relatively low compared to the other two, which suggests that the model might not be the best fit overall. Therefore, based on these values, the Nagelkerke R-squared seems to be the best choice for evaluating the model's fit. Also, a higher Cox and Snell value of 0.469 and Nagelkerke value of 0.470 indicate that the model explains a substantial amount of the variability in the outcomes. This suggests that the survival analysis and multinomial regression approach are effective in capturing the nuances of lung cancer diagnosis, contributing significantly to precision healthcare. On the other hand, the lower McFadden value of 0.091 implies that while the model is informative, there is still room for improvement in explaining the variation in the data. This indicates that further refinement and additional factors may enhance the precision and accuracy of the model for lung cancer diagnosis.

https://doi.org/10.62500/icrtsda.1.1.15

CHI-SQUARE TEST

Table 4. Chi-Square Test

	Value	df	p-value
Pearson Chi-Square	142.544[a]	114	0.036
Likelihood Ratio	138.787	114	0.057
Linear-by-Linear Association	16.284	1	0.000

df indicates the degree of freedom.

H_o: There is no association between age and ph. ecog stages.

H_1: There is an association between age and ph. ecog stages.

The comparison done is for age and ph. ecog stages using the chi-square test. The Pearson chi-square value came out to be 142.544 with 114 degrees of freedom, and the p-value was 0.036. The likelihood ratio value was 138.787 with 114 degrees of freedom, and the pvalue was 0.057. Additionally, the chi-square value for linear by linear association was 16.284 with 1 degree of freedom and the p-value was 0.000. With these p-values, we would reject the null hypothesis, suggesting that there is a significant dependency between these variables. So, we can reject H_o which means there is an association between age and ph. ecog stages. This finding could indicate that age alone may not be a strong predictor of ph. ecog stages in lung cancer diagnosis. It highlights the importance of considering other variables or factors in the model to improve the precision and accuracy of lung cancer diagnosis.

Table 5. Chi-Square Test

	Value	df	p-value
Pearson Chi-Square	1755.889[a]	1710	0.215
Likelihood Ratio	654.668	1710	1.000
Linear-by-Linear Association	0.352	1	0.553

df indicates the degree of freedom.

H_o: There is no association between age and weight loss.

H_1: There is an association between age and weight loss.

The comparison done is for age and weight loss using the chi-square test. The Pearson chisquare value came out to be 1755.889 with 1710 degrees of freedom, and the p-value was 0.215. The likelihood ratio value was 654.668 with 1710 degrees of freedom, and the pvalue was 1.000. Additionally, the chi-square value for linear by linear association was 0.352 with 1 degree of freedom and the p-value was 0.553. With these p-values, we would fail to reject the null hypothesis, suggesting that there is no significant dependency between these variables. So, we cannot reject H_o which means there is no association between age and weight loss. So, this result would highlight the significance of including age and weight loss in the analysis to improve the precision and accuracy of lung cancer diagnosis.

https://doi.org/10.62500/icrtsda.1.1.15

Table 6. Chi-Square Test

	Value	df	p-value
Pearson Chi-Square	38.354[a]	38	0.453
Likelihood Ratio	46.753	38	0.156
Linear-by-Linear Association	4.345	1	0.037

df indicates the degree of freedom.

H_o: There is no association between age and status.

H_1: There is an association between age and status.

The comparison done is for age and status using the chi-square test. The Pearson chi-square value came out to be 38.354 with 38 degrees of freedom, and the p-value was 0.453. The likelihood ratio value was 46.753 with 38 degrees of freedom, and the p-value was 0.156. Additionally, the chi-square value for linear by linear association was 4.345 with 1 degree of freedom and the p-value was 0.037. With these p-values, we would fail to reject the null hypothesis, suggesting that there is no significant dependency between these variables. So, we cannot reject H_o which means there is no association between age and weight loss. It indicates that other variables might have a more significant influence on the accuracy of lung cancer diagnosis.

KAPLAN MEIER ANALYSIS

Table 7. Means and Medians for Survival Time

	Coefficients	Confidence Interval
Mean	618.508(37.552)	544.906, 692.111
Median	740.000(116.671)	511.326, 968.674

Based on the Kaplan-Meier analysis, the mean survival estimate is 618.508 with a standard error of 37.552, and the median survival estimate is 740.000 with a standard error of 116.671. With a higher median survival estimate compared to the mean, it suggests that the survival times are skewed towards the higher end, possibly indicating that a significant portion of the group has longer survival times. The standard errors give an idea of the precision of these estimates. Overall, the results show that the group has a relatively good survival outcome, with the median survival time being higher than the mean, indicating a positively skewed distribution of survival times. Also, the confidence interval for the mean survival estimate is 544.906 to 692.111 and the median is 5111.326 to 968.674, which gives us more insight into the precision of our estimates. The wider confidence interval for the median suggests more variability in the data around the median estimate compared to the mean. Overall, it seems like there is a good amount of variability in the survival times, especially around the median estimate. It shows that survival times can vary a lot, especially near the middle estimate. This variation means that patients with lung cancer may have very different survival times, showing the different outcomes and paths of this disease. This analysis gives healthcare providers important information about how long patients may survive, helping them plan treatments better and take care of patients more effectively.

https://doi.org/10.62500/icrtsda.1.1.15

Table 8. Test of Significance for Comparison of Kaplan Meier Survival Curves

	Chi-Square	df	p-value
Log Rank (Mantel-Cox)	3.118	1	0.077
Breslow (Generalized Wilcoxon)	1.454	1	0.228
Tarone-Ware	2.012	1	0.156

df indicates the degree of freedom.

The tests for comparing the Kaplan Meier survival curves show that the Log Rank (MantelCox) test has a chi-square value of 3.118 with 1 degree of freedom and a p-value of 0.077. The Breslow (Generalized Wilcoxon) test has a chi-square value of 1.454 with 1 degree of freedom and a p-value of 0.228. Lastly, the Tarone-Ware test has a chi-square value of 2.012 with 1 degree of freedom and a p-value of 0.156. So, since none of the tests have pvalues lower than 0.05, which is the typical cutoff for statistical significance, it seems like there isn't adequate evidence to claim there's a significant variance in survival curves. The Log-Rank test has the lowest p-value, indicating it may be the most sensitive for detecting differences between the groups being compared. So, the Log Rank test seems to be the most suitable.

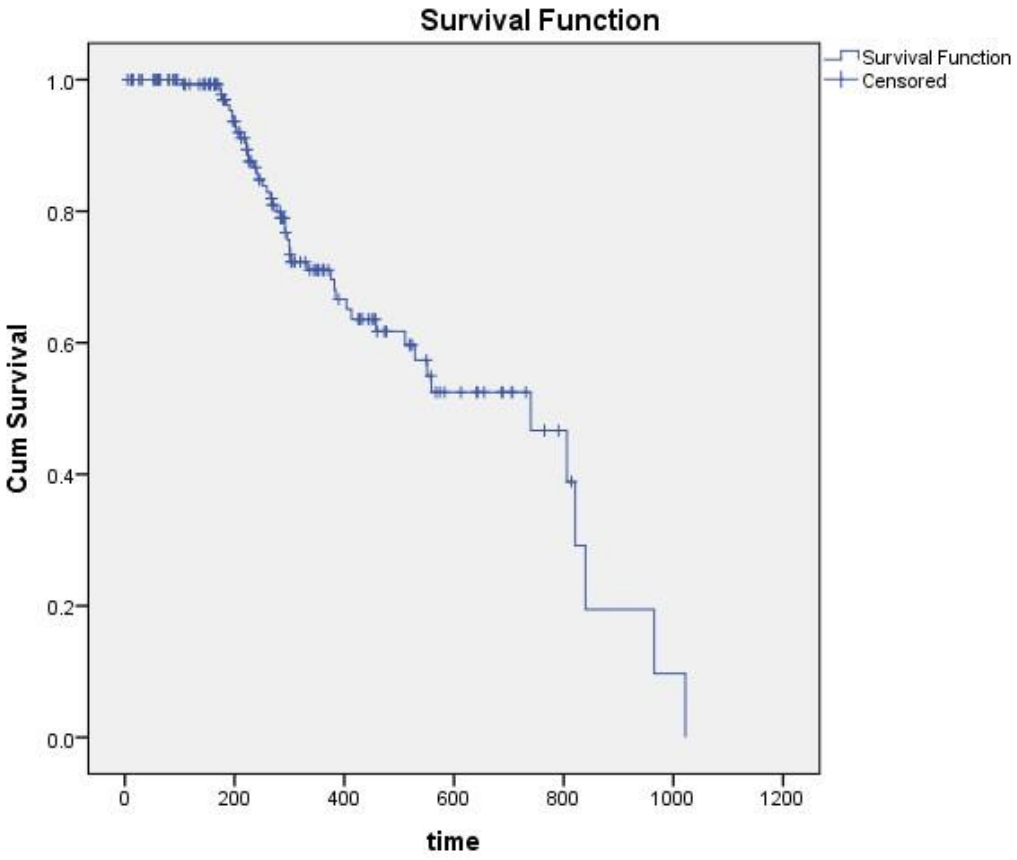

https://doi.org/10.62500/icrtsda.1.1.15

The Kaplan-Meier curve shows the cumulative survival probabilities. A flatter slope curve indicates a lower event rate and therefore a better survival prognosis. So, it tells that the survival times of patients are more consistent or similar and it suggests that patients have more uniform survival outcomes, with less variation in how long they survive. This could imply that the factors influencing survival in patients are more consistent or that the treatment provided has a more predictable impact on their survival times.

4. COMMENTS AND CONCLUSION

In conclusion, lung cancer is a significant global health concern primarily linked to smoking. Early detection, understanding molecular biomarkers, and promoting tobacco cessation are crucial for improving prognosis. Survival analysis and multinomial regression are effective tools for personalized treatment plans, but further refinement is needed for better accuracy. The analysis of age and ph. ecog stages show a significant association, emphasizing the importance of considering multiple variables for precise lung cancer diagnosis. The comparison of age and weight loss, as well as age and status, did not show significant dependencies, suggesting the need for additional factors in the analysis. The Kaplan-Meier analysis indicates a positively skewed distribution of survival times, with a good median survival estimate. The Log Rank test is the most sensitive for detecting differences in survival curves, highlighting its suitability for analysis. The Kaplan-Meier curve suggests consistent survival outcomes for patients, indicating more uniform survival times and potential predictability in treatment impact. Also, it's crucial to address the delays in treatment promptly to ensure timely and effective lung cancer treatment.

REFERENCES

1. Britannica, T. Editors of Encyclopaedia (2024, April 25). lung cancer. Encyclopedia Britannica. https://www.britannica.com/science/lung-cancer
2. Boiselle, P. M., Ernst, A., & Karp, D. D. (2000). Lung cancer detection in the 21st century: potential contributions and challenges of emerging technologies. *American Journal of Roentgenology*, *175*(5), 1215-1221.
3. Torre, L. A., Bray, F., Siegel, R. L., Ferlay, J., Lortet-Tieulent, J., & Jemal, A. (2015). Global cancer statistics, 2012. *CA: a cancer journal for clinicians*, *65*(2), 87-108.
4. Siegel, R. L., Miller, K. D., Fuchs, H. E., & Jemal, A. (2022). Cancer statistics, 2022. *CA: a cancer journal for clinicians*, *72*(1).
5. Tas, F., Ciftci, R., Kilic, L., & Karabulut, S. (2013). Age is a prognostic factor affecting survival in lung cancer patients. *Oncology letters*, *6*(5), 1507-1513.
6. Ozlü, T., & Bülbül, Y. (2005). Smoking and lung cancer. *Tuberk Toraks*, *53*(2), 200-9.

Enhancing Lung Cancer Diagnosis: Unraveling the Power of Survival Analysis and Multinomial Regression for Precision Healthcare

7. Loeb, L. A., Emster, V. L., Warner, K. E., Abbotts, J., & Laszlo, J. (1984). Smoking and lung cancer: an overview. *Cancer research*, *44*(12_Part_1), 59405958.
8. Hegmann, K. T., Fraser, A. M., Keaney, R. P., Moser, S. E., Nilasena, D. S., Sedlars, M., ... & Lyon, J. L. (1993). The effect of age at smoking initiation on lung cancer risk. *Epidemiology*, *4*(5), 444-448.
9. Mustafa, M., Azizi, A. J., IIIzam, E., Nazirah, A., Sharifa, S., & Abbas, S. (2016). Lung cancer: risk factors, management, and prognosis. *IOSR Journal of Dental and Medical Sciences*, *15*(10), 94-101.

https://doi.org/10.62500/icrtsda.1.1.15

10. Nitadori, J. I., Inoue, M., Iwasaki, M., Otani, T., Sasazuki, S., Nagai, K., ... & Group, J. S. (2006). Association between lung cancer incidence and family history of lung cancer: data from a large-scale population-based cohort study, the JPHC study. *Chest*, *130*(4), 968-975.
11. Cassidy, A., Myles, J. P., Duffy, S. W., Liloglou, T., & Field, J. K. (2006). Family history and risk of lung cancer: age-at-diagnosis in cases and first-degree relatives. *British journal of cancer*, *95*(9), 1288-1290.
12. Hamilton, W., Peters, T. J., Round, A., & Sharp, D. (2005). What are the clinical features of lung cancer before the diagnosis is made? A population based casecontrol study. *Thorax*, *60*(12), 1059-1065.
13. Snoeckx, A., Reyntiens, P., Carp, L., Spinhoven, M. J., El Addouli, H., Van Hoyweghen, A., ... & Parizel, P. M. (2019). Diagnostic and clinical features of lung cancer associated with cystic airspaces. *Journal of thoracic disease*, *11*(3), 987.
14. Onuigbo, W. I. B. (1957). Some observations on the spread of lung cancer in the body. *British Journal of Cancer*, *11*(2), 175.
15. Pandi, A., Mamo, G., Getachew, D., Lemessa, F., Kalappan, V. M., & Dhiravidamani, S. (2016). A brief review on lung cancer. *Int. J. Pharma Res. Health Sci*, *4*, 907-914.
16. Brodowicz, T., O'Byrne, K., & Manegold, C. (2012). Bone matters in lung cancer. *Annals of oncology*, *23*(9), 2215-2222.
17. Sutedja, G. (2003). New techniques for early detection of lung cancer. *European Respiratory Journal*, *21*(39 suppl), 57s-66s.
18. Collins, L. G., Haines, C., Perkel, R., & Enck, R. E. (2007). Lung cancer: diagnosis and management. *American family physician*, *75*(1), 56-63.
19. Woodard, G. A., Jones, K. D., & Jablons, D. M. (2016). Lung cancer staging and prognosis. *Lung cancer: treatment and research*, 47-75.
20. Latimer, K. M., & Mott, T. F. (2015). Lung cancer: diagnosis, treatment principles, and screening. *American family physician*, *91*(4), 250-256.
21. Lemjabbar-Alaoui, H., Hassan, O. U., Yang, Y. W., & Buchanan, P. (2015). Lung cancer: Biology and treatment options. *Biochimica et Biophysica Acta (BBA)Reviews on Cancer*, *1856*(2), 189-210.
22. Bunn Jr, P. A. (2012). Worldwide overview of the current status of lung cancer diagnosis and treatment. *Archives of pathology & laboratory medicine*, *136*(12), 1478-1481.
23. Yang, C. F. J., & D'Amico, T. A. (2012). Thoracoscopic segmentectomy for lung cancer. *The Annals of thoracic surgery*, *94*(2), 668-681.
24. Tronc, F., Grégoire, J., Rouleau, J., & Deslauriers, J. (2000). Long-term results of sleeve lobectomy for lung cancer. *European Journal of Cardio-Thoracic Surgery*, *17*(5), 550-556.
25. Brunswicker, A., Taylor, M., Grant, S. W., Abah, U., Smith, M., Shackcloth, M., ... & North West Thoracic Surgery Collaborative (NWTSC)† Argus Leah Michael Sarah Mason Sabrina Bhullar Dilraj Obale Emmanuel Fritsch NilsCristopher. (2022). Pneumonectomy for primary lung cancer: contemporary outcomes, risk factors and model validation. *Interactive CardioVascular and Thoracic Surgery*, *34*(6), 1054-1061.
26. Gildea, T. R., DaCosta Byfield, S., Hogarth, D. K., Wilson, D. S., & Quinn, C. C. (2017). A retrospective analysis of delays in the diagnosis of lung cancer and associated costs. *ClinicoEconomics and Outcomes Research*, 261-269.
27. Jensen, A. R., Mainz, J., & Overgaard, J. (2002). Impact of delay on diagnosis and treatment of primary lung cancer. *Acta Oncologica*, *41*(2), 147-152.
28. Salomaa, E. R., Sällinen, S., Hiekkanen, H., & Liippo, K. (2005). Delays in the diagnosis and treatment of lung cancer. *Chest*, *128*(4), 2282-2288.
29. Bjerager, M. (2001). Delay in diagnosis and treatment of lung cancer. *Danish Med Bull*, *53*, 453.
30. Christensen, E. D., Harvald, T., Jendresen, M., Aggestrup, S., & Petterson, G. (1997). The impact of delayed diagnosis of lung cancer on the stage at the time of operation. *European journal of cardio-thoracic surgery*, *12*(6), 880-884.

https://doi.org/10.62500/icrtsda.1.1.16

Proc. 1st International Conference on Recent Trends in Statistics and Data Analytics
Air University Islamabad, Pakistan – May 9, 2024, Vol. 1, pp. 140-147

Unveiling the world of fungal infections: Exploring Athlete's Foot, Ringworm, and Nail Fungus

Malaika Shahzadi[1], Mehwish Asghar[2] and Samia Ghulam[3]
Department of statistics, Govt. College Women University, Sialkot.

Abstract

Skin diseases caused by fungal infections, such as athlete's foot, ringworm, and nail fungus, affect millions of people worldwide. This study aims to delve into the characteristics, causes, symptoms, and treatment options for these common fungal infections. Through an extensive review of existing literature, this research explores the various types of fungal organisms responsible for these infections and their modes of transmission. Additionally, it examines the clinical manifestations and diagnostic approaches for each condition, shedding light on the distinguishing features that aid in accurate diagnosis. Furthermore, the study investigates the available treatment modalities, including topical and oral antifungal medications, and highlights the importance of preventive measures to minimize the risk of recurrence. By understanding the intricacies of these fungal infections, individuals can take proactive steps to protect their skin health and seek appropriate medical care when needed. This study serves as a comprehensive guide to enhance awareness, prevention, and management of athlete's foot, ringworm, and nail fungus, ultimately promoting better skin health and overall well-being.

Keywords:

Available treatments, antifungal medication, prevention, awareness

1. Introduction

Fungal infections are becoming more common at an alarming rate, which poses a significant challenge to medical experts. This growth is directly linked to the rise in the number of people with impaired immune systems as a result of modifications to medical practice, including the use of immunosuppressive medications and intense chemotherapy. HIV and other illnesses that impair immunity have also had a role in this issue.

Mucous membranes, keratinous tissues, and the skin are all impacted by superficial and subcutaneous fungal infections. This class includes some of the most common skin conditions that impact millions of people globally. They can have crippling consequences on a person's quality of life and, in certain cases, spread to other people or become invasive, even though they are rarely life-threatening. The majority of fungal infections that are superficial and subcutaneous are easily detected and treatable.

A more invasive organism that is endemic to a particular region or an opportunistic organism that infects an at-risk host can both be the source of systemic fungal infections. Systemic infections are linked to a high rate of morbidity and death and can even be fatal. The precise incidence of systemic infections is difficult to ascertain due to the difficulty of diagnosis and the fact that the causal agent is frequently only verified at death. Aspergillus species and Candida albicans are the most common pathogens, although other fungus, like non-albicans Candida spp., are becoming more and more significant. [1]

We take into consideration four categories of diseases: Mycotoxins; endemic, region-specific infections in North America (coccidioidomycosis, blastomycosis, and histoplasmosis); **athlete's foot and ringworm** (dermatophytosis); thrush or candidiasis (infection with Candida albicans); and aspergillosis (infection with Aspergillus fumigatus). Every illness is examined in light of evolving medical knowledge and procedures, as well as societal shifts brought about by "modernity." As a result, widespread education created the perfect environment for youngsters to develop scalp ringworm, while the popularity of collegiate athletics and advancements in personal cleanliness contributed to the spread of athlete's foot.

https://doi.org/10.62500/icrtsda.1.1.16

Along with the development of transplantation and new cancer treatment techniques, antibiotics also appeared to make the body more susceptible to more severe Candida infections. Due to population migration bringing non-immune groups susceptible to endemic mycoses, some parts of North America experienced a surge in fungal diseases as their economies developed. Mycotoxins, often known as fungus toxins, have been identified as byproducts of contemporary food transportation and storage systems. Lastly, the incidence of aspergillosis and other systemic mycoses increased in the last part of the 20th century due to the rapid development and application of new medical technologies such as immunosuppression and intensive care.[2].

Skin, hair, and nail dermatophytic infections are quite frequent and come in a wide range of forms. Inflammatory signs in the skin are frequently absent, but they can sometimes occasionally be rather noticeable, especially when zoophilic dermatophytes are to blame. It is highly difficult to differentiate onychomycosis from other causes of onychodystrophy based solely on clinical observations; in fact, only a small percentage of fungal infections may be clinically suspected as the causal agent. More information is provided about the clinical manifestation of infections of the nails, scalp, and beard, as well as infections of the skin.[3]

2. Literature survey

As people age, the percentage of those with serious skin conditions rises linearly. Approximately 70% of people over 70 have at least one skin condition. Furthermore, for a variety of infections, including those of the skin and soft tissues, the morbidity and death rate increases two to three times in the elderly (Cummings and Uttech, 1990, Gavazzi and Krause, 2002). The structure and function of an aged person's skin varies from those of other age groups. [4]

Onychomycosis and Nail Psoriasis

A chronic, recurrent immune-mediated illness, psoriasis affects 2-3% of people worldwide [1]. Nail involvement is another common symptom of psoriasis, despite skin manifestations being the most distinctive finding. While the lifetime incidence of nail psoriasis is predicted to be between 80 and 90 percent, the reported prevalence of nail involvement in psoriasis patients varies between 15% and 79% [2,3]. Pitting, trachyonychia, leukonychia, red spots in the lunula, subungual hyperkeratosis, onycholysis, splinter hemorrhages, and salmon patches are the most typical nail abnormalities associated with psoriasis [4].
The nail infection known as onychomycosis is brought on by dermatophytes, yeasts, and non-dermatophytes molds (NDMs). Nearly half of all nail anomalies are caused by this most frequent nail disorder . Ageing, gender, genetics, smoking, occlusive footwear, certain professional and hobby group activities (swimming pools, saunas, tennis, running, walking barefoot, athletes, coaches, clean workers, housewives), and nail trauma are among the documented risk factors known to increase susceptibility to onychomycosis . Color changes, onycholysis, and subungual hyperkeratosis are the most common clinical features of onychomycosis. As a result, onychomycosis and nail psoriasis can occasionally be difficult to distinguish on a clinical basis . Furthermore, since both of these entities are highly prevalent in the general population, coexistence of these two entities may also occur.
The most prevalent clinical feature Therefore, while treating psoriatic patients with aberrant nail growth, doctors are advised to employ diagnostic methods such as polymerase chain reactions, direct microscopy, and cultures to confirm or rule out onychomycosis .[5]

The Ethology and Frequency

Geographic heterogeneity in the incidence of onychomycosis appears to be significant. Age, location, type of work, travel, and personal hygiene all appear to have an impact on the disease's prevalence.
The chemicals that cause onychomycosis differ greatly depending on the location. Dermatophytes are without a doubt the most frequent causing organisms. The most frequent dermatophyte causal agent is Trichophyton rubrum, which is followed by Trichophyton mentagrophytes.

https://doi.org/10.62500/icrtsda.1.1.16

Aspergillus species were more frequently isolated than other agents among the NDM.[567] Scopulariopsis brevicaulis has also been reported as a frequent cause of onychomycosis.[6] Table 1 shows the causes of dermatophytic and NDM onychomycosis. C. albicans is the most common cause of onychomycosis caused by yeasts but other Candida species are also rarely reported. Studies show various prevalence, but roughly 90% in toenail and 50% in fingernail infections may be caused by dermatophytes.

Clinical feature

In the NDM, Aspergillus species were isolated more frequently than other agents. Scopulariopsis brevicaulis has also been reported as a frequent cause of onychomycosis.[6] Table 1 lists the causes of both dermatophytic and NDM onychomycosis; C. albicans is the most common yeast-caused onychomycosis cause, though other species of Candida are also infrequently reported. Various prevalence studies indicate that dermatophytes may be responsible for 90% of toenail and 50% of fingernail infections.

The following are the clinical forms of onychomycosis: total dystrophic onychomycosis (TDO) proximal subungual onychomycosis (PSO), endothrix onychomycosis, superficial white onychomycosis (SWO), and distal lateral subungual onychomycosis (DLSO) .[789] The nail apparatus appears to have a relatively low level of efficient cell-mediated immunity, which leaves the nail more susceptible to fungal infections.[9] Growing older also increases the incidence of onychomycosis.[10] In women, candidal onychomycosis is more common.[11]

The most prevalent type of onychomycosis is distal lateral subungual onychomycosis. First affecting the underside and lateral edges of the nail plate, the infection proceeds proximally along the nail bed, causing subungual hyperkeratosis, or the deposition of debris under the nail, and onycholysis, or the pushing up of the nail plate. PSO is a less common kind that is frequently observed in conjunction with HIV infection. Under the surface of the proximal nail fold, fungus enters through the proximal portion of the nail plate. The proximal portion of the nail discolors yellow-white, and the discoloration spreads farther down the nail bed. Additionally, SWO is a unique variation in which the nail plate is directly invaded, exhibiting flakiness and white discolouration without a nail bed.

Machine Learning Methods

Feature Extraction Using CNN Deep learning explores the possibilities of learning features directly from input data and tries to avoid hand-crafted features [12]. The main aim of Deep Learning is to achieve multiple levels of feature representation from an old one for more abstract semantics of the data. As a particular deep learning technique, Convolutional neural networks have achieved more popularity in image classification and its feature extraction. A CNN model is a combination of a few mathematical functions. In CNN, convolution is a function which takes inputs such as image and a filter or kernel to produce the output [6]. CNN is developed by using trainable layers which are stacked with each other. These layers are connected by a supervised classifier and some sets of arrays called feature detectors.

There are 3 main parts for constructing CNN: Convolutional Layer, Pooling Layer and FC layer. In CNN, the main building block is the Convolutional Layer in which feature detector is used with an input signal as shown in Fig.1.This layer calculates the output of each neuron connected in local regions and for the next input, it computes a dot product of the weights. The region where neurons are connected to the input is called filter or kernel. There is a use of ReLU i.e. Rectified Linear Unit which is used for generating non-linearity in the given image [13]. A Pool layer is placed between two consecutive convolutional layers which are common in the trade. Pool layer resizes the input size for next convolution and it is generally used for producing a reduced progressive spatial size of representation [6]. A layer that is having connections to each activation function of the previous layer is known as Fully Connected (FC) layer. A Classifier is generally used in the end because it is presented in FC Layer.

https://doi.org/10.62500/icrtsda.1.1.16

The main aim of using classifier is to analyse the proper class of image which is based on the detected features.

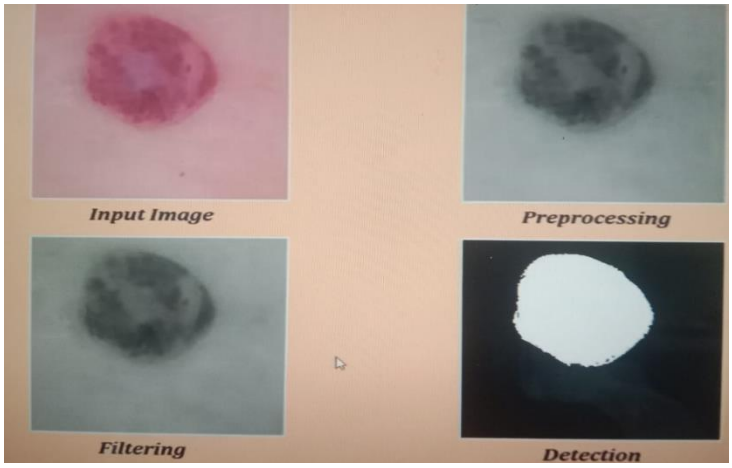

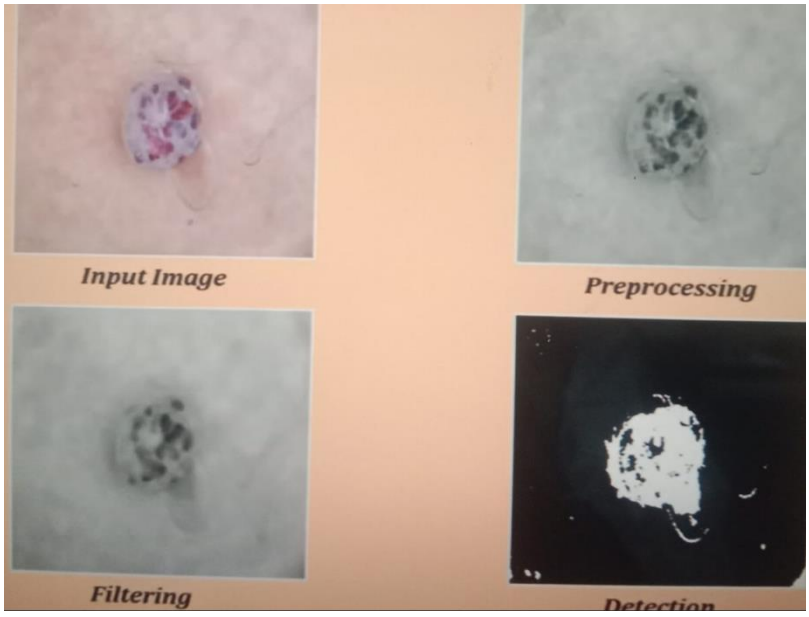

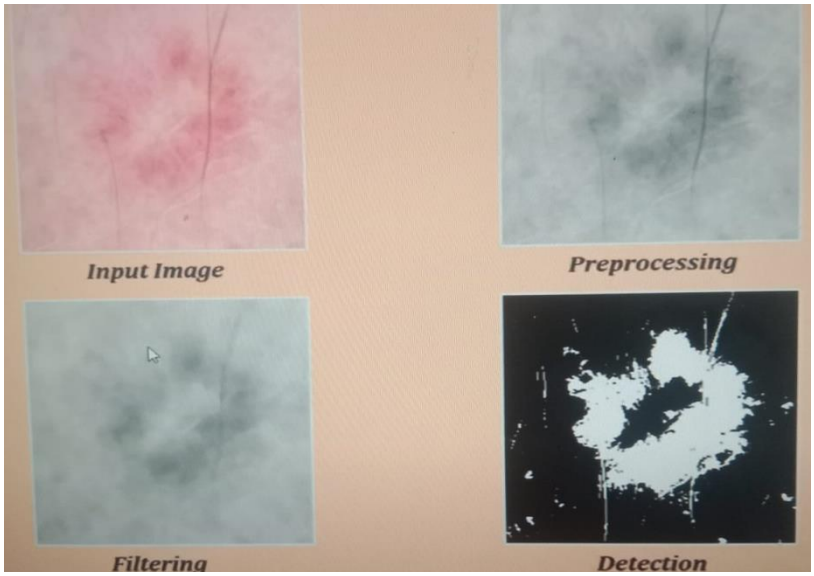

https://doi.org/10.62500/icrtsda.1.1.16

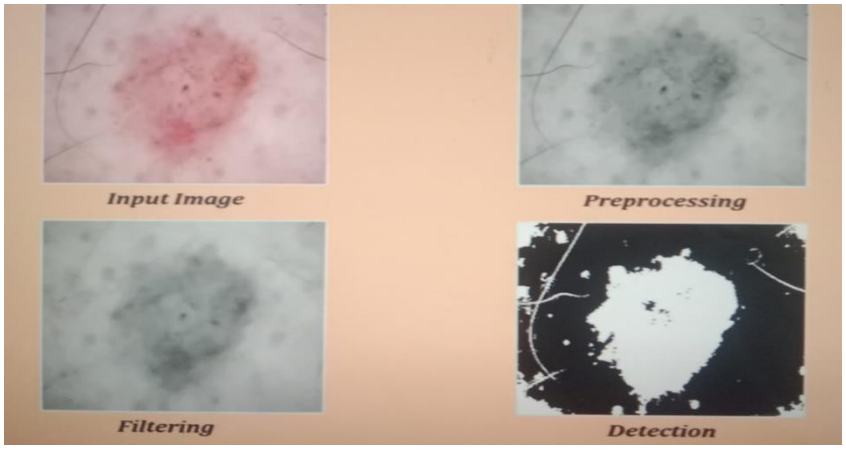

Machine learning Classifier

The process of predicting the particular class of given data point is known as Classification. Classes are referred by targets/ labels/categories in terms of classification problems. In predictive modeling, mapping function map Input Variables(X) to output variable(Y) for classification various data points..

Support Vector Machine

It is a supervised learning algorithm that is capable of making fine classifications through a separating hyperplane. In other means, trained labeled data (Supervised Learning) has been used and the algorithm returns an optimal separating hyperplane which classifies new examples.

Logistic Regression

It is a Classification model which is very simple to implement and performs efficiently on linear separable classes. It is a Binary classification algorithm but can be implemented for multi-class classification by using OvR Method.

Dataset Description

In this proposed approach, we have used skin diseases Dataset which is also known as fungal diseases on skin [19]. This dataset contains overall 1153 images of histopathological Samples stained with Hematoxylin and Eosin. The Dataset has been divided into two categories i.e Benign and Malignant with respective to sample 2,48

The nail plate becomes stained with little to no subungual hyperkeratosis or onycholysis when endonyx onychomycosis first manifests as DLSO. Over an extended length of time, all of these types may eventually result in TDO.0 and 5429.

	precision	recall	f1-score	support
0	0.64	0.61	0.63	62
1	0.80	0.64	0.71	77
2	0.75	0.53	0.62	201
3	0.70	0.29	0.41	24
4	0.66	0.43	0.52	191
5	0.86	0.97	0.91	1128
6	0.83	1.00	0.91	20
accuracy			0.82	1703
macro avg	0.75	0.64	0.67	1703
weighted avg	0.81	0.82	0.81	1703

https://doi.org/10.62500/icrtsda.1.1.16

Proposed Methodology

A model has been developed for automatic classification on the basis of Magnification which classifies the samples for benign and malignant classes. The proposed system used in this work is illustrated . Each phase is described in the following subsection:

• Data Preparation & Pre-Processing-In this phase, the dataset has been loaded into google drive and applied Data Processing steps on it.

• Feature Extraction & Classifier –In this, Features are extracted using CNN's. After removing original classifier, a traditional supervised classifier is added to it i.e. SVM and LR.

• Model Development- Here, two models are generated which may or may not have dependency between them.

• Performance measuring parameters- Performance of the model is evaluated on the basis of accuracy, precision, recall, and F-values. It is calculated by using a confusion matrix

• Classifier Output –Results are analysed on the basis of cross-validation and test scores of SVM and

LR.

Pre-Trained Deep CNN Architecture for feature extraction

In order to extract features from BreakHis Dataset, evaluation of Pre-trained CNN's Such as VGG16, VGG19, ResNet50 and Xception has been carried out [20][21][22]. The main aim of using a pre-trained model is to remove the top classifier from FC layers according to our need. The classifier which is removed from the FC layer is replaced by a traditional classifier which fits our purpose. According to below-mentioned strategies, fine-tune model is developed.

1) Training of the entire model- In this case, a pre-trained model is selected for training according to the dataset. After training of the model, it needs learning from scratch which results in the requirement of a large dataset and a lot of computational power.

2) Train a few layers and leave other layers frozen- As we know that lower layers refer to general features which are problem independent whereas higher layers refer to specific features that are problem-dependent. So, in order to solve the problems of lower and higher layers, the weights of the neural network have been modified. To avoid overfitting in modified weights, one has to leave a greater number of layers frozen for a smaller dataset which consists of a large number of parameters as input.

3) Freezing of Convolutional Base- It corresponds to an intense situation for train/freeze trade-off. Here, the concept is to use the original form of convolutional base and feed outputs of the convolutional base to classifiers. A new fixed feature extractor has been used for this purpose which is developed from a pre-trained model. This approach can solve the problem in an efficient way when low computational power and smaller datasets are used.

3. Model Construction

In this research work, count tables have been used from exploratory Data Analysis. These tables helped us for construction of model using neural network and classifiers. Firstly, the models are constructed by using scikit-learn library's function known as Grid SerchCV with Cross-validation parameter having value as 10 [16]. Two models such as Magnification Model and Cancer Class Models are produced for SVM and LR. The Extraction of features is done by using Google Colaboratory which is a free environment for research purposes and used for developments. Colab has been used for this purpose which permits a Tesla K-80 GPU instance, available for 12hrs. The models are as follows:

https://doi.org/10.62500/icrtsda.1.1.16

• Magnification Factor Model- This model gives the knowledge about magnification factor which is used during the study of whole slide imaging [15]. The magnification factors used in this dataset are 40x, 100x, 200x, 400x. Table no.3 is used for developing the model.

3. Conclusion

CNN are best suitable for fungal skin diseases. In this study, Logistic regression are important for detect the disease are present or not. Hence there is working on development of automatic, efficient, fast anf accurate which is used for detect disease. Further to needed to compute amount of disease present.

References

[1] Garber, G. (2001). An overview of fungal infections. *Drugs*, *6*-12.*1*(Suppl 1), 1

[2] Homei, A., & Worboys, M. (2013). Athlete's Foot: A Disease of Fitness and Hygiene. In *Fungal Disease in Britain and the United States 1850–2000*. Springer Nature

[3] Al-Ani, F. K., Younes, F. A., & Al-Rawashdeh, O. F. (2002). Ringworm infection of cattle and horses in Jordan. *Acta Veterinaria Brno*, *71*(1), 55-60.

[4] Laube, S. (2004). Skin infections and ageing. *Ageing research reviews*, *3*(1), 69-89..

5] Kyriakou, A., Zagalioti, S. C., Trakatelli, M. G., Fotiadou, C., Apalla, Z., Lazaridou, E., & Patsatsi, A. (2022). Fungal infections and nail psoriasis: an update. *Journal of Fungi*, *8*(2), 154

[6] kirkpatrick CH. Chronic mucocutaneous candidiasis Pediatr Infect Dis J. 2001;20:197–206

[7] Singal A, Khanna D. Onychomycosis: Diagnosis and management Indian J Dermatol Venereol Leprol. 2011;77:659–72

[8] Elewski BE. Onychomycosis: Pathogenesis, diagnosis, and management Clin Microbiol Rev. 1998;11:415–29

[9] Grover C, Khurana A. Onychomycosis: Newer insights in pathogenesis and diagnosis Indian J Dermatol Venereol Leprol. 2012;78:263–70

[10] Westerberg DP, Voyack MJ. Onychomycosis: Current trends in diagnosis and treatment Am Fam Physician. 2013;88:762

[11] Arenas R. Onychomycosis. Clinico-epidemiological mycological and therapeutic aspects Gac Med Mex. 1990;126:84–9

[12] S. Doyle, S. Agner, A. Madabhushi, M. Feldman and J. Tomaszewski, "Automated grading of breast cancer histopathology using spectral clustering with textural and architectural image features," 2008 5th IEEE International Symposium on Biomedical Imaging: From Nano to Macro, Paris, 2008, pp. 496-499.

[13] Mohamad Mahmoud Al Rahhal “Breast Cancer Classification in Histopathological Images using Convolutional Neural Network” (IJACSA) International Journal of Advanced Computer Science and Applications, Vol. 9, No. 3, 2018 [19] Spanhol, F., Oliveira, L. S., Petitjean, C., Heutte, L., A Dataset for Breast Cancer Histopathol

[14] Vibha Gupta and bhavsar Arnav,” Breat cancer Histopathological Image Classification: Is Magnification Important?” IEEE Conference on Computer Vision and Pattern Recognition Workshops (CVPRW) DOI: 10.1109/CVPRW.2017.107

https://doi.org/10.62500/icrtsda.1.1.16

[15] A study of Cross- Validation and Bootstrap for accuracy Estimation and Model Selection,Kohavi,Ron, International Joint conference on Artificial Intellgence(IJCAI),14(12):1137-43,199

https://doi.org/10.62500/icrtsda.1.1.17

Proc. 1st International Conference on Recent Trends in Statistics and Data Analytics
Air University Islamabad, Pakistan – May 9, 2024, Vol. 1, pp. 148-156

Forecasting of different Crops by Area of Punjab using Box-Jenkins Method

Maryam Arshad[1], Mehwish Asghar[2] and Naiza Arshad[3]

Department of statistics, Govt. College Women University, Sialkot[1, 2, 3]

Abstract

A crop is a plant or plant product that can be grown and harvested for profit or subsistence. By use, crops fall into six categories: food crops, feed crops, fiber crops, oil crops, ornamental crops, and industrial crops. Food crops, such as fruit and vegetables, are harvested for human consumption. The goal of this study was to provide a thorough overview of Punjab's kharif agricultural situation as it stands today in Pakistan and forecasting different crops for the next 10 years. The projected years are 2022 through 2031, and the index contained yearly time series data from 1947 to 2021. For the individual univariate series of the acreage and production of different crops in Pakistan Punjab, time series modeling employing the Box- Jinken's and ANN models was constructed. The Box and Jenkins linear time series model—also known as the ARIMA (p, d, q) model and ARMA (p, q) model—was used. It incorporates autoregression, moving average, and integration.

Keywords: ACF, AIC, PACF, SIC, ARMA, ARIMA, ANN

1. Introduction

SUGARCANE

Historically used as a source of energy for humans, sugarcane (Saccharum officinarum L.) has more recently been used to substitute fossil fuel in automobiles. Cultivated on 0.966 million hectares, sugarcane is the second largest cash crop in Pakistan and accounts for around 3.6% of the country's GDP [1]. At the moment, sugarcane makes up 11% of the value contributed of all crops and 4.8% of the planted land [2]. An important part of our nation's economy is the sugar sector.

RICE

Pakistan is the tenth-largest rice producer in the world. More than 8 percent of the global rice trade is comprised of exports from Pakistan [3]. It is a significant crop for Pakistan's agricultural economy. One significant crop for Kharif is rice. Pakistan placed 10th among the world's top rice-producing nations in 2019 with 7.5 million tons of rice produced.3.15 million hectares of land, or 11.7% of all cultivated land, Production of milled rice is expected to be 5.50 million tonnes in 2022 and 9.32 million tonnes in 2021–2022 [4].
5 year average yield: 3.6 MT/ha

GDP contribution: 0.6%

3.0% is the contribution to the agricultural value added.

Value (2022–2023): US$2.7 billion

7.48% growth rate is anticipated (CAGR 2023–2028).

Volume: 2022–2023; 4.5 million tons

Volume growth anticipated: 0.3% by 2024

Key markets: Europe, the Middle East, and Africa [5]

https://doi.org/10.62500/icrtsda.1.1.17

GROUNDNUTS

An important cash crop in Punjab's barani areas is groundnut. The 13th most significant food crop in the world is groundnuts. They rank third in terms of importance among vegetable proteins and fourth globally in terms of edible oil. High-quality edible oil (43–55%), readily digested protein (25–32%), and carbs (20%) are all abundant in groundnut seeds. Around the world, 12 percent of peanut production is utilized for seed, 37 percent is used for direct food purposes, and 50% is used for oil extraction (ICRISAT 2008). Just 0.4% of the world's groundnut crop and 0.2% of its production are found in Pakistan.It was cultivated on roughly 86974 acres in Pakistan in 2018–19, yielding a total production of 100790 tons. The area is roughly 89.8%, 8.0%, and 2.2%.[6]

MAIZE

One important food grain that is used to make many different items is maize. It makes up 0.4% of the GDP and 2.2% of the value added in agriculture. When compared to other food grains, maize, or corn, is Pakistan's most important commercial crop. The fourth-largest producer of maize is Pakistan. A variety of meteorological and soil conditions can support the growth of maize, and the Kharif (monsoon) season is ideal for planting. The warm season is ideal for maize cultivation, which can withstand temperatures as high as 35°C. It grows from sea level to a height of 3000 meters. Crops require 50–100 cm of rainfall annually, and they cannot be grown in regions with rainfall totaling more than 100 cm dish made of maize.[7]

COTTON

Pakistan's principal crop for both cash and fiber is cotton. Pakistan ranks third globally in terms of cotton consumption and production. The cotton sector plays a significant role in Pakistan's economy. It has a significant impact on the nation's foreign exchange earnings. It makes for 2% of the nation's GDP, 8.2% of value created, and 55% of the methods of generating an income. Based on textiles and cloth, cotton accounts for 40% of employment and 46% of manufacturing output. Pakistan holds a 9% share of the global textile industry and is the third largest exporter of raw cotton. Tropical and subtropical regions are ideal for growing cotton; the crop needs a temperature range of 21°C to 30°C.[8][9]

2. Methodology

2.1 Autocorrelation function (ACF)

The autocorrelation function is the measure of a time series' correlation with itself (z1, z2,..., zn). Based on the weak stationary assumption, the correlation coefficient between zt and zt-1, denoted by t, is called the lag-k autocorrelation of zt.With the aid of an ACF, the average correlation between data points in a time series and earlier values in the series that are determined for different lag lengths is quantified and presented[10].

2.2 Partial Autocorrelation Function (PACF)

The partial autocorrelation function at lag-k, represented by ϕ kk, is the correlation coefficient between z t and z t–1 after the impact of the intervening z t–1,t–2,…., z t–k+1 is removed. Regressing the time series values at all shorter lags, the partial autocorrelation function (PACF) in time series analysis offers the partial correlation of a stationary time series with its own lagged values.

2.3 Autoregressive Moving Average Model (ARMA)

The model containing p autoregressive terms and q moving-average terms is denoted by the notation ARMA(p, q). The AR(p) and MA(q) models are included in this model.[5]

https://doi.org/10.62500/icrtsda.1.1.17

$$X_t=\epsilon t+\Sigma\varphi iXt\text{-}1+\Sigma\theta_i\epsilon_{t\text{-}i}$$

Peter Whittle employed mathematical analysis (Laurent series and Fourier analysis) and statistical inference to describe the general ARMA model in his 1951 thesis.[6][7] In their 1970 book, George E. P. Box and Jenkins introduced an iterative (Box–Jenkins) approach to selecting and estimating ARMA models, which helped to popularize them. For low-order polynomials (those with degrees of three or fewer), this approach was helpful.[8].With a little more interpretation, the ARMA model is just an infinite impulse response filter applied to white noise.[11][12]

2.4 Model Building

The Box-Jenkins iterative approach to developing linear time series models consists of four stages: identification, parameter estimation, diagnostic verification, and forecast, respectively. The identification stage is the most important one. It has the correct ARIMA model in it. Diagnostic model checking is testing the model's hypotheses to identify any areas where the model is flawed.

To ascertain the goodness of fit of the proposed ARIMA model, such that

$H_o=\rho_k(a_t)=0 \text{and} H_1=\rho_k(a_t)=0$

We reject the hypothesis that the residuals are randomly distributed if Q is within the extreme 5% of the chi-square distribution's right side tail.

2.5 Neural Network

The idea of intelligent machines has been around for millennia, but in the last century, neural network technology has advanced to unprecedented levels. The University of Illinois and the University of Chicago's Warren McCulloch and Walter Pitts released "A Logical Calculus of the Ideas Immanent in Nervous Activity" in 1943. The study examined how the brain might create intricate patterns and then reduce them to a binary logic framework that only included true or false links. Neural networks function in a manner like to that of the human brain. In a neural network, an information gathering and classification mathematical function known as a "neuron" uses a particular architecture to classify and gather data. The network is quite similar to statistical techniques like regression analysis and curve fitting.

2.6 Artificial neural network

An artificial neural network employs biological neurons to mimic the functions of the human brain. Artificial neural networks do practical computations and mimic complex brain operations.

In 1943, McCulloch and Pitts proposed the first artificial neuron model.

Neural networks are widely used in biology, engineering, medicine, and finance. A fed-forward or fed-back strategy can be applied to the development of an artificial neural network. An artificial neural network has three different kinds of layers: input, hidden, and output layers .[13][14]

3. Data Analysis and Results

3.1 Data description

In order to develop a suitable model to be used to forecast the yearly area of sugarcane, rice, maize, groundnuts and cotton crops, the data for the current study were the annual area of sugarcane, rice, maize, groundnuts and cotton crops. The data were obtained from the website “AMIS.PK” for the period (1947 to 2021) [15]. The statistical programs: EViews-10 and Zaitun Time Series were utilized.

3.2 Comparison of ARIMA and ANN

For ARIMA, the normality of area of sugarcane, rice, maize, groundnuts and cotton is determined by the probability value of the Jarque-Bera test. If the probability of Jarque-Bera is greater than 0.05 so we accept the null hypothesis, which means residuals are normally distributed. By taking the first log,

https://doi.org/10.62500/icrtsda.1.1.17

in the case of the sugarcane field, we make our data stationary. The model (0,1,2) for the annual sugarcane area is then chosen based on ACF and PACF values since it has the lowest AIC and SIC values and Adjusted R-Square value are maximum. In order to make our data stationary for rice crop, we additionally use the first log and we chose the (1, 1, 2) model because here it has the lowest AIC and SIC values and Adjust R-Square has maximum value. For the groundnut crop we make our data stationary at first log so we chose (0,1,1) model since it has the lowest AIC and SIC values and Adjusted R-Square has maximum value. . For Maize crop we make our data stationary we apply second log. The model (1, 2, 1) we chose because it has lowest AIC and SIC values and Adjust R-Square value has maximum. In the order we make our data stationary for cotton therefore we chose (0, 1, 1) model as it has the lowest AIC and SIC values and Adjusted R-Square has maximum value.

In order to forecast the area of sugarcane for ANN we placed ten input layers neurons, twelve hidden layers neurons and one output layer neuron. We use the bipolar sigmoid function and compute mean absolute error (MAE) on Zaitun Time Series with a learning rate of 0.05 and momentum of 0.5. To forecast area for Rice for ANN we used

10 input layers neurons, twelve hidden layers neurons and one output layer neuron. We use the bipolar sigmoid function with a learning rate of 0.05 and momentum of 0.5 to compute mean absolute error (MAE) on Zaitun Time Series. To forecast of Groundnut for ANN we apply placed twelve input layers neurons, twelve hidden layers neurons and one output layer neuron. We utilize the bipolar sigmoid function and compute mean absolute error (MAE) on Zaitun Time Series with a learning rate of 0.05 and momentum of 0.5. To predict of maize for ANN we placed nine input layers neurons, ten hidden layers neurons and one output layer neuron. Applying the bipolar sigmoid function and computing the mean absolute error (MAE) on the Zaitun Time Series, we set the learning rate at 0.05 and the momentum at 0.5. To predict of Cotton for ANN we utilize eleven input layers neurons, ten hidden layers neurons and one output layer neuron. We use the bipolar sigmoid function and compute mean absolute error (MAE) on Zaitun Time Series with a learning rate of 0.05 and momentum of 0.5.

The comparison of the Mean Absolute Error (MAE) and Root Mean Square Error (RMSE) of ARIMA and ANN is as:

ARIMA	MAE	RMSE
Sugarcane	179.5027	228.5010
Rice	416.419	524.069
Groundnuts	52.823	62.191
Maize	2035.14	1082.707
Cotton	1056.469	1350.27

ANN	**MAE**	**RMSE**
Sugarcane	78.9620	100.517
Rice	181.194	236.239
Groundnut	16.4590	20.6775
Maize	103.578	77.87158
Cotton	290.29	380.4668

The ANN forecasted graph of sugarcane, rice, maize, groundnut and cotton crops are as:

https://doi.org/10.62500/icrtsda.1.1.17

SUGARCANE FORECASTED VALUES

Years	Forcasted
2022	1913.4199
2023	1753.4492
2024	1869.7054
2025	1956.8525
2026	1960.4897
2027	1945.4554
2028	1843.0561
2029	1813.9826
2030	1959.1809
2031	2012.7957

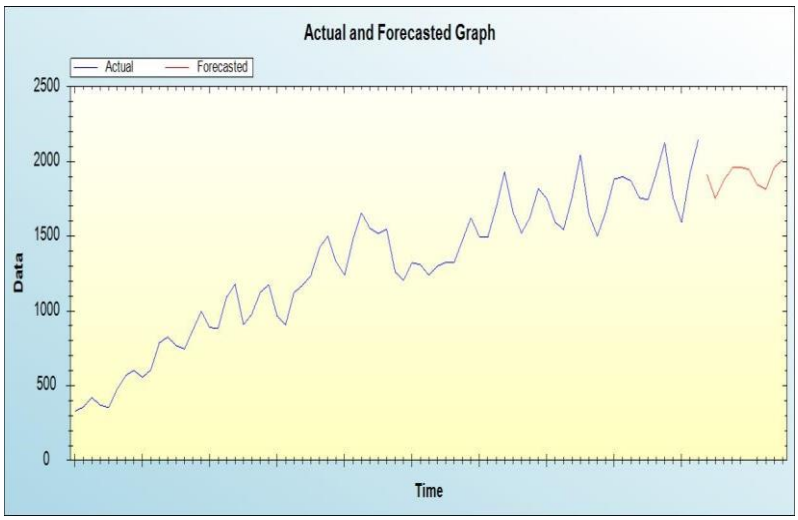

RICE FORECASTED VALUES

Years	Forcasted
2022	5892.0032
2023	5593.1194
2024	5367.2879
2025	5192.2124
2026	5072.3572
2027	4855.3913
2028	4811.7174
2029	5102.1300
2030	5367.1692
2031	5431.1162

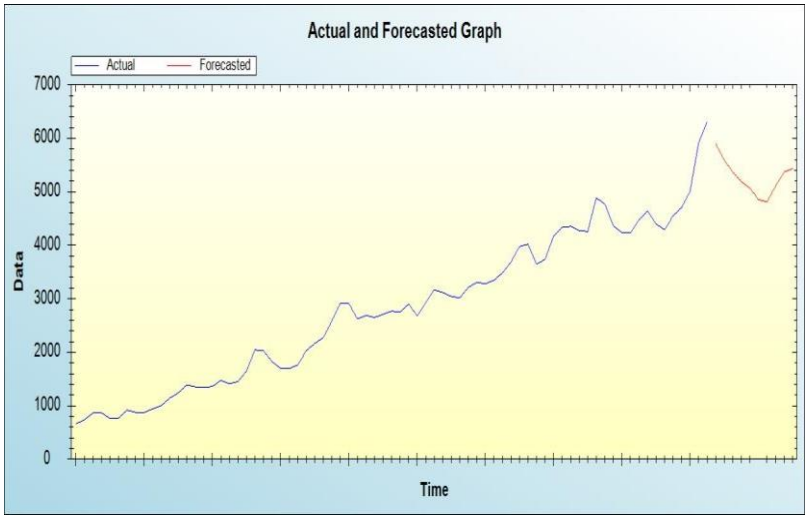

GROUNDNUTS FORECASTED VALUES

years	Forcasted values
2022	330.8805
2023	330.7624
2024	303.2422
2025	276.8133
2026	291.7028
2027	317.3387
2028	296.5332
2029	285.1891
2030	299.8804

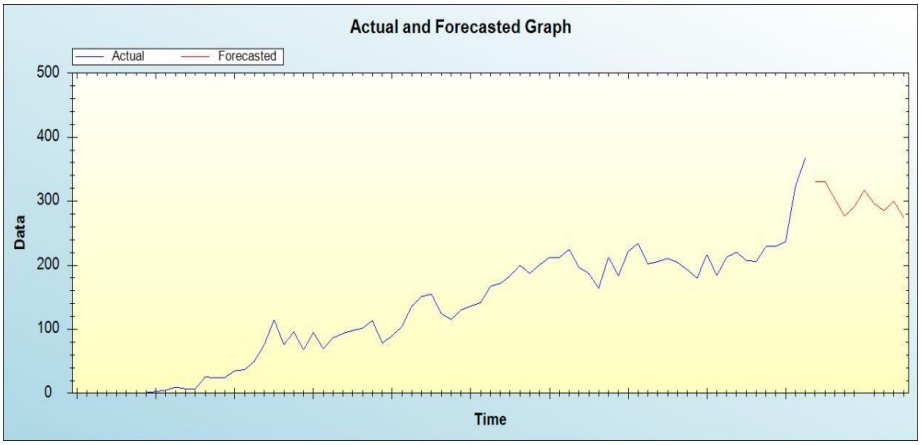

https://doi.org/10.62500/icrtsda.1.1.17

2031 274.4179

MAIZE FORECASTED VALUES

Years	Forecasted
2021	2348.6662
2022	2361.1864
2023	2372.9113
2024	2378.6640
2025	2392.5411
2026	2391.7990
2027	2396.8735
2028	2398.6905
2029	2399.0666
2030	2399.5370

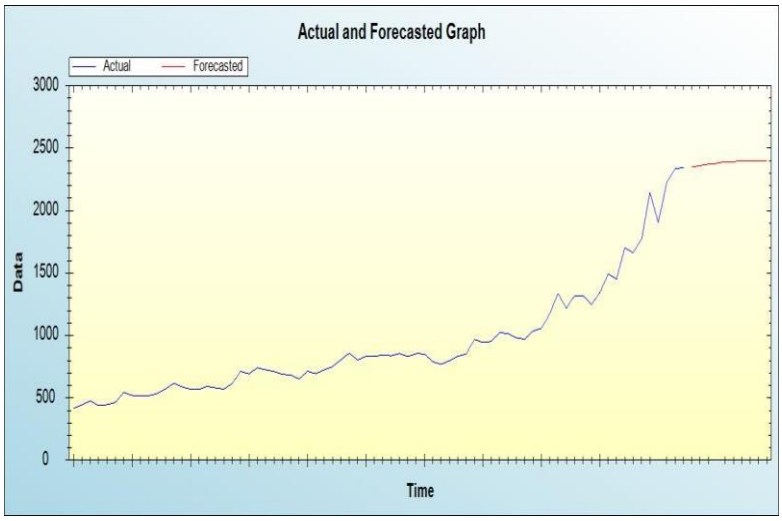

COTTON FORECASTED VALUES

Years	Forcasted
2021	4011.2958
2022	3951.9348
2023	3777.7926
2024	3267.7013
2025	3577.3539
2026	3078.2271
2027	3298.2844
2028	2889.7358
2029	2995.1735
2030	2781.1003

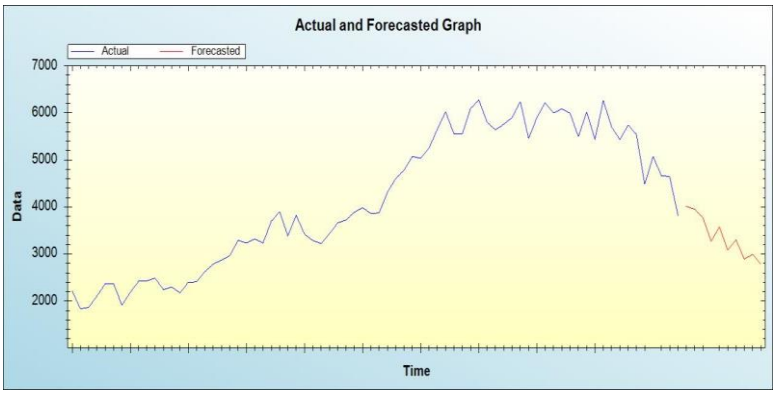

3. Conclusions

The goal of the current study was to determine if ARIMA models perform as well as artificial neural networks. According to the study, the best practical and economical model for predicting the area of sugarcane, rice, groundnuts, maize, and cotton crops in Punjab, Pakistan for the ensuing ten years is the Artificial Neural Network (ANN). The Root Mean Square Error (RMSE) and Mean Absolute Error (MAE) values decrease when ANN is used in place of ARIMA. This is a reliable indicator of the model. It is recommended that the government utilize the ANN models to forecast the area in Punjab, Pakistan for the crops of rice, cotton, groundnuts, maize, and sugarcane.

References

1. Anonymous. 2005. Economic survey on crop situation. Federal Bureau of statistics. Government of Pakistan. Islamabad: p.10.
2. Annonymous. 2005. Sugar and sugarcane statistics Annual report, PSMA: p. 63-64.

https://doi.org/10.62500/icrtsda.1.1.17

3. https://apps.fas.usda.gov/psdonline/circulars/grain-rice.pdf

4. **https://gain.fas.usda.gov/Recent%20GAIN%20Publications/Grain%20and%20Feed%20A nnual_Islamabad_Pakistan_4-3-2017.pdf**
5. **https://en.wikipedia.org/wiki/Rice_production_in_Pakistan#cite_note-2**
6. **https://aari.punjab.gov.pk/varieties_groundnut**
7. Government of Pakistan. 2007. Agriculture Statistics of Pakistan. Ministry of Food, Agriculture and Livestock, Government of Pakistan, Islamabad.
8. https://www.researchgate.net/deref/https%3A%2F%2Fdoi.org%2F10.1111%2Fpbi.12467 ?_tp=eyJjb250ZXh0Ijp7ImZpcnN0UGFnZSI6InB1YmxpY2F0aW9uIiwicGFnZSI6InB1Y mxpY2F0aW9uIn19
9. Abelson, P.H. 1998. A third technological revolution. Sci. 279: 2019.
10. ^ *Hannan, Edward James (1970). Multiple time series. Wiley series in probability and mathematical statistics. New York: John Wiley and Sons.*
11. ^ *Whittle, P. (1951). Hypothesis Testing in Time Series Analysis. Almquist and Wicksell. Whittle, P. (1963). Prediction and Regulation. English Universities Press. ISBN 08166-1147-5.*
12. *Shumway, Robert H. (2000). Time series analysis and its applications. David S. Stoffer. New York: Springer. p. 98. ISBN 0-387-98950-1. OCLC 42392178.*
13. https://home.csulb.edu/~cwallis/382/readings/482/mccolloch.logical.calculus.ideas.1943.pdf
14. https://www.ibm.com/topics/neural-networks
15. www.amis.pk

Forecasted Area of Rabi Crops in Punjab using the Box-Jenkins Methodology and ANN

https://doi.org/10.62500/icrtsda.1.1.18

Proc. 1st International Conference on Recent Trends in Statistics and Data Analytics
Air University Islamabad, Pakistan – May 9, 2024, Vol. 1, pp. 157-168

Forecasted Area of Rabi Crops in Punjab using the Box-Jenkins Methodology and ANN

Naiza Arshad[1], Mehwish Asghar[2] and Maryam Arshad[3]

Department of statistics, Govt. College Women University, Sialkot[1,2,3]

Abstract

Crops play a crucial role in global food security, with staple crops providing the bulk of calories and nutrients for billions of people worldwide. Winter crops are grown and harvested in the spring, a type of crop known as "Rabi crops". In many areas, Rabi crops are an integral part of the agricultural landscape, making a substantial contribution to both food security and economic stability. Forecasting the Rabi crops of Wheat, Masoor, Barley, Gram, Repaseed, and Punjab for the years 2022–2035 is the study's main goal. The index included the yearly time series data from 1947-1948 to 2021-2022. In this study, we forecast and assess Rabi crop yields using the robust time series analysis technique known as the Box-Jenkins methodology. The AIC and SBC model selection criteria are used to choose the best model. . It is examined that the suitable models for Rabi crops for Wheat, Masoor, Barley, Gram, and Repaseed are ARIMA (0,1,2), ARIMA (2,1,3), ARIMA (3,1,1), ARIMA (0,1,1), and ARIMA (0,1,1), respectively. When measured against other fitted models, these models have the lowest values of AIC and SBC. Additionally, the technique of artificial neural networks (ANNs) is employed to predict future values. A comparison between ARIMA and ANN is performed based on a smaller mean square error (MSE).

Keywords: ARIMA Model, Forecasting, Auto correlation function, Akaike information criteria, ANN Technique

1.Introduction

Pakistan's economy depends heavily on agriculture in a number of ways. It is essential for maintaining food security, fostering economic expansion, and offering creating jobs, decreasing poverty, and obtaining foreign currency. In addition to providing jobs for 45% of the labor force, it makes for more than 20% of the country's GDP. Approximately 64% of Pakistan's population lives in rural regions and depends on agriculture for their living, either directly or indirectly. It also gives the industrial sector access to markets for industrial goods and raw materials. Export revenue has a very high percentage of agriculture as well. Pakistan's total geographical area is 79.61 million hectares, of which 57.05 million hectares are stated to be farmed, or 22.17 million hectares, or 39% of the total area.

Gram

One of Pakistan's main Rabi crops is gram, sometimes referred to as chickpea or chana (Cicer arietinum). Pakistan's ranking according on the amount of land cultivated Chickpea comes in second. Pakistan's production, which is 581 kg ™, is quite low in relation to area when compared to several other nations [1]. Although grame is a shortduration crop that may be seeded from September to November, the optimal time to sow it is during the first week of October. In a typical environment, it attained maturity in four months or a bit longer. Once the crop reaches maturity, it can be severely damaged by rain and flooding. It has a frost allergy as well. It is a crop that can withstand heat and is fully dependent on Mother Nature. It controls water via its extensive taproots.When taken in moderation, gram is highly helpful for controlling cholesterol and aiding with digestion. It is also used as a blood thinner, bronchitis, and snake bite medication. illness, sunstroke, skin conditions, etc. Cough and cold gram leaves are used to treat discomfort.[1][2][3]

https://doi.org/10.62500/icrtsda.1.1.18

Barley

The world's fifth-largest grain crop, barley is produced annually in 136 mt on over 56 mha. Compared to 2010–11, barley output in Pakistan fell to 1.4% in 2011–12. Similarly, the area used for barley decreased from 77000 hectares in 2010–11 to 75000 ha in 2011–12 (GoP, 2010). Reduced crop yield for fodder, inadequate use of compost, inadequate foundation, and lack of plant safety are the causes of the decline in barley output and area. Human use of barley has significantly declined in recent years, whereas wheat use has increased in popularity.

Poultry feed is currently being produced fast from barley crops. Barley is thought to be dangerous since it is acclimated to marginal and stressful conditions. farmers in poverty grow an aversion crop (Bilal and Shahbaz, 2008). The most nutritious cereal, barley, has the proper amount of each and every necessary vitamin. It is well known that barley water has several therapeutic properties and aids in the quick treatment of a wide range of illnesses. It reduces or regulates body weight and serves as an appetite suppressant. Barley is an important crop all throughout the world, as evidenced by its usage in the production of malt and health tonics (Chand et al., 2008). Barley was used to make bread by the Prophet Muhammad (Sallallahu Alayhi Wasallam). (1996) said that the process of producing barley, aside from the salt, imparts expertise and information about the grain's typical use. Barley, or jou, is grown in soils that are difficult for wheat, maize, rice, and sugarcane to grow because it is a tolerant crop that can withstand hard conditions. Barley not only produces high yields with few inputs in agriculture, but it may help restore depleted soil. Barley is sown like wheat, but because of its quick development, it is ready for harvesting early. Noaman et al. have also highlighted the utilization of barley (1995).[4][5]

Rapeseed

In Pakistan, rapeseed and mustard are traditional oilseed crops that are used as the primary source of edible oil. These crops provide between 16 and 20 percent of Pakistan's total edible oilseed yield (Pakistan Economic Survey, 2015–16). 21 thousand tons of rapeseed are produced on 4 thousand hectares of land. In Punjab, where it is produced on 120.0 thousand tons of land covering 135.6 thousand hectares, rapeseed is a popular crop. Domestic edible oil consumption in the nation exceeds production, which amounts to 2.821 million tons, of which 2.1 million tons are imported and around 0.684 million tons are satisfied by local resources (Pakistan Economic Survey, 201516).

The import oil bill of Pakistan is thought to be the second biggest following petroleum (Ahmad & Associates, 2013). Less than two percent oil-soluble erucic acid and less than 20 µmol/g Oil-free meals' glucosinolates are referred to as the suggested dosage of these substances. meal made with seeds 40% of Brassica's protein is composed of balanced amino acid, but the proportion of protein content is less. more than its requirement. A substantial sum of foreign currency is being used to fund rapeseed oil imports using forced reduction in quality for human use consumption (Economic Survey of Pakistan, 2015–16).

There is a dire need to reduce the gap between domestic edible oil production and its import to maximum extent production of oil and the majority of its import. To supply the growing demand for locally produced edible oil from the growing population, new cultivars with lower erucic acid and glucosinolate contents must be developed immediately.[6][7]

Masoor

Pulses, with their 25–32% protein content, are a key contributor to Pakistan's daily diet's protein needs. Lentil (Lens culinaris Medik.) is the second most significant crop for pulses after chickpeas and is crucial to a diet high in cereals (Ramdath et al., 2020). The country's production and area of lentils are declining sharply, despite the fact that the demand for them is rising annually as a result of population

https://doi.org/10.62500/icrtsda.1.1.18

growth (Erskine et al., 2011). Over the past five years, there has been a noticeable decline in both productivity and total area.

In 2020–21, the area used for lentil production was reduced to 6.5 thousand hectares from 9.5 thousand hectares in 2019–20. The data indicates a 30.5% decrease in area. Due to a rise in the cultivars' average yield, lentil production in 2020–21 was the same as it was in 2019–20 (Anonymous, 2020–21). While the potential yield of lentil cultivars ranges between 1500 and 2000 kg ha-1, Pakistan's average crop output is noticeably lower (Aktar et al., 2016).[8][9]

Wheat

For the majority of people on the planet, wheat (Triticum aestivum L.) is their primary food source (Khan et al., 2008). It is the crop that is grown most everywhere in the globe. Since wheat is a staple food in Pakistan, it is grown on the greatest area (8.303 million hectares in 2005–06) and in practically every region of the nation. 1.9% of GDP and 13.7% of agricultural value added are contributed by it (National Coordinated Wheat Programme, NARC, Islamabad). Pakistan is ranked ninth in terms of area, fifth in terms of yield per hectare, and eighth in terms of output among the top ten nations in the world that produce wheat. Despite being a cotton zone, southern Punjab contributes around 44%.[10][11]

2. Methodology

2.1. Autocorrelation fuction (ACF)

The autocorrelation function measures how a time series (z1, z2,..., zn) correlates with itself. The correlation coefficient between zt and zt-1, denoted by t, is known as the lag-k autocorrelation of zt and is predicated on the weak stationary assumption.An ACF is used to quantify and visualize the average correlation between data points in a time series and earlier values in the series computed for different lag lengths.

2.2. Partial autocorrelation function (PACF)

The partial autocorrelation function at lag-k, represented by the symbol kk, is the correlation coefficient between z_1 and z_1-1 after the influence of the intervening Z1-1,-2,...., Zt-k+1 has been removed. In time series analysis, the partial autocorrelation function (PACF) regresses the time series values at all shorter lags and provides the partial correlation of a stationary time series with its own delayed values.

2.3. Autoregressive Moving Average Model (ARMA)

ARIMA (p, d, q) is used to represent the autoregressive moving average model,

Where p: The order of autoregressive q: The order of moving average.

d: The order of non-seasonality difference.

The general form of an ARMA model for stationary time series can be expressed as follows:

$(Bx)_t = \delta + \theta(B)a_t$

A non-stationary series must first be converted into a stationary one by taking into account pertinent differences:

$\nabla^d x_t = {}_t \quad {}_{t-s} \quad (1-B)^d x \quad = x_t - x$

https://doi.org/10.62500/icrtsda.1.1.18

$(1-B)^d$: The d^{th} difference. B: The backward shift operator.

For non-stationary time series, the general form of an ARMA model can be written as:

$\Phi(B)(1-B)^d x_t = \delta + \theta(B)a_t$ Where

$\Phi(B) = 1 - \Phi_1 B - \Phi_2 B^2 - \ldots - \Phi_p B^P$, is the autoregressive operator of order p.

$\theta(B) = 1 - \theta_1 B - \theta_2 B^2 - \ldots - \theta_p B^P$, is the moving average operator of order q.

$a_t = N I (0, \sigma_a^2)$

2.4. Model Building

The Box-Jenkins iterative technique to developing linear time series models consists of four stages: identification, parameter estimates, diagnostic verification, and forecasting. The identification stage is the most important one. It has the correct ARIMA model in it. Diagnostic model checking involves testing the model's assumptions to identify any places where the model is flawed.

To determine the quality of fit of the proposed ARIMA model, so that

$H_0 = \rho_k(a_t) = 0$

$H_1 = \rho_k(a_t) = 0$

We reject the hypothesis that the residuals are randomly distributed if Q is located in the extreme 5% of the chisquare distribution's right side tail.

2.5. Artificial Neural Network (ANN)

An artificial neural network mimics the functioning of the human brain by utilizing organic neurons. Artificial neural networks do practical computations and mimic complex brain operations. In 1943, McCulloch and Pitts proposed the first artificial neuron model.

Neural networks are widely used in biology, engineering, medicine, and finance. A feed-forward or feed-back architecture can be used to build an artificial neural network. An artificial neural network consists of three different types of layers: input, hidden, and output layers. According to Figure 1,

https://doi.org/10.62500/icrtsda.1.1.18

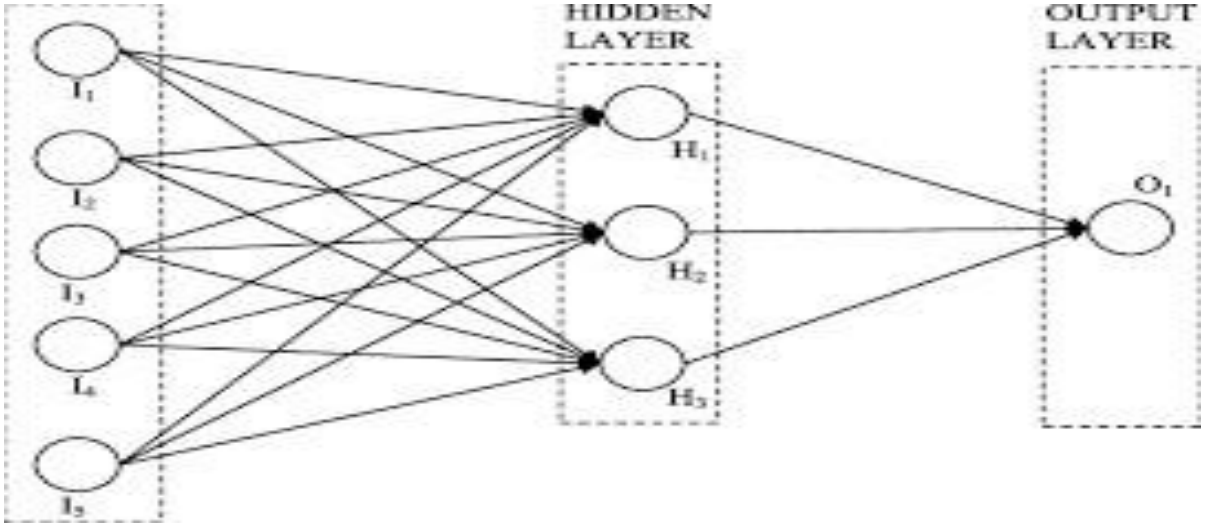

Figure 1: Artificial neural network

3. Data Analysis and Results

3.1. Data Description

In order to develop a suitable model to be used to forecast the yearly area of rabi crops, the data for the current study were the annual area of Rabi Crops. The data were obtained from the website AMIS.Pk for the period(1947-2021). The statistical program:EViews-10 and Zaitun Time Series were utilized.

3.2. Comparison of ARIMA and ANN

For ARIMA, the normality of area of the rabi crops is determined by the probability value of the Jarque-Bera test. If the probability of Jarque- Bera is greater than 0.05 so we accept the null hypothesis, which means residuals are normally distributed. By taking the first log, in the case of the rice field, we make our data stationary. The model for Gram ARIMA(0,1,1), Barley ARIMA(3,1,1),Repaseed ARIMA(0,1,1), Masoor ARIMA(2,1,3) and wheat

ARIMA(1,1,2) for the annual rabi crops is then chosen based o In order to make our data stationary for yearly rabi crops area because it has the highest adjusted R-squared value and the lowest AIC and SIC values. Using the Unit Root test, we demonstrate the stationary nature of the annual data on Rabi Crops Area. In order to forecast the area of the Rabi Crops for ANN, we placed Gram and Masoor twelve input layer neurons, ten hidden layer neurons, and one output layer neuron. Rapeseed, Barley and Wheat twelve input layers neurons, twelve hidden layer neurons, and one output layer neuron. With a learning rate of 0.005 and momentum of 0.05, we employ the bipolar sigmoid function and calculate Mean Square Error (MSE) and Mean Absolute Error (MASE) on Zaitun Time Series. Taking square root of MSE we calculate Root Mean Square Error (RMSE).The comparison of the Mean Square Error (MSE), Root Mean Square Error (RMSE) and Mean Absolute Error (MAE) of ARIMA and ANN is as:

ARIMA	MSE	RMSE	MAE
GRAM	180152.794	424.4441	376.8888
BARLEY	3208.528009	56.64387	34.1064
REPASEED	24767.96079	157.3784	138.2225
MASOOR	2769.883217	52.62968	44.0621

https://doi.org/10.62500/icrtsda.1.1.18

WHEAT	1217367.982	1103.344	920.142

Table 1: MSE, RMSE and MAE

ANN	MSE	RMSE	MAE2
GRAM	11799.23939	31.71654037	78.3828
BARLEY	1005.938933	108.6243039	18.64907
REPASEED	2511.288097	50.11275384	39.83782
MASOOR	295.223311	17.18206364	11.97115
WHEAT	160034.193880	400.0427401	314.9843

Table 2:MSE, RMSE and MAE

The ANN forecasted values and graph ot the area of gram, barley, rapeseed, masoor and wheat crops are as: Artificial Neural Network ANN Forecasted Values

Table 3: ANN forecasted value of Gram Area

Column1	Column2
2022	1758.5248
2023	1745.0952
2024	1711.942
2025	1765.1052
2026	1801.2157
2027	1815.6504
2028	1872.3316
2029	1853.0485
2030	1938.0717
2031	1969.542
2032	1963.936
2033	1929.5119
2034	1897.0544
2035	1880.6327

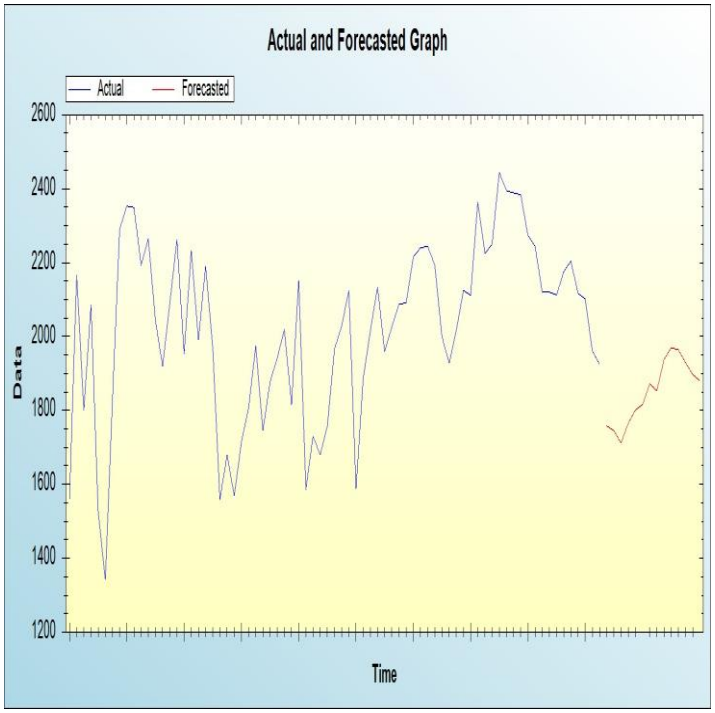

https://doi.org/10.62500/icrtsda.1.1.18

Table 4: ANN forecasted value of Barley Area

Column1	Column2
2022	21.4061
2023	25.5386
2024	28.1084
2025	24.5384
2026	24.7199
2027	25.1471
2028	23.1659
2029	23.0557
2030	25.9401
2031	28.7743
2032	28.2728
2033	27.9985
2034	26.9903
2035	28.0059

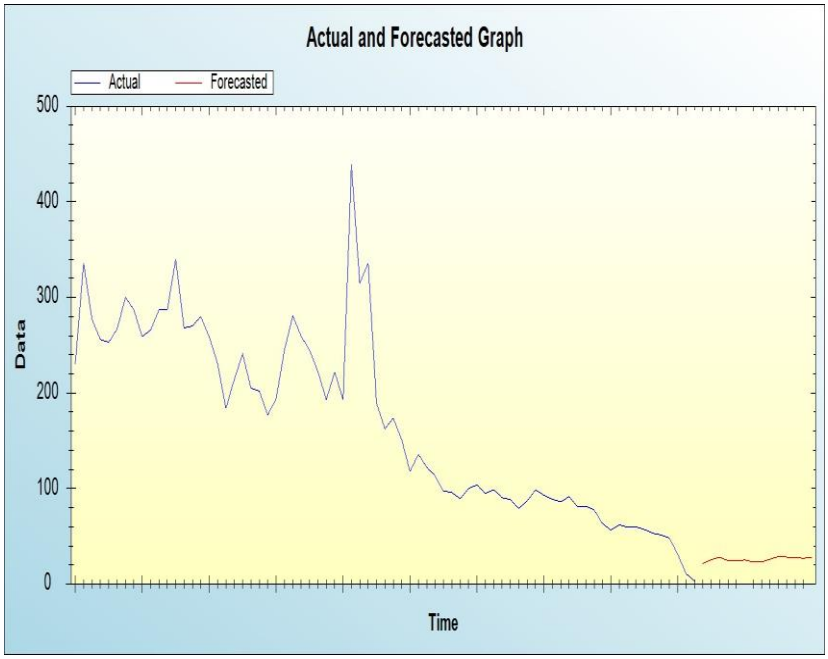

Table 5: ANN forecasted value of Rapeseed Area

Column1	Column2
2022	449.0997
2023	580.9241
2024	420.12
2025	531.4279
2026	414.3753
2027	504.9285
2028	502.166
2029	393.9072
2030	420.6486
2031	397.6999
2032	436.5489
2033	373.0011
2034	448.1864
2035	363.2818

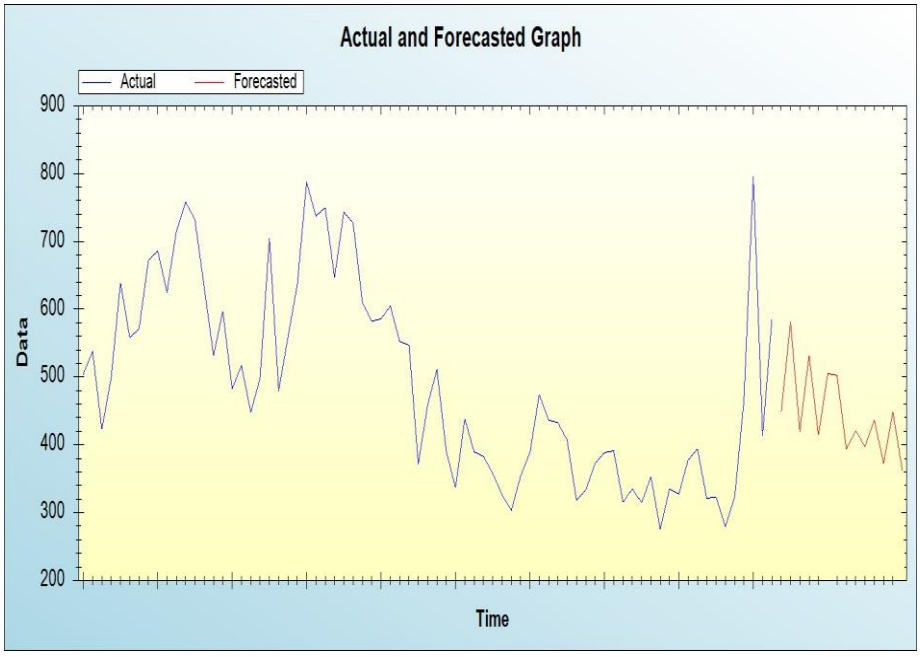

https://doi.org/10.62500/icrtsda.1.1.18

Table 6: ANN forecasted value of Masoor Area

Column1	Column2
2022	10.34
2023	10.094
2024	9.1165
2025	8.9639
2026	9.0665
2027	7.6627
2028	7.0862
2029	7.0157
2030	6.8431
2031	6.8311
2032	6.9421
2033	6.8685
2034	6.8647
2035	6.8679

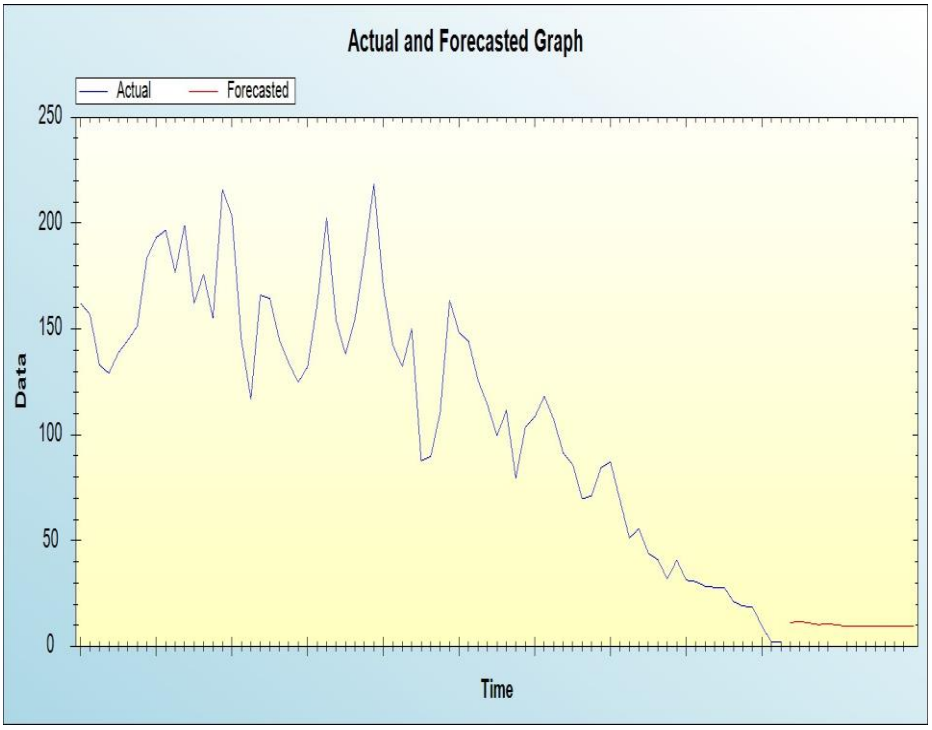

Table 7: ANN forecasted value of Wheat Area

Column1	Column2
2022	16352.2932
2023	16424.8187
2024	16481.7128
2025	16501.9566
2026	16491.985
2027	16411.4157
2028	16441.1143
2029	16383.6201
2030	16432.3074
2031	16439.8616
2032	16437.4962
2033	16437.4917
2034	16448.0469
2035	16444.7514

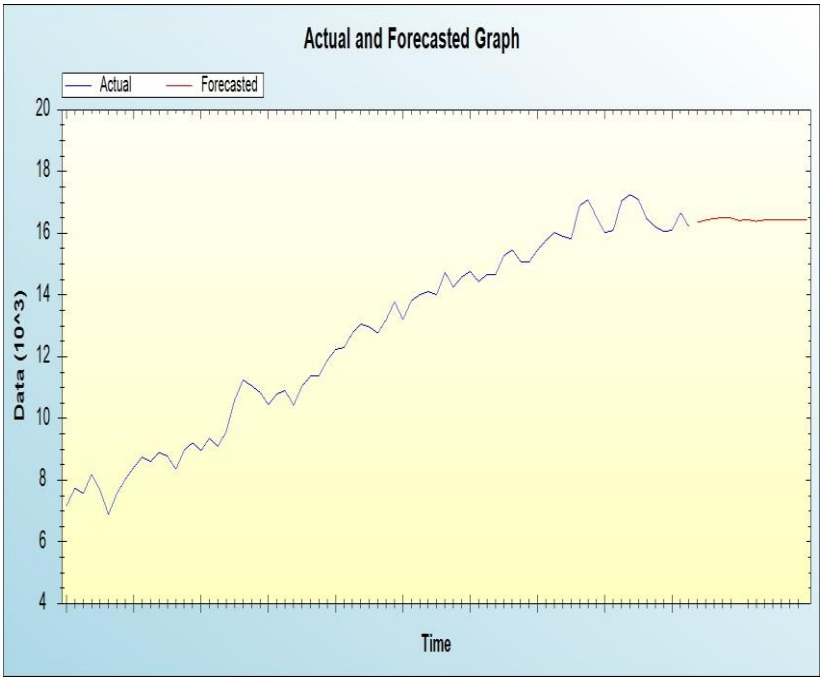

https://doi.org/10.62500/icrtsda.1.1.18

4. Conclusions

The goal of the current study was to determine if ARIMA models outperform artificial neural networks in terms of performance. According to the study, Artificial Neural Networks (ANN) are the most appropriate and frugal model for predicting the Area of Rabi Crops in Punjab, Pakistan for the next 14 years. The Mean Square Error (MSE), Root Mean Square Error (RMSE), and Mean Absolute Error (MAE) are all lower when we employ ANN rather than ARIMA. This is a reliable indicator of the model.

We advise the government to anticipate the area of Rabi Crops in Punjab, Pakistan, using artificial neural networks (ANN) models.

REFERENCE

1. NASR, N., & QAYUUM, A. (2015). A DETAILED DESCRIPTIVE STUDY OF GRAM PRODUCTION IN PUNJAB, PAKISTAN. *Journal of Global Agriculture and Ecology*, *3*(1), 38-43
2. Amir, M. W., Raza, Z., & Amin, M. (2022). Statistical Modeling and Forecasting of Gram Pulse Area and Production of Pakistan. *Journal of Quantitative Methods*, *6*(2).
3. Waqas Wakil, Muhammad Ashfaq, Sohail Ahmed. Larval population and pod infestation by helicoverpa. Pak. Entomol. 2005;27:33-36.
4. Naheed, S., Raza, I., Anwar, M. Z., Habib, N., Zahra, N., & Siddiqui, S. (2015). Forecasting area and production of barley in Punjab, Pakistan. *Pakistan Journal of Agricultural Research*, *28*(3).
5. Sobia Naheed, S. N., Irum Raza, I. R., Anwar, M. Z., Nusrat Habib, N. H., Naheed Zahra, N. Z., & Sabeen Siddiqui, S. S. (2015). Forecasting area and production of barley in Punjab, Pakistan.
6. Nadeem, M. A., Muhammad, H., Ullah, Z., & Khan, A. M. (2017). Rohi Sarsoon: A new high yielding rapeseed variety released for general cultivation in south Punjab (Pakistan). *Asian J Agri & Biol*, *5*(4), 251-256.
7. Amer, M., Aslam, M., Razaq, M., & Afzal, M. (2009). Lack of plant resistance against aphids, as indicated by their seasonal abundance in canola, Brassica napus (L.) in Southern Punjab, Pakistan. *Pak. J. Bot*, *41*(3), 1043-1051.
8. Kaukab, S., Khan, M. E., Amin, M. A., Akhter, M., Rehman, A. U., Shahid, M., ... & Rizwan, M. (2022). PUNJAB MASOOR-2020: A NEW LENTIL VARIETY WITH HIGH SEED YIELD AND RESISTANCE TO POTENTIAL FUNGAL DISEASES. *Pakistan Journal of Phytopathology*, *34*(2), 187-192
9. Tufail, M., Ahmad, M., & Ali, A. (1995). Masoor-93: an ideal combination of characters for Punjab province, Pakistan. *Lens Newsletter*, *22*(1/2), 50-52.
10. Hussain, A., Saboor, A., Khan, M. A., Mohsin, A. Q., Hassan, F., & Anwar, M. Z. (2012). Technical efficiency of wheat production in Punjab (Pakistan): A cropping zone wise analysis. *Pakistan Journal of Life and Social Sciences*, *10*(2), 130-138
11. Hussain, M., Hussain, G. H. U. L. A. M., Akhtar, L. H., Tariq, A. H., Rafiq, M. U. H. A. M. M. A. D., Aslam, M. Z., ... & Sahi, S. T. (2010). New wheat variety “Fareed-06” for irrigated areas of Punjab, Pakistan. *Pak. J. Bot*, *42*(5), 3285-3297

FORCASTING OF BAJRA PRODUCTION USING ARIMA AND ANN: A CASE STUDY OF PUNJAB PAKISTAN.

https://doi.org/10.62500/icrtsda.1.1.19

Proc. 1st International Conference on Recent Trends in Statistics and Data Analytics
Air University Islamabad, Pakistan – May 9, 2024, Vol. 1, pp. 169-174

FORCASTING OF BAJRA PRODUCTION USING ARIMA AND ANN: A CASE STUDY OF PUNJAB PAKISTAN.

Iqra Yaseen[1], Rohma Maliha[2],Samra Shehzadi[3] and Wajiha Nasir[4]

Department of statistics, Govt. College Women University, Sialkot[1,2,3,4]

Abstract

Pearl millet is the most widely used kind of millet. It has been growing across Africa and the Indian subcontinent from the beginning of time. In Pakistan's arid and dry regions, it is widely sown. Its cultivation is centered in Punjab in the arid regions of Bahawalpur and Pothwar's barani districts. For the study, we used annual data from the Punjab Crop Reporting Survey, which covered 27 years (1995-2021) . We used Box Jenkson and Artificial neural network to forecasting. From 1995 to 2021, neural networks were used for observation.for the prediction of the bajra market. We compare the both forecasting methods by Mean Square Error (MSE), Root Mean Square error (RMSE), of Mean Absolute Error (MAE).

Key words:

Bajra, Production, ARIMA, Neural Network.

1. Introduction

Bajra, sometimes know as pearl millet, is an important crop for food and agriculture, especially in areas with semi-arid and dry climates. Scientifically known as Pennisetum glaucum, this cereal grain has been farmed for millennia and has a long history of use as a staple food in many different cultures worldwide.Bajra is well known for its capacity to adapt to challenging environmental factors; it thrives in regions with little rainfall and poor soil. It is an essential crop in areas with limited water resources and difficult agricultural conditions because of its resistance to heat and drought. Bajra is essential to the nutritional security of the world because of its many uses and advantages. Bajra is grown by planting its seeds in soil that drains properly and receives lots of sunlight. It is widely grown in areas of Africa, Asia, and the Middle East, where it provides millions of people with their main source of nutrition. Utilizing both conventional and contemporary farming methods, farmers raise this hardy crop that will continue to thrive under challenging circumstances. Because it provides a variety of vital elements like fiber, protein, carbs, vitamins, and minerals, bajra is highly valued for its nutritional richness. Because it is gluten-free, anyone with celiac disease or gluten intolerance can use it. Because bajra is exceptionally high in iron and magnesium, it is useful in treating nutritional deficiencies, especially in areas where access to a variety of foods is limited.

Kakar et al. (2023) investigate that the study looks on Pakistan's cereal crop growth, instability, and trends from 1951 to 2020. The findings indicate that while bajra and jowar are trending negatively, wheat, rice, and maize are growing positively. There is less varied instability and a higher Coppock Index in wheat, rice, and maize. Non-traditional cereal crops should be promoted by public government departments for both nutritional and financial reasons. Gandhi et al. (2023) studied that the purpose of the study is to forecast pearl millet pricing and production in Rajasthan, India, utilizing annual production data up to 2029–2030 and time series data up to December 2024. Pearl millet pricing and production were forecast using the

https://doi.org/10.62500/icrtsda.1.1.19

ARIMA and SARIMA models. ARIMA (0, 1, 2) with drift for pearl millet production and ARIMA (1, 1, 1) (1, 0, 1) for pearl millet prices were the best-fitting models, respectively. According to the data, pearl millet production and prices are expected to rise in Rajasthan, pointing to a growing trend in the agriculture industry. Comprehending these variables might aid farmers in making knowledgeable choices regarding marketing and acreage distribution. Shateen et al. (2021) studied that using the ARDL technique, this study investigates the long- and short-term relationships between dual sector inflation in Pakistan from 1974 to 2020. We gathered information from the World Development Indicator and the Handbook of Statistics. A consistent rise in the average cost of goods and services, or inflation, has a big effect on the economy. It falls into one of three categories: cost-push, demand-pull, or built-in inflation. A decrease in a consumer's purchasing power per unit of money currency, or inflation, causes a real value loss. Economic growth is influenced by fiscal and monetary policies, which control it. Thapa et al. (2022) investigate that the using Box-Jenkins Autoregressive Integrated Moving Average (ARIMA) models, the study projects vegetable area, production, and productivity in Nepal from 1977/78 to 2019/20. While the ARIMA (0, 2, 0) model was optimal for vegetable productivity, the ARIMA (0, 2, 1) model was shown to be appropriate for all areas and production. Mean absolute percent error (MAPE) values were used to assess the models' performance; the MAPE values for productivity, production, and area projections were 3.80%, 2.40%, and 2.70%, respectively. According to the study, developing awareness among vegetable growers and producing precise projections are essential for developing future vegetable production plans in Nepal. Mehmood et al. (2023) investigate that using historical data from 1947 to 2021, this study attempted to anticipate the area and production of wheat crop in Pakistan from 1947 to 2021. The research employed the ARIMA linear model, which yielded the lowest RMSE and MAE values for wheat production and area. A ten-year average wheat area of 9058.10, with an anticipated annual rise of 2.87 percent, was forecasted using the ARIMA-ANN model. The mean yield of wheat was 25878.03, with a 2.34 percent predicted variation. The government will need to use these forecast projections in order to plan the industrial sector, meet trade needs, and meet food needs.

2. Methodology

The main objective of this study is to develop a significant model to forecast bajra production in Punjab Pakistan. For this purpose, yearly annual data on bajra production rates from 1995 to 2021 have been collected from Punjab crop reporting survey.

2.1: Autocorrelation function:

The autocorrelation function at lag kk, denoted as $\rho k \rho k$ (rho sub k), measures the correlation between observations in a time series that are kk time units apart. The autocorrelation function is often visualized using a correlogram, which is a plot of the autocorrelation coefficients against the lag kk. This plot helps identify patterns in the autocorrelation structure of the time series.

2.2:Partial autocorrelation:

The partial autocorrelation function at lag kk, denoted as $\phi k k \phi k k$ (phi sub kk), measures the correlation between observations in a time series that are kk time units apart, after removing the effects of the intervening lags

2.3:ARIMA Model:

The ARIMA model, which stands for Autoregressive Integrated Moving Average, is a widely used time series forecasting method that combines autoregression, differencing, and moving

https://doi.org/10.62500/icrtsda.1.1.19

average components to capture the temporal structure of a time series data. Here's are some points of the ARIMA model:

1. **Autoregressive (AR) Component**: The autoregressive component models the relationship between an observation and a number of lagged observations (also called autoregressive terms). It assumes that the value of the time series at any given point is linearly dependent on its previous values.
2. **Integrated (I) Component**: The integrated component involves differencing the time series data to make it stationary. Stationarity is a key assumption of many time series models, including ARIMA. Differencing involves computing the difference between consecutive observations to remove
3. **Moving Average (MA) Component**: The moving average component models the relationship between an observation and a residual error term based on a moving average model applied to lagged forecast errors. It captures the impact of past shocks on the current value of the time series.

   The general notation for an ARIMA model is ARIMA(p, d, q), where

   - *p* represents the order of the autoregressive component, indicating the number of lagged observations included in the model'
   - *d* represents the degree of differencing applied to the time series data to make it stationary
   - *q* represents the order of the moving average component, indicating the number of lagged forecast errors included in the model.

   3:Results and discussion:

   3.1:Data Description

   In order to develop a suitable model that could be used to the productio of bajra crops. For this purpose, yearly annual data on bajra production rates from 1995 to 2021 have been collected from Punjab crop reporting survey.

   Time series plot of bajra production in Pakistan is developed

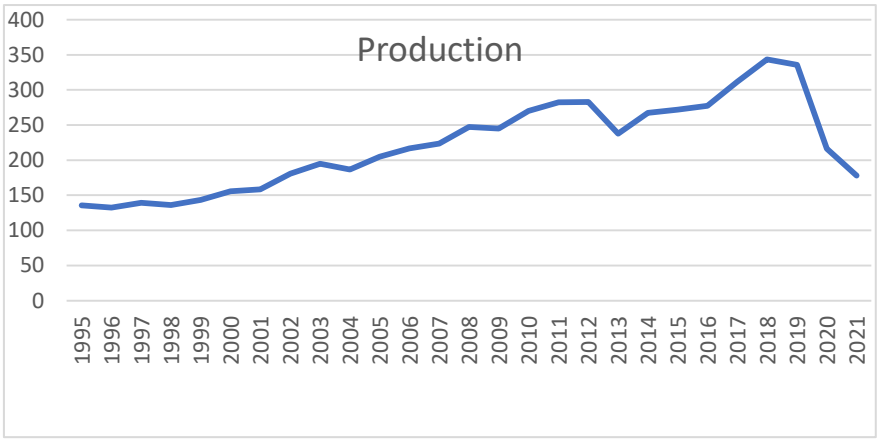

Production figures from 1995 to 2021 are displayed on the graph. It appears from the description that the trend component is the most widely utilized feature in this graph. In this instance, the trend indicates a general decrease in production levels interspersed with intervals of recovery. The trend is the long-term movement in the data across time.

https://doi.org/10.62500/icrtsda.1.1.19

Table 1: Augmented Dickey-Fuller Test

	Test Statistics	Sig
First difference	-3.490605	0.0170

The values of parameters p and q have been determined by constructing a correlogram of the first difference series. According to the correlogram, p may have a value of 0 and q might have a value of 1. An ARIMA model has been suggested based on the potential values of p and q.

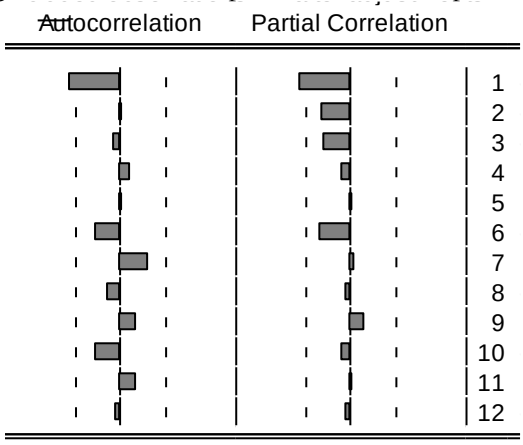

Table 2: ARIMA (0, 2, 1)

Table 2 demonstrate that, in comparison to other models, ARIMA (0, 2, 1) has lower predicting error. Consequently, ARIMA (0, 2, 1) has been our recommended model based on the Box-Jenkins Methodology.

Table 3

Model	RMSE	MSE	MAPE
(0,2,1)	9.09286	82.67950	26.69769

4 Neural Networking

Twelve input layer neurons, twelve hidden layer neurons, and one output layer neuron have all been used in a backpropagation neural network (BNP) using a bipolar sigmoid function. The time series is not represented by a parametric model in this method. The NN is used to predict the production of bajra crops, and a plot of the original data is provided along with the prediction.

https://doi.org/10.62500/icrtsda.1.1.19

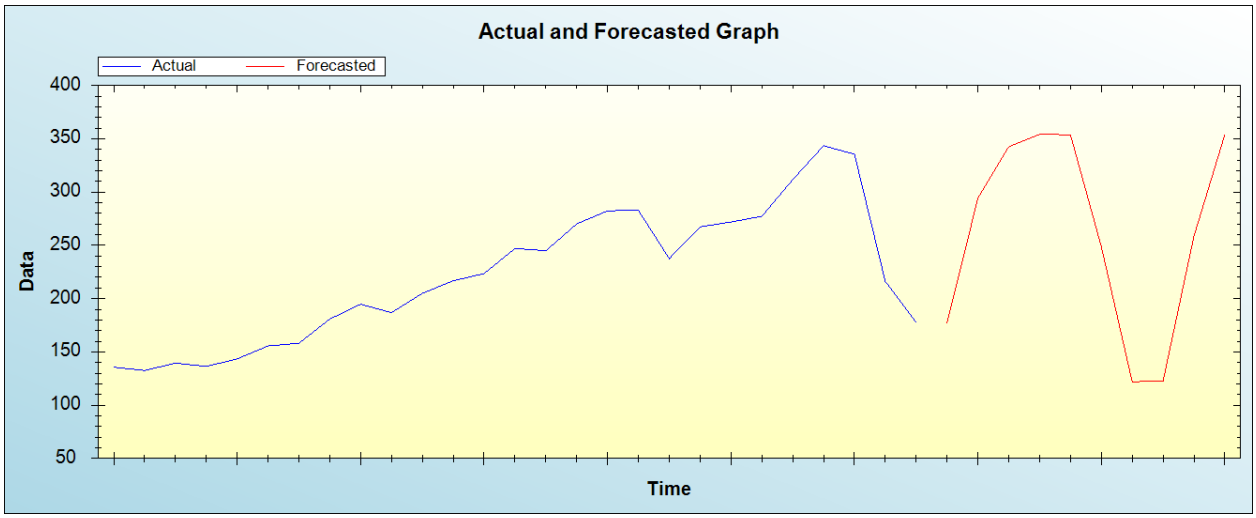

Table 4: Forecasting Error

RMSE	MSE	MAE
9.082242	82.487131	6.350939

The Table's result indicates that, in comparison to Box-Jenkins models, neural network forecasting errors have been the lowest. Thus, the annual bajra production has been forecasted using neural networking.

Table 5: Forecasted value of Bajra production

Year	Bajra production	Year	Bajra production
2022	177.3073	2027	248.6609
2023	294.1883	2028	122.1003
2024	342.5393	2029	122.5605
2025	354.2002	2030	258.5997
2026	353.7616	2031	353.8323

5 COMMENTS AND CONCLUSION

The primary aim of this research is to create a meaningful model that can predict Pakistan's annual production of bajra. The Punjab Crop Reporting Survey has provided yearly statistics on bajra production from 1995 to 2021 for this purpose. Various models in Neural Networking have been proposed using the Box-Jenkins technique. Among all the suggested approaches, it has been found that the accuracy metrics for NN, RMSE, MAE, and MAPE, are the lowest. Consequently, policymakers are advised to use NN to predict the output of bajra.

References

1. Kakar, J. S., Lodhi, A. S., Nazir, A., Akhtar, S., & Iqbal, M. A. (2023). Cereal crops production in Pakistan: Trends instability and growth. *International Journal of Agricultural Extension*, *11*(2), 201-207
2. Gandhi, T., Saravanakumar, V., Chandrakumar, M., Divya, K., & Senthilnathan, S. (2023). Forecasting pearl millet production and prices in Rajasthan, India: An ARIMA approach

https://doi.org/10.62500/icrtsda.1.1.19

3. Shaheen, R., Iqbal, S., & Javed, A. (2021). DUAL SECTOR INFLATION DYNAMICS IN PAKISTAN: AN EMPIRICAL ANALYSIS USING COINTEGRATION ANALYSIS. *The journal of contemporary issues in business and government*, *27*(5), 2737-2742
4. Mehmood, Q., Sial, M. H., Sharif, S., & Riaz, M. (2023). Development of statistical, artificial neural network and hybrid models, forecasting wheat area and production in Pakistan. *International Journal of Agricultural & Statistical Sciences*, *19*(1).
5. Thapa, R., Devkota, S., Subedi, S., & Jamshidi, B. (2022). Forecasting area, production and productivity of vegetable crops in Nepal using the Box-Jenkins ARIMA model. *Turkish Journal of Agriculture-Food Science and Technology*, *10*(2), 174-181

https://doi.org/10.62500/icrtsda.1.1.20

Proc. 1st International Conference on Recent Trends in Statistics and Data Analytics
Air University Islamabad, Pakistan – May 9, 2024, Vol. 1, pp. 175-180

FORECASTING OF JOWAR PRODUCTION USING ARIMA AND ANN: A CASE STUDY OF PUNJAB PAKISTAN

Rohma Maliha[1] , Iqra Yaseen[2] , Samra Shahzadi[3] and Wajiha Nasir[4]
Department of Statistics, Govt. College Women University, Sialkot[1, 2, 3, 4]

ABSTRACT

Jowar also known as sorghum, is the main agriculture crop of Pakistan. It is drought- tolerant and can be used for various purposes such as food, animal feed, and even biofuel production. Jowar trade annual data obtained from Punjab Crop Reporting Survey for this yearly annual data from 1995-2019 were used for model fitting and forecasting up to 2030. The best fit ARIMA model were selected based on autocorrelation function and partial autocorrelation function at lag. Neural Network also has been utilized on observation 1995-2019 for the prediction of Jowar trade. Prediction error based on Mean Square Error (MSE), Root Mean Square Error (RMSE) and Mean Absolute Error (MAE), proposed Neural Network Model found to be the best among them. Model parameter were estimated by using the E-view software, Microsoft Excel and Zaitun software.

KEYWORDS: Jowar, Production, Time series, Autoregressive Integrated Moving Average (ARIMA), Artificial Neural Networking (ANN).

1. INTRODUCTION

Jowar (Sorghum bicolor) holds significant agricultural importance in Punjab, Pakistan, contributing to food security and economic sustainability. Jowar is a hardy crop that can tolerate a wide range of environment conditions. It's grown in both tropical and subtropical regions. Jowar is primarily grown in the southern districts of Punjab, Pakistan, such as Bahawalpur, Rahim Yar Khan, and Multan. These areas have favorable climatic conditions and soil types that are suitable for jowar cultivation. The crop requires warm temperatures during the growing season and is sensitive to frost. Jowar grains are used for various purposes, including human consumption, livestock feed, and industrial applications. In many regions, it's a staple food and is used to make flatbreads, porridge, and alcoholic beverages. Jowar straw is also used as fodder for livestock and as a raw material for paper and biofuel production.

Farah et al. (2016) studied that the main crop of Sudan is sorghum, and the nation is among the major producers of the grain worldwide. Sudan is sixth globally in terms of sorghum output, behind Nigeria, China, India, and the United States. The most significant crop and animal feed is sorghum. The goal of the study is to forecast Sudan's sorghum production. The study used the best technique for the pattern time series analysis using the Box-Jenkins methodology. The four steps of this procedure are identification, estimation, diagnostic checking, and ARIMA model forecasting. Shoko et al. (2017) investigate that crop production forecasting and estimation are essential for guiding policy choices pertaining to development and food security. The current study looks at South Africa's sorghum production situation. In order to forecast sorghum production, univariate time series modeling employing the ARIMA model was created. The Box and Jenkins linear time series model also known as the ARIMA (p, d, q) model which combines integration, moving average, and autoregression was used. The sorghum yearly output series from 1960 to 2014 showed a declining tendency, however the production prediction for sorghum between 2017 and 2020 showed a growing trend. According to the analysis, ARMA (1, 0, 4) is the best-fitting model for the sorghum production series. In terms of forecasting accuracy and explaining variability, the model performed well. This study has also demonstrated that sorghum's drought-tolerant qualities may help ensure food security for households and the country. Praveen et al. (2020) studied that the effects of climate variation on land production for important food and non-food grain crops in India are evaluated in this study. We gathered

https://doi.org/10.62500/icrtsda.1.1.20

information on 15 crops from all throughout India for 50 years, from 1967 to 2016. To project the variance in agricultural production for each crop over a period of 20 years, or until 2036, using several variables, such as temperature and rainfall estimates. According to our findings, most crops' land productivity decreases as the yearly mean temperature rises. The detrimental effects of climate variation on agricultural production suggest that minor and marginal farming families those most severely impacted by climate variation may be at risk for food security. The findings indicate that a rise in temperature would have a negative impact on agricultural productivity and evaluate how vulnerable Indian agriculture is to climate change. Using the autoregressive integrated moving average model, we conducted forecasting for 20 years. It demonstrates that the productivity of several crops, including gram, sesamum (til), jowar, groundnut, sugarcane, and bajra, will rise in the future when temperature and rainfall increase. Certain crops like arhar, wheat, rice, cotton, and tea are sensitive to the climate. The yield of these crops either slightly increases or decreases with temperature. Ray et al. (2023) investigate that forecasts can be used by nations to develop data-driven strategies and make informed business decisions. A key element of agricultural diversification programs is the growth of cash crops, which reduce rural poverty and unemployment in developing countries. This study presents a comparison of the ARIMA, ETS, and NNAR models for predicting the area, production, and productivity of cotton, wheat, paddy, maize, jowar, and other crops. Data from 1980 to 2010 was utilized for model estimation (training), while data from 2011 to 2020 was used for validity testing. The models were compared using training and validation data sets (RMSE, MAE, and MASE) based on goodness of fit. By selecting the best model, forecast values for the years up to 2027 were obtained. The production of maize and jowar is expected to decline, while that of wheat, paddy, and cotton is expected to increase. The present forecast's results should help policymakers develop more aggressive future plans for food security and sustainability, as well as more effective plans for the cultivation of cash crops in India.

2. METHODOLOGY

The main goal of this study is to create a reliable model for predicting Jowar production in Punjab, Pakistan. To achieve this, annual data on Jowar production rates from 1995 to 2019 was collected from the Punjab crop reporting survey. The Box-Jenkins methodology and Neural Networking techniques were employed for this purpose. The proposed models were evaluated and compared using accuracy measures such as Root Mean Square Error (RMSE), Mean Absolute Error (MAE), and Mean Absolute Percentage Error (MAPE). This comparison helped determine the effectiveness of each model.

Autocorrelation Function (ACF)

ACF stands for Autocorrelation Function, which is a statistical tool used in time series analysis. It measures the correlation between a time series and its lagged values. In other words, it helps us understand the relationship between an observation and its past observations at different time lags. The ACF is calculated by computing the correlation coefficient between the original time series and its lagged versions. The lag refers to the time interval between the current observation and the past observation being considered. The ACF values range from -1 to 1, where a value of 1 indicates a strong positive correlation, -1 indicates a strong negative correlation, and 0 indicates no correlation .The ACF is useful in several ways.

Firstly, it helps identify the presence of any significant patterns or trends in the time series. If the ACF values are high and slowly decay over time, it suggests a strong correlation between the observations at different lags, indicating the presence of a trend. On the other hand, if the ACF values quickly decay to zero, it suggests no correlation and a lack of trend.

Secondly, the ACF can help determine the order of an autoregressive (AR) or moving average (MA) model. By examining the significant lags in the ACF plot, we can identify the appropriate lag order for the AR or MA model. For example, if the ACF values are significant at lag 1, it suggests an AR(1) model is appropriate, while significant values at lag 2 indicate an AR(2) model.

https://doi.org/10.62500/icrtsda.1.1.20

Partial Autocorrelation Function (PACF)

The PACF, or Partial Autocorrelation Function, is another statistical tool used in time series analysis. It measures the correlation between a time series and its lagged values, while controlling for the influence of intermediate lags. The PACF is calculated by removing the correlation explained by the previous lags and focusing only on the direct relationship between the current observation and a specific lag. It helps us understand the unique contribution of each lag to the overall correlation structure of the time series. Similar to the ACF, the PACF values range from 1 to 1, where a value of 1 indicates a strong positive correlation, -1 indicates a strong negative correlation, and 0 indicates no correlation. The PACF plot is useful in determining the appropriate lag order for an autoregressive (AR) model.

In the PACF plot, significant values at a particular lag indicate a strong correlation between the current observation and that specific lag, while non-significant values indicate no correlation. By examining the significant lags in the PACF plot, we can identify the appropriate lag order for the AR model.

Autoregressive Integrated Moving Average (ARIMA)

ARIMA, which stands for Autoregressive Integrated Moving Average, is a widely used statistical model for analyzing and forecasting time series data. It combines three components: autoregression (AR), differencing (I), and moving average (MA).

- **The autoregressive component (AR)** models the relationship between an observation and a certain number of lagged observations. It assumes that the current value of the time series is dependent on its past values.
- **The differencing component (I)** is used to make the time series stationary, which means removing any trends or seasonality present in the data. Differencing involves subtracting the previous value from the current value to eliminate the trend.
- **The moving average component (MA)** models the dependency between an observation and a residual error from a moving average model applied to lagged observations.

ARIMA models are commonly used for time series forecasting, as they can capture both shortterm and long-term patterns in the data. The model parameters, such as the order of autoregression (p), differencing (d), and moving average (q), are determined based on the characteristics of the time series data. By fitting an ARIMA model to historical data, we can make predictions and forecast future values of the time series. The model takes into account the patterns and dependencies observed in the data, allowing us to make informed predictions.

Box Jenkins Methodology

The Box-Jenkins methodology, also known as the Box-Jenkins approach, is a popular and powerful statistical technique used for time series analysis and forecasting. It was developed by George Box and Gwilym Jenkins in the 1970s. The Box-Jenkins methodology consists of three main steps: model identification, model estimation, and model diagnostic checking.

- In the model identification step, the appropriate ARIMA model is determined by analyzing the autocorrelation function (ACF) and partial autocorrelation function (PACF) plots of the time series. These plots help identify the order of autoregression (p), differencing (d), and moving average (q) components of the ARIMA model.
- Once the model is identified, the model estimation step involves estimating the parameters of the ARIMA model using maximum likelihood estimation or other suitable methods. This step involves fitting the model to the historical data and estimating the coefficients that best describe the relationship between the observations.
- After the model is estimated, the model diagnostic checking step is performed to assess the adequacy of the chosen model. This involves examining the residuals of the model to ensure

https://doi.org/10.62500/icrtsda.1.1.20

they are independent, normally distributed, and have constant variance. If the model fails to meet these assumptions, adjustments or alternative models may be considered.

3. RESULTS AND DISCUSSION

Time series plot of Jowar production in Pakistan is developed.

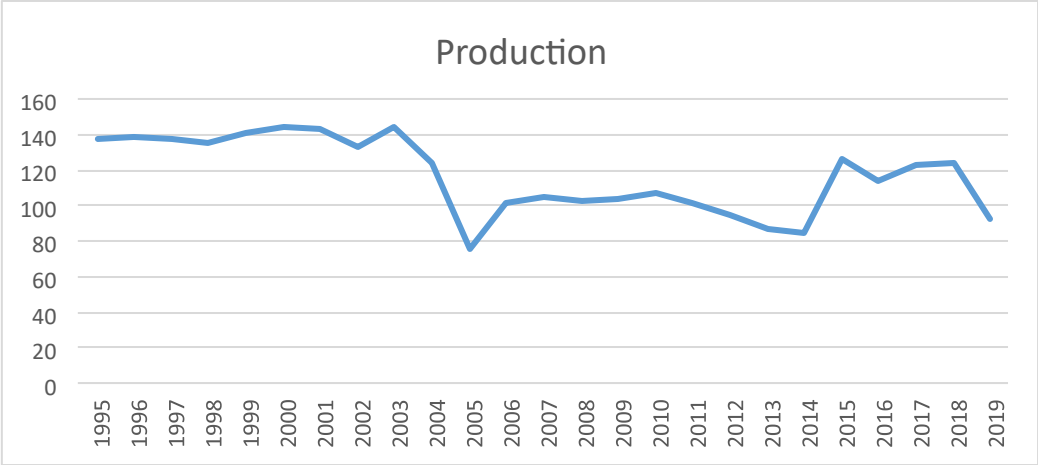

The graph shows production levels from 1995 to 2019. Based on the description provided, it seems that the trend component is the most prominent feature used in this graph. The trend is the longterm movement in the data over time, and in this case, it shows a general decline in production levels with some periods of recovery.

Table 1 Augmented Dickey-Fuller Test

	Test Statistics	**Sig**
First difference	-5.217279	0.0003

To determine the values of the parameters p and q, a correlogram of the first difference series was created. The correlogram analysis suggested that the possible value of p is 0, while the value of q is 10. Based on these possible values of p and q, an ARIMA model was proposed.

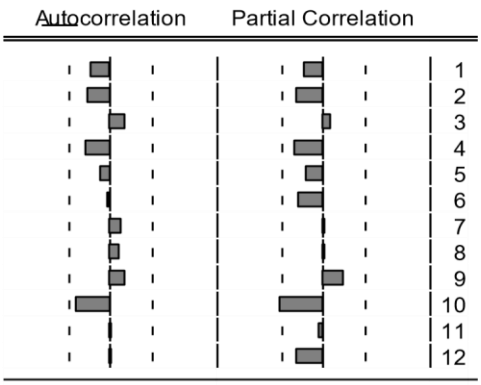

Table 2 reveal that ARIMA (0, 1, 10) has less forecasting error as compare to other. Therefore, from Box-Jenkins Methodology our suggested model has been ARIMA (0, 1, 10).

https://doi.org/10.62500/icrtsda.1.1.20

Table 2

Model	RMSE	MSE	MAE
(0,1,10)	19.71565	388.70685	15.48503

Neural Networking

In this approach, a Back Propagation Neural Network (NN) with a bipolar sigmoid function is used. The NN consists of 12 neurons in the input layer, 12 neurons in the hidden layer, and 1 neuron in the output layer. Unlike other methods, there is no specific mathematical model used to represent the time series data. The NN is applied to predict Jowar crop production, and a plot is provided to compare the original data with the NN's prediction.

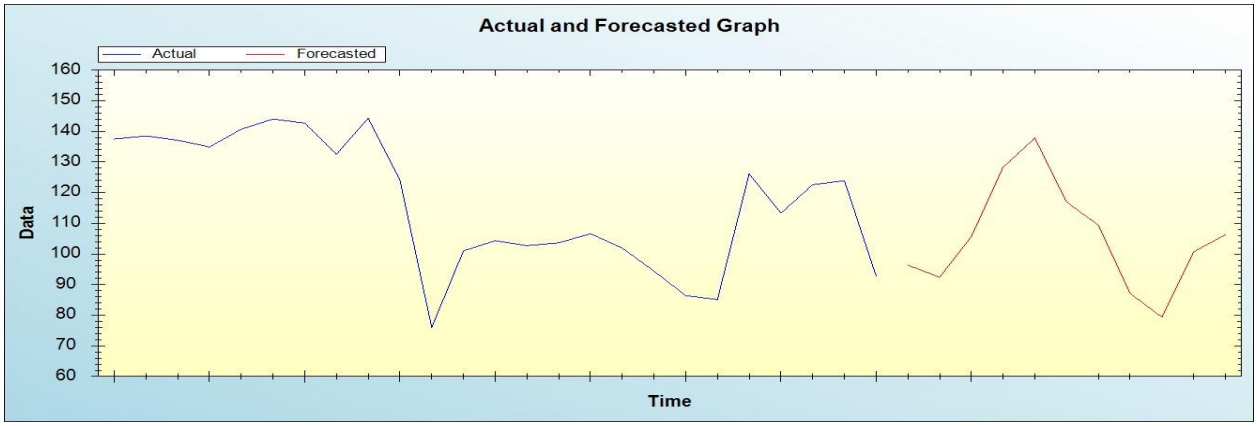

Table 3 Forecasting Error

RMSE	MSE	MAE
1.34105406	1.798426	0.990813

From the output of Table it can be seen that forecasting errors in neural networking have been least as compare to Box-Jenkins models. Therefore, neural networking has been utilized for forecasting of yearly jowar production.

Table 4

Forecasted value of Jowar production

Year	Jowar production	Year	Jowar production
2020	96.3543	2026	109.3877
2021	92.3753	2027	87.1035
2022	105.6691	2028	79.3615
2023	128.2574	2029	100.6887
2024	137.8269	2030	106.2450
2025	116.8985		

4. COMMENTS AND CONCLUSION

The main aim of this study is to create a good model for predicting how much Jowar will be produced in Pakistan each year. To do this, the researchers collected information about Jowar production from 1995 to 2019 from a survey called the Punjab Crop Reporting Survey. They used a method called Box-

https://doi.org/10.62500/icrtsda.1.1.20

Jenkins and another method called Neural Networking to come up with different models. They found that the Neural Networking model was the most accurate, with the smallest values for RMSE, MAE, and MAPE compared to the other methods. So, they suggest that the people who make policies should use the Neural Networking model to predict Jowar production.

References

1. Srivastava, A. B., Mishra, P., Singh, K. K., & Choudhri, H. P. S. (2022). Instability and production scenario of wheat production in Uttar Pradesh using ARIMA model and its role in food security. Indian Journal of Economics and Development, 18(1), 181-188.
2. Frah, E. A. (2016). Sudan production of Sorghum; forecasting 2016-2030 using autoregressive integrated moving average ARIMA model. American Journal of Mathematics and Statistics, 6(4), 175-181.
3. Shoko, R. R., & Belete, A. (2017). Efficient planning of sorghum production in South Africa-Application of the Box-Jenkin's method. Journal of Agribusiness and Rural Development, 46(4), 835-841.
4. Ray, S., Al Khatib, A. M. G., Kumari, B., Biswas, T., Nuta, A. C., & Mishra, P. (2023). Forecasting cash crop production with statistical and neural network model.
5. Bezabih, G., Wale, M., Satheesh, N., Fanta, S. W., & Atlabachew, M. (2023). Forecasting cereal crops production using time series analysis in Ethiopia. Journal of the Saudi Society of Agricultural Sciences.

https://doi.org/10.62500/icrtsda.1.1.21

Proc. 1st International Conference on Recent Trends in Statistics and Data Analytics
Air University Islamabad, Pakistan – May 9, 2024, Vol. 1, pp. 181-191

Estimation of Population mean in the presence of Non Response and Measurement Errors

Mahwish Akram[1] and Zainab Ashraf[2]
Department of Statistics, Govt. College Women University, Sialkot [1,2]

Abstract

The problem of estimating the finite population mean in simple random sampling in the presence of non-response and measurement error was considered. The estimators was proposed and its properties studied in the simultaneous presence of non-response and measurement errors. Because of this, the survey results are affected by the measurement error. we propose a method to jointly incorporate measurement error and non-response in the estimators of population mean using auxiliary information in simple random sampling. We have not only studied some available estimators but also suggested estimators in the presence of two types of non-sampling errors occurring jointly the measurement error and the non-response. This paper presents new estimators of mean estimation in presence of measurement error. Estimators are proposed and its properties are discussed with expression based comparative study.

Keywords: Population mean, Non-response, measurement error, Auxiliary information.

1. Introduction

Over the past several decades, statisticians were interested in the problem of estimating the parameters of interest in the presence of response error (measurement errors). These measurement errors make the result invalid, which are meant for no measurement error case. If measurement errors are very small and we can neglect it, then the statistical inferences based on observed data continue to remain valid. (Singh and Sharma (2015).The reasons for measurement error mainly relate to convenience, and human error. Sevilimedu and Yu, L. (2022). It may originate from various kinds of sampling methods such as simple random sampling, Various methods of estimation are used under the assumption that observations collected are true (error free). In real life this kind of situations are not tenable. These are also called measurement error. (Shukla, Pathak, and Thakur (2012). It is well known that the auxiliary information in the theory of sampling is used to increase of efficiency of estimator of population parameters. There exist situations when information is available in the form of attribute which is highly correlated with y. (Singh, Kumar, Singh, Smarandache (2011).

We have attempted to investigate the impact of measurement errors on the population ratio and product of two population means estimators in this research. In the case of measurement errors, a comparison is done between the recommended estimator and the traditional estimators. Singh and Karpe(2010).Tracy and Osahan (1994) have investigated how random nonresponse affects the accuracy of the population mean ratio estimate. Khare and Srivastava (2000) It has been thought about using the generalized estimator for population mean in the presence of nonresponse.

Assume that we have a collection of n paired observations on two qualities, X and Y, that were collected using a straightforward random sampling approach. Furthermore, it is believed that measurement error rather than the actual values of xi and yi for the i th sample units are seen (Xi, Yi). Let (xi, yi) represent the observed values rather than the real values (Xi, Yi) for the i th (i = 1.2,.., n) in a straightforward random sampling process.

$$u_i = y_i - Y_i \quad (1)$$

https://doi.org/10.62500/icrtsda.1.1.21

$vi = -xi \quad Xi$ (2)

where the measurement errors v_i and u_i are related and stochastic, with variances of σ_u^2 and σ_v^2 with mean zero. Furthermore, even if Xi and Yi have a correlation, let u_i and v_i have no correlation.

Non-response is a prevalent issue that affects postal surveys more than inperson interviews. Reaching out to the non-respondent and attempting to get as much information as you can is the standard method for resolving non-response issues.

Hansen and Hurwitz (1946) proposed a double sampling strategy that includes the following steps to estimate the population mean in the event of non-response at the initial stage:

i. The questionnaire is mailed to the sample units after a straightforward random sample of size n is selected.

ii. Through in-person interviews, a sub-sample of size r = (n2 / k), (k > 1) from the n2 non-responding units in the first step attempt is contacted.

The first attempt and the personal interviews at the second attempt. In the Hansen and Hurwitz method the population is supposed to be consisting of response stratum of size N_1 and the non-response stratum of size $N_2 = (N - N_1)$.

Let $\bar{Y} = \sum y N_i$ and $S_y^2 = \sum (y Y_i -)^2 (N-1)$ denote the mean and the population

Let $Y_1 = \sum y N_{i1}$ and $S_y^2{}_1 = \sum (y_i - Y)^2 (N_1 - 1)$ – N / N variance of the study–variable y.

indicate the respondent group's mean and variation. In a similar vein,let

$\bar{Y}_2 = \sum y N_{i2}$ and $S_y^2{}_2 = \sum (y_i - Y)^2 (N_2 - 1)$ denote the non-response group's mean

and variance. One way to express the population mean is as $Y = WY_{1\,1} + W\,Y_{2\,2}$, – – –

n

Where $W_1 = (N$ $_1$/ $N)$ and $W_2 = (N_2 N)$. The sample mean $\bar{y}_1 = \sum y\, n_i$ / is an

$i=1$ – – –

unbiased for Y, yet is as biased as $W_2 = (Y_1 - Y_2)$When calculating the population

r mean $\bar{Y}$. The mean of the sample $\bar{y}_{2r} = \sum y\, r_i$ is impartial regarding the n_2 units'

mean y_2.

Hansen and Hurwitz (1946) provided an impartial estimator of the population mean Y, which is provided by $\bar{y}^* = w_{1\,1}\bar{y} + w_{2\,2}\bar{y}_r$.

https://doi.org/10.62500/icrtsda.1.1.21

Where $w_1 = (n\ n_1), w_2 = (n_2/n)$ are the percentages of respondents and nonrespondents in the sample. The variance of $\bar{y}^*$ is given by

$V(\bar{y}^*) = \square\square\square 1\_\_\_\_\_ - nf\square\square\square Sy2 + W\,k\_\_\_\_\_(n-1)\,Sy2(2); Wheref = (n/N).$

It is well recognized from the sampling literature that using auxiliary data linked to x, which has a strong correlation with study variable y, can improve the efficiency of the estimator of the population mean of study variable y. Further Rao (1986, 90) have suggested the use of auxiliary character with known population mean in presence of nonresponse problems to increase the efficiency of the estimator. The generalized estimator for population means in presence of nonresponse has been considered by Khare and Srivastava (2000), Tiwari, Bhougal, Kumar and Rather (2022) Sabir, Sanaullah and Gupta (2022), Okafor and Lee (2000).A study has been conducted on the attributes of the suggested class of estimators. Under ideal circumstances, the mean square error values for the suggested class of estimators have been determined. There have only been a few attempts to estimate population characteristics when there are different kinds of non-sampling errors present. The majority of the older research addresses the issue of measurement error or non-response. Singh, Bhattacharyya, and Bandyopadhyay (2020). The problem has been supported by an empirical study.

Let $x_i, (i = 1,2,....,N)$ indicate a supplementary feature that is associated with the study variable $y_i, (i = 1,2,....,N)$ the auxiliary variable's population mean is

$\bar{X} = \square x_i / N$. Let X_1 and $\bar{X}_2$ indicate the response and non-response groups' r population means. Let $\bar{x}_1 = \square x_i / n_2, \bar{x}_2 = \square x_i / n_2, \bar{x}_{2r} = \square x_i / r$ indicate the n_1 responding units' mean, n_2 non-responding units' mean, and $r = (n_2 / k)$ subsampled units in turn. In order to improve estimating approaches, we combined two key ideas in this paper: non-response and measurement error in the estimate process, and we also suggested a class of estimators.

Notation:

Let $\bar{x} = \frac{1}{n}\square_{i=1} x_i$, $\bar{y} = \frac{1}{n}\square_{i=1} y_i$, be the objective estimator of X and Y the population

$\frac{1}{n}$ $\frac{2}{1}$ $\frac{1}{n}$ $y_i - \bar{y})$ are not means, correspondingly, but $s_x^2 = n\,1\square = (x_i - \bar{x})$ and $s_y = \frac{}{n-1}\square_{i=1}$ (

$i\ 1$

impartial estimators of $(\square_x^2, \square_y^2)$, respectively. In the presence of measurement error, the predicted values of s_x^2 and s_y^2 are provided by,

$$E\,s(\ )_x^2 = \square\ \square_x^2 + {}_v^2$$

$$E(s\ )^2_y = +\square\ \square_y^2 \qquad {}_u^2$$

https://doi.org/10.62500/icrtsda.1.1.21

When the error variance $\square_v^2$ is known , the unbiased estimator of $\square_x^2$, is $\square\hat{}_x^2 = s_x^2 - \square_v^2 \square 0$, and when $\square_u^2$ is known, then the unbiased estimator of $\square_y^2$ is $\square\hat{}\, y2 = -sy2 \square u2 \square 0$.

$$E\,s(\,x^2{}_2) = \square\ \square_x{}^2{}_2 + {}_v{}^2{}_2$$
$$E\,s(\,y^2{}_2) = \square\ \square_y{}^2{}_2 + {}_u{}^2{}_2$$

Define

$$\overline{y} = \square_y \quad (1+e_0 \quad)$$

$$\overline{x} = \square_x (1+e_1)$$

Such that

$E\,e(\,{}_0) = E\,e(\,{}_1) = 0$ what's more, up to the primary level of estimate (when limited population remedy factor is disregarded

$$E\,e(\,0^2) = Cny2\ \square\ \square 1 + SSu2\ \square\ \square + W\,k2(n-1)\ Cy22\ \square\ \square\ \square 1 + \frac{SSuy2222}{2}\ \square\ \square\ \square\ \square$$

$$\square \quad y\ \square \qquad \square$$

$$C2\ \square \qquad S2\ \square\ W\,k($$

$$E\,e(\,12) = nx\ \square\ \square 1 + Svx2\ \square\ \square + 2\,n - 1)Cx22\ \square\ \square\ \square\ \square 1 + \frac{SSvx2222}{}\ \square\ \square\ \square\ \square$$

$$\frac{}{n} + \frac{}{n}$$

$$\bar{p}\ C\ Cyx\ y\ \bar{x}\ W\,k2(\,-1)\ pyx2C\ Cy2$$
$$x2\ E\ e\ e(\,0\ 1) =$$

$$Cy = S\ Y\ C/\,, \quad x = Sx\,/\,X\ C, y2 = Sy2\,/\bar{Y}\ C, x2 = Sx2\,/\,\bar{X}\ p, xy = Sxy\,/\,S\ Sx\ \ y$$

2. Adapted estimator

A ratio type estimator is provided by when both measurement error and nonresponse are present in order to estimate the population mean. (Singh and Sharma (2015)

$$\overline{y}^* - \qquad\qquad t_r = \overline{x}^* X$$

(1)

Expressing the estimator tr in terms of e's

$$t_r = Y\,(1+e_0)(\bar{1}+e_1)^{-1} \qquad (2)$$

https://doi.org/10.62500/icrtsda.1.1.21

Expanding equation (6) and simplifying,

(*t*$_r$ −*Y*)=*Y e*□□ 0 − −*e*$_1$ *e e*$_{0\ 1}$ +*e*$_1$^{2}□□ (3)

and taking expectation both sides of (3), the bias of estimator tr is

Bias t( )*r* =□ *nx* □1+□*Sv*22 □□+ *ASx*22 □□□1+□*Sxv*2222 □□□□−2□□□
1n p S Sxy x y + *Apxy*2*S Sx*2 *y*2 □□□□□□□ □*S* 2
□
□□ □ *x* □ □

Squaring both sides of (3),

(*tr* −□*y*2)2 =*Y* 2 □□*e*02 +*e*12 −2*e e*0 1□□ (4)

Taking expectations of (4) and using notations, we get the MSE of estimator tr as

MSE(tr) = *n*□*Sy*2□□1+□*Suy*22 □□□□+*Sx*2 □□□1+□*Sxv*22 □□□−2*p S Sxy x y* □□□□+*A*
S□□□□□ *y*22 □□□□□1+□*Suy*2222 □□□□+*Sx*22 □□□□1+□*Sxv*2222 □□□□−2*p*
*S Sxy*2 *x*2 *y*2 □□□□ 1 □ □
□□ □

□*Sy*2 □ □2 □ □ □2 □

MSE(tr) =□□□□□1+ *Suy*2 □□□+*ASy*22 □□□1+ *Suy*222 □□□+ *Snx*2 □□□1+□*Sxv*22
□□□+*ASx*22 □□□□1+□*Sxv*2222 □□□□−2□□□ 1*np S S Ap S Sxy x y* + *xy*2*x*2 *y*2
□□□□□□□

n □

= + −*M N O*2

Where,

− −− −− *M* =□□□1*n* *S$_y$*^{2} □□□1+□*Su*22 □□□ *ASy*22
□□□1+□*Suy*2222 □□□□□□□□□□
+
□□ □ *y* □ □

− −− −− *N* =□□□1*n* 2 □1+□*Sv*22 □□+ *ASx*22
□□□1+□*Sxv*2222 □□□□□□□□□□
Sx □
□□ □ *x* □ □

O =□□1 *p S Sxy x y* + *Apxy*2*S Sx*2 *y*2 □□ □*n* □

https://doi.org/10.62500/icrtsda.1.1.21

A regression estimator is described as (Singh and Sharma (2015)

$$t_{lr} = \bar{y}^{*} + b\,X(\bar{x} - \bar{x}^{*}) \qquad (5)$$

Expressing the estimator tr in terms of e's,

$$t_{lr} = Y(1+e_0) - bXe_1$$

and expanding equation (5) and simplifying

$$(t_{lr} - Y) = (Ye_0 - bXe_1) \qquad (6)$$

Squaring both sides of (6) and after simplification,

$$(t_{lr} - Y)^2 = \square\square Y^2 e_0^2 + b^2 X^2 e_1^2 - 2bXYe_0 e_1 \square\square \qquad (7)$$

Taking expectations both sides of (7) the MSE of estimator tlr is obtained as

$$MSE\,t(_{lr}) = +M\,b\,R\,N^{2\,2} - 2bRO$$ (8) The optimum value

of b is obtained by minimizing (8) and is given by

$$b^{*} = R\,N^{1\,\square\,\square}{}_{\square}{}_{\square\square\square}{}^{O} \qquad (9)$$

Substituting the optimal value of b in equation (9), the minimum MSE of the estimator t_{lr} is obtained as

$$MSE\,t(_{lr})_{\min} = M\,\square\square 1 - \frac{\square\quad O^2\,\square}{MN}\square\square \qquad (10)$$

Substituting the optimal value of b in equation (10), the minimum MSE of the estimator t_{lr} is obtained as

$$MSE\,t(\,lr\,) = \frac{1}{n}\,Sy2\,\square\square 1 - pxy2\square\square + W k2(n-1)\square\square Sy22 + b\,S2x22 \quad -2bpxy2S \quad Sx2\;y2\,\square\square \qquad (11)$$

The ratio estimator t_p is obtained as(Singh and Sharma (2015)

$$t_p = m_1\bar{y}^{*} + m_2\,\bar{x}\bar{y}^{*}\,\bar{X} \qquad (12)$$

$t_1 = \bar{y}^{*}$(usual unbiased estimator) and for $(m\ m_1, \quad _2) = (0,1)$ $t_2 = \bar{x}\bar{y}^{*}\,\bar{X}$ (usual ratio

estimator). The estimators are generalized version of usual unbiased estimator and ratio estimator.

https://doi.org/10.62500/icrtsda.1.1.21

Expressing the estimator t_p in terms of e's

$$t_p = mY_1(1+e_0)+m\ Y_2(1+e_0)(1+e_1)^{-1} \quad (13)$$

Expanding equation (13) and simplifying,

$$(t_p - Y) = Y e_0 + m_2(- + e_1 \quad e_1^2 - e\ e_0 1) \quad (14)$$

Squaring both sides of (14) and after simplification,

$$(tp - Y)2 = Y2 \ e02 + m\ e2\ 12\ 2 - 2m\ e\ e2\ 0\ 1 \quad (15)$$

Taking expectations of (15) and using notations, the MSE of estimator tr is obtained as

$$MSE\ t(_p) = M + m\ R\ N_2{}^2 - 2m\ RO_2 \quad (16)$$ The optimum

value of m2 is obtained by minimizing (16), given by

$$m_2^* = {}^1n\ N \quad O \quad (17)$$

And $m_1^* = -1\ m_2^*$

Substituting the optimal value of m2 in equation (17) the minimum MSE of the estimator t_p is obtained a

$$MSE\ t(_p)_{\min} = M\ 1 - \frac{O^2}{MN} \quad (18)$$

Proposed class of estimator

A proposed class of estimators given by,

$$t_{pr} = m_1 y^* + m_2(X - x^*)\ X_*$$

$t_1 = y^*$ (usual unbiased estimator) and for $(m\ m_1, \quad _2) = (0,1)\ t_2 = x^* X$ (usual ratio

estimator).As a result, the suggested class of estimators is a generalized form of the standard ratio and unbiased estimator.

$$t_{pr} = mY_1(1+e_0)+m_2(X - X(1+e_0))\ \frac{X}{X(1+e1)} \quad (19)$$

Expanding equation (19) and simplifying,

$$t_{pr} = mY_1(1+ + e_0)\ m_2(X - - X \quad Xe_1)(1+e_1)^{-1} \quad (20)$$

$$(t_{pr} - Y) = Ye_0 - m\ Xe_2 \quad _1 + m\ Xe_2 \quad _1{}^2 \quad (21)$$

https://doi.org/10.62500/icrtsda.1.1.21

Squaring both sides of (21) and after simplification,

$$(t_{pr} - \bar{Y})^2 = (\bar{Y}e_0 - m\bar{X}e_2 \; _1)^2 \qquad (22)$$

Taking expectations of (22) and using notations, the MSE of estimator tr is obtained as

$$MSE\ t(_{pr}) = +M\ m\ N_2^2 - 2m\ O_2 \qquad (23)$$

The optimum value of m2 is obtained by minimizing (24), given by

$$m_2^* = {}^1 n\ N \ldots O \qquad (24)$$

3. A second proposed exponential estimator is described as

$$t_{pr1} = m_1\bar{y}^* + m\ e_2 \ldots \bar{y}^* \ldots \bar{X} \qquad (25)$$

$(m\ m_1, _2) = (0,1)$ $t_2 = \bar{x}^* \bar{y}^* \bar{X}$ (usual ratio estimator) $t_p = m_1\bar{y}^* + m_2 \frac{\bar{y}^*}{\bar{x}^*}\bar{X}$. As a result, the suggested class of estimators is a generalized form of the standard ratio estimators.

$$t_{pr1} = m\bar{Y}_1(1+e_0) + m\ e_2 \ldots \bar{Y}(1+e_0) \ldots \bar{X}(1+e1) - \bar{X} \ldots \qquad (26)$$

Expanding equation (26) and simplifying,

$$t_{pr1} = m\bar{Y}_1(1+e_0)\ m\ e_2 \ldots -\bar{Y}(1+e0)(1+e1)^{-1} \ldots \qquad (27)$$

$$t_{pr1} = m\bar{Y}_1\ (1+\ +e_0\ )\ m\ e_2 \ldots -\bar{Y}(1+e0)(1-\ +\ +e1\ \ 1e2\ \ldots \qquad (28)$$

$$= m\bar{Y}_1(1+e_0) + m_2 \left[1 + \frac{(-\bar{Y} + \bar{Y}e_1 - \bar{Y}e_1^2 - \bar{Y}e_0 + \bar{Y}e_0e_1)}{1!} + \frac{(-\bar{Y} + \bar{Y}e_1 - \bar{Y}e_1^2 - \bar{Y}e_0 + \bar{Y}e_0e_1)^2}{2!} + \ldots\right] \qquad (29)$$

$(tpr1 - \bar{Y}) = \bar{Y}e0 + m2 \ldots 1 - + \bar{Y}\ \bar{Y}e1 - \bar{Y}e12 - \bar{Y}e0 + \bar{Y}e\ e0\ 1 + 1n(\bar{Y}\ 2 + \bar{Y}\ e2\ 21 - \bar{Y}\ e2\ 41 - \bar{Y}e02 + \bar{Y}e\ e0\ 12\ 2\ ) \ldots$ (30)

Squaring both sides of (30) and after simplification,

$$(t_{pr1} - \bar{Y})^2 = (\bar{Y}e_1 - \bar{Y}e_0 + \bar{Y}e\ e_{0\ 1})^2 \qquad (31)$$

Taking expectations of (31) and using notations, the MSE of estimator tr is obtained as

$$MSE\ t(_{pr1}) = R\ N^2 + -M2RO \qquad (32)$$

https://doi.org/10.62500/icrtsda.1.1.21

The optimum value of m2 is obtained by minimizing (32), given by

$$m_2^* = {}^1n\ N \qquad (33)$$

Empirical Study

The empirical study's data came from Sangeetha and Gujarati (2007)

Where,

Table 1. Value of parameter

N	$\square_y$	$\square_x$	S_y	S_x	p	$\square_u 2$	$\square_v 2$
100	17.798428	26.630242	2.303259	93.962473	96.70980	1.913428	96.709801
$\square y2$	$\square x2$	$Sy2$	$Sx2$	R	W_2		
17.848960	28.732580	1.355194	102.35153	0.6901332	0.5		

Table 2. displaying the bias and mean square error (MSE)

Estimators	**MSE**	PRE_1	PRE_2	PRE_3	PRE_4	PRE_5
t_r	790.70243176	100	99.89	107.02	90.38	90.09
t_{lr}	798.902366431	98.97	100	107.13	90.47	89.16
t_p	846.23474809	93.43	93.34	100	84.45	84.18
t_{pr}	714.6819	110.63	110.52	118.40	100	99.67
$tpr1$	712.366409557	111	110.88	118.79	100.32	100

4. Conclusion

A class of estimators for the population mean of the research variable y was put forth. With the assumption that non-response and measurement error are present in both the study and auxiliary variables, the estimators employ auxiliary information to increase efficiency. Furthermore, it is discovered that some wellknown population mean estimators, including ratio estimator, normal regression, and ratio exponential type for population mean, belong to the suggested class of estimators. The MSEs of the suggested class of estimators were acquired in the simultaneous presence of response error and non-response up to the first order of approximation. The suggested class of estimators has the benefit that the members of the proposed class of estimators can be readily identified by their properties readily acquired from the suggested class of estimators' features.

References

Tracy, D. S., & Osahan, S. S. (1994). Random non-response on study variable versus on study as well as auxiliary variables. *Statistics*, *54*(2), 163-168.

Hansen, M. H., & Hurwitz, W. N. (1946). The problem of non-response in sample surveys. *Journal of the American Statistical Association*, *41*(236), 517529.

Kumar, M. (2011). Some Ratio Type Estimators under Measurement Errors'

https://doi.org/10.62500/icrtsda.1.1.21

Mukesh Kumar;'Rajesh Singh,"Ashish K. Singh and" Florentin Smarandache" Department of Statistics, Banaras Hindu University (UP), India "College of Management Studies, Raj Kumar Goel Institute of Technology, India" Department of Mathematics, University of New Mexico, Gallup, USA. *World Applied Sciences Journal*, *14*(2), 272-276.

Singh, H. P., & Karpe, N. (2010). Estimation of mean, ratio and product using auxiliary information in the presence of measurement errors in sample surveys. *Journal of Statistical Theory and Practice*, *4*, 111-136.

Shukla, D., Pathak, S., & Thakur, N. S. (2012). An estimator for mean estimation in presence of measurement error. *Research and Reviews: A Journal of Statistics*, *1*(1), 1-8.

Allen, J., Singh, H. P., & Smarandache, F. (2003). A family of estimators of population mean using multiauxiliary information in presence of measurement errors. *International Journal of Social Economics*, *30*(7), 837-848.

Khare, B. B., Pandey, S. K., & Srivastava, U. (2011). An improved class of twophase sampling estimators for population mean using auxiliary character in presence of non response. *Journal of Scientific Research*, *55*, 151-161.

Singh, H. P., & Tracy, D. S. (2001). Estimation of population mean in presence of random non-response in sample surveys. *Statistics*, *61*(2), 231-248.

Singh, R. S., & Sharma, P. (2015). Method of estimation in the presence of nonresponse and measurement errors simultaneously. *Journal of Modern Applied Statistical Methods*, *14*, 107-121.

Singh, G. N., Bhattacharyya, D., & Bandyopadhyay, A. (2020). Formulation of logarithmic type estimators to estimate population mean in successive sampling in presence of random non response and measurement errors. *Communications in Statistics-Simulation and Computation*, *51*(3), 901-923.

Sabir, S., Sanaullah, A., & Gupta, S. (2022). Estimation of mean considering the joint influence of measurement errors and non-response in two-phase sampling designs. *Journal of the National Science Foundation of Sri Lanka*, *50*(1).

Khare, B. B., & Srivastava, S. (1997). Transformed ratio type estimators for the population mean in the presence of nonresponse. Communications in Statistics - Theory and Methods, 26(7), 1779-1791.

Singh, H. P. and Karpe, N. (2009). A class of estimators using auxiliary information for estimating finite population variance in presence of measurement errors. Communication in Statistics - Theory and Methods, 38(5)

Wiley, D. E., & Wiley, J. A. (1970). The estimation of measurement error in panel data. *American Sociological Review*, *35*(1), 112-117.

Stefanski, L. A. (1985). The effects of measurement error on parameter estimation. *Biometrika*, *72*(3), 583-592.

Ferrari, P., Friedenreich, C., & Matthews, C. E. (2007). The role of measurement error in estimating levels of physical activity. *American journal of epidemiology*, *166*(7), 832-840.

Tiwari, K. K., Bhougal, S., Kumar, S., & Rather, K. U. I. (2022). Using randomized response to estimate the population mean of a sensitive variable under the influence of measurement error. *Journal of Statistical Theory and Practice*, *16*(2), 28.

Sevilimedu, V., & Yu, L. (2022). Simulation extrapolation method for measurement error: A review. *Statistical methods in medical research*, *31*(8), 1617-1636.

https://doi.org/10.62500/icrtsda.1.1.21

Stefanski, L. A. (1985). The effects of measurement error on parameter estimation. *Biometrika*, *72*(3), 583-592.

Liang, H., & Wu, H. (2008). Parameter estimation for differential equation models using a framework of measurement error in regression models. *Journal of the American Statistical Association*, *103*(484), 1570-1583.

Li, T., & Vuong, Q. (1998). Nonparametric estimation of the measurement error model using multiple indicators. *Journal of Multivariate Analysis*, *65*(2), 139165.

Blalock, H. M. (1970). Estimating measurement error using multiple indicators and several points in time. *American Sociological Review*, *35*(1), 101-111.

https://doi.org/10.62500/icrtsda.1.1.22

Proc. 1st International Conference on Recent Trends in Statistics and Data Analytics
Air University Islamabad, Pakistan – May 9, 2024, Vol. 1, pp. 192-197

Emotional States, Self-Management and Life-Styale among Type-I and Type-II Diabetics: A comparative Study

[1]Muqadas and [2]Dr. Amir Raza
[1,2]Department of Statistics, GC Women University Sialkot

Abstract

There has been a continuous increase in the prevalence of prediabetes and diabetes in Pakistan. The main factors include growing age, family history, and hypertension. This study details the perceived obstacles and practical approaches for type 1 and type 2 diabetes self-management among persons living in Sialkot. The data is collected using a questionnaire and a survey among the students in the Govt. College Women University, Sialkot. We have analyzed the data using descriptive and inferential statistical (Chi-Square and logistic regression) techniques to sort out the main reasons for diabetics and to determine the best ways to take care of ourselves after developing diabetes, i.e., how to control blood sugar levels, how to change our lifestyles, and to determine the proportion of people with type 1 and type 2 diabetes in order to improve general health and manage the disease. In order to better control blood sugar levels and avoid complications, this entails giving people the tools they need to recognize and manage the emotional effects of diabetes, as well as adopting good lifestyle practices, including regular exercise, a balanced diet, and stress management.

Keywords: Self-Management, Emotional-States, life-style, Descriptive Statistics & Inferential Statistics.

1. INTRODUCTION

Diabetes mellitus,a chronic metabolic disorder characterized by elevated blood glucose levels, imposes significant challenges on individuals' emotional well-being, self-management practices, and lifestyle choices. With the global prevalence of diabetes escalating rapidly, understanding the nuanced differences in these factors between Type-I and Type-II diabetes becomes imperative for tailored intervention strategies and improved patient outcomes.

In this comparative study, we delve into the nuanced differences and similarities in emotional states, self-management behaviors, and lifestyle factors among individuals with type 1 and type 2 diabetes. By examining these aspects comprehensively, we aim to shed light on the unique challenges each group faces and identify potential avenues for tailored interventions to enhance diabetes care and overall quality of life. Through a deeper understanding of the psychological and behavioral dimensions of diabetes management, we aspire to contribute to the development of more effective strategies for supporting individuals living with diabetes.

The diabetic's ability to self-manage their disease is essential to reaching optimal lycemic levels. Individuals with diabetes may need to restrict their intake of carbohydrates through food choices, modify their eating habits to incorporate healthy fats, glycemic load, and nutrition, control their blood sugar levels with the help of glucose-lowering medications, check their blood sugar levels with blood tests or sensors, get enough exercise to improve their glycemia, control their weight, or maintain good health, and plan their activities around current glucose levels and insulin requirements . Additional daily diabetes activities include assessing the meal's carbohydrate content, modifying insulin doses, and reducing increased glucose levels when rapid acting insulin is used to cover glucose spikes after meals.

Acute metabolic complications such as severe hypoglycemia or severe hyperglycemia, which increase the risk of ketoacidosis or hyperosmolar coma, are linked to suboptimal glycemic management. Persistent or recurrent hyperglycemia also raises the risk of developing serious long-term complications such as diabetic retinopathy, neuropathy, nephropathy, and foot syndrome. Consequently, it is essential

https://doi.org/10.62500/icrtsda.1.1.22

to develop and maintain effective self-behaviors to achieve favorable glycemic outcomes in order to preserve good health and avoid complications and morbidity. Evidence, however, suggests that individuals with diabetes can frequently improve their overall performance and self-management techniques this may be especially true for those who also have co-occurring mental illnesses like depression or diabetes-specific discomfort

Given that self-management is the primary factor determining how well a person with diabetes manages their condition, normal clinical practice may benefit from reflecting on and tracking relevant behaviors in individuals to identify areas for potential improvement and provide appropriate education and support.

Those with diabetes whose outcomes are persistently suboptimal may find it especially important to assess and evaluate dishete seir practices. Measuring self-handling may also be necessary for the treatment of diabetes, particularly in cases where mental variables—such as those that exacerbate the disease or obstruct the best possible care—need to be examined or the results of interventions—such as diabetes self-management education—need to be assessed. Therefore, appropriate measuring instruments are needed

Many different tools have been developed for diabetes self-management, according to several systematic reviews of the literature. However, the majority of these instruments have only been used in a limited number of studies, and the testing of measurement properties was frequently conducted on a small number of scales, with only a small number of these scales meeting rigorous appraisal criteria .These issues can make it more difficult to use the current tools for practice and research

2. METHODS

In this study, we employed both chi-square analysis and descriptive statistics crosstab analysis to compare emotional states, self-management, and lifestyle among Type-I and Type-II diabetics. Firstly, chi-square analysis was conducted to examine the association between categorical variables, such as emotional states and diabetes type. Additionally, descriptive statistics crosstab analysis was utilized to provide a detailed comparison of various factors, including self-management emotional states and lifestyle choices, between Type-I and Type-II diabetics.

3. RESULTS AND DISCUSSION

H_0:Is diet plan and wound healing are not associated

H_1: Is diet plan and wound healing are associated

TABLE-1

	Value	Df	Asymp. Sig. (2-sided)
Pearson Chi-Square	22.146[a]	6	.001
Likelihood Ratio	14.697	6	.023
Linear-by-Linear Association	7.924	1	.005
N of Valid Cases	300		

a. 5 cells (41.7%) have expected count less than 5. The minimum expected count is .07.

https://doi.org/10.62500/icrtsda.1.1.22

Conclusion: As the calculated of chi square= 22.146 is significant as the aceptive P value is .001 which less than 0.05 so we can not accepted H0 therefore diet plan and wound healing are significant associated

TABLE-2

Hypothesis

H_0: Is blood sugar and self compassion are not associated

H_1: Is blood sugar and self compassion are associated

Conclusion: As the calculated of chi square =4.826 is insignificant as the exceptive p-value is .306 which greater than 0.05 so we not accepted H_O therefore blood sugar and self compassion are not significant associated

TABLE-3

	Value	df	Asymp. Sig. (2-sided)
Pearson Chi-Square	4.826[a]	4	.306
Likelihood Ratio	4.881	4	.300
Linear-by-Linear Association	.000	1	.982
N of Valid Cases	300		

a. 2 cells (22.2%) have expected count less than 5. The minimu expected count is 3.04.

Chi-Square Tests

	Value	df	Asymp. Sig. (2-sided)
Pearson Chi-Square	16.463[a]	4	.002
Likelihood Ratio	17.163	4	.002
Linear-by-Linear Association	1.079	1	.299
N of Valid Cases	300		

a. 0 cells (0.0%) have expected count less than 5. The minimum expected count is 6.08.

Hypothesis

H_0: Is blood sugar and physical activity are not associated

H_1:Is blood sugar and physical activity are associated

Conclusion: As the calculated of chi square=16.463 is significant as the exceptive p value is .002 which less than 0.05 so we can not accepted H_0 therefore blood sugar and physical activity are significant

Discriptive statistics:

https://doi.org/10.62500/icrtsda.1.1.22

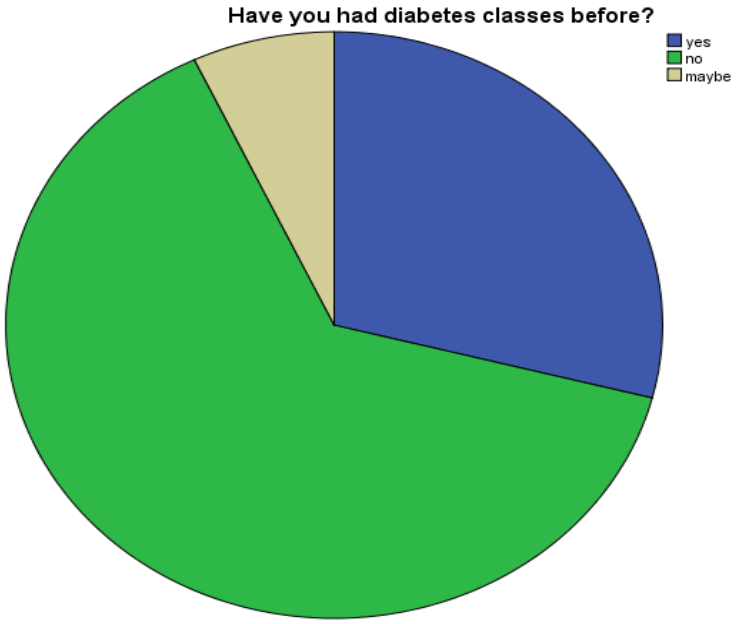

Based on the pie chart results, it seems that a majority, 64%, have not attended diabetes classes. 29% have attended them, and 7% are uncertain if they have or not.

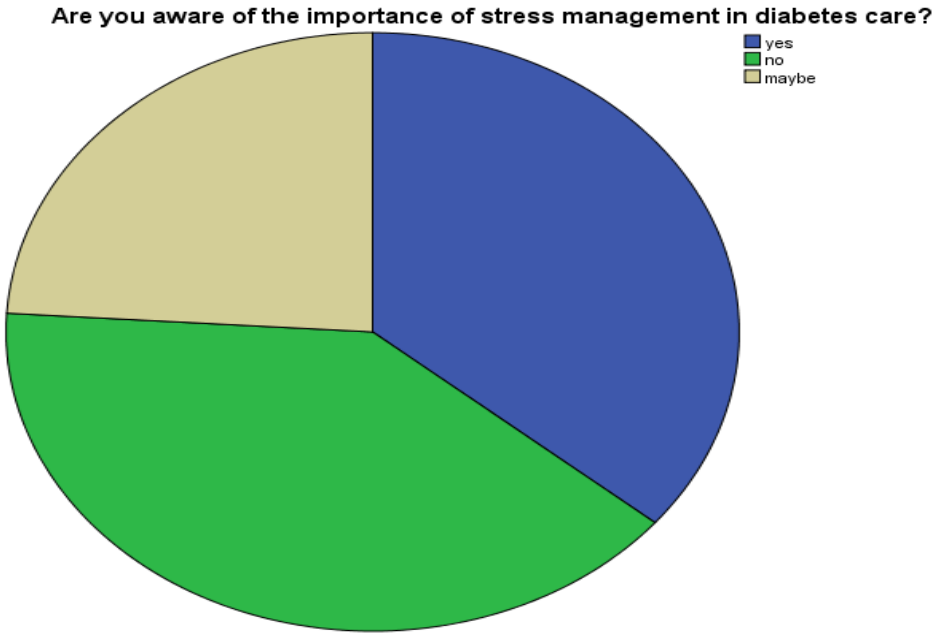

Based on the pie chart results, it seems that 40% are not aware, 36% are aware, and 24% are uncertain about the importance of stress management in diabetes care.

https://doi.org/10.62500/icrtsda.1.1.22

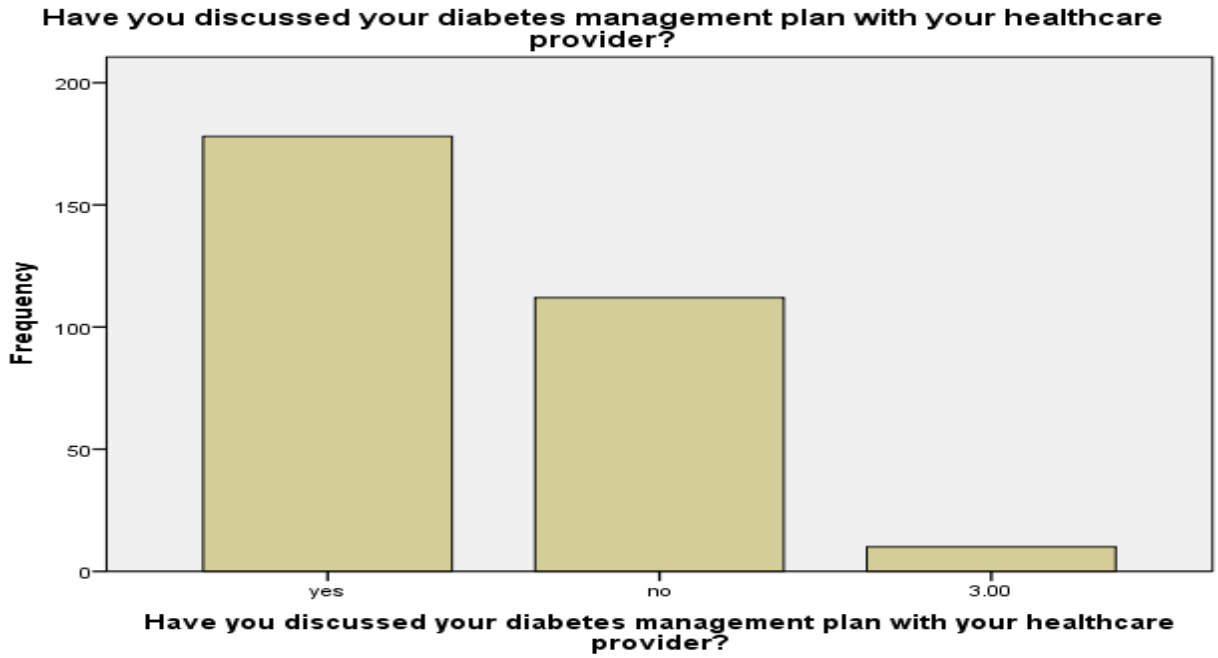

Explanation: The majority of respondents have discussed their diabetes management plan with their healthcare provider, as indicated by the higher frequency in the "yes" category compared to "no" and "maybe" categories in the bar chart.

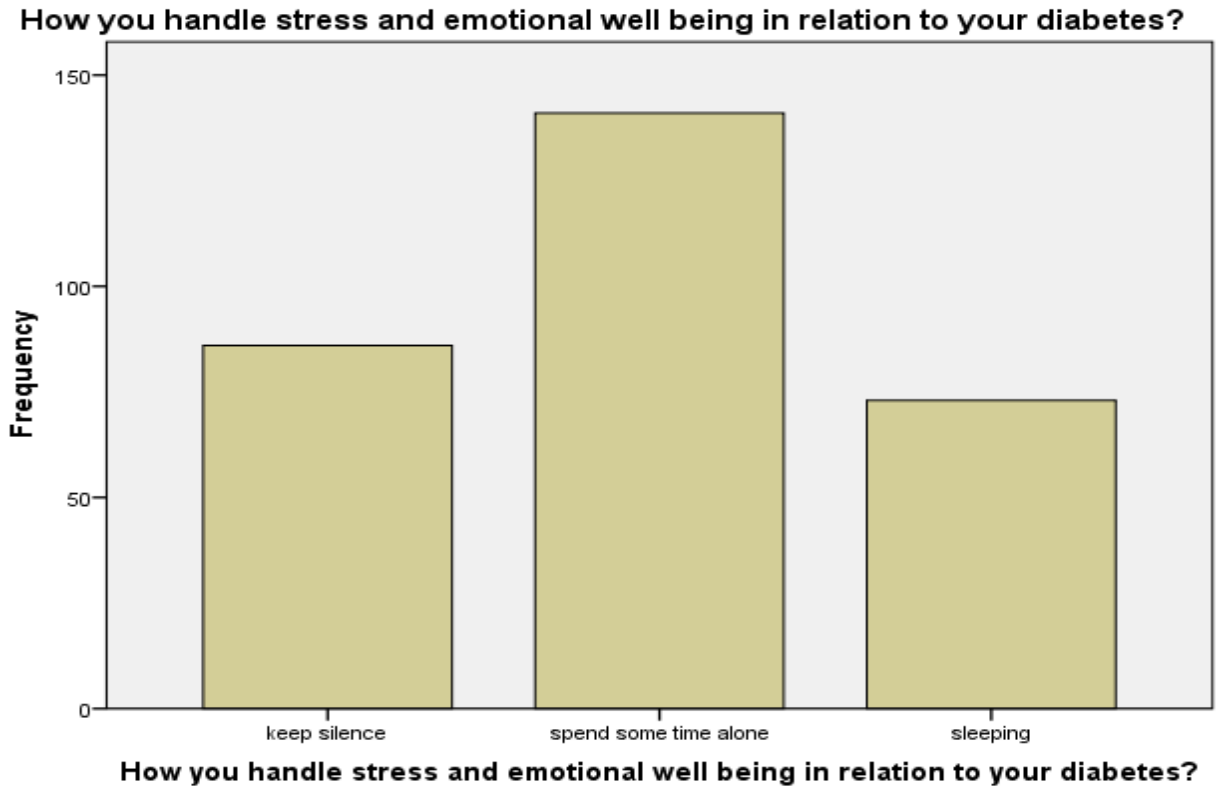

Explanation: Among the provided coping mechanisms, spending some time alone is the most common approach, followed by keeping silence and then sleeping, as indicated by the frequencies in the bar chart.

https://doi.org/10.62500/icrtsda.1.1.22

REFERENCES

1. Ruggiero, L., Glasgow, R., Dryfoos, J. M., Rossi, J. S., Prochaska, J. O., Orleans, C. T., … & Johnson, S. (1997). Diabetes self-management: self-reported recommendations and patterns in a large population. Diabetes care, 20(4), 568-576.
2. Shigaki, C., Kruse, R. L., Mehr, D., Sheldon, K. M., Ge, B., Moore, C., & Lemaster, J. (2010). Motivation and diabetes self-management. Chronic illness, 6(3), 202-214.
3. Norris, S. L., Nichols, P. J., Caspersen, C. J., Glasgow, R. E., Engelgau, M. M., Jack Jr, L., … & Task Force on Community Preventive Services. (2002). Increasing diabetes self-management education in community settings: a systematic review. American journal of preventive medicine, 22(4), 39-66.

https://doi.org/10.62500/icrtsda.1.1.23

Proc. 1st International Conference on Recent Trends in Statistics and Data Analytics
Air University Islamabad, Pakistan – May 9, 2024, Vol. 1, pp. 198-207

AN IMPROVED ESTIMATOR OF THE POPULATION VARIANCE UNDER A LINEAR SCRAMBLING MODEL

Muhammad Azeem[*1]
[1]Department of Statistics, University of Malakand, Khyber Pakhtunkhwa, Pakistan

ABSTRACT

In many sample surveys, researchers deal with estimating the parameters of a sensitive-type variable. In past few years, variance estimation of a sensitive variable has remained a topic of interest among survey researchers. Utilizing auxiliary information, this study suggests a novel estimator of the population variance by utilizing a linear scrambling model. The mean square error of the new suggested estimator has been obtained under the linear scrambling model. Further, the new variance estimator has been compared with some of the available competitor estimators using different evaluation measures. The findings suggest that the new variance estimator performs more efficiently than the available estimators. This makes the new estimator preferable for real-world survey applications.

Keywords: Auxiliary variable, efficiency, model evaluation, scrambling variable, variance estimator.

1. INTRODUCTION

In data collection on sensitive issues, the use of scrambled responses is an effective method commonly employed by survey researchers. Since the development of a basic additive and multiplicative scrambling models in the studies of Warner (1971) and Eichhorn and Hayre (1983), many research studies have presented efficient scrambling models over the past few decades. Gupta et al. (2002) suggested a scrambling technique which accommodates those survey respondents who perceive the question being asked as non-sensitive. Such respondents are generally willing to report their true response irrespective of the sensitivity of the question. Another additive scrambling technique was introduced in a research study by Diana and Perri (2011).

In order to evaluate the degree of privacy in quantitative models, Yan et al. (2008) suggested a novel evaluation metric which was later improved by Gupta et al. (2018) and Azeem (2023). The studies of Gjestvang and Singh (2009), and Narjis and Shabbir (2023) presented efficient optional scrambling models. In a recent study, Azeem and Salam (2023) utilized direct responses and scrambled responses to develop an efficient weighted mean of the two types of responses.

Originated from the study of Cochran (1940), auxiliary variables have been found very important in many research studies for enhancing the efficiency of estimates of population parameters. Das and Tripathi (1978) and Isaki (1983) suggested estimators of the population variance which utilized auxiliary information. These early studies presented estimators for non-sensitive variables only. In order to deal with sensitive variables in variance estimation, the recent studies of Gupta et al. (2020), Saleem et al. (2023), Kumar et al. (2023), and Azeem et al. (2024) suggested improved estimators of population variance.

The current paper introduces a novel estimator of the variance under the linear scrambling model of Diana and Perri (2011). Assuming the variable of interest being sensitive, the proposed estimator uses a single auxiliary variable to estimate the population variance. Using model evaluation metrics, our analysis suggests that the new proposed variance estimator performs better than the previous estimators.

https://doi.org/10.62500/icrtsda.1.1.23

2. NOTATIONS

Suppose the population under consideration has N units identified as $U_1, U_2, ..., U_N$ and let us denote the sample size by n. Further, the main sensitive variable of interest and the auxiliary variable, respectively, be denoted by Y and X. Let (x_i, y_i) represent the ith population unit for the pair of variables. Let $(\bar{x}, \bar{y})$ and $(\bar{X}, \bar{Y})$ denote, respectively, the sample and population means of (X, Y). Further, we use the notation (s_x^2, s_y^2) and (σ_x^2, σ_y^2), respectively, for the sample and population variance of (X, Y). For some positive integers, say 'r' and 's', the moment ratio can be expressed as:

$$\lambda_{rs} = \frac{\mu_{rs}}{\mu_{20}^{\frac{r}{2}} \mu_{02}^{\frac{s}{2}}}, \tag{1}$$

where

$$\mu_{rs} = \frac{1}{N-1} \sum (x_i - \bar{X})^s (y_i - \bar{Y})^r . \tag{2}$$

3. LINEAR SCRAMBLING MODEL AND AVAILABLE ESTIMATORS

Diana and Perri (2011) have developed a linear scrambling model for privacy protection which can be written as:

$$Z = TY + S, \tag{3}$$

where Z denotes the scrambled response, and T and S are scrambling variables, satisfying $E(S) = 0$, and $E(T) = 1$.

Using the model given in equation (3), the variance of Z is given as:

$$\sigma_z^2 = \sigma_T^2 \sigma_y^2 + \sigma_T^2 \mu_y^2 + \sigma_y^2 + \sigma_S^2 .$$

Solving for σ_y^2 yields:

$$\sigma_y^2 = \frac{\sigma_z^2 - \sigma_S^2 - \sigma_T^2 \bar{Z}^2}{\sigma_T^2 + 1} . \tag{4}$$

The scrambled response form of the basic estimator t_0 can be obtained by interchanging σ_z^2 and $\bar{Z}^2$ by s_z^2 and $\bar{z}^2$, respectively, to obtain:

$$t_0(R) = \frac{s_z^2 - \sigma_S^2 - \sigma_T^2 \bar{z}^2}{\sigma_T^2 + 1} . \tag{5}$$

The variance estimator of Isaki (1983) is given as:

$$t_1 = s_y^2 \left(\frac{\sigma_x^2}{s_x^2} \right). \tag{6}$$

https://doi.org/10.62500/icrtsda.1.1.23

The algebraic expressions for bias and the mean square error may be written as:

$$Bias\left(t_1\right)=\theta\sigma_y^2\left(\lambda_{04}-\lambda_{22}\right), \tag{7}$$

and

$$MSE\left(t_1\right)=\theta\sigma_y^4\left(\lambda_{40}+\lambda_{04}-2\lambda_{22}\right). \tag{8}$$

The Isaki's (1983) estimator using the linear model may be written as:

$$t_1\left(R\right)=\frac{s_z^2-\sigma_S^2-\sigma_T^2\bar{Z}^2}{\sigma_T^2+1}\left(\frac{\sigma_x^2}{s_x^2}\right). \tag{9}$$

The mathematical form of the bias of $t_1\left(R\right)$ may be obtained in the form:

$$Bias\left(t_1\left(R\right)\right)=\theta\left[\frac{2\sigma_T^2\bar{Z}^2\lambda_{12}C_z-\sigma_z^2\left(\lambda_{22}-1\right)-\sigma_T^2\bar{Z}^2C_z^2}{\sigma_T^2+1}\right], \tag{10}$$

where

$$C_z^2=C_y^2\sigma_T^2+\frac{\sigma_S^2}{\bar{Y}^2}.$$

The mean squared error of $t_1\left(R\right)$ may be expressed as:

$$MSE\left(t_1\left(R\right)\right)=\frac{\theta}{\left(\sigma_T^2+1\right)^2}\Big[\sigma_z^4\left(\lambda_{40}-1\right)-2\sigma_z^2\sigma_y^2\left(\sigma_T^2+1\right)\left(\lambda_{22}-1\right)+\sigma_y^4\left(\sigma_T^2+1\right)^2\left(\lambda_{04}-1\right)$$

$$+4C_z\left(\sigma_T^4\bar{Z}^4C_z-\sigma_z^2\sigma_T^2\bar{Z}^2\lambda_{30}+\sigma_T^2\sigma_y^2\bar{Z}^2\lambda_{12}\left(\sigma_T^2+1\right)\right)\Big]. \tag{11}$$

Gupta et al. (2020) developed a novel variance estimator which can be expressed as:

$$t_2\left(R\right)=\left[\left(\left(\frac{s_z^2-\sigma_S^2-\sigma_T^2\bar{Z}^2}{\sigma_T^2+1}\right)+\left(\sigma_x^2-s_x^2\right)\right)\left(\frac{\alpha\sigma_x^2+\beta}{w\left(\alpha\sigma_x^2+\beta\right)+\left(1-w\right)\left(\alpha\sigma_x^2+\beta\right)}\right)^g\right]. \tag{12}$$

It can be noted that the estimator given in equation (12) involves a few predetermined constants *g*, *w*, α, and β.

https://doi.org/10.62500/icrtsda.1.1.23

The mathematical form of the bias of $t_2(R)$ may be obtained as:

$$Bias\left(t_2(R)\right)=\frac{-\theta\sigma_T^2\bar{Z}^2}{\sigma_T^2+1}C_z^2-\frac{\alpha g w\theta\sigma_x^2}{\alpha\sigma_x^2+\beta}\left[\frac{\sigma_z^2\left(\lambda_{22}-1\right)-2\sigma_T^2\bar{Z}^2\lambda_{12}C_z}{\sigma_T^2+1}-\sigma_x^2\left(\lambda_{04}-1\right)\right]. \quad (13)$$

The optimum expression for MSE may be written in the form:

$$MSE\left(t_2(R)\right)_{opt}=\frac{\theta}{\left(\sigma_T^2+1\right)^2}\left[\left(\sigma_z^4\left(\lambda_{40}-1\right)+4\sigma_T^4\bar{Z}^4C_z^2-4\sigma_z^2\sigma_T^2\bar{Z}^2\lambda_{30}C_z\right)\right.$$

$$\left.-\frac{1}{\left(\lambda_{04}-1\right)}\left(\sigma_z^2\left(\lambda_{22}-1\right)-2\sigma_T^2\bar{Z}^2\lambda_{12}C_z\right)^2\right]. \quad (14)$$

4. PROPOSED VARIANCE ESTIMATOR AND ITS PROPERTIES

The proposed estimator can be formulated as:

$$t_p=\left\{s_y^2+\left(\sigma_x^2-s_x^2\right)\right\}\frac{s_x^{*2}}{\sigma_x^2}\exp\left(\frac{\sigma_x^2-s_x^2}{\sigma_x^2+s_x^2}\right), \quad (15)$$

where

$$s_x^{*2}=\frac{\left(N-1\right)\sigma_x^2-\left(n-1\right)s_x^2}{N-n}. \quad (16)$$

Theorem 1: The bias of the suggested variance estimator may be expressed as:

$$Bias\left(t_p(R)\right)\approx\frac{\theta}{2\left(\sigma_T^2+1\right)}\left[2\sigma_T^2\bar{Z}^2C_z^2-2A\sigma_z^2\left(\lambda_{22}-1\right)+4A\sigma_T^2\bar{Z}^2\lambda_{12}C_z+AB\left(\lambda_{04}-1\right)\right], \quad (17)$$

where

$$A=D+\frac{1}{2}, \quad (18)$$

$$D=\frac{n-1}{N-n}, \quad (19)$$

and

$$B=2\sigma_x^2\left(\sigma_T^2+1\right)+\sigma_z^2-\sigma_T^2\bar{Z}^2-\sigma_S^2, \quad (20)$$

https://doi.org/10.62500/icrtsda.1.1.23

Proof: We use the notations:

$$s_z^2 = \sigma_z^2\left(1+d_z\right),\ s_x^2 = \sigma_x^2\left(1+d_x\right), \text{ and } \bar{z} = \bar{Z}\left(1+e_z\right),$$

so that

$$d_z = \frac{s_z^2-\sigma_z^2}{\sigma_z^2},\ d_x = \frac{s_x^2-\sigma_x^2}{\sigma_x^2}, \text{ and } e_z = \frac{\bar{z}-\bar{Z}}{\bar{Z}}.$$

Further,

$$E\left(d_z\right) = E\left(d_x\right) = E\left(e_z\right) = 0,\ E\left(d_z^2\right) = \theta\left(\lambda_{40}-1\right),\ E\left(d_x^2\right) = \theta\left(\lambda_{04}-1\right),\ E\left(e_z^2\right) = \theta C_z^2,$$

$$E\left(d_z d_x\right) = \theta\left(\lambda_{22}-1\right),\ E\left(d_z e_z\right) = \theta\lambda_{30}C_z, \text{ and } E\left(d_x e_z\right) = \theta\lambda_{12}C_z.$$

The proposed estimator takes the form:

$$t_p\left(R\right) = \left\{\frac{\sigma_z^2\left(1+d_z\right)-\sigma_T^2\bar{Z}^2\left(1+e_z\right)^2-\sigma_S^2}{\sigma_T^2+1}+\sigma_x^2-\sigma_x^2\left(1+d_x\right)\right\}$$

$$\times\frac{\left(N-1\right)\sigma_x^2-\left(n-1\right)\sigma_x^2\left(1+d_x\right)}{\left(N-n\right)\sigma_x^2}\exp\left[\frac{\sigma_x^2-\sigma_x^2\left(1+d_x\right)}{\sigma_x^2+\sigma_x^2\left(1+d_x\right)+\alpha}\right],$$

or

$$t_p\left(R\right) = \left\{\frac{\sigma_z^2+\sigma_z^2 d_z-\sigma_T^2\bar{Z}^2-\sigma_T^2\bar{Z}^2e_z^2-2\sigma_T^2\bar{Z}^2e_z-\sigma_S^2}{\sigma_T^2+1}-\sigma_x^2 d_x\right\}$$

$$\times\frac{\sigma_x^2\left(N-1\right)-\sigma_x^2\left(n-1\right)d_x}{\left(N-n\right)\sigma_x^2}\exp\left[-\frac{1}{2}d_x\left(1+\frac{1}{2}d_x\right)^{-1}\right].$$

Ignoring higher order terms leads to:

$$t_p\left(R\right) = \left\{\frac{\sigma_z^2+\sigma_z^2 d_z-\sigma_T^2\bar{Z}^2-\sigma_T^2\bar{Z}^2e_z^2-2\sigma_T^2\bar{Z}^2e_z-\sigma_S^2}{\sigma_T^2+1}-\sigma_x^2 d_x\right\}\left(1-Dd_x\right)\left(1-\frac{1}{2}d_x+\frac{1}{4}d_x^2\right).$$

Further mathematical work yields:

$$t_p\left(R\right)-\sigma_y^2 \approx \frac{1}{2\left(\sigma_T^2+1\right)}\left[2\sigma_T^2\bar{Z}^2e_z^2-2A\sigma_z^2 d_x d_z+4A\sigma_T^2\bar{Z}^2d_x e_z+ABd_x^2\right].$$

(21)

Taking expectation on equation (21) yields:

https://doi.org/10.62500/icrtsda.1.1.23

$$E\left[t_p(R)-\sigma_y^2\right]\approx\frac{1}{2\left(\sigma_T^2+1\right)}\left[2\sigma_T^2\bar{Z}^2E\left(e_z^2\right)-2A\sigma_z^2E\left(d_xd_z\right)+4A\sigma_T^2\bar{Z}^2E\left(d_xe_z\right)+AB\cdot E\left(d_x^2\right)\right],$$

or

$$Bias\left(t_p(R)\right)\approx\frac{\theta}{2\left(\sigma_T^2+1\right)}\left[2\sigma_T^2\bar{Z}^2C_z^2-2A\sigma_z^2\left(\lambda_{22}-1\right)+4A\sigma_T^2\bar{Z}^2\lambda_{12}C_z+AB\left(\lambda_{04}-1\right)\right].$$

This completes the proof.

Theorem 2: The mean square error may be written in the form:

$$MSE\left(t_p(R)\right)\approx\frac{\theta}{\left(\sigma_T^2+1\right)^2}\left[\sigma_z^4\left(\lambda_{40}-1\right)+G^2C_z^2+H^2\left(\lambda_{04}-1\right)\right.$$

$$\left.-2G\lambda_{30}C_z+2GH\lambda_{12}C_z-2H\left(\lambda_{22}-1\right)\right],\tag{22}$$

where

$$G=2\sigma_T^2\bar{Z}^2,\tag{23}$$

and

$$H=\left(\sigma_T^2+1\right)\sigma_x^2-A\left(\sigma_z^2-\sigma_T^2\bar{Z}^2-\sigma_S^2\right).\tag{24}$$

Proof:

Ignoring higher order terms, we can write:

$$t_p(R)-\sigma_y^2\approx\frac{1}{\sigma_T^2+1}\left[\sigma_z^2d_z-Ge_z-Hd_x\right].\tag{25}$$

Squaring equation (25) and taking expectation leads to:

$$E\left[t_p(R)-\sigma_y^2\right]^2\approx\frac{1}{\left(\sigma_T^2+1\right)^2}E\left[\sigma_z^4d_z^2+G^2e_z^2+H^2d_x^2-2Gd_ze_z-2H\sigma_z^2d_zd_x+2GHd_xe_z\right].$$

Further simplification leads to the required proof:

$$MSE\left(t_p(R)\right)\approx\frac{\theta}{\left(\sigma_T^2+1\right)^2}\left[\sigma_z^4\left(\lambda_{40}-1\right)+G^2C_z^2+H^2\left(\lambda_{04}-1\right)\right.$$

$$\left.-2G\lambda_{30}C_z+2GH\lambda_{12}C_z-2H\left(\lambda_{22}-1\right)\right].$$

https://doi.org/10.62500/icrtsda.1.1.23

5. COMPARATIVE ANALYSIS

For comparison of the proposed estimator with the Isaki's (1983) estimator, the efficiency conditions can be derived as:

$$MSE\left(t_p\left(R\right)\right) < MSE\left(t_1\left(R\right)\right),$$

or

$$\left(G^2 - 4\sigma_T^4\bar{Z}^4\right)C_z^2 + \left\{H^2 - \sigma_y^4\left(\sigma_T^2+1\right)^2\right\}\left(\lambda_{04}-1\right)$$
$$< 2\left[\left(G - 2\sigma_z^2\sigma_T^2\bar{Z}^2\right)\lambda_{30}C_z + \left\{GH - 2\sigma_y^2\sigma_T^2\bar{Z}^2\left(\sigma_T^2+1\right)\right\}\lambda_{12}C_z - \left\{H - \sigma_y^2\sigma_z^2\left(\sigma_T^2+1\right)\right\}\left(\lambda_{22}-1\right)\right].$$

For comparison of the proposed estimator with the Gupta et al. (2020) estimator, the efficiency conditions can be derived as:

$$MSE\left(t_p\left(R\right)\right) < MSE\left(t_2\left(R\right)\right),$$

or

$$\left(G^2 - 4\sigma_T^4\bar{Z}^4\right)C_z^2 + \frac{1}{\lambda_{04}-1}\left[H^2\left(\lambda_{04}-1\right)^2 + \left(\lambda_{22}-1\right)\left\{\sigma_z^2 - 2H\left(\lambda_{04}-1\right)\left(\lambda_{22}-1\right)\right\}\right]$$
$$< 2\left[\left(G - 2\sigma_z^2\sigma_T^2\bar{Z}^2\right)\lambda_{30} - \left\{GH - \frac{\sigma_T^2\bar{Z}^2}{\lambda_{04}-1}\right\}\lambda_{12}\right]C_z.$$

Table 1: Mean square errors for $\sigma_x^2 = 6$, $\sigma_z^2 = 2.5$, $\sigma_y^2 = 2$, $\mu_y = 3$

Parameters	n	$t_0(R)$	$t_1(R)$	$t_2(R)$	$t_p(R)$
$\sigma_S^2 = 10$, $\sigma_T^2 = 0.5$	30	1.7463	1.0961	4.2915	0.8413
	80	0.6549	0.4110	1.6093	0.3100
	150	0.3493	0.2192	0.8583	0.1611
	500	0.1048	0.0658	0.2575	0.0412
	1000	0.0524	0.0329	0.1287	0.0140
$\sigma_S^2 = 3$, $\sigma_T^2 = 0.7$	30	1.1458	0.5421	3.8107	0.4421
	80	0.4297	0.2033	1.4290	0.1633
	150	0.2292	0.1084	0.7621	0.0852
	500	0.0687	0.0325	0.2286	0.0224
	1000	0.0344	0.0163	0.1143	0.0084
$\sigma_S^2 = 0.8$, $\sigma_T^2 = 0.9$	30	0.9030	0.3579	3.2899	0.2528
	80	0.3386	0.1342	1.2337	0.0928
	150	0.1806	0.0716	0.6580	0.0480
	500	0.0542	0.0215	0.1974	0.0119
	1000	0.0271	0.0107	0.0987	0.0037
$\sigma_S^2 = 1$, $\sigma_T^2 = 1$	30	1.0481	0.5626	3.0217	0.5300
	80	0.3930	0.2110	1.1331	0.1968
	150	0.2096	0.1125	0.6043	0.1035
	500	0.0629	0.0338	0.1813	0.0286
	1000	0.0314	0.0169	0.0907	0.0120

https://doi.org/10.62500/icrtsda.1.1.23

Table 2: δ values for $\sigma_x^2 = 6$, $\sigma_z^2 = 2.5$, $\sigma_y^2 = 2$, $\mu_y = 3$

Parameters	n	$t_0(R)$	$t_1(R)$	$t_2(R)$	$t_p(R)$
$\sigma_S^2 = 10$, $\sigma_T^2 = 0.5$	30	0.1127	0.0707	0.2769	0.0543
	80	0.0422	0.0265	0.1038	0.0200
	150	0.0225	0.0141	0.0554	0.0104
	500	0.0068	0.0042	0.0166	0.0027
	1000	0.0034	0.0021	0.0083	0.0009
$\sigma_S^2 = 3$, $\sigma_T^2 = 0.7$	30	0.1071	0.0507	0.3561	0.0413
	80	0.0402	0.0190	0.1336	0.0153
	150	0.0214	0.0101	0.0712	0.0080
	500	0.0064	0.0030	0.0214	0.0021
	1000	0.0032	0.0015	0.0107	0.0008
$\sigma_S^2 = 0.8$, $\sigma_T^2 = 0.9$	30	0.0844	0.0335	0.3075	0.0236
	80	0.0316	0.0125	0.1153	0.0087
	150	0.0169	0.0067	0.0615	0.0045
	500	0.0051	0.0020	0.0184	0.0011
	1000	0.0025	0.0010	0.0092	0.0003
$\sigma_S^2 = 1$, $\sigma_T^2 = 1$	30	0.0873	0.0469	0.2518	0.0442
	80	0.0328	0.0176	0.0944	0.0164
	150	0.0175	0.0094	0.0504	0.0086
	500	0.0052	0.0028	0.0151	0.0024
	1000	0.0026	0.0014	0.0076	0.0010

In order to evaluate the performance of different variance estimators, two important aspects – efficiency and δ values, were computed using a variety of values of parameters. The computed values of mean square error and δ have been displayed in Table 1 and Table 2, respectively, for various sample sizes. The superiority of the proposed estimator can clearly be observed in both tables.

6. COMMENTS AND CONCLUSION

This study presented an improved variance estimator for situations where the variable of interest is sensitive. The properties of the suggested estimator have been discussed along with the derivation of efficiency conditions. Table 1 reveals that the proposed estimator achieves improved efficiency over the available estimators for small and large sample sizes. An interesting finding is that both the few decades-old estimator of Isaki (1983) is more efficient than the recent estimator of Gupta et al. (2020). In fact, the Isaki's (1983) estimator is the second-best estimator of all four estimators chosen for comparison purpose. It is also observed that an increase in the sample size causes a proportional reduction in the mean squared error. Therefore, if the cost of the survey permits, a large sample size is always recommended.

Table 2 reveals that the unified metric δ provides smaller values for the proposed estimator than the available estimators. Being an important model-evaluation measure, the unified metric's smallest computed values under the suggested estimator make it useful in real-world applications. The Isaki's (1983) estimator is observed to be the second-best estimator in terms of δ values. Moreover, the small δ values for large n show the importance of the selection of large samples. Keeping in view these results, it is recommended for survey researchers to use the proposed estimator in real-world surveys when estimation of the population variance is required.

7. FUTURE RESEARCH RECOMMENDATIONS

Under the assumption of a sensitive variable of interest, the current study introduced an efficient estimator of the variance based on the linear model of Diana and Perri (2011). It is recommended for

https://doi.org/10.62500/icrtsda.1.1.23

future researchers to develop new scrambling models for used with the proposed estimator to achieve further improvement in the performance of the proposed variance estimator.

REFERENCES

1. Azeem, M. (2023). Introducing a weighted measure of privacy and efficiency for comparison of quantitative randomized response models. *Pakistan Journal of Statistics*, 39(3), 377-385.

2. Azeem, M., and Salam, A. (2023). Introducing an efficient alternative technique to optional quantitative randomized response models. *Methodology*, 19(1), 24-42. https://doi.org/10.5964/meth.9921

3. Azeem, M., Salahuddin, N., Hussain, S., Ijaz, M., and Salam, A. (2024). An efficient estimator of population variance of a sensitive variable with a new randomized response technique. *Heliyon*, 10(5), e27488. https://doi.org/10.1016/j.heliyon.2024.e27488

4. Cochran, W.G. (1940). The estimation of the yields of the cereal experiments by sampling for the ratio of grain to total produce. *The Journal of Agricultural Science*, 30, 262-275.

5. Das, A.K., and Tripathi, T.P. (1978). Use of auxiliary information in estimating the finite population variance. *Sankhya*, 40, 139-148.

6. Diana, G., and Perri, P.F. (2011). A class of estimators of quantitative sensitive data. *Statistical Papers*, 52(3), 633-650. https://doi.org/10.1007/s00362-009-0273-1

7. Eichhorn, B.H., and Hayre, L.S. (1983). Scrambled randomized response methods for obtaining sensitive quantitative data. *Journal of Statistical Planning and Inference*, **7**(4), 307-316.

8. Gjestvang, C.R., and Singh, S. (2009). An improved randomized response model: Estimation of mean. *Journal of Applied Statistics*, *36*(12), 1361-1367.

9. Gupta, S., Aloraini, B., Qureshi, M.N., and Khalil, S. (2020). Variance estimation using randomized response technique. *REVSTAT – Statistical Journal*, 18(2), 165-176.

10. Gupta, S., Gupta, B., and Singh, S. (2002). Estimation of sensitivity level of personal interview survey questions. *Journal of Statistical Planning and Inference*, 100(2), 239-247. https://doi.org/10.1016/S0378-3758(01)00137-9

11. Gupta, S., Mehta, S., Shabbir, J., and Khalil, S. (2018). A unified measure of respondent privacy and model efficiency in quantitative rrt models. *Journal of Statistical Theory and Practice*, 12(3), 506-511. https://doi.org/10.1080/15598608.2017.1415175

12. Isaki, C.T. (1983). Variance estimation using auxiliary information. *Journal of the American Statistical Association*, 78(381), 117-123.

13. Kumar, S., Kour, S.P., and Singh, H.P. (2023). Applying ORRT for the estimation of population variance of sensitive variable. *Communications in Statistics – Simulation and Computation*, 1-11. https://doi.org/10.1080/03610918.2023.2292966

14. Narjis, G., and Shabbir, J. (2021). An efficient new scrambled response model for estimating sensitive population mean in successive sampling. *Communications in Statistics – Simulation and Computation*, 52(11), 5327-5344. https://doi.org/10.1080/03610918.2021.1986528

https://doi.org/10.62500/icrtsda.1.1.23

15. Saleem, I., Sanaullah, A., Al-Essa, L.A., and Bashir, S. (2023). Efficient estimation of population variance of a sensitive variable using a new scrambling response model. *Scientific Reports*, 13, Article Number 19913. https://doi.org/10.1038/s41598-023-45427-2

16. Warner, S.L. (1971). The linear randomized response model. *Journal of the American Statistical Association*, 66(336), 884-888. https://doi.org/10.1080/01621459.1971.10482364

17. Yan, Z., Wang, J., and Lai, J. (2008). An efficiency and protection degree-based comparison among the quantitative randomized response strategies. *Communications in Statistics – Theory and Methods*, 38(3), 400-408. https://doi.org/10.1080/03610920802220785

https://doi.org/10.62500/icrtsda.1.1.24

Proc. 1st International Conference on Recent Trends in Statistics and Data Analytics
Air University Islamabad, Pakistan – May 9, 2024, Vol. 1, pp. 208-215

STATISTICAL INVESTIGATION OF THE ROOT CAUSES OF EXAMINATION MALPRACTICE IN DISTRICT CHARSADDA

Irfan Ullah[1], Zahid Khan[2], Nabeela Raziq[3], and Fatima[4]
[1]Assistant Professor Govt Postgraduate College Charsadda
[2]Lecturere Department of Statistics, University of Malakand
[3] BS scholar GPGC Charsadda
[4] BS scholar GPGC Charsadda

Abstract

Examination malpractice has badly affected the education system of the world and District Charsadda is no exemption. This research aimed to identify the root causes of examination malpractice in District Charsadda. The population of the study consisted of all Government colleges of Tehsil Charsadda. A sample of size 263, using cluster sampling, was drawn from the target population. Questionnaire was use for data collection from both boys and girls. Descriptive measures and chi square test were carried out for the statistical analysis of data. The findings of the study explored that a very high percentage of students involved due to the root causes of examination malpractice. Results obtained through chi-square test for independence suggested that 6 out of 11 factors i.e quest for making grades, ill preparation of students, overcrowded examination halls, poor stocking of college libraries, an offshoot of the ills of the society and absence of crime detection gadgets are independent of gender perception about examination malpractice and hence these are the key factors responsible for examination malpractice, while the remaining 5 factors have significant association with agreement level of gender.

Keywords: Examination malpractice, Stack Bar chart, Chi Squares test, quest for making grades, ill preparation of students.

1. INTRODUCTION

The problem of examination malpractice is a common issue, which has created many problems to the world educational system. Examination malpractice throws a very bad effect on economy because every country or any society can be developed on the bases of education. Examination is one of the main source to assess and evaluate skills and knowledge of learner. It is the key manner of judgment of the learners understanding of a certain part of knowledge. According to Black, P.; William, D.(1998) for quality education a comprehensive examination system is compulsory. The role of examination in our educational system is the most significant. It is conducted to judge the ability of students. Students also judge himself/herself that how much they learned. They also find out difficulties, weakness, and deficiencies in learning process. Examination malpractice is also defined as any illegal source which a candidate uses to get success in examination. The increase in examination malpractice is observed in examination process because candidates have not the courage to face failure in examination, they have not self-confidence, their preparation for examination is poor and incomplete and also due to their laziness. It put very bad effect into our society. Examination malpractice has destroyed educational system very badly, it blocks the mind of the youth and they don't know that how to use their mental power and achieve success. Examination malpractice disturb all systems of a country because in future we have to face corrupt leaders such as doctors , civil servants , bankers , politicians , accountants , journalists , professors etc. which has serious social , political and economical consequences. It has not only a serious effect on social, political and economic system of a country but also on the World. Examination malpractice can be divided into three categories Pre- examination Malpractices, during examination malpractices, post examination malpractices. In the free examination category it is the obtaining of question paper before the date of examination, during examination malpractices includes

https://doi.org/10.62500/icrtsda.1.1.24

copying from another candidate with or without permission , exchanging papers with other candidates , personal relationships with invigilators and supervisors , terrifying the invigilators and supervisors by use of power , impersonation , bringing such materials which is not allowed in examination hall such as cell phones , watches , calculators , use of Bluetooth , hearing aids ,receiving micro from messengers and office clerks , post examination malpractices includes obtaining marks by providing some gifts to the checker of exam papers . According to Adedokun, J. A. (2003) examination malpractice is obtaining marks by using illegal means which is not accordance with the rules and regulations of examination. Denga says that students engage in examination malpractice due to the over stress of work, frighten from parents and absence of punishment to criminals. Yakabu (1998) says that for cheating in examination candidates use different tricks they hide cheating materials in pants, shoes, text messages, saving information calculators etc. Evans et al. (1990) conducted a study to assess students' and teachers' attitudes and views of cheating activity. According to this the unsuitable behavior and attitudes of teachers with students in classroom have bad impact on students due to which students getting involved in cheating. The study also found that the increasing rate in examination malpractice is also due to those teachers who haven't emphasizing to understand the importance of education. The study also demonstrated that the involvement of students in examination malpractice is due to those teachers who are unsupportive, uninspired, or boring and those who have a lot of expectations for their students.There are many elements which are the cause of prevalence of examination malpractice including the ill distribution, improper facilities, unsuitable administration fear of lifting from success and the participation of the ineligible candidates, according to Ruwa (1997), may contribute to the incidence of cheating. According to Fayombo (2004) mostly the candidates focus on the achievement of diplomas and certificates that is why they are getting involved in examination malpractice. Cheating in examination makes it hard to judge a person fairly based on how successfully they perform in a set of inquiries, remarks, or assignments made to judge how much of a desired quality, proficiency, or information they have (Nwandiani, 2005). According to Sommers & Satel (2005), the experience of shameless violation for laws and regulations in education is simply a reflection of the overall situation in society.

According to Erakhumen (2006), basic and second cycle teachers lack sufficient experience in the fields they assert to teach because their mentors at the time lacked the necessary knowledge and were not sufficiently motivated. Also blamed for the poor performance of their students are the institution's leaders. It is also defined as getting best results by using illegal means such as carrying cheating materials in examination hall, taking help from examinees or others before the examination, during the examination, and after the examination (Fasasi, 2006).Unfairly supporting of a candidate during conduction of examination is known as examination malpractice (Wilayat, 2009).

1.1 Significance of the study

It is observed that education system in Pakistan is grades oriented. Students are adopting all means to achieve high grades and certificates. Instead of getting knowledge and skills students desire to get required qualification for a job with good grades to ensure employment. That is why examination malpractice is increasing day by day. An examination malpractice is the main concern to the educationists and to those who conduct examination. The current study is conducted to highlight the major causes of examination malpractices in District charsadda so that possible steps can be taken to prevent it.

1.2 Objectives of the study

i. To investigate the root causes of malpractice in examination in tehsil Charsadda

ii. To know the association between gender and agreement level of the root causes of examination Malpractice.

https://doi.org/10.62500/icrtsda.1.1.24

2. METHODOLOGY

In this section we are going to discuss the methods used in the study to collect the data also about the target population, size of sample, sampling technique, the process of data collection and analysis of data.

2.1 Population and Sample

The population of the study are the BS students of Government colleges in District Charsadda. The district consists of three tehsil named Tehsil Charsadda, Tangi and Shabqadar. Tehsil Charsadda was selected using cluster sampling, which is consisted of 6 Govt. colleges for boys and girls. Data have been collected from 263 students, the data was collected through questionnaire. The questionnaire consists questions about causes of examination malpractice with five options strongly disagree =1, Disagree=2, Undecided=3, Agree=4, Strongly Agree=5

2.2 STACKED BAR CHART AND CHI_SQUARE TEST

A specific kind of bar chart is a stacked bar chart which describes the composition and comparison between the categories. The stacked bar chart can be drawn in order to compare total values across categories.

Chi-square test is a statistical test used to test the agreement between the observed values and expected values when the sample size is large. The observations are classified into mutually exclusive classes. The statistic $\chi 2$ is defined as

$$\chi 2 = \sum_{i=1}^{r} \quad \sum_{j=1}^{c} \quad \frac{(O_{ij}-E_{ij})^2}{E_{ij}}$$

It has a distribution of $\chi 2$ with (r-1) (c-1) degrees of freedom, where Oi stands for the sample's observed values and Ei for expected values.

3. RESULTS AND DISCUSSION

The following results were obtained using SPSS and Excel software. The results of the objective 1 are shown both graphically and numerically.

OBJECTIVE 1: TO INVESTIGATE THE ROOT CAUSES AND CONSEQUENCES OF MALPRACTICE IN EXAMINATION IN TEHSIL CHARSADDA

Table 1 CAUSES OF EXAMINATION MALPRACTICE

S.No.	Items	SD	D	U	A	SA
1	Quest for making grades	2	3	2	65	191
		0.8%	1.1%	0.8%	24.7%	72.6%
2	Colleges environment located in a crime bidden areas	56	47	44	89	27
		21.3%	17.9%	16.7%	33.8%	10.3%
3	Ill preparation of students	16	24	26	110	87
		6.1%	9.1%	9.9%	41.8%	33.1%

https://doi.org/10.62500/icrtsda.1.1.24

4	Overcrowded examination hall encourages malpractice	27	49	38	96	53
		10.3%	18.6%	14.4%	36.5%	20.2%
5	Poor stocking of college libraries with relevant books	46	81	18	82	36
		17.5%	30.8%	6.8%	31.2%	13.7%
6	Students cannot afford textbooks materials	22	47	33	112	49
		8.4%	17.9%	12.5%	42.6%	18.6%
7	Lack of state of the art teaching and learning resources	26	45	34	88	70
		9.9%	17.1%	12.9%	33.5%	26.6%
8	Involvement of students in social activities	36	70	25	89	43
		13.7%	26.6%	9.5%	33.8%	16.3%
9	It is a part or an offshoot of the ills of the society	16	9	13	90	135
		6.1%	3.4%	4.9%	34.2%	51.3%
10	Fear of failure on the part of student	19	16	13	114	101
		7.2%	6.1%	4.9%	43.3%	38.4%
11	Lack of manpower and absence of crime detection gadgets	25	24	41	91	82
		9.5%	9.1%	15.6%	34.6%	31.2%

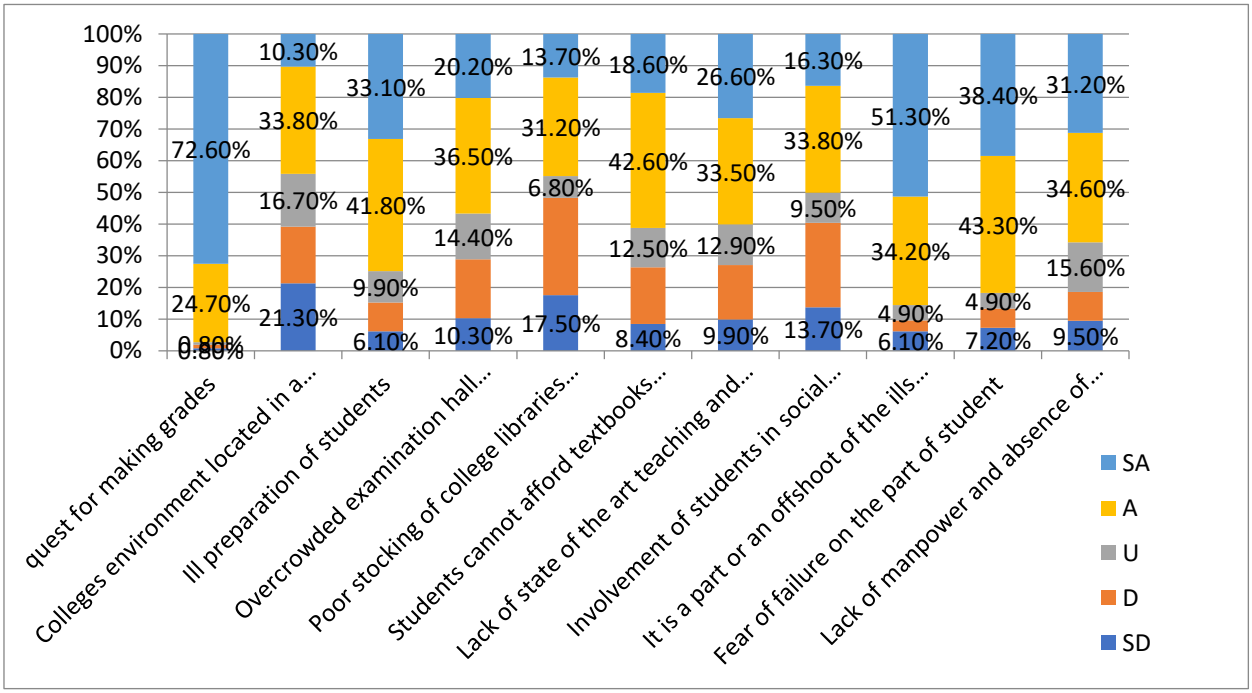

https://doi.org/10.62500/icrtsda.1.1.24

Figure 1: Stack bar chart for the observed data

Table1 shows the counts and percentages of the responses of the respondents about causes of examination malpractices. About item 1 majority of the respondents 72.6% (out of 263) responded that quest for making grades is the main cause of examination malpractice, 24.7% are agreed while 0.8% respondents haven't decided ,some of respondents (1.1%) are disagreed while few (0.8%) are strongly disagreed. About item 2 , 10.3% respondents have the view that the major cause of examination malpractice is the location of colleges environment in a crime bidden areas , 33.8% are also believed on this , while 16.7% haven't decided , 17.9% haven't consider it the main cause ,21.3% are also strongly disagreed . About item 3 , 33.1% respondents are strongly agreed they believed that ill preparation of students for an examination are contribute to examination malpractice, 41.8% are also agreed while 9.9% haven't decided , few of respondents (9.9%) disagreed while 6.1% are strongly disagreed .About item 4, 20.2% respondents are strongly agreed and 36.5% are agreed , the respondents are of the view that the examination malpractice is encourages due to the overcrowded in examination halls , while 14.4% haven't decided , 18.6% disagreed and they haven't consider it the major cause , 10.3% respondents are also strongly disagreed. About item 5, 13.7% respondents are strongly agreed and 31.2% are also agreed which shows that the poor stocking of college libraries with relevant books is the cause of examination malpractice, few respondents (6.8%) haven't decided, while 30.8% disagreed and 17.5% are strongly disagreed and they have the opinion that it is not the major cause. About item 6 , majority of the respondents are strongly agreed (42.6%) , also 18.6% respondents are strongly agreed , they have the opinion that students involved in examination malpractice because they can't afford textbooks materials , 12.5% haven't decided while 17.9% are disagreed and few respondents (8.4%) are strongly agreed and haven't consider it a part due to which examination malpractice encourages. About item 7, 26.6% respondents are strongly agreed and 33.5% are agreed which shows that the lack of state-of-the-art teaching and learning resources is the cause of examination malpractice, some of respondents (12.9%) haven't decided, 17.1% are disagreed and 9.9% are also strongly disagreed. About item 8, 16.3% respondents are strongly agreed , they have the opinion that the involvement of students in social activities encourages examination malpractice, 9.5% respondents undecided ,26.6% respondents haven't consider it the major cause, 13.7% respondents are also strongly disagreed. About item 9, majority of respondents (51.3%) are strongly agreed and 34.2% are also agreed which shows that examination malpractice play a major role in the ills of the society, 4.9% haven't decided few (3.4%) are disagreed and only 6.1% respondents are strongly disagreed. About item 10, 38.4% respondents are strongly agreed and 43.3% are agreed which shows that students involved in examination malpractice due to the fear of failure in a given examination. About item 11, 31.2% respondents are strongly agreed that loose supervision during examination resulting from lack of manpower and absence of scientific crime detection gadgets encourages students in examination malpractice.

OBJECTIVE 2:

TO KNOW THE ASSOCIATION BETWEEN GENDER AND AGREEMENT LEVEL OF THE CAUSES OF EXAMINATION MALPRACTICE

For each question hypothesis have been formulated to test the independence of gender and their perception regarding agreement level about the examination malpractice. The results are shown in table 2:

https://doi.org/10.62500/icrtsda.1.1.24

Table: 2 $\chi 2$ test results for independence of gender and agreement level

S.No	Hypothesis	Test Statistic Value	df	Significance
1	Is there a significant association between gender and perception regarding agreement level of "quest for making grades"	5.912	4	.206
2	association between gender and agreement level of "Colleges environment located in a crime bidden areas"	13.422	4	.009
3	association between gender and agreement level of "Ill preparation of students"	4.256	4	.372
4	significant association between gender and agreement level of "Overcrowded examination hall encourages malpractice"	3.140	4	.535
5	association between gender and agreement level of "Poor stocking of college libraries with relevant books"	12.060	4	.017
6	significant association between gender and agreement level of "students cannot afford textbooks materials"	12.060	4	.017
7	association between gender and agreement level of "Lack of state of the art teaching and learning resources"	17.877	4	.001
8	association between gender and agreement level of "Involvement of students in social activities"	17.221	4	.002
9	association between gender and agreement level of "It is a part or an offshoot of the ills of the society"	8.941	4	.063
10	association between gender and agreement level of "Fear of failure on the part of students"	13.337	4	.010
11	association between gender and agreement level of "Lack of manpower and absence of crime detection gadgets' "	2.007	4	.735

From the results in table 2 it is observed that the items S.No 2, 5, 6, 7, 8 and 11 are insignificant i.e the opinion of boys and girls is not the same about the factors location of colleges in crime bidden areas, Students cannot afford textbooks materials, Lack of teaching and learning resources, Involvement of students in social activities, Fear of failure on the part of student. quest for making grades, ill preparation of students, overcrowded examination halls, poor stocking of college libraries, an offshoot of the ills of the society, absence of crime detection gadgets) are independent of gender perception about the factors.

4. CONCLUSIONS

Examination malpractice is a common issue, which has affected the world educational system very badly. However, this was embarked upon the researcher to expose the causes of examination malpractice. The researcher selected all government colleges in tehsil Charsadda, A sample of size 263 was drawn from the target population. A self-developed questionnaire was used as research instrument for data collection. Descriptive statistics i.e. simple percentages and inferential statistics i.e. chi square test were applied for the statistical analysis of data. The findings of the study explored that more than half of the students (72.6%) agreed to the fact that students involved in examination malpractice in order to achieve high grades. Using chi-square test of independence it is found that 6 out of 11 factors (quest

https://doi.org/10.62500/icrtsda.1.1.24

for making grades, ill preparation of students, overcrowded examination halls, poor stocking of college libraries, an offshoot of the ills of the society, absence of crime detection gadgets) are significantly independent of gender, it means that there is no significant association between these factors and agreement level of gender and hence these are the key factors responsible for examination malpractice as the response of both males and females towards these factors are same, while 5 of the factors(location of colleges in crime bidden areas, Students cannot afford textbooks materials, Lack of teaching and learning resources, Involvement of students in social activities, Fear of failure on the part of student) have significant association with agreement level of gender which means that these factors depends upon the gender.

5. RECOMMENDATIONS

1: Students should not force to achieve high scores because every person has their own learning capability.

2: The concerned authority should appoint honest, trustworthy and devoted personnel for conducting examinations.

3: Conceptual type question papers should be included to discourage examination malpractice.

4: The students must be motivated and guided for proper preparation of examination.

5: In every examination hall finger print system should be establish to avoid impersonation.

6: Before entering in examination hall students body checking should be ensured.

REFERENCES

1. . Adedokun, J. A. (2003). Measurement & evaluation in the class room. *Sagamu: The Stronghold Educational Publishers*.
2. Adamu, A., Cobbinah, B. B., & Alhassan, R. (2021). Assessment of the Factors Causing Senior High Students Involvement in Examination Malpractice in the Takoradi Metropolis of Ghana. *Open Journal of Social Sciences*, *9*(6), 241-254.
3. Achio, S., Ameko, E., Kutsanedzie, F., Alhassan, S., & Ganaa, F. (2012). Concerns on issues of examination malpractices a case study of Accra Polytechnic. *Academic Research International*, *3*(2), 145.
4. Abdulkareem, A. Y., Fasasi, Y. A., & Akinnubi, O. P. (2012). Parents-Teachers Association and quality assurance in the management of Kwara State secondary schools, Nigeria.
5. Afolabi, O. A. (2010). Opening address by the permanent secretary, Prof. *OA Afolabi, Federal Ministry of Education at the national examination summit held at the national universities commission (NUC), Abuja on Monday, 24th May*.
6. Breslau, N., & McNally, R. J. (2006). The epidemiology of 9/11: technological advances and conceptual conundrums.
7. Badejo, A. O., & Gandonu, M. B. (2010). Predisposing factors towards examination malpractice among students in Lagos universities: Implications for counselling. *Edo Journal of Counselling*, *3*(2), 197-210.
8. Black, P., & Wiliam, D. (1998). Assessment and classroom learning. *Assessment in Education: principles, policy & practice*, *5*(1), 7-74.
9. Cornelius-Ukpepi, B. U., & Ndifon, R. A. (2012). Factors that influence examination malpractice and academic performance in primary science among primary six pupils in Cross River State, Nigeria. *Journal of Education and Practice*, *3*(9), 59-68.
10. Denga, D. I. (2004). Cultism and Academic Performance.

https://doi.org/10.62500/icrtsda.1.1.24

11. Eckstein, M. A. (2003). *Combating academic fraud: Towards a culture of integrity*. International Institute for Educational Planning.
12. Erakhumen, J. (2006). Introduction to Curriculum Research and Development.
13. Evans, E. D., & Craig, D. (1990). Adolescent cognitions for academic cheating as a function of grade level and achievement status. *Journal of Adolescent Research*, *5*(3), 325-345.
14. learning. *International Journal of Novel Research in Humanity and Social Sciences*, *2*(1), 52-62.
15. Khan, I., Khan, M. J, & Khan, J. (2012). Teachers perception regarding malpractice used in examination in urban areas of district peshawer.
16. Ikere-Ekiti. MA. Adegboye, 0. Odutoye, & J. 0. Adetunberu. *Issues on examination maipractices in Nigeria*, 62-73.
17. Makaula, F. B. (2018). Perceived causes and methods of examination malpractice in the Malawian education system: A case study of secondary schools in South East Education Division (SEED).
18. Nwadiani, M. (2005, November). Curbing examination malpractice in the Nigerian educational system. In *A lead Paper presented at the First Annual Conference of the Faculty of Education, Ambrose Alli University, Ekpoma, November* (pp. 10-12).
19. Nnam, M. U., & Inah, A. F. (2015). Empirical investigation into the causes, forms and consequences of examination malpractice in Nigerian institutions of higher Khan, I., Khan, M. J., & Khan, J. (2012). Teachers' perception regarding malpractices used in examinations in urban areas of District Peshawar.
20. Obidoa, M. A., Onyechi, K. C., & Okere, A. U. (2013). Examination malpractice and control in public secondary schools in Anambra state, Nigeria: implications for the counsellor.
21. Ruwa, M. (1997). Examination malpractices: A case study of the University of Maiduguri. *Maiduguri Journal of Educational Studies*, *3*(10), 197-208.
22. Solangi, A. F., Ahmed, M. U., Hussain, S., & Khattak, M. D. (2017). Exploring the potential of virtual learning in an open and distance learning (ODL) environment. *Pakistan Journal of Distance and Online Learning*, *3*(1), 9-22.
23. Udoh, N. A. (2011). Remote causes and counseling implications of examination malpractice in Nigeria. *Inquiries Journal*, *3*(10).
24. Wilayat, M. (2009). Examination Malpractice: Causes of examination malpractice/unfair means. *IER University of Peshawar*.
25. Yakubu, L. O. (1998). Various tricks adopted by students in perpetuating examination malpractices in tertiary institutions: A case study of Ondo State College of Education.

https://doi.org/10.62500/icrtsda.1.1.25

Proc. 1st International Conference on Recent Trends in Statistics and Data Analytics

Air University Islamabad, Pakistan – May 9, 2024, Vol. 1, pp. 216-222

Stratified Dual-rank ranked set Sampling for Estimating Population Mean

Zahid Khan

Lecturer, Department of Statistics, University of Malakand, Chakdara, Dir Lower, Pakistan

ABSTRACT

Ranked set sampling (RSS) is cost-effective sampling design widely uses in survey where the measurement of units is costly. The RSS method used ranking procedure in selection of units. The ranking is done by visual inspection or by auxiliary variable. In the present paper, 'stratified Dual-rank ranked set sampling' (SDRRSS) method is suggested to estimate population mean. Some of the properties of the mean estimator under the suggested scheme is investigated. The performance of the estimator of proposed scheme is investigated by relative efficiency (RE). A simulation study is conducted for computing such relative efficiency. The proposed method is also illustrated with practical data sample.

Key words: population mean, properties, relative efficiency, practical data

1. INTRODUCTION

Mclyntyre (1952) developed the concept of ranked set sampling (RSS) for estimation of mean pasture yield that provides higher efficiency than SRS, but their study did not furnish any empirical proof. This job is done by Takahasi and Wikamato (1968) whom furnished it with essential mathematical support. Initially, the RSS was proposed with the concept of perfect ranking of units within sets, while no matter how imperfect the ranking, Dell and Clutter (1972) exhibited that the mean of RSS remained unbiased estimator of the population mean.

Due to the fact that RSS appears to be a more cost-effective option than $S\,R\,S$, several authors have focused on proposing modified ranked set sampling methods. Moreover, the commonly used traditional simple random sampling (SRS) design is ancient in many cases. New designs are proposed in order to increase efficiency. Samawi (1996) developed stratified ranked set Sampling (SRSS) scheme. Empirical study was conducted and showed that SRSS provided more efficient estimator of population mean than ordinary SSRS design. Samawai and Saeid (2004) introduced stratified extreme ranked set sampling (SERSS) method for estimation of population mean. Ibrahim et al. (2010) proposed stratified median ranked set sampling (SMRSS) method. They showed empirically that SMRSS provides more efficient mean estimator. Al-Omari et al. (2011) introduced stratified percentile ranked set sampling (SPRSS) scheme. Their study showed that mean estimator of SPRSS was more efficient than some of modified RSS methods. Mahdizadeh and Zamanzade (2018) investigated stratified pair ranked set sampling (SPRSS) method. Their proposed scheme not only utilized fewer sampling units but also provide efficient estimator.

Khan et al. (2021) developed modified median ranked set sampling (MMRSS) which gives low MSE/variance than some of its counterpart designs. For more modified version of RSS see (Khan et al., 2020; Khan et al, 2022)

Auxiliary variable can also be used in estimator of mean in RSS. Khan et al. (2020) developed ratio estimator under RSS which show minimum MSE than some of existing estimators. The RSS can easily be used to collected data of patients. Khan et al. (2022) conducted study on estimation of anemia patients and causes of anemia using RSS method for selecting sample.

Dual-ranked set sampling proposed by Teconeli (2024) is providing very higher efficiency than simple random sampling and ranked set sampling, and it is a cost-effective alternative to double ranked set sampling estimation. In some situation the stratified sampling method is the only method which applicable for sampling survey, especially when the population is heterogenous. Thus, in this situation dual-ranked set sampling can not be applicable. In the present study the concept of dual-ranked set

https://doi.org/10.62500/icrtsda.1.1.25

sampling is extended to stratified dual-ranked set sampling method. This method will be more applicable with higher efficiently than some of the existed stratified designs.

1.1 Ranked Set Sampling

The procedure of RSS is briefly explain as; draw randomly n units each of size n and then distribute these units into n sets, each set consists of n units. Then, rank the units within each set by eye or with low-cost method. Finally, select smallest rank unit from the first set, second smallest rank unit from the second set, the processes are continued until largest ranked unit is selected from last set. The procedure is repeated r time to get rn units.

Let X be the study variable with probability density function $f_{x(x)}$, cumulative density function $F_{x(x)}$, mean μ_X and variance σ_X^2 Let $X_{11j}, X_{12j}, ..., X_{1nj}, X_{21j}, X_{22j}, ..., X_{2nj}, ..., X_{n1j}, X_{n2j}, ..., X_{nnj}$ be the n independent simple random sample each of size n from j^{th} (for $j = 1, 2, ..., r$) cycle drawn from $f_{x(x)}$. The mean and variance of RSS is as follows,

$$\bar{X}_{RSS} = \frac{\sum_{j=1}^{r}\sum_{i=1}^{n} X_{i(i:n)j}}{rn} \tag{1}$$

The variance is as follows,

$$\text{var}\left(\bar{X}_{RSS}\right) = \frac{\sigma_X^2}{rn} - \frac{1}{rn^2}\sum_{i=1}^{n}\left(\mu_{i(i:n)} - \mu\right)^2 \tag{2}$$

Where, $\mu_{i(i:n)}$ is the mean of i^{th} order statistics.

1.2 Double Ranked Set Sampling (DRSS)

The procedure of DRSS for getting sample of size n is briefly explained as follows: select n^3 units from a target population, distribute them into n sets each of size n^2 units. Apply RSS procedure to get n RSS units each of size$n$. Finally, the RSS technique is used on the already taken RSS units to obtain a double ranked set sample of size$n$. The estimator of population mean under DRSS is as follows,

$$\bar{X}_{DRSS} = \frac{1}{rn}\sum_{j=1}^{r}\sum_{i=1}^{n} X^*_{i(i:n)j'} \tag{7}$$

with variance

$$\text{var}\left(\bar{X}_{DRSS}\right) = \frac{\sigma^2}{rn} - \frac{1}{nr^2}\sum_{i=1}^{n}\left(\mu_{i(i:n)} - \mu\right)^2 \tag{8}$$

where $X^*_{i(i:n)j'}$ is the i^{th} sample unit for $i = 1, 2, ..., n$ selected by DRSS in the j^{th} cycle $j = 1, 2, ..., r$.

1.4 Dual-rank ranked set sampling

https://doi.org/10.62500/icrtsda.1.1.25

The DRRS samples can be selected by randomly drawing n^2 elements from the target population, and distributing them into n sets each of size n. By ranking the element within each set, select n element. This procedure repeated n times, as result, n sets each of size n obtained. Now, rank each set again, and pick the middle value in case of odd elements, otherwise, pick $\frac{n}{2}$ position elements from 1,2,3… sets and position $\frac{n+2}{2}$ elements from 2,4,6… sets. Repeat steps 1-5 *m* times (cycles) to draw a DRRSS sample of size $N = mn$.

2. PROPOSED SAMPLING DESIGN

The procedure SRSS for getting a sample of size n is to divide the population into H mutually exclusive and exhaustive strata. Then, select an independently n^2 elements from the target population from stratum h in r_h cycle, and distributing them into n sets each of size n. By ranking the element within each set, select n element. This procedure repeated n times, as result, n sets each of size n obtained. Now, rank each set again, and pick the $\frac{n+1}{2}$ position value in case of odd elements, otherwise, pick $\frac{n}{2}$ position elements from 1,2,3… sets and position $\frac{n+2}{2}$ elements from 2,4,6… sets. Repeat steps 1-5 *m* times (cycles) to draw a DRRSS sample of size $N = mn$. dual-ranked set sample of size $r_h n_h$ units from stratum h in r_h cycle. Let $X^{h*}_{[\frac{n+1}{2}:n]j}$ be the order statistic in the j^{th} cycle of the Stratified dual-ranked set sample collected from stratum h. The observations $X^{h*}_{[\frac{n+1}{2}:n]j}$ $(h=1,....,H;\ j=1,...r_h)$ are independent, but not identically distributed. For fixed h and i, $X^{h}_{[i]j}$'s $(j=1,...r_h)$ are identically distributed, where the common mean and variance are denoted by $\mu_{[\frac{n+1}{2}:n]h}$ and $\sigma_{[\frac{n+1}{2}:n]h}$ respectively.

The layout for selecting sample of size 3 from stratum h.

$\boxed{X^{11}_{1[1:3]}}$	$X^{11}_{2[1:3]}$	$X^{11}_{3[1:3]}$
$X^{11}_{1[2:3]}$	$\boxed{X^{11}_{2[2:3]}}$	$X^{11}_{3[2:3]}$
$X^{11}_{1[3:3]}$	$X^{11}_{2[3:3]}$	$\boxed{X^{11}_{3[3:3]}}$

$\boxed{X^{21}_{1[1:3]}}$	$X^{21}_{2[1:3]}$	$X^{21}_{3[1:3]}$
$X^{21}_{1[2:3]}$	$\boxed{X^{21}_{2[2:3]}}$	$X^{21}_{3[2:3]}$
$X^{21}_{1[3:3]}$	$X^{21}_{2[3:3]}$	$\boxed{X^{21}_{3[3:3]}}$

$\boxed{X^{31}_{1[1:3]}}$	$X^{31}_{2[1:3]}$	$X^{31}_{3[1:3]}$	
$X^{31}_{1[2:3]}$	$\boxed{X^{31}_{2[2:3]}}$	$X^{31}_{3[2:3]}$	
$X^{31}_{1[3:3]}$	$X^{31}_{2[3:3]}$	$\boxed{X^{31}_{3[3:3]}}$	

Selected elements from 1st stage ranking

$X^{11}_{1[1:3]}$	$\boxed{X^{11}_{2[1:3]}}$	$X^{11}_{3[3:3]}$
$X^{21}_{1[1:3]}$	$\boxed{X^{21}_{2[2:3]}}$	$X^{21}_{3[3:3]}$

https://doi.org/10.62500/icrtsda.1.1.25

$X^{31}_{1[1:3]}$	$X^{31}_{3[3:3]}$	$X^{31}_{3[3:3]}$

Finally, after ranking the elements obtained in stage first, the following elements of order $\frac{n+1}{2}$ are selected

$X^{11*}_{2[2:3]}$, $X^{21*}_{2[2:3]}$, $X^{31*}_{2[2:3]}$

2.1 Mean and Variance

The mean estimator under SDRRSS is given by

$$\bar{X}_{(SDRRSS)} = \sum_{j=1}^{r} \frac{N_h}{N} \bar{X}_{(SDRRSS,h)}, \quad (3)$$

where,

$\bar{X}_{(SDRRSS,h)} = \frac{1}{n_h r_h} \sum_{i=1}^{n_h} \sum_{j=1}^{r_h} X^{ih*}_{[\frac{n+1}{2}:n]j}$ is the RSS estimator of the mean in stratum h.

The variance is given by

$$\text{var}(\bar{X}_{(SDRRSS)}) = \sum_{h=1}^{H} \left(\frac{N_h}{N n_h} \right)^2 \frac{1}{r_h} \sum_{i=1}^{n_h} \sigma^2_{[\frac{n+1}{2}:n]}{}^{ih*} \quad (4)$$

Where

$$\sum_{i=1}^{n_h} \sigma^2_{[i:\frac{n+1}{2}]}{}^{ih*} = n_h \sigma_h^2 - \sum_{i=1}^{n_h} (\bar{X}_{(i,\frac{n+1}{2})h} - \mu_h)^2$$

Combining we get,

$$\text{var}(\bar{X}_{(SRSS,h)}) = \text{var}(\bar{X}_{(SSRS,h)}) - \sum_{h=1}^{H} \left(\frac{N_h}{N} \right)^2 \frac{1}{n_h^2 r_h} \sum_{i=1}^{n_h} (\bar{X}_{(\frac{n+1}{2},n_h)h} - \mu_h)^2$$

Similarly, the mean and variance for even sample sizes is as under,

$$\bar{X}_{(SDRRSS)} = \sum_{j=1}^{r} \frac{N_h}{N} \bar{X}_{(SDRRSS,h)}$$

where,

$\bar{X}_{(SDRRSS,h)} = \frac{1}{n_h r_h} \sum_{i=1}^{n_h} \sum_{j=1}^{r_h} \left(X^{ih*}_{[\frac{n}{2}:n]j} + X^{ih*}_{[\frac{n+2}{2}:n]j} \right)$ is the RSS estimator of the mean in stratum h.

The variance is given by

$$\text{var}(\bar{X}_{(SDRRSS)}) = \sum_{h=1}^{H} \left(\frac{N_h}{N n_h} \right)^2 \frac{1}{r_h} \sum_{i=1}^{n_h} \left(\sigma^2_{[\frac{n}{2}:n]h} + \sigma^2_{[\frac{n+2}{2}:n]h} \right)$$

After simplification we get

https://doi.org/10.62500/icrtsda.1.1.25

$$\text{var}(\bar{X}_{(SRSS,h)}) = \text{var}(\bar{X}_{(SSRS,h)}) - \sum_{h=1}^{H}\left(\frac{N_h}{N}\right)^2 \frac{1}{n_h^2 r_h}\sum_{i=1}^{n_h}(\bar{X}_{(i,n_h)h} - \mu_h)^2$$

3. SIMULATION STUDY

A simulation study is conducted to investigate the performance of mean estimator under SDRRSS. Both symmetric and asymmetric distributions are considered for testing the performance of SDRRSS-based mean estimator. Relative efficiency (REs) of DRRSS, SRSS and SERSS with respect to SSRS is calculated. R 4.5 software is used for simulation study. The data is collected from 2 strata: (3,3), (4,4), (5,5) 6,with n=8,10.

The equation used for REs of symmetric distribution is as under,

$$RE\left(\bar{X}_t, \bar{X}_{SRS}\right) = \frac{\text{var}\left(\bar{X}_{SRS}\right)}{\text{var}\left(\bar{X}_t\right)}$$

For asymmetric distribution, the relative efficiency is defined as,

$$RE\left(\bar{X}_t, \bar{X}_{SRS}\right) = \frac{\text{var}\left(\bar{X}_{SRS}\right)}{MSE\left(\bar{X}_t\right)}$$

Where, t=SDRRSS, SRSS

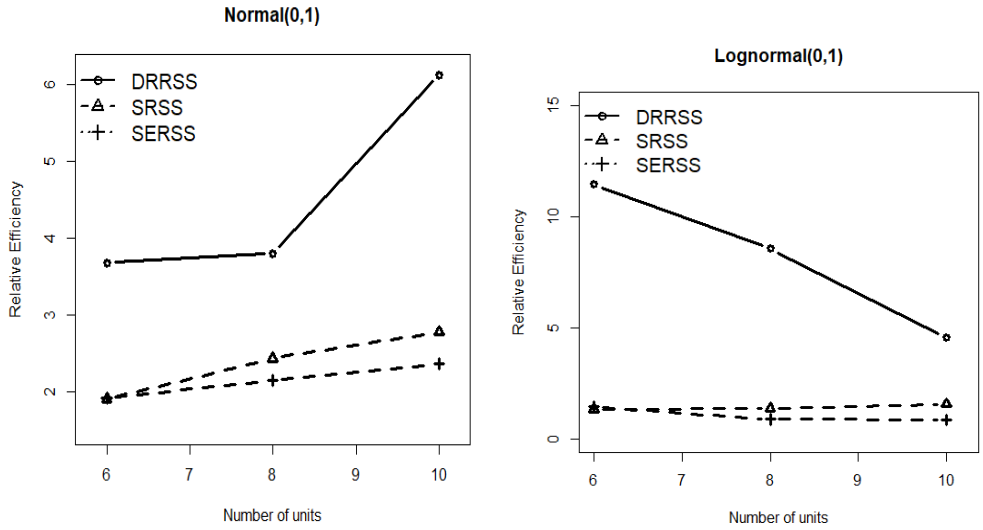

https://doi.org/10.62500/icrtsda.1.1.25

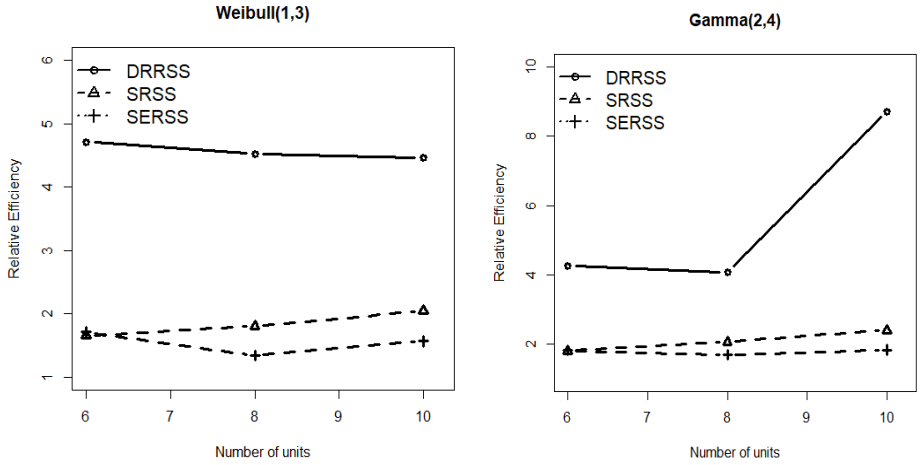

Figure 1. Relative Efficiency of Mean Estimator based on DRRSS, SRSS, SERSS relative to SSRS.

The result of simulation study is shown in Figure 1. The study is conducted for four distributions, normal, lognormal, Weibull, and gamma. In all these distributions the performance of proposed sampling method is better than SRSS and SERSS. The performance is measured on relative efficiency (RE). The higher the RE the better the sampling method.

Table 1; Relative Efficiency of SDRRSS and SRSS vs SSRS

Distribution	Strata	DRRSS	SRSS	SERSS
Normal(0,1)	(3,3)	**3.6786**	1.9039	1.9123
	(4,4)	**3.7956**	2.4325	2.1432
	(5,5)	**6.1232**	2.7756	2.3655
Lognormal(0,1)	(3,3)	**11.45**	1.3343	1.4594
	(4,4)	**8.5543**	1.3697	0.8746
	(5,5)	**4.5432**	1.5543	0.8548
Weibull(1,3)	(3,3)	**4.7123**	1.6561	1.7087
	(4,4)	**4.5232**	1.8046	1.3421
	(5,5)	**4.4665**	2.0487	1.5648
Gamma (2,4)	(3,3)	**4.26**	1.7987	1.8132
	(4,4)	**4.0723**	2.0533	1.6804
	(5,5)	**8.7132**	2.3954	1.8326

The result of simulations study is given in Table 1 indicates that the mean estimator under SDRRSS is more efficient than SRSS, and SESRS in given distributions.

https://doi.org/10.62500/icrtsda.1.1.25

4. Conclusion

In the present study a new sampling scheme, stratified dual ranked set sampling, is suggested which perform better than some of its counterpart sampling methods.

5. References

1. Taconeli, C. A. (2024). Dual-rank ranked set sampling. *Journal of Statistical Computation and Simulation*, *94*(1), 29-49.
2. McIntyre GA. A method for unbiased selective sampling using ranked sets. Aust J Agric Res. 1952;3:385–390.
3. Takahasi K,Wakimoto K. On unbiased estimates of the population mean based on the sample stratified by means of ordering. Ann Inst Stat Math. 1968;20:1–31.
4. Dell TR, Clutter JL. Ranked set sampling theory with order statistics background. Biometrics. 1972;28:545–555.
5. Khan, Z., Muhammad, A., Aftaf, M. H. and Ismail, M. (2022). Modified median ranked set sampling scheme for estimating population mean. *International Journal of Computational Intelligence in Control*, 14(9), 121-127.
6. Khan, Z., & Ismail, M. (2019). Modified Ratio Estimators of population mean based on ranked set sampling. *Pakistan Journal of Statistics and Operation Research*,15 (2), 445-449.
7. Khan, Z., Ismail, M., & Noor-ul-Amin, M. (2022). Stratified mixture ranked set sampling for estimation of population mean and median. *Pak. J. Statist*, 38(2), 197-210.
8. Khan, Z., Ismail, M., & Samawi, H. (2020**)**. Mixture ranked set sampling for estimation of population mean and median. *Journal of Statistical Computation and Simulation*, 90(4), 573-585.
9. Khan, Z., & Ali, A. (2022). Anemia and its Causes among Children in District Dir Lower Applying Ranked Set Sampling Method for Data Collection. *Research Journal of Social Sciences and Economics Review*, *3*(4), 34-37.
10. Samawi, H. M. (1996a). Stratified ranked set sample. *Pakistan Journal Of Statistics*, 12, 9-16.
11. Samawai, H. M., & Saeid, L. J. (2004). Stratified extreme ranked set sample with application to ratio estimators. *Journal of Modern Applied Statistical Methods*, 3(1), 117-133.
12. Ibrahim, K., Syam, M., & Al-Omari, A. I. (2010). Estimating the population mean using stratified median ranked set sampling. *Applied Mathematical Sciences*, 4(47), 2341-2354.
13. Al-Omari, A. I., Kamarulzaman, I., & Syam, M. I. (2011). Investigating the use of stratified percentile ranked set sampling method for estimating the population mean. *Proyecciones (Antofagasta)*, 30(3), 351-368.
14. Mahdizadeh, M., & Zamanzade, E. (2018). Stratified pair ranked set sampling. *Communications in Statistics-Theory and Methods*, 47(24), 5904-591

Investigating the Impact of ChatGPT on the Academic Performance of University Students

https://doi.org/10.62500/icrtsda.1.1.26

Proc. 1st International Conference on Recent Trends in Statistics and Data Analytics
Air University Islamabad, Pakistan – May 9, 2024, Vol. 1, pp. 223-234

Investigating the Impact of ChatGPT on the Academic Performance of University Students

[1] Shawal Naveed, [2] Areesha Pervaiz [3] Dr. Muhammad Hamid and [4] Dr. Aamir Raza

[1,2,4] Department of Statistics, Govt. College Women University, Sialkot

[3] Department of Computer Science, Govt. College Women University, Sialkot

Abstract

ChatGPT, an AI-powered language model, is increasingly used by students for writing, learning and assessments. This study explores the influence of ChatGPT on university students' academic performance, examining both its potential benefits and drawbacks. The primary objective is to assess ChatGPT's effectiveness in enhancing student learning outcomes. A quantitative approach is employed, with data collected through questionnaires. Kruskal-Walli's test, Mann-Whitney U test, Chi-square test, ordinal regression analyses and AI techniques are utilized to analyze the data. The results are extremely favorable because all the tests applied in this paper showed significant results because the p-value of every test is less than Alpha value. The results offer valuable insights for policymakers, academics and educators to promote the ethical and responsible use of artificial intelligence within the educational landscape.

Keywords:

AI, ChatGPT, Academic Performance, Education, Machine learning.

1. Introduction

ChatGPT is a chatbot made by OpenAI and it became super popular really quickly after it was launched in November 2022. By January 2023, it had over 100 million users! Because of ChatGPT's success, other companies started making similar chatbots like Gemini, Ernie Bot, and others. Microsoft even made one called Copilot based on ChatGPT's technology.

Some people worry that chatbots like ChatGPT might make people lazy or make it easy to copy stuff from the internet without understanding it. They're also concerned it could spread false information.

You can use ChatGPT online in two versions: one based on GPT-3.5 and the other on GPT-4. These are fancy names for different types of AI models. ChatGPT learns to talk like a human through practice with feedback from people. At first, it was free for everyone to try out, but now OpenAI charges for some features. If you use the free version, you get the older GPT-3.5. The newer GPT-4 version and some extra features are available for paying customers, called "ChatGPT Plus."

This study looks at how ChatGPT, a fancy chatbot that uses advanced AI technology, affects students' grades in school. ChatGPT can talk like a person and help students with their studies by giving them info and helping them learn in a personalized way. Using ChatGPT in schools has changed how students learn and get help with their studies. This study wants to see how ChatGPT helps students, what its limits are, and if there are any ethical issues with using it.

Using ChatGPT in schools encourages students to keep learning and getting better. ChatGPT helps students think and solve problems by talking to them and answering questions. Students can have conversations with Cha/tGPT, ask questions, and learn more about difficult topics. This talking back and forth helps students get smarter and better at talking and thinking about stuff.

Using ChatGPT in schools has its good points, but we need to think about some important stuff too. If students use ChatGPT too much, they might not talk to real people as much, which is important for learning. Also, there's a worry that ChatGPT might not always give the right answers or could show

https://doi.org/10.62500/icrtsda.1.1.26

biases from the info it learned from. So, we need to be careful how we use ChatGPT in schools and make sure it follows the rules and helps students learn in the best way possible.

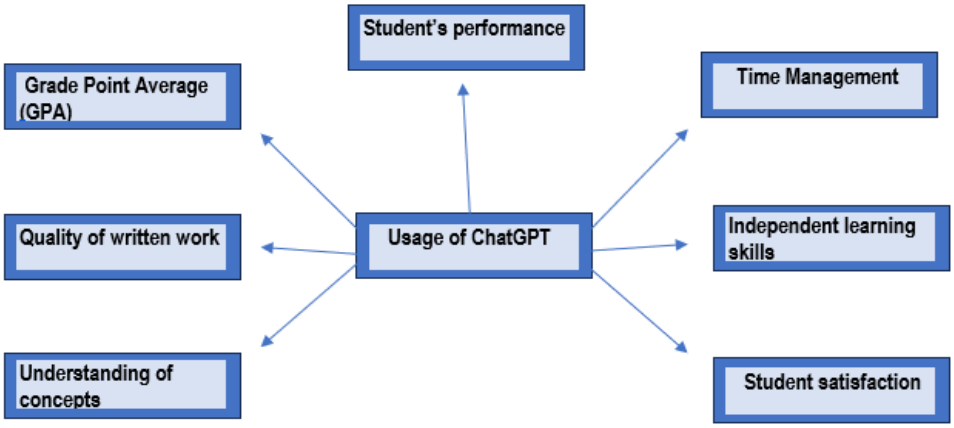

The aim of the research in the first phase is to look into how university students' academic performance is affected by the AI tool ChatGPT. As explained in more detail in the following section, ChatGPT was introduced in November 2022 and is currently a popular app among students. Furthermore, ChatGPT 4 is a premium version; hence, the most popular version is 3.5 out of the several. The final part explains that a 400-sample-size questionnaire was used for the quantitative research, and information was gathered from Government College Women University Sialkot. Various statistical techniques are used in the findings section to examine the relationship between different variables and verify that the model fits the dataset. At the 5% level of significance, it is determined that the results are statistically significant.

2. LITERATURE REVIEW

Learning Analytics (LA) was utilized as a data science approach in the educational area in this study by Rincón-Flores et al. (2020), allowing the measurement, accumulating, and analysis of learners' data and context. The K-Nearest Neighbor and Random Forest artificial intelligence algorithms were applied by the researchers to generate a predictive model for engineering students' academic performance. Given that the projections supplied by each pupil were not particularly precise, an overall grasp of group performance contributed further develop the method of instruction and consequences. Most students also claimed that they were going to be willing to make use of LA, as they felt that obtaining early access to the results of their judgments would enhance their performance in class.

Nurtayeva et al. (June 2023) explained the benefits and drawbacks of ChatGPT and other AI tools in relation to students' academic performance. The study addressed moral issues and ethical use while highlighting the advantages of individualized learning, quick feedback, and enhanced teacher-student connection.

A study on the application of ChatGPT, a generative artificial intelligence (GenAI) tool, in higher education was carried out by Elkhodr et al. (June 2023). Their study examined the possible advantages and disadvantages of using it, with an emphasis on its usefulness as a teaching tool and how it affects student experiences and learning outcomes. The researchers investigated how undergraduate and graduate ICT students perceived ChatGPT as a learning tool using three case studies. The results showed that students had a favorable attitude and thought ChatGPT was a useful and entertaining

https://doi.org/10.62500/icrtsda.1.1.26

learning tool. Many said they would be open to using these AI tools in their upcoming educational endeavors. Additionally, the study showed that students using ChatGPT had better functionality, user flow, and content understanding than students who just used.

Vargas-Murillo et al. conducted a systematic literature review (SLR) in July 2023 to investigate the use of ChatGPT in higher education. They examined papers from various journal databases using certain filtering parameters. The aim of the research was to examine ChatGPT's application, impact on learning, and opportunities and challenges related to AI-assisted learning within the framework of digital education studies. Their results suggest that ChatGPT could enhance processes related to academics and librarians. They do, however, emphasize how important it is to consider the ethical implications of such technology, since it may influence how people approach certain academic procedures and tasks. The study highlights the necessity of using ChatGPT since it can alter professional duties and procedures.

A study by Hanum Siregar et al. (July 2023) examined how students' use of Chat GPT affected their motivation to learn. An AI tool called Chat GPT, which responds to user inquiries via chat, has potential applications in a number of fields, including education, where it might help students study. Data were gathered for the study from 500 participants, who were students from a scouting community in Medan, Indonesia. The study collected data through questionnaires and surveys using a quantitative methodology. Ten questions each for the independent and dependent variables were taken from earlier research instruments and modified to characterize the variables. The hypothesis was tested using linear regression, and tests for multicollinearity, heteroscedasticity, and normality were performed, among other standard assumptions and descriptive statistics.

Two researches on ChatGPT usage among college students have been carried out by Abbas et al. (2024), with an emphasis on the approaches and conclusions. The first study confirmed validity and reliability by designing an eight-item scale to assess ChatGPT usage. A larger sample (N=494) was adopted in Study 2 to confirm the validity of the scale and investigate various additional factors like reward sensitivity and academic workload. Relationships have been examined using structural equation modeling (SEM), and the findings showed that ChatGPT usage increased in association with more workload and time pressure, but declined in likelihood with reward sensitivity. Researchers has linked the use of ChatGPT to lower scores in school, memory loss, and procrastination. Methodologically reliable insights on student use of ChatGPT and its effects on their educational achievement are provided by this study.

Abdaljaleel et al. (2024) looked into the variables affecting views toward and use of ChatGPT among undergraduates in Arab nations. They demonstrated that ease of use, favorable opinions toward technology, social influence, perceived usefulness, and low perceived dangers all had an influence on positive attitudes and consumption through the implementation of the "TAME-ChatGPT" survey to 2240 participants. Major impacts based on age, university type, country of residence, and recent

https://doi.org/10.62500/icrtsda.1.1.26

academic success have been found by multivariate analysis. The efficiency of "TAME-ChatGPT" as a tool to evaluate ChatGPT intake in higher education has been proven by the study.

A thorough evaluation of fourteen scientific studies evaluating the integration of ChatGPT into educational settings until April 10th, 2023 was done out by Albadarin et al. in April 2023. Their analysis stressed ChatGPT's functionality as a virtual assistant that promotes students' grades, learning processes, and capabilities. Findings from three investigations (21.4%), however, revealed specific drawbacks, such as impaired imagination and collaborative learning competencies as an outcome of an unreasonable reliance on ChatGPT. ChatGPT assisted professors grow more effective and productive and implement a wide range of teaching approaches. For ChatGPT to be able to use in education efficiently recommendations emphasized the demand for clear regulations, support, and planned training. The review supports further inquiry and conversation among stakeholders and policymakers, and it is a useful tool for practitioners aiming at incorporating ChatGPT into methods of instruction.

The possible benefits as well as challenges of implementing ChatGPT, a cutting-edge AI-based language model, into higher education settings were explored in a qualitative study conducted by Malik et al. (April 2023). The present study evaluated the various implications of ChatGPT on research, teaching, learning, and student assessment through semi-structured interviews with twelve prominent scholars from Asia, Europe, and North America. Results of their research demonstrate ChatGPT has the potential to boost scholastic output, stimulate original thought, and aid in the development of ideas. However, the study also brought attention to moral questions about risks of excessively depending on ChatGPT and intellectual integrity. While underlining the significance of responsible and ethical AI use in researchers, this research brings nuanced insights into the revolutionary possibilities of ChatGPT to the ongoing debate about AI integration in education.

The performance impact of ChatGPT on higher education students was examined by Chen et al. (2023) through a survey study. Probabilistic least squares (PLS) structural equation modeling was implemented for data analysis following 448 university students were polled. With technical characteristics having direct performance consequences, the assessment displayed verification for all eight of the exploratory possibilities. Remarkably, overall excellence proved out to be a significant factor that determined how it impacts on performance, altering it indirectly through compatibility, task-technology fit, and technology characteristics. Following that in prominence was related to technology amenities, with compatibility qualifying as the most crucial mediating aspect. Apart from to offering developers insight into how they can make ChatGPT services more appealing, the study offers valuable guidance to students on how to make use of the app ethically while researching.

In his exploration of the increasing utilization of artificial intelligence in education, particularly for chatbots including ChatGPT, Oranga (2023) tackles students from kindergarten to graduate. Applying ChatGPT as the main source of knowledge, this paper analyzes the pluses, obstacles, along with the drawbacks related to employing AI in education. Immediate feedback, round-the-clock connectivity,

https://doi.org/10.62500/icrtsda.1.1.26

and individualized learning are just a few of the perks. Whilst ChatGPT alongside other AI technologies can improve educational opportunities, it is important to note that these devices should not take over the duties of human educators. As chatbots operate optimally when accompanied by human supervision and guidance it promotes collaboration between them instead, guarantee trainees acquire an adequate and fruitful education.

Tewari et al. (2023) explore whether artificial intelligence is being utilized extensively in education, including a specific focus on chatbots like ChatGPT which have been employed at all levels of learning, from kindergarten to graduate school. With ChatGPT functioning as the foundational knowledge source, this investigation evaluates all the benefits, obstacles, along with the drawbacks of using AI in education. It draws attention to benefits including real-time feedback, round-the-clock connectivity, and customized learning. The report does, however, stress the value of human instructors and the idea that AI tools should not take their place. Rather, it promotes cooperation between chatbots and human teachers since joint learning is the most effective. By incorporating the benefits of both AI and human instruction, this guarantees that students obtain a thorough as well as effective education.

The research that took place in 2023 by Delello et al. polled 165 college students on their understanding and views regarding ChatGPT and AI. The outcomes demonstrated an excellent degree of familiarity (71.5% for ChatGPT, 98.2% for AI), even though reservations have been expressed over the insufficient use of AI by instructors along with potential hazards which includes plagiarism. The study emphasizes the necessity it is for administrators to update themselves and students about how artificially intelligent technology publications, whether data is processed, as well as how ethical integration of AI can enhance teaching and learning.

The Generative Pre-training Transformer (GPT), an AI-powered system that enables text-based conversational interactions, has been looked at by Jumriah et al. (2024) in their article. GPT delivers adaptable features which include educational assistance, enhancement of productivity, recommendation provision, and language translation. Personalized learning, accessibility, interactive resources, assignment and problem-solving encouragement, and more are all perks that GPT brings in the context of education. Nevertheless, it has limitations as well, such as inadequate comprehension incompetence of substitute artistic endeavors, and insufficient detail tendencies. Likewise, it demands an uninterrupted internet connection and has difficulties telling reality from opinion. Even if GPT Chat is useful for immediate information retrieval, summaries, and other research jobs, it should not entirely substitute manual research procedures. To fully reap the benefits of GPT Chat and solve present challenges, further research and development are required.

In their review, Shehri et al. (2023) dig into the use of cutting edges AI models, like ChatGPT, inside the instructive scene. ChatGPT, an imaginative language learning model created by OpenAI, shows potential for reforming training by improving showing approaches, encouraging expanded understudy

https://doi.org/10.62500/icrtsda.1.1.26

commitment, and working with customized opportunities for growth. Regardless of these promising perspectives, the expected disadvantages of ChatGPT innovation stay questionable. This paper plans to examine the effects of ChatGPT on understudies' scholarly execution, with specific regard for the job of 'brief designing' in molding these impacts. Utilizing a quantitative methodology, the exploration examines the impact of ChatGPT on understudy scholastic execution across different colleges in Pakistan. Through a web-based review conveyed among 37 understudies from different organizations, the review surveys segment subtleties and the effect of ChatGPT on scholarly execution measurements like learning, work quality, and innovativeness, with brief designing filling in as an interceding factor. SPSS investigation, combined with Cronbach's alpha to guarantee dependability and inward consistency of reactions, uncovers a huge relationship among the gathered information. Discoveries recommend a positive connection between ChatGPT utilization and scholarly execution. Nonetheless, regardless of understudies' familiarity with ChatGPT capacities, the greater part does not use it for assessment arrangement. In addition, the review highlights the intervening job of brief designing, underscoring the crucial significance of viable brief plan in enhancing the instructive advantages of computer-based intelligence advancements like ChatGPT.

Investigating the implications of involving Chat GPT (Generative Pre-trained Transformer) into technology education, Hakiki et al. (2023) conducted an experimental study at Universities Muhammadiyah Muara Bungo. The experimental group performed Chat GPT, whereas the control group followed conventional approaches. Indicating Chat GPT's favorable contribution to student learning outcomes, the experimental group's level of achievement were substantially greater, as shown by the results. The significance of what was found had been confirmed by statistical analysis applying a t-test having a 95% confidence level. This investigation highlights the way AI-powered chatbots, for instance Chat GPT, could enhance educational surroundings; consequently, more research needs to be conducted until these chatbots are widely implemented in every sort of circumstances.

The emergence of Generative Pre-trained Transformers (GPT) for instance OpenAI's ChatGPT represents an aspect of the manner in which artificial intelligence (AI) has substantially altered education in recent years. Whereas these models possess tremendous pledge, their widespread use and transparency develop concerns. They are capable of creating evidence that seems to be writing by humans as well as carry out automated conversations. The incorporation of ChatGPT into the system of education has brought about contrasting viewpoints; while it demonstrated exceptional proficiency and grabbed attention, a few see it as progressive, while others wonder about its prospective consequences for ethics and thinking critically. By addressing those procedures, the current study strives to expand the knowledge of how computational intelligence (AI) technologies have altered education in contemporary times.

The potential effects of artificial intelligence (AI) chatbots, with a particular focus on OpenAI's ChatGPT, on higher education institutions (HEIs), have been examined in the present article by

https://doi.org/10.62500/icrtsda.1.1.26

Abdillah, H. Z., Partino, P., & Madjid, A. (2023) via a systematic literature review strategy. The researchers evaluated databases including PubMed, IEEE Xplore, and Google Scholar to meticulously choose pertinent literature. They gave precedence to peer-reviewed paperwork, trustworthy news outlets, and English publications, and they omitted any mentions of tangential chatbots that utilized AI. The study intends to pinpoint significant improvements and characteristics in the installation of AI chatbots in colleges and universities through applying a meticulous approach. This will bring to light both the positive and negative aspects of this new technology.

Participants from the Croatian education system were questioned about their usage and perception of Chat GPT in a study conducted by Aleksić-Maslać, K., Borović, F., & Biočina, Z. (2024). About 265 respondents have been divided into three separate groups: lifelong learners (N3 = 33), educators (N2 = 69), and students (N1 = 163). Everyone who participated obtained surveys. The evidence demonstrates a variety of usage levels, with lifelong students and instructors having a smaller amount of acquaintance. Despite this, Chat GPT illustrated advantageous to every demographic, particularly those in educational and business purposes. Accuracy was widely respected. Students acknowledged concerns about AI replacing specialized occupations however educators and lifelong learners felt assured in their future employment possibilities. All groups evaluated a little less on ethics and general views toward Chat GPT, even if they recognized its versatility. There is a promise of further study on respondent features. For tailored instruction, Chat GPT exhibits potential overall.

In order to discover the numerous ways in which gender, grade level, major, and preceding experience fluctuate in university students' perceptions of Chat GPT, Yilmaz et al. (2023) constructed and verified an instrument. Observations from the Science and Mathematics Education Program, which encompassed 239 students, suggested a majority of positive viewpoint. Fortunately, there were substantial differences in "Perceived social influence" amongst majors and experience levels, in addition to variations in "Perceived ease of use" pertaining to gender. Higher education chat systems designed with AI have been influenced by these findings.

Although there have been numerous studies on the AI tool Chat GPT conducted in numerous other nations, the focus of our investigation will be on Chat GPT's effect on students' academic achievement. Some aspects of Chat GPT related to this subject, such as GPA, the caliber of written work, comprehension of concepts, time management, autonomous learning abilities, critical thinking and problem solving, participation and engagement, attendance, feedback from teachers or peers, student satisfaction, and recommendations, have not yet been studied in developing nations like Pakistan. In order to clarify things, we shall investigate each of these aspects.

Investigating the Impact of ChatGPT on the Academic Performance of University Students

https://doi.org/10.62500/icrtsda.1.1.26

Reference	*Tittle*	*Methodology*	*Result*	*Limitation*	*Citation*
[1]	Analysis of the Use of Chat GPT to Improve Student Performance	Descriptive Statistics , Regression	Significant+ Positive Result	>Causality >Generalizability >Technology Limitations >Ethical Considerations. >Research Design.	(Jumriah, Susilawati et al. 2024)
[2]	Effects of ChatGPT on Students Academic Performance: Mediating Role of Prompt Engineering	Correlation, Reliability	Significant+ Positive Result	>Measurement Validity. >External Factor. >Causality. >Generalizability.	(Shehri, Maham et al. 2023)
[3]	Exploring the impact of using Chat-GPT on student learning outcomes in technology learning: The comprehensive experiment	Descriptive Statistics, Z-Test, T-Test, F-Test.	Significant+ Positive Result	>Sample Size. >Generalizability. >Control Variables. >Technology Constraints. >Time Constraints.	(Hakiki, Fadli et al. 2023)
[4]	Enhancing Student Well-being through AI Chat GPT in the Smart Education University Learning Environment: A Preliminary Review of Research Literature	Descriptive Statistics	Significant Result	>Sample Size and >Representation >Quality of Existing Research >Publication Bias >Ethical Considerations	(Abdillah, Partino and Madjid 2023)
[5]	The Analysis of Chat GPT Usage Impact on Learning Motivation among Scout Students	Regression analyses, Pearson correlation, Kolmogorov-Smirnov	Significant Result	>Increased motivation >Enhanced learning outcomes	(Siregar, Hasmayni and Lubis 2023)
[6]	Exploring College Students' Awareness Of AI & ChatGPT: Unveiling Perceived Benefits and Risks	Non-Parametric Tests	Significant Result	>Sample Bias >Self-report Bias >Ethical Concerns >Limited Scope	(Delello, Sung et al. 2023)
[7]	The Influence of ChatGPT on Social Science Students: Insights Drawn from Undergraduate Students in the United States	Thematic Analysis	Significant Result	>Dependency >Accuracy >Ethical Concerns >Generalizability	(Jowarder 2023)

https://doi.org/10.62500/icrtsda.1.1.26

[8]	Challenges and Opportunities of AI-Assisted Learning: A Systematic Literature Review on the Impact of ChatGPT Usage in Higher Education	Systematic Literature Review (SLR)	Positive Result	>Bias >Privacy Concerns >Lack of Human Touch >Technical Challenges >Overreliance on Technology	(Vargas-Murillo, de la Asuncion and de Jesús Guevara-Soto 2023)

3. Methodology

This study presented the methodology used to look at how ChatGPT impacted the performance of university students. The methodology provided a structured framework for data collection, analysis, and interpretation, which was crucial in confirming the validity and trustworthiness of the study's conclusions. The site of the research included Government College Women University Sialkot, which was chosen because of its vibrant academic environment and growing emphasis on the use of technology in the classroom. The choice to focus only on female students recognized the need for doing gender-conscious research.

The approach to choosing survey respondents was purposive sampling, which is often referred to as judgmental sampling. The researcher's personal assessment was the basis for this strategy when selecting individuals from the target audience. After 400 people were contacted and asked to respond to the survey, a sizable dataset was acquired for examination(Krejcie and Morgan 1970). Due to the participation of participants from several academic departments, such as computer science, information technology, mathematics, statistics, and other related subjects, a wide range of academic backgrounds and opinions were covered in the research.

The study's questionnaire was thoughtfully created to evaluate a variety of components that contribute to academic performance, including critical thinking, problem-solving abilities, and engagement. GPA and other quantitative measures were also included. To give a complete view of students' academic practices and habits, the questionnaire covered variables such as time management, ability to learn independently, and quality of written work.

Quantitative Research

- **Survey Instrumentation:**

  A survey questionnaire was developed in order to collect quantitative data on students' use of ChatGPT, their opinions about its benefits, and their academic performance. Both closed-ended and Likert-scale items were included in the questionnaire to help gather organized information that could be statistically analyzed.

- **Sampling Strategy:**

https://doi.org/10.62500/icrtsda.1.1.26

Data from a number of departments was acquired utilizing simple random sampling, but because of errors in the dataset, purposive sampling which gets data based on judgment was employed as a replacement. A power analysis was implemented to determine the sample size needed to provide the study with adequate statistical power.

- **Data Collection:**

In order to reach a wider and more varied sample of students, the survey was conducted online through the use of an online survey platform. With the goal to increase participation rates, incentives were offered to participants who were recruited through academic forums, social media, and email invitations. Hard copy questionnaires were also used to gather information.

- **Data Analyses:**

The data was analyzed through non-parametric tests because the information collected was not normally distributed. The variables were tested using chi-square, Kruskal-Wallis, Mann-Whitney U, and ordinal regression tests. Machine learning methods will be employed to estimate the data for subsequent analyses.

4. Results

- **Chi-square Analysis**

The chi-square test is used to examine if observed frequencies are significantly different from expected frequencies or whether there is a significant association between categorical variables in a contingency table. (McHugh 2013)

- **Ordinal regression**

By predicting the probability of each ordinal result and shedding light on the ordinal character of the relationship, ordinal regression is used to evaluate the relationship between an ordinal dependent variable and one or more independent variables.(Tutz 2022)

- **Mann-Whitney U test**

When the outcome variable is ordinal or continuous and the assumptions of parametric tests, such as the t-test, are not satisfied (e.g., non-normality or uneven variances), this test is used to compare the medians of two independent groups.(McKnight and Najab 2010)

- **Kruskal-Walli's test**

https://doi.org/10.62500/icrtsda.1.1.26

The medians of three or more independent groups are compared using this test, which is an extension of the Mann-Whitney U test. It is an alternative to the one-way analysis of variance (ANOVA) test that is non-parametric.(Chen, Ma et al. 2023)

In this article, various techniques were applied to the dataset. At first, Harman's single factor test was used to detect the bias, and then reliability was checked. After this, the chi square test of independence was applied to analyze whether the two variables were independent or not. In addition, to check the strength of the relationship between dependent and independent variables, ordinal regression is used. Furthermore, two non-parametric tests (Kruskal-Walli's test and Mann-Whitney U test) were applied to check the difference between two or more independent groups.

"Reliability"

		N	*%*
Cases	***Valid***	389	99.5
	Excluded	2	.5
	Total	400	100.0

Case Processing Summary

Reliability Statistics

Cronbach's Alpha	*N of items*
.936	42

Before the analyses on the dataset, first the reliability test is applied to the dataset by using Cronbach's alpha, and the value should be greater than 0.7 for the good reliability of the dataset, so our value is 0.93, which indicates that our data is reliable.

"Common Method Bias"

Extraction Sums of Squared Loading		
Total	***% of Variance***	***Cumulative%***
12.037	30.092	30.092

Common Method Bias (CMB) plays an important role to ensure the reliability, validity and accuracy of research results especially in fields where survey research is frequently used. It is mostly used in research methodology because it may help the researchers to draw their results more accurate about the relationship between variables. Harman's single factor is a test which is used to determine whether CMB is a significant element in your research. This is because all of the questions, which measure hidden factors, are combined into a single common factor. A single factor's total variance less than 50% indicates that CMB may not have any effect on your data. It means our results shows that there is no biasness in our data. Keep in mind that Harman's strategy involves testing for CMB rather than controlling for it.

"Ordinal Regression"

		Estimate	Std. Error	Wald	df	Sig.	95% Confidence Interval	
							Lower bound	Upper bound
Threshold	[GPA1=1.00]	-.445	.419	1.130	1	.288	-1.266	.376
	[GPA1=2.00]	1.206	.394	9.389	1	.002	.435	1.977
	[GPA1=3.00]	2.852	.415	47.133	1	.000	2.037	3.666
	[GPA1=4.00]	5.301	.475	124.557	1	.000	4.370	6.232
Location	QualityOfWrittenWork1	0.364	.105	11.947	1	.001	.158	.570
	UnderstandingOfConcepts	0.393	.094	17.306	1	.000	.208	.578

Goodness-of-Fit

	Chi-Square	df	Sig.
	109.940	82	.021
	114.319	82	.011

Pseudo R-Square

Cox and Snell	.110
Nagelkerke	.117
McFadden	.042

Model	***-2 Log Likelihood***	***Chi-Square***	***df***	***Sig.***
Intercept	306.010	46.634	2	.000
Final	259.375			

Parameter Estimates

Test of Parallel Lines

Model	**-2 Log Likelihood**	**Chi-Square**	**df**	**Sig.**
Null Hypothesis	259.375	26.730	6	.000
General	232.645			

The above table indicates the results of ordinal regression, in which the dependent variable is GPA and there are two independent variables (quality of written work and understanding of concepts). In the model summary, the value of the chi-square test assesses whether the model significantly improves the prediction compared to a null model with no predictors. A significant chi-square indicates that the model provides a better fit than the null model. SPSS may provide various model fit statistics, such as the Nagelkerke R^2 or Cox & Snell R^2. These statistics indicate the proportion of variance in the outcome

https://doi.org/10.62500/icrtsda.1.1.26

variable explained by the model, so the results are statistically significant because the p value is 0.01, which is less than the 0.05 level of significance.

"Chi Square"

		How likely are you to recommend the use of ChatGPT to your peers for academic purposes?					***Total***
		Very unlikely	***Unlikely***	***Neutral***	***Likely***	***Very Likely***	
How satisfied are you overall with the use of ChatGPT in your academic journey?	***Very dissatisfied***	8	3	4	5	0	20
	Dissatisfied	6	7	17	13	3	46
	Neutral	9	11	85	54	4	163
	Satisfied	3	5	38	77	14	137
	Very Satisfied	2	2	3	10	17	34
Total		28	28	147	159	38	400

Symmetric Measure

		Value	***Asymp. Std. Error***	***Approx. T***	***Approx. Sig.***
Ordinal by Ordinal	***Kendall's Tau-b***	.355	.044	7.838	.000
	Gamma	.490	.057	7.838	.000
N of Valid Cases		***400***			

The above tables show that the two factors (student satisfaction level and student recommendations to their peers to use ChatGPT in education) are associated with each other. Kendall's tau b and Gamma are used for ordinal datasets, and the p value is 0.01, which is less than 0.05, which means that we are rejecting our null hypothesis that there is no association between two variables, so the results are statistically significant

"Kruskal-Wallis Test"

Null Hypothesis	***Test***	***Sig.***	***Decision***
The distribution of GPA is the same across categories of To what extent has ChatGPT helped you in understanding and clarifying academic concepts?	Independent Samples Kruskal-Wallis Test	.000	Reject the null hypothesis

Asymptotic significances are displayed. The significance level is .05

https://doi.org/10.62500/icrtsda.1.1.26

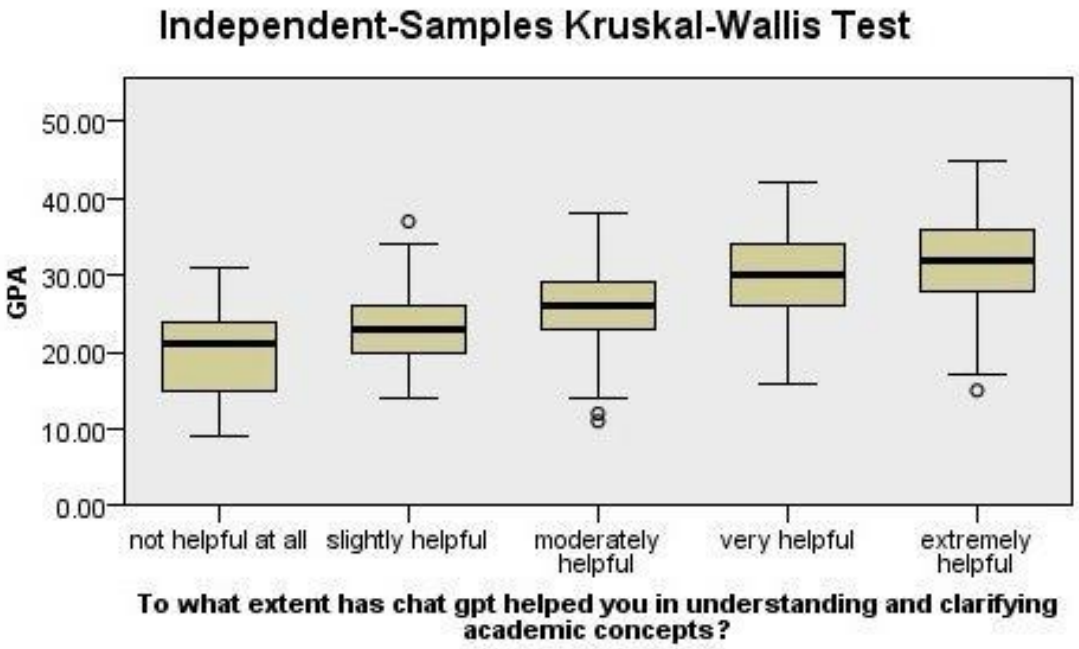

Total N	400
Test Statistics	122.617
Degree of freedom	4
Asymptotic Sig. (2-Tailed)	.000

Test Statistics

According to the results of the Kruskal-Walli's test, there was a significant difference in the distribution of GPA between the different levels of understanding and clarifying academic concepts by using ChatGPT (test statistic= 122.617, p = 0.001), and the highest mean rank of "Extremely helpful" is 297.69 with N = 335. This shows that the GPAs of the students who reported various levels of ChatGPT guidance also varied. For the most part, students with higher GPAs were those who considered ChatGPT to be more useful in explaining academic topics than those who didn't.

"Mann Whitney U-Test"

Has ChatGPT encouraged you to explore additional resources and materials beyond the provided course content?		***N***	***Mean Rank***	***Sum of Ranks***
To what degree do you feel ChatGPT has contributed to your success in exams and assessments?	***Never***	35	56.41	1974.50
	Rarely	97	70.14	6803.50
	Total	132		

Test Statistics

	To what degree do you feel ChatGPT has contributed to your success in exams and assessments?

https://doi.org/10.62500/icrtsda.1.1.26

Mann-Whitney U	1344.500
Wilcoxon W	1974.500
Z	-1.885
Asymp. Sig. (2-Tailed)	.059

The results showed a number of values, Z-value is -1.885 and p-value is 0.059 which is equal to 0.05 and hence we will reject the null hypothesis. The U statistic is a measure of the rank sum of one group relative to the other. It indicates which group tends to have higher ranks in the data. A lower U value suggests that the first group tends to have higher ranks, while a higher U value suggests the opposite. The z-score is a measure of how many standard deviations an observation is from the mean. In the context of the Mann-Whitney U test, the z-score indicates the significance of the difference between the two groups. A larger absolute z-score indicates a more significant difference.

5. Limitation

The study was impacted by a number of constraints, such as biases in the sampling process, biases in self-reporting, and external factors affecting student performance. For the purpose of providing a clear interpretation of the results, these limitations were recognized and solved during the analysis. This methodology section described an in-depth study strategy that integrated quantitative research approaches to offer comprehensive knowledge of the research topic namely, the effect of ChatGPT on student performance. The objective of this study was to provide significant insights into the subject of education and to guide future research and practice by utilizing this methodology and ethical principles.

6. Conclusion

In recent years, artificial intelligence (AI) has progressed significantly. In this era, artificial intelligence plays an important role in every field of life. Artificial Intelligence (AI) technologies, such Chat GPT, can help students enhance their GPA, comprehension of subjects, ability to learn independently, and quality of writing work. This paper investigates the impact of ChatGPT on the academic performance of university students. The result shows that there is a positive impact of using ChatGPT on student's academic performance because P-value of every test is less than Alpha value (α=0.05), which shows that the results are statistically significant. Giving learners writing prompts is essential if you want them to take advantage as much as possible of ChatGPT's educational features. Furthermore, policymakers should introduce AI tools like ChatGPT in educational institutes, and educators should teach the students advanced ways to use these tools efficiently in their studie.

https://doi.org/10.62500/icrtsda.1.1.27

Proc. 1st International Conference on Recent Trends in Statistics and Data Analytics

Air University Islamabad, Pakistan – May 9, 2024, Vol. 1, pp. 235-242

FISCAL DISCIPLINE
Public Financial Management Act 2019 (PFM Act 2019): Implementation Issues
PSDP Projects: Prioritization, Management and Utilization of Barrowed Money

DR. MUHAMMAD AFZAL

Advisor development Projects
Mo Planning, Development & Special Initiatives
Planning Commission, Islamabad

Abstract

Public Sector Development Program (PSDP) is an operational and integral part of public sector investment that is prepared in close coordination with all stakeholders. The efficient utilization of resources in viable development programs/ projects creates multiplier effect for various sectors of the economy to grow. On the other hand, it stimulates the private sector to crowd in and provide enabling environment to attract investment. The overall development goal of the PSDP is to improve the living standards of the people of Pakistan.

After 18th Amendment, the federal government has attached much priority to core projects of national significance mainly in infrastructure, production and social sector being its primary responsibility. The major chunk of PSDP 2023-24 is earmarked for infrastructure projects of energy, railway, motorways/highways, aviation, ports etc. Equal importance is given to social sectors particularly in higher education, health, governance, climate change etc. Agriculture as we all know that it a bone of the economy is also on the redar. Being the pioneer, the present government has revived the CPEC initiative and its allied projects to timely complete for developing linkages among economic hubs, promoting the trade and commerce, inter-provincial / regional connectivity. To achieve self-sufficiency in food and water resources, substantial funds have been earmarked for agriculture related projects. On the other hand, provinces are expected to undertake the projects of provincial nature from their ADPs, as they have been receiving adequate funding under 7th NFC award. However, to supplement the efforts of the provinces, federal government provides sufficient funds for provincial level subjects related to SDGs program etc. To ensure balanced regional development, special provisions have been made in federal PSDP 2023-24 to support less developed areas i.e Baluchistan, Gilgit Baltistan, AJ&K and Merged Districts of KP etc. In addition, special development initiative for Backward/Poor Districts in the Country is being launched to meet the SDGs targets.

The critical questions remain such as;

- **I*s PSDP leading to desired economic growth?***
- ***Are there adequate financing arrangements for throw-forward of projects?***
- ***What is the average lifecycle of projects?***

2 - Introduction & Background

The phenomenon of socio- economic development is directly related to successful implementation of PSDP and ADP and various government initiatives. These initiatives deal with a variety of societal needs, ranging from infrastructural development to social welfare, education, healthcare and economic growth. Understanding the impact and effectiveness with which these policies, plans, programs and projects and initiatives are implemented is a prerequisite to sustainable achievement of National Development Goals.

Historically there has existed PSDP and ADP to fund federal and provincial schemes. At both levels financial space is limited and big constraint as for as the development needs of the areas are concerned. This is also one of the reasons that the federal government is constrained to fund the provincial initiatives. Three years back the size of the PSDP was more than one trillion rupees, which

https://doi.org/10.62500/icrtsda.1.1.27

has been reduced to Rs. 700 billion, which is slightly high than the previous year. The overall development portfolio is around Rs. 2 trillion.

In light of this, the research at hand dares to evaluate PSDP/ ADP development projects, programs and government initiatives in context of Pakistan's National Development Goals. This analysis aims to dig out of these projects, translating it into a tool for an inclusive and comprehensive policymaking and informed decision-making.

3 - **Review of Literature**

- IMF Economic Review Regarding alternatives investment and banking practices for the benefit of emerging and developing economies like Pakistan:
- Khan, Mohsin S. "Islamic Interest-Free Banking: A Theoretical Analysis (Le Système Bancaire Islamique: Analyse Théorique d'un Système Qui Ne Fait Pas Appel à l'intérêt) (La Prohibición Islámica de Los Intereses Bancarios: Análisis Teórico)." *Staff Papers (International Monetary Fund)* 33, no. 1 (1986): 1–27. https://doi.org/10.2307/3866920.
- Birnbaum, Eugene A. "The Cost of a Foreign Exchange Standard or of the Use of a Foreign Currency as the Circulating Medium." *Staff Papers (International Monetary Fund)* 5, no. 3 (1957): 477–91. https://doi.org/10.2307/3866111.
- Greene, Joshua, and Delano Villanueva. "Private Investment in Developing Countries: An Empirical Analysis." *Staff Papers (International Monetary Fund)* 38, no. 1 (1991): 33–58. https://doi.org/10.2307/3867034.
- Cnossen, Sijbren. "Capacity Taxation: The Pakistan Experiment (L'impôt Sur La Capacité de Production: L'expérience Pakistanaise) (Impuesto a La Capacidad: El Experimento Pakistaní)." *Staff Papers (International Monetary Fund)* 21, no. 1 (1974): 127–69. https://doi.org/10.2307/3866694.
- Korean development 5-year plan which was replicated in lines with Pakistan's 5 year plan
- https://www.researchgate.net/publication/298670979_Korea's_Sustainable_Development_Strategy#:~:text=Like%20the%20long%2Dterm%20development,safe%2C%20sustainable%2C%20and%20strong.
- https://eng.kds.re.kr/Main/index.html

4 - **Scope of Research**

PSDP and ADP are not translated into real development due to unnecessary interventions from the political and sometimes bureaucratic corners. We have also seen that most of the projects are not approved on technical grounds due to which it is less likely to get the desired results. Further expenditures do not follow the releases, allocations and cost of the projects. There is great mismatch between these four very integral parts of the phasing of the projects. It is also pertinent to mention that the phasing of funds is not consonant with gestation period. Due to improper phasing, allocations, releases, expenditures, some of the areas of the country are historically neglected and if we conduct a survey we will find out less developed regions and districts from such areas. Balanced development as per Article 156 (2) if not focused, the dream to develop these areas will remain unrealized. These all are violations of constitution as well as PFM Act 2019.

This research is focused on the successes, challenges and implications of the PSDP (Rs. 1150 Billion for the year 2023) / ADP during a period of 10 years (2012-13 to 2022-23) with focus on the Major sectors of economy WRT to their size/ cost of projects that are Infrastructure Sector (52 percent share of Rs. 950 Billion i.e. Rs. 494 Billion) and Social Sector (25.5 percent share of Rs. 950 Billion i.e. Rs. 242.25 Billion)

i. How PSDP/ ADP funded Projects are prioritized for maximizing economic growth?
ii. What should be the mechanism to identify the key areas/ sectors for public investment at the federal and provincial level?

https://doi.org/10.62500/icrtsda.1.1.27

iii. How can national strategic projects be implemented in key priority sectors in regions where they give highest returns?
iv. Is it needs to redefine the scope of PSDP? What should be the mechanism to redefine the scope of PSDP?
v. Should we rely on public sector investment, private sector investment, foreign funded or a mix of two or three?

How can we create synergy between federally conceived and provincially conceived projects to make it National development?

5 - Research Methodology

The comprehensive evaluation of PSDP and Government Initiatives for the period 2023-24 in the context of National Development will be conducted by employing mixed method techniques for providing an insight regarding the numerical as well as non-numerical aspects of the topic at hand.

The Quantitative Technique has been employed to reflect the Financial Cost and pattern of the PSDP projects/ programs against the intended outcomes. The statistical tools and software like Microsoft Excel, Primavera and SPSS are being run on the available data for its interpretation in terms of national development to identify patterns, correlations and extrapolate the results to predict the future course of action.

The qualitative techniques are being employed to explain the contextual realities imparting towards the success or failure of PSDP projects/ programs. These contextual explanations and analysis will measure the influence and impact of various stakeholders that impact the National Development Political representatives, Media, Non-Governmental Organizations, international Agendas, Input from the UN, role of World Bank, Asian Development Bank, Islamic Development Bank and JICA.

6 - **Public Policy Relevance**

The investment made through federal as well as provincial instruments is not accruing results as we expect from it. What is the reason? Is investment made through these instruments on the right direction? What are the major constraints for formulation and execution of these instruments? Is it the responsibility of the development professionals or leftover other stakeholders to set the development agenda? On seeing the economic indicators, no doubt Pakistan is behind from the world and also in our region. Neither it wants to learn from history nor even from the neighboring countries. Does this development model is sufficient enough for our survival? What the social and economic indicators reflect in 21st century. How global challenges and meet international commitments shall be met? All these questions arise in the context of the topic and also directly relates to the realm of public policy, as all these questions will show “Action” or “Inaction” in response to a problem or some matter of concern.

There is dire need to understand the concept of public goods. Who should be beneficiaries of public goods? What responsibilities are at Federal and provincial level? Do we have sufficient resources to provide all public goods to public at affordable resources? Is there constraint of resources or mismanagement or underutilization of these resources? How the public functionaries could reach at optimal level? What could be method to maximize the utility of public buildings?

There is need to set some standards in all products, which are for our common use. The way we are constructing roads, hospital, universities, colleges, schools, they all are different in size, cost and standards. How cost effective, energy efficient, environmental friendly, earthquakes and flood resilient buildings could be constructed.

We all know that we have very limited resources and at the moment development portfolio is based on costly loans. The grim side of the picture is that we are barrowing funds from donor agencies for petty sort of works i.e maintenance of roads, rehabilitation of buildings and some time to provide supplements for our young generation which is not sustainable model at any cost. We are the society who most of the time barrow money for scholarships or to meet day-to-day needs of the nation.

https://doi.org/10.62500/icrtsda.1.1.27

The investment made through federal as well as provincial instruments is not accruing results as we expect from it. What is the reason? Is investment made through these instruments on the right direction? What are the major constraints for formulation and execution of these instruments? Is it the responsibility of the development professionals or leftover other stakeholders to set the development agenda? On seeing the economic indicators, no doubt we are for behind from the world and also in our region. Neither we want to learn from our history nor even from the neighboring countries. Do this development model is sufficient enough for our survival? What the social and economic indicators reflect in 21st century. How we would be able to meet global challenges and meet our international commitments. We are signatory of many global agreements and made commitments i.e. on health environment, labor, narcotics, SDGs etc.

For the purpose of standardization, set a direction of investment for development of the country, stimulate and promote growth and focus on export led development, made resources available for big ticket items by the federal government and give more autonomy to the provinces so they could take decision to carry their development agenda, define the lines to barrow money from development partner agencies in future, realization of federal and provincial functions, effort is being made at planning commission to prepare agreed document which will set direction for future. Define the federal and provincial development jurisdictions for the purpose optimal use of financial as well as other country resources. The other instruments which have been developed or in pipeline will also supplement to this instrument. We believe that by participation and valuable input from federal entities, provincial governments and area governments this document shall add a good amount of value.

What's Happening? In the absence of any framework at federal as well as at provincial level, the federal government ends up by performing provincial functions and approving development schemes despite the fact that financial resources have been dried. Clarity of functions and jurisdiction does not exist at federal and provincial level. Hence investment proposals from the provinces are submitted for funding from federal PSDP and federal government seems working like provincial government.

During the CDWP meetings, one of the key issues highlighted is the lack of clear distinction between federal and provincial functions for development. Projects that are submitted by provincial governments to tap funds from PSDP, forum (CDWP) feels that these activities mostly fall under the domain of provinces. There is no clear approved framework that outlines areas requiring federal investment.

The Constitution also mentions various development fora, which considers, approves/disapproves economic policies, programs and projects, and deliberates on economic issues of the country. Article 156(2) of the Constitution 1973 of the Islamic Republic of Pakistan, lays down the core functions of the National Economic Council (the, "NEC") as under:

> **"The National Economic Council (NEC)** shall review the overall economic condition of the country and shall, for advising the Federal Government and the Provincial Governments, formulate plans in respect of financial, commercial, social, and economic policies; and in formulating such plans it shall, among other factors, ensured **balanced development and regional equity** and shall also be guided by the principles of policy set in Chapter-2 of part–II."

The above role of the NEC is very clear and binding on the development agencies to set the direction of financial resources. Keeping in view the role assigned to NEC, few questions arise in every development practitioner: - What is balanced development? Does it exist in the country? What is the responsibility of state organs to embrace balanced development? There may be need to align PSDP in a way that less developed areas get the whole allocation of PSDP for the time till these areas are also better off.

There is less likely to meet the SDGs agenda and international commitment if some pockets of the country are neglected and remain undeveloped. It is necessary to have equal opportunities and benefits for these areas. We have different parameters available to judge the economic and social status

https://doi.org/10.62500/icrtsda.1.1.27

of all the districts and tehsils of the country and very recently 20 less developed districts of the country have been identified. On the basis of these evidences we can define and indicate areas where more interventions are required. The incumbent government has made very serious efforts by introducing interventions for these historically neglected areas. Although this is very fruitful effort but lot more is required for these areas.

There is need to understand the devolution concept. Historically, there were three legislative lists in the Constitution: Federal Legislative List, Provincial Legislative List and Concurrent Legislative List. Due to the introduction of 18th Amendment, the Provincial Legislative List and Concurrent Legislative List were omitted. Instead, a Federal Legislative List was introduced having two parts:

a) Part-I of the Federal Legislative List: the federal government has the constitutional powers to make laws.

b) Part-II of the Federal Legislative List: in accordance with Article 154 of the Constitution, the Council of Common Interests (CCI) shall formulate and regulate policies in relations to the matters enumerated therein and shall exercise supervision and control over related institutions.

The responsibility of the federal government has been increased manifold as for as the hand holding of the provincial and area governments is required. The federation has own more responsibility to invest more in those areas, which fall under its domain to strengthen the federating units.

PSDP/ADPs:

Historically we have these two instruments to fund federal and provincial schemes. At both levels financial space is limited and big constraint as for as the development needs of the areas are concerned. This is also one of the reasons that the federal government is constrained to fund the provincial initiatives. Below table shows the size of the PSDP and ADPS for the year 2023-24. Three years back the size of the PSDP was more than one trillion rupees, which has been reduced to Rs. 700 billion, which is slightly high than the previous year. The overall development portfolio is around Rs. 2 trillion. What are the objectives of these instruments: -?

a) PSDP is an important policy instrument for achieving the socio-economic objectives of the government at federal level

b) The provincial ADPs translate provincial economic strategies in development projects. It is the main channel for funding development schemes in provinces

Table - 1: PSDP and ADP Size 2023-24

PSDP / ADP	Rupees component	Foreign component	Total
PSDP	**875+200 VGF**	**75**	**1150**
ADP	**990**	569	1,559
-Punjab	*300*	*126*	*426*
-Sindh	*350*	*267*	*617*
-Baluchistan	*130*	*138*	*268*
-Khyber Pakhtunkhwa	*210*	*38*	*248*
Total:	**1,865**	**644**	**2,932**

Source: PSDP-ADP **(Rs. in Billion)**

The question arises why provincial schemes are funded from PSDP. As per constitution federal government can fund schemes in those areas, which are behind in development pace or less developed due geographical constraints. Provincial schemes funded over the period of time are listed below to give fare idea that this funding is provided across the board ignoring the above-mentioned constitutional provisions. The only way for prosperous Pakistan is to invest in a way that each part of the country has equal economic, social and other required opportunities. The areas, which are less populated, may not some time get proper attention due to certain reasons.

https://doi.org/10.62500/icrtsda.1.1.27

Table–2: Funding for Provincial Schemes from PSDP (2015-2024)

Year	Cost	Allocation	%age
2015-16	142.4	13.0	9.13
2016-17	114.7	17.2	15.00
2017-18	152.7	47.2	30.90
2018-19	160.0	26.9	16.80
2019-20	219.8	17.2	15.00
2020-21	248.3	99.0	39.87
2021-22	395.31	102.14	25.84
2022-23	1,196.34	262.30	21.93
2023-24	1,372.86	313.38	22.83
Total:	**4,002.41**	**898.02**	**22.44**

Source: PSDP (Rs. in Billion)

Table 3 below showing a pattern of development portfolio i.e. number of schemes their cost, expenditure 2022- 23 and allocations in 2023-24. The allocations for the less developed province is relatively less, as it should have been. This is the main reason that we could not set development agenda in a right way. This is high time to develop consensus in federating units to understand the peculiarities and needs of the areas. The development funds may also be channelized according to the requirements of the areas.

Table -3: Provincial Schemes Funded from PSDP 2023-24

(Rs. in Billion)

Province	No. of schemes	Cost	Exp. Upto 30.06.2022	Allocation 2022-23
Punjab	84	189.71	76.15	16.99
Sindh	56	285.29	108.1	36.24
Khyber Pakhtunkhwa	30	77.01	30.75	8.57
Merged districts	13	3.21	2.33	53.2
Baluchistan	140	280.11	83.43	30.98
Cross Provinces	34	331.83	62.19	120.22
Total:	**357**	**1167.16**	**362.95**	**266.20**

Source: PSDP

Deputy Chairman Planning Commission has very recently identified some issues and concept paper is developed based on these issues, which need immediate attention of policy makers to realign the public investment funding for its optimal utilization. These are very important area and few questions have also been framed that need to be responded. There is also need to explore other funding channels to provide more space to private sector and reduce the government footprint. The areas and questions are reproduced below for further deliberation by the recently notified working group under the chairmanship of Additional Secretary (Admn., Dev. &SI). Subsequently these ideas shall be shared with the provincial as well as area government through workshops.

Issues

The key issues that need to be discussed and addressed are as follows:

1. National strategic project prioritization for maximizing economic growth.

Despite the fact that federal and provincial sectoral strategies have always been present, the public investments in Pakistan have generally been considered to be haphazard and discretionary. There has been little research establishing the impact of sectoral public investments on national and provincial economic growth. Furthermore, there is also no proper estimation of the regional GDP that would

https://doi.org/10.62500/icrtsda.1.1.27

ascertain the accurate contribution of the regions to the national GDP. As a result, a substantial portion of the public investment ends up in sectors whose contribution to the national economic growth is less than optimum. To avoid suboptimal and lopsided investments, it is high time to prioritize public investments in national projects of strategic nature, which promise an all-encompassing national economic growth. Such projects should have joint ownership of the federation and provinces and should be financed through new funding mechanisms in which all federating units pool their share.

Key Questions

There is therefore a need to answer questions like:

a. What should be mechanism to identify the key areas/sectors for public investments at the federal and provincial level to optimize economic growth?
b. How can we identify which province has a comparative and competitive advantage in a particular sector so that public investment can be prioritized towards that sector?
c. How can national strategic projects be implemented in key priority sectors in regions where they promise the highest return?
d. What should be the funding mechanism and arrangements for such projects? Should the funding for such national priority projects be based on some formula like NFC?
e. Are there international examples of such national public investments available in federal state context?

2. Redefining the scope of PSDP

Over the years, the share of provincial allocations in PSDP has become substantial. The implementation of such projects is problematic due to a vague notion of project ownership. The projects at times may be used for political mileage and tilt towards any region, with federal government support, in disregard of a concern for economic efficiency and equity. To ensure transparency and to promote public investments to maximize economic growth, an option worth considering is to restrict the PSDP to the federal government only.

Key Question

What kind of mechanism should be in place through which the PSDP can be confined to projects of national economic impact and outlook like large dams, hydroelectric and nuclear power projects, railways infrastructure, national highways etc?

3. Prioritizing foreign funding

There is a need to direct foreign funding towards the identified national strategic public investment priorities that have the highest impact on increasing economic growth in the country. At present the foreign funding is often donor driven or based on provincial demands and may not support the country's strategic priority sectors.

Key Questions

a. What mechanism should be established through which the provinces can access foreign funding for the identified national strategic priority areas rather than for low priority-low impact isolated projects?
b. What financing arrangements, other than donor funding, can be explored?

4. Synergies and integration of provincial projects

Federal and Provincial projects in sectors such as health, education, infrastructure, urban services, agriculture, industries etc. are generally implemented in isolation. There is no cross learning between provinces and federal government and between provinces themselves that reduces efficiency of such investments when viewed with a lens focused on national economic growth goal. Furthermore, projects of similar nature and types are sometimes implemented using varied methodologies, with

https://doi.org/10.62500/icrtsda.1.1.27

different funding sources and amounts. Integration of such projects can help the provinces achieve economies of scale and optimize public investment spending.

Key Questions

a. How can synergies between provincial projects be created for knowledge sharing?
b. What mechanism can help achieve integration of projects across provinces vis-à-vis national GDP growth objectives?

5. Clarity on devolved subjects

The differences in comprehension of the underlying spirit of the 18th constitutional amendment and its interpretation among the constituent units of federation have a strong bearing upon overall national economic performance. These differences can potentially invoke constitutional jurisdiction of the Supreme Court of Pakistan to help resolve rifts and differences. It is therefore imperative that a clear interpretation of the 18th amendment may be developed through consensus between the federal government and the provinces.

Key questions

How can the federal government and the provinces be brought on the same page in respect of the understanding and implementation of 18th amendment so that public service delivery can be optimized?

Provincial Subjects After 18th Amendment

Police 2. Administration of Justice 3. Prisons 4. Local Government 5. Public Health & Sanitation 6. Food and Agriculture 7. Public Works 8. Population Welfare 9. Provincial Forests 10. Fisheries 11. Industries	12. Relief & Rehabilitation 13. Information 14. Education 15. Culture 16. Livestock 17. Social Welfare and Women Development 18. Tourism 19. Health 20. Sports 21. Mini Dams, Command Area Dev. & Water Distribution Network

Bibliography

The principals of policy; Constitution Islamic Republics of Pakistan 1973

18th constitutional amendment amendment

PFM Act 2019 Ministry of Finance, Government of Pakistan

PIMA-CPIMA report, prepared by the Planning Commission of Pakistan in collaboration with IMF.

Manual of development projects, Ministry of Planning Development and Special Initiatives, Planning Commission of Pakistan

PSPD documents issued from time to time by Planning Commission of Pakistan

Annual Development Plans of provincial as well as Area Government i.e. GB and AJK.

https://doi.org/10.62500/icrtsda.1.1.27

Pakistan Institute of development economics reports on development expenditure

https://doi.org/10.62500/icrtsda.1.1.28

Proc. 1st International Conference on Recent Trends in Statistics and Data Analytics
Air University Islamabad, Pakistan – May 9, 2024, Vol. 1, pp. 243-252

Applications of Perturbation Method to Solve Nonlinear Differential Equations

Muhammad Izaan Ullah Khan[1] and Khalil Ahmad[2]
Department of Mathematics, Air University, PAF-Complex E-9, Islamabad, Pakistan

ABSTRACT

In this research paper, our aim is to find analytic solutions of nonlinear differential equations using perturbation method. The method deforms a difficult problem into simple problem, which can easily solve. The results are compare with the results obtained by exact solutions and ode45. The results expose that the method is very effective, convenient and quite precise to nonlinear differential equations. We show result graphically and tabular form and plot absolute and residual errors.

1. INTRODUCTION

Nonlinear differential equations are one of the most difficult problems in mathematical modeling because of their complexity and lack of precise analytical solutions. Our main goal in this study work is to take on this obstacle headon by using the perturbation method's power to get analytic solutions for nonlinear differential equations. The perturbation method provides a methodical way to approach problems, making them easier to solve by breaking them down into smaller, more manageable ones. Our research aims to demonstrate the effectiveness, practicality, and accuracy of this approach for solving nonlinear differential equations.

The goal of our research is to contrast the results found using the perturbation approach with those found using precise analytical techniques and numerical solvers such as ode45. We examine the agreement between these findings in order to evaluate the accuracy and dependability of the perturbation approach in describing the behavior of nonlinear systems. We also provide our results in tabular and graphical representations so that a thorough display and study of the data is possible. We also carefully examine the absolute and residual errors related to the perturbation method's solutions, shedding light on the method's effectiveness and highlighting its promise as a useful tool for resolving nonlinear differential equations.

In this particular context, the perturbation method is highly significant because it provides information about the behavior of nonlinear systems that would otherwise be challenging to get using precise analytical or numerical methods. The perturbation approach facilitates the understanding of stability, bifurcations, and other critical phenomena by offering a way to comprehend the underlying dynamics of complicated systems through the systematic approximation of solutions. [3]

2. METHOD DESCRIPTION

2.1 Regular Perturbation Method

In this method assumes the solution of the ODE of the form $y(x) = y_0(x) + \varepsilon y_1(x) + \varepsilon^2 y_2(x) + \ldots$, and then substituted in the original equation to get the desired result.

To use this method the pattern is follows

2.1.1 Identify the Perturbation Parameter:

Determine a small parameter (typically denoted by ε) that scales the terms in the differential equation. This parameter represents the "size" of the perturbation or deviation from a simpler problem. [2]

2.1.2 Expansion of Solution:

https://doi.org/10.62500/icrtsda.1.1.28

Expand the solution to the differential equation as a power series in the small parameter ε. This expansion takes the form of $y(x) = y_0(x) + \varepsilon y_1(x) + \varepsilon^2 y_2(x) + \ldots$, where each term represents a correction to the leading-order approximation $y_0(x)$. [2]

2.1.3 Substitution:

Substitute the expanded solution into the original differential equation. This yields a sequence of equations at different orders of ε. [2]

2.1.4 Order-by-Order Analysis:

Equate coefficients of like powers of ε on both sides of the equation obtained from substitution. This gives a series of equations that can be solved recursively to determine each correction term in the expansion. [2]

2.1.5 Boundary or Initial Conditions:

Apply any boundary or initial conditions to determine the coefficients in the expansion. This typically involves matching coefficients of the power series to the known conditions. [2]

2.1.6 Asymptotic Analysis:

Analyze the behavior of the solution as ε approaches zero. In some cases, the series may converge to an exact solution, while in others; it may provide an asymptotic approximation valid for small ε. [2]

2.1.7) Error Estimation:

Estimate the error introduced by truncating the series at a finite order. This is important for assessing the accuracy of the approximation and determining the range of validity of the perturbation method. [2]

3. APPLICATIONS

Problem1

Gravitational Formula Correction with Regular Perturbation Method

$$\frac{d^2y}{dt^2} = \frac{-1}{(\varepsilon y+1)^2} \tag{1}$$

$$y(t + \varepsilon) = y_0(t) + \varepsilon y_1(t) + \varepsilon^2 y_2(t) + O(\varepsilon^3) \tag{2}$$

Where y_0, y_1, y_2 are unknown functions of t. (2) is known as the perturbation of the solution in terms of the parameter ε. By substituting (2) into the differential equation (1) and gathering powers of ε, we attain the following perturbation equation:

$$\frac{d^2y_0(t)}{dt^2} + \varepsilon\frac{d^2y_1(t)}{dt^2} + \varepsilon^2\frac{d^2y_2(t)}{dt^2} = \frac{-1}{\left(\varepsilon\left(\frac{dy_0}{dt} + \varepsilon\frac{dy_1}{dt} + \varepsilon^2\frac{dy_2}{dt}\right)+1\right)^2} \tag{3}$$

This equation must be satisfied for any value of ε.

Compare the order of ε^0

$$\frac{d^2y_0(t)}{dt^2} = 1 \tag{4}$$

The solution of the (4)

https://doi.org/10.62500/icrtsda.1.1.28

$$y_0(t) = +\mathrm{t} - \frac{t^2}{2} \tag{5}$$

Compare the order of ε^1

$$\left(\frac{d^2 y_1(t)}{\partial d}\right) = 2y_0(t) \tag{6}$$

The solution of the (5)

$$y_1(t) = -\frac{t^4}{12} + \frac{t^3}{3} \tag{7}$$

Compare the order of ε^2

$$\left(\frac{d^2 y_2(t)}{dt^2}\right) = 2y_1(t) \tag{8}$$

The solution of the (8)

$$y_2(t) = -\frac{t^6}{180} + \frac{t^5}{30} + t \tag{9}$$

Put the (5), (7) and (9) in the (2), we will get:

$$y(t+\varepsilon) = \mathrm{t} - \frac{t^2}{2} + \varepsilon\left(-\frac{t^4}{12} + \frac{t^3}{3}\right) + \varepsilon^2\left(-\frac{t^6}{180} + \frac{t^5}{30} + t\right) + O(\varepsilon^3) \tag{10}$$

(10) is the solution of the (1).

t	f(t)	F(t)	|F(t)-f(t)|
0	0	0	0
0.2	0.1638	0.1822	0.0184
0.4	0.3147	0.3259	0.0212
0.6	0.4224	0.4321	0.0197
0.8	0.4643	0.5017	0.0174
1	0.5	0.5352	0.0352
1.2	0.4643	0.5329	0.0486
1.4	0.4224	0.4948	0.0824
1.6	0.3147	0.4248	0.1201
1.8	0.1638	0.3093	0.1455
2	0	0.1604	0.1604

https://doi.org/10.62500/icrtsda.1.1.28

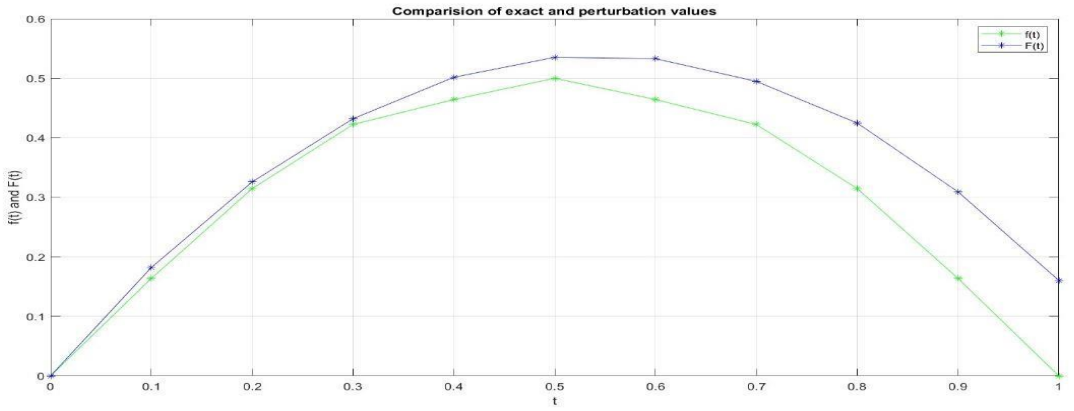

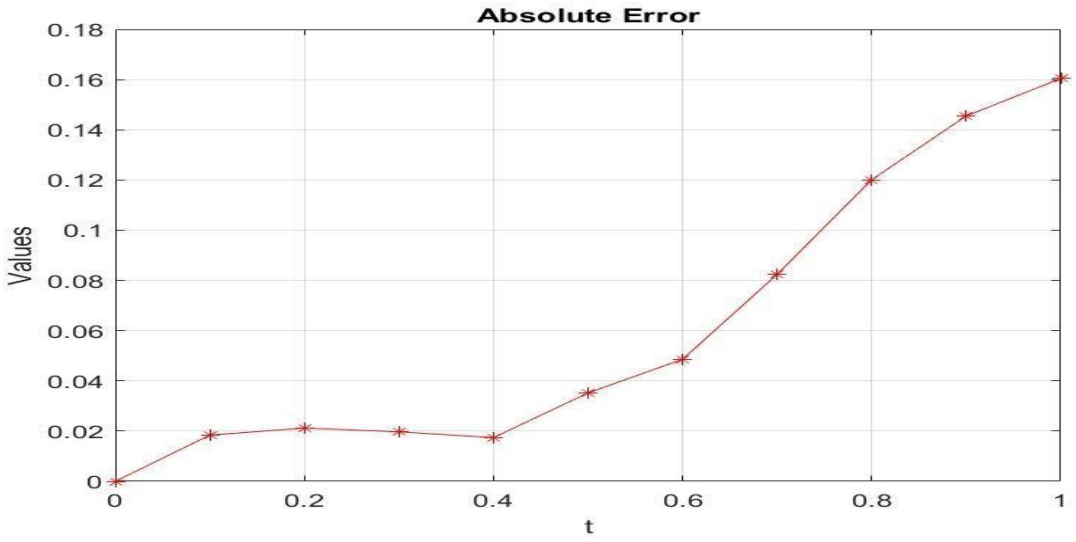

Problem 2

Consider the parameter ε is very small but not zero in the given problem

$$2\frac{d^2y}{dt^2} + 4\frac{dy}{dt} + \varepsilon y = 0 \tag{11}$$

Let us look for a series solution of the form

$$y(t + \varepsilon) = y_0(t) + \varepsilon y_1(t) + \varepsilon^2 y_2 + O(\varepsilon^3) \tag{12}$$

Where y_0, y_1, y_2 are unknown functions of t. (12) is known as the perturbation of the solution in terms of the parameter ε. By substituting (12) into the differential equation (11) and gathering powers of ε, we attain the following perturbation equation:

$$2\left(\frac{d^2y_0(t)}{dt^2} + \varepsilon\frac{d^2y_1(t)}{dt^2} + \varepsilon^2\frac{d^2y_2(t)}{dt^2}\right) + 4\left(\frac{dy_0}{dt} + \varepsilon\frac{dy_1}{dt} + \varepsilon^2\frac{dy_2}{dt}\right) + \varepsilon(y_0(t) + \varepsilon y_1(t) + \varepsilon^2 y_2) = 0 \tag{13}$$

This equation must be satisfied for any value of ε.

Compare the order of ε^0

$$2\left(\frac{d^2y_0(t)}{dt^2}\right) + 4\left(\frac{dy_0}{dt}\right) = 0 \tag{14}$$

https://doi.org/10.62500/icrtsda.1.1.28

The solution of the (14)

$$y_0(t) = \frac{1}{2} - \frac{e^{-2t}}{2} \tag{15}$$

Compare the order of ε^1

$$2\left(\frac{d^2y_1(t)}{dt^2}\right) + 4\left(\frac{dy_1}{dt}\right) + \left(y_0(t)\right) = 0 \tag{16}$$

$$2\left(\frac{d^2y_1(t)}{dt^2}\right) + 4\left(\frac{dy_1}{dt}\right) = -\left(y_0(t)\right) \tag{17}$$

The solution of the (17)

$$y_1(t) = \frac{5}{8} - \frac{5e^{-2t}}{8} - \frac{t}{8} - \frac{te^{-2t}}{8} \tag{18}$$

Compare the order of ε^2

$$2\left(\frac{d^2y_2(t)}{dt^2}\right) + +4\left(\frac{dy_2}{dt}\right) + \left(y_1(t)\right) = 0 \tag{19}$$

$$2\left(\frac{d^2y_2(t)}{dt^2}\right) + +4\left(\frac{dy_2}{dt}\right) = -\left(y_1(t)\right) \tag{20}$$

The solution of the (20)

$$y_2(t) = \frac{65}{128} - \frac{65e^{-2t}}{128} - \frac{11t}{64} - \frac{5te^{-2t}}{32} + \frac{t^2}{64} \tag{21}$$

Put the (15), (18) and (21) in the (12), we will get:

$$y(t+\varepsilon) = \left(\frac{1}{2} - \frac{e^{-2t}}{2}\right) + \varepsilon\left(\frac{5}{8} - \frac{5e^{-2t}}{8} - \frac{t}{8} - \frac{te^{-2t}}{8}\right) + \varepsilon^2\left(\frac{65}{128} - \frac{65e^{-2t}}{128} - \frac{11t}{64} - \frac{5te^{-2t}}{32} + \frac{t^2}{64}\right) \tag{22}$$

(22) is the solution of the (11).

't'	**f(t)**	**F(t)**	**|f(t)-F(t)|**
0.10000000	0.090634	0.090641	7×10^{-6}
0.20000000	0.164839	0.164855	1.6×10^{-5}
0.30000000	0.225594	0.225615	2.1×10^{-5}
0.40000000	0.275335	0.275362	2.7×10^{-5}
0.50000000	0.316059	0.316090	3.1×10^{-5}
0.60000000	0.349401	0.349436	3.5×10^{-5}
0.70000000	0.376700	0.376737	3.7×10^{-5}
0.80000000	0.399049	0.399090	4.1×10^{-5}
0.90000000	0.417347	0.417390	4.3×10^{-5}
1.00000000	0.432328	0.432373	4.5×10^{-5}

https://doi.org/10.62500/icrtsda.1.1.28

Where, Absolute error = |f(t)-F(t)|

Now, consider that ε = 0.0001 then the result will be

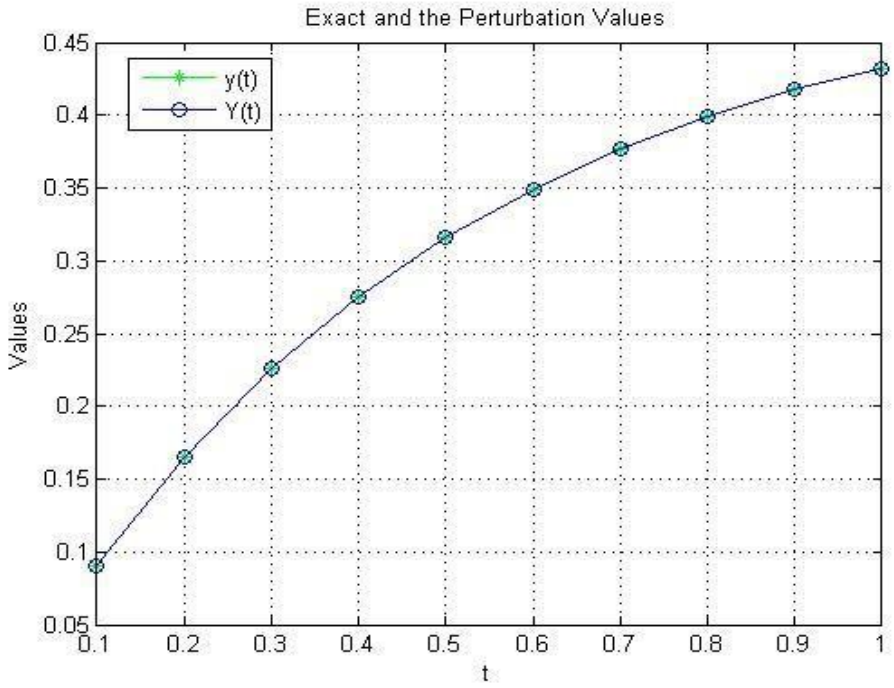

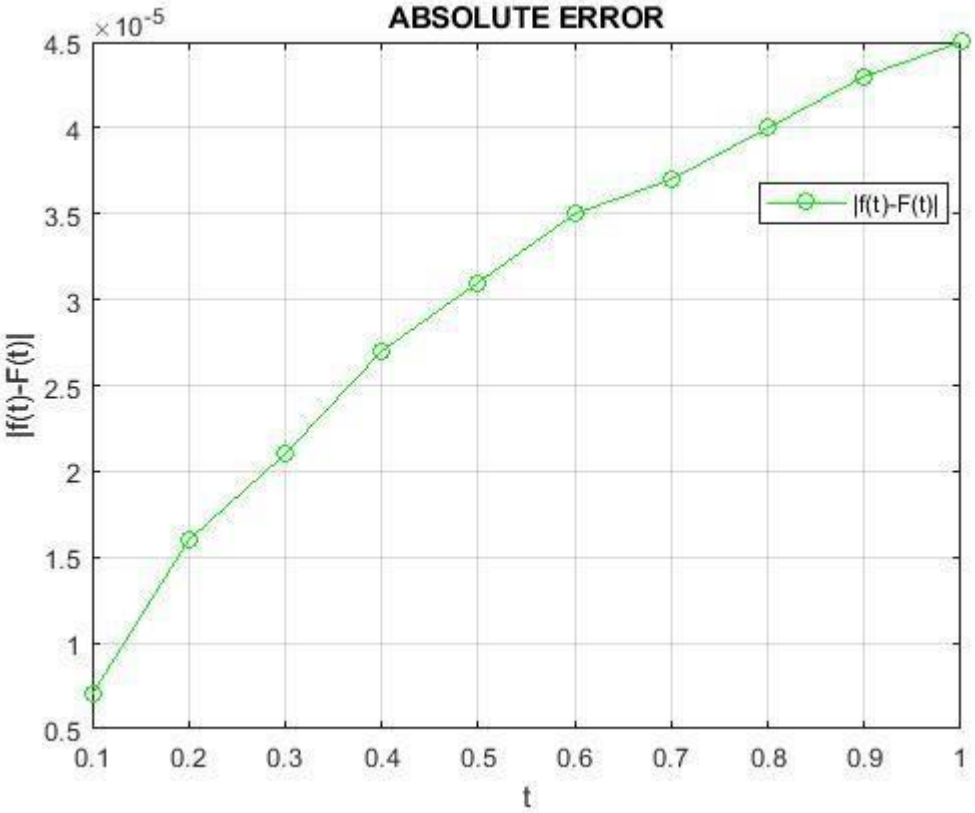

https://doi.org/10.62500/icrtsda.1.1.28

Residual Error

Residual Error = 1.0504×10^{-8}

Problem 3

Let the Problem

$$2\frac{d^2y}{dt^2} + 4\frac{dy}{dt} + \varepsilon y(1-y) = 0 \tag{23}$$

Let us look for a series solution of the form

$$y(t + \varepsilon) = y_0(t) + \varepsilon y_1(t) + \varepsilon^2 y_2 + O(\varepsilon^3) \tag{24}$$

Where y_0, y_1, y_2 are unknown functions of t. (24) is known as the perturbation of the solution in terms of the parameter ε. By substituting (24) into the differential equation (23) and gathering powers of ε, we attain the following perturbation equation:

$$2\left(\frac{d^2y_0(t)}{dt^2} + \varepsilon\frac{d^2y_1(t)}{dt^2} + \varepsilon^2\frac{d^2y_2(t)}{dt^2}\right) + 4\left(\frac{dy_0}{dt} + \varepsilon\frac{dy_1}{dt} + \varepsilon^2\frac{dy_2}{dt}\right) + \varepsilon(y_0(t) + \varepsilon y_1(t) + \varepsilon^2 y_2)(1 - y_0(t) + \varepsilon y_1(t) + \varepsilon^2 y_2) = 0 \tag{25}$$

Compare the order of ε^0

$$2\left(\frac{d^2y_0(t)}{dt^2}\right) + 4\left(\frac{dy_0}{dt}\right) = 0 \tag{26}$$

The solution of the (26)

$$y_0(t) = \frac{1}{2} - \frac{e^{-2t}}{2} \tag{27}$$

Compare the order of ε^1

$$2\left(\frac{d^2y_1(t)}{dt^2}\right) + 4\left(\frac{dy_1}{dt}\right) + (y_0(t)) - (y_0(t))^2 = 0 \tag{28}$$

$$2\left(\frac{d^2y_1(t)}{dt^2}\right) + 4\left(\frac{dy_1}{dt}\right) = -(y_0(t)) + (y_0(t))^2 \tag{29}$$

The solution of the (29)

$$y_1(t) = \frac{35}{64} - \frac{9e^{-2t}}{16} - \frac{t}{16} + \frac{e^{-4t}}{64} \tag{30}$$

Compare the order of ε^2

$$2\left(\frac{d^2y_2(t)}{dt^2}\right) + +4\left(\frac{dy_2}{dt}\right) + (y_1(t)) - 2(y_1(t))(y_0(t)) = 0 \tag{31}$$

$$2\left(\frac{d^2y_2(t)}{dt^2}\right) + +4\left(\frac{dy_2}{dt}\right) = 2(y_1(t))(y_0(t)) - (y_1(t)) \tag{32}$$

The solution of the (32)

$$y_2(t) = \frac{361}{768} - \frac{517e^{-2t}}{1024} + \frac{33te^{-2t}}{256} + \frac{9e^{-4t}}{256} - \frac{t^2e^{-2t}}{128} - \frac{e^{-6t}}{3072} \tag{33}$$

https://doi.org/10.62500/icrtsda.1.1.28

Put the (27), (30) and (33) in the (24), we will get:

$$y(t+\varepsilon) = \left(\frac{1}{2} - \frac{e^{-2t}}{2}\right) + \varepsilon\left(\frac{35}{64} - \frac{9e^{-2t}}{16} - \frac{t}{16} + \frac{e^{-4t}}{64}\right) + \varepsilon^2\left(\frac{361}{768} - \frac{517e^{-2t}}{1024} + \frac{33te^{-2t}}{256} + \frac{9e^{-4t}}{256} - \frac{t^2e^{-2t}}{128} - \frac{e^{-6t}}{3072}\right) + O(\varepsilon^3) \quad (34)$$

Where y(t) is the exact solution Y(t) is the perturbation solution and Absolute error = |y(t)-Y(t)| Now, consider that ε = 0.0001 then the result will be

t	y(t)	Y(t)	|y(t)-Y(t)|
0	0	0	0
0.10000000	0.09063470	0.09064368	8.2×10^{-7}
0.20000000	0.16483999	0.16485641	1.7×10^{-5}
0.30000000	0.22559408	0.22561659	2.4×10^{-5}
0.40000000	0.27533524	0.27536274	2.9×10^{-5}
0.50000000	0.31605977	0.31609136	3.4×10^{-5}
0.60000000	0.34940210	0.34943703	3.7×10^{-5}
0.70000000	0.37670039	0.37673805	4.0×10^{-5}
0.80000000	0.39905023	0.39909013	4.2×10^{-5}
0.90000000	0.41734862	0.41739036	4.3×10^{-5}
1.00000000	0.43232996	0.43237321	4.5×10^{-5}

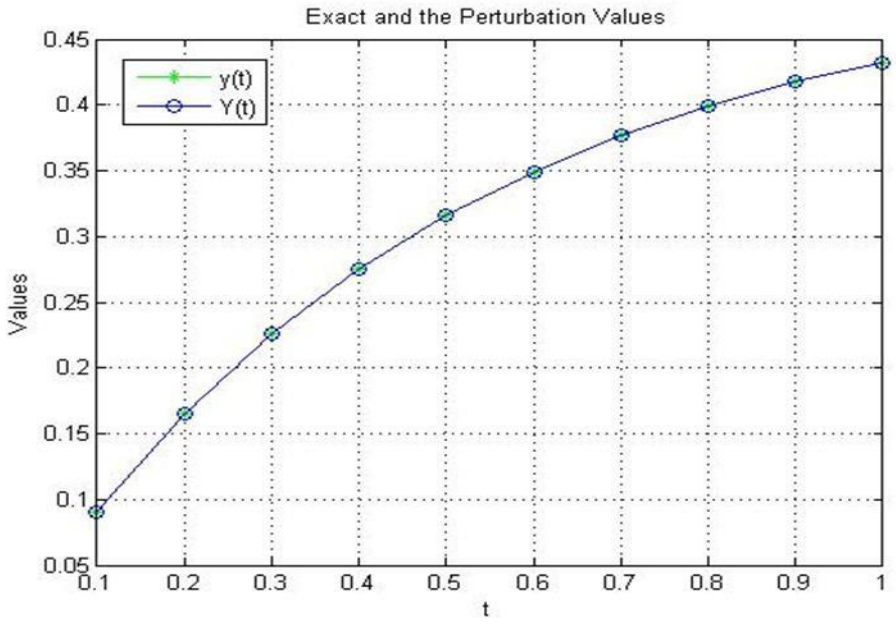

https://doi.org/10.62500/icrtsda.1.1.28

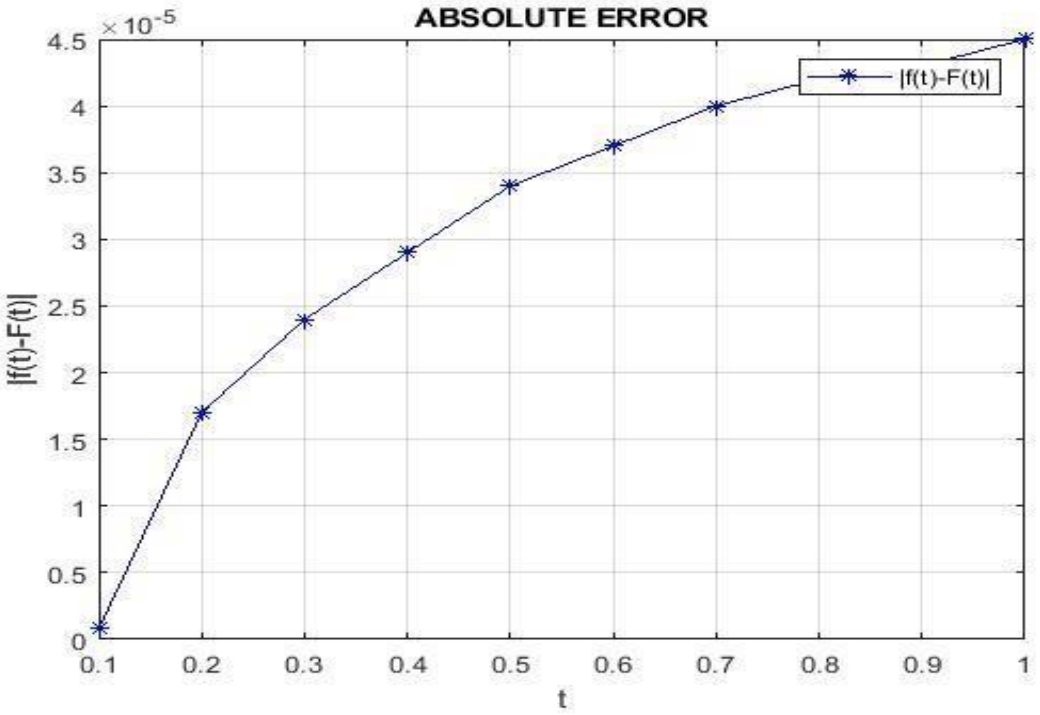

Residual Error

Residual Error = 1.1470×10^{-8}

REFERENCES

1. S. Shaw, Perturbation Techniques for Non Linear Systems, (2001).
2. Viscous Fluid Flow , McGraw-Hill Education; 4th edition (2021).
3. H. Mark Holmes, Introduction to Perturbation Methods Springer Science & Business Media,
   (2012),

https://doi.org/10.62500/icrtsda.1.1.29

Proc. 1st International Conference on Recent Trends in Statistics and Data Analytics
Air University Islamabad, Pakistan – May 9, 2024, Vol. 1, pp. 253-268

A NEW RANDOMIZED RESPONSE SCRAMBLING TECHNIQUE FOR EFFICIENT MEAN ESTIMATION OF A SENSITIVE VARIABLE

Asadullah[1], and Muhammad Azeem[*1]
[1]Department of Statistics, University of Malakand, Khyber Pakhtunkhwa, Pakistan

ABSTRACT

In survey sampling, the most important concern of the respondents is privacy when the respondents give answers to a survey team about their personal information or controversial issues. To study the human behavior and to collect reliable data, a useful and trustworthy method is the randomized response technique. In this study, we introduce a novel randomized response technique for getting information on sensitive type variables. Under the proposed technique, the mathematical properties of the mean of a sensitive variable have been studied and compared with some of the existing competitor techniques using different model-evaluation measures. The findings suggest that the proposed technique is more efficient than the already available techniques.

Keywords: Sensitive variable, privacy, mean estimator, randomized response, efficiency.

1. INTRODUCTION

In high-risk behavior studies, it is often difficult for the survey researchers to obtain efficient estimator for population parameters by asking sensitive questions directly. The sensitive questions may be related to illegal use of drugs, gambling, smoking habit, payment of income tax, and cheating in examination etc. which often yield non-responses or untruthful responses. Due to fear of punishment or loss of social stigma, the survey participants do not like to disclose their true status to others. So they often refuse to respond or give untruthful responses which resultantly become a significant factor for affecting the accuracy and reliability of estimates. In order to solve the problem of non-response and untruthful response an alternative method other than direct questioning survey method may be feasible. Warner (1965) was the first to present a method which is called randomized response technique (RRT). This technique was designed to obtain information in the form of binary responses without requiring the respondents to disclose their true status. To enhance the respondent's confidence, Greenburg et al. (1971) presented an unrelated-question model. In their proposed model, the second question of the Warner (1965) model was replaced by an unrelated question. For making the technique more efficient and applicable, many researchers have introduced various quantitative models including Warner (1971) model and Eichhorn and Hayre (1983) model.

Chaudhuri and Stenger (1992) presented a model in which they used both the additive and multiplicative models together. They used two randomization devices and the respondents were selected through simple random sampling procedure. Gupta et al. (2002), and Bar-Lev et al. (2004) introduced optional quantitative randomized response models, giving the choice to respondents to give scrambled answers if they considered that the survey question is sensitive. Further, the respondents have to give true response if the survey question is considered non-sensitive. Gjestvang and Singh (2009) proposed a quantitative additive scrambling approach for sensitive surveys. Diana and Perri (2011) presented a mixed-response model which combined both multiplicative and additive models in a single model. Hussain et al. (2014) also presented a randomized response model in which the respondents are instructed to subtract the scrambling response from the true response. Further modifications in randomized response models have been contributed by Kalucha et al.(2016), Batool et al. (2017), Tiwari and Mehta (2017), Gupta et al. (2018), and Arshad and Hussain (2019).

An improved optimal randomization model was introduced by Murtaza et al. (2020). In this model, the assumption of correlation among the random variables is used to estimate the finite population mean.

https://doi.org/10.62500/icrtsda.1.1.29

Narjis and Shabbir (2023) presented an updated additive version of the Gjestvang and Singh (2009) scrambled technique. Under this model, a randomization device spinner consists of three types of instructions asked from each respondent selected in the sample. The respondent was advised to use the tool and report the answer accordingly. Recently, another modified scrambling quantitative response model was presented by Azeem et al. (2024), which improved the existing scrambling techniques.

2. SCRAMBLED RANDOMIZED RESPONSE MODELS

In this section, some randomized response models have been discussed with which the comparisons of the proposed models are carried out. Suppose a population of interest consists of units N and a simple random sample of n size is selected from the said population. Let Y be a sensitive variable with unknown variance and mean, i.e., $Var\left(Y_i\right)=\sigma_Y^2$ and $E\left(Y_i\right)=\mu_Y$ respectively. Let W denote a random variable with mean $E\left(W\right)=\theta$, and $Var\left(W\right)=\sigma_W^2$, assumed to be known. Moreover, Suppose T be another random variable with $E\left(T\right)=1$, and $Var\left(T\right)=\sigma_T^2$. Let X be another scrambling variable with variance σ_X^2 and mean μ_X. All variables are independent of each other.

2.1. Diana and Perri (2011) Model

Under the randomized response model of Diana and Perri (2011), the reported responses are following:

$$Z=TY+W\ . \tag{1}$$

An unbiased mean estimator of the sensitive variable is as follow:

$$\hat{\mu}_{DP}=\frac{1}{n}\sum_{i=1}^{n}Z_i\ . \tag{2}$$

The variance of the $\hat{\mu}_{DP}$ is as follow:

$$Var\left(\hat{\mu}_{DP}\right)=\frac{1}{n}\left[\sigma_T^2\left(\sigma_Y^2+\mu_Y^2\right)+\sigma_Y^2+\left(\sigma_W^2+\theta^2\right)\right]. \tag{3}$$

The measure privacy level is given as:

$$\nabla_{DP}=E\left[TY+W-Y\right]^2=\sigma_T^2\left(\sigma_Y^2+\mu_Y^2\right)+\left(\sigma_W^2+\theta^2\right). \tag{4}$$

For the Diana and Perri (2011) model, the joint metric of privacy and efficiency is given below:

$$\delta_{DP}=\frac{Var\left(\hat{\mu}_{DP}\right)}{\nabla_{DP}}=\frac{1}{n}\left[\frac{\sigma_Y^2+\sigma_T^2\left(\sigma_Y^2+\mu_Y^2\right)+\left(\sigma_W^2+\theta^2\right)}{\left(\sigma_W^2+\theta^2\right)+\sigma_T^2\left(\sigma_Y^2+\mu_Y^2\right)}\right]. \tag{5}$$

2.2. Murtaza et al. (2020) Model

The observed response using the Murtaza et al. (2020) are the following:

$$Z=\begin{cases}Y, & \text{with probability } P,\\ TY+\alpha W, & \text{with probability } 1-P,\end{cases} \tag{6}$$

where α denotes a pre-defined constant fixed by the interviewer. An unbiased estimator using the above model may be expressed as:

https://doi.org/10.62500/icrtsda.1.1.29

$$\hat{\mu}_M = \frac{1}{n}\sum_{i=1}^{n} Z_i \,. \tag{7}$$

The sampling variance of the estimator $\hat{\mu}_M$ can be obtained as follows:

$$Var\left(\hat{\mu}_M\right) = \frac{1}{n}\left[\frac{\alpha+\beta}{\alpha+\beta+\gamma}\sigma_T^2\left(\sigma_Y^2+\mu_Y^2\right)+\sigma_Y^2+\alpha^2\left(\sigma_W^2+\theta^2\right)\right]. \tag{8}$$

The metric of privacy may be obtained as:

$$\nabla_M = \frac{\alpha+\beta}{\alpha+\beta+\gamma}\left[\sigma_T^2\left(\sigma_Y^2+\mu_Y^2\right)+\alpha^2\left(\sigma_W^2+\theta^2\right)\right]. \tag{9}$$

The joint metric of privacy and efficiency may be obtained as follows:

$$\delta_M = \frac{Var\left(\hat{\mu}_M\right)}{\nabla_M} = \frac{1}{n}\left[\frac{\frac{1}{n}\left[\frac{\alpha+\beta}{\alpha+\beta+\gamma}\sigma_T^2\left(\sigma_Y^2+\mu_Y^2\right)+\alpha^2\left(\theta^2+\sigma_W^2\right)+\sigma_Y^2\right]}{\frac{\alpha+\beta}{\alpha+\beta+\gamma}\left\{\sigma_T^2\left(\sigma_Y^2+\mu_Y^2\right)+\alpha^2\left(\theta^2+\sigma_W^2\right)\right\}}\right]. \tag{10}$$

2.3. Narjis and Shabbir (2023) Model

Under the Narjis and Shabbir (2023) scrambling method, the observed response may be expressed as follows:

$$Z = \begin{cases} Y-\beta S & \text{with probability } \dfrac{\alpha}{\alpha+\beta+\gamma} \\ \alpha S+Y & \text{with probability } \dfrac{\beta}{\gamma+\alpha+\beta} \\ Y & \text{with probability } \dfrac{\gamma}{\alpha+\beta+\gamma}, \end{cases} \tag{11}$$

where α, β, and γ are constants chosen by the interviewer before the survey is conducted.

An unbiased mean estimator $\hat{\mu}_{NS}$ may be written as:

$$\hat{\mu}_{NS} = \frac{1}{n}\sum_{i=1}^{n} Z_i \,, \tag{12}$$

The sampling variance of $\hat{\mu}_{NS}$ may be obtained as:

$$Var\left(\hat{\mu}_{NS}\right) = \frac{1}{n}\left[\frac{\alpha\beta(\alpha+\beta)}{(\alpha+\beta+\gamma)}\left(\sigma_W^2+\theta^2\right)+\sigma_Y^2\right], \tag{13}$$

The measure of privacy of Narjis and Shabbir (2023) quantitative model may be expressed as:

$$\nabla_{NS} = \frac{\alpha\beta(\alpha+\beta)}{\alpha+\beta+\gamma}(\sigma_W^2+\theta^2)\,. \tag{14}$$

https://doi.org/10.62500/icrtsda.1.1.29

The unified metric of privacy and efficiency are expressed as:

$$\delta_{NS} = \frac{Var\left(\hat{\mu}_{NS}\right)}{\nabla_{NS}} = \frac{1}{n}\left[\frac{\frac{\alpha\beta\left(\alpha+\beta\right)}{\left(\alpha+\beta+\gamma\right)}\left(\sigma_W^2+\theta^2\right)+\sigma_Y^2}{\frac{\alpha\beta(\alpha+\beta)}{\alpha+\beta+\gamma}(\sigma_W^2+\theta^2)}\right]. \tag{15}$$

2.4. Azeem et al. (2024) Model

Azeem et al. (2024) introduced the following optional scrambling model:

$$Z = \begin{cases} \frac{\lambda+1}{2}Y - \frac{\beta}{2}W, & \text{with probability } P_1 = \frac{\alpha}{\lambda(\alpha+\beta)}, \\ \frac{\lambda+1}{2}Y + W\frac{\alpha}{2}, & \text{with probability } P_2 = \frac{\beta}{\lambda(\alpha+\beta)}, \\ \frac{Y}{2}, & \text{with probability } P_3 = 1-\frac{1}{\lambda}. \end{cases} \tag{16}$$

An unbiased mean estimator of the sensitive variable under study is given by:

$$\hat{\mu}_{AZ} = \frac{1}{n}\sum_{i=1}^{n} Z_i \,. \tag{17}$$

The sampling variance of $\hat{\mu}_{AZ}$ is given as:

$$Var\left(\hat{\mu}_{AZ}\right) = \frac{1}{n}\left[\frac{\alpha\beta}{4\lambda}\left(\sigma_W^2+\theta^2\right)+\frac{1}{4}\left(\lambda+3\right)\left(\sigma_Y^2+\mu_Y^2\right)-\mu_Y^2\right]. \tag{18}$$

The measure of privacy of $\hat{\mu}_{AZ}$ may be expressed as:

$$\nabla_{AZ} = \frac{1}{4\lambda}(4\lambda^2+\lambda-1)(\sigma_Y^2+\mu^2)+\frac{\alpha\beta}{\lambda}(\sigma_W^2+\theta^2)\,. \tag{19}$$

The joint metric of privacy and efficiency is given as:

$$\delta_{AZ} = \frac{Var\left(\hat{\mu}_{AZ}\right)}{\nabla_{AZ}} = \frac{1}{n}\left[\frac{\frac{\alpha\beta}{4\lambda}\left(\sigma_W^2+\theta^2\right)\sigma_T^2+\frac{1}{4}(\lambda+3)\left(\sigma_Y^2+\mu_Y^2\right)-\mu_Y^2}{\frac{1}{4\lambda}(4\lambda^2+\lambda-1)(\sigma_Y^2+\mu^2)+\frac{\alpha\beta}{\lambda}(\sigma_W^2+\theta^2)}\right]. \tag{20}$$

3. PROPOSED MODELS

In this section, two quantitative randomized response models are proposed. Under the proposed models, a sample of n size is selected from the target population N and each respondent selected in the sample is given a randomization device, such is a deck of cards. Furthermore, each respondent is asked to either give the true or a scrambled response.

3.1. Proposed Model-1

The reported responses under proposed Model-1 are given as:

https://doi.org/10.62500/icrtsda.1.1.29

$$Z=\begin{cases} Y+\left(\beta+\dfrac{1}{\alpha}+1\right)W & \text{with probability } P_1=\dfrac{\alpha}{\lambda(\alpha+\beta)} \\ Y-\left(\alpha+\dfrac{1}{\beta}-1\right)W & \text{with probability } P_2=\dfrac{\beta}{\lambda(\alpha+\beta)} \\ Y-W & \text{with probability } P_3=\dfrac{1}{\lambda} \\ Y & \text{with probability } P_4=1-\dfrac{1}{\lambda}, \end{cases} \tag{21}$$

where α , β , γ and λ are predetermined positive constants.

An unbiased mean estimator of the population is given as:

$$\hat{\mu}_{P_1}=\frac{1}{n}\sum_{i=1}^{n}Z_i\,, \tag{22}$$

The variance of $\hat{\mu}_{P_1}$ is given by:

$$Var\left(\hat{\mu}_{P_1}\right)=\frac{1}{n}\left[\sigma_Y^2+\left(\frac{2}{\lambda}\right)\left(\sigma_W^2+\theta^2\right)\left\{\beta\left(\beta+2\right)+\alpha\left(\alpha-2\right)+K+U+3\right\}+2\theta\mu_Y V\right]. \tag{23}$$

3.2. Proposed Model-2

The reported responses under proposed model-2 are given as:

$$Z=\begin{cases} Y, & \text{with probability } A, \\ Y+\left(\alpha-\dfrac{\alpha}{A}\right)\bar{X}, & \text{with probability } A(1-A), \\ T\left(Y+\alpha\bar{X}\right), & \text{with probability } (1-2A+A^2). \end{cases} \tag{24}$$

4. MEAN AND VARIANCE

An unbiased mean estimator of the population is given below.

$$\hat{\mu}_{P_2}=\frac{1}{n}\sum_{i=1}^{n}Z_i\,, \tag{25}$$

The variance of $\hat{\mu}_{P_2}$ is given by:

$$Var\left(\hat{\mu}_{P_2}\right)=\frac{1}{n}\left[\sigma_Y^2+M\left\{\left(\sigma_X^2+\mu_X^2\right)\left(\frac{\alpha^2(1-A)}{A}+\left(\sigma_T^2+1\right)\alpha^2\right)+2\alpha\sigma_T^2\mu_X\mu_Y+\sigma_T^2\left(\sigma_Y^2+\mu_Y^2\right)\right\}\right] \tag{26}$$

https://doi.org/10.62500/icrtsda.1.1.29

where

$$M = 1 - 2A + A^2 .$$

Theorem 3.1: The estimators $\hat{\mu}_{P_1}$ and $\hat{\mu}_{P_2}$ are unbiased mean estimators of population mean μ_Y.

Proof: Applying expectation to both sides of equation (22) gives:

$$E\left(\hat{\mu}_{P_1}\right) = E\left(\frac{1}{n}\sum_{i=1}^{n} Z_i\right),$$

$$= \frac{1}{n}\sum_{i=1}^{n} E\left(Z_i\right),$$

$$= \frac{1}{n}\sum_{i=1}^{n}\left[\left(P_1\right)E\left\{Y + \left(\beta + \frac{1}{\alpha} + 1\right)W\right\} + P_2 E\left\{Y - \left(\alpha + \frac{1}{\beta} - 1\right)W\right\} + P_3 E\left(Y - W\right) + P_4 E\left(Y\right)\right].$$

Some further simplification yields:

$$E(\hat{\mu}_{P_1}) = \mu_Y . \tag{27}$$

In the similar way, the unbiasdeness of $\hat{\mu}_{P_2}$ can be proved.

Theorem 3.2: The variances of $\hat{\mu}_{P_1}$ and $\hat{\mu}_{P_2}$ are given by,

$$Var\left(\hat{\mu}_{P_1}\right) = \frac{1}{n}\left[\sigma_Y^2 + \left(\frac{2}{\lambda}\right)\left(\sigma_W^2 + \theta^2\right)\left\{\beta\left(\beta + 2\right) + \alpha\left(\alpha - 2\right) + K + U + 3\right\} + 2\theta\mu_Y V\right]. \tag{28}$$

Proof: The variance of Z_i can be obtained as:

$$Var\left(Z\right) = E\left(Z^2\right) - \left\{E\left(Z\right)\right\}^2 . \tag{29}$$

Now,

$$E\left(Z^2\right) = \sigma_Y^2 + \mu_Y^2 + \left(P_1 + P_2 + P_3\right)\left[\left(\sigma_W^2 + \theta^2\right)\left\{\beta\left(\beta + 2\right) + \alpha\left(\alpha - 2\right) + \frac{1}{\alpha}\left(\frac{1}{\alpha} + 2 + 2\beta\right)\right.\right.$$

$$\left.\left. + \frac{1}{\beta}\left(\frac{1}{\beta} + 2\left(\alpha - 1\right) + 3\beta\right)\right\} + 2\theta\mu_Y\left(\beta + \frac{1}{\alpha} + 1 - \alpha - \frac{1}{\beta}\right),\right.$$

or

$$E\left(Z^2\right) = \sigma_Y^2 + \mu_Y^2 + \left(\frac{2}{\lambda}\right)\left[\left(\sigma_W^2 + \theta^2\right)\left\{\beta\left(\beta + 2\right) + \alpha\left(\alpha - 2\right) + \frac{1}{\alpha}\left(\frac{1}{\alpha} + 2 + 2\beta\right)\right.\right.$$

https://doi.org/10.62500/icrtsda.1.1.29

$$+\frac{1}{\beta}\left(\frac{1}{\beta}+2(\alpha-1)+3\beta\right)\Big\}+2\theta\mu_Y\left(\beta+\frac{1}{\alpha}+1-\alpha-\frac{1}{\beta}\right)\Big]. \tag{30}$$

Now using equation (30) in equation (29), we get:

$$Var(Z)=\sigma_Y^2+\mu_Y^2+\left(\frac{2}{\lambda}\right)\Big[\left(\sigma_W^2+\theta^2\right)\Big\{\beta(\beta+2)+\alpha(\alpha-2)+\frac{1}{\alpha}\left(\frac{1}{\alpha}+2+2\beta\right)$$

$$+\frac{1}{\beta}\left(\frac{1}{\beta}+2(\alpha-1)+3\beta\right)\Big\}+2\theta\mu_Y\left(\beta+\frac{1}{\alpha}+1-\alpha-\frac{1}{\beta}\right)\Big]-\left(\mu_Y^2\right).$$

After further simplification, the above equation yields:

$$Var(Z)=\sigma_Y^2+\left(\frac{2}{\lambda}\right)\Big[\left(\sigma_W^2+\theta^2\right)\Big\{\beta(\beta+2)+\alpha(\alpha-2)+\frac{1}{\alpha}\left(\frac{1}{\alpha}+2+2\beta\right)$$

$$+\frac{1}{\beta}\left(\frac{1}{\beta}+2(\alpha-1)\right)+3\Big\}+2\theta\mu_Y\left(\beta+\frac{1}{\alpha}+1-\alpha-\frac{1}{\beta}\right)\Big]. \tag{31}$$

Let

$$K=\frac{1}{\alpha}\left(\frac{1}{\alpha}+2+2\beta\right),\ U=\frac{1}{\beta}\left(\frac{1}{\beta}+2(\alpha-1)\right),\ \text{and}\ V=\left(\beta+\frac{1}{\alpha}+1-\alpha-\frac{1}{\beta}\right)\Big].$$

Using values of K,U and V in equation (31), we get:

$$Var(Z)=\sigma_Y^2+\left(\frac{2}{\lambda}\right)\left(\sigma_W^2+\theta^2\right)\Big\{\beta(\beta+2)+\alpha(\alpha-2)+K+U+3\Big\}+2\theta\mu_Y V. \tag{32}$$

Applying variance to both sides of equation (22) yields:

$$Var\left(\hat{\mu}_{P_1}\right)=Var\left(\frac{1}{n}\sum_{i=1}^{n}Z_i\right),$$

or

$$Var\left(\hat{\mu}_{P_1}\right)=\frac{1}{n}Var\left(Z_i\right). \tag{33}$$

Using equation (32), the above equation simplifies to:

$$Var\left(\hat{\mu}_{P_1}\right)=\frac{1}{n}\Big[\sigma_Y^2+\left(\frac{2}{\lambda}\right)\left(\sigma_W^2+\theta^2\right)\Big\{\beta(\beta+2)+\alpha(\alpha-2)+K+U+3\Big\}+2\theta\mu_Y V\Big]. \tag{34}$$

In the same way the variance of $\hat{\mu}_{P_2}$ can be easily derived.

https://doi.org/10.62500/icrtsda.1.1.29

Remark 1: If the values of constants: α, β and λ are known, then unbiased estimators for the sampling variance of $\hat{\mu}_{P_1}$, and $\hat{\mu}_{P_2}$, are given as:

$$var\left(\hat{\mu}_{P_1}\right)=\frac{1}{n}s_z^2, \qquad \text{and} \qquad var\left(\hat{\mu}_{P_2}\right)=\frac{1}{n}s_z^2,$$

or

$$var\left(\hat{\mu}_{P_1}\right)=\frac{1}{(n-1)n}\sum_{i=1}^{n}\left(Z_i-\bar{Z}\right)^2, \tag{35}$$

and

$$var\left(\hat{\mu}_{P_2}\right)=\frac{1}{(n-1)n}\sum_{i=1}^{n}\left(Z_i-\bar{Z}\right)^2. \tag{36}$$

where s_z^2 and $\bar{Z}$ denote the variance and sample mean, respectively.

5. UNIFIED MEASURE OF EFFICIENCY AND PRIVACY

For assessing the privacy level offered by quantitative randomized response model, Yan et al. (2008) suggested the following measure:

$$\nabla = E\left[Z-Y\right]^2. \tag{37}$$

The unified metric of the respondent's privacy level and efficiency presented by Gupta et al. (2018) is given as:

$$\delta=\frac{MSE}{\nabla}. \tag{38}$$

Measure of privacy level offered by the proposed Model-1 is given as:

$$\nabla_{P_1}=\left(\sigma_W^2+\theta^2\right)\left[\frac{\alpha}{\lambda(\alpha+\beta)}\left\{K+\beta^2+2\beta+1\right\}+\frac{\beta}{\lambda(\alpha+\beta)}\left\{U+\alpha^2-2\alpha+1\right\}+\frac{1}{\lambda}\right]. \tag{39}$$

The unified metric of the respondent's privacy level and efficiency offered by proposed Model-1is given as:

$$\delta_{P_1}=\frac{\frac{1}{n}\left[\sigma_Y^2+\left(\frac{2}{\lambda}\right)\left(\sigma_W^2+\theta^2\right)\left\{\beta(\beta+2)+\alpha(\alpha-2)+K+U+3\right\}+2\theta\mu_Y V\right]}{\left(\sigma_W^2+\theta^2\right)\left[\frac{\alpha}{\lambda(\alpha+\beta)}\left\{K+\beta^2+2\beta+1\right\}+\frac{\beta}{\lambda(\alpha+\beta)}\left\{U+\alpha^2-2\alpha+1\right\}+\frac{1}{\lambda}\right]}. \tag{40}$$

Measure of privacy level offered by the proposed Model-2 is given as:

https://doi.org/10.62500/icrtsda.1.1.29

$$\nabla_{P_2} = M\left[\left(\sigma_X^2+\mu_X^2\right)\left\{\frac{\alpha^2(1-A)}{A}+\alpha^2\left(\sigma_T^2+1\right)\right\}+\sigma_T^2\left(\sigma_Y^2+\mu_Y^2-2\alpha\mu_X\mu_Y\right)\right]. \tag{41}$$

The unified metric of the privacy level and efficiency offered by the proposed Model-2 is given as:

$$\delta_{P_2} = \frac{\sigma_Y^2+M\left\{\left(\sigma_X^2+\mu_X^2\right)\left(\frac{\alpha^2(1-A)}{A}+\left(\sigma_T^2+1\right)\alpha^2\right)+2\alpha\sigma_T^2\mu_X\mu_Y+\sigma_T^2\left(\sigma_Y^2+\mu_Y^2\right)\right\}}{nM\left[\left(\sigma_X^2+\mu_X^2\right)\left\{\frac{\alpha^2(1-A)}{A}+\alpha^2\left(\sigma_T^2+1\right)\right\}+\sigma_T^2\left(\sigma_Y^2+\mu_Y^2-2\alpha\mu_X\mu_Y\right)\right]}. \tag{42}$$

It is known from equation (37) that:

$$\nabla_{P_1} = E\left[Z-Y\right]^2,$$

or

$$\nabla_{P_1} = P_1E\left[Z-Y\right]^2+P_2E\left[Z-Y\right]^2+P_3E\left[Z-Y\right]^2+P_4E\left[Z-Y\right]^2,$$

or

$$\nabla_{P_1} = P_1E\left[Y+W\left(\frac{1}{\alpha}+\beta+1\right)-Y\right]^2+P_2E\left[Y-W\left(\frac{1}{\beta}+\alpha-1\right)-Y\right]^2$$

$$+P_3E\left[Y-W-Y\right]^2+P_4E\left[Y-Y\right]^2,$$

or

$$\nabla_{P_1} = \left(\sigma_W^2+\theta^2\right)\left[P_1\left(\beta^2+\frac{1}{\alpha^2}+1+\frac{2}{\alpha}+\frac{2\beta}{\alpha}+2\beta\right)+P_2\left(\alpha^2+\frac{1}{\beta^2}+1-\frac{2}{\beta}+\frac{2\alpha}{\beta}-2\alpha\right)+P_3\right].$$

After further simplification, we get:

$$\nabla_{P_1} = \left(\sigma_W^2+\theta^2\right)\left[\frac{\alpha}{\lambda(\alpha+\beta)}\left\{K+\beta^2+2\beta+1\right\}+\frac{\beta}{\lambda(\alpha+\beta)}\left\{U+\alpha^2-2\alpha+1\right\}+\frac{1}{\lambda}\right]. \tag{43}$$

It is known from equation (38) that the unified metric of the respondent's privacy level and efficiency can be calculated as:

$$\delta_{P_1} = \frac{MSE}{\nabla_{P_1}}, \tag{44}$$

or

https://doi.org/10.62500/icrtsda.1.1.29

$$\delta_{P_1}=\frac{\frac{1}{n}\left[\sigma_Y^2+\left(\frac{2}{\lambda}\right)\left(\sigma_W^2+\theta^2\right)\left\{\beta\left(\beta+2\right)+\alpha\left(\alpha-2\right)+K+U+3\right\}+2\theta\mu_Y V\right]}{\left(\sigma_W^2+\theta^2\right)\left[\frac{\alpha}{\lambda\left(\alpha+\beta\right)}\left\{K+\beta^2+2\beta+1\right\}+\frac{\beta}{\lambda\left(\alpha+\beta\right)}\left\{U+\alpha^2-2\alpha+1\right\}+\frac{1}{\lambda}\right]}. \tag{45}$$

In the same way, the measure of privacy and efficiency of Model-2 can be easily derived.

6. MODEL COMPARISON

The proposed randomized Model-1 will be more precise than the Diana and Perri. (2011) model if:

$$Var\left(\hat{\mu}_{P_1}\right)<Var(\hat{\mu}_{DP}),$$

or

$$\frac{1}{n}\left[\sigma_Y^2+\left(\frac{2}{\lambda}\right)\left(\sigma_W^2+\theta^2\right)\left\{\beta\left(\beta+2\right)+\alpha\left(\alpha-2\right)+K+U+3\right\}+2\theta\mu_Y V\right]$$
$$\leq\frac{1}{n}\left[\sigma_T^2\left(\sigma_Y^2+\mu_Y^2\right)+\sigma_Y^2+\left(\sigma_W^2+\theta^2\right)\right],$$

or

$$\left[\sigma_Y^2+\left(\frac{2}{\lambda}\right)\left(\sigma_W^2+\theta^2\right)\left\{\beta\left(\beta+2\right)+\alpha\left(\alpha-2\right)-\frac{\lambda}{2}+K+U+3\right\}+2\theta\mu_Y V\right]\leq\sigma_T^2\left(\sigma_Y^2+\mu_Y^2\right).$$

The proposed Model-1 will be more precise than the Murtaza et al. (2020) model if:

$$Var\left(\hat{\mu}_{P_1}\right)<Var(\hat{\mu}_M),$$

or

$$\frac{1}{n}\left[\sigma_Y^2+\left(\frac{2}{\lambda}\right)\left(\sigma_W^2+\theta^2\right)\left\{\beta\left(\beta+2\right)+\alpha\left(\alpha-2\right)+K+U+3\right\}+2\theta\mu_Y V\right]$$
$$\leq\frac{1}{n}\left[\frac{\alpha+\beta}{\alpha+\beta+\gamma}\sigma_T^2\left(\sigma_Y^2+\mu_Y^2\right)+\sigma_Y^2+\alpha^2\left(\sigma_W^2+\theta^2\right)\right],$$

or

$$\left[\left(\frac{2}{\lambda}\right)\left(\sigma_W^2+\theta^2\right)\left\{\beta\left(\beta+2\right)+\alpha\left(\alpha-2\right)-\frac{\lambda\alpha^2}{2}+K+U+3\right\}+2\theta\mu_Y V\right]$$
$$\leq\left[\frac{\alpha+\beta}{\alpha+\beta+\gamma}\sigma_T^2\left(\sigma_Y^2+\mu_Y^2\right)\right].$$

The proposed Model-1 will be more precise than the Narjis and Shabbir. (2023) model if:

$$Var\left(\hat{\mu}_{P_1}\right)<Var(\hat{\mu}_{NS}),$$

https://doi.org/10.62500/icrtsda.1.1.29

or

$$\frac{1}{n}\left[\sigma_Y^2+\left(\frac{2}{\lambda}\right)\left(\sigma_W^2+\theta^2\right)\left\{\beta\left(\beta+2\right)+\alpha\left(\alpha-2\right)+K+U+3\right\}+2\theta\mu_Y V\right]$$
$$\leq\frac{1}{n}\left[\frac{\alpha\beta\left(\alpha+\beta\right)}{\left(\alpha+\beta+\gamma\right)}\left(\sigma_W^2+\theta^2\right)+\sigma_Y^2\right],$$

or

$$\left[\left(\frac{2}{\lambda}\right)\left(\sigma_W^2+\theta^2\right)\left\{\beta\left(\beta+2\right)+\alpha\left(\alpha-2\right)+K+U+3\right\}+2\theta\mu_Y V\right]\leq\left[\frac{\alpha\beta\left(\alpha+\beta\right)}{\left(\alpha+\beta+\gamma\right)}\left(\sigma_W^2+\theta^2\right)\right]$$

.

The proposed Model-1 will be more precise than the Azeem et al. (2024) model if:

$$Var\left(\hat{\mu}_{P_1}\right)<Var(\hat{\mu}_{AZ}),$$

or

$$\frac{1}{n}\left[\sigma_Y^2+\left(\frac{2}{\lambda}\right)\left(\sigma_W^2+\theta^2\right)\left\{\beta\left(\beta+2\right)+\alpha\left(\alpha-2\right)+K+U+3\right\}+2\theta\mu_Y V\right]$$
$$\leq\frac{1}{n}\left[\frac{\alpha\beta}{4\lambda}\left(\sigma_W^2+\theta^2\right)+\frac{1}{4}\left(\lambda+3\right)\left(\sigma_Y^2+\mu_Y^2\right)-\mu_Y^2\right],$$

or

$$\left[\sigma_Y^2+\left(\frac{2}{\lambda}\right)\left(\sigma_W^2+\theta^2\right)\left\{\beta\left(\beta+2\right)-\frac{\alpha\beta}{8}+\alpha\left(\alpha-2\right)+K+U+3\right\}+2\theta\mu_Y V\right]$$
$$\leq\left[\frac{1}{4}\left(\lambda+3\right)\left(\sigma_Y^2+\mu_Y^2\right)-\mu_Y^2\right].$$

The proposed Model-2 will be more precise than the Diana and Perri (2011) model if:

$$Var(\hat{\mu}_{p_2})\leq Var\left(\hat{\mu}_{DP}\right),$$

or

$$\frac{1}{n}\left[\sigma_Y^2+M\left\{\left(\sigma_X^2+\mu_X^2\right)\left(\frac{\alpha^2(1-A)}{A}+\left(\sigma_T^2+1\right)\alpha^2\right)+2\alpha\sigma_T^2\mu_X\mu_Y+\sigma_T^2\left(\sigma_Y^2+\mu_Y^2\right)\right\}\right]$$
$$\leq\frac{1}{n}\left[\sigma_T^2\left(\sigma_Y^2+\mu_Y^2\right)+\sigma_Y^2+\left(\sigma_W^2+\theta^2\right)\right],$$

or

$$M\left\{\left(\sigma_X^2+\mu_X^2\right)\left(\frac{\alpha^2(1-A)}{A}+\left(\sigma_T^2+1\right)\alpha^2\right)+2\alpha\sigma_T^2\mu_X\mu_Y+\sigma_T^2\left(\sigma_Y^2+\mu_Y^2\right)\left(1-\frac{1}{M}\right)\right\}\leq\left(\sigma_W^2+\theta^2\right).$$

https://doi.org/10.62500/icrtsda.1.1.29

The proposed Model-2 will be more precise than the Murtaza et al. (2020) model if:

$$Var(\hat{\mu}_{p_2}) \le Var\left(\hat{\mu}_M\right),$$

or

$$\frac{1}{n}\left[\sigma_Y^2 + M\left\{\left(\sigma_X^2+\mu_X^2\right)\left(\frac{\alpha^2(1-A)}{A}+\left(\sigma_T^2+1\right)\alpha^2\right)+2\alpha\sigma_T^2\mu_X\mu_Y+\sigma_T^2\left(\sigma_Y^2+\mu_Y^2\right)\right\}\right]$$

$$\le \frac{1}{n}\left[\frac{\alpha+\beta}{\alpha+\beta+\gamma}\sigma_T^2\left(\sigma_Y^2+\mu_Y^2\right)+\sigma_Y^2+\alpha^2\left(\sigma_W^2+\theta^2\right)\right],$$

or

$$\left[M\left\{\left(\sigma_X^2+\mu\ \right)\left(\frac{\alpha^2(\ -A}{A}+\left(\sigma\ \ +1\right)\alpha\ \right)+\ \ \alpha\sigma\ \mu\ \ \mu\ \ +\sigma\ \left(\sigma\ \ +\mu\ \right)\left(\ \ -\frac{A\ \alpha+\beta}{\gamma M}\right)\right\}\right]$$

$$\le \alpha^2\left(\sigma_W^2+\theta^2\right).$$

The proposed Model-2 will be more precise than the Narjis and Shabbir. (2023) model if:

$$Var(\hat{\mu}_{p_2}) \le Var\left(\hat{\mu}_{NS}\right),$$

or

$$\frac{1}{n}\left[\sigma_Y^2 + M\left\{\left(\sigma_X^2+\mu_X^2\right)\left(\frac{\alpha^2(1-A)}{A}+\left(\sigma_T^2+1\right)\alpha^2\right)+2\alpha\sigma_T^2\mu_X\mu_Y+\sigma_T^2\left(\sigma_Y^2+\mu_Y^2\right)\right\}\right]$$

$$\le \frac{1}{n}\left[\frac{\alpha\beta(\alpha+\beta)}{(\alpha+\beta+\gamma)}\left(\sigma_W^2+\theta^2\right)+\sigma_Y^2\right],$$

or

$$M\left\{\left(\sigma_X^2+\mu_X^2\right)\left(\frac{\alpha^2(1-A)}{A}+\left(\sigma_T^2+1\right)\alpha^2\right)+2\alpha\sigma_T^2\mu_X\mu_Y+\sigma_T^2\left(\sigma_Y^2+\mu_Y^2\right)\right\}$$

$$\le \frac{1}{n}\left[\frac{\alpha\beta A(\alpha+\beta)}{\gamma}\left(\sigma_W^2+\theta^2\right)\right].$$

The proposed Model-2 will be more precise than the Azeem et al. (2024) model if:

$$Var(\hat{\mu}_{p_2}) \le Var\left(\hat{\mu}_{AZ}\right),$$

or

$$\frac{1}{n}\left[\sigma_Y^2 + M\left\{\left(\sigma_X^2+\mu_X^2\right)\left(\frac{\alpha^2(1-A)}{A}+\left(\sigma_T^2+1\right)\alpha^2\right)+2\alpha\sigma_T^2\mu_X\mu_Y+\sigma_T^2\left(\sigma_Y^2+\mu_Y^2\right)\right\}\right]$$

https://doi.org/10.62500/icrtsda.1.1.29

$$\leq \frac{1}{n}\left[\frac{\alpha\beta}{4\lambda}\left(\sigma_W^2+\theta^2\right)+\frac{1}{4}(\lambda+3)\left(\sigma_Y^2+\mu_Y^2\right)-\mu_Y^2\right],$$

or

$$\sigma_Y^2+\mu_Y+M\left\{\left(\sigma_X+\mu_X\right)\left(\frac{\alpha^2(\ -A}{A}+\left(\sigma_T+1\right)\alpha\ \right)+2\alpha\sigma_T\mu_X\mu_Y+\left(\sigma_T-\frac{(\lambda+3)}{4M}\right)\left(\sigma_Y+\mu_Y\right)\right\}$$

$$\leq \frac{\alpha\beta}{4\lambda}\left(\sigma_W^2+\theta^2\right).$$

7. EMPIRICAL COMPARISON

The variances of the mean and the combined metric of privacy and efficiency under the proposed models, the Azeem et al (2024) model, the Narjis and Shabbir (2023) model, the Murtaza et al. (2020) model, and the Diana and Perri (2011) randomized response model, are displayed in Table 1 and Table 2, for various values of parameters and constants.

Table 1: Variances of the mean under the proposed and existing models for $n = 1000$

	μ_Y	γ	σ_X^2	θ	$Var(\hat{\mu}_{DP})$	$Var(\hat{\mu}_M)$	$Var(\hat{\mu}_{NS})$	$Var(\hat{\mu}_{AZ})$	$Var(\hat{\mu}_{P_1})$	$Var(\hat{\mu}_{P_2})$
$\alpha = 4,\ \lambda = 50$	0.6	2	0.1	9	0.081356	1.297842	0.4868	8.11706	0.0769077	0.004096
		3	0.2	8	0.064356	1.02583733	0.3420666	6.41706	0.0607752	0.005056
		4	0.3	7	0.049356	0.7858336	0.23588	4.91706	0.0465477	0.006016
		5	0.4	6	0.036356	0.57783054	0.1577272	3.61706	0.0342252	0.006976
	0.7	2	0.1	9	0.081356	1.297842	0.4868	8.11706	0.0769077	0.004096
		3	0.2	8	0.064369	1.025846	0.3420666	6.41865	0.0606952	0.003245
		4	0.3	7	0.049369	0.7858414	0.23588	4.91865	0.0464777	0.004205
		5	0.4	6	0.036369	0.57783763	0.1577272	3.6186525	0.0341652	0.005165
$\alpha = 3.5,\ \lambda = 60$	0.6	2	0.1	9	0.081356	0.99371606	0.4165133	8.52396	0.0561611	0.004519
		3	0.2	8	0.064356	0.78546123	0.2905352	6.73896	0.0444053	0.005254
		4	0.3	7	0.049356	0.60170742	0.1991842	5.16396	0.0340359	0.005989
		5	0.4	6	0.036356	0.44245433	0.1325666	3.79896	0.0250529	0.006724
	0.7	2	0.1	9	0.081369	0.9937256	0.4165133	8.5258775	0.0561182	0.003356
		3	0.2	8	0.064369	0.78546964	0.2905352	6.7408775	0.0443672	0.004091
		4	0.3	7	0.049369	0.60171494	0.1991842	5.1658775	0.0340026	0.004826
		5	0.4	6	0.036369	0.44246114	0.1325666	3.8008775	0.0250244	0.005561
$\alpha = 4,\ \lambda = 70$	0.6	2	0.1	9	0.081356	1.297842	0.4868	11.36386	0.0549912	0.004096
		3	0.2	8	0.064356	1.02583733	0.3420666	8.98386	0.0434680	0.005056
		4	0.3	7	0.049356	0.7858336	0.23588	6.88386	0.0333055	0.006016
		5	0.4	6	0.036356	0.57783054	0.1577272	5.06386	0.0245037	0.006976
	0.7	2	0.1	9	0.081369	1.29785175	0.4868	11.366102	0.0549269	0.002285
		3	0.2	8	0.064369	1.025846	0.3420666	8.9861025	0.0434108	0.003245
		4	0.3	7	0.049369	0.7858414	0.23588	6.8861025	0.0332555	0.004205
		5	0.4	6	0.036369	0.57783763	0.1577272	5.0661025	0.0244608	0.005165

https://doi.org/10.62500/icrtsda.1.1.29

Table 2: Values of δ for the proposed and existing models for $n = 1000$

	μ_Y	γ	σ_X^2	θ	δ_{DP}	δ_M	δ_{NS}	δ_{AZ}	δ_{P_1}	δ_{P_2}
$\alpha = 4, \lambda = 50$	0.6	2	0.1	9	0.0010043	0.001333524	0.00100041	0.197431	0.00094147	0.00016205
		3	0.2	8	0.0010055	0.001500265	0.00100058	0.167140	0.00094075	0.00026589
		4	0.3	7	0.0010072	0.001667043	0.00100084	0.136610	0.00094028	0.00036973
		5	0.4	6	0.0010098	0.001833887	0.00100127	0.106656	0.00094048	0.00047357
	0.7	2	0.1	9	0.0010045	0.001333521	0.00100041	0.170398	0.00093689	5.9068E-05
		3	0.2	8	0.0010057	0.001500259	0.00100058	0.142874	0.00093560	0.00016353
		4	0.3	7	0.001007	0.001667032	0.00100084	0.115664	0.00093440	0.00026799
		5	0.4	6	0.0010102	0.001833869	0.00100127	0.089470	0.00093363	0.00037245
$\alpha = 3.5, \lambda = 60$	0.6	2	0.1	9	0.0010043	0.00136389	0.00100048	0.197316	0.00049803	0.00029445
		3	0.2	8	0.0010055	0.001545809	0.00100068	0.163503	0.00049943	0.00039875
		4	0.3	7	0.0010072	0.001727779	0.00100100	0.130845	0.00050183	0.00050305
		5	0.4	6	0.001009	0.001909839	0.00100151	0.100106	0.00050609	0.00060735
	0.7	2	0.1	9	0.0010045	0.001363886	0.00100048	0.167071	0.00049519	0.00021331
		3	0.2	8	0.0010057	0.0015458	0.00100068	0.13743	0.00049623	0.00031830
		4	0.3	7	0.0010075	0.001727764	0.00100100	0.109219	0.00049817	0.00042329
		5	0.4	6	0.0010102	0.001909812	0.00100151	0.083022	0.00050183	0.00052829
$\alpha = 4, \lambda = 70$	0.6	2	0.1	9	0.0010043	0.001333524	0.00100041	0.233792	0.00094554	0.00016205
		3	0.2	8	0.0010055	0.001500265	0.00100058	0.192523	0.00094589	0.00026589
		4	0.3	7	0.0010072	0.001667043	0.00100084	0.153146	0.00094700	0.00036973
		5	0.4	6	0.0010098	0.001833887	0.00100127	0.116507	0.00094962	0.00047357
	0.7	2	0.1	9	0.001004	0.001333521	0.00100041	0.196854	0.00094096	5.9068E-05
		3	0.2	8	0.0010057	0.001500259	0.00100058	0.161053	0.00094075	0.00016353
		4	0.3	7	0.0010075	0.001667032	0.00100084	0.127328	0.00094112	0.00026799
		5	0.4	6	0.0010102	0.001833869	0.00100127	0.096321	0.00094277	0.00037245

8. COMMENTS AND CONCLUSION

Two new randomized response models have been introduced in this paper. The result shows that the proposed models are more efficient than the Azeem et al. (2024) model, the Narjis and Shabbir (2023) model, the Murtaza et al. (2020) and the Diana and Perri (2011) randomized response model, in terms of both efficiency and overall performance when privacy protection and efficiency are simultaneously considered. Observing the above two tables, it is clear that the proposed response models are more efficient than the Azeem et al. (2024) model, the Narjis and Shabbir (2023) model, the Murtaza et al. (2020) and the Diana and Perri (2011) randomized response models. From the comparison of models, it is evident that the proposed Model-2 is more precise than the existing models. Moreover, Model-2 is more precise than Model-1. It is also clearly observed from the tables that as the values of α and λ decrease, the variances of the mean estimator under the proposed randomized response models also decrease. Likewise, we also observe that the values of δ decrease as the values of α and λ decrease.

The proposed models are simple and easy as they don't need the respondents to have full command on Mathematics. The respondent who simply knows multiplication and addition of numbers using an electronic calculator can easily calculate and report his/her response. Based on the results, the proposed models are recommended for practical use for data collection on sensitive issues.

https://doi.org/10.62500/icrtsda.1.1.29

REFERENCES

1. Arshad, W., and Hussaın, Z. (2019). On Generalized Additive Scrambled Response Modeling in Sensitive Surveys. *Gazi University Journal of Science*, 32(1), 372-383.

2. Azeem, M., Hussain, S., Ijaz, M., and Salahuddin, N. (2024). An improved quantitative randomized response technique for data collection in sensitive surveys. *Quality & Quantity*, 58(1), 329-341.

3. Bar-Lev, S. K., Bobovitch, E., and Boukai, B. (2004). A note on randomized response models for quantitative data. *Metrika*, 60(3), 255-260.

4. Batool, F., Shabbir, J., and Hussain, Z. (2017). On the estimation of a sensitive quantitative mean using blank cards. *Communications in Statistics-Theory and Methods*, 46(6), 3070-3079.

5. Chaudhuri, A., and Stenger, H, (1992). *Sampling Survey*. Marcel Dekker, New York.

6. Diana, G., and Perri, P. F. (2011). A class of estimators for quantitative sensitive data. *Statistical Papers*, 52, 633-650.

7. Eichhorn, B. H., and Hayre, L. S. (1983). Scrambled randomized response methods for obtaining sensitive quantitative data. *Journal of Statistical Planning and Inference*, 7(4), 307-316.

8. Greenberg, B. G., Kuebler Jr, R. R., Abernathy, J. R., and Horvitz, D. G. (1971). Application of the randomized response technique in obtaining quantitative data. *Journal of the American Statistical Association*, 66(334), 243-250.

9. Gjestvang, C. R., and Singh, S. (2009). An improved randomized response model: Estimation of mean. *Journal of Applied Statistics*, 36(12), 1361-1367.

10. Gupta, S., Gupta, B., and Singh, S. (2002). Estimation of sensitivity level of personal interview survey questions. *Journal of Statistical Planning and Inference*, 100(2), 239-247.

11. Gupta, S., Mehta, S., Shabbir, J., and Khalil, S. (2018). A unified measure of respondent privacy and model efficiency in quantitative RRT models. *Journal of Statistical Theory and Practice*, 12, 506-511.

12. Hussain, Z., Al-Sobhi, M. M., and Al-Zahrani, B. (2014). Additive and subtractive scrambling in optional randomized response modeling. *PLOS ONE*, 9(1), e83557.

13. Kalucha, G., Gupta, S., and Shabbir, J. (2016). A two-step approach to ratio and regression estimation of finite population mean using optional randomized response models. *Hacettepe Journal of Mathematics and Statistics*, 45(6), 1819-1830.

14. Murtaza, M., Singh, S., and Hussain, Z. (2020). An innovative optimal randomized response model using correlated scrambling variables. *Journal of Statistical Computation and Simulation*, 90(15), 2823-2839.

15. Narjis, G., and Shabbir, J. (2023). An efficient new scrambled response model for estimating sensitive population mean in successive sampling. *Communications in Statistics-Simulation and Computation*, 52(11), 5327-5344.

16. Tiwari, N., and Mehta, P. (2017). Additive randomized response model with known sensitivity level. *International Journal of Computational and Theoretical Statistics*, 4(02), 83-93.

https://doi.org/10.62500/icrtsda.1.1.29

17. Warner, S. L. (1965). Randomized response: A survey technique for eliminating evasive answer bias. *Journal of the American Statistical Association*, 60(309), 63-69.

18. Warner, S. L. (1971). The linear randomized response model. *Journal of the American Statistical Association*, 66(336), 884-888.

https://doi.org/10.62500/icrtsda.1.1.30

Proc. 1st International Conference on Recent Trends in Statistics and Data Analytics
Air University Islamabad, Pakistan – May 9, 2024, Vol. 1, pp. 269-286

Detection and Classification of COVID-19 and Lung Diseases from Chest X-Rays based on Transfer Learning with Fine Tuning

Ansar Rahman[a,1], Shams-ul-Islam[b,1] , Safdar Munir[c,2], M Saleem[d,3], and SajjadKhan[e,1]
[1]Department of Mathematics, COMSATS University Islamabad, Park Road Islamabad 44000, Pakistan
[2]Department of Robotics and Artificial Intelligence, School of Mechanical & Manufacturing Engg (SMME), National University of Science and Technology (NUST), H-12 Campus, Islamabad, 44000, Pakistan.
[3]Department of Science and Humanities, Sir Syed CASE Institute of Technology, Sector B-17, Islamabad, 44000, Pakistan.

ABSTRACT

COVID-19 spread fast over the globe and evolved into a pandemic. It hurts everyday life, public health, and international trade. In order to stop the pandemic from spreading and to manage the immediately impacted individuals, positive patients must be found as quickly as possible. The accurate diagnosis of COVID- 19 can be aided by the use of advanced AI techniques connected to radiological imaging. As images from radiography can spot infections like pneumonia. In this study, a transfer learning-based method for accurately and automatically analyzing CXR images to detect COVID-19 and other lung disorders is introduced. Using pre-trained ResNet50 TL model weights, we developed a transfer learning technique to distinguish COVID- 19 vs. normal, lung opacity (non-CoVID), and viral pneumonia patients from chest X-ray photographs. ResNet50 model weights that have already been trained using natural image datasets were employed. We utilized ImageNet weights specifically. Pretrained imageNet weights are fed into the ResNet50 model. In addition, we added three fully connected layers to the ResNet50 model to further refine it. We are mainly focused on four-class classification, i.e., comparison of COVID-19, lung opacity, viral pneumonia, and normal cases. For two-class, three-class, and specifically four-class classifications, our proposed model obtained overall accuracy of 99.17%, 98%, and 97.33%, respectively.

Keywords: Covid-19, CXRs images, Transfer Learning, ResNet50, Fine Tuning

1. Introduction

In late 2019, researchers found the virus known as SARS-CoV-2. CoronaVirus Disease 2019, also known as COVID-19, was brought on by the virus that had its origins in China. In March 2020, WHO categorized the condition as an epidemic [1, 2]. Dyspnea, a high temperature, a runny nose, and a cough are some of the diseases' more common symptoms. While reverse transcription polymerase chain reaction (RT-PCR) test kits are the primary method for diagnosing COVID-19, other important alternative methods for detection include chest X-rays, ultrasounds, and other types of medical imaging, such as CT, MRI, PET, and ultrasound. As RT-PCR produces a lot of false-negative findings because of its low sensitivity. To resolve this issue, COVID-19 is identified and diagnosed using radiological imaging methods, such as CT and chest X-rays [3]. As lung disease abnormalities, such as COVID-19, can be detected by both CT and CXR [4, 5]. In this study, chest radiographs are preferred over CT scans. This is because most hospitals have X-ray machines. X-ray machines are less expensive than CT scanners. In addition, X-Rays emit significantly less ionizing radiation than CT scans [6]. CXR imaging analysis for abnormalities can most frequently be used to diagnose these instances [7]. Diagnosis for

https://doi.org/10.62500/icrtsda.1.1.30

pneumonia and other lung conditions are made using chest X-rays [8]. Several biological health activities and difficulties, including tumor identification, and pneumonia recognition utilizing CXR, are using AI today [9, 10, 11]. Deep learning's effectiveness is largely attributable to its capacity to learn levels of representations (i.e., features) from unprocessed data which helps models to achieve superior generalization. Particularly, convolutional neural networks play a key role in computer vision, where deep learning has been successful. The CNN learns the hierarchy of image feature extracts or filters at different levels of abstraction with accurate assumptions about the natural images [12] and much fewer parameters than feed-forward networks [13]. Deep learning techniques are capable of reporting visual features that are hidden in the original photos. The analysis center commonly uses convolutional neural networks (CNN) since they are particularly useful for feature learning and extraction [14]. The different types of lung nodules were identified using CNN, which was also utilized to study pediatric pneumonia and perform automatic labeling [15, 16, 17]. Deep learning approaches on CXRs are gaining popularity since deep CNNs are readily available and provide promising results in a variety of applications. The majority of studies in the literature can be divided into two categories (COVID-19 vs normal cases). However, only a small number of studies covered multi-classes. Furthermore, the most recent studies in this field propose the classification of three classes. This study provides the classification of two, three, and four classes (Covid-19, Normal, Viral Pneumonia, and Lung Opacity). Furthermore, unlike the majority of the research, each class evaluates and compares itself to other classes. By instantly retraining deep CNN networks, the transfer learning technique has substantially aided the process. Due to their extensive understanding of this field, radiologists also carry out a vital function by completing the accurate investigation, radiology AI systems can assist. The objective of this research is to utilize Deep TL techniques for the detection of Covid-19 and other lung disorders from chest X-ray images. To classify X-ray images, various datasets are available. In this study, we make use of a dataset with four classes i.e. Covid-19, Normal, Viral Pneumonia, and Lung Opacity. In this paper, we developed a COVID-19 detection model using the transfer learning technique on a well-known CNN model called ResNet50. Additionally, we fine-tuned ResNet50 by adding fully connected layers. Based on pre-trained convolutional neural networks, a variety of transfer learning techniques are used to classify different lung illnesses and automatically diagnose COVID-19 from CXRs [18]. In this work, we undergo independent training to determine the following;

Covid-19 in comparison to normal cases.

Comparison of Normal, Covid-19, and Viral Pneumonia.

Comparison of Covid-19, Lung Opacity, Viral Pneumonia, and normal cases.

This paper's key contributions are as follows;

As RT-PCR has a lower sensitivity, CXR images are used in this paper for the detection and classification of Covid-19 and other lung diseases to detect and diagnose COVID-19.

The goal of this work is to provide an automated deep transfer learning-based method for the diagnosis of infection in chest X-rays. The creation of a state-of-art automated COVID-19 diagnosis system based on a pre-trained deep transfer learning model with fine-tuning is proposed. The created model utilizes the ResNet50 model ImageNet weights to identify COVID-19 patients from Chest X-Rays.

Successfully employed a general upscale technique to enhance the resolution of chest X-ray images from the standard size of 224x224 pixels to 324x324 pixels, resulting in improved visual details and aiding in the accurate detection and classification of COVID-19 and lung diseases,

The proposed method is a four-class problem to classify the X-ray images of Normal, Viral Pneumonia, Lung Opacity, and Covid-19 patients.

https://doi.org/10.62500/icrtsda.1.1.30

2. Literature Review

Deep learning algorithms have recently been applied to quickly analyze chest X-rays. Rather than a chest computed tomography scan, it was chosen. because of its portability and low ionizing radiation exposure. Wang et al. [19] developed a deep convolutional neural network (CNN) to identify COVID-19 cases from chest X-rays using 13,975 chest X-ray images for training. Their model achieved a high classification accuracy of 98.9%. Sethy et al. [20] utilized the ResNet-50 model along with SVM for COVID-19 categorization. The resulting model achieved a classification accuracy of 95.348%. These findings suggest that CNN models, especially ResNet-50, can be effective for identifying CXRs of patients with COVID-19. Farooq and Hafeez [21] created a model named as COVIDResNet. COVIDResNet's accuracy was 96.23%. Asnaoui et al. [22] reported on a study wherein eight different TL algorithms were compared with one another in order to detect Covid-19. 5856 CXRs were used for model training. Inception-V3 and MobileNet-V2 both offered a classification accuracy of 96%. A transfer learning method was utilized by Apostolopoulos and Mpesiana [23] for Covid-19 detection. They made use of 504 normal pictures, 714 viral pneumonia images, and 224 verified COVID-19 images. For the binary class, the model's accuracy was 98.75%. Das and Kumar [24] utilized a deep TL based approach to identify COVID-19 infection in CXRs. Their dataset comprised 1427 X-ray scans, including 224 COVID-19 cases, 700 cases of common bacterial pneumonia, and 504 healthy cases. The model's training accuracy was 99.5% while its testing accuracy was 97.4%. Farooq et al. [25] proposed a model that utilized pre-trained ResNet followed by three stages of fine-tuning on a dataset of 6009 photos, including 68 COVID-19 cases. Their algorithm achieved 96.23% accuracy for four-class classification. In [26] Zhang et al. present a deep learning method that can distinguish between COVID-19 CXR radiographs and normal CXR radiographs. Pre-trained ResNet forms the network's backbone. The 1430 normal CXR images and the 100 COVID-19 images are split into training and testing groups, respectively, with 50% of each group being utilized for each. The detection rate of this approach is 96% for COVID-19 patients and 70.65% for non-COVID-19 cases. Abbas et al. [27] proposed the use of their previously developed CNN, DeTraC-Net, along with pre-trained VGG19 for the categorization of COVID-19 CXRs pictures into instances of normal and severe acute respiratory illness. Their model achieved an accuracy of 97.35%. Narin et al. [28] used three pre-trained network models, ResNet50, InceptionV3, and Inception-ResNetV2, to diagnose COVID-19 from CXR radiographs. They evaluated the effectiveness of their suggested model using 50 COVID-19 CXRs and 50 normal CXRs and achieved 98% accuracy with ResNet50. Taresh and Zhu [29] evaluated the performance of pre-trained CNNs in automatically diagnosing COVID-

19 from CXRs. Their dataset included 1200 CXR images from COVID-19 patients, 1345 CXRs from viral pneumonia patients, and 1341 CXR images from healthy subjects. VGG16 model performed well by achieving the maximum accuracy of 98.29%. Panahi and Askari [30] proposed a Deep Residual Neural Network for COVID-19 Detection from Chest X-ray Images. By using 1800 CXRs for four-class classification the achieved an accuracy of 92.1%. Arpan and Surya [31] introduce COVID-19 AI Detector (CovidAID), a cutting-edge model using deep neural networks to prioritize patients for the right tests. Their model predicts the COVID-19 infection with 90% accuracy and 100% sensitivity (recall) using the publicly available covid- chest x-ray dataset. Ahmad and Zeinab [32] developed a COVIDetection Net based on deep learning to automatically detect COVID-19. Their model achieved an accuracy of 94.44% for four-class classification. Mahmood Khan et.al [33] proposed a transfer learning approach using ResNet101 for COVID-19 detection. They achieved 87.01% accuracy for four-class classification purpose. Hossain et al. [34] proposed a TL with fine tuning Based ResNet50 model for COVID-19 Detection. Their model achieved validation accuracy of 99.17% for binary classification. Sanjay and Abhishek [35] proposed a trained output based transfer learning (TOTL)

https://doi.org/10.62500/icrtsda.1.1.30

based model for the detection of COVID-19. They used four different datasets. They Achieved accuracy of 96.82%, 98.43%, 96.6%, and 96.47% for datasets 1, 2, 3, and 4 respectively.

In this paper, we proposed a network based on transfer learning. We used pre-trained weights of ResNet50

for transfer learning purposes. Additionally, we fine-tuned ResNet50 by adding three fully connected layers. We also used dropout layers to overcome overfitting. The proposed Model gives excellent results for multi- class classification purposes (four-class).

3. Proposed Methodology

This study presented a transfer learning approach to differentiate between chest radiographs of Covid-19 patients and those with normal findings, lung opacity (Non-Covid), and viral pneumonia. The block diagram of proposed methodology is shown in Fig 1. The pre-trained ResNet50 transfer learning model weights were utilized for this purpose. A chest X-ray dataset was employed and randomly divided into training and validation sets. Pre-trained ResNet50 model weights were obtained from natural image datasets, particularly ImageNet. The model was fine-tuned by integrating three fully connected layers, after which it was applied to the chest radiographs for classification as follows;

- Covid-19 in comparison to normal cases.
- Comparison of Normal, Covid 19, and Viral Pneumonia.
- Comparison of Covid-19, Lung Opacity, Viral Pneumonia, and normal cases.

3.1. Dataset description

In the proposed work, we make use of a dataset with four classes containing Covid-19, Normal, Lung Opacity, and Viral Pneumonia from the Kaggle source created by Tawsifur Rahman and two collaborators [1] . This database was generated by a group of researchers working with medical professionals from various worldwide sources during various time frames. The images in the dataset are grayscale, but have three channels with repeated RGB values. Table 1 shows the distribution of images across different classes, but the dataset is imbalanced. To address this issue, we create balanced subsets of the dataset by selecting a subset of classes. https://www.kaggle.com/tawsifurrahman/covid19-radiographydatabase.[1]

Table 2 represents the datasets division into train and validation sets for different classes. Training and validation phases will use 80% and 20% of the prepared dataset, respectively. We used a training set of the data for training the model and validation sets are used for model validation. Some images from this dataset are shown in Fig.2 belonging to different four classes.

In recent studies, data preprocessing, data augmentation, and data transformation are the most commonly used techniques for different architectures. In our work, we used data transformation by resizing images into 324 x 324-pixel resolution and Data augmentation as a prepossessing technique.

https://doi.org/10.62500/icrtsda.1.1.30

Table 1: COVID-19 Radiography Database

COVID-19	Normal	Lung Opacity	Viral Pneumonia	Total
3616	10192	60 12	1345	21165

Table 2: **Dataset Utilized**

Class Name	COVID-19	Normal	Lung Opacity	Viral Pneumonia	Total
Train	720	720	720	720	2880
Validation	180	180	180	180	720

3.2. *Data Augmentation*

Data augmentation is a popular approach utilized in deep learning to expand a training dataset's size by utilizing different modifications on the existing data. By utilizing this technique, the performance of deep learning models is often improved. Essentially, data augmentation involves generating new training examples by applying different alterations to the already existing ones. In order to enhance data, it may be rotated, translated, scaled, cropped, flipped, or even subjected to the addition of noise.

In this instance, we are augmenting existing photographs with new ones to use as training data, using a number of different parameters. Using the rotation-range argument, we can randomly rotate the photographs within a 30-degree range, giving us more room to play with the orientation of the items in the pictures. The photos can be randomly shifted horizontally and vertically by adjusting the width-shift and height-shift range parameters. This makes the model more adaptable by introducing randomness into the positions of objects in the photos. To counteract potential bias in the training data caused by the orientation of the objects in the photos, the horizontal-flip parameter randomly flips the images horizontally.

We are able to produce a training dataset that is more varied and robust by implementing these aug- mentation factors. We used Keras ImageDataGenerator API for augmenting CXRs images.

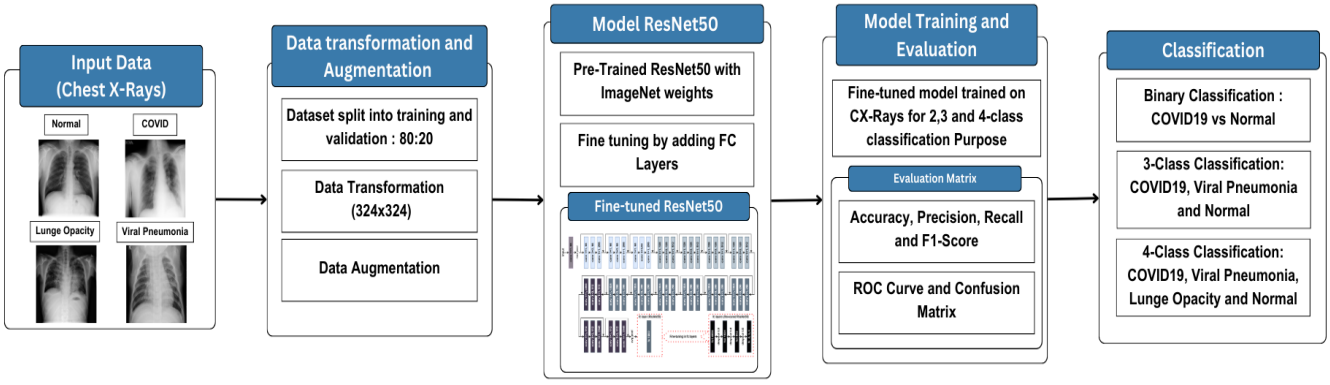

https://doi.org/10.62500/icrtsda.1.1.30

Figure 1: Block Diagram of Proposed Methodology

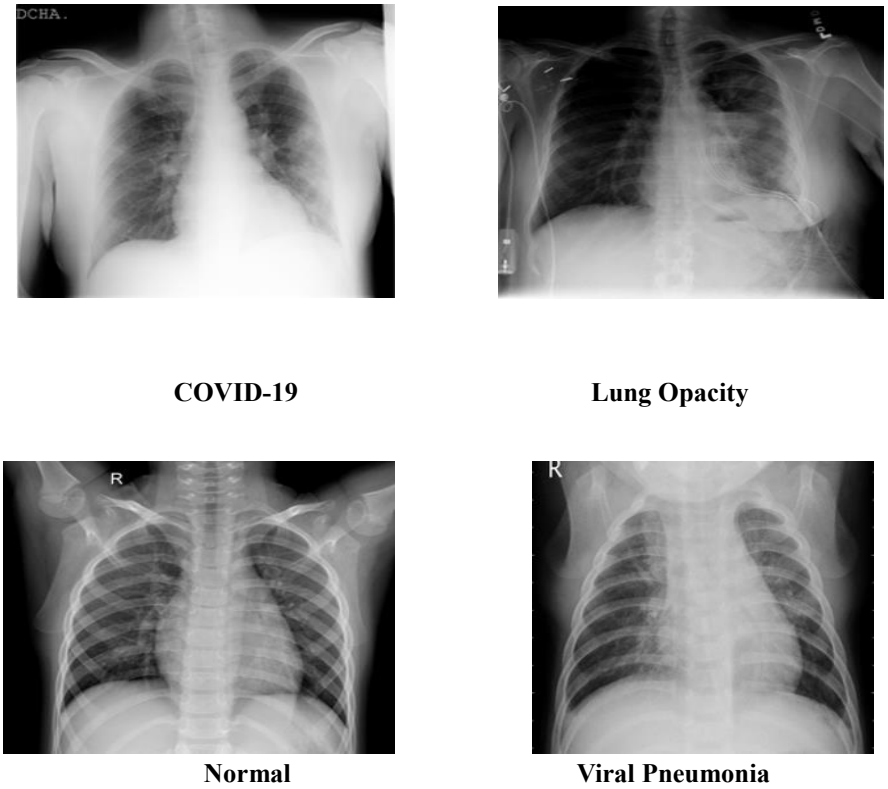

Figure 2: (Sample Images from Dataset)

3.3. *ResNet50*

ResNet50 is a deep neural network architecture that belongs to the family of Residual Networks (ResNets). It was proposed by researchers at Microsoft Research in 2015 and is composed of 50 layers. The ResNet50 architecture is based on the concept of residual learning, which is achieved by adding shortcut connections, also known as skip connections, that allow the gradient to flow more easily through the network. By using this method, it becomes feasible to train neural networks with a very high number of layers, without encountering issues related to vanishing or exploding gradients.

ResNet50 is commonly utilized as a pre-existing model for TL in a range of computer vision tasks, including image classification, object detection, and semantic segmentation. The efficacy of this approach has been validated through its ability to achieve top-performing results on diverse benchmark datasets, such as the large-scale image recognition challenge, ImageNet.

Vanishing Gradients

After the initial success of the first CNN-based architecture (AlexNet) in securing victory in the Im- ageNet 2012 competition, subsequent winning architectures have focused on increasing the depth of deep neural networks to lower the error rate. Nonetheless, deep learning faces a prevalent challenge known as the vanishing gradient problem that can occur when the number of layers is increased, causing the gradient to become either too small or too large. This causes the training and testing error rates to increase as well, particularly when using a large number of layers.

https://doi.org/10.62500/icrtsda.1.1.30

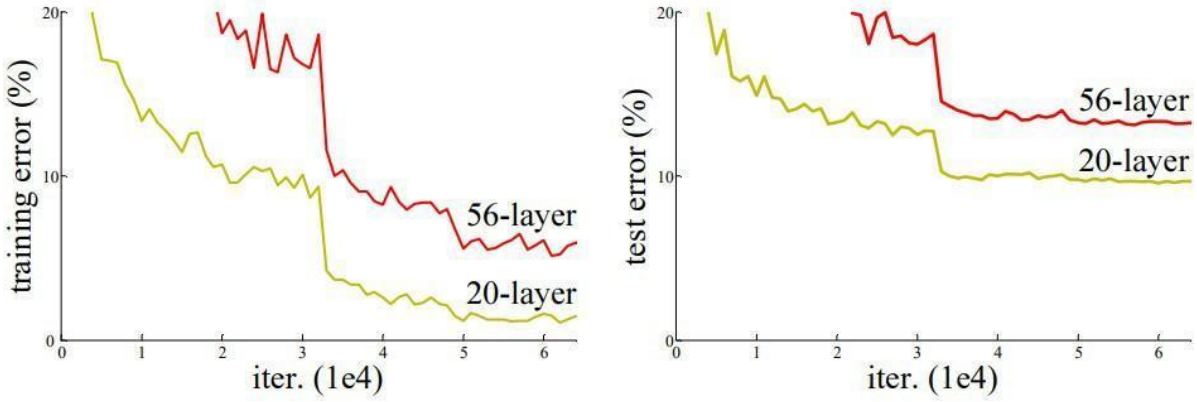

Figure 3: Comparison of 20-layer vs 56-layer architecture

After examining the error rate, the researchers discovered that a CNN with 56 layers had a higher error rate for both the training and test sets of data compared to a 20-layer CNN architecture as shown in Fig. 3, which is possibly due to the problem of vanishing or exploding gradients. In 2015, Microsoft Research scientists proposed a novel architecture called Residual Network (ResNet), which introduced a solution to this problem by using residual connections.

Residual Network:

ResNet addresses the issue of vanishing gradients by introducing Residual Blocks, which employ skip connections to connect the activations of a layer to deeper layers by bypassing certain intermediary layers, thus forming a residual block. Several residual blocks are stacked together to construct ResNets. The key idea behind ResNet is to enable the network to adapt to the residual mapping instead of solely learning the underlying mapping across the layers. In other words, instead of attempting to learn H(x), the initial mapping, ResNets enable the network to fit the residual mapping, which is achieved through the use of skip connections.

$$F(x) = H(x) - x \text{ which gives } H(x) = F(x) + x \quad (3.1)$$

Using skip connections in ResNets offers several advantages, including the ability to bypass layers that may hinder the performance of the network through regularization. ResNet overcomes the challenges posed by vanishing or exploding gradients by facilitating the training of deep neural networks without encountering such issues. The skip connections facilitate the flow of information through the network as shown in Fig. 4, making it easier for the gradient to propagate and preventing it from vanishing or exploding as the number of layers increases. This is particularly useful when working with large datasets or complex problems where deep networks are required to achieve high accuracy.

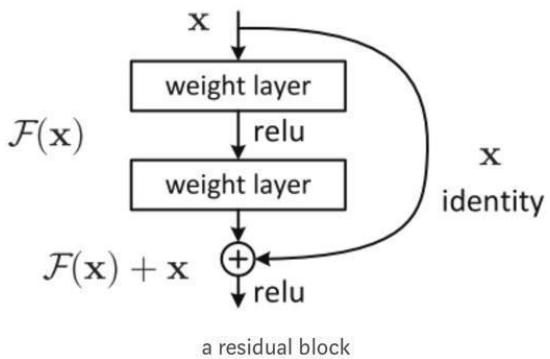

a residual block

https://doi.org/10.62500/icrtsda.1.1.30

Figure 4: (Skip (Shortcut) connection)

Transfer Learning:

Transfer learning is a widely adopted technique in deep learning, which involves leveraging an existing model as a foundation for a new task instead of initiating the model development process from scratch. The pre-existing model has already learned a range of features from a large dataset, usually in a different domain or for a different task. These learned features can be transferred to the new task, either by adjusting the pre-trained model on the new task or by employing the pre-trained model as a feature extractor. In this study, we fine-tuned a pre-trained model by transferring the learned features to the new task. Fine-tuning in transfer learning refers to the process of using a pre-trained neural network as the starting point for training a new model on a new task. In the course of fine-tuning, the parameters of the pre-trained network are updated with new data specific to the new task, while keeping the pre-trained weights fixed to a certain extent. The goal of fine-tuning is to utilize the knowledge learned by the pre-trained network and adjust it to more effectively do the new duty, thus lowering the quantity of training data needed and accelerating convergence. Transfer learning can minimize the quantity of training data needed for the new task, speed up the training process, and often lead to better performance than training a model from scratch.

In our proposed method, we utilized ResNet50 as the pre-trained weights for our work with some fine-tuning. Our methodology can be summarized in the following subsections.

3.4. Pre-trained ResNet50

Presently, state-of-the-art computer vision solutions are offered by artificial intelligence research based on deep learning. CNN, a deep learning technique, is increasingly favored in a variety of fields for image identification applications. Using only a little amount of preprocessing, CNNs can detect visual patterns directly in pixel images. A number of cutting-edge models, such as ResNet50, VGG16, DenseNet201, AlexNet, Inception v3, and GoogleNet, have gained popularity. These models have been trained on large datasets comprising diverse image categories. Transfer learning techniques utilized pre-trained weights of state-of-the- art architecture. In this study, we make use of ResNet50 for transfer learning purposes. The building block of the 50-layer ResNet has a bottleneck design. The number of parameters and matrix multiplications are decreased by employing a bottleneck residual block that uses 1x1 convolutions. This considerably speeds up the training process for each layer. Instead of using simply two layers, it employs a stack of three. Fine-tuned ResNet50 architecture is presented in Fig .

The following components make up the 50-layer ResNet architecture; The stride size is 2 and the kernel size is 7 7 for the first convolution layer with 64 unique kernels. A max pooling layer with a 2-sized stride. The following convolution consists of three convolution layers, each of which i.e. (1x1, 64 kernels), (3x3, 64 kernels), and (1x1, 256 kernels) is repeated three times. 12 further layers, iterated four times, with (1x1,128 kernels), (3x3, 128 kernels), and (1x1, 512 kernels). There are three conv levels (1x1, 256 kernels), (3x3, 256 kernels), and (1x1, 1024 kernels) that are repeated six times each, as well as three further conv layers i.e. (1x1, 512 kernels), (3x3, 512 kernels), and (1x1, 2048 kernels) are repeated three times. It is then followed by average polling (avg pool). A FC layer with 1000 output features makes up the ResNet50 model's last component.

https://doi.org/10.62500/icrtsda.1.1.30

We utilized ImageNet weights of the ResNet50 model for classification purposes. Rather, using the ResNet50 model as such, we fine-tuned the ResNet50 model. As visual features are typically retrieved and learned in the early layers of CNN-based architecture. To benefit from an existing architecture, the earliest layers are left alone, and adjustments can be made to the last layers. Consequently, we made a modification to the architecture by replacing the last fully connected layer with three new fully connected layers. The initial fully connected layer consists of 4096 features and is succeeded by a dropout layer with a dropout probability of 0.3. Following that, the second fully connected layer comprises 1024 features, accompanied by a dropout layer with a dropout probability of 0.4. Subsequently, the third fully connected layer involves 512 features, along with a dropout layer with a dropout probability of 0.5. Furthermore, we integrated a Batch-normalization Layer before each dropout layer for normalization purposes. Finally, based on specific requirements for two, three, and four-class classification, we employed a fully connected layer that consists of 2, 3, and 4 features, respectively. fine-tuned ResNet50 model is shown in Fig. 5.

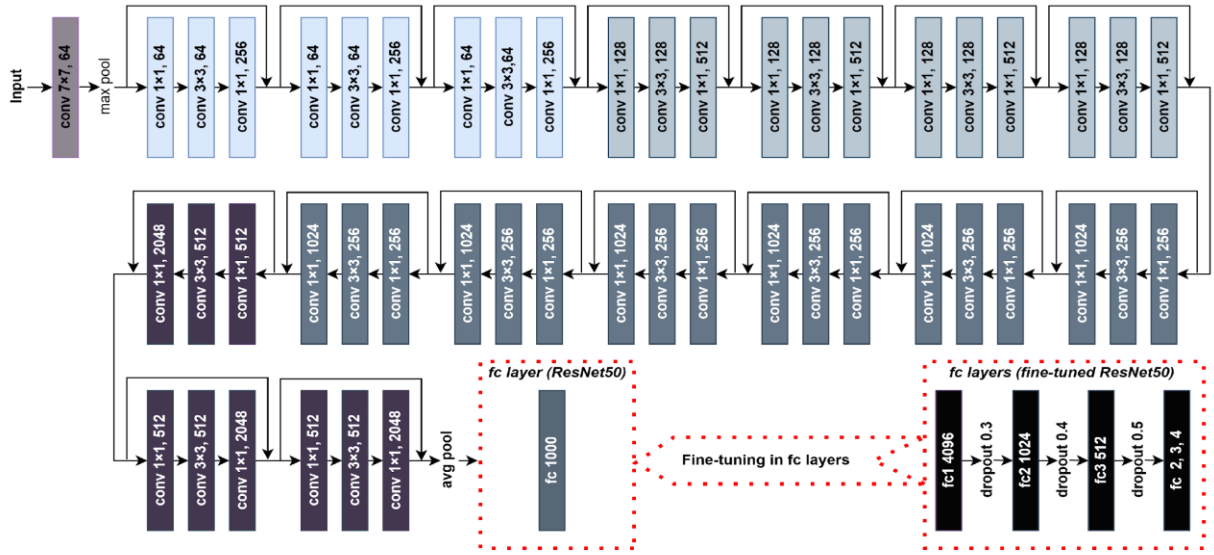

Figure 5: Fine-tuned ResNet50 Architecture

The ResNet50 model was fine-tuned in this study, as described earlier. The pre-trained ResNet50 model weights obtained from ImageNet were employed. Since medical image datasets, such as chest radiographs and CT scans, require specialized training, researchers are exploring various transfer learning techniques to address this challenge. Transfer learning models developed using the ImageNet dataset are frequently employed in the interpretation of medical image. The proposed fine-tuned ResNet50 transfer learning architecture is shown in Table 3. The building blocks, represented in brackets along with the number of stacked blocks, are used.

Table 3: Architecture of Fine-tuned ResNet50

Layer Name	Output size	Layer
conv1	164 X 164	7 X 7, 64, stride 2

https://doi.org/10.62500/icrtsda.1.1.30

$conv2_X$	81 X 81	3 X 3 max pool, stride 2 [1 X 1, 64 3 X 3, 64 1 X 1, 256] X 3
$conv3_X$	41 X 41	[1 X 1, 128 3 X 3, 128 1 X 1, 512] X 4
$conv4_X$	21 X 21	[1 X 1, 256 3 X 3, 256 1 X 1, 1024] X 6
$conv5_X$	11 X 11	[1 X 1, 512 3 X 3, 512 1 X 1, 2048] X 3
fc1	1 X 1	Average pool features = 4096
fc2	1 X 1	Dropout 0.3 features = 1024
fc3	1 X 1	Dropout 0.4 features = 512
fc4	1 X 1	Dropout 0.5 features = 2, 3, 4

4. Results and Discussion

In this research study, we analyzed and characterized three distinct modalities that utilized X-ray images.

These modalities consisted of two-class, three-class, and four-class classifications.

In the two-class modality, we trained and validated our model to distinguish between Covid-19 cases and normal cases. We employed deep transfer learning techniques to develop a model that could accurately differentiate between the two classes using X-ray images. For the three-class modality, we expanded our model to include viral pneumonia cases in addition to Covid-19 and normal cases. We trained and evaluated our model using X-ray images to compare and distinguish between these three classes. In the four-class modality, we further expanded our model to include lung opacity cases in addition to the three classes in the previous modality. We trained and evaluated our model using X-ray images to compare and distinguish between these four classes. The performance evaluation of the proposed network for the four distinct categories involved a detailed analysis of its accuracy, precision, recall, and F1 score. The results of this

https://doi.org/10.62500/icrtsda.1.1.30

analysis, which are presented in the following subsections, shed light on the effectiveness of our proposed model in the diagnosis of respiratory diseases. Overall, our study's findings demonstrate the potential of using deep transfer learning to achieve accurate and timely diagnosis of respiratory diseases by leveraging X-ray images

4.1. Covid-19 in comparison to normal cases

For the job of binary-class classification, our suggested model attained an impressive total accuracy of 99.17%. We observed that the loss decreases as the epochs progress, which shows how successful our suggested model is. To visualize the accuracy and loss trends over the course of the training process, We plotted the graphs for loss and accuracy in relation to validation as shown in Fig 6 and 7 . These graphs demonstrated that there is initial variation between epochs, but that our network's performance stabilizes as time goes on.

The confusion matrix for this state was evaluated to get insight into our model's performance, and the results are shown in Fig 8. Confusion matrices provide a thorough breakdown of the TP, TN, FP, and FN outcomes, allowing us to evaluate the model's performance. As a result of this breakdown, we can evaluate our model's efficacy with greater specificity. To provide a more comprehensive evaluation of our model's efficacy, we computed a number of performance metrics beyond just accuracy, including precision, recall, and F1 scores. In order to compare the TPR and FPR and choose the best threshold for classification, we also showed ROC curves in Fig 9.

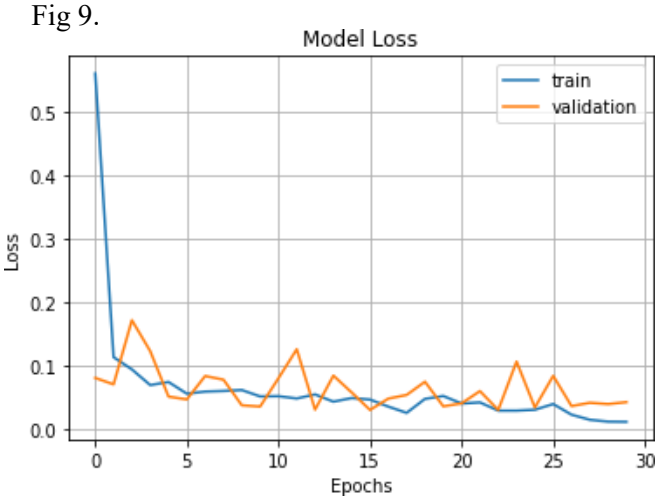

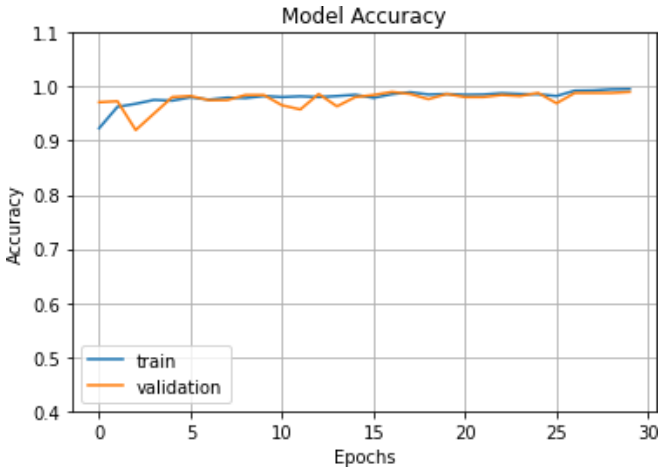

Figure 6: (Training Accuracy vs Validation Accuracy)

Figure 7: (Training Loss vs Validation Loss)

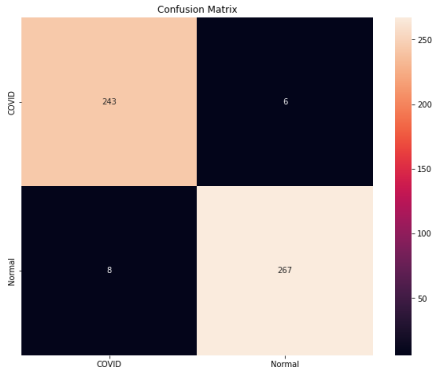

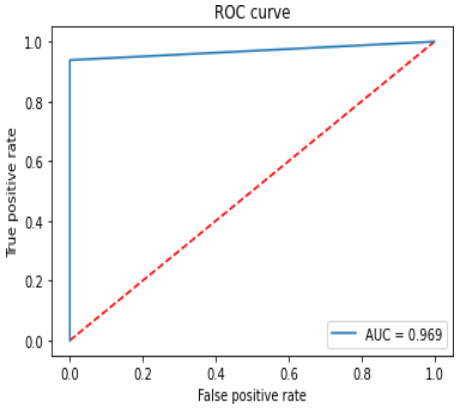

https://doi.org/10.62500/icrtsda.1.1.30

Figure 8: (Confusion Matrix) **Figure 9: (ROC-Curve**

4.2. *Comparison of Normal, Covid-19, and Viral Pneumonia*

Our suggested models acquired a remarkable accuracy of 98% for the three-class classification, which included Normal, Covid 19, and Viral pneumonia. In Figs. 10 and 11, we plot the loss and accuracy graphs against validation to see how they change over the duration of training. Our model's best fit is depicted by the straight-line connecting accuracy and validation accuracy, while the line connecting loss and validation loss gradually declines and smoothes out after an initial period.

In order to better comprehend our model's efficacy, we examined the confusion matrix for this state, shown in Fig. 12. Using the confusion matrix, we were able to assess the TP, TN, FP, and FN of the model. We didn't stop with only measuring accuracy when evaluating the efficacy of our model; we also computed other performance metrics like precision, recall, and F1 scores. For a visual representation of the trade-off between sensitivity and specificity, we also generated ROC curves, as shown in Fig. 13. The ROC curves help us compare the TPR and FPR and settle on the best categorization threshold to use.

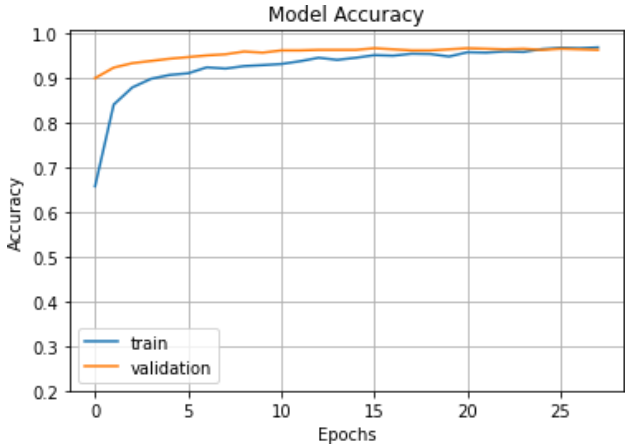

Figure 10: (Training Accuracy vs Validation Accuracy)

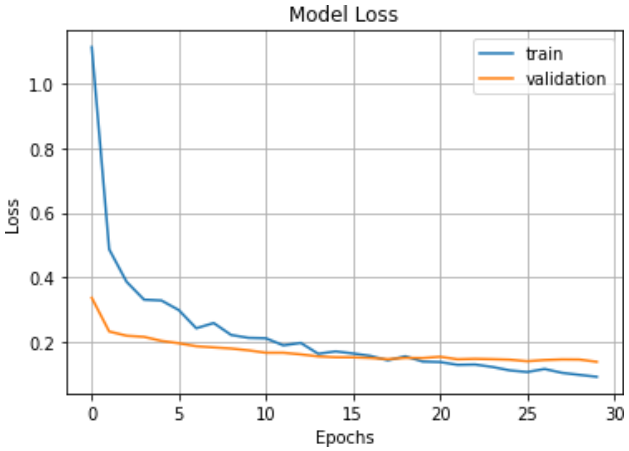

Figure 11: (Training Loss vs Validation Loss)

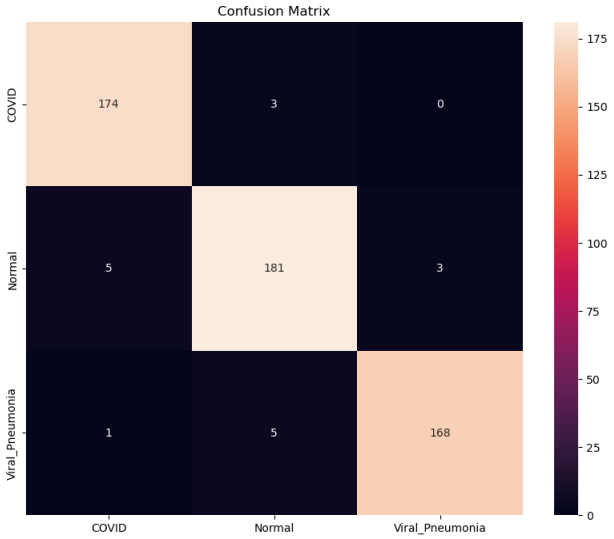

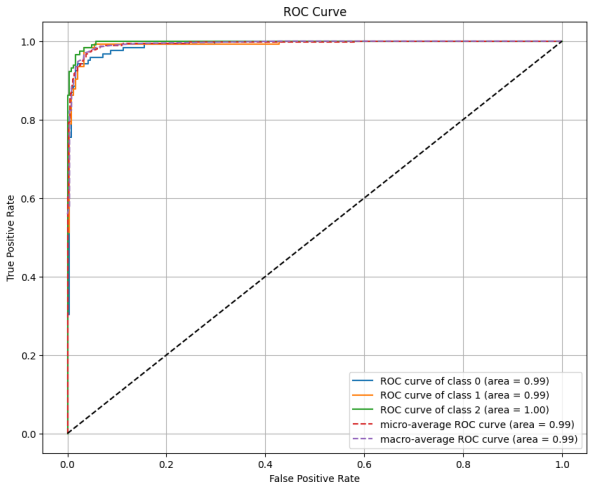

https://doi.org/10.62500/icrtsda.1.1.30

Figure 12: (Confusion Matrix) **Figure 13: (ROC-Curve**

Comparison of Covid-19, Lung Opacity, Viral Pneumonia, and Normal cases

In this study, we mainly focused on four-class classification, which is an area of research that has received less attention compared to two or three-class classification. For this challenge, our suggested model attains remarkable accuracy of 97.33%.

In Fig 14 and 15 we plotted accuracy and loss curves. The accuracy and loss curves indicated that the model was well-fitted and stable. The accuracy versus validation accuracy graph exhibits how the model performs on both the training set (training-accuracy) and validation set (validation-accuracy) over the course of increasing numbers of training epochs. A well-fitted model should have a high accuracy and validation accuracy, and the two curves should be close together. Loss and validation loss are plotted against one another as the number of training epochs grows; loss refers to the loss on the training set, while validation loss refers to the loss on the validation set. Both the loss and validation loss should be small, and the two curves should be somewhat close for a model to be considered well-fit. The loss against validation loss graph in the scenario shown in the paragraph appears to illustrate that the model begins with a large loss but improves as the number of training epochs grows, eventually stabilizing at a low loss. Similarly, when plotting accuracy against validation accuracy, we see that both metrics stay quite high and in close proximity to one another, indicating strong performance. In order to better comprehend our model's efficacy, we examined the confusion matrix for this state, shown in Fig. 16. We were able to assess the model's TP, TN, FP, and FN using the information provided by the confusion matrix. To further illustrate the trade-off between sensitivity and specificity, ROC curves are given in Fig. 17.

In conclusion, we show that our proposed model for four-class classification is effective, based on our

research. These outcomes point to a model that is well-fit and has good performance on both the training and validation sets. We also calculated precision, recall, and F1 score to assess the model's efficacy, and the results are displayed in Table 4. Here label 0, 1, 2 and 3 represents Covid, Normal, Viral-Pneumonia and Lung-Opacity respectively. Our suggested network's performance is compared in detail to that of other networks proposed in previous studies in Table 5. The table provides data demonstrating the advantages of our proposed network over those of other recently proposed networks

Table 4: **Results Comparison**

Models	Classes	Accuracy	Reference
Pre-trained ResNet50	two-class	98	[27]
TL based model	two-class	98.75	[23]
Fine-tuned ResNet50	two-class	99.17	[34]
COVID-ResNet	three-class	96.23	[21]
Automated Deep TL	three-class	97.4	[24]

https://doi.org/10.62500/icrtsda.1.1.30

VGG16	three-class	98.29	[29]
Deep Residual NN	four-class	92.1	[30]
COVIDetection Net	four-class	94.44	[32]
ResNet50 with fine-tuning	four-class	96.23	[25]

Table 5: **Classification Report**

	2-class		3-class			4-class			
Labels	0	1	0	1	2	0	1	2	3
Precision	0.99	0.99	0.96	0.99	0.99	0.98	0.99	0.98	0.97
Recall	0.98	0.99	0.98	0.99	0.96	0.97	0.98	0.96	0.98
F1-Score	0.99	0.99	0.97	0.99	0.97	0.98	0.97	0.96	0.97

https://doi.org/10.62500/icrtsda.1.1.30

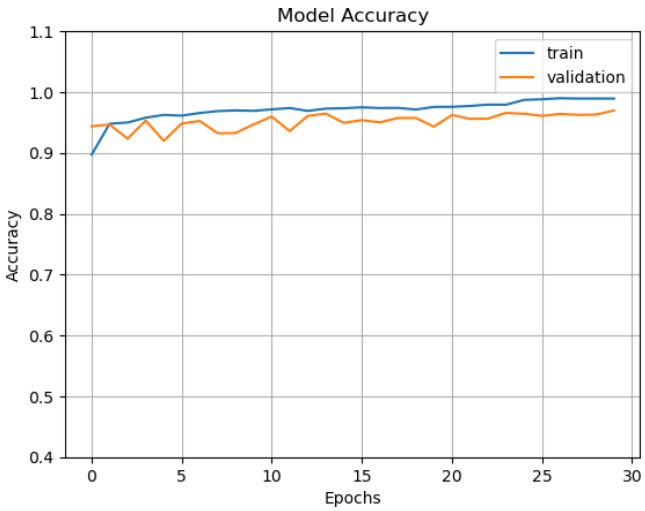

Figure 14: (Training Accuracy vs Validation Accuracy)

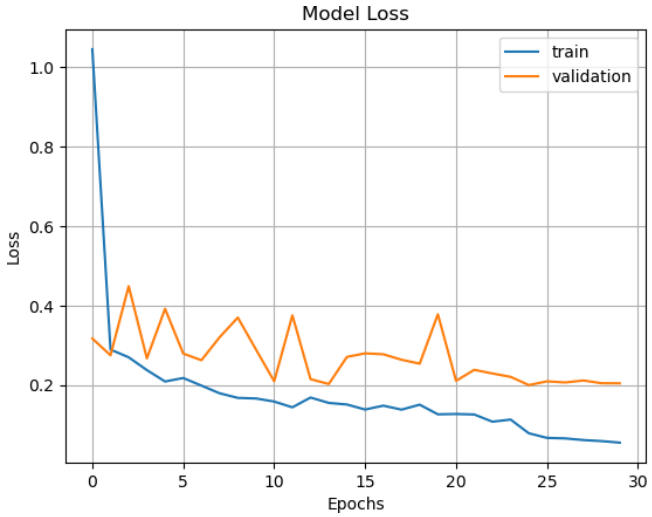

Figure 15: (Training Loss vs Validation Loss)

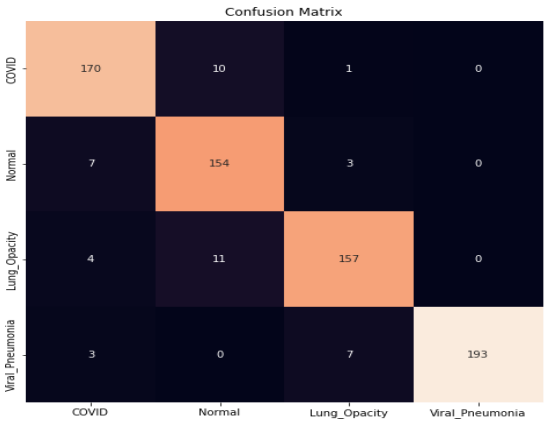

Figure 16: (Confusion Matrix)

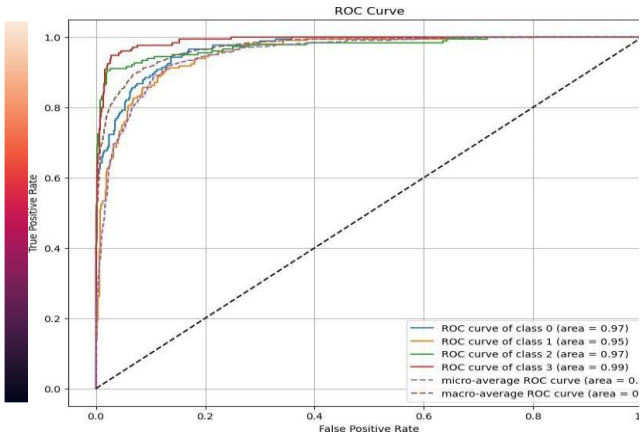

Figure 17: (ROC-Curve)

https://doi.org/10.62500/icrtsda.1.1.30

5. Conclusion and Future work

This study used a pre-trained ResNet-50 model with fine-tuning through the inclusion of three fully connected layers for two, three, and four class classifications to investigate the possibility of deep TL techniques for detecting and classifying COVID-19 and lung illnesses. The study's findings indicated a high overall accuracy of 99.17%, 98%, and 97.33% for classifications into two, three, and four classes, respectively. These results imply that deep transfer learning methods can be very helpful in medical picture analysis and may help in the diagnosis of a wide range of ailments, especially COVID-19 and lung conditions. Pre-trained models, like ResNet-50, can significantly cut down on the time and resources required for training, enabling more effective and precise model creation. Additionally, the model's efficacy in identifying and categorizing COVID-19 and lung disorders can be enhanced by fine-tuning it through the addition of fully linked layers. In conclusion, the study demonstrated that COVID-19 and lung illnesses can be accurately detected and classified using a pre-trained ResNet-50 model with fine-tuning by the inclusion of three fully connected layers. The model's precision can, however, be impacted by the size, consistency, and quality of the dataset as well as any potential biases. However, this study lays the foundation for future research to investigate the application of deep learning models and techniques in medical picture processing as well as the creation of larger and more varied datasets. Deep learning is ultimately a promising field for future research and application because it has the ability to help with the detection and treatment of various conditions, such as COVID-19 and lung ailments.

Future research can focus on a number of areas to improve the effectiveness of deep learning methods for medical picture processing. To aid in the training and testing of models, larger and more diverse datasets containing information from various demographics and imaging modalities can be useful. The effectiveness of several deep learning models, such as CNNs, RNNs, and GANs, in identifying and categorizing lung illnesses, such as COVID-19, may also be evaluated. Furthermore, the model's performance may be assessed using real-world data, and models that can be used in clinical situations can be constructed.

In addition to these efforts, the model's decision-making process can be improved by employing XAI methods to make it more explicit and understandable. Furthermore, a broader range of respiratory illnesses can be utilized to evaluate the model's performance, allowing for more precise diagnosis and therapy. These areas of research can complement each other and the efforts mentioned above, leading in the development of more powerful deep learning models for medical image processing

References

1. Cucinotta, D., & Vanelli, M. (2020). WHO declares COVID-19 a pandemic. Acta Bio Medica: Atenei Parmensis, 91(1), 157.
2. Rustam, F., Reshi, A. A., Mehmood, A., Ullah, S., On, B. W., Aslam, W., & Choi, G. S. (2020). COVID-19 future forecasting using supervised machine learning models. IEEE access, 8, 101489-101499.
3. Ng, M. Y., Lee, E. Y., Yang, J., Yang, F., Li, X., Wang, H., ... & Kuo, M. D. (2020). Imaging profile of the COVID-19 infection: radiologic findings and literature review. Radiology: Cardio- thoracic Imaging, 2(1).

https://doi.org/10.62500/icrtsda.1.1.30

4. Cascella, M., Rajnik, M., Aleem, A., Dulebohn, S. C., & Di Napoli, R. (2022). Features, evaluation, and treatment of coronavirus (COVID-19). Statpearls [internet].
5. American College of Radiology. (2020). ACR recommendations for the use of chest radiography and computed tomography (CT) for suspected COVID-19 infection.
6. Latif, S., Usman, M., Manzoor, S., Iqbal, W., Qadir, J., Tyson, G., ... & Crowcroft, J. (2020). Leveraging data science to combat COVID-19: A comprehensive review. IEEE Transactions on Artificial Intelligence, 1(1), 85-103.
7. Cennimo, D. J. (2020). Coronavirus disease 2019 (COVID-19) clinical presentation. vol, 8, 101489-101499.
8. Al-Awadhi, A. M., Alsaifi, K., Al-Awadhi, A., & Alhammadi, S. (2020). Death and contagious infectious diseases: Impact of the COVID-19 virus on stock market returns. Journal of behavioral and experimental finance, 27, 100326.
9. Kallianos, K., Mongan, J., Antani, S., Henry, T., Taylor, A., Abuya, J., & Kohli, M. (2019). How far have we come? Artificial intelligence for chest radiograph interpretation. Clinical radiology, 74(5), 338-345.
10. Rahman, T., Chowdhury, M. E., Khandakar, A., Islam, K. R., Islam, K. F., Mahbub, Z. B.,... & Kashem, S. (2020). Transfer learning with deep convolutional neural network (CNN) for pneumonia detection using chest X-ray. Applied Sciences, 10(9), 3233.
11. Tahir, A. M., Chowdhury, M. E., Khandakar, A., Al-Hamouz, S., Abdalla, M., Awadallah, S.,... & Al-Emadi, N. (2020). A systematic approach to the design and characterization of a smart insole for detecting vertical ground reaction force (vGRF) in gait analysis. Sensors, 20(4), 957.
12. Lakhani, P., & Sundaram, B. (2017). Deep learning at chest radiography: automated classification of pulmonary tuberculosis by using convolutional neural networks. Radiology, 284(2), 574-582.
13. Laal, M. (2013). Innovation process in medical imaging. Procedia-Social and Behavioral Sciences, 81, 60-64.
14. Krizhevsky, A., Sutskever, I., & Hinton, G. E. (2017). Imagenet classification with deep convo- lutional neural networks. Communications of the ACM, 60(6), 84-90.
15. Choe, J., Lee, S. M., Do, K. H., Lee, G., Lee, J. G., Lee, S. M., & Seo, J. B. (2019). Deep learning–based image conversion of CT reconstruction kernels improves radiomics reproducibility for pulmonary nodules or masses. Radiology, 292(2), 365-373.
16. Kermany, D. S., Goldbaum, M., Cai, W., Valentim, C. C., Liang, H., Baxter, S. L., ... & Zhang, K. (2018). Identifying medical diagnoses and treatable diseases by image-based deep learning. Cell, 172(5), 1122-1131.
17. Negassi, M., Suarez-Ibarrola, R., Hein, S., Miernik, A., & Reiterer, A. (2020). Application of artificial neural networks for automated analysis of cystoscopic images: a review of the current status and future prospects. World journal of urology, 38(10), 2349-2358.
18. Majeed, T., Rashid, R., Ali, D., & Asaad, A. (2020). Covid-19 detection using cnn transfer learning from x-ray images. Medrxiv, 12, 2020
19. Wang, L., Lin, Z. Q., & Wong, A. (2020). Covid-net: A tailored deep convolutional neural network design for detection of covid-19 cases from chest x-ray images. Scientific Reports, 10(1), 1-12.
20. Sethy PK, Behera SK. Detection of coronavirus disease (COVID-19) based on deep features. Preprints 2020:2020030300.
21. Farooq, M., & Hafeez, A. (2020). Covid-resnet: A deep learning framework for screening of

https://doi.org/10.62500/icrtsda.1.1.30

covid19 from radiographs. arXiv preprint arXiv:2003.14395.

22. El Asnaoui, K., Chawki, Y., & Idri, A. (2021). Automated methods for detection and classification pneumonia based on x-ray images using deep learning. In Artificial intelligence and blockchain for future cybersecurity applications (pp. 257-284). Springer, Cham.
23. Apostolopoulos, I. D., & Mpesiana, T. A. (2020). Covid-19: automatic detection from x-ray images utilizing transfer learning with convolutional neural networks. Physical and engineering sciences in medicine, 43(2), 635-640.
24. Das, N. N., Kumar, N., Kaur, M., Kumar, V., & Singh, D. (2020). Automated deep transfer learning-based approach for detection of COVID-19 infection in chest X-rays. Irbm.
25. Farooq, M., & Hafeez, A. (2020). Covid-resnet: A deep learning framework for screening of covid19 from radiographs. arXiv preprint arXiv:2003.14395.
26. Zhang, J., Xie, Y., Pang, G., Liao, Z., Verjans, J., Li, W., ... & Xia, Y. (2020). Viral pneumonia screening on chest X-rays using confidence-aware anomaly detection. IEEE transactions on medical imaging, 40(3), 879-890.
27. Abbas, A., Abdelsamea, M. M., & Gaber, M. M. (2021). Classification of COVID-19 in chest X- ray images using DeTraC deep convolutional neural network. Applied Intelligence, 51, 854-864.
28. Narin, A., Kaya, C., & Pamuk, Z. (2021). Automatic detection of coronavirus disease (covid-19) using x-ray images and deep convolutional neural networks. Pattern Analysis and Applications, 24(3), 1207-1220.
29. Taresh, M. M., Zhu, N., Ali, T. A. A., Hameed, A. S., & Mutar, M. L. (2021). Transfer learning to detect covid-19 automatically from x-ray images using convolutional neural networks. International Journal of Biomedical Imaging, 2021.
30. Panahi, A., Askari Moghadam, R., Akrami, M., & Madani, K. (2022). Deep Residual Neural Network for COVID-19 Detection from Chest X-ray Images. SN Computer Science, 3(2), 1-10.
31. Mangal, A., Kalia, S., Rajgopal, H., Rangarajan, K., Namboodiri, V., Banerjee, S., & Arora, C. (2020). CovidAID: COVID-19 detection using chest X-ray. arXiv preprint arXiv:2004.09803.
32. Elkorany, A. S., & Elsharkawy, Z. F. (2021). COVIDetection-Net: A tailored COVID-19 detec- tion from chest radiography images using deep learning. Optik, 231, 166405.
33. Mahmood Khan, R. N., Hussain, L., Alluhaidan, A. S., Majid, A., Lone, K. J., Verdiyev, R.,... & Duong, T. Q. (2022). COVID-19 lung infection detection using deep learning with trans- fer learning and ResNet101 features extraction and selection. Waves in Random and Complex Media, 1-24.
34. Hossain, M. B., Iqbal, S. H. S., Islam, M. M., Akhtar, M. N., & Sarker, I. H. (2022). Transfer learning with fine-tuned deep CNN ResNet50 model for classifying COVID-19 from chest X-ray images. Informatics in Medicine Unlocked, 30, 100916.

https://doi.org/10.62500/icrtsda.1.1.30

35. Kumar, S., & Mallik, A. (2022). COVID-19 Detection from Chest X-rays Using Trained Output Based Transfer Learning Approach. Neural processing letters, 1-24.

https://doi.org/10.62500/icrtsda.1.1.31

Proc. 1st International Conference on Recent Trends in Statistics and Data Analytics
Air University Islamabad, Pakistan – May 9, 2024, Vol. 1, pp. 287-295

Harmonizing Genotype Selection Strategies: Advancements of Multi Environmental Trails Analysis in Crop Development

Behnam Bakhshi* and Mohammad Reza Naroui Rad

Horticulture Crops Research Department, Sistan Agricultural and Natural Resources Research and Education Center, AREEO, Zabol, Iran.

Abstract

Selecting optimal methods for identifying superior genotypes remains a primary challenge for plant breeders. This review aimed to classify various univariate and multivariate selection indices using strategies such as Variance-based, AMMI (Additive Main effects and Multiplicative Interaction)-based, BLUP (Best Linear Unbiased Prediction)-based, and GE/T (Genotype × Environment/Trait)-based approaches to determine the most effective genotypes in terms of stability, yield, and agronomic traits. This review categorized these statistic methods to five general methodologies: univariate performance selection index (UPSI: mean performance), univariate stability selection indices (USSIs: Var, Shukla, ASV, MASV, MASI, and WAASB), multivariate performance selection indices (MPSIs: GT, GYT, GYSI, and FAI-BLUP), univariate performance and stability selection indices (UPSSIs: CV, HMGV, RPGV, WAASBY, and GGE), and multivariate performance and stability selection index (MPSSI: MTSI). This study introduces an optimized model of USSIs (O-USSIs) aimed at enhancing genetic gain, demonstrating the efficiency of O-USSIs in selecting high-yielding and stable genotypes. Additionally, this study introduces GYSI as an efficient method to identify high-yielding and stress tolerant genotypes simultaneously. These methods facilitate the ranking of genotypes based on stress tolerance, high yielding, and stability, thereby assisting plant breeders in genotype selection.

Keywords: Agronomic traits, High-yielding, Multi Environmental Trials, Stability, Stress Tolerance, Statistical Methods

1. Introduction

Yield enhancement stands as the primary objective within breeding programs, yet stability and the performance of agronomic traits also hold significant importance for augmenting selection efficiency (1). Selection indices represent vital practical tools in this domain, having been introduced as early as 1936 (2) and continuously refined since. A pivotal aspect of releasing a new cultivar lies in its broad adaptability. Broad adaptability signifies increased stability against inherent variability in an ecosystem, while specific adaptability denotes the notable yield of genotypes within a particular environment (3). In the presence of genotype by environment (G×E) interaction, evaluating genotypes across multiple locations or years, termed as multi-environment trials (METs), becomes imperative (4, 5). The collective impact of genotype (G), environment (E), and G×E interaction within an environment dictates a genotype's performance (4). Previous studies have utilized stability indices, including parametric (6-8), non-parametric (9), Additive Main Effects And Multiplicative Interaction (AMMI) (8, 10-12), and GGE-biplot (9, 13-17), in selecting oilseed rape genotypes. Recently, these statistical methods were applied and compared in oilseed rape to elucidate the relationship between mean yield and stability (18).

The majority of studies typically assess the mean yield and stability of a single trait, often focusing solely on grain yield. However, univariate selection, either through direct selection or trait-based selection for high yield, may lead to unintended alterations in other agronomic traits (19). Evidence

https://doi.org/10.62500/icrtsda.1.1.31

suggests that multivariate selection, considering several traits simultaneously, is more effective than univariate approaches (20). Therefore, for accurate selection and recommendation of the best genotypes, selection based on multiple traits should be prioritized (19).

Desirable traits for oilseed rape improvement and sustainable grain production often include reduced days to maturity (early maturity), moderate plant height, extended flowering period, increased pod number per plant, higher grain number per pod, and greater thousand-grain weight (21-23). Various selection indices have been developed to assist breeders in considering multiple traits, such as genotype by trait (GT) (24), genotype by yield*trait (GYT) (25), ideotype-design index (FAI-BLUP) (26), and multi-trait stability index (MTSI) (27). However, few studies have been conducted to identify superior oilseed rape genotypes using multiple traits.

The GT biplot methodology has been employed to explore the interrelationships among different traits of winter oilseed rape genotypes (28). Recently, new oilseed rape lines were evaluated based on multiple traits using GT and GYT biplot analysis (29).

Despite advancements in understanding selection indices, a comprehensive review comparing various multivariate and univariate selection indices in oilseed rape genotypes has not been undertaken thus far. Consequently, this study endeavors to compare and amalgamate different categories of selection indices, including Variance-based, AMMI (Additive Main effects and Multiplicative Interaction)-based, BLUP (Best Linear Unbiased Prediction)-based, and GE/T (Genotype × Environment/Trait)-based approaches. By doing so, this research aims to provide novel insights into how univariate or multivariate genotype selection for performance and stability can be optimized to maximize the efficacy of genotype selection within plant breeding programs.

2. Results

Selection indices

In genotype selection, agronomic traits and stability stand as the primary objectives for plant breeders. Evaluation of indices can be conducted in either multivariate or univariate approaches, both of which are employed in assessing performance- and stability-based selection indices.

This review categorizes different groups of selection indices, such as GE/T-, BLUP-, AMMI-, and Variance-based methodologies, based on their efficiency in evaluating stability, yield, and agronomic traits performance. As a result, the selection indices were classified into five general methods: Univariate Performance Selection Index (UPSI), Univariate Stability Selection Indices (USSIs), Multivariate Performance Selection Indices (MPSIs), Univariate Performance and Stability Selection Indices (UPSSIs), and Multivariate Performance and Stability Selection Indices (MPSSI) (see Table 2).

Univariate performance selection index (UPSI)

Univariate Performance Selection Index (UPSI) can be derived by calculating the mean performance of each environmental trial and subsequently utilizing this information for ranking genotypes based on mean grain yield.

Univariate stability selection indices (USSIs)

In this study, variance-based stability parameters including environmental variance (Var) and Shukla's stability variance (Shukla) (31, 32), AMMI-based stability parameters such as AMMI stability value (ASV), modified AMMI stability value (MASV), and modified AMMI stability index (MASI) (33-35), as well as BLUP-based stability parameters such as the weighted average of absolute scores (WAASB) (36), are categorized as Univariate Stability Selection Indices (USSIs).

Selection for desirable traits by estimation of multivariate performance selection indices (MPSIs)

To identify genotypes with desirable traits, multivariate performance selection indices (MPSIs) including genotype by trait (GT), genotype by yield*trait (GYT), genotype by yield*stress index (GYSI), and Ideotype-design index (FAI-BLUP) could be employed for genotype selection. GT analysis

https://doi.org/10.62500/icrtsda.1.1.31

involved computing the mean values of agronomic traits data from various environments. Additionally, each evaluated trait was adjusted in relation to grain yield to balance their importance according to breeder's goals using GYT. Based on FAI-BLUP analysis, ideal values for the ideotype design could be defined for each trait, considering the minimum, mean, and maximum values of the dataset. This approach allows breeders to set target values for each trait. In this review, a modified GYT biplot approach called genotype by yield*stress index (GYSI) biplot is introduced, where stress tolerant indices replaced the traits. Various stress tolerant and susceptibility indices, including Tolerance Index, Stress Susceptibility Index, Yield Stability Index, Harmonic Mean, Geometric Mean Productivity, Mean Productivity, and Stress Tolerance Index, could be incorporated to create the GYSI ranking. Using this methodology, each stress index was either multiplied or divided by grain yield to construct the GYSI table. For stress indices where higher values are desirable (e.g., YSI, HM, GMP, MP, and STI), they were multiplied by grain yield (e.g., GY*YSI). Conversely, for stress indices where higher values are undesirable (e.g., TOL and SSI), grain yield was divided by the trait (e.g., GY/TOL). Thus, a larger value in the GYSI table indicates greater desirability.

Table 1. The stress tolerance indices that could be utilized in GYSI calculation

Indices	Abbreviation	Formula	Desirable value	References
Tolerance Index	TOL	$Yp - Ys$	Low	(37)
Mean Productivity	MP	$\frac{(Yp + Ys)}{2}$	High	(37)
Stress Tolerance Index	STI	$\frac{Yp \times Ys}{(\bar{Y}p)^2}$	High	(38)
Geometric Mean Productivity	GMP	$\sqrt{Yp \times Ys}$	High	(38)
Harmonic Mean Productivity	HM	$\frac{2(Yp \times Ys)}{(Yp + Ys)}$	High	(39)
Yield Stability Index	YSI	$\frac{Ys}{Yp}$	High	(40)
Stress Susceptibility Index	SSI	$\frac{(1 - \frac{Ys}{Yp})}{(1 - (\frac{\bar{Y}s}{\bar{Y}p}))}$	Low	(41)

To ranking genotypes, the GYSI data shroud be standardized for each yield-stress index combination as represented using the following formula and then integrated to calculate superiority index (SI) for each genotype. High SI values of yield-stress index combinations represent high-yielding and drought tolerance simultaneously. Finally, genotypes with the positive SI values (above average) could be considered as high yielding and stress tolerant genotypes.

$$\textit{Standardized yield-stress index value} = \frac{\text{Genotype yield\_stress index value} - \text{Yield\_stress index mean of all genotypes}}{\text{Yield\_stress index Standard deviation of all genotypes}}$$

Simultaneous selection for stable and high-yielding genotypes

UPSI and USSIs are both viable strategies for genotype selection based on mean grain yield and genotype stability, respectively. However, their independent and sometimes conflicting results can complicate genotype selection. To address this limitation, three approaches are introduced in this review

1. Subscription of UPSI and USSIs results: Subscribing to the top five ranked USSIs and UPSI can be considered an appropriate method to identify high-yielding and stable genotypes simultaneously.

2. Yield involvement in USSIs calculation (O-USSIs): This method involves incorporating yield performance into USSIs calculation, resulting in the identification of high-yielding and stable genotypes

https://doi.org/10.62500/icrtsda.1.1.31

simultaneously, known as optimized USSIs (O-USSIs). These O-USSIs could be calculated using the following formula:

$$O\text{-}USSI = \alpha \frac{\bar{Y}i.}{\bar{Y}..} + \beta \frac{\frac{1}{USSIi}}{\frac{1}{g}\sum_{1}^{g}\frac{1}{USSIi}}$$

where *O-USSI* is the USSI of the i[th] genotype; $\bar{Y}i.$ is the mean grain yield of the i[th] genotype of testing environments; $\bar{Y}..$ is the overall mean grain yield; USSIi is the stability parameter value of i[th] genotype; g is the examined number of genotypes. α and β are the weights assigned for grain yield and stability, which are considered 70 and 30% in this study, respectively. More weight was assigned to grain yield due to its importance (43). Accordingly, the high-yielding and stable genotypes were ranked upside.

3-Univariate performance and stability selection *indices* (UPSSIs)*:* Yield performance data could be analyzed using the GGE method (GGE-biplot), employing principal component analysis (PCA) of environment-centered data to rank genotypes based on their superiority indices. Similarly, WAASBY was introduced as another superiority index-based model, ranking genotypes by weighting between yield performance and WAASB stability index. Additionally, HMGV, RPGV, and coefficient of variability (CV) were also introduced as other methods to identify high-yielding and stable genotypes (44,45,46).

***Multivariate performance and stability selection indices* (MPSSI)**

Using scores determined through exploratory factor analysis, the Multi-trait Stability Index (MTSI) was derived based on the ideotype-genotype Euclidean distance. MTSI is categorized as a BLUP-based Multi-trait Performance and Stability Selection Index (MPSSI), which simultaneously enables genotype selection based on high trait performance (including grain yield and other agronomic traits) as well as high stability (27).

Estimation of genetic gain (GS)

For each selection index, the genetic gain (GS) for the examined traits could be calculated using the following formula:

$$GS_{j(i)} = \left(H_k^2 \times (X_{sj(i)} - X_{.j})\right) \times 100/X_{.j}$$

Where H_k^2 is the broad-sense heritability of trait *k*, $X_{sj(i)}$ is the average of the selected genotypes (top 5 ranked genotypes for each method) for trait *k* with selection based on i index, $X_{.j}$is the original population average of trait *k.*

3. Conclusion

This research comprehensively considered a diverse array of selection indices, encompassing Var, Shukla, CV, ASV, MASV, MASI, WAASB, GT, GYT, GYSI, FAI-BLUP, HMGV, RPGV, WAASBY, GGE, and MTSI, each addressing specific selection parameters such as stability, yield performance, or other agronomic traits. Through these selection indices, various rankings and genetic gains were obtained. A novel aspect of this research was the classification of these selection indices based on several criteria, including whether the index is multivariate or univariate, its ability to evaluate stability, yield performance, and agronomic traits. Consequently, five primary genotype selection strategies were developed: UPSI, USSIs, UPSSIs, MPSI, and MPSSI. Given the increasing necessity for evaluating genotypes in multi-environment trials, this study recommends utilizing the introduced integrated approach to provide accurate recommendations for the best-performing genotypes

https://doi.org/10.62500/icrtsda.1.1.31

Index type	Statistic	Symbol	Formula	Desirable value	References
UPSI	Mean	Y	$\overline{X}$	max	
USSIs	Environmental variance (Var)	Var	$\sum(R_{ij} - M_i)^2/(e-1)$	min	(31)
	Shukla's stability variance	Shukla	$\left[\frac{p}{(p-2)(q-1)}\right] W^2 - \frac{\sum W_i^2}{(p-1)(p-2)(q-1)}$	min	(47)
	AMMI stability value	ASV	$\sqrt{\left(\frac{SS_{IPCA1}}{SS_{IPCA2}}(IPCA1)\right)^2 + (IPCA$	min	(33)
	Modified AMMI stability value	MASV	$\sqrt{\sum_{n=1}^{N-2}\left(\left(\frac{SSIPCA_n}{SSIPCA_{n+1}}\right)(IPCA_n\right.}$	min	(34)
	Modified AMMI stability index	MASI	$\sqrt{\sum_{n=1}^{N} IPCA_n^2 \times \theta_n^2}$	min	(35)
	Weighted average of absolute scores	WAASB	$\frac{\sum_{n=1}^{p}\lvert IPCA_{in} \times EP_n\rvert}{\sum_{n=1}^{p} EP_n}$	min	(36)
UPSIs	Coefficient of variability	CV	$\frac{SD_x}{\overline{X}} \times 100$	min	(46)
	Harmonic mean of genotypic values	HMGV	$\frac{e}{\sum_{j=1}^{e}(\frac{1}{GV_{ij}})}$	min	(45)
	Relative performance of genotypic values	RPGV	$\frac{1}{e}[\frac{\sum_{j=1}^{e} GV_{ij}}{M_j}]$	min	(45)
	Weighted average of the stability (WAASB) and mean performance (Y)	WAASBY	$\frac{(rY_i \times \theta_y) + (rW_i \times \theta_w)}{\theta_y + \theta_w}$	max	(36)

https://doi.org/10.62500/icrtsda.1.1.31

	Genotype + Genotype × Environment interaction	GGE	$\mu + e_j + \sum_{n=1}^{N} \lambda_n \Upsilon_{in} \delta_{jn} + \varepsilon_{ij}$	min	(48)
MPSSI	Multi-trait stability index	MTSI	$\left[\sum_{j=1}^{f} (R_{il} - R_{lj})^2\right]^{0.5}$	min	(27)
MPSIs	Genotype by trait	GT	$\frac{T_{ik} - \overline{T}_k}{S_k}$	min	(24)
	Genotype by yield*trait	GYT	$\frac{T_{ik} - \overline{T}_k}{S_k}$	min	(25)
	Genotype by yield*stress tolerant index	GYSI	$\frac{T_{ik} - \overline{T}_k}{S_k}$	+min	(49)
	Ideotype-design index	FAI-BLUP	$\frac{\frac{1}{d_{il}}}{\sum_{i=1,j=1}^{i=n;j=m} \frac{1}{d_{il}}}$	max	(26)

Table 2: different groups of selection indices calculated in this study.

θ: percentage sum of square explained by the nth IPCAs effects. θ_y: weights of mean performance. θ_w: weights of stability. μ: Grand mean. λ_n: The eigenvalue of the principal component analysis axis. Υ_{in} *and* δ_{jn}: genotype and environment principal components scores for axis n. ε_{ij}: Residual effect ~ N (0, σ^2). d_{il}= Genotype-ideotype distance from the i^{th} genotype to the l^{th} ideotype based on standardized mean Euclidean distance. e: number of environments. e_j: Environmental deviation from the grand mean. EP_n: the amount of the variance explained by the n^{th} IPCA. GV_{ij}: the genetic value of i^{th} genotype in j^{th} environment. IPCA: Interaction principal component axis. M_i: mean performance of genotype across all environments. M_j: the mean performance in the j^{th} environment. N: number of principal components retained in the model. R_{ij}: performance of i^{th} genotype in the j^{th} environment. R_l: l^{th} score of the ideotype. rY_i: rescaled values (0-100) for grain yield. rW_i: rescaled values the stability (WAASB). S_k: the standard deviation for the trait or yield-trait combination j. SD_x: Standard deviation of a genotype mean across environments. SS: sum of squares. T_{ik}: the original value of i^{th} genotype for the trait or k^{th} yield-trait combination in the GT or GYT table. $\overline{T_k}$: mean across genotypes for the trait or k^{th} yield-trait combination. W^2: Wricke's ecovalence. $\overline{X}$: genotype means.

References

1. Rincker K, Nelson R, Specht J, Sleper D, Cary T, Cianzio SR, et al. Genetic improvement of US soybean in maturity groups II, III, and IV. Crop science. 2014;54(4):1419-32.

2. Smith HF. A discriminant function for plant selection. Annals of eugenics. 1936;7(3):240-50.

https://doi.org/10.62500/icrtsda.1.1.31

3. Wade L, McLaren C, Quintana L, Harnpichitvitaya D, Rajatasereekul S, Sarawgi A, et al. Genotype by environment interactions across diverse rainfed lowland rice environments. Field Crops Research. 1999;64(1-2):35-50.

4. Yan W, Hunt L. Biplot Analysis of Multi-environment Trial Data. Quantitative genetics, genomics, and plant breeding2002. p. 162-77.

5. Yan W, Tinker NA. Biplot analysis of multi-environment trial data: Principles and applications. Canadian journal of plant science. 2006;86(3):623-45.

6. Tahira AR, Amjad M. Stability analysis of rapeseed genotypes targeted across irrigated conditions of Pakistan. International Journal of Agriculture Innovations and Research. 2013;2:208-12.

7. Marjanović-Jeromela A, Marinković R, Mijić A, Jankulovska M, Zdunić Z, Nagl N. Oil yield stability of winter rapeseed (Brassica napus L.) genotypes. Agric Conspec Sci. 2008;73(4):217-20.

8. Oghan HA, Sabaghnia N, Rameeh V, Fanaee HR, Hezarjeribi E. Univariate stability analysis of genotype× environment interaction of oilseed rape seed yield. Acta Universitatis Agriculturae et Silviculturae Mendelianae Brunensis. 2016;64(5):1625-34.

9. Rahnejat SS, Farshadfar E. Evaluation of phenotypic stability in canola (Brassica napus) using GGE-biplot. Int J Biosci. 2015;6(1):350-6.

10. Agahi K, Ahmadi J, Oghan HA, Fotokian MH, Orang SF. Analysis of genotype× environment interaction for seed yield in spring oilseed rape using the AMMI model. Crop Breed Appl Biotechnol. 2020;20.

11. Bocianowski J, Liersch A, Nowosad K. Genotype by environment interaction for alkenyl glucosinolates content in winter oilseed rape (Brassica napus L.) using additive main effects and multiplicative interaction model. Current Plant Biology. 2020;21:100137.

12. Nowosad K, Liersch A, Poplawska W, Bocianowski J. Genotype by environment interaction for oil content in winter oilseed rape (Brassica napus L.) using additive main effects and multiplicative interaction model. Indian Journal of Genetics and Plant Breeding. 2017;77(02):293-7.

13. Miah MA, Rasul MG, Mian MAK, Rohman M. Evaluation of rapeseed lines for seed yield stability. International Journal of Agronomy and Agricultural Research. 2015;7(6):12-9.

14. Mortazavian S, Azizinian S. GGE biplot analysis for visualization of mean performance and stability of rapeseed yield in Iran. 2013.

15. Shojaei SH, Mostafavi K, Khodarahmi M, Zabet M. Response study of canola (Brassica napus L.) cultivars to multi-environments using genotype plus genotype environment interaction (GGE) biplot method in Iran. African Journal of Biotechnology. 2011;10(53):10877-81.

16. Mashayekh A, Mohamadi A, Gharanjick S. Evaluation of canola genotypes for yield stability in the four regions in Iran. Bulletin of Environment, Pharmacology and Life Sciences. 2014;3(11):123-8.

17. Escobar M, Berti M, Matus I, Tapia M, Johnson B. Genotype× environment interaction in canola (Brassica napus L.) seed yield in Chile. Chilean Journal of Agricultural Research. 2011;71(2):175.

18. Amiri Oghan H, Bakhshi B, Rameeh V, Faraji A, Askari A, Fanaei HR. Comparison of Ammi, Parametric and Non-Parametric Models in Identifying High-Yielding and Stable Oilseed Rape Genotypes. Turkish Journal Of Field Crops. 2022;27(2):224-34.

19. Olivoto T, Nardino M, Meira D, Meier C, Follmann DN, de Souza VQ, et al. Multi-trait selection for mean performance and stability in maize. Agronomy Journal. 2021;113(5):3968-74.

20. Bakhshi B. Heat and drought stress response and related management strategies in oilseed rape. Agrotechniques in Industrial Crops. 2021;1(4):170-81.

21. Zheng M, Terzaghi W, Wang H, Hua W. Integrated strategies for increasing rapeseed yield. Trends Plant Sci. 2022.

22. Hu Q, Hua W, Yin Y, Zhang X, Liu L, Shi J, et al. Rapeseed research and production in China. The Crop Journal. 2017;5(2):127-35.

23. Diepenbrock W. Yield analysis of winter oilseed rape (Brassica napus L.): a review. Field crops research. 2000;67(1):35-49.

24. Yan W, Rajcan I. Biplot analysis of test sites and trait relations of soybean in Ontario. Crop science. 2002;42(1):11-20.

25. Yan W, Frégeau-Reid J. Genotype by yield* trait (GYT) biplot: a novel approach for genotype selection based on multiple traits. Scientific reports. 2018;8(1):1-10.

26. Rocha JRdASdC, Machado JC, Carneiro PCS. Multitrait index based on factor analysis and ideotype-design: Proposal and application on elephant grass breeding for bioenergy. Gcb Bioenergy. 2018;10(1):52-60.

27. Olivoto T, Lúcio AD, da Silva JA, Sari BG, Diel MI. Mean performance and stability in multi-environment trials II: Selection based on multiple traits. Agronomy Journal. 2019;111(6):2961-9.

28. Dehghani H, Omidi H, Sabaghnia NJAJ. Graphic analysis of trait relations of rapeseed using the biplot method. 2008;100(5):1443-9.

29. Gholizadeh A, Oghan HA, Alizadeh B, Rameeh V, Payghamzadeh K, Bakhshi B, et al. Phenotyping new rapeseed lines based on multiple traits: Application of GT and GYT biplot analyses. Food Science & Nutrition. 2022.

30. Olivoto T, Lúcio ADC. metan: An R package for multi-environment trial analysis. Methods in Ecology and Evolution. 2020;11(6):783-9.

31. Roemer J. Sinde die ertagdreichen Sorten ertagissicherer. Mitt DLG. 1917;32(1):87-9.

32. Shukla G. Some statistical aspects of partitioning genotype environmental components of variability. Heredity. 1972;29(2):237-45.

33. Purchase J, Hatting H, Van Deventer C. Genotype× environment interaction of winter wheat (Triticum aestivum L.) in South Africa: II. Stability analysis of yield performance. South African Journal of Plant and Soil. 2000;17(3):101-7.

34. Zali H, Farshadfar E, Sabaghpour SH, Karimizadeh R. Evaluation of genotype× environment interaction in chickpea using measures of stability from AMMI model. Annals of Biological Research. 2012;3(7):3126-36.

https://doi.org/10.62500/icrtsda.1.1.31

35. Ajay B, Aravind J, Abdul Fiyaz R, Bera S, Narendra K, Gangadhar K, et al. Modified AMMI Stability Index (MASI) for stability analysis. Groundn Newsl. 2018;18:4-5.

36. Olivoto T, Lúcio AD, da Silva JA, Marchioro VS, de Souza VQ, Jost E. Mean performance and stability in multi-environment trials I: combining features of AMMI and BLUP techniques. Agronomy Journal. 2019;111(6):2949-60.

37. Rosielle A, Hamblin J. Theoretical aspects of selection for yield in stress and non-stress environment. Crop science. 1981;21(6):943-6.

38. Fernandez GC. Effective selection criteria for assessing plant stress tolerance. Adaptation of food crops to temperature and water stress. 1993:13-181992257270.

39. Schneider KA, Rosales-Serna R, Ibarra-Perez F, Cazares-Enriquez B, Acosta-Gallegos JA, Ramirez-Vallejo P, et al. Improving common bean performance under drought stress. Crop Science. 1997;37(1):43-50.

40. Bouslama M, Schapaugh W. Stress tolerance in soybean. Part 1: evaluation of three screening techniques for heat and drought tolerance. Crope Science. 1984;24:933-7.

41. Fischer R, Maurer R. Drought resistance in spring wheat cultivars. I. Grain yield responses. Australian Journal of Agricultural Research. 1978;29(5):897-912.

42. Rao A, Prabhakaran V. Use of AMMI in simultaneous selection of genotypes for yield and stability. Journal of the Indian Society of Agricultural Statistics. 2005;59(1):76-82.

43. Anuradha N, Patro T, Singamsetti A, Sandhya Rani Y, Triveni U, Nirmala Kumari A, et al. Comparative study of AMMI-and BLUP-based simultaneous selection for grain yield and stability of finger millet [Eleusine coracana (L.) Gaertn.] genotypes. Frontiers in Plant Science. 2022;12:786839.

44. Yan W, Hunt L, Sheng Q, Szlavnics Z. Cultivar evaluation and mega-environment investigation based on the GGE biplot. Crop Science. 2000;40(3):597-605.

45. De Resende M. SELEGEN-REML/BLUP: sistema estatístico e seleção genética computadorizada via modelos lineares mistos. 2007.

46. Francis T, Kannenberg L. Yield stability studies in short-season maize. I. A descriptive method for grouping genotypes. Canadian Journal of Plant Science. 1978;58(4):1029-34.

47. Shukla G. Some statistical aspects of partitioning genotype-environmental components of variability. Heredity. 1972;29(2):237-45.

48. Yan W, Kang MS. GGE biplot analysis: A graphical tool for breeders, geneticists, and agronomists: CRC press; 2002.

49. Bakhshi, B., & Shahmoradi, S. S. Simultaneous selection of high-yielding and drought-tolerant barley landraces using GT, GYT and GYSI methodologies. Cereal Research Communications, 51(1), 237-248. 2023.

Harmonizing Genotype Selection Strategies: Advancements of Multi Environmental Trails Analysis in Crop Development

https://doi.org/10.62500/icrtsda.1.1.31

https://doi.org/10.62500/icrtsda.1.1.32

Proc. 1st International Conference on Recent Trends in Statistics and Data Analytics
Air University Islamabad, Pakistan – May 9, 2024, Vol. 1, pp. 296-309

Future of E-Governance in Pakistan

Ayesha Nazuk [a], Asad Ullah Noman Erkin[b], Misbah Noor[b] and Rija Zahid[b]

[a] Faculty member, School of Social Sciences and Humanities (S^3H), National University of Sciences and Technology (NUST), Sector H-12, Islamabad, 44000, Pakistan

[b] B.S Economics graduates, School of Social Sciences and Humanities (S^3H), National University of Sciences and Technology (NUST), Sector H-12, Islamabad, 44000, Pakistan

Abstract

As digitalization grows more prevalent in society, the need for governments to step-up and adopt electronic governance (e-governance) grows dire in order to promote efficiency, transparency, and citizen engagement. Given a developing country like Pakistan's unique set of problems, such as low literacy rates, concerning internet infrastructure, and a struggling cybersecurity framework, topped with a rapidly evolving digital landscape, the country faces hurdles in its path towards successful e-governance implementation. This study aims to investigate the potential of e-governance in Pakistan and identify the key challenges hindering its adoption and effectiveness. Utilizing a mixed-methods approach, this study combines qualitative interviews and a quantitative survey to gather insights from key stakeholders such as the Government Officials, policy makers, and citizens across various sectors and regions in Pakistan. Through extensive qualitative analysis the study elucidates the multifaceted challenges impeding the effective adoption and implementation of e-governance in Pakistan, these challenges encompass infrastructural limitations, cybersecurity vulnerabilities, digital literacy gaps, institutional resistance to change, and capacity constraints within governmental agencies. Whereas the quantitative survey assesses the current state of e-governance, its perception and usability from a user perspective. By juxtaposing qualitative and quantitative findings, this research provides a comprehensive understanding of the potential transformative impacts of e-governance on Pakistan's governance landscape. Our findings pointed out that despite the fact that people believe e-governance is a promising resource for national socio-economic development, there is hesitation in adopting it due to obstacles like cyber-security concerns and a lack of deeper grasp of the services provided. **Keywords:** E-governance, Cybersecurity, Digital services, Internet infrastructure

1. Introduction

Information and Communication Technologies (ICT) are crucial in enabling individuals and organisations to optimise the effectiveness of their goals in the contemporary day. This is particularly accurate when considering the potential of this phenomenon to enhance governments, as it generates a wide range of advantages for both the nation and its citizens. Firstly, it facilitates governments in streamlining their administrative process and serves as a means to include the public in decision-making. Furthermore, it enhances the overall welfare of the nation by promoting openness and providing a comprehensive understanding of the functioning of these administrative procedures. This, in turn, helps to reduce corruption and replace outdated methods of government.

We compared the pros and cons of cyber governance in this report. It examines how countries that have implemented such systems are doing. This paper also polls Pakistanis' views on

https://doi.org/10.62500/icrtsda.1.1.32

internet usage, exposure, comprehension of E-governance, and government trust. This includes qualitative and quantitative data collection and analysis to produce policy-relevant results.

1.1 Research Objectives:

I. To examine the determinants that impact the acceptance and implementation of e-governance platforms among citizens in Pakistan.

II. To comprehend the primary cybersecurity obstacles linked to the deployment of e-governance in Pakistan.

2. E-Governance

The exchanges between citizens, corporations, and the government are outlined in e-governance models. Typical models consist of:

2.2.1 Government-to-Citizen (G2C):

Under the G2C paradigm, individual citizens receive services and information directly from government entities. This covers services such as accessing public health information, paying taxes online, and acquiring birth certificates.

2.2.2. Government-to-Business (G2B):

Under this framework, enterprises and businesses communicate with government agencies. This frequently entails business registration, computerized procurement systems, and licensing and regulatory procedures.

2.2.3. Government-to-Government (G2G):

Improving data exchange and interactions between governments is the main goal of the G2G paradigm. This concept decreases redundancy and boosts administrative efficiency by streamlining interagency cooperation and communication.

3. Literature Review

The United Nation (UN) has a measure known as the E-Government Development Index (EGDI) in place which gives a performance rating of a nation's use of ICT in accessing and involving its people. It consists of three pivotal provisions of online services, telecommunication capacity, and human capital as its dimensions. The EDGI has a range from 0 to 1 with four different classifying levels, Pakistan's EDGI score is roughly 0.42 which falls into the category of middle values, indicating room for improvement. However, what is alarming is that out of the 193 UN countries, Pakistan's e-governance rank is 150, hinting that the road to improvement is a long one (*EGOVKB* |United Nations, 2022).

A critical issue in the discussion of e-governance is the threat of cybercrime. Cybersecurity researchers have dedicated their time in the prevention of unauthorized access of programs, databases, networks, and systems, but as time has progressed the volume and complexity of cybercrime has increased. It presents itself as a threat to Pakistan as little steps have been taken towards mitigating it. As a developing country, Pakistan's implementation of cyber-services is slowly underway. Existing legislation on cybercrime is ill-equipped to deal with it comprehensively in its growing threat. Moreover, according to leading industry experts in the Federal Investigation Agency (FIA), Pakistan lacks skilled and qualified professionals to efficiently tackle cases. Going forward, policies towards national defense must not limit

https://doi.org/10.62500/icrtsda.1.1.32

themselves to borders and tangible threats, but must also account for national cyber security (Awan & Memon, 2016).

Pakistan's first step in introducing legal sanctity and security in the IT sector came in the form of the Electronics Transaction Ordinance (ETO) passed in 2002, which mostly dealt with the realm of e-commerce. It was followed by the Prevention of Electronic Crimes or Cyber Crimes Ordinance in 2007 which not only criminalized the acts of cyberstalking, cyberterrorism, and forgery of e-documents, but also subjugated all cybercriminals who committed these crimes in Pakistan, regardless of their nationalities, to their appropriate penalties. Based on the 2007 ordinance, came the predominant law dealing with all sorts of cybercrimes in the country, the Prevention of Electronic Crimes Act (PECA) in 2016. This law works against 23 offenses including hate speech, electronic theft, and fraud but only three of these offenses, cyber terrorism and offense related to dignity and modesty of natural persons, are cognizable. PECA is procedural and regulatory in nature, giving the sole authority of investigation to the FIA. PECA is a great step in providing legislation against cybercrime, but further laws need to be promulgated and implemented in order to strengthen cybersecurity in Pakistan (Adil, 2023).

4. Theoretical Framework

In order to facilitate this research, the foundational concept and model used is the Technology Acceptance Model (Davis, 1989) also known as TAM. The model associates two factors as to why people would choose to use a piece of technology, and those are:

1. Perceived usefulness
2. Perceived ease of use

According to the model, whether a piece of technology is actually useful or easy to use is not a matter of the technology itself but rather the perception of it. These perceptions are subject to change depending on an individual's experience with the technology, their age, and even their gender. Perceiving a technology as useful will increase the odds that an individual will want to make use of it and this occurs when they are able to incorporate the technology to supplement their work. Whereas the ease of use is determined by the difficulty faced when opting to make use of said technology.

At the core of it, this framework allows for us to inquire and study the adoption of technology throughout numerous domains in order to acknowledge and understand why users behave the way they do and what type of challenges we may face along with any benefits that may be brought about.

To understand and examine the role of government officials and employees in the implementation of a new e-system, the "Institutional Theory" is used. The main focus of institutional theory is on institutions and how they mold and impact people and organizational behavior. The mechanisms by which structures—such as plans, regulations, customs, and practices—become accepted as the standards for social conduct are examined by the Institutional Theory. Institutional Theory's various components describe how these pieces are produced, disseminated, accepted, and modified over time and space, as well as how they eventually fade into obscurity. Within the framework of this research, Institutional Theory can be applied to investigate how the government influenced Pakistan's adoption and execution of e-governance. It assists in analyzing how institutional elements, rules, and laws affect whether e-governance projects succeed or fail (Hassan, 2008).

Combined together, these models offer a thorough knowledge of Pakistan's adoption, application, and cybersecurity of e-governance. It takes into account the viewpoints of the

https://doi.org/10.62500/icrtsda.1.1.32

general public, public servants, and the larger institutional environment. User acceptability can be analyzed by integrating TAM and the Institutional Theory clarifies the larger organizational and governmental influences.

5. Methodology

5.1. Research Design:

The primary objective of this study is to understand the potential and challenges of E-Governance in Pakistan. To simplify our analysis, we look at e-governance adoption, user perceptions, and cybersecurity in Pakistan. This study uses a mixed-methods approach that combines quantitative and qualitative research approaches. A survey was conducted as part of the quantitative component to understand how the general public perceives e-governance in Pakistan. The qualitative component includes in-depth interviews with government officials and workers who are involved in the implementation of e-governance programmes.

5.2. Survey for Public:

As part of the quantitative aspect of this research, a structured questionnaire with demographic information and questions assessing e-governance awareness, perceptions, experiences, access, and suggestions for improvement was used. Sample size of 200 was set to represent the general public of Pakistan which utilized convenience sampling.

5.3. In-depth Interviews

As part of the qualitative aspect of this study, Face-to-face interviews were conducted with Government Officials and employees using a set of predefined questions tailored for each ministry. One of the main aims was to understand the role of e-governance within the ministries, particularly in relation to improving efficiency especially considering the challenges posed by Pakistan's internet infrastructure. The inductive investigation was grounded in Institutional Theory. It delved deeply into the concept to let the theory naturally arise from the data, guided by theoretical sensitivity and without any bias.

5.4. Transcription of Interviews

All participants of the interviews were free to communicate in Urdu or English, whichever language they felt most comfortable in. The majority of the officials in this study spoke in English. The interviews were recorded with given consent which were then later transcribed twice by different researchers. These transcriptions were then cross-checked to ensure validity. The final step was to then sort these transcriptions into a sheet which allowed for grouping of themes and further analysis under the methods of the framework.

5.5 Data Analysis:

In order to analyze the collected qualitative data, Braun and Clarke's (2006) analysis method is utilized. This is used to carry out a thematic analysis for qualitative data, which allows for the identification of certain patterns that may be present. These patterns can then be further studied and reported.

This methodology entails certain steps to be carried out in order for the analysis to be conducted. It involves first acquiring a detailed understanding of any data received, after which codes are generated that act as labels for any section of the data that is pertinent to the research questions. These codes are then further sorted amongst themselves based on similar patterns to form themes. A detailed evaluation of these themes is carried out in order to confirm their sufficiency where they are finalized or renamed and converted to subthemes if found to be lacking. Once there is adequate detail as to what each theme is to dictate then the final analysis is carried out, linking sections of the data to their respective themes.

https://doi.org/10.62500/icrtsda.1.1.32

5.6. Integration of framework:
The quantitative study of user acceptance and adoption of e-governance will be guided by the Technology Acceptance Model (TAM) and Unified Theory of Acceptance and Use of Technology (UTAUT). Similarly, through our in-depth qualitative interviews, we will apply the Institutional Theory to comprehend the function of Government Officials in the execution of e-governance.

6.0. Findings

The research findings and results are presented in this section. They include insights from both quantitative surveys and qualitative interviews.

6.1. Survey for Public:
The results from the survey are graphically presented below:

E_Governance_Awareness **(EGA)**: The survey revealed a moderate level of awareness of e-governance services in Pakistan, with **56%** respondents indicating some familiarity with the e-governance concepts and services.

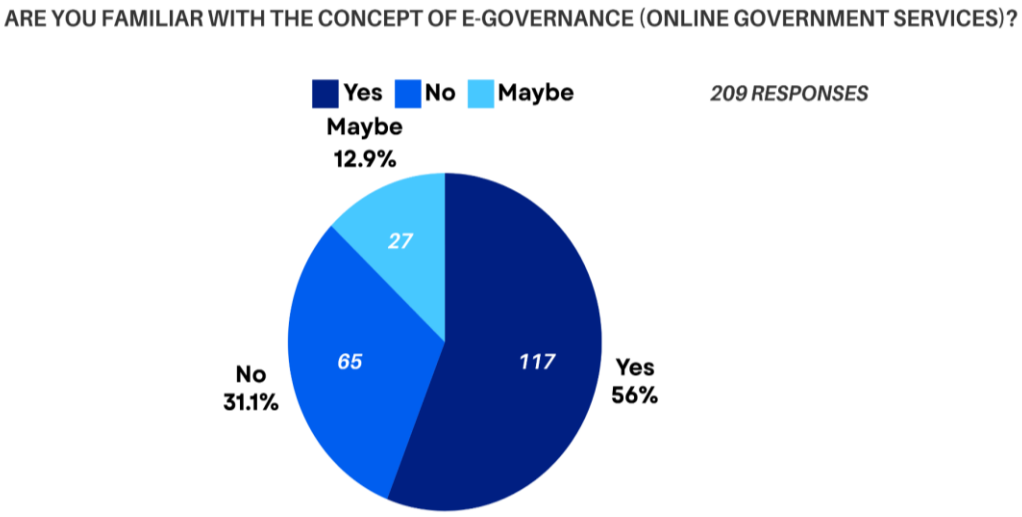

Fig. 6.1. Diagram of response distribution of a question from the survey.

Awareness of Services **(AS):** Participants demonstrated varying levels of awareness regarding specific e-governance services, with higher awareness observed for basic services such as online utility bill payments and tax filings, compared to more complex services like E-Police Reporting.

https://doi.org/10.62500/icrtsda.1.1.32

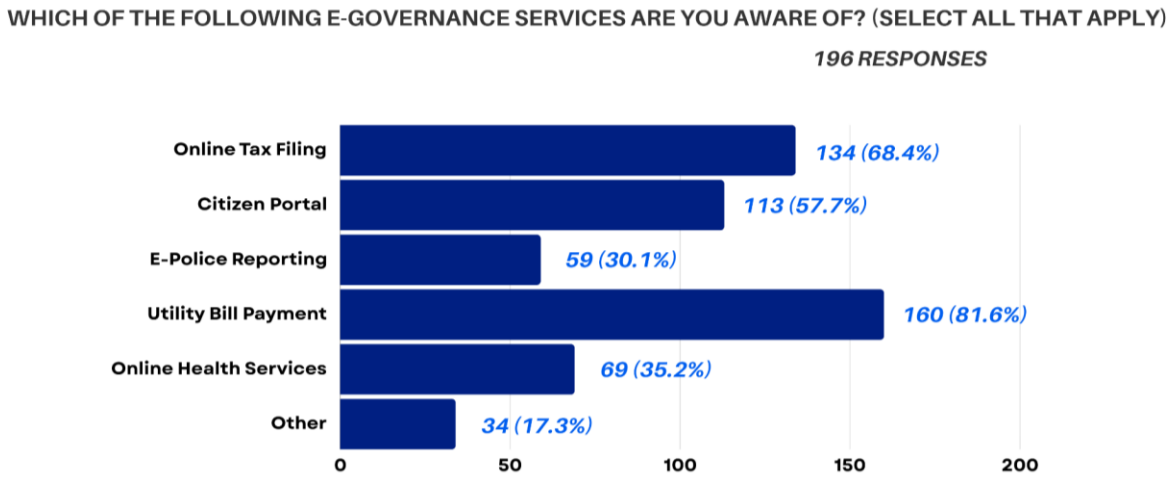

Fig. 6.2. Diagram of the response of awareness of e-governance services.

E_Governance_Usage **(EGU)**: Actual usage of e-governance services was adequate in lieu of the number of respondents aware of them, with only **60.2%** of respondents reporting personal usage of e-governance platforms.

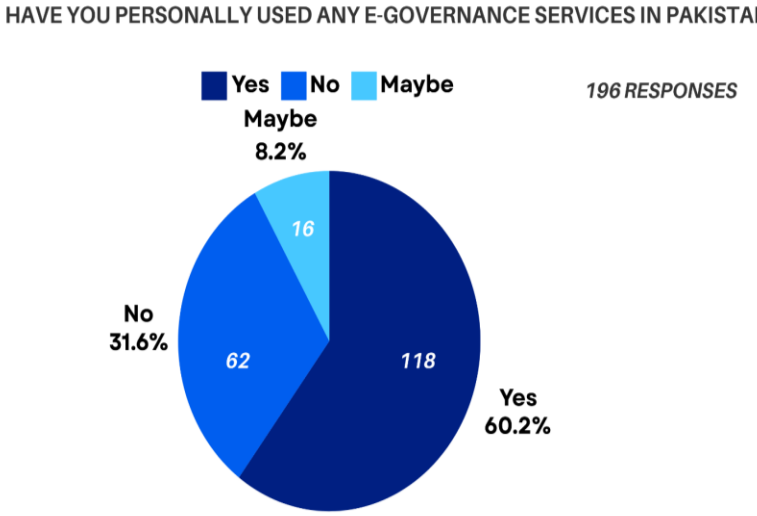

Fig. 6.3. Diagram showing the usage statistics of e-governance services from the survey.

Satisfaction_Level **(SL)**: Among users of e-governance services, satisfaction levels were mixed, with some expressing satisfaction with the convenience and efficiency of online services, while others reported dissatisfaction due to technical glitches and usability issues. Aggregating the values, we get an average satisfaction score of **3.41 out of 5**, with 5 translating to fully satisfied.

https://doi.org/10.62500/icrtsda.1.1.32

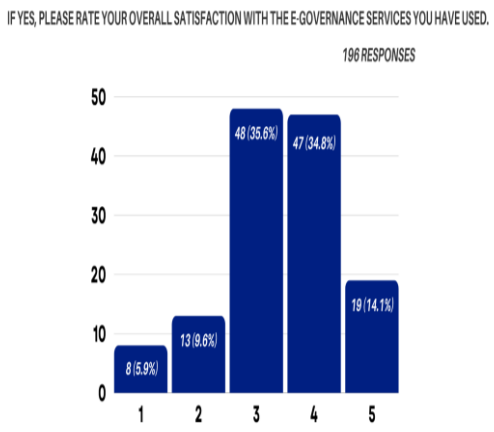

Fig. 6.4. Diagram representing satisfaction rating (out of 5) given to e-governance services.

Perceived_Impact **(PI)**: Respondents generally perceived e-governance as having a positive impact on improving government services and efficiency, with **34.7%** responding with "Very Positive" and **49%** responding with "Positive."

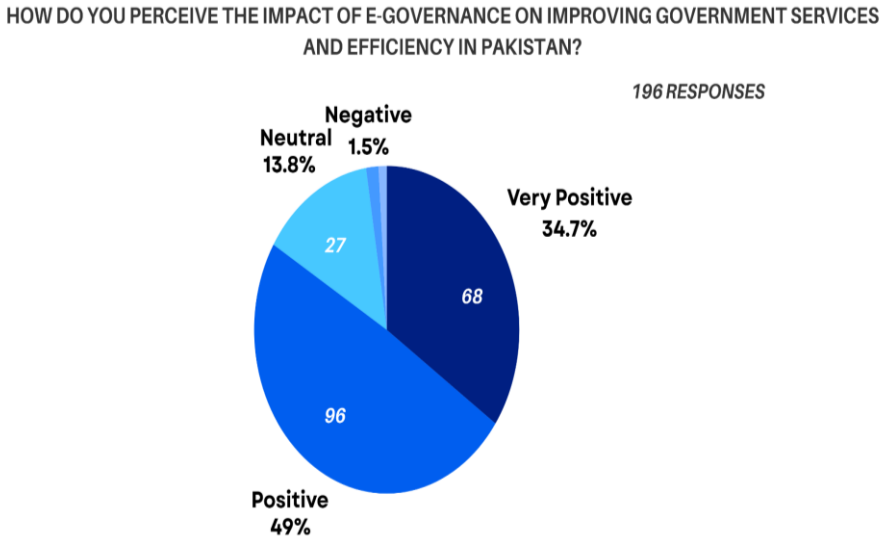

Fig. 6.5. Diagram showing the perceived impact of e-governance services on efficiency.

https://doi.org/10.62500/icrtsda.1.1.32

Internet_Access **(IA)**: Access to reliable internet infrastructure did not emerge as a significant barrier to e-governance adoption, with **87.8%** of respondents having reliable access. It is important to note that this response might be biased given the online nature of this survey limiting the respondent profile to people with the internet.

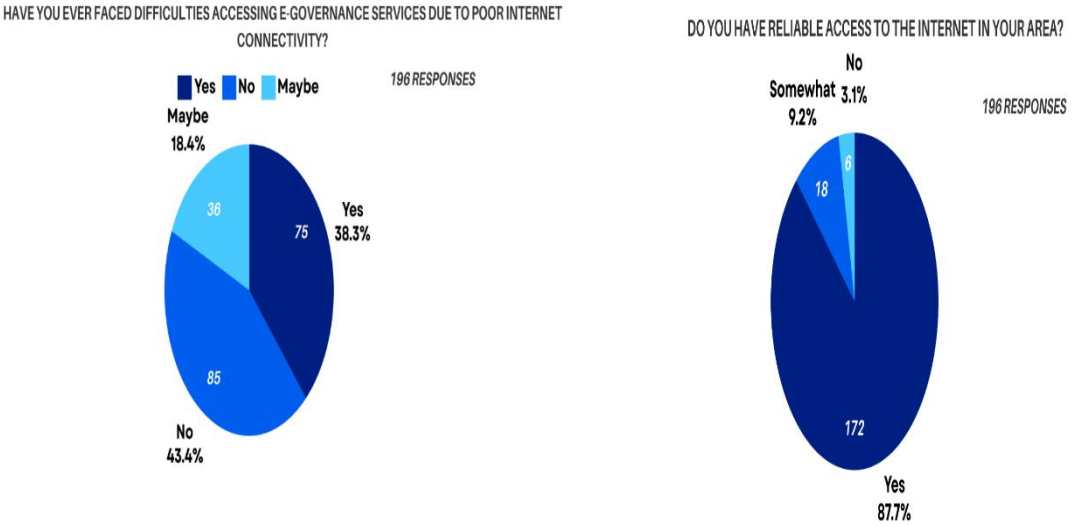

Fig. 6.6. Diagram showing the reliability of internet access of survey participants.

Connectivity_Difficulties **(CD):** Regarding connectivity problems, respondents' experiences with e-governance services were divided; 43.4% had never encountered them, while 38.4% said that bad internet access had negatively impacted their experience.

Fig. 6.7. Diagram displaying the portion of respondents who had difficulty with their internet connection.

Government_Effectiveness **(GE)**: Perceptions of government effectiveness in utilizing technology for public services varied among respondents, with most having a neutral view.

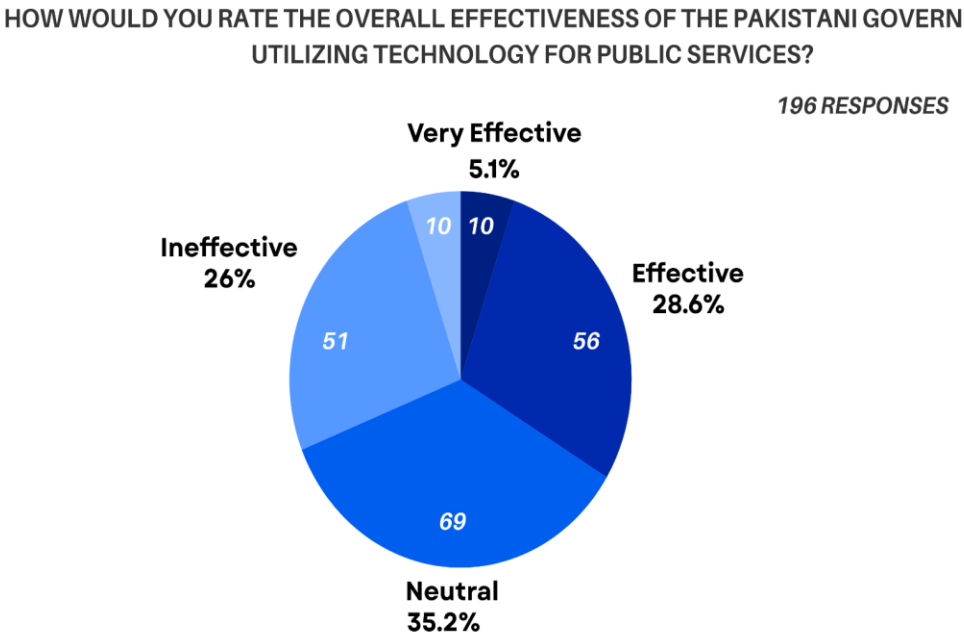

https://doi.org/10.62500/icrtsda.1.1.32

Fig. 6.8. Diagram showing the rating of overall effectiveness of e-governance services from respondents.

Tech_Contribution_Transparency **(TCT):** A vast majority of respondents believe that technology can contribute to a more transparent and accountable government in Pakistan with **45.4%** of respondents strongly agreeing and **43.9%** agreeing to the positive impact of technology in accountability and transparency.

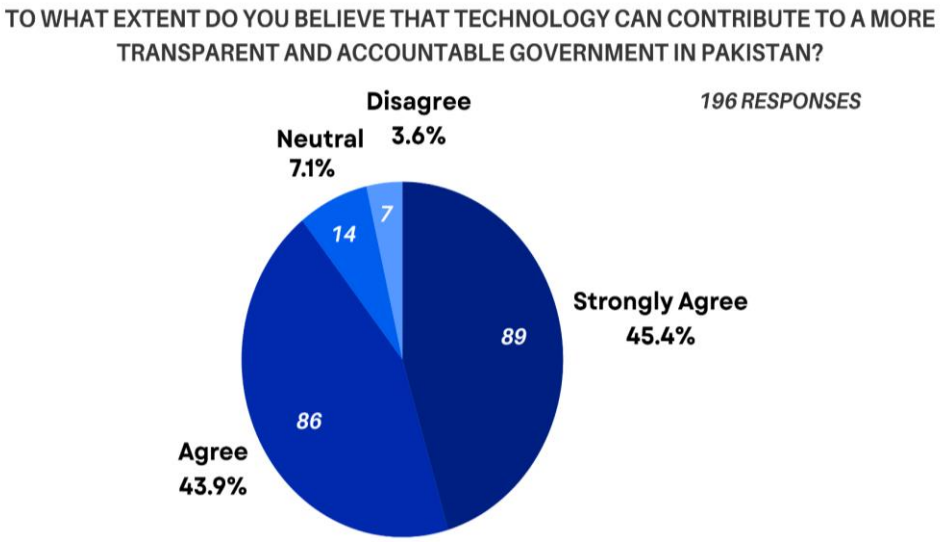

Fig. 6.9. Diagram representing respondents' belief in the connection of technology and transparency.

Respondent	Gender	Age	Total professional experience (In years)	Total organizational experience (In years)	Ministry	Education
B01	Male	44	19	19	Customs	Masters
B02	Male	43	14	12	Human Rights	Doctorate
B03	Female	57	32	30	Economics Affairs	Masters
B04	Male	38	16	16	Foreign Affairs	Masters
B05	Male	39	16	14	Finance	Masters
B06	Male	46	19	19	President Office	Masters
B07	Male	40	16	16	Prime Minister Office	Masters
B08	Male	37	14	14	Economic Affairs	Masters
B09	Female	58	33	31	Information Technology	Masters

https://doi.org/10.62500/icrtsda.1.1.32

Confidence_in_Cybersecurity **(CC):** A majority of respondents reported having no or little confidence in their data being secure while using e-services and platforms provided by the government.

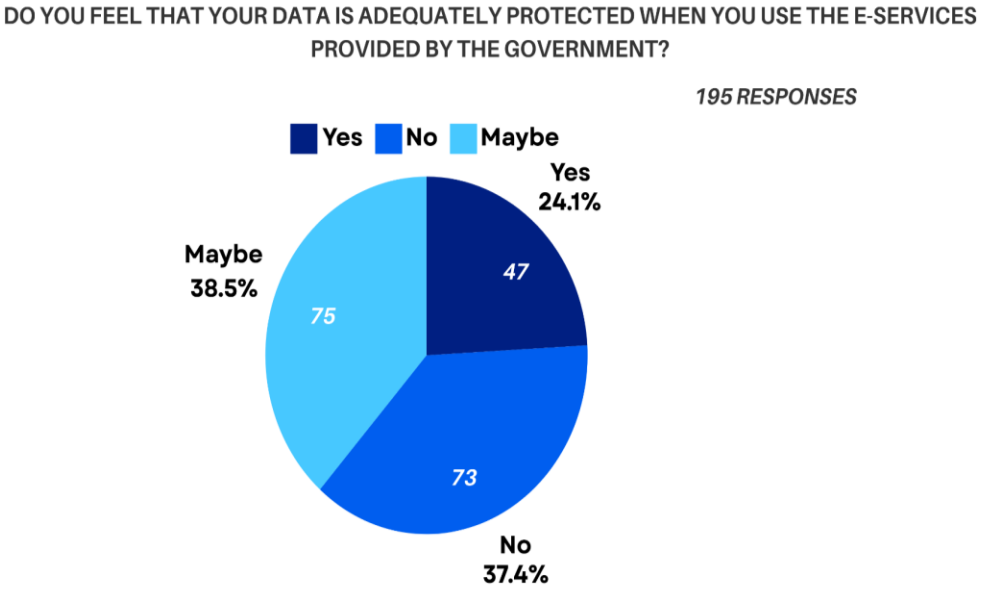

Fig. 6.10. Diagram showing respondents feelings of security of e-governance services.

6.2. In-depth Interviews:
The demographic profile of all participants involved in the in depth interviews is provided below:

Table 6.1: Demographic profile of interview participants

The major findings derived from the in-depth interviews fall under the following themes: Cyber-security concerns and Weaknesses, E-Governance Mechanisms and Challenges, Awareness and Training Needs, Transparency and Accountability, and Infrastructure and Accessibility.

(a) Cyber Security Concerns and Weaknesses:

A range of worries were raised about cyber security, as one participant states "*cyber security is one of my concerns. We don't have enough cyber security professionals on the set up which will be protecting our data*," (B05). Additionally, concerns were presented about internet infrastructure, inadequate information security protocols, problems with identity theft, and gaps in the cyber security framework.

(b) E-Governance Mechanisms and Challenges:

Participants share their thoughts on the efficiency of e-governance systems in their ministries, emphasizing both the positive aspects and potential areas for development. As interviewees talk about their journey of adopting e-office they share "*they were not habitual of using the e-office. But now all feel comfortable, and they prefer that files should be routed through e-office.*" (B02). Hence the necessity for clearly defined cyber Standard Operating Procedures (SOPs), frequent website updates, cost optimization through e-governance, and the integration of IT into fiscal policy becomes ardently clear.

(c) Awareness and Training Needs:

https://doi.org/10.62500/icrtsda.1.1.32

The necessity for training programmes to advance IT and cyber security expertise, as well as raising stakeholder knowledge of e-governance, is a recurring subject. It is highlighted as participants mention "*we need training in place*" (B05) and "*benefits should be trickled down. And for that purpose, we need training of the people, training of the masses.*" (B02). An Official shared, *"Appropriate staff needs to be hired moving forward that is IT literate"* (B09). The necessity of proactive approaches to cyber security and the flexibility of working techniques to keep up with technological changes are stressed by the participants.

(d) Transparency and Accountability:

While talking about the increased transparency through the digital mode of governance one participant states, *"The press conferences, the finance minister, the finance secretary and all the activities done by the high ups of finance usually are uploaded on the website. And the website is updated periodically. It has different sections which bares information regarding different activities carried out by different wings. That is, budget wing, the data of budget wing, the whole budget, the necessary rules and regulations that are framed by the finance division, and the distribution of resources, of course"* (B05).

(e) Infrastructure and Accessibility:

Problems with inadequate internet infrastructure and information accessibility present themselves as major obstacles to the adoption and execution of e-governance projects. This is shown by the mention of "*limited resources"* and *"lacking infrastructure*" (B01). While talking about the weak internet and weak training of officials, one Government Official states, *"And second thing is the quality of internet. Quality of internet and training of the officials and officers as well. So that they may be useful for the overall utility of the business. So, this area needs more deliberations and more interventions"* (B02).

7.0. Discussion

The findings of this study can be mapped on to existing literature as it can be observed that there are parallels present in themes such as cyber security concerns and mechanisms. The findings about the necessity of training and literacy are consistent with the literature, especially Chandio et al.'s (2018) work, which emphasized the critical role that literacy plays in gaining access to e-government services. The discussions made by Chandio et al. in regard to the importance of ICT literacy complemented the views that were shared during the interviews about the necessity of training programs on IT and cybersecurity knowledge for furthering information technology. The survey participants' worries about cybersecurity fall into line with the Pakistani cybersecurity literature: Awan & Memon (2016) emphasized the increasing threat of cybercrime in Pakistan and noted that there is a lack of qualified personnel to address these issues. In this light, it becomes more evident how important strengthening the cybersecurity framework of the government is— as it directly serves to safeguard government installations and data while building the public's trust.

From the findings of this study, we can draw the following policy proposals which aim to supplement the e-governance framework while advancing e-governance in Pakistan:

1. Investing in ICT Literacy and Training
2. Improvement of Cybersecurity Infrastructure
3. Enhancement of E-Government Systems
4. Encouragement of Accountability and Transparency

https://doi.org/10.62500/icrtsda.1.1.32

5. Infrastructure Development and Accessibility

6. Participation in Global Best Practices

7. Policy Coherence and Coordination

8. Mechanisms for observation, assessment, and feedback

In the grand scheme of things, addressing these issues and embracing technology-based governance could help Pakistan boost citizen confidence, foster transparency, and elevate government service delivery. In laying the groundwork for a more efficient, transparent, and responsive governance setup, Pakistan can pivot attention on cybersecurity — funding education plus awareness initiatives — and improving infrastructure in a bid to enhance accessibility.

References

Akhtar, S. (2020). Regional Cooperation through Connectivity: Lessons for South Asia and Pakistan. In S. S. Aneel, U. T. Haroon, & I. Niazi (Eds.), *Corridors of Knowledge for Peace and Development* (pp. 13–16). Sustainable Development Policy Institute. http://www.jstor.org/stable/resrep24374.9

Awan, J., & Memon, S. (2016). Threats of cyber security and challenges for Pakistan. In *International Conference on Cyber* Warfare *and Security* (p. 425). Academic Conferences International Limited. Retrieved from https://www.researchgate.net/publication/318850748_Threats_of_Cyber_Security_and_Challenges_for_Pakistan Accessed April 15, 2024

Bosman, I. (2021). *COVID-19 and E-Governance: Lessons from South Africa*. South African Institute of International Affairs. http://www.jstor.org/stable/resrep29596

Chertoff, M., Simon, T., & Global Commission on Internet Governance. (2017). The Impact of the Dark Web on Internet Governance and Cyber Security. In *Cyber Security in a Volatile World* (pp. 29–36). Centre for International Governance Innovation. http://www.jstor.org/stable/resrep05239.7

Cybersecurity Framework | NIST. (2024, March 8). NIST. Retrieved from https://www.nist.gov/cyberframework Accessed April 15, 2024

Davis, F. D. (1989). Perceived Usefulness, Perceived Ease of Use, and User Acceptance of Information Technology. *MIS Quarterly, 13*(3), 319–340. https://doi.org/10.2307/249008

Dawes, S. S. (2008). The Evolution and Continuing Challenges of E-Governance. *Public Administration Review*, *68*. https://www.jstor.org/stable/25145732

Ghayur, A. (2006). Towards Good Governance: Developing an e-Government. *The Pakistan Development Review*, *45*(4), 1011–1025. http://www.jstor.org/stable/41260665

Greene, T. (2020, March 12). *What is the internet backbone and how it works*. Network World. Retrieved from https://www.networkworld.com/article/968484 Accessed April 15, 2024

Gruber, H., Koutroumpis, P., Mayer, T., & Nocke, V. (2011). Mobile telecommunications and the impact on economic development. *Economic Policy*, *26*(67), 387–426. http://www.jstor.org/stable/41261993

Hassan, Shahidul & Gil-Garcia, J. Ramon. (2008). Institutional Theory and E-Government Research. 349-360. 10.4018/978-1-59904-857-4.ch034. https://www.researchgate.net/publication/292702879_Institutional_Theory_and_E-Government_Research

Iftikhar, P. (2019). Pakistan and the Digital Economy: Future Directions. In S. S. Aneel, U. T. Haroon, & I. Niazi (Eds.), *70 Years Of Development: The Way Forward* (pp. 188–202). Sustainable Development Policy Institute. http://www.jstor.org/stable/resrep24393.16

Jaeger, P. T., & Thompson, K. M. (2003). E-government around the world: Lessons, challenges, and future directions. Government information quarterly, 20(4), 389-394.

https://www.academia.edu/17834528/E_government_around_the_world_lessons_challenges_and_future_directions?sm=b

Jun, N., Wang, F., & Wang, D. (2014). E-government use and perceived government transparency and service capacity: Evidence from a Chinese Local Government. *Public Performance & Management Review*, *38*(1), 125-151. https://www.jstor.org/stable/24735276

Lachow, I. (2011). The Stuxnet Enigma: Implications for the Future of Cybersecurity. *Georgetown Journal of International Affairs*, 118–126. http://www.jstor.org/stable/43133820

Melitski, J., & Calista, D. (2016). E-government and e-governance best practices in cities and countries compared between 2003 and 2012: Fad or diffused innovation? *Public Administration Quarterly*, *40*(4), 913–948. http://www.jstor.org/stable/26383376

Mujahid, Y. H., & Siddiqui, S. R. (2002). Digital Opportunity Initiative for Pakistan [with Comments]. *The Pakistan Development Review*, *40*(4), 911-928. https://www.jstor.org/stable/41260370

Rubasundram, G. A., & Rasiah, R. (2019). Corruption and Good Governance: An Analysis of ASEAN's E-Governance Experience. *Journal of Southeast Asian Economies*, *36*(1), 57-70. https://www.jstor.org/stable/26664253

Saunders, M., Lewis, P., & Thornhill, A. (2007). Research Methods for Business Students, (6th ed.) London: Pearson.

Shad, M. R. (2019). Cyber Threat Landscape and Readiness Challenge of Pakistan. *Strategic Studies*, *39*(1), 1–19. https://www.jstor.org/stable/48544285

Sumanjeet (2006). E-governance: An overview in the Indian context. *The Indian Journal of Political Science*, *67*(4), 857-866. https://www.jstor.org/stable/41856269

Teşu, M. D., & Haltofová, B. (2012). Developing e-government for better public services within European Union. *Theoretical and Empirical Researches in Urban Management*, 7(2), 79-88. https://www.jstor.org/stable/24873318

United Nations. (n.d.). *EGOVKB > about > overview > E-government development index*. United Nations. https://publicadministration.un.org/egovkb/en-us/About/Overview/-E-Government-Development-Index

Venkatesh, V., Morris, M. G., Davis, G. B., & Davis, F. D. (2003). User Acceptance of Information Technology: Toward a Unified View. MIS Quarterly, 27(3), 425–478. https://doi.org/10.2307/30036540

https://doi.org/10.62500/icrtsda.1.1.33

Proc. 1st International Conference on Recent Trends in Statistics and Data Analytics
Air University Islamabad, Pakistan – May 9, 2024, Vol. 1, pp. 310-322

On the risk of premature transfer from intensive care and coronary care unit

M. S. Bataineh
Department of Mathematics, University of Sharjah, P. O. Box 27272, Sharjah, United Arab Emirates.

Abstract

Hospitals' Intensive Care and Coronary Care Unit (ICU and CCU) are limited and critical resources. The efficient utilization of ICU and CCU capacity significantly impacts both the welfare of patients and the hospital's efficiency and effectiveness. When ICU and CCU become full, an existing patient might be transferred out to a general medical or surgical ward to make room for the new arrival. This study analyzes the admission and discharge of one particular ICU and CCU in a public hospital. The queuing theory will be used to develop a model that predicts the proportion of patients from each category that would be prematurely transferred as a function of the size of the unit, number of categories, mean arrival rates, and length of stay. A numerical example was introduced to demonstrate the operating characteristics, for any given unit size, can be predicted using estimates of the arrival rate for each category (high and low) of patients and the average length of stay for each category. The case study results for the hospital under study illustrates that the efficiency level was acceptable because the proportion of patients from the high risk transferred or turned away is 0.0008, and the proportion of all patients transferred from the unit is 0.0063. Also, it is clear from the results that the increase in the arrival rate affect the distribution of the number of beds used where the number of beds must increase to maintain the current efficiency.

1. Introduction

The intensive care and coronary care units (ICU and CCU), as with other emergency care facilities, are almost available inside every hospital. They are expensive to operate due to the need for high-level of medical and monitoring equipment to provide adequate patient care for life-threatening contingencies. They are staffed by highly trained physicians and nurses who specialize in caring for critically ill patients. Also, they are distinguished from general hospital wards by a higher staff-to-patient ratio and the access to advanced medical resources and equipment. Patients admitted can be classified as medical ICU or surgical ICU patients who are admitted after surgery (Choi and Lee 2016). Medical ICU patients are admitted for reasons such as severe injuries caused by a tragic accident, critical short-term situations like heart attacks or blood poisoning. Due to the variability of demand for admission and the limited capacity of such units, it is inevitable that from time to time there will be insufficient capacity to both complete the treatment of existing patients and to admit new patients. Either a new referral is refused admission, or existing patients are prematurely transferred out of intensive care and coronary care to make room.

Intensive care and coronary care units have a system of classifying patients into a number of risk categories, which are low, medium and high risk. This system means that during the periods of high demand, it is necessary to prevent the premature transfer of higher-risk patients out of the ICU and CCU. Consequently, when these units become full, it is a common practice to transfer the patients perceived to be in a lower risk category out of the unit and into a general ward to make a bed available. There are two main reasons for such a procedure. Firstly, very little is likely to be known about the medical history or condition of the patient at the time of referral and secondly, if heart failure should occur then the necessary equipment and expertise needs to be immediately available. Unfortunately, if the unit is full, it may be necessary to prematurely transfer a patient who has been diagnosed as having had a heart attack but whose condition appears to be stable out in order to accommodate a referral whose diagnosis, following tests, may turn out to be nothing more serious than acute indigestion (see Wharton (1996)).

https://doi.org/10.62500/icrtsda.1.1.33

In this work, the description concentrates on the analytical model based on queuing theory in which the controllable parameters are the overall mean arrival rate and length of stay, the number of diagnostic categories, and the proportion of patients in each diagnostic category and the number of beds in the unit. The output includes the proportion of patients form each category (high and low risk) that are likely to be transferred prematurely if all arrivals are admitted.

The remainder of this paper is organized as follows. Section 2 presents a review of the state-of-the-art literature pertaining to the problem at hand. Section 3 provides the modeling of the ICU unit. A numerical example is introduced in section 4. Section 5 provides a case study of applying the developed model on a public hospital. Lastly, concluding remarks are presented in Section 6 along with suggestions for future research avenues.

2. Literature Review

Management and planning of the Intensive Care Unit (ICU) is significantly important due to its interaction with the different connected departments within the hospital and how it influences the admission and discharge processes and the scheduling of these connected departments. Several research works have investigated ICU related problems and different approaches were used including optimization, simulation, and queuing theory. This review will focus on the use of queuing theory to support ICU management decisions.

Bai et al. 2018 reviewed the literature on how Operations Research/Management Science (OR/MS) supports ICU management. They focused on the ICU management problem (single department management problem) and classify the literature from multiple angles, including decision horizons, problem settings, and modeling and solution techniques. Lakshmi and Appa Iyer (2013) reviewed the literature of applying the queuing theory in health care management. They examined and classified the literature according to the system operation and system analysis. Systems operation included the emergency department, intensive care unit, obstetrics and neonatal unit, geriatrics and mental health care unit. Systems analysis included Leaving without treatment ratio (LWTR), variable arrival rate (VAR), priority queue discipline (PQD), minimum waiting time (MWT).

The multiple input streams, where it was first traced on the hospital application. Balintfy (1952) considered a census-predictor model by formulating the system as a Markov process. Three different categories of patients (good, fair, and poor) were used to classify the patient's state. Blumberg (1961) considers only one patient type. Using the Poisson distribution for the demand process and deterministic service behavior, he develops tables useful in studying the effects of various allocation policies under different conditions. Weckwerth (1966) employs a similar modeling approach and assumes that the negative exponential distribution satisfactorily characterises a patient's length of stay in the hospital.

Young (1962) was the first to discuss the cut-off model, in which low priority customers are kept waiting if the number of servers busy when he arrives is at or above a specified cut-off level, models for admissions and discharges were given. Kolesar (1970), following the work of Young, developed a Markovian decision model for hospital admission schedules. Describing the state of the system as the number of beds occupied at the start of a given period, he introduced a linear programming model that exploits the Markovian structure in providing a basis for determining an optimal control policy for scheduling admissions. Benn (1966) solved a priority assignment problem in railroad transportation, and the results are published in Jaiswal (1968, pp. 204-214). The same model was later put forward by Shonick and Jackson (1973) to assist in finding how many hospital beds were needed to serve the emergency and regular patients.

Ridge et al. (1998) describe a simulation model for bed capacity planning in Intensive Care. They developed a queuing model for the purposes of validating the simulation model. They used an M/M/c model with priority to emergency patients to analyze a 6-bed intensive care unit (ICU). Kim et al. (1999) analyzed the admission-and-discharge processes of the ICU unit by using queuing and simulation models. They used an M/M/c queueing model to analyze the capacity of the 14-bed ICU and evaluated three different ways of computing the overall average service time for the queueing model.

https://doi.org/10.62500/icrtsda.1.1.33

The results provide insights into the operation management issues of an ICU facility to help improve both the unit's capacity utilization and the quality of care provided to its patients. Green (2002) used queueing analysis to estimate bed unavailability in intensive care units (ICUs) and obstetrics units. The results indicate that as many as 40% of all obstetrics units and 90% of ICUs have insufficient capacity to provide an appropriate bed when needed. This contrasts sharply with the expectations deduced according to standard average occupancy targets. Shmueli et al. (2003) presented a model for optimizing admissions to the ICU with the objective of maximizing the expected incremental number of lives saved by operating an ICU. They use queuing theory to model the probability distribution of the number of occupied ICU beds. McManus et al. (2004) used queueing theory to construct a mathematical model of patient flow, compared predictions from the model to observed performance of the unit, and explored the sensitivity of the model to changes in unit size.

Griffths and Price-Llyod (2006) proposed an M/H/c/∞ queueing model in conjunction with a simulation model of the ICU environment were they emphasized on adequately representing the high variation in the patient length of stay. Seshaiah and Thiagaraj (2011) develop a queueing network model with blocking and reneging to study how the wait times in emergency care units are influenced by the number of available beds in ICUs and general units. They determined the adequate bed counts in each of the two units through an approximate logical method and simulation, so as to guarantee certain access standards. Chan and Yom-Tov (2011) examined the queueing dynamics of an ICU where patients may be readmitted. They developed a state-dependent Erlang-R queueing network where the service times and readmission probabilities depend on whether the ICU is full.

After examining the above relevant literature, next, we highlight the contribution of this work which is developing a model that predicts the proportion of patients from each category that would be prematurely transferred as a function of the size of the unit, number of categories, mean arrival rates, and length of stay. The model can be used by Hospital managers as a decision tool for planning and managing the ICU unit.

3. ICU Unit Modelling

In order to develop the model, it has been assumed that the referral rates are Poisson distributed, and the distributions of the duration of stay are exponential. In analyzing the steady-state behavior of the systems with Poisson distributed arrival rates and exponentially distributed service times the most commonly used approach is to obtain and solve a set of differential-difference equations relating system states over time.

Consider an ICU unit with *C* beds and *k* risk categories, where *k* is the least important risk category. The patients with risk category *j*, (*j* = 1, 2, …, *k)* has a Poisson arrival rate of λ_j and exponential service time of rate μ_j. Let $\rho_j = \frac{\lambda_j}{\mu_j}$ be the workload parameter for category j risk and $P(n_1, n_2, \ldots\ldots\ldots, n_k)$ be the probability of n_j patients in the unit from categories *j, j*=1, 2, …, *k,* where $n_j \geq 0, \sum_{j=1}^{k} n_j \leq C$ and = 0 otherwise. For simplicity, we write P (0, 0, …, 0)= P_0 and $P(n_1, n_2, \ldots, n_k)$ = $P_{\boldsymbol{u}}$, where **u** is a vector with *j*th component n_j (*j =1, 2, ...,* k). The steady-state equations for this model are

$$\sum_{j=0}^{k}\left(\lambda_j + n_j\mu_j\right) P_{\boldsymbol{u}} = \sum_{j=1}^{k}\left(n_j + 1\right)\mu_j P_{\boldsymbol{u}+\boldsymbol{v}} + \sum_{j=1}^{k}\lambda_j P_{\boldsymbol{u}-\boldsymbol{v}} \,. \qquad (2.1)$$

Where, **v** is a vector with all zero components except for a one at position *j* corresponding to priority *j*. The steady-state can be stated as follows and as shown in Theorem 1 and its proof.

https://doi.org/10.62500/icrtsda.1.1.33

$$P_{\mathbf{u}} = \prod_{j=1}^{k} \frac{\rho_j^{n_j}}{n_j!} P(0,0,...,0). \tag{2.2}$$

Theorem 3.1

When categories 1, 2, …, k have different service times, the probability distribution of the customers in the system at the steady-state is

$$P_u = \left(\prod_{j=1}^{k} \frac{\rho_j^{n_j}}{n_j!} \right) P_0 \text{ Where, } \quad P_0 = \left[\sum_{\substack{(n_1,n_2,....,n_k) \\ \sum_{j=1}^{k} n_j \le C}} \prod_{j=1}^{k} \frac{\rho_j^{n_j}}{n_j!} \right]^{-1}$$

Proof:

To prove the theorem we need to show that (2.2) satisfies (2.1). Let $P_u = D\prod_{j=1}^{k} \frac{\rho_j^{n_j}}{n_j!}$ then we show that D should be

$$\left[\sum_{\substack{(n_1,n_2,....,n_k) \\ \sum_{j=1}^{k} n_j \le C}} \prod_{j=1}^{k} \frac{\rho_j^{n_j}}{n_j!} \right]^{-1}$$

in order to satisfy the summability – to – one criterion. Let $\Re(\boldsymbol{u}) = \prod_{j=1}^{k} \frac{\rho_j^{n_j}}{n_j!}$, then substituting $P_u = D\Re(\boldsymbol{u})$ into (2.1) gives

$$D\Re(\boldsymbol{u}) \sum_{j=1}^{k} (\lambda_j + n_j \mu_j) = D\Re(\boldsymbol{u}) \sum_{j=1}^{k} \lambda_j + D\Re(\boldsymbol{u}) \sum_{j=1}^{k} n_j \mu_j$$

Since the left-hand side is the same as the right hand-side, i.e. $P_u = D\prod_{j=1}^{k} \frac{\rho_j^{n_j}}{n_j!}$. Now to evaluate *D*, we have: $\sum_{\substack{(n_1,n_2,....,n_k) \\ \sum_{j=1}^{k} n_j \le C}} P_u = 1.$

Thus, $D = \left[\sum_{\substack{(n_1,.....,n_k) \\ \sum_{j=1}^{k} n_j \le C}} \prod_{j=1}^{k} \frac{\rho_j^{n_j}}{n_j!} \right]^{-1}$.

https://doi.org/10.62500/icrtsda.1.1.33

One of particular interest is the proportion of patients in each category who are (prematurely) transferred out of the unit in order to make room for incoming (undiagnosed) arrivals. If T_m denotes the probability that a patient in category *m* is prematurely transferred then PT_m is the proportion of time or probability that the unit is full with patients of type *m* and above and that

$$T_m = \sum_{\substack{(n_1,\ldots,n_m,0,\ldots,0) \\ \sum_{j=1}^{m} n_j = C}} P(n_1, n_2, \ldots, n_k) - \sum_{\substack{(n_1,\ldots,n_{m-1},0,\ldots,0) \\ \sum_{j=1}^{m-1} n_j = C}} P(n_1, n_2, \ldots, n_k) \qquad 2.3$$

It follows that the proportion of patients from category *m* are prematurely transferred PT_m is given by

$$PT_m = \left(\sum_{\substack{(n_1,\ldots,n_j,0,\ldots,0) \\ \sum_{i=1}^{j} n_i = C}} P_{\mathbf{u}} - \sum_{\substack{(n_1,\ldots,n_{j-1},0,\ldots,0) \\ \sum_{i=1}^{j-1} n_i = C}} P_{\mathbf{u}} \right) \frac{\sum_{i=1}^{j} \lambda_i}{\sum_{i=1}^{j} \lambda_i - \sum_{i=1}^{j-1} \lambda_i} \qquad 2.4$$

Corollary 3.1

The probability of dropping a customer from priority category *j* out of the system is given by

$$\sum_{\substack{(n_1,\ldots,n_j,0,\ldots,0) \\ \sum_{i=1}^{j} n_i = C}} P_{\mathbf{u}} - \sum_{\substack{(n_1,\ldots,n_{j-1},0,\ldots,0) \\ \sum_{i=1}^{j-1} n_i = C}} P_{\mathbf{u}}$$

Proof:

Let T_j be the probability that a customer of category *j* is dropped out of the system, then

$$\begin{aligned} T_j &= \Pr\{\text{The system is full by categories } 1, 2, \ldots, j \text{ and } n_j > 0\} \\ &= \Pr\{\text{The system is full by categories } 1, 2, \ldots, j\} \\ &\quad \times \Pr\{n_j > 0 \mid \text{system is full by categories } 1, 2, \ldots, j\} \\ &= \Pr\{\text{The system is full by categories } 1, 2, \ldots, j\text{-}1\} \\ &\quad \times \left(1 - \frac{\Pr\{\text{The system is full by categories } 1, 2, \ldots, j\text{-}1\}}{\Pr\{\text{The system is full by categories } 1, 2, \ldots, j\}}\right) \\ &= \Pr\{\text{The system is full by categories } 1, 2, \ldots, j\} - \\ &\quad \Pr\{\text{The system is full by categories } 1, 2, \ldots, j - 1\} \end{aligned}$$

https://doi.org/10.62500/icrtsda.1.1.33

$$= \sum_{\substack{(n_1,\ldots,n_j,0,\ldots,0) \\ \sum_{i=1}^{j} n_i = C}} P_{\mathbf{u}} - \sum_{\substack{(n_1,\ldots,n_{j-1},0,\ldots,0) \\ \sum_{i=1}^{j-1} n_i = C}} P_{\mathbf{u}} \quad .$$

Observe that from the above corollary, the proportion of customers of category *j* that are dropped from the system is given by

$$\left(\sum_{\substack{(n_1,\ldots,n_j,0,\ldots,0) \\ \sum_{i=1}^{j} n_i = C}} P_{\mathbf{u}} - \sum_{\substack{(n_1,\ldots,n_{j-1},0,\ldots,0) \\ \sum_{i=1}^{j-1} n_i = C}} P_{\mathbf{u}} \right) \frac{\sum_{i=1}^{\ell} \lambda_i}{\sum_{i=1}^{j} \lambda_i - \sum_{i=1}^{j-1} \lambda_i} .$$

4. Illustrative Example

For any given set of parameters λ_j and μ_j (j =1,2) and *C*, the steady-state probabilities can be obtained by using equations 2.1 and 2.2. Consider, for example, a unit for which the arrival rates of high and low-risk patients are independently and Poisson distributed with means of 1 and 2 patients per day respectively and let the length of stay of high and low-risk patients be exponentially distributed with means 3 and 2 days respectively. For illustration, assume that the number of beds available is 5 beds.

The probability distributions for the number of patients in the unit from diagnostic categories up to and including the k^{th} category *k* (*k* = 1, 2) is given in Table 1 below.

	No. of patients in coronary care					
Categories	0	1	2	3	4	5
High & low	0	3	7	18	30	42
High	5	16	25	25	18	11

Table 1: Probability distribution (%) of patients

The distribution of the number of all categories of patients in the unit is in effect the distribution of bed occupancy in the unit. Hence the unit is full 42% of the time, and it follows that 42% of all patients are transferred prematurely; it is full 11% of the time with patients from high risk. It follows that 31% of premature transfers are from low risk, and 11% are from high risk. From Table 1, the proportions of category 2 and 1 transferred prematurely are 93% and 33% respectively.

5. **Case Study**

The ICU and CCU in the hospital under study have 9 beds and provide services for a population of 100,000 residents. In general, the patients are referred to the hospital in CCU by their general practitioners, accidents or by themselves. The patients treated in the critical care unit are categorized into six groups as follows.

https://doi.org/10.62500/icrtsda.1.1.33

I. ICU / high dependency,
II. Cardiac Monitoring,
III. Heart attack,
IV. Chest pain,
V. Overdose,
VI. Other acute diagnoses.

Then the Hospital admission and serving policy is,

1. Prior to admission to the intensive or coronary care unit the patients are categorized into one of follows two categories:
    - High Risk (that includes numbers I, II and III mentioned above), and
    - Low Risk (which includes numbers IV, V and VI).
2. Patients admitted to the unit will stay and not to be released until a satisfactory/full recovery.
3. When the unit is full (full capacity occupied), the new patient will be diagnosed, categorized and transferred elsewhere, as shown in the flow-chart in Figure 1

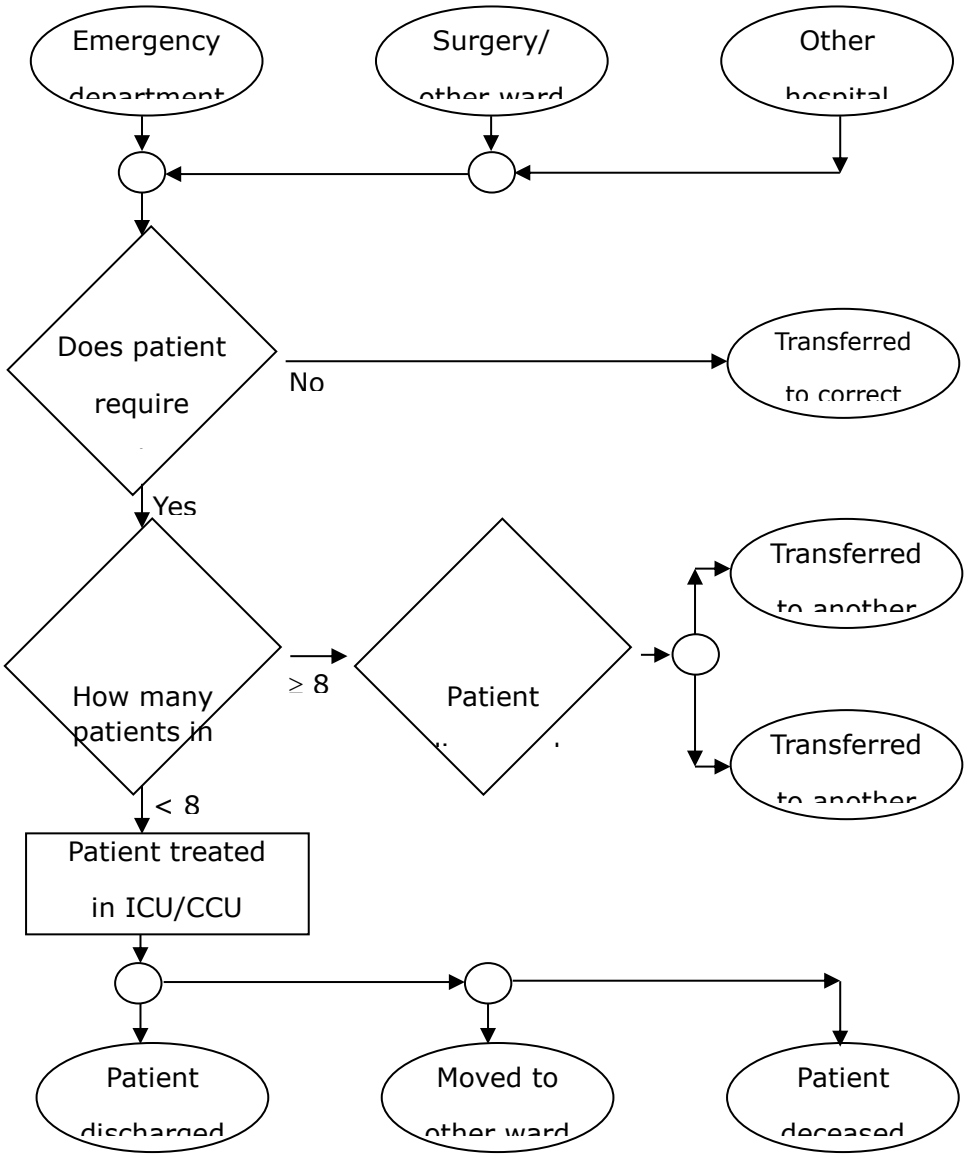

https://doi.org/10.62500/icrtsda.1.1.33

Figure 1: Hospital flowchart

The data available are daily recorded over one year for the number of admissions per day, the final diagnoses of all the patients admitted and the bed occupancies. To estimate the model parameters, it was found that the admissions per day over a period of 365 days for the two categories (high and low) were Poisson distribution with mean 1.52 and 1.422 per day receptively. The actual and theoretical pairs for both high and low risk are shown in Table 2, Table 3, Figure 2 and Figure 3 below.

Table 2: Admissions per day (high risk)

No. of Admission	0	1	2	3	4	5	6
Actual frequency	82	125	91	34	23	9	2
Theoretical	80	121	92	46	18	5	1

Table 3: Admissions per day (low risk)

No. of Admission	0	1	2	3	4	5	6	7
Actual frequency	94	119	89	42	13	7	0	1
Theoretical	88	125	89	42	15	4	1	0

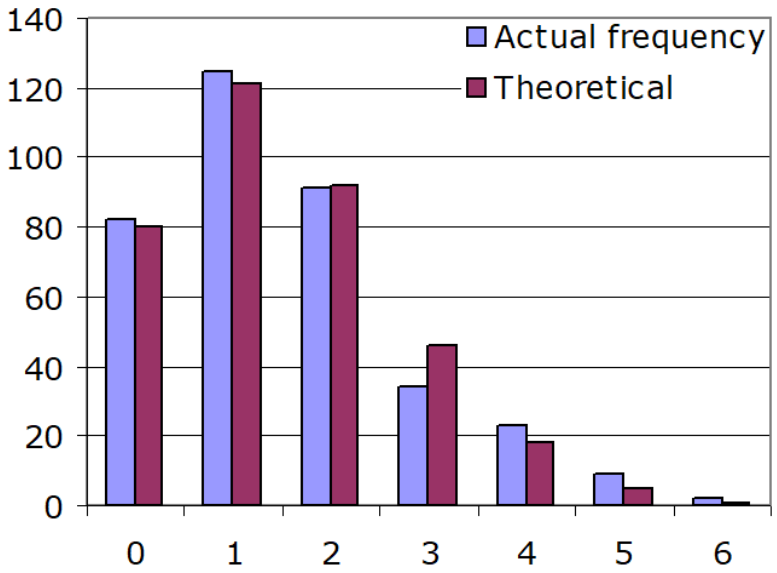

Figure 2: Admissions per day (high risk)

https://doi.org/10.62500/icrtsda.1.1.33

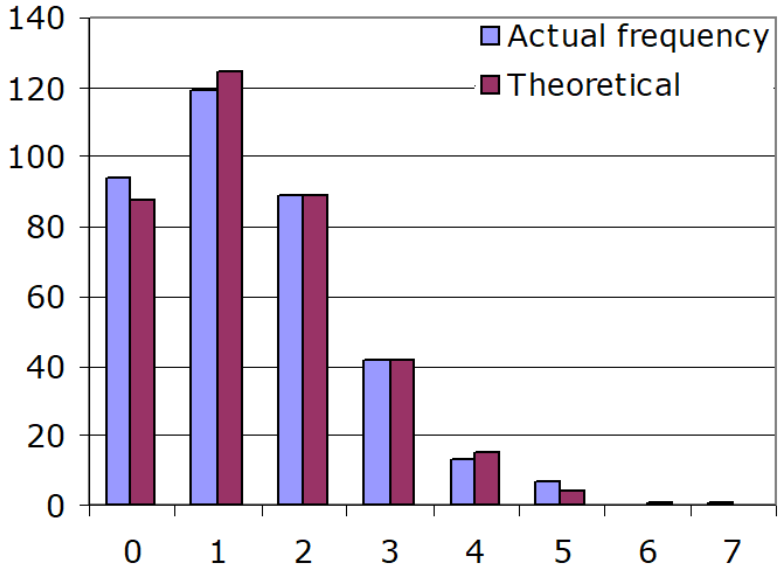

Figure 3: Admissions per day (low risk)

Among the 1097 patients admitted over a one-year period, the final diagnoses were 502 low risk and 595 high risk. Lengths of stay in the unit over the period of 365 days were found to be exponentially distributed for the low and high risk with mean 1.196 and 2.04 respectively. The actual and theoretical distributions are shown in Table 4, Table 5, Figure 4 and Figure 5 below.

Table 4: Mean stay of high risk

No. of days	0	1	2	3	4	5	6	7	8	9	10	11	12	13	14	15	16
Actual frequency	135	170	106	88	39	16	11	14	4	1	5	3	1	0	1	0	1
Theoretical (rounded)	290	178	109	67	41	25	15	9	6	3	2	1	1	1	0	0	0

Table 5: Mean stay of low risk

No. of days	0	1	2	3	4	5	6	7	8	9	10
Actual frequency	170	199	70	28	18	6	6	3	1	0	1
Theoretical (rounded)	420	182	79	34	15	6	3	1	1	0	0

https://doi.org/10.62500/icrtsda.1.1.33

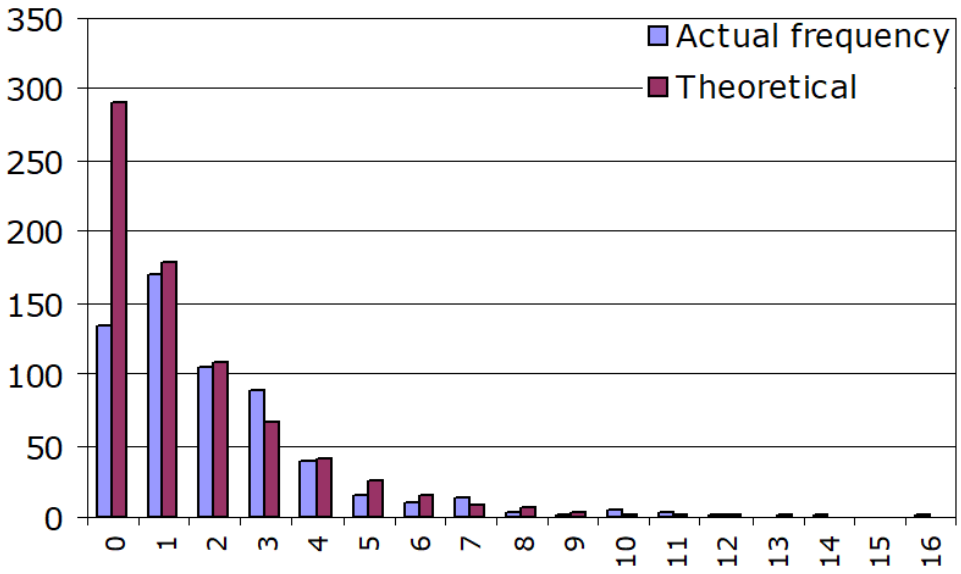

Figure 4: Mean stay of high risk

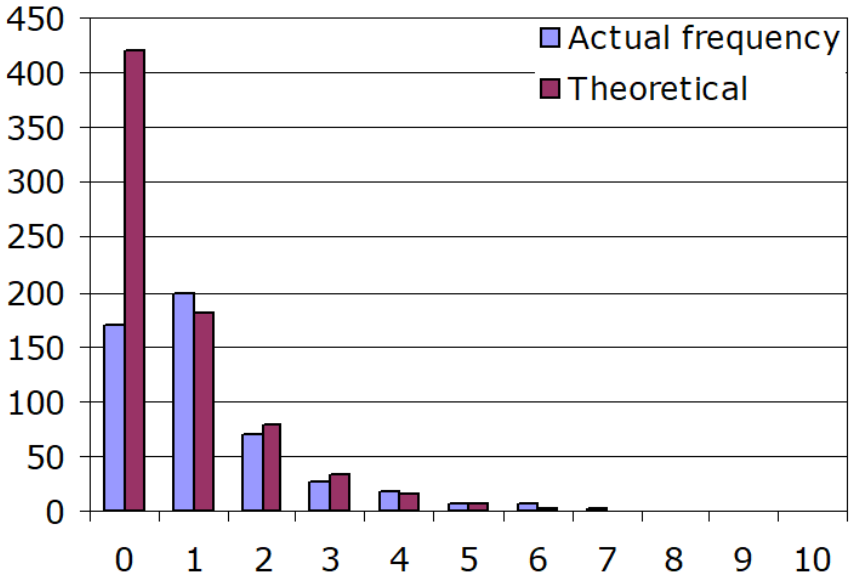

Figure 5: Mean stay of low risk

The distribution of actual bed occupancy is shown in Figure 6. This distribution appears as a normal distribution with a mean of 7.0438 and a standard deviation of 1.7011. Using a chi-square test, it is clearly shown that the distribution for the bed occupancy level is Normal distribution, the actual and theoretical distributions are presented in Table 6 as well as in Figure 6.

Table 6: Bed occupancy

No. of beds	1	2	3	4	5	6	7	8	9	10	11
Actual frequency	0	1	6	21	36	68	92	64	52	20	5
theoretical (rounded)	0	1	5	17	42	71	86	73	44	19	6

https://doi.org/10.62500/icrtsda.1.1.33

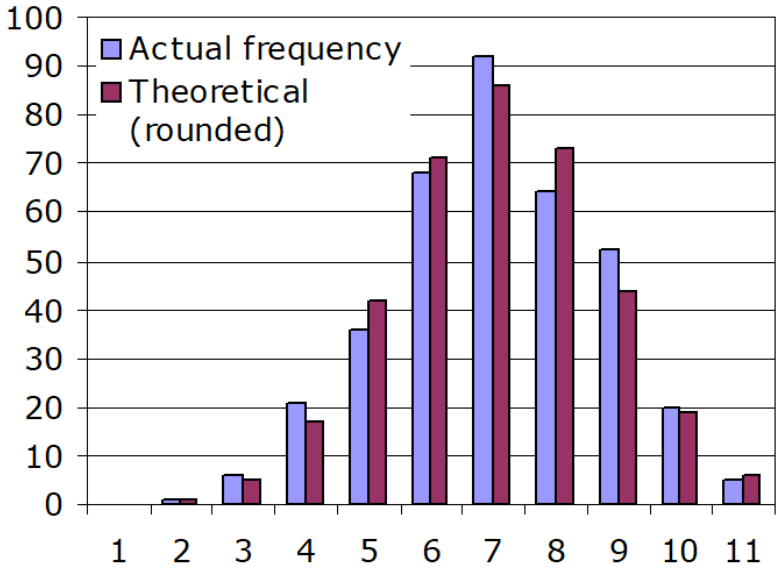

Figure 6: Bed occupancy

One can notice there are occasions where the bed occupancy level exceeds the current bed capacity. That happened on 25 occasions throughout the year, i.e. 6.8 % of the time. In other words, management accepts that the unit's capacity is adequate 93.2 % of the time. Since this is the case, and to predict the required bed capacity level for future patient demands, we will assume a significance level of 95 %.

Since the hospital under study is satisfied with the current efficiency of the unit, we are going to estimate our current probabilities of "x" amount of beds used on any one day shown in Table 7.

Beds Used (BU)	Frequency (Fr)	Probability = BU/Fr
7	92	0.2521
8	64	0.1753
9	52	0.1425
10	20	0.0548
11	5	0.0137

Table 7: Probability distribution of bed used on one day

As shown earlier, the bed occupancy level has a normal distribution with a mean of approximately 7 patients (rounded down from 7.0438) and a standard deviation of 2 patients (rounded up from 1.7011). Since our sample is large and spans a year of patient traffic, we will assume that these values hold true for the entire population.

We will now examine the days of the year, which have a bed occupancy level greater than and equal to the average. We selected at random, 1 day from each of the days, where the bed occupancy level exceeded 6 patients. These days were then examined in detail, and the results are shown in the tables (1-5) in Appendix (1).

Thus, with 8 beds available (9 beds in the unit) some 0.0093 of all patients are transferred prematurely, if it can be assumed, however, that patients are accurately diagnosed soon after admission then only 0.00008 of high risk and 0.00922 of low risk would be transferred prematurely.

https://doi.org/10.62500/icrtsda.1.1.33

The main purpose of this section is to demonstrate that queuing theory can be applied to give insights into the steady-state behavior and operating characteristics of service systems with pre-emptive service disciplines.

For illustration, the model has been used to obtain estimates of the proportion of patients transferred prematurely form a coronary care unit in which patients are classified into two categories (high and low risk).

In order to complete the current study and to justify its results, we have to test our assumptions and to justify the use of the model. To test whether the number of patients of both categories of risk that arrive each day is random, we fitted a Poisson distribution to the number of patients per day. A chi-square test has shown that the fit was significant at the 99 % confidence level. To test whether the length of stay for the two categories is exponential, a chi-square test showed that the fit was not at the 99 % confidence level for the two categories.

However, as seen in Figure 3 and 4, the observed frequency for 0 days differ greatly from the expected frequency. This results in a large value for chi-square, thus greatly influencing the sum of chi-square on closer examination of these observations. It was determined that patients who were admitted for less than one day were in fact in the ward for only a very short time. This raises suspicion that perhaps these patients were not as serious as first diagnosed and did not require the specialized treatment from this unit. Under this assumption, the chi-square test showed that the fit was significant at the 99 % confidence level for both categories. Thus, the system behavior within each category should have been modeled as multiple server queueing system with Poisson arrivals and exponential distribution.

6. Discussions and Conclusion

Emergency services are subject to highly variable demand. Under this situation, we have to balance the cost of providing more capacity than is needed on average against the risk to patients who must otherwise be refused admission to or transferred prematurely from intensive care in order to admit new patients for observation and diagnosis.

The decision as to where the balance lies between the costs of providing more facilities than the average required and the cost to patients otherwise put at risk remains a matter of clinical judgment. The proposed model, however, at least reduces some of the uncertainty about the effect of unit size on the numbers and diagnostic categories of patients put at risk by premature transfer.

When coronary care units become full, it is common practice to make at least one bed available for new arrivals by transferring the patient perceived to be at least risk to a general medical or surgical ward. In deciding how many beds should be provided it is clearly necessary to make some assumption about the relationship between the number of beds available and the proportion of high-risk patients who would be prematurely transferred out of intensive care.

The numerical example we introduced demonstrates the operating characteristics for any given size of unit can be predicted using estimates of the arrival rate for each category (high and low) of patients and the average length of stay for each category.

The case study illustrates that the efficiency level of the (CCU) in the hospital under study was acceptable because the proportion of patients from the high risk transferred or turned away is 0.0008, and the proportion of all patients transferred from the unit is 0.0063.

Increases in the arrival rate affect the distribution of the number of beds used. From this, it can be seen that, for these increases, the unit's number of beds must increase to maintain its current efficiency. One must address the fact that in the future, there is a high chance that the arrival rate will increase, due to the significant growth of the local population. As a result, the current critical care unit would no longer be optimal due to the decrease in the ability of the units to cope with demand in the future.

https://doi.org/10.62500/icrtsda.1.1.33

References

Bai, J., Fügener, A., Schoenfelder, J., and Brunner, J. (2018). "Operations research in intensive care unit management: a literature review". *Health Care Management Science* 21:1–24.

Bailey, N.T.J. (1952). "A Study of Queues and Appointment System in Hospital Out- patient Department with Special Reference to Waiting Time". *Journal of the Royal Statistical Society: Series B* 14: 185-194.

Benn, B.A. (1966). "Hierarchical Car Pool Systems in Railroad Transportation". *Ph.D.thesis, case Institute of technology, Cleveland, Ohio.*

Blumberg, M.S.(1961). "DPF Concept Helps Predict Bed Needs". *Modern Hospital* 97: 75-81.

Chan, C. and Yom-Tov, G. (2011). "Intensive care unit patient flow with read-missions: a state-dependent queueing network". *2011 MSOM Annual Conference Ann Arbor,Michigan* pp.1–3

Choi, M. and Lee, H. (2016). "Critical Patient Severity Classification System predicts outcomes in intensive care unit patients". *Nursing in critical care* 21: 206-213.

Cooper, R.B. (1972). "*Introduction to Queueing Theory*". Macmillan, New York.

Green, L. (2002). "How many hospital beds?". *Inquiry* 39: 400-412.

Griffths, J. and Price-Llyod, N. (2006). "A queuing model of activities in an intensive care unit". *IMA Journal of Management Mathematics* 17: 277-288.

Harris, R.A (1985). "Hospital bed requirements planning". *European Journal of Operational Research,* 25: 21-126.

Kim, S., Horowitz, I., Young, K., and Buckley, T. (1999). "Analysis of capacity management of the intensive care unit in ahospital". *European Journal of Operational Research* 115: 36-46.

Kolesar, P.(1970). "A Markovian Model for Hospital Admission scheduling". *Management Science* 16: 384-396.

Lakshmi, C. and Appa Iyer, S. (2013). "Application of queueing theory in health care: A literature review". *Operations Research for Healthcare* 2: 25-39.

Liyanage, L. and Gale, M. (1995). "Quality improvement for the Campbell town hospital emergency service". *International conference on systems, Man and Cybernetics* 3: 1997-2002.

McClain, J.O. (1976). "The Planning Using Queueing Theory Models of Hospital Occupancy: A Sensitivity Analysis". *Inquiry* 13: 167-176.

McManus, M., Long, M., Cooper, A., and Litvak E. (2004). "Queueing theory accurately models the need for critical care resources". *Anesthesiology* 100: 1271-1276.

National health strategy. (1992). "A Study of Hospital Outpatient and Emergency Department Services". Paper 10.

Ridge, J., Jones, S. Nielsen, M., and Shahani, A. (1998). "Capacity planning for intensive care units". *European Journal of Operational Research* 105: 346-355.

https://doi.org/10.62500/icrtsda.1.1.33

Seshaiah, C. and Thiagaraj, H. (2011). "A queueing network congestion model inhospitals". *European Journal of Scientific Research* 63: 419-427.

Shmueli, A., Sprung, C., and Kaplan, E. (2003). "Optimizing admissions to an intensive care unit". *Health Care Management Science* 6: 131-136.

Shonick, W. and Jackson, J.R. (1973). "An Improved Stochastic Model forOccupancy- Related Random Variables in General- Acute Hospital". *Operations Research* 21: 952-965.

Sissouras, A.A. and Moores, B. (1975). "The Optimum Number of Beds in a Coronary Care Uint". *Omega* 4: 59-65.

Weckwerth, V.E. (1966). "Determining Bed Needs from Occupancy and CensusFigures". *Hospital* 40: 52-54.

Wharton, F. (1996). "On The Risk Of Premature Transfer From Coronary Care Units". *Omega, Int.J. Mgmt. Sci*. 24: 413-423.

A SHORT SURVEY OF THE EXACTLY SOLVABLE DIFFERENTIAL EQUATIONS IN PHYSICAL CHEMISTRY

https://doi.org/10.62500/icrtsda.1.1.34

Proc. 1st International Conference on Recent Trends in Statistics and Data Analytics
Air University Islamabad, Pakistan – May 9, 2024, Vol. 1, pp. 323-330

A SHORT SURVEY OF THE EXACTLY SOLVABLE DIFFERENTIAL EQUATIONS IN PHYSICAL CHEMISTRY

Nosheen Zareen khan[1], Seyedeh-Razieh Mirrajei [2] and Masoud Saravi[3]
Department of Mathematics University of Sharjah, UAE
[2] Education Office of Amol, Amol, Iran
[3] University of Shomal, Amol, Iran.

ABSTRACT

This paper presents a survey of mathematical models in several areas of chemistry using Differential Equations (DEs). Wherever required, ideas and analytical methods have been illustrated with modelling examples. Although, in general, students of chemistry have a more limited mathematical background than physics or engineering students but in this paper, we tried to present applications with explaining the underlying methods. In this manner, we have tried to have a better understanding how solve them. We emphasis that this paper is useful for the researchers in the field of chemistry, hence some objective and new contribution may not clear for the readers in other fields. Main goal of this paper is to familiarize reader to applications of DEs on chemistry.

Keywords: Ordinary and Partial Differential Equation, Closed-form solution, Schrödinger equations

1. INTRODUCTION

Differential equations arise in many areas of chemistry, and it is therefore to know how to solve the more commonly occurring ones. Although several textbooks have been written on exploitation of analytical methods for solving such equations but most of them may mention only one or two examples related to modeling in chemistry [1],[2],[3],[4],[5],[6],[11]. The range in complexity from simple equations describing elementary kinetic processes to the Schrödinger equation in three dimensions.
A differential equation is a mathematical equation for an unknown function of one or several variables that relates the values of the function itself and its derivatives of various order. The *order* of a differential equation is defined to be that of the highest order derivative it contains, and the *degree* of a differential equation is defined as the power to which the highest order derivative is raised. If the degree of unknown function or its derivatives is not one, then DE is called *nonlinear* otherwise is *linear*. We classify differential equations into two categories. Those which only involve functions of a single variable are *ordinary differential equations* (ODEs) whereas if they describe a function of two or more variables are called *partial differential equations* (PDEs).

Hence in following DEs, first three equations are ODEs of order one but equations (5), (6) and (7) are order two. The rest are PDEs of order two. All have degree one. Note that equations (2) and (3) are nonlinear.

$$\frac{dx}{dt} = -kt, \tag{1}$$
$$\frac{dx}{dt} = k_1(1-x)(2-x) - k_2x^2, \tag{2}$$
$$y'(x) = a(x) + b(x)y(x) + c(x)y^2(x). \tag{3}$$
$$(1-x^2)y'' - 2xy' + \lambda(\lambda+1)y = 0, \tag{4}$$
$$xy'' + (1-x)y' + \lambda y = 0, \tag{5}$$

https://doi.org/10.62500/icrtsda.1.1.34

$$y'' - x2y' + 2\lambda y = 0, \quad (6)$$

$$\frac{\partial^2 u}{\partial t^2} = c^2 \frac{\partial^2 u}{\partial x^2}, \quad (7)$$

$$\frac{\partial u}{\partial t} = c^2 \left(\frac{\partial^2 u}{\partial x^2} + \frac{\partial^2 u}{\partial y^2}\right), \quad (8)$$

$$\frac{\partial^2 u}{\partial x^2} + \frac{\partial^2 u}{\partial y^2} + \frac{\partial^2 u}{\partial z^2} = 0, \quad (9)$$

$$\frac{\partial^2 \psi}{\partial x^2} + \frac{\partial^2 \psi}{\partial y^2} + \frac{\partial^2 \psi}{\partial z^2} + \frac{8\pi^2 m(E-V)\psi}{h^2} = 0, \quad (10)$$

The equations (1)-(2), are describing elementary kinetic processes of first order reactions, successive first order reactions and second order reactions respectively. Eq. (3) is Riccati equation which is widely used in many areas of quantum mechanics, and particularly in quantum chemistry (e.g, the theory of neutron transport). Of all first order nonlinear DE, it occupies perhaps the most important place. It is closely related to the general linear second order equation. In 1760, Euler proved that the Riccati first-order nonlinear differential equation can be equivalently reduced to a second-order linear homogeneous differential equation (see, e.g.,[1], [2], [3]). Therefore, there exists a correspondence between Riccati and Schrödinger equation of the linear second-order ODE type.

If $a(x) = 0$ then we have Bernouli differential equation. Eq. (4) is Lauguerre equation appears in the description of wave function of the hydrogen atom. Eq. (5), known as Legendre equation occurs in numerous physical applications and particularly in problems with axial symmetry when they are expressed in spherical polar coordinates. In quantum mechanichs the study of Schrödinger equation for the case a harmonic oscillator leads to Eq. (6) which is known as Hermite equation

Eq. (7) is the one-dimensional wave equation. Eq. (8) arises in the theory of heat conduction, also in the diffusion of neutrons in an atomic pile to produce nuclear energy. Eq. (9) is the famous 3-dimensional Laplace's equation which has a wide range of application in heat, electricity, potential theory, gravitation, and aerodynamic. Eq. (10) is time-independent Schrödinger equation in three dimensions for the particle in a rectangular box.

The laws governing chemical kinetics can be written as systems of ordinary differential equations. In the case of complex reactions with several different participating molecules, these equations are nonlinear and present interesting mathematical properties (stability, periodicity, bifurcation, etc.).

In this paper that are in some way representative in chemistry we try to examine a number of them which can be solved theoretically to find a closed-form solution for them, if exist. However, there are many unsolved DEs in pure and applied chemistry that some of them are of great importance.

Next section discusses the methods that can be useful to solve some of DEs in chemistry but bear in mind that in nonlinear or even linear cases, most of them must be solved numerically.

2. Description of the Methods

If we could write the first order ODEs given by $y'(x) = f(x, y)$ in the form

$$P(x)dx + Q(y)dy = 0, \quad (11)$$

then we say the variables are *separable,* and the solution can be obtained by integrating both sides of (11) with respect to *x.* Thus,

$$\int P(x)\,dx = \int Q(y)\frac{dy}{dx}dy,$$

or for simplicity one can write

$$\int P(x)\,dx = \int Q(y)\,dy.$$

We assume the integrations can be done by some methods of integrations.

https://doi.org/10.62500/icrtsda.1.1.34

The variables of equations 1 and 3 are separable, thus can easily be solved.

Suppose in (9) the variables are not separable. That is.

$$P(x,y)dx + Q(x,y)dy = 0. \tag{12}$$

If equations are so-called *exact, i.e.,* $\frac{\partial Q}{\partial x} = \frac{\partial P}{\partial x}$ then it can be solved by integration. If not we have to find a factor called *integrating factor f(x,y)*, that usually is not unique, to make it exact. Unfortunately, finding such integrating factors is not easy and sometimes impossible. But if we restrict the integrating factor to be a single variable function in terms of *x* or y, we can find the solutions. Equation 2 is a linear first order ODE. The general form of a linear first order ODE is given by

$$y'(x) + p(x)y(x) = q(x). \tag{13}$$

This is not an exact one, but it can be shown that its integrating factor is given by $\int e^{p(x)}dx$,

In the previous section we mentioned two important equations, Bernoulli and Riccati equations. The general form of a Bernoulli equation is given by

$$y'(x) + p(x)y(x) = q(x)y^n(x), \tag{14}$$

where *n* is a real number. Applications of this equation are in the study of population dynamics and in hydrodynamic stability. When $n \neq 0, 1$, the equation is nonlinear. For this case, if we set $z = y^{1-n}$, then equation inverts to a linear first order ODE and can easily be solved.

Recall Eq. (3),

$$y'(x) = a(x) + b(x)y(x) + c(x)y^2(x).$$

As we said, this equation is known as Riccati equation which cannot be solved by elementary methods but if a particular solution $y_1(x)$ is known, then the solution of this ODE can be obtained through the substitution $(x) = y_1(x) + \frac{1}{z(x)}$, where $z(x)$ is the general solution of

$$z'(x) + \big(2q(x) - p(x)\big)z(x) = -q(x).$$

We mentioned that there exists the correspondence between Riccati and Schrödinger equations (see, e.g., [7]). To demonstrate this correspondence, let us define the following transformation.

$$y(x) = -c(x)\frac{\psi'(x)}{\psi(x)},$$

which leads to

$$a(x)\psi''(x) - \big(a'(x) + a(x)b(x)\big)\psi'^{(x)} + a^2(x)c(x)\psi(x) = 0. \tag{15}$$

This is a well-known second order linear differential equation which may be solved by an analytical method. If we know two independent solutions of (15) then the solution of Riccati equation can be written in terms of the general solution. But in general, to obtain the solution of this equation by analytical methods is difficult, and in most cases are impossible. But if we impose more on coefficient functions, we may find closed form solution if exists. For example, let $a(x), b(x)$ and $c(x)$ be constants.

3. Examples

This section deals with some examples that have been taken from several textbooks. We try to consider some which are not complicated to readers. In this manner, we solved or, at least we guided how to solve them.

Example 1**:** It has been established empirically that radioactive elements decompose at approximately a fixed rate, called the *decay rate.* That is, if $m(t)$ is the mass of the substance present at any time, then

https://doi.org/10.62500/icrtsda.1.1.34

the rate of change per unit mass, $(\frac{dm}{dt}/m)$, is a constant. The *half-life* of a substance is the amount of time it takes for it to decay to one-half of its amount. Question: Show that the hale-life H of a radioactive substance can be determined from two measurements $m_1 = m(t_1)$ and $m_2 = m(t_2)$ of the amounts present at time t_1 and t_2 by the formula, $H = \frac{(t_2 - t_1)\ln 2}{\ln(m_1/m_2)}$..

Example 2**:** In the reversible second-order reaction

$$A + B \rightleftarrows 2C$$

if the initial concentrations os A and B are 1 and 2, respectively, the rate of formation of C is given by

$$\frac{dx}{dt} = k_1(1 - x)(2 - x) - k_2x^2, \tag{16}$$

where x is concentration of C at time t and k_1 and k_2 are constants. The equation (4) has two variables: concentration of intermediate product X and time variable t. Given at time $t = 0, x = 0$ and at equilibrium (i.e. when $\frac{dx}{dt} = 0$), $x = \frac{1}{2}$, we wish to derive a relation between time and concentration. Although this is a nonlinear first-order ODE but can analytically be solved. If we consider right hand side of this equation as a polynomial of degree 2, then one may write

$$k_1(1 - x)(2 - x) - k_2x^2 = (x - a)(b - x).$$

Since the variables are separable, we can easily find the solution. Imposing $\frac{dx}{dt} = 0$ when $x = \frac{1}{2}$, leads to $t = \frac{1}{5k_1}\ln\left[\frac{(x+2)}{2(1-x)}\right]$.

If constant term in the kinetic equation of reaction given by (16), i.e. $2k_1$, replaced by a function in term of time then to find the analytical solution of this type of equation is impossible. According to what kind function will be chosen then the different discussion may be used (see, e.g., [9]).

Remark 1: The Schrödinger equation can be solved exactly for only a few simple systems: the particle in a box, the harmonic oscillator, the rigid rotator, the hydrogen atom, and a few others [10]. Nevertheless, approximate solutions can be obtained for a very large variety system, and these solutions have contributed inestimably to the practical application of quantum theory to development of chemical principles.

Example 3**:** Using an electron as the particle, Schrödinger equation (in atomic units) for the particle in a box may be written as $-\frac{\boldsymbol{h^2}}{\boldsymbol{2m}}\frac{\boldsymbol{d^2\psi}}{\boldsymbol{dx^2}} = E\psi$ such that $V = 0$ for $0 \le x \le a$, otherwis $V = \infty$, where E is the energy of particle, m is the mass and h is Planck's constant. This equation can be rewritten as $\frac{\boldsymbol{d^2\psi}}{\boldsymbol{dx^2}} + \frac{2mE}{h^2}\psi = 0$, which is a linear second-order ODE with constant coefficients. Such equations can easily be solved by finding roots of a quadratic equation where its coefficients are the same coefficients of given ODE. For this equation it is not difficult to show that the general solution is: $\psi(x) = A\cos\lambda x + B\sin\lambda x$, where $\lambda^2 = \frac{2Em}{h^2}$.

Since $\psi(0) = 0$ then $A = 0$. That is, $\psi(x) = B\sin\lambda x$. In order $\psi(x)$ vanishes at $x = a$ we obtain $B\sin\lambda a = 0$. This leads to $\lambda = \frac{n\pi}{a}$. Hence, $\psi(x) = B\sin\frac{n\pi}{a}x$. There remains only the constant B to be determined. The probability of finding the particle somewhere within the box must be unity. Since wave functions of a particle in a box are orthogonal then

$$\int \psi_m^*(x)\psi_n(x)d\xi = \begin{cases} 0 & \text{if } n \neq m \\ 1 & \text{if } n = m. \end{cases}$$

https://doi.org/10.62500/icrtsda.1.1.34

Therefore

$$\int_0^a \psi_n^*(x)\psi_n(x)d\xi = 1 \to \int_0^a B^2 \sin^2\frac{n\pi}{a}dx = \frac{1}{2}aB^2 = 1 \to B = \sqrt{\frac{2}{a}}.$$

Thus, the solution is $\psi_n(x) = \sqrt{\frac{2}{a}}\sin\frac{n\pi}{a}x, \;\; n = 1,2,\dots.$

Moreover, since $\lambda^2 = \frac{2Em}{h^2}$, then $(\frac{n\pi}{a})^2 = \frac{2Em}{h^2}$. i.e., $E_n = \frac{1}{8m}(\frac{nh}{a})^2, \;\; n = 0,1,2,\dots.$

The number *n*, which labels the wave functions and energy, is called a *quantum number*. When the quantum number is specified, we can quote the corresponding energy and and wave function using these relations.

A powerful technique used to solve many of PDEs encountered in physical applications in which the domains of interest are finite. It is the method of *separation of variables.* Even though it has limitations, it is widely used. It involves the idea of reducing a more difficult problem to several simpler problems; here we shall reduce a PDE to several ODEs for which we already have a method of solution. Then, hopefully, by satisfying the initial and boundary conditions, a solution to PDE can be found. In this method according to a PDE whose dependent variable is *u* and its independent variables are *x* and *t*, for example, this method involves assuming a solution of the form *u=XT* where *X* and *T* are function of *x* and *t*, respectively and are to be determined. To illustrate the details of the method, let us consider the following example,.

Example 4**:** In the nuclear theory, the following PDE plays a key role:

$$\frac{\partial^2 u}{\partial x^2} + \frac{\partial^2 u}{\partial y^2} + \frac{\partial^2 u}{\partial z^2} + B^2 u = 0$$

where *u*(*x, y, z)* is known as *neutron flux.* It is the sum of the distance travelled per second per cubic centimetres at (*x, y, z*) by bombarding neutrons. B^2 is a positive constant and is called *buckling.* For a certain value of B^2 (known as matrial buckling), the arrangement of the material is critical.in this example, we shall find relations between dimensions and minimum volume of the reactors filled with material such that (11$0 is satisfied. We assume that the rector has the shape of a rectangular box having sides as *a, b, c*. the origin is taken as the center of the box and the axes are parallel to its edges. Since, outside the reactor there is no flux, then the boundary conditions are

$$u = 0 \text{ at } x = \pm\frac{a}{2}, \;\; y = \pm\frac{b}{2}, \;\; z = \pm\frac{c}{2}.$$

Moreover, we assume that *u*(*x, y, z)* is symmetric with respect to coordinate planes. Since in this equation we have three independent variables hence by product method we let the solution of equation is of the form

$$u = X(x)Y(y)Z(z). \tag{17}$$

Substitute in (114) and simplify. We obtain

$$\frac{X"}{X} + \frac{Y"}{Y} + \frac{Z"}{Z} + B^2 = 0. \tag{18}$$

Equate the first fraction to $-\lambda^2$ and solve the resulting equation to obtain

$$X = A_1\cos\lambda x + B_1\sin\lambda x.$$

https://doi.org/10.62500/icrtsda.1.1.34

Due to (17) and symmetry, the condition $u = 0$ demands that $X = 0$ when $x = \pm\frac{a}{2}$. This leads to that $B_1 = 0$ and $\lambda = \frac{(2n+1)\pi}{2a}$. Therefore, choosing $\frac{\pi}{2a}$ for λ, we get $X = A_1 \cos\frac{\pi}{a}x$. Applying the same method to each fraction, we obtain $Y = A_2 \cos\frac{\pi}{b}y$ and $Z = A_3 \cos\frac{\pi}{c}z$. Hence, Eq. (116) reduces to $u = A\cos\frac{\pi}{a}x\cos\frac{\pi}{b}y\ \cos\frac{\pi}{c}z$, where the constant A depends on the power output of reactor. Substituting this in Eq. (18), we can obtain the value of B^2 as

$$B^2 = \frac{\pi^2}{a^2} + \frac{\pi^2}{b^2} + \frac{\pi^2}{c^2}. \tag{19}$$

Obviously, the volume of the reactor will be minimum if it has the shape of a cubic. Therefore, for a given value of B^2 the volume will be $\frac{\pi^3 3\sqrt{3}}{B^2}$ because from Eq. (19) we get $a = b = c = \frac{\pi\sqrt{3}}{3}$.

Example 5**:** Equation (10) is the Schrödinger equation for a particle in a three-dimensional box such that $V = 0$ for $0 \le x \le a,\ 0 \le y \le b,\ 0 \le z \le c$, otherwis $V = \infty$, where E, m and h been introduced in example 3. We consider this equation for $a \ne b \ne c \ne 0$. If we apply the same technique which been used in previous example, we can write

$$\frac{X"}{X} + \frac{Y"}{Y} + \frac{Z"}{Z} = -\frac{8\pi^2 mE}{h^2}.$$

Since as x appears only in $\frac{X"}{X}$, then when x varies only $\frac{X"}{X}$ can change. Similarly, for $\frac{Y"}{Y}$ and $\frac{Z"}{Z}$. But the sum of $\frac{X"}{X}$, $\frac{Y"}{Y}$, $\frac{Z"}{Z}$ is a constant; therefore $\frac{X"}{X}$ must itself be a constant. We write it $-\frac{8\pi^2 mE_x}{h^2}$. Similarly, $\frac{Y"}{Y}$ and $\frac{Z"}{Z}$ must be constant and are $-\frac{8\pi^2 mE_y}{h^2}, -\frac{8\pi^2 mE_z}{h^2}$ respectively, such that $E_x + E_y + E_z = E$. Thus

$$X'' + \frac{8\pi^2 \mathrm{mE_x}}{\mathrm{h^2}}\mathrm{X} = 0,\ \ Y'' + \frac{8\pi^2 mE_y}{h^2}Y = 0,\ \ Z'' + \frac{8\pi^2 mE_z}{h^2}Z = 0.$$

We have, $X = A_1 \cos\lambda x + B_1 \sin\lambda x$. But if we apply boundary conditions that state $\psi = 0$ at $x = 0$ and $x = a$, we obtain $A_1 = 0\ and\ \lambda = \frac{n_x\pi}{a}$. Thus $X = B_1 \sin\frac{n_x\pi}{a}x$. In the same manner we get $Y = B_2 \sin\frac{n_y\pi}{b}y$ and $Z = B_3 \sin\frac{n_z\pi}{c}z$. Hence,

$$\psi = B \sin\frac{n_x\pi}{a}x \sin\frac{n_y\pi}{b}y \sin\frac{n_z\pi}{c}z.$$

Now if we use the same argument as in example 3 it is not difficult to show that $B = \frac{8}{\sqrt{abc}}$.

We may wish to write the complete solution as follow.

$$\psi_{n_x,n_y,n_z}(x,y,z) = \frac{8}{\sqrt{abc}}\sin\frac{n_x\pi}{a}x \sin\frac{n_y\pi}{b}y \sin\frac{n_z\pi}{c}z,$$

$$E_{n_x,n_y,n_z} = \frac{h^2}{8}\left[\left(\frac{n_x}{a}\right)^2 + \left(\frac{n_y}{b}\right)^2 + \left(\frac{n_z}{c}\right)^2\right],\ n_x = 1,2,\ldots;\ n_y = 1,2,\ldots;\ n_z = 1,2,\ldots\ .$$

As we can see, many of the features of the one-dimensional problem are reproduced in three-dimensional.

Remark 2**:** It is possible to solve all PDEs that have been introduced in this paper by a general method, the separation of variables. The wave equation given by Eq. (7) can, however, be solved by an appropriate transformation of variables. By introducing tow new independent variables $\zeta = x - ct$, $\eta = x + ct$. One can show that these substitutions lead to

https://doi.org/10.62500/icrtsda.1.1.34

$$\frac{\partial^2 u}{\partial \zeta \partial \eta} = 0.$$

Integration with respect to ζ and η, respectively gives

$$u(\zeta, \eta) = f(\zeta) + g(\eta)$$

or, equivalently

$$u(x, t) = f(x - ct) + g(x + ct).$$

This is *D'Alembert solution* of wave equation.

The problem of the structure of hydrogen atom is the most important problem in the field of atomic and molecular structure. Bahr's treatment of the hydrogen atom marked the beginning of the old quantum theory of atomic structure, and wave mechanics had its inception in Schrodinger 's first paper, in which he gave the solution of the wave equation for the hydrogen atom. Since the most differential equations concerning physical phenomenon could not be solved by analytical method hence, the solutions of the wave equation are based on polynomial (series) methods. Even if we use series method, sometimes we need an appropriate change of variable, and even when we can, their closed form solution may be so complicated that using it to obtain an image or to examine the structure of the system is impossible. For example, if we consider Schrodinger equation, i.e., we come to a three-term recursion relations, which work with it takes, at least, a little bit time to get a series solution. For this reason, we use a change of variable such as or when we consider the orbital angular momentum, it will be necessary to solve. As we can observe, working with this equation is tedious. Another two equations which occur in the hydrogen atom wave equations, are Legendre and Laguerre equations, which can be solved only by power series methods.

It should be clear that when the DEs are nonlinear, nevertheless most of them are difficult to solve their behavior are considerably more complex. Nonlinear equations can lead to oscillatory solutions and can also exhibit the phenomenon of *chaos*. Chaotic systems are systems that are highly sensitive to small changes in the parameters of the equations or in the initial conditions. Basically, this means that the behavior of a chaotic system can be unpredictable, since such small changes can occur in the form of small errors in determining the parameters (rounding to the nearest tenth or hundredth) or in specifying the initial conditions and these small changes can cause the system to evolve in time in a very different way.

3. Conclusions

Results in this paper show that we can apply DEs in several areas of chemistry and find relations between elements which have been considered in such problems, particularly in nuclear theory. Through the paper we emphasized analytical methods to obtain closed-form solutions for them. But most of DEs may be nonlinear or even linear which must be solved numerically. Our next goal is to consider such problems.

Acknowledgment

The authors would like to thank the anonymous reviewers. Our thanks also go to Prof. Dr A. Rostami for his useful comments and suggestions for the improvement of this paper.

https://doi.org/10.62500/icrtsda.1.1.34

REFERENCES

1. ALDONA KRUPSKA, Mathematical description of the nonlinear chemical reactions with oscillatory inflow to the reaction field, *J. Chem. Sci.* Vol. 127, No. 6, June 2015, pp. 1025–1034.
2. D. R. Bates (2ed), *Quantum Theory, Vol 1, Academic. New York,* 1961.
3. Haley S. B.: *Am. J. Phys.* 1997, *65*, 237.
4. J. Kevorkian, Partial Differential Equations; Analytical Solution Techniques, Thomson Publishing Group, 1990.
5. M. Hermann, M. Saravi, A First course in Ordinary Differential Equations: Analytical and Numerical Methods, Springer, 2014.
6. M. Tenenbaum, H. Pollard, Ordinary Differential Equations. Harper& Row and Joan Weatherhill,1964.
7. R. Tajammal, M. A. Rana, N. Z. Khan and M. Shoaib, "Slip effect on combined heat and mass transfer in three dimensional MHD porous flow having heat," *2018 15th International Bhurban Conference on Applied Sciences and Technology (IBCAST)*, Islamabad, Pakistan, 2018, pp. 635-644, doi: 10.1109/IBCAST.2018.8312291.
8. Stephenson, An Introduction to Partial Differential Equations for Science Student, Longman, London (2nd edn, 1970).
9. T.M. Creese/ R.M. Haralick, Differential Equations for Engineers, McGraw-Hill, Inc,1978.
10. William E. Boyce, Richard C. Diprima, Elementary Differential Equations and Boundary Value Problems, third edition, John Wiley& Sons, Inc,1977.
11. W.E. Williams, Partial Differential Equations, Oxford University Press, 1980.

https://doi.org/10.62500/icrtsda.1.1.35

Proc. 1st International Conference on Recent Trends in Statistics and Data Analytics
Air University Islamabad, Pakistan – May 9, 2024, Vol. 1, pp. 331-340

A Novel Framework: Evaluating Stack-Based Windows Memory Mitigations

Moiz Abdullah[1], Khwaja Mansoor[2] and Syed Shujjah Abu Bakar[3]
Dept. of Cyber Security, Air University Islamabad Pakistan
Dept. of Cyber Security, Air University Islamabad Pakistan
Dept. of Cyber Security, Air University Islamabad Pakistan

ABSTRACT

In recent decades, technological advancements have revolutionized the way humans interact with the digital realm, reshaping the entire human experience. The technology has revolutionized but has created serious risks about memory security. This paper investigates the present strength of the Stack based exploit mitigations in the Windows operating system specifically focusing on memory security. Through several attacks at the stack region of memory along with comprehensive analysis, this study uncovers the potential risks and consequences of the weak stack-based memory mitigations present. The objective is to raise awareness about these stack-based memory attacks and possible implications urging a need for a robust security testing framework which particularly tests the present security of Windows stack based exploit mitigations while providing with a comprehensive security report. Certain improvements and advanced security mechanisms are crucial to guard the memory pages. As memory is becoming more advanced and complex part of the computer systems, addressing these challenges is paramount to ensuring user privacy, data integrity and overall security of the Windows memory.

1. INTRODUCTION

Memory errors and their exploitation have remained an issue for the tech enthusiasts for a long time. Despite many years of research, the bugs continue to prevail which place a question mark on the system security. Stack is a common target region for hackers, crackers and even for backdoor creators. Many bugs exist which are actively exploited. The individuals driven by malicious intents and curiosity have found ways to bypass the present stack mitigations. The question arises whether the stack-based memory exploits are still a threat to the user's privacy and data integrity. This pushes to get into the wonders of this highly neglected domain. [7]

The significance of using Address Space layout randomization in operating systems for protection against Return Oriented Programming (ROP) attacks is highly regarded. The challenge of less memory space in IOT devices is taken care of where implementing function-based address space layout randomization is an appropriate choice. [12]

Memory corruption bugs are critical for the software industry, and they provide the pathway for cybercrime. Even though the effort to detect and prevent this sort of issue is continued, absolute elimination is impossible as of yet. For example, there is Microsoft Enhanced Mitigation Experience Toolkit (EMET) that offers run-time mitigations against vulnerable statically linked binary applications. Conversely, criminals have developed ways to bypass EMET. [13]

The memory war rages on as offensive researchers develop new attacks, while defensive researchers create protections. According to the MITRE ranking, memory corruption bugs rank among the top three most dangerous software errors. Even Google Chrome, a secure web browser written in C++, fell victim to exploits during hacking contests. Over the past 30 years, various defenses have emerged, including stack cookies, exception handler validation, Data Execution Prevention, and Address Space Layout Randomization. However, attack vectors persist. The battle continues to secure our systems against memory-based threats. [15]

https://doi.org/10.62500/icrtsda.1.1.35

In recent years, the buffer overflow bugs have been one of the major reason for half of the cyber advisories registered with the CERT. The overflow of buffer can be caused when function prototypes have been specified in a wrong way or when functions are implemented incorrectly. In case of both the types of data, there is the situation of more data being written in the buffer, as a result which buffer's end is overwritten thus resulting in the problem of buffer overflow. The overflow refers to the surplus code that is written towards the top of any process location. It then gets control of that process instruction and runs the injected code immediately. The addresses are modified in almost every case which is made possible by the program that utilizes the return address on the stack and by the overwriting of function pointers in memory space of the process. [2]

This research focuses on the memory security aspects of the highly working computer systems. Establishing a virtual environment, Potential threats were explored and identified by creating an environment where attackers could bypass the present stack-based exploit mitigations, leak memory addresses in particular, control execution flow while instructing the instruction pointer at a choice of own location leading towards code execution. The exploit examples include return pointer overflows, Structured Exception Handling (SEH) exploits and Denial of Service (DOS) Exploits. The virtual environment consisted of a windows 11 operating system, different applications with variable versions and an attacker's machine. Custom Python based framework having the capability to assess the state of present stack mitigations and run exploits against different applications including the executable debugging and attacks were conducted to simulate real-world scenarios and analyze the current Windows stack memory mitigations after assessing them effectively. The study starts with scanning the present vulnerable applications on a windows 11 operating system while employing exploitation techniques like stack overflows, structured exception handling (SEH) exploits in the stack region level corruption to assess the security of present stack-based memory mitigations. After successful exploitation, it led to the research idea of having a more secure and stronger mitigation. This approach is directed towards the analysis of the cause leading to failure of present stack-based exploit mitigations.

Research Contributions

- Examine potential security weaknesses in the present stack-based exploit mitigations, with a particular focus on assessing the cause of failure. Attack Simulation was performed to identify weaknesses in the security architecture of the Windows exploit mitigations.
- Identify potential risks that jeopardize user privacy and data integrity.
- Raise awareness of how vulnerable systems are to memory-based attacks.
- Invaluable Insights that will assist in the development of strong and reliable security mitigations along with future research.

Organization of the Chapter

The paper is organized as: section II provides a literature review. Section III provides a details overview of system configurations, deployment architecture, exploitation bugs, and framework used for simulating attacks. Section IV offers in-depth insights into the results obtained and simulations conducted for various attacks. Section V is conclusion and future directions.

2. RELATED WORK: REVIEW OF THE LITERATURE

In 2020, The authors devised a scheme to not only a detection procedure but also a manipulation method which would handle fraudulent traffic. Unlike the preceding methods which got into the module process and work with ones that are already compiled executables, this method was transparent and had the ability to work per-process even when applied to the whole system. A mirror functional version becomes the one who executes the original task, though in a way all the overflow-over-the-bound happens within the allocated memory (stack frame). Second of such techniques assumes manipulation

https://doi.org/10.62500/icrtsda.1.1.35

of the process's memory stack through binary substitution of key stack elements prior to further execution. These library libraries had performance overhead in the ownership range from zero to 15 percent. [2]

In 2021, the authors described how ASLR can be used as a helping vector for successful memory exploitation. Four BadASLR categories were proposed by them: (i) helping heap spraying attack with free chunk reclamation; (ii) helping frame-pointer null poisoning attack with stack pivoting; (iii) bringing back the exploitability of invalid pointer referencing bug; and (iv) introducing wild-card ROP gadgets in x86/x64 position independent code environment. The authors also described real world bug bounty cases. [8]

In 2021, The authors provided a significance of Memory corruption vulnerabilities and their importance. The authors used information of static global variables derived through analysis of executable binary files and dynamic memory usage information obtained by tracking memory related functions called during real time execution of the process. The authors proposed a method that detects memory defects in which the location causing the defect is different from the actual location. [14]

In 2022, the authors developed an innovative mechanism known as Window Canaries (WC), which is utilized as an alternative of the Stack Canaries for architectures that have a register window, which is a special area that protects return addresses and stack pointers, without requiring additional instruction to be added to each function with the potential of exploiting the unintended code. This served a technical implementation proposing the meaning of the approach for a Tensalite LX processor with the register window option as well as its performance assessment and discussion of its benefits and drawbacks. [9]

In 2022, The authors described Stack based buffer overflows in detail and the mitigation techniques which mitigate the exploits in parallel to describing techniques used by hackers to bypass these mitigations to fully take control over the target system. They discussed about exploit mitigations and described how ASLR has led to randomizing the base addresses while attackers have found a way around to this mitigation via ROP and known half part of the address. [4]

In 2022, The authors offered a technique for enhancing symbolic execution efficiency and identifying four categories of memory vulnerabilities: use after free, heap-based buffer overflows, stack-based buffer overflows, and double after free. They assessed the approach using benchmark programs as well. The four stages of the suggested method were testing unit extraction, test unit processing, learning, simulation, and test data generation. [1]

In 2022, The authors described the significance of using Address Space layout randomization in operating systems for protection against rop attacks. They addressed the challenge of less memory space in IOT devices where they implemented function-based address space layout randomization. They also applied optimizations to tackle overhead created by memory management. [12]

In 2023, The authors explained how the AVX instruction set is used by contemporary x86 processors to increase performance; nevertheless, this raises security issues when masked load/store instructions are implemented with vulnerable features. A Stronger re-randomization technique such as randomizing every memory address is required to successfully mitigate the presented attack. [5]

In 2023, The authors provided significance of Operating systems and analysis of their vulnerabilities. They focused on enhancing the understanding trends, severity and common weaknesses of the Operating Systems. Two refined datasets were used by the authors. OS versions were one, while OS categories were the other. [3]

In 2023, The authors described a pointer that isn't shielded by stack canaries or stack guard, which exposes the esp32 microcontroller. They describe the exploitation of vulnerability and mitigations. The authors used development boards for evaluation instead of simulations. [10]

In 2023, The authors described that page-by-page permissions can be controlled to make the code unreadable and focused on dependency issue where a special user can be denied access where code is

https://doi.org/10.62500/icrtsda.1.1.35

unreadable. An Anti-read, which stores code pages in a designated memory pool and effectively manages their rights in accordance with requirements was also suggested. Whenever a malicious user tries to read the code, he/she gets randomized code. [11]

In 2023, The authors mainly emphasized on control flow hijacking vulnerabilities and exploits while proposing an automatic way of generating binary exploits based on crash inputs termed as CAEG Crash based automatic Exploit generation. The model addresses two challenges of regenerating crash state and producing control flow hijacking exploits automatically. [6]

3. METHODOLOGY

To achieve our project objectives, a well-planned methodology was carefully developed. Firstly, an effective environment was established where we followed standard procedures commonly employed by both malicious actors and ethical hackers. The initial phased involved gathering different memory based exploits related to the stack..This process enlightened the focus on the very commonly targeted region of memory and involved obtaining of open source exploits from exploit database and National vulnerability database (NVD). These platforms also identified the present vulnerabilities in different applications. After this phase, comes the target operating system which was windows 11. This target was selected as the operating system consists of Windows Defender Exploit Guard (WDEG) which was released just after the Enhanced mitigations experience toolkit (EMET) including Data Execution Prevention (DEP), Address Space Layout Randomization (ASLR), Control Flow Guard (CFG), Structured Exception Handling Overwrite Protection. This operating system ensured that if bypassed, the mitigations need improvements for sure. After selecting the target OS, the next phase was to set target applications. These applications were vulnerable and were properly set up in the Windows 10 Operating system. The details of the vulnerable applications with versions are provided in the forthcoming section III C" Vulnerable Applications".

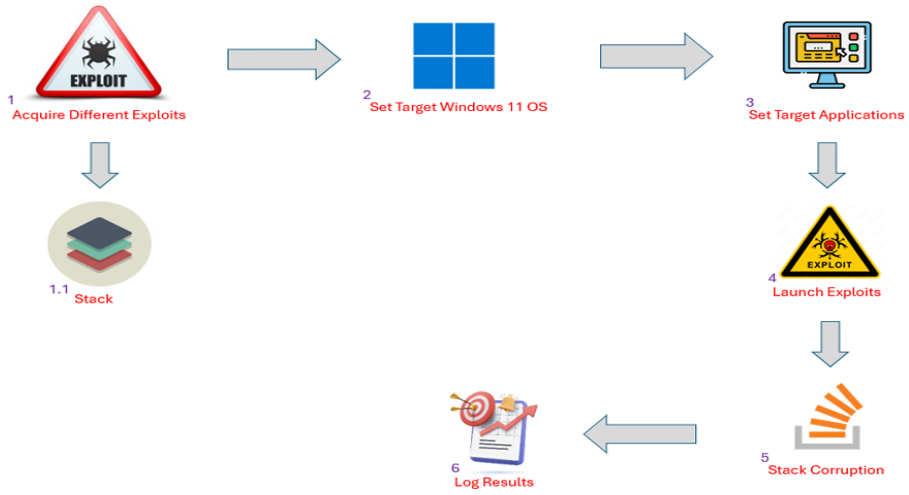

Figure 5: A Methodological Diagram to assess Stack based Exploit Mitigations

The next phase is to launch different memory-based exploits against different selected vulnerable applications. This phase leads to stack corruption further leading towards the arbitrary code execution. The launching of exploits is done through a python-based framework which automates the process of launching different exploits on target operating system against the target vulnerable applications. The details of framework are provided in the forthcoming section III D" Custom

https://doi.org/10.62500/icrtsda.1.1.35

Framework". The results are eventually properly logged to assess the present security of the Stack based exploit mitigations.

A. System Configuration and Network Topology

The attacker machine used for the study is a Kali Linux instance hosted on a Windows 10 operating system as the host, running through VMware Workstation 16. The target machine used is a Windows 11 operating system instance hosted on the same windows 10 operating system as the host, running through VMware workstation 16. The build number of target OS used is 22000 while having the kernel version 10. Both machines are configured to be on the same network. The virtual network adapter utilized was configured for Network Address Translation (NAT) which enabled seamless communication between the two virtual machines and the external network. Despite sharing hardware resources, both virtual machines have distinct MAC and IP addresses. The network configuration encompasses an IP address range of 192.168.0.0. There is a dedicated network interface card (NIC) used specifically TP-Link N300 Wireless Nano USB Adapter (TL-WN823N). The IP addresses are assigned as 192.168.0.105 to the attacker machine and the target device is assigned the IP address of 192.168.0.102 with 192.168.0.1 serving as the gateway IP address linked to the TP-Link Archer A7 AC1750 Smart Router.

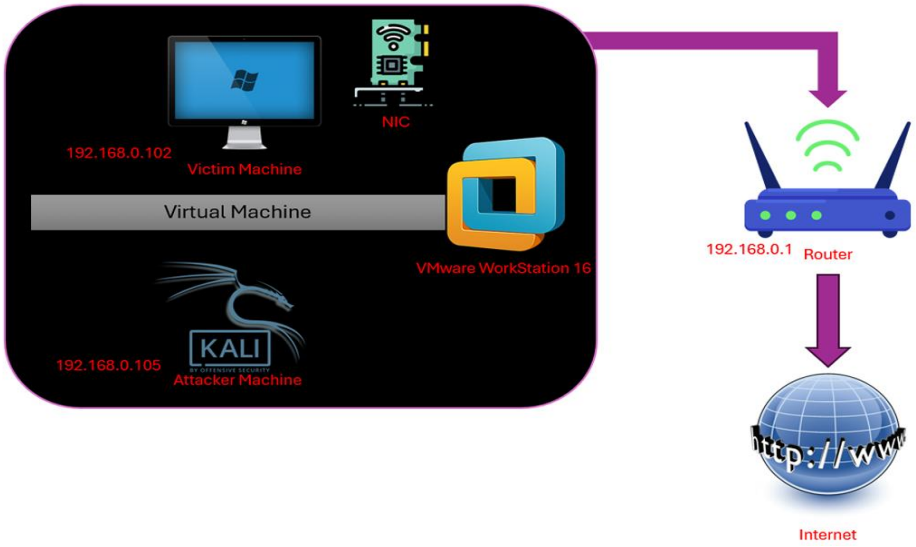

Figure 6: Overview of Network Setup

Figure 2 provides an overview of a comprehensive network setup implemented in our simulation.

B. Memory Exploits

The memory-based exploits collected are of one target type of Stack based exploits. The stack exploits consist of 5 return pointer overflows, 3 Structured Exception Handling (SEH) Overflows and 2 Denial of Service (DOS) based Exploits.

https://doi.org/10.62500/icrtsda.1.1.35

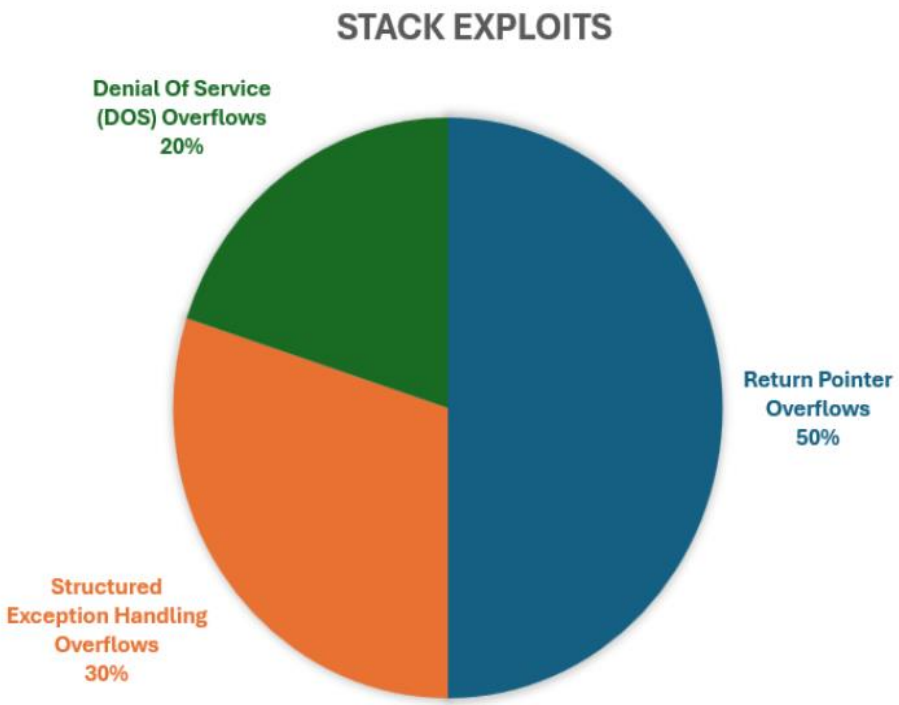

Figure 7: Overview of Stack Exploits

An overview of Stack based exploits is provided in Figure 3 which represents 50 percent of the return pointer overflow bugs, 30 percent of the Structured Exception Handling overflow bugs and 20 percent of the Denial of Service (DOS) overflow bugs.

C. Applications and Versions

Different applications were taken against which the exploits were to be launched. These applications were properly installed and deployed on Windows 11 target machine.

https://doi.org/10.62500/icrtsda.1.1.35

TABLE I
APPLICATIONS FOR STACK BASED MEMORY EXPLOITS

Applications	Versions
FreeFloat FTP Server	1
DVD X player	5.5
Kolibri Server	2
Allok Video Converter	4.6
Easy File Sharing Web Server	7.2
AVS Audio Converter	10.3
Triologic Media Player	8
Easy File Sharing Web Server 2	7.2
Xlight FTP Server	3.9
FTP Navigator	8.03

Table I represents different stacks applications which are taken for exploitation. These applications are vulnerable and lead to unexpected behavior while causing a high severity risk.

D. Custom Framework

A custom framework was built in python by using the python Integrated Development and Learning Environment (IDLE). This framework automated the task of launching exploits one by one on the Windows 11 target virtual machine against different vulnerable applications which eventually lead to memory corruption. Specifically, python libraries such as kernel32 and virtual alloc were used to interact with certain processes in order to effectively perform the exploitation and represent the possible outcomes. Python based Framework efficiently accessed different exploits from different folders named as stack exploits which represented different vulnerabilities.

E. Deployment and Simulation

Before initiating the testing phases, the instances were properly deployed. The simulated environment contains a comprehensive deployment of instances where a Windows operating system is used as the target operating system carrying vulnerable applications. Before initiating the simulated test, it was very important to identify the present state of the exploit mitigations which was confirmed via the Windows Defender Exploit Guard. The exploits were made ready via the custom Framework and the shell-codes were also kept as per requirement. The simulation consisted of netcat used as a listener and msfvenom to generate shellcodes. The simulated environment was made all ready with virtualization technology. Within the simulated environment, it was very important to target the stack region of the memory as there are different exploits for different memory regions.

The Figure 4 represents the deployment model which represents the simulated environment that has Windows 11 target machine, kali-linux attacker machine and the Exploits gathering, organizing and launching of exploits while providing comprehensive details of received results.

https://doi.org/10.62500/icrtsda.1.1.35

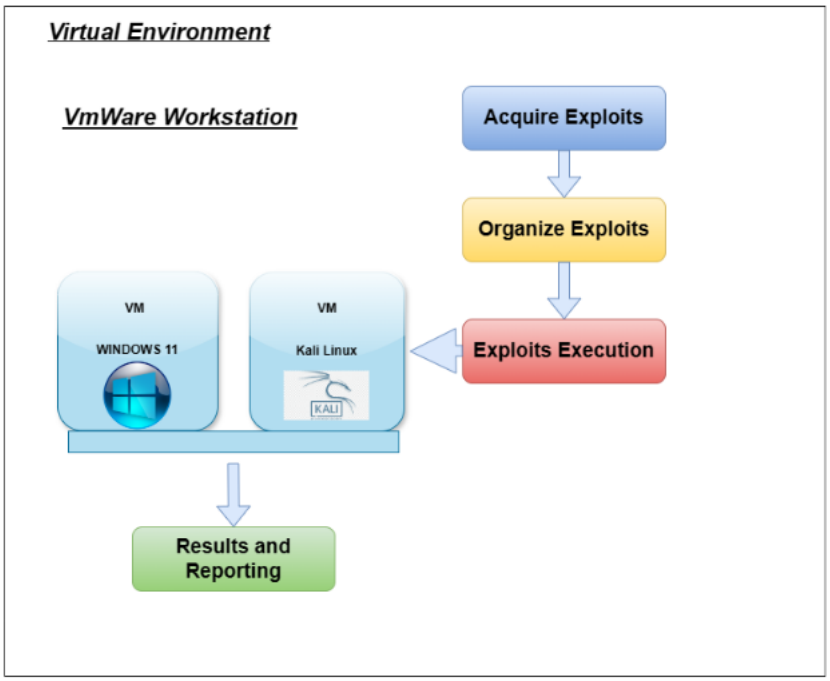

Figure 8: Overview of Deployment for Simulated Environment

4. RESULTS

This section covers a wide range of Stack based memory exploits launched against different vulnerable applications that corrupted Stack based memory region particularly causing unexpected behavior. The Memory based Stack region was corrupted with 5 exploits having return pointer overflow bug, 3 exploits having Structured Exception Handling bug and 2 exploits having Denial of service overflows. The payload used is of a reverse shell which was generated via msfvenom. The shellcode is generated while taking out the bad characters to make the exploit execution smoother. Netcat is used for receiving the reverse connection upon successful execution of the exploit. Instead of a reverse shell, popping a calculator or notepad is also an option. Just the shellcode needs to be replaced. Reverse Shell shellcode is used in order to simulate the exact adversarial environment. The exploit results were properly logged after launching the exploits one by one. The consequence included return pointer overflow stack exploitation first, then Structured Exception Handling (SEH) overflows and lastly, the Denial of Service (DOS) based exploits.

Figure 5 displays where the tested exploits are shown which include successful exploits, failed exploits and unexpected behavior exploits. 5 return pointer overflow exploits, 3 Structured Exception Handling (SEH) exploits and 2 Denial of service (DOS) based exploits of the stack memory region were tested. All of the exploits were successful against the vulnerable applications on the Windows 11 operating system having Windows defender exploit guard activated. There was no failure of exploits. This shows that the present exploit mitigations are not up to the mark and need serious consideration. The successful exploits are described below:

https://doi.org/10.62500/icrtsda.1.1.35

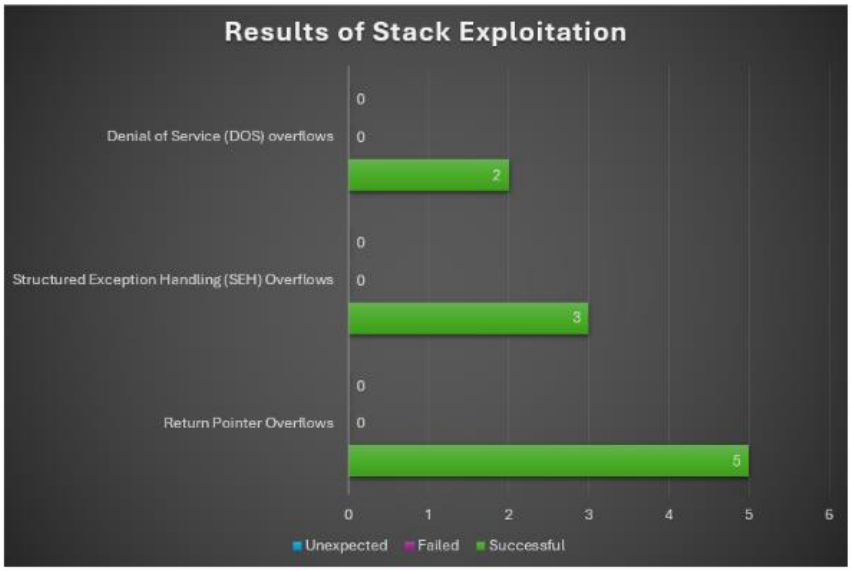

Figure 9: Results of Stack Exploits Launched Against Applications

- 5 Return Pointer Overflow stack Exploits based on return pointer overflows which were of Free float ftp server, DVD X player, kolibri HTTP Server, Allok video converter and easy file sharing web server were successful by overwriting the instruction pointer and leading to code execution. DVD X Player and Allok video converter were local exploits where the input file was used as assisting in the triggering of the vulnerability whereas all of the other exploits were remote exploits which lead to exploitation of the target system remotely. The control flow was very easily hijacked which lead to replacement of the instruction pointer with the intents of the ethical hacker via an adversarial perspective which lead to a reverse shell of the device. The payload used was of a reverse shell generated by msfvenom.
- 3 Structured Exception Handling (SEH) Overflow stack Exploits based on Structured Exception Handling (SEH) Overflows were successful because the corrupted SEH Chain was overwritten properly on the choice of the hacker leading to code execution. The SEH overflow exploits were of triologic Media player, AVS Audio Converter and Easy File sharing web server. All of these applications were vulnerable to SEH corruption. The instruction pointer was hijacked by exploitation of the SEH chain leading to code execution. The Easy File sharing web server had a remote exploit whereas the two of the others had a local exploit requiring a file to perform the exploitation. The payload used was of a reverse shell which gave direct access to the system.
- 2 Denial of Service (DOS) based stack Exploits were successful. Both were remote DOS exploits which led to the crashing of the application. The crash occurred because the buffer was overflowed, and the stack pointers moved to unknown locations. However, the instruction pointer was not compromised to hijack the execution flow. This led to a new observation that the DOS vulnerabilities in different applications need different approaches for security. The exploits were of Xlight FTP Server and FTP navigator.

The results were properly logged for further analysis of the cause leading to present exploit mitigations failure. The success of exploits shows that the present stack-based exploit mitigations are not up to the mark leading to serious security concerns.

https://doi.org/10.62500/icrtsda.1.1.35

TABLE II
STATE OF EXPLOITATION

Applications	Exploit Results
FreeFloat FTP Server	Success
DVD X player	Success
Kolibri Server	Success
Allok Video Converter	Success
Easy File Sharing Web Server	Success
AVS Audio Converter	Success
Triologic Media Player	Success
Easy File Sharing Web Server 2	Success
Xlight FTP Server	Success
FTP Navigator	Success

The table II represents the results of various stack-based memory exploits launched against different target applications. The results are properly evaluated which represent that the various stack-based memory exploits were successful creating an alarming situation while raising awareness regarding it's seriousness. The successful of these exploits serves as an eye-opening call for the researchers and developers worldwide. This also includes the fact about the Denial-of-service exploits which are not technically catered by protecting applications from getting exploited at the binary level.

5. COMMENTS AND CONCLUSION

The research highlights the potential Windows Stack based memory security risks and threats including the user's privacy concerns as well as the data integrity. The study highlights the present need to work further on the present exploit mitigations in Windows operating system to counter the latest threats.

Memory was the target of a wide range of memory-based attacks which corrupted the stack region leading to code execution. In particular, it led to the whole system compromise. The memory-based attacks were thoroughly examined. By employing a custom framework, many stack based memory exploits were collected, attacks were launched at the memory of Windows 11 Operating system causing potential harm and device compromise just like a real adversarial environment.

The research emphasizes the need for strong security measures for the memory security and exploit mitigations. As the innovation in technology increases, the threats and risks also rise. This study raises awareness of the fact that systems can be compromised where a user has a vulnerable application in his or her system by an attacker with the correct tools and required skills. Since the pointers are always disclosed and the present mitigations are not up to the mark, there exists a need to create and deploy a more secure as well as stronger memory-based exploit mitigation. Also, the Denial of service based. Memory exploits cannot be countered via working normally on the binary level.

Further research is crucial in this regard.

REFERENCES

1. Sara Baradaran, Mahdi Heidari, Ali Kamali, and Maryam Mouzarani. A Unit-Based Symbolic Execution Method for Detecting Memory Corruption Vulnerabilities in Executable Codes. International Journal of Information Security, 22(5):1277–1290, 2023.

2. Arash Baratloo, Michael Karaul, and Zvi M. Kedem. Transparent and flexible network security with ipchains. In Proceedings of the 2000 USENIX Annual Technical Conference, June 2000.

https://doi.org/10.62500/icrtsda.1.1.35

3. Manish Bhurtel and Danda B Rawat. Unveiling the Landscape of Operating System Vulnerabilities. Future Internet, 15(7):248, 2023.

4. Muhammad Arif Butt, Zarafshan Ajmal, Zafar Iqbal Khan, Muhammad Idrees, and Yasir Javed. An In-depth Survey of Bypassing Buffer Overflow Mitigation Techniques. Applied Sciences, 12(13):6702, 2022.

5. Hyunwoo Choi, Suryeon Kim, and Seungwon Shin. AVX Timing SideChannel Attacks Against Address Space Layout Randomization. In 2023 60th ACM/IEEE Design Automation Conference (DAC), pages 1–6. IEEE, 2023.

6. Zhenwei Ge, Chao Zhang, Zhongyuan Qin, Xin Sun, and Wen Wang. CAEG: Crash-based Automatic Exploit Generation. In International Conference on Cyber Security, Artificial Intelligence, and Digital Economy (CSAIDE 2023), volume 12718, pages 51–57. SPIE, 2023.

7. Ralf Hund, Carsten Willems, and Thorsten Holz. Practical Timing Side Channel Attacks Against Kernel Space ASLR. In 2013 IEEE Symposium on Security and Privacy, pages 191–205. IEEE, 2013.

8. Daehee Jang. Badaslr: Exceptional Cases of ASLR Aiding Exploitation. Computers & Security, 112:102510, 2022.

9. Peter Kai. Window canaries: Re-thinking stack canaries for architectures with register windows. IEEE Xplore, Volume Number, 2022.

10. Kai Lehniger and Peter Langendorfer. Through the Window: Exploita- ¨ tion and Countermeasures of the ESP32 Register Window Overflow. Future Internet, 15(6):217, 2023.

11. YongGang Li, JiaZhen Cai, Yu Bao, and Yeh-Ching Chung. What You Can Read is What You Can't Execute. Computers & Security, 132:103377, 2023.

12. Lan Luo, Xinhui Shao, Zhen Ling, Huaiyu Yan, Yumeng Wei, and Xinwen Fu. FASLR: Function-based ASLR via TrustZone-M and MPU for Resource-Constrained IoT Systems. IEEE Internet of Things Journal, 9(18):17120–17135, 2022.

13. Zoltan L. N ´ emeth. Modern binary attacks and defences in the windows ´ environment—fighting against microsoft emet in seven rounds. In 2015 IEEE 13th International Symposium on Intelligent Systems and Informatics (SISY), pages 275–280. IEEE, 2015.

14. Jihyun Park, Byoungju Choi, and Yeonhee Kim. Automated Memory Corruption Detection Through Analysis of Static Variables and Dynamic Memory Usage. Electronics, 10(17):2127, 2021.
15. Laszlo Szekeres, Mathias Payer, Tao Wei, and Dawn Song. Sok: Eternal War in Memory. In 2013 IEEE Symposium on Security and Privacy, pages 48–62. IEEE, 2013.

https://doi.org/10.62500/icrtsda.1.1.36

Proc. 1st International Conference on Recent Trends in Statistics and Data Analytics
Air University Islamabad, Pakistan – May 9, 2024, Vol. 1, pp. 341-356

ALGEBRAIC ASPACTS OF ξ- PYTHAGOREAN FUZZY SUBGROUP

Areej Fatima, Naveed Hussain*, Muhammad Usman, Mobeen Aslam, and Nadia Ramzan

Department of Mathematics and Statistics, University of Agriculture Faisalabad, Pakistan

ABSTRACT

The notion of a Pythagorean fuzzy set over a certain linear operator ξ- Pythagorean fuzzy set (ξ-PFS) is proposed and various set theoretical properties of notion are explored. The union and intersection of any two ξ- Pythagorean fuzzy sets (ξ- PFS's) is proved to be ξ- Pythagorean fuzzy set (ξ- PFS). The above idea is applied to explain the concept of ξ-Pythagorean fuzzy subgroup (PFSG) in addition to every Pythagorean fuzzy subgroup (PFSG) is ξ- Pythagorean fuzzy subgroup (ξ- PFSG) is established. A certain condition is established under which a given ξ- Pythagorean fuzzy set (PFS) is ξ- Pythagorean fuzzy subgroup (PFSG). Moreover, it is established that the intersection of any two ξ- Pythagorean fuzzy subgroups (ξ-PFSG's) is to be proved ξ- Pythagorean fuzzy subgroup (ξ-PFSG). In addition, thoughts of ξ- Pythagorean fuzzy cossets, ξ- Pythagorean fuzzy normal subgroups (PFNSG) are defined and proved every Pythagorean fuzzy normal subgroup is ξ- Pythagorean fuzzy normal subgroup (PFNSG). Besides, the conception of ξ- Pythagorean fuzzy homomorphism between any two ξ- Pythagorean fuzzy subgroups (ξ- PFSG's) is presented and the effect of defined homomorphism is investigated in the framework of its image and preimage.

Keywords. Fuzzy set; Fuzzy coset; Pythagorean fuzzy set; fuzzy subgroup; fuzzy homomorphism.

1. INTRODUCTION

In a crisp set, a component is either an individual from the set or not, idea of partial membership does not exist. In such sets, a member is either entirely present within the set or entirely absent from it. Using a crisp set, you can model or depict a variety of real-world objects, including set of students, set of pens, set of workers and set of copies. The term Crisp indicates dichotomous that is, yes or no kind rather than more or less category. In straight twofold logic, for instance a sentence can either be true or untrue, with no between ground. In set theory, either an element is a member of a set or it is not: in optimization, a solution can only be either practical or not. Crisp sets and fuzzy sets are components of different set theories; crisp sets use bi-valued logic whereas fuzzy sets deal with infinite valued logics [14].

In real world situations, we might run over the circumstances where we are unable to conclude whether the claim is valid or bogus. The term fuzzy mean things which are not quite clear. Real-world circumstances are frequently ambiguous or uncertain in a variety of ways. Due to lack of shortage, it's possible that the system's future state won't be fully known. The mentioned type of vagueness has long been handled correctly by probability theory and statistics. Fuzziness is prevalent in many aspects of daily life, containing in manufacturing, medicine manufacturing besides others. However, it is especially prevalent in all domains where human judgement, assessment, and decision-making is crucial. These are ranges of decision making, logics, learning and so forth [13].

A valuable tool for describing situations when data is ambiguous or imprecise is fuzzy set theory. Such cases are handled with fuzzy sets, which assign an object's degree of set membership. Numerous physical problems have been successfully solved thanks to fuzzy logic's ability to explain steady adaptations from membership to non-membership and the other way around. Fuzzy logic gives thinking that is incredibly flexible. The aforementioned specific theory addresses ambiguous concepts by using phonetic elements rather than quantitative factors. It has played a key role in many fields like, software engineering, activity research, auto transmission, man-made reasoning and control designing.

https://doi.org/10.62500/icrtsda.1.1.36

Inaccuracy is a crucial component of every decision-making procedure. Different tools and strategies have been developed to deal with the unreliable domain of collective decision-making [27].

Pythagorean fuzzy domain is the modern method for manipulating unreliability in numerous decision-making problems. The fuzzy sets serve as a starting point for research into the career placements issue since they generalise both fuzzy and intuitionistic fuzzy sets with a wide variety of presentations. Pythagorean fuzzy set provides new techniques to deal with fuzziness as well as vagueness with high accuracy also exactness equated to intuitionistic fuzzy set. The concepts of group theory are applied in many fields of social and natural sciences. A vital aspect of analysing molecular structures is group symmetry. The concept of Pythagorean fuzzy subgroup helps us to counter the decay rate of Isotope molecules [15].

The following results would be addressed in this paper:

Theorem 1.1. Union and intersection of any two ξ – Pythagorean fuzzy sets (ξ – PFS's) is ξ – pythagorean fuzzy set (ξ – PFS).

Theorem 1.2. The following conditions are satisfied in each β^{ξ} – Pythagorean fuzzy subgroup (ξ – PFSG). For $e \in G$ (identity of G)

i. $\varphi^2\beta^{\xi}(e) \geq \varphi^2\beta^{\xi}(p)$
ii. $\psi^2\beta^{\xi}(e) \leq \psi^2\beta^{\xi}(p), \forall\, p \in G.$
iii. $\beta^{\xi}(pq^{-1}) = \beta^{\xi}(e) \Rightarrow \beta^{\xi}(p) = \beta^{\xi}(q), \forall\, p, q \in G.$

Theorem 1.3. Every Pythagorean fuzzy subgroup of a group G is ξ – pythagorean fuzzy subgroup. Moreover, intersection of two ξ – pythagorean fuzzy subgroups of a group G is also ξ – pythagorean fuzzy subgroup of G.

Theorem 1.4. Let β be a Pythagorean fuzzy set of a group G which satisfies the conditions

$$\varphi^2\beta(p^{-1}) = \varphi^2\beta(p) \; and \; \psi^2\beta(p^{-1}) = \psi^2\beta(p) \; for \; any \; p \in G.$$

Moreover, $\xi < min\{x, 1-y\}$,

$$x = min\{\varphi^2\beta(p) : \forall\, p \in G\} \quad \text{and} \quad y = max\{\psi^2\beta(p) : \forall\, p \in G\}$$

Then β is ξ – pythagorean fuzzy subgroup of G.

Theorem 1.5. If β is pythagorean fuzzy normal subgroup (PFNSG) of a group G then β is also ξ – PFNSG of G. Furthermore, every ξ – pythagorean fuzzy normal subgroup β^{ξ} of G admits the following properties

$$\varphi^2\beta^{\xi}(pq) = \varphi^2\beta^{\xi}(qp)$$

and

$$\psi^2\beta^{\xi}(pq) = \psi^2\beta^{\xi}(qp)$$

Theorem 1.6. Let β^{ξ} be a ξ – PFNSG β^{ξ} of a group G such that $\xi < min\{x, 1-y\}$,

$x = \upsilon\{\varphi^2\beta(p): \forall p \in X\}$ and $y = \sigma\{\psi^2\beta(p): \forall p \in X\}$

Then β^{ξ} be a ξ – PFNSG of G.

Theorem 1.7. Let G/β^{ξ} the set of all distinct ξ – Pythagorean fuzzy right cossets of ξ – PFNSG β^{ξ} of G.

$$G/\beta^{\xi} = \{\beta^{\xi}p : p \in G\}$$

The binary operation ∇ defined on the set G/β^{ξ} as follows, is a well-defined operation.

$$\beta^{\xi}p \nabla \beta^{\xi}q = \beta^{\xi}pq, \quad \forall\, p, q \in G$$

https://doi.org/10.62500/icrtsda.1.1.36

Furthermore, the set G/β^{ξ} forms a group under the operation ∇.

Theorem 1.8. Let β^{ξ} be ξ – PFSG of a group G and f be a surjective homomorphism from group G to G′ then $f(\beta^{\xi})$ is ξ – PFSG of a group G′. Moreover, if β^{ξ} be ξ – PFNSG of a group G then $f(\beta^{\xi})$ is ξ – PFNSG of a group G′.

Theorem 1.9. Let β^{ξ} be ξ – PFSG of a group G′ and f be a bijective homomorphism from group G to G′ then $f^{-1}(\beta^{\xi})$ is ξ – PFSG of a group G. Moreover, if β^{ξ} be ξ – PFNSG of a group G′ then $f^{-1}(\beta^{\xi})$ is ξ – PFNSG of a group G.

2. BASIC CONCEPTS

Definition 2.1. [25] A fuzzy set (FS) η is a set whose elements have degree of membership.

Definition 2.2. [20] A fuzzy set η of a group G is called a fuzzy subgroup if η admits:

(i) $\eta(p_1p_2) \geq \eta(p_1) \wedge \eta(p_2)$
(ii) $\eta(p_1^{-1}) \geq \eta(p_1), \forall\, p_1, p_2 \in G.$

Definition 2.3. [24] An object $\beta = \{(p, \varphi(p), \psi(p))\}$of a universe X represented as pythagorean fuzzy set (PFS), where $0 \leq \varphi(p) \leq 1$ be the degree of membership, $0 \leq \psi(p) \leq 1$ is the degree of non-membership of $p \in X$, which hold the axiom

$0 \leq \varphi^2(p) + \psi^2(p) \leq 1.$

Definition 2.4. The cut set of a Pythagorean fuzzy set β of X is designated by $\beta(\rho, \delta)$ and is interpreted in this way:

$$\beta(\rho,\delta) = \{p \in X | \varphi^2\beta(p) \geq \rho, \psi^2\beta(p) \leq \delta, 0 \leq \rho^2 + \delta^2 \leq 1, 0 \leq \rho \leq 1, 0 \leq \delta \leq 1\}.$$

Definition 2.5. A Pythagorean fuzzy set β of a group G is designated as a Pythagorean fuzzy subgroup (PFSG) of G if β fulfils the following requirements:

(i) $\varphi^2\beta(p_1p_2) \geq \varphi^2\beta(p_1) \wedge \varphi^2\beta(p_2)\ and\ \psi^2\beta(p_1p_2) \leq \psi^2\beta(p_1) \vee \psi^2\beta(p_2), \forall\, p_1, p_2 \in G$
(ii) $\varphi^2\beta(p_1^{-1}) \geq \varphi^2\beta(p_1)\ and\ \psi^2\beta(p_1^{-1}) \leq \psi^2\beta(p_1), \forall\, p_1 \in G.$

Definition 2.6. For any Pythagorean fuzzy subgroup β and a fixed element $p_1 \in G$. The pythagorean fuzzy left coset of β in G is denoted by $p_1\beta$ and is described as follows:

$$(p_1\varphi\beta)^2(p) = \varphi^2\beta(p_1^{-1}p)\ ,\ (p_1\psi\beta)^2(p) = \psi^2\beta(p_1^{-1}p), \forall\, p \in G.$$

Definition 2.7. [21] Let β be a Pythagorean fuzzy subgroup of a group G. Formerly β is a Pythagorean fuzzy normal subgroup (PFNSG) of the group G if and only if each Pythagorean fuzzy left cosset of G contains a corresponding Pythagorean fuzzy right cosset. Equivalently,

$$p_1\beta = \beta p_1, \forall p_1 \in G.$$

3. PROOF OF THEOREMS

The propositions will ultimately be used to support the key results of this study.

Proposition 3.1. Intersection of any two ξ – pythagorean fuzzy sets (ξ – PFS's) is ξ – pythagorean fuzzy set (ξ – PFS).

Proof. For any two ξ – pythagorean fuzzy sets ${\beta_1}^{\xi}$ and ${\beta_2}^{\xi}$ of a universe X, we have

$$\varphi^2{}_{(\beta_1 \cap \beta_2)^{\xi}}(p) = \upsilon(\varphi^2{}_{(\beta_1 \cap \beta_2)}(p), \xi)$$

$$= \upsilon\{min(\varphi^2{}_{\beta_1}(p), \varphi^2{}_{\beta_2}(p)), \xi)$$

$$= min\{\upsilon(\varphi^2{}_{\beta_1}(p), \xi), \upsilon(\varphi^2{}_{\beta_2}(p), \xi)\}$$

https://doi.org/10.62500/icrtsda.1.1.36

$$= min\,(\varphi^2{}_{\beta_1{}^{\xi}}(p), \varphi^2{}_{\beta_2{}^{\xi}}(p))$$

$$\varphi^2{}_{(\beta_1 \cap \beta_2)^{\xi}}(p) = \varphi^2{}_{\beta_1{}^{\xi} \cap \beta_2{}^{\xi}}(p), \forall\, p \in X$$

Hence,

$$\varphi^2{}_{(\beta_1 \cap \beta_2)^{\xi}} = \varphi^2{}_{\beta_1{}^{\xi} \cap \beta_2{}^{\xi}}$$

Moreover,

$$\psi^2{}_{(\beta_1 \cap \beta_2)^{\xi}}(p) = \sigma\,(\psi^2{}_{(\beta_1 \cap \beta_2)}, 1 - \xi)$$

$$= min\,(\psi^2{}_{\beta_1{}^{\xi}}(p), \psi^2{}_{\beta_2{}^{\xi}}(p))$$

$$\psi^2{}_{(\beta_1 \cap \beta_2)^{\xi}}(p) = \psi^2\beta_1^{\xi}(p) \cap \psi^2\beta_2^{\xi}(p), \forall\, p \in X$$

Hence,

$$\psi^2{}_{(\beta_1 \cap \beta_2)^{\xi}} = \psi^2{}_{\beta_1{}^{\xi} \cap \beta_2{}^{\xi}}$$

Consider,

$$(\beta_1 \cap \beta_2)^{\xi} = (\varphi^2{}_{(\beta_1 \cap \beta_2)^{\xi}}, \psi^2{}_{(\beta_1 \cap \beta_2)^{\xi}}) = (\varphi^2{}_{\beta_1{}^{\xi} \cap \beta_2{}^{\xi}}, \psi^2{}_{\beta_1{}^{\xi} \cap \beta_2{}^{\xi}})$$

This shows that

$$(\beta_1 \cap \beta_2)^{\xi} = \beta_1^{\xi} \cap \beta_2^{\xi}$$

Proposition 3.2. Union of any two ξ – Pythagorean fuzzy sets (ξ – PFS's) is ξ – PFS.

Proof. For any two ξ – Pythagorean fuzzy sets β_1^{ξ} and β_2^{ξ} of a universe X, we have

$$\varphi^2{}_{(\beta_1 \cup \beta_2)^{\xi}}(p) = \upsilon\,(\varphi^2{}_{(\beta_1 \cup \beta_2)}(p), \xi)$$

$$= \upsilon\{max\,(\varphi^2{}_{\beta_1}(p), \varphi^2{}_{\beta_2}(p)), \xi)$$

$$= max\,\{\upsilon\,(\varphi^2{}_{\beta_1}(p), \xi), \upsilon\,(\varphi^2{}_{\beta_2}(p)), \xi)\}$$

$$= max\,(\varphi^2{}_{\beta_1{}^{\xi}}(p), \varphi^2{}_{\beta_2{}^{\xi}}(p))$$

$$\varphi^2{}_{(\beta_1 \cup \beta_2)^{\xi}}(p) = \varphi^2{}_{\beta_1{}^{\xi} \cup \beta_2{}^{\xi}}(p), \forall\, p \in X$$

Hence,

$$\varphi^2{}_{(\beta_1 \cup \beta_2)^{\xi}} = \varphi^2{}_{\beta_1{}^{\xi} \cup \beta_2{}^{\xi}}$$

Moreover,

$$\psi^2{}_{(\beta_1 \cup \beta_2)^{\xi}}(\mathrm{p}) = \sigma\,(\psi^2{}_{(\beta_1 \cup \beta_2)}, 1 - \xi)$$

$$= \sigma\{max\,(\psi^2{}_{\beta_1}(p), \psi^2{}_{\beta_2}(p)), 1 - \xi)$$

$$= max\,(\psi^2{}_{\beta_1{}^{\xi}}(p), \psi^2{}_{\beta_2{}^{\xi}}(p))$$

$$\psi^2{}_{(\beta_1 \cup \beta_2)^{\xi}}(p) = \psi^2{}_{\beta_1{}^{\xi} \cup \beta_2{}^{\xi}}(p), \forall\, p \in X$$

Hence,

https://doi.org/10.62500/icrtsda.1.1.36

$$\psi^2{}_{(\beta_1 \cup \beta_2)^\xi} = \psi^2{}_{\beta_1{}^\xi \cup \beta_2{}^\xi}$$

Consider,

$$(\beta_1 \cup \beta_2)^\xi = (\varphi^2{}_{(\beta_1 \cup \beta_2)^\xi}, \psi^2{}_{(\beta_1 \cup \beta_2)^\xi}) = (\varphi^2{}_{\beta_1{}^\xi \cup \beta_2{}^\xi}, \psi^2{}_{\beta_1{}^\xi \cup \beta_2{}^\xi})$$

This shows that

$$(\beta_1 \cup \beta_2)^\xi = \beta_1^\xi \cup \beta_2^\xi$$

Proposition 3.3. Every Pythagorean fuzzy subgroup of a group G is ξ – Pythagorean fuzzy subgroup.

Proof. Let $p, q \in G$ be any two elements of a group G and using the fact that β is pythagorean fuzzy subgroup of G, we have

$$\varphi^2{}_{\beta^\xi}(pq) = \upsilon\left(\varphi^2{}_\beta(pq), \xi\right)$$

$$\geq \upsilon\left\{min\left(\varphi^2{}_\beta(p), \varphi^2{}_\beta(q)\right), \xi\right\}$$

$$= min\left\{\varphi^2{}_{\beta^\xi}(p), \varphi^2{}_{\beta^\xi}(q)\right\}$$

Implies that

$$\varphi^2{}_{\beta^\xi}(pq) \geq min\left\{\varphi^2{}_{\beta^\xi}(p), \varphi^2{}_{\beta^\xi}(q)\right\}$$

Moreover,

$$\psi^2{}_{\beta^\xi}(pq) = \sigma\left(\psi^2{}_\beta(pq), 1-\xi\right)$$

$$\leq \sigma\left\{max\left(\psi^2{}_\beta(p), \psi^2{}_\beta(q)\right), 1-\xi\right\}$$

$$= max\left\{\psi^2{}_{\beta^\xi}(p), \psi^2{}_{\beta^\xi}(q)\right\}$$

Implies that

$$\psi^2{}_{\beta^\xi}(pq) \leq max\left\{\psi^2{}_{\beta^\xi}(p), \psi^2{}_{\beta^\xi}(q)\right\}$$

Now

$$\varphi^2{}_{\beta^\xi}(p^{-1}) = \upsilon\left(\varphi^2{}_\beta(p^{-1}), \xi\right)$$

$$= \upsilon\left(\varphi^2{}_\beta(p), \xi\right)$$

$$= \varphi^2{}_{\beta^\xi}(p)$$

Implies that

$$\varphi^2{}_{\beta^\xi}(p^{-1}) = \varphi^2{}_{\beta^\xi}(p)$$

Similarly,

$$\psi^2{}_{\beta^\xi}(p^{-1}) = \sigma\left(\psi^2{}_\beta(p^{-1}), 1-\xi\right)$$

$$= \psi^2{}_{\beta^\xi}(p)$$

Implies that

https://doi.org/10.62500/icrtsda.1.1.36

$$\psi^2{}_{\beta^\xi}(p^{-1}) = \psi^2{}_{\beta^\xi}(p)$$

Hence, β is ξ – Pythagorean fuzzy subgroup of G.

Proposition 3.4. Intersection of two ξ – Pythagorean fuzzy subgroups of a group G is also ξ – pythagorean fuzzy subgroup of G.

Proof. For any two ξ – Pythagorean fuzzy subgroups ${\beta_1}^\xi$ and ${\beta_2}^\xi$ of a group G, we have

$$\varphi^2{}_{(\beta_1 \cap \beta_2)^\xi}(pq) = \upsilon\,(\varphi^2{}_{(\beta_1 \cap \beta_2)}\,(pq), \xi)$$

$$= min\,\left(\varphi^2{}_{{\beta_1}^\xi}\,(pq), \varphi^2{}_{{\beta_2}^\xi}\,(pq)\right)$$

$$\geq min\,\left\{min\,\left(\varphi^2{}_{{\beta_1}^\xi}\,(p), \varphi^2{}_{{\beta_1}^\xi}\,(q)\right), min\,\left(\varphi^2{}_{{\beta_2}^\xi}\,(p), \varphi^2{}_{{\beta_2}^\xi}\,(q)\right)\right\}$$

$$= min\left(\varphi^2{}_{(\beta_1 \cap \beta_2)^\xi}(p), \varphi^2{}_{(\beta_1 \cap \beta_2)^\xi}(q)\right)$$

Thus,

$$\varphi^2{}_{(\beta_1 \cap \beta_2)^\xi}(pq) \geq min\,\left(\varphi^2{}_{(\beta_1 \cap \beta_2)^\xi}(p), \varphi^2{}_{(\beta_1 \cap \beta_2)^\xi}(q)\right) \tag{1}$$

Similarly,

$$\psi^2{}_{(\beta_1 \cap \beta_2)^\xi}(pq) = \sigma(\psi^2{}_{(\beta_1 \cap \beta_2)}\,(pq), 1 - \xi)$$

$$= min\,\left(\psi^2{}_{{\beta_1}^\xi}\,(pq), \psi^2{}_{{\beta_2}^\xi}\,(pq)\right)$$

$$\leq min\,\left\{max\,\left(\psi^2{}_{{\beta_1}^\xi}\,(p), \psi^2{}_{{\beta_1}^\xi}\,(q)\right), max\,\left(\psi^2{}_{{\beta_2}^\xi}\,(p), \psi^2{}_{{\beta_2}^\xi}\,(q)\right)\right\}$$

$$= max\left(\psi^2{}_{(\beta_1 \cap \beta_2)^\xi}(p), \psi^2{}_{(\beta_1 \cap \beta_2)^\xi}(q)\right)$$

Thus,

$$\psi^2{}_{(\beta_1 \cap \beta_2)^\xi}(pq) \leq max\,\left(\psi^2{}_{(\beta_1 \cap \beta_2)^\xi}(p), \psi^2{}_{(\beta_1 \cap \beta_2)^\xi}(q)\right) \tag{2}$$

Moreover,

$$\varphi^2{}_{(\beta_1 \cap \beta_2)^\xi}(p^{-1}) = \upsilon\,(\varphi^2{}_{(\beta_1 \cap \beta_2)}\,(p^{-1}), \xi)$$

$$= min\,\left(\varphi^2{}_{{\beta_1}^\xi}\,(p^{-1}), \varphi^2{}_{{\beta_2}^\xi}\,(p^{-1})\right)$$

$$= \varphi^2{}_{{\beta_1}^\xi \cap {\beta_2}^\xi}(p)$$

$$= \varphi^2{}_{(\beta_1 \cap \beta_2)^\xi}(p)$$

Thus,

$$\varphi^2{}_{(\beta_1 \cap \beta_2)^\xi}(p^{-1}) = \varphi^2{}_{(\beta_1 \cap \beta_2)^\xi}(p) \tag{3}$$

Similarly,

$$\psi^2{}_{(\beta_1 \cap \beta_2)^\xi}(p^{-1}) = \sigma(\psi^2{}_{(\beta_1 \cap \beta_2)}\,(p^{-1}), 1 - \xi)$$

$$= min\,\left(\psi^2{}_{{\beta_1}^\xi}\,(p^{-1}), \psi^2{}_{{\beta_2}^\xi}\,(p^{-1})\right)$$

$$= \psi^2{}_{{\beta_1}^\xi \cap {\beta_2}^\xi}(p)$$

https://doi.org/10.62500/icrtsda.1.1.36

$$= \psi^2{}_{(\beta_1 \cap \beta_2)^\xi}(p)$$

Thus,

$$\psi^2{}_{(\beta_1 \cap \beta_2)^\xi}(p^{-1}) = \psi^2{}_{(\beta_1 \cap \beta_2)^\xi}(p) \qquad (4)$$

From relations (1), (2), (3) and (4), we conclude that ${\beta_1}^\xi \cap {\beta_2}^\xi$ is ξ – pythagorean fuzzy subgroup of G.

Remark 3.1. Union of two ξ – PFSG's of a group G need not to be ξ – PFSG of G.

Proposition 3.5. If β is a Pythagorean fuzzy normal subgroup (PFNSG) of a group G then β is also ξ – pythagorean fuzzy normal subgroup of G.

Proof. For Pythagorean fuzzy normal subgroup β of a group G, $p\beta = \beta p$ for any $p \in G$.
Consider,

$$\begin{aligned} \varphi^2{}_{\beta^\xi}(p^{-1}g) &= \upsilon(\varphi^2{}_\beta(p^{-1}g), \xi) \\ &= \upsilon(\varphi^2{}_\beta(gp^{-1}), \xi) \\ &= \varphi^2{}_{\beta^\xi}(gp^{-1}) \end{aligned}$$

Thus,

$$\varphi^2{}_{\beta^\xi}(p^{-1}g) = \varphi^2{}_{\beta^\xi}(gp^{-1})$$

Similarly,

$$\begin{aligned} \psi^2{}_{\beta^\xi}(p^{-1}g) &= \sigma\left(\psi^2{}_\beta(p^{-1}g), 1-\xi\right) \\ &= \sigma(\psi^2{}_\beta(gp^{-1}), 1-\xi) \\ &= \psi^2{}_{\beta^\xi}(gp^{-1}) \end{aligned}$$

Thus,

$$\psi^2{}_{\beta^\xi}(p^{-1}g) = \psi^2{}_{\beta^\xi}(gp^{-1})$$

Consequently, β is also ξ – Pythagorean fuzzy normal subgroup of G.

Proposition 3.6. Every ξ – Pythagorean fuzzy normal subgroup β^ξ of G admits the following properties

$$\varphi^2{}_{\beta^\xi}(pq) = \varphi^2{}_{\beta^\xi}(qp)$$

and

$$\psi^2{}_{\beta^\xi}(pq) = \psi^2{}_{\beta^\xi}(qp)$$

Proof. For ξ – Pythagorean fuzzy normal subgroup β^ξ of G, we have

$$p\beta^\xi = \beta^\xi p, \ \forall\, p \in G$$

This implies that

$$p\beta^\xi(q^{-1}) = \beta^\xi p(q^{-1}), \ \forall\, q \in G$$

Consider,

$$\begin{aligned} \varphi^2{}_{p\beta^\xi}(q^{-1}) &= \varphi^2{}_{\beta^\xi p}(q^{-1}) \\ \upsilon\left(\varphi^2{}_\beta(p^{-1}q^{-1}), \xi\right) &= \upsilon\left(\varphi^2{}_\beta(q^{-1}p^{-1}), \xi\right) \\ \varphi^2{}_{\beta^\xi}(p^{-1}q^{-1}) &= \varphi^2{}_{\beta^\xi}(q^{-1}p^{-1}) \\ \varphi^2{}_{\beta^\xi}((qp)^{-1}) &= \varphi^2{}_{\beta^\xi}((pq)^{-1}) \\ \varphi^2{}_{\beta^\xi}(qp) &= \varphi^2{}_{\beta^\xi}(pq) \end{aligned}$$

https://doi.org/10.62500/icrtsda.1.1.36

Moreover,

$$\psi^2{}_{p\beta^\xi}(q^{-1}) = \psi^2{}_{\beta^\xi p}(q^{-1})$$
$$\sigma\left(\psi^2{}_{\beta}(p^{-1}q^{-1}), 1-\xi\right) = \sigma\left(\psi^2{}_{\beta}(q^{-1}p^{-1}), 1-\xi\right)$$
$$\psi^2{}_{\beta^\xi}(p^{-1}q^{-1}) = \psi^2{}_{\beta^\xi}(q^{-1}p^{-1})$$
$$\psi^2{}_{\beta^\xi}((qp)^{-1}) = \psi^2{}_{\beta^\xi}((pq)^{-1})$$

$\psi^2{}_{\beta^\xi}(qp) = \psi^2{}_{\beta^\xi}(pq) \quad \forall$ p,q ∈ G.

This conclude the proof.

Proposition 3.7. Let G/β^ξ the set of all ξ – Pythagorean fuzzy right cossets of ξ– Pythagorean fuzzy normal subgroup β^ξ of G.

$$G/\beta^\xi = \{\beta^\xi p : p \in G\}$$

The binary operation ∇ defined on the set G/β^ξ as follows, is a well-defined operation.

$\beta^\xi p \nabla \beta^\xi q = \beta^\xi pq, \quad \forall$ p, q ∈ G

Proof. Let $\beta^\xi p = \beta^\xi p'$ and $\beta^\xi q = \beta^\xi q'$.

Then

$$[\beta^\xi p \nabla \beta^\xi q](g) = \beta^\xi pq(g) = \left(\varphi^2{}_{\beta^\xi pq}(g), \psi^2{}_{\beta^\xi pq}(g)\right), \text{g} \in \text{G}$$

Consider,

$$\varphi^2{}_{\beta^\xi pq}(g) = \upsilon\left(\varphi^2{}_{\beta}g(pq)^{-1}, \xi\right)$$
$$= \varphi^2{}_{\beta^\xi p'}(gq^{-1})$$
$$= \varphi^2{}_{\beta^\xi q}(p'^{-1}g)$$
$$= \varphi^2{}_{\beta^\xi q'}(p'^{-1}g)$$

$$= \upsilon\left(\varphi^2{}_{\beta}g(p'q')^{-1}, \xi\right)$$
$$= \varphi^2{}_{\beta^\xi p'q'}(g)$$

Thus,

$$\varphi^2{}_{\beta^\xi pq}(g) = \varphi^2{}_{\beta^\xi p'q'}(g)$$

Moreover,

$$\psi^2{}_{\beta^\xi pq}(g) = \sigma\left(\psi^2{}_{\beta}g(pq)^{-1}, 1-\xi\right)$$
$$= \psi^2{}_{\beta^\xi p'}(gq^{-1})$$
$$= \psi^2{}_{\beta^\xi q}(p'^{-1}g)$$
$$= \psi^2{}_{\beta^\xi q'}(p'^{-1}g)$$

$$= \sigma\left(\psi^2{}_{\beta}g(p'q')^{-1}, 1-\xi\right)$$

https://doi.org/10.62500/icrtsda.1.1.36

$$= \psi^2{}_{\beta^{\xi}p'q'}(g)$$

Thus,

$$\psi^2{}_{\beta^{\xi}pq}(g) = \psi^2{}_{\beta^{\xi}p'q'}(g)$$

Consequently, the operation ∇ defined on the set G/β^{ξ} is a well-defined operation.

Proposition 3.8. The set G/β^{ξ} of all distinct ξ – Pythagorean fuzzy right cossets of ξ – Pythagorean fuzzy normal subgroup β^{ξ} of a group G forms a group under the operation ∇.

Proof. Consider the set G/β^{ξ} defined in the previous proposition.

In view of previous proposition, the set G/β^{ξ} satisfies the closure property.

Associativity

$$[\beta^{\xi}p \nabla \beta^{\xi}q] \nabla \beta^{\xi}r = [\beta^{\xi}pq \,] \nabla \beta^{\xi}r$$

$$= \beta^{\xi}pqr$$

$$= \beta^{\xi}p \nabla [\beta^{\xi}qr]$$

$$= \beta^{\xi}p \nabla [\beta^{\xi}\mathrm{q} \nabla \beta^{\xi}\mathrm{r}], \forall\ \mathrm{p}, \mathrm{q}, \mathrm{r} \in \mathrm{G}$$

Identity

For every $\beta^{\xi}p \in G/\beta^{\xi}$ there exist $\beta^{\xi}e \in G/\beta^{\xi}$ such that

$$\beta^{\xi}p \nabla \beta^{\xi}e = \beta^{\xi}pe = \beta^{\xi}p$$

and

$$\beta^{\xi}e \nabla \beta^{\xi}p = \beta^{\xi}ep = \beta^{\xi}p$$

This implies that $\beta^{\xi}e$ is the identity element of G/β^{ξ}.

Inverse

It is easy to note that inverse of each element of G/β^{ξ} exist as if for every $\beta^{\xi}p \in G/\beta^{\xi}$ there exist $\beta^{\xi}p^{-1} \in G/\beta^{\xi}$ such that

$$\beta^{\xi}p \nabla \beta^{\xi}p^{-1} = \beta^{\xi}pp^{-1} = \beta^{\xi}e$$

and

$$\beta^{\xi}p^{-1} \nabla \beta^{\xi}p = \beta^{\xi}p^{-1}p = \beta^{\xi}e$$

Consequently, $\left(G/\beta^{\xi}, \nabla\right)$ is a group.

Proposition 3.9. Let β^{ξ} be ξ – Pythagorean fuzzy subgroup of a group G and f be a surjective homomorphism from G to G' then $f\left(\beta^{\xi}\right)$ is ξ– Pythagorean fuzzy subgroup of a group G'.

Proof. In view of given condition, for any two elements $q_1, q_2 \in \mathrm{G}'$ then there exist elements $p_1, p_2 \in \mathrm{G}$ such that

$f(p_1) = q_1 \quad , \quad f(p_2) = q_2$

Consider,

$$f\left(\beta^{\xi}\right)(q_1q_2) = \left(\varphi^2{}_{f(\beta^{\xi})}(q_1q_2), \psi^2{}_{f(\beta^{\xi})}(q_1q_2)\right)$$

https://doi.org/10.62500/icrtsda.1.1.36

Where

$$\varphi^2{}_{f(\beta^\xi)}(q_1q_2) = \varphi^2{}_{(f(\beta))^\xi}(q_1q_2)$$

$$= \varphi^2{}_{\beta^\xi}(p_1p_2)$$

$$\geq min\left\{\varphi^2{}_{\beta^\xi}(p_1), \varphi^2{}_{\beta^\xi}(p_2)\right\}$$

$$= min\left\{\vee\left\{\varphi^2{}_{\beta^\xi}(p_1): f(p_1) = q_1\right\}, \vee\left\{\varphi^2{}_{\beta^\xi}(p_2): f(p_2) = q_2\right\}\right\}$$

$$= min\left\{\varphi^2{}_{f(\beta^\xi)}(q_1), \varphi^2{}_{f(\beta^\xi)}(q_2)\right\}$$

Thus

$$\varphi^2{}_{f(\beta^\xi)}(q_1q_2) \geq min\left\{\varphi^2{}_{f(\beta^\xi)}(q_1), \varphi^2{}_{f(\beta^\xi)}(q_2)\right\}$$

Moreover,

$$\psi^2{}_{f(\beta^\xi)}(q_1q_2) = \psi^2{}_{(f(\beta))^\xi}(q_1q_2)$$

$$= \sigma\left(\psi^2{}_{f(\beta)}(f(p_1)f(p_2)), 1-\xi\right)$$

$$= \sigma\left(\psi^2{}_{\beta}(p_1p_2), 1-\xi\right)$$

$$= \psi^2{}_{\beta^\xi}(p_1p_2)$$

$$\leq max\left\{\psi^2{}_{\beta^\xi}(p_1), \psi^2{}_{\beta^\xi}(p_2)\right\}$$

$$= max\left\{\wedge\left\{\psi^2{}_{\beta^\xi}(p_1): f(p_1) = q_1\right\}, \wedge\left\{\psi^2{}_{\beta^\xi}(p_2): f(p_2) = q_2\right\}\right\}$$

$$= max\left\{\psi^2{}_{f(\beta^\xi)}(q_1), \psi^2{}_{f(\beta^\xi)}(q_2)\right\}$$

Thus

$$\psi^2{}_{f(\beta^\xi)}(q_1q_2) \leq max\left\{\psi^2{}_{f(\beta^\xi)}(q_1), \psi^2{}_{f(\beta^\xi)}(q_2)\right\}$$

Further,

$$f(\beta^\xi)(q^{-1}) = \left(\varphi^2{}_{f(\beta^\xi)}(q^{-1}), \psi^2{}_{f(\beta^\xi)}(q^{-1})\right)$$

Where

$$\varphi^2{}_{f(\beta^\xi)}(q^{-1}) = \varphi^2{}_{(f(\beta))^\xi}(q^{-1})$$

$$= \varphi^2{}_{f(\beta^\xi)}(q)$$

Implies that

$$\varphi^2{}_{f(\beta^\xi)}(q^{-1}) = \varphi^2{}_{f(\beta^\xi)}(q)$$

Moreover,

$$\psi^2{}_{f(\beta^\xi)}(q^{-1}) = \psi^2{}_{(f(\beta))^\xi}(q^{-1})$$

https://doi.org/10.62500/icrtsda.1.1.36

$$= \psi^2{}_{f(\beta^\xi)}(q)$$

Implies that

$$\psi^2{}_{f(\beta^\xi)}(q^{-1}) = \psi^2{}_{f(\beta^\xi)}(q)$$

Consequently, $f(\beta^\xi)$ is ξ – pythagorean fuzzy subgroup of a group G′.

Proposition 3.10. Let β^ξ be ξ – Pythagorean fuzzy normal subgroup of a group G and f be a surjective homomorphism from group G to G′then $f(\beta^\xi)$ is ξ – pythagorean fuzzy normal subgroup of a group G′.

Proof. In view of given condition, for any two elements $q_1, q_2 \in$ G′ then there exist elements $p_1, p_2 \in$ G such that

$f(p_1) = q_1 \quad , \quad f(p_2) = q_2$

Consider,

$$(f(\beta))^\xi(q_1q_2) = \left(\varphi^2{}_{(f(\beta))^\xi}(q_1q_2), \psi^2{}_{(f(\beta))^\xi}(q_1q_2)\right)$$

Where

$$\varphi^2{}_{(f(\beta))^\xi}(q_1q_2) = \upsilon\left(\varphi^2{}_{f(\beta)}(f(p_1)f(p_2)), \xi\right)$$

$$= \varphi^2{}_{\beta^\xi}(p_1p_2)$$

$$= \varphi^2{}_{\beta^\xi}(p_2p_1)$$

$$= \upsilon\left(\varphi^2{}_{f(\beta)}(q_2q_1), \xi\right) = \varphi^2{}_{(f(\beta))^\xi}(q_2q_1)$$

Moreover,

$$\psi^2{}_{(f(\beta))^\xi}(q_1q_2) = \sigma\left(\psi^2{}_{f(\beta)}(f(p_1)f(p_2)), 1-\xi\right)$$

$$= \psi^2{}_{\beta^\xi}(p_1p_2)$$

$$= \psi^2{}_{\beta^\xi}(p_2p_1)$$

$$= \psi^2{}_{\beta^\xi}(q_2q_1)$$

Consequently, $f(\beta^\xi)$ is ξ – pythagorean fuzzy normal subgroup of a group G′.

Proposition 3.11. Let β^ξ be ξ – Pythagorean fuzzy subgroup of a group G′ and f be a bijective homomorphism from group G to G′ then $f^{-1}(\beta^\xi)$ is ξ – Pythagorean fuzzy subgroup of a group G.

Proof. Given that f is a bijective homomorphism from group G to G′. For elements $q_1, q_2 \in$ G′ there exist elements $p_1, p_2 \in$ G such that

$f(p_1) = q_1 \quad , \quad f(p_2) = q_2$

Consider,

$$f^{-1}(\beta^\xi)(p_1p_2) = \left(\varphi^2{}_{f^{-1}(\beta^\xi)}(p_1p_2), \psi^2{}_{f^{-1}(\beta^\xi)}(p_1p_2)\right)$$

Where

https://doi.org/10.62500/icrtsda.1.1.36

$$\varphi^2{}_{f^{-1}(\beta^\xi)}(p_1p_2) = \varphi^2{}_{\beta^\xi}(f(p_1p_2))$$

$$\geq min\left\{\varphi^2{}_{f^{-1}(\beta^\xi)}(p_1), \varphi^2{}_{f^{-1}(\beta^\xi)}(p_2)\right\}$$

Thus

$$\varphi^2{}_{f^{-1}(\beta^\xi)}(p_1p_2) \geq min\left\{\varphi^2{}_{f^{-1}(\beta^\xi)}(p_1), \varphi^2{}_{f^{-1}(\beta^\xi)}(p_2)\right\}$$

Moreover,

$$\psi^2{}_{f^{-1}(\beta^\xi)}(p_1p_2) = \psi^2{}_{\beta^\xi}(f(p_1p_2))$$

$$\leq max\left\{\psi^2{}_{f^{-1}(\beta^\xi)}(p_1), \psi^2{}_{f^{-1}(\beta^\xi)}(p_2)\right\}$$

Thus

$$\psi^2{}_{f^{-1}(\beta^\xi)}(p_1p_2) \leq max\left\{\psi^2{}_{f^{-1}(\beta^\xi)}(p_1), \psi^2{}_{f^{-1}(\beta^\xi)}(p_2)\right\}$$

Moreover,

$$f^{-1}(\beta^\xi)(p^{-1}) = \left(\varphi^2{}_{f^{-1}(\beta^\xi)}(p^{-1}), \psi^2{}_{f^{-1}(\beta^\xi)}(p^{-1})\right)$$

where,

$$\varphi^2{}_{f^{-1}(\beta^\xi)}(p^{-1}) = \varphi^2{}_{\beta^\xi}(f(p^{-1}))$$

$$= \varphi^2{}_{\beta^\xi}(f(p))$$

$$= \varphi^2{}_{f^{-1}(\beta^\xi)}(p)$$

Implies that

$$\varphi^2{}_{f^{-1}(\beta^\xi)}(p^{-1}) = \varphi^2{}_{f^{-1}(\beta^\xi)}(p)$$

Similarly

$$\psi^2{}_{f^{-1}(\beta^\xi)}(p^{-1}) = \psi^2{}_{\beta^\xi}(f(p^{-1}))$$

$$= \psi^2{}_{\beta^\xi}(f(p))$$

$$= \psi^2{}_{f^{-1}(\beta^\xi)}(p)$$

Implies that

$$\psi^2{}_{f^{-1}(\beta^\xi)}(p^{-1}) = \psi^2{}_{f^{-1}(\beta^\xi)}(p)$$

Consequently, $f^{-1}(\beta^\xi)$ is ξ – pythagorean fuzzy subgroup of a group G.

Proposition 3.12. Let β^ξ be ξ– pythagorean fuzzy normal subgroup of a group G′ and f be a bijective group homomorphism from group G to G′ then $f^{-1}(\beta^\xi)$ is ξ – pythagorean fuzzy normal subgroup of a group G.

Proof. Given that f is a bijective group homomorphism from group G to G′. For elements $q_1, q_2 \in$ G′ there exist elements $p_1, p_2 \in$ G such that

$f(p_1) = q_1$, $f(p_2) = q_2$

https://doi.org/10.62500/icrtsda.1.1.36

Consider,

$$f^{-1}(\beta^{\xi})(p_1p_2) = \left(\varphi^2{}_{f^{-1}(\beta^{\xi})}(p_1p_2), \psi^2{}_{f^{-1}(\beta^{\xi})}(p_1p_2)\right)$$

Where

$$\varphi^2{}_{f^{-1}(\beta^{\xi})}(p_1p_2) = \varphi^2{}_{\beta^{\xi}}(f(p_1p_2))$$
$$= \varphi^2{}_{f^{-1}(\beta^{\xi})}(p_2p_1)$$

Thus,

$$\varphi^2{}_{f^{-1}(\beta^{\xi})}(p_1p_2) = \varphi^2{}_{f^{-1}(\beta^{\xi})}(p_2p_1)$$

Moreover,

$$\psi^2{}_{f^{-1}(\beta^{\xi})}(p_1p_2) = \psi^2{}_{\beta^{\xi}}(f(p_1p_2))$$
$$= \psi^2{}_{f^{-1}(\beta^{\xi})}(p_2p_1)$$

Thus,

$$\psi^2{}_{f^{-1}(\beta^{\xi})}(p_1p_2) = \psi^2{}_{f^{-1}(\beta^{\xi})}(p_2p_1)$$

Consequently, $f^{-1}(\beta^{\xi})$ is ξ – pythagorean fuzzy normal subgroup of a group G.

Proof of theorem 1.1.

Proof. The proof of theorem 1.1 can be follows from proposition 3.1 and 3.2.

Proof of theorem 1.2.

Proof.

i. We know that

$$\varphi^2{}_{\beta^{\xi}}(e) = \varphi^2{}_{\beta^{\xi}}(pp^{-1})$$
$$\geq min(\varphi^2{}_{\beta^{\xi}}(p), \varphi^2{}_{\beta^{\xi}}(p^{-1}))$$
$$= \varphi^2{}_{\beta^{\xi}}(p)$$

Hence,

$\varphi^2{}_{\beta^{\xi}}(e) \geq \varphi^2{}_{\beta^{\xi}}(p)$, for all p $\in$ G

ii. We know that

$$\psi^2{}_{\beta^{\xi}}(e) = \psi^2{}_{\beta^{\xi}}(pp^{-1})$$
$$\leq max(\psi^2{}_{\beta^{\xi}}(p), \psi^2{}_{\beta^{\xi}}(p^{-1}))$$
$$= \psi^2{}_{\beta^{\xi}}(p)$$

Hence,

$$\psi^2{}_{\beta^{\xi}}(e) \leq \psi^2{}_{\beta^{\xi}}(p), \text{for all p} \in \text{G}$$

iii. We know that

$$\varphi^2{}_{\beta^{\xi}}(p) = \varphi^2{}_{\beta^{\xi}}(pe)$$
$$\geq min(\varphi^2{}_{\beta^{\xi}}(pq^{-1}), \varphi^2{}_{\beta^{\xi}}(\text{q}))$$

https://doi.org/10.62500/icrtsda.1.1.36

$$= \varphi^2{}_{\beta^\xi}(q)$$

$$\varphi^2{}_{\beta^\xi}(p) \geq \varphi^2{}_{\beta^\xi}(q) \quad (1)$$

Similarly,

$$\varphi^2{}_{\beta^\xi}(q) = \varphi^2{}_{\beta^\xi}(qp^{-1}p)$$

$$\geq min(\varphi^2{}_{\beta^\xi}(qp^{-1}), \varphi^2{}_{\beta^\xi}(\mathrm{p}))$$

$$= \varphi^2{}_{\beta^\xi}(p)$$

$$\varphi^2{}_{\beta^\xi}(q) \geq \varphi^2{}_{\beta^\xi}(p) \quad (2)$$

From (1) and (2), we have

$\varphi^2{}_{\beta^\xi}(p) = \varphi^2{}_{\beta^\xi}(q)$, for all p $\in$ G

Similarly,

$$\psi^2{}_{\beta^\xi}(p) = \psi^2{}_{\beta^\xi}(pe)$$

$$\leq max(\psi^2{}_{\beta^\xi}(pq^{-1}), \psi^2{}_{\beta^\xi}(\mathrm{q}))$$

$$= \psi^2{}_{\beta^\xi}(q)$$

$$\psi^2{}_{\beta^\xi}(p) \leq \psi^2{}_{\beta^\xi}(q) \quad (3)$$

Similarly,

$$\psi^2{}_{\beta^\xi}(q) = \psi^2{}_{\beta^\xi}(qp^{-1}p)$$

$$\leq max(\psi^2{}_{\beta^\xi}(qp^{-1}), \psi^2{}_{\beta^\xi}(\mathrm{p}))$$

$$= \psi^2{}_{\beta^\xi}(p)$$

$$\psi^2{}_{\beta^\xi}(q) \leq \psi^2{}_{\beta^\xi}(p) \quad (4)$$

From (3) and (4), we have

$\psi^2{}_{\beta^\xi}(p) = \psi^2{}_{\beta^\xi}(q)$, $for\ all$ p $\in$ G

Consequently,

$\beta^\xi(pq^{-1}) = \beta^\xi(e) \Rightarrow \beta^\xi(p) = \beta^\xi(q)$

Proof of theorem 1.3.

Proof. It follows from the proposition 3.3 and 3.4.

Proof of theorem 1.4.

Proof. In view of given condition, we have

$\xi < min\{x, 1-y\}$

$\Rightarrow$ $\mathrm{x} > \xi$ and $\xi < 1 - \mathrm{y}$

https://doi.org/10.62500/icrtsda.1.1.36

$\Rightarrow \quad \min\left\{{\varphi^2}_\beta(p): \forall\, p \in \mathrm{G}\right\} > \xi \quad$ and $\quad \max\left\{{\psi^2}_\beta(p): \forall\, p \in \mathrm{G}\right\} < 1-\xi$

$\Rightarrow \quad {\varphi^2}_\beta(p) > \xi \quad$ and $\quad {\psi^2}_\beta(p) < 1-\xi, \quad \forall\, p \in \mathrm{G}.$

Therefore,

${\varphi^2}_{\beta^\xi}(pq) \geq min\left\{{\varphi^2}_{\beta^\xi}(p), {\varphi^2}_{\beta^\xi}(q)\right\}$ and ${\psi^2}_{\beta^\xi}(pq) \leq max\left\{{\psi^2}_{\beta^\xi}(p), {\psi^2}_{\beta^\xi}(q)\right\}$

Further, according to given conditions, we have

${\varphi^2}_\beta(p^{-1}) = {\varphi^2}_\beta(p)$ and ${\psi^2}_\beta(p^{-1}) = {\psi^2}_\beta(p)$, hold for all $p \in \mathrm{G}$

So,

${\varphi^2}_{\beta^\xi}(p^{-1}) = {\varphi^2}_{\beta^\xi}(p) \quad$ and $\quad {\psi^2}_{\beta^\xi}(p^{-1}) = {\psi^2}_{\beta^\xi}(p)$

Hold. Hence, β is ξ – PFSG of G.

Proof of theorem 1.5.

Proof. It can be follows from proposition 3.5 and 3.6.

Proof of theorem 1.6.

Proof. Since $\xi < min\{x, 1-y\}$

$\Rightarrow \quad \mathrm{x} > \xi \quad$ and $\quad \mathrm{y} < 1-\xi$

$\Rightarrow \quad \upsilon\left\{{\varphi^2}_\beta(p): \forall\, p \in \mathrm{X}\right\} > \xi \quad$ and $\quad \sigma\left\{{\psi^2}_\beta(p): \forall\, p \in \mathrm{X}\right\} < 1-\xi$

$\Rightarrow \quad {\varphi^2}_\beta(p) > \xi, \quad \forall\, p \in \mathrm{X} \quad$ and $\quad {\psi^2}_\beta(p) < 1-\xi, \quad \forall\, p \in \mathrm{X}$

Therefore,

${\varphi^2}_{\beta^\xi p}(g) = \upsilon\left\{{\varphi^2}_\beta(gp^{-1}), \xi\right\} = \Theta$ and ${\psi^2}_{\beta^\xi p}(g) = \sigma\left\{{\psi^2}_\beta(gp^{-1}), 1-\xi\right\} = \Theta'$

Similarly,

${\varphi^2}_{p\beta^\xi}(g) = \upsilon\left\{{\varphi^2}_\beta(p^{-1}g), \xi\right\} = \Theta$ and ${\psi^2}_{p\beta^\xi}(g) = \sigma\left\{{\psi^2}_\beta(p^{-1}g), 1-\xi\right\} = \Theta'$

From the above discussion, we have

${\varphi^2}_{\beta^\xi p}(g) = {\varphi^2}_{p\beta^\xi}(g)$ and ${\psi^2}_{\beta^\xi p}(g) = {\psi^2}_{p\beta^\xi}(g)$

Thus,

$\beta^\xi p = p\beta^\xi, \forall\, \mathrm{p} \in \mathrm{G}$

Hence, β^ξ is a ξ – PFNSG of G.

Proof of theorem 1.7.

Proof. The proof of theorem 1.7 can be follows from proposition 3.7 and 3.8.

Proof of theorem 1.8.

Proof. It can be follows from proposition 3.9 and 3.10.

Proof of theorem 1.9.

Proof. The proof of theorem 1.9 can be follows from position 3.11 and 3.12.

https://doi.org/10.62500/icrtsda.1.1.36

4. COMMENTS AND CONCLUSION

In this work we explain the concept of ξ-Pythagorean fuzzy subgroup (PFSG) in addition prove that every Pythagorean fuzzy subgroup (PFSG) is ξ- Pythagorean fuzzy subgroup (ξ- PFSG). Also established conditions under which given ξ- Pythagorean fuzzy set (PFS) is ξ- Pythagorean fuzzy subgroup (PFSG). Further prove that the intersection of any two ξ- Pythagorean fuzzy subgroups (ξ-PFSG's) is ξ- Pythagorean fuzzy subgroup (ξ-PFSG). We also defined ξ- Pythagorean fuzzy cossets, ξ-Pythagorean fuzzy normal subgroups (PFNSG), ξ- pythagorean fuzzy homomorphism and proved that every Pythagorean fuzzy normal subgroup is ξ- Pythagorean fuzzy normal subgroup (PFNSG), also, the Pythagorean fuzzy homomorphism two ξ- Pythagorean fuzzy subgroups (ξ- PFSG's) is presented.

REFERENCES

https://doi.org/10.62500/icrtsda.1.1.36

Addis, G.M. (2018). Fuzzy homomorphism theorems on groups: *Korean J. Mat,* 26,373-385.

1. Ajmal, N. and A.S. Prajapati. (1992). Fuzzy cosets and fuzzy normal subgroups. *Inf. Sci*,64,17-25.
2. Akram, M. and S. Naz. (2019). A novel decision-making approach under complex Pythagorean fuzzy environment. *Math. Comput. App*, 24,73.
3. Anthony, J. and H. Sherwood. (1979). Fuzzy groups redefined. *J. Math. Anal. Appl.* 69,124-130.
4. Atanassov, K. (1986). Intuitionistic fuzzy sets. *Fuzzy Sets. Syst*, 20,87-96.
5. Bhunia, S. and G. Ghorai. (2021). A new approach to fuzzy group theory using (α, β)-Pythagorean fuzzy sets. *Songklanakarin J. Sci. Technol*, 43,295-306.
6. Biswas, R. (1990). Fuzzy subgroups and anti fuzzy subgroups. *Fuzzy Sets. Syst*, 35,121-124.
7. Chakraborty, A. and S. Khare. (1993). Fuzzy homomorphism and algebraic structures. *Fuzzy Sets. Syst*, 59,211-221.
8. Choudhury, F.P., A. Chakraborty and S. Khare. (1988). A note on fuzzy subgroups and fuzzy homomorphism. *J. Math. Anal. Appl*, 131,537-553.
9. Das, P.S. (1981). Fuzzy groups and level subgroups. *J. Math. Anal. Appl*, 84,264-269.
10. Dixit, V., R. Kumar and N. Ajmal. (1990). Level subgroups and union of fuzzy subgroups. *Fuzzy Sets. Syst*, 37,359-371.
11. Ejegwa, P.A. (2019). Pythagorean fuzzy set and its application in career placements based on academic performance using max–min–max composition. *Complex. Intel. Syst*, 5,165-175.
12. Klir, G.J., U. St. Clair and B. Yuan. (1997). Fuzzy set theory: *Fou. Appl.* Prentice-Hall, Inc, 10, 1-29.
13. Lee, K.H. (2004). First course on fuzzy theory and applications. *Springer Sci. Busi. Media*, 27, 13-109.
14. Mordeson, J.N., K.R. Bhutani and A. Rosenfeld. (2005). Fuzzy group theory. *Springer*, 182,1-80.
15. Mukherjee, N. and P. Bhattacharya. (1984). Fuzzy normal subgroups and fuzzy cosets. *Inf. Sci*, 34,225-239.
16. Mukherjee, N. and P. Bhattacharya. (1986). Fuzzy groups: some group-theoretic analogs. *Inf. Sci*, 39,247-267.
17. Onasanya, B. (2016). Review of some anti fuzzy properties of some fuzzy subgroups. *Ann. Fuzzy Math. Inf*, 11,899-904.
18. Peng, X. and Y. Yang. (2015). Some results for Pythagorean fuzzy sets. *Int. J. Intel. Syst*, 30,1133-1160.
19. Rosenfeld, A. (1971). Fuzzy groups. *J. Math. Anal. Appl*, 35,512-517.
20. Tarnauceanu, M. (2015). Classifying fuzzy normal subgroups of finite groups. *Iran. J. Fuzzy. Syst*, 12:107-115.
21. Umer Shuaib, M.S. (2019). On some properties of o-anti fuzzy subgroups. *Comput. Sci*, 14,215-230.
22. Umer Shuaib, M.S. and W. Asghar. (2018). On some characterizations of o-fuzzy subgroups. *Comput. Sci*, 13,119-131.
23. Yager, R.R. (2013). Pythagorean fuzzy subsets. *Int. J. Intell. Syst*, 28,436-452.
24. Zadeh, L.A. (1965). Fuzzy sets. *Inf. Control*, 8,338-353.
25. Zhan, J. and Z. Tan. (2004). Intuitionistic M-fuzzy groups. *Soochow J. Math*, 30,85-90.
26. Zimmermann, H.-J. (2011). Fuzzy set theory—and its applications. *Springer Sci. Business Media*, 4,1-43.

https://doi.org/10.62500/icrtsda.1.1.37

Proc. 1st International Conference on Recent Trends in Statistics and Data Analytics
Air University Islamabad, Pakistan – May 9, 2024, Vol. 1, pp. 357-374

Algebraic Aspects of δ-Picture Fuzzy Subgroups

Najam Ul Sahar[1], Fatima Ehsan[2], Naveed Hussain[3]*, Sawaira Arshad[4], and Khansa Pervaz[5]
Department of Mathematics and Statistics, University of Agriculture Faisalabad, Pakistan

ABSTRACT

This study proposes the idea of a Picture fuzzy (PF) set over a specific linear operator δ-PF set and investigates some set theoretical aspects of the idea. It is demonstrated that a (δ-PF) set is the union and intersection of any two (δ-PF) sets. In addition to every PF subgroup being δ-PF subgroup established, the following notion is applied to illustrate the concept of δ-PF subgroup. A specific set of requirements is defined for a particular δ-PF set to be a δ-PF subgroup. Furthermore, it is proven that any two δ-PF subgroups that intersect must be a δ-PF subgroup. Furthermore, concepts related to δ-PF cosets and δ-PF subgroup are established and demonstrated, demonstrating that each PF normal subgroup is a δ-PF subgroup. Additionally, we will explore several significant algebraic aspects of the concept of δ-PF quotient subgroup and successfully utilize the idea of δ-PF normal subgroup to introduce the ideology of this subgroup.

Keywords. Fuzzy Set; Fuzzy Coset; Picture Fuzzy Set; Fuzzy Subgroup; Fuzzy Normal Subgroup, Fuzzy Quotient Subgroup.

1. INTRODUCTION

The established fuzzy set (FS) theory is useful for building decisions in unpredictable environments. Numerous direct and indirect extensions of FSs have been developed and also effectively implemented in the majority of real-life problems in [17]. A recently developed tool for those who deal with uncertainty is a picture FS, which is extension of intuitionistic FS and may represent uncertainty in scenarios with many replies of this kind: Yes, refrain from, no in [11]. Cuong discussed some properties of picture FSs and proposed distance measures between picture FSs [2]. Cuong and Hai researched the basic logic operators of fuzzy: disjunctions, conjunctions, negations, and consequences on image FSs, as well as developed fundamental crucial steps for fuzzy inference procedures in picture fuzzy systems in [7].

Atanassov proposed intuitionistic FSs in [2]. Sharma investigated the t-intuitionistic fuzzy subgroup in [16]. Over time, several academics have conducted numerous studies on FSs and intuitionistic FSs. The intuitionistic FS considers the measures of membership and non membership in such a way the sum doesn't exceed unity. The intuitionistic FS did not consider an indicator of neutrality. Cuong and colleagues introduced the concept of picture FS, which combines a measure of neutrality membership along with intuitionistic FS. As a result, image FS may be considered an instant generalisation of intuitionistic FS by combining three components, particularly positive, neutral, and negative, as described in [5]. Garg and Arora introduced t-norm operations-based Maclaurin Symmetric means aggregation operators for tackling decision-making issues in a dual reluctant fuzzy soft set in [12].

Cuong and colleagues investigate certain categories of recognizable picture FS t-norms and picture FS t-conorms for picture FSs in [8]. In 2015, certain recognizable t-norms and t-conorms operators were developed and first described in [7, 9]. Using the concept of quasi coincidence between fuzzy point and a FS, various fuzzy subgroup ideas are proposed, and their acceptability is evaluated [3]. Wei implemented the concepts of intuitionistic FS, interval-valued intuitionistic FS and image FSs. Additionally, construct several similarity measure (SM) across image FSs, such as a cosine similarity measure, a weighted cosine SM, a set-theoretic SM and a weighted grey SM in [16].

Theorem 1.1. Intersection of any two δ-PF sets is δ-PF set.

Theorem1.2. Union of any two δ-PF sets is δ-PF set.

https://doi.org/10.62500/icrtsda.1.1.37

Theorem 1.3. Every PF subgroup(G) admits the following properties $\mu_{B^\delta}(x) \leq \mu_{B^\delta}(e)$, $\xi_{B^\delta}(x) \leq \xi_{B^\delta}(e)$ and $\upsilon_{B^\delta}(x) \geq \upsilon_{B^\delta}(e)$.

Theorem 1.4. If A^δ and B^δ are δ-PF subgroup of a group *G*, then $A^\delta \cap B^\delta$ is a δ-PF subgroup of *G*.

Theorem 1.5. If B^δ is δ-PF subgroup of a group *G*. Then B^δ is δ-PF subgroup of $G \Leftrightarrow C_{\alpha,\gamma,\beta}(B^\delta)$ is δ-NSG of group G, $\forall\ \alpha, \gamma, \beta \in [0,1]$ with $\alpha + \gamma + \beta \leq 1$.

Theorem 1.6. If A^δ and B^δ are δ-PF normal subgroups of a group *G*. Then $A^\delta \cap B^\delta$ is δ-PF normal subgroups of a group *G*.

Theorem1.7. Let B^δ be a δ-PFNSG of *G*. Then the set G_{B^δ}={m ∈ G:$\mu_{B^\delta}(m) = \mu_{B^\delta}(e), \xi_{B^\delta}(m) =$, $\xi_{B^\delta}(e)$, $\upsilon_{B^\delta}(m) = \upsilon_{B^\delta}(e)$} is a $\delta -$ NSG of G.

Theorem 1.8. Every δ-PF normal subgroups admits the following characteristics

1) $mB^\delta = nB^\delta \iff m^{-1}n \in G_{B^\delta}$
2) $B^\delta m = B^\delta n \iff mn^{-1} \in G_{B^\delta}$

Theorem 1.9. Every δ-PF normal subgroups satisfies the following relation
If $mB^\delta = uB^\delta$ and $nB^\delta = vB^\delta$ then $mnB^\delta = uvB^\delta$.

Theorem 1.10. For any δ-PF normal subgroups B^δ of *G*, there exist a natural epimorphism $\varphi: G \to {}^{G}/_{G_{B^\delta}}$,defined by $p \to pB^\delta, p \in G$ with $ker\varphi = G_{B^\delta}$.

Theorem 1.11. Let B^δ be δ-PF normal subgroups and G_{B^δ} be of *G*. Then, there exist an isomorphism between ${}^{G}/_{B^\delta}$ and ${}^{G}/_{G_{B^\delta}}$.

2. BASIC CONCEPTS

Definition 2.1. [13] If X is a universal set and x be any particular element of X. The FS B is a collection of order pairs $B = \{(x, \mu_B(x)) | x \in X\}$, where $\mu_B(x): X` \longrightarrow [0,1]$ is said to be membership f_n.

Definition 2.2. [4] A fuzzy subset μ of a group G is said to be fuzzy subgroup of G if

$$\mu_B(x, y) \geq min(\mu_B(x), \mu_B(y))$$

$$\mu_B(x^{-1}) \geq \mu_B(x), \forall x, y \in G$$

Definition 2.3. [5] A picture FS B on a universe X is an object of the form

$$B = \{(x, \mu_B(x), \xi_B(x), \upsilon_B(x)) | x \epsilon X\}\ ,$$

Where $\mu_B(x) \in [0,1]$ is called the "degree of positive membership of x in B", $\xi_B(x) \in [0,1]$ is called the "degree of neutral membership of x in B", and where μ_B , ξ_B and υ_B satisfy the following condition:

$$(\forall x \in X)\ \ (\mu_B(x) + \xi_B(x) + \upsilon_B(x) \leq 1)$$

Then for $x \in X$, $1 - (\mu_B(x) + \xi_B(x) + \upsilon_B(x))$ could be called the "degree of refusal membership of x in B".

Let PF set(X) denote the set of all the PF sets on a universe X.

Definition 2.4. [16] The α,β function of picture FS B of a universe X is denoted by

$$C_{\alpha,\beta} = \{x \epsilon X \mid \mu_B(x) \geq \alpha, \upsilon_B(x) \leq \beta\}$$

Definition 2.5. [14] Let G be a group and B be a picture fuzzy subset of G. Then B is a picture fuzzy subgroup of G if:

https://doi.org/10.62500/icrtsda.1.1.37

1. $\mu_B(xy) \geq \min(\mu_B(x), \mu_B(y)), \upsilon_B(xy) \leq \max(\upsilon_B(x), \upsilon_B(y))$
2. $\mu_{B^\delta}(x^{-1}) = \mu_{B^\delta}(x)$ *and* $\upsilon_{B^\delta}(x^{-1}) = \upsilon_{B^\delta}(x)\ \forall\ x, y \in G$.

Definition 2.6. [1] Consider a PF subgroup B and *x* be a fix point of a group G. The PF right coset of B in G by the element x is defined as

$$Bx(g) = \{(x, \mu_{Bx}(g), \xi_{Bx}(g)) | x \epsilon G\}$$

Where

$$\mu_{Bx}(g) = \mu_B(gx^{-1}) \text{ and } \xi_{Bx}(g) = \xi_B(gx^{-1})$$

Similarly, the PF left coset of B in G by the element x is defined as

$$xB(g) = \{(x, \mu_{xB}(g), \xi_{xB}(g)) | x \epsilon G\}$$

Where

$$\mu_{xB}(g) = \mu_B(x^{-1}g) \text{ and } \xi_{xB}(g) = \xi_B(x^{-1}g)$$

Definition 2.7. Let B be PF subgroup of G then B is called PF normal subgroup of G if and only if

$xB = Bx$,$\forall\ x \in G$.

Definition 2.8. Let B be a PF normal subgroup of a group G. The set of all distinct PF left or right cosets of B in G is represented by ${}^{G}/_{B}$. This set forms a group under the following binary operation.

Let $xB, B \in {}^{G}/_{B}$ then $xB * yB = (x * y)B, \forall x, y \in G_B$.

This group is called quotient group of G with respect to PF subgroup B.

Definition 2.9. Let B be a PF set of universe P and δ∈[0,1]. The PF set B^{δ} is called δ-PF set of universe with respect to PF set B and is defined as

$$B^{\delta} = (\mu_{B^\delta}, \xi_{B^\delta}, \upsilon_{B^\delta})$$

Where,

$$\mu_{B^\delta}(x) = min(\mu_B(x), \delta), \xi_{B^\delta}(x) = min(\xi_B(x), \delta), \upsilon_{B^\delta}(x) = max(\upsilon_B(x), \delta)$$

Definition 2.10. The α,γ,β function of δ- PF set B^{δ} of a universe X is denoted by

$$C_{\alpha,\gamma,\beta} = \{x \epsilon X \mid \mu_{B^\delta}(x) \geq \alpha, \xi_{B^\delta}(x) \geq \gamma, \upsilon_{B^\delta}(x) \leq \beta\}$$

Definition 2.11. A δ-PF set B^{δ} of a group G is called δ- PF subgroup of G if B^{δ} admits the following conditions:

1. $\mu_{B^\delta}(xy) \geq min\{\mu_{B^\delta}(x), \mu_{B^\delta}(y)\}$, $\xi_{B^\delta}(xy) \geq min\{\xi_{B^\delta}(x), \xi_{B^\delta}(y)\}$ *and* $\upsilon_{B^\delta}(xy) \leq max\{\upsilon_{B^\delta}(x), \upsilon_{B^\delta}(y)\}$
2. $\mu_{B^\delta}(x^{-1}) = \mu_{B^\delta}(x)$, $\xi_{B^\delta}(x^{-1}) = \xi_{B^\delta}(x)$ *and* $\upsilon_{B^\delta}(x^{-1}) = \upsilon_{B^\delta}(x)\ \forall\ x, y \in G$.

Definition 2.12. Consider a δ-PF subgroup B^{δ} and *x* be a fix point of a group G. The δ-PF right coset of B^{δ} in G by the element x is defined as

$$B^{\delta}x(g) = \{(x, \mu_{B^{\delta}{}_x}(g), \xi_{B^{\delta}{}_x}(g), \upsilon_{B^{\delta}{}_x}(g)) | x \epsilon G\}$$

Where

$$\mu_{B^{\delta}{}_x}(g) = \mu_{B^\delta}(gx^{-1}), \xi_{B^{\delta}{}_x}(g) = \xi_{B^\delta}(gx^{-1}) \text{ and } \upsilon_{B^{\delta}{}_x}(g) = \upsilon_{B^\delta}(gx^{-1})$$

https://doi.org/10.62500/icrtsda.1.1.37

Similarly, the PF left coset of B^{δ} in G by the element x is defined as

$$xB^{\delta}(g) = \{(x, \mu_{xB^{\delta}}(g), \xi_{xB^{\delta}}(g), \upsilon_{xB^{\delta}}(g)) | x \in G\}$$

Where

$$\mu_{xB^{\delta}}(g) = \mu_{B^{\delta}}(x^{-1}g), \xi_{xB^{\delta}}(g) = \xi_{B^{\delta}}(x^{-1}g) \; and \; \upsilon_{xB^{\delta}}(g) = \upsilon_{B^{\delta}}(x^{-1}g)$$

Definition 2.13. Let B^{δ} be δ-PF subgroup of G then B^{δ} is called δ-PF normal subgroup of G if and only if

$xB^{\delta} = B^{\delta}x$,$\forall\, x \in G$.

Definition 2.14. Let B^{δ} be a δ-PF normal subgroup of a group G. The set of all distinct PF left or right cosets of B^{δ} in G is represented by $G/_{B^{\delta}}$. This set forms a group under the following binary operation.

Let $xB^{\delta}, yB^{\delta} \in G/_{B^{\delta}}$ then $xB^{\delta} * yB^{\delta} = (x * y)B^{\delta}, \forall x, y \in G_{B^{\delta}}$.

This group is called quotient group or the factor group of G with respect to δ-PF normal subgroup B^{δ}.

3. PROOF OF THEOREMS

Proof of Theorem 1.1

Proof. For any two δ-PF set B_1^{δ} and B_2^{δ} of a set X we have

$\mu_{(B_1 \cap B_2)^{\delta}}(x) = \min\{\mu_{(B_1 \cap B_2)}(x), \delta\}$

$= \min\{\min\{\mu_{B_1}(x), \mu_{B_2}(x)\}, \delta\}$

$= \min[\min\{\mu_{B_1}(x), \delta\}, \min\{\mu_{B_2}(x), \delta\}]$

$= \min[\min\{\mu_{B_1}(x), \delta\}, \min\{\mu_{B_2}(x), \delta\}]$

$= \min\{\mu_{B_1{}^{\delta}}(x), \mu_{B_2{}^{\delta}}(x)\}$

$\mu_{(B_1 \cap B_2)^{\delta}}(x) = \mu_{B_1{}^{\delta}}(x) \cap \mu_{B_2{}^{\delta}}(x)$, for all x∈X .

Hence,

$$\mu_{(B_1 \cap B_2)^{\delta}} = \mu_{B_1{}^{\delta}} \cap \mu_{B_2{}^{\delta}}$$

$\upsilon_{(B_1 \cap B_2)^{\delta}}(x) = \max\{\upsilon_{(B_1 \cap B_2)}(x), \delta\}$

$= \max\{\min\{\upsilon_{B_1}(x), \upsilon_{B_2}(x)\}, \delta\}$

$= \max[\min\{\upsilon_{B_1}(x), \delta\}, \min\{\upsilon_{B_2}(x), \delta\}]$

$= \min[\max\{\upsilon_{B_1}(x), \delta\}, \max\{\upsilon_{B_2}(x), \delta\}]$

$= \min\{\upsilon_{B_1{}^{\delta}}(x), \upsilon_{B_2{}^{\delta}}(x)\}$

$\upsilon_{(B_1 \cap B_2)^{\delta}}(x) = \upsilon_{B_1{}^{\delta}}(x) \cap \upsilon_{B_2{}^{\delta}}(x)$, for all x∈X .

Hence,

https://doi.org/10.62500/icrtsda.1.1.37

$$\upsilon_{(B_1 \cap B_2)^\delta} = \upsilon_{B_1{}^\delta} \cap \upsilon_{B_2{}^\delta}$$

Similarly, one can easily show that

$$\xi_{(B_1 \cap B_2)^\delta} = \xi_{B_1{}^\delta} \cap \xi_{B_2{}^\delta}$$

Consequently,

$$(B_1 \cap B_2)^\delta = B_1{}^\delta \cap B_2{}^\delta .$$

Proof of Theorem 1.2

Proof. For any two δ-PF set $B_1{}^\delta$ and $B_2{}^\delta$ of a set X we have

$\mu_{(B_1 \cup B_2)^\delta}(x) = \min \{\mu_{(B_1 \cup B_2)}(x), \delta\}$

$= \min \{\max \{\mu_{B_1}(x), \mu_{B_2}(x)\}, \delta\}$

$= \min [\max \{\mu_{B_1}(x), \delta\}, \max \{\mu_{B_2}(x), \delta\}]$

$= \max [\min \{\mu_{B_1}(x), \delta\}, \min \{\mu_{B_2}(x), \delta\}]$

$= \max \{\mu_{B_1{}^\delta}(x), \mu_{B_2{}^\delta}(x)\}$

$\mu_{(B_1 \cup B_2)^\delta}(x) = \mu_{B_1{}^\delta}(x) \cup \mu_{B_2{}^\delta}(x)$, for all x∈X .

Hence,

$$\mu_{(B_1 \cup B_2)^\delta} = \mu_{B_1{}^\delta} \cup \mu_{B_2{}^\delta}$$

$\upsilon_{(B_1 \cup B_2)^\delta}(x) = \max \{\upsilon_{(B_1 \cup B_2)}(x), \delta\}$

$= \max \{\max \{\upsilon_{B_1}(x), \upsilon_{B_2}(x)\}, \delta\}$

$= \max [\max \{\upsilon_{B_1}(x), \delta\}, \max \{\upsilon_{B_2}(x), \delta\}]$

$= \max [\max \{\upsilon_{B_1}(x), \delta\}, \max \{\upsilon_{B_2}(x), \delta\}]$

$= \max \{\upsilon_{B_1{}^\delta}(x), \upsilon_{B_2{}^\delta}(x)\}$

$\upsilon_{(B_1 \cup B_2)^\delta}(x) = \upsilon_{B_1{}^\delta}(x) \cup \upsilon_{B_2{}^\delta}(x)$, for all x∈X .

Hence,

$$\upsilon_{(B_1 \cup B_2)^\delta} = \upsilon_{B_1{}^\delta} \cup \upsilon_{B_2{}^\delta}$$

Similarly, one can easily show that

$$\xi_{(B_1 \cup B_2)^\delta} = \xi_{B_1{}^\delta} \cup \xi_{B_2{}^\delta}$$

Consequently,

$$(B_1 \cup B_2)^\delta = B_1{}^\delta \cup B_2{}^\delta .$$

Proof of Theorem 1.3

Proof. Consider

https://doi.org/10.62500/icrtsda.1.1.37

$\mu_{B^\delta}(e) = \mu_{B^\delta}(xx^{-1}) \geq \min\{\mu_{B^\delta}(x), \mu_{B^\delta}(x^{-1})\} = \mu_{B^\delta}(x)$

$\Rightarrow \quad \mu_{B^\delta}(e) \geq \mu_{B^\delta}(x)$

Similarly,

$\xi_{B^\delta}(e) = \xi_{B^\delta}(xx^{-1}) \geq \min\{\xi_{B^\delta}(x), \xi_{B^\delta}(x^{-1})\} = \xi_{B^\delta}(x)$

$\Rightarrow \quad \xi_{B^\delta}(e) \geq \xi_{B^\delta}(x)$

Now,

$\upsilon_{B^\delta}(e) = \upsilon_{B^\delta}(xx^{-1}) \leq \max\{\upsilon_{B^\delta}(x), \upsilon_{B^\delta}(x^{-1})\} = \upsilon_{B^\delta}(x)$

$\Rightarrow \quad \upsilon_{B^\delta}(e) \leq \upsilon_{B^\delta}(x).$

Proof of Theorem 1.4

Proof. By theorem 1.1 $A^\delta \cap B^\delta$ is a δ-PF subgroup of G iff $C_{\alpha,\gamma,\beta}(A^\delta \cap B^\delta)$ is a subgroup of G.

As $C_{\alpha,\gamma,\beta}(A^\delta \cap B^\delta) = C_{\alpha,\gamma,\beta}(A^\delta) \cap C_{\alpha,\gamma,\beta}(B^\delta)$ and both $C_{\alpha,\gamma,\beta}(A^\delta)$ and $C_{\alpha,\gamma,\beta}(B^\delta)$ are subgroups of G and intersection of two subgroups of a group is a subgroup of G.

This implies that,

$C_{\alpha,\gamma,\beta}(A^\delta \cap B^\delta)$ is a subgroup of and hence $A^\delta \cap B^\delta$ is δ-PF subgroup of G.

Proof of Theorem 1.5

Proof. Let $x,y \in G$ and

$\alpha = \mu_{B^\delta}(x) \wedge \mu_{B^\delta}(y), \gamma = \xi_{B^\delta}(x) \wedge \xi_{B^\delta}(y)$ and $\beta = \upsilon_{B^\delta}(x) \vee \upsilon_{B^\delta}(y)$. Then

$\mu_{B^\delta}(x) \geq \alpha, \xi_{B^\delta}(x) \geq \gamma, \ \upsilon_{B^\delta}(x) \leq \beta$ and $\mu_{B^\delta}(y) \geq \alpha, \xi_{B^\delta}(y) \geq \gamma, \upsilon_{B^\delta}(y) \leq \beta.$

That is $x \in C_{\alpha,\gamma,\beta}(B^\delta)$, $y \in C_{\alpha,\delta,\beta}(B^\delta)$

$\Rightarrow xy \in C_{\alpha,\gamma,\beta}(B^\delta)$, $yx \in C_{\alpha,\gamma,\beta}(B^\delta)$

Therefore,

$\mu_{B^\delta}(xy) = \mu_{B^\delta}(yx), \xi_{B^\delta}\xi(xy) = \xi_{B^\delta}(yx)$ and $\upsilon_{B^\delta}(xy) = \upsilon_{B^\delta}(yx)$ (As $C_{\alpha,\gamma,\beta}(B^\delta)$ is $\delta - \text{NSG}$)

Hence B^δ is δ-PF normal subgroup of *G*.

Conversely,

Let $x \in C_{\alpha,\gamma,\beta}(B^\delta)$ and $g \in G$. Then $\mu_{B^\delta}(x) \geq \alpha, \xi_{B^\delta}(x) \geq \gamma, \ \upsilon_{B^\delta}(x) \leq \beta$. Moreover, since B^δ is δ-PF normal subgroup of *G* therefore

$$\mu_{B^\delta}(g^{-1}xg) = \mu_{B^\delta}(x), \ \xi_{B^\delta}(g^{-1}xg) = \xi_{B^\delta}(x) \ and \ \upsilon_{B^\delta}(g^{-1}xg) = \upsilon_{B^\delta}(x)$$

This implies that

$$\mu_{B^\delta}(g^{-1}xg) \geq \alpha, \xi_{B^\delta}(g^{-1}xg) \geq \gamma \ and \ \upsilon_{B^\delta}(g^{-1}xg) \leq \beta$$

So, $g^{-1}xg \in C_{\alpha,\gamma,\beta}(B^\delta)$.

Hence $C_{\alpha,\gamma,\beta}(B^\delta)$ is $\delta - \text{NSG}$.

https://doi.org/10.62500/icrtsda.1.1.37

Proof of Theorem 1.6

Proof. By theorem 1.5 $A^{\delta} \cap B^{\delta}$ is a δ-PF subgroup of G iff $C_{\alpha,\gamma,\beta}(A^{\delta} \cap B^{\delta})$ is a subgroup of G.

As $C_{\alpha,\gamma,\beta}(A^{\delta} \cap B^{\delta}) = C_{\alpha,\gamma,\beta}(A^{\delta}) \cap C_{\alpha,\gamma,\beta}(B^{\delta})$ and both $C_{\alpha,\gamma,\beta}(A^{\delta})$ and $C_{\alpha,\gamma,\beta}(B^{\delta})$ are subgroups of G and intersection of two subgroups of a group is a subgroup of G.

This implies that,

$C_{\alpha,\gamma,\beta}(A^{\delta} \cap B^{\delta})$ is a subgroup of and hence $A^{\delta} \cap B^{\delta}$ is δ-PF subgroup of G.

Proof of Theorem 1.7

Proof. One can easily observe that $G_{B^{\delta}} \neq \emptyset \; as \; e \in G_{B^{\delta}}$. For any 2 elements m, n ∈ $G_{B^{\delta}}$ we have

$$\mu_{B^{\delta}}(mn^{-1}) \geq \min\{\mu_{B^{\delta}}(m), \mu_{B^{\delta}}(n^{-1})\}$$

$$= \mu_{B^{\delta}}(e)$$

$$\Rightarrow \quad \mu_{B^{\delta}}(mn^{-1}) \geq \mu_{B^{\delta}}(e)$$

Similarly,

$$\xi_{B^{\delta}}(mn^{-1}) \geq \min\{\xi_{B^{\delta}}(m), \xi_{B^{\delta}}(n^{-1})\}$$

$$= \xi_{B^{\delta}}(e)$$

$$\Rightarrow \quad \xi_{B^{\delta}}(mn^{-1}) \geq \xi_{B^{\delta}}(e)$$

Moreover,

$$\upsilon_{B^{\delta}}(mn^{-1}) \leq \max\{\upsilon_{B^{\delta}}(m), \upsilon_{B^{\delta}}(n^{-1})\}$$

$$= \upsilon_{B^{\delta}}(e)$$

$$\Rightarrow \quad \upsilon_{B^{\delta}}(mn^{-1}) \leq \upsilon_{B^{\delta}}(e)$$

This shows that $\mu_{B^{\delta}}(mn^{-1}) \geq \mu_{B^{\delta}}(e), \xi_{B^{\delta}}(mn^{-1}) \geq \xi_{B^{\delta}}(e), \upsilon_{B^{\delta}}(mn^{-1}) \leq \upsilon_{B^{\delta}}(e)$.

But in the view of theorem 1.3 we have $\mu_{B^{\delta}}(mn^{-1}) \leq \mu_{B^{\delta}}(e), \xi_{B^{\delta}}(mn^{-1}) \leq \xi_{B^{\delta}}(e), \upsilon_{B^{\delta}}(mn^{-1}) \geq \upsilon_{B^{\delta}}(e)$.

From the above discussion, we have $mn^{-1} \in G_{B^{\delta}}$.

This means that $G_{B^{\delta}}$ is subgroup of *G*.

Furthermore, for any element $m \in G_{B^{\delta}}$ and $g \in G, we \; have$

$$\mu_{B^{\delta}}(g^{-1}mg) = \mu_{B^{\delta}}(m) = \mu_{B^{\delta}}(e)$$

Similarly,

$$\xi_{B^{\delta}}(g^{-1}mg) = \xi_{B^{\delta}}(m) = \xi_{B^{\delta}}(e)$$

Moreover,

$$\upsilon_{B^{\delta}}(g^{-1}mg) = \upsilon_{B^{\delta}}(m) = \upsilon_{B^{\delta}}(e)$$

It follows that $g^{-1}mg \in G_{B^{\delta}}$. Hence, $G_{B^{\delta}}$ is a δ-NSG of *G*.

https://doi.org/10.62500/icrtsda.1.1.37

Proof of Theorem 1.8

Proof.

1) Let $mB^{\delta} = nB^{\delta}$ where $m,n \in G$

$\Longrightarrow mB^{\delta}(n) = nB^{\delta}(n)$

The application of definition 2.5 in the above relation yields that

$\mu_{B^{\delta}}(m^{-1}n) = \mu_{B^{\delta}}(n^{-1}n)$, $\xi_{B^{\delta}}(m^{-1}n) = \xi_{B^{\delta}}(n^{-1}n)$ and $\upsilon_{B^{\delta}}(m^{-1}n) = \upsilon_{B^{\delta}}(n^{-1}n)$

$\Longrightarrow \mu_{B^{\delta}}(m^{-1}n) = \mu_{B^{\delta}}(e)$, $\xi_{B^{\delta}}(m^{-1}n) = \xi_{B^{\delta}}(e)$ and $\upsilon_{B^{\delta}}(m^{-1}n) = \upsilon_{B^{\delta}}(e)$

The application of theorem 1.7 in the above relation yields that $m^{-1}n \in G_{B}^{\delta}$.

Conversely, suppose that $m^{-1}n \in G_{B}^{\delta}$. This implies that

$\mu_{B^{\delta}}(m^{-1}n) = \mu_{B^{\delta}}(e)$, $\xi_{B^{\delta}}(m^{-1}n) = \xi_{B^{\delta}}(e)$ and $\upsilon_{B^{\delta}}(m^{-1}n) = \upsilon_{B^{\delta}}(e)$

$\Longrightarrow \mu_{B^{\delta}}(m^{-1}n) = \mu_{B^{\delta}}(n^{-1}n)$

$mB^{\delta}(n) = nB^{\delta}(n)$

Similarly, we can easily prove the required arguments for $\xi_{B^{\delta}}$ and $\upsilon_{B^{\delta}}$.

Consequently, $mB^{\delta} = nB^{\delta}$.

2) Let $B^{\delta}m = B^{\delta}n$ where $m,n \in G_{B^{\delta}}$.

$\Longrightarrow B^{\delta}m(m) = B^{\delta}n(m)$

The application of definition 2.5 in the above relation yields that

$\mu_{B^{\delta}}(mm^{-1}) = \mu_{B^{\delta}}(mn^{-1})$, $\xi_{B^{\delta}}(mm^{-1}) = \xi_{B^{\delta}}(mn^{-1})$ and $\upsilon_{B^{\delta}}(mm^{-1}) = \upsilon_{B^{\delta}}(mn^{-1})$

$\Longrightarrow \mu_{B^{\delta}}(mn^{-1}) = \mu_{B^{\delta}}(e)$, $\xi_{B^{\delta}}(mn^{-1}) = \xi_{B^{\delta}}(e)$ and $\upsilon_{B^{\delta}}(mn^{-1}) = \upsilon_{B^{\delta}}(e)$

The application of theorem 1.7 in the above relation yields that $mn^{-1} \in G_{B}^{\delta}$.

Conversely, suppose that $mn^{-1} \in G_{B}^{\delta}$. This implies that

$\mu_{B^{\delta}}(mn^{-1}) = \mu_{B^{\delta}}(e)$, $\xi_{B^{\delta}}(mn^{-1}) = \xi_{B^{\delta}}(e)$ and $\upsilon_{B^{\delta}}(mn^{-1}) = \upsilon_{B^{\delta}}(e)$

$\Longrightarrow \mu_{B^{\delta}}(mn^{-1}) = \mu_{B^{\delta}}(mm^{-1})$

$nB^{\delta}(m) = mB^{\delta}(m)$

Similarly, we can easily prove the required arguments for $\xi_{B^{\delta}}$ and $\upsilon_{B^{\delta}}$.

Consequently, $nB^{\delta} = mB^{\delta}$.

https://doi.org/10.62500/icrtsda.1.1.37

Proof of Theorem 1.9

Proof

Since $mB^{\delta} = uB^{\delta}$ and $nB^{\delta} = vB^{\delta}$ the application of theorem 1.7 in the above relations yield that $m^{-1}u, n^{-1}v \in G_{B^{\delta}}$.

Consider

$$(mn)^{-1}(uv) = (n^{-1}m^{-1})(uv)$$

$$= n^{-1}(m^{-1}u)v$$

$$= n^{-1}(m^{-1}u)(nn^{-1})v$$

$$= [n^{-1}(m^{-1}u)n](n^{-1}v) \in G_{B^{\delta}}$$

Hence $(mn)^{-1}(uv) \in G_{B^{\delta}}$. The application of theorem 1.8 in the above relation yields that $mnB^{\delta} = uvB^{\delta}$.

Proof of Theorem 1.10

Proof.For any element $p, q \in G$ we have $\varphi(pq) = pB^{\delta}qB^{\delta} = \varphi(p)\varphi(q)$.

Therefore, φ is homomorphism. Moreover, obvious φ is surjective. Now,

$$ker\varphi = \{p \in g : \varphi(p) = eB^{\delta}\}$$

$$= \{p \in g : pB^{\delta} = eB^{\delta}\}$$

$$= \{p \in g : pe^{-1} \in G_{B^{\delta}}\}$$

$$= G_{B^{\delta}}$$

In the subsequent result, we demonstrate an isomorphic correspondence between quotient group of G by δ-PF normal subgroup B^{δ} and quotient group G by $G_{B^{\delta}}$.

Proof of Theorem 1.11

Proof. Define a mapping φ: ${}^{G}/_{B^{\delta}} \to {}^{G}/_{G_{B^{\delta}}}$ as $\left(mB^{\delta}\right) = mG_{B^{\delta}}, m \in G$.

For any $mB^{\delta}, nB^{\delta} \in {}^{G}/_{B^{\delta}}$ we have

$$\varphi\left(mB^{\delta}nB^{\delta}\right) = \varphi(mnB^{\delta})$$

$$= mnG_{B^{\delta}}$$

$$= mG_{B^{\delta}}nG_{B^{\delta}}$$

$$= \varphi(mB^{\delta})\varphi(nB^{\delta})$$

This shows that φ is homomorphism.

Moreover, for any $mB^{\delta}, nB^{\delta} \in {}^{G}/_{B^{\delta}}$, we have

https://doi.org/10.62500/icrtsda.1.1.37

$$\varphi(mB^{\delta}) = \varphi(nB^{\delta})$$

$$mG_{B^{\delta}} = nG_{B^{\delta}}$$

$$\Rightarrow n^{-1}mG_{B^{\delta}} = nG_{B^{\delta}}$$

Which shows that $n^{-1}m \in G_{B^{\delta}}$.

By applying theorem 1.10. in the above relation yields that $mB^{\delta} = nB^{\delta}$. Furthermore, the surjective case is easily understood. Consequently, φ is an isomorphism between $G/_{B^{\delta}}$ and $G/_{G_{B^{\delta}}}$.

4. COMMENTS AND CONCLUSION

This study elucidates the notion of the δ-Picture fuzzy subgroup (PFSG) and establishes the inverse relationship between each Picture fuzzy subgroup (PFSG) and its δ-Picture fuzzy subgroup (δ- PFSG). Additionally, conditions under which a particular δ-Picture fuzzy subgroup (PFSG) is a δ-Picture fuzzy set (PFS) were created. Additionally demonstrate that any two δ-Picture fuzzy subgroups (δ-PFSGs) that intersect are also δ-Picture fuzzy subgroups (δ-PFSG). Additionally, we established the definitions of δ-Picture fuzzy cosets, δ-Picture fuzzy normal subgroups (PFNSG), and δ-Picture fuzzy quotient subgroup. Furthermore, we demonstrated that each Picture fuzzy normal subgroup is a δ-Picture fuzzy normal subgroup (PFNSG).

REFERENCES

1. Addis, G. M. (2021). L-fuzzy cosets in universal algebras. *Mathematica Slovaca*, 71, 573-594.
2. Atanassov, K. T., and Atanassov, K. T. (1999). Intuitionistic fuzzy sets. *Physica-Verlag HD*,1-137.
3. Bhakat, S. K., and Das, P. (1992). On the definition of a fuzzy subgroup. *Fuzzy sets and systems*, 51, 235-241.
4. Biswas, R. (1989). Intuitionistic fuzzy subgroups. In Mathematical Forum, 10, 37-46.
5. Cuong, B. C., and Kreinovich, V. (2013). Picture fuzzy sets-a new concept for computational intelligence problems. *IEEE*,1-6.
6. Cuong, B. C., and Kreinovich, V. (2014). Picture fuzzy sets. *Journal of computer science and cybernetics*, 30,409-420.
7. Cuong, B. C., and Pham, V. H. (2015). Some fuzzy logic operators for picture fuzzy sets. *IEEE*, 132-137.
8. Cuong, B. C., and Pham, V. H. (2015). Some fuzzy logic operators for picture fuzzy sets. *IEEE*,132-137.
9. Cuong, B. C., Kreinovitch, V., and Ngan, R. T. (2016). A classification of representable t-norm operators for picture fuzzy sets. *IEEE*,19-24.
10. Cuong, B. C., Ngan, R. T., and Hai, B. D. (2015). An involutive picture fuzzy negator on picture fuzzy sets and some De Morgan triples.*IEEE*,126-131.
11. Dogra, Shovan and Pal, Madhumangal.(2023). Picture fuzzy subgroup. *Kragujevac Journal of Mathematics*, 47, 911-933.
12. Dutta, P., and Ganju, S. (2018). Some aspects of picture fuzzy set. *Transactions of A. Razmadze Mathematical Institute*, 172,164-175.
13. Garg, H., and Arora, R. (2020). Maclaurin symmetric mean aggregation operators based on t-norm operations for the dual hesitant fuzzy soft set. *Journal of Ambient Intelligence and Humanized Computing*, 11, 375-410.
14. Klir, G., and Yuan, B. (1995). Fuzzy sets and fuzzy logic.New Jersey.: *Prentice hall*, 4,1-12.
15. Li, X. S., Yuan, X. H., and Lee, E. S. (2009). The three-dimensional fuzzy sets and their cut sets. *Computers & Mathematics with Applications*, 58, 1349-1359.

https://doi.org/10.62500/icrtsda.1.1.37

16. Sharma, P. K. (2012). t-Intuitionistic fuzzy subgroups. *International Journal of Fuzzy Mathematics and Systems*, 3, 233-243.
17. Wei, G. (2018). Some similarity measures for picture fuzzy sets and their applications. *Iranian Journal of Fuzzy Systems*, 15,77-89.
18. Zadeh, L. A. (1965). Fuzzy set theory. *Information and control*, 8, 338-353.

https://doi.org/10.62500/icrtsda.1.1.38

Proc. 1st International Conference on Recent Trends in Statistics and Data Analytics
Air University Islamabad, Pakistan – May 9, 2024, Vol. 1, pp. 375-380

Application and Simulation Analysis of Hotelling's T^2 Control Chart for Monitoring Drinking Water Quality

Muskan Ahsan[1], Muhammad Kashif[2*] and Muhammad Usman[3]

Department of Mathematics and Statistics, University of Agriculture Faisalabad, Pakistan

ABSTRACT

This research aims to assess the efficiency of a drinking water treatment system by employing Hotelling's T^2 statistic. While traditional control charts are commonly used in engineering to enhance quality by pinpointing specific sources of variation, they typically assume independent observations. This study focuses on demonstrating the effectiveness of multivariate control charts in overseeing water quality at a treatment facility in Faisalabad, Pakistan. The variables examined include Turbidity, Nitrate (N), Fluoride (F), Arsenic (As), and iron (Fe) residue. Specifically, multivariate control charts, Hotelling's T^2, are utilized. These statistics are computed through various methods such as the sample covariance matrix, successive differences estimator, and minimum volume ellipsoid estimator. During the analysis, certain control charts exhibit out-of-control signals, prompting the removal of corresponding samples. After this adjustment, the multivariate control charts return to a controlled state. Subsequent Monte Carlo simulation confirms the efficacy of these charts in detecting mean changes, with all control charts remaining in control throughout the simulation. Moreover, multivariate T^2 charts demonstrate superior performance when applied to independent observations.

1. INTRODUCTION

Water, an indispensable natural resource, plays a pivotal role in sustaining life on Earth, particularly surface water, which serves as a primary source for various human activities (Tyagi *et al.*, 2013). Recognizing its critical importance, this study embarks on the development of multivariate Hotelling T^2 control charts utilizing data sourced from the Pakistan Council of Research in Water Resources (PCRWR) (Rasheed *et al.*, 2021). The objective is to assess the quality of tap water across five key properties: turbidity, nitrate, fluoride, arsenic, and iron (Susanty *et al.*, 2018).

To ensure a comprehensive analysis, samples were systematically selected to represent all days of the year, providing a robust dataset for analysis. Originally introduced by Hotelling in 1947, the Hotelling's T^2 chart has been extensively discussed and employed by numerous researchers, such as (Alt, 1978), (Alt and Smith, 1988), (Alt, 1985),(Roberts, 2000), and (Kashif *et al.*, 2023). Subsequently, multivariate Hotelling T^2 control charts were meticulously constructed for each of these properties. Additionally, 22 fresh samples were meticulously collected, analyzed, and plotted on the control charts to further refine the understanding of water quality dynamics and validate the effectiveness of the control measures implemented (LOWRY and MONTGOMERY, 1995).

In the realm of process management, the primary objective revolves around promptly detecting any assignable causes of process shifts, thereby facilitating timely investigation and corrective action to enhance process performance. This imperative necessitates the utilization of effective monitoring tools, with control charts serving as invaluable instruments for online process monitoring (Imran *et al.*, 2024).

https://doi.org/10.62500/icrtsda.1.1.38

These control charts, also referred to as process or quality control charts, offer graphical representations that indicate whether a data sample falls within the expected range of variation. Through their application, the aim is to uphold the quality and integrity of tap water, ensuring its suitability for diverse uses while concurrently safeguarding public health and environmental sustainability (LOWRY and MONTGOMERY, 1995).

The implementation of the T^2 control chart entails leveraging the sample covariance matrix, as elucidated by Sullivan and Woodall in 1996. Hotelling's T-squared T^2 statistic emerges as a powerful multivariate analysis technique, specifically designed to assess differences between groups concerning continuous variables (Williams *et al.*, 2006).

By quantifying the distance between group means relative to within-group variability, this statistic finds utility in a myriad of fields, including quality control, environmental monitoring, and experimental design. To evaluate its effectiveness, a Monte Carlo simulation study was conducted, comparing its performance when applied to the data against one-step ahead forecast errors (Capilla, 2009). Furthermore, for comparative analysis, the performance of the chart with multivariate independent observations, possessing identical mean and covariance matrix as the original data, was scrutinized.

Throughout the analysis, certain control charts exhibited out-of-control signals, necessitating the removal of corresponding samples to restore stability. Following this adjustment, the multivariate control charts reverted to a controlled state, affirming the robustness of the control measures. Subsequent Monte Carlo simulations corroborated the efficacy of these charts in detecting mean changes, with all control charts maintaining stability throughout the simulation. Additionally, the superior performance of multivariate T^2 charts when applied to independent observations underscored their effectiveness in ensuring water quality control (Mohd Hashim *et al.*, 2020).

2. [MATERIAL AND METHODS]

The data set:

In this research, the T^2 control chart is applied to a dataset acquired from a drinking treatment plant situated in Faisalabad, Pakistan, covering the duration of the year 2023. The study focuses on annual measurements of turbidity, nitrate levels, fluoride concentration, arsenic content, and iron concentration to showcase the utility of the control chart. Accordingly, the dataset is structured to include individual observations, each comprising data points for these five characteristics (Conceição *et al.*, 2018). These observations can be effectively summarized using a mean vector and a variance-covariance matrix, providing insights into the central tendencies and interrelationships among the parameters under examination (Tracy *et al.*, 1992).

$$\bar{\boldsymbol{X}}=\begin{bmatrix}0.48\\6.41\\0.88\\3.78\\0.78\end{bmatrix}$$

$$\sum=\begin{bmatrix}0.1426 & -0.8168 & -0.0788 & 0.0734 & -0.0911\\ -0.8168 & 57.3009 & 0.6788 & -0.0512 & -4.5169\\ -0.0788 & 0.6788 & 0.6946 & 0.9435 & -0.2599\\ 0.0734 & -0.5116 & 0.9435 & 8.7242 & -0.3729\\ -0.0911 & -4.5169 & -0.2599 & -0.3729 & 5.9132\end{bmatrix}$$

Constructing Hotelling's T^2 Control Charts

Hotelling's $\boldsymbol{T^2}$ chart, a technique introduced by Hotteling in 1947, serves as a significant method for overseeing product quality via multivariate analysis (Montgomery, 2019). Additionally, it proves adept at pinpointing multivariate outliers (Mostajeran *et al.*, 2018).

https://doi.org/10.62500/icrtsda.1.1.38

In this discussion, we explore random vectors conforming to a multivariate normal distribution with defined parameters, denoting the dataset as X. The $\boldsymbol{T^2}$ statistic, as established by Hotelling in 1974, is expressed through Equation (1).

$$\boldsymbol{T^2 = (y - \bar{y})' Z^{-1} (y - \bar{y})} \qquad [\mathbf{1}]$$

In this context, where y signifies the data vector, y¯ denotes the mean vector, and Z represents the covariance matrix, the control limit for the $\boldsymbol{T^2}$ chart,

under the assumption of the original data following a normal distribution, is determined by Equation (2) and (3).

1.Upper Control Limit (UCL) = $\frac{[v(w+1)(w-1)]}{[w- wv]}, F(\alpha, v, w - v)$ [2]

When the number of observations surpasses 100, a suggested control limit is calculated for monitoring process stability and performance.

1. Upper Control Limit (UCL) = $\frac{v(w-1)}{w-v}, F(\alpha, v, w - v)$ [3]
   (mashuri2021, save).

2. MATERIAL AND METHODS

Establishing the upper control limit for the hotelling's T^2 control chart involves the application of equation [3], yielding a value of 11.65. This threshold holds crucial importance as it signifies substantial deviations from the anticipated behavior of the data points. With this limit determined, we can now move forward with the implementation of the hotelling's T^2 control chart (Ibrahim *et al.*, 2017).

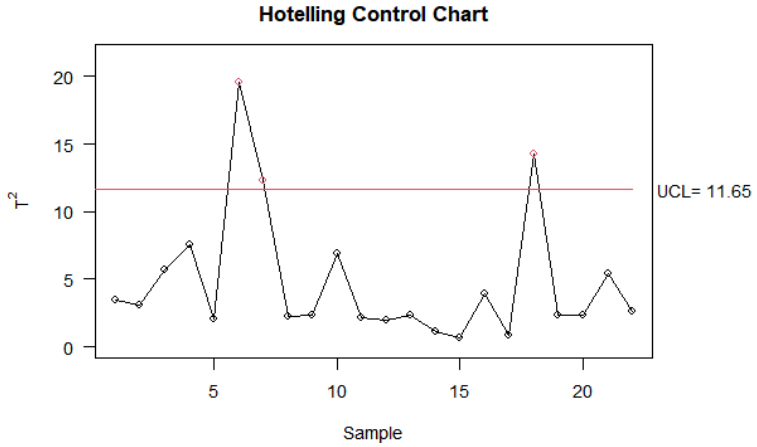

This suggests the presence of three signals indicating that the process is out of control. To address this issue, we will remove these samples and then proceed to generate new Hotelling control charts.

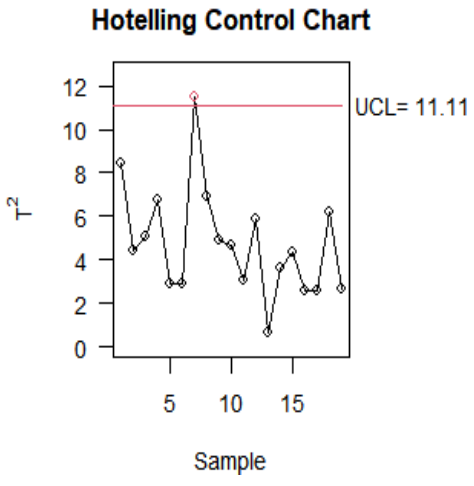

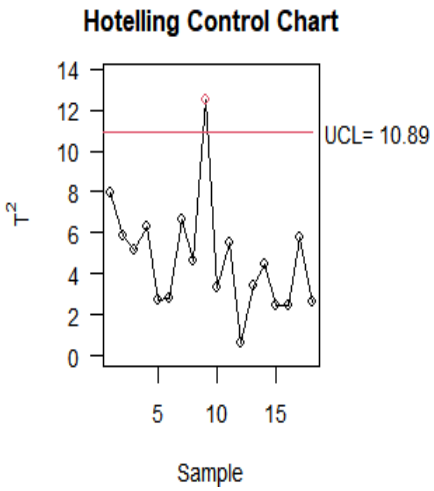

https://doi.org/10.62500/icrtsda.1.1.38

Figure 2. Multivariate Hotelling T^2 control chart of 19 samples

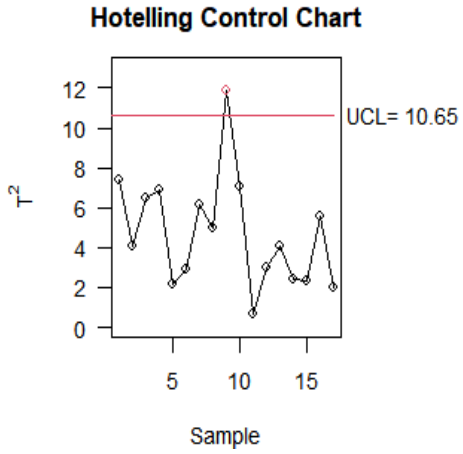

Figure 3. Multivariate Hotelling T^2 control chart of 18 samples

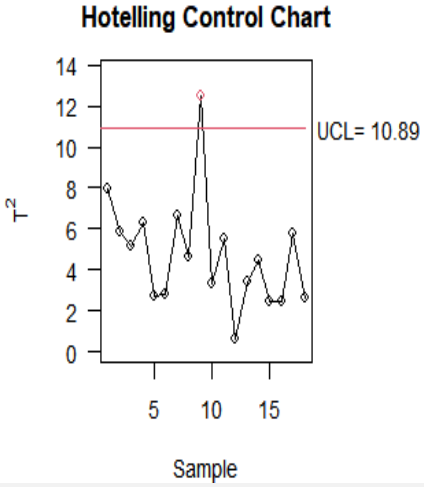

Figure 4. Multivariate Hotelling T^2 control chart of 17 samples

Figure 5. Multivariate Hotelling T^2 control chart of 16 samples

In Figure 2, we observe a sample of 19 observations, followed by the creation of a Hotelling T^2 control chart. Here, we detect one out-of-control signal, prompting its removal. This process is repeated in Figure 3, where again one value is out-of-control. Similarly, in Figure 4, after repeating the process, we encounter the same situation. However, in Figure 5, all processes are found to be in control.

Simulated control charts:

In the course of our study, we are currently engaged in the creation of simulated Hotelling's T^2 control charts, a critical aspect of quality control analysis. Employing sample sizes ranging from 25 to 100 observations, we aim to explore the effectiveness of these charts across varying dataset sizes. To establish the upper control limit (UCL) for each chart, Equation 2 serves as our guiding principle, enabling us to tailor control limits to the unique characteristics of each simulated dataset.

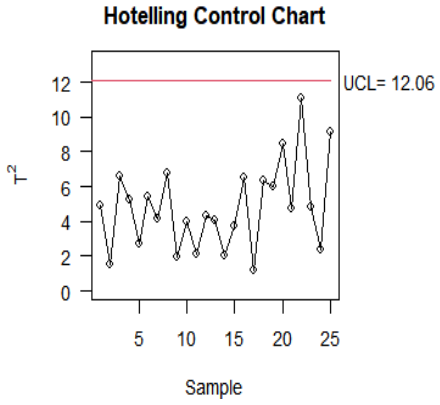

Figure 6. Multivariate Hotelling T^2 control chart of 25 samples

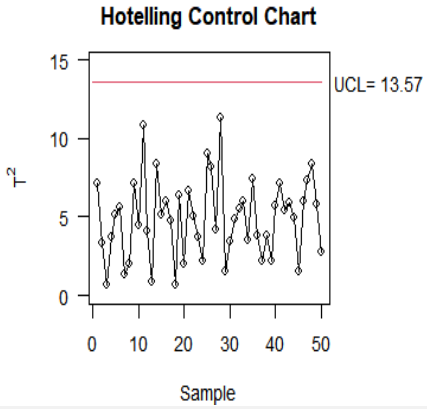

Figure 7. Multivariate Hotelling T^2 control chart of 50 samples

https://doi.org/10.62500/icrtsda.1.1.38

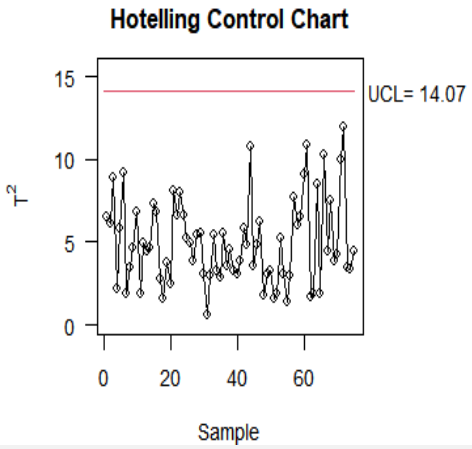

Figure 8. Multivariate Hotelling T^2 control chart of 75 samples

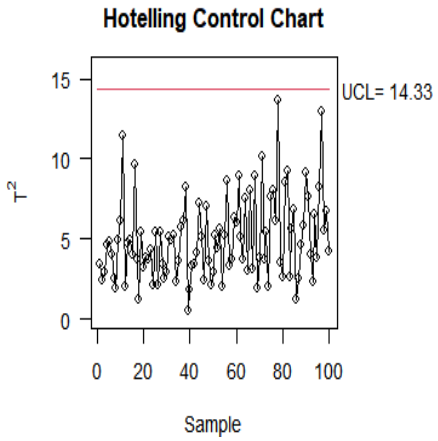

Figure 9. Multivariate Hotelling T^2 control chart of 100 samples

None of the simulated control charts display any out-of-control signals, signifying consistent stability throughout the analyses. This suggests that the implemented processes are effectively maintained within acceptable bounds, validating the reliability of the control measures.

6. COMMENTS AND CONCLUSION

Comments:

1. Objective Clarity: The research aims at evaluating the efficiency of a drinking water treatment system using Hotelling's T^2 statistic, offering a clear objective for the study.

2. Multivariate Approach: The study's focus on multivariate control charts is appropriate for assessing water quality, considering the interconnectedness of various parameters.

3. Methodological Rigor: The study employs various methods for computing Hotelling's T^2 statistic, demonstrating a comprehensive approach to data analysis.

4. Signal Detection: The detection and removal of out-of-control signals during the analysis show the researchers' diligence in maintaining data integrity.

5. Simulation Analysis: The use of Monte Carlo simulation to confirm the efficacy of control charts enhances the robustness of the findings.

Conclusion:

The study successfully demonstrates the effectiveness of multivariate Hotelling's T^2 control charts in assessing drinking water quality. Through rigorous analysis and signal detection procedures, the research ensures the reliability of the findings. The absence of out-of-control signals in both real and simulated data further validates the stability and effectiveness of the implemented control measures. Overall, this research contributes valuable insights into the application of multivariate control charts for monitoring water quality, with implications for enhancing public health and environmental sustainability.

REFERENCES

https://doi.org/10.62500/icrtsda.1.1.38

1. Alt, F.B. 1978. ECONOMIC DESIGN OF CONTROL CHARTS FOR CORRELATED, MULTIVARIATE OBSERVATIONS.
2. Alt, F.B. 1985. Multivariate quality control. Encycl. Stat. Sci. 6:110–122.
3. Alt, F.B. and N.D. Smith. 1988. 17 multivariate process control. Handb. Stat. 7:333–351.
4. Capilla, C. 2009. Application and Simulation Study of the Hotelling's T2 Control Chart to Monitor a Wastewater Treatment Process. Environ. Eng. Sci. 26:333–342.
5. Conceição, K.Z., M.A.V. Boas, S.C. Sampaio, M.B. Remor and D.I. Bonaparte. 2018. STATISTICAL CONTROL OF THE PROCESS APPLIED TO THE MONITORING OF THE WATER QUALITY INDEX Analyzing the physical-chemical and biological characteristics allows the evaluation of the water quality of a water body . Thus , the objective of this study was to d. 4430:951–960.
6. Ibrahim, S., M. Ahmed and E.K. Abusabah. 2017. Construction of Control Charts for Drinking Water Treatment in Medani Station of Water Purification , Gezira State , Sudan Key words : Control Charts , Quality , Water Treatment , Surface Water . 1 . Introduction : Water is an important natural resource o. 86:68–86.
7. Imran, M., H.L. Dai, F.S. Zaidi, X. Hu, K.P. Tran and J. Sun. 2024. Analyzing out-of-control signals of T2 control chart for compositional data using artificial neural networks. Expert Syst. Appl. 238:122165.
8. Kashif, M., A.M. Almarashi, M. Aslam and M.I. Khan. 2023. Water Waste Monitoring Using Neutrosophic Multivariate T 2 Control Chart. Water. Air. Soil Pollut. 234:1–13.
9. LOWRY, C.A. and D.C. MONTGOMERY. 1995. A review of multivariate control charts. IIE Trans. 27:800–810.
10. Mohd Hashim, S.R., A. Andrew and W.A. Malandi. 2020. An application of univariate and multivariate control charts in monitoring water quality. ASM Sci. J. 13:1–7.
11. Montgomery, D.C. 2019. Introduction to statistical quality control. John wiley & sons.
12. Mostajeran, A., N. Iranpanah and R. Noorossana. 2018. An Explanatory Study on the Non-Parametric Multivariate T2 Control Chart. J. Mod. Appl. Stat. Methods 17:1–27.
13. Rasheed, H., F. Altaf, K. Anwaar and M. Ashraf. 2021. Drinking Water Quality in Pakistan: Current Status and Challenges. Pakistan Council of Research in Water Resources (PCRWR), Islamabad. All rights Reserv. by PCRWR. authors Encourag. fair use this Mater. non-commercial Purp. with proper Cit. 141.
14. Roberts, S.W. 2000. Control chart tests based on geometric moving averages. Technometrics 42:97–101.
15. Susanty, A., M.M. Ulkhaq and D. Amalia. 2018. Using multivariate control chart to maintain the quality of drinking water in accordance with standard. Int. J. Appl. Sci. Eng. 15:83–94.
16. Tracy, N.D., J.C. Young and R.L. Mason. 1992. Multivariate control charts for individual observations. J. Qual. Technol. 24:88–95.
17. Tyagi, S., B. Sharma, P. Singh and R. Dobhal. 2013. Water quality index (WQI) is valuable and unique rating to depict the overall water quality status in a single term that is helpful for the selection of appropriate treatment technique to meet the concerned issues. However, WQI depicts the composite influ. Am. J. water Resour. 1:34–38.
18. Williams, J.D., W.H. Woodall, J.B. Birch and J.O.E.H. Sullivan. 2006. On the Distribution of Hotelling ' s T 2 Statistic Based on the Successive Differences Covariance Matrix Estimator. J. Qual. Technol. 38:217–229.

https://doi.org/10.62500/icrtsda.1.1.39

Proc. 1st International Conference on Recent Trends in Statistics and Data Analytics
Air University Islamabad, Pakistan – May 9, 2024, Vol. 1, pp. 381-391

EVALUATING THE EFFICIENCY OF A WASTEWATER TREATMENT PLANT THOROUGH CAPABILITY INDICES

Arfa[1], Muhammad Kashif[2*] and Muhammad Zafar Iqbal[3]

Department of Mathematics and Statistics, University of Agriculture Faisalabad, Pakistan

ABSTRACT

In traditional wastewater treatment plant (WWTP) assessments, the effectiveness is typically estimated through the percentage removal of Chemical Oxygen Demand (COD), Biochemical Oxygen Demand (BOD), Total Suspended Solids (TSS) and Total Disolved Solids (TDS). The challenge with the conventional approach lies in the absence of a direct comparison between the distribution of these characteristics at the outlet and the specified bounds set by monitoring groups like the Central Pollution Control Board (CPCB).Addressing this gap, the introduction and application of Process Capability Indices (PCIs) based on Probability and Multivariate Process Capability Indices (MPCIs) had been presented in literature to assess how well the wastewater treatment process aligns with the established specifications. While PCIs have been extensively employed in evaluating manufacturing processes, the aim was to extend their utility to the field of environmental engineering. The objective of this study is to apply these indices on two data sets to quantify and to improve the performance of wastewater. From the perspective of environmental engineers, the paper emphasizes the need for assessing the effectiveness of the application of capability indices in wastewater treatment processes and subsequently implementing operation improvements founded on happening these findings. Measuring wastewater treatment process capability analysis utilizing suitable capability indices, drawing insights from secondary data collected through PCRWR website. The results highlight that the application of appropriate capability indices enhances the efficiency of measuring wastewater treatment processes as compared to the conventional practices.

1. INTRODUCTION

The primary goal of wastewater treatment is to purify water by removing pollutants, coarse particles, toxins, and harmful microorganisms, resulting in clean water, or effluent, suitable for discharge into the environment. According to World Vision, over 770 million individuals worldwide do not have access to clean and pure water for drinking and domestic purposes (Silva, 2023).Addressing the significant environmental threat posed by low-quality treatment plants and untreated wastewater necessitates a swift expansion of highly effective, high-capacity wastewater treatment facilities. It is equally important to enhance the efficiency of existing plants. The enhancement of treated wastewater quality not only benefits the environment but also contributes to mitigating water scarcity. The improvement of wastewater treatment efficacy involves initiating a process capability study that employs relevant capability indicators. Statisticians use analysis of process capability, employing capability indices, to assess the proficiency of a process aligns with standards or specifications. Emphasizing that a high-quality wastewater treatment process aligns with the effluent discharge standards mandated by the CPCB is crucial in evaluating wastewater treatment processes using capacity indices (Danu, 2022).To ensure the efficacious functioning of a wastewater treatment plant (WWTP), it is essential to implement sophisticated data monitoring procedures. These procedures involve measuring various parameters, including BOD, COD, dissolved oxygen (DO), TSS, TDS. Additionally, accurate monitoring of pH and temperature is imperative. When assessing the effectiveness of a process, environmental engineers examine variables such as pH, NH4-N, NTotal, fecal coliform, and others in the outflow. They analyze the percentage of BOD, TSS, and other pollutants removed by the wastewater treatment (Rahmat *et al.*, 2022). The assessed demonstration of a sewage treatment plant utilizing the technique of activated Sludge revealed a BOD removal skill of 94.56% and a TSS removal ability of

https://doi.org/10.62500/icrtsda.1.1.39

93.72% (Khadse and Khadse, 2020). In another evaluation, the plant demonstrated a COD deduction efficacy of 69.39% and a BOD eliminate capableness of 62.78% (Chandrakant *et al.*, 2015). Indian standards dictate that the effluent discharged from a wastewater treatment plant should have a BOD not exceeding 10 mg/l and a COD not exceeding 50 mg/l (Khadse and Khadse, 2020). The formulas for calculating BOD and COD removal efficiency consider the values at the inlet and outlet stages. However, these formulas don't incorporate limit specifications for certain attributes during act assessment. The common practice of evaluating performance lacks a direct comparison between the distribution of wastewater treatment process characteristics at the exit phase and release water discharge principles or boundary specification set by the CPCB for these individualities. Recognizing this gap, this paper proposes and utilizes capability indices to compare the result of the wastewater treatment procedure using the process guidelines, quantifying how capably the procedure works. PCIs are employed in industrial settings to gauge the extent to which a process generates data within specified tolerance limits. Typically utilized in Statistical Process Control (SPC) programs, these indices are designed for characteristics that are independent of each other. An established protocol in SPC involves confirming that statistical control is being maintained by the method before initiating a process capability analysis. The manufacturing industry commonly relies on several widely utilized univariate PCIs, such as CP and CPK. These indices are introduced to offer numerical assessments of both process capability and performance, serving as valuable tools for quality assurance. In recent SPC literature, there has been a notable surge of interest in PCIs. Various authors, including Kane and Marcucci and Beazley (Raeisi, 2009) have contributed significantly to this growing body of literature. PCIs have found extensive application in assessing the quality performance of industrial operations. Moreover, their utility extends to the effectual assessment of environmental performance, as highlighted in references (Corbett and Pan, 2002) . Over the past three decades, scientists have devised MPCIs to assess the potency of multivariate processes (Castaldi *et al.*, 2008). Notably, MPCIs leverage multivariate statistical principles, allowing simultaneous consideration of variables and their correlation structure. A recent study (Danu, 2022) has undertaken a comparative analysis of the advantages of both PCIs and MPCIs. Meeting the water demands of households, farms, and factories poses a considerable challenge given the current distribution of water resources. To fulfill these needs, global practices often involve desalinating ocean water or recycling treated wastewater. Water pollution stems from various sources, including both discrete and diffuse contributors. Point sources, such as industrial effluents and sewage discharge, contribute to contamination, as do non-point sources like improper waste disposal, resource mismanagement, pesticide use, agricultural runoff, and accidental spillage of toxic substances. While stringent regulations can address contamination from point sources, combating non-point source pollution requires consumer education and awareness campaigns. Effectively managing water resources necessitates addressing both point and non-point causes of pollution, recognizing that the latter can be significantly mitigated or eliminated.

2. [MATERIALS AND METHODS]

2.1 Study area

PCIS AND MPCIS

Univariate PCIs in the traditional context.

Upper capability indices(CPU) and Lower capability indices(CPL) for PCIs are derived based on the following rules:

1. It is presumed that the process is under statistical stability.

2. Tolerance limits (LSL or USL) define the acceptable range for a quality characteristic.

3. Process measurements (X) are supposed to obey a normal distribution with a mean μ and variance σ^2.The probability density function for this normal distribution is given by:

$$f(x;\mu,\sigma) = \frac{1}{\sigma\sqrt{2\pi}}\, e^{-}\frac{1}{2}\left(\frac{x-\mu}{\sigma}\right), -\infty < x, \mu < \infty \quad \sigma > 0$$

https://doi.org/10.62500/icrtsda.1.1.39

The Capability Indices, namely the CPU and CPL, are defined as:

The upper capability index, given a specified USL, is determined by:

$$\text{CPU} = \frac{\text{USL}-\mu}{3\sigma} \quad (1)$$

In the same way the index of lower capability, provided a specified LSL, is determined by:

$$\text{CPL} = \frac{\text{LSL}-\mu}{3\sigma} \quad (2)$$

If a quality characteristic's tolerance region is defined by both LSL and USL, Cpk is the widely employed capability index, clarify as the min(CPU,CPL) (Khadse and Khadse, 2020).

Requirements for capabilities: A process is deemed incapable when its capability index is below one, indicating inadequacy with respect to specifications. In such cases, adjustments to the σ and/or μ are necessary. Conversely, a technique is considered able to if its capability index is equal to or exceeds 1.The size of the index of capability provides insight into how capable the process aligns with ethics or terms. A capability index value falling between (1.33, 1.50) signifies satisfactory process performance, while a value exceeding 1.5 is indicative of excellent performance.

In practical applications, the factors μ and σ are substituted with the estimation of these $\hat{\mu}$ and $\hat{\sigma}$ figured from sample $X_1, X_2, \ldots, X_n$.

$\hat{\mu} = \bar{X} = \frac{1}{n}\sum_{i=1}^{n} X_i$ and

$\hat{\sigma} = S = \sqrt{\frac{1}{n-1}\sum_{i=1}^{n}(X_i - \bar{X})^2}$.

B. Probability-based PCIs offer a valuable approach to measuring process performance, addressing the challenges associated with constructing indices for both univariate and multivariate setups. In comparison to traditional PCIs and MPCIs(Khadse and Shinde, 2009), probability-based PCIs are particularly beneficial. Given the assumptions we introduce alternative formulations for CPU and CPL below. These unusual forms represent a refined variety of CPU and CPL, providing a smoother characterization of process capability.

$$CPU_{(p)} = -\frac{1}{3}\Phi^{-1}\left(\frac{1-p}{2}\right); \quad (3)$$

Where p=P(X< USL|μ,σ^2)

$$CPL_{(p)} = -\frac{1}{3}\Phi^{-1}\left(\frac{1-p}{2}\right); \quad (4)$$

Where p=P(X> LSL|μ,σ^2)

At this time Φ^{-1} represents the quantile normal distribution standard function. The PCIs, CPU(p) and CPL(p), are projected via $\hat{p}$ by substituting the estimators $\hat{\mu}$ and $\hat{\sigma}$ for the parameters μ and σ.

Remark 1: In the case where a region for acceptance for a worth feature is defined by LSL and USL, an alternative formulation of Cpk is expressed as follows:

$C_{pk(p)}$ Cpk (p) = $-\frac{1}{3}\Phi^{-1}\left(\frac{1-p}{2}\right)$;

Where p=P(LSL<X<USL||μ,σ^2)

The series of a chance element in a normal distribution extends from -∞ near ∞, and utilizing the density function of probability of $-\infty < X < \infty$ is equal to 1. However, in instances of highly capable processes, computational limitations may arise, leading to the situation where the parameter p defined in equations "(3)," "(4)," and Remark 1 equates to 1. In such cases, it is advisable to set p slightly below one, for instance, p=0.99999999.

https://doi.org/10.62500/icrtsda.1.1.39

C. MPCIs based on probability

We introduce Multivariate Process Capability Indices (MPCIs) as another to the multiple versions of CPU(p) and CPL(p). Specifically, we denote these as MCPU(p) and MCPL(p), respectively. The definition of these indices relies on the following assumptions:

1. The task is in a state of statistical control.

2. Each quality traits is associated with a single specification constraints.

3. The quality characteristics, denoted as Xi for i = 1, 2,3, ..., m, follow a Multivariate Normal Distribution (MND) with a mean array μ and a matrix of variance-covariance Σ. The probability density function of the m-dimensional normal distribution for the vector X which is random expressed as follows:

$$f(x) = \frac{1}{(2\pi)^{\frac{m}{2}} |\Sigma|^{\frac{1}{2}}} e^{-(x-\mu)'\Sigma^{\frac{-1}{2}}(x-\mu)/2}$$

$$-\infty<x_i, \mu_i<\infty;\ (i=1,2,3,\ldots..,m)$$

Consider the matrix Σ, which is positive definite

We introduce MPCIs as another to the multiple versions of CPU(p) and CPL(p). Specifically, we denote these as MCPU(p) and MCPL(p), respectively. The definition of these indices relies on the following assumptions:

1. The task is in a state of statistical control.

2. Each quality traits is associated with a single specification constraints.

3. The quality characteristics, denoted as Xi for i = 1, 2,3, ..., m, follow a MND with a mean μ and a variance-covariance Σ. The probability density function with the m-dimensions normal distribution for the pertaining to the random vector X is expressed as follows:

$$f(x) = \frac{1}{(2\pi)^{\frac{m}{2}} |\Sigma|^{\frac{1}{2}}} e^{-(x-\mu)'\Sigma^{\frac{-1}{2}}(x-\mu)/2}$$

$$-\infty<x_i, \mu_i<\infty;\ (i=1,2,3,\ldots..,m)$$

Consider the matrix Σ, which is positive definite(Khadse and Khadse, 2020).

$$MCPU_{(p)} = -\frac{1}{3}\Phi^{-1}\left(\frac{1-p}{2}\right); \quad (5)$$

Where p=P(X< USL|μ, Σ)

$$MCPL_{(p)} = -\frac{1}{3}\Phi^{-1}\left(\frac{1-p}{2}\right); \quad (6)$$

Where p=P(X> LSL|μ, Σ)

3. [RESULTS AND DISCUSSION]

Application of capability analysis in real world studies.

The analysis of capability the wastewater treatment process is conducted based on secondary data extracted from Hudiara Drain(Haq and Ashraf, 2023) and Jhelum District(Hifza *et al.*, 2020)

A. Hudiara Drain study

The wastewater quality in Hudiara Drain reveals consistently elevated levels of BOD and COD throughout the year, exceeding permissible limits at all points along its length. At the entry point in Pakistan (Lallo), average BOD and COD values measured 300 mg/l and 500 mg/l, respectively. Even

https://doi.org/10.62500/icrtsda.1.1.39

within the exit point into the Ravi River (Khurdpur), comparable high levels were observed. Exceedances were particularly notable in February 2021 and May 2020. Numerous studies consistently confirm that BOD and COD levels surpass NEQS limits, emphasizing inadequate treatment of sewage and industrial effluents from both Indian and Pakistani sources. On the other hand, Total Dissolved Solids (TDS), with values peaking in July and reaching their lowest in January. There are different variables in Hudiara Drain data but we use 3 variables and 20 number of observations per variable in our analysis.

Table 1. Data on BOD, COD, and TDS outlet from Hudiara Drain

sample	BOD	COD	TDS
1	287	498	868
2	196	335	917
3	288	481	1038
4	250	477	804
5	237	426	1081
6	221	438	788
7	223	422	1230
8	245	453	660
9	245	451	1175
10	224	416	1028
11	258	466	1280
12	258	484	717
13	232	424	1090
14	234	416	989
15	223	405	870
16	235	455	850
17	281	464	999
18	235	382	835
19	250	394	1029
20	265	481	1035

Capability analysis: In the assessment of waste water treatment method capability using PCIs and MPCIs, we consider the subsequent effluent standards aimed at WWTP, as established via the CPCB(Khadse and Khadse, n.d.).

Table II. Effluent Permissible limits for WWTP

Characteristics	Characteristics limits
BOD	300
COD	500
TDS	1300

The statistics has been verified for outliers employing Grubbs' Test, and the resulting deviations have been identified at a significance level of 5%. There is no outlier in this case.

The histogram shows the distribution of BOD data with a mean of approximately 243.1 mg/1 and a standard deviation of about 23.8 mg/1. The data appears to be slightly skewed to the right, indicating that there are more observations with lower BOD values than higher ones. The red dashed line represents the Upper Specification Limit (USL) for BOD, which is set at 300 mg/1. This limit is often used to define the maximum acceptable BOD level for a specific application or regulatory requirement. From the histogram, we can see that most of the BOD values fall below the USL, indicating that the majority of the observations are within the acceptable range. However, there are a few data points that exceed the USL, suggesting potential issues with BOD levels in those instances. Overall, the histogram provides a visual representation of the BOD distribution and highlights the relationship between the data and the specified upper limit.

https://doi.org/10.62500/icrtsda.1.1.39

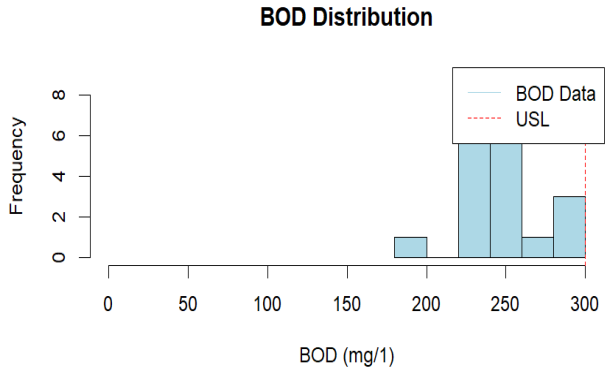

Figure: Histogram of BOD Distribution

Table IV. Sample Mean and SD

Factors	Mean	SD
BOD	244.35	23.65158
COD	438.40	40.65827
TDS	964.15	166.27253

Table V. Correlation matrix

	BOD	COD	TDS
BOD	1.000		
COD	0.7993	1.000	
TDS	0.04328	-0.0638	1.000

Table VI. PCIs based on estimated probabilities

parameters	$\hat{p} = P(X < USL \setminus \hat{\mu}, \hat{\sigma})$	$C\hat{P}U_{(P)}$
BOD	0.9907	0.8668
COD	0.9351	0.61537
TDS	0.9783	0.7652

The estimation of Probability-based MPCI is conducted using equation "(5)," and the obtained values, along with the estimation procedure, are presented.

we take mean vector and variance covariance matrix in Hudiara Drain study, At this point, X= (BOD,COD,TSS) ' monitors multivariate normal distribution through

$$\hat{\mu}=\begin{bmatrix}244.35\\438.40\\964.15\end{bmatrix} \text{ and}$$

$$\hat{\Sigma}=\begin{bmatrix}559.3974 & 768.6421 & 170.2079\\768.6421 & 1653.0947 & -431.5895\\170.2079 & -431.5895 & 27646.5553\end{bmatrix}$$

The estimated probability $\hat{p}$=P(X<(300,500,1300)′)= 0.91299 is calculated using the R software with the `mvtnorm` package (Genz *et al.*, 2020). The resulting estimated value of the Multivariate Capability Index $\widehat{MCPU}(p)$ = 0.57047.

Now In previous, determined the fact estimate of MCPU(p). To establish a 95% confidence interval for MCPU(p), a simulation technique is employed in step five. This involves generating 5000 samples from the forecast multivariate normal distribution per a sample size of 20. For each produced sample, p is

https://doi.org/10.62500/icrtsda.1.1.39

estimated, and subsequently, MCPU(p) is computed ensuing stage four. Through this process, 5000 estimated points of MCPU(p) are obtained. The 2.5th and 97.5th percentiles of these valued serve as the lesser and higher bounds, respectively, of the confidence interval (CI) for MCPU(p) is (0.43229, 0.758443)

Interpretation:

The 95% confidence interval for the MCPU(p) suggests that, based on the given multivariate data, there is a high probability (95%) that the true Maximum Cumulative Probability of non-conformity falls between the estimated lower and upper bounds. This provides a range for the potential extreme values in the dataset, aiding in the assessment of outliers and the understanding of the data's variability. In this case, the wastewater treatment plant is deemed incapable of meeting the effluent discharge standards set by the CPCB. This determination is based on the estimated values of the Multivariate Process Capability Index (MPCI), specifically $M\hat{C}PU(p)$, which is considerably lower than the desirable value of 1.

B. Jhelum District study

This study calculates the show efficacy of Wastewater test results of four tehsils of Jhelum District. Data collected on PCRWR website with pdf (wastewater Assesment and Treatment need Analysis of District Jehlum) . This study include BOD, COD,TSS and TDS. In this study we have different variables but in the analysis we use 4 variables and 42 number of observation per variable(Hifza *et al.*, 2020).

sample	TDS	TSS	COD	BOD
1	964.8	207	146	70
2	671.4	513	50	22
3	118200	12	17760	450
4	696.6	6	114	52
5	1212	66	165	95
6	9588	315	97	65
7	13080	342	175	97
8	1368	1164	110	49
9	1770	672	232	97
10	8196	218	182	92
11	4920	225	53	20
12	1242	162	73	35
13	9756	1156	219	87
14	1073	520	3700	1460
15	1572	1215	531	232
16	792.6	1005	85	50
17	96384	210	4460	77
18	9690	333	301	74
19	107670	240	9900	78
20	505	170	73	42
21	771	340	220	90
22	1143	550	538	236
23	1075	60	97	45
24	1027.8	310	260	270
25	1248	247	446	245
26	1119.6	260	325	157
27	1074.6	90	105	54
28	988.2	250	251	105
29	1314	240	372	195

https://doi.org/10.62500/icrtsda.1.1.39

30	1476	380	266	117
31	1176.6	90	276	137
32	1157.4	150	294	147
33	1734	980	573	310
34	2370	400	1055	512
35	2310	740	783	403
36	2076	840	934	451
37	2019	250	125	53
38	990	260	345	165
39	310.2	30	42	10
40	1006.8	180	292	135
41	183	30	50	18
42	179	672	65	32

Capability analysis: When assessing the capability of the waste water treatment procedure using PCIs and MPCI, we consider the waste standards established for WWTP in the CPCB (Khadse and Khadse, n.d.,2020).

Table II. Effluent Discharged Standards for WWTP

Characteristics	Characteristics limits
TDS	3500
TSS	200
COD	150
BOD	80

Data has been tested on behalf of outlier utilizing Grubbs' test and succeeding outliers are detected at a significance level of 5%."

Table III. Outliers consuming Grubb's Test

Variable	Sample numbers	Outlier
TDS	3	118200
TSS	15	1215
COD	3	17760
BOD	14	1460

Therefore more analysis sample num. 3 , sample num.15 and sample num. 14 omitted since the dataset.

The information has been assessed to multivariate normality using Royston H test. The test indicates that the data doesn't deviate significantly from a MND at the 5% significance, as the detected p value is 0.001.Since decide that X= (BOD,COD,TSS,TDS) ' follows MND and variables BOD,COD and TDS has a normal distribution.

Table IV. Sample mean and standard deviation

parameters	Mean	SD
TDS	7570.66	22502.54
TSS	368.03	312.13
COD	619.21	1682.97
BOD	127.92	119.97

Table V. Correlation matrix

Parameters	TDS	TSS	COD	BOD
TDS	1.0000	-0.0848	0.9286	-0.1068
TSS	-0.0848	1.0000	-0.0535	0.2904
COD	0.9286	-0.0535	1.0000	0.0442

https://doi.org/10.62500/icrtsda.1.1.39

BOD	-0.1068	0.2904	0.0442	1.0000

Table VI. PCIs based on estimated probabilities

Variable	$\hat{p}$ = P(X<USL\$\hat{\mu}$, $\hat{\sigma}$)	C$\hat{P}$U (p)
TDS	0.428224	0.1884793
TSS	0.295178	0.1262731
COD	0.3902009	0.1701201
BOD	0.3447804	0.148841

The estimation of the Probability-based Multivariate Process Capability Index (MPCI) is conducted using equation "(5)," and the obtained value, along with the approximation procedure, is presented under.

Now, X= (BOD,COD,TSS,TDS)' has multivariate normal distribution having

$$\hat{\mu}=\begin{bmatrix}7570.6564\\368.0256\\619.2051\\127.9231\end{bmatrix} \text{ and}$$

$$\hat{\Sigma}=\begin{bmatrix}506364471.6 & -595859.71 & 35167464.288 & -288369.638\\ -595859.7 & 97424.82 & -28095.926 & 10873.844\\ 35167464.3 & -28095.93 & 2832399.009 & 8915.595\\ -288369.6 & 10873.84 & 8915.595 & 14393.389\end{bmatrix}$$

$\hat{\boldsymbol{p}}$=P(X<(3500,200,150,80)′)= 0.04445963. That chance is calculated applying R Studio exhibiting mvtnorm package (Genz *et al.*, 2020).$\widehat{\boldsymbol{MCPU}}(\boldsymbol{p})$ = 0.01858**.**

In previous phase, there are recorded the estimate point of MCPU(p). To establish a 95% confidence interval for MCPU(p), a simulation technique is employed in step five. This involves generating 5000 number ofsamples from the multivariate normal distribution predicted with a sample size of 39. For every made sample, p is estimated, and subsequently, MCPU(p) is computed following step 4. This process yields 5000 point estimates of MCPU(p). The lower and higher bounds of the CI for MCPU(p) are determined by computing the 2.5th and 97.5th percentiles of these estimated values. Following step 5, the resulting 95% CI for MCPU(p) is (0.005987643,0.03748111).

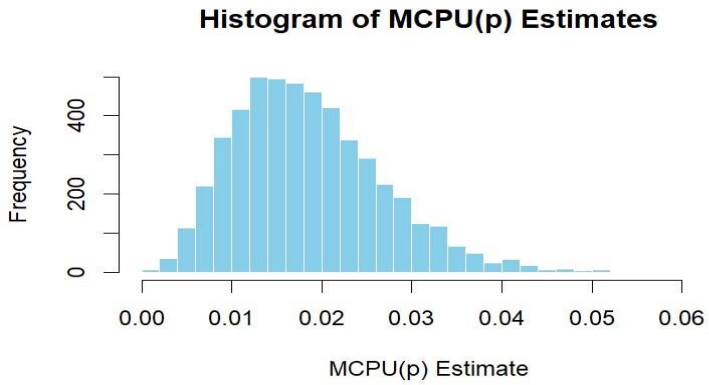

Figure: Histogram of MCPU estimator

Interpretation: The histogram shows the distribution of MCPU(p) estimates based on 5000 simulated samples from a multivariate normal distribution. Each estimate is calculated using the formula $MCPU_{(p)}$

https://doi.org/10.62500/icrtsda.1.1.39

= qnorm$(1 - P_sample)/2)/(-3)$, where P_sample is the probability of the sample falling below the upper specification limit (USL).The x-axis represents the MCPU(p) estimates, and the y-axis represents the frequency of each estimate in the simulated samples. The histogram is divided into 30 bins to visualize the distribution.And we can observe in the histogram the central tendency and spread of the MCPU(p) estimates. The shape of the histogram provides insights into the variability and skewness of the estimates. The 2.5th and 97.5th percentiles of the estimates are also calculated and can be used to understand the range of likely values for MCPU(p).Overall, the histogram provides a visual representation of the distribution of MCPU(p) estimates, which can be valuable for understanding the performance of the estimator in your context.

6. COMMENTS AND CONCLUSION

The conventional method of assessing the performance of a wastewater treatment plant lacks a direct comparison between the distribution of the wastewater treatment process at the passage stage and the sewage discharge principles or specification limits established by the CPCB. Recognizing this gap, this paper introduces and utilizes probability-driven PCIs and MPCIs. These indices compare the output of the waste water treatment method with the process provisions, quantifying the manner in which suitable the process achieves. Capability indices, generally applied in estimating the quality performance of industrial processes, prove effective in assessing wastewater treatment plant performance. Two WWTP are studied over capability analysis using the clear probability-based PCIs and MPCIs. Mutually plants are found to be unable of meeting CPCB standards. While both plants fall short of the standards, the WWTP in Gadli village, Kaithal town, Haryana, India, demonstrates slightly better capability compared to the plant in Sector 8, Charkop, Mumbai, Maharashtra, India. This observation is supported by the larger estimated Multivariate Process Capability Index (MPCI) for the former plant. Root cause analysis is essential to identify the reasons for the low capability and improve the performance of these plants. The proposed definitions of probability-based PCIs and MPCIs can be extended to non-multivariate normal processes, considering the conforming probability basis. Large samples are necessary for obtaining accurate and precise estimates of PCIs or MPCIs.

REFERENCES

1. Castaldi, P., G. Garau and P. Melis. 2008. Maturity assessment of compost from municipal solid waste through the study of enzyme activities and water-soluble fractions. *Waste Manag.* 28:534–540.
2. Chandrakant, G., P. Jaswanth, S. Reddy and G. Kiranmal. 2015. Design & performance evaluation of wastewater treatment plant-D at Tirumala. *Int. J. Sci. Eng. Res.* 6:1672–1688.
3. Corbett, C.J. and J.-N. Pan. 2002. Evaluating environmental performance using statistical process control techniques. *Eur. J. Oper. Res.* 139:68–83.
4. Danu, R. 2022. An Innovative Condition Assessment Method for Wastewater Treatment Facilities to Promote Long-Term Sustainability in Management and Operations. *Math. Stat. Eng. Appl.* 71:592–601.
5. Genz, A., F. Bretz, T. Miwa, X. Mi, F. Leisch, F. Scheipl, B. Bornkamp, M. Maechler, T. Hothorn and M.T. Hothorn. 2020. Package 'mvtnorm.' *J. Comput. Graph. Stat.* 11:950–971.
6. Hifza, R., N. Farah, A. Fauzia, I. Saiqa and M. Ashraf. 2020. Wastewater assessment and treatment needs analysis of District Jhelum. *Pakistan Counc. Res. Water Resour.* 52.
7. Haq, Z.U. and M. Ashraf, (2023). A Closer Look at the Hudiara Drain: Threats to the Ecosystem Health. Pakistan Council of Research in Water Resources (PCRWR) Islamabad, pp.29.
8. Khadse, K.G. and A.K. Khadse. 2020. Assessment of Wastewater Treatment Plant Performance using Capability Indices. 9:267–272.
9. Khadse, K.G. and A.K. Khadse. n.d. Assessment of Wastewater Treatment Plant Performance using Capability Indices.

10. Khadse, K.G. and R.L. Shinde. 2009. Probability-based process capability indices. *Commun. Stat. Comput.* 38:884–904.
11. Raeisi, S. 2009. Multivariate process capability indices on the presence of priority for quality characteristics. 5:27–36.
12. Rahmat, S., W.A.H. Altowayti, N. Othman, S.M. Asharuddin, F. Saeed, S. Basurra, T.A.E. Eisa and S. Shahir. 2022. Prediction of Wastewater Treatment Plant Performance Using Multivariate Statistical Analysis: A Case Study of a Regional Sewage Treatment Plant in Melaka, Malaysia. *Water* 14:3297.
13. Shakir, S.K., A. Azizullah, W. Murad, M.K. Daud, F. Nabeela, H. Rahman, S. ur Rehman and D.-P. Häder. 2017. Toxic metal pollution in Pakistan and its possible risks to public health. *Rev. Environ. Contam. Toxicol. Vol. 242* 1–60.
14. Silva, J.A. 2023. Wastewater treatment and reuse for sustainable water resources management: a systematic literature review. *Sustainability* 15:10940.

https://doi.org/10.62500/icrtsda.1.1.40

Proc. 1st International Conference on Recent Trends in Statistics and Data Analytics
Air University Islamabad, Pakistan – May 9, 2024, Vol. 1, pp. 392-400

SOLUTION OF ELECTRO-OSMOTIC COUETTE–POISEUILLE FLOW OF MHD POWER-LAW NANOFLUID WITH ENTROPY GENERATION

Saba Liaquat[1], Dr. Madiha Ghamkhar[2], Asra Ayub[3], Saira Iftikhar[4] and Dr. Muhammad Zafar Iqbal[5]

Department of Mathematics and Statistics, University of Agriculture Faisalabad, Pakistan

ABSTRACT

The primary goal of this research is to create a novel mathematical model for the electro-osmotic flow of Couette-Poiseuille nanofluids. The base fluid will be considered the power-law model, which is coated with aluminum oxide (Al_2O_3) nanoparticles. While the lower wall stays fixed, the flow is created by the top wall moving uniformly in the axial direction, and a mathematical solution for the behavior of a nonlinear ordinary differential equation flow is discovered. A constant pressure gradient, magnetic field, and the effects of entropy formation are evaluated. Furthermore, the physical characteristics of the most significant major elements, including the magnetic parameter, electro-osmotic parameter, power law fluid parameter, Brinkman number, Nusselt number are adequately outlined by various graphs and tables. The obtained results are compared with the literature.

Keywords: electro-osmotic flow; power law fluid; nanoparticles; MHD; entropy generation.

1. INTRODUCTION

In laboratories and technical applications for manufacturing, conventional fluids are commonly employed. A variety of tests and measures are being established to enhance heat transmission properties. The attachment of fluids into nanoparticles significantly improved in a manufacturing environment. We discussed the thermal conductivity measurements and enhancements of a variety Nano-fluids. And base heat transfer was used (Al_2O_3 ,MgO , ZnO, SiO_2, and TiO_2) suspended in carrier fluids (water, mineral oil, and ethylene glycol),etc.(Choi and Eastman) have made pioneering contributions to Nano-fluids.

In addition, power-laws have drawn interest of numerous scientists because they accurately explain the fluid behaviour of shear-dependent fluids. The hydrodynamic interaction of two swimmers in a power-law fluid was recently studied (Ouyang *et al.*).

Microchannels and electric-powered fluid use electro-osmotic flow, also referred to as electro-osmosis. Investigations were made into how non-Newtonian fluids affected electro-osmotic flow (Zhao and Yang).(Kang *et al.*) examined dynamic feature of the electro-osmosis in a cylindrical micro-capillary. (Das and Chakraborty) proposed mathematical models for the thermo solutal transport of unconventional liquids under the effect of electro-osmosis.

Furthermore, several scientists have carried out encouraging studies on nanoparticles. (Makinde and Chinyoka) examined the unsteady flow and transmission of a dusty fluid between two parallel plates with variable viscosity and electric conductivity. In vertical channels with asymmetric heating, (Malvandi and Ganji) have studied impact of Nano-particle movement on hydro-magnetic mixed convection of aluminum oxide Nano-fluid. (Vasu and De) investigated a mathematical model of electro-osmosis in a rectangular, narrow channel. (Ellahi *et al.*) studied heat transfers in power-law Nano-fluids. (Sarkar and Ganguly) presented heat transfer properties of thermally completely transformed magnetohydrodynamic flows in small channels.

Numerous applications, including diffusion and Joule heating, have recently motivated prominent writers to research entropy formation. (Bhatti *et al.*, 2017) demonstrate the effects of MHD-generated entropy production on electro-osmosis. (Nuwairan and Souayeh) studied Gold Nanoparticle

https://doi.org/10.62500/icrtsda.1.1.40

Transport during MHD electro-osmosis in a Peristaltic microchannel for Biomedical Treatment. The non-dimensional problems have been solved numerically. They performed a numerical analysis of entropy generation in nanofluids flowing through wavy walls and suspended with nanoparticles in water as the base fluid (Cho and Chen).

(Escandón *et al.*) determined a semi-analytical solution that was used for the entropy generation of complex fluids in micro-channels. (Ranjit and Shit) studied entropy production in electro-osmosis by evenly distributed peristaltic transport. (Xie and Jian) observed the entropy generation of magneto-hydrodynamic electro-osmotic flow. Graphs were used to evaluate how physical variables affected the amount of flow.

2. PROBLEM DESIGN

2.1. PHYSICAL CONSIDERATION

Consider the uniform and incompressible Nano-fluids that flow over horizontally parallel plates. The wall at y = a is moving with constant speed U*, whereas the second wall remains fixed at $\bar{y} = -a$. The electric double layer potential is represented by: the bottom wall's zeta potential is represented by ξ_1, the upper wall's zeta potential is represented by ξ_2, and the channel's overall width is represented by 2a. The homogeneous transverse magnetic field is denoted as B_0.

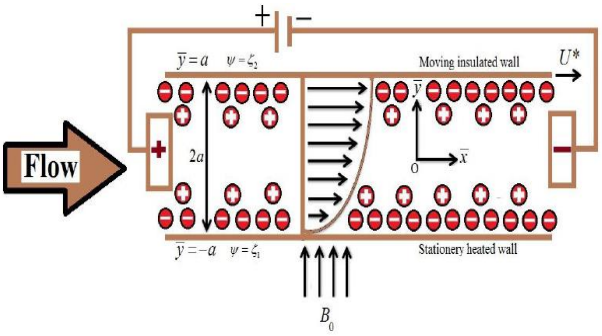

Figure 4.1

2.2. ELECTRICAL POTENTIAL DISTRIBUTION

Gouy-Chapman proposed the diffuse double-layer model. They took ionized thermal motion into consideration. Counter-ions are typically driven away from the surface by thermal variations. According to Gouy and Chapman, the poission equation can be used to define the electric double layer (ELD) potential for a planer surface:

$$\frac{\partial^2 \bar{\psi}}{\partial \bar{x}^2} + \frac{\partial^2 \bar{\psi}}{\partial \bar{y}^2} = -\frac{\bar{\rho}_e(\bar{y})}{\varepsilon\varepsilon_0} \tag{1}$$

The EDL potential distribution for a symmetrical ionic solution can be calculated using the non-linear Poisson-Boltzmann equation, in these circumstances can be transformed as follows equation (1) becomes:

$$\nabla^2\psi = k^2\psi, k = \left(\frac{2n_0 z^2 e^2}{k_B T \varepsilon\varepsilon_0}\right)^{1/2}. \tag{2}$$

Different materials and zeta potentials are used to create the channels plates.

$$\bar{\psi} = \zeta_1 \, at \, \bar{y} = -a \, and \, \bar{\psi} = \zeta_2 \, at \, \bar{y} = a. \tag{3}$$

The electrical potential within the influence of (3) can be investigated as follows:

https://doi.org/10.62500/icrtsda.1.1.40

$$\bar{\psi}(\bar{y}) = \frac{\zeta_1 Sinh(\bar{\kappa}(a-\bar{y})) + \zeta_2 Sinh(\bar{\kappa}(a+\bar{y}))}{Sin(2a\kappa)} \tag{4}$$

Beyond a charged particle, the external electric force $\bar{p}_e E$, known as electro-kinetic force, is generated. In addition to electric charge density $\bar{p}_e(\bar{y})$, it is defined as:

$$\bar{\rho}_e(\bar{y}) = -\varepsilon \bar{\kappa}^2 \frac{\zeta_1 Sinh(\bar{\kappa}(a-\bar{y})) + \zeta_2 Sinh(\bar{\kappa}(a+\bar{y}))}{Sin(2a\kappa)} \tag{5}$$

2.3. POWER LAW MODEL

The power law fluid model listed below is utilized in the present investigation.

$$\tau = \mu_{nf}(\frac{\partial \bar{u}}{\partial \bar{y}})^{n-1}(\frac{\partial \bar{u}}{\partial \bar{y}}) = \{\mu_{nf}(\frac{\partial \bar{u}}{\partial \bar{y}})^n \; for \; \frac{\partial \bar{u}}{\partial \bar{y}} > 0, -\mu_{nf}(\frac{\partial \bar{u}}{\partial \bar{y}})^n \; for \; \frac{\partial \bar{u}}{\partial \bar{y}} < 0. \tag{6}$$

where τ is shear stress, n is index of movement behavior, μ_{nf} is Nano-fluid viscosity, δ is index of consistency

$$\mu_{nf} = (123\phi^2 + 7.3\phi + 1)\,\mu_f \tag{7}$$

In the discussion that follows, the base fluid's viscosity is assumed to be

$$\mu_f = \delta(\frac{\partial \bar{u}}{\partial \bar{y}})^{n-1}. \tag{8}$$

When n = 1, a fluid is said to be Newtonian, while n<1 and n > 1 indicate, correspondingly, the shear-thinning and shear-thickening of fluids. The following shear stress for the non-Newtonian power-law model:

$$\tau = \delta(123\phi^2 + 7.3\phi + 1)(\frac{\partial \bar{u}}{\partial \bar{y}})(\frac{\partial \bar{u}}{\partial \bar{y}})^{n-1}. \tag{9}$$

2.4. GOVERNING EQUATIONS

An upper wall's movement causes the electro-osmotic flow to occur in the channel, whereas an applied electric field causes the flow around the channel's walls. Current flow is governed by the following equations:

$$\nabla.V = 0 \tag{10}$$

$$(V.\nabla)V = \frac{1}{\rho_{nf}}(-\nabla p + \nabla.\tau + Bodyforce) \tag{11}$$

$$(V.\nabla)T = \alpha_{nf}\nabla^2 T + \frac{1}{(\rho Cp)_{nf}\sigma_{nf}} J^2 + \frac{1}{(\rho Cp)_{nf}}\Gamma \tag{12}$$

where V is velocity, T is temperature, Γ is viscous of dissipation. Magnetic, electrical, and buoyancy effects are all part of the body force.

https://doi.org/10.62500/icrtsda.1.1.40

$$Body\ force = (J \times B) + \bar{\rho}_e E + (\rho\beta)_{nf}\, g(T - T_w), \tag{13}$$

where $(J \times B)$ is Lorentz force, $\bar{\rho}_e E$ is External Electric force, $(\rho\beta)_{nf}\, g(T - T_w)$ is Buoyancy force and

$$\Gamma = \mu_{nf} \left(\frac{\partial \bar{u}}{\partial \bar{y}}\right)^2. \tag{14}$$

It results in the following joules of heating effects when Lorentz force is applied:

$$J \times B = (-\sigma_{nf}\, B_0 \bar{u}, 0, 0) and \frac{1}{\sigma_{nf}} J^2 = \sigma_{nf} B_0^{\,2} \bar{u}^2, \tag{15}$$

After removing the axial heat conductions at the walls, the governing equation becomes

$$\frac{\partial \bar{P}}{\partial \bar{x}} = \mu_{nf} \frac{\partial^2 \bar{u}}{\partial \bar{y}^2} - \sigma_{nf} B_0^{\,2} \bar{u} + (\rho\beta)_{nf} (T - Tw) g + \bar{\rho}_e(\bar{y}) E_x. \tag{16}$$

$$\bar{u} \frac{\partial T}{\partial \bar{x}} = \alpha_{nf} \frac{\partial^2 T}{\partial \bar{y}^2} + \frac{\sigma_{nf} B_0^{\,2}}{(\rho C_p)_f} \bar{u}^2 + \frac{\mu_{nf}}{(\rho C_p)_{nf}} \left(\frac{\partial \bar{u}}{\partial \bar{y}}\right)^2. \tag{17}$$

The boundary conditions are as follows:

$$(At\ upper\ wall): \bar{u} = U^*, k_f \frac{\partial T}{\partial \bar{y}} = 0\ at\ \bar{y} = a,$$
$$(At\ lower\ wall): \bar{u} = 0, -k_f \frac{\partial T}{\partial \bar{y}} = q_w\ at\ \bar{y} = -a. \tag{18}$$

The effective density, Heat capability, Thermal and Electrical conductivities of a Nano fluid are respectively given

$$\frac{\rho_{nf}}{\rho_p} = \left[(1-\phi)\frac{\rho_f}{\rho_p} + \phi\right]. \tag{19}$$

$$\frac{(\rho C_p)_{nf}}{(\rho C_p)_p} = \left[(1-\phi)\frac{(\rho C_p)_f}{(\rho C_p)_p} + \phi\right]. \tag{20}$$

$$\frac{(k)_{nf}}{(k)_f} = (4.97\phi^2 + 2.72\phi + 1). \tag{21}$$

$$\frac{\sigma_{nf}}{\sigma_f} = \left[1 + \frac{3(\frac{\sigma_p}{\sigma_f} - 1)\phi}{(\frac{\sigma_p}{\sigma_f} + 2) - (\frac{\sigma_p}{\sigma_f} - 1)\phi}\right]. \tag{22}$$

The following dimensionless transformations

$$\bar{y} = ay, \bar{u} = u_m u, U^* = u_m U, \bar{p} = p_f u_m^{\,2} p(a/u_m)^n, \theta = \frac{T - T_w}{q_w a / f},$$
$$\bar{\rho_e} = -(\varepsilon\zeta 1/a^2)\rho_e, \kappa = \bar{\kappa}/a, \bar{\psi} = \bar{\psi}/\zeta, \tag{23}$$

https://doi.org/10.62500/icrtsda.1.1.40

Transform Equations (16) and (17) by using (23) in the dimensionless form as:

$$(123\phi^2+7.3\phi+1)n(\frac{\partial \bar{u}}{\partial \bar{y}})^{n-1}\frac{\partial^2 \bar{u}}{\partial \bar{y}^2}-A^4M^2u+A_3Gr\theta+B_u\rho_e-\mathrm{Re}\,P=0. \tag{24}$$

$$(4.97\phi^2+2.72\phi+1)\frac{\partial^2\theta}{\partial y^2}+Br(123\phi^2+7.3\phi+1)(\frac{\partial \bar{u}}{\partial \bar{y}})^{n+1}-\gamma B_1u+BrM^2A_4u^2=0. \tag{25}$$

$$u=U,\frac{\partial\theta}{\partial y}=0 \quad aty=1(upper\ wall),$$
$$u=0,\frac{\partial\theta}{\partial y}=-1\ aty=-1(Lower\ wall). \tag{26}$$

In which

$$Gr=\frac{(\rho\beta)_f gq_w a^3}{\delta k_f u_m}\left(\frac{a}{u_m}\right)^{n-1},Re=\frac{\rho_f u_m a}{\delta}\left(\frac{a}{u_m}\right)^{n-1},M^2=\frac{\sigma_f B_0{}^2a^2}{\delta}\left(\frac{a}{u_m}\right)^{n-1},$$

$$Br=\frac{\delta u_m{}^2}{q_w a}\left(\frac{a}{u_m}\right)^{1-n},U_{Hs}=-\frac{\varepsilon\zeta 1E_x}{\delta}\left(\frac{a}{u_m}\right)^{n-1},\beta_u=\frac{U_{Hs}}{u_m},$$
$$\gamma=\frac{k_f u_m a}{\alpha_f q_w}\frac{\partial T}{\partial x},\rho e(y)=\kappa^2(\frac{Sinh(\kappa(1-y))+R\zeta Sinh(\kappa(1+y))}{Sin(2\kappa)}),$$
$$\alpha_f=\frac{(\rho Cp)_f}{k_f},A_4=\frac{\sigma_{nf}}{\sigma_f},A_3=\frac{(\rho\beta)_{nf}}{(\rho\beta)_f},B_1=\frac{(\rho C_p)_{nf}}{(\rho C_p)_f},R\zeta=\zeta 2/\zeta 1. \tag{27}$$

Assuming $u_m=-(a^2/2\mu_f)\partial p/\partial \bar{x}$ are the highest speeds that may be reached b/w two plates, respectively, and that β_u is the ratio of the highest fluid speed to the electro-osmotic speed, U_{Hs}. Table 1 below provides an illustration of the Thermo-physical characteristics of alumina and the base fluid, polyvinyl chloride (PVC).

Table: 2.1 Physical properties of PVC and Al_2O_3

roperties		Cp (J kg^{-1}K^{-1})	×10^{-5}(K^{-1})	(kg m^{-3})	Wm^{-1}K^{-1})	(Ns m^{-2})
AL_2O_3		775	8.6×10^{-1}	3980	45	……
	2%	4117.56	21.9	006.24	0.586	0.0015
	3%	4085.34	21.8	010.25	0.579	0.00107
PVC	4%	4053.12	21.8	014.27	0.572	0.00114
	5%	4020.9	21.8	018.29	0.718	0.00114
	6%	3988.68	21.8	022.31	0.559	0.00116
	7%	3956.46	21.7	026.33	0.552	0.00119

https://doi.org/10.62500/icrtsda.1.1.40

2.5. ENTROPY GENERATION

The entropy generation of local volumetric rate can be described as:

$$S_G = \frac{k_{nf}}{T^2_w}\left(\frac{\partial \bar{T}}{\partial \bar{y}}\right)^2 + \frac{\mu_{nf}}{T_w}\left(\frac{\partial \bar{u}}{\partial \bar{y}}\right)^2 + \frac{\sigma_{nf} B^2_0 \bar{u}^2}{T_w} + \frac{\rho_e(\bar{y}) E_x}{T_w}. \tag{28}$$

The characteristic entropy generation can be written as follows:

$$S_0 = \frac{q^2_w}{k_f T^2_w}. \tag{29}$$

Using (23), the creation of non-dimensional total entropy becomes

$$Ns = \left(4.97\phi^2 + 2.72\phi + 1\right)\left(\frac{\partial \theta}{\partial y}\right)^2 + \frac{Br}{\Omega}\left(\left(123\phi^2 + 7.3\phi + 1\right)\left(\frac{\partial u}{\partial y}\right)^{n+1} + A_4 M^2 u^2 + \beta_u \rho_e u\right) \tag{30}$$

where M is magnetic field, Br is Brinkman number, B_u is volumetric volume expansion, ρ_e is dimensional electric charge density, Ω is dimensionless temperature difference. These parameters are as follows:

$$M^2 = \frac{\sigma_f B_0^2 a^2}{\delta}\left(\frac{a}{u_m}\right)^{n-1}, Br = \frac{\delta u_m^2}{q_w a}\left(\frac{a}{u_m}\right)^{1-n},$$
$$\beta_u = \frac{U_{Hs}}{u_m}, \quad p_e = -\frac{\varepsilon \zeta 1 E_x}{a^2} p_e, \; \Omega = \frac{q_w a}{k_f T_w}. \tag{31}$$

$$\text{Be} = \frac{\text{Entropy due to heat transfer}}{\text{Total entropy geeration}}, \tag{32}$$

$$Be = \frac{\left(4.97\phi^2 + 2.72\phi + 1\right)\left(\frac{\partial \theta}{\partial y}\right)^2}{\left(4.97\phi^2 + 2.72\phi + 1\right)\left(\frac{\partial \theta}{\partial y}\right)^2 + \frac{Br}{\Omega}\left(\left(123\phi^2 + 7.3\phi + 1\right)\left(\frac{\partial u}{\partial y}\right)^{n+1} + A_4 M^2 u^2 + \beta_u \rho_e u\right)}. \tag{33}$$

3. DISCUSSION OF RESULTS

A magnetized power-rule Nano-fluid beside the parallel walls is the subject of current research into flow and entropy. At the same pressure, the effects of the Nano-fluid can be determined using the upper plate's motion and the electric body force. Systematic research is done on flow and entropy production in a Nano-fluid's magnetized power law in the horizontal channel. Heat is generated by the lower(inferior) wall, while the temperature is sustained by the upper(superior) wall. The Gouy-Chapman model, commonly referred to as the ionic cloud model, differs from the Helmholtz model in several ways. The Helmholtz model predicts constant differential capacitance, which means that it does not change with potential. However, this problem has been fixed in the Gouy-Chapman model.

Figures provide a graphic representation of the special effects of various significant constraints. We get different results, By using different parameters, which can be explained as φ = 0.03, n = 0.764 (PVC 3%), M = 2, γ = 10, β_u = 0.3, Gr = 2.366, κ = 8, Br = 1and Re = 442.956.The effects of modified magnetic parameter (M) on temperature distribution of nanofluid are shown in Figures 2. They

https://doi.org/10.62500/icrtsda.1.1.40

demonstrate that as the magnetic factor rises, the temperature profile rises. Figure 3 illustrates the relationship between temperature and volume fraction. By raising the volume fraction, the temperature profile rises. Different concentrations of PVC on the temperature field Figure 4 show that when PVC increases, the velocity distribution increases. Figure 5 demonstrates how a channel's flow exceeds and increases to its maximum value. The effect of magnetic field (M) on entropy generation is shown in Figure 6. It can be seen that when M rises, left side of the entropy generation lowers with the least amount of energy loss at y = - 0.25; thereafter, increasing behaviour is seen. Figure 7 illustrates the effect of Brinkmann number (Br) on entropy production, showing that as Br rises, entropy generation drops on the left-side and reaches its smallest energy loss at y = 0 before increasing in a tendency on the left side. Figure 8 illustrates the effect of $Br\Omega^{-1}$ (dimensionless temperature factor) on entropy generation, and it shows that entropy generation reduces on the lower wall and takes the lowest energy loss (at y = 0.5).

Figure: 3.1 Result of Magnetic parameter (M) on temperature

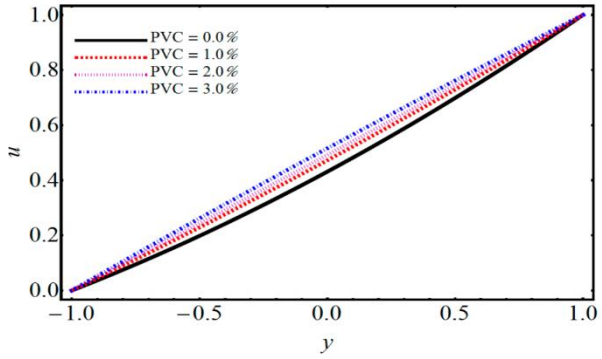

Figure: 3.2 Result of φ on temperature

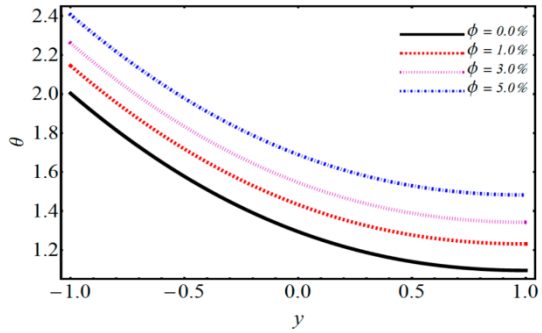

https://doi.org/10.62500/icrtsda.1.1.40

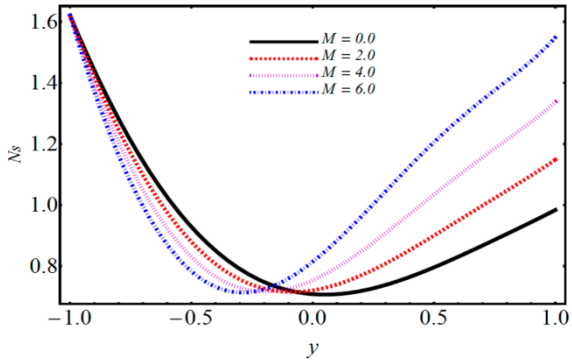

Figure: 3.3 Result of PVC concentration on velocity

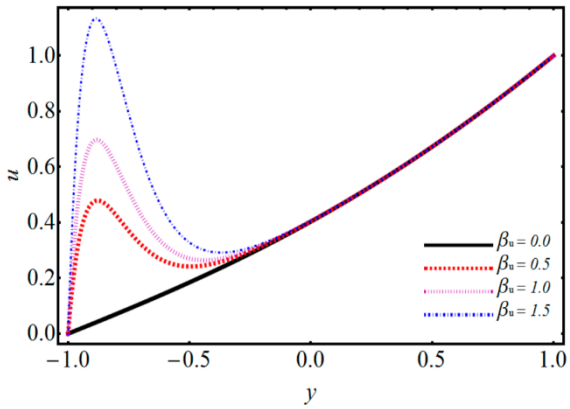

Figure: 3.4 Result of β_u on velocity

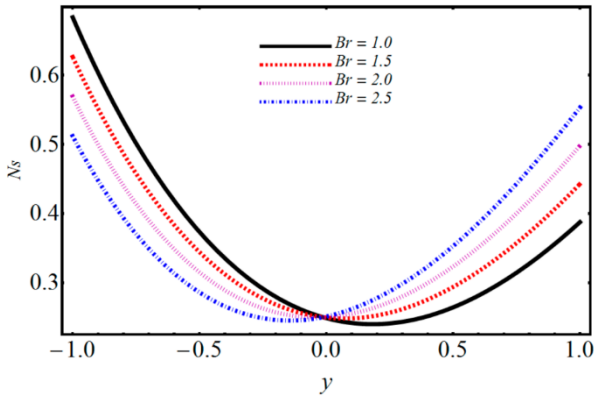

Figure: 3.5 Result of the magnetic parameter on entropy generation

https://doi.org/10.62500/icrtsda.1.1.40

Figure: 3.6 Result of Brinkman number Br on entropy generation

Figure: 3.7 Result of $Br\Omega^{-1}$ on entropy generation

4. COMMENTS AND CONCLUSION

The effects of entropy generation on Nano-fluid power law over a parallel channel (horizontal) are studied in this research. In this approach one movable wall and the other is stationary are existing. The effect of a mixed an electrical double layer and convection magnetic field has joined

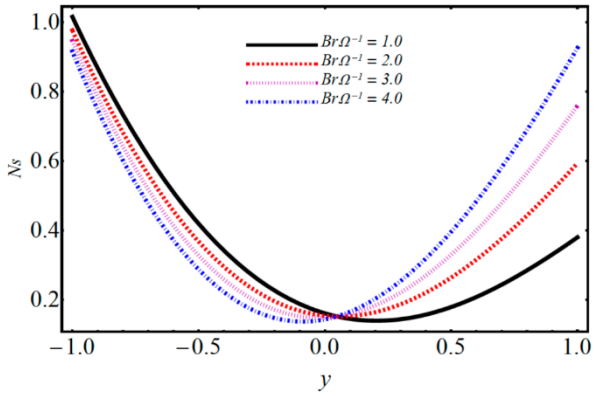

for momentum conduct. By moving the upper wall, flow is created in an axial direction. The key conclusions are as follows:

• The velocity of the Nano-fluid falls as the nanoparticle volume fraction and magnetic parameter increase, but the temperature profile rises.

• While a drop in temperature is being observed, the velocity profile is increasing with increasing PVC.

• For rising values and ratio between u_m and U_{Hs}, temperature and velocity demonstrate similar behaviour.

• When a magnetic parameter snowballs, the Nusselt number rises; however, it falls when the Brinkman number, volume fraction, electro-osmotic variables, the ratio of U_{Hs} to u_m, and other parameters rise.

• The entropy generation rises with rise of magnetic field M volumetric volume expansion β, and κ, whereas it falls with an increase of Brinkman number and $Br\Omega^{-1}$.

• Entropy generation has a dual behavior for both increasing and decreasing R_ζ values.

REFERENCES

1) Bhatti, M.M., Sheikholeslami. M. and Zeeshan. A. (2017). Entropy analysis on electro-kinetically modulated peristaltic propulsion of magnetized nanofluid flow through a microchannel. *Entropy*, 19,481.

2) Cho, C.C. and Chen. C.L. (2012). Natural convection heat transfer performance in complex-wavy-wall enclosed cavity filled with nanofluid. *International Journal of Thermal Sciences*, 60, 255-263.

3) Choi, S.U. and Eastman. J.A. (1995). Enhancing thermal conductivity of fluids with nanoparticles, Argonne National Lab.(ANL), Argonne, IL (United States).

4) Das, S. and Chakraborty. S. (2006). Analytical solutions for velocity, temperature and concentration distribution in electroosmotic microchannel flows of a non-Newtonian bio-fluid. *Analytica chimica acta*, 559, 15-24.

https://doi.org/10.62500/icrtsda.1.1.40

5) Ellahi, R., Hassan. M. and Zeeshan. A. (2016). A study of heat transfer in power law nanofluid. *Thermal Science*, 20, 2015-2026.
6) Escandón, J., Bautista. O. and Mendez. F. (2013). Entropy generation in purely electroosmotic flows of non-Newtonian fluids in a microchannel. *Energy*, 55, 486-496.
7) Kang, Y., Yang. C. and Huang. X. (2002). Dynamic aspects of electroosmotic flow in a cylindrical microcapillary. *International Journal of Engineering Science*, 40, 2203-2221.
8) Makinde, O.D. and Chinyoka. T. (2010). MHD transient flows and heat transfer of dusty fluid in a channel with variable physical properties and Navier slip condition. *Computers & Mathematics with Applications*, 60, 660-669.
9) Malvandi, A. and Ganji. D. (2015). Effects of nanoparticle migration on hydromagnetic mixed convection of alumina/water nanofluid in vertical channels with asymmetric heating. *Physica E: Low-dimensional Systems and Nanostructures*, 66, 181-196.
10) Nuwairan, M.A. and Souayeh. B. (2022). Simulation of gold nanoparticle transport during MHD electroosmotic flow in a peristaltic micro-channel for biomedical treatment. *Micromachines*, 13, 374.
11) Ouyang, Z., Lin. J. and Ku. X. (2019). Hydrodynamic interaction between a pair of swimmers in power-law fluid. *International Journal of Non-Linear Mechanics*, 108, 72-80.
12) Ranjit, N. and Shit. G. (2017). Entropy generation on electro-osmotic flow pumping by a uniform peristaltic wave under magnetic environment. *Energy*, 128, 649-660.
13) Sarkar, S. and Ganguly. G. (2015). Fully developed thermal transport in combined pressure and electroosmotically driven flow of nanofluid in a microchannel under the effect of a magnetic field. *Microfluidics and Nanofluidics*, 18, 623-636.
14) Vasu, N. and De. S. (2010). Electroosmotic flow of power-law fluids at high zeta potentials. *Colloids and Surfaces A: Physicochemical and Engineering Aspects*, 368, 44-52.
15) Xie, Z. and Jian. Y. (2018). Entropy generation of magnetohydrodynamic electroosmotic flow in two-layer systems with a layer of non-conducting viscoelastic fluid. *International Journal of Heat and Mass Transfer*, 127, 600-615.
16) Zhao, C. and Yang. C. (2011). An exact solution for electroosmosis of non-Newtonian fluids in microchannels. *Journal of Non-Newtonian Fluid Mechanics*, 166, 1076-1079.

https://doi.org/10.62500/icrtsda.1.1.41

Proc. 1st International Conference on Recent Trends in Statistics and Data Analytics
Air University Islamabad, Pakistan – May 9, 2024, Vol. 1, pp. 401-408

Numerical solution of Higher order Emden-Fowler Equation using Adomian Decomposition Method

Adnan Maqsood[1], Dr. Madiha Ghamkhar[2*], Asra Ayub[3] and Dr. Ghulam Farid[4]
Department of Mathematics and Statistics, University of Agriculture Faisalabad, Pakistan

ABSTRACT

The Adomian decomposition technique is an efficient method for solving initial value problems of different order differential physical equations like Schrodinger Equation, Hermit equation, heat equation, wave equation. This method is simple, rapid, and easy to use in which the convergent series solution to a specific answer of all issues is provided. Several extensions of Adomian decomposition technique have also been established by the researchers and are available in literature. Due to a variety of applications in many areas of Physics, Mathematics, and Engineering the Adomian decomposition technique is a hot topic among the researchers of 19th century. In this work, an extension of ADM will be discussed. This extension will be involving Emden-Fowler type equation. Basic kinds of Emden-Fowler type of differential equations of different orders will also be explored. Also, linear, and non-linear IVP's of different orders ordinary differential Emden-Fowler type equations will be investigated.

Keywords : ADM , Emden-Fowler equation, ordinary differential equations, Initial conditions.

1. INTRODUCTION

The ADM technique is a valuable methodology to solve a wide range of linear and non - linear, ODE or PDE, and has been used in many fields of science and technology. In ADM technique, recursion produces a convergent series of analytical approximations. In certain situations, the solution converges smoothly for values of the independent variable more than the initial values. The decomposition approach can be helpful for solving a broad range of problems since it produces a fast convergent series solution. It has several significant benefits over traditional approximate methods as it is mathematically efficient and delivers analytic. Verifiable answer without the need for perturbation, linearization, or huge computations that discretization methods like finite difference entail. The resulting solutions are physically more realistic since it solves non-linear issues that need to be investigated on the mathematical framework, but it seems reasonable to say that while this is still ongoing research, the decomposition method appears to be valuable for physicists and engineers working on real-world problems for many reasons. (Singh *et al.,* 2020)

2. DESCRIPTION OF METHOD (ADM)

Consider the following Emden-Fowler governing equation.

$$u^{-n}\frac{d}{du}u^{n-m}\frac{d}{du}u^{m}v+g(u,v)=0 \tag{2.1}$$

General differential operator for this equation is given below:

$$L(.)=u^{-p}\ \frac{d}{du}u^{p-m}\frac{d}{du}u^{m}\frac{d^{i-1}}{du^{(i-1)}}(.) \tag{2.2}$$

Equation (2.1) can be written as follows

$$Lv=-g(u,v) \tag{2.3}$$

General Inverse operator L^{-1} for equation (2.1) is

https://doi.org/10.62500/icrtsda.1.1.41

$$L^{-1}(.)=\underbrace{\int_{a_0}^{u}\int_{a_1}^{u}\int_{a_2}^{u}\ldots\int_{a_{p-1}}^{u}}_{(i-1)}u^{-m}\int_{a_p}^{u}u^{m-p}\int_{0}^{u}u^{p}\underbrace{dududu\ldots dududu.}_{(i+1)} \tag{2.4}$$

Apply L^{-1} on equation (2.3) and get

$$L^{-1}\ (Lv)=\ L^{-1}\ (\ -g(u,v)\ )$$

$$v(u)=\alpha(u)-L^{-1}(g(u,v)) \tag{2.5}$$

The solution $v(u)$ and the function $g(u,v)$ of Adomian technique are given by infinite series.

$$v(u)=\sum_{p=0}^{\infty}v_p(u) \tag{2.6}$$

And Adomian polynomial is also given in infinite series form as follows

$$g(u,v)=\sum_{p=0}^{\infty}D_p \tag{2.7}$$

To formulate Adomian polynomials, specific methods have shown

The algorithm is as follows:

$$D_0=G(v_0),\qquad D_1=v_1G'(v_0)$$

$$D_2=v_2G'(v_0)+\frac{1}{2!}v_1^{\,2}G''(v_0)$$

$$D_3=v_3G'(v_0)+v_1v_2G''(v_0)+\frac{1}{3!}v_1^{\,3}G'''(v_0)$$

After putting these in equation (2.6)

$$\sum_{p=0}^{\infty}v_p(u)=\alpha(u)+L^{-1}\sum_{P=0}^{\infty}D_P \tag{2.9}$$

The component $v(u)$ can be written by ADM as given below.

$$v_0=\alpha(u)\ ,\ \ v_1=L^{-1}D_0,\quad v_2=L^{-1}D_1\ ,\quad v_3=L^{-1}D_2$$

3. GENERAL EMDEN-FOWLER EQUATION AND KINDS

We will use the following governing equation for elaborating kinds of said equation.

$$u^{-n}\frac{d}{du}u^{n-k}\frac{d}{du}u^{k}v+g(u,v)=0 \tag{3.1}$$

Where $n\geq 1$ for different values of "k".

https://doi.org/10.62500/icrtsda.1.1.41

Kinds of Emden-Fowler type are listed below

First kind: 1st kind can be derived by putting $k = 1, 2, 3...$ in equation (3.1).

$$v^{(k+1)} + \frac{p+n}{u} v^{(k)} + \frac{p(n-1)}{u^2} v^{(k-1)} + g(u,v) = 0 \quad (3.2)$$

2nd kind: 2nd kind can be derived by putting $p = -n$ in (3.2)

$$v^{(k+1)} - \frac{n(n-1)}{u} v^{(k-1)} + g(u,v) = 0 \quad (3.3)$$

3rd kind: 3rd kind can be derived by putting $p = 0$ in (3.2)

$$v^{(k+1)} + \frac{n}{u} v^{(k)} + g(u,v) = 0 \quad (3.4)$$

4. NUMERICAL PROBLEMS OF THE METHOD

Problem 1: Consider the Emden-Fowler 1st kind equation

$$v^4 + \frac{9}{u} v''' + \frac{15}{u^2} v'' = 1 + u^2 + \frac{20}{u} + v \quad (4.1)$$

General form of Emden-Fowler 1st kind equation

$$v^{(k+1)} + \frac{p+n}{u} v^{(k)} + \frac{p(n-1)}{u^2} v^{(k-1)} + g(u,v) = 0$$

Initial conditions are given below

$$v(0) = 0, \quad v'(0) = 0$$
$$v''(0) = 0, \quad v'''(0) = 0$$

Exact solution of above equations is given $= u^5$

$$Lv = 1 + u^2 + \frac{20}{u} + v \quad (4.2)$$

$$L^{-1}(Lv) = L^{-1}(1 + u^2 + \frac{20}{u} + v)$$

When we use initial conditions on both sides of equation yields

$$v(u) = L^{-1}(1 + u^2 + \frac{20}{u}) + L^{-1}(v)$$

Substitute the series $v_n(u)$ *for* $v(u)$ in equation we get

$$\sum_{n=0}^{\infty} v_n(u) = L^{-1}(1 + u^2 + \frac{20}{u}) + L^{-1} \sum_{n=0}^{\infty} D_n(u) \quad (4.3)$$

https://doi.org/10.62500/icrtsda.1.1.41

$$v_{n+1} = L^{-1}(D_n)$$

$$v_0 = \frac{5u^3}{36} + \frac{u^4}{420} + \frac{u^6}{1890} \tag{4.4}$$

$$v_1 = \frac{u^7}{24192} + \frac{u^8}{2328480} + \frac{u^{10}}{24324300}$$

(4.5)

$$v_2 = L^{-1}(v_1)$$

$$v_2 = \frac{u^{11}}{447068160} + \frac{u^{12}}{59935075200} + \frac{u^{14}}{1128890763000} \tag{4.6}$$

$$v(u) = \frac{5u^3}{36} + \frac{u^4}{420} + \frac{u^6}{1890} + \frac{u^7}{24192} + \frac{u^8}{2328480} + \frac{u^{10}}{24324300} + \frac{u^{11}}{447068160} + \frac{u^{12}}{59935075200} \tag{4.7}$$

Table 4.1 Comparison of absolute error (1st kind)

X	Exact	ADM	Absolute Error
0.0	0.00000	0.00000000000	0.00000000000
0.1	0.00001	0.00013912751	-0.00012912751
0.2	0.00032	0.00111495502	-0.00079495502
0.3	0.00243	0.00376968046	-0.00133968046
0.4	0.01024	0.00895207619	0.00128792380
0.5	0.03125	0.01751851076	0.01373148923
0.6	0.07776	003033441428	0.04742558571
0.7	0.16807	0.04827620789	0.11979379210
0.8	0.32768	0.07223371851	0.25544628148
0.9	0.5904	0.10311309944	0.48737690055
1.0	1.0000	0.14184027777	0.85815972222

Figure 4.1 Comparison between Exact and ADM solution (1st kind)

Problem 2: Consider the following (3rd kind) Emden-Fowler equation

$$v^4 + \frac{5}{u}v''' = 48 + u^8 - v^2$$

(4.1)

Emden-Fowler 3rd kind equation

$$v^{(k+1)} + \frac{n}{u}v^{(k)} + g(u,v) = 0$$

Initial conditions for this problem are given below

https://doi.org/10.62500/icrtsda.1.1.41

$$v(1)=1,\ v'(\frac{1}{2})=\frac{1}{2},\ v''(\frac{1}{6})=\frac{1}{3},\ v'''(0)=0$$

$$k=3\ ,\ n=5$$

Exact solution of above equations is given $=u^4$

$$Lv=48+u^8-v^2 \tag{4.2}$$

$$L^{-1}(Lv)=L^{-1}(48+u^8-v^2)$$

When we use initial conditions on both sides of equation yields

$$v(u)=L^{-1}(48+u^8)-L^{-1}(v^2)$$

Substitute the series $v_n(u)\ for\ v(u)$ in equation we get

$$\sum_{n=0}^{\infty}v_n(u)=L^{-1}(48+u^8)+L^{-1}\sum_{n=0}^{\infty}D_n(u) \tag{4.3}$$

$$v_{n+1}=-L^{-1}(D_n),\quad n\geq 0$$

$$D_0=v_0{}^2,\qquad D_1=2v_0v_1$$

$$D_2=v_1{}^2+2v_0v_2\ ,\qquad D_3=2v_1v_2+2v_0v_3$$

The calculated solution components for above series are given as

$$v_0=L^{-1}(48+u^8)$$

$$v_0=-7.53137\times10^{-5}-4.43809\times10^{-7}u-8.26909\times10^{-11}u^2+u^4+7.5757576\times10^{-5}u^{12}$$

$$v_1=L^{-1}(v_0{}^2)$$

$$v_1=7.52447\times10^{-5}+4.39215\times10^{-7}u+5.75308\times10^{-11}u^2-1.1817\times10^{-10}u^4$$
$$-1.1817\times10^{-10}u^4-3.71388\times10^{-13}u^5-4.36296\times\times10^{-16}u^6$$
$$-6.99028\ \times10^{-20}u^7-7.4716\times10^{-8}u^8+\ldots-1.12301\times10^{-14}u^{28} \tag{4.4}$$

$$v_2=L^{-1}(2v_0v_1)$$

$$v_2=-6.88768\times10^{-8}-4.55044\times10^{-9}u-5.44271\times10^{-12}u^2$$
$$-2.36123\times10^{-10}u^4-7.38591\times10^{-13}u^5-8.56178\times10^{-16}u^6$$
$$-1.17813\ \times10^{-19}u^7+7.46475\times10^{-8}u^8+\ldots-5.09824\times10^{-25}u^{44} \tag{4.5}$$

$$v(u)=-1.37876\times10^{-7}-9.14463\times10^{-9}u-3.06027\times10^{-11}u^2+u^4$$
$$-1.10998\times10^{-12}u^5-1.29247\times10^{-15}u^6-1.87716\ \times10^{-19}u^7$$
$$+1.49363\times10^{-7}u^8+\ldots-5.09824\times10^{-25}u^{44} \tag{4.6}$$

Table 4.1 Comparison of absolute error (3rd kind)

https://doi.org/10.62500/icrtsda.1.1.41

X	EXACT	ADM	ABSOLUTE ERROR
0.0	0.0000	0.0000001378	0.0000001378
0	0.0001	0.0000998612	0.0000001387
0.2	0.0016	0.0015998602	0.0000001397
0.3	0.0081	0.0080998593	0.0000001406
0.4	0.0256	0.0255998584	0.0000001415
0.5	0.0625	0.0624998575	0.0000001424
0.6	0.1296	0.1295998566	0.0000001433
0.7	0.2401	0.2400998557	0.0000001442
0.8	0.4096	0.4095998547	0.0000001452
0.9	0.6561	0.6560998538	0.0000001461
1.0	1.0000	0.9999998529	0.0000001470

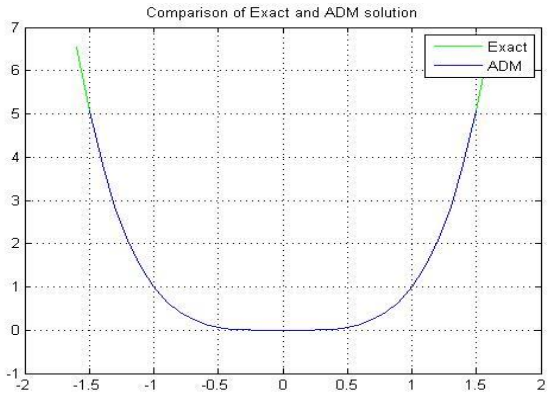

Figure 4.1 Comparison of Exact and ADM solution (3rd kind)

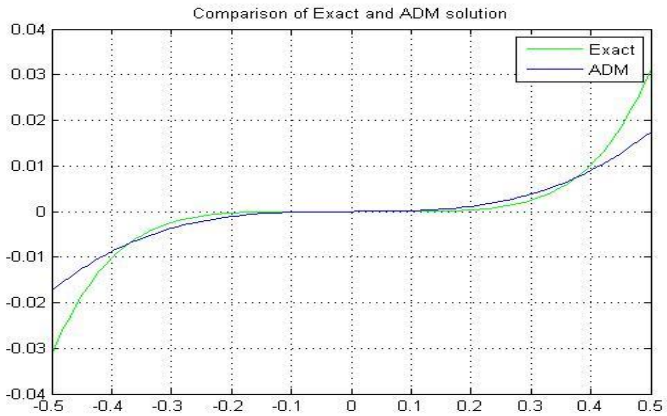

https://doi.org/10.62500/icrtsda.1.1.41

5. COMMENTS AND CONCLUSION

In this work, we have discussed application of Adomian DM on Emden-Fowler type ordinary linear and non-linear equations and provide numerical solution as well as the efficiency of Adomian decomposition technique to solve Emden-Fowler type equations. We have created a variety of order-varying Emden-Fowler type equations. To demonstrate our approach, we treated both linear and non-linear problems using the Adomian decomposition technique. The results demonstrate the ADM's reliability and quick convergence. Also this method is very rapid, easy to use and less time consuming.

REFERENCES

1) Adomian, G. (1991). A review of the decomposition method and some recent results for nonlinear equations. *Computational Mathematics and its Applications*, 21, 101-127.
2) Adomian, G. and Rach, R. (1983). Inversion of nonlinear stochastic operators. *Journal* of *Mathematical Analysis* and *Applications*, 91, 36-46.
3) Alaqel, S.A. and Hasan. Y.Q. (2020). A Novel Modification of Adomian Decomposition Method for Singular BVPs of Emden-Fowler Type Higher-Order Emden-Fowler Equation. ***Journal of Advances in Mathematics and Computer Science*,** 35, 84–100.
4) Alaqel, S.A. and Hasan. Y.Q. (2020). Solutions of emden-fowler type equations of different order by adomian decomposition method. *Advances in Mathematics*: Scientific *Journal,* 9, 969–978.
5) Antar, M.A. (2001). Steady and transient numerical analysis of the performance of annular fins. The *International Journal of Energy Research,* 25, 1197–1206.
6) Biazar, J. and Hosseini. K. (2016). A modified Adomian decomposition method for singular initial value Emden-Fowler type equations. *International Journal of Applied Mathematical Research,* 5, 69-75.
7) Fowler, R.H. (1931). Further studies of Emden's and similar differential equations. The Quarterly *Journal* of *Mathematics*, 2, 259–288
8) Hossen, K.A.A. (2020). On Solutions of Emden-Fowler Equation. *American Journal* of *Computational* and Applied *Mathematics*, 10, 90–99.
9) Mall, S. and Chakraverty. S. (2015). Numerical solution of nonlinear singular initial value problems of Emden-Fowler type using Chebyshev Neural Network method. Neurocomputing, 149, 975–982.
10) Muatjetjeja, B. and Khalique. C.M. (2011). Exact solutions of the generalized Lane-Emden equations of the first and second kind. Pramana - J. Phys. 77:545–554.
11) Mubarak, A., S. Mutaish and F. Education-aden. (2018). Adjusted Adomian Decomposition Method for Solving Emden-Fowler Equations of Various Order. *MAYFEB Journal* of *Mathematics,* 3, 1–10.

https://doi.org/10.62500/icrtsda.1.1.42

12) Parand, K., Hemami. M. and Hashemi-Shahraki. S. (2017). Two Meshfree Numerical Approaches for Solving High-Order Singular Emden–Fowler Type Equations. *International Journal of Applied* and *Computational Mathematics*, 3, 521–546.

13) Singh, R., Guleria. G. and Singh. M. (2020). Haar wavelet quasilinearization method for numerical solution of Emden–Fowler type equations. *Mathematics* and *Computers* in *Simulation,* 174, 123–133.

https://doi.org/10.62500/icrtsda.1.1.42

Proc. 1st International Conference on Recent Trends in Statistics and Data Analytics
Air University Islamabad, Pakistan – May 9, 2024, Vol. 1, pp. 409-424

VIBRATION FREQUENCY ANALYSIS OF FOUR LAYERED CANTILEVER CYLINDRICAL SHELL

Madiha Ghamkhar[1*], Asra Ayub[2], Fatima Irshad[3], and Ghulam Farid[4]
Department of Mathematics and Statistics, University of Agriculture Faisalabad, Pakistan

ABSTRACT

In this study, vibration frequency analysis of a four layered cantilever cylindrical shell is studied where the 1st and 4th layers are made up of isotropic material and the 2nd and 3rd layers are of functionally graded materials. Sander's shell theory is used for the displacement relations of strain and curvature displacement. Using the Rayleigh Ritz mathematical approach, the shell frequency equation is obtained. The characteristic beam functions are used to calculate axial model dependency. Results for natural frequencies against the circumferential wave number with increasing thickness, length and power exponent law are obtained for a four layered cantilever cylindrical shell with the help of MATLAB software. Furthermore, the accuracy of this methodology is checked with numerous results.

1. INTRODUCTION

In the domain of technology and engineering, cylindrical shells are important components. For its basic geometrical design, the vibrations of cylindrical shells are researched thoroughly. There are numerous studies on them in the open literature. Rayleigh (1882) [1] examined Sophie's work on circular cylindrical shell vibration. Love (1888) [2] presented the first linear shell theory at the turn of the nineteenth century, based on Krichhoff's platform idea. All other shell theories are constructed from this idea by changing some physical concepts. Arnold and Warburton (1949) [3], first investigated the vibration of cylindrical shells. Sharma and Johns (1971) [4] analyzed the cylindrical shell oscillations under clamped-free boundary constraints with the Ritz method. Numerous approaches to the vibrational behavior of thin shells are being investigated by several researchers. These methods vary from the Rayleigh-Ritz-based energy methods to analytic approaches in which closed-form results are respectively employed. Soedal (1980) [5] developed a novel frequency formulation for a cylindrical shell with clamped-clamped, clamped-free and free-free edge constraints using an analysis model and the Donnell-Mushtari-Vlasov equation. Chung (1981) [6] used Sander's shell equation to investigate cylindrical shell oscillations by clamping, freeing and simply supporting them. Ludwig and Krieg (1981) [7] utilized an adaptive approach to establish the frequencies and periods of thin cylindrical shells, using the shell theory of Flugge. Lam and Loy (1995) [8] used the Ritz method to investigate the impact of constraints on the free vibration properties of a multi-layered cylindrical shell. Loy and Lam (1997) [9] studied the thin cylindrical container's vibration using ring supports during the length of the container, which required no side rebound. In order to investigate radial buckling of cylindrical shells, Bhutta *et al.* (2015) [10] studied the tri-laying cylindrical shell concept with an interlayer of FGM and extremely isotropic type layers. Zhang *et al.* (2006) [11] introduced cylinder shell vibrational behavior using the local DQM adaptive approach. Li and Batra (2006) [12] investigated the three-layer circular cylindrical shell's bending that is simply supported by an axially compressive force. Sofiyev *et al.* (2006) [13] examined the oscillation and stability study for the tri-layered conic shell, with an FGM central layer. Sheng and Wan (2008) [14] used the first-order shear deformation theory (FSDT) to study

https://doi.org/10.62500/icrtsda.1.1.42

the vibration, bending and dynamic stability of FGM cylindrical shells. Mehparvar (2009) [15] examined the oscillations of a FGM cylindrical rotating shell. Iqbal *et al.* (2009) [16] used the method of wave propagation to evaluate the oscillations in the circular shells of functionally graded materials. Iqbal *et al.* (2009) [17] investigated the vibrational properties of a functional-graded, circular shell, filled with fluid, using a technique of wave propagation. Arshad *et al.* (2010) [18] investigated the frequency response of cylindrical two-layered shells with one layer consisting of functionally graded material as well as the other layer of isotropic material. Isvandzibaei *et al.* (2014) [19] investigated the oscillation behavior of FGM cylinder shells through the inner pressure and ring support impacts. Sarkheil *et al.* (2016) [20] investigated the oscillation of bi-layered cylindrical shells composed of two distinct materials using Sander's thin shell theory.

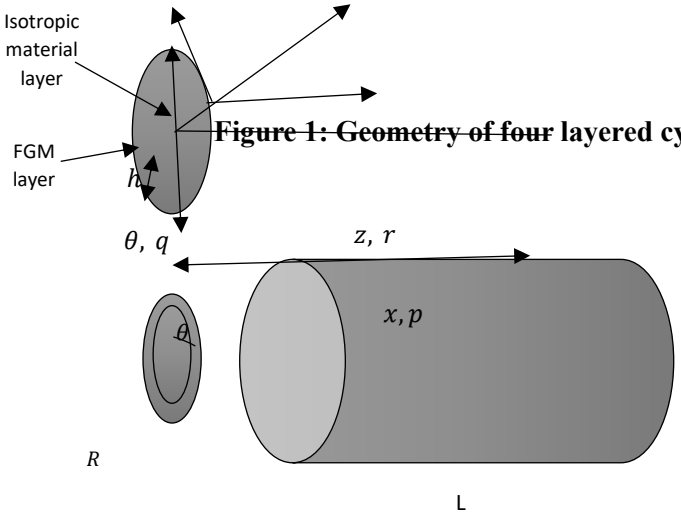

Figure 1: Geometry of four layered cylindrical shell

2. THEORETICAL CONSIDERATIONS

Consider a four layered cantilever cylindrical shell with radius R, thickness h and length L as shown in Figure 1. The central surface of the cylindrical shell is oriented to an orthogonal co-ordinate scheme $(x, \theta$ and $z)$ where x, θ and z lie in the axial, circumferential and radial shell directions. And the shell displacements in x, θ and z directions are (p, q, r) respectively.

The fundamental relationship between stress and strain is defined through generalized Hooke's law as follows:

$$[\sigma] = [Q][\varepsilon]. \tag{1}$$

Where $[\sigma]$ is the stress vector, $[Q]$ is the reduced stiffness and $[\varepsilon]$ is the strain vector. The vectors of stress and stress are described as:

$$[\sigma] = \begin{bmatrix} \sigma_x \\ \sigma_\theta \\ \sigma_{x\theta} \end{bmatrix}, \quad [\varepsilon] = \begin{bmatrix} \varepsilon_x \\ \varepsilon_\theta \\ \varepsilon_{x\theta} \end{bmatrix}. \tag{2}$$

Where, σ_x is stress in x-direction, σ_θ is stress in θ-direction and $\sigma_{x\theta}$ is shear stress in $x\theta$-direction. Similarly ε_x is the x-direction strain, ε_θ is the θ-direction strain and $\varepsilon_{x\theta}$ is the $x\theta$-direction shear strain. The reduced stiffness matrix is defined as:

https://doi.org/10.62500/icrtsda.1.1.42

$$[Q]=\begin{bmatrix} Q_{11} & Q_{12} & 0 \\ Q_{21} & Q_{22} & 0 \\ 0 & 0 & Q_{66} \end{bmatrix}. \tag{3}$$

For isotropic materials, the entries of reduced stiffness are stated as

$$Q_{11}=\frac{E}{1-\mu^2},\ Q_{22}=\frac{E}{1-\mu^2},\ Q_{12}=\frac{\mu E}{1-\mu^2},\ Q_{66}=\frac{E}{2\left(1+\mu^2\right)}, \tag{4}$$

(Loy *et al.,*1999) [21].

Here, Young's modulus and Poisson ratio are represented by E and μ.

By using Love shell theory, the relationships for strain and curvature are defined as:

$$\varepsilon_x=\varepsilon_1+z\tau_1,\ \ \varepsilon_\theta=\varepsilon_2+z\tau_2,\ \ \varepsilon_{x\theta}=\varepsilon_{12}+2z\tau_{12}. \tag{5}$$

Where, $\varepsilon_1,\varepsilon_2,\varepsilon_{12}$ are the surface relations of the strains and τ_1,τ_2,τ_{12} are the surface relations of the curvatures.

Using the expression (5) in expressions (2), (3) and (1), we have

$$\begin{aligned} \sigma_x&=Q_{11}\left(\varepsilon_1+z\tau_1\right)+Q_{12}\left(\varepsilon_2+z\tau_2\right), \\ \sigma_\theta&=Q_{21}\left(\varepsilon_1+z\tau_1\right)+Q_{22}\left(\varepsilon_2+z\tau_2\right), \\ \sigma_{x\theta}&=Q_{66}\left(\varepsilon_{12}+2z\tau_{12}\right). \end{aligned} \tag{6}$$

The force and moment resultants of a thin cylindrical shell are defined as

$$\begin{aligned} \left\{N_x,N_\theta,N_{x\theta}\right\}&=\int_{-\frac{h}{2}}^{\frac{h}{2}}\left\{\sigma_x,\sigma_\theta,\sigma_{x\theta}\right\}dz, \\ \left\{M_x,M_\theta,M_{x\theta}\right\}&=\int_{-\frac{h}{2}}^{\frac{h}{2}}\left\{\sigma_x,\sigma_\theta,\sigma_{x\theta}\right\}z\,dz. \end{aligned} \tag{7}$$

Here N_x,N_θ and $N_{x\theta}$ are the axial, circumferential and radial direction force components. M_x,M_θ and $M_{x\theta}$ are the axial, circumferential and radial direction moment components. By applying expressions (7) and (6), then

$$[N]=[\mathrm{O}][\tau].$$

(8) Where $[N]$, $[\tau]$ and $[\mathrm{O}]$ are defined as

https://doi.org/10.62500/icrtsda.1.1.42

$$[N]=\begin{bmatrix} N_x \\ N_\theta \\ N_{x\theta} \\ M_x \\ M_\theta \\ M_{x\theta} \end{bmatrix}, [\tau]=\begin{bmatrix} \varepsilon_1 \\ \varepsilon_2 \\ \varepsilon_{12} \\ \tau_1 \\ \tau_2 \\ 2\tau_{12} \end{bmatrix}, [\mathrm{O}]=\begin{bmatrix} A_{11} & A_{12} & 0 & B_{11} & B_{12} & 0 \\ A_{12} & A_{22} & 0 & B_{12} & B_{22} & 0 \\ 0 & 0 & A_{66} & 0 & 0 & B_{66} \\ B_{11} & B_{12} & 0 & D_{11} & D_{12} & 0 \\ B_{12} & B_{22} & 0 & D_{12} & D_{22} & 0 \\ 0 & 0 & B_{66} & 0 & 0 & D_{66} \end{bmatrix}. \quad (9)$$

Where A_{ij}, B_{ij} and D_{ij} denote the extensional, coupling and bending stiffness respectively, $i=1,2,6;$ and are expressed as

$$A_{ij}=\int_{-\frac{h}{2}}^{\frac{h}{2}} Q_{ij}dz\ ,\ B_{ij}=\int_{-\frac{h}{2}}^{\frac{h}{2}} Q_{ij}zdz\ ,\ D_{ij}=\int_{-\frac{h}{2}}^{\frac{h}{2}} Q_{ij}z^2dz\ . \quad (10)$$

Formulation of Strain Energy

The formulation of strain energy υ for a CS is defined as

$$\upsilon=\frac{1}{2}R\int_0^L\int_0^{2\pi}[\tau]'[\mathrm{O}][\tau]d\theta dx. \quad (11)$$

By using the expression (9), υ is reviewed like

$$\begin{aligned}\upsilon=\frac{R}{2}\int_0^L\int_0^{2\pi}\{&A_{11}\varepsilon_1^2+A_{22}\varepsilon_2^2+2A_{11}\varepsilon_1\varepsilon_2+A_{66}\varepsilon_{12}^2+2B_{11}\varepsilon_1\tau_1+2B_{12}\varepsilon_1\tau_2+2B_{12}\varepsilon_2\tau_1+2B_{22}\varepsilon_2\tau_2\\&+4B_{66}\varepsilon_{12}\tau+D_{11}\tau_1^2+D_{22}\tau_2^2+2D_{12}\tau_1\tau_2+4D_{66}\tau_{12}^2\}d\theta dx.\end{aligned} \quad (12)$$

Shell kinetic energy κ_s is stated as:

$$\kappa_s=\frac{R}{2}\int_0^L\int_0^{2\pi}\rho_t\left[\left(\frac{\partial u}{\partial t}\right)^2+\left(\frac{\partial v}{\partial t}\right)^2+\left(\frac{\partial w}{\partial t}\right)^2\right]d\theta dx. \quad (13)$$

Where the dot is just above the quantity, the time derivative of the amount is indicated. Mass density shell ρ_s and mass density for any duration of unit ρ_t is illuminated as:

$$\rho_t=\int_{-\frac{h}{2}}^{\frac{h}{2}}\rho_s dz. \quad (14)$$

Here ρ_s is the mass density shell.

Displacement Relations of Strain and Curvature

Various shell theories were introduced to determine the cylindrical shell's free vibration. Love's shell theory is basic first-order. Budiansky and Sanders (1963) [22] introduced the displacement relations of strain and curvature from the linear thin shell theory of first-order. According to this theory, the displacement relations of strain and curvature are given by

https://doi.org/10.62500/icrtsda.1.1.42

$$\{\varepsilon_1,\varepsilon_2,\varepsilon_{12}\}=\left\{\frac{\partial p}{\partial x},\frac{1}{R}\left(\frac{\partial q}{\partial\theta}+r\right),\left(\frac{\partial q}{\partial x}+\frac{1}{R}\frac{\partial p}{\partial\theta}\right)\right\},$$

$$\{\tau_1,\tau_2,2\tau_{12}\}=\left\{-\frac{\partial^2 r}{\partial x^2},-\frac{1}{R^2}\left(\frac{\partial^2 r}{\partial\theta^2}-\frac{\partial q}{\partial\theta}\right),-\frac{2}{R}\left(\frac{\partial^2 r}{\partial x\partial\theta}-\frac{3}{4}\frac{\partial q}{\partial x}+\frac{1}{4R}\frac{\partial p}{\partial\theta}\right)\right\}. \quad (15)$$

By using the expression (15) in (12), υ is reviewed like

$$\begin{aligned}\upsilon=\frac{R}{2}\int_0^L\int_0^{2\pi}\Bigg[&A_{11}\left(\frac{\partial p}{\partial x}\right)^2+\frac{A_{22}}{R^2}\left(\frac{\partial q}{\partial\theta}+r\right)^2+\frac{2A_{12}}{R}\left(\frac{\partial p}{\partial x}\right)\left(\frac{\partial q}{\partial\theta}+r\right)+A_{66}\left(\frac{\partial q}{\partial x}+\frac{1}{R}\frac{\partial p}{\partial\theta}\right)^2\\&-2B_{11}\left(\frac{\partial p}{\partial x}\right)\left(\frac{\partial^2 r}{\partial x^2}\right)-\frac{2B_{12}}{R^2}\left(\frac{\partial p}{\partial x}\right)\left(\frac{\partial^2 r}{\partial\theta^2}-\frac{\partial q}{\partial\theta}\right)-\frac{2}{R}B_{12}\left(\frac{\partial q}{\partial\theta}+r\right)\left(\frac{\partial^2 r}{\partial x^2}\right)-\frac{2}{R^3}B_{22}\\&\left(\frac{\partial q}{\partial\theta}+r\right)\left(\frac{\partial^2 r}{\partial\theta^2}-\frac{\partial q}{\partial\theta}\right)-\frac{4B_{66}}{R}\left(\frac{\partial q}{\partial x}+\frac{1}{R}\frac{\partial p}{\partial\theta}\right)\left(\frac{\partial^2 r}{\partial x\partial\theta}-\frac{3}{4}\frac{\partial q}{\partial x}+\frac{1}{4R}\frac{\partial p}{\partial\theta}\right)+D_{11}\left(\frac{\partial^2 r}{\partial x^2}\right)^2\\&+\frac{D_{22}}{R^4}\left(\frac{\partial^2 r}{\partial\theta^2}-\frac{\partial q}{\partial\theta}\right)^2+\frac{2D_{12}}{R^2}\left(\frac{\partial^2 r}{\partial x^2}\right)\left(\frac{\partial^2 r}{\partial\theta^2}-\frac{\partial q}{\partial\theta}\right)+\frac{4D_{66}}{R^2}\left(\frac{\partial^2 r}{\partial x\partial\theta}-\frac{3}{4}\frac{\partial q}{\partial x}+\frac{1}{4R}\frac{\partial p}{\partial\theta}\right)^2\Bigg]d\theta dx.\end{aligned} \quad (16)$$

Lagrange Energy Functional

The Lagrange energy functional L_f is the difference between shell kinetic and strain energies for a cylindrical shell as:

$$L_f=\kappa_s-\upsilon. \quad (17)$$

Here κ_s is the shell kinetic energy and υ is the strain energy.

Rayleigh-Ritz Method

The most common methods for analyzing shell vibration are the energy variation methods, e.g., Rayleigh Ritz and Galerkin. The Rayleigh Ritz method minimizes energy variation, although coefficients of a series representing displacement deformations are concerned. In order to get normal cylinder shell frequencies, the Rayleigh-Ritz process is used.

Axial Modal Dependency

The equations for modal displacement deformations are considered as a combination of space and time variables. That leads to a set of ordinary differential equations for the axial space variable's three unknown functions. The axial modal dependency is approximated by several forms of functions. Now relationships become supposed in the displacement fields:

$$p(x,\theta,t)=X_m P(x)\cos(n\theta)\sin\omega t,$$

$$q(x,\theta,t)=Y_m Q(x)\sin(n\theta)\cos\omega t,$$

$$r(x,\theta,t)=Z_m R(x)\cos(n\theta)\sin\omega t. \quad (18)$$

Where X_m, Y_m and Z_m represent the amplitudes of vibration in the x,θ and z direction respectively. The mode form axial and circumferential wave numbers are denoted by m and n. The angular frequency of the shell wave vibration is denoted by ω. $P(x)$, $Q(x)$ and $R(X)$ are indicates

https://doi.org/10.62500/icrtsda.1.1.42

the axial model dependency in the longitudinal, circumferential and transverse directions respectively. Here we take

$$P(x)=\frac{d}{dx}(\zeta(x)),\ Q(x)=\zeta(x),\ \ R(x)=\zeta(x). \tag{19}$$

The beam function $\zeta(\mathrm{x})$ is taken as in the following form

$$\zeta(\mathrm{x})=\beta_1\cosh(\eta_m x)+\beta_2\cos(\eta_m x)-\varsigma_m\beta_3\sinh(\eta_m x)-\varsigma_m\beta_4\sin(\eta_m x). \tag{20}$$

Here values of β_i are modified the conditions of the edge $(i=1,2,3,4)$, η_m indicate the origins of such transcendental equations and ς_m parameters based on a values of η_m.

Derivation of Frequency Equation

Substitution of expressions for the cylindrical shell's strain and kinetic energy, the expression for maximum strain energy and kinetic energy are achieved by using the concept of maximizing of energy.

$$\begin{aligned}L_{f(\max)}=\frac{\pi R}{2}\Bigg[h_s\rho\int_0^1\Big\{&\omega^2\left(X_mP(x)\right)^2\cos^2\omega t+\omega^2\left(Y_mQ(x)\right)^2\sin^2\omega t+\omega^2\left(Z_mR(x)\right)^2\cos^2\omega t\Big\}\\
&-\int_0^1\Bigg\{A_{11}\left(X_mP_x(x)\sin\omega t\right)^2+\frac{A_{22}}{R^2}\left(Y_mQ(x)n\cos\omega t+Z_mR(x)\sin\omega t\right)^2+\frac{2A_{12}}{R}\\
&\left(X_mP_x(x)\sin\omega t\right)\left(Y_mQ(x)n\cos\omega t+Z_mR(x)\sin\omega t\right)+A_{66}\Big(Y_mQ_x(x)\cos\omega t\\
&-\frac{1}{R}X_mP(x)n\sin\omega t\Big)^2-2B_{11}\left(X_mP_x(x)\sin\omega t\right)\left(Z_mR_{xx}(x)\sin\omega t\right)-\frac{2B_{12}}{R^2}\\
&\left(X_mP_x(x)\sin\omega t\right)\left(-Z_mR(x)n^2\sin\omega t-Y_mQ(x)n\cos\omega t\right)-\frac{2B_{12}}{R}\\
&\left(Y_mQ(x)n\cos\omega t+Z_mR(x)\sin\omega t\right)\left(Z_mR_{xx}(x)\sin\omega t\right)-\frac{2B_{22}}{R^3}\\
&\left(Y_mQ(x)n\cos\omega t+Z_mR(x)\sin\omega t\right)\left(-Z_mR(x)n^2\sin\omega t-Y_mQ(x)n\cos\omega t\right)\\
&-\frac{4B_{66}}{R}\Big(Y_mQ_x(x)\cos\omega t-\frac{1}{R}X_mP(x)n\sin\omega t\Big)\left(-Z_mR_x(x)n\sin\omega t\right.\\
&\left.-\frac{3}{4}Y_mQ_x(x)\cos\omega t-\frac{1}{4R}X_mP(x)n\sin\omega t\right)+D_{11}\left(Z_mR_{xx}(x)\sin\omega t\right)^2\\
&+\frac{D_{22}}{R^4}\left(-Z_mR(x)n^2\sin\omega t-Y_mQ(x)n\cos\omega t\right)^2+\frac{2D_{12}}{R^2}\left(Z_mR_{xx}(x)\sin\omega t\right)\\
&\left(-Z_mR(x)n^2\sin\omega t-Y_mQ(x)n\cos\omega t\right)+\frac{4D_{66}}{R^2}\left(-Z_mR_x(x)n\sin\omega t\right.\\
&\left.-\frac{3}{4}Y_mQ_x(x)\cos\omega t-\frac{1}{4R}X_mP(x)n\sin\omega t\right)^2\Bigg\}dx\Bigg].\end{aligned} \tag{21}$$

Minimized Lagrangian Energy Functional

The reduced Lagrangian energy functional with concerning the amplitudes X_m, Y_n and Z_m of vibration as follows,

https://doi.org/10.62500/icrtsda.1.1.42

$$\frac{\partial L_{f(\max)}}{\partial X_m} = \frac{\partial L_{f(\max)}}{\partial Y_m} = \frac{\partial L_{f(\max)}}{\partial Z_m} = 0. \tag{22}$$

The eigenvalue form of shell frequency equations for cylindrical shell are expressed as

$$\begin{aligned} c_{11}X_m + c_{12}Y_m + c_{13}Z_m - h_s\rho\omega^2 I_2 X_m = 0, \\ c_{12}X_m + c_{22}Y_m + c_{23}Z_m - h_s\rho\omega^2 I_4 Y_m = 0, \\ c_{13}X_m + c_{23}Y_m + c_{33}Z_m - h_s\rho\omega^2 I_4 Z_m = 0. \end{aligned} \tag{23}$$

The form of the matrix of the above equation is:

$$\left\{ \begin{bmatrix} c_{11} & c_{12} & c_{13} \\ c_{12} & c_{22} & c_{23} \\ c_{13} & c_{23} & c_{33} \end{bmatrix} - h_s\rho\omega^2 \begin{bmatrix} I_2 & 0 & 0 \\ 0 & I_4 & 0 \\ 0 & 0 & I_4 \end{bmatrix} \right\} \begin{bmatrix} X_m \\ Y_m \\ Z_m \end{bmatrix} = 0. \tag{24}$$

Here the expressions for the terms c_{ij}, I_2 and I_4 are given below in the Appendix.

3. CLASSIFICATION OF MATERIALS

In the present study, a cylindrical shell is fabricated from four layers. The internal and external layers are fabricated from isotropic materials while the central layers are fabricated from FG materials: nickel, zirconia, stainless-steel and aluminum. The shell thickness is split into four layers. Internal, intermediates and exterior layers thickness are h_1, h_2, h_3 and h_4 respectively. Each layer is of thickness $\frac{h}{4}$

.

To observe the effect of material parameters for FGMs, the volume fraction law is applied to cylindrical shells. The trigonometry volume fraction law of the two components of a shell that has a first FGM layer for a cylindrical shell is defined by the relation:

$$V_{f1} = \sin^2\left[\left(\frac{z-h_1}{h_2-h_1}\right)^N\right], \quad V_{f2} = \cos^2\left[\left(\frac{z-h_1}{h_2-h_1}\right)^N\right], \quad 0 \le N \le \infty. \tag{25}$$

These relationships fulfill the VFL i.e. $V_{f2} + V_{f1} = 1$. Then the effective material quantities $\mathrm{E}^{(FGM)}$, $\mu^{(FGM)}$ and $\rho_s^{(FGM)}$ of the resultant material are expressed as

$$\begin{aligned} E^{(FGM)2} &= (\mathrm{E}_2 - \mathrm{E}_3)\sin^2\left(\frac{z+2h/5}{2h/5}\right)^N + \mathrm{E}_3, \\ \mu^{(FGM)2} &= (\mu_2 - \mu_3)\sin^2\left(\frac{z+2h/5}{2h/5}\right)^N + \mu_3, \\ \rho_s^{(FGM)2} &= (\rho_{s2} - \rho_{s3})\sin^2\left(\frac{z+2h/5}{2h/5}\right)^N + \rho_{s3}. \end{aligned} \tag{26}$$

https://doi.org/10.62500/icrtsda.1.1.42

For the 2nd layer, the above expressions at $z=-2h/5$ become:

$$\mathrm{E}^{(FGM)}=\mathrm{E}_3,\ \mu^{(FGM)}=\mu_3,\ \rho_s^{(FGM)}=\rho_{s3}.$$

$$E^{(FGM)3}=\left(\mathrm{E}_4-\mathrm{E}_5\right)\sin^2\left(\frac{z}{2h/5}\right)^N+\mathrm{E}_5,$$

$$\mu^{(FGM)3}=\left(\mu_4-\mu_5\right)\sin^2\left(\frac{z}{2h/5}\right)^N+\mu_5,$$

$$\rho_s^{(FGM)3}=\left(\rho_{s4}-\rho_{s5}\right)\sin^2\left(\frac{z}{2h/5}\right)^N+\rho_{s5}. \tag{27}$$

For the 3rd layer, the above expressions at $z=0$ becomes: $\mathrm{E}^{(FGM)}=\mathrm{E}_5,\ \mu^{(FGM)}=\mu_5,\ \rho_s^{(FGM)}=\rho_{s5}.$

For the 2nd layer, the material properties at $z=0$ becomes:

$$E^{(FGM)2}=\left(\mathrm{E}_2-\mathrm{E}_3\right)\sin^2(1)+\mathrm{E}_3,$$

$$\mu^{(FGM)2}=\left(\mu_2-\mu_3\right)\sin^2(1)+\mu_3,$$

$$\rho_s^{(FGM)2}=\left(\rho_{s2}-\rho_{s3}\right)\sin^2(1)+\rho_{s3}. \tag{28}$$

And for the 3rd layer, the material properties at $z=2h/5$ becomes:

$$E^{(FGM)3}=\left(\mathrm{E}_4-\mathrm{E}_5\right)\sin^2(1)+\mathrm{E}_5,$$

$$\mu^{(FGM)3}=\left(\mu_4-\mu_5\right)\sin^2(1)+\mu_5,$$

$$\rho_s^{(FGM)3}=\left(\rho_{s4}-\rho_{s5}\right)\sin^2(1)+\rho_{s5}. \tag{29}$$

Thus, the shell is consisted of purely stainless steel at $z=-2h/5$ for the 2nd layer and nickel at $z=0$ for the 3rd layer, and the properties of material are combination of zirconia and stainless steel for the 2nd layer at $z=0$ and the properties of material are combination of aluminum and nickel for the 3rd layer at $z=2h/5$. The modified stiffness moduli are illustrated as:

$$A_{ij}=A_{ij}(iso)+A_{ij}(FGM)+A_{ij}(FGM)+A_{ij}(iso),$$

$$B_{ij}=B_{ij}(iso)+B_{ij}(FGM)+B_{ij}(FGM)+B_{ij}(iso),$$

$$D_{ij}=D_{ij}(iso)+D_{ij}(FGM)+D_{ij}(FGM)+D_{ij}(iso). \tag{30}$$

Here $i,j=1,2,6$ and (iso) denotes the 1st and 4th isotropic layers and (FGM) denotes the 2nd and 3rd functionally graded material layers. Their values are given in Appendix.

https://doi.org/10.62500/icrtsda.1.1.42

4. RESULTS AND DISCUSSION

The results for the variation in natural frequencies with different thickness, length and power exponent law against the circumferential wave number (n) for a cantilever four layered cylindrical shell are illustrated in tables and figures. In table 1, given the variation in natural frequencies for the cantilever four layered cylindrical shell when $(m=2,\ N=10,\ L=20,\ R=1)$ is applied. For n=1, the natural frequency increases horizontally from 40.2391 to 40.2390 by increasing the thickness as 0.001, 0.005, 0.007, 0.01, 0.05, 0.07 and 0.08. For n=2, the natural frequency increases horizontally from 13.8976 to 15.0363 by increasing the thickness as 0.001, 0.005, 0.007, 0.01, 0.05, 0.07 and 0.08. For n=3, the natural frequency increases horizontally from 6.6687 to 17.6559 by increasing the thickness as 0.001, 0.005, 0.007, 0.01, 0.05, 0.07 and 0.08. When circumferential wave numbers increase vertically from 1 to 10 then natural frequency increases horizontally from 40.2391 to 212.0190 by increasing the thickness as 0.001, 0.005, 0.007, 0.01, 0.05, 0.07 and 0.08.

N	h=0.001	h=0.005	h=0.007	h=0.01	h=0.05	h=0.07	h=0.08
1	40.2391	40.2391	40.2391	40.2391	40.2390	40.2390	40.2390
2	13.8976	13.8975	13.8975	13.8974	14.0698	14.5704	15.0363
3	6.6687	6.6687	6.6692	6.6722	9.2179	14.1747	17.6559
4	3.8602	3.8615	3.8664	3.8886	12.8277	24.3055	31.5863
5	2.5044	2.5112	2.5323	2.6227	19.9483	38.8832	50.7468
6	1.7523	1.7747	1.8395	2.0971	29.0848	56.9388	74.3574
7	1.2933	1.3516	1.5084	2.0507	39.9768	78.3310	102.3063
8	0.9932	1.1212	1.4272	2.3206	52.5710	103.0309	134.5700
9	0.7866	1.0293	1.5245	2.7832	66.8534	131.0303	171.1417
10	0.6385	1.0426	1.7409	3.3703	82.8197	162.3267	212.0190

Table 1. Variation in natural frequencies with different thickness against n for cantilever four layered cylindrical shell when $(m=2,\ N=10,\ L=20,\ R=1)$.

In table 2, given the variation in natural frequencies for cantilever four layered cylindrical shell when $(m=3,\ N=15,\ h=0.005,\ R=1)$ is applied. For n=1, the natural frequency decreases horizontally from 125.3000 to 3.6622 by increasing the length as 10, 20, 30, 40, 50, 60 and 70. For n =2, the natural frequency decreases horizontally from 50.9604 to 1.1678 by increasing the length as 10, 20, 30, 40, 50, 60 and 70. For n =3, the natural frequency decreases horizontally from 25.5825 to 0.5546 by increasing the length as 10, 20, 30, 40, 50, 60 and 70. When circumferential wave numbers increase vertically from 1 to 10 then natural frequency decreases horizontally from 125.3000 to 0.8287 by increasing the length as 10, 20, 30, 40, 50, 60 and 70.

N	L=10	L=20	L=30	L=40	L=50	L=60	L=70
1	125.3000	40.2129	19.0408	10.9725	7.1042	4.9652	3.6622
2	50.9604	13.8885	6.2825	3.5563	2.2828	1.5879	1.1678
3	25.5825	6.6643	2.9860	1.6850	1.0808	0.7524	0.5546
4	15.0688	3.8590	1.7260	0.9774	0.6327	0.4481	0.3394
5	9.8595	2.5096	1.1319	0.6575	0.4472	0.3414	0.2842
6	6.9344	1.7735	0.8306	0.5248	0.4027	0.3487	0.3228
7	5.1424	1.3507	0.6984	0.5126	0.4487	0.4235	0.4123
8	3.9779	1.1204	0.6843	0.5797	0.5478	0.5359	0.5308
9	3.1952	1.0286	0.7521	0.6952	0.6789	0.6730	0.6705

https://doi.org/10.62500/icrtsda.1.1.42

10	2.6672	1.0419	0.8732	0.8418	0.8331	0.8300	0.8287

Table 2. Variation in natural frequencies with different length against *n* for a cantilever four layered cylindrical shell when $(m=3,\ N=15,\ h=0.005,\ R=1)$.

In table 3, given the variation in natural frequencies for cantilever four layered cylindrical shell when $(m=1,\ h=0.005,\ L=10,\ R=1)$ is applied. For *n*=1, the natural frequency decreases horizontally from 126.9141 to 125.3008 by increasing the power exponent law as 1, 2, 3, 4, 5, 10 and 15. For *n*=2, the natural frequency decreases horizontally from 51.6149 to 50.9604 by increasing the power exponent law as 1, 2, 3, 4, 5, 10 and 15. For *n*=3, the natural frequency decreases horizontally from 25.9108 to 25.5825 by increasing the power exponent law as 1, 2, 3, 4, 5, 10 and 15. When circumferential wave numbers increased vertically from 1 to 10 then natural frequency decreases horizontally from 126.9141 to 2.6672 by increasing the power exponent law as 1, 2, 3, 4, 5, 10 and 15.

N	*N*=1	*N*=2	*N*=3	*N*=4	*N*=5	*N*=10	*N*=15
1	126.9141	126.1997	125.8928	125.7228	125.6145	125.3828	125.3008
2	51.6149	51.3250	51.2005	51.1316	51.0876	50.9936	50.9604
3	25.9108	25.7654	25.7030	25.6684	25.6463	25.5992	25.5825
4	15.2621	15.1765	15.1397	15.1194	15.1064	15.0786	15.0688
5	9.9860	9.9300	9.9059	9.8926	9.8841	9.8660	9.8595
6	7.0232	6.9839	6.9670	6.9576	6.9516	6.9389	6.9344
7	5.2083	5.1791	5.1666	5.1597	5.1553	5.1458	5.1424
8	4.0287	4.0063	3.9967	3.9913	3.9879	3.9805	3.9779
9	3.2356	3.2180	3.2103	3.2060	3.2032	3.1973	3.1952
10	2.7004	2.6861	2.6797	2.6762	2.6739	2.6689	2.6672

Table 3. Variation in natural frequencies with different power exponent law against *n* for a cantilever four layered cylindrical shell when $(m=1,\ h=0.005,\ L=10,\ R=1)$

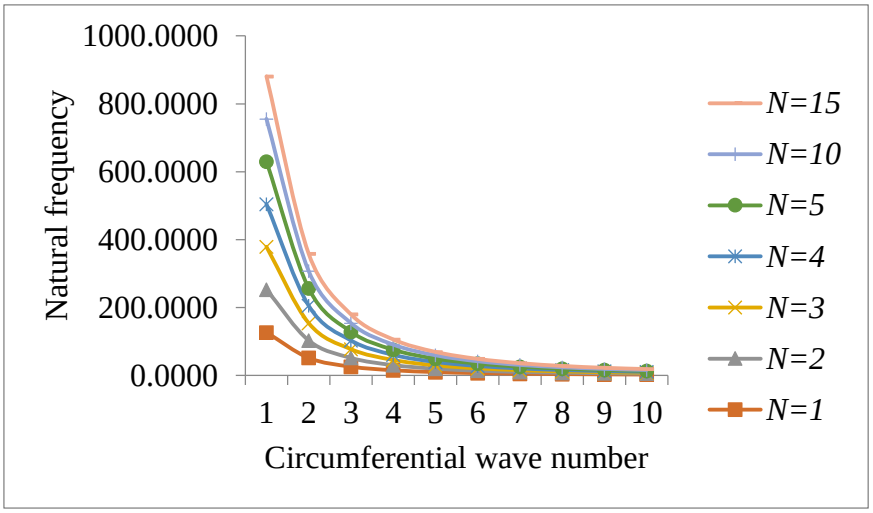

Figure 1: Variation in natural frequencies with different power exponent law against *n* for cantilever four layered cylindrical shell when $(m=2,\ h=0.005,\ L=10,\ R=1)$

https://doi.org/10.62500/icrtsda.1.1.42

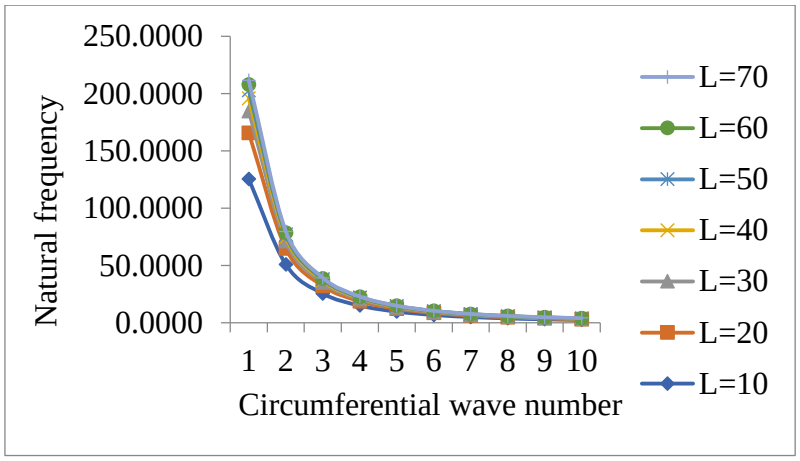

Figure 2: Variation in natural frequencies with different length against *n* for cantilever four layered cylindrical shell when $(m=1,\ N=10,\ h=0.002,\ R=1)$.

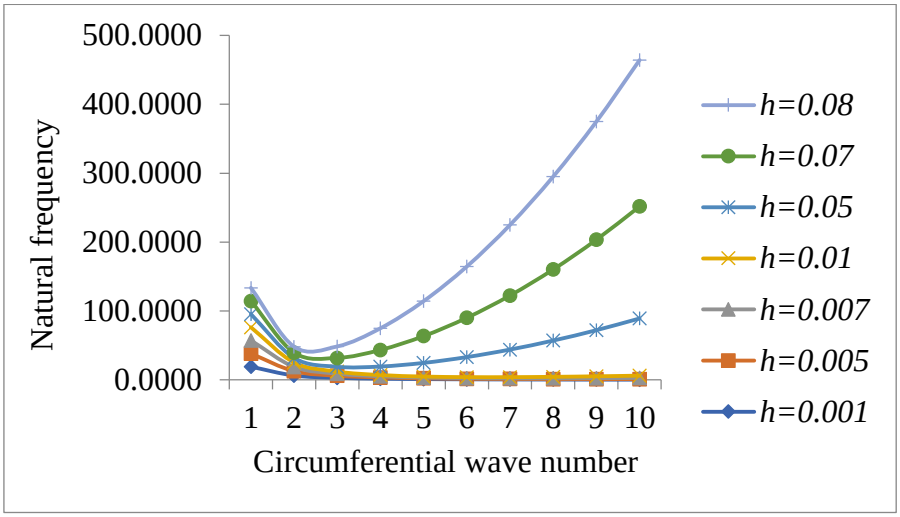

Figure 3: Variation in natural frequencies with different thickness against *n* for cantilever four layered cylindrical shell when $(m=3,\ N=5,\ L=30,\ R=1)$.

Figures 1, 2 and 3 illustrate the variation in natural frequencies against *n* for the cantilever four layered cylindrical shell. In figures 1 and 2, the natural frequency of cantilever four layered cylindrical shell with $(m=2,\ h=0.005,\ L=10,\ R=1)$ and $(m=1,\ N=10,\ h=0.002,\ R=1)$ is maximum at N=1 and L=1, after that the natural frequency decreases with increasing the power exponent law and length against *n*. In figure 3, the natural frequency of cantilever four layered cylindrical shell with $(m=3,\ N=5,\ L=30,\ R=1)$ is increased at h=1, then decreased at h=2 and h=3 and then continuously increased for various values of *h* against *n*.

For authenticity of the current work, results for the cantilever four layered cylindrical shell, are compared with others available in the literature, as shown in figure 4 and figure 5. In which frequency parameters are compared with those presented in Iqbal *et al.* (2009) and Bhutta *et al.* (2015).

In figure 4, given the comparison of natural frequencies against *n* for a cylindrical shell clamped-clamped boundary conditions *(*m=1, h=0.002, L=20, R=1*)*. In a three-layered cylindrical shell, the

https://doi.org/10.62500/icrtsda.1.1.42

behavior of the natural frequency against wave numbers at N=1 is unique, according to Iqbal *et al.* (2009). Like for all wave numbers, its behavior is decreasing. According to the present analysis, in a four layered cylindrical shell, the behavior of natural frequency against wave numbers is also unique, as at all wave numbers it decreases smoothly.

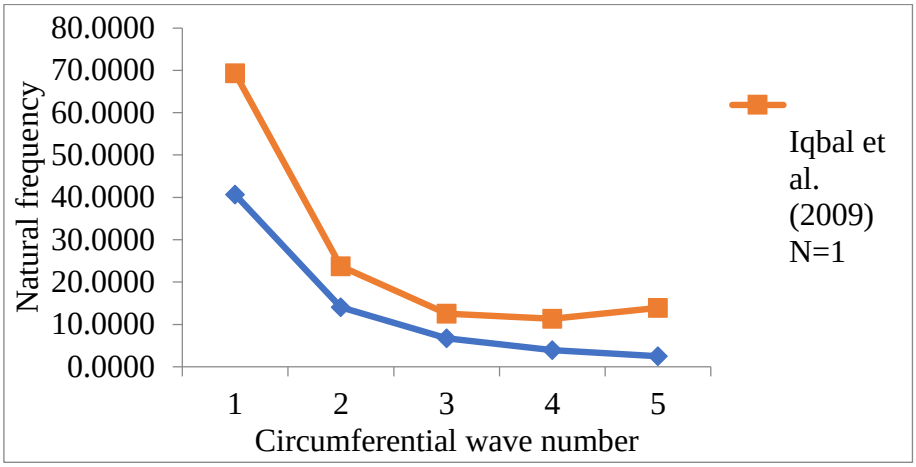

Figure 4: Comparison of natural frequencies with different power exponent law against n for a cantilever four layered cylindrical shell when $(m=1,\ h=0.002,\ L=20,\ R=1)$.

In figure 5, given the comparison of natural frequencies against n for a cylindrical shell clamped-clamped boundary conditions (m=1, h=0.002, L=20, R=1). In a three-layered cylindrical shell, the behavior of the natural frequency against wave numbers at N=1 and N=5 has fluctuated, according to Bhutta *et al.* (2015). At some wave numbers, its behavior is increasing, while at others, it is decreasing. But according to the present analysis, in a four-layered cylindrical shell, the behavior of natural frequency against wave numbers is unique, as at all wave numbers it decreases smoothly.

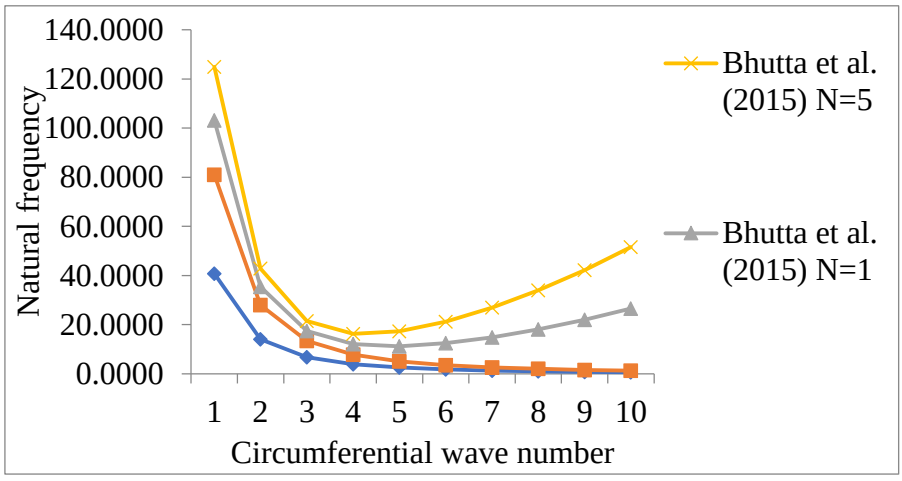

Figure 5: Comparison of natural frequencies with different power exponent law against n for a cantilever four layered cylindrical shell when $(m=1,\ h=0.002,\ L=20,\ R=1)$.

https://doi.org/10.62500/icrtsda.1.1.42

5. CONCLUSION

In the current study, vibration frequency analysis of cantilever four layered cylindrical shell is complete with different thickness, power exponent law and length of the shell's layers. For the displacement relations of strain and curvature, the Sander shell theory is used. Using the Rayleigh Ritz approach, the shell frequency equation is obtained. For present Cs, results show the behavior of natural frequencies with clamped-clamped boundary conditions. It is observed that natural frequencies are improved by increasing the thickness $(0.001 \le h \le 0.08)$ against circumferential wave number $(1 \le n \le 10)$. By increasing the power exponent law $(1 \le N \le 15)$ and length $(10 \le L \le 70)$ against circumferential wave number $(1 \le n \le 10)$, natural frequencies are reduced. Thickness, length and power exponent law have an effect on the natural frequencies of the cylindrical shell. Also, circumferential wave number has an effect on the natural frequencies of the cylindrical shell. The frequencies increased and decreased by circumferential wave number.

REFERENCES

1. Rayleigh, J.W.S. (1882). Theory of Sound. Macmillan, London.
2. Love, A.E.H. (1888). XVI. The small free vibrations and deformation of a thin elastic shell. Philosophical Transactions of the Royal Society of London (A.), 179, 491-546.
3. Arnold, R.N. and Warburton, G.B. (1949). Flexural vibrations of the walls of thin cylindrical shells having freely supported ends. Proceedings of the Royal Society of London. Series A. *Mathematical and Physical Sciences*, 197, 238-256.
4. Sharma, C.B. and Johns, D.J. (1971). Vibration characteristics of a clamped-free and clamped-ring-stiffened circular cylindrical shell. *Journal of Sound and Vibration*, 14:459-474.
5. Soedel, W. (1980). A new frequency formula for closed circular cylindrical shells for a large variety of boundary conditions. *Journal of Sound and Vibration*, 70, 309-317.
6. Chung, H. (1981). Free vibration analysis of circular cylindrical shells. *Journal of Sound and Vibration*, 74, 331-350.
7. Ludwig, A. and Krieg, R. (1981). An analytical Quasi-exact method for calculating eigen vibrations of thin circular cylindrical shells. *Journal of Sound and Vibration*, 74, 155-174.
8. Lam, K.Y. and Loy, C.T. (1995). Effects of boundary conditions on frequencies of a multi-layered cylindrical shell. *Journal of Sound and Vibration*, 188, 363-384.
9. Loy, C.T. and Lam, K.Y. (1997). Vibration of cylindrical shells with ring support. *International Journal of Mechanical Sciences*, 39, 455-471.
10. Bhutta, Z.G., Naeem, M.N. and Imran, M. (2015). On Vibration of Three-Layered Cylindrical Shell with Functionally Graded Middle Layer. *American Journal of Applied Mathematics*, 3, 32.
11. Zhang, L., Xiang, Y. and Wei, G.W. (2006). Local adaptive differential quadrature for free vibration analysis of cylindrical shells with various boundary conditions. *International Journal of Mechanical Sciences*, 48, 1126-1138.
12. Li, S.R. and Batra, R.C. (2006). Buckling of axially compressed thin cylindrical shells with functionally graded middle layer. *Thin-Walled Structures*, 44, 1039-1047.
13. Sofiyev, A.H., Deniz, A., Akcay, I.A. and Yusufoğlu, E.L.Ç.İ.N. (2006). The vibration and stability of a three-layered conical shell containing an FGM layer subjected to axial compressive load. *Acta Mechanica*, 183, 129-144.
14. Sheng, G.G. and Wang, X. (2008). Thermal vibration, buckling and dynamic stability of functionally graded cylindrical shells embedded in an elastic medium. *Journal of Reinforced Plastics and Composites*, 27, 117-134.

https://doi.org/10.62500/icrtsda.1.1.42

15. Mehrparvar, M. (2009). Vibration analysis of functionally graded spinning cylindrical shells using higher order shear deformation theory. *Journal of Solid Mechanics*, 1, 159-170.
16. Iqbal, Z., Naeem, M.N. and Sultana, N. (2009). Vibration characteristics of FGM circular cylindrical shells using wave propagation approach. *Acta Mechanica*, 208, 237-248.
17. Iqbal, Z., Naeem, M.N., Sultana, N., Arshad, S.H. and Shah, A.G. (2009). Vibration characteristics of FGM circular cylindrical shells filled with fluid using wave propagation approach. *Applied mathematics and mechanics*, 30, 1393-1404.
18. Arshad, S.H., Naeem, M.N., Sultana, N., Iqbal, Z. and Shah, A.G. (2010). Vibration of bilayered cylindrical shells with layers of different materials. *Journal of Mechanical Science and Technology*, 24, 805-810.
19. Isvandzibaei, M.R., Jamaluddin, H. and Hamzah, R.R. (2014). Analysis of the vibration behavior of FGM cylindrical shells including internal pressure and ring support effects based on Love-Kirchhoff theory with various boundary conditions. *Journal of Mechanical Science and Technology*, 28, 2759-2768.
20. Sarkheil, S., Foumani, M.S. and Navazi, H.M. (2016). Free vibration of bi-material cylindrical shells. Proceedings of the Institution of Mechanical Engineers, Part C: *Journal of Mechanical Engineering Science*, 230, 2637-2649.
21. Loy, C.T., Lam, K.Y. and Reddy, J.N. (1999). Vibration of functionally graded cylindrical shells. *International Journal of Mechanical Sciences*, 41, 309-324.
22. Budiansky, B. and Sanders, Jr. J.L. (1963). On the 'best' first order linear shell theory. *In Progress in applied mechanics*, 192, 129–140.

Appendix

$$C_{11} = A_{11}\left(\sin^2 \omega t\right) I_1 + \frac{n^2}{R^2}\left(\sin^2 \omega t\right)\left(A_{66} - \frac{B_{66}}{2R} + \frac{D_{66}}{4R^2}\right) I_2 .$$

$$C_{12} = \frac{n}{R}\left(\sin \omega t \cdot \cos \omega t\right)\left(A_{12} + \frac{B_{12}}{R}\right) I_3 + \frac{n}{R}\left(\sin \omega t \cdot \cos \omega t\right)\left(-A_{66} - \frac{3B_{66}}{2R} + \frac{B_{66}}{2R} - \frac{3D_{66}}{4R^2}\right) I_2 .$$

$$C_{13} = \frac{1}{R}\left(\sin^2 \omega t\right)\left(A_{12} + \frac{n^2 B_{12}}{R}\right) I_3 - B_{11}\left(\sin^2 \omega t\right) I_1 - \frac{n^2}{R^2}\left(\sin^2 \omega t\right)\left(B_{66} + \frac{D_{66}}{R}\right) I_2 .$$

$$C_{22} = \frac{nB_{12}}{R^2}\left(\sin \omega t \cdot \cos \omega t\right) I_3 + \frac{n^2}{R^2}\left(\cos^2 \omega t\right)\left(A_{22} + \frac{2B_{22}}{R} + \frac{D_{22}}{R^2}\right) I_4 + \frac{3}{R}\left(\cos^2 \omega t\right)\left(\frac{3D_{66}}{4R} + A_{66} + B_{66}\right) I_2 .$$

$$C_{23} = \frac{n}{R}\left(\sin \omega t \cdot \cos \omega t\right)\left(2B_{66} + \frac{3D_{66}}{R}\right) I_2 - \frac{n}{R}\left(\sin \omega t \cdot \cos \omega t\right)\left(B_{12} + \frac{D_{12}}{R}\right) I_3 + \frac{n}{R^2}\left(\sin \omega t \cdot \cos \omega t\right)$$
$$\left(A_{22} + \frac{n^2 B_{22}}{R} + \frac{B_{22}}{R} + \frac{n^2 D_{22}}{R^2}\right) I_4 .$$

$$C_{33} = D_{11}\left(\sin^2 \omega t\right) I_1 + \frac{4n^2 D_{66}}{R^2}\left(\sin \omega t\right) I_2 - \frac{1}{R}\left(\sin \omega t\right)\left(\frac{2n^2 D_{12}}{R} + 2B_{12}\right) I_3$$
$$+ \frac{1}{R^2}\left(\sin^2 \omega t\right)\left(A_{22} + \frac{2n^2 B_{22}}{R} + \frac{n^4 D_{22}}{R^2}\right) I_4 .$$

Where

https://doi.org/10.62500/icrtsda.1.1.42

$$I_1=\int_0^1\left(P_x(x)\right)^2dx,\ I_2=\int_0^1\left(P(x)\right)^2dx,$$

$$I_3=\int_0^1P_x(x)Q(x)dx,\ I_4=\int_0^1\left(Q(x)\right)^2dx.$$

$$A_{11}=A_{22}=\frac{h\mathrm{E}_1}{10\left(1-\mu_1^2\right)}+\frac{2h\left(\mathrm{E}_2-\mathrm{E}_3\right)}{5\left(1-\mu_2^2\right)}y_1+\frac{2h\mathrm{E}_3}{5\left(1-\mu_2^2\right)}+\frac{2h\left(\mathrm{E}_4-\mathrm{E}_5\right)}{5\left(1-\mu_4^2\right)}y_1+\frac{2h\mathrm{E}_5}{5\left(1-\mu_4^2\right)}+\frac{h\mathrm{E}_6}{10\left(1-\mu_6^2\right)},$$

$$A_{12}=A_{21}=\frac{h\mu_1\mathrm{E}_1}{10\left(1-\mu_1^2\right)}+\frac{2h\mu_2\left(\mathrm{E}_2-\mathrm{E}_3\right)}{5\left(1-\mu_2^2\right)}y_1+\frac{2h\mu_2\mathrm{E}_3}{5\left(1-\mu_2^2\right)}+\frac{2h\mu_4\left(\mathrm{E}_4-\mathrm{E}_5\right)}{5\left(1-\mu_4^2\right)}y_1+\frac{2h\mu_4\mathrm{E}_5}{5\left(1-\mu_4^2\right)}+\frac{h\mu_6\mathrm{E}_6}{10\left(1-\mu_6^2\right)},$$

$$A_{66}=\frac{h\mathrm{E}_1}{20\left(1+\mu_1\right)}+\frac{h\left(\mathrm{E}_2-\mathrm{E}_3\right)}{5\left(1+\mu_2\right)}y_1+\frac{h\mathrm{E}_3}{5\left(1+\mu_2\right)}+\frac{h\left(\mathrm{E}_4-\mathrm{E}_5\right)}{5\left(1+\mu_4\right)}y_1+\frac{h\mathrm{E}_5}{5\left(1+\mu_4\right)}+\frac{h\mathrm{E}_6}{20\left(1+\mu_6\right)},$$

$$B_{11}=B_{22}=-\frac{9h^2\mathrm{E}_1}{200\left(1-\mu_1^2\right)}+\frac{4h^2\left(\mathrm{E}_2-\mathrm{E}_3\right)}{25\left(1-\mu_2^2\right)}\left(y_2-y_1\right)-\frac{4h^2\mathrm{E}_3}{50\left(1-\mu_2^2\right)}+\frac{4h^2\left(\mathrm{E}_4-\mathrm{E}_5\right)}{25\left(1-\mu_4^2\right)}y_2+\frac{4h^2\mathrm{E}_5}{50\left(1-\mu_4^2\right)},$$

$$+\frac{9h^2\mathrm{E}_6}{200\left(1-\mu_6^2\right)},$$

$$B_{12}=B_{21}=-\frac{9h^2\mathrm{E}_1\mu_1}{200\left(1-\mu_1^2\right)}+\frac{4\mu_2h^2\left(\mathrm{E}_3-\mathrm{E}_2\right)}{25\left(1-\mu_2^2\right)}\left(y_2-y_1\right)-\frac{4h^2\mu_2\mathrm{E}_3}{50\left(1-\mu_2^2\right)}+\frac{4\mu_4h^2\left(\mathrm{E}_4-\mathrm{E}_5\right)}{25\left(1-\mu_4^2\right)}y_2+\frac{4h^2\mu_4\mathrm{E}_5}{50\left(1-\mu_4^2\right)}$$

$$+\frac{9\mu_6\mathrm{E}_6h^2}{200\left(1-\mu_6^2\right)},$$

$$B_{66}=-\frac{9h^2\mathrm{E}_1}{400\left(1+\mu_1\right)}+\frac{2h^2\left(\mathrm{E}_2-\mathrm{E}_3\right)}{25\left(1+\mu_2\right)}\left(y_2-y_1\right)-\frac{2h^2\mathrm{E}_3}{50\left(1+\mu_2\right)}+\frac{2h^2\left(\mathrm{E}_4-\mathrm{E}_5\right)}{25\left(1+\mu_4\right)}y_2+\frac{2h^2\mathrm{E}_5}{50\left(1+\mu_4\right)}$$

$$+\frac{9h^2\mathrm{E}_6}{400\left(1+\mu_6\right)},$$

$$D_{11}=D_{22}=\frac{61h^3\mathrm{E}_1}{3000\left(1-\mu_1^2\right)}+\frac{8h^3\left(\mathrm{E}_2-\mathrm{E}_3\right)}{125\left(1-\mu_2^2\right)}\left(y_3+y_1-2y_2\right)+\frac{8h^3\mathrm{E}_3}{375\left(1-\mu_2^2\right)}+\frac{8h^3\left(\mathrm{E}_4-\mathrm{E}_5\right)}{125\left(1-\mu_4^2\right)}y_3+\frac{8h^3\mathrm{E}_5}{375\left(1-\mu_4^2\right)}$$

$$+\frac{61h^3\mathrm{E}_6}{3000\left(1-\mu_6^2\right)},$$

$$D_{12}=D_{21}=\frac{61h^3\mu_1\mathrm{E}_1}{3000\left(1-\mu_1^2\right)}+\frac{8h^3\mu_2\left(\mathrm{E}_2-\mathrm{E}_3\right)}{125\left(1-\mu_2^2\right)}\left(y_3+y_1-2y_2\right)+\frac{8h^3\mu_2\mathrm{E}_3}{375\left(1-\mu_2^2\right)}+\frac{8h^3\mu_4\left(\mathrm{E}_4-\mathrm{E}_5\right)}{125\left(1-\mu_4^2\right)}y_3+\frac{8h^3\mu_4\mathrm{E}_5}{375\left(1-\mu_4^2\right)}$$

$$+\frac{61h^3\mu_6\mathrm{E}_6}{3000\left(1-\mu_6^2\right)},$$

https://doi.org/10.62500/icrtsda.1.1.42

$$D_{66}=\frac{61h^3\mathrm{E}_1}{6000\left(1+\mu_1\right)}+\frac{4h^3\left(\mathrm{E}_2-\mathrm{E}_3\right)}{125\left(1+\mu_2\right)}\left(y_3+y_1-2y_2\right)+\frac{4h^3\mathrm{E}_3}{375\left(1+\mu_2\right)}+\frac{4h^3\left(\mathrm{E}_4-\mathrm{E}_5\right)}{125\left(1+\mu_4\right)}y_3+\frac{4h^3\mathrm{E}_5}{375\left(1+\mu_4\right)}$$

$$+\frac{61h^3\mathrm{E}_6}{6000\left(1+\mu_6\right)}.$$

https://doi.org/10.62500/icrtsda.1.1.43

Proc. 1st International Conference on Recent Trends in Statistics and Data Analytics
Air University Islamabad, Pakistan – May 9, 2024, Vol. 1, pp. 425-429

Analysis of statistical data in determining productivity and efficiency of input allocation in wheat fields of sistan region

Mahmood Mohammadghasemi*[1], Ahmad Ghasemi[2] and Mohammadreza Narooi Rd[3]
Iran, Sistan and Baluchestan Province - Zabul, Sistan Agricultural Education and Natural Resources Research Center.

ABSTRACT

Wheat is main crop and has a major role from aspect income in sistan. Exactly more than 80 percent wheat production of province is belonged to sistan Differences efficiency and productivity between to productions is one of important recognition ways strength and weakness current condition of agriculture. Because with use efficiency of production factor has possibility high production and improvement income with ought Increases in basic resource and or uses of new technology in result to can increase operation in unit level very increase. The result with use of Excel & Eviews software, showed if the average level under cultivated one percentage increase the amount of produced will increase 1 / 1 percent. Negative coefficient indicates that using of water input has been used in uneconomic area. Also maximum and minimum average productivity related to inputs of under cultivated area and water. Average productivity of under cultivated area showed that the average per hectare under cultivation product is produced 2365/35 kilogram. Thus the average efficiency inputs water, fertilizer and labor show that a per cubic meter of water, one kg of fertilizer and each of labor, respectively, each 0.198, 7 / 73, 485/11 kg wheat can be achieved Among of them, Average productivity of inputs: water, fertilizer and labor Showed that one unit extra of inputs water, fertilizer and labor respectively making to increase 0.198, 7.73 and 485.11 (kg) in production wheat. Marginal productivity of fertilizer and labor were get 0.108, 28.564. Furthermore criterions of VMPXi /PXi show that consumption water in uneconomic area and another input used less than optimum. Total productivity equal to 4.65 that is showing that one unit extra of total input make increase 4.65 kg in production. Under cultivated area, water, labor and fertilizer have significant effect on producing this crop, but are used of the mention factors uneconomically.

Key word: sistan area, water, statistical data, Wheat

1. INTRODUCTION

Deficit of sources and productivity is one of the important limited factors in agricultural (Mohamadghasemi, 2017). Al through before decade had was various ways for increase production of agricultural products such as increase under cultivated area, but limitations such unavailable suitable land for cultivation, investment, water and other factor cause pay attention more on use from methods increment productivity production factor. The 90 percentage increase of agriculture production is cause improve productivity of production factor. Therefore require to scientific study on productivity of agriculture production factor (sardarshahraki etal, 20120).

Investigation for economic review of application of factors in production of cotton in garmsar city from estimated of transcendental production function.

Result had showed that farmers with under cultivation area rather perform economic usually in consumption factor while consumption of often production factor was in third of production (Mohamadghasemi et al, 2021).

https://doi.org/10.62500/icrtsda.1.1.43

In review of productivity and allocation of grape production factor in khorasan province there used from third degree and several sentences of production function. Result was indicated that 47 % of gardener that used water more than optimum. And 95, 56 and 43 % from garden and whole there respectively in use of poison, nitrogen fertilizer, phosphor fertilizer and land was less than optimum (karim et al, 2020).

Study of expensive operation agriculture research and broad casting in American with use of cobb-douglas equation for final evaluation of sowed operation were get result that research and broad casting is cause of increasing operation output factors (Zeng et al., 2014).

Study of operation factors for wheat production with use of production equation in penjab showed one percent increase in number educated person and in area cultivation because respectively1.23 and 0.437 percent increase in agriculture operation (Rogkos et al, 2021).

Bialy, 2002 in one research on cow milk production found out amount of capital, job power and research potential have positive effect on milk production. With atteation of self sufficiency of wheat was need yesterday, and will had tomorrow development there fore achieve to this aim there are two ways: Increase of cultivation area or increase of yield in unit of area. Statistics is showed in sistan region under cultivation in year 2007-2008 for wheat was 298610 hectare in irrigated cultivation. Also statistics show that Wheat yield in farm condition was low than research condition. Such as research yield is 8T/ ha and farm yield is 2T/ ha

2. [METHOD]

There are two manners for calculating of productivity. First econometrics method and second non parametric. In econometrics method productivity will be estimated by two equations of production and cost. Second method is method criterion of productivity determination with use of mathematical planning or calculating of index number.

In this study has been used from econometrics method and have to bring review productivity and optimum allocation of production factors in wheat cultivation with estimation of production function , while that have calculated with total factor productivity index by use from non parametric method. Results showed that cobb-douglas production equation is better. There fore introduce total form of cobb-douglas function to below:

The logarithm form of mention function expression to below

That in mention relation Y is total amount of out put, X amount of input used in process of out put and A and B is function coefficient. In more economic study usually have rested calculated two type of productivity, partial productivity and total productivity.

Average production is mean of output that calculated by follow equation.

Marginal productivity is showed change in total production lieu to change one unit of input. Another word marginal productivity expression amount of change in total out put in live change in one unit of factor used

In order to determine of circumstance allocative of production factor use of concept value of marginal productivity each of factor.

In high relation, PY target price of production if value of marginal productivity on factor equal to price

In this case amount of consumption factor (with assumption competitive market) will be optimum limitation. If value of marginal productivity of factor equal to value of that factor exception to this is that factor allocation to set desired limit and another word that allocation efficiency equal to 100 percent and circumstance an allocation optimum of factor production decrease that productivity. If value of

https://doi.org/10.62500/icrtsda.1.1.43

marginal productivity of variable input larger than this price, ( ) in this case allocation of factor wasn't efficiency. Therefor must use of more units from variable input in production product. Conversely allocation efficiency using of factor is better decrease consumption of factor.

We can not measure reality of production unit by partially productivity of production factors. Therefore use from criterion total productivity of factor production for assessment operation of units production. Total factor production (TFP) definition to face ration of index quantity of output to index quantity of factors (salami 1376 and Jain 1992). For calculating of total productivity with attention to different units of factors and also……..

Also for access to total productivity of factor in production unit has been used from of kendrik index.

TFPi: index of total productivity of jom production unit

Yi: amount of total out put obtain in jom production unit

SS: average shear of cost factor in total costs of units

Xji: amount of factor in jom unit production

Data in this study has collected by desing and complete questionnaire from farmers in sistan (2007). Sam plewith use from kocvan equation was used from 280 operation and sampling with two stage random method.

3. [OBSERVATİON AND RESULTS:]

The result from estimate of cubb-douglas production function display in table 1. Coefficient in production function is production elasticity. As coefficient of area under cultivation show if under cultivation area in unit wheat in this study so that average one percentage increase, production increasing equal to 1/1 percentage. The negative coefficient of water factor statement this is that use from this factor in region an economic. Coefficients obtain for fertilizer and labor show the former wheat use of this two factor in two regions economic that is logical region.

Significant F was in level less than one percent statement this is that in sum model is significant. R2 adjustment show that , 5 percentage form change of wheat accounting in units case of examination with use from explanatory variables current in model.

With perform azmoons appear that mode haven't difficult from point of view collineavity, and heteroscedasticity difficult of auto – correlation model removed after distinction. Exactly DW amareh is 2.077.

Average and marginal productivity with use from relations (3) and (4) calculated for all factors and introduce those results in 2 schedules.

Just as observation in & schedule, maximum and minimum productivity related to under cultivation area and water.

Average productivity of under cultivation area had showed that on the average (middingly) in live of one hectare under cultivation production 35/2365 produce. Thus average productivity of factors: water, fertilizer and labor has showed that in live of on (m3) water, one kg fertilizer and each labor to average 485/11, 7/73, 128% kg obtain wheat produce. Thus result showed that maximum marginal productivity relation to laud factor and equal to z, 4/21 . There for in live of increase on hectare under cultivation area increasing wheat produce equal to z, 4121 . Negative marginal productivity of water expresses that farmer's wheat in area in use of this factor are in uneconomic area.

Marginal productivity of fertilizer and labor is 0/10 and 28/5. Also one unit extra of this inputs respectively make to increasing in production to amount 0.108 and 28/5 kg. Criterion VMPxi/pxi had showed that consumption water was in uneconomic area and another input used less than optimum. Thus should consumption this factor by farmers increase until come to optimum limitation

https://doi.org/10.62500/icrtsda.1.1.43

6. COMMENTS AND CONCLUSION

Search of economic behavior of wheat producers in the region Sistan through estimation production function showed that the most efficacious factors in wheat production is surface under cultivation, water level, fertilizers and labor so that if surface under cultivation increase a percentage equivalent of production will increase rate to 1/1 percent. Negative coefficient of water input indicates that this input used in non-economic area. The most and least average productivity depended to inputs surface under cultivation and water. Also the results show that the most marginal productivity related to the land input and is equivalent to 21/2604. Thus to increase the per hectare surface under cultivation is added rate to equal to21 / 2604 kg to wheat product. In addition, VMPxi/pxi had showed that consumption water was in uneconomic area and another input used less than optimum. Therefore, the equivalent total productivity advantage 65 / 4 means that the per a using total input unit (total building by) produce in region farms on the average 65 / 4 kg wheat production.

Suggestions:

Considering the results of this study, are will be offered, several recommendations, mostly derived from results of analysis:

- Considering that surface under cultivation has the most tension between the production factors therefore suggested that is interest rates to increase productivity right solution used in this context that appears to consider inheritance law reform the consolidation of lands creating cooperative in order to increase the surface under cultivation appropriate.

- Review in about efficient allocation factors suggests non-economic consumption of water. Therefore suggested to the education and awareness to the farmers in this area and create proper platforms for efficiency savings in water consumption as regular network of irrigation and drainage and clearing of lands that enhance water use efficiency water consumption brings to the optimum level.

- Amounts of using fertilizer and work force input show that farmers in area use of this input in the production economic region but different from optimum level. There fore for gain maximum benefit, it is necessary that shall be changed amount of use above inputs.

Table. 1estimate of cubb-douglas production function

variable	coefficient	Std.Error	Significant
Fix coefficient	9.195	1.046	0.000
Under cultivation area(hecter)		1.101	0.118 0.000
Water(m3)	-0.179	0.112	0.109
Fertilizer(kg)	0.014	0.007	0.056
labor	0.059	0.021	0.006
AR(1)	0.194	0.059	0.001

https://doi.org/10.62500/icrtsda.1.1.43

Table2 Average and marginal productivity

factor	Average productivity	Marginal productivity
Under cultivation area(hecter)		2365.352604.21
Water(m3)	0.198	-0.035
Fertilizer(kg)	7.73	0.108
Labor	485.11	28.564

REFERENCES

1. Karim and Others, 2020., Management Challenges and Adaptations with Climate Change in Iran Forests, Caspian Journal of Environmental Science. 18 (1), 2020.
2. Mohammadghasemi,M.,(2017). Water Resources Management of Hirmand River Basin for Agricultural Productiones Using Stochastic Dynamic Programming.iournal hydroscinces and environment.vol.1.20-24. Issn:2345-5608
3. Mohammadghasemi, M., Karim, M. H., Dahmardeh, M., & Ghasemi, A. (2021). The Prospect of Investment in Medicinal Plants at Sistan Region1. Journal of Medicinal plants and By-product, 10(2). 127-132.
4. Ragkos; A., Ambas V.(2021). Examining the potential of an irrigation work to improve sustainability in a rural area. Water Supply 21 (6) 2959–2973.
5. Sardar Sharaki, Karim MH., 2020. The Economic Efficiency Trend of Date Orchards in Saravan County, Iran. Econ. Rev. 22(4), 1093-1112.
6. Sardar Sharaki, Karim MH., 2020. The Economic Efficiency Trend of Date Orchards in Saravan County, Iran. Econ. Rev. 22(4), 1093-1112.
7. Zeng, X., Hu, T., Guo, X., & Li, X. (2014). Water transfer triggering mechanism for multi-reservoir operation in inter-basin water transfer-supply project.Water Resources Management, 28(5), 1293-1308.

Cutting room fabric losses and their degree of prevalence: A support to sustainability

https://doi.org/10.62500/icrtsda.1.1.45

Proc. 1st International Conference on Recent Trends in Statistics and Data Analytics
Air University Islamabad, Pakistan – May 9, 2024, Vol. 1, pp. 430-436

A Theoretical Approach to Study Drinking Epidemic

Kashaf Ishfaq[1] , Iqra Shahid[2] , Muhammad Imran Aslam[3] , Muhammad Rizwan[4] , Yasir Nadeem Anjam[5] and Muhammad Arshad[6]
[,1,2,3,5,6]Department of Applied Sciences, National Textile University, Faisalabad 37610, Pakistan
[4]Ministry of Food Security and Research, Isalamabad.

Abstract

The aim of this study is to explore the dynamics of drinking epidemic model. The focuses of the study are attained by the employment of fractal-fractional order through the launch of Atangana Baleanu Caputo operator. The behavioral versatility of the population under examination is induced by proposing four mutually exclusive compartments that is; susceptible class, heavy drinker class, drinkers in treatment class and recovered class. The theoretical environment of the proposed synergy is elaborated with respect to wide range of parametric setting involving varying values of order and dimensions. The temporal dynamics of every stratum of the population under consideration is then explored with respect to each parametric setting. The attainment of numerical solutions is facilitated by the application of Adam Bashforth iterative technique, whereas the existence of the solution along with uniqueness is argued within the framework of fixed point theory. Also, nonlinear functional analysis is tossed to demonstrate the Ulam-Hyer's stability. The outcomes of this study convincingly argue the utility of the fractal-fractional order setup in the elaboration of drinking epidemic dynamics prevailed in a population. Keywords: Epidemic model; fractal-fractional; Ulam–Hyers stability; iterative technique. 1. Introduction The misuse of alcohol is acknowledged as a leading contributor to the onset of more than 200 diseases, injuries, and various health ailments. Alcohol addiction is closely associated with heightened risks encountering health issues, spanning mental and behavioral disorders such as alcohol dependence to significant non- communicable illnesses like liver cirrhosis, specific cancers, and cardiovascular conditions [1]. Preprint submitted to . May 6, 2024 Approximately 3.3 million fatalities annually are attributed to drinking, with the majority of these deaths transpiring without primary intervention [2]. Over the past twenty years, researchers have diligently endeavored to identify the factors responsible for the proliferation of the phenomenon within society. The researchers have devised various epidemiological models aimed at pin- pointing the causes of alcoholism and strategies for containing the their transmission within the community [3, 4, 5]. Fractional-order mathematical models play a crucial role and offer numerous benefits in capturing the dynamic characteristics of real-world phenomena. Moreover, they exhibit greater precision and reliability compared to tradi- tional integer-order derivatives, thanks to their additional capabilities in representing hereditary and memory effects [6]. It was Riemann and Liouville who initially formalized the RL fractional derivative, marking a significant advancement in the field. Building upon this innovative concept, Caputo and Fabrizio introduced a fresh definition for fractional order derivatives incor- porating an exponential kernel, coined as the Caputo-Fabrizio fractional derivative [7]. Abdon Atangana and Dumitru Baleanu, proposed a novel definition for the arbitrary order derivative utilizing the Mittag- Leffler kernel, a non-local and nonsingular kernel, termed as the AB fractional derivative in the spirit of Caputo's and Riemann-Liouville's formulations independently [8]. The utilization of fractional operators finds widespread appli- cation across nearly every scientific domain. An instance of this is demonstrated in the implementation of the ABC fractional modeling approach for a time-variable predator-prey model, as detailed in [9]. Similarly, sana qureshi (2019) explores the utilization of fractional calculus to accurately model the dynamics of blood ethanol levels, incor- porating the complex non-linear behaviors observed in real-world scenarios [10]. Moreover, Saima Rashid in (2022) investigates the application of fractal-fractional calculus to model the intricate dynamics of media addiction, capturing the nonlinear behavior inherent in addictive behaviors [11]. Moreover, Lei Zhang (2022) analysis of a fractional-order smoking model with relapse and harmonic mean type incidence rate under the ABC operator" examines the dynamics of smoking behavior incorporating relapse phenomena and complex incidence rates using fractional calculus [12]. Recognizing the delicacy of the problem, our aim in this

https://doi.org/10.62500/icrtsda.1.1.45

paper is to construct and analyze a mathematical model focusing at the prevalence of drinking in a population. The population understudy is stratified into four compartments such as; susceptible class, drinking class, heavy drinking class and recovered class. The proposed model employs fractal-fractional order derivatives through the Atangana-Baleanu Caputo (ABC) operator, ensuring a comprehensive representation of complex dynamics in the context of alcohol-related diseases. Initial scrutiny of the model establishes the validity of solutions via fixed-point theory, ensuring both existence and uniqueness. Sub2 sequent analysis using Ulam-Hyres stability via nonlinear functional analysis confirms solution stability, a critical aspect in understanding the model's behavior. Recognizing the significance of the research, a novel fractional Adam-Bashforth iterative numerical scheme is introduced for numerical simulations, further validated through MATLAB simulations. The numerical outcomes, plotted across various fractional orders and fractal dimensions, reveal distinct patterns compared to integer orders, emphasizing the model's sensitivity to these parameters. This underscores the efficacy of the fractional approach in capturing nuanced aspects of alcohol-induced diseases, providing valuable insights for intervention strategies and policy formulation. The structure of this article is meticulously divided into five sections for a clear delineation of content. Section 2 delineates the methodologies and materials employed. Section 3 focuses on a rigorous analysis of existence and Ulam-Hyers stability within the theoretical framework. Section 4 provides a numerical evaluation that substantiates the theoretical findings. The final section offers a comprehensive discussion and concludes with insights into the proposed model. 2. Methods and material 2.1. Description of the Model This study investigates a mathematical model to understand the propagation of alcohol consumption within the human population at any given time t. The model divides the total population into four compartments: Susceptible individuals A(t), Heavy drinkers individuals P(t), Drinkers in treatment Z(t) and Recovered individuals R(t). Based on the above mentioned consideration, we have the compartmental flow diagram depicted in Figure 1. Thus, the total human population N(t) at any given time t is expressed as: N(t) = A(t) + P(t) + Z(t) + R(t). Therefore, the basic model for the drinking epidemic is controlled by a system of nonlinear differential equations. dA dt = Π − βAP − μA + σR, dP dt = βAP − (μ + γ1 + θ)P, dZ dt = θP − (μ + γ2 + γ)Z, dR dt = γZ − (μ + σ)R, (1) 3 A P Z R β θ σ γ Π μ (μ + γ1) (μ + γ2) μ Figure 1: Schematic diagram for the transmission of drinking dynamics model. In accordance with the conditions: A(0) ≥ 0, P(0) ≥ 0, Z(0) ≥ 0, R(0) ≥ 0, 0 < a, p ≤ 1. Each term that impacts the system, as outlined in model (1), is described in Table 1.. Table 1: Description of each term of the equations of the model (1). Parameter Description Π Recruitment rate of the susceptible people β Transmission rate from susceptible class to heavy drinker people σ Transmission rate from recovered people to susceptible people μ Natural death rate γ1 Drinking induced death rate of heavy drinker people θ Proportion of drinking entering of drinker in treatment class γ2 Drinking induced death rate of drinker in treatment people γ Recovered rate of drinker in treatment people 2.2. Fractional Expansion of the Model This modification facilitates a more thorough exploration of the long-term memory effects characteristic of alcohol consumption dynamics. This sophisticated approach yields a more precise representation, crucial 4 for navigating the complexities and evolving patterns prevalent in real-world scenarios of alcohol use. Definition 2.1. Consider a continuous and differentiable function W(t) defined over the interval (c, d), characterized by a fractional order 0 < a ≤ 1 and a fractal dimension 0 < p ≤ 1. This function can be delineated in terms of an ABC framework as follows: ABCD a,p (W(t)) = ABC(a) (1 − a) d dsp Z t 0 W(s)ka −η (1 − a) t − sa a ds. In this context, ABC(a) denotes a 'normalization mapping' defined such that ABC(0) = ABC(1) = 1, which functions as the normalization constant. Here, ka a represents a well-defined mapping known as the 'Mittag-Leffler' function, which includes the exponent mapping as a particular instance [?]. Definition 2.2. Consider the expression for a continuous function W(t) defined over the interval (c, d). The fractal-fractional order integral of W(t), characterized by a fractal order 0 < a ≤ 1 and a fractal dimension 0 < p ≤ 1, can be articulated in the ABC framework as follows: ABCI a 0 (W(t)) = (1 − a) ABC(a) t p−1W(t) + ap ABC(a)Γ(a) Z t 0 (t − s) a−1 s p−1W(s)ds. (2) Lemma 2.2.1. Let's express the solution to the provided problem considering 0 < p, a ≤ 1, ABCD a 0 (W(t)) = pt p−1Y(t, W(t)), t ∈ [0, T], W(0) = W0, 0 < a, p ≤ 1, is provided by W(t) = W0 + (1 − a) ABC(a) t p−1Y(t, W(t)) + pa ABC(a)Γ(a) Z t 0 (t − s) a−1 s p−1Y(s, W(s))ds. Definition 2.3. [15] (Contractions Mapping). Suppose B is a Banach space. Then the operator T : X → X is a contraction if, kT(x) − T(y)k ≤ Mkx − yk, ∀x, y, ∈ X, 0 < M < 1. Lemma 2.3.1. [15] (Banach's fixed point theorem). If a Banach space B contains a non-empty open subset D, then any contraction mapping q from D into itself possesses a unique fixed point. Lemma 2.3.2. [15] (Krasnoselskii's fixed points theorem). The

https://doi.org/10.62500/icrtsda.1.1.45

Banach space B has a non-empty, closed, convex subset D. Let F1 and F2 be two operators satisfying the following conditions: 5 (i) F1 x + F2y ∈ D, ∀x, y ∈ D, (ii) The operator F1 is both compact and continuous (iii) The operator F2 is a contraction mapping. Then, there exists ∈ D such that F1v + F2v = v. Theorem 2.4. [16] Every sequence that contracts is a Cauchy sequence, thus ensuring convergence in a complete metric space. Theorem 2.5. Let B ⊆ R and Ψ : B → R n be continuously differentiable mappings, where s ∈ B. Then, for each compact subset B of B, the function Ψ satisfies a Lipschitz condition. The associated Lipschitz constant, denoted by L, is defined as L > 0, representing the supremum of the norm of the derivat L = sup s∈B dΨ ds . Subsequently, for t ≥ 0, we introduce the proposed nonlinear deterministic mathematical model (1) for alcohol consumption. This model employs the fractal-fractional order derivative via the ABC fractional order operator, which is characterized by a fractional order 0 < a ≤ 1 and a dimension 0 < p ≤ 1. ABCD a,p t A(t) = Π − βAP − μA + σR, ABCD a,p t P(t) = βAP − (μ + γ1 + θ)P, ABCD a,p t Z(t) = θP − (μ + γ2 + γ)Z, ABCD a,p t R(t) = γZ − (μ + σ)R, (3) with the initial conditions A(0) ≥ 0, P(0) ≥ 0, Z(0) ≥ 0, R(0) ≥ 0, 0 < a, p ≤ 1. The system (3) operates independently, which allows it to be described in a simple way: □ □□□□□□ □□□□□□ ABCD a,p t V(t) = M(V(t)), 0 < t < tf < ∞, V(0) = V0. (4) 6 Here, V :, [0, +∞) → R4 and M :,R 4 → R4 are vector-valued functions defined as: V(t) = □ □□□□□□□□□□□□□□□□□□□□□□□□□□ A(t) P(t) Z(t) R(t) □ □□□□□□□□□□□□□□□□□□□□□□□□□□ , V0 = □ □□□□□□□□□□□□□□□□□□□□□□□□□□ A0 P0 Z0 R0 □ □□□□□□□□□□□□□□□□□□□□□□□□□□ , M(V(t)) = □ □□□□□□□□□□□□□□□□□□□□□□□□□□ Π − βAP − μA + σR βAP − (μ + γ1 + θ)P θP − (μ + γ2 + γ)Z γZ − (μ + σ)R □ □□□□□□□□□□□□□□□□□□□□□□□□□□ . Theorem 2.6. The function M(V) in (4) exhibits Lipschitz continuit Proof. Let E denote a convex compact subset of E = n (t, V) | 0 ≤ t ≤ tf , V ∈ R4 o . Let V1, YV2 ∈ E. Then, according to the mean value theorem, there exists W ∈ (V1, V2) such that, M(V1(t)) − M(V2(t)) V1(t) − V2(t) = M0 (W(t)), or M(V1(t)) − M(V2(t)) = M0 (W(t)) · (V1(t) − V2(t)), | M(V1(t)) − M(V2(t)) | = | M0 (W(t)) · (V1(t) − V2(t)) |, ≤ || M0 (W) ||∞ ||V1 − V2||∞. As M ∈ C 1 [0, , tf] over the convex compact set E, there exists a positive constant τ such that: || M0 (W) ||∞ ≤ τ. Hence, | M(V1(t)) − M(V2(t)) | ≤ τ||V1 − V2||∞, sup t∈[0, tf] | M(V1) − M(V2) | ≤ τ||V1 − V2||∞, || M(V1) − M(2) ||∞ ≤ τ||V1 − V2||∞. Thus, M(W) is Lipschitz. 7 3. Theoretical Insights into the Model 3.1. Theory Of Existance We now turn our attention to investigating the existence of the proposed model. Let us define a Banach space W = Y × Y × Y × Y × Y × Y, where Y = H([0, T],R) represents the function space. The norm in this space is defined as follows: kXk = kWk = maxt∈[0,T] X(t) Specifically, kXk = kWk = maxt∈[0,T] |A(t)| + |P(t)| + |Z(t)| + |R(t)| . To establish the existence and uniqueness of the model formulated in (3), we utilize the fixed-point theorem. It is important to note that the integral is differentiable, which allows us to express the model (3) as follows: ABCD a (A(t)) = pt p−1M1(A(t), t) = Π − βAP − μA + σR, ABCD a (P(t)) = pt p−1M2(P(t), t) = βAP − (μ + γ1 + θ)P, ABCD a (Z(t)) = pt p−1M3(Z(t), t) = θP − (μ + γ2 + γ)Z, ABCD a (R(t)) = pt p−1M4(R(t), t) = γZ − (μ + σ)R, (5) The system (5) operates independently; therefore, it can be summarized briefly as: □ □□□□□□ □□□□□□ ABCD a 0 (W(t)) = pt p−1Y(t, W(t)), t ∈ [0, T], W(0) = W0, 0 < w,r ≤ 1, (6) and solution to equation (6) can be expressed as: W(t) = W0 + (1 − a) ABC(a) t p−1Y(t, W(t)) + ra ABC(a)Γ(a) Z t 0 (t − s) a−1 s p−1Y(s, W(s))ds. (7) Where, W(t) = □ □□□□□□□□□□□□□□□□□□□□□□□□□□ A(t) P(t) Z(t) R(t) □ □□□□□□□□□□□□□□□□□□□□□□□□□□ , W0 = □ □□□□□□□□□□□□□□□□□□□□□□□□□□ A0 P0 Z0 R0 □ □□□□□□□□□□□□□□□□□□□□□□□□□□ , Y(t, W(t)) = □ □□□□□□□□□□□□□□□□□□□□□□□□□□ M4(A, P, Z, R, t) M4(A, P, Z, R, t) M4(A, P, Z, R, t) M4(A, P, Z, R, t) □ □□□□□□□□□□□□□□□□□□□□□□□□□□ . 8 Let's reformat system (3) into a fixed-point form. We define the mapping T : V → V as follows: T(W)(t) = W0 + (1 − a) ABC(a) t p−1Y(t, W(t)) + pa ABC(a)Γ(a) Z t 0 (t − s) a−1 s p−1Y(s, W(s))ds. (8) Assume T = E + M, where E(W) = W0 + (1 − a) ABC(a) t p−1Y(t, W(t)), M(W) = ra ABC(a)Γ(a) Z t 0 (t − s) a−1 s p−1Y(s, W(s))ds. (9) Subsequently, we will conduct a qualitative analysis of the provided system using fixed-point theory. (V1) There exists a constant LY, MY, such that, |Y(t, W)| ≤ LY|W| + MY. (V2) There exists a positive constant LY such that for any v, v¯ ∈ W provided that, |Y(t, v) − Y(t, v¯)| ≤ LY[|v − v¯|]. Theorem 3.1. If conditions (W1, W2) are satisfied, the system (7) has at least one solution. Then, the system (3) produces an equivalent number of solutions under the condition that (1−a) ABC(a) t

https://doi.org/10.62500/icrtsda.1.1.45

p−1LY < 1. Proof. We establish the theorem through two outlined steps as follows: Step I: Let ¯v ∈ W where W = v ∈ W : ||v|| ≤ φ, , φ > 0 represents a convex closed set. Therefore, for the operator E defined in (9), one has: ||E(v) − E(¯v)|| = (1 − a) ABC(a) t p−1maxt∈[0,T] |Y(t, v(t)) − Y(t, v¯(t))|, ≤ (1 − a) ABC(a) t r−1LY||v − v¯||. (10) Hence, the operator E is closed and, therefore, a contraction. Step II:We will now verify the relative compactness of the operator M, demonstrating its continuity and boundedness. It is evident that the operator M is well-defined over the entire domain, given that Y is |N(v)|| = maxt∈[0,τ] || pa ABC(a)Γ(a) Z t 0 (t − s) a−1 s r−1Y(s, W(s))ds , ≤ pa ABC(a)Γ(a) Z t 0 (s) a−1 (1 − s) p−1 |Y(s, W(s))|ds, ≤ p[LY|W| + NYT a+p−1] ABC(a)Γ(a) B(a, p) . (11) 9 The symbol B(a, p) denotes the beta function. Consequently, given equation (11), the operator M is established to be bounded. To demonstrate "equi-continuity," assume t1 > t2 where both are within [0, τ], we observe: |M(W(t2)) − M(W(t1))| = pa ABC(a)Γ(a) Z t2 0 (t2 − x) a−1 x p−1Y(x,w(x))dx − Z t1 0 (t1 − x) a−1 x p−1Y(x, W(x))dx, ≤ p[LY|W| + NYT a+p−1]B(a, r) ABC(a)Γ(a) [t a 2 − t a 1]. (12) As t2 approaches t1, the right-hand side of (12) tends to zero. Furthermore, owing to the continuity of the operator M, we have: |M(W(t2)) − M(W(t1))| → 0, as t2 → t1. Thus, we have demonstrated that M is both bounded and continuous, thereby confirming its uniform continuity. According to the Arzela-Ascoli theorem, a subset W of W associated with M is compact if and only if it is closed, bounded, and equicontinuous. Given that M exhibits relative compactness and complete continuity, it satisfies these criteria. In light of equations (3) and (7), we conclude that the system possesses at least one solution. To establish the uniqueness of the solution for the model (3), we employ the fixed-point method as detailed in [15]. Theorem 3.2. Under assumption (V2) and the uniqueness of solution for (7), we assert that the system (3) also possesses a unique solution if the condition (1−a)t p−1LY ABC(a) + p[LYT a+r+1]B(w,r) ABC(a)Γ(a) < 1 is satisfied. Proof. Let the operator T : W → W by T(W)(t) = W0(t) + Y(t, W(t)) − Y0(t) (1 − a) ABC(a) t p−1 + pa ABC(a)Γ(a) Z t 0 (t − x) a−1 t p−1Y(x, W(x))dx, t ∈ [0, τ]. Let v, v¯ ∈ W, then ||T(v) − T(¯v)|| ≤ (1 − a) ABC(a) t p−1maxt∈[0,τ] Y(t, v(t)) − Y(t, v¯(t)) + pa ABC(a)Γ(a) maxt∈[0,τ] Z t 0 (t − x) a−1 t p−1Y(x, v(x))dx − Z t 0 (t − x) a−1 t p−1Y(x, v¯(x))dx, ≤ Θ||v − v¯||, (13) 10 and Θ = (1 − a)t p−1LY ABC(a) + p[LYT w+r+1]B(a, p)LY ABC(a)Γ(a) . (14) Upon examining (13), it becomes apparent that the operator T acts as a contraction. Consequently, equation (7) admits a unique solution. Therefore, the system described in (3) also possesses a unique solution.

3.2. Ulam-Hyers Stability The objective of this section is to establish the Ulam-Hyers (UH) stability for the proposed model (3). Definition 3.3. The suggested model is said to be Ulam-Hyers (UH) stable if there exists a constant ℵa,p > 0 such that for any % > 0 and for every function W ∈ C([0, T],R), the following condition is satisfied: ABCD a,p t W(t) − ψ(t, W(t)) ≤ %, t ∈ [0, T], (15) and there exists a unique solution φ ∈ C([0, T],R) such that, W − φ(t) ≤ ℵa,p %, t ∈ [0, T]. (16) Consider a small perturbation φ(t) ∈ C([0, T],R) with φ(0) = 0. We define: • |φ(t)| ≤ %, for % > 0; • ABCD a,p t W(t) = Y(t, W(t)) + φ(t). Lemma 3.3.1. The solution to the perturbed problem ABCD a,r t W(t) = Y(t, W(t)) + ψ(t), W(0) = W0, (17) satisfies the following relation W(t) − W0(t) + [Y(t, W(t)) − ψ0(t)] (1 − a) ABC(a) t p−1 + pa ABC(a)Γ(a) Z t 0 (t − x) a−1 x p−1Y(x, W(x))dx , ≤ Γ(a)t p−1 + pT a+p−1 ABC(aΓ(a) B(a, p)% = $a,p%. (18) Proof. For the sake of simplicity, we will not delve into the proof.

Theorem 3.4. Under assumption (V2) and in light of equation (18), the solution to equation (7) demonstrates Ulam-Hyers stability. Consequently, the analytical solution to the proposed system attains UlamHyers stability provided that Θ < 1. 11 Proof. Let v ∈ W denote a unique solution and ¯v ∈ W be any solution of equation (7), then |v(t) − v¯(t)| = |W(t) − W0(t) + [Y(t, v¯(t)) − Y0(t)] (1 − a) ABC(a) t p−1 + pa ABC(a)Γ(a) Z t 0 (t − x) a−1 x p−1Y(x, v¯(x))dx , ≤ |W(t) − W0(t) + [Y(t, W(t)) − Y0(t)] (1 − a) ABC(a) t p−1 + pa ABC(a)Γ(a) Z t 0 (t − x) a−1 x p−1Y(x, W(x))dx + W0(t) + [Y(t, W(t)) − Y0(t)] (1 − a) ABC(a) t p−1 + pa ABC(a)Γ(a) Z t 0 (t − x) a−1 x p−1Y(x, W(x))dx − W0(t) + [(t, v¯(t)) − Y0(t)] (1 − a) ABC(a) t p−1 + pa ABC(a)Γ(a) Z t 0 (t − x) a−1 x p−1Y(x, v¯(x))dx , ≤ Ya,p + (1 − a) ABC(a) LYt p−1 ||v − v¯|| + pT a+r−1 ABC(a)Γ(a) B(a, p)||v − v¯||, ≤ Ya,p + Θ||v − v¯||. (19) From equation (19), we can express it as follows: |v(t) − v¯(t)| ≤ Ya,r 1 − Θ |v(t) − v¯(t)|. (20) Based on equation (20), we deduce that the solution to equation (7) exhibits Ulam-Hyers stability. Consequently, generalized Ulam-Hyers stability can be established by employing YW(%) = $a,p% with YW(0) = 0. This demonstrates that the solution to the proposed problem is both Ulam-Hyers stable and generalized Ulam-Hyers stable.

https://doi.org/10.62500/icrtsda.1.1.45

4. Numerical Evaluation of the Model In this section, we focus on computing the numerical solutions for the system (3) characterized by arbitrary fractal orders. This is achieved using the ABC derivative, a prominent method within fractalfractional calculus. We employ iterative schemes to approximate the solution of the designated model. For this purpose, fractal-fractional ABC techniques are utilized to obtain an approximate solution that can be graphically represented. Consequently, we continue with the formulation as specified in expression (5): ABCD a (A(t)) = pt p−1M1(S(t), t), ABCD a (P(t)) = pt p−1M2(C(t), t), ABCD a (Z(t)) = pt p−1M3(L(t), t), ABCD a (R(t)) = pt p−1M4(H(t), t). (21) 12 The symbols Mi , i = 1, 2, 3, 4 are defined in (5). Next, by applying the fractal-fractional integral in the ABC sense to the first equation of (5), we obtain: A(t) − A(0) = (1 − a) ABC(a) t p−1 M1(A(t), t) + pa ABC(a)Γ(a) Z t 0 (t − x) a−1 x p−1M1(A(x), x)dx. (22) We now present the numerical solution of equation (22) using a novel approach for discrete time instances t = tk+1, k = 0, 1, 2, ... The initial equation of the system, as previously described, is then articulated as follows: A(tk+1) − A(0) = (1 − a) ABC(a) (t p−1 k+1) M1(A(tk), tk) + Pa ABC(a)Γ(a) Z tk+1 0 (tk+1 − x) a−1 x p−1M1(A(x), x)dx, = (1 − a) ABC(a) (t p−1 k+1) M1(A(tk), tk) + pa ABC(a)Γ(a) X k q=0 Z tq+1 q (tk+1 − x) a−1 x p−1M1(A(x), x)dx. (23) Next, we estimated the function M1 over the interval [tq, tq+1] using the interpolation polynomial as follows: M1 M1 Δ (t − tq−1) − R1 Δ (t − tq), (24) which suggests that A(tk+1) = A(0) + (1 − a) ABC(a) (t p−1 k+1) M1(A(tk), tk) + pa ABC(a)Γ(a) X k q=0 M1(A(tk), tk) Δ × Z tq+1 q (t − tq−1)(tq+1 − t) a−1 t p−1 q dt − M1(A(tk), tk) Δ Z tq+1 q (t − tq)(tk+1 − t) a−1 t p−1 q dt , A(tk+1) = A(0) + (1 − a) ABC(a) (t p−1 k+1) M1(A(tk), tk) + pa ABC(a)Γ(a) X k q=0 t p−1 q M1(A(tq), tq) Δ Iq−1,a − t p−1 q−1M1(A((tq−1), tq−1)) Δ Iq,a . (25) Now, computing Iq−1,a and Iq,a , we derive: Iq−1,a = Z tq+1 q (t − tq−1)(tk+1 − t) a−1 dt, = − 1 a (tq+1 − tq−1)(tk+1 − tq+1) σ − (tq − tq−1)(tk+1 − tq) σ , − 1 a(a − 1) (tk+1 − tq+1) a+1 − (tk+1 − tq) a+1 , (26) 13 and Iq,a = Z tq+1 q (t − tq)(tk+1 − t) a−1 dt, = − 1 a (tq+1 − tq)(tk+1 − tq+1) a − 1 a(a − 1) (tk+1 − tq+1) − (tk+1 − tq) η+1 . (27) Put tq = qΔ; yields Iq−1,a = − Δ a+1 a (q + 1 − (q − 1))(k + 1 − (q + 1))a − (q − (q − 1))(k + 1 − q) a , − Δ a+1 a(a − 1) (k + 1 − (q + 1))a+1 − (k + 1 − q) a+1 , = Δ a+1 a(a − 1) − 2(a + 1)(k − q) a + (a + 1)(k + 1 − q) a − (k − q) a+1 + (k + 1 − q) a+1 , = Δ a+1 a(a − 1) (k − q) a − 2(a + 1) − (k − q) + (k + 1 − q) a a + 1 + k + 1 − q , = Δ a+1 a(a − 1)(k + 1 − q) a (k − q + 2 + a) − (k − q) a (k − q + 2a + 2) . (28) Now for Iq,a , we have Iq,a = − Δ a+1 a (q + 1 − q)(k + 1 − (q + 1))a − Δ a+1 a(a − 1) (k + 1 − (q + 1))a+1 − (k + 1 − q) a+1 , = Δ a+1 a(a − 1) − (a + 1)(k − q) a − (k − q) a+1 + (k + 1 − q) a+1 , = Δ a+1 a(a − 1) (k − q) a − (a + 1) − (k − q) + (k + 1 − q) a+1 , = Δ a+1 a(a − 1) (k + 1 − q) a+1 − (k − q) a (k − q + 1 + a) . (29) Upon substituting the values from (28) and (29) into (25), we obtain: □ □□□□□□□□□□□□□□□□□□□□ □□□□□□□□□□□□□□□□□□□□ A(tk+1) = A(0) + (1 − a) ABC(a) (t p−1 k+1) M1(A(tk), tk) + pa ABC(a)Γ(a) X k q=0 t p−1 q M1(A(tq), tq) Δ × Δ a+1 a(a − 1) (k + 1 − q) a (k − q + 2 + a) − (k − q) a (k − q + 2 + 2a) − t p−1 q−1M1(A((tq−1), tq−1)) Δ Δ a+1 a(a − 1) (k + 1 − q) a+1 − (k − q) a (k − q + 1 + a) . (30) 14 Similarly, the remaining terms for the corresponding compartments of the devised model can be expressed as follows: □ □□□□□□□□□□□□□□□□□□□□ □□□□□□□□□□□□□□□□□□□□ P(tk+1) = P(0) + (1 − a) ABC(a) (t p−1 k+1) M2(P(tk), tk) + pa ABC(a)Γ(a) X k q=0 t p−1 q M2(P(tq), tq) Δ × Δ a+1 a(a − 1) (k + 1 − q) a (k − q + 2 + a) − (k − q) a (k − q + 2 + 2a) − t p−1 q−1M2(P((tq−1), tq−1)) Δ Δ a+1 a(a − 1) (k + 1 − q) a+1 − (k − q) a (k − q + 1 + a) . (31) □ □□□□□□□□□□□□□□□□□□□□ □□□□□□□□□□□□□□□□□□□□ Z(tk+1) = Z(0) + (1 − a) ABC(a) (t p−1 k+1) M3(Z(tk), tk) + pa ABC(a)Γ(a) X k q=0 t p−1 q M3(3(tq), tq) Δ × Δ a+1 a(a − 1) (k + 1 − q) a (k − q + 2 + a) − (k − q) a (k − q + 2 + 2a) − t p−1 q−1M3(Z((tq−1), tq−1)) Δ Δ a+1 a(a − 1) (k + 1 − q) a+1 − (k − q) a (k − q + 1 + a) . (32) □ □□□□□□□□□□□□□□□□□□□□ □□□□□□□□□□□□□□□□□□□□ R(tk+1) = R(0) + (1 − a) ABC(a) (t p−1 k+1) M4(R(tk), tk) + pa ABC(a)Γ(a) X k q=0 t p−1 q M4(R(tq), tq) Δ × Δ a+1 a(a − 1) (k + 1 − q) a (k − q + 2 + a) − (k − q) a (k − q + 2 + 2a) − t p−1 q−1M4(R((tq−1), tq−1)) Δ Δ a+1 a(a − 1) (k + 1 − q) a+1 − (k − q) a (k − q + 1 + a) . (33) 4.1. Simulation and Discussion This section is dedicated to analyzing the proposed fractal-fractional model, with a particular focus on how the model parameters interact and collectively influence the transmission dynamics of drug addiction within society. Numerical simulations are conducted under specific initial conditions and parameter settings for the compartments (A(0) = 135, P(0) = 90, Z(0) = 77, R(t) = 49, Π = 0.25, β = 0.7, σ = 0.1, μ = 0.25, γ1 = 0.35, γ2 = 0.3, θ = 0.7, γ = 0.09) [15]. 15 0 50 100 150 200 250 300 350 400 0.5 0.55 0.6 0.65 0.7 0.75 0.8 0.85 0.9 0.95 1 a1= 0.65 , p1=0.03 a2= 0.70 , p2=0.04 a3= 0.75 , p3=0.05 a4= 0.80 , p4=0.06 Figure 2: Graphical representation of the susceptible class A(t) in the proposed model under various fractional orders and dimensions. 0 50 100 150 200 250 300 350 400 0 0.05 0.1 0.15 0.2 0.25 a1= 0.65 , p1=0.03 a2= 0.70 ,

https://doi.org/10.62500/icrtsda.1.1.45

p2=0.04 a3= 0.75 , p3=0.05 a4= 0.80 , p4=0.06 Figure 3: Graphical representation of the heavy drinkers class P(t) in the proposed model under various fractional orders and dimensions. 16 0 50 100 150 200 250 300 350 400 0 0.02 0.04 0.06 0.08 0.1 0.12 0.14 0.16 0.18 a1= 0.65 , p1=0.03 a2= 0.70 , p2=0.04 a3= 0.75 , p3=0.05 a4= 0.80 , p4=0.06 Figure 4: Graphical representation of the drinkers in treatments class Z(t) in the proposed model under various fractional orders and dimensions. 0 50 100 150 200 250 300 350 400 0 0.01 0.02 0.03 0.04 0.05 0.06 0.07 0.08 0.09 0.1 a1= 0.65 , p1=0.03 a2= 0.70 , p2=0.04 a3= 0.75 , p3=0.05 a4= 0.80 , p4=0.06 Figure 5: Graphical representation of the recovered class P(t) in the proposed model under various fractional orders and dimensions. We explore various fractional orders (a) and dimensions (p) for the independent variable t, with the condition that a , p. This arrangement allows for the independent variation of fractal order and dimen17 sion. Specifically, we consider a = 0.65, 0.70, 0.75, 0.80 and p = 0.03, 0.04, 0.05, 0.06. The trajectories of compartmental classes in the drug addiction transmission model exhibit noticeable changes due to these manipulations. Each combination of a and p results in distinct patterns and behaviors observed in Figures 2 to 5. The time span covers t ∈ [0, 400] units, representing days. This investigation helps us understand how the interaction between fractional order and dimension influences the model dynamics over time. As illustrated in Figure 2, there is a noticeable decrease in the number of susceptible individuals A at lower fractional orders. This decline highlights the sensitivity of the model to the parameter adjustments in the fractional derivative component. Figure 3 details the dynamics of heavy drinkers P(t), where the primary characteristics observed are the varying slopes for different fractional orders. This indicates a dependence on fractional dimensions which maintain stability over time. Initially, there is a sharp decrease in the population of heavy drinkers, attributed to heightened susceptibility to adverse drinking behaviors. As the model progresses, a stabilization occurs, indicating an equilibrium state that reflects consistent exposure under varied parametric conditions. This behavior demonstrates that both lower and higher fractional orders facilitate a more detailed analysis and utilization of the available information, alongside the observed stability in transmission rates over time.In Figure 4, the pattern of increase followed by a gradual decrease in mild drinking behaviors among treatments Z(t) is presented. This trend suggests an initial effectiveness of interventions which diminishes over time. Finally, Figure 5 explores the dynamics among individuals susceptible to narcotic drinking behaviors who have subsequently recovered R(t). A pronounced initial decline is noted for lower fractional orders, reflecting the impact of the fractional order on recovery dynamics. 5. Conclusion Alcohol addiction, medically termed alcoholism, is a persistent and often advancing condition marked by an individual's reliance on and abuse of alcohol. This dependency can result in numerous adverse effects, including personal health complications, relationship strains, social setbacks, impaired decision-making, accidents, diminished enthusiasm for life, and an overall decline in quality of life. Individuals grappling with alcohol addiction often struggle to regulate their alcohol intake and may experience intense cravings for alcohol. Key characteristics of alcohol addiction encompass compulsive drinking, a loss of control over consumption, physical reliance, and continued alcohol use despite evident harm. Fundamentally, an ABC operator is defined to assist the determining of optimal protocols while dealing with complex multi-frontiers problem. Many researchers have appreciated the utility of these methods to gain better control over the 18 ongoing stochastic processes. The findings of this research competently argue the utility of ABC operator in the study of transmissions dynamic of drinking disease. For all pre-defined compartments, the trend in susceptible class indicates that susceptibility decrease rapidly at lower fractional order. Moreover, the behavior of heavy drinkers displays distinct slopes corresponding to different fractional orders. Furthermore, the growth and decline patterns of mild drinking in treatments demonstrate the dynamic nature of this compartment, with rapid increase followed by gradual decrease. Similarly, in recovered compartment the rapid growth and subsequent decline of individuals suggests a consistent recovery process within the model. References [1] Li, S., Samreen, L. S., Ullah, S., Riaz, M. B., Awwad, F. A., & Teklu, S. W. (2024). Global dynamics and computational modeling approach for analyzing and controlling of alcohol addiction using a novel fractional and fractal–fractional modeling approach. Scientific Reports, 14(1), 5065. [2] World Health Organization. (2019). Global status report on alcohol and health 2018. World Health Organization. [3] Din, A., Li, Y., Khan, T., & Zaman, G. (2020). Mathematical analysis of spread and control of the novel corona virus (COVID-19) in China. Chaos, Solitons & Fractals, 141, 110286. [4] Atangana, A. (2020). Modelling the spread of COVID-19 with new fractal-fractional operators: can the lockdown save mankind before vaccination?.Chaos, Solitons & Fractals, 136, 109860. [5] Din, A., & Li, Y. (2020). Controlling heroin addiction via age-structured

modeling. Advances in Difference Equations, 2020, 1-17. [6] Khan, F. M., Khan, Z. U., Lv, Y. P., Yusuf, A., & Din, A. (2021). Investigating of fractional order dengue epidemic model with ABC operator. Results in Physics, 24, 104075. [7] Caputo, M., & Fabrizio, M. (2015). A new definition of fractional derivative without singular kernel. Progress in Fractional Differentiation & Applications, 1(2), 73-85. [8] ur Rahman, M., Arfan, M., Shah, K., & Gomez-Aguilar, J. F. (2020). Investigating a nonlinear dynam- ´ ical model of COVID-19 disease under fuzzy caputo, random and ABC fractional order derivative. Chaos, Solitons & Fractals, 140, 110232. 19 [9] Khan, A., Alshehri, H. M., Gomez-Aguilar, J. F., Khan, Z. A., & Fern ´ andez-Anaya, G. (2021). A ´ predator–prey model involving variable-order fractional differential equations with Mittag-Leffler kernel. Advances in Difference Equations, 2021, 1-18. [10] Qureshi, S., Yusuf, A., Shaikh, A. A., Inc, M., & Baleanu, D. (2019). Fractional modeling of blood ethanol concentration system with real data application. Chaos: An Interdisciplinary Journal of Nonlinear Science, 29(1). [11] Rashid, S., Ashraf, R., & Bonyah, E. (2022). Nonlinear dynamics of the media addiction model using the fractal-fractional derivative technique. Complexity, 2022. [12] Zhang, L., Saeed, T., Wang, M. K., Aamir, N., & Ibrahim, M. (2022). ANALYSIS OF A FRACTIONAL ORDER SMOKING MODEL WITH RELAPSE AND HARMONIC MEAN TYPE INCIDENCE RATE UNDER ABC OPERATOR. Fractals 30(05), 2240140. [13] Anjam, Y. N., Shahid, I., Emadifar, H., Arif Cheema, S., & ur Rahman, M. (2024). Dynamics of the optimality control of transmission of infectious disease: a sensitivity analysis. Scientific Reports, 14(1), 1041. [14] Atangana, A. (2020). Modelling the spread of COVID-19 with new fractal-fractional operators: can the lockdown save mankind before vaccination?. Chaos, Solitons & Fractals, 136, 109860. [15] Adu, I. K., Osman, M. A., Yang, C. (2017). Mathematical model of drinking epidemic. Br. J. Math. Computer Sci, 22(5). [16] Kreyszig, E. (1991). Introductory functional analysis with applications (Vol. 17). John Wiley & Sons. 20

https://doi.org/10.62500/icrtsda.1.1.45

Proc. 1st International Conference on Recent Trends in Statistics and Data Analytics
Air University Islamabad, Pakistan – May 9, 2024, Vol. 1, pp.437-445

Cutting room fabric losses and their degree of prevalence: A support to sustainability

S. A. Cheema[1], A. Rasheed[2], T. Kifayat[3], M. Hussain[4] and I. L. Hudson[5]
[1]Department of Applied Sciences, School of Sciences, National Textile University Faisalabad, Pakistan.
[2]Department of Clothing, National Textile University Faisalabad, Pakistan.
[3] Department of Computer Sciences, Shaheed Zulfikar Ali Bhutto Institute of Science and Technology Islamabad, Pakistan.
[4]Department of Economics, Macquarie University, Australia.

[5]Department of Statistics, Faculty of Computing, The Islamia University of Bahawalpur, Pakistan.

Abstract

The cutting room fabric losses remain one of the leading contributors towards the pyramid of wastages of apparel industry. The role of these losses in hindering the sustainable outlook of clothing industry and disturbing the ecological harmony is well lamented in relevant circles. However, yet they remain least targeted entities in textile sphere as they are anticipated as unavoidable component of production process. The fundamental aim of this research is to explore the dynamics of these cut and sew losses along with the enumeration of comparative hierarchy prevailed among these wastages. The objectives of this study are facilitated by the employment of well-directed experiment while focusing four sub-categories of losses including; width loss, splice loss, buffer loss and remnant loss. width loss, splice loss, buffer loss and remnant loss. Also, the experimental environment was further enriched by considering various influencers such as; garment type, garment style, sizes, spreading table length, marker width, fabric roll length, %age excess fabric, edge alignment and fabric quality. Thus, 1728 realizations regarding above documented pre-consumer losses were assembled. The observed data was then used to elaborate a latent model capable of assessing the comparative burden hierarchy associated with each loss. The focuses are achieved by exploiting the well celebrated probabilistic formation of Maxwell. The proposed latent synergy is persuaded with respect to Bayesian framework. The utility of the devised mechanism is demonstrated by offering relevant statistical delicacies such as; prevalence probabilities, influence parameters and associated risks. The outcomes of this research highlight the dominance of buffer loss upon other contemporaries.

***Keywords**:* Apparel industry; cutting room losses; latent model;

1. INTRODUCTION

The year 2020-21 reported 448 billion U.S. dollars contribution of apparel industry in global trade. According to [1] these trade aggregates were adjusted to accommodate the adverse effects of COVID-19 pandemic inflicting 6% reduction as compare to the average trade volume of previous years. The estimates of fiber consumption reveal myriad of increments over the time, for example per capita fiber consumption is estimated to increase up to 10.4 kg from 3.7 kg per person in year 2008 as compared to year 1950 [2]. The meet of paramount consumption of fabric requires equally aggressive fiber production which is estimated to grow by 3.7% annually [3]. Unfortunately, the crisp of fast fashion industry is doomed by the production of associated apparel wastages. The estimated volume of fashion disposals for year 2015 remained 92 million tons which through conservative projections reveals

https://doi.org/10.62500/icrtsda.1.1.45

alarming increase of additional 56 million tons till the year 2030 [4]. The challenges delivered by the apparel wastes are of multidimensional complexity encapsulating, socio-economic exploitation [5, 6], threatening global food production-supply chain [7, 8], distorting the ecological balance [9, 10] and posing health hazards [11, 12]. The United Nations ranked apparel industry as second most polluting industry, single handedly emitting 8% of all carbon emissions [13]. Also, it is estimated that 20% of global wastewater, almost 93 billion cubic meters of water annually, is contributed by the textile industry [14]. Other than these external hazards, one of the major challenges to gain sustainable growth of the industry remains internal that is sharp rise in the cost of merchandizes. The estimates of contribution of fabric cost to the total cost of saleable final merchandize vary over the range of 25 % to 40% [15]. Broadhead, advocated this fact with utmost clarity by documenting that;

"No other single refinement in production can provide substantial cost saving as easily as fabric control."

see [16]. The fabric waste, commonly stratified into two categories that is (i)- pre-consumer waste - encapsulating fabric store, cutting room, production floor, printing floor and finishing floor and (ii)- post-consumer waste – covering throughout consumer use to end-of-use disposal, occurs at various stages of long and burdensome supply chain [17]. To fulfil required expectations, the significance of the material cost and eagerness to reach optimal resolve has long been a well cherished topic of scientific rigors [18, 19]. One may witness streams of resolves, such as recycling, reuse and balanced supply-consumption attitudes, available in the literature to overcome the adversities inflicted by the post-consumer wastages. For interesting and knowledgeable account of novel strategies, one may consult to [20 - 25]. However, the pre-consumer waste usually go unchecked, may be because discarding the apparel leftovers does not affect the capacity of manufacturer of ready-to-wear merchandizes as the leftover cost is considered an unavoidable component of production process [26]. But, the legitimacy of pursuing pre-consumer waste is not only embedded in potential financial gain but a deeper understating of the waste can prevent the wastage reach to landfill. Among contemporary pre-consumer disposals, cutting room wastages earned the notoriety of being the dominant losses as well as unavoidable despite the best efforts of the industry [27]. With aforementioned stacks, the challenge of controlling and understanding of the dynamics of fabric wastages remain attractive pursuit for professional and commercial research circles.

Recognizing the unwavering need of in-depth understanding of pre-consumer losses, this research instigates an elaborative investigation into the cut and sew wastages with respect to four categories such as, buffer loss, splice loss, width loss and remnant loss. Moreover, by interlocking experimental realizations and theoretical subject knowledge, this research derives novel mathematical functionals quantifying the waste volume inflicted by contemporary losses. Additionally, this article devises an interesting mechanism to assess the comparative degree of waste burden associated with each loss. The targets are achieved by exploiting latent model capable of incorporating stochastic outlook of rival losses through an elegant functional form. Section 2 documents these developments in details. Section 3, of this research is dedicated to comprehensive discussion of the outcomes of this experiment based scientific inquiry. Lastly, section 4 comprehends major findings of the study along with some future research attractions.

2. METHODOLOGY

2.1. Experimental Plan

One of the most striking features of this research remains its insistence on well-designed experimental plan. Four cut and sew losses such as, width loss, splice loss, buffer loss and remnant loss are studied in a synchronized, systematic and exploratory fashion. The assessments of all pre-described losses are realized with respect to nine covariates - thought to determining the losses such as, garment type, garment style, sizes, spreading table length, marker width, fabric roll length, excess fabric, edge alignment and fabric quality. The experimental environment is further enriched by incorporating different levels of each associated covariates. At first, full factorial experimental layout was adopted to create 108

https://doi.org/10.62500/icrtsda.1.1.45

markers while taking five factors that is, garment type, garment style, sizes, spreading table length, marker width, along with their pre-defined levels into consideration. Thus, developed markers were then exercised while accommodating the remaining four covariates and their levels as blockings to generate 1728 primary experimental realizations of fabric wastage in square meters unit. The order quantity and the fabric width were controlled at constant levels of 1000 units and 1.527 meters, respectively. The primary unit of analysis was considered to be denim trouser. Table 1 comprehends the details of subtleties and their related levels considered to determine the cut and sew losses.

Table 1: Covariates and their levels determining the pre-consumer cutting room fabric losses

Sr. #	***Covariates***	***Level 1***	***Level 2***	***Level 3***
1	Garment Type	Men's trouser	Women's trouser	----
2	Garment style	Basic	Fashion	----
3	Sizes	1	3	5
4	Spreading table length (m)	12	24	36
5	Marker width (m)	57	58	59
6	Fabric rolls length (m)	100	200	----
7	Excess (cutting) (%)	5	10	----
8	Edge alignment	With end cutter	Without end cutter	----
9	Fabric quality	Poor	Good	----

2.2. Proposed Scheme

Let us say that a pairwise comparison is persuaded among k apparel losses based on n realizations, where pair of stimuli elicits a continuous discriminal process. The latent prevalence between $i'th$ loss and loss j are then thought to follow Maxwell distribution over the consistent support in the population, such as;

$$f(x_i) = \sqrt{\frac{2}{\pi}} x_i^2 \frac{e^{\frac{-x_i^2}{2\theta_i^2}}}{\theta_i^3}, x_i > 0, \theta_i > 0 \quad (1)$$

and

$$f(x_j) = \sqrt{\frac{2}{\pi}} x_j^2 \frac{e^{\frac{-x_j^2}{2\theta_j^2}}}{\theta_j^3}, x_j > 0, \theta_j > 0. \quad (2)$$

where, θ_i and θ_j are scale parameters quantifying the rate of prevalence in a Euclidian space. The utility of aforementioned probabilistic model in tackling the positively skewed physical phenomena is well documented in multi-disciplinary research literature [28, 29]. In our study, we exploit the scale parameter of the Maxwell distribution to quantify the comparative dominance of losses under consideration. Without losing the generality, the axiomatic formation of the statement *"loss i dominates the loss j"* is written as;

$$p_{ij} = P(X_i > X_j) = F(X_i - X_j), \quad (3)$$

https://doi.org/10.62500/icrtsda.1.1.45

where, p_{ij} denote the influence probability associated with $i'th$ loss in comparison to the $j'th$ loss such that $p_{ij} \in (0,1)$. Further, $F(X_i - X_j)$ is cumulative distribution function (cdf) of the Maxwell distribution given in equations (1) and (2), assessing the absolute difference lying in stimuli dictating the contemporary losses. By solving the equation (3) the influence probabilities are simplifies as;

$$p_{ij} = \frac{2}{\pi}\int_0^{\infty}\int_{b_j}^{\infty}\frac{b^2{}_i b^2{}_j}{\theta^3{}_i \theta^3{}_j} e^{-\frac{1}{2}\left(\frac{b^2{}_i}{2\theta^2{}_i}-\frac{b^2{}_j}{2\theta^2{}_j}\right)} db_i db_j,$$

which provides the simplified form such as;

$$p_{ij} = 1 + \frac{2}{\pi}\left[\frac{\theta_i\theta_j(\theta^2{}_i-\theta^2{}_j)}{(\theta^2{}_i+\theta^2{}_j)^2} - \arctan\left(\frac{\theta_i}{\theta_j}\right)\right]. \quad (4)$$

It is trivial to verify that the influence probability of loss j over loss i is calculable as $p_{ji} = 1 - p_{ij}$, and is written as,

$$p_{ji} = 1 + \frac{2}{\pi}\left[\frac{\theta_i\theta_j(\theta^2{}_j-\theta^2{}_i)}{(\theta^2{}_i+\theta^2{}_j)^2} + \arctan\left(\frac{\theta_j}{\theta_i}\right)\right].$$

The pairwise comparison of losses resultant from the above documented inquiry that *"Does loss i dominate the loss j?"* will generate a binary string of permissible responses of "yes" or "no" against every item. Therefore, the likelihood function when k losses are compared with respect to n happenings, is given as;

$$L(\underline{\boldsymbol{\theta}}; \mathbf{X}) = \prod_{i<j}^{k} \frac{n!}{r_{ij}!(n-r_{ijj})!} p_{ij}{}^{r_{ij}} p_{ji}{}^{n-r_{ij}}, \quad (5)$$

where, $\underline{\boldsymbol{\theta}}$ is a vector of scale parameters of Maxwell distribution and is nominated as worth parameters dictating the comparative influence of each loss. Whereas $\boldsymbol{X}$ is the loss matrix, n represents the total number of comparisons and r_{ij} denotes the number of dominant cases of loss i in comparison to the loss j.

Estimation of Prevalence Parameters: The estimation of worth parameters is launched under Bayesian paradigm capable of incorporating the historic information available about the phenomenon under study. For the demonstration purposes, this study consider Jefferys prior assisting the incorporation of prior data. The Jeffreys prior for k apparel losses is written as follows:

$$p_J(\theta_1, \theta_2, \theta_3, \ldots., \theta_k) \propto \sqrt{\det[I(\theta_1, \theta_2, \theta_3, \ldots., \theta_k)]}.$$

https://doi.org/10.62500/icrtsda.1.1.45

Where,

$$\det[I(\theta_1,\theta_2,\theta_3,\ldots.,\theta_k)] = (-1)^{k-1}\begin{vmatrix} E\left[\frac{\partial^2 \ln L(.)}{\partial\theta_1^2}\right] & E\left[\frac{\partial^2 \ln L(.)}{\partial\theta_1\,\partial\theta_2}\right]\ldots & E\left[\frac{\partial^2 \ln L(.)}{\partial\theta_1\,\partial\theta_{k-1}}\right] \\ E\left[\frac{\partial^2 \ln L(.)}{\partial\theta_2\,\partial\theta_1}\right] & E[\frac{\partial^2 \ln L(.)}{\partial\theta_2^2}]\ \ldots & E\left[\frac{\partial^2 \ln L(.)}{\partial\theta_2\,\partial\theta_{k-1}}\right] \\ \vdots & \vdots & \vdots \\ E\left[\frac{\partial^2 \ln L(.)}{\partial\theta_{k-1}\,\partial\theta_1}\right] & E\left[\frac{\partial^2 \ln L(.)}{\partial\theta_{k-1}\,\partial\theta_2}\right]\ldots & E\left[\frac{\partial^2 \ln L(.)}{\partial\theta_{k-1}^2}\right] \end{vmatrix}.$$

The estimability issue for k worth parameters is resolved by using the constraint such as, $\theta_k = 1 - \sum_{i=1}^{k-1}\theta_i$. The joint posterior distribution under the Jefferys prior is given as,

$$P(\theta_1,\theta_2,\ldots,\theta_k|\underline{x}) = \frac{1}{C_j}P(\theta_1,\theta_2,\ldots,\theta_k)\prod_{i<j}^{k} p_{ij}^{\,r_{ij}}p_{ji}^{\,n-r_{ij}}, \tag{6}$$

with the normalizing constant, say C_j, as,

$$C_j = \int_{\theta_1=0}^{1}\int_{\theta_2=0}^{1-\theta_1}\ldots\int_{\theta_k=0}^{1-\sum_{i=1}^{k-1}\theta_i} P(\theta_1,\theta_2,\ldots,\theta_k)\prod_{i<j}^{k} p_{ij}^{\,r_{ij}}p_{ji}^{\,n-r_{ij}}\,d\theta_1 d\theta_2\ldots d\theta_{k-1}.$$

As the joint posterior distribution of equation (6) is not of closed form, therefore Bayes estimates governing the apparel losses are attained by employing Gibbs sampler - one of the prominent methods of Markov chain Monte Carlo (MCMC) and commonly used to handle complex multiple integrals. We employed the Gibbs sampler to attain the marginal posterior distribution of the worth parameters by iteratively conditioning on interim values in a continuing cycle. Let $P(\underline{\theta};\underline{x})$ be the joint posterior density, where $\underline{\theta} = (\theta_1,\theta_2,\ldots,\theta_k)$. Then the conditional densities are given by, $P(\theta_1 I\theta_2,\theta_3\ldots,\theta_k), P(\theta_2 I\theta_1,\theta_3\ldots,\theta_k)\ldots P(\theta_k I\theta_1,\theta_2\ldots,\theta_{k-1})$. According to the Gibbs sampler, we assume initial values such as $\left({\theta_2}^{(0)},{\theta_3}^{(0)},\ldots,{\theta_k}^{(0)}\right)$ and pursue the conditional distribution of θ_1 such that $P\left({\theta_1}^{(1)} I{\theta_2}^{(0)},{\theta_3}^{(0)},\ldots,{\theta_k}^{(0)}\right)$. The iterative procedure will continue until it converges. For demonstration purposes, we provide the expression for the marginal posterior distribution of $k'th$ worth parameter θ_k, under the Jefferys Prior,

$$P(\theta_k|\underline{x}) = \int_{\theta_1=0}^{1-\theta_k}\int_{\theta_2=0}^{1-\theta_1-\theta_k}\ldots\int_{\theta_k=0}^{1-\sum_{i=1}^{k-2}\theta_i-\theta_k}\frac{1}{C_j}P(\theta_1,\theta_2,\ldots,\theta_k)\prod_{i<j}^{k} p_{ij}^{\,r_{ij}}p_{ji}^{\,n-r_{ij}}\,d\theta_1 d\theta_2\ldots d\theta_{k-1}$$

3. RESULTS AND DISCUSSION

3.1. Data Summary

Table 2 enumerates the distributional summaries of all four losses realized through the experiments. We report numerous statistics indicating various splits of the apparel wastage data highlighting aggregated propensity of influence of the each loss. Based on 1728 experimental realizations the average width loss is estimated to be 67.32 m^2. The mean of splice loss is quantified as 2.98 m^2 over the pre-described factorial setting. Where the average value of buffer loss remains 1927.29 m^2 across the defined experimental setting. Lastly, the remnant loss shows an average of 96.43 m^2. These findings clearly establish the comparative overwhelming dominance of the buffer loss. In fact, the minimum

https://doi.org/10.62500/icrtsda.1.1.45

observed value associated with buffer loss remains gigantically higher than the maximal values of remaining losses, cumulatively. Next, in procession we witness remnant loss which is consistently followed by the width loss. The most accommodating behavior is reflected in the analysis of the splice loss. These sparkling differences imposed by the contemporary losses deserve further in-depth investigation exploring the role of underlying covariate structure in deriving these disparities. Further, the asymmetric nature of all losses can be anticipated by noticing the underlying discrepancies among their averages and median values. The skewed (positively) distributional outlook of the losses is depicted through Figure 1.

Table 2: Summary statistics of all pre-consumer cutting room fabric losses

Losses	***Min.***	***Q1***	***Mean***	***SD***	***Median***	***Q3***	***Max.***
Width Loss	24.97	42.17	67.32	33.01	55.82	85.58	160.12
Splice Loss	1.09	2.14	2.98	1.04	2.74	3.45	6.32
Buffer Loss	1036.82	1528	1927	455.26	1756.02	2464.66	3023.87
Remnant Loss	34.05	60.4	96.43	40.94	96.48	114.76	207.4

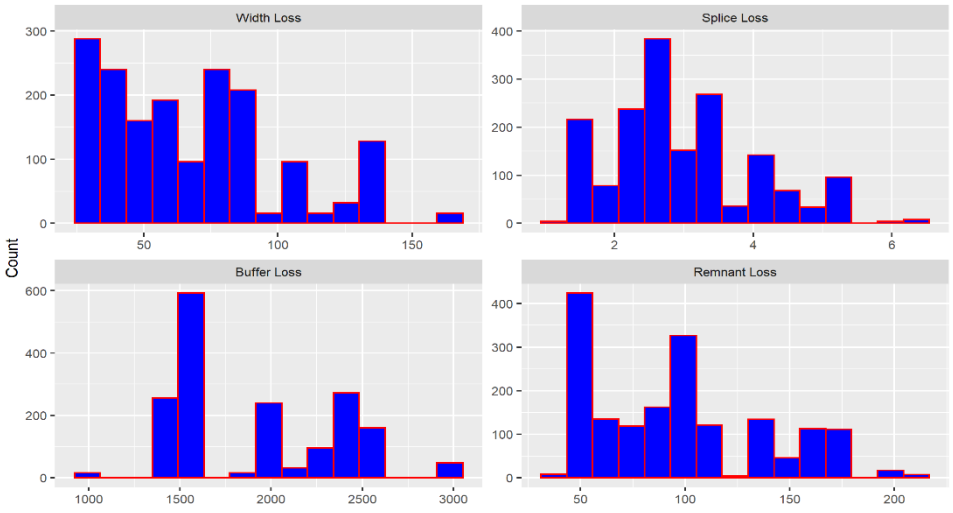

Figure 1: Distributional outlook of the losses under study

3.2. Degree of Influence and Burden Hierarchy

We start by documenting the estimated influence matrix with respect to four contemporary losses. The estimated results are based on the apparel losses data composed of 1728 observation generating four losses. Thus, we are specified with the comparative assessment of four losses when quantified with

https://doi.org/10.62500/icrtsda.1.1.45

respect to 1728 realizations. Table 3 does the job by summarizing the estimated pairwise influence probabilities, where, *W* stands for width loss, *S* for splice loss, *B* for buffer loss and *R* for remnant loss.

Table 3: Estimated influence matrix

Probabilities	*Pairs*					
	$W^{(i)} \leftrightarrow S^{(j)}$	$W^{(i)} \leftrightarrow B^{(j)}$	$W^{(i)} \leftrightarrow R^{(j)}$	$S^{(i)} \leftrightarrow B^{(j)}$	$S^{(i)} \leftrightarrow R^{(j)}$	$B^{(i)} \leftrightarrow R^{(j)}$
$\hat{p}_{ij}$	0.9553	0.0342	0.4326	0.0007	0.0331	0.9538
$\hat{p}_{ji}$	0.0447	0.9658	0.5674	0.9993	0.9669	0.0462

the estimates of influence probabilities associated with all six possible pairs of losses document the comparative dominance of the prevalent degree of losses. at first, the hazard of width loss in comparison to splice loss is overwhelmed with influence difference of almost 0.90 and odds of 21:1. further, when width loss is compared with buffer loss, the supremacy belongs to buffer loss with probability difference of almost 0.93 and odds of 1:28. similarly, remnant loss remained slightly more noticeable in comparison to width loss with 0.13 difference in terms of influence probabilities where odds remained 1:1.3. moreover, the weight of buffer loss stays almost 99% more perceptible in comparison to the splice loss with astonishing odds of 1:1428. alike patterns are witnessed when splice loss is compared with remnant loss. the burden of remnant loss is almost 93% higher than that of splice loss with estimated odds of 1:29. lastly, buffer loss loads 90% more than remnant loss with odds of 20:1.

now, we report the estimates of worth parameters calculated under three different loss functions using marginal posterior distributions and by employing gibbs sampling. table 4 clearly determines the underlying burden hierarchy of losses under study.

Table 4: Estimate of worth parameters and their associated risks under various loss functions

	LOSSES			
	WIDTH LOSS	**SPLICE LOSS**	**BUFFER LOSS**	**REMNANT LOSS**
$\hat{\theta}^{(worth)}$	0.162	0.040	0.589	0.185

The two revelations remained undisputed regardless of the used loss functions – (i) – burden hierarchy of the losses under study and, – (ii) – the efficacy of squared error loss function in retaining the extent of information in the data by offering minimum of the risks. With respect to all loss functions, we witnessed the natural ordering of the losses such that, $\hat{\theta}_B > \hat{\theta}_R > \hat{\theta}_W > \hat{\theta}_S$. Thus based on newly proposed comparative scheme of latent Bayesian paradigm, we can say that, with respect to the Jefferys prior, the highest value of the worth parameter is associated with the buffer loss, which is around 0.59 on average. The buffer loss is then followed by remnant loss in terms of load ranking with average estimated value of around 0.19. Next in line remained width loss with estimated worth parameter of 0.16, on average. The minimal value of the hazard parameter is associated with the splice loss brand which has the lowest average estimate of the degree of burden such as 0.05. Figure 2, provides the pictorial display of the marginal posterior distributions of estimated worth parameters associated with all losses. One may appreciate the legitimacy of the devised scheme by noticing the symmetry and compactness of the distributional display.

https://doi.org/10.62500/icrtsda.1.1.45

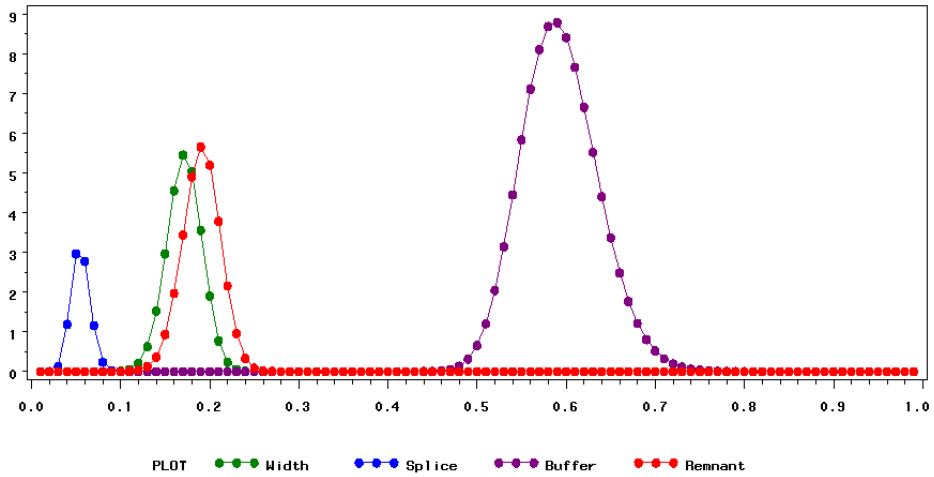

Figure 2: Display of the marginal posterior distributions of the worth parameters with respect to all four losses.

4. COMMENTS AND CONCLUSION

Apparel wastages, aside from posing serious concerns towards the sustainable growth of clothing industry, leave notable environmental footprints of the industry which go beyond emission. The fabric wastages, ritualistically send to landfill, are found to contribute in soil contamination and water pollution. The apparel wastages are usually classified into pre-consumer and post-consumer stratifications. This research fundamentally aims at one of the leading and yet ignored constituent of the pre-consumer waste that is cut and sew waste – commonly produced in cutting room. This systematic and synchronized investigative effort is based on well-structured experimental plan quantifying the cutting room losses. Through meticulously persuaded full factorial design, this research focuses on four losses that is, buffer loss, width loss, splice loss and remnant loss. The findings of this study are based on 1728 realizations of all four aforementioned losses. The research takes into account the well thought loss influencers such as garment type, garment style, sizes, spreading table length, marker width, fabric roll length, excess fabric, edge alignment and fabric quality. Based on these losses' realizations, this study novely propose mathematical functionals deriving the production of considered losses. Additionally, by the application of sophisticated probabilistic tools, this research materialize the competitive degree of dominance of the losses and thereby delineates the burden hierarchy prevalent among contemporary losses. It is estimated that with respect to all factors considered to be influencing the loss generation, buffer loss dominates cutting room wastages with notable distinction. The buffer loss is followed by remnant loss which is then closely trailed by width loss. The splice loss is estimated to contribute minimally toward the cutting room waste generation. The influence parameter associated with buffer loss indicates that 59% of the total cut and sew loss is nominated as being buffer loss. Further, remnant loss remains responsible for the generation of 19% of the total loss, whereas width loss accounts for 16% of the total cutting room loss. Lastly, splice loss constitutes 5% of the total loss and thus inflicting minimal damages among all competing losses.

In future, it will be interesting to pursue strategies meticulously targeting the reduction in the production of the most dominant buffer loss. Also, the quintile-based analysis of the produced losses is worth exploring with respect to the pre-defined determinants of the wastage governance.

REFERENCES

1. World Trade Organization, “World Trade Statistical Review 2021”, 2021.
2. Sanchis-Sebastiá, M., Ruuth, E., Stigsson, L., Galbe, M. and Wallberg, O., Novel Sustainable Alternatives for the Fashion Industry: A Method of Chemically Recycling Waste Textiles via Acid Hydrolysis. “Waste Manag.” 2021, 121, 248–254.
3. Pensupa, N., Leu, S.-Y., Hu, Y., Du, C., Liu, H., Jing, H., Wang, H. and Lin, C.S.K., Recent Trends in Sustainable Textile Waste Recycling Methods: Current Situation and Future Prospects. “Top. Curr. Chem.” 2017, 375, 76.
4. Bilgic, H. and Baykal, D. P., The effects of fabric type, fabric width and model type on the cost of unit raw material in terms of apparel, “IOP Conf. Ser. Mater. Sci. Eng.”, 2017, 254, 17.
5. Yeşilpinar, S. and Aytaç, V., An Approach Aimed at Fabric Consumption in Shirt Production. Textile Research Journal, 2009, 79, 5, 461–467.
6. Ng, S. F., Hui, C. L., Lo, T. Y. and Chan, S. H., Fabric Loss during Spreading: A Comparative Study of the Actual Loss in Manufacturing Men's Shirts, The Journal of The Textile Institute, 2001, 92:3, 269-279
7. Broadhead, R., Accurate fabric costs – improving fabric yield estimates, *www.techexchange.com*, 2010.
8. Stanescu, M. D., State of the Art of Post-Consumer Textile Waste Upcycling to Reach the Zero Waste Milestone. “Environ. Sci. Pollut. Res.” 2021, 28, 14253–14270.
9. Bailey, K., Basu, A. and Sharma, S., The Environmental Impacts of Fast Fashion on Water Quality: A Systematic Review. Water, 2022, 14, 1073.
10. Thunberg Calls out Climate Impact of Fashion Brands in Vogue Interview. BBC News 9 August 2021. Available online: https: //www.bbc.com/news/world-europe-58145465
11. Moazzem, S., Wang, L., Daver, F. and Crossin, E., Environmental Impact of Discarded Apparel and Landfilling and Recycling. Resources, Conservation and Recycling, 2021, 166, 105338.
12. Lewis, T., Apparel Disposal and Reuse, Sustainable Apparel: Woodhead Publishing Series in Textile, 2015, 233-250.
13. Caulfield, K., Sources of Textile Waste in Australia, 2009. Accessed: Sep. 28, 2021. [Online]. Available: https://studylib.net/doc/18791293/sources-of-textile-waste-in-australia
14. Domina, T. and Koch, K. The textile waste lifecycle, Cloth. Text. Res. J., 1997, 15, 2, 96–102.
15. Rissanen, T. Zero-Waste Faison Design, University of Technology, Sydney, 2013. doi: 10.1007/978-3-7643-8140-0_108.
16. Redress, “Ecochic Design Award: Sourcing Textile Waste,” 2017.
17. Enes, E., Adaption of Zero-Waste Pattern Design Method to Fashion Industry with the Case of Turkey, Phd Thesis in Design Studies. Izmir University of Economics, 2019.
18. Rissanen, T., From 15% to 0: Investigating the creation of fashion without the creation of fabric waste, Creat. Des. meets Technol. Eur., 2005, 1–10.
19. Glock, R. E. and Kunze, G. I., Preproduction operations, *Apparel Manufacturing*, 2004, 389–425.

https://doi.org/10.62500/icrtsda.1.1.46

Proc. 1st International Conference on Recent Trends in Statistics and Data Analytics
Air University Islamabad, Pakistan – May 9, 2024, Vol. 1, pp. 446-

Modeling the corruption dynamics: A theoretical approach

Muhammad Imran Aslam[1] , Iqra Shahid[2] , Kashaf Ishfaq[3] , Yasir Nadeem Anjam[4] and Ammara Nawaz Cheema[5]

[1,2,3,4]Department of Applied Sciences, National Textile University, Faisalabad 37610, Pakistan

[5]Department of Mathematics, Air University Islamabad, Pakistan

Abstract

This article aims at the encapsulation of corruption dynamics prevailing in a population. The focuses of the study are attained through the proposition of a versatile deterministic model. The devised model is examined with respect to Caputo-Fabrizio fractional order framework. The research is instigated by the stratifying the population of interest into five compartments such as; susceptible class, exposed class, corrupted class, recovered class and honest class. The legitimacy of the suggested scheme is established through the persuasion of relevant delicacies such as, positivity, invariance of region, points of equilibrium, basic reproduction number along with stability analysis. The utility of the proposed synergy is persuaded by nominating various fractional orders of the sense of Caputo- Fabrizio derivatives. The investigative environment is further enriched by considering numerous inter-connected compartmental parameters delineating the degree of vulnerability of the population under study towards corruption. Furthermore, the dynamics of each compartment, consequent upon the predefined set of fractional order, are rigorously sight-seen with respect to an elaborative set of time values. The findings of this research are found to competently argue the applicability along with utility of the fractional order derivative approach in the estimation of corruption transmission. Keywords: Capruto-Fabrizio fractionals; Corruption model; Transmission dynamics; Stability analysis. 1. Introduction The phenomenon of corruption is a multifaceted societal, political, and economic issue impacting individuals holding positions in both public and private sectors. It is often described as an endemic affliction within society due to its highly enticing, tempting, and infectious nature, characterized by a disturbingly Preprint submitted to . May 6, 2024 indulgent pattern [1]. It is evident that insecurity, greed, limited media freedom, low-income levels, and governmental instability are primary contributors to corruption. As evidenced by the findings in [2], corruption is not merely an outcome but a significant instigator of conflict, actively contributing to its escalation through multiple channels. Corruption hurts how well democracy works, makes the economy grow slower and makes governments less stable [3]. Also, corruption can twists the rules of law, democracy, human rights, and hinders economies from growing because it scares away foreign investors. Small businesses often can not even get started because corruption makes it too hard and expensive. It takes away important things from citizens like clean water, safety, good schools, and chances to improve their lives. Corruption can have notable effects on people's minds and feelings. Corruption can also make people feel like they have less control over their lives, which can lead to stress and anxiety. Efforts to comprehend the mathematical aspects of how corruption spread are receiving substantial attention and resources. Corruption Mathematical Models Using Caputo-Fabrizio Fractional Order Corruption, a pervasive societal issue, has been the subject of numerous mathematical modeling studies aiming to comprehend its dynamics and devise effective mitigation strategies. In recent years, the utilization of the Caputo-Fabrizio fractional order has emerged as a promising approach to capture the intricacies of corruption dynamics. For example, Fang (2022) has launched a non-linear evolution model for drinking behavior under caputo-Fabrizio derivative when health intervention is employed [4]. Similarly, Muhammad AsadUllah (2024) studied the utility of Mathematical simulations and sensitivity visualization of fractional-order disease models, when interest lies in the explanation of primary infection mechanism [5]. Furthermore, in recent times, there has been an increasing emphasis on exploring fractional order strategies to achieve more effective management of corruption transmission. For example, Nosrati Sahlan has investigated the existence, uniqueness, stability, and numerical aspects of a novel mathematical model of HIV/AIDS transmission incorporating a fractal fractional order derivative has garnered significant scholarly attention [6].Fundamentally, Muhammad Aslam Noor is defined to assist the determining fractional protocols while dealing with complex multi-frontier problems. They researched on Monkeypox transmission

https://doi.org/10.62500/icrtsda.1.1.46

dynamics, incorporating Caputo-Fabrizio fractal-fractional derivatives, has explored control strategies to curb its spread. Studies have investigated the effectiveness of interventions in containing the virus within society. These analyses contribute valuable insights for public health measures aimed at managing Monkeypox outbreaks [7]. Many researchers have appreciated the utility of these methods to gain better control over the ongoing stochastic processes. For example, Kubra (2024) advocated the deterministic mathematical models of 2 SARS-CoV-2, utilizing fractal-fractional operators, has examined transmission dynamics and control measures. Comparative studies have evaluated the efficacy of various intervention strategies in mitigating the spread of the virus. These analyses provide insights into the dynamics of COVID-19 and inform public health responses to the pandemic [8]. Additionally [9], global dynamic of fractional order for controlling the outbreak of malaria transmission model. Motivated by the importance of the aforementioned issue, this study adds to the current body of literature concerning the utility of the fractional Caputo-Fabrizio derivative by proposing a novel mathematical framework adopt at elucidating the dynamics of corruption within a community.The main goal of utilizing the Caputo-Fabrizio derivative is to extend the traditional calculus framework to better capture the complex dynamics of real-world phenomena characterized by memory-dependent and non-local behaviors. By introducing a fractional-order derivative with the Caputo-Fabrizio formulation, researchers aim to provide a more accurate representation of various processes. This derivative enables the modeling of systems with long-range dependencies and non-local interactions, facilitating a deeper understanding of intricate phenomena and enhancing predictive capabilities in diverse domains. The population under study is classified into five mutually exclusive classes namely, susceptible class, exposed class, corrupted class, recovered class, and honest class. Firstly, we will thoroughly examine the developed model to ensure its validity by demonstrating pivotal delicacies such as positivity, invariant region, equilibrium points, reproduction number, and stability analysis. Along with showing complete stability analyses at equilibrium points to evaluate both local and global stability. The study under review is organized into five detailed sections. Section 2 elaborates on the methodologies and materials utilized in the model, encompassing the estimation of equilibrium points, the determination of the basic reproduction number, and stability analysis. In Section 3, the fractional order analysis of the proposed model is introduced, accompanied by analytical solutions derived through the Laplace Adomian decomposition method. Section 4 provides a concise review of numerical simulations resulting from the previously described techniques. Finally, Section 5 summarizes the principal conclusions of the study and explores prospective directions for future research. 3 2. Methods and Materiel 2.1. The Model Mathematical models of corruption are developed to provide a systematic approach to understanding the mechanics and impacts of corrupt behaviors within diverse sectors, allowing for the evaluation and formulation of effective anti-corruption strategies. Let us consider that, for any time $t \geq 0$, the population under study, say N(t),classified into five distinct groups. Susceptible individuals A(t) include those who either completely abstain from corrupt practices or are involved in them. Exposed individuals E(t) are those who have come into contact with corruption through others but have not themselves engaged in corrupt activities. Corrupt individuals P(t) are actively involved in corruption. Recovered individuals R(t) represent those who have previously participated in corrupt activities but have since ceased their involvement. Lastly, honest individuals M(t) are characterized by their inherent truthfulness and are considered incapable of engaging in corrupt behavior. The schematic diagram of the corruption model is depicted in Figure 2.1. A E P M R π d d d d d η νγ1 γ2 (1 − ν)γ1 (1 − φ)ω ξ φω Figure 2.1: Schematic diagram for the transmission of corruption dynamics. Thus, the whole population at any time t is given by, $N(t) = A(t) + E(t) + P(t) + R(t) + M(t)$. 4 The foundational corruption dynamic model is to be governed through a system of non-linear differential equations, such as $dA\,dt = \pi + (1 - \varphi)\omega R - \mu\eta AP - (\xi + d)A$, $dE\,dt = \mu\eta AP - (\gamma 1 + d)E$, $dP\,dt = \nu\gamma 1E - (\gamma 2 + d)P$, $dR\,dt = \gamma 2P + (1 - \nu)\gamma 1E - (\omega + d)R$, $dM\,dt = \xi A + \varphi\omega R - dM$, (2.1) subject to the initial conditions: $A(0) = A0 \geq 0$, $E(0) = E0 \geq 0$, $P(0) = P0 \geq 0$, $R(0) = R0 \geq 0$, $M(0) = M0 \geq 0$. Descriptions of each parameter of the proposed model are provided below in Table 1. Table 1: Description of parameters of model (2.1) Parameters Description μ Probability of corruption being transmitted per contact η Rate at which susceptible individuals will interact with exposed individuals γ1 Rate at which individuals who have been exposed to corruption become corrupted ω Rate at which individuals who have recovered become honest π Recruitment rate of susceptible humans ξ Proportion of individuals that joins the honest population from susceptible population d Mortality rate for the entire human population ν proportion of individuals who join the corrupted sub-population from the exposed compartment φ Proportion of

https://doi.org/10.62500/icrtsda.1.1.46

individuals who move from the recovered compartment to the honest sub-population. γ2 Rate at which corrupted individuals become recovered 5 2.2. Analytical view In this section, we provide the fundamental definitions and relevant results from fractional calculus that are essential for analyzing the proposed model. Definition 2.1. The Caputo-Fabrizio (CF) fractional order derivative of a function f(t) of order α (where 0 < α < 1) is defined as: CFD α t f(t) = N(α) 1 − α Z t 0 exp − α 1 − α (t − τ) f 0 (τ) dτ, where f 0 (t) is the first derivative of f , and M(α) is a normalization function, often chosen as M(α) = 1 − α. Definition 2.2. The Caputo-Fabrizio (CF) fractional integral for a function f by α(0, 1) is described as: CF I α t [f(t)] = 1 − α N(α) + α N(α) Z t 0 f(τ) dτ, t ≥ 0. Definition 2.3. The Laplace transform of the Caputo-Fabrizio (CF) fractional order derivative Dα f(t) of a function f(t), where α is the fractional order 0 < α < 1, is given by: L{D α f(t)} = s αF(s) − αs α−1 1 − α f(0). where F(s) = L{f(t)} is the Laplace transform of f(t) and f(0) is the initial value of f(t). Definition 2.4. The fractional derivative of He's is stated as: D β t = 1 Γ(w − β) d w dtw Z t t0 (s − t) w−β−1 [f0(s) − f(s)] ds 2.3. Theoretical view 2.3.1. Positivity The devised model are demonstrated by considering compartmental space such as R 5 + = ((A,E, P, R, M) ∈ R5 ; A(0) ≥ 0,E(0) ≥ 0, P(0) ≥ 0, R(0) ≥ 0, M(0) ≥ 0) . Where, Int R 5 + denotes the interior of R 5 + . 6 2.3.2. Invariance of Region This is achieved by considering the population as, N(t) = A(t) + E(t) + P(t) + R(t) + M(t). (2.2) Now, differentiate (2.2) respecting the solution of the model (2.4) provides dN dt = dA dt + dE dt + dP dt + dR dt + dM dt . (2.3) Consequently, substituting all state equations from the model (2.1) into equation (2.3) results in the following derivation: dN dt = π − dN. Integrating the above equation on both sides and taking t → ∞. The aforementioned character is demonstrated by introducing a region, closed set B such as, B = (A,E, P, R, M) ∈ R 5 : A + E + P + R + M ≤ π d . It is discernible that B possesses positive invariance, serving as an attractor for all solutions delineated by system (2.1). Consequently, the system articulated in (2.1) demonstrates both mathematical and biological well-posedness within the designated region B. 2.3.3. Equilibrium Points For the calculation of the equilibrium points of the corruption model, taking L.H.S of the model equal to zero. π + (1 − φ)ωR − μηAP − (ξ + d)A = 0, μηAP − (γ1 + d)E = 0, νγ1E − (γ2 + d)P = 0, γ2P + (1 − ν)γ1E − (ω + d)R = 0, ξA + φωR − dM = 0 (2.4) The corruption free equilibrium point, E0, is obtained by allowing E = 0, P = 0 and R = 0 such as, E0 = π ξ + d , 0, 0, 0, ξπ d(ξ + d) ! . 7 Additionally, the endemic equilibrium point E ∗ is written as; E ∗ = (A ∗ ,E ∗ , P ∗ , R ∗ , M∗), where, A ∗ = (γ1 + d)(γ2 + d) νηγ1μ , E ∗ = (γ2 + d)(ω + d)[1 − R0] νγ1μηφ(γ1 + d)(γ2 + d)(k + d) , P ∗ = (ω + d)[1 − R0] μηφ(γ1 + d)(γ2 + d)(k + d) , R ∗ = [d(ν − 1) − γ2][R0 − 1] νμηφ(γ1 + d)(γ2 + d)(k + d) , M∗ = ξ(γ1 + d)(γ2 + d) dνηγ1μ + ωφ[d(ν − 1) − γ2][R0 − 1] dνμηφ(γ1 + d)(γ2 + d)(k + d) . and φ = νγ1d(φ − 1) − (ω + d)(γ1 + d)(γ2 + d) − γ1(1 + φ)(γ2 + d). 2.3.4. Reproduction Number We employ the next-generation matrix method [10, 11], to compute the reproduction number. The matrices F and V are used to depict the recruitment of new corrupt individuals and to represent the internal and external transmission terms associated with the compartments of individuals engaged in corruption, we gain F = 0 πμη ξ+d 0 0 0 0 0 0 0 0 0 0 0 0 0 , V = γ1 + d 0 0 0 −νγ1 γ2 + d 0 0 −(1 − ν)γ1 −γ2 ω + d 0 0 0 −φω d . 8 The basic reproduction number is now calculated as the spectral radius of the next-generation matrix F V−1 such as, FV−1 = νμγ1ηπ (γ1+d)(γ2+d)(ξ+d) πμη (ξ+d)(γ2+d) 0 0 0 0 0 0 0 0 0 0 0 0 0 0 0 . Thus the basic reproduction number, R0, is solved as R0 = νγ1μηπ (γ1 + d)(γ2 + d)(ξ + d) . If R0 > 1, it suggests that corruption is likely to increase and spread through the population, becoming more endemic. Conversely, an R0 < 1 indicates that corruption is likely to decline over time. 2.4. Stability Analysis 2.4.1. Local Stability Local stability concentrates on minor perturbations surrounding an equilibrium state. This analysis assists in assessing whether the system will revert to the equilibrium or diverge from it following minimal disturbances. Theorem 2.5. The corruption-free equilibrium point of the said problem is locally asymptotically stable with the condition R0 < 1, whereas unstable for R0 > 1. Proof. The Jacobian matrix of corruption-free equilibrium point for the devised model is given as, J(E0) = −μηP − (ξ + d) 0 −μηA (1 − φ)ω 0 μηP −γ1 − d μηA 0 0 0 νγ1 −d − γ2 0 0 0 (1 − ν)γ1 γ2 −(ω + d) 0 ξ 0 0 φω −d . The evaluation of the jacobian at the corruption-free equilibrium provides, J(E0) =

https://doi.org/10.62500/icrtsda.1.1.46

$-(\xi + d)$ 0 $-\mu\eta\pi$ ξ+d $(1 - \varphi)\omega$ 0 0 $-\gamma 1 - d$ $\mu\eta\pi$ ξ+d 0 0 0 $\nu\gamma 1$ $-d - \gamma 2$ 0 0 0 $(1 - \nu)\gamma 1$ $\gamma 2$ $-(\omega + d)$ 0 ξ 0 0 $\varphi\omega$ $-d$. 9 The resultant eigenvalues are $\lambda 1 = -(\xi + d) < 0$, $\lambda 2 = -d < 0$, where as, $|J(E0) - \lambda I| =$ $-\gamma 1 - d - \lambda$ $\mu\eta\pi$ ξ+d 0 $\nu\gamma 1$ $-d - \gamma 2 - \lambda$ 0 $(1 - \nu)\gamma 1$ $\gamma 2$ $-(\omega + d) - \lambda$ = 0, $|J(E0) - \lambda I| =$ $-a1 - \mu$ a2 0 a3 $-a4 - \mu$ 0 a5 $\gamma 2$ $-a6 - \mu$ = 0. Here, $a1 = \gamma 1 + d$, $a2 = \mu\eta\pi$ ξ+d , $a3 = \nu\gamma 1$, $a4 = d + \gamma 2$, $a5 = (1 - \nu)\gamma 1$, $a6 = \omega + d$. Now we get, λ 3 $-$ (a1 + a4 + a6)λ 2 $-$ (a1a4 + a1a6 + a4a6)λ + (a2a3a6 $-$ a1a4a6) = 0. By Using the Routh-Hurwitz [12] standards for third-order polynomials, it is verified that, (a1 + a4 + a6) > 0, (a2a3a6 $-$ a1a4a6) > 0, i f (a2a3a6$-$a1a4a6) a2a3a6 < 1. On substitution, we get R0 = $\nu\gamma 1\mu\eta\pi$ $(\gamma 1 + d)(\gamma 2 + d)(\xi + d) < 1$, and, [a1 + a4 + a6] $-$ μ[a1a4 + a1a6 + a4a6] > (a2a3a6 $-$ a1a4a6) if R0 < 1. This completes the proof while highlighting the fact that corruption transmission can be avoided if the initial size of the corrupted people falls inside the corruption-free equilibrium point area of attraction. Theorem 2.6. The endemic equilibrium, E $*$, is locally asymptotically stable with the condition R0 > 1, where as unstable for R0 < 1. Proof. The Jacobian matrix is computed as J(E $*$) = $-\mu\eta P - (\xi + d)$ 0 $-\mu\eta A$ $(1 - \varphi)\omega$ 0 $\mu\eta P$ $-\gamma 1 - d$ $p\eta A$ 0 0 0 $\nu\gamma 1$ $-d - \gamma 2$ 0 0 0 $(1 - \nu)\gamma 1$ $\gamma 2$ $-(\omega + d)$ 0 ξ 0 0 $\varphi\omega$ $-d$. 10 The eigenvalues are written as $\lambda 1 = -d < 0$, where, $|J(E *) - \lambda I| =$ $-(q1 + q2 + \mu)$ 0 $-q1$ q3 q1 q4 $- \mu$ q1 0 0 q5 $-(q6 + \mu)$ 0 0 q7 $\gamma 2$ $-(q8 + \mu)$, and q1 = $\mu\eta P$, q2 = $(\xi + d)$, q3 = $(1 - \varphi)\omega$, q4 = $(\gamma 1 + \nu)$, q5 = $\nu\gamma 1$, q6 = $d + \nu$, q7 = $(1 - \nu)\gamma 1$, q8 = $(\omega + d)$. On simplification, we get, $|J(E *) - \lambda I| = \lambda$ 4 + (q1 + q2 $-$ q4 + q6 + q8)λ 3 + (q1q6 $-$ q1q4 $-$ q1q5 + q1q8 $-$ q2q4 + q2q6 $-$ q4q6 $-$q4q8 + q6q8)λ 2 + (q1q6q8 + q1q2q5 $-$ q1q3q7 $-$ q1q4q6 $-$ q1q4q8 $-$ q1q5q8 $-$ q2q4q6 $-$ q2q4q8 +q2q6q8 $-$ q4q6q8)λ $-$ (q1q2q5q8 + q1q3q5q2 + q1q3q6q7 + q1q4q6q8 + q2q4q6q8) = 0. Therefore, the above equation can be written as $|J(E *) - \lambda I|$ = n0λ 4 + n1λ 3 + n2λ 2 + n3λ 1 + n4 = 0, where, n0 = 1, n1 = (q1 + q2 $-$ q4 + q6 + q8), n2 = (q1q6 $-$ q1q4 $-$ q1q5 + q1q8 $-$ q2q4 + q2q6 $-$ q4q6 $-$ q4q8 + q6q8), n3 = (q1q6q8 + q1q2q5 $-$ q1q3q7 $-$ q1q4q6 $-$ q1q4q8 $-$ q1q5q8 $-$ q2q4q6$-$ q2q4q8 + q2q6q8 $-$ q4q6q8), n4 = (q1q2q5q8 + q1q3q5q2 + q1q3q6q7 + q1q4q6q8 + q2q4q6q8). On the employment of Routh-Hurwitz criterion [12] for fourth-order polynomials, n0 > 0, n1 > 0, n1n2 $-$ n0n3 > 0, (n1n2 $-$ n0n3)n3 $-$ n 2 1 n4 > 0 and n4 > 0, only if R0 > 1. One may notice that the eigenvalues are non-positive indicating the local asymptotic stability of E $*$ according to Hurwitz criteria. ———— 11 2.4.2. Global Stability Global stability examines system responses to significant disturbances and across diverse initial conditions. It evaluates whether the system consistently converges to an equilibrium state irrespective of initial states. Theorem 2.7. The said problem is globally asymptotically stable at corruption-free equilibrium E0 for R0 < 1, whereas remains unstable otherwise. Proof. The global stability of the developed model at point E0 originated through the construct of the Lyapunov function such as, V(t) = (A $-$ A $*$) + E + P. (2.5) Next, the time derivative of (2.5) is calculated and applied to the system of the equation given in (2.1), we get, dV dt = dA dt + dE dt + dP dt , = $\pi - \mu\eta AP - (\xi + d)A + \mu\eta AP - (\gamma 1 + d)E + \nu\gamma 1E - (\gamma 2 + d)P$, = π $(d + \xi)$ $(d + \xi)$ $-$ $(\xi + d)A - \gamma 1E - dE + \nu\gamma 1E - \gamma 2P - dP$, = $(\xi + d)A * - (\xi + d)A - d(E + P) - \gamma 1E + \nu\gamma 1E - \gamma 2P$, = $(\xi + d)(A * - A) - d(E + P) - \gamma 1(E - \nu E) - \gamma 2P$, = $-$ $(\xi + d)(A - A *) + d(E + P) + \gamma 1(E - \nu E) + \gamma 2P$ < 0. It is provable that the dV dt < 0 for R0 < 1. Also A = A $*$ and E = P = 0. The invariant principle of LaSalle's [13] suggests that E0 is globally asymptotically stable. ———— Theorem 2.8. The endemic equilibrium state E $*$ = (A $*$,E $*$, P $*$, R $*$, M$*$) of the model (2.1) is globally asymptotically stable with the condition R0 > 1, otherwise it is unstable. Proof. The global stability is established by defining the Lyapunov function at endemic equilibrium points such as, Q = 1 2 (A $-$ A $*$) + (E $-$ E $*$)(P $-$ P $*$) 2 (2.6) After calculating the time derivatives of equation (2.6) and using them in model (2.1), one get dQ dt = (A $-$ A $*$) + (E $-$ E $*$)(P $-$ P $*$) $\times$ $\pi - (\xi + d)A - (\gamma 1 + d)E + \nu\gamma 1E - (\gamma 2 + d)P$, dQ dt = (A $-$ A $*$) + (E $-$ E $*$)(P $-$ P $*$) $\times$ $(d + \xi)R0A * - (\xi + d)A - (\gamma 1 + d)E + \nu\gamma 1E - (\gamma 2 + d)P$, 12 where, $\gamma 1 + d = \eta 1$, $\gamma 2 + d = \eta 2$, $\xi + d = \eta 3$. dQ dt = (A $-$ A $*$) + (E $-$ E $*$)(P $-$ P $*$) $\times$ $\eta 3R0A * - \eta 3A - \eta 1E + \nu\gamma 1E - \eta 2P$, dQ dt = (A $-$ A $*$) + (E $-$ E $*$)(P $-$ P $*$) $\times$ $\eta 3(R0A * - A) - E(\eta 1 + \nu\gamma 1) - \eta 2P$, dQ dt = $-$ (A $-$ A $*$) + (E $-$ E $*$)(P $-$ P $*$) $\times$ $\eta 3(A - R0A *) + E(\eta 1 + \nu\gamma 1) + \eta 2P$ < 0. One may notice that dQ dt < 0 for all (A $*$,E $*$, P $*$, R $*$, M$*$), where as

https://doi.org/10.62500/icrtsda.1.1.46

dQ dt = 0 holds only for A ∗ = A,E ∗ = E, P ∗ = P. Subsequently, the endemic equilibrium E ∗ is the only positively invarient set contained in (A,E, P, R, M), A ∗ = A,E ∗ = E, P ∗ = P . Consequently, the positive E ∗ is asymptotically globally stable. 3. Fractional Analysis of the Model The Caputo-Fabrizio fractional derivative, a modern adaptation in this field, is distinguished by its nonsingular kernel, which simplifies mathematical formulations and broadens their practical application. This application demonstrates that using lower fractional orders leads to a more rapid convergence of the density across all compartments. Consequently, the fractional extension of Model (2.1) offers a more nuanced understanding of the dynamics within the system. □ □□□□□□□□□□□□□□□□□□□□□□□□□□□ □□□□□□□□□□□□□□□□□□□□□□□□□□□ CFD k t (A(t)) = π + (1 − φ)ωR(t) − μηA(t)P(t) − (ξ + d)A(t), , CFD k t (E(t)) = μηA(t)P(t) − (γ1 + d)E(t), CFD k t (P(t)) = νγ1E(t) − (γ2 + d)P(t), CFD k t (R(t)) = γ2P(t) + (1 − ν)γ1E(t) − (ω + d)R(t), CFD k t (M(t)) = ξA(t) + φωR(t) − dM(t).. (3.1) Here the initial conditions are given as: A(0) = A0 ≥ 0, E(0) = E0 ≥ 0, P(0) = P0 ≥ 0, R(0) = R0 ≥ 0, M(0) = M0 ≥ 0. 3.1. Solution of the Corruption Model We employ a hybrid approach that integrates the Laplace transform with the Adomian Decomposition Method (LADM), in conjunction with the Caputo-Fabrizio fractional order derivative. Along with initial 13 conditions, we deal with the general approach used for developing the solution for model (3.1) in the discussion. □ □□□□□□□□□□□□□□□□□□□□□□□□□□ □□□□□□□□□□□□□□□□□□□□□□□□□□□ L[CFD k t (A(t))] = L[π + (1 − φ)ωR(t) − μηA(t)P(t) − (ξ + d)A(t)], L[CFD k t (E(t))] = L[μηA(t)P(t) − (γ1 + d)E(t)], L[CFD k t (P(t))] = L[νγ1E(t) − (γ2 + d)P(t)], L[CFD k t (R(t))] = L[γ2P(t) + (1 − ν)γ1E(t) − (ω + d)R(t)], L[CFD k t (M(t))] = L[ξA(t) + φωR(t) − dM(t)]. (3.2) Now, we apply the definition of (CFFD) on the L.H.S of the system (3.2) and by using initial condition □ □□□□□□□□□□□□□□□□□□□□□□□□□□ □□□□□□□□□□□□□□□□□□□□□□□□□□□ L[CFD k t (A(t))] = A(0) s + s+k(1−s) s L[π + (1 − φ)ωR(t) − μηA(t)P(t) − (ξ + d)A(t)], L[CFD k t (E(t))] = E(0) s + s+k(1−s) s L[μηA(t)P(t) − (γ1 + d)E(t)], L[CFD k t (P(t))] = P(0) s + s+k(1−s) s L[νγ1E(t) − (γ2 + d)P(t)], L[CFD k t (R(t))] = R(0) s + s+k(1−s) s L[γ2P(t) + (1 − ν)γ1E(t) − (ω + d)R(t)], L[CFD k t (M(t))] = M(0) s + s+k(1−s) s L[ξA(t) + φωR(t) − dM(t)]. (3.3) Assuming that the outcome for the given compartments A(t),E(t), P(t), R(t) and M(t) for infinite series is given as: □ □□□□□□□□□□□□□□□□□□□□□□□□□ □□□□□□□□□□□□□□□□□□□□□□□□□□ Ak(t) = P∞ k=0 Ak(t), Ek(t) = P∞ k=0 Ek(t), Pk(t) = P∞ k=0 Pk(t), Rk(t) = P∞ k=0 Rk(t), Mk(t) = P∞ k=0 Mk(t), (3.4) These non-linear terms of the Adomian polynomial A(t)P(t) = P∞ k=0 Gk(t) are as shown in: (Gk(t) = 1 m! d m dμ m [Pm k=0 μ kAk(t) Pm k=0 μ kPk(t)]|μ=0, (3.5) 14 Now we apply the equation (3.2) and (3.3) into (3.4), and we can get □ □□□□□□□□□□□□□□□□□□□□□□□□□□ □□□□□□□□□□□□□□□□□□□□□□□□□□□ L[P∞ k=0 Ak(t)] = A(0) s + s+k(1−s) s L[π + (1 − φ)ωRk(t) − μη P∞ k=0 Gk(t) − (ξ + d) P∞ k=0 Ak(t)], L[P∞ k=0 Ek(t)] = E(0) s + s+k(1−s) s L[μη P∞ k=0 Gk(t) − (γ1 + d) P∞ k=0 Ek(t)], L[P∞ k=0 Pk(t)] = P(0) s + s+k(1−s) s L[νγ1 P∞ k=0 Ek(t) − (γ2 + d) P∞ k=0 Pk(t)], L[P∞ k=0 Rk(t)] = R(0) s + s+k(1−s) s L[γ2 P∞ k=0 Pk(t) + (1 − ν)γ1 P∞ k=0 Ek(t) − (ω + d) P∞ k=0 Rk(t)], L[P∞ k=0 Mk(t)] = M(0) s + s+k(1−s) s L[ξ P∞ k=0 Ak(t) + φω P∞ k=0 Rk(t) − d P∞ k=0 Mk(t)]. (3.6) Now we put k = 0, 1, 2, 3..., k + 1. and like terms are comparing on both side and we get, A(0) = m1,E(0) = m2, P(0) = m3, R(0) = m4, M(0) = m5 Furthermore, we may get this by examining equivalent components 15 on both sides. □ □□□ □□□□□□□□□□□□□□□□□□□□□□□□□□□□□□□□□□□□□ □□□ □□□□□□□□□□□□□□□□□□□□□□□□□□□□□□□□□□□□□ L[A0(t)] = m1 s , L[E0(t)] = m2 s , L[P0(t)] = m3 s , L[R0(t)] = m4 s , L[M0(t)] = m5 s , L[A1(t)] = s+k(1−s) s L[π + (1 − φ)ωR0(t) − μηG0(t) − (ξ + d)A0(t)], L[E1(t)] = s+k(1−s) s L[μηG0(t) − (γ1 + d)E0(t)], L[P1(t)] = s+k(1−s) s L[νγ1E0(t) − (γ2 + d)P0(t)], L[R1(t)] = s+k(1−s) s L[γ2P0(t) + (1 − ν)γ1E0(t) − (ω + d)R0(t)], L[M1(t)] = s+k(1−s) s L[ξA0(t) + φωR0(t) − dM0(t)]. L[A2(t)] = s+k(1−s) s L[π + (1 − φ)ωR1(t) − μηG1(t) − (ξ + d)A1(t)], L[E2(t)] = s+k(1−s) s L[μηG1(t) − (γ1 + d)E1(t)], L[P2(t)] = s+k(1−s) s L[νγ1E1(t) − (γ2 + d)P1(t)], L[R2(t)] = s+k(1−s) s L[γ2P1(t) + (1 − ν)γ1E1(t) − (ω + d)R1(t)], L[M2(t)] = s+k(1−s) s L[ξA1(t) + φωR1(t) − dM1(t)]. . . . L[Ak+1(t)] = s+k(1−s) s L[π + (1 − φ)ωRk(t) − μηGk(t) − (ξ + d)Ak(t)], L[Ek+1(t)] = s+k(1−s) s L[μηGk(t) − (γ1 + d)Ek(t)], L[Pk+1(t)] = s+k(1−s) s L[νγ1Ek(t) − (γ2 + d)Pk(t)], L[Rk+1(t)] = s+k(1−s) s L[γ2Pk(t) + (1 − ν)γ1Ek(t) − (ω + d)Rk(t)], L[Mk+1(t)] = s+k(1−s) s L[ξAk(t) + φωRk(t) − dMk(t)]. (3.7) 16 As a result, using equation (3.7) for the inverse Laplace transform, we obtained □

https://doi.org/10.62500/icrtsda.1.1.46

□□ □□□ □□□ □□□ A0(t) = m1,E0(t) = m2, P0(t) = m3, R0(t) = m4, M0(t) = m5, A1(t) = [1 + k(t − 1)][π + (1 − φ)ωm4 − μηm1m3 − (ξ + d)m1], E1(t) = [1 + k(t − 1)][μηm1m3 − (γ1 + d)m2], P1(t) = [1 + k(t − 1)][νγ1m2 − (γ2 + d)m3], R1(t) = [1 + k(t − 1)][γ2m3 + (1 − ν)γ1m2 − (ω + d)m4], M1(t) = [1 + k(t − 1)][ξm1 + φωm4 − dm5]. A2(t) = π[1 + k(t − 1)] + (1 − φ)ωh14 − [μη(h11m3 + h13m1) − (ξ + d)h11][k 2 t 2 − 2k 2 t + 2kt + (k − 1)2], E2(t) = [μη(h11m3 + h13m1) − (γ1 + d)h12][k 2 t 2 − 2k 2 t + 2kt + (k − 1)2], P2(t) = [νγ1h12 − (γ2 + d)h13][k 2 t 2 − 2k 2 t + 2kt + (k − 1)2], R2(t) = [γ2h13 + (1 − ν)γ1h12 − (ω + d)h14][k 2 t 2 − 2k 2 t + 2kt + (k − 1)2], M2(t) = [1 + k(t − 1)][ξh11 + φωh14 − dh15][k 2 t 2 − 2k 2 t + 2kt + (k − 1)2]. (3.8) Also, the following parameters can be calculated in the same method, and the value indicates the independent variables in the above equations: □ □□□□□□□□□□□□□□□□□□□□□□□□□□□ □□□□□□□□□□□□□□□□□□□□□□□□□□□□ h11(t) = [1 + k(t − 1)][π + (1 − φ)ωm4 − μηm1m3 − (ξ + d)m1], h12(t) = [1 + k(t − 1)][μηm1m3 − (γ1 + d)m2], h13(t) = [1 + k(t − 1)][νγ1m2 − (γ2 + d)m3], h14(t) = [1 + k(t − 1)][γ2m3 + (1 − ν)γ1m2 − (ω + d)m4], h15(t) = [1 + k(t − 1)][ξm1 + φωm4 − dm5]. (3.9) Similarly, higher-order power terms can be documented, and terms previously mentioned in earlier sections have already been identified. Consequently, the methods documented above prove valuable in evaluating solutions for nonlinear fractional-order systems. 17 4. Results and Discussion In this section, we perform numerical simulations for the problem at hand to complement the analytical results obtained using the previously documented techniques. The simulation outputs include a quantitative point analysis, with model parameters selected based on their biological feasibility. Additionally, we have made specific assumptions regarding the parameter values of the proposed model (3.1), as follows: □ □□□□□□□□□□□□□□ □□□□□□□□□□□□□ m1 = 10000, m2 = 0, m3 = 100, m + 4 = 0, m + 5 = 100, π = 85, φ = 0.1, ω = o.35, μ = 0.036, η = 0.0234, ξ = 0.03, d = 0.0160, γ1 = 0.3, γ2 = 0.007, ν = 0.3. (4.1) By employing the above documented parametric values, the subsequent terms of the considered model (3.1) are determined: □ □□□ □□□ □□□ A0(t) = 10000, E0(t) = 0, P0(t) = 100, R0(t) = 0, M0(t) = 100, A1(t) = (459.24)[1 + k(t − 1), E1(t) = (84.24)[1 + k(t − 1)], P1(t) = (−2.3)[1 + k(t − 1)], R1(t) = (0.7)[1 + k(t − 1)], M1(t) = (298.4)[1 + k(t − 1)]. A2(t) = (−7.77)[k 2 t 2 − 2k 2 t + 2kt + (k − 1)2], E2(t) = (360.49)[k 2 t 2 − 2k 2 t + 2kt + (k − 1)2], P2(t) = (5.09)[k 2 t 2 − 2k 2 t + 2kt + (k − 1)2], R2(t) = (−11.94)[k 2 t 2 − 2k 2 t + 2kt + (k − 1)2], M2(t) = (9.031)[k 2 t 2 − 2k 2 t + 2kt + (k − 1)2]. (4.2) 18 Furthermore, the solution to the first few terms of the proposed model is also shown as follows: □ □□□□□□□□□□□□□□□□□□□□□□□□□□□ □□□□□□□□□□□□□□□□□□□□□□□□□□□ A(t) = 1000 − (459.24)[1 + k(t − 1)] − (7.77)[k 2 t 2 − 2k 2 t + 2kt + (k − 1)2], E(t) = 0 − (84.24)[1 + k(t − 1)] − (360.49)[k 2 t 2 − 2k 2 t + 2kt + (k − 1)2], P(t) = 100 − (2.3)[1 + k(t − 1)] − (5.09)[k 2 t 2 − 2k 2 t + 2kt + (k − 1)2], R(t) = 0 − (0.7)[1 + k(t − 1)] − (11.94)[k 2 t 2 − 2k 2 t + 2kt + (k − 1)2], M(t) = 100 − (298.4)[1 + k(t − 1)] − (9.031)[k 2 t 2 − 2k 2 t + 2kt + (k − 1)2]. (4.3) For the graphical representation of the numerical results, MATLAB software is utilized. The graphs shown in the figures below are generated using the initial compartmental conditions and parameter values established for the devised model [14]: A(0) = 10000, E(0) = 0, P(0) = 100, R(0) = 0, M(0) = 100, π = 85, φ = 0.1, ω = o.35, μ = 0.036, η = 0.0234, ξ = 0.03, d = 0.0160, γ1 = 0.3, γ2 = 0.007, ν = 0.3. 0 20 40 60 80 100 0 2000 4000 6000 8000 10000 = 0.50 = 0.55 = 0.60 = 0.65 = 0.70 Figure 4.1: Graphically representation of susceptible compartment A(t) of proposed model with respect to arbitrary fractional orders. 19 0 20 40 60 80 100 0 1000 2000 3000 4000 5000 = 0.50 = 0.55 = 0.60 = 0.65 = 0.70 Figure 4.2: Graphically representation of exposed compartment E(t) of proposed model with respect to arbitrary fractional orders. 0 20 40 60 80 100 0 1000 2000 3000 4000 = 0.50 = 0.55 = 0.60 = 0.65 = 0.70 Figure 4.3: Graphically representation of corrupted compartment P(t) of proposed model with respect to arbitrary fractional orders. 20 0 20 40 60 80 100 0 500 1000 1500 2000 = 0.50 = 0.55 = 0.60 = 0.65 = 0.70 Figure 4.4: Graphically representation of recovered compartment R(t) of proposed model with respect to arbitrary fractional orders. 0 20 40 60 80 100 0 500 1000 1500 2000 = 0.50 = 0.55 = 0.60 = 0.65 = 0.70 Figure 4.5: Graphically representation of honest compartment M(t) of proposed model with respect to arbitrary fractional orders. The Figures 4.1 − 4.5 depicts the

https://doi.org/10.62500/icrtsda.1.1.46

impact of varying fractional orders on the dynamics of each compartment while considering wide range of time intervals. The figure 4.1 refers the behavior of susceptible class. One may notice the utility of fractional scheme by pursing variable slope of the compartment associated with varying orders. The sharper slopes remain consistently associated with the lower fractional orders. Further, 21 figure 4.2 represents the temporal behavior of exposed class. It is to be noticed that the lower fractional orders competently indicate the vulnerability of the class. Moreover,figure 4.3 delineates the behavior of corrupted class with respect to varying fractional orders. The varying degree of influence of corrupted class associated with varying fractional orders remain observable phenomena. Similarly, the recovered class is encapsulated by offering the disply of Figure 4.4. The variable degree of recovery can be noticed in relation to the variable fraction orders. Lastly, the Figure 4.5 is designated for the deception of the transmission dynamics associated with honest class. The influence of fractional order proposition can be witnessed through the variable slopes highlighted the extent of transmittance. 5. Conclusion This research targeted the encapsulation of dynamics of corruption prevailing in a population. The objectives are net by proposing a new deterministic model pursueded by the application of fractional order scheme. The suggested technique is rigorously analyzed while considering a range of fractional orders. Moreover, each fractional order is explored over the time intervals to approximate the temporal behavior of the suggested mechanism. The findings of this research competently argue the utility of fractional order schemes in the study of transmission dynamics of the corruption. For all pre-defined compartments, the degree of prevalence is noticed to be associated with varying levels of fractional. These outcomes determine the capability of fractional order mechanism in using the available information more rigorously. The usefulness of the proposed methodology becomes even more obvious in case of lesser magnitude of information available to the investigated. In future, it will be interesting to explore the applicability of fractional order derivatives when high frequency data is posed. References [1] Nwajeri, U. K., Asamoah, J. K. K., Ugochukwu, N. R., Omame, A., & Jin, Z. (2023). A mathematical model of corruption dynamics endowed with fractal–fractional derivative. Results in Physics, 52, 106894. [2] Deglow, A., & Fjelde, H. (2021). The quality of government and civil conflict. [3] MacLachlan, K. (2019). Corruption as Statecraft: Using Corruption Practices as Foreign Policy Tools. Retrieved, 29, 2023. 22 [4] Jin, F., Qian, Z. S., Chu, Y. M., & ur Rahman, M. (2022). On nonlinear evolution model for drinking behavior under Caputo-Fabrizio derivative. J. Appl. Anal. Comput, 12(2), 790-806. [5] Ullah, M. A., Raza, N., & Nazir, T. (2024). Mathematical simulations and sensitivity visualization of fractional order disease model describing human immunodeficiency. Alexandria Engineering Journal, 87, 1-16. [6] Wu, Y., Nosrati Sahlan, M., Afshari, H., Atapour, M., & Mohammadzadeh, A. (2024). On the existence, uniqueness, stability, and numerical aspects for a novel mathematical model of HIV/AIDS transmission by a fractal fractional order derivative. Journal of Inequalities and Applications, 2024(1), 36.. [7] Kubra, K. T., and Ali, R. (2023). Analysis of Monkey Pox Transmission Dynamics in Society with Control Strategies Under Caputo-Fabrizio Fractal-Fractional Derivative. Modelling in fractional-order systems with applications in engineering, 83. [8] Kubra, K. T., Ali, R., Alqahtani, R. T., Gulshan, S., & Iqbal, Z. (2024). Analysis and comparative study of a deterministic mathematical model of SARS-COV-2 with fractal-fractional operators: a case study. Scientific Reports, 14(1), 6431. [9] Helikumi, M., & Lolika, P. O. (2022). Global dynamics of fractional-order model for malaria disease transmission. ARJOM, 18(9), 82-110. [10] Van den Driessche, P., & Watmough, J. (2002). Reproduction numbers and sub-threshold endemic equilibria for compartmental models of disease transmission. Mathematical biosciences, 180(1-2), 29- 48. [11] Van den Driessche, P. (2017). Reproduction numbers of infectious disease models. Infectious disease modelling, 2(3), 288-303. [12] Merkin, D. R. (2012). Introduction to the Theory of Stability, Springer Science & Business Media, 24. [13] La Salle, J. P. (1976). The stability of dynamical systems. Society for Industrial and Applied Mathematics. [14] Alemneh, H. T. (2020). Mathematical modeling, analysis, and optimal control of corruption dynamics. Journal of Applied Mathematics, 2020, 1-13. 23 [15] He, J. H., Jiao, M. L., Gepreel, K. A., & Khan, Y. (2023). Homotopy perturbation method for strongly nonlinear oscillators. Mathematics and Computers in Simulation, 204, 243-258. 24

https://doi.org/10.62500/icrtsda.1.1.48

. 1st International Conference on Recent Trends in Statistics and Data Analytics
Air University Islamabad, Pakistan – May 9, 2024, Vol. 1, pp. 453-461

A New Estimator Using Cumulative Distribution Function in Simple Random Sampling

Kalim Ullah[1], Gamze Ozel Kadilar[2], Ammara Nawaz Cheema[3], Muhammad Asif [4] and Zawar Hussain[5]

[1]Foundation University Medical College, Foundation University School of Health Sciences, DHA-I, Islamabad 44000, Pakistan.
[2]Department of Statistics, Hacettepe University, Turkey
[3,4]Air University PAF complex, Sector E-9, Islamabad, Pakistan.
[5]Department of Statistics, Islamia University, Bahawalpur, Pakistan.

ABSTRACT

In this work, the sample size has been used to enhance the estimability of the population distribution function of the main variable. In order to estimate the cumulative distribution function (CDF) of populations, an estimator of generalized ratio type has been proposed. We identified the ideal value of the characterizing scalar that minimizes the mean squared error (MSE), as well as the least value of the MSE of the proposed estimator mean squared error associated with this optimal value. We compared the suggested estimator to the mean per unit estimate and other leading estimators aiming at the estimation of the population distribution function of population. Moreover, the comparative performance evaluation was conducted. The legitimacy of the estimator was established by calculating the bias and MSE of the estimator. The findings of this research highlight the efficacy of the devised scheme of estimating population cumulative distribution function in diverse settings of scientific inquiries.

Keywords*:* Cumulative distribution function; auxiliary information; efficiency

1. INTRODUCTION

The incorporation of appropriate auxiliary information increases the accuracy of estimators of anonymous population parameters in survey sampling (s). Several population parameter estimators exist in the literature, together with the population distribution function, median, mean, total, quantiles, and so on, and each requires supplemental information on more than one auxiliary variable in addition to the information on the examined variable. Many studies related to population mean estimation exist in the literature. In terms of population mean estimates, Murthy [1], Sisodia and Dwivedi [2], Srivastava and Jhajj [3], Rao [4], Singh [5, Singh [6], Kadilar and Cingi [7], Kadilar and Cingi [8], Gupta and Shabbir [9], Grover and Kaur [10], Lu [12], Grover and Kaur [11], Muneer et al. [13], Shabbir and Gupta [14], and Gupta [15].

To determine the proportion of observed values less than or equal to a specified value, it is necessary to assess the finite population cumulative distribution function (CDF). There are certain circumstances under which CDF must be estimated. A nutritionist, for example, may be interested in the percentage of people who consume at least 25% of their calories from saturated fat. Several authors have used one or more auxiliary variables to approximate the CDF using information from the literature. CDF estimators proposed by Chambers and Dunstan [17] require information about the study as well as auxiliary variables. Ratio or regression/difference methods can be used to estimate CDFs, as described by Rao et al. [18] and Rao [19]. The CDF can be estimated using auxiliary information using a kernel technique proposed by Kuk [20]. To compute the CDF, Ahmed and Abu-Dayyeh [21] used information on auxiliary variables. A calibration technique was implemented by Rueda et al. [22] to calculate the CDF in an improved manner. An approach to estimating the CDF and quintiles using a survey was investigated by Singh et al. [23]. The CDF can be predicted using a variety of estimators in a non-

https://doi.org/10.62500/icrtsda.1.1.48

response scenario by Yaqub and Shabbir [24]. As part of their effort to estimate highway accident rates by accident severity, Zeng et al. [25] assessed the severity of injuries suffered by delivery drivers involved in rural traffic accidents. The multinomial Tobit model [26] was based on the random parameter. According to Yaqub and Shabbir [24], a generalized family of estimators is available for evaluating the CDF following a non-response. Although Chen et al. [28] utilised an imbalanced mixed logit model in panel data setup with real-phenomena driving environment big dataset to analyse hourly crash possibilities, Dong et al. [27] employed a mixed logit model to study the differences between individual and multi-vehicle road accident probabilities. Yet, Zeng et al. [30] achieved spatial combined statistical modelling for regional sunlight and nightly crash incidences by using Bayesian bivariate conditional auto-regressive model. According to Zeng et al. [29], accident rates should be modelled jointly by sternness at the area level. On the other hand, these estimators only used one auxiliary variable.

Our study provides an estimator that uses the distribution function and the sample size of auxiliary information for estimating the CDF, similar to Gupta and Yadav (2018). A bias and mean squared error (MSE) is calculated for the old and new CDF estimates using the first-order estimation. In theoretical and numerical analyses, the anticipated estimators were found to be more accurate. Estimating the CDF of a finite population, this method is more accurate than the current updated estimators.

2. MATERIALs AND METHODS

2.1. NOTATIONS

Let us assume that a finite population of size N consists of $Z = \{Z_1, Z_2, \ldots, Z_N\}$ units. Let further that Y_i and X_i stand in for the research variable and the auxiliary variable for the ith population unit i^{th} $(i = 1, 2, \ldots, N)$. Assuming that the SRSWOR method was used to sample this population of size n, which uses basic random sampling without replacement. The following notations are defined:

- $I(Y_i \leq y)$: Y-based indicator variable, where $y = \overline{Y}, \widetilde{Y}, Q_{1(y)}$ and $Q_{3(y)}$. Here, $\overline{Y}$ is the mean, $\widetilde{Y}$ is the median, $Q_{1(y)}$ is the first quartile and $Q_{3(y)}$ is the third quartile of Y-based indicator variable, respectively.
- $I(X_i \leq x)$: Indicator variable based on X, where $x = \overline{X}, \widetilde{X}, Q_{1(x)}$ and $Q_{3(x)}$. Here, $\overline{X}$ is the mean, $\widetilde{X}$ is the median, $Q_{1(x)}$ is the first quartile and $Q_{3(x)}$ is the third quartile of Based on an indicator variable X, respectively.
- $F(y) = \sum_{i=1}^{N} I(Y_i \leq y)/N$: The function of Y's population distribution,
- $\hat{F}(y) = \sum_{i=1}^{n} I(Y_i \leq y)/n$: The function of Y's sample distribution,
- ${S_1}^2 = \sum_{i=1}^{N}\left(I(Y_i \leq y) - F(y)\right)^2/(N-1)$,
- $F(x) = \sum_{i=1}^{N} I(X_i \leq x)/N$: Population distribution function X,
- $\hat{F}(x) = \sum_{i=1}^{n} I(X_i \leq x)/n$ The sample distribution function of X, ${S_2}^2 = \sum_{i=1}^{N}\left(I(X_i \leq x) - F(x)\right)^2/(N-1)$,
- $D_1 = S_1/F(y)$, $D_2 = S_2/F(x)$, $D_3 = \sum_{i=1}^{N}\left(I(Y_i \leq y) - F(y)\right)\left(I(X_i \leq x) - F(x)\right)/(N-1)$,
- $\gamma = \left(\frac{1}{n} - \frac{1}{N}\right)$: Finite population correction (fpc).

We also define the following error terms:

$$\Psi_0 = \frac{\left(F(y) - \hat{F}(y)\right)}{F(y)}, \Psi_1 = \frac{\left(F(x) - \hat{F}(x)\right)}{F(x)}.$$

Here, we have $E(\Psi_i) = 0$, for i= 0, 1, $E\left({\Psi_0}^2\right) = \gamma {D_1}^2$, $E\left({\Psi_1}^2\right) = \gamma {D_2}^2$ and $E(\Psi_0\Psi_1) = \gamma D_1 D_2 D_3$.

2.2. EXISTING ESTIMATORS

In this section, some finite population mean estimators are modified in order to assess the finite CDF in case of simple random sampling. Under the first order of approximation, the MSEs and bias of these modified estimators are calculated.The usual sample estimators, $F(y)$, and its variance are defined, respectively, as follows:

$$\hat{F}_1(y) = \frac{\sum_{i=1}^{n} I(Y_i \leq y)}{n}, \text{var}\left(\hat{F}(y)\right) = \gamma F^2(y) {D_1}^2. \quad (1)$$

https://doi.org/10.62500/icrtsda.1.1.48

Cochran (1940) adapted ratio estimator $F(y)$, defined by

$$\hat{F}_2(y) = \hat{F}(y)\frac{F(x)}{\hat{F}(x)}. \quad (2)$$

The mathematical expression for MSE and bias of $\hat{F}_2(y)$ are, respectively, given as

$$Bias\left(\hat{F}_2(y)\right) = \gamma F(y)\left({D_2}^2 - D_1D_2D_3\right), \quad (3)$$

$$MSE\left(\hat{F}_2(y)\right) = \gamma \mathrm{F}^2(y)\left({D_1}^2 + {D_2}^2 - 2D_1D_2D_3\right). \quad (4)$$

If $D_3 > D_2/(2D_1)$, then $\hat{F}_2(y)$ is better than $\hat{F}_1(y)$ in terms of the MSE. Thus, biases and the MSE of above estimators are, respectively, written as

$$Bias\left(\hat{F}_i(y)\right) = \gamma F(y)\left({\Phi_j}^2 D_2{}^2 - D_1D_2D_3\right), \quad (5)$$

$$MSE\left(\hat{F}_i(y)\right) = \gamma \mathrm{F}^2(y)\left({D_1}^2 + {\Phi_j}^2 D_2{}^2 - 2\Phi_j D_1D_2D_3\right).$$

$$i = 3, 4, \ldots, 9 \text{ and } j = 1,2,\ldots,7. \quad (6)$$

These estimators are summarized in Table 1.

Table 1. Estimators, their Constants, MSEs and Biases

Estimators	**Constant**	**Bias**	**MSE**
$\hat{F}_3(y) = \hat{F}(y)\left(\frac{F(x)+D_2}{\hat{F}(x)+D_2}\right)$ Sisodia and Dwivedi [31]	${\Phi}_1 = \left(\frac{F(x)}{F(x)+D_2}\right)$	$\gamma F(y)\left({\Phi_1}^2 D_2 - 2\Phi_1 D_1D_2D_3\right)$	$\gamma \mathrm{F}^2(y)\left({D_1}^2 + {\Phi_1}^2 D_2{}^2 - 2\Phi_1 D_1D_2D_3\right)$
$\hat{F}_4(y) = \hat{F}(y)\left(\frac{F(x)D_2+\beta_2}{\hat{F}(x)D_2+\beta_2}\right)$ Upadhyaya and Singh [39]	${\Phi}_2 = \left(\frac{F(x)D_2}{F(x)D_2+\beta_2}\right)$	$\gamma F(y)\left({\Phi_2}^2 D_2 - 2\Phi_2 D_1D_2D_3\right)$	$\gamma \mathrm{F}^2(y)\left({D_1}^2 + {\Phi_2}^2 D_2{}^2 - 2\Phi_2 D_1D_2D_3\right)$
$\hat{F}_5(y) = \hat{F}(y)\left(\frac{F(x)+D_3}{\hat{F}(x)+D_3}\right)$ Singh and Tailor [35]	${\Phi}_3 = \left(\frac{F(x)}{F(x)+D_3}\right)$	$\gamma F(y)\left({\Phi_3}^2 D_2 - 2\Phi_3 D_1D_2D_3\right)$	$\gamma \mathrm{F}^2(y)\left({D_1}^2 + {\Phi_3}^2 D_2{}^2 - 2\Phi_3 D_1D_2D_3\right)$
$\hat{F}_6(y) = \hat{F}(y)\left(\frac{F(x)+\beta_2}{\hat{F}(x)+\beta_2}\right)$ Singh et.al [35]	${\Phi}_4 = \left(\frac{F(x)}{F(x)+\beta_2}\right)$	$\gamma F(y)\left({\Phi_4}^2 D_2 - 2\Phi_4 D_1D_2D_3\right)$	$\gamma \mathrm{F}^2(y)\left({D_1}^2 + {\Phi_4}^2 D_2{}^2 - 2\Phi_4 D_1D_2D_3\right)$
$\hat{F}_7(y) = \hat{F}(y)\left(\frac{F(x)+\beta_1}{\hat{F}(x)+\beta_1}\right)$ Yan and Tian [40]	${\Phi}_5 = \left(\frac{F(x)}{F(x)+\beta_1}\right)$	$\gamma F(y)\left({\Phi_5}^2 D_2 - 2\Phi_5 D_1D_2D_3\right)$	$\gamma \mathrm{F}^2(y)\left({D_1}^2 + {\Phi_5}^2 D_2{}^2 - 2\Phi_5 D_1D_2D_3\right)$
$\hat{F}_8(y) = \hat{F}(y)\left(\frac{F(x)+M_d}{\hat{F}(x)+M_d}\right)$ Subramani and Kumarpandiyan [37]	${\Phi}_6 = \left(\frac{F(x)}{F(x)+M_d}\right)$	$\gamma F(y)\left({\Phi_6}^2 D_2 - 2\Phi_6 D_1D_2D_3\right)$	$\gamma \mathrm{F}^2(y)\left({D_1}^2 + {\Phi_6}^2 D_2{}^2 - 2\Phi_6 D_1D_2D_3\right)$
$\hat{F}_9(y) = \hat{F}(y)\left(\frac{F(x)+n}{\hat{F}(x)+n}\right)$ Jerajuddin and Kishun [15]	${\Phi}_7 = \left(\frac{F(x)}{F(x)+n}\right)$	$\gamma F(y)\left({\Phi_7}^2 D_2 - 2\Phi_7 D_1D_2D_3\right)$	$\gamma \mathrm{F}^2(y)\left({D_1}^2 + {\Phi_7}^2 D_2{}^2 - 2\Phi_7 D_1D_2D_3\right)$

3. PROPOSED ESTIMATOR

https://doi.org/10.62500/icrtsda.1.1.48

3.1. The Estimator

On the lines of Jerajuddin and Kishun [15] of population mean through CDF. Our study proposes the subsequently generalized estimator for population through CDF utilizing information regarding the sample length as,

$$\hat{F}_{Pr}(y) = \hat{F}(y)\left[\delta + (1-\delta)\left(\frac{F(x)+n}{\hat{F}(x)+n}\right)\right], \quad (7)$$

Where δ is appropriately chosen constant, which is chosen in such a way that minimizes the MSE of proposed estimator. After rewriting Eq. (7) in terms of Ψ_i, the resultant estimator is obtained as;

$$\hat{F}_{Pr}(y) = F(y)(1+\Psi_0)\left[\delta + (1-\delta)\left(\frac{F(x)+n}{F(x)(1+\Psi_1)+n}\right)\right] = F(y)(1+\Psi_0)\left[\delta + (1-\delta)\left(\frac{1}{1+\frac{F(x)}{(F(x)+n)}\Psi_1}\right)\right] = F(y)(1+\Psi_0)[\delta + (1-\delta)(1+{}^{\Phi}\Psi_1)^{-1}]. \quad (8)$$

Here, we define ${}^{\Phi} = \frac{F(x)}{(F(x)+n)}$. We assume that$|\Psi_1| < 1$, so that $(1+{}^{\Phi}\Psi_1)^{-1}$ may be expanded. Now, expanded the right-hand side of (8), we have, $\hat{F}_{Pr}(y) = F(y)(1+\Psi_0)\left[\delta + (1-\delta)\left((1-{}^{\Phi}\Psi_1 + {}^{\Phi 2}{\Psi_1}^2)\right)\right] = F(y)(1+\Psi_0)\left[1-{}^{\Phi}\Psi_1 + {}^{\Phi 2}{\Psi_1}^2 + {}^{\Phi}\delta\Psi_1 - {}^{\Phi 2}\delta{\Psi_1}^2\right]$

Keeping the terms up to the first order of approximation, we obtain

$$\hat{F}_{Pr}(y) = F(y)\left[1+\Psi_0 - {}^{\Phi}\Psi_1 - {}^{\Phi}\Psi_0\Psi_1 + {}^{\Phi 2}{\Psi_1}^2 + {}^{\Phi}\delta\Psi_1 + {}^{\Phi}\delta\Psi_0\Psi_1 - {}^{\Phi 2}\delta{\Psi_1}^2\right], \quad (9)$$

Subtracting $F(y)$ from both sides of (9), we get

$$\left(\hat{F}_{Pr}(y) - F(y)\right) = F(y)\left[\Psi_0 - {}^{\Phi}\Psi_1 - {}^{\Phi}\Psi_0\Psi_1 + {}^{\Phi 2}{\Psi_1}^2 + {}^{\Phi}\delta\Psi_1 + {}^{\Phi}\delta\Psi_0\Psi_1 - {}^{\Phi 2}\delta{\Psi_1}^2\right], \quad (10)$$

Applying the expectations on dual sides of (10) and putting the values of different expectations, we obtain the bias of $\hat{F}_{Pr}(y)$

$$Bias\left(\hat{F}_{Pr}(y)\right) = \gamma F(y)\left[-{}^{\Phi}D_1D_2D_3 + {}^{\Phi 2}{D_1}^2 + {}^{\Phi}\delta D_1D_2D_3 - {}^{\Phi 2}\delta\,{\mathrm{D}_1}^2\right]. \quad (11)$$

Taking square on dual sides of (10) and hold the terms up to the first order of approximation, we obtain,

$$\left(\hat{F}_{Pr}(y) - F(y)\right)^2 = \mathrm{F}^2(y)\left[{\Psi_0}^2 + {}^{\Phi 2}{\Psi_1}^2 - 2{}^{\Phi}\Psi_0\Psi_1 + {}^{\Phi 2}\delta^2{\Psi_1}^2 + 2{}^{\Phi}\delta\Psi_0\Psi_1 - 2{}^{\Phi}\delta^2{\Psi_1}^2\right], \quad (12)$$

Applying the expectation on dual sides of (12) and putting the values of different expectations, we obtain the mean square error of $\hat{F}_{Pr}(y)$, up to the first order of approximation, as

$$MSE\left(\hat{F}_{Pr}(y)\right) = \gamma\mathrm{F}^2(y)\left[{D_1}^2 + {}^{\Phi 2}{D_2}^2 - 2{}^{\Phi}D_1D_2D_3 + {}^{\Phi 2}\delta^2{D_2}^2 + 2{}^{\Phi}\delta D_1D_2D_3 - 2{}^{\Phi}\delta^2\,{\mathrm{D}_2}^2\right], \quad (13)$$

Differentiate (13) with respect to "Φ" we get ${}^{\Phi} = \frac{\delta^2{D_1}^2 - \delta D_1D_2D_3}{\delta^2{D_1}^2} = \frac{C_1}{C_2}$. Thus, the minimum *MSE* of $\hat{F}_{Pr}(y)$ is obtained as

$$MSE_{min}\left(\hat{F}_{Pr}(y)\right) = \gamma\mathrm{F}^2(y)\left[{D_1}^2 + {}^{\Phi 2}{D_2}^2 - 2{}^{\Phi}D_1D_2D_3 - \frac{{C_1}^2}{C_2}\right]. \quad (14)$$

3.2. EFFICIENCY COMPARISON

The offered estimator is compared with the usual prevailing estimators by comparing their *MSEs*. The theoretical conditions for these comparisons are obtained below.

- From (14) and (1), we have $Var(\hat{F}(y)) - MSE_{min}\left(\hat{F}(y)\right) > 0\gamma\mathrm{F}^2(y){D_1}^2 - \gamma\mathrm{F}^2(y)\left[{D_1}^2 + {}^{\Phi 2}{D_2}^2 - 2{}^{\Phi}D_1D_2D_3 - \frac{{C_1}^2}{C_2}\right] > 0.\left[{}^{\Phi 2}{D_2}^2 - 2{}^{\Phi}D_1D_2D_3\right] < \frac{{C_1}^2}{C_2}$.
- From (14) and (4), we have $MSE\left(\hat{F}_2(y)\right) - MSE_{min}\left(\hat{\bar{Y}}_{Pr}\right) > 0\ \gamma\mathrm{F}^2(y)\left({D_1}^2 + {D_2}^2 - 2D_1D_2D_3\right) - \gamma\mathrm{F}^2(y)\left[{D_1}^2 + {}^{\Phi 2}{D_2}^2 - 2{}^{\Phi}D_1D_2D_3 - \frac{{C_1}^2}{C_2}\right] > 0.\ \left(({}^{\Phi 2} - 1){D_2}^2 + ({}^{\Phi} - 1)2D_1D_2D_3\right) < \frac{{C_1}^2}{C_2}$.

https://doi.org/10.62500/icrtsda.1.1.48

- From (14) and (6), we have $MSE\left(\hat{F}_i(y)\right) - MSE_{min}\left(\hat{\bar{Y}}_{Pr}\right) > 0\ \gamma F^2(y)\left({D_1}^2 + {\Phi_j}^2{D_2}^2 - 2^{\Phi_j}D_1D_2D_3\right) - \gamma F^2(y)\left[{D_1}^2 + {\Phi 2}{D_2}^2 - 2^{\Phi}D_1D_2D_3 - \frac{{C_1}^2}{C_2}\right] > 0\ \left(\left({\Phi_j}^2 - {\Phi 2}\right){D_2}^2 + \left({\Phi_j} - {\Phi}\right)2D_1D_2D_3\right) < \frac{{C_1}^2}{C_2}$.

4. EMPIRICAL EVALUATION

The proposed estimator is evaluated against existing estimators by utilizing three different real data sets. The comparative decisions are based on *MSE* and *PRE* criteria. The datasets used in this study for comparative analysis are detailed below and descriptive statistics of the all datasets are given in Table 2, respectively.

Dataset 1: Source: Singh [34]
Y: The number of fish trapped by a marine entertaining fisherman in the year 1995,
X: The number of fish trapped by a marine entertaining fisherman in the year 1994.
Dataset 2: Source: Kadilar and Cingi [22]
In Turkey, Y is the number of teachers, X is the number of classes
Dataset 3: Source: Gujarati [9]
Y: represents the number of eggs produced in 1990 (millions), and X: represents the price per dozen (cents) in 1990.

Table 2. Summary statistics of all data sets

Dataset I						
Parameter	Value	Parameter	$\bar{Y}, \bar{X}$	$Q_{1(y)}, Q_{1(x)}$	$\tilde{Y}, \tilde{X}$	$Q_{3(y)}, Q_{3(x}$
N	69	$F(y)$	0.7246377	0.2608696	0.5072464	0.7536232
n	10	$F(x)$	0.7681159	0.2608696	0.5072464	0.7536232
Γ	0.08550725	D_1	0.6209575	1.695582	0.9928314	0.5759607
		D_2	0.5534675	1.695582	0.9928314	0.5759607
		D_3	0.6606858	0.8496732	0.9420168	0.7658371
		β_1	-1.27058	1.089162	-0.02898855	-1.177177
		β_2	2.614387	2.186275	1.00084	2.385747
		Md	0.343791	0.3867652	0.7305565	0.3652783
Dataset II						
Parameter	Value	Parameter	$\bar{Y}, \bar{X}$	$Q_{1(y)}, Q_{1(x)}$	$\tilde{Y}, \tilde{X}$	$Q_{3(y)}, Q_{3(x}$
N	923	$F(y)$	0.7703142	0.255688	0.5016251	0.7497291
n	180	$F(x)$	0.7692308	0.2502709	0.5005417	0.7497291
Γ	0.0044721	D_1	0.5463469	1.707095	0.9972954	0.5780805
		D_2	0.5534675	0.5480195	1.731739	0.9994587
		D_3	0.6606858	0.8930209	0.8711024	0.8461553

https://doi.org/10.62500/icrtsda.1.1.48

		β_1	-1.270585	-1.278019	1.153033	-0.00216684
		β_2	2.614387	2.633333	2.329486	1.000005
		Md	0.3437913	0.3421385	0.3710516	0.7404969
Dataset III						
Parameter	Value	Parameter	$\bar{Y}, \bar{X}$	$Q_{1(y)}, Q_{1(x)}$	$\tilde{Y}, \tilde{X}$	$Q_{3(y)}, Q_{3(x}$
N	50	$F(y)$	0.68	0.26	0.5	0.74
n	5	$F(x)$	0.58	0.26	0.5	0.74
γ	0.18	D_1	0.6929589	1.704183	1.010153	0.5987669
		D_2	0.5534675	0.8596024	1.704183	1.010153
		D_3	0.6606858	-0.1494137	-0.03950104	-0.12
		β_1	-1.27058	-0.3241764	1.094306	0
		β_2	2.614387	1.10509	2.197505	1
		Md	0.343791	0.622692	0.385476	0.7413

MSEs and PREs of estimators utilizing datasets 1 to 3 are presented in Tables 3 and 4. As seen in Tables 3 and 4, the proposed estimator can be concluded to be more efficient than their prevailing counterparts.

Table 3. MSEs of estimators for all data sets

	For $\{y = \bar{Y},\ x = \bar{X}\}$			For $\{y = Q_{1(y)}, x = Q_{1(x)}\}$		
Estimator	Population 1	Population 2	Population 3	Population 1	Population 2	Population 3
$\hat{F}_1(y)$	0.01731285	0.000792114	0.03996735	0.01672968	0.000852022	0.03533878
$\hat{F}_2(y)$	0.01067654	0.000170006	0.1162843	0.005029838	0.000222996	0.07346939
$\hat{F}_3(y)$	0.01010797	0.000235199	0.05591924	0.01323638	0.000675859	0.03632754
$\hat{F}_4(y)$	0.01472999	0.000611466	0.05051786	0.01241944	0.000637384	0.03680225
$\hat{F}_5(y)$	0.01032615	0.000306086	0.1715127	0.01097464	0.000559622	0.08776509
$\hat{F}_6(y)$	0.01339178	0.00051203	0.05235287	0.01388916	0.000714189	0.0360297
$\hat{F}_7(y)$	0.08062446	0.004759318	0.3896828	0.01186085	0.000611355	0.03717721
$\hat{F}_8(y)$	0.009790685	0.000191705	0.06141532	0.00799257	0.000387731	0.04219708
$\hat{F}_9(y)$	0.01592834	0.000786089	0.04217177	0.01601771	0.000849933	0.03556312
$\hat{F}_{Pr}(y)$	**0.009755691**	**0.000160414**	**0.0390751**	**0.004651778**	**0.000205491**	**0.03528364**
	For $\{y = \tilde{Y}, x = \tilde{X}\}$			For $\{y = Q_{3(y)}, x = Q_{3(x)}\}$		
Estimator	Population 1	Population 2	Population 3	Population 1	Population 2	Population 3
$\hat{F}_1(y)$	0.02168662	0.001119234	0.04591837	0.01611006	0.00084004	0.03533878
$\hat{F}_2(y)$	0.002514919	0.000345129	0.10285714	0.007544757	0.000184318	0.08816327
$\hat{F}_3(y)$	0.01035023	0.000610985	0.05460081	0.007299546	0.000263295	0.05580101
$\hat{F}_4(y)$	0.01043953	0.000611263	0.05478772	0.01269347	0.000626077	0.03926786
$\hat{F}_5(y)$	0.01004274	0.000568999	0.13991746	0.007834579	0.000331812	0.14135602
$\hat{F}_6(y)$	0.01039734	0.000611125	0.05469388	0.01111497	0.000525651	0.04198631
$\hat{F}_7(y)$	0.00274703	0.000346672	0.10285714	0.1110166	0.006523587	0.15297354
$\hat{F}_8(y)$	0.008584943	0.0005365	0.05780771	0.006798648	0.000215369	0.06211278
$\hat{F}_9(y)$	0.01976469	0.001113979	0.04729971	0.01445991	0.00083385	0.03818037

https://doi.org/10.62500/icrtsda.1.1.48

$\hat{F}_{Pr}(y)$	**0.002442007**	**0.000317886**	**0.04525714**	**0.006661406**	**0.000174207**	**0.03317578**

Table 4. PREs of estimators for all data sets

	For $\{y = \bar{Y},\ x = \bar{X}\}$			For $\{y = Q_{1(y)}, x = Q_{1(x)}\}$		
Estimator	Population 1	Population 2	Population 3	Population 1	Population 2	Population 3
$\hat{F}_1(y)$	100	100	100	100	100	100
$\hat{F}_2(y)$	162.1578	465.9341	34.37037	332.6087	382.0802	48.1
$\hat{F}_3(y)$	171.2791	336.784	71.47334	126.3917	126.0649	97.2782
$\hat{F}_4(y)$	117.5347	129.5433	79.11528	134.7055	133.6748	96.02341
$\hat{F}_5(y)$	167.6603	258.7876	23.30285	152.4395	152.2496	40.26518
$\hat{F}_6(y)$	129.2797	154.7007	76.34223	120.4513	119.2993	98.08234
$\hat{F}_7(y)$	21.47344	16.64342	10.25638	141.0496	139.3662	95.05493
$\hat{F}_8(y)$	176.8298	413.1936	65.07716	209.3154	219.7454	83.74697
$\hat{F}_9(y)$	108.6921	100.7664	94.77274	104.4449	100.2458	99.36917
$\hat{F}_{Pr}(y)$	**177.4641**	**493.7937**	**102.2834**	**359.6405**	**414.627**	**100.15628**
	For $\{y = \bar{Y}, x = \bar{X}\}$			For $\{y = Q_{3(y)}, x = Q_{3(x)}\}$		
Estimator	Population 1	Population 2	Population 3	Population 1	Population 2	Population 3
$\hat{F}_1(y)$	100	100	100	100	100	100
$\hat{F}_2(y)$	862.3188	324.2946	44.64286	213.5266	455.7564	40.08333
$\hat{F}_3(y)$	209.5279	183.1851	84.09832	220.6995	319.0488	63.33
$\hat{F}_4(y)$	207.7356	183.1019	83.81142	126.9162	134.17531	89.99414
$\hat{F}_5(y)$	215.9432	196.7022	32.81818	205.6276	253.1675	24.99984
$\hat{F}_6(y)$	208.5786	183.1433	83.95522	144.9402	159.8095	84.16738
$\hat{F}_7(y)$	789.457	322.8513	44.64286	14.5114	12.87697	23.10123
$\hat{F}_8(y)$	252.6123	208.6176	79.43294	236.9598	390.0478	56.89453
$\hat{F}_9(y)$	109.7241	100.4718	97.07959	111.4119	100.74232	92.55744
$\hat{F}_{Pr}(y)$	**888.0653**	**352.0864**	**101.46104**	**241.8417**	**482.2079**	**106.5198**

5. COMMENTS AND CONCLUSION

In this work, under a simple random sampling technique, we provided an estimator for evaluating the finite population cumulative distribution function (CDF). Additional information regarding the distribution function and the size of the ancillary variable was required by the suggested estimator. The suggested estimator's bias and MSE were calculated using first-order estimate. Based on theoretic and empirical comparisons, the proposed estimator can be concluded to be more efficient than their prevailing counterparts. As a result, we advocate utilizing the proposed estimator with the DF and sample size of the ancillary variable to estimate the finite population DF in simple random sampling.

Extending the provided estimator to two-phase and stratified two-phase sample techniques would be interesting. Furthermore, knowledge regarding multi-auxiliary variables could be used to generalize the suggested estimator.

REFERENCES

1. Ahmed, M. S., & Abu-Dayyeh, W. (2001). Estimation of finite-population distribution function using multivariate auxiliary information. *Statistics in Transition*, *5*(3), 501-507.
2. Alam, S., & Shabbir, J. (2020). Calibration estimation of mean by using double use of auxiliary information. *Communications in Statistics-Simulation and Computation*, DOI: 10.1080/03610918.2020.1749660.
3. Baghel, S., & Yadav, S. K. (2020). Restructured class of estimators for population mean using an auxiliary variable under simple random sampling scheme. *Journal of Applied Mathematics, Statistics and Informatics*, *16*(1), 61-75.
4. Cochran, W. G. (1940). The estimation of the yields of cereal experiments by sampling for the ratio of grain to total produce. *The journal of agricultural science*, *30*(2), 262-275.
5. Chambers, R. L., & Dunstan, R. (1986). Estimating distribution functions from survey data. *Biometrika*, *73*(3), 597-604.
6. Chen, F., & Chen, S. (2011). Injury severities of truck drivers in single-and multi-vehicle accidents on rural highways. *Accident Analysis & Prevention*, *43*(5), 1677-1688.
7. Dong B, Ma X, Chen F, Chen S. Investigating the differences of single-vehicle and multivehicle accident

https://doi.org/10.62500/icrtsda.1.1.48

probability using mixed logit model. *Journal of Advanced Transportation*. 2018 Jan 1;2018. https://doi.org/10.1155/2018/7905140 PMID: 32908973.
8. Gupta, S., & Shabbir, J. (2008). On improvement in estimating the population mean in simple random sampling. *Journal of Applied Statistics*, *35*(5), 559-566.
9. Gujarati, D. N. (2009). *Basic Econometrics*. Tata McGraw-Hill Education, New York.
10. Grover, L. K., & Kaur, P. (2011). Ratio type exponential estimators of population mean under linear transformation of auxiliary variable: theory and methods. *South African Statistical Journal*, *45*(2), 205-230.
11. Grover, L. K., & Kaur, P. (2014). A generalized class of ratio type exponential estimators of population mean under linear transformation of auxiliary variable. *Communications in Statistics-Simulation and Computation*, *43*(7), 1552-1574.
12. Gupta, R. K., & Yadav, S. K. (2018). Improved estimation of population mean using information on size of the sample. *American Journal of Mathematics and Statistics*, *8*(2), 27-35.
13. Gupta, R. K., & Yadav, S. K. (2018). Improved estimation of population mean using information on size of the sample. *American Journal of Mathematics and Statistics*, *8*(2), 27-35.
14. Hussain, I., & Haq, A. (2019). A new family of estimators for population mean with dual use of the auxiliary information. *Journal of Statistical Theory and Practice*, *13*(1), 23.
15. Jerajuddin, M., & Kishun, J. (2016). Modified ratio estimators for population mean using size of the sample selected from population. *IJSRSET*, *2*(2), 10-16.
16. Javed, M., Irfan, M., & Pang, T. (2019). Hartley-Ross type unbiased estimators of population mean using two auxiliary variables. *Scientia Iranica*, *26*(6), 3835-3845.
17. Jaroengeratikun, U., & Lawson, N. (2019). A combined family of ratio estimators for population mean using an auxiliary variable in simple random sampling. *Journal of Mathematical and Fundamental Sciences*, *51*(1), 1-12.
18. Kuk, A. Y. (1993). A kernel method for estimating finite population distribution functions using auxiliary information. *Biometrika*, *80*(2), 385-392.
19. Khan, L., & Shabbir, J. (2016). Hartley-Ross type unbiased estimators using ranked set sampling and stratified ranked set sampling. *The North Carolina Journal of Mathematics and Statistics*, *2*, 10-22.
20. Khan, L., & Shabbir, J. (2017). Generalized exponential-type ratio-cum ratio estimators of population mean in ranked set and stratified ranked set sampling. *Journal of Statistics and Management Systems*, 20(1), 133-151.
21. Kadilar, C., & Cingi, H. (2004). Estimator of a population mean using two auxiliary variables in simple random sampling. *International Mathematical Journal*, *5*, 357-367.
22. Kadilar, C., & Cingi, H. (2006). Improvement in estimating the population mean in simple random sampling. *Applied Mathematics Letters*, *19*(1), 75-79.
23. Lu J. Efficient estimator of a finite population mean using two auxiliary variables and numerical application
24. in agricultural, biomedical, and power engineering. Mathematical Problems in Engineering. 2017 Jan 1;2017. https://doi.org/10.1155/2017/2696108 PMID: 29578548
25. Murthy, M. N. (1967). *Sampling: Theory and Methods*. Statistical Publication Society, London.
26. Muneer, S., Shabbir, J., & Khalil, A. (2017). Estimation of finite population mean in simple random sampling and stratified random sampling using two auxiliary variables. *Communications in Statistics-Theory and Methods*, *46*(5), 2181-2192.
27. Rao, J. N. K., Kovar, J. G., & Mantel, H. J. (1990). On estimating distribution functions and quantiles from survey data using auxiliary information. *Biometrika*, 365-375.
28. Rao, T. J. (1991). On certail methods of improving ration and regression estimators. *Communications in Statistics-Theory and Methods*, *20*(10), 3325-3340.
29. Rao, J. N. K. (1994). Estimating totals and distribution functions using auxiliary information at the estimation stage. *Journal of official statistics*, *10*(2), 153.
30. Rueda M, Martı´nez S, Martı´nez H, Arcos A. (2007). Estimation of the distribution function with calibration methods. *Journal of statistical planning and inference. 137(2):435–48.*
31. Sisodia, B.V.S. & Dwivedi, V.K. (1981). A Modified Ratio Estimator Using Coefficient Of Variation Of Auxiliary Variable, Jour. of Indian. Soc. of Agri. Stat., 33(1), 13–18.
32. Srivastava, S. K., & Jhajj, H. S. (1983). A class of estimators of the population mean using multiauxiliary information. *Calcutta Statistical Association Bulletin*, *32*(1-2), 47-56.
33. Singh, H. P., & Tailor, R. (2003). Use of known correlation coefficient in estimating the finite population mean. *Statistics in transition*, *6*(4), 555-560.
34. Singh, S. (2003). *Advanced Sampling Theory With Applications: How Michael Selected Amy* (Vol. 2). Springer Science & Business Media.
35. Singh, H. P., & Tailor, R. (2005). Estimation of finite population mean with known coefficient of variation

https://doi.org/10.62500/icrtsda.1.1.48

of an auxiliary character. *Statistica*, *65*(3), 301-313.
36. Singh, H. P., Singh, S., & Kozak, M. (2008). A family of estimators of finite-population distribution function using auxiliary information. *Acta applicandae mathematicae*, *104*(2), 115-130.
37. Subramani, J. (2013). A new modified ratio estimator for estimation of population mean when median of the auxiliary variable is known. *Pakistan Journal of Statistics and Operation Research*, 137-145.
38. Shabbir, J., & Gupta, S. (2017). Estimation of finite population mean in simple and stratified random sampling using two auxiliary variables. *Communications in Statistics-Theory and Methods*, *46*(20), 10135-10148.
39. Upadhyaya, L. N., & Singh, H. P. (1999). Use of transformed auxiliary variable in estimating the finite population mean. *Biometrical Journal: Journal of Mathematical Methods in Biosciences*, *41*(5), 627-636.
40. Yan, Z., & Tian, B. (2010). Ratio method to the mean estimation using coefficient of skewness of auxiliary variable. In *International Conference on Information Computing and Applications* (pp. 103-110).
41. Yaqub, M., Shabbir, J., & Gupta, S. N. (2017). Estimation of population mean based on dual use of auxiliary information in non-response. *Communications in Statistics-Theory and Methods*, *46*(24), 12130-12151.
42. Zeng, Q., Wen, H., Huang, H., Pei, X., & Wong, S. C. (2017). A multivariate random-parameters Tobit model for analyzing highway crash rates by injury severity. *Accident Analysis & Prevention*, *99*, 184-191.
43. Zeng, Q., Guo, Q., Wong, S. C., Wen, H., Huang, H., & Pei, X. (2019). Jointly modeling area-level crash rates by severity: a Bayesian multivariate random-parameters spatio-temporal Tobit regression. *Transportmetrica A: Transport Science*, *15(2), 1867-1884.*
44. Zeng, Q., Wen, H., Wong, S. C., Huang, H., Guo, Q., & Pei, X. (2020). Spatial joint analysis for zonal daytime and nighttime crash frequencies using a Bayesian bivariate conditional autoregressive model. *Journal of Transportation Safety & Security*, *12(4), 566-585.*

https://doi.org/10.62500/icrtsda.1.1.48

Proc. 1st International Conference on Recent Trends in Statistics and Data Analytics
Air University Islamabad, Pakistan – May 9, 2024, Vol. 1, pp. 462-469

Spatial evenness and pandemics: A demonstration of bio-diversity conceptualization

S. A. Cheema[1], A. A. Khan[2], A. Hussain[3], T. Munir[4] and Z. Hussain[5]

[1]Department of Applied Sciences, School of Sciences, National Textile University Faisalabad, Pakistan.
[2]Department of Statistics, Government Post Graduate College Kohat KPK, Pakistan.
[3]Govermant College Khayaban-e-Sir Syed Rawalpindi, Pakistan.
[4]Department of Anaesthesiology, The Aga Khan University Hospital Karachi, Pakistan.
[5]Department of Statistics, Faculty of Computing, The Islamia University of Bahawalpur, Pakistan.

ABSTRACT

In the wake of the realization of the pressure exerted by humankind on ecosystem, the urge of understanding the degree of bio-diversity crises is also gaining momentum. Broadly speaking, the diversity tools aim at the patterns of species' co-occurrence and abundance while distinguishing the biological abundance and ecological equivalence. The context of this study is to aid the ongoing efforts voicing the loss of species' richness especially on spatial scale. The aforementioned objectives are facilitated by assembling a set of decorated evenness assessment tools available in the literature. The conceptual overview is then enriched by enlisting numerous multi-parametric criteria scooping the *required* and *desirable* features necessary for a diversity measure to maintain. The extent of appropriateness of each measure is explored with respect to featured legitimacy criteria while proposing three categories that is; good, poor, and fail. By doing so, this study encapsulates the performance of eight of bio-diversity while targeting the multi-disciplinary research rigors. Lastly, an interesting application venue is explored while considering the death data consequent upon the initial COVID-19 transmissions. The degree of evenness of number of deaths is enumerated while stratifying the globe into six assemblages as per definition of WHO. The regions are Western Pacific (WPR), Europe (EUR), South-East-Asia (SEAR), Eastern Mediterranean (EMR), Americas (AMR) and Africa (AFR).

Keywords: Bio-diversity; ecological patterns; species evenness;

1. INTRODUCTION

Probabilistic models, over the time, have proved convincing tools in supporting the better understanding of the randomness prevalent in the real life phenomena. The efficacy of distributional approach in summarizing the complex stochastic processes has been appreciated by many researchers by delineating its applicability in diverse fields of inquiry. The validity of probabilistic schemes in imaging ubiquitous information, characterized with extremities, volatilities, and group structures, is well celebrated. For example in, health sciences [1], information theory [2], artificial intelligence [3], and behavioral sciences [4]. The aforementioned studies provide a glimpse of promising nature of probabilistic models in few research fields among many. Therefore, it is of no surprise that we witness that a notable amount of literature, focusing the study of stochastic nature of the flow of transmissible

https://doi.org/10.62500/icrtsda.1.1.48

COVID 19, is being documented, during the ongoing global health hazard [5]. A careful review of the literature reveals that the research efforts exploring the clinical nature of the virus and the mathematical dynamics of the transmission, strongly coincide with each other [6]. The objectives of ongoing model-focused research can be categorized along four major lines, (i) – overall projection, (ii) – emergence re-emergence patterns, (iii) – turning point detection, and (iv) – pandemic final size. Since destructive nature of Coronavirus depends on various parameters, such as, degree of genetic immunity, personal hygiene, travelling history, therefore, models under consideration are far from perfection but their utility in developing comprehensive framework to confront the pandemic is undisputed [7].

The objectives of this research, advance on going COVID 19 related research literature, mainly on two fronts. Firstly, we investigate the extent of regional spatial evenness in the distributions of number deaths, reported during the pandemic, around the globe. Secondly, we pursue the best fit probabilistic model capable of explaining the underlying stochastic attributes of the distributions. Our findings are based on the CDC daily global updates of number death due to COVID 19, dated from 3rd of Feb. 2020 to 21st of Jul. 2020. Moreover, to facilitate the comparative understanding of the pandemic flow, we classify the global death data into six regions, defined by WHO, that is, Western Pacific (WPR), Europe (EUR), South-East-Asia (SEAR), Eastern Mediterranean (EMR), Americas (AMR) and Africa (AFR). Fig. 1 provides the region-specific outlook of the distributional trends observant in all regions during the pandemic, using death data. The distributional complexities, such as, outliers, varying extent of volatility, point inflations and group structures, in regional data, are immediately noticeable. Further, regions vividly differ in terms of suffering due to COVID 19 related deaths. The average number of deaths in AMR is higher than the maximum number deaths, reported in all other regions and at any day, during the pandemic episode. The only exception to this tendency is EUR, which then, remains second most effected regions among six defined regions. Another interesting realization about EUR is the presence of outliers as well as the exceeding degree of variability. The AMR and EUR are followed by SEAR, which is then, closely tailed by EMR. The AFR and WPR standout as the least effected regions, but pose all anticipated distributional challenges by presenting the existence of outliers. In general, the maximum number of deaths recorded in all regions stay lower than the second quartile of the AMR and EUR.

Inspired by the above documented realizations, we start our investigation by exploring the spatial evenness in the distribution of the regional death data. The evenness is considered as one of the vital features of the study of abundance among species in the analysis of distributions of biological communities. The evenness indices provide simple but effective tools to explore the organisms' habitat distributions with respect to space [8], [9]. It is to be noted that with our theoretical framework, we try to quantify species diversity (COVID 19 related deaths) among six biological habitats (regions). In order to execute our analysis, we use eight most commonly employed evenness indices, latest and classics, available in the literature of biological sciences. Moreover, to further validate our framework, we assemble a list of desirable features that are required to maintain by any index to be the legitimate evenness index. The features are quantified with respect to the death data. Furthermore, a pairwise regional analysis is also conducted to attain a deeper understanding of the spatial disparities. The next section (section 2) is dedicated for the explanation and compilation of the resultant outcomes. We observe that the distributions of number of deaths due to COVID 19 are not spatially even.

https://doi.org/10.62500/icrtsda.1.1.48

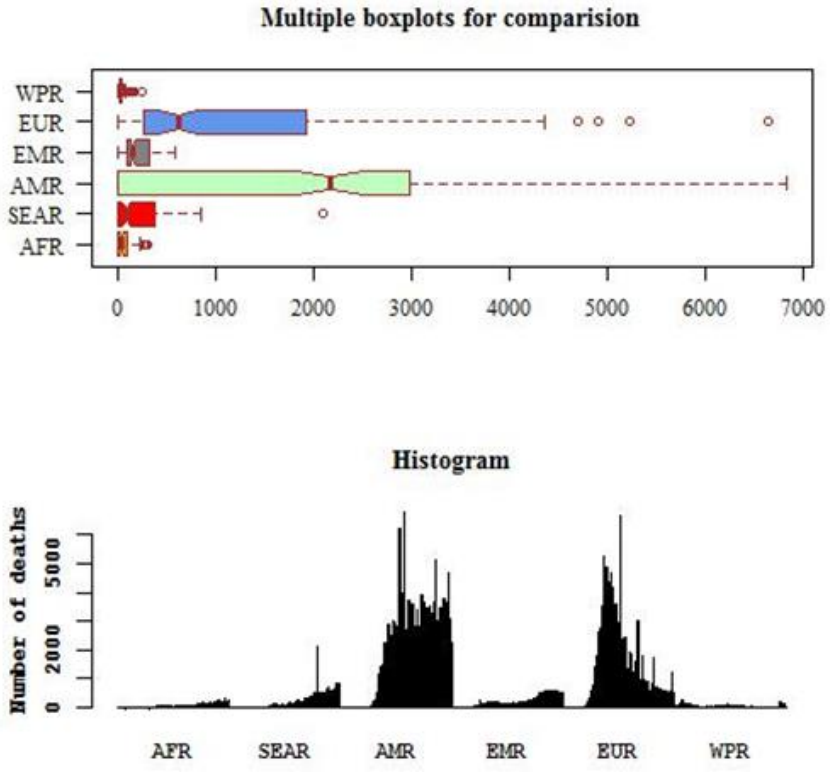

Figure 1: Distributional display of the regional death trends due to COVID 19 pandemic.

2. MATERIALS AND METHODS

2.1. The Evenness Indices

Let us say, S, be the number of sites to sample the information. Let also, x_s, be the abundance of the specie at $s'th$ site, such that, $\sum x = \sum_{s=1}^{S} x_s$ and $p_s = x_s / \sum x$. Further, let us define, $H' = -\sum_{s=1}^{S} p_s \ln(p_s)$, and $D = \sum_{s=1}^{S} p_s^2$. We now consider the indices given below;

$$E_{Heip} = \frac{e^{H'} - 1}{S - 1}, \tag{1}$$

$$E_{\text{var}} = 1 - \frac{2}{\pi} \arctan \frac{\left\{ \sum_{s=1}^{S} \left(\ln(x_s) - \sum_{t=1}^{S} \ln(x_t) / S \right)^2 \right\}}{S}, \tag{2}$$

$$E = \frac{\sum_{s=1}^{S} \min(p_s, 1/S) - 1/S}{1 - 1/S}, \tag{3}$$

https://doi.org/10.62500/icrtsda.1.1.48

$$E_{\frac{1}{D}} = \frac{1/D}{S}, \tag{4}$$

$$E_{-\ln D} = \frac{-\ln D}{\ln S}, \tag{5}$$

$$E_{Mcl} = \frac{\sum x - \sqrt{\sum_{s=1}^{S} x_s^2}}{\sum x - \sum x / \sqrt{S}}, \tag{6}$$

$$E_{1-D} = \frac{1-D}{1-1/S}, \tag{7}$$

and,

$$J' = \frac{H'}{\ln(S)}. \tag{8}$$

2.2. Criteria

We assemble from the literature, a number of criteria that an evenness index is required to meet [13]. Based on their importance, we categorize these criteria into two classes, that is, (i) – requirements, which are essential to maintain, and (ii) – features, that are desirable. We report four requirements and ten features required by any evenness index to maintain.

Requirements: The requirements are listed as below;

(i) The evenness index is required to be independent from community richness.

(ii) Marginal reduction in abundance of most minor, should results in decreasing value of the index.

(iii) Added variability should notify a decline in the index value.

(iv) The index should be unit robust.

Features: Now, we list the desirable features as follows;

(i) The index is desirable to gain its maximum value when abundance is equal.

(ii) The maximum value of 1 is desirable.

(iii) In case of maximum inequality in abundance, the index is expected to produce minimum value.

(iv) The unrealistically uneven abundance is not necessary before the index value is low.

(v) The minimum index value is desirable to be 0.

(vi) The minimum value remains attainable with any number of organisms under study.

(vii) For intermediate abundance values, the index is expected to produce middle value of the scale.

(viii) The index remains interpretable in case of series of changes in evenness.

(ix) The index is desirable to be symmetric.

https://doi.org/10.62500/icrtsda.1.1.48

(x) The index is likely to produce lower values, in case of skewed abundance distribution.

Tab. 1, summarizes the performance of eight indices with respect to aforementioned criteria.

Table 1: Summarizing the legitimacy of evenness indices to study the spatially non-explicit distributions of COCID – 19 death data. Key is: ✓ = Good; □ = Poor; ■ = Fails

		Requirements				Features									
Index	**Range**	**1**	**2**	**3**	**4**	**1**	**2**	**3**	**4**	**5**	**6**	**7**	**8**	**9**	**10**
E_{Heip}	(0,1)	□	✓	✓	✓	✓	✓	✓	✓	✓	✓	□	✓	■	✓
E_{var}	(0,1)	✓	✓	✓	✓	✓	✓	✓	□	✓	✓	□	✓	✓	□
E	(0,1)	□	✓	✓	✓	✓	✓	✓	■	✓	□	✓	□	■	✓
$E_{\frac{1}{D}}$	(0,1)	✓	✓	✓	✓	✓	✓	✓	■	✓	✓	□	✓	■	✓
$E_{-\ln D}$	(0,1)	□	✓	✓	✓	✓	✓	✓	✓	✓	✓	□	✓	■	✓
E_{Mcl}	(0,1)	■	✓	✓	✓	✓	✓	✓	✓	✓	✓	■	✓	■	✓
E_{1-D}	(0,1)	□	✓	✓	✓	✓	✓	✓	✓	✓	✓	■	✓	■	✓
J'	(0,1)	□	✓	✓	✓	✓	✓	✓	✓	✓	✓	■	✓	■	✓

3. EMPIRICAL EVALUATION – APPLICATION TO COVID-19 DATA

AFTER DOCUMENTING THE DEGREE OF LEGITIMACY OF ALL ABOVE CONSIDERED EVENNESS INDICES, WE NOW PROCEED BY APPLYING THEM TO THE COVID 19 REGIONAL DEATH DATA TO QUANTIFY THE EXTENT OF EVENNESS IN THE SPATIALLY NON-EXPLICIT DISTRIBUTION OF DEATH COUNTS. TAB. 2 PROVIDES THE ESTIMATED VALUES OF EVENNESS INDICES.

Table2: Estimated values of evenness indices using COVID – 19 regional data.

	Indices							
	E_{Heip}	E_{var}	E	$E_{\frac{1}{D}}$	$E_{-\ln D}$	E_{Mcl}	E_{1-D}	J'
Values	0.1429	0.3133	0.4153	0.4741	0.5834	0.4885	0.77811	0.6929

It is to be noted that like most of the metrics, these indices are most useful when interpreted relatively. We observed that, indices responded to differences in exploring the spatial stochastic intensities. We observe three varying extent of evenness, ranging from lower to higher, with respect to different indices. For example, E_{Heip} and E_{var} indices, reveal lower degree of evenness in the non-explicit regional distributions, whereas, indices E, $E_{\frac{1}{D}}$, $E_{-\ln D}$ and E_{Mcl}, project moderation in the evenness of death counts due to COVID 19 pandemic. On the other hand two indices, E_{1-D} and J', approximate a higher level of evenness in death data across the regions. These mixed findings indicate the underlying distributional complexities, such as extremities, clustering and high influential points as well as the possibility of potential confounder, in the study of distributional aspects of the COVID 19 data. All these challenges remained anticipated in the exploratory analysis of the data, displayed through the Fig. 1. Provoked by these realizations, we further launch a pairwise (bi-regional) analysis to attain a better understanding of the spatially non-explicit distributional perspectives. All the above

https://doi.org/10.62500/icrtsda.1.1.48

documented indices are then employed on all possible regional pairs. Thus, we have fifteen regional pairs for each index. Tab. 3 compiles the results of the pairwise investigation.

Table 3: A bi-regional comparison of the spatially non-explicit distributional evenness of the COVID 19 death data.

Pairs		Indices							
		E_{Heip}	E_{var}	E	$E_{\frac{1}{D}}$	$E_{-\ln D}$	E_{Mcl}	E_{1-D}	J'
WPR	EUR	0.1343	0.1942	0.0551	0.5283	0.0794	0.0927	0.1071	0.1819
	SEAR	0.4388	0.4976	0.2369	0.6319	0.3379	0.3773	0.4176	0.5248
	EMR	0.4732	0.5339	0.2611	0.6468	0.3715	0.4125	0.454	0.5589
	AMR	0.1140	0.1749	0.0452	0.5231	0.0652	0.0762	0.0883	0.1557
	AFR	0.8785	0.9153	0.6497	0.8907	0.8329	0.8561	0.8773	0.9096
EUR	SEAR	0.5877	0.6531	0.3481	0.7018	0.4891	0.5324	0.5751	0.6669
	EMR	0.5487	0.6129	0.3173	0.6821	0.4479	0.491	0.5339	0.631
	AMR	0.9898	0.9934	0.8989	0.9899	0.9853	0.9877	0.9898	0.9926
	AFR	0.2394	0.2944	0.1112	0.5586	0.1599	0.1842	0.2099	0.3096
SEAR	EMR	0.9969	0.998	0.9444	0.9969	0.9955	0.9963	0.9969	0.9978
	AMR	0.5176	0.5806	0.2936	0.6671	0.416	0.4584	0.501	0.6018
	AFR	0.6899	0.7539	0.4365	0.7590	0.6022	0.6431	0.6825	0.7569
EMR	AMR	0.4811	0.5422	0.2668	0.6504	0.3793	0.4206	0.4624	0.5667
	AFR	0.7308	0.7919	0.4757	0.7844	0.6497	0.6883	0.7251	0.7914
AMR	AFR	0.2045	0.2607	0.0917	0.5479	0.1321	0.1528	0.1749	0.2684

Now, we interpret the outcomes of Tab. 3. The, regional pairs, (WPR, AFR), (EUR, AMR), (EUR, EMR), (SEAR, AFR) and (EMR, AFR), regardless of the index, reveals higher extent of distributional evenness, in comparison to other pairs. These findings also verify the understanding based on initial exploratory analysis. Further, (WPR, SEAR), (WPR, EMR), (EUR, SEAR), (SEAR, AMR) and (SEAR, AMR), approximate moderate tendencies in the non-explicit evenness of COVID 19 related death counts' regional distribution. It becomes clearer that the overall mix results of evenness, were largely associated with these pairs. On the other hand, less evenness is observed, regardless of the index among the pairs of (WPR, EUR), (WPR, AMR), (EUR, AFR) and (AMR, AFR). These outcomes are also summarized in simple principal component plot, given in Fig. 2. Lastly, we observed that the index $E_{\frac{1}{D}}$ remains tend to provide higher values of distributional evenness in all cases. These realizations modestly implicate that pandemic related risk structures varies with respect to space and therefore a priority-based approach can be useful to surpass the viral flow.

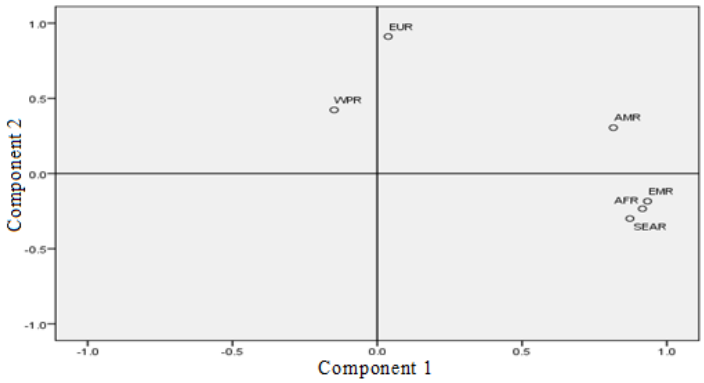

https://doi.org/10.62500/icrtsda.1.1.48

Figure 2: The display of simple principal component plot to highlight the underlying groups in the COVID 19 regional death data.

4. COMMENTS AND CONCLUSION

We observed that, the AMR region stand out as the most eccentric case study. It not only presented the distributional complexities but also dominates the group structure observant in the data by demonstrating the higher tendencies in defining the over spatial un-evenness of the data. Further, the region also remained a case of most vague fitting for all considered statistical models. The AMR is followed by EUR, with respect to the most number of reported deaths. However, proposed less complex distributional structure than the AMR. Further, SEAR, AFR and EMR, projected closely homogeneous group structures while explaining the extent of spatially non-explicit distributional evenness. Lastly, the WPR remained least effected region with minimal distributional challenges, among all six regions.

At this stage, it seems appropriate to document few limitations of this study. Firstly, evenness indices and more generally the spatially non-explicit measures, are built to demonstrate one dimensional standpoint and therefore remain tends to oversimplify the complex information structure. For more sophisticated exploration, one is suggested to consult spatially explicit measures, such as, quadrate variance methods, kriging and difference-based indices. Secondly, this study only explores the extent of spatial discrepancies/evenness and not the why of unevenness. For this purpose, one need to add relevant covariates, such as population density, number of flights, robustness of health services, demographics etc., through appropriate functional forms, linear and non-linear.

REFERENCES

[1] J. Arino, F. Brauer, P. V. Driessche, J. Watmough and J. Wu, “Simple model for containment of a pandemic,” Journal of the Royal Society Interface, vol. 3, no. 8, pp. 453-457, 2006.

[2] Z. Ren, D. Zheng, Y. Lei and L. Tian, “Applying stack bidirectional LSTM model to intrusion detection,” Computers, Material & Continua, vol. 65, no. 1, pp. 321-336, 2020.

[3] Z. Ezziane, “Applications of artificial intelligence in bioinformatics: A review,” Expert Systems with Applications, vol. 30, no. 1, pp. 2-10, 2006.

[4] C. Strobl, F. Wickelmaier and A. Zeileis, “Accounting for individual differences in Bradley-Terry models by means of recursive partitioning,” Journal of Educational and Behavioral Statistics, vol. 36, no. 2, pp. 135-153, 2011.

[5] J. Arino and S. Portet, “A simple model for COVID - 19,” Infectious Disease Modelling, vol. 5, pp. 309-315, 2020.

[6] Y. R. Guo, Q. D. Cao, Z. S. Hong, Y. Y. Tan, S. D. Chen et al., “The origin, transmission and clinical therapies on coronavirus disease 2019 (COVID-19) outbreak–an update on the status,” Military Medical Research, vol. 7, no. 1, pp. 1–10, 2020.

[7] A. J. Kucharski, T. W. Russell, C. Diamond, Y. Liu, J. Edmunds et al., “Early dynamics of transmission and control of COVID-19: a mathematical modelling study,” The Lancet Infectious Diseases, vol. 20, no. 5, pp. 553–558, 2020.

[8] Y. Zhang, H. Y. H Chen and P. B. Reich, “Forest productivity increases with evenness, species richness and trait variation: a global meta-analysis,” Journal of Ecology, vol. 100, no. 3, pp. 742-749, 2012.

[9] X.P. Laura, E. S. Daniel, K. P. Julia and A. T. Stanley, “Quantifying spatial pattern with evenness indices,” Ecological Applications, vol. 15, no. 2, pp. 507–520, 2005.

https://doi.org/10.62500/icrtsda.1.1.48

[10] H. K. Lim, W. K. Li and P. L. H. Yu, "Zero-inflated Poisson regression mixture model," Computational Statistics & Data Analysis, vol. 71, pp. 151-158, 2014.

[11] D. Lambert, "Zero-inflated Poisson regression, with an application to defects in manufacturing," Technometrics, vol. 34, no. 1, pp. 1-14, 1992.

[12] A. L. Byers, H. Allore, T. M. Gill and P. N. Peduzzi, "Application of negative binomial modeling for discrete outcomes: A case study in aging research," Journal of Clinical Epidemiology, vol. 56, no. 6, pp. 559-564, 2003.

[13] B. Smith and B. J. Wilson, "A consumer's guide to evenness indices," Oikos, vol. 76, no. 1, pp. 70-82, 1996.

https://doi.org/10.62500/icrtsda.1.1.49

Proc. 1st International Conference on Recent Trends in Statistics and Data Analytics
Air University Islamabad, Pakistan – May 9, 2024, Vol. 1, pp. 470-482

On the risk of premature transfer from intensive care and coronary care unit

Mohammad Saleh Bataineh[1] and Nosheen Zareen Khan[1*]
[1]Department of Mathematics, University of Sharjah, UAE

ABSTRACT

Hospitals' Intensive Care and Coronary Care Unit (ICU and CCU) are limited and critical resources. The efficient utilization of ICU and CCU capacity significantly impacts both the welfare of patients and the hospital's efficiency and effectiveness. When ICU and CCU become full, an existing patient might be transferred out to a general medical or surgical ward to make room for the new arrival. This study analyzes the admission and discharge of one particular ICU and CCU in a public hospital. The queuing theory will be used to develop a model that predicts the proportion of patients from each category that would be prematurely transferred as a function of the size of the unit, number of categories, mean arrival rates, and length of stay. A numerical example was introduced to demonstrate the operating characteristics, for any given unit size, can be predicted using estimates of the arrival rate for each category (high and low) of patients and the average length of stay for each category. The case study results for the hospital under study illustrates that the efficiency level was acceptable because the proportion of patients from the high risk transferred or turned away is 0.0008, and the proportion of all patients transferred from the unit is 0.0063. Also, it is clear from the results that the increase in the arrival rate affect the distribution of the number of beds used where the number of beds must increase to maintain the current efficiency.

1. INTRODUCTION

The intensive care and coronary care units (ICU and CCU), as with other emergency care facilities, are almost available inside every hospital. They are expensive to operate due to the need for high-level of medical and monitoring equipment to provide adequate patient care for life-threatening contingencies. They are staffed by highly trained physicians and nurses who specialize in caring for critically ill patients. Also, they are distinguished from general hospital wards by a higher staff-to-patient ratio and the access to advanced medical resources and equipment. Patients admitted can be classified as medical ICU or surgical ICU patients who are admitted after surgery (Choi and Lee 2016). Medical ICU patients are admitted for reasons such as severe injuries caused by a tragic accident, critical short-term situations like heart attacks or blood poisoning. Due to the variability of demand for admission and the limited capacity of such units, it is inevitable that from time to time there will be insufficient capacity to both complete the treatment of existing patients and to admit new patients. Either a new referral is refused admission, or existing patients are prematurely transferred out of intensive care and coronary care to make room.

Intensive care and coronary care units have a system of classifying patients into a number of risk categories, which are low, medium and high risk. This system means that during the periods of high demand, it is necessary to prevent the premature transfer of higher-risk patients out of the ICU and CCU. Consequently, when these units become full, it is a common practice to transfer the patients perceived to be in a lower risk category out of the unit and into a general ward to make a bed available. There are two main reasons for such a procedure. Firstly, very little is likely to be known about the medical history or condition of the patient at the time of referral and secondly, if heart failure should occur then the necessary equipment and expertise needs to be immediately available. Unfortunately, if the unit is full, it may be necessary to prematurely transfer a patient who has been diagnosed as having had a heart attack but whose condition appears to be stable out in order to accommodate a referral whose diagnosis, following tests, may turn out to be nothing more serious than acute indigestion (see Wharton (1996)).

https://doi.org/10.62500/icrtsda.1.1.49

In this work, the description concentrates on the analytical model based on queuing theory in which the controllable parameters are the overall mean arrival rate and length of stay, the number of diagnostic categories, and the proportion of patients in each diagnostic category and the number of beds in the unit. The output includes the proportion of patients form each category (high and low risk) that are likely to be transferred prematurely if all arrivals are admitted.

The remainder of this paper is organized as follows. Section 2 presents a review of the state-of-the-art literature pertaining to the problem at hand. Section 3 provides the modeling of the ICU unit. A numerical example is introduced in section 4. Section 5 provides a case study of applying the developed model on a public hospital. Lastly, concluding remarks are presented in Section 6 along with suggestions for future research avenues.

2. Literature Review

Management and planning of the Intensive Care Unit (ICU) is significantly important due to its interaction with the different connected departments within the hospital and how it influences the admission and discharge processes and the scheduling of these connected departments. Several research works have investigated ICU related problems and different approaches were used including optimization, simulation, and queuing theory. This review will focus on the use of queuing theory to support ICU management decisions.

Bai et al. 2018 reviewed the literature on how Operations Research/Management Science (OR/MS) supports ICU management. They focused on the ICU management problem (single department management problem) and classify the literature from multiple angles, including decision horizons, problem settings, and modeling and solution techniques. Lakshmi and Appa Iyer (2013) reviewed the literature of applying the queuing theory in health care management. They examined and classified the literature according to the system operation and system analysis. Systems operation included the emergency department, intensive care unit, obstetrics and neonatal unit, geriatrics and mental health care unit. Systems analysis included Leaving without treatment ratio (LWTR), variable arrival rate (VAR), priority queue discipline (PQD), minimum waiting time (MWT).

The multiple input streams, where it was first traced on the hospital application. Balintfy (1952) considered a census-predictor model by formulating the system as a Markov process. Three different categories of patients (good, fair, and poor) were used to classify the patient's state. Blumberg (1961) considers only one patient type. Using the Poisson distribution for the demand process and deterministic service behavior, he develops tables useful in studying the effects of various allocation policies under different conditions. Weckwerth (1966) employs a similar modeling approach and assumes that the negative exponential distribution satisfactorily characterises a patient's length of stay in the hospital.

Young (1962) was the first to discuss the cut-off model, in which low priority customers are kept waiting if the number of servers busy when he arrives is at or above a specified cut-off level, models for admissions and discharges were given. Kolesar (1970), following the work of Young, developed a Markovian decision model for hospital admission schedules. Describing the state of the system as the number of beds occupied at the start of a given period, he introduced a linear programming model that exploits the Markovian structure in providing a basis for determining an optimal control policy for scheduling admissions. Benn (1966) solved a priority assignment problem in railroad transportation, and the results are published in Jaiswal (1968, pp. 204-214). The same model was later put forward by Shonick and Jackson (1973) to assist in finding how many hospital beds were needed to serve the emergency and regular patients.

Ridge et al. (1998) describe a simulation model for bed capacity planning in Intensive Care. They developed a queuing model for the purposes of validating the simulation model. They used an M/M/c model with priority to emergency patients to analyze a 6-bed intensive care unit (ICU). Kim et al. (1999) analyzed the admission-and-discharge processes of the ICU unit by using queuing and simulation models. They used an M/M/c queueing model to analyze the capacity of the 14-bed ICU and evaluated three different ways of computing the overall average service time for the queueing model. The results provide insights into the operation management issues of an ICU facility to help improve

https://doi.org/10.62500/icrtsda.1.1.49

both the unit's capacity utilization and the quality of care provided to its patients. Green (2002) used queueing analysis to estimate bed unavailability in intensive care units (ICUs) and obstetrics units. The results indicate that as many as 40% of all obstetrics units and 90% of ICUs have insufficient capacity to provide an appropriate bed when needed. This contrasts sharply with the expectations deduced according to standard average occupancy targets. Shmueli et al. (2003) presented a model for optimizing admissions to the ICU with the objective of maximizing the expected incremental number of lives saved by operating an ICU. They use queuing theory to model the probability distribution of the number of occupied ICU beds. McManus et al. (2004) used queueing theory to construct a mathematical model of patient flow, compared predictions from the model to observed performance of the unit, and explored the sensitivity of the model to changes in unit size.

Griffths and Price-Llyod (2006) proposed an M/H/c/∞ queueing model in conjunction with a simulation model of the ICU environment where they emphasized on adequately representing the high variation in the patient length of stay. Seshaiah and Thiagaraj (2011) develop a queueing network model with blocking and reneging to study how the wait times in emergency care units are influenced by the number of available beds in ICUs and general units. They determined the adequate bed counts in each of the two units through an approximate logical method and simulation, to guarantee certain access standards. Chan and Yom-Tov (2011) examined the queueing dynamics of an ICU where patients may be readmitted. They developed a state-dependent Erlang-R queueing network where the service times and readmission probabilities depend on whether the ICU is full.

After examining the above relevant literature, next, we highlight the contribution of this work which is developing a model that predicts the proportion of patients from each category that would be prematurely transferred as a function of the size of the unit, number of categories, mean arrival rates, and length of stay. The model can be used by Hospital managers as a decision tool for planning and managing the ICU unit.

3. ICU Unit Modelling

In order to develop the model, it has been assumed that the referral rates are Poisson distributed, and the distributions of the duration of stay are exponential. In analyzing the steady-state behavior of the systems with Poisson distributed arrival rates and exponentially distributed service times the most commonly used approach is to obtain and solve a set of differential-difference equations relating system states over time.

Consider an ICU unit with C beds and k risk categories, where k is the least important risk category. The patients with risk category j, (j = 1, 2, …, k) has a Poisson arrival rate of λ_j and exponential service time of rate μ_j. Let $\rho_j = \frac{\lambda_j}{\mu_j}$ be the workload parameter for category j risk and $P(n_1, n_2, \ldots\ldots\ldots, n_k)$ be the probability of n_j patients in the unit from categories j, j=1, 2, …, k, where $n_j \geq 0, \sum_{j=1}^{k} n_j \leq C$ and = 0 otherwise. For simplicity, we write P (0, 0, …, 0)= P_0 and $P(n_1, n_2, \ldots, n_k)$ = $P_{\boldsymbol{u}}$, where **u** is a vector with jth component n_j (j =1, 2, ..., k). The steady-state equations for this model are

$$\sum_{j=0}^{k}\left(\lambda_j + n_j\mu_j\right) P_{\boldsymbol{u}} = \sum_{j=1}^{k}\left(n_j + 1\right)\mu_j P_{\boldsymbol{u}+\boldsymbol{v}} + \sum_{j=1}^{k}\lambda_j P_{\boldsymbol{u}-\boldsymbol{v}} \,. \tag{2.1}$$

Where, **v** is a vector with all zero components except for a one at position j corresponding to priority j. The steady-state can be stated as follows and as shown in Theorem 1 and its proof.

https://doi.org/10.62500/icrtsda.1.1.49

$$P_{\mathbf{u}} = \prod_{j=1}^{k} \frac{\rho_j^{n_j}}{n_j!} P(0,0,...,0). \tag{2.2}$$

Theorem 3.1

When categories 1, 2, …, k have different service times, the probability distribution of the customers in the system at the steady-state is

$$P_u = \left(\prod_{j=1}^{k} \frac{\rho_j^{n_j}}{n_j!} \right) P_0 \text{ Where, } \quad P_0 = \left[\sum_{\substack{(n_1,n_2,....,n_k) \\ \sum_{j=1}^{k} n_j \le C}} \prod_{j=1}^{k} \frac{\rho_j^{n_j}}{n_j!} \right]^{-1}$$

Proof:

To prove the theorem we need to show that (2.2) satisfies (2.1). Let $P_{\boldsymbol{u}} = D \prod_{j=1}^{k} \frac{\rho_j^{n_j}}{n_j!}$ then we show that D should be

$$\left[\sum_{\substack{(n_1,n_2,....,n_k) \\ \sum_{j=1}^{k} n_j \le C}} \prod_{j=1}^{k} \frac{\rho_j^{n_j}}{n_j!} \right]^{-1}$$

in order to satisfy the summability – to – one criterion. Let $\Re(\boldsymbol{u}) = \prod_{j=1}^{k} \frac{\rho_j^{n_j}}{n_j!}$, then substituting $P_{\boldsymbol{u}} = D\Re(\boldsymbol{u})$ into (2.1) gives

$$D\Re(\boldsymbol{u}) \sum_{j=1}^{k} (\lambda_j + n_j \mu_j) = D\Re(\boldsymbol{u}) \sum_{j=1}^{k} \lambda_j + D\Re(\boldsymbol{u}) \sum_{j=1}^{k} n_j \mu_j$$

Since the left-hand side is the same as the right hand-side, i.e. $P_{\boldsymbol{u}} = D \prod_{j=1}^{k} \frac{\rho_j^{n_j}}{n_j!}$. Now to evaluate *D*, we have: $\sum_{\substack{(n_1,n_2,....,n_k) \\ \sum_{j=1}^{k} n_j \le C}} P_{\boldsymbol{u}} = 1.$

https://doi.org/10.62500/icrtsda.1.1.49

Thus, $$D = \left[\sum_{\substack{(n_1,\ldots,n_k) \\ \sum_{j=1}^{k} n_j \le C}} \prod_{j=1}^{k} \frac{\rho_j^{n_j}}{n_j!} \right]^{-1}.$$

One of particular interest is the proportion of patients in each category who are (prematurely) transferred out of the unit in order to make room for incoming (undiagnosed) arrivals. If T_m denotes the probability that a patient in category *m* is prematurely transferred then PT_m is the proportion of time or probability that the unit is full with patients of type *m* and above and that

$$T_m = \sum_{\substack{(n_1,\ldots,n_m,0,\ldots,0) \\ \sum_{j=1}^{m} n_j = C}} P(n_1, n_2, \ldots, n_k) - \sum_{\substack{(n_1,\ldots,n_{m-1},0,\ldots,0) \\ \sum_{j=1}^{m-1} n_j = C}} P(n_1, n_2, \ldots, n_k) \qquad 2.3$$

It follows that the proportion of patients from category *m* are prematurely transferred PT_m is given by

$$PT_m = \left(\sum_{\substack{(n_1,\ldots,n_j,0,\ldots,0) \\ \sum_{i=1}^{j} n_i = C}} P_{\mathbf{u}} - \sum_{\substack{(n_1,\ldots,n_{j-1},0,\ldots,0) \\ \sum_{i=1}^{j-1} n_i = C}} P_{\mathbf{u}} \right) \frac{\sum_{i=1}^{j} \lambda_i}{\sum_{i=1}^{j} \lambda_i - \sum_{i=1}^{j-1} \lambda_i} \qquad 2.4$$

Corollary 3.1

The probability of dropping a customer from priority category *j* out of the system is given by

$$\sum_{\substack{(n_1,\ldots,n_j,0,\ldots,0) \\ \sum_{i=1}^{j} n_i = C}} P_{\mathbf{u}} - \sum_{\substack{(n_1,\ldots,n_{j-1},0,\ldots,0) \\ \sum_{i=1}^{j-1} n_i = C}} P_{\mathbf{u}}$$

Proof:

Let T_j be the probability that a customer of category *j* is dropped out of the system, then

$$\begin{aligned} T_j &= \Pr\{\text{The system is full by categories } 1, 2, \ldots, j \text{ and } n_j > 0\} \\ &= \Pr\{\text{The system is full by categories } 1, 2, \ldots, j\} \\ &\quad \times \Pr\{n_j > 0 \mid \text{system is full by categories } 1, 2, \ldots, j\} \\ &= \Pr\{\text{The system is full by categories } 1, 2, \ldots, j\text{-}1\} \\ &\quad \times \left(1 - \frac{\Pr\{\text{The system is full by categories } 1, 2, \ldots, j\text{-}1\}}{\Pr\{\text{The system is full by categories } 1, 2, \ldots, j\}}\right) \end{aligned}$$

https://doi.org/10.62500/icrtsda.1.1.49

$$= \Pr\{\text{The system is full by categories } 1, 2, \ldots, j\} -$$

$$\Pr\{\text{The system is full by categories } 1, 2, \ldots, j-1\}$$

$$= \sum_{\substack{(n_1,\ldots,n_j,0,\ldots,0) \\ \sum_{i=1}^{j} n_i = C}} P_{\mathbf{u}} - \sum_{\substack{(n_1,\ldots,n_{j-1},0,\ldots,0) \\ \sum_{i=1}^{j-1} n_i = C}} P_{\mathbf{u}} \quad .$$

Observe that from the above corollary, the proportion of customers of category j that are dropped from the system is given by

$$\left(\sum_{\substack{(n_1,\ldots,n_j,0,\ldots,0) \\ \sum_{i=1}^{j} n_i = C}} P_{\mathbf{u}} - \sum_{\substack{(n_1,\ldots,n_{j-1},0,\ldots,0) \\ \sum_{i=1}^{j-1} n_i = C}} P_{\mathbf{u}} \right) \frac{\sum_{i=1}^{\ell} \lambda_i}{\sum_{i=1}^{j} \lambda_i - \sum_{i=1}^{j-1} \lambda_i} .$$

4. Illustrative Example

For any given set of parameters λ_j and μ_j (j =1,2) and C, the steady-state probabilities can be obtained by using equations 2.1 and 2.2. Consider, for example, a unit for which the arrival rates of high and low-risk patients are independently and Poisson distributed with means of 1 and 2 patients per day respectively and let the length of stay of high and low-risk patients be exponentially distributed with means 3 and 2 days respectively. For illustration, assume that the number of beds available is 5 beds.

The probability distributions for the number of patients in the unit from diagnostic categories up to and including the k^{th} category k (k = 1, 2) is given in Table 1 below.

	No. of patients in coronary care					
Categories	0	1	2	3	4	5
High & low	0	3	7	18	30	42
High	5	16	25	25	18	11

Table 1: Probability distribution (%) of patients

The distribution of the number of all categories of patients in the unit is in effect the distribution of bed occupancy in the unit. Hence the unit is full 42% of the time, and it follows that 42% of all patients are transferred prematurely; it is full 11% of the time with patients from high risk. It follows that 31% of premature transfers are from low risk, and 11% are from high risk. From Table 1, the proportions of category 2 and 1 transferred prematurely are 93% and 33% respectively.

5. **Case Study**

The ICU and CCU in the hospital under study have 9 beds and provide services for a population of 100,000 residents. In general, the patients are referred to the hospital in CCU by their general practitioners, accidents or by themselves. The patients treated in the critical care unit are categorized into six groups as follows.

https://doi.org/10.62500/icrtsda.1.1.49

VII. ICU / high dependency,
VIII. Cardiac Monitoring,
IX. Heart attack,
X. Chest pain,
XI. Overdose,
XII. Other acute diagnoses.

Then the Hospital admission and serving policy is,

1. Prior to admission to the intensive or coronary care unit the patients are categorized into one of follows two categories:
    - High Risk (that includes numbers I, II and III mentioned above), and
    - Low Risk (which includes numbers IV, V and VI).
2. Patients admitted to the unit will stay and not to be released until a satisfactory/full recovery.
3. When the unit is full (full capacity occupied), the new patient will be diagnosed, categorized and transferred elsewhere, as shown in the flow-chart in Figure 1

https://doi.org/10.62500/icrtsda.1.1.49

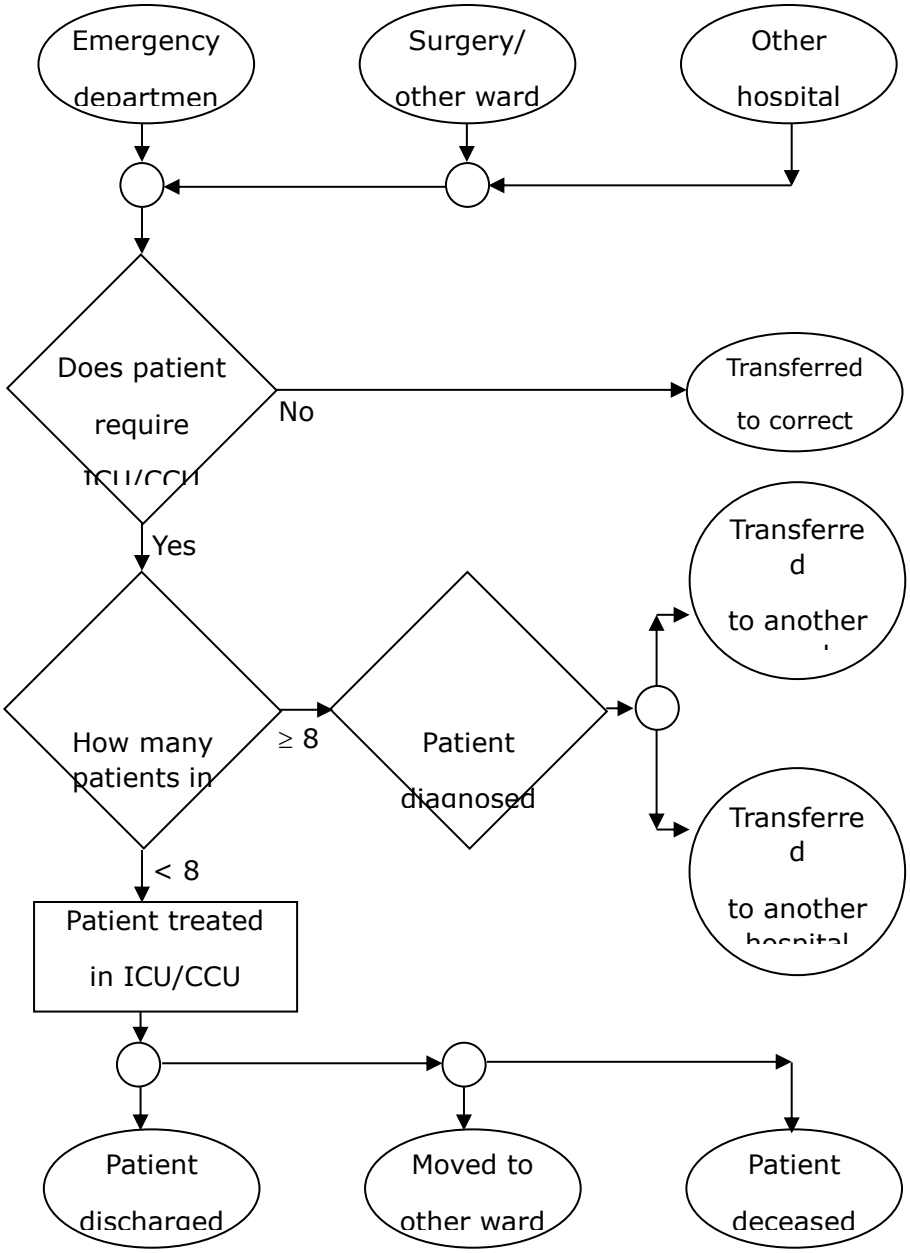

Figure 1: Hospital flowchart

The data available are daily recorded over one year for the number of admissions per day, the final diagnoses of all the patients admitted and the bed occupancies. To estimate the model parameters, it was found that the admissions per day over a period of 365 days for the two categories (high and low) were Poisson distribution with mean 1.52 and 1.422 per day receptively. The actual and theoretical pairs for both high and low risk are shown in Table 2, Table 3, Figure 2 and Figure 3 below.

https://doi.org/10.62500/icrtsda.1.1.49

Table 2: Admissions per day (high risk)

No. of Admission	0	1	2	3	4	5	6
Actual frequency	82	125	91	34	23	9	2
Theoretical	80	121	92	46	18	5	1

Table 3: Admissions per day (low risk)

No. of Admission	0	1	2	3	4	5	6	7
Actual frequency	94	119	89	42	13	7	0	1
Theoretical	88	125	89	42	15	4	1	0

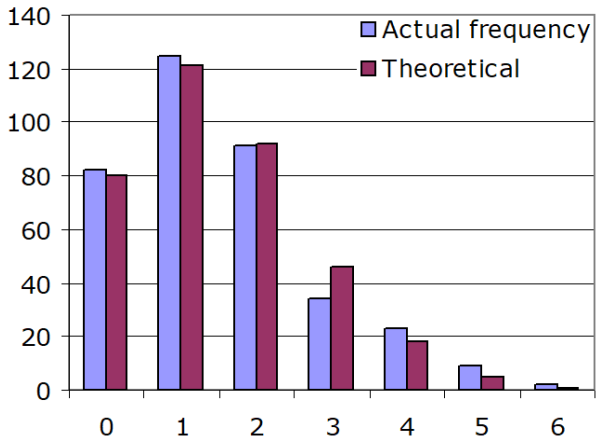

Figure 2: Admissions per day (high risk)

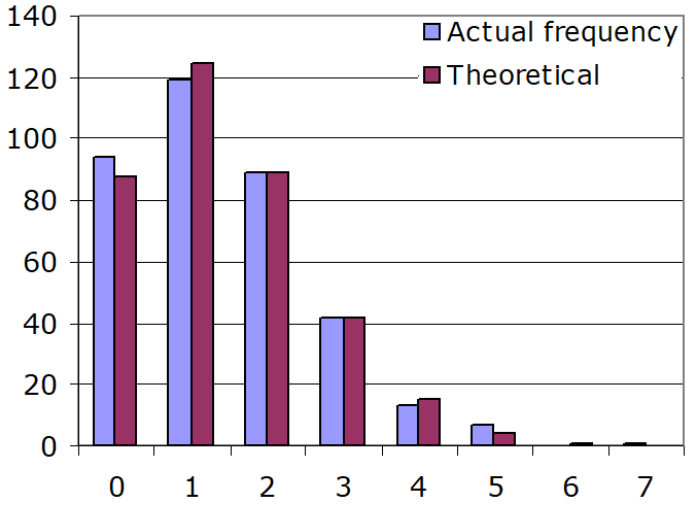

Figure 3: Admissions per day (low risk)

Among the 1097 patients admitted over a one-year period, the final diagnoses were 502 low risk and 595 high risk. Lengths of stay in the unit over the period of 365 days were found to be exponentially distributed for the low and high risk with mean 1.196 and 2.04 respectively. The actual and theoretical distributions are shown in Table 4, Table 5, Figure 4 and Figure 5 below.

https://doi.org/10.62500/icrtsda.1.1.49

Table 4: Mean stay of high risk

No. of days	0	1	2	3	4	5	6	7	8	9	10	11	12	13	14	15	16
Actual frequency	135	170	106	88	39	16	11	14	4	1	5	3	1	0	1	0	1
Theoretical (rounded)	290	178	109	67	41	25	15	9	6	3	2	1	1	1	0	0	0

Table 5: Mean stay of low risk

No. of days	0	1	2	3	4	5	6	7	8	9	10
Actual frequency	170	199	70	28	18	6	6	3	1	0	1
Theoretical (rounded)	420	182	79	34	15	6	3	1	1	0	0

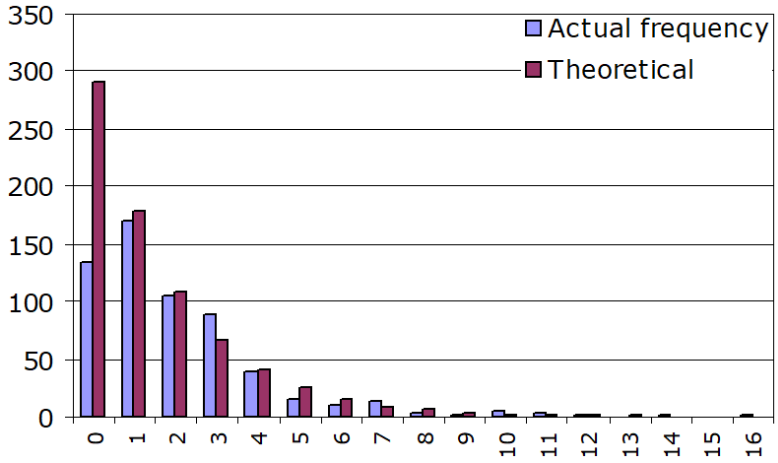

Figure 4: Mean stay of high risk

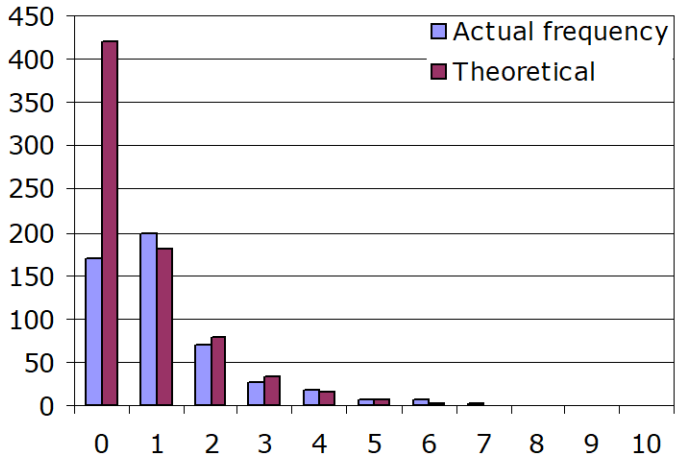

Figure 5: Mean stay of low risk

The distribution of actual bed occupancy is shown in Figure 6. This distribution appears as a normal distribution with a mean of 7.0438 and a standard deviation of 1.7011. Using a chi-square test,

https://doi.org/10.62500/icrtsda.1.1.49

it is clearly shown that the distribution for the bed occupancy level is Normal distribution, the actual and theoretical distributions are presented in Table 6 as well as in Figure 6.

Table 6: Bed occupancy

No. of beds	1	2	3	4	5	6	7	8	9	10	11
Actual frequency	0	1	6	21	36	68	92	64	52	20	5
theoretical (rounded)	0	1	5	17	42	71	86	73	44	19	6

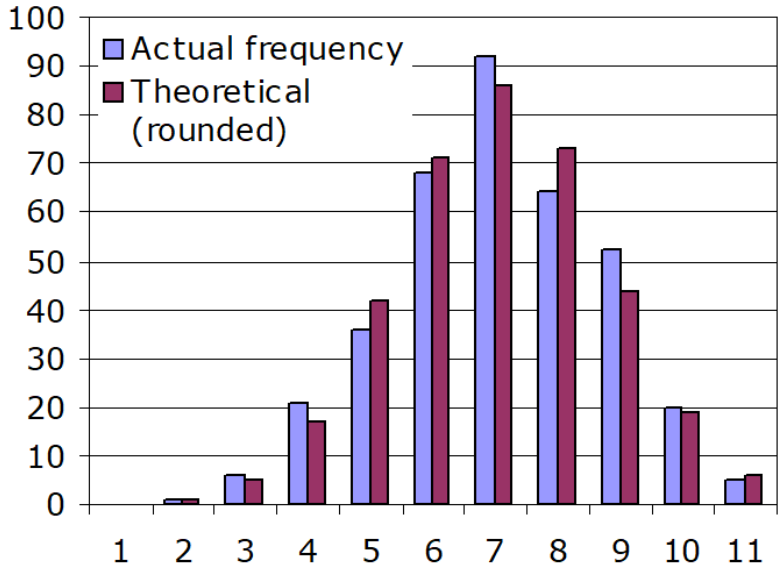

Figure 6: Bed occupancy

One can notice there are occasions where the bed occupancy level exceeds the current bed capacity. That happened on 25 occasions throughout the year, i.e. 6.8 % of the time. In other words, management accepts that the unit's capacity is adequate 93.2 % of the time. Since this is the case, and to predict the required bed capacity level for future patient demands, we will assume a significance level of 95 %.

Since the hospital under study is satisfied with the current efficiency of the unit, we are going to estimate our current probabilities of “x” number of beds used on any one day shown in Table 7.

https://doi.org/10.62500/icrtsda.1.1.49

Beds Used (BU)	Frequency (Fr)	Probability = BU/Fr
7	92	0.2521
8	64	0.1753
9	52	0.1425
10	20	0.0548
11	5	0.0137

Table 7: Probability distribution of bed used on one day

As shown earlier, the bed occupancy level has a normal distribution with a mean of approximately 7 patients (rounded down from 7.0438) and a standard deviation of 2 patients (rounded up from 1.7011). Since our sample is large and spans a year of patient traffic, we will assume that these values hold true for the entire population.

We will now examine the days of the year, which have a bed occupancy level greater than and equal to the average. We selected at random, 1 day from each of the days, where the bed occupancy level exceeded 6 patients. These days were then examined in detail, and the results are shown in the tables (1-5) in Appendix (1).

Thus, with 8 beds available (9 beds in the unit) some 0.0093 of all patients are transferred prematurely, if it can be assumed, however, that patients are accurately diagnosed soon after admission then only 0.00008 of high risk and 0.00922 of low risk would be transferred prematurely.

The main purpose of this section is to demonstrate that queuing theory can be applied to give insights into the steady-state behavior and operating characteristics of service systems with pre-emptive service disciplines.

For illustration, the model has been used to obtain estimates of the proportion of patients transferred prematurely form a coronary care unit in which patients are classified into two categories (high and low risk).

In order to complete the current study and to justify its results, we have to test our assumptions and to justify the use of the model. To test whether the number of patients of both categories of risk that arrive each day is random, we fitted a Poisson distribution to the number of patients per day. A chi-square test has shown that the fit was significant at the 99 % confidence level. To test whether the length of stay for the two categories is exponential, a chi-square test showed that the fit was not at the 99 % confidence level for the two categories.

However, as seen in Figure 3 and 4, the observed frequency for 0 days differs greatly from the expected frequency. This results in a large value for chi-square, thus greatly influencing the sum of chi-square on closer examination of these observations. It was determined that patients who were admitted for less than one day were in fact in the ward for only a very short time. This raises suspicion that perhaps these patients were not as serious as first diagnosed and did not require the specialized treatment from this unit. Under this assumption, the chi-square test showed that the fit was significant at the 99 % confidence level for both categories. Thus, the system behavior within each category should have been modeled as multiple server queueing system with Poisson arrivals and exponential distribution.

6. Discussions and Conclusion

Emergency services are subject to highly variable demand. Under this situation, we have to balance the cost of providing more capacity than is needed on average against the risk to patients who must otherwise be refused admission to or transferred prematurely from intensive care in order to admit new patients for observation and diagnosis.

https://doi.org/10.62500/icrtsda.1.1.49

The decision as to where the balance lies between the costs of providing more facilities than the average required and the cost to patients otherwise put at risk remains a matter of clinical judgment. The proposed model, however, at least reduces some of the uncertainty about the effect of unit size on the numbers and diagnostic categories of patients put at risk by premature transfer.

When coronary care units become full, it is common practice to make at least one bed available for new arrivals by transferring the patient perceived to be at least risk to a general medical or surgical ward. In deciding how many beds should be provided it is clearly necessary to make some assumption about the relationship between the number of beds available and the proportion of high-risk patients who would be prematurely transferred out of intensive care.

The numerical example we introduced demonstrates the operating characteristics for any given size of unit can be predicted using estimates of the arrival rate for each category (high and low) of patients and the average length of stay for each category.

The case study illustrates that the efficiency level of the (CCU) in the hospital under study was acceptable because the proportion of patients from the high risk transferred or turned away is 0.0008, and the proportion of all patients transferred from the unit is 0.0063.

Increases in the arrival rate affect the distribution of the number of beds used. From this for these increases, the unit's number of beds must increase to maintain its current efficiency. One must address the fact that in the future, there is a high chance that the arrival rate will increase, due to the significant growth of the local population. As a result, the current critical care unit would no longer be optimal due to the decrease in the ability of the units to cope with demand in the future.

REFERENCES

1. Bai, J., Fügener, A., Schoenfelder, J., and Brunner, J. (2018). "Operations research in intensive care unit management: a literature review". *Health Care Management Science* 21:1–24.
2. Bailey, N.T.J. (1952). "A Study of Queues and Appointment System in Hospital Out- patient Department with Special Reference to Waiting Time". *Journal of the Royal Statistical Society: Series B* 14: 185-194.
3. Benn, B.A. (1966). "Hierarchical Car Pool Systems in Railroad Transportation". *Ph.D.thesis, case Institute of technology, Cleveland, Ohio.*
4. Blumberg, M.S.(1961). "DPF Concept Helps Predict Bed Needs". *Modern Hospital* 97: 75-81.
5. Chan, C. and Yom-Tov, G. (2011). "Intensive care unit patient flow with read-missions: a state-dependent queueing network". *2011 MSOM Annual Conference Ann Arbor,Michigan* pp.1–3
6. Choi, M. and Lee, H. (2016). "Critical Patient Severity Classification System predicts outcomes in intensive care unit patients". *Nursing in critical care* 21: 206-213.
7. Cooper, R.B. (1972). "*Introduction to Queueing Theory*". Macmillan, New York.
8. Green, L. (2002). "How many hospital beds?". *Inquiry* 39: 400-412.
9. Griffths, J. and Price-Llyod, N. (2006). "A queuing model of activities in an intensive care unit". *IMA Journal of Management Mathematics* 17: 277-288.
10. Harris, R.A (1985). "Hospital bed requirements planning". *European Journal of Operational Research,* 25: 21-126.
11. Kim, S., Horowitz, I., Young, K., and Buckley, T. (1999). "Analysis of capacity management of the intensive care unit in ahospital". *European Journal of Operational Research* 115: 36-46.
12. Kolesar, P., (1970). "A Markovian Model for Hospital Admission scheduling". *Management Science* 16: 384-396.
13. Lakshmi, C. and Appa Iyer, S. (2013). "Application of queueing theory in health care: A literature review". *Operations Research for Healthcare* 2: 25-39.

https://doi.org/10.62500/icrtsda.1.1.49

14. Liyanage, L. and Gale, M. (1995). "Quality improvement for the Campbell town hospital emergency service". *International conference on systems, Man and Cybernetics* 3: 1997-2002.
15. McClain, J.O. (1976). "The Planning Using Queueing Theory Models of Hospital Occupancy: A Sensitivity Analysis". *Inquiry* 13: 167-176.
16. McManus, M., Long, M., Cooper, A., and Litvak E. (2004). "Queueing theory accurately models the need for critical care resources". *Anesthesiology* 100: 1271-1276.
17. National health strategy. (1992). "A Study of Hospital Outpatient and Emergency Department Services". Paper 10.
18. Ridge, J., Jones, S. Nielsen, M., and Shahani, A. (1998). "Capacity planning for intensive care units". *European Journal of Operational Research* 105: 346-355.
19. Seshaiah, C. and Thiagaraj, H. (2011). "A queueing network congestion model inhospitals". *European Journal of Scientific Research* 63: 419-427.
20. Shmueli, A., Sprung, C., and Kaplan, E. (2003). "Optimizing admissions to an intensive care unit". *Health Care Management Science* 6: 131-136.
21. Shonick, W. and Jackson, J.R. (1973). "An Improved Stochastic Model forOccupancy- Related Random Variables in General- Acute Hospital". *Operations Research* 21: 952-965.
22. Sissouras, A.A. and Moores, B. (1975). "The Optimum Number of Beds in a Coronary Care Uint". *Omega* 4: 59-65.
23. Weckwerth, V.E. (1966). "Determining Bed Needs from Occupancy and CensusFigures". *Hospital* 40: 52-54.
24. Wharton, F. (1996). "On The Risk Of Premature Transfer From Coronary Care Units". *Omega, Int.J. Mgmt. Sci*. 24: 413-423.
25. Young, J. P. (1962). "A Queueing Theory Approach to the control of Hospital Inpatient Census". *Ph.D. Dissertation, School of Engineering The Johns Hopkins University*, Baltimore.

https://doi.org/10.62500/icrtsda.1.1.50

Proc. 1st International Conference on Recent Trends in Statistics and Data Analytics
Air University Islamabad, Pakistan – May 9, 2024, Vol. 1, pp. 483-489

Examining the important factors of infant mortality in Pakistan

Maryam Sadiq[1*] and Sidra Younas[1]
[1]Department of Statistics, University of Azad Jammu and Kashmir, Muzaffarabad, Pakistan.

ABSTRACT

A high infant mortality rate is a symbol of a socially and economically deprived society. Different international reports show that Pakistan has an infant mortality rate of 51.5 per 1000 live births. Using a survival analysis approach, the present study contributed to the discourse of significant factors by studying the effect of potential socio-demographic determinants of infant mortality by using the data acquired from the Pakistan Demographic and Health Survey 2017-18. The hazard ratio is found to be significantly associated with the mother's educational level, income level, gender of child, preceding and succeeding birth intervals, total pregnancy outcomes, and size of child at birth. The observed significant factors highlighted the need to formulate appropriate strategies to enhance maternal education level and prevent low preceding and succeeding birth intervals to improve infant survival in Pakistan.

Keyword: Infant mortality, survival analysis, Pakistan.

1. INTRODUCTION

Infant mortality has been related to a diverse range of adverse health impacts and a low quality of life. This issue has remained a major health problem in low-income and lower-middle income countries, affecting their social and economic progress as well as the psychological and mental development of society. Different international reports show that Pakistan has an infant mortality rate of 51.5 per 1000 live births in 2023. The three successive Pakistan Demographic and Health Surveys declared a decreasing trend in infant mortality rate. In Pakistan, the rate of infant deaths has been reduced from 78 to 51.5 deaths per 1,000 live births during 2002-2018. Despite the fact that Pakistan has improved the infant survival rate, this issue still needs consideration to meet the Millennium Development Goal, defined as 31 deaths per 1000 live births. In under-developed countries with low quality of health care facilities and utilization, it is a hard task to easily achieve the goal of high infant survival. The policymakers and researchers concentrated on determining the significant factors of infant mortality to improve the quality of life and decrease the infant mortality rate. Several past studies examined the association of infant mortality with demographic, economic, socio-demographic, and other factors. Several recent researchers examined the effect of lifestyle (Foggin et al. 2001, Kandala et al. 2006), employment of health facilities (Atari and Mkandawire 2014), demographic and environmental determinants (Fatima-Tuz-Zahura et al. 2017), and socioeconomic variables (Folasade 2000), on infant mortality utilizing various statistical methods. Sadiq et al. (2022) used the Partial least squares spline modeling approach to that region of residence, age of mother at birth, wealth index, mother's occupation, domestic violence, mother's autonomy, cousin marriage are observed to be significant factors of infant mortality. Considering the lack of limited work on Pakistani children, this research is conducted to examine the important risk factors of infant mortality in Pakistan.

2. METHODS

2.1 ABOUT THE DATA

The dataset for analysis is obtained from Pakistan Demographic and Health Survey (PDHS) 2017-18. The survey provided comprehensive information about children regarding demographic, social, financial and health characteristics. Time and survival status are considered as an outcome variable with censoring time of 12 months. The sample of 310 infants with complete information and 7 potential explanatory variables including mother's educational level, income level of family, gender of child,

https://doi.org/10.62500/icrtsda.1.1.50

succeeding and preceding birth interval, total pregnancy outcomes, size of child at birth are considered for final analysis.

2.2. Statistical Analysis

The commonly used classical survival analysis techniques include the **Kaplan-Meier Curve** and the Cox proportional hazards (PH) regression (Kleinbaum and Klein 2006, Hosmer and Lemeshow 1999). Let $S(t)$ be the probability of survival of an individual up to and including time *t* and let T denotes the time of occurance of an event (death), then the probability that the time of event is greater than some time t is

$$S(t)=P(T>t)$$

where the survival times are always positive.

The **Kaplan-Meier Curve** is an estimator for S(t) which is given as

$$\hat{S}(t) = \prod_{t_i<t} 1 - \frac{d_i}{m_i}$$

Where m_i is the number of observations at risk at time t_i, and d_i is the number of samples who died at that time.

The Cox proportional hazards (PH) regression model is a traditional and general technique of classical survival time analysis which is employed to determine the association of explanatory variables with the survival by uncovering hazard quantities. The Cox model is mathematically written as

$$h(t, x, \beta) = h_o(t)\exp(\beta' x_i) \qquad (1)$$

Where $h_o(t)$ denotes the baseline hazard function at time t, β' is a vector of unknown parameters and x_i is a vector of covariates. The hazard ratio for a single independent binary variable is

$$HR(t) = \frac{h_1(t)}{h_o(t)} = e^{\beta_1}$$

The Cox regression model assumes that the hazards are proportional

The **hazard ratio** (e^{β_1}) remains constant over time *t* and fulfill the assumption. The βs are the regression coefficient estimates where β>0 indicates more risk (hazard) than reference and hence poor survival, and a β<0 denotess less risk than baseline and greater survival.

3. RESULTS

The Kaplan-Meier (KM) Curve is considered initially as a suitable semi-parametric method to evaluate the cumulative survival probabilities of covariates. Figure1 graphically represented the KM plot indicating infant survival probabilities for size of child at birth.

https://doi.org/10.62500/icrtsda.1.1.50

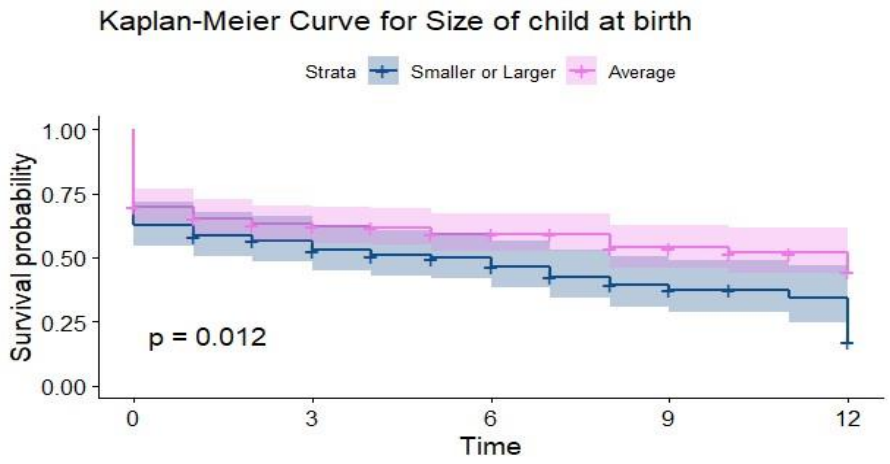

Fig1: The Kaplan-Meier curve for estimating survival probability for size of child at birth.

The Fig1 indicated that the size of child at the time of birth is a significant factor of infant mortality with higher survival probability for infant having average size at the time of birth compared to larger and smaller size. The graphical display highlighted the highest mortality rate for infants having smaller or larger size at the time of 12 months.

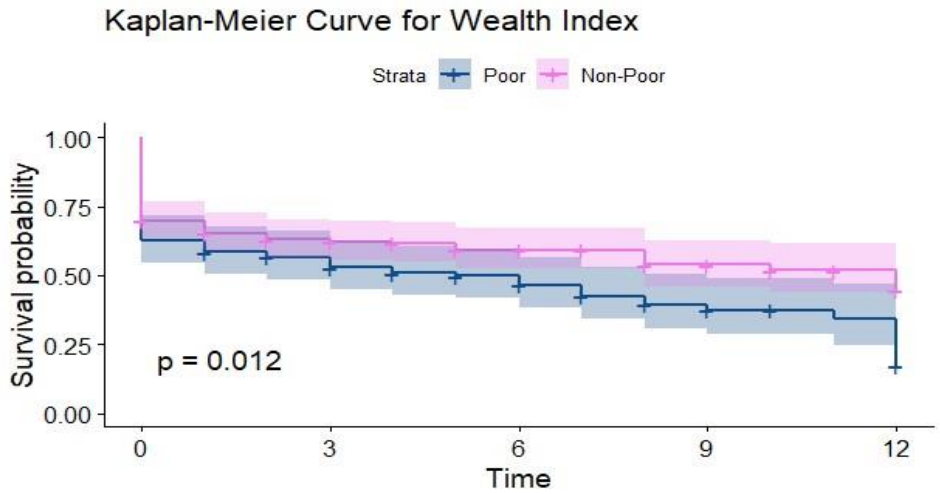

Fig2: The Kaplan-Meier curve for estimating survival probability for wealth index of child's family.

Fig2 is a visual display of the KM plot indicating infant survival probabilities for the income level of a child's family. The plot showed that family income is a significant determinant of infant survival with lower survival probability for infants belonging to poor families compared to middle income and rich families.

Fig3 represented the KM plot indicating a significant association between infant survival and the education level of the mother. The plot showed that infants belonging to literate mothers have a higher survival probability compared to infants belonging to illiterate mothers. This survival probability for newborns of illiterate mothers is further reduced by attaining the age of 12 months.

https://doi.org/10.62500/icrtsda.1.1.50

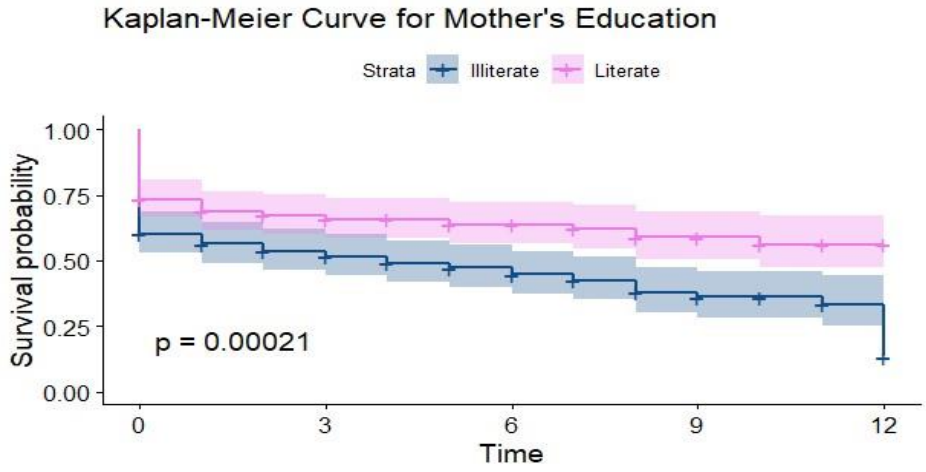

Fig3: The Kaplan-Meier curve for estimating survival probability for mother's education level.

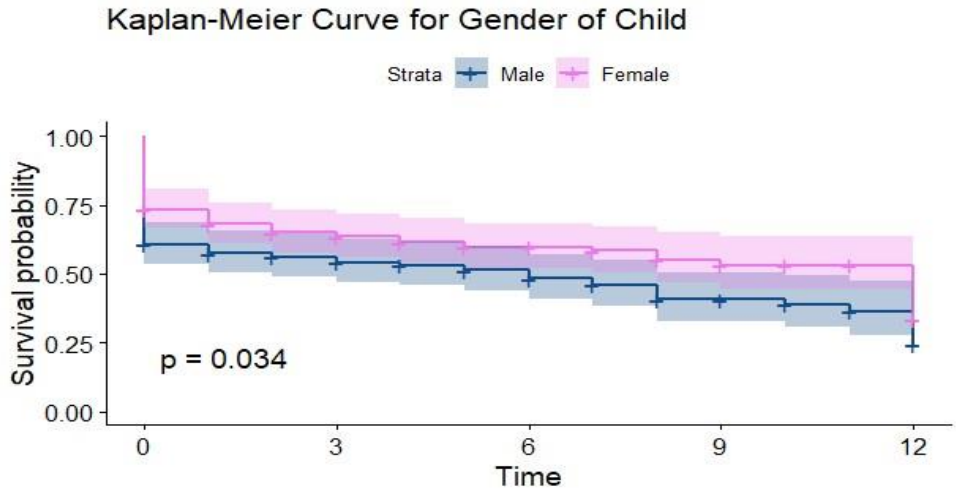

Fig4: The Kaplan-Meier curve for estimating survival probability for gender of child.

The visual display of the KM plot in Fig4 indicated significant relationship of gender of infants with mortality, showing a higher survival probability of female newborns compared to males.

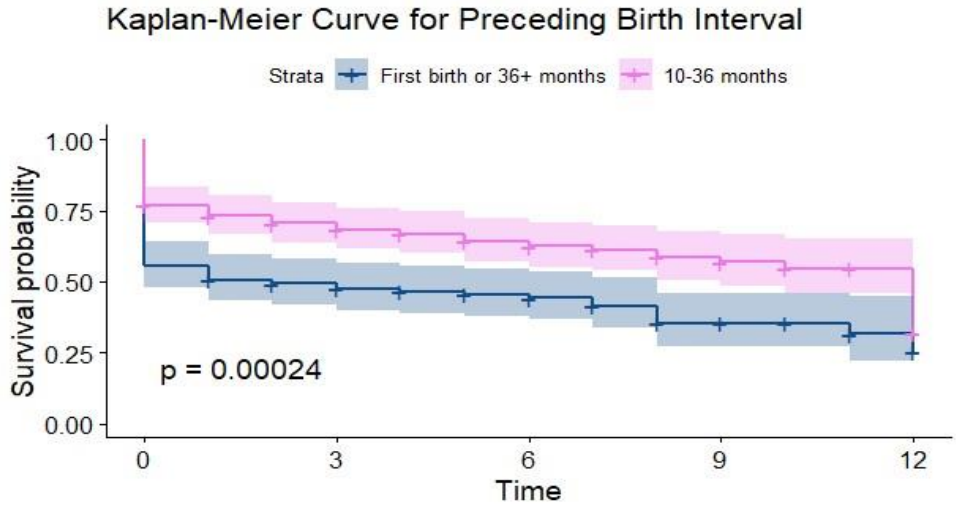

Fig5: The Kaplan-Meier curve for estimating survival probability for preceding birth interval of child.

https://doi.org/10.62500/icrtsda.1.1.50

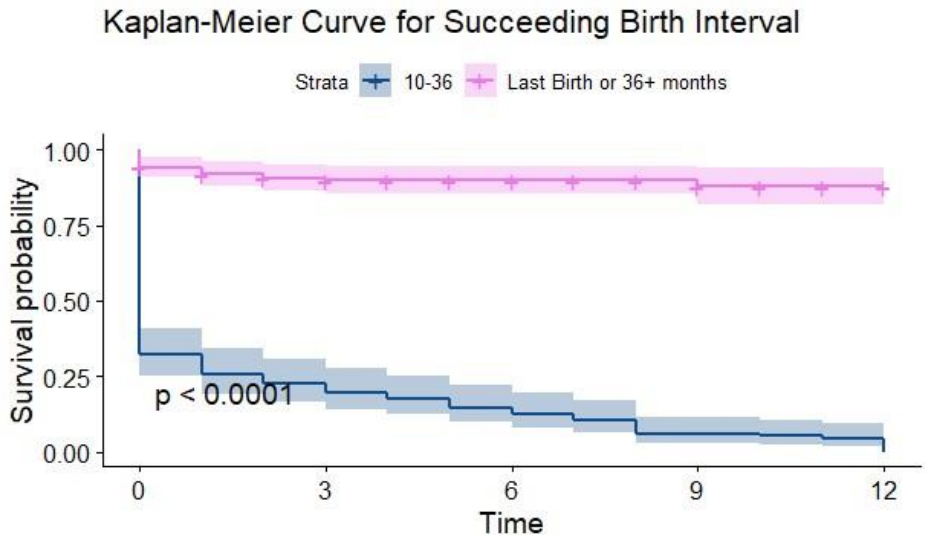

Fig6:The Kaplan-Meier curve for estimating survival probability for succeeding birth interval of child.
Figure 5 represented the KM plot showing the strong effect of the preceding birth interval on infant survival. Contrary to literature, the plot indicated that infants having 10-36 months preceding birth interval have a higher survival probability compared to infants having a preceding birth interval of more than 36 months or first birth.
The association between succeeding birth interval and infant mortality is presented in Fig6. The KM curve indicated that infants with 10-36 months succeeding birth interval have the least survival probability compared to infants with more than 36 months succeeding birth interval or last birth. Interestingly, the plot showed a much higher survival probability for larger birth intervals.

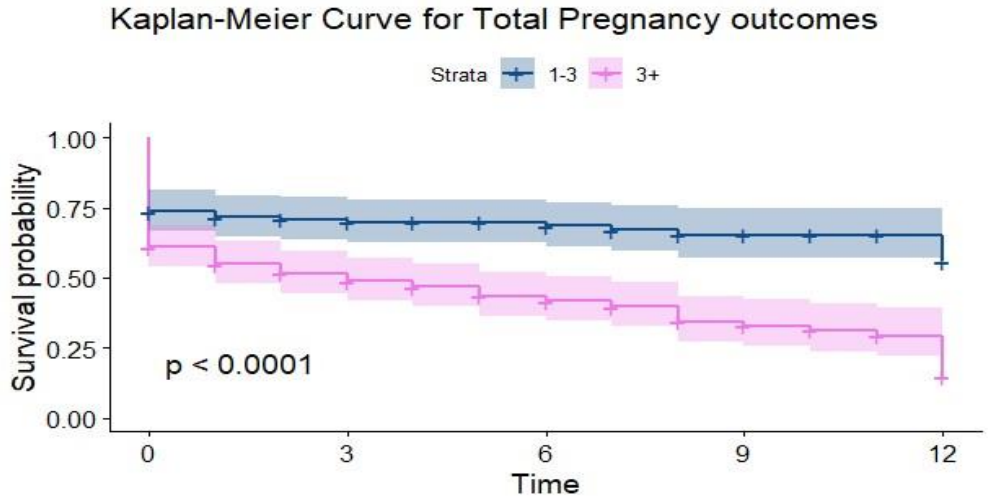

Fig7: The Kaplan-Meier curve for estimating survival probability for total pregnancy outcomes of child's mother.
Figure 7 indicated that the total pregnancy outcome is a significant factor of infant mortality with higher survival probability for infants whose mothers have 1-3 pregnancy outcomes ever compared to infants whose mothers have more pregnancy outcomes.

Finally, the Cox regression model is executed as a semi-parametric model after fulfilling the assumptions of proportional hazard, independence, linearity, no multicollinearity, and no outliers.

https://doi.org/10.62500/icrtsda.1.1.50

Table1: The Hazard ratios for infant survival in Pakistan using a proportional hazards Cox regression model.

Variables	Hazard ratio	p-value	95 % CI
Mother's age	**0.83**	**0.04**	**0.67-1.02**
Mother's Educational level	**0.68**	**0.01**	**1.08- 1.72**
Wealth index	**0.74**	**0.07**	**0.53- 1.02**
Gender of child	**1.30**	**0.01**	**1.13 -1.99**
Preceding birth interval	**1.44**	**0.02**	**1.02 -2.59**
Succeeding Birth interval	**1.72**	**0.01**	**1.26 -2.36**
Size of child at birth	**1.64**	**0.03**	**1.04 -2.59**
Total Pregnancy Outcomes	**0.68**	**0.01**	**1.08- 1.72**

Table1 showed the hazard ratios, probability values and 95% confidence interval (CI) for considered explanatory variables. The results showed that mother's educational level, income level of family, gender of child, succeeding and preceding birth intervals, total pregnancy outcomes, and size of child at birth are related to infant survival. The analysis further showed that educated mothers have a nearly 20% increased survival probability compared to uneducated mothers. The infants belonging to poor families have a nearly 30% increased hazard compared to non-poor families. Female infants have an approximately 30% reduction in mortality hazard compared to male infants. Infants with 10-36 months preceding birth interval are 1.3 times more likely to die compared to infants with 36+ months preceding birth interval or first birth. Infants with 10-36 months preceding birth interval are 1.4 times more likely to die compared to infants with 36+ months preceding birth interval or last birth. The infants having non-average birth weight are 1.72 times more likely to die compared to infants with average birth weight. The infants whose mothers have 3+ pregnancy outcomes are 1.64 times more likely to die compared to infants whose mothers have 1-3 pregnancy outcomes.

6. CONCLUSION AND RECOMMENDATIONS

The current study uses the Kaplan-Meier and the Cox model to determine the important socio-demographic variables of newborn mortality. The study reported that mother's educational level, income level of family, gender of child, succeeding and preceding birth intervals, total pregnancy outcomes, and size of child at birth are significant determinants of infant survival. The study further suggested that other diverse factors related to environment, geographic variations, biomedical, and socioeconomic might be observed to further inspect infant mortality for optimizing the quality of life. More efficient statistical approaches with modern data gathering approaches concerning infant survival must be considered in the future.

REFERENCES

NIPS, I. Pakistan demographic and health survey 2017-18, Islamabad.[online].

Foggin, P., Armijo-Hussein,N., Marigaux,C., Zhu,H. and Liu,z.(2001). *Risk factors and child mortality among the Miao in Yunnan, Southwest China*, Social Science and Medicine, 53, 1683–1696.

Atari,D.O. and Mkandawire,P. (2014). *Spatial variation of management of childhood diarrhea in Malawi*, Health and place, 29, 84–94.

Folasade,I.B. (2000). *Environmental factors, situation of women and child mortality in Southwestern Nigeria*, Social Science and Medicine, 51,1473–1489.

https://doi.org/10.62500/icrtsda.1.1.50

Kandala,N.B., Magadi,M.A., Madise,N.J. (2006). *An investigation of district spatial variations of childhood diarrhoea and fever morbidity in Malawi*, Social Science and Medicine 62, 1138–1152.

Sadiq,M., Alnagar,D.K.F., Abdulrahman,A.T. and Alharbi,R. (2022). *The partial least squares spline model for public health surveillance data*. Computational and Mathematical Methods in Medicine.

Fatima-Tuz-Zahura,M., Mohammad,K.A., Bari,W. (2017). *Log-logistic proportional odds model for analyzing infant mortality in bangladesh*. Asia Pacific Journal of Public Health.

Kleinbaum,D.G. and Klein,M. (2006). *Survival analysis: a self-learning text*. Springer Science and Business Media.

Hosmer Jr,D.W. and Lemeshow,S. (1999). *Applied survival analysis: Regression modelling of time to event data*.

https://doi.org/10.62500/icrtsda.1.1.51

Proc. 1st International Conference on Recent Trends in Statistics and Data Analytics
Air University Islamabad, Pakistan – May 9, 2024, Vol. 1, pp. 490-504

SOME WEIGHTED INEQUALITIES FOR HOUSDORFF OPERATORS AND COMMUTATORS ON MORREY HERZ SPACE

AMNA AJAIB1, ALINA WASIF2, MALAIKA ZAHID3, and RABAILRAHMAN4
2DEPARTMENT OF MATHEMATICS, FAZAIA BILQUIS COLLEGE OF EDUCATION FOR WOMEN PAF BASE NUR KHAN, PAKISTAN

Abstract.

This research explores the boundedness of Hausdorff operators in weighted central Morrey spaces, enhancing understanding of these spaces and their interaction with operator theory, providing sharp bounds for powerweighted central Morrey spaces.The n-dimensional Hausdorff operator can be expressed as follows

$$H_{(\psi,A)}f(x) = \int_{\mathbb{R}^n} \frac{\psi(y)}{|y|^n} f(A(y)x)\, dy$$

Further, our paper investigates Hausdorff operators and symbol functions in weighted spaces, enhancing understanding of operators and commutators in function spaces with different weightings and structures.

1. Introduction

In recent times, significant interest has been directed toward the Hausdorff operator, largely attributable to the groundbreaking research conducted by Liflyand and M´oricz, as documented in [14]. In their paper, the focus was on the one-dimensional Hausdorff operator [1].

$$H_\psi f(x) = \int_0^\infty \frac{\psi(t)}{t}\ f(x)\, dt$$

where ψ is a locally integrable function on the positive half-line. The Hausdorff operator, through its kernel function ψ, establishes connections with several classical operators in analysis. These include the Cesaro operator, Hardy–Littlewood–Polya operator, Riemann–Liouville fractional integral operator, and Hardy–Littlewood average operator[11].

Brown and Moricz, along with Lerner and Liflyand, independently extended the Hausdorff operator to high-dimensional spaces by considering a locally integrable function ψ on R^n.

In the field of harmonic analysis, exploring weighted inequalities for Hausdorff commutators and operators within Morrey-Herz spaces is a significant and intricate area of research. These weighted inequalities offer a nuanced understanding of how

---

1

[1,2,3,4]Department of Mathematics, Fazaia Bilquis College of Education for Women,PAF Nur Khan
Corresponding Author: dr.amnaajaib@gmail.com
alinawasif2002@gmail.com malaikazahid02@gmail.com
rehmanrabail12345@gmail.com

Key words and phrases. Housdorff operator, Commutators, central space,central-BMO functions, wighted central Morrey spaces,sharp bounds.

weight functions influence the behavior of Hausdorff operators within Morrey-Herz spaces.

Morrey spaces, which are generalizations of Lebesgue spaces, provide a broad framework for analyzing functions with locally controlled growth. When combined with Herz spaces, which capture oscillatory behavior, this union offers fertile ground for investigating how Hausdorff operators behave under various weightings. The ndimensional Hausdorff operator[1] can be expressed as follows

https://doi.org/10.62500/icrtsda.1.1.51

$$H_{(\psi,A)}f(x) = \int_{\mathbb{R}^n} \frac{\psi(y)}{|y|^n} f(A(y)x)\,dy$$

where A(y) is an n × n matrix satisfying non-singularity conditions almost everywhere in the support of a fixed integrable function ψ.

This research helps us understand the examination of traditional operators such as the Cesaro and Hardy–Littlewood–Polya operators, expanding their utility and understanding within a wider framework. Additionally, the exploration of weighted inequalities for Hausdorff commutators and operators on Morrey-Herz spaces not only enhances the theoretical comprehension of these mathematical concepts but also discovers practical applications across various fields like signal processing, image analysis, and partial differential equations.

In this complex domain, the extension of the Hausdorff operator to higher dimensional spaces,adds an extra layer of complexity to the analysis. As we delve into the specifics of weighted inequalities, the interplay between the Hausdorff operators and the weight functions will unfold, revealing profound implications for the broader landscape of harmonic analysis within Morrey-Herz spaces.The Hausdorff operator associated to the kernel function ψ is then defined by

$$H_\Omega(A,f)(x) = \int_{\mathbb{R}^n} \Omega(t)|t|^n \prod_{i=1}^{m} f_i(A_i(t)x)\,dt \quad \text{where } x \in \mathrm{R}^n.$$

where $\Omega : \mathrm{R}^n \to [0,\infty)$, and $A_i(t)$, for $i = 1,\ldots,m$, are $n \times n$ is an invertible matrices for almost every t in the support of Ω. Additionally, $f_1,f_2,\ldots,f_m : \mathrm{R}^n \to \mathrm{C}$ are measurable functions.

Our main result can be stated as:

Theorem 1.1. *Let* $1 \le q_1,q_2 < \infty$, $\lambda < 0$. *Suppose that* $w \in A_1$ *with the critical index* r_w *for the reverse H¨older condition, and assume that* $q_1 > \frac{q_2 r_w}{r_w - 1}$ *Then for any* $1 < \delta < r_w$, *we have*

$$\|H\psi,Af\|M^{\cdot}_{q_2,\lambda}(\mathrm{R}n;w) \preceq G1\|f\|M^{\cdot}_{q_1,\lambda}(\mathrm{R}n;w),$$

where $H_{\psi,A}$ *is a certain operator,* δ *is a parameter, and* G_1 *is a constant.*

$$G_1 = \left(\int_{\mathbb{R}^n} \frac{\psi(y)}{|y|^n} \|A(y)\|_{M^{p,\lambda}}\,dy\right) + \left(\int_{\mathbb{R}^n} \frac{\psi(y)}{|y|^n} \|A(y)\|_{M^{p,\lambda}} \|A(y)\|^{\delta}_{H^q}\,dy\right).$$

Theorem 1.2. *For* $1 \le q < \infty$, $-\frac{1}{q} \le \lambda < 0$, *and* $0 < \alpha < \infty$, *the expression is given by:*

For $0 < \alpha < \infty$, *the inequality is given by:*

$$\|\mathrm{H}\psi,Af\|M^{\cdot}_{q,\lambda}(\mathrm{R}n;v) \preceq G2\|f\|M^{\cdot}_{q,\lambda}(\mathrm{R}n,v).$$

where,

$$G_2 = \int_{\mathbb{R}^n} \frac{\psi(y)}{|y|^n} \left|\det A^{-1}(y)\right|^{1/q} \|A(y)^{-1}\|^{(n+\alpha)(\lambda+1/q)}_{M^{p',\lambda'}} \|A^{-1}(y)\|^{\alpha/q}_{H^q}\,dy.$$

- *If* $-n < \alpha \le 0$, *then the inequality is given by:*

https://doi.org/10.62500/icrtsda.1.1.51

$\|HA,f\|Mq,\lambda(Rn;v) \preceq G3\|f\|Mq,\lambda(Rn,v)$, *where* G_3 *is*

defined as

$$G_3 = \int_{\mathbb{R}^n} \frac{\psi(y)}{|y|^n} \left|\det A^{-1}(y)\right|^{1/q} \|A(y)^{-1}\|_{M^{p',\lambda'}}^{n(\lambda+1/q)+\alpha\lambda} dy.$$

Theorem 1.3. *Let* $1 \le q < \infty$, $-\frac{1}{q} \le \lambda < 0$, $-n < \alpha < \infty$, *and* ψ *be a non negative function. Suppose that there is a constant C independent of y such that* $|\det A^{-1}(y)| \le C|\det A(y)|^{-1}$ *for all* $y \in supp(\psi)$. *Then,* $H_{\psi,A}$ *is bounded on* $Mq,\lambda(\mathrm{R}^n;v)$ *if and only if*

$$G_4 = \int_{\mathbb{R}^n} \frac{\psi(y)}{|y|^n} \|A(y)\|_{M^{p,\lambda}}^{(n+\alpha)\lambda} dy < \infty.$$

Theorem 1.4. *Let* $1 \le q < \infty$, $1 \le s < q_1 < \infty$, $\frac{1}{s} = \frac{1}{q_1} + \frac{1}{q_2}$, *and* $\lambda < 0$. *Suppose that w* $\in A_1$ *with the critical index* r_w *for the reverse Ho¨lder condition, and suppose that* $s > \frac{qr_w}{r_w - 1}$. *Then for any* $1 < \delta < r_w$,

$$\|H\psi,Abf\|M\dot{}\ q,\lambda(\mathrm{R}n;w) \preceq G5\|b\|CMO\dot{}q2(\mathrm{R}n,w)\|f\|M\dot{}\ q1,\lambda(\mathrm{R}n,w),$$

$$G_5 = \int_{\|A(y)\|<1} \frac{|\psi(y)|\|A(y)^{-1}\|^{1/q_1}}{|y|^n \|A(y)\|^{-n\lambda - n/q_1}} \left(1 + \frac{\det A^{-1}(y)|^{1/q_2}}{\|A(y)\|^{-n/q_1}}\right) \log \frac{2}{\|A(y)\|} dy$$
$$+ \int_{\|A(y)\|\ge 1} \frac{|\psi(y)|\|A(y)^{-1}\|^{1/q_1}}{|y|^n \|A(y)\|^{-n/q_1 - n\delta(\delta-1)/\delta}} \left(1 + \frac{\det A^{-1}(y)|^{1/q_2}}{\|A(y)\|^{-n/q_1}}\right) \log \frac{2}{\|A(y)\|} dy.$$

Theorem 1.5. *Let* $1 \le q < q_1 < \infty$, $\frac{1}{q} = \frac{1}{q_1} + \frac{1}{q_2}$, $-\frac{1}{q} \le \lambda < 0$. *Then:*

(1) *If* $0 < \alpha < \infty$,

$$\|H\psi,Ab \quad f\|M\dot{}\ q,\lambda(\mathrm{R}n;v) \preceq G6\|b\|CMO\dot{}\ q2\ (\mathrm{R}n,v)\|f\|M\dot{}$$

$q1,\lambda(\mathrm{R}n,v)$, *where*

$$G_6 = \int_{\mathbb{R}^n} \frac{|\psi(y)||\det A^{-1}(y)|^{1/q_1}\|A(y)^{-1}\|^{\alpha/q_1}}{|y|^n \|\det A(y)\|^{-(n+\alpha)(\lambda+1/q_1)}} \left(1 + \frac{|\det A^{-1}(y)|^{1/q_2}\|A^{-1}(y)\|^{\alpha/q_2}}{\|A(y)\|^{(-n+\alpha)/2}}\right)$$
$$\times \left(\frac{\log 2}{\|A(y)\|}\zeta_{\{\|A(y)\|<1\}} + \log 2\|A(y)\|\zeta_{\|A(y)\|\ge 1}\right) dy.$$

(a) *If* $-n < \alpha \le \infty$

$$\|H\psi,Ab \quad f\|M\dot{}\ q,\lambda(\mathrm{R}n;v) \preceq G7\|b\|CMO\dot{}\ q2\ (\mathrm{R}n,v)\|f\|M\dot{}$$

$q1,\lambda(\mathrm{R}n,v)$, *where,*

$$G_7 = \int_{\mathbb{R}^n} \frac{|\psi(y)||\det A^{-1}(y)|^{1/q_1}}{|y|^n \|\det A(y)\|^{-(n+\alpha)(\lambda+1/q_1)}} \left(1 + \frac{|\det A^{-1}(y)|^{1/q_2}}{\|A(y)\|^{(-n/q_2)}}\right.$$
$$\left.\times \left(\frac{\log 2}{\|A(y)\|}\zeta_{\{\|A(y)\|<1\}} + \log 2\|A(y)\|\zeta_{\|A(y)\|\ge 1}\right) dy.\right. \quad !$$

The operators $H_{\psi,A}{}^{b,1}$ *and* $H_{\psi,A}{}^{b,2}$ *are defined as follows:*

https://doi.org/10.62500/icrtsda.1.1.51

$$H^{b,1}_{\psi,A} f = \int_{\|A(y)\|<1} \frac{\psi(y)|}{|y|^n} (b(x) - b(A(y)x)) f(A(y)x)\, dy,$$

$$H^{b,2}_{\psi,A} f = \int_{\|A(y)\|\geq 1} \frac{\psi(y)|}{|y|^n} (b(x) - b(A(y)x)) f(A(y)x)\, dy.$$

Theorem 1.6. *Let* $1 < q < q_1 < \infty$, $\frac{1}{q} = \frac{1}{q_1} + \frac{1}{q_2}$, $-\frac{1}{q} < \lambda < 0$, *and* ψ *be a nonnegative function. Suppose that there is a positive constant C independent of y such that* $|\det A^{-1}(y)| \leq C|\det A(y)|^{-1}$ *for all* $y \in supp(\psi)$, *In addition, if* $\frac{\psi(y)}{|y|^n}$ *is integrable, then:*

(1) $H^{b,1}_{\psi,A}$ *is bounded from* $Mq^{\cdot}{}_{1},\lambda(\mathrm{R}^n;v)$ *to* $Mq,\lambda^{\cdot}$ $(\mathrm{R}^n;v)$ *if and only if*

$$G_8 = \int_{\|A(y)\|<1} \frac{\psi(y)}{|y|^n} \|A(y)\|^{(n+\alpha)\lambda}_{M^{p,\lambda}} \log 2|\det A(y)|\, dy < \infty.$$

(2) $H^{b,2}_{\psi,A}$ *is bounded from* $Mq^{\cdot}{}_{1},\lambda(\mathrm{R}^n;v)$ *to* $Mq,\lambda^{\cdot}$ $(\mathrm{R}^n;v)$ *if and only if*

$$G_9 = \int_{\|A(y)\|<1} \frac{\psi(y)}{|y|^n} \|A(y)\|^{(n+\alpha)\lambda}_{M^{p,\lambda}} \log 2\|A(y)\|\, dy < \infty.$$

THE THEOREMS LISTED BELOW ARE DOCUMENTED IN [1]

Theorem 1.7. *Let* $1 \leq q_1, q_2 < \infty$, $\lambda < 0$. *Suppose that* $w \in A_1$ *with the critical index* r_w *for the reverse H¨older condition, and assume that* $q_1 > \frac{q_2 r_w}{r_w - 1}$ *Then for any* $1 < \delta < r_w$, *we have*

$$\|H\Phi,Af\|M^{\cdot}\, q_2,\lambda(\mathrm{R}n;w) \preceq G1\|f\|M^{\cdot}\, q_1,\lambda(\mathrm{R}n;w),$$

where $H_{\Phi,A}$ *is a certain operator,* δ *is a parameter, and* G_1 *is a constant.*

$$G_1 = \left(\int_{\{|A(y)|<1\}} \frac{|\Phi(y)|}{|y|^n} |\det A^{-1}(y)|^{1/q_1} \|A(y)\|^{\lambda + n/q_1}\, dy \right.$$

$$+ \left. \int_{\{|A(y)|\geq 1\}} \frac{|\Phi(y)|}{|y|^n} |\det A^{-1}(y)|^{1/q_1} \|A(y)\|^{n/q_1 + n\lambda(\delta-1)/\delta}\, dy \right).$$

Theorem 1.8. *For* $1 \leq q < \infty$, $-\frac{1}{q} \leq \lambda < 0$, *and* $0 < \alpha < \infty$, *the expression is given by:*

For $0 < \alpha < \infty$, *the inequality is given by:*

$$\|\mathrm{H}\Phi,Af\|M^{\cdot}\, q,\lambda(\mathrm{R}n;v) \preceq G2\|f\|M^{\cdot}\, q,\lambda(\mathrm{R}n,v).$$

where,

$$G_2 = \int_{\mathbb{R}^n} \frac{\Phi(y)}{|y|^n} \left|detA^{-1}(y)\right|^{1/q} \|A(y)^{-1}\|^{(n+\alpha)(\lambda+1/q)} \|A^{-1}(y)\|^{\alpha/q}\, dy.$$

• *If* $-n < \alpha \leq 0$, *then the inequality is given by:*

$$\|\mathrm{H}A,f\|Mq,\lambda(Rn;v) \leq G3\|f\|Mq,\lambda(Rn,v),\ \textit{where } G_3 \textit{ is}$$

defined as

$$G_3 = \int_{\mathbb{R}^n} \frac{\Phi(y)}{|y|^n} \left|detA^{-1}(y)\right|^{1/q} \|A(y)^{-1}\|^{n(\lambda+1/q)+\alpha\lambda} dy.$$

https://doi.org/10.62500/icrtsda.1.1.51

Theorem 1.9. *Let* $1 \le q < \infty$, $-\frac{1}{q} \le \lambda < 0$, $-n < \alpha < \infty$, *and* Φ *be a non negative function. Suppose that there is a constant* C *independent of* y *such that* $|\det A^{-1}(y)| \le C|\det A(y)|^{-1}$ *for all* $y \in supp(\Phi)$. *Then,* $H_{\Phi,A}$ *is bounded on* $M_{q,\lambda}(\mathrm{R}^n;v)$ *if and only if*

$$G_4 = \int_{\mathbb{R}^n} \frac{\Phi(y)}{|y|^n} \|A(y)\|^{(n+\alpha)\lambda}\, dy < \infty.$$

Theorem 1.10. *Let* $1 \le q < \infty$, $1 \le s < q_1 < \infty$, $\frac{1}{s} = \frac{1}{q_1} + \frac{1}{q_2}$, *and* $\lambda < 0$. *Suppose that* $w \in A_1$ *with the critical index* r_w *for the reverse Hölder condition, and suppose that* $s > \frac{qr_w}{r_w - 1}$. *Then for any* $1 < \delta < r_w$,

$$\|\mathcal{H}^b_{\Phi,A} f\|_{\dot{M}^{q,\lambda}(\mathbb{R}^n;w)} \preceq G_5 \|b\|_{C\dot{M}O^{q_2}(\mathbb{R}^n,w)} \|f\|_{\dot{M}^{q_1,\lambda}(\mathbb{R}^n,w)},$$

Theorem 1.11. *Let* $1 \le q < q_1 < \infty$, $\frac{1}{q} = \frac{1}{q_1} + \frac{1}{q_2}$, $-\frac{1}{q} \le \lambda < 0$. *Then:*

(1) *If* $0 < \alpha < \infty$,

$$\|\mathcal{H}^b_{\Phi,A} f\|_{\dot{M}^{q,\lambda}}(\mathbb{R}^n;\nu) \le G_6 \|b\|_{C\dot{M}O^{q_2}}(\mathbb{R}^n,\nu) \|f\|_{\dot{M}^{q_1,\lambda}}(\mathbb{R}^n,\nu),$$

where

$$G_6 = \int_{\mathbb{R}^n} \frac{|\Phi(y)||\det A^{-1}(y)|^{1/q_1} \|A(y)^{-1}\|^{\frac{\alpha}{q_1}}}{|y|^n \|\det A(y)\|^{-(n+\alpha)(\lambda+1/q_1)}} \left(1 + \frac{|\det A^{-1}(y)|^{1/q_2} \left\|A^{-1}(y)\right\|^{\alpha/q_2}}{\|A(y)\|^{(}-n+)/2}\right.$$
$$\left. \times \left(\frac{\log 2}{\|A(y)\|}\zeta_{\{\|A(y)\|<1\}} + \log 2\|A(y)\|\zeta_{\|A(y)\|\ge 1}\right) dy.\right.$$

(a) *If* $-n < \alpha \le \infty$

$$\|\mathrm{H}\Phi b, Af\|_{M^{\cdot}\, q,\lambda}(\mathrm{R}n;v) \le G7\|b\|_{CMO^{\cdot}\, q2}\,(\mathrm{R}n,v)\|f\|_{M^{\cdot}\, q1,\lambda}(\mathrm{R}n,v),$$

$$G_5 = \int_{\|A(y)\|<1} \frac{|\Phi(y)|\|A(y)^{-1}\|^{1/q_1}}{|y|^n \|A(y)\|^{-n\lambda - n/q_1}} \left(1 + \frac{\det A^{-1}(y)|^{1/q_2}}{\|A(y)\|^{-n/q_1}}\right) \log \frac{2}{\|A(y)\|}\, dy$$
$$+ \int_{\|A(y)\|<1} \frac{|\Phi(y)|\|A(y)^{-1}\|}{|y|^n \|A(y)\|^{-n/q_1 - n}}$$

where,

$$G_7 = \int_{\mathbb{R}^n} \frac{|\Phi(y)||\det A^{-1}(y)|^{1/q_1}}{|y|^n \|\det A(y)\|^{-(n+\alpha)(\lambda+1/q_1)}} \left(1 + \frac{|\det A^{-1}(y)|^{1/q_2}}{\|A(y)\|^{(-n/q_2)}}\right.$$
$$\left. \times \left(\frac{\log 2}{\|A(y)\|}\zeta_{\{\|A(y)\|<1\}} + \log 2\|A(y)\|\zeta_{\|A(y)\|\ge 1}\right) dy.\right.$$

The operators $H_{b,1,\Phi,A}$ *and* $H_{b,2,\Phi,A}$ *are defined as follows:*

$$H^{b,1}_{\Phi,A} f = \int_{\|A(y)\|<1} \frac{\Phi(y)|}{|y|^n} (b(x) - b(A(y)x))\, f(A(y)x)\, dy,$$
$$H^{b,2}_{\Phi,A} f = \int_{\|A(y)\|\ge 1} \frac{\Phi(y)|}{|y|^n} (b(x) - b(A(y)x))\, f(A(y)x)\, dy.$$

Theorem 1.12. *Let* $1 < q < q_1 < \infty$, $\frac{1}{q} = \frac{1}{q_1} + \frac{1}{q_2}$, $-\frac{1}{q} < \lambda < 0$, *and* Φ *be a nonnegative function. Suppose that there is a positive constant* C *independent of* y *such that* $|\det A^{-1}(y)| \le C|\det A(y)|^{-1}$ *for all* $y \in supp(\Phi)$, *In addition, if* $\frac{\Phi(y)}{|y|^n}$ *is integrable, then:*

https://doi.org/10.62500/icrtsda.1.1.51

(1) $H^{b,1}_{\Phi,A}$ *is bounded from* $Mq^{\cdot}{}_{1},\lambda(\mathrm{R}^n;v)$ *to* $Mq,\lambda^{\cdot}$ $(\mathrm{R}^n;v)$ *if and only if*

$$G_8 = \int_{\|A(y)\|<1} \frac{\Phi(y)}{|y|^n} |||A(y)\|^{(n+\alpha)\lambda} \log 2|\det A(y)|\, dy < \infty .$$

(2) $H^{b,2}_{\Phi,A}$ *is bounded from* $Mq^{\cdot}{}_{1},\lambda(\mathrm{R}^n;v)$ *to* $Mq,\lambda^{\cdot}$ $(\mathrm{R}^n;v)$ *if and only if*

$$G_9 = \int_{\|A(y)\|<1} \frac{\Phi(y)}{|y|^n} |||A(y)\|^{(n+\alpha)\lambda} \log 2\|A(y)|||\, dy < \infty .$$

2. Preliminaries

Let us denote $B(x,r)$*, the ball in* R^n *centered at x with radius r, by B. Moreover,* $|B|$ *denotes the Lebesgue measure of B. In 1938, the local behavior of solutions to certain kind of PDE's was estimated by Morrey , he introduced a new function space, what is called Morrey space. In* [2]*, the Morrey space* $M^{q,\lambda}(\mathrm{R}^n)$ *was defined as the set of locally integrable functions f satisfying.*

$$\|f\|_{M^{q,\lambda}(\mathbb{R}^n)} = \sup_B \left(\frac{1}{|B|^{1+\lambda q}} \int_B |f(x)|^q dx \right)^{1/q} < \infty ,$$

with $1 \le q < \infty$ *and* $-1/p < \lambda < 0$*. The authors in recently introduced the central Morrey space* $M^{\cdot\, q,\lambda}(\mathrm{R}^n)$ *which, for* $-1/p < \lambda < 0$*, can be defined by*

$$\|f\|_{\dot{M}^{q,\lambda}(\mathbb{R}^n)} = \sup_{R>0} \left(\frac{1}{|B(0,R)|^{1+\lambda q}} \int_{B(0,R)} |f(x)|^q dx \right)^{1/q} < \infty .$$

On the other hand, function spaces with weighted norms also play a vital role in many branches of mathematical analysis. The theory of A_p *weights started in 1972 with Muckenhoupt work and was modified by several mathematicians . A weight is a nonnegative, locally integrable function on* R^n*.And we denote by* $\omega(B)$ *the weighted measure of B, i.e* $\omega(B) = {}^{\mathrm{R}}{}_B\, \omega(x)dx$*, and by* p' *the conjugate index of p, satisfying* $1/p + 1/p' = 1$*. We say that* $\omega \in A_p$*,* $1 < p < \infty$*, if for every ball B there exist a constant C such that*

$$\left(\frac{1}{|B|} \int_B \omega(x)dx \right) \left(\frac{1}{|B|} \int_B \omega(x)^{-1/(p-1)} dx \right)^{p-1} \le C.$$

We say that $\omega \in A_1$*, if for every ball B there exist a constant C such that*

$$\left(\frac{1}{|B|} \int_B \omega(x)dx \right) \le C \operatorname*{ess\,inf}_{x\in B} \omega(x) .$$

For $p = \infty$*, we define* $A_\infty = {}^{\mathrm{S}}{}_{1\le p<\infty} A_p$*. Furthermore,* $A_p \subset A_q$ *for all* $p < q$ *and for* $1 < p < \infty$*, if* $\omega \in A_p$ *then* $w \in A_s$ *for some* $1 < s < p$*.*

The history of Morrey-Herz spaces involves the evolution and integration of ideas from several areas of mathematical analysis, including Morrey spaces, Herz spaces, and harmonic analysis.Morrey spaces were introduced by Charles B. Morrey Jr. in the 1950s as a generalization of Sobolev spaces. Morrey's work focused on studying the local behavior of functions, particularly in the context of elliptic and parabolic partial differential equations.Herz spaces, also known as Herz-Sobolev spaces, were introduced by Friedrich Ernst Peter Herz in the 1960s. Herz's work extended the classical Sobolev spaces by incorporating oscillatory behavior of functions. Herz spaces are important in the study of singular integral operators and oscillatory integrals.

The integration of ideas from Morrey spaces and Herz spaces led to the development of Morrey-Herz spaces. These spaces combine the local regularity properties of Morrey

https://doi.org/10.62500/icrtsda.1.1.51

spaces with the oscillatory behavior captured by Herz spaces.Morrey-Herz spaces have found applications in diverse areas of analysis, including the study of partial differential equations, singular integral operators, and Fourier analysis on locally compact groups.

3. Proof of the main results

In this section we shall prove the main result stated in section one. However, we need some useful propositions for this purpose.

Proposition 3.1. *(*[1]*) Let f be a nonnegative locally integrable function. If w* ∈ A_p*, where p* ≥ 1

$$\frac{1}{|B(x_0,R)|}\int_{B(x_0,R)} f(x)\,dx \le C\left(\frac{1}{w(B(x_0,R))}\int_{B(x_0,R)} f^p(x)w(x)\,dx\right)^{1/p}.$$

Let w be a weight function on R^n*. For any measurable set E* ⊂ R^n*, the weighted Lebesgue space* $L^p(E;w)$ *is defined as*

$$\|f\|_{L^p(E;w)} = \left(\int_E |f(x)|^p w(x)\,dx\right)^{1/p} < \infty.$$

Proposition 3.2. [28, 29] *Let w* ∈ $A_p \cap RH_r$*, where p* ≥ 1 *and r* > 1*. Then, there exist constants* $D_1, D_2 > 0$ *such that*

$$D_1\frac{|E|^p}{|B|} \le \frac{w(E)}{w(B)} \le D_2\frac{|E|^{(r-1)/r}}{|B|}.$$

For any measurable subset E of the ball B, in general, for any λ > 1*, we have* $w(B(x_0,\lambda R)) \le \lambda^n w(B(x_0,R))$.

Proposition 3.3. *(*[1]*) Let α be a real number, Q be a nonsingular matrix, and x* ∈ R^n*. We have the following results:*

(i) *For v(Qx), we have:*

$$v(Qx) = \begin{cases} \|Q\|^{\alpha} v(x) \\ \|Q^{-1}\|^{-\alpha} v(x) \end{cases} \quad \text{if } \alpha > 0, \text{ if } \alpha \le 0.$$

(ii) *For* $v(B(0,\|Q\|R))$*, we have:*

$$v(B(0,\|Q\|R)) = |\det Q|^{n+\alpha} v(B(0,R)).$$

After stating these Propositions , we will now prove our main results. First six main results have a changed value of sharp bounds, whereas in the next six results [1] *the sharp bounds are different.*

Proof of Theorem 1.1

For a fixed ball B ⊂ R^n*, by the Minkowski inequality*

$$\|H_{\psi,A}f\|_{L^{q_2}(\mathbb{B};w)} = \left(\int_B \left|\frac{1}{|B|}\int_B |f(A(y)x)|^{\frac{1}{q_2}} w(x)\,dx\right|^{q^2} dy\right)^{\frac{1}{q^2}}$$

https://doi.org/10.62500/icrtsda.1.1.51

$$\leq \left(\int \mathbb{R}^{\kappa} \frac{|A(y)|}{|y|^n} \left(\int_B |f(A(y)x)|^{\frac{1}{q^2}} w(x)\, dx \right)^{q^2} dy \right)^{\frac{1}{q^2}}$$

.

In view of the condition $q_1 > \frac{q_2 rw}{(rw-1)}$, *there exists* $1 < r < rw$ *such that* $q_1 = \frac{q_2 r}{r-1}$.
An application of the Ho¨lder inequality and the reverse H¨older condition yields

$$\|f(A(y)\cdot)\|_{L^{q_2}(B;w)} \leq \left(\int_B |f(A(y)x)|^{q_1}\, dx \right)^{\frac{1}{q_1}} \left(\int_B w(x)^r\, dx \right)^{\frac{1}{rq_2}} \left(\int_{\det A^{-1}(y)} \frac{1}{|B|^{1/q_1} w(B)^{1/q_2}}\, dx \right.$$

!

By virtue of Proposition 3.1, one has

$$\left(\int_{A(y)B} |f(x)|^{q_1}\, dx \right)^{\frac{1}{q_1}} \preceq (B(0, \|A(y)\|R))^{1/q_1} \left(\frac{1}{\|B(0, \|A(y)\|R)\|^{1/q_1}} \int_{B(0,\|A(y)\|R)} |f(x)|^{q_1} w(x)\, dx \right)^{\frac{1}{q_1}}$$

$$\left(\|A(y)\|^{\frac{n}{q_1}} |B(0,\mathbb{R})|^{\frac{1}{q_1}} w\left(\mathbb{B}(0, \|A(y)\|\mathbb{R})\right)^{\lambda} \|\mathfrak{V}\|_{\dot{M}^{q_1,\lambda}(\mathbb{R};w)'} \right)$$

We thus conclude from above results that

$$\|H_{\psi,A} f\|_{\dot{M}^{q_2,\lambda}(R^n;w)}$$

$$\preceq \|f\|_{\dot{M}^{q_1,\lambda}(R^n,w)} \int_{\mathbb{R}^n} |\psi(y)||y|^n \left|\det A^{-1}(y)\right|^{1/q_1} \|A(y)\|^{n/q_1} \left(\frac{w(B(0,\|A(y)\|R))}{w(B(0,R))} \right)^{\lambda} dy$$

$$\preceq \|f\|_{\dot{M}^{q_1,\lambda}(R^n,w)} \times \int_{\|A(y)\|<1} |\psi(y)||y|^n \left|\det A^{-1}(y)\right|^{1/q_1} \|A(y)\|^{n/q_1} \left(\frac{w(B(0,\|A(y)\|R))}{w(B(0,R))} \right)^{\lambda} dy$$

$$+ \int_{\|A(y)\|\geq 1} |\psi(y)||y|^n \left|\det A^{-1}(y)\right|^{1/q_1} \|A(y)\|^{n/q_1} \left(\frac{w(B(0,\|A(y)\|R))}{w(B(0,R))} \right)^{\lambda} dy$$

Since $\lambda < 0$, Proposition 3.2 implies that, if $A(y) < 1$,

$$\left(\frac{w(B(0,\|A(y)\|R))}{w(B(0,R))} \right)^{\lambda} \left(\frac{|B(0,\|A(y)\|R)|}{|B(0,R)|} \right)^{\lambda} = \|A(y)\|^{n\lambda}$$

and, if ‖A(y)‖ 1,

$$\left(\frac{w(B(0,\|A(y)\|R))}{w(B(0,R))} \right)^{\lambda} \left(\frac{|B(0,\|A(y)\|R)|}{|B(0,R)|} \right)^{\lambda(\delta-1)/\delta} = \|A(y)\|^{n\lambda(\delta-1)/\delta}$$

for any $1 < \delta < r_w$. Therefore, from it is easy to see that, for any $1 < \delta < r_w$,

$$\|H_{\psi,A} f\|_{\dot{M}^{q_2,\lambda}(R^n;w)}$$

$$\preceq \|f\|_{\dot{M}^{q_1,\lambda}(R^n,w)} \left(\int_{\|A(y)\|<1} |\psi(y)||y|^n \left|\det A^{-1}(y)\right|^{1/q_1} \|A(y)\|^{n\lambda+n/q_1}\, dy \right)$$

$$+ \int_{\|A(y)\|\geq 1} |\psi(y)||y|^n \left|\det A^{-1}(y)\right|^{1/q_1} \|A(y)\|^{n/q_1+n\lambda(\delta-1)/\delta}\, dy$$

The proof of Theorem 1.1 is completed.

Proof of Theorem 1.2

In view of the Minkowski inequality, change of variables and Proposition 3.3, we have

https://doi.org/10.62500/icrtsda.1.1.51

$$\left(\frac{1}{v(B(0,R))^{1+\frac{\lambda}{q}}}\int_{B(0,R)}|H_{\psi,A}f|^q v(x)\,dx\right)^{1/q} \qquad \text{if } \alpha>0,$$
$$\preceq v(B(0,R))^{-\left(\lambda+\frac{1}{q}\right)}\int_{R^n}\left|\frac{\psi(y)}{|y|^n}\right||f(A(y)x)|^q\,v(x)\,dx\,dy$$
$$\simeq v(B(0,R))^{-(\lambda+1/q)}$$
$$\int_{R^n}\left|\frac{\psi(y)}{|y|^n}\right|\left|\det A^{-1}(y)\right|^{1/q}\left(\int_{A(y)B}|f(x)|^q v(A^{-1}(y)x)\,dx\right)^{1/q}dy$$
$$\preceq \|f\|_{\dot{M}^{q,\lambda}(R^n,v)}$$
$$\times\begin{cases}\int_{R^n}\left|\frac{\psi(y)}{|y|^n}\right|\left|\det A^{-1}(y)\right|^{1/q}\|A(y)\|^{(n+\alpha)(\lambda+1/q)}\|A^{-1}(y)\|^{\alpha/q}\,dy\\ \int_{R^n}\left|\frac{\psi(y)}{|y|^n}\right|\left|\det A^{-1}(y)\right|^{1/q}\|A(y)\|^{n(\lambda+1/q)+\alpha\lambda}\,dy\end{cases}\qquad \text{if } \alpha\le 0.$$

$$\|H\psi,A\|_{\dot{M}^{q,\lambda}(R^n,v)\to\dot{M}^{q,\lambda}(R^n,v)}\preceq\begin{cases}G_2\\ G_3\end{cases}$$ Therefore, we conclude that if $\alpha>0$, if $\alpha\le 0$.

Thus we finish the proof of Theorem 1.2

Proof of Theorem 1.3

If $\|A^{-1}(y)\|\preceq\|A(y)\|^{-1}$ then from the equation below,
$\|D|^{-n}\le|\det(D^{-1})|\le\|D^{-1}|^{n}$
we deduce that,
$\|A(y)^{-n}\|\simeq|detA^{-1}(y)|\simeq\|A^{-1}(y)\|^n$

Here we will prove the necessary part of Theorem 1.3, as the sufficient part can easily be obtained from Theorem 1.2. We divide our proof into the following two cases.
If $-\frac{1}{q}<\lambda<\infty$

in this case, we select $f_0\in \dot{M}^{p,\lambda}(\mathrm{R}^n;v)$ such that $f_0(x)=|x|^{(n+\alpha)\lambda}$. It is easy to see that $\|f0\|\dot{M}$

$p,\lambda(\mathrm{R}n;v)=|Sn-1|-\lambda(n+\alpha)\lambda(1+\lambda q)-1/q$, where $|Sn-1|$ denotes the volume of the unit

$$\succeq\int_{|}x\|>1,\|x\|_{-(n+\alpha)/q}$$
$$\succeq\int_{|x|>1}(|x|^{-(n+\alpha)/q-\epsilon}\int_{\|A(y)\|\succeq 1/|x|\frac{\psi(y)}{|y|^n}\|A(y)\|^{(-n+\alpha)/q-\epsilon)q}v(x)dx=\int_{\|A(y)\|>\epsilon}\frac{\psi(y)}{|y|^n}\|A(y)\|^{-(n+\alpha)/q-\epsilon}dy\Big)^q(\epsilon^{\epsilon})q\|f_{\epsilon}\|_q L^q($$

sphere S^{n-1}.

On the other hand, making use of the fact that $(n+\alpha)\lambda<0$, we obtain H
$_{\psi,A}f_0(x)=\int_{\mathbb{R}^n}\frac{\psi(y)}{|y|^n}\|A(y)x\|^{(n+\alpha)\lambda}\,dy$
$\succeq|x|^{(n+\alpha)\lambda}\quad\int_{\mathbb{R}^n}\frac{\psi(y)}{|y|^n}\|A(y)\|^{(n+\alpha)\lambda}dy,$
this implies that

$\|H\psi,A\|\dot{M}^{\cdot}\qquad q,\lambda(Rn,v)\to Mq,\lambda^{\cdot}\qquad(Rn,v)$
$\succeq\int_{\mathbb{R}^n}\frac{\psi(y)}{|y|^n}\|A(y)\|^{(n+\alpha)\lambda}\,dy$ **as required.**

Case 2. . If = –1/q, 0 ¡∈< 1,**we take**$f_{\epsilon}(x)=|x|^{-(n+\alpha)/q-\epsilon}\zeta\{|x|>1\}$.

https://doi.org/10.62500/icrtsda.1.1.51

A simple computation yields $\|f_{\in}\|_q = |S^{n-1}| \in (q)$ Now,

$\|H_{\psi,A(f)}\|^q{}_{Lq(Rn,v)}$

by letting $\in \longrightarrow 0$, *wehave*

$$\|H_\psi\|_{Lq}(\mathbb{R}^n, v) \to L^q(\mathbb{R}^n, v) \succeq \int_{\mathbb{R}^n} \frac{\psi(y)}{|y|^n} \|A(y)\|^{(-\frac{n+\alpha}{q})}\, dy$$

With this we complete the proof of Theorem 1.3

Proof of Theorem 1.4

As before, we fix a ball $B \subseteq \mathrm{R}^n$. Using the Minkowski inequality, we obtain

$$\|H_{b,\psi,A}f\|L^q(B;w) = \left(\int B \left\| \left(\int_{\mathbb{R}^n} \frac{\psi(y)}{|y|^n} (b(x) - b(A(y)x)) f(A(y)x) dy \right) \right\|_{q,w(x)} dx \right)^{1/q}$$

$$\leq \int_{\mathbb{R}^n} \left| \frac{\psi(y)}{|y|^n} \left(\int_B |(b(x) - b(A(y)x)) f(A(y)x)|^q w(x) dx \right)^{1/q} \right| dy$$

$$\leq \int_{\mathbb{R}^n} \left| \frac{\psi(y)}{|y|^n} \left(\int_B |(b(x) - b_{B,w}) f(A(y)x)|^q w(x) dx \right)^{1/q} \right| dy$$

$$+ \int_{\mathbb{R}^n} \left| \frac{\psi(y)}{|y|^n} \left(\int_B |(b_{B,w} - b_{A(y)B,w}) f(A(y)x)|^q w(x) dx \right)^{1/q} \right| dy$$

$$+ \int_{\mathbb{R}^n} \left| \frac{\psi(y)}{|y|^n} \left(\int_B |(b(A(y)x) - b_{A(y)B,w}) f(A(y)x)|^q w(x) dx \right)^{1/q} \right| dy = I_1 + I_2 + I_3$$

Let's start estimating I_1. For this purpose, we first compute the inner norm $\|(b(\cdot) - b_{B,w})f(A(y)\cdot)\|_{Lq(B;w)}$. The condition $s > qr_w/(r_w - 1)$ implies that there is $1 < r < r_w$ such that $s = qr' = qr/(r-1)$. By the H¨older inequality and the reverse H¨older condition, we obtain

$$\|(b(\cdot) - b_{B,w}) f(A(y)\cdot)\| L^q(B;w) \leq \left(\int B |(b(x) - b_{B,w}) f(A(y)x)|^s dx \right)^{1/s} \left(\int_B w(x)^r dx \right)^{1/(rq)}$$

$$\preceq |B|^{-1/s} w(B)^{1/q} \left(\int_B |(b(x) - b_{B,w}) f(A(y)x)|^s dx \right)^{1/s}$$

In view of the condition $1/s = 1/q1 + 1/q2$, we have

$$\|(b(\cdot) - b_{B,w}) f(A(y)\cdot)\| L^q(B;w) \preceq |B|^{-1/s} w(B)^{1/q} \left(\int B |b(x) - b_{B,w}|^{q2} dx \right)^{1/q2} \left(\int_B |f(A(y)x)|^{q1} dx \right)^{1/q1}$$

$$\preceq \left| \det A^{-1}(y) \right|^{1/q1} |B|^{-1/s} w(B)^{1/q} \left(\int_B |b(x) - b_{B,w}|^{q2} dx \right)^{1/q2} \left(\int_{A(y)B} |f(x)|^{q1} dx \right)^{1/q}$$

By virtue of Proposition 3.1, it is easy to see that

https://doi.org/10.62500/icrtsda.1.1.51

$$\left(\int_B \|b(x)-b_{B,w}\|_{q2}\,dx\right)^{1/q2} |B|^{1/q2}\|b\|_C \dot{M}_O^{q2}(R^n,w)$$

Substituting the result from above inequalities in 1.1,1.4 , one has

$$\|(b(\cdot)-b_{B,w})f(A(y)\cdot)\|L^q(B;w)$$

$$\preceq w(B)^{\frac{1}{q}}|\det A^{-1}(y)|^{\frac{1}{q2}}\,\|A(y)\|^{n/q1}\,w(A(y)B)^{\lambda}\|b\|_C\dot{M}_O^{q2}(R^n,w)\,\|f\|\,\dot{M}^{q1,\lambda}(R^n,w)$$

Therefore, we obtain

$$I_1 \preceq w(B)^{\lambda+1/q}\|b\|C\dot{M}_O^{q2}(R^n,w)\|f\|\dot{M}^{q1,\lambda}(R^n,w)$$

$$\times\int_{\mathbb{R}^n}\frac{\psi(y)}{|y|^n}\left|\det A^{-1}(y)\right|^{\frac{1}{q1}}\|A(y)|^{\frac{n}{q1}}\left(\frac{w(B(0,\|A(y)\|R))}{w(B(0,R))}\right)^{\lambda}dy$$

Making use of the inequalities in 1.2,1.4, we get

$$I_1 \preceq w(B)^{\lambda+1/q}\|b\|C\dot{M}_O^{q2}(R^n,w)\|f\|\dot{M}^{q1,\lambda}(R^n,w)$$

$$\times \int_{\{|\alpha(y)|<1\}} |\det A(y)|-1/q1|\alpha(y)|-n\lambda+n/q1\,dy$$

$$+\int_{\{|\alpha(y)|\geq 1\}} |\det A(y)|-1/q1|\alpha(y)|-n\lambda(\delta-1)/\delta+n/q1\,dy$$

Proof of Theorem 1.5

(i) As in the previous theorem $\|Hb\psi,Af\|Lq(B;v) \leq$

$$J1 + J2 + J3,$$

where J_1, J_2, and J_3 assume the form of I_1, I_2, and I_3, respectively, but with $w(\cdot)$ replaced by $v(\cdot)$.

$$J^1 \leq \int_{R^n}|\tfrac{\psi(y)}{|y|^n}\left(\int_B|b(x)-b_{B,v}|^{q2}\,v(x)\,dx\right)^{1/q2}\left(\int_B|f(A(y)x)|^{q1}\,v(A^{-1}(y)x)\,dx\right)^{1/q1}dy$$

$$\leq v(B)1/q2\|b\|CMO^{\cdot}q2(Rn,v)$$

$$\times\int_{R^n}|\tfrac{\psi(y)}{|y|^n}\left|\det A^{-1}(y)\right|^{1/q1}$$

In view of Proposition 3.3 it is easy to see that

$$J1 \leq v(B)\lambda+1/q\|b\|CMO^{\cdot}q2(Rn,v)\|f\|M^{\cdot}\,q1,\lambda(Rn,v)$$

$$\times\int_{R^n}|\tfrac{\psi(y)}{|y|^n}\left|\det A^{-1}(y)\right|^{1/q1}\left\|A(y)\right\|^{(n+\alpha)(\lambda+1/q)}\left\|\left\|A^{-1}(y)\right\|^{\alpha/q}$$

The expression for J_2 can be written as

$$J^2 = \int_{R^n}|\tfrac{\psi(y)}{|y|^n}\,\|f(A(y)\cdot)\|\,L^q(B;v)|bB,v-bA(y)B,v|\,dy.$$

In order to estimate J_2 we first compute $[\|f(A(y)\cdot)_{Lq(B;v)}$.

For this purpose a change of variables following the H¨older inequality and Proposition 3.3 gives us

https://doi.org/10.62500/icrtsda.1.1.51

$\|f(A(y)\cdot)\|L^q(B;v)$
$= (\mathrm{R}_B |f(A(y)x|^q v(x)dx)^{1/q}$

$=\det A-1(y)1/qv(A-1(y)x)dx)1/q$

$\preceq \det A^{-1}(y)^{1/q} \left\|A^{-1}(y)\right\|^{\alpha/q}\|f\|_{L^q(A(y)B;v)}$

$\preceq \left|\det A^{-1}(y)\right|^{1/q} \left\|A^{-1}(y)\right\|^{\alpha/q}\|f\|_{L^{q_1}(A(y)B;v)v(A(y)B)^{1/q2}}$

$\preceq \nu(B)^{\lambda+1/q}|\det A^{-1}(y)^{1/q}\|A(y)\|^{(n+\alpha)(\lambda+1/q)} \left\|A^{-1}(y)\right\|^{\alpha/q}\|f\|_{\dot{M}^{q1,\lambda}(R^n,v)}$

Therefore ,

$J2 \preceq v(B)\lambda+1/q\|f\|M^{\cdot}\ q1,\lambda(Rn,v)$
$\times \int_{\mathbb{R}^n} |\psi(y)| \left|\det A^{-1}(y)\right|^{1/q} \|A^{-1}(y)\|^{\alpha/q}|y|^n\|A(y)\|^{-(n+\alpha)(\lambda+1/q)}|b_{B,v} - b_{A(y)B,v}|\}, dy.$

By denoting $\varrho(y) = \det A-1(y)1/q\|A-1(y)\|\alpha/q|y|n\|A(y)\|-(n+\alpha)(\lambda+1/q)|bB,v - bA(y)B,v|dy,$

we decompose J_2 as

$$J2 \preceq v(B)\lambda+1/q\|f\|M^{\cdot}\ q1,\lambda(Rn,v)$$

Hence,

$$J_3 \preceq v(B)^{\lambda+\frac{1}{q}}\|\mathbf{b}\|_{CMO^{\cdot}q_2(R^n,v)}\|f\|_{M^{\cdot}q_1,\lambda(R^n,v)} \times \int_{\mathbb{R}^n} \left|\frac{\psi(y)}{|y|^n}\right| \left|\det A^{-1}(y)\right|^{1/q} \|A(y)\|^{(n+\alpha)(\lambda+1/q)}\|A^{-1}(y)\|^{\alpha/q}\, dy$$

Combining the estimates J_1, J_2, and J_3, we obtain

$$\|H\mathbf{b},A\|M^{\cdot}\ q1,\lambda(Rn,w) \leq G6\|\mathbf{b}\|_{CMO^{\cdot}q2(Rn,w)}\|f\|M^{\cdot}q_1,\lambda(Rn,v)$$

This completes the proof of part (i). (ii) Using Proposition 3.3 along with an argument as given above, the proof of this part becomes simpler. We thus finish the proof of Theorem 1.5.

Proof of Theorem 1.6

If$\|A^{-1}(y)\| \preceq \|A(y)\|^{-1}$, then (3.7) [1] is valid. The sufficient part of Theorem 1.6 can easily be obtained from Theorem 1.5. Next we will show the necessary part. For $-1/q < \lambda < 0$, choose $f_0(x) = |x|^{(n+\alpha)\lambda}$. It is easy to see that $f_0 \in M^{\cdot\, q1,\lambda}(R^n;v)$ and $\|f_0\|M^{\cdot\, q1,\lambda}(R^n;v) = |S^{n-1}|^{-\lambda}(n+\alpha)\lambda(1+\lambda q1)^{-1/q1}$. Assume that$H\psi,A^{b,1}$ is bounded from$M^{\cdot\, q1,\lambda}$ to $C^{MOq^{\cdot}2}(R^n,v)$ Noting that $(n+\alpha)\lambda < 0$, we have

$$H^{bo,1}_{\psi,A,}f_0(x) = \int_{\|A(y)\|<1} \frac{\psi(y)}{|y|^n}\|A(y)\|^{(n+\alpha)\lambda}\log(\frac{|A(y)x|}{|x|})^{-1}dy$$

$\succeq f0(x)\mathrm{R}\|A(y)\|<1\ |y|nA(y)(n+\alpha)\lambda\ \log1\|A(y)\|dy$ Hence,

$$\|H^{bo,1}_{\psi,A}\|_{M^{q1,\lambda}(R^n,v)\to M^{q,\lambda}(R^n,v)} \succeq \int_{\|A(y)\|<1} \frac{\psi(y)}{|y|^n}\|A(y)\|^{(n+\alpha)\lambda}\log\frac{1}{\|A(y)\|}dy.$$

https://doi.org/10.62500/icrtsda.1.1.51

Therefore, we obtain

$$\int_{\|A(y)\|<1} \frac{\psi(y)}{|y|^n} \|A(y)\|^{(n+\alpha)\lambda} \log \frac{1}{\|A(y)\|} < \infty.$$

On the oher hand

$$\int_{\|A(y)\|\leq 1/2} \frac{\psi(y)}{|y|^n} \|A(y)\|^{(n+\alpha)\lambda} dy \leq \int_{\|A(y)\|\leq 1/2} \frac{\psi(y)}{|y|^n} \|A(y)\|^{(n+\alpha)\lambda} \log \frac{1}{\|A(y)\|} dy.$$

since $\frac{\psi(y)}{|y|^n}$ **is integrable and** $(n+\alpha)\lambda < 0$

$$\int_{1/2\leq \|A(y)\|\leq 1} \frac{\psi(y)}{|y|^n} \|A(y)\|^{(n+\alpha)\lambda} dy \leq \infty.$$

From (4.11) and (4.12), we have

$$\|A(y)\|<1 \frac{\psi(y)}{|y|^n} \|A(y)\|^{(n+\alpha)\lambda} dy \leq \infty$$

It is important to note that

$$G_8 = \int_{\|A(y)\|<1} \frac{\psi(y)}{|y|^n} \|A(y)\|_{M^{p,\lambda}}^{(n+\alpha)\lambda} \log 2|\det A(y)|\, dy < \infty.$$

Then, combining (4.10) and (4.13)[1], we have $G_8 \leq \infty$.

(ii) **In this case we replace** $b_0(x)$ *by* $\log \frac{1}{|x|}$, then by an argument similar to above the proof can be obtained easily.

4. Conclusion

Finally, we explore the boundedness of the Hausdorff operator in weighted central Morrey spaces in this study. The exact limits for Hausdorff operators and associated commutators in the Morrey Herz space have been correctly obtained. Moreover, we get similar results for the commutators of Hausdorff operators, in particular when the symbol functions are in weighted central-BMO spaces. By our research, we have added to our knowledge of the behavior of Hausdorff operators in these particular function spaces, illuminating their boundedness characteristics and opening up new avenues for mathematical study. Our findings open up new avenues for this kind of study by providing insightful information on the interactions between operators and function spaces.

References

[1] Hussain, A., Ajaib, A. (2018). Some weighted inequalities for Hausdorff operators and commutators. Journal of Inequalities and Applications, 2018, 1-19.

[2] Van Duong, D. (2021). Hausdorff operator and commutator on weighted Morrey–Herz spaces on p-adic fields.*Analysis and Mathematical Physics*, 11(1), 31.

[3] Hausdorff, F. (1921). Summation methoden und Momentfolgen. I. *Math. Z., 9*, 74–109.

[4] Goldberg, R.R. (1960). Convolutions and general transforms on L_p. *Duke Math. J., 27*, 251–259.

[5] Georgakis, C. (1992). The Hausdorff mean of a Fourier-Stieltjes transform. *Proc. Am. Math. Soc., 116*, 465–471.

[6] Andersen, K., Sawyer, E. (1988). Weighted norm inequalities for the Riemann–Liouville and Weyl fractional integral operators. *Trans. Am. Math. Soc., 308*, 547–558.

https://doi.org/10.62500/icrtsda.1.1.51

[7] Miyachi, A. (2004). Boundedness of the Ces`aro operator in Hardy space. *J. Fourier Anal. Appl., 10*, 83–92.

[8] Fu, Z.W., Gong, S.L., Lu, S.Z., Yuan, W. (2015). Weighted multilinear Hardy operators and commutators. *Forum Math., 27*, 2825–2851.

[9] Brown, G., Mo´ricz, F. (2002). Multivariate Hausdorff operators on the spaces $L_p(R^n)$. *J. Math. Anal. Appl., 271*, 443–454.

[10] Carton-Lebrun, C., Fosset, M. (1984). Moyennes et quotients de Taylor dans BMO. *Bull. Soc. Roy. Sci. Li´ege, 53*, 85–87.

[11] Xiao, J. (2001). L_p and BMO bounds of weighted Hardy–Littlewood averages. *J. Math. Anal. Appl., 262*, 660–666.

[12] Chuong, N.M., Hung, H.D. (2014). Weighted L_p and weighted BMO-bounds for a new generalized weighted Hardy–Ces`aro operator. *Integr. Transforms Spec. Funct., 25*, 697–710.

[13] Chuong, N.M., Duong, D.V., Dung, K.H. (2017). Multilinear Hausdorff operators on some function spaces with variable exponent (2017). *arXiv:1709.08185*.

[14] Liflyand, E., M´oricz, F. (2000). The Hausdorff operator is bounded on the real Hardy space $H^1(R)$. *Proc. Am. Math. Soc., 128*, 1391–1396.

[15] M´oricz, F. (2005). Multivariate Hausdorff operators on the spaces $H^1(R^n)$ and $BMO(R^n)$. *Anal. Math., 31*, 31–41.

[16] Rim, K.S., Lee, J. (2006). Estimates of weighted Hardy–Littlewood averages on the *p*-adic vector spaces. *J. Math. Anal. Appl., 324*, 1470–1477.

[17] Liflyand, E. (2008). Boundedness of multidimensional Hausdorff operators on $H^1(R^n)$. *Acta. Sci. Math. Szeged., 74*, 845–851.

[18] Hussain, A., Gao, G. (2013). Multidimensional Hausdorff operators and commutators on Herz-type spaces. *J. Ineq. Appl., 2013*, 594.

[19] Tang, C., Xue, F., Zhou, Y. (2011). Commutators of weighted Hardy operators on Herz-type spaces. *Ann. Pol. Math., 101*, 267–273.

[20] Ruan, J., Fan, D. (2016). Hausdorff operators on the power weighted Hardy spaces. *J. Math. Anal. Appl., 433*, 31–48.

[21] Wu, J.L., Zhao, W.J. (2016). Boundedness for fractional Hardy–type operator on variableexponent Herz–Morrey spaces. *Kyoto J. Math., 56(4)*, 831–845.

[22] Hardy, G. H., Littlewood, J. E., Po´lya, G. (1952). *Inequalities*. Cambridge university press.

[23] Hausdorff, F. (1921). Summation methoden und Momentfolge, *I. Mathematical Zeitschrift, 9, 74–109*.

[24] Chuong, N. M. (2018). Pseudodifferential operators and wavelets over real and p-adic fields. *Springer International Publishing.*

[25] Chuong, N. M., Duong, D. V., Dung, K. H. (2019). Some estimates for p-adic rough multilinear Hausdorff operators and commutators on weighted Morrey–Herz type spaces. *Russian Journal of Mathematical Physics, 26(1), 9-31.*

[26] Chuong, N. M., Van Duong, D., Hung, H. D. (2016). Bounds for the weighted Hardy-Cesa`ro operator and its commutator on Morrey-Herz type spaces. *Zeitschrift fu¨r Analysis und ihre Anwendungen, 35(4), 489-504.*

[27] Chen, J., Fan, D., Li, J. (2012).Hausdorff operators on function spaces. *Chinese Annals of Mathematics, Series B, 33(4), 537-556.*

[28] Garc´ıa-Cuerva, J., De Francia, J. R. (2011). Weighted norm inequalities and related topics. Elsevier.

https://doi.org/10.62500/icrtsda.1.1.51

[29] Gundy, RF, Wheeden, RL: Weighted integral inequalities for nontangential maximal function, Lusin area integral, and Walsh-Paley series. Stud. Math. 49, 107-124 (1974).

[30] Fu, Z., Lu, S., Zhao, F. (2011). Commutators of n-dimensional rough Hardy operators. *Science China Mathematics, 54, 95-104.*

[31] Gao, G. (2012). Boundedness for commutators of n-dimensional rough Hardy operators on Morrey–Herz spaces. *Computers Mathematics with Applications, 64(4), 544-549.*

[32] Lu, S., Ding, Y., Yan, D. (2007). Singular integrals and related topics. *World Scientific.*

[33] Chen, J., Dai, J., Fan, D., Zhu, X. (2018). Boundedness of Hausdorff operators on Lebesgue spaces and Hardy spaces. *Science China Mathematics, 61, 1647-1664.*

[34] Alvarez, J., Lakey, J., Guzm´an-Partida, M. (2000). Spaces of bounded lambda-central mean oscillation, Morrey spaces, and lambda-central Carleson measures. *Collectanea Mathematica, 51(3), 1-47*

https://doi.org/10.62500/icrtsda.1.1.52

Proc. 1st International Conference on Recent Trends in Statistics and Data Analytics

Air University Islamabad, Pakistan – May 9, 2024, Vol. 1, pp. 505-519

BEHAVIOUR OF HAUSDROFF OPERRATOR ON WEIGHTED CBMO HERZ SPACE AND P-ADIC SPACE

AMNA AJAIB*, ALINA HUSSAIN*, MUNEEBA NAVEED*, HAMAIL SHOUKAT*

[2]DEPARTMENT OF MATHEMATICS, FAZAIA BILQUIS

COLLEGE OF EDUCATION FOR WOMEN PAF BASE NUR

KHAN, PAKISTAN

Abstract

In this article, we study the commutators of Hausdorff operators and proved their boundedness on the Heisenberg group in the setting of the Herz space and p-adic.We obtained the study of the Hausdorff operator on padic function spaces of power weighted type, such as Lebesgue spaces, and Herz type spaces. Furthermore,We also discuss the sharpness of our results,given certain conditions on the norm of the matrix C.

1. Introduction

First described in [4], the matrix Hausdorff operators defined in Euclidean space with n dimensions were described as follows:

$$Z(1.1)\ H_{\eta,C}f(x) = \int_{Rn} \eta(t)f(xC(t))dt$$

$H_{\eta,C}$ is bounded on Hardy spaces, as proved by Lerner and Liflyand in [4], Considering account the dual of Hardy space H^1 and bounded mean oscillation (BMO) space. In [5], comparable boundedness of $H_{\eta,C}$ was further reexamined through the use of atomic decomposition of Hardy spaces. The works mentioned above have significance since they represent the initial efforts to investigate The Hausdorff operators in high dimensions on $H_R{}^1{}_n$. These findings were expanded upon on $H_n{}^p$ spaces with $0 < p < 1$ by Liflyand and Miyachi [6].

Chen et al. [7] altered the form of (1.1) in 2012 by exchanging $\frac{\eta_t(t)}{n}$ for the kernel function $\eta(t)$:

$$H_{\eta,C}f(x) = \int_{R^n} \frac{\eta(t)}{|t|^n} f(xC(t))dt \quad (1.2)$$

As a subcase, when $C_t(t) = [\frac{1}{|t|}, \frac{1}{|t|}, \ldots, \frac{1}{|t|}]$, They provide an alternative interpretation of the Hausdorff operator in dimension n:

$$H_\eta f(x) = \int_{R^n} \frac{\eta(t)}{|t|^n} f(\frac{x}{|t|})dt \quad (1.3)$$

Among their conclusions is the boundedness of Hausdorff operators on Herz and Herz-type Hardy spaces, local Hardy spaces, and Hardy spaces. We conclude that these operators outperform Hardy spaces on Herz-type Hardy spaces. In the same year, Chen et al. [8], along with other co-authors, extended the problem on the boundedness of $H_{\eta,C}$ to the product of Hardy-type spaces. Boundedness

---

[1]*Department of Mathematics, Fazaia Bilquis College PAF Base Nur Khan, Rawalpindi, Pakistan

https://doi.org/10.62500/icrtsda.1.1.52

*Corresponding Author: dr.amnaajaib@gmail.com, muneebanaveed18@gmail.com, alinahussain2001@gmail.com, Hamailshouket5@gmail.com

Key words and phrases. Hausdorff Operator, Commutaors, Boundedness CBMO function, Padic Functinal space, Herz space, Weights.

1

results were extended for Hausdorff operators on $H_R{}^1{}_n$ in [9]. The continuity of (1.2) on block spaces, Hardy-Morrey spaces, Morrey spaces, and rectangularly defined spaces has also been the subject of some research ([10], [11], [12], and [13], respectively). Comparably, [14]–[16] present some findings about the boundedness of H_η.

Similarly, commutators to integral operators are of significance because of their numerous applications in function space characterization and partial differential equation theory (see, for example, [17]–[19]).In [20], An effort has been made to study the boundedness of commutators of $H_{\eta,C}$,given by:

$$H^b_{\eta,C} f(x) = \int_{R^n} \frac{\eta(t)}{|t|^n} (b(xC(t))) f(xC(t)) dt \tag{1.4}$$

In addition, we determine function spaces where the symbol function b belongs to either the central BMO space or the Lipschitz space, as was previously studied [21, 22, 23], and analyze the commutators of H_η when the matrix $C(t)$ is diagonal. We recommend that interested readers consult the review papers [24, 25] to obtain a comprehensive understanding of the history and upcoming advancements of Hausdorff operators.

p-adic analysis has developed in significance over time since it has many applications in several branches of mathematical sciences, including mathematical physics. In their 1989 book [26], Vladimirov et al. presented a foundation for p-adic quantum mechanics. They introduced concepts such as p-adic stochastic processes, p-adic pseudo-differential operators, and p-adic quantum theory. This volume included, among other things, a thorough reconstruction of Schwartz's theory of distributions over p-adic fields. Several operator theory and function space generalizations have been made in the subject of harmonic analysis on p-adic fields since the publication of this book.

On the other hand, the study of one-dimensional Fourier analysis has greatly improved thanks to Hausdorff summability methods, also referred to as Hausdorff operators. In particular, these techniques have helped analyze the summability aspects of classical Fourier series. However, the work [27] is the source of the current flurry of interest in the study of Hausdorff operators on function spaces. In their paper, they demonstrated that the 'operator',

$$H_\eta f(x) = \int_0^\infty \frac{\eta(t)}{t} f(\frac{x}{t}) dt$$

The paper [28] modified these results for the real Hardy spaces H^p(R), where $0 < p < 1$, by adding certain smoothness criteria on the kernel function η. Aside from its summability qualities, this operator can be seen as a generalization of a few classical operators, including the Hardy operator, the adjoint Hardy operator, and the Ces`aro operator. These traits have motivated researchers to study the behavior of H_η in high-dimensional Euclidean spaces R^n. In this context, an expansion of (1.1) was presented in [29] and it is expressed as following.

$$H_{\eta,C} f(x) = \int_{Rn} \eta(t) f(C(t)x) dt$$

https://doi.org/10.62500/icrtsda.1.1.52

where $\eta \in L^1_{loc}(R^n)$ and $C(t)$ is an $n \times n$ matrix such that $\det C(t) \neq 0$ almost everywhere in the support of η.

Here it is important to draw attention to certain recent developments in the theory of the Hausdorff operator. A summary of the literature demonstrates that the Hardy spaces H^1 [30, 31, 32], where its boundedness is thoroughly explored, receive far more attention than H^p spaces where $0 < p < 1$ [33, 34]. A thorough prior explanation of the boundedness of the Hausdorff operator on Hardy spaces can be found in the paper [35]. Another area of extensive research is the boundedness of the Hausdorff operator on various function spaces. Numerous contemporary works, such as [36, 37, 38, 39] and [40], are cited in this article without any specific historical context.

The Hausdorff operator on p-adic function spaces is mostly studied by Volosivets [41, 42]. Let us suppose the following: $n \times n$ matrix $C(t)$ is nonsingular virtually everywhere with continuous components $c_{ij}(t) : \mathbb{Q}_p^n \to \mathbb{Q}_p$; $f(x)$ is continuous on $\mathbb{Q}_p^n$; and $\eta(t)$ is measurable on $\mathbb{Q}_p^n$. Then the following formula determines the Hausdorff operator:

$$H_{\eta,C}f(x) = \int_{Qn_p} \eta(t) f(C(t)x)dt$$

Whenever the integral on the right-hand side exists in the Lebesgue sense.

Volosivets in [41] investigated the boundedness of $H_{\eta,C}$ in the real Hardy spaces $H^1(Q^n_p)$ for the matrix $C(t)$ of the form $C(t) = c(t)E$, where E is the identity matrix. Later, in [42], he replaced limits on its norm in $\mathbb{Q}_p^n$ for the condition on the form of the matrix C, and established the boundedness of $H_{\eta,C}$ in $H^1(\mathbb{Q}_p^n)$ and BMO$(\mathbb{Q}_p^n)$.

Motivated by the aforementioned work, this paper examines the Hausdorff operator on p-adic function spaces of power-weighted type, including Lebesgue spaces, Morrey spaces, and Herz-type spaces. In contrast to [41, 42], we employ a different methodology to establish our results. Additionally, by imposing certain conditions on the norm of the matrix A, we discuss the sharpness of our results. These findings are significant in that $H\eta,C$ reduces to the p-adic Hardy-Littlewood operator and p-adic modified Hardy operator if $C(t)$ is a diagonal matrix and η is suitably chosen. Furthermore, the analysis presented in this paper can be applied to demonstrate the boundedness of $H_{\eta,C}$ and its commutators on other weighted function spaces of p-adic nature,[2].

In essence, the study of the Hausdorff operator on Herz spaces and p-adic spaces represents a fertile area of research with wide-ranging applications across mathematics and its diverse applications. By unraveling the properties and interactions of the Hausdorff operator in these spaces, mathematicians can advance our understanding of function spaces, operator theory, and mathematical analysis, paving the way for innovative discoveries and applications in various fields.In conclusion, the Hausdorff operator is a powerful tool for analyzing functions in Herz spaces and p-adic numbers. Its properties and applications make it a useful tool for studying the smoothness and decay properties of functions in these spaces. Further research on the Hausdorff operator and its applications is likely to lead to new insights and discoveries in harmonic analysis, functional analysis, and number theory. Our main result can be stated as:

Theorem 1.1. *Let us suppose that* $1 \leq p, q_1, q_2 \leq \infty$ *and* $\gamma_1, \gamma_2 \in R$ *with* $\gamma_1 < 0$. *Let* $\frac{1}{s} = \frac{1}{q_1} + \frac{1}{q}$ *and* $\frac{\gamma_1}{Q} + \frac{1}{q_1} = \frac{\gamma_1}{Q} + \frac{1}{q_2}$. *Additionally, let w belong to* C_1 *along with* r_w *for the reverse H¨older condition and* $s > \frac{q_2 r_w}{(r_w - 1)}$.

https://doi.org/10.62500/icrtsda.1.1.52

(i)If $\frac{1}{q_1} + \frac{\gamma_1}{Q} \geq 0$*, then for any* $1 < \delta < r_w$*,*

$$\left\|T^b_{\eta,C} f\right\|_{K^{\gamma_2,p}_{q_2}(\mathbb{Q}^n_p;w)} \leq K_1 \|b\|_{CMO^q(\mathbb{Q}^n_p;w)} \|f\|_{K^{\gamma_1,p}_{q_1}(\mathbb{Q}^n_p;w)}.$$

where

$$K_1 = \int_{||C(t)||<1} \frac{|\eta(t)|}{|y|^Q_h}(1+|detC^{-1}(t)|^{\frac{1}{q}}||C(t)||^{\frac{Q}{q}})|detC^{-}1(t)|^{\frac{1}{q_1}}||C(t)||^{-\gamma_1} log\frac{2}{||C(t)||}dt+$$
$$\int_{||C(t)||<1} \frac{|\eta(t)|}{|y|^Q_h}(1+|detC^{-1}(t)|^{\frac{1}{q}}||C(t)||^{\frac{Q}{q}})|detC^{-}1(t)|^{\frac{1}{q_1}}||C(t)||^{Q/q_1-(\gamma_1+Q/q_1)(\delta-1)/\delta} log2||C(t)||dt$$

(ii)If $\frac{\gamma_1}{Q} + \frac{1}{q_1} < 0$*, then for any* $1 < \delta < r_w$*,*

$$\left\|T^b_{\eta,C} f\right\|_{K^{\gamma_2,p}_{q_2}(\mathbb{Q}^n_p;w)} \leq K_2 \|b\|_{CMO^q(\mathbb{Q}^n_p;w)} \|f\|_{K^{\gamma_2,p}_{q_2}(\mathbb{Q}^n_p;w)}.$$

where

$$K_2 = \int_{||C(t)||<1} \frac{|\eta(t)|}{|y|^Q_h}(1+|detC^{-1}(t)|^{\frac{1}{q}}||C(t)||^{\frac{Q}{q}})|detC^{-}1(t)|^{\frac{1}{q_1}}||C(t)||^{-\gamma_1} log2||C(t)||dt+$$
$$\int_{||C(t)||<1} \frac{|\eta(t)|}{|y|^Q_h}(1+|detC^{-1}(t)|^{\frac{1}{q}}||C(t)||^{\frac{Q}{q}})|detC^{-}1(t)|^{\frac{1}{q_1}}||C(t)||^{Q/q_1-(\gamma_1+Q/q_1)(\delta-1)/\delta} log\frac{2}{||C(t)||}dt$$

Theorem 1.2. *Let* $1 \leq p \leq \infty$ *and* $\beta > -n$*. If* $\frac{1}{q_2} = \frac{1}{q_1} + \frac{1}{q}$ *and* $\frac{\gamma_2}{Q} + \frac{1}{q} = \frac{\gamma_1}{Q}$*, then we have*

$$\left\|T^b_{\eta,C} f\right\|_{K^{\gamma_2,p}_{q_2}(\mathbb{Q}^n_p;u)} \leq K_3 \|b\|_{CMO^q(\mathbb{Q}^n_p;w)} \|f\|_{K^{\gamma_1,p}_{q_1}(\mathbb{Q}^n_p;w)}.$$

where K_3 *is*

$$K_3 = \begin{cases} \int_{\mathbb{Q}^n} \theta(t)(1+\log_2(\|C^{-1}(t)\|\|C(t)\|))\,dt, \\ \int_{\mathbb{Q}^n} \theta(t) G(C^{-1}(t), \gamma_1(Q+\beta)/Q)\,dt, \end{cases} \quad \text{if } \gamma_1 = 0, \text{ if } \gamma_1 \neq 0,$$

and

$$\theta(y) = \frac{|\psi(t)|}{|t|^Q_h}|detC^{-1}(t)|^{1/q_1}\left(\log\frac{2}{||C(t)||\chi_{||C(t)||<1}} + \log 2||C(t)||\chi_{[||C(t)||<1]}\right)$$
$$\times G(C^{-1}(t), \beta/q_1)(1+|detC^{-1}(t)|^{1/q} G(C^{-1}(t), \beta/q)||C(t)||^{(Q+\beta)/q}.$$

In the next section, we give some definitions and notations. However, theorem is proved in the last section.

2. **Some Definitions and Notations**

In 1972, Muckenhoupt explored the study of the maximum H-Littlewood function in the weighted space L^p, creating the theory of weights A_p. A comprehensive investigation was then conducted by G.C and R-de Francia.

Definition 2.1

When a $M > 0$ exists and for any ball $b \subset \mathrm{R}^n$, We claim that W is part of the Muckenhoupt class $A_p(\mathrm{R}^n)$, $1 < r < \infty$.

$$\left(\frac{1}{|b|}\int_b W(t)dt\right)\left(\frac{1}{|b|}\int_b W(t)^{\frac{r'}{r}}dt\right)^{\frac{r'}{r}} \leq M$$

Also, $W \in A_1$ if $\exists$ a constant $M > 0$ such that for every ball $b \subset \mathrm{R}^n$:

https://doi.org/10.62500/icrtsda.1.1.52

$$\frac{1}{|b|}\left(\int_b W(t)dt\right) \leq M \operatorname{essinf}_{t\in b} W(t)$$

Definition 2.2

We can define W to belong to the reverse H¨older class $\in RH_r(\mathrm{R}^n)$ if there is a finite constant $M > 0$ and $r > 1$ such that for every ball $b \subset \mathrm{R}^n$.

$$\left(\frac{1}{|b|}\int_b W^r(t)dt\right)^{1/r} \leq \frac{M}{|b|}\int_b W(t)dt$$

Definition 2.3

Let $\gamma \in \mathrm{R}$, $0 < l,r < \infty$, and μ be a positive number. Then the weighted Herz space $K_{l,q}^{\gamma,\mu}(w, Q_n^p)$ is given as:

$$K_{l,r}^{\gamma,l}(w, Q_n^p) = \{f \in L_{\mathrm{loc}}^r(w, Q_n^p \setminus \{0\}) : \|f\|_{K_{l,r}^{\gamma,l}(w,Q_n^p)} < \infty\}$$

where

$$||f||_{K_{l,r}^{\gamma,l}(w,Q_n^p)} = \sum_{k=-\infty}^{\infty} w(B_k)^{\frac{\gamma l}{n}} ||f\chi_k||_{L^r(w,Q_n^p)}^l$$

Remark:

Obviously $K_{l,r}^{\gamma,r}(w,Q^p{}_n) = L^r(w,Q^p{}_n)$

Definition 2.4

Let w be a weight function on $Q^p{}_n$, $1 \leq s < \infty$, and $\mu \geq -\frac{1}{s}$. The weighted p-adic Morrey space $L^{s,\mu}(Q_n^p; w)$ is defined as:

$$L^{s,\mu}(Q_n^p; w) = \{f \in L_{\mathrm{loc}}^s(Q_n^p; w) : ||f||_{L^{s,\mu}(Q_n^p;w)} < \infty\}$$

where

$$||f||_{L^{s,\mu}(Q_n^p;w)} = \sup_{b\in Q_n^p, \alpha\in\mathbb{Z}} \left(\frac{1}{w(B_\alpha(b))^{1+\mu s}} \int_{B_\alpha(b)} |f(x)|^s w(x)\, dx\right)^{\frac{1}{s}}$$

Proposition 2.1

Let $W \in A_p \cap RH_r(\mathrm{R}^n)$, $r \geq 1$ and $q \geq 1$. Then, there exist constants $M_1, M_2 > 0$ such that:

$$M_1\left(\frac{|e|}{|b|}\right)^r \leq \left(\frac{w(e)}{w(b)}\right) \leq M_2\left(\frac{|e|}{|b|}\right)^{q-1/q}$$

for any measured subset e of a ball b. Generally, for any $\mu > 1$:

$$w(b(x_0,\mu R) \leq \mu^{Qq} w(b(x_0,R))$$

https://doi.org/10.62500/icrtsda.1.1.52

Proposition 2.2

Let $W \in A_p(\mathrm{R}^n)$, $1 \leq Q < \infty$, then for any $f \in L_{\mathrm{loc}}{}^1(\mathrm{R}n)$ and any ball $b \subset \mathrm{R}n$:

$$\frac{1}{|b|}\int_b |f(t)|dt \leq M\left(\frac{1}{w|b|}\int_b |f(t)|^q w(t)dt\right)^{1/q}$$

The weighted Lebesgue space $L^q(E;w)$ is the space of all functions f satisfying the norm requirement for any measurable set $E \subset \mathrm{R}n$:

$$||f||_{L^q(E;w)} = \left(\int_B |f(t)|^q w(t)dt\right)^{1/q} < \infty$$

Lemma 2.1

Assume that $2(m + 1) \times (2m + 1)$ matrix M is invertible matrix. Then,

$||M||^{-Q} \leq |detM^{-1}| \leq ||M^{-1}||^{Q}$ where

$||M|| = \sup x\epsilon \mathrm{R}n, x\neq 0\ |Mx|h/|x|h$

In addition, we'll use the notation $v(\cdot)$ as rather than $w(\cdot)$ when the A_p weights decrease to the power function, i.e.,$v(\cdot) = |.|_h^{\beta}$. In such instance, a simple computation yields:

$v(b_k) = \int_{|t|_g \leq 2^k} |t|_g^{\beta}\, dt = \frac{w_Q 2^{k(Q+\beta)}}{\beta+Q}$

Moreover, we use the piecewise defined function G in the situation of boundedness of $T_{\eta C}{}^b$ on the power-weighted Herz space:

$$G(M,\delta\beta) = \begin{cases} ||M||^{\omega\gamma} & \text{if } \gamma > 0 \\ ||M^{-1}||^{-\omega\gamma} & \text{if } \gamma \leq 0. \end{cases},$$

where M is any invertible matrix, $\gamma\epsilon$R and ω is any non-negative number.Then, it is easy to see that H satisfies:

$H(M,\gamma(1/q + 1/p)) = H(M,\gamma/q)H(M,\gamma/p)$ where $p,q\epsilon Z^{+}$

Lemma 2.2

Let $W \in w^{\beta}$, $\beta > -n$. Then, for any $\gamma \in \mathrm{Z}$, we have $w(B_\gamma) = p(n + \beta)^{\gamma} \cdot w(B_0)$ and

$$w(S_\gamma) = p(n + \beta)^{\gamma} \cdot w(S_0).$$

For convenience in use, we adopt the following notation here and in the sequel:

$$G(M,\delta) \leq= \begin{cases} ||M||^{\beta} w(x) & \text{if } \beta > 0, \\ ||M^{-1}||^{-\beta} w(x) & \text{if } \beta \leq 0. = G(D,\beta)w(x) \end{cases}$$

where M is any invertible matrix and $\delta \in \mathrm{R}$.

https://doi.org/10.62500/icrtsda.1.1.52

Lemma 2.3

Let F be an n n matrix with entries $f_{ij} \in Qp$ Then the norm of F_r, regarded as an operator from $Q^p{}_n$ to $Q^p{}_n$ is defined as:

$||F|| = \max 1 \le i \le n \max 1 \le j \le n |fij|p$

Lemma 2.4

Let $W \in w_\alpha$, $\alpha > -n$. Then for any $\gamma \in Z$,we have $w(B\gamma) = p(n+\alpha)\gamma w(B0)$

and $w(S\gamma) = p(n+\alpha)\gamma w(S0)$

For convenience in use, we adopt the following notation here and in the sequel:

$$G(F, \delta\alpha) = \begin{cases} F^{\delta\alpha} & \text{if } \alpha > 0 \\ ||F^{-1}||^{-\delta\alpha} & \text{if } \alpha \le 0. \end{cases},$$

where F is any nonsingular matrix $\alpha \in R$ and δ is a non-zero positive number.

It's simple to observe that:

$M(F, \alpha(\frac{1}{q} + \frac{1}{p})) = M(F, \frac{\alpha}{q})M(F, \frac{\alpha}{p})$

where $p,q \in Z^+$

Proposition 2.3

Suppose$\alpha > -n$, $W(t) = |t|^{\frac{\alpha}{p}}$. E is any nonsingular matrix and $t \in Q^p{}_n$,then $^{(}F^{\delta\alpha}W(t)$ if $\alpha > 0$,

$w(Ft) \le$

$||F^{-1}||^{-\delta\alpha}W(t)$ if $\alpha \le 0$.

Lemma 2.5

Assume that $f \in L(Q^p{}_n)$ and $C : Q^p{}_n$ Then

$$^{R}Q_pn\, f(x)dx = {}^{R}Qpn\, |\det C|_p f(Cy)dy$$

Lemma 2.6

$\rightarrow Q^p{}_n$ is a nonsingular linear transform.

https://doi.org/10.62500/icrtsda.1.1.52

Let$\alpha > -n$, $W(t) = |t|^{\frac{\alpha}{p}}$. F is any non-singular matrix,then we have

$W(FB_\gamma(a)) \leq M(F,\alpha)|\det F|_p w(B_\gamma(a))$

3. **Proof of the main results**

In this section we shall prove the main result stated in section one. However, we need some useful lemmas for this purpose.

After stating these lemmas, we will now prove our main results.

Proof of Theorem 3.1

Here, we need to prove that

$\left(\sum_{k=-\infty}^{\infty} w(B_k)^{\frac{\gamma_2 p}{Q}} \|T^b_{\eta,C} f\|^p_{L^{q_2}(E_k,w)}\right)^{\frac{1}{p}} \preceq \|f\|_{K^{\gamma_1,p}_{q_1}(\mathbb{Q}_p^n;w)}$

By essential splitting and the Minkowski inequality, an upper bound for the inner norm $\|^{T}{}_{\eta,C}{}^{b} f\|_{Lq_2(Ek,w)}$ can be obtained as:

$$\begin{aligned}
\|T^b_{\eta,C} f\|_{L^{q_2}(E_k,w)} &= \left\| \int_{\mathbb{Q}_p^n} \frac{\eta(t)}{|t|_h^Q} (b(x) - b(C(t)x)) f(C(t)x)\, dt \right\|_{L^{q_2}(E_k,w)} \\
&\leq \int_{\mathbb{Q}_p^n} \frac{\eta(t)}{|t|_h^Q} \|(b(x) - b(C(t)x)) f(C(t)x)\|_{L^{q_2}(E_k,w)}\, dt \\
&\leq \int_{\mathbb{Q}_p^n} \frac{\eta(t)}{|t|_h^Q} \|(b(x) - b_{B_k}) f(C(t)x)\|_{L^{q_2}(E_k,w)}\, dt \\
&\quad + \int_{\mathbb{Q}_p^n} \frac{\eta(t)}{|t|_h^Q} \left\|(b(C(t)x) - b_{\|C(t)\|B_k}) f(C(t)x)\right\|_{L^{q_2}(E_k,w)}\, dt \\
&\quad + \int_{\mathbb{Q}_p^n} \frac{\eta(t)}{|t|_h^Q} \left\|(b_{B_k} - b_{\|C(t)\|B_k}) f(C(t)x)\right\|_{L^{q_2}(E_k,w)}\, dt \\
&= P_1 + P_2 + P_3
\end{aligned} \tag{3.1}$$

We first compute $\|(b(x) - b(C(t)x))f(C(t)x)\|_{Lq_2(Ek,w)}$, with the goal of achieving P_1.If $s > \frac{q_2 r_w}{(r_w - 1)}$, then $1 < r < r_w$ must exist in order for $s = q_2 r'$.Thus, based on the reverse H¨older condition and the H¨older inequality, we get

$$\|(b(.) - b_{BK})f(C(t).)\|_{Lq_2(Ek,w)} = \left(\int_{Ek} |(b(x) - b_{Bk})f(C(t)x)|^s dx\right)^{1/s} \left(\int_{Ek} w(x)^r dx\right)^{1/rq_2}$$

$$\preceq |Bk|^{-1/s} w(Bk)^{1/q_2} \|b(.) - bBk)f(C(t).)\|_{Ls(Ek)}. \tag{3.2}$$

Now, using the condition $\frac{1}{s} = \frac{1}{q_1} + \frac{1}{q}$, We are able to

$\|(b(\cdot) - b_{BK})f(C(t)\cdot)\|_{Ls(Ek)} \leq \|b(\cdot) - b_{BK}\|_{Lq(Bk)}\, \|f(C(t)\cdot)\|_{Lq_1(Bk)}$

Changing any of the variables combined with Proposition 2.2 in the second(3.3) factor results in the right side of inequality (3.3).

https://doi.org/10.62500/icrtsda.1.1.52

$$\begin{aligned}\|f(C(t)\cdot)\|_{L^{q_1}(B_k)} &= |detC^{-1}(t)|^{1/q_1}\Big(\int_{C(t)B_k}|f(x)|^{q_1}dx\Big)^{1/q_1}\\ &\preceq |detC^{-1}(t)|^{1/q_1}|B(0,2^k||C(t)||)|^{1/q_1}\times\Big[\frac{1}{w(B(0,2^k||C(t)||))}\\ &\int_{(B(0,2^k||C(t)||}|f(x)^{q_1}w(x)dx\Big]^{1/q_1}\\ &\preceq \left(|\det C^{-1}(t)|\,||C(t)||^Q|B_k|\right)^{\frac{1}{q_1}}\ w(||C(t)||B_k)^{-\frac{1}{q_1}}\ \|f\|_{L^{q_1}(||C(t)||B_k;w)}\end{aligned}\tag{3.4}$$

In view of Proposition 2.4, the additional element on the right side of inequality (3.3) yields

$$\|b(\cdot)-b_{BK}\|_{Lq(Bk)}\preceq |B_k|^{1/q}\,\|b\|_{CMOq(Qnp,w)}\tag{3.5}$$

When combined, inequality (3.2)–(3.5) produces

$$\begin{aligned}&\|(b(\cdot)-b_{BK})f(C(t)\cdot)\|_{Lq2(Ek;w)}\\ &\preceq \|b\|_{CMO^q(\mathbb{Q}_p^n,w)}\,\|f\|_{L^{q_1}(||C(t)||B_k;w)}\left(|\det C^{-1}(t)|\,||C(t)||^Q\right)^{\frac{1}{q_1}}\ \frac{w(B_k)^{1/q_2}}{w(||C(t)||B_k)^{1/q_1}}\end{aligned}$$

Hence, we obtain the following estimate for P_1:

$$P_1\preceq \|b\|_{CMO^q(\mathbb{Q}_p^n,w)}\int_{\mathbb{Q}_p^n}\frac{\eta(t)}{|y|_h^Q}\left(|\det C^{-1}(t)|\,||C(t)||^Q\right)^{\frac{1}{q_1}}\ \frac{w(B_k)^{1/q_2}}{w(||C(t)||B_k)^{1/q_1}}\ \|f\|_{L^{q_1}(||C(t)||B_k;w)}\,dt$$

Next, we use the estimate provided by P_2 to fix

$$P_2=\int_{\mathbb{Q}_p^n}\frac{\eta(t)}{|y|_h^Q}\left\|(b(C(t).)-b_{\|C(t)\|B_k})f(C(t).)\right\|_{L^{q_2}(E_k,w)}\,dt$$

Since $s=q_2r'$,therefore, we infer from (3.2) that

$$\begin{aligned}&\left\|(b(C(t)\cdot)-b_{\|C(y)\|B_k})f(C(t)\cdot)\right\|_{L^{q_2}(E_k,w)}\\ &\preceq |B_k|^{-1/s}w(B_k)^{1/q_2}\left\|(b(C(t)\cdot)-b_{\|C(t)\|B_k})f(C(t)\cdot)\right\|_{L^s(E_k)}\end{aligned}\tag{3.6}$$

Using H¨older's inequality, Proposition 2.2, and the change of variables formula, we have

$$\begin{aligned}&\left\|(b(C(t)\cdot)-b_{\|C(t)\|B_k})f(C(t)\cdot)\right\|_{L^s(E_k,w)}\\ &=|detC^{-1}(t)|^{1/s}\Big(\int_{C(t)B_k}|(b(x)-b_{||C(t)||B_k})f(x)|^s dx\Big)^{1/s}\preceq |detC^{-1}(t)|^{1/s}|||C(t)||B_k|^{1/s}\\ &\qquad\Big(\frac{1}{w(||C(t)||B_k}\int_{||C(t)||B_k}|(b(x)-b_{||C(t)||B_k})f(x)|^s w(x)dx\Big)^{1/s}\end{aligned}\tag{3.7}$$

$$\preceq |detC{-}1(t)|1/s|Bk|1/s||C(t)||Q1/sw(||C(t)||Bk){-}1/s$$

$$\times(\mathrm{R}||C(t)||Bk\,|b(x)-b||C(t)||Bk|qw(x)dx)1/q(\mathrm{R}||C(t)||Bk\,|f(x)|q1w(x)dx)1/q1$$

$$\preceq |detC^{-1}(t)|^{1/s}|B_k|^{1/s}||C(t)||^{Q1/s}w(||C(t)||B_k)^{-1/q1}||f||_{L}q_1(||C(t)||B_k;w)||b||_{CMO}q(_{Q}np;w)$$

The following form has been assumed by the expression for P_2 by virtue of (3.6) and (3.7):

$$P_2\preceq \|b\|_{CMO^q(\mathbb{Q}_p^n,w)}\int_{\mathbb{Q}_p^n}\frac{\eta(t)}{|y|_h^Q}\left(|\det C^{-1}(t)|\,||C(t)||^Q\right)^{\frac{1}{s}}\ \frac{w(B_k)^{1/q_2}}{w(||C(t)||B_k)^{1/q_1}}\ \|f\|_{L^{q_1}(||C(t)||B_k;w)}\,dt$$

Now, the estimation of P_3, given by

https://doi.org/10.62500/icrtsda.1.1.52

$P_3 = \int_{\mathbb{Q}_p^n} \frac{\eta(t)}{|t|_h^Q} ||fC(t).)||_{Lq_2(E_k)} |b_{B_k} - b_{||C(t)||B_k}| dt,$

requires the bounds for $||fC(t).)||_{Lq2(Ek)}$ and $|b_{Bk} - b_{||C(t)||Bk}|$.

First, we suppose that $||fC(t).)||_{Lq2(Ek)}$. In view of the condition $s = q_2 r'$, we use the H¨older inequality and the reverse H¨older condition to obtain

$$\begin{aligned} ||fC(t).)||_{Lq2(Ek,w)} &\leq \Big(\int_{B_k} |f(C(t)x)|^{q2} w(x)dx \Big)^{1/q2} \\ &\leq \Big(\int_{Bk} |f(C(t)x)|^s dx \Big)^{1/s} \Big(\int_{Bk} w(x)^r dx \Big)^{1/rq2} \qquad (3.8) \\ &\preceq |Bk|^{1/s} w(Bk)^{1/q2} ||fC(t).)||_{Ls(Bk)} \end{aligned}$$

Moreover, inequality (3.4) and the constraint $1/s = 1/q + 1/q_1$ enable us to write

$$\begin{aligned} ||fC(t).)||_{Ls(Bk)} = |B_k|^{1/q} ||fC(t).)||_{Lq1(Bk)} &\preceq |B_k|^{1/s} (|\det C^{-1}(t)|||C(t)||^Q)^{1/q1} \\ & w(||C(t)||B_k)^{-1/q1} \, ||f||_{Lq1}(||C(t)||B_k;w) \qquad (3.9) \end{aligned}$$

We replace the result in the formula for P_3 by combining inequalities (3.8) and (3.9), which now becomes

$$P_3 \preceq \int_{\mathbb{Q}_p^n} \frac{\eta(t)}{|t|_h^Q} \left(|\det C^{-1}(t)| \, ||C(t)||^Q \right)^{\frac{1}{q_1}} \frac{w(B(0,2^k))^{1/q_2}}{w(||C(t)||B_k)^{1/q_1}} \, \|f\|_{L^{q_1}(w(||C(t)||B_k),w)}$$

$$|b_{B_k} - b_{||C(t)||B_k}| dt$$

Now, it turns to bound $|b_{Bk} - b_{||C(t)||Bk}|$.In order to do this, we divided the integral as follows:

$$P3 \preceq \mathrm{R}||C(t)||<1 \, |bBk - b||C(t)||Bk|\psi(t)dt + \mathrm{R}||C(t)||\geq 1 \, |bBk - b||C(t)||Bk|\psi(t)dt = P31 + P32$$

where, for convenience use, we applied the following notation:

$$\psi(t) = \frac{\eta(t)}{|y|_h^Q} \left(|\det C^{-1}(t)| \, ||C(t)||^Q \right)^{\frac{1}{q_1}} \frac{w(B(0,2^k))^{1/q_2}}{w(||C(t)||B_k)^{1/q_1}} \, \|f\|_{L^{q_1}(||C(t)||B_k;w)}$$

Additional integral decomposition for P_{31} generates:

$$P_{31} = \sum_{j=0}^{\infty} \int_{2^{-j-1} \leq ||C(t)|| < 2^{-j}} \psi(t) \{ \sum_{i=1}^{j} |b_{2^{-i}B_k} - b_{2^{-i+1}B_k}| + |b_{2^{-j}B_k} - b_{||C(t)||B_k}| \} dt$$

Using Proposition 2.2, the first expression contained in curly brackets can be essentially represented in the following way:

https://doi.org/10.62500/icrtsda.1.1.52

$$
\begin{aligned}
|b_{2^{-i}B_k} - b_{2^{-i+1}B_k}| &\leq \frac{1}{|2^{-i}B_k|}\int_{2^{-i}B_k}|b(t) - b_{2^{-i+1}B_k}|dt \\
&\leq \frac{1}{w(2^{-i}B_k)}\int_{2^{-i}B_k}|b(t) - b_{2^{-i+1}B_k}|w(t)dt \\
&\leq \frac{1}{w(2^{-i}B_k)}[\int_{2^{-i+1}B_k}|b(t) - b_{2^{-i+1}B_k}|^q w(t)dt]^{1/q}[\int_{2^{-i+1}B_k} w(t)dt]^{1/q'} \\
&\leq \frac{w(2^{-i+1}B_k)}{w(2^{-i}B_k)}[\frac{1}{w(2^{-i+1}B_k)}\int_{2^{-i+1}B_k}|b(t) - b_{2^{-i+1}B_k}|^q w(t)dt]^{1/q} \\
&\preceq ||b||_{CMO^q(\mathbb{Q}_p^n;w)}
\end{aligned}
$$

Similarly, In the expression of P_{31}, for the second term inside the curly brackets, we have

$$|b2^{-j}B_k - b||C(t)||B_k| \preceq ||b||CMO^q(\mathrm{Q}^n{}_p;w)$$

Therefore, we complete the estimation of P_{31} by writing

$P_{31} \preceq ||b||_{CMO^q(\mathbb{Q}_p^n;w)} \sum_{j=0}^{\infty}\int_{2^{-j-1}\leq||C(t)||<2^{-j}} \psi(t)(j+1)dt \preceq ||b||_{CMO^q(\mathbb{Q}_p^n;w)}$

$\int_{||C(t)||<1}\psi(t)log\frac{2}{||C(t)||}dt$

Similarly, the integral P_{32} yields us with

$$
\begin{aligned}
P_{32} &= \int_{||C(t)||\geq 1} \psi(t)|b_{Bk} - b_{\|}C(t)_{\|}B_k|dt \\
&= \sum_{j=0}^{\infty}\int_{2^j\leq||C(t)||<2^{j+1}} \psi(t)\,\mathrm{X}|b2iBk - b2{-}i{+}1Bk| + |b2j{+}1Bk - b||C(t)||Bk|\;\; dt\, j{=}0 \\
&\preceq ||b||_{CMOq(\mathrm{Q}np;w)} \int_{||C(t)||\geq 1}\psi(t)log2||C(t)||dt
\end{aligned}
$$

A combination of expressions for $P_1, P_2, P_{31} and P_{32}$ gives

$$
\begin{aligned}
||T^b_{\eta,C}f||_{L^{q_2}(E_k,w)} \preceq ||b||_{CMO^q(\mathbb{Q}_p^n;w)} &\int_{\mathbb{Q}_p^n}\frac{\eta(t)}{|y|_h^Q}\left(|\det C^{-1}(t)|\,||C(t)||^Q\right)^{\frac{1}{q_1}} \\
&\times (1 + |detC^{-1}(y)|^{1/q}||C(t)||^{Q/q})\frac{w(B(0,2^k))^{1/q_2}}{w(||C(t)||B_k)^{1/q_1}}\,\|f\|_{L^{q_1}(||C(t)||B_k;w)} \\
&\times max\{log\frac{2}{||C(t))||}, log(2||C(t)||)\}dt
\end{aligned}
$$

In view of the concept of the Herz space, factors with index k in the equation of $\psi(t)$ are crucial. Therefore, in order to proceed and avoid repeating extraneous

https://doi.org/10.62500/icrtsda.1.1.52

aspects of the Herz space, we must modify and rename the equation for ψ. Thus, we will use this notation in the remaining parts of this work:

$$\psi(t) = \frac{\eta(t)}{|y|_h^Q}\left(|\det C^{-1}(t)|\,||C(t)||^Q\right)^{\frac{1}{q_1}}\left(1+|detC^{-1}(y)|^{1/q}||C(t)||^{Q/q}\right)$$
$$max\{log\frac{2}{||C(t))||}, log(2||C(t)||)\}$$

Then,

$$\|T^b_{\eta,C}f\|_{L^{q_2}(E_k,w)} \leq ||b||_{CMO^q(\mathbb{Q}_p^n;w)} \int_{\mathbb{Q}_p^n} \psi(t)\frac{w(B_k)^{1/q_2}}{w(||C(t)||B_k)^{1/q_1}}\,\|f\|_{L^{q_1}(||C(t)||B_k;w)}\,dt$$

In conclusion, we examine the notion of Herz space and utilize the Minkowski inequality to obtain

$$\begin{aligned}&\left\|T^b_{\phi,C}f\right\|_{K^{\alpha_2,p}_{q_2}(\mathbb{Q}_p^n;w)}\\ &= \left\{\sum_{k=-\infty}^{\infty} w(B_k)^{\frac{\alpha_2}{Q}}\left\|T^b_{\phi,C}f\right\|_{L^p_{q_2}}(E_k;w)\right\}^{1/p}\\ &\preceq ||b||_{CMO^q(\mathbb{Q}_p^n;w)}\int_{\mathbb{Q}_p^n}\psi(t)\{(\sum_{k=-\infty}^{\infty}\frac{w(B_k)^{\gamma_2/Q+1/q_2}}{w(||C(t)||B_k)^{1/q_1}}\,\|f\|_{L^{q_1}(||C(t)||B_k;w)})^p\}^{1/p}dt\end{aligned} \tag{3.10}$$

The terms inside the curly brackets of inequality (3.10) and inequality (3.9) in [25] are similar; the differences between the two inequality can be found in the integrands outside of the curly brackets and the constant multiple $||b||_{CMO^q(\mathbb{Q}^np;w)}$ outside of the integral. So, inequality (3.10) can be written in the following way:

$$\begin{aligned}&\left\|T^b_{\psi,C}f\right\|_{K^{\gamma_2,p}_{q_2}(\mathbb{Q}_p^n;w)}\\ &\preceq ||b||_{CMO^q(\mathbb{Q}_p^n;w)}\sum_{j=-\infty}^{\infty}\int_{2^{j-1}<||C(t)||\leq 2^j}\psi(t)\{[\sum_{j=-\infty}^{\infty}[(\frac{w(B_k)}{w(B_{k+j})})^{\gamma_1/Q+1/q_1}\\ &\qquad\times\sum_{l=-\infty}^{j}[(\frac{w(B_{k+j})}{w(B_{k+l})})^{\gamma_1/Q}w(B_{k+l})^{\gamma_1/Q\|f\|_{L^{q_1}(E_{k+l};w)}}]^p\}^{1/p}dt\end{aligned} \tag{3.11}$$

where the final inequality is obtained by using the condition $\frac{\gamma_1}{Q}+\frac{1}{q_1}=\frac{\gamma_1}{Q}+\frac{1}{q_2}$. We apply Proposition 2.1 to have $l \leq j$ and $\gamma_1 < 0$ under the given conditions.

$$\frac{w(B_{k+j})}{w(B_{k+l})})^{\gamma_1/Q} \preceq \frac{|B_{k+j}|}{|B_{k+l}|}^{\gamma_1(\delta-1)/(Q\delta)} = 2^{(j-l)\gamma_1(\delta-1)/\delta} \tag{3.12}$$

for any $1 < \delta < r_w$.

In proposition 2.1, if $\frac{1}{q_1}+\frac{\gamma_1}{Q} \geq 0$, then

$$\frac{w(B_k)}{w(B_{k+j})})^{\gamma_1/Q+1/q_1} \preceq \begin{cases}\{2^{-jQ(\gamma_1/Q+1/q_1)}, & \text{if } j\leq 0,\\ 2^{-jQ(\gamma_1/Q+1/q_1)(\delta-1)/\delta} & \text{if } j>0,\end{cases} \tag{3.13}$$

and if $\frac{\gamma_1}{Q}+\frac{1}{q_1} < 0$, then

$$\frac{w(B_k)}{w(B_{k+j})})^{\gamma_1/Q+1/q_1} \preceq \begin{cases}\{2^{-jQ(\gamma_1/Q+1/q_1)(\delta-1)/\delta} & \text{if } j\leq 0,\\ 2^{-jQ(\gamma_1/Q+1/q_1)}, & \text{if } j>0,\end{cases} \tag{3.14}$$

for any $1 < \delta < r_w$.

https://doi.org/10.62500/icrtsda.1.1.52

Thus,for $\frac{1}{q_1} + \frac{\gamma_1}{Q} \geq 0$,, from inequalities (3.11)–(3.13), for any $1 < \delta < r_w$,we have

$$\begin{aligned}\left\|T^b_{\psi,C}f\right\|_{K^{\gamma_2,p}_{q_2}(\mathbb{Q}^n_p;w)} &\preceq \|b\|_{CMO^q(\mathbb{Q}^n_p;w)} \sum_{j=-\infty}^{\infty} \int_{2^{j-1}<||C(t)||\leq 2^j} \psi(t)||C(t)||^{-\gamma_1 - Q/q_1} \\ &\times \sum_{l=-\infty}^{j} 2^{\gamma_1(j-1)(\delta-1)/\delta} \{ \sum_{k=-\infty}^{\infty} w(B_{k+l})^{\gamma_1 p/Q} \|f\|_{L^{q_1}(E_{k+l};w)} \}^{1/p} dt \\ &+ \|b\|_{CMO^q(\mathbb{Q}^n_p;w)} \sum_{j=-1}^{\infty} \int_{2^{j-1}<||C(t)||\leq 2^j} \psi(t)||C(t)||^{\gamma_1 + Q/q_1(\delta-1)/\delta}\end{aligned}$$

If we swap out $\psi(t)$ for its value in the inequality above, we obtain

$$\begin{aligned}\left\|T^b_{\psi,C}f\right\|_{K^{\gamma_2,p}_{q_2}(\mathbb{Q}^n_p;w)} &\preceq \|b\|_{CMO^q(\mathbb{Q}^n_p;w)} \|f\|_{L^{q_1}(E_{k+l};w)} \\ &\times \int_{||C(t)||<1} \frac{|\eta(t)|}{|y|^Q_h} (1 + |detC^{-1}(t)|^{\frac{1}{q}} ||C(t)||^{\frac{Q}{q}}) |detC^{-}1(t)|^{\frac{1}{q_1}} ||C(t)||^{-\gamma_1} log \frac{2}{||C(t)||} dt \\ &+ \int_{||C(t)||<1} \frac{|\eta(t)|}{|y|^Q_h} (1 + |detC^{-1}(t)|^{\frac{1}{q}} ||C(t)||^{\frac{Q}{q}}) \\ &\times |detC^{-}1(t)|^{\frac{1}{q_1}} ||C(t)||^{Q/q_1 - (\gamma_1 + Q/q_1)(\delta-1)/\delta} log 2||C(t)||dt\end{aligned}$$

This complete Theorem 3.1's proof. **Proof of Theorem 3.1**

Following the proof of Theorem 3.1, we write:

$\|T_{\eta,C}{}^b f\|_{Lq_2(E_k,w)} \leq I1 + I2 + I3,$

The previous theorem states that $I_1, I_2 and I_3$ are equal to P_1, P_2 and P_3. However, instead of $w(.)$, $u(.) = |.|^{\gamma}_h$ has been used. Next, we get by applying Holder inequality and the change of variables.

$$\begin{aligned}I_1 &\leq \int_{\mathbb{Q}^n_p} \frac{|\eta(t)|}{|t|^Q_h} \left(\int_{E_k} |(b(x) - b_{B_k})|^q u(x)dx \right)^{1/q} \left(\int_{E_k} |(fC(t)x|^{q_1} u(x)dx \right)^{1/q_1} dt \\ &\leq u(B_k)^{1/q} \|b\|_{CMO^q(\mathbb{Q}^n_p;u)} \int_{\mathbb{Q}^n_p} \frac{|\eta(t)|}{|t|^Q_h} |detC^{-1(t)}|^{1/q_1} \left(\int_{C(t)E_k} |f(z)|^{q_1} u(C^{-1}(t)z)dz \right)^{1/q_1} dt\end{aligned}$$

Using Proposition 2.3, we get

$$\begin{aligned}l_1 &\leq u(B_k)^{1/q} \|b\|_{CMO^q(\mathbb{Q}^n_p;u)} \int_{\mathbb{Q}^n_p} \frac{|\eta(t)|}{|t|^Q_h} |detC^{-1(t)}|^{1/q_1} \left(\int_{C(t)E_k} |f(x)|^{q_1} G(C^{-1}(t), \beta/q_1) u(x)dx \right)^{1/q_1} dt \\ &\leq u(B_k)^{1/q} \|b\|_{CMO^q(\mathbb{Q}^n_p;u)} \int_{\mathbb{Q}^n_p} \frac{|\eta(t)|}{|t|^Q_h} |detC^{-1}(t)|^{1/q_1} G(C^{-1}(t), \beta/q_1) \|f\|_{L^{q_1}(||C(t)||B_k;u)} dt.\end{aligned}$$

Next, the expression for I_2 can be written as:

$$I_2 = \int_{\mathbb{Q}^n_p} \frac{|\eta(t)|}{|t|^Q_h} ||(b(C(t).) - b_{||C(t)||B_k}) f(C(t).)||_{L^{q_2}(E_k;u)} dt. \quad (3.15)$$

Changing variables and using the condition $q_2/q + q_2/q_1 = 1$, we get

$||(b(C(t).) - b||C(t)||Bk)f(C(t).)||Lq2(Ek;u)$

https://doi.org/10.62500/icrtsda.1.1.52

$$= ({}^{\mathrm{R}}{}_{E}k\ |(b(C(t)x) - b_{\|C(t)\|Bk})f(C(t)x)|^{q2}u(x)dx)^{1/q2} = |detC^{-1}(t)|^{1/q2}$$

$$G(C-1(t),\beta/q2)(\mathrm{R}C(t)Ek\ |(b(x) - b\|C(t)\|Bk)f(x)|q2u(x)dx)1/q2 \quad (3.16)$$

$$\leq |detC-1(t)|1/q2G(C-1(t),\beta/q2)(\mathrm{R}C(t)Ek\ |(b(x) - b\|C(t)\|Bk)|qu(x)dx)1/q$$

$$(\mathrm{R}C(t)Ek\ |f(x)|q1u(x)dx)1/q1$$

$$= |detC^{-1}(t)|^{1/q2}G(C^{-1}(t),\beta/q_2)u(\|C(t)\|B_k)^{1/q}\|b\|_{CMO}q(\mathrm{Q}np;u)\|f\|_{L}q_1(\|C(t)\|B_k;u)$$

It is easy to see that $u(\|C(t)\|B_k) = \|C(t)\|^{Q+\beta}u(B_k)$.Inequality (3.15) becomes the following using (3.16):

$$I_2 = u(B_k)^{1/q}||b||_{CMO^q(\mathbb{Q}_p^n;u)} \int_{\mathbb{Q}_p^n} \frac{|\eta(t)|}{|t|_h^Q}|detC^{-1}(t)|^{1/q_2}G(C^{-1}(t),\beta/q)G(C^{-1}(t),\beta/q_1)$$

$$\|C(t)\|^{(Q+\beta)/q}\|f\|_{L}q_1(C(t)E_k;u)dt$$

The estimation of I_3 is still awaiting. Applying the H¨older inequality and Proposition 2.3 to change the variables, we obtain

$$I_3 = \int_{\mathbb{Q}_p^n} \frac{|\eta(t)|}{|t|_h^Q} \left\|(b_{B_k} - b_{\|C(t)\|B_k})f(C(t).)\right\|_{L^{q_2}(E_k,u)}\ dt$$

$$= \int_{\mathbb{Q}_p^n} \frac{|\eta(t)|}{|t|_h^Q}||f(C(t)x)||_{L^{q_2}(E_k,u)}|b_{B_k} - b_{\|C(t)\|B_k}|dt$$

$$\leq \int_{\mathbb{Q}_p^n} \frac{|\eta(t)|}{|t|_h^Q}|detC^{-1}(t)|^{1/q_2}G(C^{-1}(t),\beta/q_2)u(\|C(t)\|B_k)^{1/q}||f||_{L^{q_1}(C(t)E_k;u)} \quad |b_{B_k} - b_{\|C(t)\|B_k}|dt.$$

Next, if $\|C(t)\| < 1$, then there exists an integer $j \geq 0$,such that

$2^{-j-1} \geq \|C(t)\| < 2^{-j}$,

Therefore,

$$|b_{B_k} - b_{\|C(t)\|B_k}| \leq \sum_{i=1}^{j} |b_{2^{-i}B_k} - b_{2^{-i+1}B_k}| + |b_{2^{-j}B_k} - b_{C(t)B_k}|$$

$$\leq \|b\|_{CMO^q(\mathbb{Q}_p^n;u)}\ log\frac{2}{\|C(t)\|}$$

Similarly, for$\|C(t)\| \geq 1$, we have

$$|bBk - b\|C(t)\|Bk| \leq \|b\|CMOq(\mathrm{Q}np;u)\ log2\|C(t)\|$$

Hence,

$$I_3 \preceq u(B_k)^{1/q}||b||_{CMO^q(\mathbb{Q}_p^n;u)} \int_{\mathbb{Q}_p^n} \frac{|\eta(t)|}{|t|_h^Q}|detC^{-1}(t)|^{1/q_1}G(C^{-1}(t),\beta/q_2)$$

$$\times G(C^{-1}(t),\beta/q)||C(t)||^{(Q+\beta)/q}(log\tfrac{2}{\|C(t)\|}\chi_{[\|C(t)\|<1]}+log2\|C(t)\|_{\chi_{\|C(t)\|\geq 1}})||f||_{L^{q_1}(C(t)E_k;u)}dt$$

Thus, combining I_1,I_2*and*I_3, we get

$$\left\|T^b_{\eta,C}\right\|_{L^{q_2}(E_k;v)} \preceq u(B_k)^{1/q}||b||_{CMO^q(\mathbb{Q}_p^n;u)} \int_{\mathbb{Q}_p^n} \frac{|\eta(t)|}{|t|_h^Q}|detC^{-1}(t)|^{1/q_1}$$

$$\times\ G(C^{-1}(t),\beta/q_1)(1 + |detC^{-1}(t)|^{1/q}G(C^{-1}(t),\beta/q)||C(t)||^{(Q+\beta)/q}$$

$$\times\ (log\frac{2}{\|C(t)\|}\chi_{[\|C(t)\|<1]} + log2\|C(t)\|_{\chi_{\|C(t)\|\geq 1}})||f||_{L^{q_1}(C(t)E_k;u)}dt.) \quad (3.17)$$

https://doi.org/10.62500/icrtsda.1.1.52

Hence, the definition of E_k and (2.2) imply that

$$C(t)E_k \subset \{x : \|C^{-1}(t)\|^{-1}2^{k-1} < |x|_h < \|C(t)\|2^k\}.$$

Now, there exists an integer l such that for any $t \in supp(\phi)$, we have

$$2^l < \|C^{-1}(t)\|^{-1} < 2^{l+1}. \tag{3.18}$$

Finally, the inequality $\|C^{-1}(t)\|^{-1} \leq \|C(t)\|$ implies that there exists a nonnegative integer m satisfying:

$$2^{l+m} < \|C(t)\| < 2^{l+m+1}. \tag{3.19}$$

We infer from (3.18) and (3.19) that:

$$log_2(\|C(t)\|\|C^{-1}(t)\|/2) < m < log_2(2\|C(t)\|\|C^{-1}(t)\|).$$

Therefore,

$$C(t)Ek \subset \{x : 2l+k-1 < |x|h < 2k+l+m+1\}.$$

Hence,

$$\|f\|_{L^{q_1}(C(t)E_k;u)} \leq \sum_{j=1}^{l+m+1} \|f\|_{L^{q_1}(E_{k+j};u)}. \tag{3.20}$$

When inequality (3.20) is combined with inequality (3.17), we get

$$\left\|T^b_{\eta,C}\right\|_{L^{q_2}(E_k;u)} \preceq u(B_k)^{1/q} \|b\|_{CMO^q(\mathbb{Q}_p^n;u)} \int_{\mathbb{Q}_p^n} \theta(t) \sum_{j=1}^{l+m+1} \|f\|_{L^{q_1}(E_{k+j};u)}\, dt. \tag{3.21}$$

where

$$\theta(t) = \frac{|\psi(t)|}{|t|_h^Q} |detC^{-1}(t)|^{1/q_1} \left(\log \frac{2}{\|C(t)\|\chi_{\|C(t)\|<1}} + \log 2\|C(t)\|\chi_{[\|C(t)\|<1]}\right)$$
$$\times G(C^{-1}(t), \beta/q_1)(1 + |detC^{-1}(t)|^{1/q} G(C^{-1}(t), \beta/q)\|C(t)\|^{(Q+\beta)/q}.$$

Using the Minkowski inequality and the condition $\frac{\gamma_2}{Q} + \frac{1}{q} = \frac{\gamma_1}{Q}$ yields

$$\left\|T^b_{\eta,C}\right\|_{K^{\gamma_2,p}_{q_2}(\mathbb{Q}_p^n;u)}$$
$$\preceq \|b\|_{CMO^q(\mathbb{Q}_p^n;u)} \{\sum_{k=-\infty}^{\infty} (u(B_k)^{1/q+\gamma_2/Q} \int_{\mathbb{Q}_p^n} \theta(t) \sum_{j=1}^{l+m+1} \|f\|_{L^{q_1}(E_k;u)} dt)^p\}^{1/p}$$
$$\preceq \|b\|_{CMO^q(\mathbb{Q}_p^n;u)} \int_{\mathbb{Q}_p^n} \theta(t) \sum_{j=1}^{l+m+1} u(B_{-j})^{\gamma_1/Q} \{\sum_{k=-\infty}^{\infty} (u(B_{k+j})^{\gamma_1/Q} \|f\|_{L^{q_1}(E_{k+j};u)})^p\}^{1/p} dt$$
$$\preceq \|b\|_{CMO^q(\mathbb{Q}_p^n;u)} \|f\|_{K^{\gamma_1,p}_{q_1}(\mathbb{Q}_p^n;u)} \int_{\mathbb{Q}_p^n} \theta(t) \sum_{j=1}^{l+m+1} u(B_{-j})^{\gamma_1/Q}$$

It is easy to see that

$$\sum_{j=1}^{l+m+1} u(B_{-j})^{\gamma_1/Q} \simeq sum_{j=1}^{l+m+1} 2^{-j\gamma_1(Q+\beta)/Q}.$$

Next, for $\gamma_1 = 0$,

$$\gamma_1 \overset{j}{\neq} 0$$
$$\sum_{=1}^{l+m+1} 2^{-j\gamma_1(Q+\beta)/Q} = m + 2 \preceq 1 + log_2(2\|C(t)\|\|C^{-1}(t)\|),$$

for

$$-1 \quad \gamma_1(Q+\beta)/Q$$

https://doi.org/10.62500/icrtsda.1.1.52

$$^{P}l_j+_{=1}m+1\ 2-j\gamma_1(Q+\beta)/Q \simeq 2-l\gamma_1(Q+\beta)/Q\|C\quad(t)\|\qquad,\quad \text{if } \gamma_1>0,\quad (\\ \leq \qquad\qquad \|C-1(t)\|-\gamma_1(Q+\beta)/Q,\text{if } \gamma_1<0,$$

$$= G(C^{-1}(t),\gamma_1(Q+\beta)/Q).$$

Therefore,

$$\left\|T^b_{\eta,C}\right\|_{K^{\gamma_2,p}_{q_2}(\mathbb{Q}^n_p;u)}$$

$$\preceq \|b\|_{CMO^q(\mathbb{Q}^n_p;u)}\|f\|_{K^{\gamma_1,p}_{q_1}(\mathbb{Q}^n_p;u)}\begin{cases}\int_{\mathbb{Q}^n_p}\theta(t)(1+log_2(2||C(t)||||C^{-1}(t)||))dt, & \text{if } \gamma_1=0,\\ \int_{\mathbb{Q}^n}\theta(t)G(C^{-1}(t),\gamma_1(Q+\beta)/Q)dt, & \text{if } \gamma_1\not=0,\end{cases}$$

$$p$$

$$= K3\|b\|CMOq(\mathrm{Q}np;u)\ \|f\|Kq^{\gamma}11^{,p}(\mathrm{Q}np;u)\ .$$

Thus, we completed the Theorem's proof.

4. Conclusion

In this article, we proved the boundedness property of the commutator associated with the matrix Hausdorff operator within the context of the Heisenberg group, focusing specifically on the Herz space and p-adic space. Exploring potential avenues for future research, the aim to extend their findings to include the boundedness analysis of the same operator within weighted Herz spaces.

References

[1] Ajaib, A., & Hussain, A. (2020). Weighted CBMO estimates for commutators of matrix Hausdorff operator on the Heisenberg group. Open Mathematics, 18(1), 496–511.

[2] Hussain, A., & Sarfraz, N. (2019). The Hausdorff operator on weighted p-adic Morrey and Herz type spaces. p-Adic Numbers, Ultrametric Analysis and Applications, 11, 151-162.

[3] Sarfraz, N., & Hussain, A. (2019). Estimates for the commutators of p-adic Hausdorff operator on Herz-Morrey spaces. Mathematics, 7(2), 127.

[4] Lerner, A. K., & Liflyand, E. (2007). Multidimensional Hausdorff operators on the real Hardy space. Journal of the Australian Mathematical Society, 83(1), 79-86.

[5] Liflyand, E. (2008). Boundedness of multidimensional Hausdorff operators on $H^1(R^n)$ Acta Sci. Math.(Szeged), 74(3-4), 845.

[6] Liflyand, E. (2018). Hausdorff operators in Hp spaces, 0¡ p.

[7] Chen, J., Fan, D., & Li, J. (2012). Hausdorff operators on function spaces. Chinese Annals of Mathematics, Series B, 33(4), 537-556..

[8] Chen, J. C., Fan, D. S., & Zhang, C. J. (2012). Boundedness of Hausdorff operators on some product Hardy type spaces. Applied Mathematics-A Journal of Chinese Universities, 27(1), 114-126.

https://doi.org/10.62500/icrtsda.1.1.52

[9] Chen, J., & Zhu, X. (2014). Boundedness of multidimensional Hausdorff operators on H1 (Rn). Journal of Mathematical Analysis and Applications, 409(1), 428-434.

[10] Burenkov, V. I., & Liflyand, E. R. (2017). On the boundedness of Hausdorff operators on Morrey-type spaces. Eurasian Mathematical Journal, 8(2), 97-104.

[11] Damtew, B. M. (2016). Boundedness of multidimensional Hausdorff operator on HardyMorrey and Besov-Morrey spaces. Journal of Inequalities and Applications, 2016, 1-11.

[12] Ho, K. P. (2016). Hardy-Littlewood-P´olya inequalities and Hausdorff operators on block spaces. Math. Inequal. Appl, 19(2), 697-707.

[13] Espinoza-Villalva, C., & Guzma´n-Partida, M. (2016). Continuity of Hardy type operators on rectangularly defined spaces. Journal of Mathematical Analysis and Applications, 436(1), 29-38.

[14] Hussain, A., & Gao, G. (2013). Multidimensional Hausdorff operators and commutators on Herz-type spaces. Journal of Inequalities and Applications, 2013, 1-12.

[15] Zhao, G., & Lou, Q. (2018). Hausdorff Operators on Modulation Spaces M_{p,p^s}. Journal of Function Spaces, 2018, 1-7.

[16] Zhao, G., & Guo, W. (2019). Hausdorff operators on Sobolev spaces W k, 1. Integral Transforms and Special Functions, 30(2), 97-111..

[17] Gu¨rbu¨z, F. (2017). Some estimates for generalized commutators of rough fractional maximal and integral operators on generalized weighted Morrey spaces. Canadian Mathematical Bulletin, 60(1), 131-145.

[18] Gurbuz, F. (2016). Multi-sublinear operators generated by multilinear fractional integral operators and commutators on the product generalized local Morrey spaces. arXiv preprint arXiv:1602.07468.

[19] Gurbuz, F. (2020). Generalized weighted Morrey estimates for Marcinkiewicz integrals with rough kernel associated with Schrodinger operator and their commutators. CHINESE ANNALS OF MATHEMATICS SERIES B, 41(1), 77-98.

[20] Hussain, A., & Ajaib, A. (2018). Some results for the commutators of generalized Hausdorff operator. arXiv preprint arXiv:1804.05309.

[21] Hussain, A., & Gao, G. L. (2014). Some new estimates for the commutators of n-dimensional Hausdorff operator. Applied Mathematics-A Journal of Chinese Universities, 29, 139-150.

[22] Wu, X. (2015). Necessary and sufficient conditions for generalized Hausdorff operators and commutators. Annals of Functional Analysis, 6(3), 60-72.

[23] Hussain, A., & Ahmed, M. (2017). Weak and strong type estimates for the commutators of Hausdorff operator. Math. Inequal. Appl, 20(1), 49-56.

[24] Chen, J. C., Fan, D. S., & Wang, S. L. (2013). Hausdorff operators on Euclidean spaces.
Applied Mathematics-A Journal of Chinese Universities, 28(4), 548-564.

https://doi.org/10.62500/icrtsda.1.1.52

[25] Liflyand, E. R. (2013). Hausdorff operators on Hardy spaces. Eurasian Mathematical Journal, 4(4), 101-141.

[26] Vladimirov, V. S., Volovich, I. V., & Zelenov, E. I. (1994). p-adic Analysis and Mathematical Physics.

[27] Liflyand, E., & Mo´ricz, F. (2000). The Hausdorff operator is bounded on the real Hardy space H^1(R). Proceedings of the American Mathematical Society, 128(5), 1391-1396.

[28] Liflyand, E., & Miyachi, A. (2009). Boundedness of the Hausdorff operators in H^p spaces, 0¡ p¡ 1. Studia Mathematica, 3(194), 279-292.

[29] A. Lerner and E. Liflyand, "Multidimensional Hausdorff operators on the real Hardy spaces," J. Austr. Math. Soc. 83, 79–86 (2007).

[30] Chen, J. C., He, S. Y., & Zhu, X. R. (2017). Boundedness of Hausdorff operators on the power weighted Hardy spaces. Applied Mathematics-A Journal of Chinese Universities, 32, 462-476.

[31] Huy, D. Q., & Ky, L. D. (2017). The multi-parameter Hausdorff operators on H^1 and L^p. arXiv preprint arXiv:1705.02548.

[32] Xiao, J. (2001). Lp and BMO bounds of weighted Hardy–Littlewood averages. Journal of Mathematical Analysis and Applications, 262(2), 660-666.

[33] Chen, J., Dai, J., Fan, D.,& Zhu, X. (2018). Boundedness of Hausdorff operators on Lebesgue spaces and Hardy spaces. Science China Mathematics, 61, 1647-1664.

[34] Liflyand, E., & Miyachi, A. (2019). Boundedness of multidimensional Hausdorff operators in H^p spaces, $0 < p < 1$. *Transactions of the American Mathematical Society*, **371**(7), 4793-4814.

[35] Liflyand, E. R. (2013). Hausdorff operators on Hardy spaces. Eurasian Mathematical Journal, 4(4), 101-141.

[36] Burenkov, V. I., & Liflyand, E. R. (2017). On the boundedness of Hausdorff operators on Morrey-type spaces. Eurasian Mathematical Journal, 8(2), 97-104.

[37] D. Fan and F. Zhao, "Sharp constants for multivariate Hausdorff q-inequalities," J. Aust. Math. Soc. 106 (2), 274–286 (2018).

[38] Hussain, A., & Ajaib, A. (2018). Some weighted inequalities for Hausdorff operators and commutators. Journal of Inequalities and Applications, 2018, 1-19.

[39] Ruan, J., Fan, D., & Wu, Q. (2017). Weighted Herz space estimates for Hausdorff operators on the Heisenberg group.

[40] Volosivets, S. S. (2017). Weak and strong estimates for rough Hausdorff type operator defined on p-adic linear space. p-Adic Numbers, Ultrametric Analysis and Applications, 9, 236-241.

[41] Volosivets, S. S. (2010). Multidimensional Hausdorff operator on p-adic field. P-Adic Numbers, Ultrametric Analysis, and Applications, 2, 252-259.

https://doi.org/10.62500/icrtsda.1.1.52

[42] Volosivets, S. S. (2013). Hausdorff operators on p-adic linear spaces and their properties in Hardy, BMO, and H¨older spaces. Mathematical Notes, 93(3), 382-39

https://doi.org/10.62500/icrtsda.1.1.52

DOUBLE GENERAL INTEGRAL TRANSFORM FOR SOLVING HYPERBOLIC BOUNDARY VALUE PROBLEM

https://doi.org/10.62500/icrtsda.1.1.53

Proc. 1st International Conference on Recent Trends in Statistics and Data Analytics

Air University Islamabad, Pakistan – May 9, 2024, Vol. 1, pp. 520-525

DOUBLE GENERAL INTEGRAL TRANSFORM FOR SOLVING HYPERBOLIC BOUNDARY VALUE PROBLEM

AMNA AJAIB,AYESHA BIBI*, and AYESHA ZAHID
DEPARTMENT OF MATHEMATICS, FAZAIA BILQUIS COLLEGE OF EDUCATION FOR WOMEN PAF BASE NUR KHAN, PAKISTAN

Abstract

In this paper, we use formulas and properties of parabolic boundary value problem and implement them to solve hyperbolic boundary value problems using double general integral transform. These problems typically have initial conditions along with boundary conditions specified at different points in the domain. Solving hyperbolic boundary value problems can be challenging due to the complex nature of the equations involved.

1. Introduction

Transforms have been successively used since the 1780s. [7] Many integral transforms such as Laplace transform, Sumudu transform, Aboodh transform, Elzaki transform, Maghoub transform, Natural transform, and Kamal transform have been developed by many academicians to solve Ordinary differential equations, Partial differential equations, Integral equations, Integro-differential equations, system of differential equations, boundary value problems[1].

An Integral transform is a Mathematical technique that converts a given function or data from one domain into another by using integral equations[14]. Integral transforms, help to change the representation of functions, making it easier to analyze complex systems and solve various types of Differential Equations. They often shift the problem from one domain to a different domain, where the analysis or solution may be more convenient[11]. Integral transformations is a really effective way to solve Partial differential equations[2]. Partial differential equation are math tools that help describe a lot of things in physics and other sciences, making them super useful. They're like magic tools that turn complex equations into simpler ones for easier solving[4]. General integral transform is given as:

$$T\{f(t)\} = m(s)\int_0^{\infty} f(t)e^{-n(s)}dt$$

2. Preliminaries

2.1. **Double General Integral Transform.** A double general integral transform is a mathematical operation that converts a two-dimensional function into a different representation, often used for solving complex problems in mathematics and engineering. It is defined as:

Let $f(x,y)$ be an integrable function defined for the variables x and y in the first quadrant $p^1(s)$ 6= 0, $p_2(s)$ 6= 0 and $q_1(s)$, $q_2(s)$ are positive real functions; we define the double general integral transform $T_2\{f(x,y)\}$ by the formula

[1] Department of Mathematics, Fazaia Bilquis College of Education for Woman, PAF NurKhan *Corresponding Author: ayeshaaabibi2002@gmail.com

Key words and phrases. Double General Integral Transform, Ordinary Differential Equation, Partial Differential Equation, Parabolic Boundary Value Problem, Hyperbolic Boundary Value Problem, Inverse Transform.

DOUBLE GENERAL INTEGRAL TRANSFORM FOR SOLVING HYPERBOLIC BOUNDARY VALUE PROBLEM

https://doi.org/10.62500/icrtsda.1.1.53

$$T_2\{f(x,y)\} = m_1(s)m_2(s)\int_0^{\infty}\int_0^{\infty} e^{-(n_1(s)x+n_2(s)y)}f(x,y)dxdy$$

Provided that the integral exists for some $q_1(s)$, $q_2(s)$.

[1]The double general integral transform is a valuable tool for solving boundary value problems in Partial Differential Equations, including elliptic, parabolic, and hyperbolic problems cite4. Researchers are actively exploring different integral transforms to address these issues, and the double general integral transform has been used to solve parabolic boundary value problems, particularly those involving heat equations. [6]This approach has proven to be effective and useful in obtaining solutions for parabolic boundary value problem.

2.2. **Properties of Double General Integral Transform.**

2.2.1. *Linearity Property.* $T_2\{af(x,y) + bg(x,y)\} = aT_2\{f(x,y)\} + bT_2\{g(x,y)\}$

Proof

$L.H.S = T_2\{af(x,y) + bg(x,y)\}$

$= m_1(s)m_2(s)\int_0^{\infty}\int_0^{\infty} e^{-(n_1(s)x+n_2(s)y)}af(x,y)dxdy$

$+ \int_0^{\infty}\int_0^{\infty} e^{-(n_1(s)x+n_2(s)y)}bg(x,y)dxdy)$

$= m_1(s)m_2(s)\int_0^{\infty}\int_0^{\infty} e^{-(n_1(s)x+n_2(s)y)}f(x,y)dxdy$

$+ b\int_0^{\infty}\int_0^{\infty} e^{-(n_1(s)x+n_2(s)y)}g(x,y)dxdy$

$= a(m_1(s)m_2(s)\int_0^{\infty}\int_0^{\infty} e^{-(n_1(s)x+n_2(s)y)}f(x,y)dxdy)$

$+ b(m_1(s)m_2(s)\int_0^{\infty}\int_0^{\infty} e^{-(n_1(s)x+n_2(s)y)}g(x,y)dxdy)$

$= aT_2f(x,y) + bT_2g(x,y)$

$= R.H.S$

2.2.2. *Shifting Property.* If $T_2\{f(x,y)\} = \tau(s)$ then

$T_2\{e^{(ax+by)}f(x,y)\} = \tau(s,a,b) = m_1(s)m_2(s)\int_0^{\infty}\int_0^{\infty} e^{-(n_1(s)+a)x+(n_2(s)+b)y}f(x,y)dxdy$

Proof

$T_2\{e^{(ax+by)}f(x,y)\} = \tau(s,a,b)$

That is $T_2\{e^{-(ax+by)}f(x,y)\} = m_1(s)m_2(s)\int_0^{\infty}\int_0^{\infty} e^{[-(n_1(s)+a)x+(n_2(s)+b)y]}f(x,y)dxdy$

$L.H.S = T_2\{e^{-(ax+by)}f(x,y)\}$

$= m_1(s)m_2(s)\int_0^{\infty}\int_0^{\infty} e^{-(n_1(s)x+n_2(s)y)} + e^{(ax+by)}f(x,y)dxdy$

$= m_1(s)m_2(s)\int_0^{\infty}\int_0^{\infty} e^{-(n^1(s)x+n^2(s)y+ax+by)}f(x,y)dxdy$

https://doi.org/10.62500/icrtsda.1.1.53

$= m_1(s)m_2(s)\int_0^\infty \int_0^\infty e^{-(n_1(s)+a)x+(n_2(s)+b)y} f(x,y)dxdy$
$= R.H.S$

2.2.3. *Change of Scale Property.* If $T_2\{f(x,y)\} = \tau(s)$ then $T_2\{f(ax,by)\} = {}_{ab}^{1}\tau(s,a,b)$

Proof

L.H.S = $T_2\{f(ax,by)\}$

$= T_2\{f(x,y)\} = m_1(s)m_2(s)\int_0^\infty \int_0^\infty e^{-(n_1(s)x+n_2(s)y)} f(ax,by)dxdy$

substituting $ax = u$ and $by = v$ we get $x \to 0$, $u \to 0$ and $y \to 0$, $v \to 0$
also as $x \to \infty$, $u \to \infty$ and $y \to \infty$, $v \to \infty$
$adx = du \Rightarrow dx = \frac{du}{a}$ and $bdy = dv \Rightarrow dy = \frac{dv}{b}$
Put value in above equation

$= m_1(s)m_2(s)\int_0^\infty \int_0^\infty e^{-(n_1(s)\frac{u}{a}+n_2(s)\frac{v}{b})} f(u,v)\frac{du}{a}\frac{dv}{b}$

$= \frac{1}{ab}m_1(s)m_2(s)\int_0^\infty \int_0^\infty e^{-((\frac{n_1(s)}{a})u+(\frac{n_2(s)}{b}v))} f(u,v)dudv$

$= \frac{1}{ab}[m_1(s)m_2(s)\int_0^\infty \int_0^\infty e^{-((\frac{n_1(s)}{a})u+(\frac{n_2(s)}{b}v))} f(u,v)dudv]$

$= \frac{1}{ab}[m_1(s)m_2(s)\int_0^\infty \int_0^\infty e^{-(r_1(s)u+r_2(s)v)} f(u,v)dudv]$

where $r_1(s) = \frac{n_1(s)}{a}$ and $r_2(s) = \frac{n_2(s)}{b}$

$= \frac{1}{ab}\tau(s,a,b)$
$= R.H.S$

3. Proof of the Main Results

We will demonstrate the primary finding from part one in this section. But for this, we need a few helpful theorems[2].

3.1. **Theorem i.** Let $f(x,y)$ be a function of two variables. If the first ordered partial derivative $\frac{\partial f}{\partial x}$ and $\frac{\partial f}{\partial y}$ exists and $f(0,y)$ be given $m_1(s)$,and $n_1(s)$ are positive real functions then

$$T_2\{\frac{\partial f}{\partial x}(x,y)\} = -m_1(s)T\{f(0,y)\} + n_1(s)T_2\{f(x,y)\}$$

where $T\{f(0,y)\}$ is the new general integral transform of the $f(0,y)$.

3.2. **Theorem ii.**Let $f(x,y)$ be a function of two variables. If the first ordered partial derivative $\frac{\partial f}{\partial x}$ and $\frac{\partial f}{\partial y}$ exists and $f(x,0)$ be given.$m_2(s)$ and $n_2(s)$ are positive real functions then

$$T_2\{\frac{\partial f}{\partial y}(x,y)\} = -m_2(s)T\{f(x,0)\} + n_2(s)T_2\{f(x,y)\}$$

where $T\{f(x,0)\}$ is the new general integral transform of the $f(x,0)$.

Function $f(x,y)$	Double General Integral Transform $T_2\{f(x,y)\}$
1	$\frac{m_1(s)m_2(s)}{n_1(s)n_2(s)}$
$e^{(ax+by)}$	$\frac{m_1(s)m_2(s)}{(n_1(s)-a)(n_2(s)-b)}$

DOUBLE GENERAL INTEGRAL TRANSFORM FOR SOLVING HYPERBOLIC BOUNDARY VALUE PROBLEM

https://doi.org/10.62500/icrtsda.1.1.53

$e^{(\iota(ax+by))}$	$\frac{m_1(s)m_2(s)}{(n_1(s)-\iota a)(n_2(s)-\iota b)}$
$\cosh(ax+by)$	$\frac{1}{2}[\frac{m_1(s)m_2(s)}{(n_1(s)-a)(n_2(s)-b)}+\frac{m_1(s)m_2(s)}{(n_1(s)+a)(n_2(s)+b)}]$
$\sinh(ax+by)$	$\frac{1}{2}[\frac{m_1(s)m_2(s)}{(n_1(s)-a)(n_2(s)-b)}-\frac{m_1(s)m_2(s)}{(n_1(s)+a)(n_2(s)+b)}]$
$\cos(ax+by)$	$\frac{1}{2}[\frac{m_1(s)m_2(s)}{(n_1(s)-\iota a)(n_2(s)-\iota b)}+\frac{m_1(s)m_2(s)}{(n_1(s)+\iota a)(n_2(s)+\iota b)}]$
$\sin(ax+by)$	$\frac{1}{2}[\frac{m_1(s)m_2(s)}{(n_1(s)-\iota a)(n_2(s)-\iota b)}-\frac{m_1(s)m_2(s)}{(n_1(s)+\iota a)(n_2(s)+\iota b)}]$
$(xy)^q, q>0$	$\frac{(\Gamma(q+1))^2 m_1(s)m_2(s)}{(n_1(s)n_2(s))^{k+1}}$
$x^p y^q, p>0, q>0$	$\frac{\Gamma(p+1)\Gamma(q+1)(m_1(s)m_2(s))}{(n_1(s))^{p+1}(n_2(s))^{q+1}}$

3.3. **Theorem iii.** Let (x,y) be a function of two variables. If the first and second partial derivative $\frac{\partial f}{\partial x}, \frac{\partial f}{\partial y}, \frac{\partial^2 f}{\partial x^2}$ and $\frac{\partial^2 f}{\partial y^2}$ are exists and $f(0,y), f_x(0,y)$be given. $m_1(s), m_2(s), n_1(s)$ and $n_2(s)$ are positive real functions then

$$T_2\{\frac{\partial^2}{\partial x^2}f(x,y)\} = -m_1(s)[T\{f_x(0,y)\} + n_1(s)T\{f(0,y)\}] + n_1(s)^2 T_2\{f(x,y)\}$$

where,$T\{f_x(0,y)\}, T\{f(0,y)\}$ is the new general integral transform of the $\{f_x(0,y)\}, f(0,y)$ respectively.

3.4. **Theorem iv.** Let (x,y) be a function of two variables. If the first and second ordered partial derivative $\frac{\partial f}{\partial x}, \frac{\partial f}{\partial y}, \frac{\partial^2 f}{\partial x^2}$ and$\frac{\partial^2 f}{\partial y^2}$ are exists and $f(x,0), f_x(0,y)$be given. $m_1(s), m_2(s), n_1(s)$ and $n_2(s)$ are positive real functions then

$$T_2\{\frac{\partial^2}{\partial y^2}f(x,y)\} = -m_2(s)[T\{f_y(x,0)\} + n_2(s)T\{f(x,0)\}] + n_1(s)^2 T_2\{f(x,y)\}$$

where,$T\{f_y(x,0)\}, T\{f(x,0)\}$ is the new general integral transform of the $\{f_y(x,0)\}, f(x,0)$ respectively.

4. Application

The DGIT will be used in this section to address the Hyperbolic Boundary Value Problem[3].

4.1. **Example 1.** $\{\frac{\partial^2 u}{\partial x^2}\} + \{\frac{\partial^2 u}{\partial y^2}\} = 0$ under some restrictions. $u(x,b) = 0$ $u(a,y) = 0$ $u(0,y)$ is equal to 0. and $u(x,0) = \sin x$

Solution

https://doi.org/10.62500/icrtsda.1.1.53

$T_2\{\frac{\partial^2 u}{\partial x^2}\} + T_2\{\frac{\partial^2 u}{\partial y^2}\} = 0$

$L.H.S = T_2\{\frac{\partial}{\partial x}u_x(x,y)\} + T_2\{\frac{\partial}{\partial y}u_y(x,y)\}$

$= -m_1(s)T\{u_x(0,y)\}+n_1(s)T_2\{u_x(x,y)\}-m_2(s)T\{u_y(x,0)\}+n_2(s)T_2\{u_y(x,y)\}$

$= n_1(s)T_2\{u_x(x,y)\}+n_2(s)T_2\{u_y(x,y)\}+n_1(s)T_2\{\frac{\partial u}{\partial x}(x,y)\}+n_2(s)T_2\{\frac{\partial}{\partial y}u(x,y)\}$

$= n_1(s)[-m_1(s)T\{u(0,y)\}+n_1(s)T_2\{u(x,y)\}]+n_2(s)[-m_2(s)T\{u(x,o)\}+ n_2(s)T_2\{u(x,y)\}]$

$= n_1(s)n_1(s)T_2\{u(x,y)\} - n_2(s)m_2(s)T\{sinx\} + n_2(s)n_2(s)T_2\{u(x,y)\} = 0$

$T_2\{u(x,y)\}[n_1(s)^2 + n_2(s)^2] = n_2(s)m_2(s)[\frac{m_1(s)}{n_1(s)^2+1}]$

$T_2\{u(x,y)\} = \frac{n_2(s)m_2(s)m_1(s)}{[n_1(s)^2+n_2(s)^2][n_1(s)^2+1]}$

If $n_2(s) = 1$ and $m_1(s) = m_2(s)$, then

$T_2\{u(x,y)\} = \frac{m_1(s)m_1(s)}{[n_1(s)^2+1][n_1(s)^2+1]}$

Apply inverse ,we get $\{u(x,y)\} = sin^2x$

4.2. **Example 2.** $\{\frac{\partial^2 u}{\partial x^2}\} + \{\frac{\partial^2 u}{\partial y^2}\} = 0$ under some restrictions. $u(0,y) = 0$ $u(a,y) = 0$ $u(x,b)$ is equal to zero. and $u(x,0) = sinx$

Solution

$T_2\{\frac{\partial}{\partial x}u_x(x,y)\} + T_2\{\frac{\partial}{\partial y}u_y(x,y)\}$

$\Rightarrow -m_1(s)T\{u_x(0,y)\}+n_1(s)T_2\{u_x(x,y)\}-m_2(s)T\{u_x(x,0)\}+n_2(s)T_2\{u_x(x,y)\}$

$\Rightarrow -m_1(s)T\{u_x(0,y)\} + n_1(s)[-m_1(s)T\{u(0,y)\} + n_1(s)T_2\{u(x,y)\}] - m_2(s)T\{u_x(x,0)\} + n_2[-m_2(s)T\{u(x,0)\} + n_2(s)T_2\{u(x,y)\}] = 0$

$\Rightarrow -n_1(s)m_1(s)T_2\{u(x,y)\}-m_2(s)[T\{cosx\}]-n_2(s)m_2(s)T\{sinx\}+n_1(s)^2T_2\{u(x,y)\} = 0$

$\Rightarrow T_2\{u(x,y)\}[-n_1(s)^2 + n_2(s)^2] = m_2(s)T\{cosx\} + n_2(s)m_2(s)T\{sinx\}$

$= m_2(s)[\frac{m_1(s)n_1(s)}{(n_1(s))^2+1}] + n_2(s)m_2(s)[\frac{m_1(s)}{n_1(s)^2+1}]$

$= \frac{m_1(s)m_2(s)n_1(s)}{(n_1(s))^2+1} + \frac{m_1(s)m_2(s)n_2(s)}{(n_1(s))^2+1}$

$\Rightarrow T_2\{u(x,y)\} = \frac{-m_1(s)m_2(s)[n_1(s)+n_2(s)]}{[(n_1(s))^2+1][n_1(s)^2-n_2(s)^2]}$

$= \frac{-m_1(s)m_2(s)[n_1(s)+n_2(s)]}{[(n_1(s)^2+1][n_1(s)-n_2(s)][n_1(s)+n_2(s)]}$

$\Rightarrow T_2\{u(x,y)\} = \frac{-m_1(s)m_2(s)}{[n_1(s)^2][n_1(s)-n_2(s)]}$

if $m_1(s) = m_2(s)$

if $n_1(s) = 1$

https://doi.org/10.62500/icrtsda.1.1.53

$$\Rightarrow T_2\{u(x,y)\} = -[sinx][\frac{n_1(s)}{m_1(s)-1}]$$

$$\Rightarrow \{u(x,y)\} = -e^t sinx$$

5. Conclusion

DGIT aims to streamline the problem into a set of ordinary differential equations, offering greater ease of manipulation. As a valuable asset, DGIT facilitates the resolution of hyperbolic boundary value problems across diverse scientific and engineering domains. By effecting a domain transformation and simplifying the equations, DGIT offers insights into solution behavior

References

[1] Kaklij, D. & Patil, D. (2022). A Double new general integral Transform. Available at SSRN 4023023.

[2] Patil, D., Thakare, P. D., & Patil, P. R. (2022). A double general integral transform for the solution of parabolic boundary value problems. Available at SSRN 4145866.

[3] Alderremy, A. A., & Elzaki, T. M. (2018). "On the new double integral transform for solving singular system of hyperbolic equations. Journal of Nonlinear Sciences and Applications", 11(10), 1207-1214.

[4] Elzaki, T. M., Ahmed, S. A., Areshi, M., & Chamekh, M. (2022). Fractional partial differential equations and novel double integral transform. Journal of King Saud University-Science, 34(3), 101832.

[5] Alderremy, A. A., & Elzaki, T. M. (2018). On the new double integral transform for solving singular system of hyperbolic equations. Journal of Nonlinear Sciences and Applications, 11(10), 1207-1214.

[6] Atangana, A., & Alkaltani, B. S. T. (2016). A novel double integral transform and its applications. J. Nonlinear Sci. Appl, 9, 424-434.

[7] Saadeh, R. (2022). Applications of double ARA integral transform. Computation, 10(12), 216.

[8] Kashuri, A., Fundo, A., & Liko, R. (2013). On double new integral transform and double Laplace transform. European Scientific Journal, 9(33).

[9] Patil, D. (2022). Application of integral transform (Laplace and Shehu) in chemical sciences. DP Patil, Application Of Integral Transform (Laplace And Shehu) In Chemical Sciences, Aayushi International Interdisciplinary Research Journal, Special, (88).

[10] Meddahi, M., Jafari, H., & Yang, X. J. (2022). Towards new general double integral transform and its applications to differential equations. Mathematical Methods in the Applied Sciences, 45(4), 1916-1933.

[11] Patil, D. (2021). The New Integral Transform Soham Transform.

[12] Patil, D. (2022). Dualities between double integral transforms. Elzaki TM (2011). The new integral transforms Elzaki transform", Global Journal of Pure and Applied Mathematics, 7(1), 57-64.

[13] Patil, D. (2018). Comparative study of Laplace, Sumudu, Aboodh, Elzaki and Mahgoub transforms and Applications in boundary value problems.

[14] Patil, D., Suryawanshi, Y., & Nehete, M. (2022). Application of Soham transform for solving Volterra integral equations of first kind.

[15] Patil, D., Vispute, S., & Jadhav, G. (2022). Applications of Emad-Sara transform for general solution of telegraph equation. International Advanced Research Journal in Science, Engineering and Technology, 9(6).

[16] Sedeeg, A. K., Mahamoud, Z., & Saadeh, R. (2022). Using double integral transform (LaplaceARA transform) in solving partial differential equations. Symmetry, 14(11), 2418.

[17] Kushare, S. R., Patil, D. P., & Takate, A. M. (2021). The new integral transform,Kushare transform. International Journal of Advances in Engineering and Management, 3(9), 15891592.

https://doi.org/10.62500/icrtsda.1.1.54

Proc. 1st International Conference on Recent Trends in Statistics and Data Analytics
Air University Islamabad, Pakistan – May 9, 2024, Vol. 1, pp. 526-531

FORCASTING OF BAJRA PRODUCTION USING ARIMA AND ANN: A CASE STUDY OF PUNJAB PAKISTAN.

Iqra Yaseen[1], Rohma Maliha[2],Samra Shehzadi[3] and Wajiha Nasir[4]

Department of statistics, Govt. College Women University, Sialkot[1,2,3,4]

Abstract

Pearl millet is the most widely used kind of millet. It has been growing across Africa and the Indian subcontinent from the beginning of time. In Pakistan's arid and dry regions, it is widely sown. Its cultivation is centered in Punjab in the arid regions of Bahawalpur and Pothwar's barani districts. For the study, we used annual data from the Punjab Crop Reporting Survey, which covered 27 years (1995-2021) . We used Box Jenkson and Artificial neural network to forecasting. From 1995 to 2021, neural networks were used for observation.for the prediction of the bajra market. We compare the both forecasting methods by Mean Square Error (MSE), Root Mean Square error (RMSE), of Mean Absolute Error (MAE).

Key words:

Bajra, Production, ARIMA, Neural Network.

1. Introduction:

Bajra, sometimes know as pearl millet, is an important crop for food and agriculture, especially in areas with semi-arid and dry climates. Scientifically known as Pennisetum glaucum, this cereal grain has been farmed for millennia and has a long history of use as a staple food in many different cultures worldwide.Bajra is well known for its capacity to adapt to challenging environmental factors; it thrives in regions with little rainfall and poor soil. It is an essential crop in areas with limited water resources and difficult agricultural conditions because of its resistance to heat and drought. Bajra is essential to the nutritional security of the world because of its many uses and advantages. Bajra is grown by planting its seeds in soil that drains properly and receives lots of sunlight. It is widely grown in areas of Africa, Asia, and the Middle East, where it provides millions of people with their main source of nutrition. Utilizing both conventional and contemporary farming methods, farmers raise this hardy crop that will continue to thrive under challenging circumstances. Because it provides a variety of vital elements like fiber, protein, carbs, vitamins, and minerals, bajra is highly valued for its nutritional richness. Because it is gluten-free, anyone with celiac disease or gluten intolerance can use it. Because bajra is exceptionally high in iron and magnesium, it is useful in treating nutritional deficiencies, especially in areas where access to a variety of foods is limited.
Kakar et al. (2023) investigate that the study looks on Pakistan's cereal crop growth, instability, and trends from 1951 to 2020. The findings indicate that while bajra and jowar are trending negatively, wheat, rice, and maize are growing positively. There is less varied instability and a

https://doi.org/10.62500/icrtsda.1.1.54

higher Coppock Index in wheat, rice, and maize. Non-traditional cereal crops should be promoted by public government departments for both nutritional and financial reasons. Gandhi et al. (2023) studied that the purpose of the study is to forecast pearl millet pricing and production in Rajasthan, India, utilizing annual production data up to 2029–2030 and time series data up to December 2024. Pearl millet pricing and production were forecast using the ARIMA and SARIMA models. ARIMA (0, 1, 2) with drift for pearl millet production and ARIMA (1, 1, 1) (1, 0, 1) for pearl millet prices were the best-fitting models, respectively. According to the data, pearl millet production and prices are expected to rise in Rajasthan, pointing to a growing trend in the agriculture industry. Comprehending these variables might aid farmers in making knowledgeable choices regarding marketing and acreage distribution. Shateen et al. (2021) studied that using the ARDL technique, this study investigates the long- and short-term relationships between dual sector inflation in Pakistan from 1974 to 2020. We gathered information from the World Development Indicator and the Handbook of Statistics. A consistent rise in the average cost of goods and services, or inflation, has a big effect on the economy. It falls into one of three categories: cost-push, demand-pull, or built-in inflation. A decrease in a consumer's purchasing power per unit of money currency, or inflation, causes a real value loss. Economic growth is influenced by fiscal and monetary policies, which control it.

Thapa et al. (2022) investigate that the using Box-Jenkins Autoregressive Integrated Moving Average (ARIMA) models, the study projects vegetable area, production, and productivity in Nepal from 1977/78 to 2019/20. While the ARIMA (0, 2, 0) model was optimal for vegetable productivity, the ARIMA (0, 2, 1) model was shown to be appropriate for all areas and production. Mean absolute percent error (MAPE) values were used to assess the models' performance; the MAPE values for productivity, production, and area projections were 3.80%, 2.40%, and 2.70%, respectively. According to the study, developing awareness among vegetable growers and producing precise projections are essential for developing future vegetable production plans in Nepal. Mehmood et al. (2023) investigate that using historical data from 1947 to 2021, this study attempted to anticipate the area and production of wheat crop in Pakistan from 1947 to 2021. The research employed the ARIMA linear model, which yielded the lowest RMSE and MAE values for wheat production and area. A ten-year average wheat area of 9058.10, with an anticipated annual rise of 2.87 percent, was forecasted using the ARIMA-ANN model. The mean yield of wheat was 25878.03, with a 2.34 percent predicted variation. The government will need to use these forecast projections in order to plan the industrial sector, meet trade needs, and meet food needs.

2. Methodology:

The main objective of this study is to develop a significant model to forecast bajra production in Punjab Pakistan. For this purpose, yearly annual data on bajra production rates from 1995 to 2021 have been collected from Punjab crop reporting survey.

2.1: Autocorrelation function:

The autocorrelation function at lag k k, denoted as ρ k ρk (rho sub k), measures the correlation between observations in a time series that are k k time units apart. The autocorrelation function is often visualized using a correlogram, which is a plot of the

https://doi.org/10.62500/icrtsda.1.1.54

autocorrelation coefficients against the lag k k. This plot helps identify patterns in the autocorrelation structure of the time series.

2.2:Partial autocorrelation:

The partial autocorrelation function at lag k k, denoted as $\phi k k$ ϕkk (phi sub kk), measures the correlation between observations in a time series that are k k time units apart, after removing the effects of the intervening lags

2.3:ARIMA Model:

The ARIMA model, which stands for Autoregressive Integrated Moving Average, is a widely used time series forecasting method that combines autoregression, differencing, and moving average components to capture the temporal structure of a time series data. Here's are some points of the ARIMA model:

1. **Autoregressive (AR) Component**: The autoregressive component models the relationship between an observation and a number of lagged observations (also called autoregressive terms). It assumes that the value of the time series at any given point is linearly dependent on its previous values.
2. **Integrated (I) Component**: The integrated component involves differencing the time series data to make it stationary. Stationarity is a key assumption of many time series models, including ARIMA. Differencing involves computing the difference between consecutive observations to remove
3. **Moving Average (MA) Component**: The moving average component models the relationship between an observation and a residual error term based on a moving average model applied to lagged forecast errors. It captures the impact of past shocks on the current value of the time series.

The general notation for an ARIMA model is ARIMA(p, d, q), where

- p represents the order of the autoregressive component, indicating the number of lagged observations included in the model'
- d represents the degree of differencing applied to the time series data to make it stationary
- q represents the order of the moving average component, indicating the number of lagged forecast errors included in the model.

3:Results and discussion:

3.1:Data Description

In order to develop a suitable model that could be used to the productio of bajra crops. For this purpose, yearly annual data on bajra production rates from 1995 to 2021 have been collected from Punjab crop reporting survey.

Time series plot of bajra production in Pakistan is developed

https://doi.org/10.62500/icrtsda.1.1.54

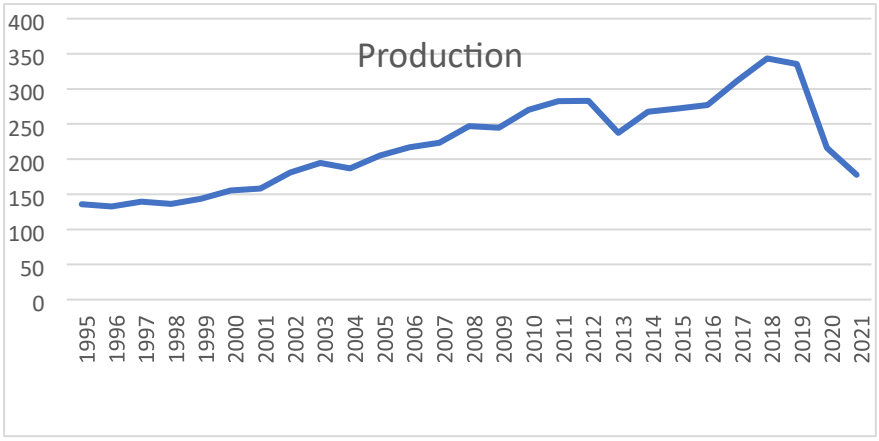

Production figures from 1995 to 2021 are displayed on the graph. It appears from the description that the trend component is the most widely utilized feature in this graph. In this instance, the trend indicates a general decrease in production levels interspersed with intervals of recovery. The trend is the long-term movement in the data across time.

Table 1

Augmented Dickey-Fuller Test

	Test Statistics	Sig
First difference	-3.490605	0.0170

The values of parameters p and q have been determined by constructing a correlogram of the first difference series. According to the correlogram, p may have a value of 0 and q might have a value of 1. An ARIMA model has been suggested based on the potential values of p and q.

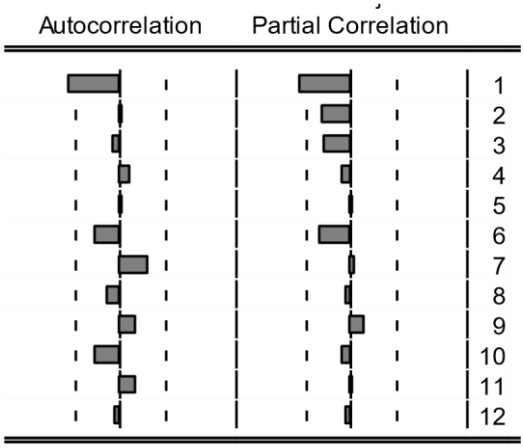

Table 2: ARIMA (0, 2, 1)

https://doi.org/10.62500/icrtsda.1.1.54

Table 2 demonstrate that, in comparison to other models, ARIMA (0, 2, 1) has lower predicting error. Consequently, ARIMA (0, 2, 1) has been our recommended model based on the Box-Jenkins Methodology.

Table 3

Model	RMSE	MSE	MAPE
(0,2,1)	9.09286	82.67950	26.69769

4:Neural Networking:

Twelve input layer neurons, twelve hidden layer neurons, and one output layer neuron have all been used in a backpropagation neural network (BNP) using a bipolar sigmoid function. The time series is not represented by a parametric model in this method. The NN is used to predict the production of bajra crops, and a plot of the original data is provided along with the prediction.

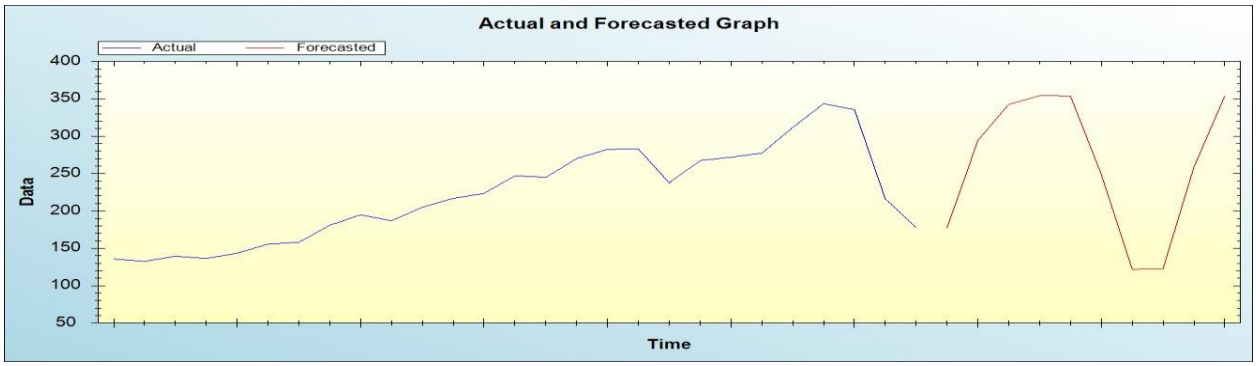

Table 4

Forecasting Error

RMSE	MSE	MAE
9.082242	82.487131	6.350939

The Table's result indicates that, in comparison to Box-Jenkins models, neural network forecasting errors have been the lowest. Thus, the annual bajra production has been forecasted using neural networking.

Table 5

Forecasted value of Bajra production

Year	Bajra production	Year	Bajra production
2022	177.3073	2027	248.6609
2023	294.1883	2028	122.1003
2024	342.5393	2029	122.5605
2025	354.2002	2030	258.5997
2026	353.7616	2031	353.8323

https://doi.org/10.62500/icrtsda.1.1.54

5:COMMENTS AND CONCLUSION:

The primary aim of this research is to create a meaningful model that can predict Pakistan's annual production of bajra. The Punjab Crop Reporting Survey has provided yearly statistics on bajra production from 1995 to 2021 for this purpose. Various models in Neural Networking have been proposed using the Box-Jenkins technique. Among all the suggested approaches, it has been found that the accuracy metrics for NN, RMSE, MAE, and MAPE, are the lowest. Consequently, policymakers are advised to use NN to predict the output of bajra.

References:

1. Kakar, J. S., Lodhi, A. S., Nazir, A., Akhtar, S., & Iqbal, M. A. (2023). Cereal crops production in Pakistan: Trends instability and growth. *International Journal of Agricultural Extension*, *11*(2), 201-207
2. Gandhi, T., Saravanakumar, V., Chandrakumar, M., Divya, K., & Senthilnathan,
   S. (2023). Forecasting pearl millet production and prices in Rajasthan, India: An ARIMA approach
3. Shaheen, R., Iqbal, S., & Javed, A. (2021). DUAL SECTOR INFLATION DYNAMICS IN PAKISTAN: AN EMPIRICAL ANALYSIS USING COINTEGRATION ANALYSIS. *The journal of contemporary issues in business and government*, *27*(5), 2737-2742
4. Mehmood, Q., Sial, M. H., Sharif, S., & Riaz, M. (2023). Development of statistical, artificial neural network and hybrid models, forecasting wheat area and production in Pakistan. *International Journal of Agricultural & Statistical Sciences*, *19*(1).
5. Thapa, R., Devkota, S., Subedi, S., & Jamshidi, B. (2022). Forecasting area, production and productivity of vegetable crops in Nepal using the Box-Jenkins ARIMA model. *Turkish Journal of Agriculture-Food Science and Technology*, *10*(2), 174-181.

https://doi.org/10.62500/icrtsda.1.1.55

Proc. 1st International Conference on Recent Trends in Statistics and Data Analytics
Air University Islamabad, Pakistan – May 9, 2024, Vol. 1, pp. 532-545

THE MATHEMATICAL MODELING FOR COVID-19 TRANSMISSION DYNAMICS AND IMPACT OF WATER POLLUTION ON IT IN PAKISTAN

AMNA AJAIB [1], MAHNOOR NAZ [2] and AYESHA KHURRAM [3]
[1,2]DEPARTMENT OF MATHEMATICS, FAZAIA BILQUIS COLLEGE OF EDUCATION FOR WOMEN PAF BASE NUR KHAN, PAKISTAN
[1]AIR UNIVERSITY, SERVICE ROAD E9/E8 ISLAMABAD 44000, PAKISTAN
[3]FAZAIA BILQUIS COLLEGE OF EDUCATION FOR WOMEN PAF BASE NUR KHAN, PAKISTAN

Abstract. Coronavirus has been broadcasted a pandemic by the World Health Organization(WHO).630,471 confirmed cases and 13,863 deaths have been observed in Pakistan as of March 23rd, 2021. From February 15th to March 15th, 2021, we collected data to investigate the Covid-19 transmission disease and its effect on water pollution. Drinking water is one of the most common ways that people are exposed to toxins. We looked at the levels of toxins in drinking water that affect the immune system and, as a result, we were more likely to become infected with this epidemic disease. We also calculated the fundamental reproductive number and demonstrated the disease persistence criteria for $Ro > 1$. Our result demonstrates that a higher concentration of pollutants per population leads to exposure to transmission diseases.

1. Introduction

Pakistan is ranked third among countries to severe water shortages, according to the International Monetary Fund (IMF). The Pakistan Council of Research in Water Resources (PCRWR) predicted in May 2018 that by 2025, Pakistan will have very little to no clean water. Just 20 percent of the country's population currently has access to safe drinking water. The remaining 80 percent of the population is reliant on contaminated water, which is largely contaminated by sewage (feaces, complete coliforms, E.coli colonies), which is subsequently contaminated by fertilizer, pesticides, and industrial effluents. Water contamination is responsible for nearly 80 percent of all diseases and 30 percent of all deaths. A solitary E. coli bacterium will increase into trillions in a shriveled pipeline in seven days, and such lines are utilized for water supply with practically no treatment. Utilization of such defiled water has brought about the passings of many individuals, just as bone and tooth sicknesses, loose bowels, diarrhea, typhoid, hepatitis, malignant growth, and other waterborne infections.
Around 60 million people in Pakistan are at risk of being poisoned by high levels of

Key words and phrases. COV ID − 19, World Health Organization;Transmission Disease; Drinking Water; Disease Persistence Criteria; concentration of pollutants; reproductive number; Pandemic, Toxins; Mathematical Modeling; Transmission Rate; Crude Mortality Rate; Fatality Rate; Water Pollution; Reproductive Rate.

2021 *Mathematics Subject Classification*. Primary 42B35; Secondary 42B30, 46E30, 22E25
amnaarshad2@outlook.com (A. Ajaib); mahnooroo1552@gmail.com (M. Naz).

https://doi.org/10.62500/icrtsda.1.1.55

arsenic in their drinking water, making it the world's largest mass poisoning. Cancer, restrictive pulmonary disease, skin lesions, cardiovascular disorders, diabetes mellitus, gangrene, neurological impairments, and problems with the endocrine glands, immunity, liver, kidney, and bladder, as well as socioeconomic risks, can all be caused by arsenic poisoning. Unfortunately, the people who are at risk also have little access to epidemiological data on arsenic toxicity, alternative drinking water or health measures.[9]

Harmful metals incorporate cadmium, beryllium, aluminum, uranium, mercury, lead, bismuth, barium, antimony, arsenic, and different components. Higher levels of these metal ions are highly toxic to organisms, including humans and plants, and their water solubility is one of the main environmental concerns Pakistan's environmental problems are largely linked to the country's recent decades of unequal economic and social growth.[8]

As a result, metal pollution is expected to put a lot of pressure on the coastal marine ecosystem. The disposal of sewage and industrial wastes is a major problem. It is sometimes drained to agricultural fields, where it is used to grow crops such as vegetables. Heavy metal pollution in wastewater irrigation poses a number of risks to the environment. It also poses a variety of health risks to humans through the ingestion of pathogenic microorganisms and heavy metals, as well as exposure to them.[8]

On March 11, 2020, the World Health Organization (WHO) declared the ongoing novel coronavirus or SARS-CoV-2 outbreak a pandemic. According to Worldometer data as of March 31, 2021, there were 128,941,489 total affirmed cases, 2818833 affirmed passings, and 104,034,816 recovered cases worldwide. The novel coronavirus has already surpassed the previous records of two life-threatening outbreaks, namely the Severe Acute Respiratory Syndrome Coronavirus (SARS-CoV) and the Middle East Respiratory Syndrome Coronavirus (MERS-CoV), presenting the greatest danger to global public health and the economy since World War *II*. COVID-19 is a genus of enveloped non-segmented single-abandoned RNA infections that have a place with the request Nidovirales, family Coronaviridae, and subfamily Orthocoronavirinae, and are generally dispersed among vertebrates and people. SARS-CoV-2 is an infectious disease caused by a novel coronavirus. In December 2019, a local pneumonia outbreak was first detected in Wuhan, Hubei Province, China, and mainland China became the epicentre of COVID-19. The majority of the early stages were typically integrated into the Huanan wholesale seafood industry, which often traded live animals. Fever, dry cough, sore throat, breathlessness, and exhaustion are all symptoms of this contagious corona virus disease. With human migration through air,the disease has now spread throughout the world as well as the territories of the world, making Europe and USA as new epicenters. COVID-19 is the third zoonotic human-to-human transmission to emerge in the twenty-first century, following SARSCoV, which spread to 37 nations, and MERSCoV, which spread to 27 nations.[13]

On February 26, 2020, the main instance of COVID-19 was accounted for in Pakistan. Because of the appearance of pioneers from Iran across the Taftan Border, the quantity of affirmed cases has been rapidly expanding since March 15, 2020. Besides, the declaration and execution of the lockdown in Pakistan occurred in under a day, causing bedlam as evacuees dashed back to the places where they grew up, deteriorating blockage and making social distance outlandish. Moreover, from March 15 to 25, 2020, the quantity of cases expanded from 53 to 1078. From that point forward, the quantity of cases in different areas of the nation has expanded quickly step by step. As of July 20, 2020, there have been a sum of 265,083 affirmed cases in Pakistan, with 5599 individuals kicking the bucket so far. As per the most recent information, Sindh region had 42.63 percent (113,007) affirmed cases, trailed by Punjab territory with 34.02 percent.[14]

Manifestations of COVID-19

Coronavirus influences various individuals in various ways. Most tainted individuals will create gentle to direct ailment and recuperate without hospitalization. Most normal indications are fever, dry hack, sluggishness. More uncommon indications are a throbbing painfulness, sore throat, looseness of the bowels, conjunctivitis, migraine, loss of taste or smell, a rash on skin, or staining of fingers or toes.

https://doi.org/10.62500/icrtsda.1.1.55

Genuine indications are trouble breathing or windedness, chest torment or tension, loss of discourse or movement.

Look for sure fire clinical consideration assuming you have genuine indications. Continuously call prior to visiting your primary care physician or wellbeing office, People with gentle side effects who are generally solid ought to deal with their manifestations at home. On normal it takes 5 to 6 days from when somebody is tainted with the infection for manifestations to show, but it can require as long as 14 days.

2. Current Situation in Pakistan

Water Availability

Nature has provided Pakistan with an abundance of land and ground water supplies. Unlikely, anthropogenies tasks such as townsfolk growth, inappropriate employment reduces amount and degrades consistency. Conferring to Sir Jamshed Iqbal(Pakistan's Chairman), Pakistan had a per capita water supply of 5,600 cubic meters[10] at the time of independence, which has declined by over 406 percentage from 5,260 meter cube in 1951 and 1,038 meter cube in 2010. If current persists, water supply will fall in between 877 meter cube per year by 2020, then to 660 by 2025 and would fall even lower to a distributing normal of 575 cubic feet by 2050 as illustrated in figure.[10]

COVID-19 Active Cases

According to Pakistan's Ministry of Health, there were 3277 confirmed positive cases in the country on 6 April, 2020 with 18 serious infected specimens and 50 fatalities. Punjab had the most affirmed cases (1493), trailed by Sindh(881), KPK(405), Balochistan(192), GB(210), federal(82) and Azad Jammu and Kashmir(15). Until this point, 16 individuals have kicked the bucket in Khyber Pakhtunkhwa , trailed by Punjab(15), Sindh(15), Gilgit Baltistan(3) and Balochistan(3).[1] Sindh province has recovered 85 sick patients, followed by KP(30), Baluchistan(17), Punjab(17 to 25), GB(9) and AJK each have one comeback. Pakistan has a 1.3 percent death rate and 4.8 percent recovery rate.

As indicated by WHO, there were total 654,591 active cases in different provinces of Pakistan from Feb,2021 to March,2021. Punjab had the most active cases that is (22,392), followed by Sindh (4445), KPK(78560, Balochistan(263), GB(37), Federal(8120) and AJK(1334) as shown in figure below.[7]

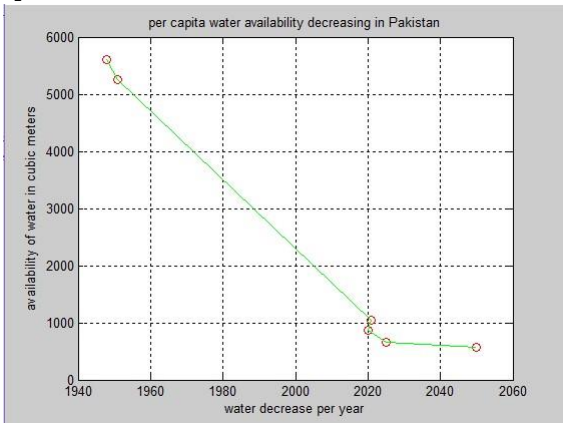

Figure 1. Pakistan's per capita water supply is rapidly dwindling

https://doi.org/10.62500/icrtsda.1.1.55

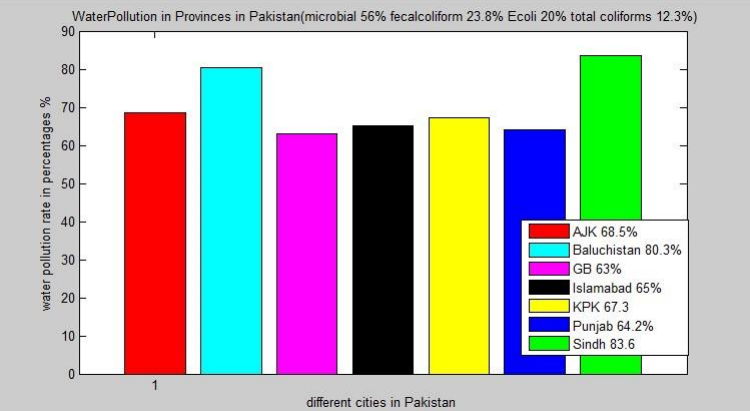

Figure 2. Actice Cases of COVID-19 pandemic in Pakistan

Reproductive Number Criteria

Even when public health experts utilize active monitoring and contact tracing to try to discover all affected people, counting the number of cases of infection during an epidemic can be challenging. During an epidemic of a newly developing infectious virus that is propagating through an entirely susceptible population, assessing the real R0 value is conceivable.There are seldom enough data gathering systems in place to catch an epidemic in its early phases, when R_0 can be calculated most reliably. As a result, R_0 is almost typically calculated retrospectively using epidemiological data or from mathematical models.[20]

R_0 is most importantly used to determine the reproductive rate of a pandemic or epidemic infectious disease.Whenever the reproductive number is greater than 1 $R_0 > 1$, it means that the disease has much potential to spread but if $R_0 < 1$ then the infectious disease is under control.

The range of basic reproductive number for $COV\,ID-19$ is from 2.4 to 3.4.

3. Mathematical Modeling for COVID-19

Predictive Mathematical Models for epidemics[24],[25] are critical for understanding the path of an epidemic and planning effective control actions. For humanto-human transmission, one often used [26]model, which outlines the individuals pass through three totally unrelated disease stages: Susceptible, Infected and Recovered.

More complicated models can depict the dynamic spread of certain diseases more precisely. Several models for COVID-19 pandemic have been created. Some researchers expanded an SEIR model by taking hazard insight and combined number of cases into account[27], suggested a discrete-time SIR model that includes dead individuals.[28]

In article[29], author created a control-oriented SIR modelthat emphasizes the impact of delayes and analyses the results of various containment approaches[29] and it was also estimated the clinical severity of COVID-19[30] using transmission dynamics. Stochastic transmission models have been developed also taken into account in [31],[32]. In this paper, we talked about an original mean-field epidemiological model for COVID-19 pandemic in Pakistan, which expands the standard SIR model proposed by [33] for SARS.

SIDARTHE model is a model which we use in this paper to distinguishes between the detected and undetected cases of the respective infection, as well as between differentseriousness if illness(SOI), non-perilous cases(asymptomatic and paucisymptomatic; minor and moderate contamination) and conceivably hazardous cases(major and outrageous disease) that require ICU admission.

The whole populace is partitioned into eight sickness stages: S, susceptible(uninfected); I, infected(asymptomatic or pauci-suggestive contaminated, unseen); D, diagnosed(infected asymptomatically, distinguished); R, recognized(symptomatic infected, identified); A,

https://doi.org/10.62500/icrtsda.1.1.55

ailing(symptomatic infected, undiscovered); T, threatened(viewed as beset with dangerous disease); H, recovered(healed); Extinct(E).[7]

Methods

The numerical model SIDARTHE dynamical framework is comprised of eight conventional differential conditions that depict the populace's movement through time in each stage.

$$S'(t) = -S(t)(\alpha * I(t) + \beta * D(t) + \gamma * A(t) + \delta * R(t)) \quad (3.1)$$

$$I'(t) = S(t)(\alpha * I(t) + \beta * D(t) + \gamma * A(t) + \delta * R(t) - (\epsilon + \zeta + \lambda) * I(t)) \quad (3.2)$$

$$D'(t) = \epsilon * I(t) - (\eta + \rho)D(t) \quad (3.3)$$

$$A'(t) = \zeta * I(t) - (\theta + \mu + \kappa) * A(t) \quad (3.4)$$

$$R'(t) = \eta * D(t) + \theta * A(t) - (\nu + \xi) * R(t) \quad (3.5)$$

$$T'(t) = \mu * A(t) + \nu * R(t) - (\sigma + \tau) * T(t) \quad (3.6)$$

$$H'(t) = \lambda * I(t) + \rho * D(t) + \kappa * A(t) + \xi * R(t) + \sigma * T(t) \quad (3.7)$$

$$E'(t) = \tau * T(t) \quad (3.8)$$

where the capital latin letters(state factors) mirror the percent of the populace in each stage and every one of the boundaries assessed are positive numbers addressed by Greek letters. The communications between various periods of contamination are portrayed graphically.

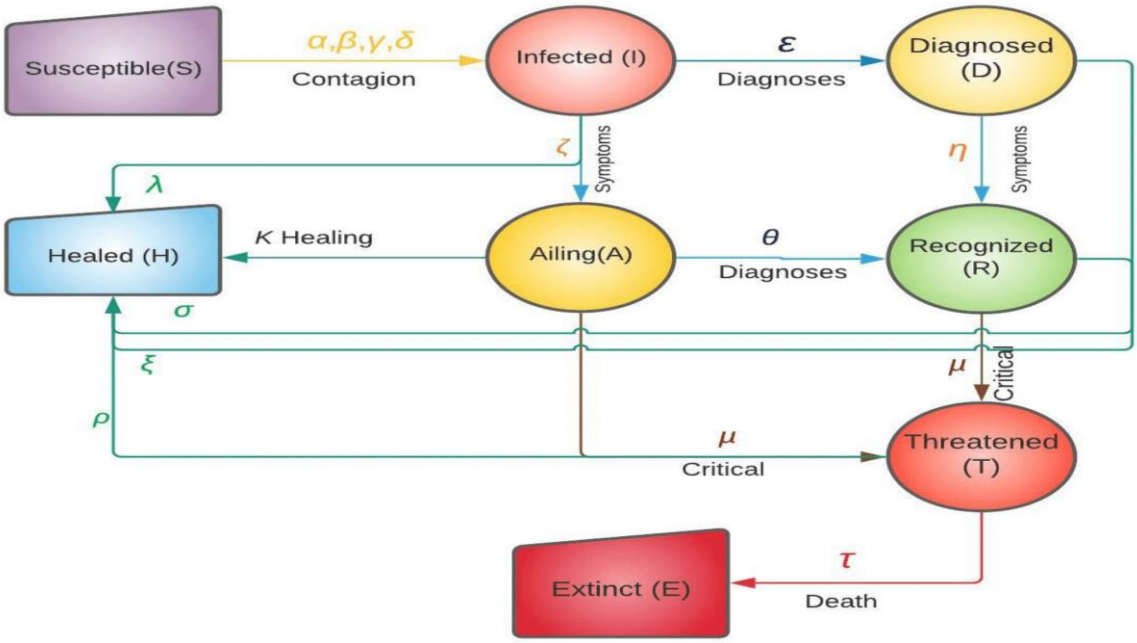

Figure 3. The Transmission Dynamics Model for COVID-19

https://doi.org/10.62500/icrtsda.1.1.55

The following are the parameters:

- The transmission rates(the probability of sickness move in a solitary contact duplicated by the normal number of contacts per individual) attributable to contacts between defenseless subject and a tainted, analyzed, debilitated or perceived subject are meant by α,β,γ and δ separately
- ϵ and θ capture the detection likelihood rate in relation to asymptomatic and symptomatic instances, respectively
- In the absence of special treatment, ζ and η signify the likelihood rate at which an infected patient, whether unaware or conscious of being infected, develops clinically significant symptoms
- μ and ν is the rate at which undiscovered and identified infected patients acquire life-threatening symptoms; they are equivalent if there is no known special therapy that is effective against the disease
- τ signifies the mortality rate (for infected people with life-threatening symptoms), which can be lowered with better treatment
- λ,κ,ξ,ρ and σ signify the rate of recovery for the five groups of infected people. These indicators can be raised as a result of improved therapies and viral immunity[7]

Modeling options are discussed. We leave out the likelihood rate of being susceptible again after recovering from the infection in the model since it appears to be minimal based on early evidence. Given the lack of accessible data, definitive proof concerning immunity is unattainable at this time.Immunity may also be transient. Albeit a few information suggest that SARS-CoV-2 reinfection is conceivable, the recognition of viral RNA in respiratory examples might reflect constancy rather than genuine repeat.[7]

At last, the SIDARTHE model is a mean-field model, which catches the normal impact of events that influence the entire populace. Social blending propensities are found the middle value of all through the entire populace, paying little heed to age, and incorporated into our virus boundaries. Our methodology, then again, is absolutely adaptable and adjusted to fuse highlights, for example, age characterization, which would require partitioning every factor in the model into N factors assuming that there are N age classes are considered. Another potential future advancement is to stretch out the model to anticipate the simultaneous development of different infections that, because of the pandemic crisis, might be misjudged, belittled, or not treated suitably in light of the fact that the medical care framework is overburdened, bringing about an expanded number of guarantee passings not straightforwardly connected to the infection.

4. Investigation of Mathematical Model

The selected SIDARTHE Model consists of eight differential equations of a bilinear system.The system is positive: if all state variables are started with non-negative values at time 0, they will take non-negative values for $t \geq 0$. H(t) and E(t) are cumulative variables that are independent of each other and their own start circumstances. The system is compartmentalized and displays mass conservation: as can be seen right away,

$$\frac{dS}{dt} + \frac{dI}{dt} + \frac{dD}{dt} + \frac{dA}{dt} + \frac{dR}{dt} + \frac{dT}{dt} + \frac{dH}{dt} + \frac{dE}{dt} = 0 \qquad (4.1)$$

https://doi.org/10.62500/icrtsda.1.1.55

Thus the amount of the relative multitude of factors is consistent on the grounds that these factors means the all out populace. In this way, we can expect to be that

$$S(t) + I(t) + D(t) + A(t) + R(t) + T(t) + H(t) + E(t) = 1 \quad (4.2)$$

where 1 denote the total population including deceased.
At time $t = 0$ euation(1.10) becomes

$$S(0) + I(0) + D(0) + A(0) + R(0) + T(0) + H(0) + E(0) = 1 \quad (4.3)$$

we can show that the variables converges to an equilibrium.

$$S^{-} \geq 0, I^{-} = 0, D^{-} = 0, A^{-} = 0, R^{-} = 0, T^{-} = 0, H^{-} \geq 0, E^{-} \geq 0 \quad (4.4)$$

with $S^{-} + H^{-} + E^{-} = 1$.

Subsequently, just the powerless, restored, and expired populaces are in the long run present, showing that the scourge has passed. All the conceivable harmony is given by (S,0,0,0,0,0,H,E) with $S^{-} + H^{-} + E^{-} = 1$.

We partition the framework into three subsystems to more readily comprehend its conduct: the first incorporates just factor S (relating to powerless people), the second incorporates factors I, D, A, R, and T (comparing to contaminated people), which are non-zero just during the transient, and the third incorporates factors H and E (comparing to tainted people) (addressing recuperated and outdated). We'll focus on the second subsystem. We consider this the IDART subsystem. A key finding is that the excess factors S, H, and E are at balance when (and just when) the tainted people I+D+A+R+T are zero. H and E (which are monotonically developing) merge to their asymptotic qualities H and E, separately, and S (which is monotonically declining) meets to S if and provided that I, D, A, R, and T combine to zero.[7]

Subsequently we characterize the IDART sub-framework as: $\begin{bmatrix} I & D & A & R & T \end{bmatrix}^T$ Hence we can rewrite the subsystem IDART as:

$$x^{\cdot}(t) = Fx(t) + Bu(t) \quad (4.5)$$

$$\dot{x}(t) = \begin{bmatrix} -r_1 & 0 & 0 & 0 & 0 \\ \epsilon & -r_2 & 0 & 0 & 0 \\ \zeta & \eta & -r_3 & 0 & 0 \\ 0 & 0 & \theta & -r_4 & 0 \\ 0 & 0 & \mu & \nu & -r_5 \end{bmatrix} x(t) + \begin{bmatrix} 1 \\ 0 \\ 0 \\ 0 \\ 0 \end{bmatrix} u(t \quad (4.6)$$

$$y_S = c^T x(t) = \begin{bmatrix} \alpha & \beta & \gamma & \delta & 0 \end{bmatrix} x(t \quad (4.7)$$

$$y_H(t) = f^T x(t) = \begin{bmatrix} \lambda & \kappa & \xi & \rho & \sigma \end{bmatrix} x(t) \quad (4.8)$$

$$y_E(t) = d^T x(t) = \begin{bmatrix} 0 & 0 & 0 & 0 & \tau \end{bmatrix} x(t \quad (4.9)$$

$$r_1 = \epsilon + \zeta + \lambda,\ r_2 = \eta + \rho,\ r_3 = \theta + \mu + \kappa,\ r_4 = \nu + \xi$$

whereand $r_5 = \sigma + \tau$ and u(t) is a feedback signal.We get the time-varying asymptotic feedback whenever S(t) converges to S^{-}, H(t) converges to H^{-} and E(t) converges to E^{-}.The remaining these three variables must satisfy the following differential equation:

$$S^{\cdot}(t) = -S(t)y_S(t) \quad (4.10)$$

$$H^{\cdot}(t) = y_H(t) \quad (4.11)$$

$$E^{\cdot}(t) = y_E(t) \quad (4.12)$$

Theorem 4.1. *Whenever $S(t) < S^{*}(t)$,the IDART subsystem with powerless populace is asymptotically in equilibrium state.*

https://doi.org/10.62500/icrtsda.1.1.55

$$S^* = \frac{r_1 r_2 r_3 r_4 r_5}{\alpha(r_2 r_3 r_4) + \beta(\epsilon)(r_3 r_4) + \gamma(\zeta)(r_2 r_4) + \delta(\eta(\epsilon)(r_3) + \zeta(\theta)(r_2))}$$

Proof. At equilibrium state ($S,^{-}$ 0,0,0,0,0,$H,^{-}$ E^{-}), the matrix F in equation(1.14)becomes a jacobian matrix with eight differential equations let

$$J = \begin{bmatrix} 0 & -\alpha\bar{S} & -\beta\bar{S} & -\gamma\bar{S} & -\delta\bar{s} & 0 & 0 & 0 \\ 0 & \epsilon & -r2 & 0 & 0 & 0 & 0 & 0 \\ 0 & \zeta & 0 & -r3 & 0 & 0 & 0 & 0 \\ 0 & 0 & \eta & \theta & -r4 & 0 & 0 & 0 \\ 0 & 0 & 0 & \mu & \nu & -r5 & 0 & 0 \\ 0 & \lambda & \rho & \kappa & \xi & \sigma & 0 & 0 \\ 0 & 0 & 0 & 0 & 0 & \tau & 0 & 0 \end{bmatrix} \begin{bmatrix} 0 & \alpha\bar{S} - r_1 & \beta\bar{S} & \gamma\bar{S} & \delta\bar{S} & 0 & 0 & 0 \\ 0 & 0 & 0 & 0 & 0 & 0 & 0 & 0 \\ 0 & 0 & 0 & 0 & 0 & 0 & 0 & 0 \\ 0 & 0 & 0 & 0 & 0 & 0 & 0 & 0 \\ 0 & 0 & 0 & 0 & 0 & 0 & 0 & 0 \\ 0 & 0 & 0 & 0 & 0 & 0 & 0 & 0 \\ 0 & 0 & 0 & 0 & 0 & 0 & 0 & 0 \end{bmatrix} \quad (4.13)$$

where J matrix has three null eigen values and five eigen values which are the roots of the given polynomials.Let A denote the matrix of the IDART subsystem.

$$A = \begin{bmatrix} \alpha\bar{S} - r1 & \beta\bar{S} & \gamma\bar{S} & \delta\bar{S} & 0 \\ \epsilon & -r_2 & 0 & 0 & 0 \\ \zeta & 0 & -r_3 & 0 & 0 \\ 0 & \eta & \theta & -r_4 v & \\ 0 & 0 & \mu & & \\ & & & 0 & \\ & & & & -r_5 \end{bmatrix} \quad (4.14)$$

computing eigen values for this matrix as the variable S multiplied by identity matrix of same order then subtract matrix A from it, we get

$$P(S) = det(SI - A) = \begin{vmatrix} S - \alpha\bar{S} + r_1 & \beta\bar{S} & \gamma\bar{S} & \delta\bar{S} & 0 \\ \epsilon & S + r_2 & 0 & 0 & 0 \\ \zeta & 0 & s + r_3 & 0 & 0 \\ 0 & \eta & \theta & S + r_4 & 0 \\ 0 & 0 & \mu & \nu & S + r_5 \end{vmatrix} \quad (4.15)$$

Then find the determinant of the above matrix by co-factor method.

$$P(S) = D(S) - SN^{-}(S) \quad (4.16)$$

where

$$D(S) = (-\alpha S^{-} + S + r_1)(S + r_2)(S + r_3)(S + r_4)(S + r_5) \text{ and } N(S) = -\beta\epsilon S^{-}(S + r_3)(S + r_4)(S + r_5) - \gamma\zeta S^{-}(S + r_2)(S + r_4)(S + r_5) - \delta\epsilon\eta S^{-}(S + r_3)(S + r_5) - \delta\zeta\theta S^{-}(S + r_2)(S + r_5)$$

After putting S^{-} equals to zero D(S) becomes,

https://doi.org/10.62500/icrtsda.1.1.55

$$D(S) = (S + r_1)(S + r_2)(S + r_3)(S + r_4)(S + r_5)$$

Since $\bar{S} = 0$, so there are no more population in r_1 as r_1 is a sum of asymptomatic individuals, not aware infected individuals and recoveries.Hence we can assume that $r_1 = 0$ N(S) becomes

$$N(S) = -\bar{S}\{(S + r_2)\{\alpha(S + r_2)(S + r_3)(S + r_4) + \beta\epsilon(S + r_3)(S + r_4) + \gamma\zeta(S + r_2)(S + r_4) + \delta\{\eta\epsilon(S + r_3) + \zeta\theta(S + r_2)\}\}\}$$

Now by transferring the function from U(T) to y(S).we have,

$$G(S) = \frac{N(S)}{D(S)} \tag{4.17}$$

Because the system is positive.Hence the H_∞ of G(S) is equal to the static gain as

$$G(0) = \frac{N(0)}{D(0)} \tag{4.18}$$

$$\bar{S}^* = \frac{1}{G(0)} = \frac{r_1 r_2 r_3 r_4 r_5}{\alpha(r_2 r_3 r_4) + \beta(\epsilon)(r_3 r_4) + \gamma(\zeta)(r_2 r_4) + \delta(\eta(\epsilon)(r_3) + \zeta(\theta)(r_2))}$$

as required. □

5. Mathematical Computation and Results

This section contains the main results of this study.

Our First Result is:

Basic Reproduction Rate (R_0) The basic reproductive number R_0, which is a function of individual contact rates, transmission probability (chance of transmission per contact), and infectiousness duration, characterises the contagiousness and transmissibility of viruses.[18]

This contrasts with the time-varying reproductive number (Rt), which represents shifting levels of immunity in the population as well as the influence of control measures restricting transmission and is defined as the number of persons infected by an infectious individual at a certain moment in time.[19]

The scientific literature for any particular infectious agent may have a variety of R_0 values. The period of contagiousness once a person becomes infected, the chance of infection per encounter between a susceptible individual and an infectious person or vector, and the contact rate are all commonly used to estimate the R_0 value.Moreover, other parameters can be added to represent more complicated transmission cycles.[20]

In previous section, we find the value of G(0) by finding eigenvalue values of the given matrix which is actually the reciprocal of basic reproductive number formula.For this specific model R_0 is:

$$R_0 = \frac{1}{G(0)} = \frac{\alpha(r_2 r_3 r_4) + \beta(\epsilon)(r_3 r_4) + \gamma(\zeta)(r_2 r_4) + \delta(\eta(\epsilon)(r_3) + \zeta(\theta)(r_2))}{r_1 r_2 r_3 r_4 r_5}$$

Rearranging and solving the above equation, we get

$$R_0 = \frac{\alpha + \frac{\beta\epsilon}{r_2} + \frac{\gamma\zeta}{r_3} + \delta\left(\frac{\eta\epsilon}{r_2 r_4} + \frac{\zeta\theta}{r_3 r_4}\right)}{r_1} \tag{5.1}$$

Through this formula we can find out the basic reproductive number of any infectious disease. B y setting different different parameters used in above formula according to current situation in Pakistan, we calculate the Basic Reproductive Rate through MATLAB, which gives the result as

$$R_0 = 2.5926 \tag{5.2}$$

https://doi.org/10.62500/icrtsda.1.1.55

According to Reproductive Rate Criteria, the above equation shows that $R_0 > 1$ which ultimately means that the corona virus infectious disease still have the ability to spread. Hence, we should take special interventions and measures so that we save our nation from this infectious disease.

Our Second Result is:

Case Fatality Rate and Crude Mortality Rate

In Epidemiology, Case Fatality Rate is sometimes called case-fatality ratio or risks, is basically the rate of occurrence of death from an accident or from infectious disease. Crude Mortality Rate is sometimes called Death Rate, it means that those who are currently sick may get serious illness and die as a result of their infection. Knowing the COVID-19 mortality risk can help you make better decisions. Thus we calculate the CFR and CMR of the pandemic disease SARS-Cov-2 for the data gathered from WHO and other health related websites in the time period of 15 February,2021 to 15 March,2021. Hence CMR percentage is **2.23**. We show the graphical representation of CFR and CMR through MATLAB code as illustrated below

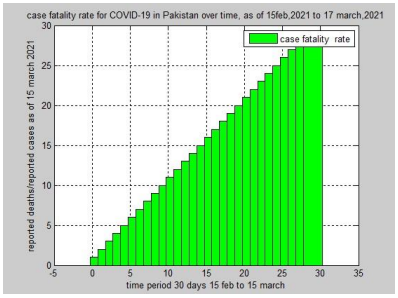

Figure 4. Case Fatality Rate for SARS-Cov-2

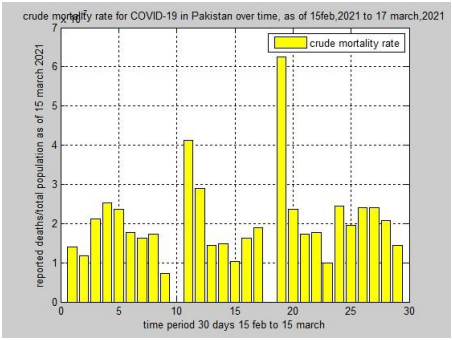

Figure 5. Crude Mortality Rate for SARS-Cov-2

Our Third Result is:

Disease Rate

Water Pollution is viewed as one of the significant medical issues in Pakistan. The Covid pandemic has radically changed our lifestyle, and the treat of COVID-19 spreading has made another level uneasiness. Utilization of synthetics and sanitizers on a normal basis.

The larger part of the COVID-19 items that were used at the gathering. The dynamic part *Quanternary Ammonia* is the EPA rules. Hydrogen peroxide, isopropanol, ethanol, sodium hypochlorite, octanoic corrosive, dodecylbenzenesulfonic corrosive, chlorine dioxide, phenolic,

https://doi.org/10.62500/icrtsda.1.1.55

triethylene glycol, L-lactic corrosive, dichloroisocyanurate dihydrate glycolic corrosive or hypochlorous corrosive are a portion of the other dynamic substances found in blends.

Graphs shows different pollutant rates in drinking water gathered from different areas of Pakistan. Further it shows the disease percentage in different provinces of Pakistan, those diseases which are due to drinking polluted and contaminated water, which eventually weak our immune systems that leads to threatened about SRS-Cov-2 pandemic disease.

Our forth Result is:

Comparison Between COVID-19 and Water Pollution

Numerous toxins that were recently respected solely as far as their ability to modify

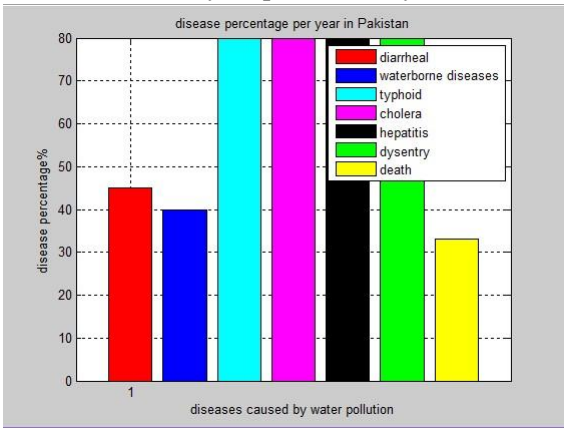

Figure 6. Disease percentage per year

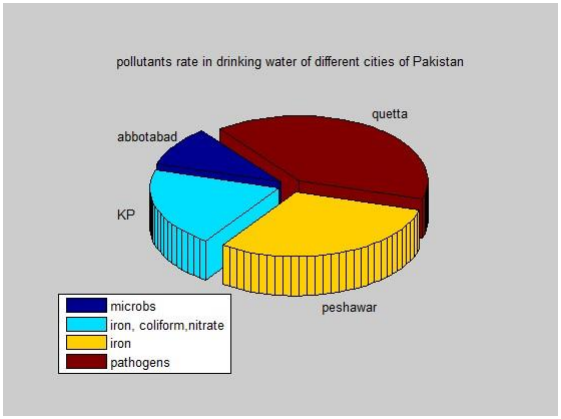

Figure 7. Water pollutants Rate

endocrine framework of late been connected in the initiation of different immunological pathways engaged with both the turn of events and support of auto-invulnerable illnesses. Estrogen has additionally been connected to reactivity incitement plays a fundamental capacity in the resistant framework by impacting provocative middle person reactions and humoral immunity.[37] Here is chart which depicts the current circumstance of COVID-19 and Water contaminations. In above figure, we see that there are 58.8 percent water pollutants and 1334 active cases in AJK, 80.3 percent water pollutants and 263 active cases in Baluchistan, 53 percent water pollutants and 37 active cases in GB, 65 percent water pollutants and 8102 active cases registered in Islamabad, 67.3 percent water

https://doi.org/10.62500/icrtsda.1.1.55

pollutants and 7056 active cases in KPK province, 64.2 percent water pollutants and 22392 active cases present in Punjab province and 83.6 percent water pollutants and 4446 active cases in Sindh. Further, we note that the Punjab province suffer with very high percentage of corona virus infectious disease and also have highest percentage of water pollutants. So, we can observe that water pollution affects our immune system which ultimately results in increasing the risk of COVID-19 pandemic.

https://doi.org/10.62500/icrtsda.1.1.55

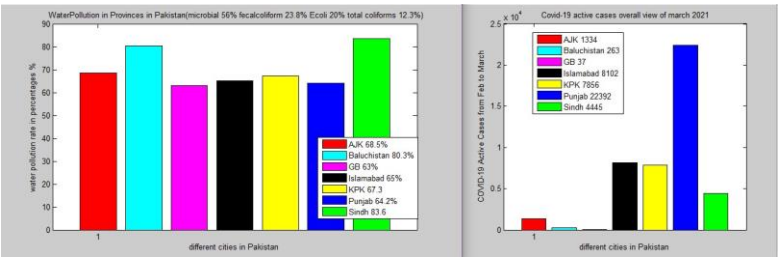

Figure 8. Comparison of COVID-19 and Water Pollutants in Pakistan

6. Conclusion and Future Strategies

Conclusion

In Pakistan, Water Contamination is one of the most serious hazards to public health. The quality of drinking water is poorly maintained and regulated. Pakistan is ranked 80th out of 122 countries in terms of drinking water quality. Through out the country, drinking water sources, including surface and ground water, are contaminated coliforms, hazardous metals and pesticides.

Because of pressing necessity to address and comprehend the impact of various environmental exposures on COVID-19. Metals, for example, are important pollutants in drinking water. According to prior reports, PFAS and plasticizers are both harmful. Immunotoxicity, which could raise concerns about COVID-19 causes respiratory problems.

The main causes leading to the deterioration of water quality are human activities such an improper disposal of municipal and industrial effluents and indiscriminate application of agrochemicals in agriculture. Microbiological and chemical pollutants are the primary causes of different health disorders, either alone or in combination. As a result, the health hazards associated with pollutants in drinking water, particularly long term exposures, are of crucial concern and research concentrating on the efforts of combination of these chemicals are still scare, even if a COVID-19 vaccine is discover, the presence of contaminants in drinking water could be a problem.[37] **Future Strategies**

The model allows us to mimic and anticipate the dynamic evolution once the model parameters have been determined using the available clinical data. To assess the likely underestimating or over estimation of the epidemic based on current statistics that are significantly subjected to the epidemic to sway. Since the analyzed gathering goes through isolation and is along these lines more averse to hurt the defenseless gathering, analyze endeavors can limit the disease peak.

Although prohibitive measures that decrease the speed of SARS-COV-2 can lessen the COVID-19 death rate, the CFR remains basically steady in various situations, unaffected by the extint of social limitation and testing. Abundance case casualty might in any case be an issue for COVID-19 patients, thus endeavors ought to focus on building up more compelling COVID-19 treatment procedures. The ebb and flow circumstance will acclimate to address interminable enhancements as new meds and antibodies are endeavored and explored.[7]

Furthermore, we can likewise refine our drinking techniques by self-sanitization strategy or by establishing cleansing plants in various spaces of Pakistan where the dangers of sicknesses are exceptionally high to control the pandemic Corona infection irresistible illness.

References

[1] West, Larry ,*World Water Day: A Billion People Worldwide Lack Safe Drinking Water*,March 26, 2006.
[2] Beaudry, Frederic,*Nutrients, a Major Source of Water Pollution* Treehugger,*www.treehugger.com/water – pollution – nutrients* – 1204127.
[3] Pink, Daniel H. (April 19, 2006). *Investing in Tomorrow's Liquid Gold.* Yahoo. Archived from the original on April 23, 2006.

https://doi.org/10.62500/icrtsda.1.1.56

[4] Nathanson, J. A. (2020, December 22).*Water pollution*, Encyclopedia Britannica. https://www.britannica.com/science/water-pollution.

[5] zUN-Water (2018) World Water Development Report 2018:Nature-based Solutions for Water, Geneva, Switzerland.

[6] Moss B. (2008). Water pollution by agriculture. Philosophical transactions of the Royal Society of London. Series B, Biological sciences, 363(1491), 659?666. https://doi.org/10.1098/rstb.2007.2176.

[7] Nabi, G., Ali, M., Khan, S. et al. The crisis of water shortage and pollution in Pakistan: risk to public health, biodiversity, and ecosystem. Environ Sci Pollut Res 26, 10443?10445 (2019). https://doi.org/10.1007/s11356-019-04483-w.

[8] Amir Waseem, Jahanzaib Arshad, Farhat Iqbal, Ashif Sajjad, Zahid Mehmood, Ghulam Murtaza, *Pollution Status of Pakistan: A Retrospective Review on Heavy Metal Contamination of Water, Soil, and Vegetables*, BioMed Research International, vol. 2014, Article ID 813206, 29 pages, 2014. https://doi.org/10.1155/2014/813206.

[9] Ahmed, A., Shafique, I. *Perception of household in regards to water pollution: an empirical evidence from Pakistan*, Environ Sci Pollut Res 26, 8543?8551 (2019). https://doi.org/10.1007/s11356-019-04273-4.

[10] Daud MK, Muhammad N, Shafaqat A, Muhammad R, Raees AB, Muhammad BS, Muhammad UA, Shahzad ASC et al , *Drinking water quality status and contamination in Pakistan*,*BioMedResInt*2017 : 7908183,2017.

[11] Amir Waseem , Jahanzaib Arshad, Farhat Iqbal, Ashif Sajjad, Zahid Mehmood, and Ghulam Murtaza,*Pollution Status of Pakistan: A Retrospective Review on Heavy Metal Contamination of Water, Soil, and Vegetables*,BioMed Research International 2013?Current,Volume 2014 ,Article ID 813206,03 Sep 2014.

[12] Nabeela, F., Azizullah, A., Bibi, R. et al. *Microbial contamination of drinking water in Pakistan?a review.*, Environ Sci Pollut Res 21, 13929?13942 (2014).*https* : *//doi.org/*10.1007/*s*11356 – 014 – 3348 – *z*

[13] https://openwho.org/courses/introduction-to-ncov

[14] Shafi, M., Liu, J., Ren, W.(2020). Impact of COVID-19 pandemic on micro, small, and medium-sized Enterprises operating in Pakistan, https://www.sciencedirect.com/science/article/pii/S2590051X20300071

[15] [COVID-19 outbreak: current scenario of Pakistan Author links open overlay panelA.Waris1U.K.Atta2M.Ali1A.Asmat3A.Baset https://www.sciencedirect.com/science/article/pii/S2052297520300330]

[16] Jefferson T, Spencer EA, PlAijddemann A, Roberts N, Heneghan C. Analysis of the Transmission Dynamics of COVID-19: An Open Evidence Review. *https* : *//www.cebm.net/evidence – synthesis/transmission – dynamics – of – covid* – 19/

[17] https://covid19.who.int/region/emro/country/pk

[18] National Information Technology Board in collaboration with ECOM PK (Pvt.) Ltd/ https://covid.gov.pk

[19] Abrar M. Pakistan eases lockdown as Covid-19 kills 46 in single-day spike. Pakistan Today. 08 May 2020. https://www.pakistantoday.com.pk/2020/05/07/govt-announces-to-exitlockdown

[20] Ali A, Zhongren M, Baloch Z. Covid-19 in Pakistan and potential repercussions for the world: is the infection on the verge of endemicity? BMJ 2020;369:m1909. doi:10.1136/bmj.m1909 pmid: 32409494

[21] Ali A, Ma Z, Bai J. Aftermath of torrential rains and covid-19 in Pakistan. BMJ 2020;370:m3776. doi: 10.1136/bmj.m3776 pmid: 32994213

[22] Government of Pakistan. Pakistan statistics. http://covid.gov.pk/

[23] Giordano, G., Blanchini, F., Bruno, R. et al. Modelling the COVID-19 epidemic and implementation of population-wide interventions in Italy. Nat Med 26, 855?860 (2020). https://doi.org/10.1038/s41591-020-0883-7

[24] Anderson,R.M., May,R.M.Infectious Diseases of Humans (Oxford Univ.Press, 1991)

[25] Brauer,F., Castillo-Chavez, C.Mathematical Models in Population Biology and Epidemiology 2nd edn (Springer, 2012)

[26] Kermack,W. O., McKendrick,A. G. A contribution to the mathematical theory of epidemics. Proc. R. Soc. Lond. 115, 700?721 (1927)

[27] Lin, Q. et al. A conceptual model for the coronavirus disease 2019 (COVID-19) outbreak in Wuhan, China with individual reaction and governmental action. Int. J. Inf. Dis. 93, 211?216 (2020).

[28] Anastassopoulou,C., Russo, L., Tsakris, A. , Siettos,C. Data-based analysis, modelling and forecasting of the COVID-19 outbreak. PLoS One 15, e0230405 (2020).

[29] Casella, F. Can the COVID-19 epidemic be managed on the basis of daily data? Preprint at https://arxiv.org/abs/2003.06967 (2020).

[30] Wu, J. et al. Estimating clinical severity of COVID-19 from the transmission dynamics in Wuhan, China. Nat. Med. 26, 506?510 (2020)

[31] Hellewell, J. et al. Feasibility of controlling COVID-19 outbreaks by isolation of cases and contacts. Lancet Global Health 8, e488?e496 (2020).

[32] Kucharski, A. J. et al. Early dynamics of transmission and control of COVID-19: a mathematical modelling study. Lancet Global Health https://doi.org/10.1016/1473-3099(20)30144-4 (2 [33] Gumel, A. B. et al. Modelling strategies for controlling SARS outbreaks.Proc. R. Soc. B Biol. Sci. https://doi.org/10.1098/rspb.2004.2800 (2004).

[34] Sy KTL, White LF, Nichols BE (2021) Population density and basic reproductive number of COVID-19 across United States counties. PLoS ONE 16(4): e0249271. https://doi.org/10.1371/journal.pone.0249271

[35] Cori A, Ferguson NM, Fraser C, Cauchemez S. A New Framework and Software to Estimate Time-Varying Reproduction Numbers During Epidemics. American Journal of Epidemiology. 2013;178(9):1505?12. pmid:24043437

[36] Delamater,*P.L.,Street,E.J.,Leslie,T.F.,Y ang,Y.T.,Jacobsen,K.H.*(2019). Complexity of the basic reproduction number (R0). Emerging infectious diseases, 25(1), 1.

https://doi.org/10.62500/icrtsda.1.1.56

[37] Quinete, N., Hauser-Davis, R.A.(2021). Drinking water pollutants may affect the immune system: concerns regarding COVID-19 health effects. Environmental science and pollution research international,28(1), 1235 to 1246. *https* : *//doi.org/*10.1007/*s*11356–020–11487–4

IMPROVED SCRAMBLING TECHNIQUE FOR APPLICATIONS IN SAMPLE SURVEYS ON SENSITIVE VARIABLES

https://doi.org/10.62500/icrtsda.1.1.60

Proc. 1st International Conference on Recent Trends in Statistics and Data Analytics

Air University Islamabad, Pakistan – May 9, 2024, Vol. 1, pp. 546-555

UNVEILING THE SPECTRUM: ASSESSING SCHOOL TEACHERS' AWARENESS REGARDING AUTISM IN SIALKOT, PAKISTAN

Kanwal Shehzadi[a], Mehwish Asghar[b], Ayesha Fatima[a]

[a] Department of Zoology, Government College Women University, Sialkot.

[b] Department of Statistics, Government College Women University, Sialkot.

ABSTRACT

Autism Spectrum disease (ASD) is a neurodevelopmental illness that causes impaired communication, social interaction, and repetitive and restricted behaviors. Autism's cause is unknown, however genetic and environmental factors have been identified. Parents exhibit concern for their child as early as 18 months, and diagnosis typically occurs between 3-5 years of age. The current study was conducted in Sialkot, Punjab, Pakistan, to analyze school teachers' knowledge and perceptions of autistic students in both public and private institutions. A cross-sectional study of 110 teachers was done utilizing purposive sampling and a self-administered questionnaire. The questionnaire aimed to investigate teachers' knowledge and perceptions about autism. The acquired data was analyzed using SPSS (Version 26). The results showed that there is not a significant difference between theawareness levels of public and private teachers (P>0.05). The overall level of awareness among school teachers has also increased over time. The reported results are quite different from the previous studies conducted in Pakistan which portrayed low level of awareness about autism among school teachers. However, the change in trend about knowledge and perception regarding autism is attributed to the area where the study was conducted and also due to increasing awareness activities.

Keywords: Autism, ASD, Perception, Awareness, Teaching sector

1. INTRODUCTION

Autism spectrum disorder (ASD) refers to a group of early-onset, lifelong, heterogeneous neurodevelopmental conditions with complex mechanisms of emergence. The term "spectrum" reflects the wide variation in the type and severity of symptoms observed in individuals with ASD. Some autistic individuals can be definitively diagnosed with autism as early as 2–3 years of age and the mean age of diagnosis for autistic children is still 4–5 years. It is important to stress that more adults are getting assessed for possible autism. Although young people are frequently recommended to participate in leisure activities including play, sports, hobbies, and social activities, children with ASD tend to spend time in passive play and maladaptive behaviors and they are less likely to spontaneously participate in organized leisure activities such as sports (Memari et al., 2015).

Individuals with ASD must have an early diagnosis and intervention in order to have access to the right services and support. By being aware of the early warning signs and symptoms of ASD, educators, families, and healthcare providers can act before the condition worsens and improves social communication, behaviour, and cognitive development. (Zwaigenbaum et al., 2015). In order to create inclusive learning environments, teachers and administrators need to be aware of the unique needs and learning styles of children with ASD. If they have a solid grasp of ASD, teachers can support the social, intellectual, and emotional development of children with ASD by applying evidence-based strategies and adaptations.

https://doi.org/10.62500/icrtsda.1.1.56

Healthcare providers not only offer comprehensive medical care and support, but they are also essential in identifying ASD. To appropriately tailor therapies and support services, healthcare providers need to be aware of the diagnostic criteria, co-occurring disorders, and traits that set apart individuals with autism spectrum disorders. (Baio, 2018). Understanding ASD helps employers and community members develop inclusive social environments and workplaces. Communities that increase awareness and acceptance of ASD can give persons with the illness equitable opportunities to participate in the workforce, social interactions, and community life. (Hagner & Cooney, 2005). To create policies and promote services and supports, it is essential to understand the varied needs and experiences of people with ASD. Policymakers may create laws and allot funds that support fairness, inclusiveness, and lifelong access to services by hearing the perspectives of people with ASD and their families. (Matson & Kozlowski, 2011).

Kanner and Asperger separately recorded instances of children exhibiting odd social behaviours and communication problems around the beginning of the 20th century. One of the earliest clinical presentations of autism was made in 1943 when Leo Kanner released a study describing a group of kids with "autistic disturbances of affective contact." (Kanner, 1943). And Asperger's work on "autistic psychopathy," which subsequently became known as Asperger's condition, was published in 1944 by Hans Asperger. In 1980, the DSM-III added autism as a diagnostic category for the first time. Pervasive developmental disorder not otherwise specified (PDD-NOS) and Asperger's syndrome were added as subcategories of ASD in the revised DSM-IV and DSM-IV-TR diagnostic criteria. 2013 saw the DSM-5 eliminate distinct diagnoses like Asperger's syndrome and PDD-NOS in favour of combining all autism-related diseases under the general label Autism Spectrum Disorder. (Asperger, 1944).

The difficulties with interpreting and utilising verbal and nonverbal cues of communication are central to Autism Spectrum Disorder. Having trouble understanding and sustaining partnerships. Less empathy and social reciprocity. (Shah, Banner, Heginbotham, & Fulford, 2014). Engaging in repetitive motions or tasks, such rocking, flapping one's hands, or aligning things. Resistance to change and adherence to customs and traditions. The word "hyper reactivity" refers to an increased sensitivity to touch, taste, smell, and visual stimuli, over-stimulated by sensory information, leading to avoidance or sensually oriented activity. (Lord, Elsabbagh, Baird, & Veenstra-Vanderweele, 2018). There is a lot of diversity in the severity of symptoms and functional impairment of ASD due to the wide range of presentations. Some individuals with ASD may have little symptoms and be quite functional, whereas others may have severe deficiencies that require substantial assistance. Different presentations of Autism Spectrum Disorder (ASD) are attributed to variances in cognitive capacities, language development, and adaptive functioning. (Johnson & Myers, 2007).

A full assessment carried out by a multidisciplinary team of psychologists, paediatricians, speech-language pathologists, and occupational therapists is usually required for the diagnosis of ASD. To determine whether core symptoms and accompanying characteristics of ASD are present, clinicians consult standardised diagnostic criteria described in diagnostic manuals such as the DSM-5 or ICD-10. Data from
developmental histories, parent/caregiver interviews, direct observations, and standardised testing can all be used to make a diagnosis. Screening tools like the Modified Checklist for Autism in Toddlers (M-CHAT) are widely used to identify early signs of ASD in children. Assessment covers a wide range of categories, including social communication skills, language development, adaptive behaviour, cognitive functioning, and sensory processing. In order to differentiate ASD from disorders such as ADHD, intellectual disability, or language impairment, clinicians may consider other neurodevelopmental and psychiatric problems that may exhibit similar symptoms. (Robins et al., 2014)

Research has indicated that the genesis of Autism Spectrum Disorder (ASD) is complex, involving both hereditary and environmental elements. (Shah et al., 2014). Advances in neuroimaging have illuminated the neurological differences associated with ASD, including modifications in brain connectivity and anatomy. (Geschwind, 2009). The prevalence of ASD has dramatically increased over the past few decades, raising awareness and knowledge in the process. A plethora of advocacy groups and support organisations have surfaced to furnish persons with Autism Spectrum Disorder (ASD) and their families with resources and services (Baio, 2018).

A higher severity of autism is diagnosed when the general public does not grasp the condition. The purpose of this pilot study was to determine the level of autism understanding among instructors in Sialkot, Punjab, Pakistan. Instructors play a critical role in shaping children's futures and empowering them to take control of

https://doi.org/10.62500/icrtsda.1.1.56

their environment. This study aims to assess educators' understanding of autism and the role that support networks and educational establishments play in raising awareness.

2. MATERIALS AND METHODS

2.1. Study area:

This study was conducted in Sialkot City, which is located between 32° 24° and 32°37°N and 73°59° and 75°02°E. Gujrat District and the State of Jammu and Kashmir lie in the north, whereas Gujranwala District is in the west. Narowal District touches Sialkot in the south. As per Punjab Development Statistics, the population of District Sialkot in 2023 will be 4,499,334 with an average growth rate of 2.44. The total number of primary schools for boys is around 348, whereas 847 primary schools are there for girls, leading to a total of 1222 primary schools in Sialkot. The teachers of these primary schools were the target population for this study ("District Profile," 2023)

2.2. Data Collection Tool

A cross-sectional study was carried out with school teachers using simple random sampling (SRS). A questionnaire on autism symptoms, diagnosis, and treatment was sent to 110 teachers, following (Ullah, Aqdas, Khan, Nabi, & Aziz, 2015) design. Half of the teachers were chosen from public schools and half from private schools.

2.3. Data Analysis:

The collected data was analyzed with SPSS (version 26). We estimated frequencies and percentages for both public and private teachers. The data was analysed using a Chi-Square test to identify differences between public and private school teachers. The mean value for the right number of responses from both categories was also determined. P-values less than 0.05 were regarded as significant.

3. RESULTS AND DISCUSSION

Data from 110 teachers in public and private schools were analyzed. Figure 1 displays the age distribution of the recruited respondents. Figure 2 illustrates that teachers in the public and private sectors have varying levels of education. Out of 110 responders, 51 gained knowledge from media (4 print and 47 electronic), 11 teachers from training, 13 from seminars and workshops, 27 from fellow teachers and friends, and 8 from other sources. Figure 5 depicts the source of information for the recruited teachers.

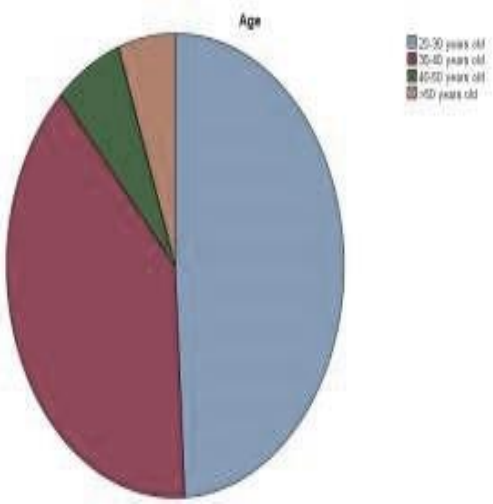

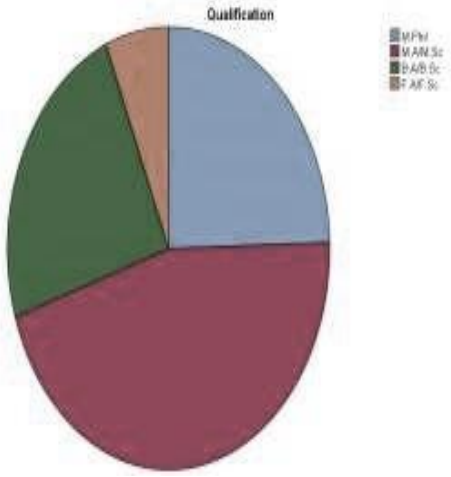

https://doi.org/10.62500/icrtsda.1.1.56

Fig. 1. Age ranges of the recruited teachers

Fig.2. Qualification of the recruited teachers

https://doi.org/10.62500/icrtsda.1.1.56

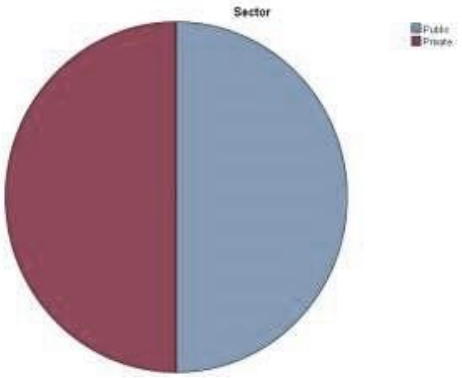

Fig. 3. Teaching sector of recruited teachers

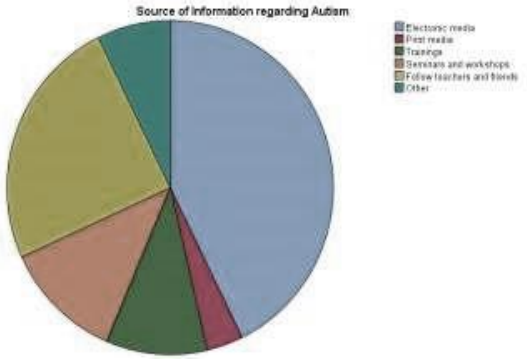

Fig. 4. Source of Information for the recruited teachers regarding Autism

The questionnaire included 13 questions to assess knowledge and 3 questions about the recruited subjects' perceptions about autism. Only 31 public and 17 private school instructors were aware that autism is an inherited condition. Autism, according to 48 public and 45 private school instructors, is a mental and learning condition. Only one question about an autistic child's general eating habits resulted in a statistically significant difference (0.046) between the replies of public and private school teachers. The remaining questions revealed no statistical difference between the responses of public and private school teachers. The overall level of awareness of public and private school teachers combined was higher than that depicted in the previous studies.

Table 1. Knowledge Regarding Autism

Questions	ıblic		Private		Total	lue	P-Value (T-test)
	n	%age	n	%age	N	%age	
Autism is an inherited disorder	31	56.4	17	50.9	59	53.6	0.000
Autism is a learning and mental disorder	48	87.3	45	81.8	93	84.5	0.000
Signs of Autism show between 0 and 3 Years	38	69.1	38	69.1	76	69.1	0.000
An autistic child is not social	49	89.1	49	89.1	98	89.1	0.000

https://doi.org/10.62500/icrtsda.1.1.56

An autistic child has poor communication skills and cannot express himself	49	89.1	49	89.1	98	89.1	0.000
Verbally, an autistic child will have a hard time phrasing a sentence	48	88.9	50	90.9	98	89.1	0.000
Nonverbally, an autistic child does repetitive gestures to express himself	46	83.6	52	94.5	98	89.1	0.000
The attention span of an autistic child is Deficient	42	76.4	44	80.0	86	78.2	0.000
General interests of an autistic child are Restricted	46	85.2	44	80	90	82.6	0.000
An autistic child maintains minimal eye contact with others	50	92.6	48	87.3	98	89.1	0.000
General eating habits of an autistic child are normal	45	83.3	36	66.7	81	75.0	0.000
An autistic child is resistant to change	49	89.1	49	89.1	98	89.1	0.000
An autistic child throws frequent bouts of Anger	51	92.7	47	85.5	98	89.1	0.000

Table 2 shows teacher's perceptions of autism. Both public and private school instructors reported high levels of awareness of autism across all three items. There were no significant differences in P values between public and private school teachers across all questions. A total of 40 public and 42 private school teachers believe autism cannot be treated just with medication and requires cognitive and behavioral therapy. 44 public and 43 private school teachers believe autistic students should be taught in special schools. When asked about specific training, 46 public and 50 private school teachers believe it is necessary for managing autistic students.

Table 2. Perception regarding Autism

Questions	Public		Private		Total		P-Value (χ^2)	P-Value (T-test)
	n	%age	n	%age	N	%age		
Autism is not treatable	40	72.7	42	76.4	82	74.5	0.662	0.000

https://doi.org/10.62500/icrtsda.1.1.56

using medication alone

Autistic child should be taught inspecial school	80.0	43	78.2	87	79.1	0.815	0.000
Managing a child with autism comeswith prior training	83.6	50	90.9	96	87.3	0.252	0.000

Table 3. Comparison of Responses from Public and Private Sector Teachers

	Total no. of questions (total no. of responses)	Total no. of correct responses (%)	Average no. of correct responses per subject	*P*- Value
Comparison of Knowledge				
Public	(715)	507 (70.90)	9.21	0.500
Private	(715)	568 (79.44)	10.32	
Total	(1430)	1075 (75.17)	9.771	
Comparison of Perception				
Public	(165)	130 (78.78)	2.36	0.500
Private	(165)	135 (81.81)	2.45	
Total	(330)	265 (80.30)	2.40	
Comparison of Knowledge and Perception (Combined)				
Public	(880)	637 (72.38)	11.58	0.500
Private	(880)	703 (79.88)	12.78	
Total	(1760)	1340 (76.13)	12.18	

The correct responses of the teachers for both knowledge and perceptions were compared, as given in Table 3. The responses of the teachers for both categories were compared and categorized individually as well as combined. The average correct response per public school teacher was 9.21 while 10.32 per private school teacher. There is not a significant difference between the responses of public and private school teachers. This analysis showed that now in the current era, both public and private school teachers are much qualified having better knowledge and perception about autism.

4. DISCUSSION

ASD is considered the most common multifactorial disorder affecting children today (Sacrey et al., 2015). Currently, the high percentage of ASD among children requires preschool teachers to recognize children's abnormal development and identify them at an early stage followed by referral to specialists (Sallows & Graupner, 2005) . A preschool teacher has a high chance of detecting this type of disorder among his or her students and could identify the student's situation to refer them for appropriate assessment towards obtaining early intervention services (Drusch, 2015). An important part of the early identification of children with ASD is preschool teachers, as they are considered reliable resources for intervention issues (Fantuzzo et al., 1999). Due to their role in dealing with parents to point them toward intervention services. Furthermore, preschool teachers deal with children daily and have been educated in child development.

https://doi.org/10.62500/icrtsda.1.1.56

(Dunlap et al., 2006). Due to these specific characteristics, preschool teachers should have the best qualities to identify children who do not exhibit signs of normal development at an early age (Able, 2012).

According to findings by other researchers, the primary factor influencing preschool instructors' capacity to report children who exhibit behavioural challenges is a lack of information and expertise in addressing such cases (Dunlap et al., 2006). According to a different research, some preschool instructors lacked the necessary knowledge and abilities to deal with troublesome behaviour, and it was suggested that they receive training (Fox & Smith, 2007).

The study emphasizes how important it is for educators to have sufficient understanding of autism spectrum disorder (ASD) in order to assist autistic students in regular classroom settings (Barbaro & Dissanayake, 2013). A study conducted in Singapore (Lian et al., 2008) on 503 preschool teachers found that educators lacked knowledge, attitudes, and practices regarding behavioural and developmental concerns in children. A Cross-sectional Survey from Pakistan, and South Asia (Ayub et al., 2017) showed that 73 educators—with a mean age of 34 and a gender split of 66%—responded. There were awareness and knowledge gaps. Of the instructors surveyed, 52 (71.2%) reported knowing anything about autism, and 23 (44.2%) of them thought of autism as a neurological/mental illness. However, our results are quite different from previous studies reporting a higher awareness rate about autism among school teachers. However, the change in trend about knowledge and perception regarding autism is attributed to the time of conveying the study and also due to increasing awareness activities.
In recent years, an increase in awareness regarding autism is observed. In 2020, a study was conducted in Nigeria in order to assess the school teachers' awareness regarding autism. The results shockingly showed that 96.2% of the participants were aware of the disorder *(Omolayo, Auta, Akinyemi, & Dennis, 2020).* Likewise, another study conducted in 2022 regarding primary school teachers' knowledge of autism spectrum disorders and their attitudes towards inclusive education revealed the same results i.e. high awareness level (Aihie & Uwaoluetan, 2022).

Likewise, our results show that the school teachers have significant awareness regarding autism, $P<0.05$. This is due to their experiences and observation of the children who are already present in the schools and also information in the news and social media about autism. The present study also shows that the largest proportion of the respondents had come to know about autism from social media. The current study also reveals that there is no significant difference between the awareness levels of public and private school teachers. These results are also supported by the fact that according to the Pakistan Economic Survey 2022/23 presented in the Senate, the country's literacy rate is 62.8%. The survey revealed the literacy rate of Punjab to be the highest among provinces, with a percentage of 66.3% leading to the recruitment of well-educated teachers in both public and private sectors resulting in no significant difference between the awareness levels of public and private sector teachers regarding autism (Khattak, 2024).

5. CONCLUSION

Our research concluded that there is much awareness regarding autism among school teachers in Sialkot, Pakistan. Understanding Autism Spectrum Disorder is essential for creating inclusive, supportive, and equitable environments for individuals with ASD and their families. In conclusion, teachers are knowledgeable about autism spectrum disorder (ASD). Through various studies and research initiatives, we are seeing a growing understanding among educators of the complexities and nuances of autism spectrum disorders. Teachers also improve in their ability to recognize the signs and symptoms of autism,

https://doi.org/10.62500/icrtsda.1.1.56

adapt lessons to meet the different needs of students with autism and work well with other stakeholders to create a learning environment. Through education, awareness, research, and advocacy efforts, society can promote acceptance, access to services, and opportunities for individuals with ASD to thrive and contribute meaningfully to their communities.

5. REFERENCES

1. Asperger, H. (1944). Die „Autistischen psychopathen" im kindesalter. *Archiv für psychiatrie und nervenkrankheiten, 117*(1), 76-136.
2. Ayub, A., Naeem, B., Ahmed, W. N., Srichand, S., Aziz, K., Abro, B., . . . Ali, S. (2017). Knowledge and perception regarding autism among primary school teachers: A cross-sectional survey from Pakistan, South Asia. *Indian journal of community medicine, 42*(3), 177-179.
3. Baio, J. (2018). Prevalence of autism spectrum disorder among children aged 8 years—autism and developmental disabilities monitoring network, 11 sites, United States, 2014. *MMWR. Surveillance Summaries, 67*.
4. Barbaro, J., & Dissanayake, C. (2013). Early markers of autism spectrum disorders in infants and toddlers prospectively identified in the Social Attention and Communication Study. *Autism, 17*(1), 64-86.
5. Geschwind, D. H. (2009). Advances in autism. *Annual review of medicine, 60*, 367-380.
6. Hagner, D., & Cooney, B. F. (2005). "I do that for everybody": Supervising employees with autism. *Focus on autism and other developmental disabilities, 20*(2), 91-97.
7. Johnson, C. P., & Myers, S. M. (2007). Identification and evaluation of children with autism spectrum disorders. *Pediatrics, 120*(5), 1183-1215.
8. Kanner, L. (1943). Autistic disturbances of affective contact. *Nervous child, 2*(3), 217-250.
9. Lian, W. B., Ying, S. H. K., Tean, S. C. H., Lin, D. C. K., Lian, Y. C., & Yun, H. L. (2008). Pre-school teachers' knowledge, attitudes and practices on childhood developmental and behavioural disorders in Singapore. *Journal of Paediatrics and Child Health, 44*(4), 187-194.
10. Lord, C., Elsabbagh, M., Baird, G., & Veenstra-Vanderweele, J. (2018). Autism spectrum disorder. *The lancet, 392*(10146), 508-520.
11. Matson, J. L., & Kozlowski, A. M. (2011). The increasing prevalence of autism spectrum disorders. *Research in autism spectrum disorders, 5*(1), 418-425.
12. Memari, A. H., Panahi, N., Ranjbar, E., Moshayedi, P., Shafiei, M., Kordi, R., & Ziaee, V. (2015). Children with autism spectrum disorder and patterns of participation in daily physical and play activities. *Neurology research international, 2015*.
13. Robins, D. L., Casagrande, K., Barton, M., Chen, C.-M. A., Dumont-Mathieu, T., & Fein, D. (2014). Validation of the modified checklist for autism in toddlers, revised with follow-up (M-CHAT-R/F). *Pediatrics, 133*(1), 37-45.
14. Shah, A., Banner, N., Heginbotham, C., & Fulford, B. (2014). 7. American Psychiatric Association (2013) Diagnostic and Statistical Manual of Mental Disorders, 5th edn. American Psychiatric Publishing, Arlington, VA. 8. Bechara, A., Dolan, S. and Hindes, A.(2002) Decision-making and addiction (Part II): myopia for the future or hypersensitivity to reward? Neuropsychologia, 40, 1690–1705. 9. Office of Public Sector Information (2005) The Mental Capacity Act 2005. http://www. *Substance Use and Older People, 21*(5), 9.

https://doi.org/10.62500/icrtsda.1.1.56

15. Ullah, S., Aqdas, I., Khan, N., Nabi, G., & Aziz, T. (2015). Awareness Regarding Autism in Schools' Teachers at District Lower Dir, Khyber Pakhtunkhwa, Pakistan. *Universal Journal of Medical Science, 3*(3), 55-59.
16. Zwaigenbaum, L., Bauman, M. L., Choueiri, R., Kasari, C., Carter, A., Granpeesheh, D., . . . Fein, D. (2015). Early intervention for children with autism spectrum disorder under 3 years of age: recommendations for practice and research. *Pediatrics, 136*(Supplement_1), S60-S81.
17. Able, H. (2012). Preschool Teachers' Perceptions of Factors Influencing their Referral Decisions for Young Children with Severe behavior Problems DISSERTATION. *The University of North Carolina: Chapel Hill, NC, USA*.
18. Aihie, O. N., & Uwaoluetan, O. (2022). Primary school teachers' knowledge of autism spectrum disorders and their attitudes towards inclusive education. *Journal of Teaching and Teacher Education, 10*(01).
19. Asperger, H. (1944). Die „Autistischen psychopathen" im kindesalter. *Archiv für psychiatrie und nervenkrankheiten, 117*(1), 76-136.
20. Ayub, A., Naeem, B., Ahmed, W. N., Srichand, S., Aziz, K., Abro, B., . . . Ali, S. (2017). Knowledge and perception regarding autism among primary school teachers: A cross-sectional survey from Pakistan, South Asia. *Indian journal of community medicine, 42*(3), 177-179.
21. Baio, J. (2018). Prevalence of autism spectrum disorder among children aged 8 years—autism and developmental disabilities monitoring network, 11 sites, United States, 2014. *MMWR. Surveillance Summaries, 67*.
22. Barbaro, J., & Dissanayake, C. (2013). Early markers of autism spectrum disorders in infants and toddlers prospectively identified in the Social Attention and Communication Study. *Autism, 17*(1), 64-86.
23. District Profile. (2023, 2024). *District Sialkot, Government of Punjab*. Retrieved from https://sialkot.punjab.gov.pk/
24. Drusch, S. J. (2015). The early identification of autism spectrum disorder in preschool settings.
25. Dunlap, G., Strain, P. S., Fox, L., Carta, J. J., Conroy, M., Smith, B. J., . . . McCart, A. (2006). Prevention and intervention with young children's challenging behavior: Perspectives regarding current knowledge. *Behavioral Disorders, 32*(1), 29-45.
26. Fantuzzo, J., Stoltzfus, J., Lutz, M. N., Hamlet, H., Balraj, V., Turner, C., & Mosca, S. (1999). An evaluation of the special needs referral process for low-income preschool children with emotional and behavioral problems. *Early Childhood Research Quarterly, 14*(4), 465-482.
27. Fox, L., & Smith, B. J. (2007). Promoting Social, Emotional and Behavioral Outcomes of Young Children Served under IDEA. Issue Brief. *Technical Assistance Center on Social Emotional Intervention for Young Children*.
28. Geschwind, D. H. (2009). Advances in autism. *Annual review of medicine, 60*, 367-380.
29. Hagner, D., & Cooney, B. F. (2005). "I do that for everybody": Supervising employees with autism. *Focus on autism and other developmental disabilities, 20*(2), 91-97.
30. Johnson, C. P., & Myers, S. M. (2007). Identification and evaluation of children with autism spectrum disorders. *Pediatrics, 120*(5), 1183-1215.
31. Kanner, L. (1943). Autistic disturbances of affective contact. *Nervous child, 2*(3), 217-250.
32. Khattak, A. (2024). *Breakdown of Literacy Rates of All Provinces*. Retrieved from https://propakistani.pk/2024/01/05/breakdown-of-literacy-rates-of-all-

https://doi.org/10.62500/icrtsda.1.1.56

provinces/#:~:text=According%20to%20the%20Pakistan%20Economic,with%20a%20percentage%20of%2066.3%25.
33. Lian, W. B., Ying, S. H. K., Tean, S. C. H., Lin, D. C. K., Lian, Y. C., & Yun, H. L. (2008). Pre-school teachers' knowledge, attitudes and practices on childhood developmental and behavioural disorders in Singapore. *Journal of Paediatrics and Child Health*, *44*(4), 187-194.
34. Lord, C., Elsabbagh, M., Baird, G., & Veenstra-Vanderweele, J. (2018). Autism spectrum disorder. *The lancet*, *392*(10146), 508-520.
35. Matson, J. L., & Kozlowski, A. M. (2011). The increasing prevalence of autism spectrum disorders. *Research in autism spectrum disorders*, *5*(1), 418-425.
36. Memari, A. H., Panahi, N., Ranjbar, E., Moshayedi, P., Shafiei, M., Kordi, R., & Ziaee, V. (2015). Children with autism spectrum disorder and patterns of participation in daily physical and play activities. *Neurology research international*, *2015*.
37. Omolayo, B., Auta, M., Akinyemi, E., & Dennis, U. (2020). Knowledge and awareness of autism spectrum disorder among teachers in Ekiti State, Nigeria. *African Journal of Teacher Education*, *9*(2), 43-61.
38. Robins, D. L., Casagrande, K., Barton, M., Chen, C.-M. A., Dumont-Mathieu, T., & Fein, D. (2014). Validation of the modified checklist for autism in toddlers, revised with follow-up (M-CHAT-R/F). *Pediatrics*, *133*(1), 37-45.
39. Sacrey, L.-A. R., Zwaigenbaum, L., Bryson, S., Brian, J., Smith, I. M., Roberts, W., . . . Novak, C. (2015). Can parents' concerns predict autism spectrum disorder? A prospective study of high-risk siblings from 6 to 36 months of age. *Journal of the American Academy of Child & Adolescent Psychiatry*, *54*(6), 470-478.
40. Sallows, G. O., & Graupner, T. D. (2005). Intensive behavioral treatment for children with autism: Four-year outcome and predictors. *American journal on mental retardation*, *110*(6), 417-438.
41. Shah, A., Banner, N., Heginbotham, C., & Fulford, B. (2014). 7. American Psychiatric Association (2013) Diagnostic and Statistical Manual of Mental Disorders, 5th edn. American Psychiatric Publishing, Arlington, VA. 8. Bechara, A., Dolan, S. and Hindes, A.(2002) Decision-making and addiction (Part II): myopia for the future or hypersensitivity to reward? Neuropsychologia, 40, 1690–1705. 9. Office of Public Sector Information (2005) The Mental Capacity Act 2005. http://www. *Substance Use and Older People*, *21*(5), 9.
42. Zwaigenbaum, L., Bauman, M. L., Choueiri, R., Kasari, C., Carter, A., Granpeesheh, D., . . . Fein, D. (2015). Early intervention for children with autism spectrum disorder under 3 years of age: recommendations for practice and research. *Pediatrics*, *136*(Supplement_1), S60-S81.

Knowledge, awareness and attitude of graduates and postgraduates females about premarital screening and genetic counselling

https://doi.org/10.62500/icrtsda.1.1.57

Proc. 1st International Conference on Recent Trends in Statistics and Data Analytics
Air University Islamabad, Pakistan – May 9, 2024, Vol. 1, pp. 556-568

Knowledge, awareness and attitude of graduates and postgraduates females about premarital screening and genetic counselling

Aneeza Hameed[*a], Aniqa Rafique[*a], Mehwish Asghar[*b]
a Department of Zoology, Government College Women University Sialkot, Pakistan
b Department of Statistics, Government College Women University, Sialkot.

ABSTRACT

Premarital screening is a global activity which aims to minimize the spread of genetically inherited, sexually transmitted and infectious diseases whereas Genetic counseling is a process which advice the expected parents who are at risk of getting genetic diseases in their future child. Pakistan is a country with high rate of genetic diseases but premarital screening and genetic counseling is not compulsory in Pakistan and only a limited data on awareness of community population about premarital screening and genetic counseling (PMSGC) is available. Therefore the study was conducted from January 2024 to February 2024 among 200 graduate and postgraduate participants to evaluate the level of knowledge, awareness and attitude about PMSGC. The data was collected by using a pretested and self-administered questionnaire survey form consisting of four main parts .The first, second, third and fourth part was about socio demographic characteristics, knowledge, awareness and attitude level of respondents about PMSGC respectively. The data was analyzed by using IBM SPSS (Statistical package for social science) software version 26.0 and Chi square test was used to find out association between level of education and knowledge, awareness and attitude of respondent towards PMSGC. The results showed a non-significant association between level of education and knowledge, awareness, attitude towards PMSGC as the p value was >0.05.hence the study conclude that knowledge, awareness and attitude towards premarital screening and genetic counseling is Independent of level of education.

Keywords: premarital screening, genetic counseling, knowledge, perception, graduates, postgraduates

1. INTRODUCTION

Marriage is necessary to build happy, strong and stable relationships of families and in many cultures it is considered as an important tradition. Premarital screening and genetic counseling are two approaches which play central role in making healthy and stable families. The process of screening couples for inherited blood abnormalities and infectious diseases who are expecting to marry in near future is called premarital screening. According to national society of genetic counsellors, genetic counselling is a process of serving people to understand and adapt medical, psychological and heritable implications of genetic contribution to disease [1]. Premarital screening and genetic counselling is a worthwhile preventive medicine approach as its aim to reduce the spread of diseases such as sickle-cell anemia and thalassemia which are considered genetic blood diseases and infectious diseases such as AIDS/HIV, hepatitis B and hepatitis C by raising awareness in people about the concept of comprehensive healthy marriage, reducing pressure on blood banks and health institutions, avoiding psychological and social problems for families [2].

Pakistan is an Islamic country in south Asia with a population of over 243 million people, making it the fifth most populous nation in the world. Two-thirds of marriages in Pakistan are consanguineous due to strong sociocultural, economic and religious reasons, leading to high rate of recessively inherited disorders. Many studies have confirmed that cousin marriages increase the risk of genetic and hereditary diseases. High rate of poverty, illiteracy, unavailable medical services and lack of population screening and genetic counselling services lead to increased incidence of genetic diseases in country [3]. There is also high rate

https://doi.org/10.62500/icrtsda.1.1.57

of mental retardation and congenital birth defects. Transmission of infectious diseases such as hepatitis C and AIDS also have high incidence rate. Blood disorder such as β-thalassemia carried by 5-7% i.e. more than 10 million of the population are the most common disorders in Pakistan because mostly people don't prefer premarital screening [4].

Premarital testing programs are mandatory in many countries but depending on culture, tradition and religion, ethical dilemmas are present. Regardless of these ethical concerns, premarital screening is best technique to improve individual quality of life and prevent disease transmission [5]. Premarital screening includes simple blood tests in which couple blood is utilized to do different tests such as complete blood count (CBC), sickle cell test, HIV, HBV and HCV screening and hemoglobin electrophoresis [6]. Through introduction of premarital genetic counselling as a part of healthcare system, the rate of genetic diseases can be reduced. Genetic technologies have potential to decrease the probability of disease development through earliest detection of disease, surveillance of target and preventive measures and provide benefits in future medicine through use of personalized interventions [7,8]. PMSGC should be practiced in Pakistan to reduce this rapidly increasing burden of hereditary diseases. The process of premarital screening and genetic counselling should educate couples and provide them effective and accurate information and in this way strength their relations [9].

Health care professionals are highly efficient and capable to understand premarital testing and genetic counseling and translate these strategies into language which is easily understood by general public. So graduate and post graduate students who are becoming parents in near future must have knowledge about the tests involved in premarital screening and having information about genetics help them in taking the decision about future life i.e. opting clinical screenings, specific treatments and thinking about offspring [10].Awareness about appropriate time to perform testing procedures and anyone have family history of diseases must know the cause whether it is due to consanguineous marriage or not play integral part in marriage decision. But due to different cultural, ethical and religious values, individuals show different attitude toward PMSGC. To encourage public to improve their knowledge and attitude toward premarital testing and genetic counselling which help them in decision making and in this way reduce the prevalence rate of hereditary and infectious diseases in the country, community-based health education campaigns should be run[10,11].

Many researchers have done a lot of work to find out the knowledge and awareness of people along with their attitude towards premarital screening and genetic counseling. A research was conducted to find out the knowledge, awareness and attitude of Medical Students Concerning Genetics and Premarital Screening. He distributed an online, self-administered survey to 302 students from phase 1, 2 and 3 of College of Medicine KSAU-HS, Jeddah Campus with a mean age of 21.68 .The results showed that majority of the students about 86% had a good prior knowledge about genetic counseling and maximum students agreed to make PMS obligatory before marriage and considered PMS as a preventive measure against hereditary diseases showing a positive attitude toward PMS [12].

Another study was performed in Al Riyadh area to find out knowledge, awareness and attitude about premarital screening. He took 564 participants from age above 18 years .the results showed that the respondents had a good Knowledge and moderate awareness about it showing a need for more educational programs regarding PMSGC [13].A study among Taif university students to investigate knowledge, attitude and practices towards national premarital screening program showed that 94% respondents were aware that hereditary diseases are transmitted through genes and moat participants believed that PMS ensures partners health [14].According to university students of north Jordan had a moderate knowledge and positive attitude towards premarital screening [15]. Another study performed in the KSA in 2018 among the unmarried Western population has revealed an overall positive attitude towards premarital screening [16].

https://doi.org/10.62500/icrtsda.1.1.57

However in Pakistan less research have been conducted on awareness about premarital screening and genetic counseling in 2012 a research was conducted to investigate awareness among parents of thalassemia patients and he found out that the awareness was inadequate about thalassemia and it's preventive measures [17].Another research was performed to evaluate awareness about thalassemia among urban population and results showed a low level of knowledge about thalassemia among Urban population of Pakistan [18]. But no study have been conducted about knowledge awareness and attitude about premarital screening and genetic counseling among graduates and postgraduates in Pakistan.

The main objective of this study to evaluate graduates and postgraduates' knowledge and awareness about premarital screening and which tests are involved. To check the knowledge how much they know about genetic counseling and what is appropriate time to perform these procedures. To evaluate the attitude of graduate and post graduate students toward the practice of premarital testing and genetic counseling.

Hypothesis: H_0: There is no significant association between level of education and knowledge awareness about premarital screening and genetic counseling and attitude towards it.

H_a: There is a significantly positive association between level of education and knowledge awareness about premarital screening and genetic counseling and attitude towards it.

2. METHODOLOGY

Study design: A study was conducted to assess the knowledge, awareness and attitude about genetic counseling and premarital screening among graduates and Postgraduates of government College women university Sialkot from January 2024 to February 2024.

Sampling technique: Simple random sampling technique was used to collect data to ensure a representative sample. As in simple random sampling each individual from the target population has an equal chance of being selected.

Sample size: The calculated sample size was 200. The prevalence about knowledge, awareness and attitude was estimated to be of 50% with 95% confidence interval and 5% error.

Inclusion Criteria: All married, coming to married and Single women who are from the ages of 15 and 30 were included in this study.

Exclusion Criteria: Participants who were under the age of 15, over age of 30 and undergraduates were excluded from study.

Data collection: Data was collected by using questionnaire survey. The researchers primarily used questionnaires from previously published studies [13, 19] and to fulfill the objectives of the study the researchers then modified the adopted questionnaires and added an additional portion regarding the knowledge about genetic counseling. The added part was then reviewed by researchers themselves and a field expert to ensure the content validity. The questionnaire consisted of 4 main parts; the first part included 8 questions about socio-demographic characteristics of participants. In it the subjects were also asked about consanguinity and a family history of hereditary diseases, the second part consisted of 7 questions which provided information about knowledge of participants. In this part the participants were asked about genetic counseling and when it is need. The respondents were provided with three options "Yes", "No", "uncertain" for each question .The third part was about awareness of PMSGC program it relied on response of participants about 12 questions. In it the awareness of participants regarding the appropriate time of screening and where it is carried out was checked .The opinion of participants regarding whether the risk of hereditary diseases may increase with cousin marriage and whether premarital screening decrease the rate of spread of genetic diseases were asked. The fourth part assessed attitude of participants exploring their beliefs and opinion about premarital screening by using Likert scale. They were asked about

https://doi.org/10.62500/icrtsda.1.1.57

misunderstanding that premarital screening is against Islamic rules, whether the laws make it compulsory for every future couple to perform premarital screening and whether the religious people should embrace the idea of premarital screening. It took about. 5-10 minutes for completion of questionnaire

Statistical analysis:

The collected data was then reviewed, coded and analyzed by using IBM SPSS (Statistical package for social science) software version 26.0. A scoring system was used for sociodemographic, knowledge, awareness and attitude portions. 2 point was given for every "yes", 1 for "No" and 0 for "Uncertain" answer in case of knowledge. However, the third and fourth part was relied using a Likert scale ranging from strongly agree=5 and strongly disagree=1.Frequency and percentages were used to describe categorical data. Chi square was used to perceive association between qualitative variables i.e. education (graduates and postgraduates) and knowledge, awareness and attitude about premarital screening and genetic counseling Pearson chi-squared test, a p-value ≤ 0.05 was used to report the statistical significance.

Ethical Considerations:

The research topic was discussed with each participant separately and upon approval consent was obtained verbally. The researchers gave right to participants to quit from study without giving reason at any time. Private and personal information was kept confidential during and after study and was only reachable by researchers.

3. RESULTS

The socio-demographic characteristics of participants are presented in table 1. The overall study population was graduate and postgraduate female students who fill the questionnaire in Sialkot, Pakistan. The total strength of participants was 200 and predominant number (70%) were in the age 21-30 and 30% were between ages 15-20.

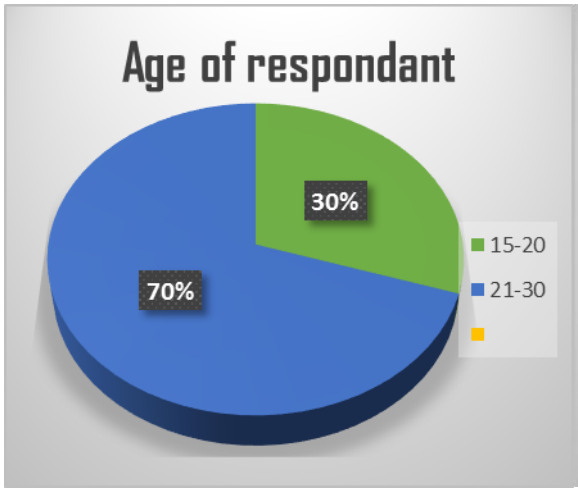

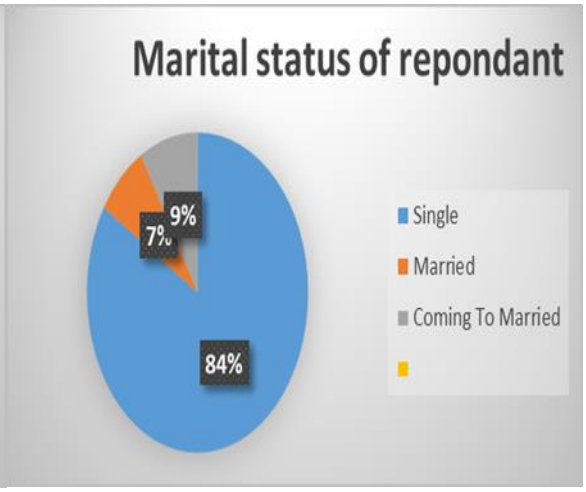

Figure 1: Age of Respondent **Figure 2: Marital Status of Respondent**

For the participant place of residence, 54% were from urban and 46% were from rural. Mostly females were fall in single category with the percentage 83.5%, coming to married females were 8.5% and lowest ratio of married females whose percentage was only 7.5%.

https://doi.org/10.62500/icrtsda.1.1.57

Table1: socio-demographic characteristics of participants, Sialkot, Pakistan (n=200)

Age of respondent	Frequency	Percent
15-20	60	30.0
21-30	140	70.0
Total	200	100.0

Marital Status of Respondent	Frequency	Percent
Single	167	83.5
Married	15	7.5
Coming To Married	17	8.5
Total	200	100.0

Education of Respondent	Frequency	Percent
Graduate	149	74.5
Post Graduate	51	25.5
Total	200	100.0

Area of Respondent	Frequency	Percent
Urban	108	54.0
Rural	92	46.0
Total	200	100.0

Major of Respondent	Frequency	Percent
Biology Related	66	33.0
Non Biology Related	134	67.0
Total	200	100.0

Family History of Respondent	Frequency	Percent
Yes	28	14.0
No	171	85.5
Total	200	100.0

Cousin Marriage of Respondent	Frequency	Percent
Yes	32	16.0
No	168	84.0
Total	200	100.0

Premarital Examination of Respondent	Frequency	Percent
Yes	19	9.5
No	180	90.0
Total	200	100

https://doi.org/10.62500/icrtsda.1.1.57

The percentage of graduate students were 74.5% and postgraduate students were 25.5% with 33% of biology related fields and 67% non-biology related fields.

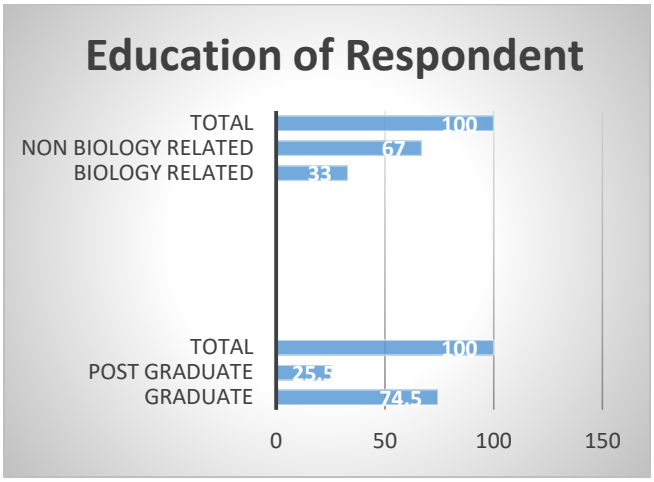

Figure 3: education of respondent

14% participants had family history of genetic disease and 85.5% showed that they had not any family history of genetic diseases. The study shows only 32 (16%) of the respondent reported that there was relative relation between them and their partners (cousin marriages) and 84% participants had not any relation with cousins. Only 9.5% respondents preferred premarital examination and 180 participants out of 200 had not preferred PMS. Majority of students both graduates and post graduates were familiar with genetic counselling.

TABLE 2: knowledge of participants about premarital screening and genetic counselling, Sialkot, Pakistan (n=200)

Questions	Yes	No	Uncertain
Do you know what is genetic counseling	156(78%)	31(15.5%)	12(6%)
Do you know when genetic counseling is needed	131(65.5%)	61(30.5%)	8(4%)
One should seek genetic counseling if there is family history of genetic disease	153(76.5%)	31(15.5%)	16(8%)
One should seek genetic counseling when couple has given birth to child with mental retardation or genetic disease	147(73.5%)	35(17.5%)	18(9%)
Genetic counseling is needed when the women willing to become pregnant is below thirty years of age	103(15.5%)	50(25.0%)	47(23.5%)
If the husband and wife are first cousins then genetic counseling is needed	155(77.5%)	22(11%)	23(11.5%)
Genetic counseling is used for the interpretation of results of prenatal diagnosis	119(59.5%)	30(15%)	51(25.5%)

The data showed out of 200 participants 156 had knowhow about genetic counselling, 12 were uncertain and 31 participants were unaware about counselling in table 2. Table 3 check the knowledge of participants in association with education of participants and non-significant association was observed between the

https://doi.org/10.62500/icrtsda.1.1.57

level of knowledge and education status because P value calculated was 0.236 which is >0.05. Figure 4 showed that 76.5% graduates had knowledge about genetic counselling , 16.8% were unaware and 6.7% were uncertain. 82.4% postgraduates had knowledge about genetic counselling , 11.8% were unaware and 3.9% were uncertain.

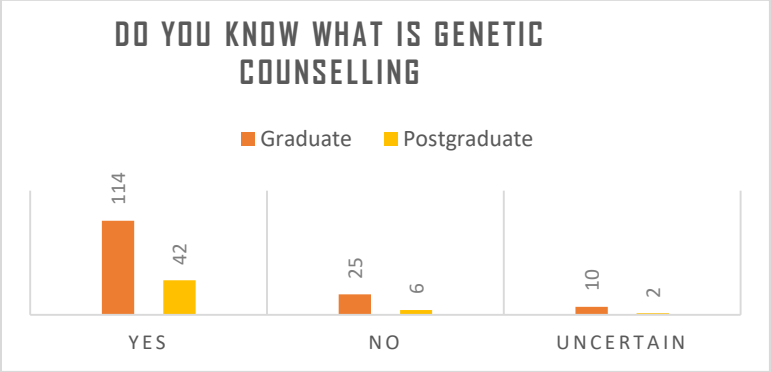

Figure 4: knowledge about genetic counselling

This showed that postgraduates had good knowledge than graduates, with 114 (76.5%) out of 149 compared to postgraduates with 42(82.4%) out of 50. Postgraduates (74.5%) had better knowledge about when genetic counselling is needed as compared to graduates (62.4%). If there is a family history of disease then genetic counselling is needed is better understood by postgraduates (82.4%) than graduates (74.5%). Postgraduates (80.4%) showed more positive knowledge if early child is with mental retardation or genetic disease then go for genetic counselling as compare to graduates (71.1%). Genetic counseling is needed when the women willing to become pregnant is below thirty years of age, this is incorrect question because it is mostly needed above the age of thirty, this is better known by postgraduates as compare to graduates because 31.4% postgraduates marked NO and 22.8% graduates marked No option. Graduates 73.2% had less knowledge as compared to postgraduates 90.2% about genetic counselling is needed when the husband and wife are first cousins. 74.5% of postgraduates had better knowledge about Genetic counseling is used for the interpretation of results of prenatal diagnosis as compared to graduates 54.4% (**table 3).**

Table 3: level of knowledge in association with education of participants (graduates and postgraduates), Sialkot, Pakistan (n=200)

Questions	Categories	Graduate	Postgraduate	Significance
Do you know what is genetic counseling	Yes	114(76.5%)	42(82.4%)	0.241*
	No	25(16.8%)	6(11.8%)	
	uncertain	10(6.7%)	2(3.9%)	
Do you know when genetic counseling is needed	Yes	93(62.4%)	38(74.5%)	0.218*
	No	51(34.2%)	10(19.6%)	
	uncertain	5(3.4%)	3(5.9%)	
One should seek genetic counseling if there is family history of genetic disease	Yes	111(74.5%)	42(82.4%)	0.393*
	No	24(16.1%)	7(13.7%)	

https://doi.org/10.62500/icrtsda.1.1.57

	uncertain	14(9.4%)	2(3.9%)	
One should seek genetic counseling when couple has given birth to child with mental retardation Or genetic disease	Yes No uncertain	106(71.1%) 29(19.5%) 14(9.4%)	41(80.4%) 6(11.8%) 4(7.8%)	0.400*
Genetic counseling is needed when the women willing to become pregnant is below thirty years of age	Yes No uncertain	81(54.4%) 34(22.8%) 34(22.8%)	22(43.1%) 16(31.4%) 13(25.5%)	0.340*
If the husband and wife are first cousins then genetic counseling is needed	Yes No Uncertain	109(73.2%) 20(13.4%) 20(13.4%)	46(90.2%) 2(3.9%) 3(5.9%)	0.040
Genetic counseling is used for the interpretation of results of prenatal diagnosis	Yes No uncertain	81(54.4%) 27(18.1%) 41(27.5%)	38(74.5%) 3(5.9%) 10(19.6%)	0.026
Total average of p value				0.236*

Value marked * are considered as statistically insignificant

Out of 200 participants, 80(40%) were agree that they have heard about premarital screening, 38(19%) were strongly agree, 41were neutral and 29, 12 participants were disagree and strongly disagree. Mostly respondents had awareness about time when this screening should be performed **(Table 4).**

Table 4: Awareness of participants toward Premarital screening and Genetic counselling, Sialkot, Pakistan (n=200)

Questions	**Strongly agree**	**Agree**	**Neutral**	**Disagree**	**Strongly disagree**
Have you heard about Premarital screening test	38 (19%)	80 (40%)	41 (20.5%)	29 (14.5%)	12 (6%)
Is Premarital screening test include Thalassemia test	32 (16%)	56 (28%)	83 (41.5%)	22 (11%)	7 (3.5%)
Is premarital screening test include sickle cell disease	49 (24.5%)	65 (32.5%)	62 (31.5%)	18 (9%)	6 (3%)
Is premarital screening Test Include AIDS Test	46 (23%)	74 (37%)	55 (27.5%)	14 (7%)	11 (5.5%)
Treatment of hereditary blood disease is readily available	41 (20.5%)	64 (32%)	63 (31.5%)	25 (12.5%)	7 (3.5%)
The appropriate time for Genetic Counseling and Premarital Screening before the engagement	49 (24.5%)	68 (34.0%)	49 (24.5%)	28 (14%)	6 (3%)
The appropriate time for genetic counseling and premarital screening after the engagement	32 (16%)	53 (26.5%)	54 (27.0%)	44 (22%)	17 (8.5%)

https://doi.org/10.62500/icrtsda.1.1.57

The main cause of hereditary diseases is cousin marriages	55 (27.5%)	65 (32.5%)	48 (24%)	24 (12%)	8 (4%)
Knowing the health history of those coming to marriage helps provide early treatment and prevents many complications for offspring	85 (42.5%)	69 (34.5%)	34 (17%)	8 (4%)	4 (2%)
premarital screening is avoiding me to have children with hereditary disease	45 (22.5%0	68 (34%)	59 (29.5%)	16 (8%)	12 (6%)
premarital screening safe and has no complications	45 (22.5%)	59 (29.5%0	68 (34.0%)	24 (12%)	4 (2%)
I know where premarital screening carried out.	27 (13.5%)	36 (18%)	63 (31.5%)	48 (24%)	26 (13%)

The statistical analysis finds out non-significant relationship between level of awareness and level of education (p=0.285) which is greater than 0.05 in table 5. Graduates (40.3%) and postgraduates (39.2%) were agree that they have heard about about premarital screening test. 47.7% graduates had not awareness about premarital screening include thalassemia or not and 8.7% were agree and 8.7% were disagree. Postgraduates also showed neutral 23.5% behavior, 17.6% agreed and 35.3% disagreed. 30.2%% graduates had not awareness about premarital screening include sickle cell disease test or not and 7.4%% were agree and 31.5% were disagree. Postgraduates also showed neutral 33.3% behavior, 35.3% agreed and 13.7% disagreed. Premarital screening test Include AIDS test was understood by graduates and postgraduates. Graduates and postgraduates had awareness about the appropriate time for Premarital Screening and Genetic Counseling. Graduates were 28.9% agree and 24.7% strongly disagree that premarital screening is safe and has no complications and this percentage was somehow similar with postgraduates- 31.4% were agree and 17.6% were strongly disagree **(table 5).**

Table5: level of Awareness About Genetic Counseling and Premarital Screening in association with variable- education (graduate and postgraduate), Sialkot, Pakistan (n=200)

Questions	Categories	Strongly agree	Agree	Neutral	Disagree	Strongly disagree	significance
Have you heard about Premarital screening test	Graduate Postgraduate	28(18.8%) 10(19.6%)	60(40.3%) 20(39.2%)	34(22.8%) 7(13.7%)	20(13.4%) 9(17.6%)	7(4.7%) 5(9.8%)	0.452*
Is Premarital screening test include Thalassemia test	Graduate Postgraduate	6(4.0%) 1(2.0%)	13(8.7%) 9(17.6%)	71(47.7%) 12(23.5%)	13(8.7%) 18(35.3%)	6(4.0%) 11(21.6%)	0.025
Is premarital screening test include sickle cell disease	Graduate Postgraduate	6(4.0%) 9(17.6%)	11(7.4%) 18(35.3%)	45(30.2%) 17(33.3%)	47(31.5%) 7(13.7%)	40(26.8%) 0(0.0%)	0.253*
Is premarital screening Test Include AIDS Test	Graduate Postgraduate	36(24.2%) 10(19.6%)	55(36.9%) 19(37.3%)	41(27.5%) 14(27.5%)	8(5.4%) 6(11.8%)	9(6%) 2(3.9%)	0.579*

https://doi.org/10.62500/icrtsda.1.1.57

Treatment of hereditary blood disease is readily available	Graduate Postgraduate	38(25.5%) 3(5.9%)	43(28.9%) 21(41.2%)	46(30.9%) 17(33.3%)	15(10.1%) 10(19.6%)	7(4.7%) 0(0.0%)	0.007
The appropriate time for Genetic Counseling and Premarital Screening before the engagement	Graduate Postgraduate	40(26.8%) 9(17.6%)	46(30.9%) 22(43.1%)	42(28.2%) 7(13.7%)	15(10.1%) 13(25.5%)	6(4%) 0(0.0%)	0.005
The appropriate time for genetic counseling and premarital screening after the engagement	Graduate Postgraduate	25(16.8%) 7(13.7%)	34(22.8%) 19(37.3%)	47(31.5%) 7(13.7%)	28(18.8%) 16(31.4%)	15(10.1%) 2(3.9%)	0.017
The main cause of hereditary diseases is cousin marriages	Graduate Postgraduate	39(26.2%) 16(31.4%)	49(32.9%) 16(31.4%)	40(26.8%) 8(15.7%)	15(10.1%) 9(17.6%0	6(4%) 2(3.9%)	0.381*
Knowing the health history of those coming to marriage helps provide early treatment and prevents many complications for offspring	Graduate Postgraduate	66(44.3%) 19(37.3%)	48(32.2%) 21(41.2%)	27(18.1%) 7(13.7%)	4(2.75%) 4(7.8%)	4(2.7%) 0(0.0%)	0.226*
premarital screening is avoiding me to have children with hereditary disease	Graduate Postgraduate	35(23.5%) 10(19.6%)	50(33.6%) 18(35.3%)	44(29.5%) 15(29.4%)	11(7.4%) 5(9.8%)	9(6%) 3(5.9%)	0.967*
premarital screening safe and has no complications	Graduate Postgraduate	36(24.2%) 9(17.6%)	43(28.9%) 16(31.4%)	54(36.2%) 14(27.5%)	12(8.1%) 12(23.5%)	4(2.7%) 0(0.0%)	0.031
I know where premarital screening carried out.	Graduate Postgraduate	23(15.4%) 4(7.8%)	27(18.1%) 9(17.6%)	49(32.9%) 14(27.5%)	32(21.5%) 16(31.4%)	18(12.1%) 8(15.7%)	0.418*
Total average of p value							0.285*

Value marked * are considered as statistically insignificant

https://doi.org/10.62500/icrtsda.1.1.57

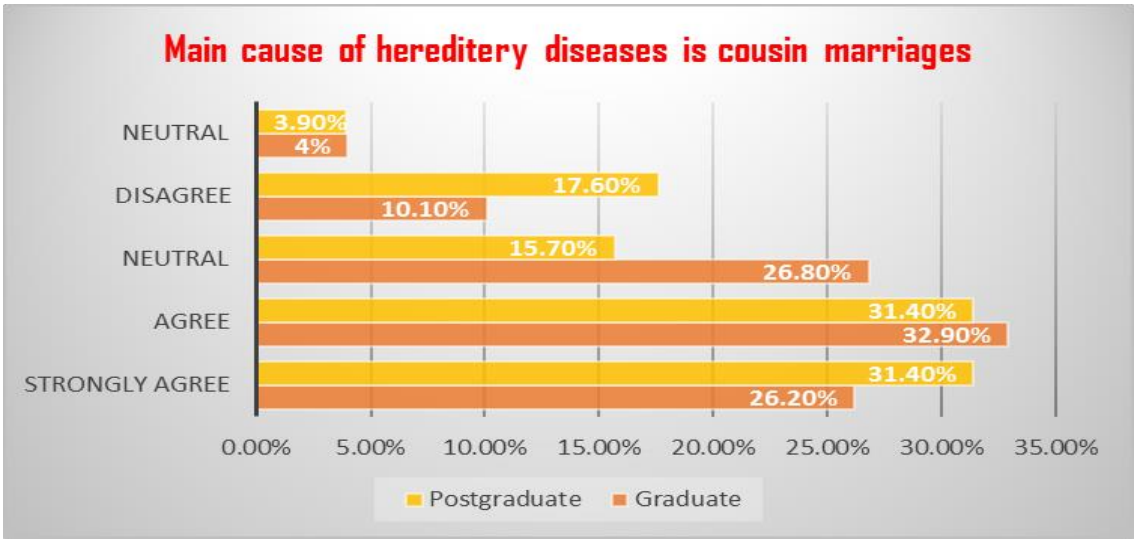

Figure 5: awareness of graduates and postgraduates about reason of hereditary diseases is cousin marriages.

Table 6: Attitude of participants toward Premarital Screening and Genetic Counseling, Sialkot, Pakistan (n=200)

Questions	Strongly agree	Agree	Neutral	Disagree	Strongly disagree
It is important to raise awareness about PMS before marriage to reduce genetic diseases	108 (54%)	76 (38%)	6 (3%)	7 (3.5%)	3 (1.5%)
I support PMSGC	66 (33.0%)	83 (41.5%)	37 (18.5%)	9 (4.5%)	5 (2.5%)
PMS disrupts young man or women from marriage	32 (16%)	60 (30%)	67 (33.5%0	34 (17%)	7 (3.5%)
If I have a hereditary disease, I do not refuse to marry a person who is a carrier for the same genetic disease	39 (19.5%)	59 (29.5%)	43 (21.5%0	45 (22.5%)	14 (7%)
Test results that shows presence of genetic disease should change the marriage decision	57 (28.5%)	77 (38.5%)	45 (22.5%)	14 (7%)	7 (3.5%)
I support adding the family's medical history to the PMSGC	57 (28.5%)	77 (38.5%)	40 (20%)	22 (11%)	4 (2%)
I support the addition of a psychiatric examination such as schizophrenia and depression to PMSGC	57 (28.5%)	61 (30.5%)	57 (28.5%)	19 (9.5%)	6 (3%)
PMS is against Islamic rules	31 (15.5%)	29 (14.5%)	94 (47%)	32 (16%)	14 (7%)
Religious people should adopt the ideas of PMS in their discussion	42 (21%)	73 (36.5%)	59 (29.5%)	17 (8.5%)	9 (4.5%)
The law that obligate all future couples to do PMS is important	46 (23.0%)	70 (35.0%)	56 (28.0%)	23 (11.5%)	5 (2.5%)

https://doi.org/10.62500/icrtsda.1.1.57

It is important to apply a law that stops upon discovery of presence of discovery of a genetic disease	38 (19%)	58 (29%)	64 (32%)	31 (15.5%)	9 (4.5%)
PMS breaks personal privacy	39 (19.5%)	43 (21.5%)	60 (30%)	47 (23.5%)	11 (5.5%)

Out of 200 participants, 108(54%) were strongly agree that it is important to raise awareness about premarital screening to reduce genetic diseases. About 67(33.5%) were neutral and 60 participants agreed that PMS disrupts young man or woman from marriage. 39 respondents strongly agreed that premarital screening breaks personal privacy, 47 participants disagreed with this statement and 60 (30%) were neutral **(Table 6).** Figure 6 shows that 73(49%) graduates were neutral about premarital screening is against Islam, 23 respondents strongly agreed, 18 were agree and 23(15.4%) were disagree. Postgraduates were fall in percentage such as 41.2% were neutral, 21.6% were agree, 15.7% were strongly agree, 17.6% and 3.9% participants disagreed and strongly disagreed respectively.

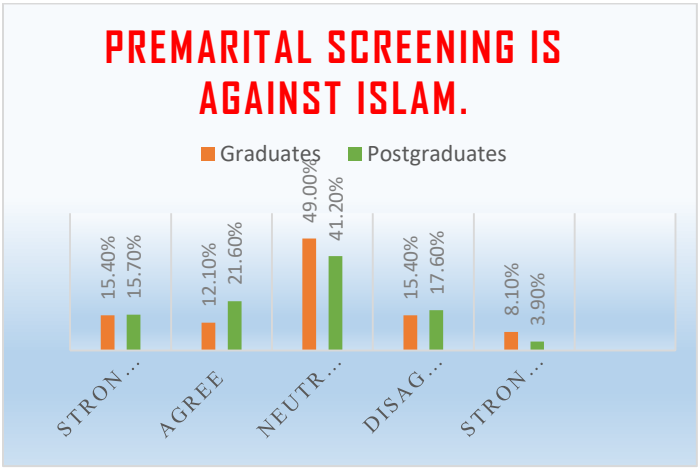

Figure 6: premarital screening against Islamic rules

Table 7: level of Attitude toward Premarital Screening and Genetic Counseling in association with education (graduates and postgraduates) Sialkot, Pakistan (n=200)

Questions	Categories	Strongly agree	Agree	Neutral	Disagree	Strongly disagree	Significance
It is important to raise awareness about PMS before marriage to reduce genetic diseases	Graduates Postgraduates	82(55.0%) 26(51.0%)	54(36.2%) 22(43.1%)	3(2%) 3(5.9%)	7(4.7%) 0(0%)	3(2%) 0(0%)	0.206*
I support PMSGC	Graduates Postgraduates	45(30.2%)	66(44.3%)	29(19.5%) 8(15.7%)	4(2.7%) 5(9.8%)	5(3.4%) 0(0%)	0.057*

https://doi.org/10.62500/icrtsda.1.1.57

		21(41.2%)	17(33.3%)				
PMS disrupts young man or women from marriage	Graduates Postgraduates	24(16.1%) 8(15.7%)	42(28.2%) 18(35.3%)	51(34.2%) 16(31.4%)	25(16.8%) 9(17.6%)	7(4.7%) 0(0%)	0.533*
If I have a hereditary disease, I do not refuse to marry a person who is a carrier for the same genetic disease	Graduates Postgraduates	34(22.8%) 5(9.8%)	40(26.8%) 19(37.3%)	31(20.8%) 12(23.5%)	31(20.8%) 14(27.5%)	13(8.7%) 1(2.0%)	0.090*
Test results that shows presence of genetic disease should change the marriage decision	Graduates Postgraduates	42(28.2%) 15(29.4%)	55(36.9%) 22(43.1%)	36(24.2%) 9(17.6%)	12(8.1%) 2(3.9%)	4(2.7%) 3(5.9%)	0.532*
I support adding the family's medical history to the PMSGC	Graduates Postgraduates	44(29.5%) 13(25.5%)	56(37.6%) 21(41.2%)	27(18.1%) 13(25.5%)	18(12.1%) 4(7.8%)	4(2.7%) 0(0.0%)	0.499*
I support the addition of a psychiatric examination such as schizophrenia and depression to PMSGC	Graduates Postgraduates	43(28.9%) 14(27.5%)	44(29.5%) 17(33.3%)	43(28.9%) 14(27.5%)	13(8.7%) 6(11.8%)	6(4%) 0(0%)	0.617*
PMS is against Islamic rules	Graduates Postgraduates	23(15.4%) 8(15.7%)	18(12.1%) 11(21.6%)	73(49.0%) 21(41.2%)	23(15.4%) 9(17.6%)	12(8.1%) 2(3.9%)	0.420*
Religious people should adopt the ideas of PMS in their discussion	Graduates Postgraduates	33(22.1%) 9(17.6%)	55(36.9%) 18(35.3%)	46(30.9%) 13(25.5%)	9(6%) 8(15.7%)	6(4%) 3(5.9%)	0.266*
The law that obligate all future couples to do PMS is important	Graduates Postgraduates	40(26.8%) 6(11.8%)	51(34.2%) 19(37.3%)	37(24.8%) 19(37.3%)	18(12.1%) 5(9.8%)	3(2%) 2(3.9%)	0.154*
It is important to apply a law that stops upon discovery of presence of discovery of a genetic disease	Graduates Postgraduates	32(21.5%) 6(11.8%)	43(28.9%) 15(29.4%)	42(28.2%) 22(43.1%)	24(16.1%) 7(13.7%)	8(5.4%) 1(2%)	0.226*
PMS breaks personal privacy	Graduates Postgraduates	22(14.8%) 17(33.3%)	31(20.8%) 12(23.5%)	47(31.5%) 13(25.5%)	39(26.2%) 8(15.7%0	10(6.7%) 1(2%)	0.031
Total average of p value							0.303*

Value marked * are considered as statistically insignificant

https://doi.org/10.62500/icrtsda.1.1.58

The collected data showed the overall attitude score of participants from Sialkot area. A non-significant association was observed between the level of attitude and level of education because P value (0.303) which is greater than 0.05 in table 7. The results present the acceptance of participants toward premarital screening and genetic counselling because 66 (33.0%) participants were strongly agree and 83 (41.5%) participants were agree for support of premarital screening and genetic counselling out of 200.

4. DISCUSSION

The importance of premarital counselling as a public health measure have begun to realize by many nations. Newly married couples can learn about reproductive health and marriage by understanding premarital screening and genetic counselling. Two-thirds of marriages in Pakistan are consanguineous due to strong sociocultural, economic and religious reasons, leading to high rate of recessively inherited disorders. Many studies have confirmed that cousin marriages increase the risk of genetic and hereditary diseases. High rate of poverty, illiteracy, unavailable medical services and lack of population screening and genetic counselling services lead to increased incidence of genetic diseases in country [3]. There is also high rate of mental retardation and congenital birth defects. Transmission of infectious diseases such as hepatitis C and AIDS also have high incidence rate. Blood disorder such as β-thalassemia carried by 5-7% i.e. more than 10 million of the population are the most common disorders in Pakistan because mostly people don't prefer premarital screening. Therefore there was a great need to carry out this study to assess the knowledge, awareness and attitude of educated community (female graduates and postgraduates) in Sialkot, Pakistan. A total of 200 participants were enrolled in the study, all of the participants were females. High proportion of the participants (70%) were in the age group of 21-30, this result is similar to other reported studies including study that was conducted at hospital King Khalid University Hospital between February 21, 2017, and March 7, 2018. Unmarried participants were in high proportion (83.5%) and proportion of married participants was only 7.5% in the present study. The study was conducted in university students with highest number of graduates (149 out of 200).

Out of 200 participants, 180 participants had not preferred PMS but 149 participants respond that they support PMSGC. This showed that they were only in favor of PMS but did not prefer to perform these testing procedures so this represented their negative attitude. 14% respondent reported that they had family history of genetic diseases, these findings are somehow similar to conducted study in Abha by Al-Khaldi et al where 10% respondents reported that they had family history of genetic diseases [20].The data showed out of 200 participants 156 had knowhow about genetic counselling, 12 were uncertain and 31 participants were unaware about counselling. Postgraduates (74.5%) had better knowledge about when genetic counselling is needed as compared to graduates (62.4%). Postgraduates had also showed better understanding as compare to graduates with respect to best time for genetic counselling, either it is used for prenatal diagnosis or not and its importance when partners are close relatives (consanguineous marriage).

In this study, regarding the target diseases by PMS, only 88 participants out of 200 knew that thalassemia test includes in PMS which show lack of awareness in public and this result was similar to result of [18] who conducted study to evaluate awareness about thalassemia among urban population and results showed a low level of knowledge about thalassemia among Urban population of Pakistan. Participants had moderate awareness (120 out of 200) about AIDS test include in PMS, there is a need of awareness campaigns in public to avoid hereditary and infectious diseases transfer from generation to generation. 120 participants out of 200 considered that main cause of hereditary diseases is cousin marriages. 104 participants agreed that premarital screening is safe and has no complications but due to lack of awareness only 63 participants know where premarital screening is carried out, so this shows that there is a great need to plan such services which increase knowledge and awareness in public.

This study shows a positive attitude of participants toward premarital screening and genetic counselling because 74.5% respondents support PMSGC. The result is similar to study results which was conducted at KKUH, where 72.2% of university-educated participants had a positive attitude [21]. 92 participants agreed that PMS disrupt young man and woman from marriage and almost 67 respondents were neutral. 30% participants were agree that PMS is against Islamic rules and 47% showed neutral attitude so 57% participants agreed that religious people should adopt the ideas of PMS in their discussion. However, 41% considered PMS breaks personal privacy so they had fears for carrying out PMS.

5. CONCLUSION

https://doi.org/10.62500/icrtsda.1.1.58

Pakistan is among the few countries with high prevalence rate of genetic diseases so the present study looked at the level of level of knowledge, awareness and attitude about premarital screening and genetic counseling among graduates and postgraduate females of Sialkot. This study results highlighted that the sample population showed a good level of knowledge and awareness about PMSGC. The respondents also showed an overall positive attitude towards premarital screening with majority of respondents believing that premarital screening is a preventive measure against hereditary genetic diseases. Respondents also agreed that it should be obligatory to get premarital examination done before marriage. These responses showed the importance of this program with maximum people supporting it. The statistical analysis showed that the association between level of knowledge, awareness, attitude and level of education is non-significant. As the p value for knowledge (0.236), awareness (0.258) and attitude (0.303) is greater than level of significance 0.05.So the researchers claim that there is significantly positive association between these two categorical variables is rejected and the null hypothesis which states that is no association is accepted The present study conclude that level of education and knowledge, awareness and attitude of respondents are independent.

6. RECOMMENDATIONS

Despite the fact that the respondents had a basic knowledge and awareness about premarital screening and genetic counseling and showed a positive attitude towards PMSGS, the results revealed that there is a lack of acceptance for PMSGS among the participants as only 9.5% of the respondents agreed that they will get premarital screening done before marriage, while the 90.5% of the participants refused to have a self-premarital examination. This lack of acceptance comes from cultural norms and religious beliefs that are rooted in our society, as some people believe that this program is against Islamic rules and should not be carried out. So, the researchers recommend that religious scholars should address this topic to raise awareness among the people.

References

1. Resta, R. G. (2006). *Defining and redefining the scope and goals of genetic counseling.* Paper presented at the American Journal of Medical Genetics Part C: Seminars in Medical Genetics.
2. Gosadi, I. M. (2019). National screening programs in Saudi Arabia: overview, outcomes, and effectiveness. *Journal of infection and public health, 12*(5), 608-614.
3. Baig, S. M., Azhar, A., Hassan, H., Baig, J. M., Aslam, M., Ud Din, M. A., . . . Zaman, T. (2006). Prenatal diagnosis of β-thalassemia in Southern Punjab, Pakistan. *Prenatal diagnosis, 26*(10), 903-905.
4. Khaliq, S. (2022). Thalassemia in Pakistan. *Hemoglobin, 46*(1), 12-14.
5. Alahmad, G., Hifnawy, T., Abbasi, B., & Dierickx, K. (2016). Attitudes toward medical and genetic confidentiality in the Saudi research biobank: An exploratory survey. *International journal of medical informatics, 87*, 84-90.
6. Rahman, M. M., Naznin, L., Giti, S., Islam, M. S., & Khatun, N. (2014). Premarital health screening a review and update. *Journal of Armed Forces Medical College, Bangladesh, 10*(1), 103-109.
7. Etchegary, H., Cappelli, M., Potter, B., Vloet, M., Graham, I., Walker, M., & Wilson, B. (2009). Attitude and knowledge about genetics and genetic testing. *Public health genomics, 13*(2), 80-88.
8. Oliveri, S., Masiero, M., Arnaboldi, P., Cutica, I., Fioretti, C., & Pravettoni, G. (2016). Health orientation, knowledge, and attitudes toward genetic testing and personalized genomic services: preliminary data from an Italian sample. *BioMed research international, 2016*.
9. Kigin, M. L. (2005). At-Risk Individuals' Awareness, Motivation, Roadblocks to Participation in Premarital Interventions, and Behaviors Following Completion of the RELATionship Evaluation (RELATE).
10. Al-Farsi, O. A., Al-Farsi, Y. M., Gupta, I., Ouhtit, A., Al-Farsi, K. S., & Al-Adawi, S. (2014). A study on knowledge, attitude, and practice towards premarital carrier screening among adults attending primary healthcare centers in a region in Oman. *BMC Public Health, 14*, 1-7.
11. Al Kindi, R., Al Rujaibi, S., & Al Kendi, M. (2012). Knowledge and attitude of university students towards premarital screening program. *Oman medical journal, 27*(4), 291.
12. D, R. R. (2006;). Defining and redefining the scope and goals of genetic counselling. A. *Am J Med Genet 2, 142C*(4), 269-275.
13. Aljulifi, M. Z., Almutairi, M. A. S., Ahmad, M. S., Abdall, S. M., Alelaiwi, M. M. M., Almutairi, F. L. M., . . . Albaker, A. B. (2022). Awareness and acceptance of premarital screening test and genetic

https://doi.org/10.62500/icrtsda.1.1.58

counseling program in Riyadh area, Saudi Arabia. *Pakistan Journal of Medical & Health Sciences, 16*(02), 875-875.
14. Melaibari, M., Shilbayeh, S., & Kabli, A. (2017). University students' knowledge, attitudes, and practices towards the national premarital screening program of Saudi Arabia. *Journal of Egyptian Public Health Association, 92*(1), 36-43.
15. Alkhaldi, S. M., Khatatbeh, M. M., Berggren, V. E., & Taha, H. A. (2016). Knowledge and attitudes toward mandatory premarital screening among university students in North Jordan. *Hemoglobin, 40*(2), 118-124.
16. Binshihon, S. M., Alsulami, M. O., Alogaibi, W. M., Mohammedsaleh, A. H., Mandourah, H. N., Albaity, B. S., & Qari, M. H. (2018). Knowledge and attitude toward hemoglobinopathies premarital screening program among unmarried population in western Saudi Arabia. *Saudi medical journal, 39*(12), 1226.
17. Ishaq, F., Hasnain Abid, F., Akhtar, A., & Mahmood, S. (2012). Awareness among parents of ββ-Thalassemia major patients, regarding prenatal diagnosis and premarital screening. *Journal of the College of Physicians and Surgeons Pakistan, 22*(4), 218-221.
18. Ebrahim, S., Raza, A. Z., Hussain, M., Khan, A., Kumari, L., Rasheed, R., . . . Zaheer, R. (2019). Knowledge and Beliefs regarding thalassemia in an urban population. *Cureus, 11*(7).
19. Nahla Khamis, I., Jamel, B., Hussein, A. B., Jawaher, A. A., Adnan, A. B., Mahdi, Q., . . . Hashim, F. (2013). Premarital screening and genetic counseling program: knowledge, attitude, and satisfaction of attendees of governmental outpatient clinics in Jeddah.
20. Al-Khaldi, Y. M., Al-Sharif, A. I., Sadiq, A. A., & Ziady, H. H. (2002). Attitudes to premarital counseling among students of Abha Health Sciences College. *Saudi medical journal, 23*(8), 986-990.
21. Al-Qattan, H. M., Amlih, D. F., Sirajuddin, F. S., Alhuzaimi, D. I., Alageel, M. S., Bin Tuwaim, R. M., & Al Qahtani, F. H. (2019). Quantifying the levels of knowledge, attitude, and practice associated with sickle cell disease and premarital genetic counseling in 350 Saudi adults. *Advances in Hematology, 2019*.

https://doi.org/10.62500/icrtsda.1.1.58

Proc. 1st International Conference on Recent Trends in Statistics and Data Analytics
Air University Islamabad, Pakistan – May 9, 2024, Vol. 1, pp. 569-588

SMART HELMET WITH INTEGRATED GLOBAL SYSTEM FOR MOBILE COMMUNICATION, VITALS and HAZARDOUS EVENT DETECTION

Farwa Suman and Dr. Jahanzeb Gul

Abstract

Every year, thousands of bike riders lose their precious lives in road accidents due to the unavailability of first aid, absence of accident reporting or dearth of emergency services. Therefore, taking under consideration the social responsibility, we have designed a Smart Helmet with integrated GSM (Global System for Mobile Communication) and GPS (Global Positioning System) technologies. The aim of this project is to inform the concerned authorities as well as the family members of the rider about his location of accident and his vitals through an auto-generated text message. The proposed Smart Helmet consists of ADXL-345, Fire, MQ-2 and sensors for the detection of Accident, fire, smoke and pulse rate respectively. Whereas, using a Neo-6m-GPS,we can track the location of the rider at the time of accident and SIM900L to send information about the hazardous event through text message. All of these sensors and modules communicate through Arduino-Mega-2560. The integration of these smart sensors turns an ordinary helmet into a smart helmet. All of these components programmed. Together leading to safe motorcycle riding and immediate medical assistance in case of emergency.

Keywords: smart helmet , Navigation, Vital and hazardous event detection, 3D printing .

I. INTRODUCTION

1.1 Background and Motivation

Every year, a tragic number of fatalities occur in road accidents in Pakistan. Mostly, bike riders and racers are the subject of these accidents. The statistics of road accidents are very alarming and demand immediate remedial measures. According to Pakistan Bureau of Statistics (PBS), from 2009 to 2020, there are 104,105 accidents reported in Pakistan out of which 44,959 are fatal while 59,146 are non-fatal accidents. In these accidents, 55,141 people passed away while 126,144 got injured. In addition to this, a figure of 120,501 vehicles were involved in these accidents leading to a huge material loss [6]. The data reveals that the cause of death in most of the cases is the belated response by the concerned authorities. Due to the unavailability of first aid, absence of accident reporting, dearth of emergency services or due to lack of immediate medical assistance, either the person dies or at least leads to some severe injury.

There is a list of reasons for such road accidents including over-speeding, violation of traffic rules etc. In order to address this, proper laws must be implemented by the government. But this is a long process. The need of the hour is to come up with such a solution that can provide immediate safety to the subject. In developed countries, there is much emphasis on smart emergency management along with the smart devices to avoid any injury in case of road accidents, but in Asian countries, we are still far behind.

In order to avoid any possible injury as a result of road accidents, we proposed a system capable of offering protection, security, and safety for bike riders. The system has integrated GSM & GPS technology which instantly notifies the emergency contacts of the accident's location via the

https://doi.org/10.62500/icrtsda.1.1.58

database. And con jointly completely different sensors like MQ2 sensor to detect smoke flame sensor to detect fire and accelerometer which measures the change in tilt in X,Y and Z axes to detect accident respectively.

1.2 Sustainable Development Goals

One of the Sustainable Development Goals (SDGs) is good health and well-being. This project ensures the safety of the rider when riding a bike and thus fulfills the SDG of the wellbeing of the two-wheeler riders.

1.3 Literature Review

In 2005, the creator [2] designed a smart helmet to ensure that bike riders must wear a helmet. It includes two separate sections; one is a transmitter section while the other is the receiver. Both these sections communicate wirelessly. A transmitter is placed on the helmet while a receiver circuit is mounted on the ignition system of the bike. The bike is ignited only when the rider is wearing a helmet. Based on a Radio Frequency Signal (RF) link system, the transmitter-receiver module operates on a frequency of 434MHz. Instead of using any microcontroller, it has employed HT12E and HT12D ICs as encoder and decoder respectively. As the rider wears a helmet, the transmitter sends an RF signal. The signal from the RF transmitter reaches the encoder in the form of address bits and control bits constituting parallel data. The data is encoded into serial bits by the encoder. This encoded data is received by the RF receiver decodes the serial data into parallel data and this data is sent them to the output data pins. A comparison of the serial input data with local addresses three times continuously in search of error or any unmatched codes. The input data is decoded only if there is no error allowing the switching of the relay on leading to the ignition of the bike.

Another helmet has also been designed previously that not only checks the buckling of the helmet on the rider's head but also checks the breath of the rider to avoid any accident as a result of alcohol drinking. The alcohol sensor and the helmet checking switch both are fitted within the helmet. The microcontroller reads the data from these two sensors. Only if the helmet is authenticated and there is no alcohol detected, the data is fetched to the encoder that converts the analog data from the sensors into a binary data and transfers it to the transmitter that transmits it. This transmitted data is received by the receiver on the bike unit. The receiver feeds the data to the decoder that decodes the digital data and delivers it to the microcontroller that drives the engine of the bike through relay. The bike gets started only if the motorcyclist is wearing his helmet properly and is non-alcoholic. [3]

However, in Microcontroller and Sensor Based Smart Biking System for Driver's Safety by S. J. Swathi, not only the safety of the driver was taken into consideration but also the security system for the bike had also been designed. This smart helmet is designed for three main functionalities. Firstly, it checks whether the rider is wearing the helmet or not. The ignition system will work only if the motorcyclist is wearing a helmet. Secondly, it has integrated sensors in it that check the alcoholic condition of the driver eliminating the act of driving if there is any iota of alcoholic condition. Thirdly, ensuring the security of the helmet it has an inbuilt password system. For controlling all the timing and control unit of the system, Atmega-8 Microcontroller is used. Two sensors have been utilized, one is a proximity sensor that detects the presence of helmet on the motorcyclist's head, while the other is a gas sensor that detects the presence of alcohol in its surrounding as well as the presence of any other released gases in the environment. This sensor turns the ignition system off in case of any alcohol or other harmful gases in the proximity. In

https://doi.org/10.62500/icrtsda.1.1.58

addition to this, the security system of the helmet has been achieved by the RFID (Radio Frequency Identification) technology. An LCD is also mounted over the helmet for displaying messages. The data collected by the sensors is in the form of analog signals which are converted into Digital signal by the inbuilt analog to digital converter of the Atmega-8 microcontroller and feeds the digital data to the microcontroller. When the RFID tag of the rider matches with the tag of the helmet, only then the access to the bike is given eliminating the risk of bike theft. The bike module starts its operation only when the sensors of the helmet module allow it. [4]

Moreover, another smart helmet includes the feature of accident detection along with GSM technology to inform about the calamity. In addition to the helmet authentication by using PIR (Proximity Infrared Sensor) sensor and alcohol detection by using MQ3R sensor for alcohol detection, it has also incorporated an accelerometer, ADXL33 for fall detection. The basic purpose of the accelerometer is to detect the happening of any accident by detecting the acceleration in all the three axes utilizing the Micro electromechanical System (MEMS) technology. In case of any accident detected by the accelerometer, the microcontroller activates the GSM (Global System for Mobile System) for sending message alert to the rider's family. The GSM is based on the

Hayes AT-Command set using GSMK modulation technique. It also provides safety zones to the user by employing an IR sensor that illuminates an LED and rings the buzzer as it detects any object very close to the rider. [5]

In another proposed system, the creator has presented a cost-effective approach towards building a smart helmet using the Internet of Things (IOT) system. In this system, along with the MQ3 sensor for alcohol detection and Ultrasonic sensor for determining any potholes and humps irrespective of any smoke or dust in the surrounding, it has a unique addition of Light Dependent Resistor (LDR) to detect the presence or absence of light in its vicinity. LDR reads the analog data of 0-5V and converts this data into digital data values (0-1023). This digital data is used to turn the relay on which in return allows to turn the torch on when the light intensity is low. In case of accident detection by the accelerometer, the mounted Global Positioning System (GPS) provides the rider's location along with the time of accident. This GPS data is delivered to the subject's family via text message through the GSM module. Moreover, the IoT system truly fills the gap between the physical world and the technological advancements. It allows the devices to communicate and connect through the internet eliminating the need for any physical amalgamation. In the nutshell, the design of such a smart helmet with a wide range of features is achieved in an extremely moderate price of nearly 4000 Indian Rupees. [4]

Another advanced design [6] of smartly built helmets has an additional feature of manifesting the rear view to the motorcyclist. A raspberry pi camera has been integrated to the front of the helmet horizontally inclined at 10^{o}. It also checks the speed of the rider continuously. For speed monitoring, a GPS module has been employed. If the rider exceeds a specific speed limit, a series of bright red LEDs just glows up just above the front end of the display. However, for the accident detection of the subject, Arduino based infrared heart rate sensor, KY-039, had been placed to the left ear of the motorcyclist when the helmet is being put on. This sensor has an infrared blaster and infrared receiver in it. When the infrared rays pass through the ears, the blood within the blood vessels absorbs it. Thus, more Infrared radiation absorption indicates more heart rate whereas less absorption is an indication of the decreased heart rate. In case of accident, the heart rate pattern exhibits irregularity that gets detected by the sensor and it triggers the GSM module to send message alert to the family member of the rider as well as the nearby ambulance system. Moreover,

https://doi.org/10.62500/icrtsda.1.1.58

there is also a turn indicator using the 3-axis gyroscope (MPU-6050) which detects the sideway movements of the head of the rider. It has a USB port for charging the Helmet.

Such helmets have already been in use that allow the recording of the vital signals of the body. [7] The engineers have designed it with the aim of providing an efficient way to record the biological signals in an effective but non-invasive way. Multiple fabric electrodes have been integrated within the helmet allowing good contact with the skin of the subject. There were three electrodes in contact with the forehead of the subject. Two on lower jaw one being placed at the right side while the other placed on the left side of the jaw. Moreover, two electrodes were also placed on the mastoids while one electrode placed in the center serves as the common ground electrode. Using the ECG signal, the heart rate is determined by employing the R peaks of the ECG. MedTex130 conductive fabric has been used for the development of the electrodes within the inner lining of the helmet. The two electrodes on the forehead dispense the information about the brain activity with reference to the electrode on the left jaw. Whereas the potentials from the electrodes placed on the right and left mastoids along with the electrodes placed on the right and left sides of the lower jaw are measured taking the left forehead electrode as the reference electrode. (Records vital signals only. Doesn't tell anything about the helmet authentication or alcoholic condition etc.)

In many cases, the subjects get to lose their lives due to the unavailability of proper medical assistance. The patient may run short of oxygen, and there are no oxygen cylinders available at hand. To grapple with such emergency situations, a novel smart helmet must be designed to not only reduce the time between the occurrence of the accident and the advent of medical assistance, but also it paves a way to provide information about the biological parameters of the subject. Although such helmets do exist that provide us with the information about the bio-signals [5], but these helmets are not designed for regular use by the public. These helmets can be put on only when we need to acquire these signals.

In the nutshell, [1] although provided an efficient way to check whether the helmet is being properly buckled up by the rider, but it has no mechanism to check the condition of the rider. Whereas [2] offers an additional feature of alcoholic condition checking of the rider but nothing about the accident happening. However, the [3] adds the security system feature while [7] records vital signals only but doesn't tell anything about the helmet authentication or alcoholic condition etc. so in our project we are designing a unique system incorporating both the security system along with the biological information.

1.4 Problem Statement

The purpose of this project is to design a Smart helmet for the bike riders that can provide smart assistance in case of accident. When accident happens, an ordinary helmet provides only physical protection to the victim whereas, he is unable to call for help and ultimately this results in either severe injury of the rider or the death of the rider. Whereas this smart helmet provides both physical protection to the rider as well as integrated GPS and GSM technologies. In case of accident, this smart helmet informs about the accident, along with his location, his pulse rate, fire, and smoke in his vicinity through an auto generated text message to his family. Thus, the life of the rider can be saved by immediately providing medical help.

1.5 Objectives of the Project

There are four main objectives for this project as:

https://doi.org/10.62500/icrtsda.1.1.58

•Fabrication of Smart Helmet with integrated electronic module

•Fabrication of a commercially optimized prototype with its applications by bike riders

•To develop such a smart helmet that integrates Biological Parameters along with GPS and GSM

•Integration of live GPS tracking and text message generation about the incident

1.6 Cost Analysis

In this project, the detailed prices of the components are mentioned as per their prices described online. As we have used a number of components that either burnt during testing or we moved towards better choices, we have mentioned only those components that are utilized in the final prototype.

Item Name	Type	No. of Units	Per Unit Cost (in Rs)	Total (in Rs)
Arduino Mega 2560	Equipment	3	4200	12600
ADXL345	Equipment	5	400	2000
Flame Sensor	Equipment	3	200	600
MQ2 Gas Sensor	Equipment	3	530	1590
TTP223 Touch Sensor	Equipment	3	100	300
MAX 30100 pulse Oximeter	Equipment	3	500	1500
Neo 6m GPS	Equipment	5	1700	8500
SIM900A	Equipment	6	4500	27000
3D Printing	Equipment	1	20000	20000
Documentation, Software Subscription	Miscellaneous	1	10000	10000
			Total in (Rs)	84090

Table 8: Cost Analysis of components

II. DESCRIPTION

2.1 Description of the Project

A significant fraction of fatalities occurs because of the person's injury not being reported in time and his inability to be rescued due to the delayed hospital admission.

In order to avoid any possible injury as a result of road accidents, we have proposed a system capable of offering protection, security, and safety for bike riders. An ordinary helmet provides only physical protection whereas a smart helmet also provides smart protection. The system has integrated GSM & GPS technology which instantly notifies the emergency contacts of the accident's location and conjointly completely different sensors like MQ-2 sensor to detect smoke, flame sensor, to detect fire and accelerometer which measures the change in tilt in X,Y and Z axes respectively.

2.2 Methodology

The developing of a Smart Helmet prototype is divided into three main steps as:

- Individual Component Testing and Communication
- Patching of Components
- 3D Modeling and 3D Printing of the Smart Helmet

https://doi.org/10.62500/icrtsda.1.1.58

Step 1: Individual Component Testing and Communication:

First of all, we started with individual testing of components. Each sensor was tested first with the Arduino 2560. When each of the components worked properly, we displayed its results on the LCD. Then we started combining the components and started by communicating two components and then in group.

Step 2**:Patchingof Components:**

Then we combined all these individual components and patched them on Vero-board for final patching. The final hardware deliverable was a circuit with many sensors and electronic components ready to be placed inside of the helmet as shown in figure 2.

Step 3**: 3D Modeling and 3D Printing:**

At last, we designed a 3D model of the box to be placed above the helmet inside which all the circuitry needs to be placed. The model was designed on SOLIDWORKS software. Then it was 3D printed using PLA material and placed over the ordinary helmet. 2.3 Block Diagram

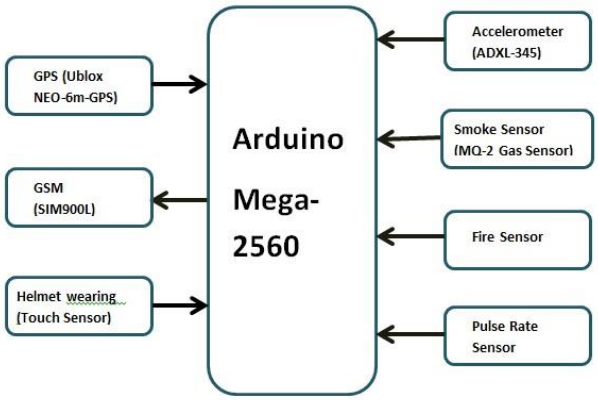

Figure 10: Block diagram of methodology.

2.**4 Product Specifications**

Table 4: Product Specifications of the Smart Helmet

Components	Current Specification	Voltage Specification
Arduino Mega 2560	**40mA**	**7V**
ADXL345	**30µA**	**5V**
Neo 6m GPS	**45mA**	**2.7V - 3.6V**
SIM900L	**2A**	**4V**
MQ2 Gas Sensor	**800mW**	**5V**
Pulse Rate Sensor	**< 4mA**	**3.3V - 5V**

https://doi.org/10.62500/icrtsda.1.1.58

2.5 Preliminary Design and Calculations

First of all, the components were tested with LCD display as shown below:

Figure 1: Testing of components on LCD, without GSM

Then these components were patched together as shown in the figure below:

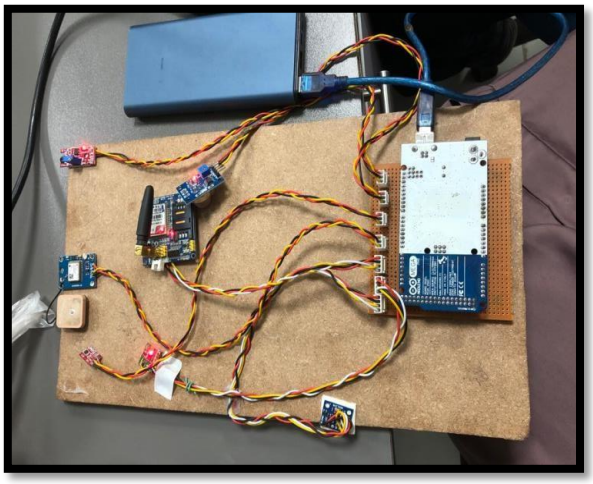

Figure 11: Hardware circuitry after patching.

III. MODELING AND SIMULATION

3.1 SolidWorks Modeling

All the electronic components need to be placed inside of a box so that all the circuitry is enclosed and can be replaced if any one of the components gets damaged as a result of an accident. In this project, we have designed a small box to be placed over the ordinary helmet for all the electronic components.

This is designed precisely by considering the minutest details of the components that are to be placed inside. Specific measurements of the sensors are taken, and then necessary space required for the wires to be placed inside is also measured and then the final dimensions of the box have been finalized leaving no extra space and making efficient use of every inch of the smart helmet.

This box for Smart helmet is designed using SolidWorks Software.

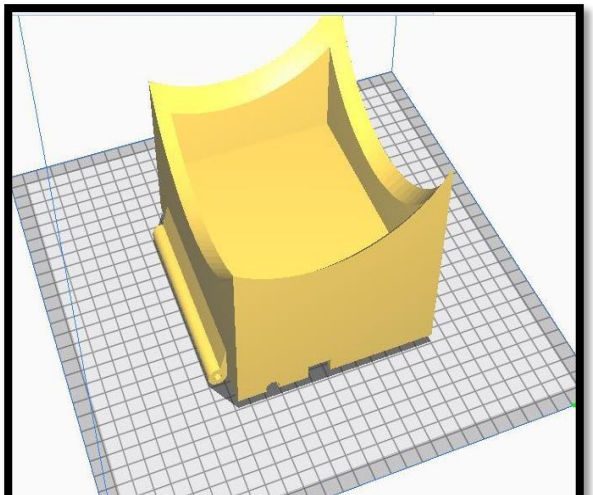

https://doi.org/10.62500/icrtsda.1.1.58

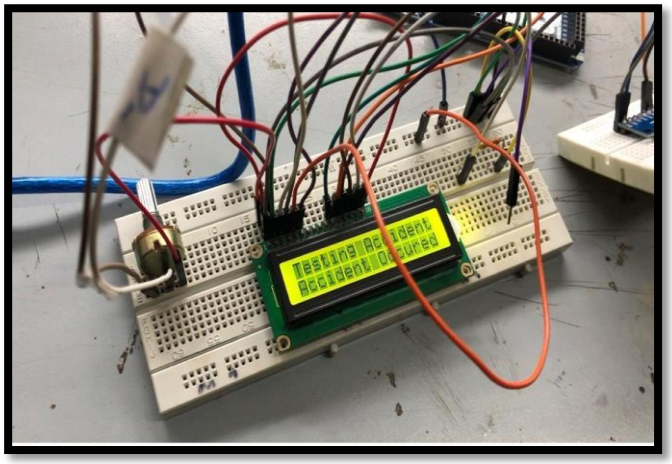

Figure 12: SOLIDOWORKS Model

The front view of the helmet after the placement of the sensors in it is shown in the figure below.

As demonstrated in the picture below that in the upper part of the lid two small holes are left. One is for the contact of the smoke sensor with the environment while the other is for GPS antenna to effectively catch GPS coordinates.

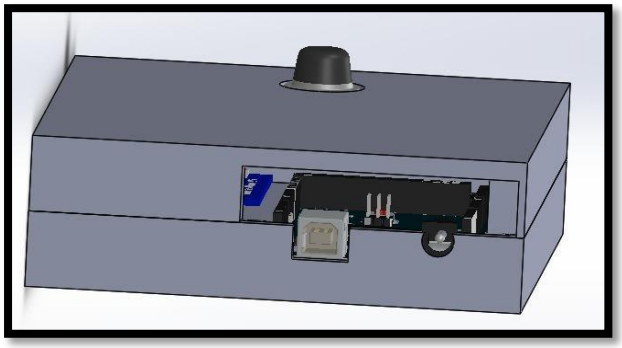

Figure 13: Box with sensors and circuitry inside

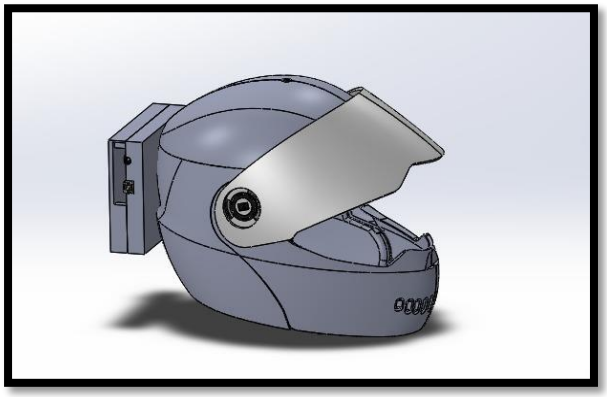

Figure 14: 3D Model of the box when placed on the helmet.

https://doi.org/10.62500/icrtsda.1.1.58

3.2 3D Model Analysis

After designing the 3D model, we had chosen PLA material for its 3D printing. As the components placed inside the box are heavy the deigned box must be sturdy enough to bear its weight along with providing protection to the circuitry. In case any one of the components of the circuit needs to be changed, the box also has a lid that can be opened to change any components.

3.3 Flowchart of the Smart Helmet

IV. EXPERIMENTAL SETUP

This chapter covers topics related to hardware. Here is mentioned hardware description and components we have used.

4.1 Hardware Description

The hardware of the Smart helmet consists of the electronic circuitry placed inside the 3D modeled box and the physical helmet.

All the electronic components of the helmet have been placed inside of the back enclosure. Only 2 sensors are outside this enclosure. One is inside the helmet over the head of the rider, the touch sensor that checks either the helmet is worn or not. Second is the pulse rate sensor that needs a contact with the ear lobe.

4.2 Components

Following components have been employed for the fabrication of the Smart helmet with integrated smart features and GPS tracking.

Table 5: Components used and their description.

No.	Component	Description
1.	Arduino Mega 2560	Microcontroller
2.	Accelerometer ADXL345	Accident detection sensor
3.	Fire and Smoke sensor (MQ2)	Fire and smoke detection sensors
4.	Touch sensor TTP223	Detects the wearing of helmet
5.	Heart Rate Sensor (MAX30100)	the pulse rate of the bike rider
6.	Neo-6m-GPS	es the location of the bike rider
7.	SIM900A GSM Module	Sends SMS in case of accident

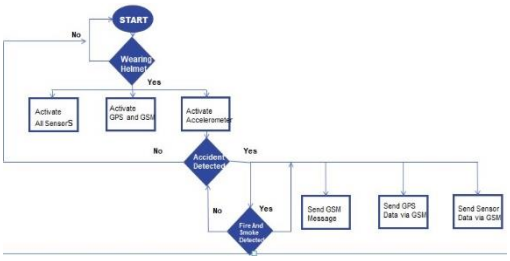

List of Components and their Specifications used for fabricating the Smart Helmet

Table 6: Component Specifications

https://doi.org/10.62500/icrtsda.1.1.58

	Specification	Normal Range	Components
GPS	Neo-6mGPS	Horizontal position accuracy GPS 2.5 m SBAS 2.0 m	-
GSM	SIM-900A	900 and 1800 MHz frequency bands	-

https://doi.org/10.62500/icrtsda.1.1.58

Accelerometer	ADXL-345	X_axis=-1 Y_axis=-1 Z_axis=-1	**x_lower_bound = -120;** **x_upper_bound = 120;** **y_lower_bound = -100;** **y_upper_bound = 100;**
Fire Sensor	760 – 1100 nano		**Detection angle**

https://doi.org/10.62500/icrtsda.1.1.58

		meter	**is 600 degrees, the flame may be detected from 100 cm-**
Smoke Sensor	MQ-2 Gas Sensor	200 to 10000ppm	**300 ppm**
Microcontroller	Arduino-Mega-2560	-	-
Touch Se	**TTP223**	**Sensora**	-

https://doi.org/10.62500/icrtsda.1.1.58

ns	**ng**
or	**e is**

The detailed description of the hardware is given below,

- Arduino-Mega-2560

The Arduino Mega 2560 is a microcontroller board based totally at the ATmega2560. It has 54 virtual input/output pins (of which 15 can be used as PWM outputs), sixteen analog inputs, 4 UARTs (hardware serial ports), a sixteen MHz crystal oscillator, a USB connection, an electricity jack, an ICSP header, and a reset button. It carries everything that has to help the microcontroller; without a doubt we just need to connect it to a laptop with a USB cable or electricity it with a AC-to-DC adapter or battery to get started out. The Mega 2560 board is compatible with maximum shields designed for the Uno and the former forums Duemilanove or Diecimila. The Mega 2560 is an replace to the Arduino Mega, which it replaces. Basically, we need an arduino for communicating serially between GPS and GSM modules. The Arduino Mega has 4 serial ports in contrast to only 1 serial port in Arduino Uno. Also, it has the greatest number of digital pins making it more efficient and having the best processing capability

Figure 7: Arduino Mega 2560

- Neo-6m-GPS

It can track up to 22 satellites on over 50 channels and achieve the industry's highest degree of tracking sensitivity i.e., -161 dB, whilst consuming just 45 mA present day. In contrast to other GPS modules, it could carry out five region updates in a second with 2.5m horizontal role accuracy. The U-blox 6 positioning engine additionally has a Time-To-First-restore (TTFF) of less than 1 second. It contains the pins needed for communication with the microcontroller over the UART. The module supports baud rates from 4800bps to 230400bps with a default baud of 9600. The GPS chip from U-blox – NEO-6M lies at the centre of the module.

https://doi.org/10.62500/icrtsda.1.1.58

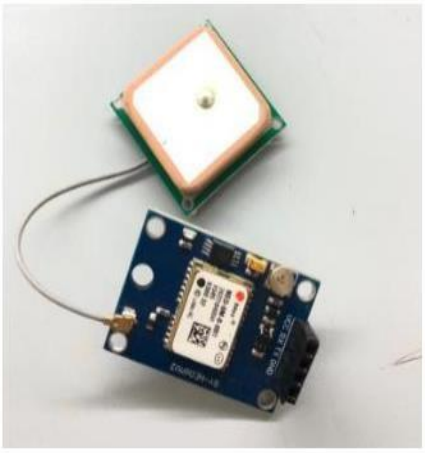

Figure 8: Neo 6m GPS

- SIM900A GSM Module

SIM900A GSM Module is a small module that provides GPRS/GSM technology for use in mobile sim-based communication. SMS and mobile calls can easily be sent or received employing the 900 and 1800MHz frequency bands. The baud rate ranges from 1200 to 115200 bps. However, in the smart helmet application, it only “sends” the message. The SIM socket on the back side supports any 2G Micro SIM card. On the top right of the SIM900A module is an LED that indicates the status of the cellular network. It blinks at different rates depending on which state it is in.

- If it blinks every 1s, this means that the module is running but the connection to the cellular network has not yet been made.
- If it blinks every 3s, this means that the module has successfully established connection with the cellular network and can now send/receive SMS.

This module works on AT Commands. In this project, GSM is employed to send a text message about the occurrence of accident, the location of the rider, presence of fire or smoke in the vicinity of the rider and his pulse to already defined number using AT-Commands. Following table gives idea of AT-Command used to send message using GSM.

Table 7: AT Commands

Command	Description
AT	If it returns ok, it means that the module is working properly
AT+CMGF=1	This is for SMS Configuration.
AT+CMGF=	It is used to define

https://doi.org/10.62500/icrtsda.1.1.58

''Phone number''		
	number of receiver who receive the message.	the will text
0*1A	This is a termination. Before sending it out, you should check the option send a Hex	

Figure 9 : SIM 900A

- Heart Rate Sensor (MAX30100)

Having applications in wearable health monitoring systems or gadgets, the MAX30100 is an integrated circuit (IC) that measures pulse oximetry and heart rate. It uses Red and infrared LEDs in order to detect the heart rate. Furthermore, this category of sensors uses low-noise analogue signal processing methods. The MAX30100 can run on either 1.8V or 3.3V power sources. Therefore, it can easily be programmed to shut down consuming very small standby current making it possible to leave the power supply connected all the time. It is often utilized in wearable, medical monitoring, and fitness assistant technology. The pin layout of MAX30100 as well as the top and bottom views of the chip is shown in Figure below.

https://doi.org/10.62500/icrtsda.1.1.58

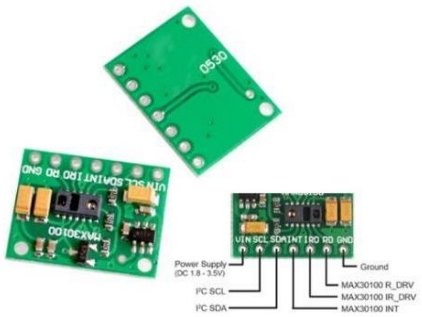

Figure 10: Pulse rate sensor

- ADXL-345

ADXL345 Accelerometer is based on the principle of measuring the acceleration or change in velocity in all the three axes; x, y, and z-axes. Due to its digital nature, ADXL345 is easy to interface. It is based on the SPI or I2C protocol. ADXL345 can not only measure static acceleration but dynamic accelerations also.

Figure 11: ADXL345

- MQ-2 Gas Sensor

The proposed Smart Helmet has the MQ-2 smoke sensor is sensitive to smoke and to the following flammable gases:

- LPG
- Butane
- Propane
- Methane
- Alcohol
- Hydrogen

It has a varying resistance based on the type of the gas. By changing the sensitivity of the built-in potentiometer of the sensor, the accuracy of detection can be adjusted. The output of the flame sensor

https://doi.org/10.62500/icrtsda.1.1.58

changes as the amount of smoke or gas present in the air varies. The relationship of voltage to gas concentration in the air is described below:

- Increased output voltage when high gas concentrations
- Decreased output voltage when lower gas Concentrations

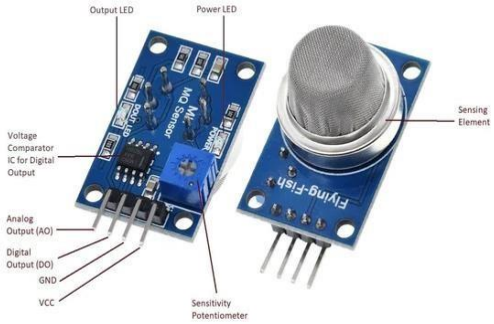

Figure 12: MQ2 gas sensor

- Fire Sensor

Fire sensor detects the fire based on the wavelength of the light source of the flame. If the wavelength is between 760 and 1100 nanometer, it detects the flame in its vicinity. When it comes to the placement of the sensor, it must be placed by a certain distance from the source so that light falls on it and it could detect the presence of the fire. It is capable of detecting flame even from a distance of 1m employing a detection angle of 600 degrees. Its output maybe an analogue signal or a digital signal. The pinout of the fire sensor is shown below.

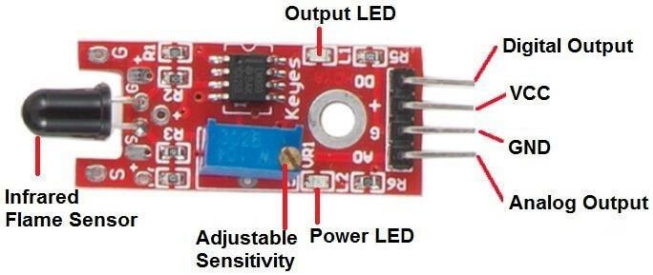

Figure 13: Fire sensor

- Touch Sensor - TTP223

The TTP223 is a Capacitive Touch Sensor. It is based on an IC sensor module. It allows a single integrated touch sensing area of 11 x 10.5mm with sensor range of ~5mm.

https://doi.org/10.62500/icrtsda.1.1.58

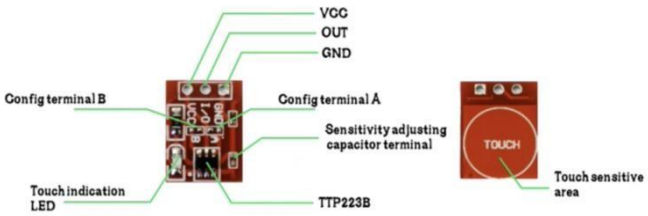

Figure 14: Touch Sensor

V. RESULTS AND DISCUSSION

This chapter covers topics related to outcomes and result of project. It also includes that our project has impact on society. Its marketability and acceptability as a product have also been discussed.

5.1 Results

The objectives approved for the project were successfully achieved. On testing of the smart helmet, following messages were generated by the smart helmet when it detected accident.

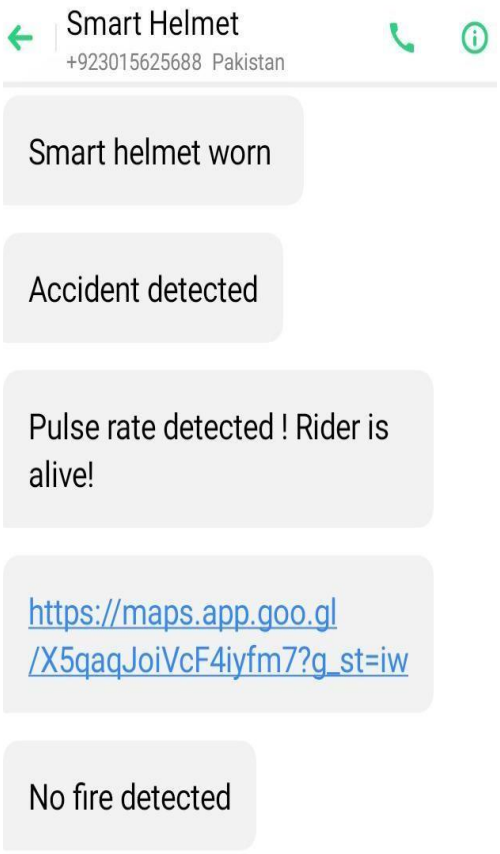

Figure 15: Text Message Generation in case of accident

5.2 Prototype Development:

https://doi.org/10.62500/icrtsda.1.1.58

For initial prototype development and initial testing, we had placed all the sensors over an ordinary helmet first. In the second phase after getting the 3D printed model, we placed these components inside the box and then performed further testing.

Actual Smart Helmet:

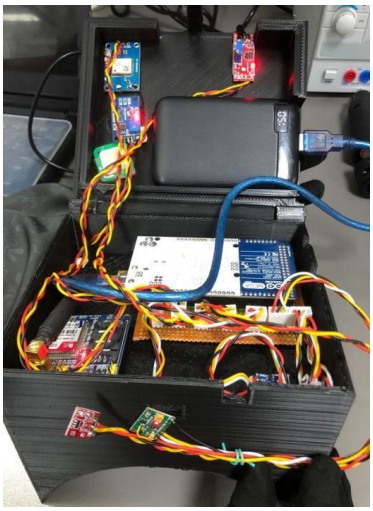

Figure 16: Smart helmet box with circuitry inside

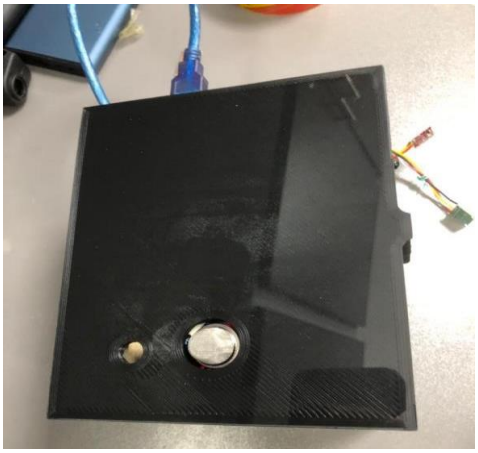

Figure 17: Helmet Outer look

https://doi.org/10.62500/icrtsda.1.1.58

Figure 18: Final Smart Helmet

5.3 Discussion

In this project, there are three main objectives of the designed system which we have achieved. Firstly, the wearing of the helmet is checked to activate other modules. Then if the accident is detected, the GSM will be activated and the data from GPS and other sensors will be sent through GSM.

5.4 Project Outcomes

Following are the outcomes of the project:

- Integrating real-time GPS tracking with the generation of incident-related SMS messages
- Development of a smart helmet with an integrated electronic module
- Development of a prototype with commercial optimization and bike riders' usage
- Designing of a smart helmet with biological parameters
- Safe motorcycle riding
- Immediate reporting in case of accident
- Resultantly, provision of medical help in case of emergency
- And hence, a great many lives could be saved.
- Fewer fatalities in case of road accidents

5.5 Project Impact

The impact of this project is in innovation where we are trying to make Smart Helmet with integrated GSM, vitals, and Hazardous Event Detection. The applications are directed mostly on ensuring the safety of motorcyclists when riding a bike.

https://doi.org/10.62500/icrtsda.1.1.58

- Marketability and Acceptability as a Product

Smart helmet plays an important role in providing safety of the motorcyclist. When smart helmets are used to their maximum capacity, the number of casualties fall. The use of existing helmets and the development of new helmets with smart features will constantly increasing.

- Impact on Society

Smart helmet ensures the safety of the bike rider. The importance of safety during vehicle riding has risen with the advancement of science and technology in all spheres of life, and the major focus is now on lowering the alerting time when an accident occurs so that the rescue team can attend to the injured faster.

VI. CONCLUSIONS AND FUTURE RECOMMENDATIONS

6.1 Conclusions

In this project, we successfully designed smart helmet hardware with integrated sensors that use GSM and GPS. To start the ignition of the vehicle, the project mandates the wearing of a helmet. It also detects fire and smoke, also the pulse rate of the bike rider as in case of an accident. An accelerometer monitors the changing axis value, and if the value exceeds the predefined range in case of an accident, a brief message with the rider's location is sent via GSM module to the predefined number. In this instance, we were able to find a partial solution to the issue of rising death rate in accidents due to lack of medical help.

6.2 Future Recommendations

In this project, a smart helmet has been fabricated using microcontroller, GSM, GPS modules, and a collection of sensors to determine the rider's location and send an SMS if there is occurrence of accident. The results of additional research will be used to create a model with more sophisticated features. For example,

- In future, a mobile application can also be developed that as well could keep a record of the bike rider’s driving, his weak areas to predict accident etc.
- The smart helmet could also be modified by the addition of an EEG recording to detect whether he is drowsy or not and in case he is drowsy, a vibrator can make him awake by giving vibrations over his head along with the alert notifications.

ACKNOWLEDGMENT

First of all, we thank Almighty Allah for giving us the strength and will to overcome the difficulties and hurdles while working on this project.

We feel immense gratitude for the opportunity to work on a project with our prestigious professors. We express from our heart deepest gratitude to our supervisor Dr. Jahanzeb Gul for his continuous

https://doi.org/10.62500/icrtsda.1.1.58

support, keen supervision and valuable pieces of advice that helped us a lot in the project. His words of motivation and guidance kept us all on the right track. No words can adequately describe our thanks and indebtedness to co-supervisor Dr. Zia MohyUdDin in helping us out.

REFERENCES

[1] https://www.thenews.com.pk/print/910436-alarmingfigures-of-traffic-accidents-need attention

[2] Journal, I., Agarwal, N., Singh, A. K., Singh, P. P., &Sahani, R. (2015). IRJET-SMART HELMET SMART HELMET.International Research Journal of Engineering and Technology.www.irjet.net

[3] Vijayan, S., Govind, V. T., Mathews, M., Surendran, S., & Sabah, M. (2014). ALCOHOL DETECTION USING SMART HELMET SYSTEM dheerajmishra ALCOHOL DETECTION USING SMART HELMET SYSTEM.In International Journal of Emerging Technology in Computer Science & Electronics (IJETCSE) (Vol. 8).

[4] Swathi, S. J., Raj, S., &Devaraj, D. (2019, April 1). Microcontroller and Sensor Based Smart Biking System for Driver's Safety.IEEE International Conference on Intelligent Techniques in Control, Optimization and Signal Processing, INCOS 2019.https://doi.org/10.1109/INCOS45849.2019.8951409

[5] Penta, M., Jadhav, M., &Girme, P. (2015). BIKE RIDER'S SAFETY USING HELMET.In Int. J. Elec&Electr.Eng&Telecoms.www.ijeetc.com

[6] Ahmed, A., Khan, M. M., Dey, R., & Nanda, I. (2022). Smart Helmet with Rear View and Accident Detection System for Increased Safety.0673– 0678.https://doi.org/10.1109/ccwc54503.2022.9720833

[7] IEEE Engineering in Medicine and Biology Society, Cerutti, S., Patton, J., Annual international conference of the IEEE Engineering in Medicine and Biology Society 37 2015.08.25-29 Milano, & EMBC 37 2015.08.25-29 Milano. (n.d.).2015 37th annual international conference of the IEEE Engineering in Medicine and Biology Society (EMBC) 25 - 29 Aug. 2015, Milano / conference chairs Sergio Cerutti ... Jim Patton, ed. in chief for conference editorial board.

[8] Nandhini, M. v, &Priya, P. G. (n.d.). IoT based Smart Helmet for Ensuring Safety in Industries. www.ijert.org

[9] Bozdal, M., & Irmak, E. (n.d.). Smart lifesaving helmet for miners.https://www.researchgate.net/publication/347947681

[10] Suriyakrishnaan, K., Gandhi, R. A., Babu, R., Sakthivel, S., & Dev, S. (2021). Smart Safety Helmet in Coal Mining Using Arduino.In Turkish Journal of Computer and Mathematics Education (Vol. 12, Issue 11).

[11] A. Mane, Prof. M. Pawar, A real-time EEG based drowsiness detection with brain-computer interface for vehicular system, International Journal of Advanced Research in Computer and Communication Engineering, Vol. 7, Issue 1, pp. 195, 2018

[12] Arachchige, U., &Jayasinghe, S. (n.d.). A smart helmet with a built-in drowsiness and alcohol detection system.https://www.researchgate.net/publication/342610875

[13] Tayag, M. I., & Asuncion De VigalCapuno, M. E. (2019). Smart Motorcycle Helmet: Real-Time Crash Detection With Emergency Notification, Tracker and AntiTheft System Using Internet-of-Things Cloud Based Technology. International Journal of Computer Science and Information Technology, 11(03), 81–94. https://doi.org/10.5121/ijcsit.2019.11

https://doi.org/10.62500/icrtsda.1.1.59

Proc. 1st International Conference on Recent Trends in Statistics and Data Analytics
Air University Islamabad, Pakistan – May 9, 2024, Vol. 1, pp. 589-597

The impact of Instagram on young Adult's social comparison, popularization and mental health

Laiba khalid[1] and Mehwish Asghar[2] *

Abstract

This paper explores believable issues such as Social Comparison, Popularization, and Mental Health and their relation- ship with Instagram use, focusing on young adults living in Pakistan. Participants (N = 762) were recruited to fill up a questionnaire, and the self-reported data was used to test our hypothesis. The study followed a correlational, non-experimental approach to investigate the mediation models as proposed. Structural Equational Modelling eluded a positive and significant relationship between age and the social issues with control variables as the frequency and time spent on Instagram. Moreover, it was found that social comparison can lead to popularization and mental health issues. Gender was, however, found to have insignificant relation with three parameters. Qualitative analysis was supported to find important implications for all Instagram stakeholders. Discussions were drawn indicating the need to raise awareness regarding these issues to enjoy social media while safeguarding the user's well-being. The paper provides critical key findings delving into the realms of these parameters, and such implications are further discussed to understand its reflection in online spaces.

Keyword :

Social media, Instagram popularization, Mental health, Social comparison

Introduction

Social media, including platforms like Instagram, facilitates the exchange of information and ideas within virtual communities. With approximately 3.6 billion active users globally, it's a significant part of modern life, particularly for young people. Instagram, specifically popular among youngsters, boasts 2.4 billion active users worldwide, with a sizable user base in Pakistan.

However, excessive social media usage, especially during adolescence, poses mental health risks. Nearly one in five adolescents suffer from mental health issues like depression and suicidal thoughts, partly due to the unrealistic beauty standards perpetuated by filters and augmented reality tools. Social comparison, particularly with idealized images presented in the media, fuels dissatisfaction with one's body and appearance, especially among those already vulnerable to mental health concerns.

People mostly compare themselves to their peers rather than celebrities when seeking acceptance and evaluating themselves. This constant comparison and jealousy can lead to depression and have adverse effects on physical and mental health. Thus, while social media offers connectivity and expression, its negative impacts on self-esteem and mental well-being highlight the need for balanced usage and critical awareness.

Social media, particularly platforms like Instagram, heavily influence body dissatisfaction and disordered eating among young women. The number of likes, comments, and followers directly impacts one's perception of social acceptance, potentially leading to anxiety and depression if engagement is low. Instagram's focus on visual content intensifies this effect, as users tend to compare themselves to

https://doi.org/10.62500/icrtsda.1.1.59

influencers and celebrities, striving for social approval. Appearance-related discomfort fuels the demand for cosmetic surgery. The prevalence of mental health issues among youth, such as anxiety and depression, has risen significantly, partly attributed to social media use. While it can offer support and connection, social media also facilitates cyberbullying, exacerbating mental health problems. Efforts to leverage social media for mental health support and treatment are promising but need further exploration

In this paper, we present and discuss the results of a survey con- ducted to identify the psychological impact of Instagram on young adults for factors such as social comparison, popularization, and mental health. The main objectives of our research study were:

- To determine whether Instagram usage influences these factors on young adults.
- To determine whether gender plays a significant role in influencing factors such as social comparison, popularization and mental health, based on recorded responses .
- To find the co-relation between popularization, mental health, and social comparison.
- Provide meaningful information/suggestions highlighting further improvements that can be achieved based on the recorded response

The study examined the relationship between social media impact, particularly on Instagram, and mental health, focusing on social comparison and popularization factors. Using Structural Equation Modeling (SEM) and ANOVA tests, significant correlations were identified. SEM was chosen for its ability to analyze multiple interrelated factors simultaneously. Additionally, qualitative analysis through Cluster Density View was employed to grasp the qualitative aspects. Despite the inherent uncertainties in qualitative analysis, the findings complemented the statistical results. The surge in social media use during the pandemic has intensified mental health concerns, with social media usage and loneliness being significant factors. Given the evolving societal needs, the study provides valuable insights into the implications of social media on mental health.

Descriptive Statistics.

Variables	Count (N = 762)	Percentage
Age		
Less than 18	375	49.20%
18–21	285	37.40%
22–25	85	11.20%
26–29	11	1.40%
More than 29	6	0.80%
Gender		
Male	528	69.30%
Female	234	30.70%
Instagram followers		
0–200	320	42.00%
201–400	184	24.10%
401–600	88	11.50%
More than 600	170	22.30%
Instagram usage		
0–2 h	439	57.60%
2–4 h	208	27.30%
4–6 h	66	8.70%
More than 6 h	49	6.40%

https://doi.org/10.62500/icrtsda.1.1.59

Data collection

The survey data was collected between 20 January 2024 to 10 feb 2024. A short time duration ensured that the questionnaire was forwarded to the appropriate samples by taking care of those who are participating in our study is from India since our research is bounded with the Indian context. A web link to the online questionnaire was disseminated through various social networking platforms such as Instagram, WhatsApp, LinkedIn, Facebook, and selective emails. A written consent in the online survey was provided to all participants, stating that the participants' privacy will not be compromised. The entire questionnaire was divided into four sections. Section I consists of demographic information. Section II consists of the psychological effect of Instagram on colourism, Section III consists of the psychological effect of Instagram on mental health, and Section IV consists of the psychological effect of Instagram on social comparison. The questionnaires are majorly taken from the study. The selection of the questions was done based on the parameters like Instagram usage, time spent on Instagram, age, gender, and relevancy. Section I had 5 demographic and Instagram related questions, Section II had 10 questions that were related to the psychological effect of Instagram on colourism, Section III had 10 questions that were related to the psychological effect of Instagram on mental-health, and Section IV had 10 questions that were related to the psychological effect of Instagram on social comparison. The details of the questionnaires are listed in table 8.

Data analysis

A total of 762 individuals of Pakistan descent have participated in this survey. The demographic analysis of the population includes 69.30% Female and 30.70% male in the age group of up to 35 years old. To support RQ1-RQ3, we performed structural equation modeling (SEM). Structural equation modeling is a multivariate statistical analysis technique used to analyze structural relationships. It is the combination of factor analysis and multiple regression analysis. This method is preferred because it estimates the multiple and interrelated dependence in a single analysis

Results and analysis

Hypotheses statements

In totality, with the extensive literature survey, we predict the following:

H1: hypothesis 1 (H1)

Instagram directly or indirectly affects factors such as colourism, mental health and social comparison. The Number of hours that an individual uses Instagram and the number of followers that an individual has on Instagram will act as the mediating variables to understand the indirect effects.

https://doi.org/10.62500/icrtsda.1.1.59

H2: hypothesis 2 (H2)

Gender does not play a significant role in influencing factors such as colourism, mental health, and social comparison in the usage of Instagram.

H3: hypothesis 3 (H3)

The factors colourism, mental health and social comparison are co- related. In other words, the usage of Instagram directly or indirectly contributes to the increase or decrease of the other.

Descriptive statistical result:

The survey aimed to understand the diversity of skin tones in Pakistan culture by asking participants to choose a tone resembling theirs. Results revealed a variety of tones, with "Natural" and "Ivory" being the most common. Other tones like "Warm Ivory" and "Porcelain" were also present. The study also explored Social Comparison, Colourism, and Mental Health through Likert scale questions. Mental Health responses indicated that people generally feel happy using Instagram but less likely to feel depressed, sad, or anxious due to emotional problems on the platform.

Responses of participants to Social Comparison and Use of Instagram.

	Strongly Agree		**Agree**		**Neutral**		**Disagree**		**Strongly Disagree**		
	N	%	N	%	N	%	N	%	N	%	Mean
I take into consideration how my followersrespond to my posts	166.00	22.87	293.00	40.36	172.00	23.69	82.00	11.29	49.00	6.75	3.76
I feel motivated when I look at others post	205.00	28.24	317.00	43.66	161.00	22.18	59.00	8.13	20.00	2.75	4.01
I compare my posts with others	119.00	16.39	179.00	24.66	173.00	23.83	174.00	23.97	117.00	16.12	3.16
I try to copy other people's social habits asperceived from Instagram	91.00	12.53	170.00	23.42	175.00	24.10	182.00	25.07	144.00	19.83	2.99
I feel confident with my physical appearance	223.00	30.72	295.00	40.63	145.00	19.97	65.00	8.95	34.00	4.68	3.99
I believe that people portray themselves differently on Instagram compared to real life	296.00	40.77	286.00	39.39	118.00	16.25	40.00	5.51	22.00	3.03	4.24
I believe people will respect me only if I am good looking and/or successful	172.00	23.69	210.00	28.93	164.00	22.59	120.00	16.53	96.00	13.22	3.48
I feel down about myself or envy things that they have or wish I would have been to places looking at specific Instagram posts	124.00	17.08	228.00	31.40	194.00	26.72	134.00	18.46	82.00	11.29	3.39
I judge others based on the number of followers and likes	99.00	13.64	140.00	19.28	151.00	20.80	165.00	22.73	207.00	28.51	2.82
I believe Instagram is a way for me to keep up with my friends and feel more involved in their lives	224.00	30.85	281.00	38.71	145.00	19.97	69.00	9.50	43.00	5.92	3.94

https://doi.org/10.62500/icrtsda.1.1.59

Social Comparison: The highest average was found to be for the item "I believe that people portray themselves differently on Instagram compared to real-life" at 4.24 and the least was found to be for the item "I judge others based on the number of followers and likes" at 2.82 indicating disagreement. All the 10 items lie above the mid spectrum range (2.5). The item "I feel motivated when I look at others post" was also at a considerable higher score at a 4.0.

Table 10

Responses of participants to Social Colourism and Use of Instagram.

	Strongly Agree		**Agree**		**Neutral**		**Disagree**		**Strongly Disagree**		
	N	%	N	%	N	%	N	%	N	%	**Mean**
I am happy with my skin tone	429.00	59.09	199.00	27.41	101.00	13.91	20.00	2.75	13.00	1.79	4.54
I feel that light-complexioned people appear more confident on Instagram	147.00	20.25	250.00	34.44	193.00	26.58	101.00	13.91	71.00	9.78	3.56
I feel more confident when I am at least one shade lighter than my natural skin tone	148.00	20.39	202.00	27.82	167.00	23.00	119.00	16.39	126.00	17.36	3.32
I use filters to make myself appear lighter in the images that I post on Instagram	112.00	15.43	164.00	22.59	186.00	25.62	134.00	18.46	166.00	22.87	3.04
I often find myself wishing that I had a lighter skin tone for my images	127.00	17.49	179.00	24.66	154.00	21.21	123.00	16.94	179.00	24.66	3.08
I am bullied on Instagram for my skin tone	67.00	9.23	100.00	13.77	150.00	20.66	139.00	19.15	306.00	42.15	2.44
I am influenced by skin lightening products as endorsed on Instagram	90.00	12.40	111.00	15.29	167.00	23.00	146.00	20.11	248.00	34.16	2.67
I believe fair skin tone is popularised by celebrities and has influenced the perception of people	242.00	33.33	238.00	32.78	147.00	20.25	72.00	9.92	63.00	8.68	3.87
I receive comments and feedback regarding my skin tone on my pictures	68.00	9.37	121.00	16.67	162.00	22.31	159.00	21.90	252.00	34.71	2.59
I believe that a growing obsession with 'fairness' is a healthy trend	129.00	17.77	162.00	22.31	147.00	20.25	101.00	13.91	223.00	30.72	2.97

Colourism: The loftiest score was found for the item "I am happy with my skin tone" at a score of 4.54 and the lowest mean was for the item "I am bullied on Instagram for my skin tone" at a rating of 2.44 as portrayed in Table 10.

https://doi.org/10.62500/icrtsda.1.1.59

Table 11

Responses of participants to Mental Health and Use of Instagram.

	Strongly Agree		Agree		Neutral		Disagree		Strongly Disagree		
	N	%	N	%	N	%	N	%	N	%	Mean
I believe that Instagram has a positive impact on my life	146.00	20.11	227.00	31.27	250.00	34.44	98.00	13.50	41.00	5.65	3.62
I am able to truly express myself on Instagram without worrying what others may think	183.00	25.21	234.00	32.23	154.00	21.21	128.00	17.63	63.00	8.68	3.63
I feel happy when I use Instagram	226.00	31.13	259.00	35.67	217.00	29.89	39.00	5.37	21.00	2.89	4.02
Instagram makes me feel good about myself and my bodyimage	186.00	25.62	187.00	25.76	252.00	34.71	98.00	13.50	39.00	5.37	3.68
I feel under pressure to fit into a particular image or post specific pictures to remain popular on Instagram	138.00	19.01	177.00	24.38	203.00	27.96	139.00	19.15	105.00	14.46	3.29
I get affected by the Number of likes I get and it influenceshow I feel about the picture or about myself	132.00	18.18	198.00	27.27	169.00	23.28	150.00	20.66	113.00	15.56	3.27
I have an online persona (I am a different person online)	113.00	15.56	164.00	22.59	185.00	25.48	163.00	22.45	137.00	18.87	3.08
I feel confident about sharing updates on Instagram	188.00	25.90	239.00	32.92	191.00	26.31	93.00	12.81	51.00	7.02	3.73
I feel depressed, sad, or anxious in work or daily life due to emotional problems on Instagram	84.00	11.57	131.00	18.04	170.00	23.42	178.00	24.52	199.00	27.41	2.

https://doi.org/10.62500/icrtsda.1.1.60

I am addicted to Instagram	132.00	18.18	175.00	24.10	207.00	28.51	134.00	18.46	114.00	15.70	3.25

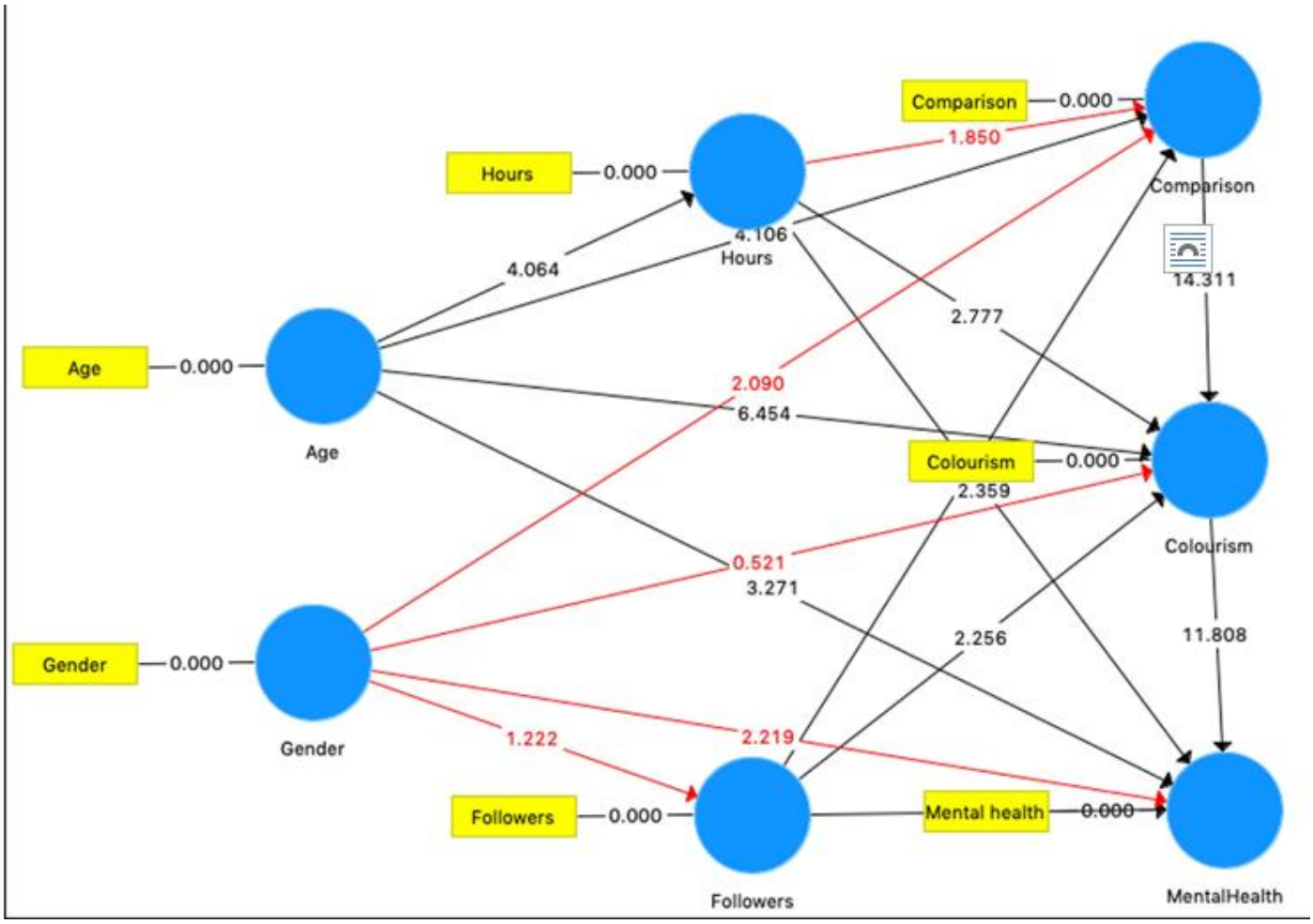

Path analysis remains one of the top choices for perform-ing SEM amongst statistical researchers and students. In their paper,
explored the advantages of SEM over other multivariate analysis such as Latent Regression models .

https://doi.org/10.62500/icrtsda.1.1.60

Summary of hypothesis testing.

	T statistics	p-value	confidence interval	
Age -> Colourism	7.98	0	−0.32	−0.19
Age -> Comparison	4.31	0	−0.2	−0.08
Age -> Hours	4.06	0	−0.22	−0.08
Age -> Mental Health	6.84	0	−0.29	−0.16
Colourism -> Mental Health	11.81	0	0.37	0.52
Comparison -> Colourism	14.31	0	0.42	0.55
Comparison -> Mental Health	7.52	0	0.16	0.27
Followers -> Colourism	4.14	0	0.08	0.23
Followers -> Comparison	4.73	0	0.1	0.24
Followers -> Mental Health	5.8	0	0.14	0.29
Gender -> Colourism*	0.34	0.74	−0.05	0.08
Gender -> Comparison*	1.85	0.07	0	0.12
Gender -> Followers*	1.22	0.22	−0.11	0.02
Gender -> Mental Health*	1.96	0.05	0	0.13
Hours -> Colourism	3.3	0	0.04	0.16
Hours -> Comparison*	1.85	0.06	−0.01	0.13
Hours -> Mental Health	3.5	0	0.05	0.18

Let us first consider the age and its correlation with social comparison, colourism, and Mental Health. Age is found to be negatively associated with Social Comparison (β=0.13, p<0.05), Colourism (β=0.13, p<0.05) and Mental Health (β=0.1, p<0.05). This indicates that users of Insta gram of the higher age bracket have a significant and negative rela- tionship with these issues. It also was found that people of higher age bracket tend to use Instagram lesser (β=0.15, p<0.05) by 1.5 h.

As far as Instagram usage goes, it can be effectively culminated by the Number of followers and hours an individual spends on Instagram. The relationship between the number of hours a person spends on Instagram and Social Comparison was found to have no statistical difference (β=0.06, p>0.05). This means less or more hours spent on Instagram do not directly or indirectly influence Social Comparison. The Number of hours spent positively relates to Colourism (β=0.08, p<0.05)and Mental Health (β=(0.07+0.05)=0.12, p<0.05). Individual spending more time on Instagram is more prone to be affected by colourism by 8% and, linearly, mental health issues by 12%.

https://doi.org/10.62500/icrtsda.1.1.60

Similarly, the relationship between the 'Number of followers' and the three factors also share a positive and significant relationship. A higher number of followers indicate that a person is more likely to expe- rience Social Comparison (β =0.16, p<0.05) by 16%, colourism (β =0.17,p<0.05) by 17% and ultimately Mental Health (β =0.22, p<0.05) issues by 22%.

ANOVA summary.

Source	DF	Sum of Square	Mean Square	F Statistic	P-value
Groups (between groups)	2	48.12	24.06	26.93	<0.0001
Error (within groups)	2283	2039.42	0.89		
Total	2285	2087.54	0.91		

Summary of participants responses for qualitative analysis.

Term	business	lot	friend	fun	entertainment	touch	person	story	post
Occurrences	4	3	11	3	5	5	6	5	3
Relevance	1.62	1.26	1.21	1.20	1.04	0.82	0.79	0.57	0.49

The ANOVA conducted in the study was validated using Levene's test to ensure homogeneity of variances, which yielded substantial power (1.0), indicating homogeneous variances. Additionally, the assumption of normally distributed groups (N > 30) was supported by the Shapiro-Wilk Test. However, despite these validations, the study acknowledges that its measurement items are not perfect representations of the constructs. To address this, a structural modeling framework was employed to analyze individual changes over time. The findings revealed that Instagram users experiencing social comparison are likely to encounter colorism and mental health problems, with mental health being indirectly affected. Notably, those facing colorism have a surprising 48% chance of experiencing mental health issue

Qualitative analysis, while not as precise as traditional methods, can complement statistical findings. In this study, participants were interviewed and asked about their use of Instagram. Their responses were analyzed using VOS viewer software, which visualizes similarities in text data. Two clusters of terms emerged: one related to social aspects like "friend" and "person," and another related to business like "business" and "post." The analysis suggests that people mainly use Instagram for socializing and entertainment, but there's also potential for it to become a marketplace. While qualitative analysis doesn't give definitive results like statistics, it provides insights into user behavior

DISCUSSION

With the rise in the use of Instagram amassing 500+ million users flocking to the app result from forms lionZEDETE][]';L\active users monthly), Instagram has a rubber-stamped impact on daily life of a lot of the population. Instagram is often perceived as a reel of "perfect" highlights. People primarily use it to

https://doi.org/10.62500/icrtsda.1.1.60

share images, videos and now it is also a source to consume and spread information faster than ever. According to), humans try to find expla- nations or judgement behind any particular event as it ascends meaning to their life.) talks about the locus of causality being in- ternal and external attributions. Internal attributions are related to their behavior or ability.

Conclusion

Some people say that it can be harmful because it exposes users to unrealistic standards of beauty and Perfect lifestyles. Others argue that it can be beneficial because it allows people to connect with each other and share their lives openly.

As mental health is such an important topic these days, you would think that all social media platforms would be taking steps to ensure their users' well-being. Unfortunately, that's not the case - and in fact, some platforms are actually making things worse. Take Instagram, for example. With its focus on perfection and likes, it's no wonder that this platform is one of the worst for mental health.

https://doi.org/10.62500/icrtsda.1.1.60

References

1) Abrams, J. A., Belgrave, F. Z., Williams, C. D., & Maxwell, M. L. (2020). African American Adolescent Girls' beliefs about skin tone and colorism. *Journal of Black Psychology*. 10.1177/0095798420928194.
2) Adams, E. A., Kurtz-Costes, B. E., & Hoffman, A. J. (2016). Skin tone bias among African Americans: Antecedents and consequences across the life span. *Developmental Review*. 10.1016/j.dr.2016.03.002.
3) Ahn, J., Son, H., & Chung, A. D. (2021). Understanding public engagement on twitter using topic modeling: The 2019 Ridgecrest earthquake case. *International Journal of Informa- tion Management Data Insights, 1*(2), Article 100033. 10.1016/j.jjimei.2021.100033.
4) Anand, K., Urolagin, S., & Mishra, R. K. (2021). How does hand gestures in videos impact social media engagement - Insights based on deep learning. *In- ternational Journal of Information Management Data Insights, 1*(2), Article 100036. 10.1016/j.jjimei.2021.100036.
5) Anderson, J. C., & Gerbing, D. W. (1988). Structural equation modeling in prac- tice: A review and recommended two-step approach. *Psychological Bulletin*. 10.1037/0033-2909.103.3.411.
6) Chua, T. H. H., & Chang, L. (2016). Follow me and like my beautiful selfies: Singapore teenage girls' engagement in self-presentation and peer comparison on social media. *Computers in Human Behavior*. 10.1016/j.chb.2015.09.011.
7) Clement, J. (n.d.). *Distribution of Instagram Users Worldwide as of October 2020, by Age Group*. Statista.
8) Copeland, L., & Lyu, J. (2020). Millennial Consumer's on Instagram: Implications for Lux-ury Brands *vs*. Celebrity Influencers: An abstract. 10.1007/978-3-030-42545-6_19.
9) Coyne, S. M., Rogers, A. A., Zurcher, J. D., Stockdale, L., & Booth, M. (2020). Does time spent using social media impact mental health?: An eight year longitudinal study. *Computers in Human Behavior*. 10.1016/j.chb.2019.106160.
10) Cronbach, L. J. (1951). Coefficient alpha and the internal structure of tests. *Psychometrika*.
11) 10.1007/BF02310555.
12) de Vries, D. A., Möller, A. M., Wieringa, M. S., Eigenraam, A. W., & Hamelink, K. (2018). Social comparison as the thief of Joy: Emotional consequences of Viewing Strangers' instagram posts. *Media Psychology*. 10.1080/15213269.2016.1267647.
13) Dubey, A. D., Alam, M., & Rekha, R. R. (2018). What's your status? Investigating the effects of social media on the students of Fiji National University. *Education and Information Technologies*. 10.1007/s10639-018-9744-0.

https://doi.org/10.62500/icrtsda.1.1.60

14) Festinger, L. (1954). A Theory of Social Comparison Processes. *Human Relations*.10.1177/001872675400700202.
15) Fuller, T. (2020). *A Vision of Pale Beauty Carries Risks for Asia's Women*. The Newyork Times https://www.nytimes.com/2006/05/14/world/ asia/14thailand.html.

IMPROVED SCRAMBLING TECHNIQUE FOR APPLICATIONS IN SAMPLE SURVEYS ON SENSITIVE VARIABLES

https://doi.org/10.62500/icrtsda.1.1.60

Proc. 1st International Conference on Recent Trends in Statistics and Data Analytics
Air University Islamabad, Pakistan – May 9, 2024, Vol. 1, pp. 600-610

IMPROVED SCRAMBLING TECHNIQUE FOR APPLICATIONS IN SAMPLE SURVEYS ON SENSITIVE VARIABLES

Abdul Basit[1], Muhammad Azeem[1*], Abdul Salam[1], and Habib Ullah Khan[1]

[1]Department of Statistics, University of Malakand, Khyber Pakhtunkhwa, Pakistan
[*]Corresponding Author Email: azeemstats@uom.edu.pk

ABSTRACT

In various surveys, there are several reasons due to which respondents hesitate to report their true information especially when they are asked to report their responses on sensitive issues. In such a situation, the survey participants may provide wrong information or may even refuse to provide information. Such refusals and untruthful reporting can be reduced to a large extent by utilizing the randomized response technique. In this study, an improved randomized scrambling model is presented which gains improved efficiency over the available models. Moreover, the unified metric of respondent-privacy and mean square error under the new model is also less than that of the available scrambling methods. The development in terms of percent relative efficiency and the unified metric is proved for several values of the population parameters. Our findings make the proposed model ideal for use with real-world surveys.

Keywords: Mean estimator, scrambling variable, efficiency, randomized response, sensitive variable.

1. INTRODUCTION

Reliable data collection has an important role in judging the quality of any research study. In survey sampling, several techniques are available to collect data from the respondents. These include direct personal investigation, indirect personal investigation, collection through enumerators, collection through questionnaires, and internet-based surveys, among others. Generally, the response rate using these traditional methods is good enough when the nature of characteristics of interest is non-sensitive. However, there are many social surveys in which there is need to collect data on sensitive characteristics. For example, the grades achieved in a certain examination, abortion, the number of cigarettes consumed in a day, illegal income, and the payable volume of income tax. In such situations, the researchers often get refusals and false information from the respondents. The large number of untruthful reports by the survey participants may influence the estimates of the population parameters badly, by giving misleading results.

In the case of data collection on sensitive characteristics, Warner (1965) suggested a technique that safeguards the privacy of the respondents, motivating them to report truthful information. This method, called the randomized response technique, helps in increasing the rate of honest reporting, and reduces the non-response rate. Warner (1971) suggested a scrambling procedure to obtain data on quantitative characteristics. As opposed to the additive model of Warner (1971), Eichhorn and Hayre (1983) introduced multiplicative scrambling for sensitive surveys. Gupta et al. (2002) suggested a scrambling technique to keep the option of true response for survey participants who perceive the question as non-sensitive. The Gupta et al. (2002) method utilized an additive scrambling variable to randomize the responses. Bar-Lev et al. (2004) presented a multiplicative scrambling-based optional technique, adding the true response option to the Eichhorn and Hayre (1983) model. Yan et al. (2008) suggested a metric for measuring the privacy level in a given model. Gjestvang and Singh (2009) developed another additive-type scrambling method for efficient estimation of the mean. Diana and Perri (2011) suggested a linear combination type quantitative scrambling model which improved the previous models. Al-Sobhi et al. (2016) proposed another randomized technique that utilizes an additive-subtractive scrambling approach. Gupta et al.

https://doi.org/10.62500/icrtsda.1.1.60

(2018) proposed a metric for assessing the overall quality of quantitative models which considers both model efficiency and privacy level.

Gupta et al. (2020) studied variance estimation under the randomized response technique. Murtaza et al. (2021) proposed an additive optional model that utilized the assumption of correlated variables. Narjis and Shabbir (2023) incorporated the option of true response into the Gjestvang and Singh (2009) technique for development in efficiency and degree of privacy. Khalil et al. (2021) studied the effect of observational errors on the estimator of the mean. A versatile optional scrambling model to gain improvement over the Diana and Perri (2011) procedure was developed by Gupta et al. (2022).

Azeem et al. (2023) presented a new modification of the Narjis and Shabbir (2023) model by adding the choice of reporting half of the true value. They concluded that their model was efficient than the Narjis and Shabbir (2023) model in terms of both efficiency and the respondents' privacy protection. Recently, Azeem (2023) introduced exponential-type random noise for efficient estimation of the mean. Azeem and Salam (2023) developed a randomization strategy that uses direct response as well as scrambled response.

2. SOME EXISTING MODELS

Consider a probability sample of n units to be obtained by utilizing a simple random sampling design from a finite population containing N units. Further, Y denotes the quantitative sensitive variable of interest, and suppose S and T denote the additive-type scrambling and multiplicative-type scrambling variables respectively. Also, let the population means and variances of variable Y, S, and T are $E(Y)=\mu_y$, $E(S)=\theta$, $E(T)=1$, $V(Y_i)=\sigma_y^2$, $V(S)=\sigma_s^2$ and $V(T)=\sigma_s^2$, where σ_y^2, σ_s^2 and σ_T^2 respectively. It is further assumed that there is no dependency between all three variables, which safeguards privacy protection. To collect data by utilizing a quantitative scrambling model, the random/scrambling numbers for the variable(s) may be obtained by using an appropriate probability distribution, with parameters being pre-defined constants chosen by the researcher, according to the population characteristics. For instance, if the data on students' grades is needed on a scale 0 to 4, one can set the mean of the distribution between 0 and 4, as GPA often varies from 0 to 4. Likewise, if data on monthly expenditure is needed, the average of the distribution can be specified in hundreds or thousands of units, according to the currency of a country. The resulting random numbers may be displayed on a pack of 100 cards, every card containing a statement with a single random number. Each respondent is given the pack cards and a calculator and is directed to randomly select a card and then follow the given instructions on the chosen card to randomize his/her response. Survey participants are asked not to display the cards picked by them to the investigator, ensuring their privacy and motivating them to provide the information.

2.1 Warner's (1971) Model

The additive scrambling randomization technique suggested by Warner (1971) is as follows:

$$Z = Y + S, \tag{1}$$

where Z is the reported response. An unbiased estimator using the Warner (1971) technique can be expressed as:

$$\hat{\mu}_W = \frac{1}{n}\sum_{i=1}^{n} Z_i . \tag{2}$$

The expression for sampling variance of $\hat{\mu}_W$ is given by:

$$Var(\hat{\mu}_W) = \frac{1}{n}\left(\sigma_Y^2 + \sigma_S^2\right). \tag{3}$$

2.2 The Eichhorn and Hayre (1983) Model

https://doi.org/10.62500/icrtsda.1.1.60

The multiplicative scrambling randomization technique proposed by Eichhorn and Hayre (1983) is given as follows:

$$Z = TY\,. \tag{4}$$

The expression of the unbiased estimator of the population mean, under the Eichhorn and Hayre (1983) randomization technique, is as follows:

$$\hat{\mu}_{EH} = \frac{1}{n}\sum_{i=1}^{n} Z_i\,. \tag{5}$$

The expression for sampling variance of $\hat{\mu}_{EH}$ is as follows:

$$Var\left(\hat{\mu}_{EH}\right) = \frac{\sigma_Y^2}{n} + \frac{\sigma_T^2\left(\sigma_Y^2 + \mu_Y^2\right)}{n}. \tag{6}$$

2.3 The Gupta et al. (2002) Model

The combination of both true and additive scrambling response method suggested by Gupta et al. (2002) is given as follows:

$$Z = \begin{cases} Y, & \text{with probability } p \\ Y + S, & \text{with probability } 1-p. \end{cases} \tag{7}$$

An unbiased estimator using the Gupta et al. (2002) model can be expressed as:

$$\hat{\mu}_{G1} = \frac{1}{n}\sum_{i=1}^{n} Z_i\,, \tag{8}$$

The expression for sampling variance of $\hat{\mu}_{G1}$ is as follows:

$$Var\left(\hat{\mu}_{G1}\right) = \frac{1}{n}\left[\sigma_Y^2 + (1-p)\sigma_S^2\right]. \tag{9}$$

2.4 The Narjis and Shabbir (2023) Scrambling Model

Under the scrambling method of Narjis and Shabbir (2023), the observed response can be expressed as:

$$Z_{NS} = \begin{cases} Y_i - \beta S, & \text{with probability } P_1 = \dfrac{\alpha}{\alpha+\beta+\gamma}, \\ Y_i + \alpha S, & \text{with probability } P_2 = \dfrac{\beta}{\alpha+\beta+\gamma}, \\ Y_i, & \text{with probability } P_3 = \dfrac{\gamma}{\alpha+\beta+\gamma}, \end{cases} \quad i = 1, 2, 3, \ldots, n, \tag{10}$$

where α, β and γ denote some pre-defined constants. An unbiased estimator using the Narjis and Shabbir (2023) technique can be expressed as:

$$\hat{\mu}_{NS} = \frac{1}{n}\sum_{i=1}^{n} Z_{NS}. \tag{11}$$

The expression for sampling variance of $\hat{\mu}_{NS}$ is as follows:

https://doi.org/10.62500/icrtsda.1.1.60

$$Var(\hat{\mu}_{NS}) = \frac{1}{n}\left[\frac{\alpha\beta(\alpha+\beta)(\sigma_s^2+\theta^2)}{\alpha+\beta+\gamma}+\sigma_Y^2\right]. \tag{12}$$

3. PROPOSED MODEL

An efficient optional scrambling technique is introduced by improving the Narjis & Shabbir (2023) model. The proposed optional randomized response model (ORRT) provides a pack of 100 cards as a randomization device, for each respondent in the sample. These cards have printed statements based on subtractive-type scrambling, additive-type scrambling, and multiplicative-type scrambling, in addition to the true response option. A card is selected at random by the respondent and reports the scrambled response according to the instructions given on the selected card. The suggested randomization technique is easy to apply in practical surveys. Those respondents who don't have a strong background in Mathematics can easily randomize their responses, using a simple calculator.

The observed responses under the suggested Model are expressed as:

$$Z_p = \begin{cases} TY_i - \beta S, & \text{with probability } P_{11} = \dfrac{\alpha}{\alpha+\beta+\gamma+\lambda}, \\ TY_i + \alpha S, & \text{with probability } P_{12} = \dfrac{\beta}{\alpha+\beta+\gamma+\lambda}, \\ TY_i, & \text{with probability } P_{13} = \dfrac{\gamma}{\alpha+\beta+\gamma+\lambda}, \\ Y_i, & \text{with probability } P_{14} = \dfrac{\lambda}{\alpha+\beta+\gamma+\lambda}, \end{cases} \quad i = 1, 2, 3, \ldots, n, \tag{13}$$

where, α, β, γ and λ denote the constants determined by the interviewer. Using the suggested model, an unbiased estimator of the mean takes the form:

$$\hat{\mu}_p = \frac{1}{n}\sum_{i=1}^{n} Z_P \,. \tag{14}$$

4. MEAN AND SAMPLING VARIANCE

The proof of unbiasedness of the estimator along with the algebraic derivation of the sampling variance under the proposed model are given below.

Theorem 1: $\hat{\mu}_{p1}$ is an unbiased estimator of μ_Y under the proposed model.

Proof: By taking expectation on Eq. (14), we get:

$$E(\hat{\mu}_p) = E\left(\frac{1}{n}\sum_{i=1}^{n} Z_p\right) = \frac{1}{n}\sum_{i=1}^{n} E(Z_p). \tag{15}$$

Now,

$$E(Z_{p1}) = P_{11}E(TY_i - \beta S) + P_{12}E(TY_i + \alpha S) + P_{13}E(TY_i) + P_{14}E(Y_i), \tag{16}$$

or

$$= P_{11}\{1(\mu_Y) - \beta\theta\} + P_{12}\{1(\mu_Y) + \alpha\theta\} + P_{13}\{1(\mu_Y)\} + P_{14}\{\mu_Y\},$$

or

$$= \mu_Y\{P_{11} + P_{12} + P_{13} + P_{14}\} + \theta\{P_{11}\beta - P_{12}\alpha\},$$

or

https://doi.org/10.62500/icrtsda.1.1.60

$$= \mu_Y + \theta\left\{\frac{\alpha\beta - \alpha\beta}{\alpha+\beta+\gamma+\lambda}\right\},$$

or

$$E(Z_p) = \mu_Y . \tag{17}$$

Now putting Eq. (17) in Eq. (15) gives:

$$E(\hat{\mu}_p) = \frac{1}{n}\sum_{i=1}^{n}\mu_Y ,$$

or

$$E(\hat{\mu}_p) = \mu_Y . \tag{18}$$

Theorem 2: The algebraic expression for variance of $\hat{\mu}_{p1}$ using the proposed model is obtained as:

$$Var(\hat{\mu}_p) = \frac{1}{n^2}\sum_{i=1}^{n} Var(Z_p) = \frac{1}{n}\left[\frac{\alpha\beta(\alpha+\beta)(\theta^2+\sigma_s^2)+(\alpha+\beta+\gamma)\sigma_T^2(\mu_Y^2+\sigma_Y^2)}{\alpha+\beta+\gamma+\lambda} + \sigma_Y^2\right]. \tag{19}$$

Proof: By taking variance of Eq. (14), we get:

$$Var(\hat{\mu}_p) = Var\left(\frac{1}{n}\sum_{i=1}^{n} Z_p\right) = \frac{1}{n^2}\sum_{i=1}^{n} Var(Z_p). \tag{20}$$

Now

$$Var(Z_p) = E(Z_p^2) - \{E(Z_p)\}^2 . \tag{21}$$

$E(Z_p^2)$ can be simplified as:

$$E(Z_p^2) = \left[P_{11}E(TY_i - \beta S)^2 + P_{12}E(TY_i + \alpha S)^2 + P_{13}E(TY_i)^2 + P_{14}E(Y_i)^2\right],$$

or

$$= \begin{bmatrix} P_{11}\{(1+\sigma_T^2)(\mu_Y^2+\sigma_Y^2) - \beta(\theta^2+\sigma_s^2)\} + P_{12}\{(1+\sigma_T^2)(\mu_Y^2+\sigma_Y^2) \\ +\alpha(\theta^2+\sigma_s^2)\} + P_{13}\{(1+\sigma_T^2)(\mu_Y^2+\sigma_Y^2)\} + P_{14}(\mu_Y^2+\sigma_Y^2) \end{bmatrix},$$

or

$$= \begin{bmatrix} (\mu_Y^2+\sigma_Y^2)\{P_{1q}+P_{12}+P_{13}+P_{14}\} +^2 (\theta^2+\sigma_s^2)\{P_{11}\beta + P_{12}\alpha\} \\ +\sigma_T^2(\mu_Y^2+\sigma_Y^2)\{P_{11}+P_{12}+P_{13}\} \end{bmatrix},$$

or

$$E(Z_p^2) = \left[\mu_Y^2 + \sigma_Y^2 + \frac{\alpha\beta(\alpha+\beta)(\theta^2+\sigma_s^2)+(\alpha+\beta+\gamma)\sigma_T^2(\mu_Y^2+\sigma_Y^2)}{\alpha+\beta+\gamma+\lambda}\right]. \tag{22}$$

Using Eq. (22) and Eq. (18) in Eq. (21), we get:

$$Var(Z_p) = \left[\mu_Y^2 + \sigma_Y^2 + \frac{\alpha\beta(\alpha+\beta)(\theta^2+\sigma_s^2)+(\alpha+\beta+\gamma)\sigma_T^2(\mu_Y^2+\sigma_Y^2)}{\alpha+\beta+\gamma+\lambda} - \mu_Y^2\right]. \tag{23}$$

Using Eq. (23) in Eq. (20) gives:

$$Var(\hat{\mu}_{p1}) = \frac{1}{n^2}\sum_{i=1}^{n} Var(Z_p) = \frac{1}{n}\left[\frac{\alpha\beta(\alpha+\beta)(\theta^2+\sigma_s^2)+(\alpha+\beta+\gamma)\sigma_T^2(\mu_Y^2+\sigma_Y^2)}{\alpha+\beta+\gamma+\lambda} + \sigma_Y^2\right].$$

https://doi.org/10.62500/icrtsda.1.1.60

5. MODEL-PERFORMANCE MEASURES

The most common measure used for comparing the quality (in terms of efficiency) of two models is relative efficiency (RE). The mathematical expression of RE is given as:

$$RE = \frac{Var(\hat{\mu}_{y1})}{Var(\hat{\mu}_{y2})}, \tag{24}$$

where $Var(\hat{\mu}_{y1})$ and $Var(\hat{\mu}_{y2})$ are the variances of the estimators of population mean under 1st model and 2nd Model respectively. RE < 1 indicates that the first model is more efficient in terms of the variance than the 2nd model, and vice versa. In a situation where the sample mean is biased for the population under a specific model, then we used mean square error (MSE) instead of the sampling variance of that estimator.

The Yan et al. (2008) metric of respondents' privacy is given as:

$$\nabla = E[Z - Y]^2, \tag{25}$$

For a given randomized response model, a large value of ∇ indicates a high level of respondent-privacy. Another metric of model evaluation was suggested by Gupta et al. (2018), which is given as follows:

$$\delta = \frac{Var(\hat{\mu}_y)}{\nabla}. \tag{26}$$

A model with a smaller value of δ is interpreted as the better model with regard to both aspects i.e., efficiency and privacy level of the respondents.

The privacy measure using the Gjestvang & Singh (2009) technique can be obtained as:

$$\nabla_{GS} = \alpha\beta(\sigma_S^2 + \theta^2). \tag{27}$$

The unified measure using the Gjestvang & Singh (2009) scrambling technique can be obtained as:

$$\delta_{GS} = \frac{Var(\hat{\mu}_{GS})}{\nabla_{GS}} = \frac{1}{n}\left[1 + \frac{\sigma_Y^2}{\alpha\beta(\sigma_S^2 + \theta^2)}\right]. \tag{28}$$

Using the model of Narjis & Shabbir (2023), the privacy measure takes the form:

$$\nabla_{NS} = \frac{\alpha\beta(\alpha+\beta)(\sigma_S^2 + \theta^2)}{\alpha+\beta+\gamma}. \tag{29}$$

Likewise, the unified measure based on the Narjis & Shabbir (2023) method can be expressed as:

$$\delta_{NS} = \frac{Var(\hat{\mu}_{NS})}{\nabla_{NS}} = \frac{1}{n}\left[1 + \frac{(\alpha+\beta+\gamma)\sigma_Y^2}{\alpha\beta(\alpha+\beta)(\sigma_S^2 + \theta^2)}\right]. \tag{30}$$

The privacy measure under the suggested model may be obtained as:

$$\nabla_p = \frac{\alpha\beta(\alpha+\beta)(\sigma_s^2 + \theta^2) + (\alpha+\beta+\gamma)\sigma_T^2(\sigma_Y^2 + \mu_Y^2)}{\alpha+\beta+\gamma+\lambda}. \tag{31}$$

The unified measure using the suggested model can be expressed as:

$$\delta_{p1} = \frac{1}{n}\left[1 + \frac{(\alpha+\beta+\gamma+\lambda)\sigma_Y^2}{\alpha\beta(\alpha+\beta)(\sigma_s^2 + \theta^2) + (\alpha+\beta+\gamma)\sigma_T^2(\sigma_Y^2 + \mu_Y^2)}\right]. \tag{32}$$

6. A REAL-WORLD SURVEY USING THE SUGGESTED MODEL

https://doi.org/10.62500/icrtsda.1.1.60

A real-world survey was conducted to apply the proposed model for the collection of students' GPA data. A sample of size 60 students from the population of size 152 students was drawn using SRS design, from the undergraduate students presently enrolled in the Economics department of the University of Malakand, Pakistan. The objective of the study was to estimate the mean μ_y of the student's grades in the examination. The university follows the grading system on a scale of 4.0. Moreover, using a normal distribution with parameters 5 and 0.5, 100 random numbers were generated for the additive-type random variable *S*. Also, another set of 100 random numbers was obtained for the multiplicative-type random variable *T* by utilizing a normal distribution with both parameters equal to 1. Following the procedure of our proposed model, a deck of 100 cards utilizing the value of the scrambling variables *S* and *T*, consisting of four options, was used as a randomization tool. Every student in the sample was instructed to randomize his/her true response by selecting a card at random from the provided deck of 100 cards, and then follow the directions printed on the chosen card. The survey participants were directed to randomize their responses secretly and hide the card chosen by them from the survey researcher. Moreover, the values of constants were taken as $\alpha = 5$, $\beta = 2$, $\gamma = 1$, and $\lambda = 6$. The probabilities of selection of various cards were calculated as: $P_{11} = \frac{5}{5+2+1+6} = 0.36$, $P_{12} = \frac{2}{5+2+1+6} = 0.14$, $P_{13} = \frac{1}{5+2+1+6} = 0.07$, and $P_{14} = \frac{6}{5+2+1+6} = 0.43$. Putting these values in Eq. (13), the observed response model can be written as:

$$Z_p = \begin{cases} TY_i - 2S, & \text{with probability} \quad P_{11} = 0.36, \\ TY_i + 5S, & \text{with probability} \quad P_{12} = 0.14, \\ TY_i, & \text{with probability} \quad P_{13} = 0.07, \\ Y_i, & \text{with probability} \quad P_{14} = 0.43. \end{cases} \quad i=1,2,\ldots,n. \qquad (33)$$

According to the function in Eq. (33), each card of the deck showed one of the following four statements printed on it:

- **i.** A total of 36 % of the cards displayed the statement: "Subtract 2 times *S* from *T* times your true GPA and report the number you get".
- **ii.** A total of 14 % of the cards displayed the instruction: "Add 5 times *S* to *T* times your GPA and report the number you get".
- **iii.** A total of 7 % of the cards displayed the instruction: "Report *T* times *S* to your GPA".
- **iv.** The remaining 43 % of the cards displayed the statement: "Report your true GPA".

The responses observed from the 60 respondents have been given in Table 1.

Table 1: Observed Randomized Responses Using the Suggested Model

-2.17	5.79	-0.48	3.67	-0.13	1.77
1.99	1.93	20.56	1.96	3.93	-0.54
5.89	-0.56	4.80	12.40	1.92	5.91
2.00	1.93	1.92	3.90	4.95	2.27

https://doi.org/10.62500/icrtsda.1.1.60

1.79	-1.59	12.07	-1.32	3.94	6.39
3.47	-2.00	-2.66	6.71	3.82	21.63
2.20	-1.64	2.93	-2.62	1.81	1.88
1.69	-3.41	1.56	1.97	-1.86	13.21
-3.65	5.66	-0.38	20.83	2.79	1.95
-2.49	6.91	13.78	8.14	3.83	6.36

Due to the scrambling process of the responses, it can be observed that some of the reported responses are negative or even exceed the upper limit of the grading scale. The observed responses under the suggested model have a mean of 3.629, compared to the population mean of 3.69. This suggests that compared to the proposed Model, the proposed Model provided a more accurate estimate of the population mean.

7. SIMULATION STUDY

In order to compare the suggested model with the Narjis & Shabbir (2023) technique, a simulation study was carried out. The values of the percentage relative efficiency sampling variance of the mean presented in Table 2 were averaged over 1000 repeated samples. One may notice from the table that the proposed model is more precise than the Narjis & Shabbir (2023) technique.

Table 2: Comparison of PRE of the Proposed model vs. the Narjis & Shabbir model for $n = 100$, $\sigma_T^2 = 0.02$

α	β	γ	λ	$\sigma_S^2 = 2.25,\ \theta = 20$	$\sigma_S^2 = 3,\ \theta = 25$	$\sigma_S^2 = 5,\ \theta = 30$	$\sigma_S^2 = 8,\ \theta = 35$
10	0.5	15	5	204.476	200.00	209.229	215.363
			6	244.735	239.638	251.456	259.171
		20	5	169.14	158.563	171.359	180.493
			6	195.882	180.686	198.959	212.782
15	0.5	15	5	183.403	199.597	209.811	216.871
			6	234.39	225.498	238.144	246.694
		20	5	184.476	172.286	187.987	199.020
			6	228.3	215.038	237.394	253.01
20	0.5	15	5	231.965	221.114	237.037	247.634
			6	257.613	247.879	267.752	280.477
		20	5	240.402	215.323	248.802	272.449
			6	237.925	210.28	246.365	273.86

Moreover, the simulated values of ∇ for the suggested optional randomized response model and Narjis & Shabbir (2023) model are presented in Table 3 using various values of the parameters. Observing Table 3 it is clear the proposed model offers a high level of the respondents' privacy protection as compared to the Narjis & Shabbir (2023) model.

https://doi.org/10.62500/icrtsda.1.1.60

Table 3: Comparison of Privacy Measure of Proposed Model with Available Models

$n=100$, $\sigma_T^2=0.02$											
α	β	γ	λ	$\sigma_S^2=2.25,\ \theta=20$		$\sigma_S^2=3,\ \theta=25$		$\sigma_S^2=5\ \theta=30$		$\sigma_S^2=8,\ \theta=35$	
				∇_{NS}	∇_{P1}	∇_{NS}	∇_{P1}	∇_{NS}	∇_{P1}	∇_{NS}	∇_{P1}
10	0.5	15	5	441.534	445.694	688.939	709.556	992.789	1006.129	1352.561	1356.995
			6	440.890	445.853	688.069	709.524	991.432	1006.361	1350.542	1357.578
		20	5	434.176	446.812	677.515	712.013	976.283	1008.643	1330.003	1359.791
			6	435.873	449.248	679.809	714.199	979.862	1013.327	1335.327	1368.028
15	0.5	15	5	978.894	990.578	1493.010	1529.585	2151.904	2188.298	2932.400	2969.198
			6	973.142	980.609	1493.417	1519.422	2152.503	2172.782	2933.229	2946.551
		20	5	945.934	955.153	1476.344	1506.173	2127.187	2152.168	2897.568	2916.602
			6	951.190	953.273	1483.548	1502.055	2138.342	2147.549	2914.019	2911.578
20	0.6	15	5	1670.230	1682.807	2605.263	2639.053	3754.952	3786.763	5116.753	5146.616
			6	1678.677	1676.283	2616.891	2628.845	3772.916	3772.376	5143.173	5126.892
		20	5	1648.157	1665.449	2573.648	2614.436	3707.200	3749.261	5048.147	5092.480
			6	1650.587	1674.440	2577.005	2626.776	3712.376	3768.381	5055.74	5120.64

Also, to compare the overall quality of the suggested optional randomized response model and Narjis & Shabbir (2023) model the values of δ are presented in Table 4 using various values of the parameters. Observing Table 4, it is clear that the suggested model is more efficient than the Narjis & Shabbir (2023). It is clear from Table 4 that the proposed randomization technique has smaller values of δ as compared to the Narjis and Shabbir (2023) model, which indicates that the overall quality of the proposed model is better than the Narjis and Shabbir (2023) model.

Table 4: Comparison of Joint Measure of Proposed Model with Available Models

$n=100$, $\sigma_T^2=0.02$											
α	β	γ	λ	$\sigma_S^2=2.25,\ \theta=20$		$\sigma_S^2=3,\ \theta=25$		$\sigma_S^2=5,\ \theta=30$		$\sigma_S^2=8,\ \theta=35$	
				δ_{NS}	δ_{P1}	δ_{NS}	δ_{P1}	δ_{NS}	δ_{P1}	δ_{NS}	δ_{P1}
10	0.5	12	5	0.00973	0.00471	0.00939	0.00456	0.00918	0.00433	0.00904	0.00418
			6	0.00954	0.00386	0.00924	0.00374	0.00906	0.00355	0.00893	0.00343
		20	5	0.00430	0.00247	0.00407	0.00244	0.00394	0.00223	0.00385	0.00209
			6	0.00426	0.00211	0.00403	0.00212	0.0039	0.0019	0.00381	0.00175
15	0.5	15	5	0.00941	0.00507	0.00431	0.00211	0.00422	0.00198	0.00416	0.00190
			6	0.00950	0.00402	0.00432	0.00188	0.00423	0.00176	0.00417	0.00168
		20	5	0.00205	0.00110	0.00192	0.00109	0.00186	0.00098	0.00182	0.00091
			6	0.00202	0.00088	0.00190	0.00087	0.00183	0.00077	0.00179	0.00071
		15	5	0.00189	0.00081	0.00181	0.00081	0.00177	0.00074	0.00175	0.00070

https://doi.org/10.62500/icrtsda.1.1.60

20	0.5		6	0.00186	0.00072	0.00179	0.00072	0.00174	0.00065	0.00172	0.00061
		20	5	0.00080	0.00033	0.00073	0.00033	0.00070	0.00028	0.00069	0.00025
			6	0.00076	0.00032	0.00070	0.00033	0.00068	0.00027	0.00067	0.00024

8. DISCUSSION AND CONCLUSION

The primary goal of the randomized response survey procedure is to protect the respondents' privacy while obtaining a viable technique for the data collection of secret and sensitive variables. In the currently available literature, several varieties of the randomized response technique (RRT) models are available for the collection of data on sensitive issues. In any particular situation, the choice of a randomized response strategy is greatly dependent on two major considerations: efficiency of the model, and respondents' privacy. In this paper, a new improved optional RRT model has been developed by adding the option of multiplicative-type scrambling responses.

In the proposed randomized response technique, the option of multiplicative-type scrambling responses is used to adapt the Narjis and Shabbir (2023) randomized response technique. A real-world data of 60 students' examination grades was collected through the model which are shown in Table 1. Mathematical proof for the unbiasedness of the estimator and the algebraic expressions for the variance and the unified metric of privacy and efficiency under the suggested technique were derived.

The percentage relative efficiency of the proposed model with Narjis and Shabbir (2023) model has been presented in Table 2, showing the findings of the comparative analysis of the proposed ORRT model with Narjis and Shabbir (2023) optional technique, for various choice of parameters and constants. Table 3 shows the values of ∇ using the suggested ORRT model and Narjis and Shabbir (2023) randomization technique, using various choices of constants and parameters. From the results shown in Table 3, it is clear that for various choices of α, β, γ and λ, the suggested ORRT model has maximum values of ∇ than the Narjis and Shabbir (2023) randomization strategy, which shows that the proposed model offered high level of privacy protection to the respondents than the Narjis and Shabbir (2023) model. Moreover, Table 4 presents values of δ using the suggested ORRT model and Narjis and Shabbir (2023) technique. It may be clearly noticed that for various choices of α, β, γ and λ, the suggested model is more efficient than the Narjis and Shabbir (2023) technique.

9. FUTURE WORK

The present research study proposed a new ORRT model under which the mean estimator was proved to be more efficient than the estimator based on the already Narjis and Shabbir (2023) model. It may be interesting if variance estimation under the suggested ORRT models is analyzed by the future researchers.

REFERENCES

1. Azeem, M. (2023). Using the exponential function of scrambling variable in quantitative randomized response models. *Mathematical Methods in the Applied Sciences*, 46(13), 13882-13893.

2. Azeem, M., and Salam, A. (2023). Introducing an efficient alternative technique to optional quantitative randomized response models. *Methodology*, 19(1), 24-42.

3. Azeem, M., Hussain, S., Ijaz, M., and Salahuddin, N. (2024). An improved quantitative randomized response technique for data collection in sensitive surveys. *Quality & Quantity*, 58(1), 329-341.

https://doi.org/10.62500/icrtsda.1.1.60

4. Bar-Lev, S. K., Bobovitch, E., and Boukai, B. (2004). A note on randomized response models for quantitative data. *Metrika*, 60(3), 255-260.

5. Diana, G., and Perri, P. F. (2011). A class of estimators for quantitative sensitive data. *Statistical Papers*, 52, 633-650.

6. Eichhorn, B. H., and Hayre, L. S. (1983). Scrambled randomized response methods for obtaining sensitive quantitative data. *Journal of Statistical Planning and inference*, 7(4), 307-316.

7. Gjestvang, C. R., and Singh, S. (2009). An improved randomized response model: Estimation of mean. *Journal of Applied Statistics*, 36(12), 1361-1367.

8. Gupta, S., Gupta, B., and Singh, S. (2002). Estimation of sensitivity level of personal interview survey questions. *Journal of Statistical Planning and inference*, 100(2), 239-247.

9. Gupta, S., Mehta, S., Shabbir, J., and Khalil, S. (2018). A unified measure of respondent privacy and model efficiency in quantitative RRT models. *Journal of Statistical Theory and Practice*, 12, 506-511.

10. Gupta, S., Qureshi, M. N., and Khalil, S. (2020). Variance estimation using randomized response technique. *REVSTAT-Statistical Journal*, 18(2), 165-176.

11. Gupta, S., Zhang, J., Khalil, S., and Sapra, P. (2022). Mitigating lack of trust in quantitative randomized response technique models. *Communications in Statistics-Simulation and Computation*, 1-9. https://doi.org/10.1080/03610918.2022.2082477

12. Khalil, S., Zhang, Q., and Gupta, S. (2021). Mean estimation of sensitive variables under measurement errors using optional RRT models. *Communications in Statistics-Simulation and Computation*, 50(5), 1417-1426.

13. Hussain, Z., Al-Sobhi, M. M., Al-Zahrani, B., Singh, H. P., and Tarray, T. A. (2016). Improved randomized response in additive scrambling models. *Mathematical Population Studies*, 23(4), 205-221.

14. Murtaza, M., Singh, S., and Hussain, Z. (2021). Use of correlated scrambling variables in quantitative randomized response technique. *Biometrical Journal*, 63(1), 134-147.

15. Narjis, G., and Shabbir, J. (2023). An efficient new scrambled response model for estimating sensitive population mean in successive sampling. *Communications in Statistics-Simulation and Computation*, 52(11), 5327-5344.

16. Warner, S. L. (1965). Randomized response: A survey technique for eliminating evasive answer bias. *Journal of the American Statistical Association*, 60(309), 63-69.

17. Warner, S. L. (1971). The linear randomized response model. *Journal of the American Statistical Association*, 66(336), 884-888.

18. Yan, Z., Wang, J., and Lai, J. (2008). An efficiency and protection degree-based comparison among the quantitative randomized response strategies. *Communications in Statistics-Theory and Methods*, 38(3), 400-408.